



2ND NATIONAL CONFERENCE ON CHEMICAL TECHNOLOGY

NCCT 2023

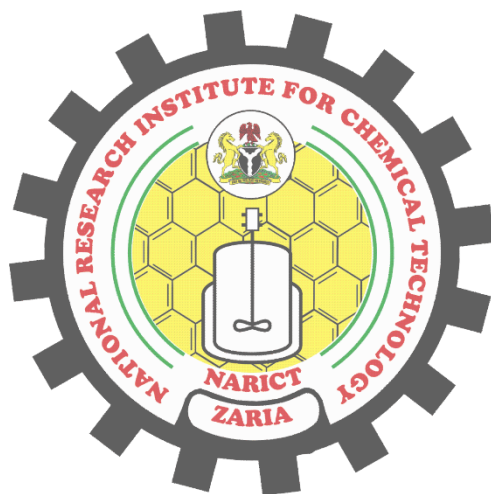
BOOK OF PROCEEDINGS

THEME:

**New Frontiers and Opportunities in Chemical
Technology for Sustainable Growth Paths in
Chemical Industry**

14th - 17th Nov. 2023

**NATIONAL RESEARCH INSTITUTE FOR CHEMICAL TECHNOLOGY
KM 4, OLD KANO ROAD, BASAWA, ZARIA, NIGERIA**



**2ND NATIONAL CONFERENCE ON
CHEMICAL TECHNOLOGY**

BOOK OF PROCEEDINGS

14TH – 17TH NOVEMBER 2023

**NATIONAL RESEARCH INSTITUTE FOR
CHEMICAL TECHNOLOGY**

KM. 4, OLD BASAWA ROAD, ZARIA, NIGERIA



HIS EXCELLENCY
BOLA AHMED TINUBU GCFR
PRESIDENT, COMMANDER-IN-CHIEF OF THE ARMED FORCES
FEDERAL REPUBLIC OF NIGERIA.



CHIEF UCHE GEOFFREY NNAJI
HONOURABLE MINISTER
FEDERAL MINISTRY OF INNOVATION, SCIENCE AND TECHNOLOGY



**PROFESSOR JEFFREY TSWARE BARMINAS
DIRECTOR-GENERAL/ CHIEF EXECUTIVE OFFICER
NATIONAL RESEARCH INSTITUTE FOR CHEMICAL
TECHNOLOGY, ZARIA**

NCCT 2023 CENTRAL ORGANIZING COMMITTEE

Technical Sub-Committee

1. Dr. Elijah Adegbe – Chair
2. Mr. Ephraim Audu
3. Engr. Chibueze N. Emejuro
4. Mr. Ismail Ibrahim
5. Mr Bashir Mohammed Aliyu
6. Ms Peculiar Okoro
7. Ms. Elizabeth Winful - Secretary

Logistics Sub-Committee

1. Dr. Ukannah S. Pendo - Chair
2. Mr. Danmallam Ahmed Adamu
3. Engr Joseph O. Otsai
4. Mr Victor Kajang
5. Mrs Ifeoma Oneli
6. Mr. Akuvada Ilyasu - Secretary

Welfare Sub-Committee

1. Mrs. Ugochi J. Okoduwa - Chair
2. Mrs. Aishat Ayoola Osigbesan
3. Mrs. Chioma N. Chibuzo- Anakor
4. Mr. Martins Kokoete Ukpong
5. Mr. Gero Mohammed - Secretary

Publicity Sub-Committee

1. Mr. Balli Gauje - Chair
2. Mr. Lawal Olamilekan Muritala
3. Mr. Ibrahim S. Umar
4. Mr. Simon A. Istifanus
5. Mr. Jibrin Abdulkadir
6. Mr. Abubakar Abdullahi
7. Mrs. Aishat Osigbesan - Secretary

Finance Sub-Committee

1. Mrs Hauwa M. Aliyu - Chair
2. Mr. Mohammed A. Suleiman
3. Ms Monica Odeh
4. Mr Jamilu Habibu
5. Mr. Yusuf O. Usman - Secretary

Engr. Dr. Opeoluwa O. Fasanya
Central Organizing Committee
Chairman

Mr. Olanipekun Idowu
Central Organizing Committee
Secretary

Brief on the National Conference on Chemical Technology (NCCT)

The National Research Institute for Chemical Technology was established in 1988 with a mission “to attain international expertise in chemicals related to environmental interventions, petrochemicals, chemical analysis, chemical process design, modelling and simulation, engineering fabrications and design, chemical analytical instrumentation and quality control and a vision “to be recognized as a research institute of international repute in the provision of innovative research and development in the processing and conversion of indigenous raw materials into valuable chemicals and petrochemical products for industrial application”.

In pursuance of the above, the National Conference on Chemical Technology (NCCT) was borne out of a passion of the National Research Institute for Chemical Technology (NARICT) as the only Research Institute for Chemical Technology in Nigeria, to contribute her quota to National development by bringing researchers, scientists, engineers, captains of industries together via a scientific conference under a theme that captures and accommodates all scientific fields and proffer solutions to pressing issues affecting the economy, health, agriculture, industry, education and other sectors of the nation.

The 1st National conference on Chemical Technology held between the 7th -10th August, 2017 with the theme “The Role of Chemical Technology in a Diversifying Economy”. The aim of the conference was to provide a platform for academics, researchers, engineers and industries to present their research results and development activities in Environmental Science and Engineering, Waste management, Chemical and Food processing, Material science and Nanotechnology and Green and Clean Energy. This conference attracted participation from the Academia, Research Institutes and the Industry. There were 12 technical sessions and 68 papers were presented.

With the aim of the 1st NCCT in mind, the 2nd edition held on the 14th-17th November, 2023 with the theme “New Frontiers and Opportunities in Chemical Technology for Sustainable Growth Paths in Chemical Industry”. This time the conference was hybrid and attracted international participation from across the globe with 2 keynote speakers, 5 plenary speakers and over a hundred papers presented on site and virtually in the 12 technical sessions and more than three hundred participants.

**COMMUNIQUE ISSUED AT END OF 2ND NATIONAL CONFERENCE ON
CHEMICAL TECHNOLOGY (NCCT2023) HELD AT NATIONAL RESEARCH
INSTITUTE FOR CHEMICAL TECHNOLOGY, BASAWA, ZARIA FROM 14TH –
17TH NOVEMBER, 2023**

The 2nd National Conference on Chemical Technology was held at the National Research Institute for Chemical Technology, Zaria, from 14th – 17th November 2023 with the theme: New Frontiers and Opportunities in Chemical Technology for Sustainable Growth Paths in Chemical Industry.

The opening ceremony was presided over by Prof. Paul A. Mamza – President and Chairman of the Council, African Association of Polymer Scientists and Engineers, while the welcome address was delivered by the Chief Host and Director General/Chief Executive Officer of National Research Institute for Chemical Technology – Prof. Jeffrey Tsware Barminas. The occasion was graced by eminent personalities amongst whom are the Honourable Minister of the Federal Ministry of Innovation, Science and Technology ably represented by the Technical Adviser Strategy and Planning, Prof. Nnaayelugo Ike-Muonso, the Chief of Air Staff ably represented by the Commandant of Air Force Institute of Technology, AVM Rabe Musa, the DG/CEO of Nigerian Institute of Leather and Science Technology, Prof. M.K. Yakubu, the Emir of Zazzau represented by the Madakin Gona Zazzau, Engr. Jamilu Muhammad amongst others.

The Chairman of the occasion, Prof. Paul A Mamza in his speech said with the new global trends and universal shift to a knowledge-based economy, the Nigerian government must prioritize and invest heavily in Science and Technology, especially in the area of Chemical Technology research and development if Nigeria must stand a chance of being counted amongst the comity of progressive nations. He further noted that scientists, engineers, and technologists must continue to discuss, collaborate, coordinate, and put their efforts together to take their rightful place in the quest for the nation's development.

The Chief Host, the DG/CEO of NARICT; Professor Jeffrey Tsware Barminas in his welcome address stated that the chemical industry has become a veritable tool for the development of any nation and that National Research Institute for Chemical Technology under his stewardship has carried out cutting edge researches and developed an array of products for a circular economy, green chemistry, renewable energy among others which can be categorized into those suitable for uptake by Small and Medium Enterprises (SMEs), Micro Small and Medium enterprises (MSMEs), cottage industries etc.

The Minister in his address said the timing for the Conference is apt and in line with Mr President's eight (8) points agenda for economic recovery. He noted that innovations, science and technology are a sure way to drive the government's economic recovery agenda that will place Nigeria on the path of sustainable growth and development.

Two keynote papers were expertly delivered by Prof. Joydeep Dutta, KTH Stockholm, Sweden and Prof. Naveen Kumar, DTU, New Delhi, India respectively.

The plenary papers addressed all the sub-themes of the conference and this was followed by twelve (12) technical sessions with well over three hundred (300) participants from all walks of life including physical and virtual participants from across Nigeria, Australia, Sweden, India, Ireland and Turkey.

Following the extensive and thought-provoking deliberations, the Conference recommends the following;

- i. NARICT is the only Chemical Technology Institute in Nigeria and a flagship agency under the Federal Ministry of Innovations, Science and Technology to spearhead the development of a National Chemical Technology Policy which would provide the required framework to develop the chemical technology subsector as the critical driver for industrialization and national growth.
- ii. Government at all levels should create an enabling environment for the commercialization of Scientific and Technological research findings.

- iii. The government should fund Innovation, Science and Technology research and ensure the revival of the ailing chemical industries in Nigeria.
- iv. The need for curriculum review and research being tailored towards product-driven and solving of societal problems in Research institutes and educational institutions
- v. The adoption of new technologies such as the use of Computational tools, Green Chemistry and Machine Learning models in our research for better output.
- vi. There is a need for a paradigm shift from the use of fossil fuels to renewable sources of energy to curb the menace of global warming.
- vii. Building local capacity and reviving chemical industries with new technologies to facilitate speedy economic recovery through industrialization.
- viii. Bridging the gap between industries and the institution through effective communication of R&D.
- ix. The Nigerian chemical industry needs to embrace sustainable growth paths which involve strategies and practices that prioritize environmental, social and economic considerations

TABLE OF CONTENT

TITLE PAGE.....	II
NCCT 2023 CENTRAL ORGANIZING COMMITTEE	VI
CONFERENCE COMMUNIQUE	VIII
TABLE OF CONTENT	X
P005 - AGRICULTURAL WASTE UTILIZATION FOR THE PRODUCTION OF PAPER-BAGS: A POTENTIAL SUBSTITUTE FOR PLASTICS BAGS AND PACKAGING	1
P007 - EVALUATION OF SORGHUM AND MILLET KUNUN-ZAKI ICE CREAM ENRICHED WITH FRESH MANGO AND BANANA FRUITS	9
P008 - PROXIMATE ANALYSIS OF SOME PROCESSED CASSAVA PRODUCTS OBTAINED WITHIN LAFIA METROPOLIS OF NASARAWA STATE	18
P009 - BIOACTIVE COMPONENTS AND ANTIOXIDANT ACTIVITIES OF TOASTED PEARL MILLET-AVOCADO SEEDS FLOUR BLENDS	25
P010 - SYNTHESIS AND CHARACTERIZATION OF SILICA NANOPARTICLES FROM COCONUT HUSK.....	32
P015 - OPTIMIZATION OF BIODIESEL PRODUCTION FROM BUSHEL KENTUCKY SEED OIL USING SULPHATED TIN OXIDE CATALYST.....	39
P018 - PROCESSES OF ENERGY CONVERSION, TRANSFORMATION AND SOCIO-ECONOMIC UTILIZATION OF AGRO-WASTES TO BRIQUETTES: A COMPREHENSIVE REVIEW	47
P20 - EVALUATION OF BIOETHANOL PRODUCTION POTENTIAL FROM GUINEA CORN HUSK USING <i>SACCHAROMYCES CEREVISIAE</i> AND <i>SACCHAROMYCES CARLBERGENSIS</i>	53
P025 - DEVELOPMENT OF DESKTOP TELEOPERATED MANIPULATOR: A NEW RESEARCH DIRECTION IN EXPERIMENTING IN A LABORATORY IN HAZARDOUS ENVIRONMENT- A REVIEW	59
P026 -WEIGHT LOSS AND ELECTROCHEMICAL TECHNIQUES TO ASSESS THE CORROSION INHIBITION POTENTIAL OF ETHANOL EXTRACT OF ACACIA NILOTICA POD ON MILD STEEL IN ACIDIC MEDIUM	68
P027 - EFFECT OF PROCESS VARIABLES ON METHYL ESTER PRODUCTION USING CHITOSAN AS HETEROGENEOUS CATALYST.....	77
P028 - BIOGENIC SYNTHESIS AND CHARACTERIZATION OF SULPHUR NANOPARTICLES FROM SULPHUR-RICH AGRORESIDUES (ONION AND CABBAGE PEELS)	88
P029 - <i>TERMINALIA CATAPPA</i> AS INHIBITOR AGAINST IMPROVISED FERROUS IMPLANT IN CORROSIVE MEDIA VIA EXPERIMENTAL APPROACH	94
P030 - PHYTOCHEMICAL AND ELEMENTAL ASSESSMENT OF SOME SELECTED HERBAL MIXTURES USED IN TREATING GASTRIC ULCER IN KADUNA METROPOLIS	105
P031 - THE IMPACT OF ARTIFICIAL INTELLIGENCE ON RESEARCH INNOVATION: NIGERIAN PERSPECTIVE	112
P032 - GASIFICATION OF MAIZE COBS AND ITS CHARACTERIZATION FOR ENERGY GENERATION	120
P033 - PRODUCTION AND ASSESSMENT OF ALUMINUM SULPHATE CRYSTALS (ALUM) FROM RECYCLED ALUMINUM FOILS AS COAGULANT IN WATER TREATMENT.....	126
P35 - <i>SARGASSUM</i> SEAWEEDES IN THE BLUE ECONOMY: A MINI REVIEW OF THEIR POTENTIAL AND APPLICATIONS IN CHEMICAL INDUSTRIES	135

P036 - MECHANOCHEMISTRY: A GREEN CHEMISTRY FOR GREEN TECHNOLOGY	145
P038 - A COMPARATIVE PROXIMATE AND MINERAL ANALYSIS OF BRANDED YOGHURTS AND NONO (LOCAL FULANI) YOGHURT SOLD IN ZARIA, KADUNA STATE, NIGERIA	151
P039 - NUTRACEUTICALS AND NATURAL PRODUCTS IN THE LIGHT OF METABOLOMICS TECHNOLOGIES- A CUTTING-EDGES APPROACH TO DRUG DISCOVERY AND REPOSITIONING.....	158
P040 - MODIFICATION OF UREA FORMALDEHYDE RESIN ADHESIVE USING NANO BIOCHAR DERIVED FROM BAMBOO WASTE AND IT'S APPLICATION IN PARTICLE BOARD PRODUCTION	162
P041 - SORPTION STUDIES, OPTIMIZATION AND EFFECT OF REUSABILITY ON THE USE OF WASTE POLYPROPYLENE PLASTICS AS SORBENTS FOR OIL SPILL CLEAN UP	169
P043 - EMISSIONS BASED ENVIRONMENTAL IMPACT ANALYSIS FROM A POWER-COOLING ORGANIC RANKINE CYCLE WITH EJECTOR SYSTEM	178
P044 - PHYTOCHEMICAL, ANTIOXIDANT AND ANTIMICROBIAL POTENTIALS OF METHANOLIC AND HEXANE EXTRACTS OF TERMINALIA CATAPPA, POLYANTHA LONGIFOLIA AND EUCALYPTUS CITODORA PLANT LEAVES	188
P045 - ZEOLITE (ZSM-5) DOPED HYDROXYAPATITE BIO-COMPOSITES DERIVED FROM CATFISH SKELETONS FOR BONE REPAIRS; SYNTHESIS AND BIOMECHANICAL CHARACTERIZATION	198
P046 - ADSORPTIVE APTITUDES OF TWO (2) NIGERIAN CLAYS FOR AQUEOUS CU, PB AND ZN METALS.....	207
P048 - EFFECT OF ABSTRACTION TEMPERATURE AND TIME ON THE PERCENTAGE YIELD OF OIL EXTRACTED FROM LEMON PEELS VIA HYDRO-DISTILLATION TECHNIQUE	213
P049 - APPLICATION OF CHEMICAL TECHNOLOGY IN FOOD PRODUCTION, PROCESSING, AND PRESERVATION IN NIGERIA: CHALLENGES AND CONCERNS	218
P050 -THERMAL ANALYSIS OF A DEVELOPED NANO CUO BASED-NEEM OIL CUTTING FLUID FOR MACHINING TI-6AL-4V	222
P051 - ANTIFUNGAL COMPOUNDS PRODUCED BY LACTIC ACID BACTERIA: LANTIPLANTIBACILLUS PLANTARUM OQ224994.1 FROM SOIL SAMPLES OF NATURE GARDEN AHMADU BELLO UNIVERSITY ZARIA.	231
P052 - RESISTOTYPING OF ESCHERICHIA COLI AND LISTERIA SPP. ISOLATED FROM MILK AND MILK PRODUCTS SOLD AROUND ZARIA	242
P053 - EVALUATION OF BIOGAS PRODUCTION FROM THE DIGESTION & CO-DIGESTION OF POULTRY DROPPINGS, PIG MANURE, AND BREWERY-SPENT GRAIN USING ENZYMES AMYLASE.	252
P054 - PARTICLE SIZE AND SIZE DISTRIBUTION OPTIMIZATION OF PALLADIUM NANOPARTICLES BIOSYNTHESIZED USING SIDA ACUTA LEAF EXTRACT AS REDUCTANT: TAGUCHI-GREY RELATIONAL APPROACH.....	260
P056 - SUSTAINABLE HYDROGEN PRODUCTION USING CERIUM-ENHANCED COPPER-ZINC-MCM41 CATALYSTS.....	274
P057 - MENTHOL-BASED HYDROPHOBIC DEEP EUTECTIC SOLVENT FOR THE DEGRADATION OF PHENOLIC POLLUTANTS IN REFINERY EFFLUENT	283
P060 - TREATMENT OF PHENOLIC WASTEWATER WITH ZERO-VALENT IRON IMMOBILIZED ON POWDERED ACTIVATED CARBON COATED WITH CHITOSAN	294
P062 - DETERMINATION OF ACTIVITY CONCENTRATION, HAZARD INDICES AND ABSORBED DOSE RATES OF SOME RADIONUCLIDES FOUND IN SELECTED FERTILIZERS USED IN YOLA	302
P064 - GAS DYNAMICS THROUGH METAL FOAM: INNOVATIVE EXPERIMENTAL SETUP AND INSIGHTS.....	311
P065 - METAL FOAMS AND AIR FLOW: EXPERIMENTAL FINDINGS AND INSIGHTS	318

P066 - INVESTIGATION ON THE EFFECT OF IRON OXIDE (FeO ₃) PIGMENT ON THE PRODUCTION OF COLOURED CEMENT FOR CONCRETE WORKS	325
P067 - PREPARATION OF HIERARCHICAL FE-ZSM-5 FOR THE SELECTIVE CATALYTIC CRACKING OF CRUDE OIL	333
P068 - ANALYSIS OF ACID OPTIONS IN THE PURIFICATION OF SPENT MOTOR ENGINE OIL USING ACIDIFIED CLAY	340
P070 - BATCH ADSORPTION OF HEAVY METAL IONS FROM PHARMACEUTICAL WASTEWATER USING COCONUT SHELL AND GROUNDNUT HULL ACTIVATED CARBON	348
P071 - INSIGHT INTO THE DEACTIVATION OF FRESH FCC CATALYST FROM A TYPICAL FCC UNIT OF A PETROLEUM REFINERY.....	355
P072 - BIOGAS SYNTHESIS FROM HUMAN EXCRETA USING ZIRCONIA DOPED SILICA CATALYST	361
P074 - DETERMINATION OF BIOMASS AND LIPID PRODUCTIVITY OF <i>CHLORELLA VULGARIS</i> FOR BIODIESEL PRODUCTION.....	370
P075 - PREVALENCE OF URINARY SCHISTOSOMIASIS AMONG PUPILS OF SELECTED PRIMARY SCHOOLS IN JOS SOUTH LOCAL GOVERNMENT AREA, PLATEAU STATE	376
P076 - PRODUCTION OF HYDROCHAR AS ADSORBENTS FOR REMOVAL OF HEAVY METALS FROM PHARMACEUTICAL WASTEWATER	383
P077 - PHYSICO-CHEMICAL AND FUNCTIONAL PROPERTIES OF TAMARIND (<i>TAMARINDUS INDICA</i>) SEED KERNEL STARCH	390
P078 - SILATION TECHNIQUES AS A VIABLE TECHNIQUE FOR THE DEVELOPMENT OF SUPER ADSORBENT FOR OIL SPILL CLEANUP: A REVIEW	395
P079 - DETERMINATION OF LD50, FECUNDITY AND LOCOMOTOR EFFECT OF AQUEOUS BEETROOT (<i>BETA VULGARIS</i>) PLANT EXTRACT IN THE PRODUCTION OF COLORANT FOR FOOD AND PHARMACEUTICAL INDUSTRY USING <i>DROSOPHILA MELANOGASTER</i>	400
P080 - ASSESSMENT OF THE EFFICACY OF SOME SELECTED PLANTS AS DERIVED BIO-PESTICIDES IN THE CONTROL OF COWPEA PESTS ON THE FIELD	407
P081 - STUDY OF THE EFFECTS OF PROCESS CONDITIONS ON BLEACHING OF PALM OIL USING ACTIVATED CLAY	412
P082 - PHYSICO-CHEMICAL AND FUNCTIONAL PROPERTIES OF TAMARIND (<i>TAMARINDUS INDICA</i>) SEED KERNEL STARCH	422
P083 - SLAUGHTERHOUSE EFFLUENT: ENVIRONMENTAL IMPACTS, PRE-TREATMENTS, AND APPLICATIONS	429
P084 - PRODUCTION OF FIRE RETARDANT FROM KAOLIN AND INDUSTRIAL EFFLUENT FOR NIGERIAN BUILDING CONSTRUCTION INDUSTRY.....	437
P085 - ASSESSING THE ECOLOGICAL AND ENVIRONMENTAL IMPACTS OF OIL SPILLS FROM REFINERIES ON SOIL AND WATER – A MINI REVIEW	447
P86 - ENHANCING PALM OIL REFINING USING ACTIVATED CARBON DERIVED FROM A LOW-RANK COAL (LRC)	460
P087 - CHEMICAL SAFETY MEASURES SURVEY ON HAZARDOUS CHEMICALS UTILIZED IN SMALL-SCALE BUSINESSES IN THE THREE MOST AGRARIAN STATES OF SOUTHWEST NIGERIA	467
P088 - ASSESSMENT OF FIRE RETARDANCY PROPERTIES OF BIOLOGICALLY AND CHEMICALLY EXTRACTED JUTE FIBRES USING SURFACE EMBEDMENT	474

P089 - ASSESSMENT OF FUNCTIONAL COTTON FABRIC PRODUCED USING CHEMICALLY SYNTHESIZED SILVER-NANO COATING	480
P090 - DEVELOPMENT OF SELF IGNITED FIRE EXTINGUISHER BALL: A REVIEW	488
P091 - THE PRESENCE OF ALKALOIDS AND ANTI-MALARIAL ACTIVITY OF <i>P. GUAJAVA</i> LEAVES EXTRACT	493
P092 - CONFIGURATION OF SOLID OXIDE FUEL CELL USING BIOFUEL OBTAINED FROM SUGARCANE BAGGASSE	498
P093 - A REVIEW ON SUSTAINABLE LOW-DENSITY POLYETHYLENE (LDPE) WASTE MANAGEMENT: POSSIBILITES FOR NIGERIA	507
P094 - ANTIMICROBIAL ACTIVITIES OF CALOTROPIS PROCERA: A REVIEW	517
P095 - EFFECT OF ACETYLATION AND FATTY ACID TREATMENT ON OLEOPHILICITY OF KENAF FIBRES	524
P096 - SYNTHESIS OF HIERARCHICAL ZSM-5 ZEOLITE WITH IMPROVED MESOPOROSITY	530
P097 - DEMULSIFICATION EFFICIENCY OF THREE FATTY ACID BASED DEMULSIFIERS ON NIGERIAN CRUDE OIL EMULSIONS	542
P098 - APPLICATION OF DEEP EUTECTIC SOLVENTS IN REMEDIATION OF CONTAMINATED WATER – A MINI REVIEW	548
P099 - COMPUTATIONAL ESTIMATION OF HEXANE SELECTED THERMODYNAMIC PROPERTIES: USING PROCESS AND ATOMIC-SCALE SIMULATIONS IN CONTRAST WITH EXPERIMENTS	561
P100 - CORROSION MITIGATION STRATEGIES: INTEGRATING CLUSTER MODEL STABILITY & MATERIAL SCREENING FOR ENHANCED METAL PROTECTION IN ATOMIC-SCALE SIMULATIONS	566
P101 - ANTIMICROBIAL PROPERTIES OF GARLIC (<i>ALLIUM SATIVUM</i>): A MINI REVIEW	573
P102 - THE PHYSICAL PROPERTIES AND EFFECT OF ACRYLIC POLYMER DISPERSIONS ON WATER VAPOUR PERMEABILITY OF FINISHED LEATHERS	582
P103 - REVIEW ON PHEROMONES IN AGRICULTURE:	594
DISCOVERY, SYNTHESIS, AND ADVANCEMENTS FOR SUSTAINABILITY, ECONOMICS, AND CROP ENHANCEMENT	594
P104 - PHYSICOCHEMICAL CHARACTERIZATION OF LAUNDRY WASTEWATER AND ITS ENVIROCHEMICAL IMPACT ON SOILS AND WATER	599
P105 - EXTRACTION OF BITUMEN FROM TAR SANDS OBTAINED FROM LODA, ONDO STATE, NIGERIA FOR APPLICATIONS IN CONSTRUCTIONS AND PETROCHEMICALS	604
P106 - ENHANCEMENT OF THE ANTIBACTERIAL ACTIVITIES OF AMPICILLIN BY SCHIFF BASE FORMATION AND COMPLEXING WITH METAL(II)-IONS OF CU, FE AND ZN.	611
P107 - PRODUCTION AND CHARACTERIZATION OF ORGANIC POTASH FROM AGRICULTURAL WASTES IN FOOD AND FERTILIZER APPLICATIONS: A CASE STUDY OF CORNCOB AND GUINEA CORN HUSK	617
P108 - EFFECT OF OPTIMUM PROCESS CONDITIONS FOR DETOXIFICATION OF PHORBOL ESTER (PE) AND ANTI-NUTRIENTS REDUCTION OF <i>JATROPHA CURCAS</i> SEED CAKE (JSC) BY <i>LENZITES BETULINA</i>	626
P109 - THE INDUCED DAMAGE TO LIVER AND KIDNEY OF WISTAR RAT BY SPENT VEGETABLE OIL AND THE AMELIORATING POTENTIALS OF COCONUT OIL	635
P110 - DESIGN OF 200KG/DAY ZEOLITE ODOUR ABATEMENT PILOT PLANT FROM KAOLIN (CLAY)	642
P111 - THEORETICAL INVESTIGATION OF THE EFFECTS OF SOLVENTS ON ELECTRONIC AND NON-LINEAR OPTICAL PROPERTIES OF SUMANENE MOLECULE BASED ON DFT	649
P112 - SYNTHESIS OF AZO DYE AND ITS IRON COMPLEX DERIVED FROM 3-AMINOPHENOL	657

P113 - ISOLATION AND CHARACTERIZATION OF <i>ASPERGILLUS NIGER</i> AND <i>SACCHAROMYCES CEREVISIAE</i> FOR BIOETHANOL	662
P114 - PRODUCTION OF BIOETHANOL FROM SAWDUST USING CO-CULTURE OF <i>ASPERGILLUS NIGER</i> AND <i>SACCHAROMYCES CEREVISIAE</i>	669
P115 - EFFECT OF SULPHURIC ACID CONCENTRATION ON COPPER LEACHING FROM METAL SCRAPS FOR COPPER SULPHATE SYNTHESIS.....	670
P116 - OPTIMIZATION OF THE EPOXIDATION PROCESS PARAMETERS OF BAOBAB SEED OIL	675
P118 - DEVELOPMENT OF BEEHIVE-GINGER/SISAL POLYESTER HYBRID COMPOSITE FOR BUILDING AND FURNITURE INDUSTRIES	683
P119 - EFFECT OF DIFFERENT PROCESSING METHODS ON THE PROXIMATE AND FUNCTIONAL PROPERTIES OF <i>DETARIUM SENEGALENSE</i> (TALLOW) SEED FLOUR	690
P120 - ISOLATION AND AUTHENTICATION OF RHIZOBIA FROM RHIZOSPHERE AND ROOT NODULES OF SOYBEAN PLANTS	695
P121 - ASSESSMENT OF ELEMENTAL COMPOSITIONS OF EXTRACTED DATE PALM (<i>PHOENIX DACTYLIFERA L</i>) SYRUP VARIETIES OBTAINED FROM WUKARI MARKET, TARABA STATE	705

P005 - AGRICULTURAL WASTE UTILIZATION FOR THE PRODUCTION OF PAPER-BAGS: A POTENTIAL SUBSTITUTE FOR PLASTICS BAGS AND PACKAGING

Tyohemba, R.L.^{1&2*}, Ajegi, J.O.³, Inyanda, D.O.⁴, Akura, J.M.², Awua, V.T.² & Adai, G.A.²

¹Centre for Food Technology & Research, Benue State University Makurdi, ²Department of Chemistry, Benue State University Makurdi, ³Department of Chemistry, College of Education Oju, Benue State, ⁴Department of Chemistry & Biochemistry, Federal Polytechnic Nasarawa, Nasarawa State.

Corresponding author email: rtyohemba@bsum.edu.ng

ABSTRACT

With the world reeling from increasing environmental degradation resulting from plastic pollution and overexploitation of forest resources, eco-friendly alternatives are being sought after. In the current research, the potential of some agricultural residues as alternatives to plastic and wood were investigated. The Kraft pulping process was successfully employed to extract cellulosic materials from banana stems, pawpaw stems, and soybeans straw. The yield of pulp (cellulose) was 41.2%, 42.5% and 43.4% for banana stems, pawpaw stem and soybeans straw respectively, whereas the moisture content, ash content, and pulp consistency ranged between 6.2 – 9.3%, 0.39 – 1.74%, and 25.50 – 28.5% respectively. FTIR analyses of the materials confirmed presence of cellulose while the SEM revealed the materials comprise of highly compacted thin sheets of carbon fibres on its surface. XRD results showed the presence of crystals with two major diffraction peaks at $2\theta = 15^\circ$ and 24° for pawpaw stem and soybeans straw respectively; and three major diffraction peaks at $2\theta = 27^\circ$, 45° and 52° in banana stem, indicating the presence of crystalline structural formation. The pulps obtained from all three waste products were tested for their suitability in certain applications. While those from banana and pawpaw stems showed great prospects as paper and packaging materials such as shopping bags, soybeans straw appeared more suitable for use as feedstock for particleboards production. The results from the study indicate that these agricultural wastes have potential as substitutes for non-biodegradable plastic packaging, and can potentially reduce the reliance on forests for the production of pulp.

KEYWORDS

Pulp, agricultural waste, paper, cellulose, packaging bags

1.0 INTRODUCTION

Over the ages, the pulp and paper mills have remained an essential part of the global economy, providing a wide variety of products for various applications. Due to rapid industrial development and urbanization, the consumption of paper has increased exponentially in the past decades, especially in high-income countries such as the United States, many in the European Union, Japan, and China (Worku, Bachheti, Bachheti, Rodrigues Reis, & Chandel, 2023).

Along with the exponential increase in the use of cellulose/pulp products comes a corresponding increase in the use of forest resources to produce pulp. The pulp and paper industry rely primarily on the use of fibrous wood, with approximately 300 million tonnes of paper is produced worldwide

daily (Alam, Rikta, Hasnine, & Ahmed, 2004). This overdependence on fibrous wood has been linked to significant environmental problems, including deforestation, soil erosion, greenhouse gas emissions, and global warming. Other raw material that also bear cellulosic fiber structures, such as non-woody plants, could therefore be considered for the manufacturing of pulp and paper to mitigate the environmental problems associated with its use (Mousavi, Hosseini, Resalati, Mahdavi, & Garmaroody, 2013). It has been suggested that agricultural residues and weed plant residues can cater to the growing demand for paper in the packaging sector, as well as hygiene and sanitation products such as paper towels, toilet paper, and disposable makeup wipes, among others (Kashyap, Solanki, Kamboj, & Pandey, 2020). In India, for instance, agricultural residues account for approximately 28% of the total feedstock used in

the pulp and paper industry (Adel et al., 2016), supplied mainly from bagasse, wheat and rice straws, cotton stalks, and other agricultural residues.

Agricultural residues are defined as the by-product or waste of agricultural activities which are generated in huge amounts after each harvesting season. The Rapid increase in the world's population has resulted in high demand of food which has in turn lead to the production of large amount of the agricultural waste. Most of the residues are burnt in the open by farmers resulting in air pollution, while others are simply dumped in open fields, equally polluting the environment. Several researchers have explored the possibility of producing pulp from agricultural residues including wheat and rye straw (Salehi, Kordsachia, & Patt, 2014), okra stalks (Omer, Khider, Elzaki, Mohieldin, & Shomeina, 2019), chilli pepper and pea stems (Gonzalo et al., 2017), and wheat straw, barley straw, and cotton stalk (Kadam, Forrest, & Jacobson, 2000).

Notwithstanding the ethical propriety and environmental/economic benefits to using agricultural residues as alternatives to woods, certain challenges tend to limit their adoption. The specific physical and chemical characteristics of non-wood fibres play an essential role in their viability as substitutes for wood (ATEŞ, Deniz, KIRCI, Atik, & Okan, 2015). For instance, straw, like many other agricultural residues, usually possess high water contents, reaching up to 70% on a weight basis in some cases, which needs to be dropped to levels around or below 25% to avoid microbial spoilage (Rousu, Rousu, & Anttila, 2002). Drying straw fibres presents unique challenges, since its fibres are typically shorter than those in softwoods, they generally drain more slowly. Also, the high silica content of straw fibres, which makes the pulp recovery process challenging, is one of the most significant issues with the chemical pulping of agricultural residues (PAN & LEARY, 2000). A case in point is bamboo, with a comparatively high ash and silicon content which tends to hinder the recovery process for alkaline spent liquor and quality of some high-grade pulp products such as dissolving pulp. Efforts have however been made to resolve these limitations. One of such notable developments is the lime-alkali-oxygen pulping process. In this process used for straw, adding lime solves the silica problems. When lime is added to the cooking liquor, silica reacts to form calcium silicate, which is insoluble in

water and therefore separable from the broth (Abd El-Sayed, El-Sakhawy, & El-Sakhawy, 2020).

In Nigeria, a lot of potentials exist with regards to sustainable pulp production. Nigeria is rich in agricultural residues, such as rice husk, bagasse, banana, pawpaw, date palm rachis and leaves, millet and sesame stalks, sorghum, wheat and soybeans straw, okra, as well as sunflower. Each of these non-wood materials can be a suitable candidate for pulp and paper manufacturing (Saeed, Liu, Chen, & Lucia, 2017). Despite the amount of work done with respect to the subject matter, little evidence exists to suggest banana stems, pawpaw stems and soybeans straws have been investigated. Therefore, the current effort investigates the suitability of locally available banana stems, pawpaw stems and soybeans straw for the extraction of pulp and production of paper and particle boards for furniture making.

2.0 MATERIALS AND METHODS

2.1. Sample collection and preparation

The agricultural residues used for the current studies were obtained from different harvested fields within Makurdi local government area of Benue state, Nigeria. The residues were cut into chips measuring 4-5 cm in length, and then washed carefully to remove sand and dust particles. Thereafter, they were separately left under the sun for three days to dehydrate and then placed in an oven to dry to a constant weight.

2.2. Preparation of white liquor

White liquor is a solution of sodium sulfide and sodium hydroxide which dissolves the lignin that binds cellulose fibers together. The liquor was prepared by mixing 0.1 M NaOH and 0.2 M Na₂S in a 3:1 ratio under room temperature in a 500 mL beaker. The mixture is kept for 2 hrs while stirring at intervals for proper homogenization before usage (Gonzalez et al., 2023).

2.3. Pulping

The foremost goal of pulping is delignification. The oven dried samples were pulped using Kraft pulping method as described by Paula et al [17], with slight modifications. Exactly 50 g of the oven dried samples were carefully weighed into 250 mL conical flasks and the white liquor introduced into the flasks until its content was half submerged in the liquor. The flasks were then sealed, and the system heated on a hot plate with a magnetic stirrer at

200 °C for 1 hour. The resultant broths were then allowed to cool to room temperature and then filtered over Whatman No. 1 filter paper. The residue left on the filter paper was cleaned with water to a neutral pH and then kept in a fume hood to dry.

2.4. Pulp yield

The yield was calculated using the following formula

$$\text{Yield of pulp (\%)} = \frac{\text{Mass of pulp obtained}}{\text{Mass of sample used}} \times 100 \quad (1)$$

2.5. Determination of moisture content

Exactly 2.0 g of sample were introduced into a pre-weighed crucible and the weight of the crucible plus sample recorded.

The crucibles and their contents were then placed in a moisture oven at 105 °C for 3 h. Thereafter, they were carefully transferred to a desiccator and allowed to cool to a stable temperature. The final mass was then taken using an analytical balance.

The moisture content was calculated as follows:

$$\% \text{ Moisture} = \frac{\text{weight loss}}{\text{Sample weight}} \times 100 \quad (2)$$

$$\% \text{ Moisture} = \frac{W2 - W3}{W2 - W1} \times 100 \quad (3)$$

Where W1 = weight of empty crucible

W2 = weight of crucible + pulp sample before drying.

W3 = weight of crucible + pulp sample after drying.

2.6. Pulp consistency

The consistency of the pulp was determined from the predetermined weight of the ash. The consistency was calculated using the formula:

$$\text{Pulp consistency (\%)} = \frac{\text{Dry weight of sample}}{\text{Total weight of sample}} \times 100 \quad (6)$$

2.7. Characterization of pulp

Characterization of the produced pulp was done to confirm its formation and to check some of its characteristics.

2.7.1 SEM analysis

Scanning electron microscopy (SEM) was used to assess the morphological features of the pulps produced. The films of the sample were prepared on a carbon coated copper grid by dropping a very small amount of the sample mixture on the grid which were then allowed to dry by placing under a mercury lamp for 5 min. The samples were analyzed at an accelerating voltage of 15 kV.

2.7.2 X-ray diffraction Analysis (XRD)

Powdered samples were pelletized and sieved to 0.074 mm. These were later taken in an aluminum alloy grid (35 mm x 50 mm) on a flat glass plate and covered with a paper. Wearing hand gloves, the samples were compacted by gently pressing them with the hand.

Each sample was run through the Rigaku D/Max-IIIc X-ray diffractometer developed by the Rigaku Int. Corp. Tokyo, Japan and set to produce diffractions at scanning rate of 20/min in the 2 to 500 at room temperature with a cuka radiation set at 40 kV and 20 ma. The diffraction data obtained was compared to that of the standard data of minerals from the mineral powder diffraction library.

2.7.3 FTIR analysis of pulp

The chemical composition of the synthesized cellulosic materials was studied using FTIR spectrometer. The samples were analyzed in the range of 4000 cm⁻¹ - 400 cm⁻¹.

2.8. Production of paper and particle board

For paper production, the blended pulp from babana and pawpaw stems was transferred into a mould after the addition of some formation-aid to ensure the smooth flow of the fibre and even spread of the pulp over the mould after which the mould and deckle were removed from the tub and the water allowed to drain completely. The form on the moulder was removed and the drained pulp was transferred into a pellon material and allowed to dry completely under the sun to form a solid paper.

To produce the particle board, the pulp obtained from the soybean straw was used. To improve the density and impart some desirable mechanical properties on the end product, the pulp was beaten for about 20 minutes during which time distilled water was being added intermittently. Starch and calcium carbonate were added as adhesive to enhance particle bonding and surface properties respectively. After thorough blending using a mechanical blender, the mixture was poured into a

decker and molder and dried in an oven until it hardens.

3.0 RESULTS AND DISCUSSION

3.1. Physicochemical properties of pulp produced from agricultural wastes

The results of the pulp yield and some properties of the pulp produced are presented in the following tables and figures below:

Table 1. Physicochemical properties (%) of produced pulp from agricultural wastes

S/N	Parameter	Banana stem	Pawpaw stem	Soya beans straw
1	Pulp yield	41.22±0.3	42.50±0.5	43.4±0.1
2	Moisture content	6.2±0.7	7.3±0.2	9.3±0.4
3	Ash content	0.39±0.4	1.74±0.5	1.68±0.1
4	Consistency	26.20±0.1	25.50±0.3	28.5±0.4

*Values are means±SD of triplicate determinations

3.1.1 Pulp yield

The yield of the pulp obtained from the pawpaw stem was estimated to be 42.50 %, 43.4% for soybean straw, while that obtained from banana stem was 41.22%. These figures are slightly comparable to the results obtained by Plazonic, et al., (Plazonić, Barbarić-Mikočević, & Antonović, 2016) in a similar study using wheat straw. These relatively high yield shows that pawpaw and banana stems are a good source of pulp, and by extension favorable substitute for wood in the paper industry.

3.1.2 Moisture content

From the results obtained, the moisture content of the cellulosic material produced from banana and pawpaw stems were 6.3% and 7.3% respectively which was slightly lower than the 9.3% for soybean straw. In comparison, Fasoyiro, et al., (Fasoyiro, Ashaye, Adeola, & Samuel, 2005) reported 3.56 % moisture content in cellulose. Moisture content of 24% or more is said to be deleterious to fibrous materials as it promotes the growth of microbes which ultimately destroys the material (Kadam et al., 2000). This low degree of moisture suggests that the resultant cellulosic material could be suitable for producing materials for long term applications such as packaging and paper bags.

3.1.3 Ash content

The ash content gives a measure of the total mineral content of a material. The ash composition of the pulp was found to be 0.39% for banana stems and 1.74% in pawpaw stems, while it was 1.68% in soybean straw. These low ash contents are indicative of the predominance of cellulosic organic

molecules as compared to mineral constituents. It also gives a fair estimate of the suitability of the derived fibres for the intended purpose.

3.1.4 Pulp consistency

The pulp consistency is one of the most important pulp and paper variables. It affects pulp mill washing and screening efficiency, as well as bleaching reactions. In the paper mill it affects refining, chemical additives, paper forming, and the uniformity of the sheet (Olejnik, 2013). In the current study, the pulp produced had a consistency of 25.50%, 26.2%, and 28.5% for pawpaw stems, banana stems, and soybean straw respectively, comparable to the figure, 26.77%, reported by Ford et al., (Ford, Mendon, Thames, & Rawlins, 2010) in their study.

3.2. Characterization of pulp produced from agricultural waste materials

3.2.1 SEM characterization

Figures 1(a – c), 2(a – c), and 3(a – c) show the SEM images of the fibres obtained from the pawpaw stem, banana stem, and soybean straws respectively. While both banana and pawpaw stems show some similarity in the nature of the fibres in that they comprise of scattered smooth thin sheets of fibres, soybean straw appears coarse and densely packed. These properties impart some degree of flexibility and rigidity respectively on whatever bulk material they are used to fabricate. The SEM micrograph of the cellulose is similar with the report by Asrofi et al., (Asrofi, Abrial, Kasim, & Pratoto, 2017).

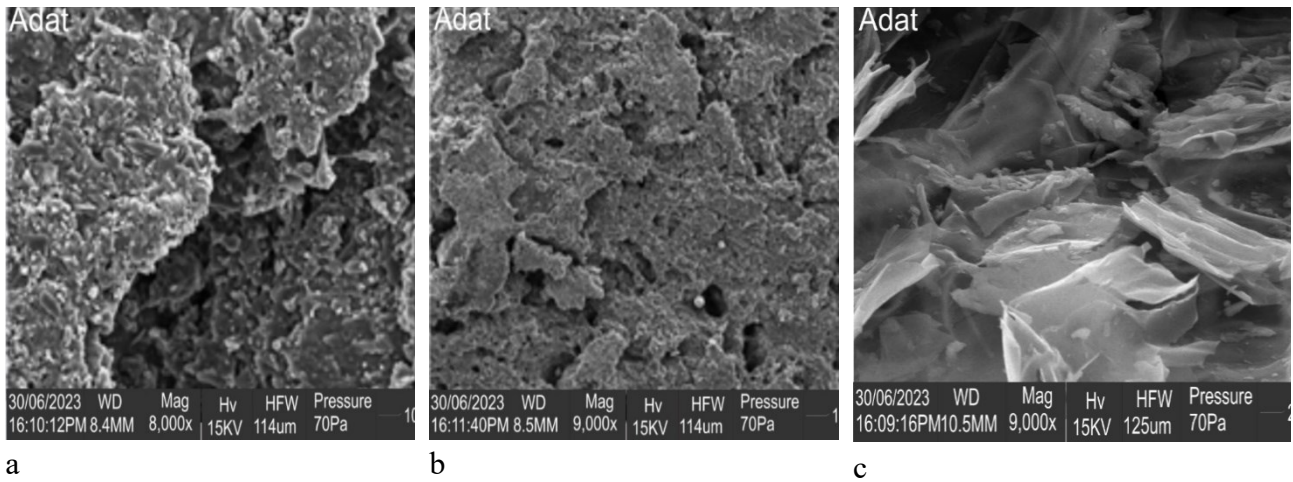


Fig. 1(a – c): Scanning electron microscopy images of cellulose fibres obtained from pawpaw stems.

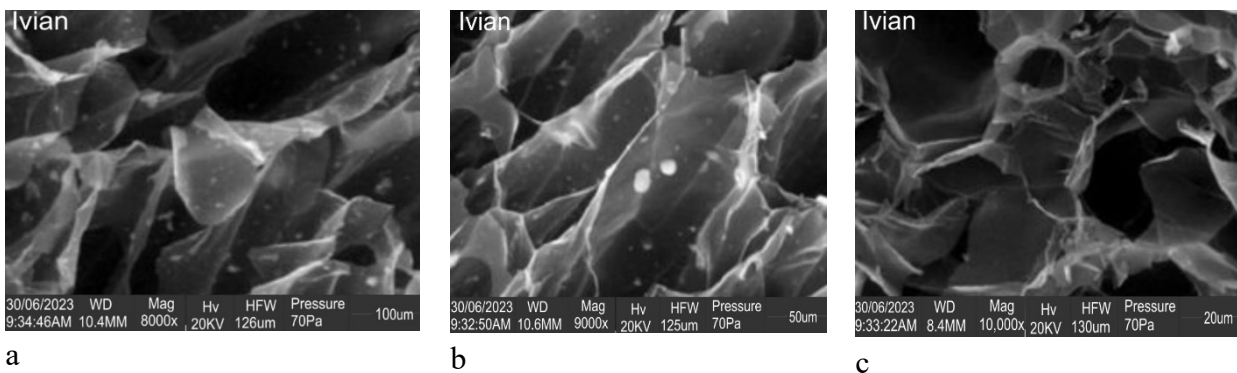


Fig. 2(a – c): Scanning electron microscopy images of cellulose fibres obtained from pawpaw stems.

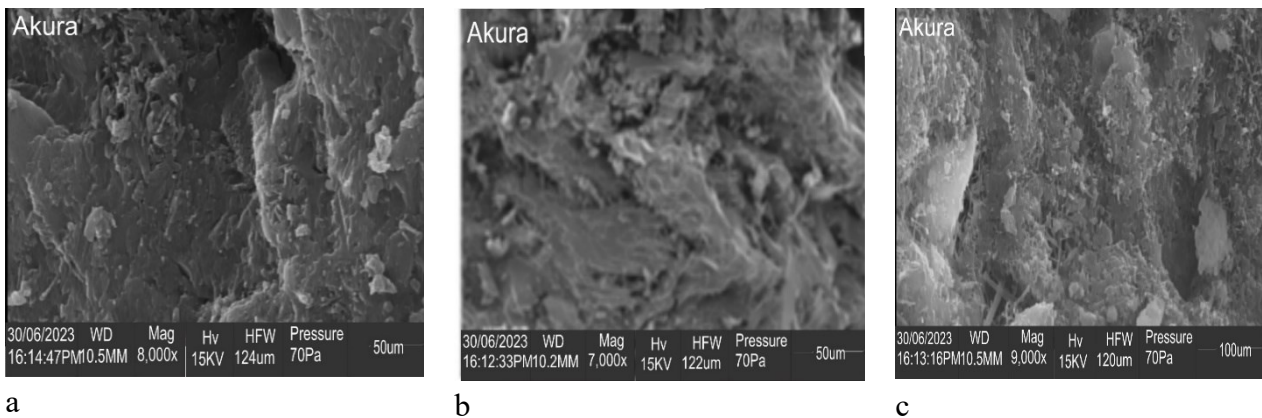


Fig. 3(a – c): Scanning electron microscopy images of cellulose fibres obtained from pawpaw stems

3.2.2 XRD analysis

The main purpose of X-ray diffraction was to identify the crystalline structure of the bio material. The X-ray powder diffraction (XRD) analysis of the various pulps share quite dissimilar features. While the spectrum of banana stem (Fig 4a) and soybean (Fig. 4b) straw show two major diffraction peaks at $2\theta = 15^\circ$ and 24° , that of pawpaw (Fig. 4c) presented three intense peaks at $2\theta = 15^\circ$, 44° , and 53° . These peaks define the features of crystalline

cellulose and are characteristic of Si in form of SiO_2 in the pulp as an inorganic component (Sarker, Azargohar, Dalai, & Venkatesh, 2020). It is suspected that the removal of hemicellulose and lignin contents induced a realignment of the crystalline spheres resulting in a steady increase in the index of crystallinity. Ford et al., (Ford et al., 2010) reported XRD peaks about $2\theta = 26^\circ$, 36.4° , and 50.5° and deduced that the extracted cellulose possesses a crystalline rather than amorphous structure.

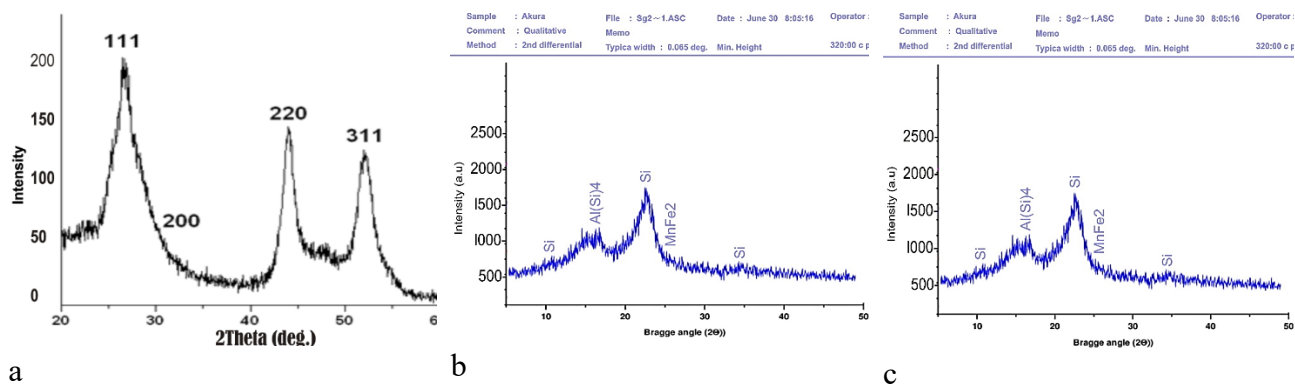


Fig. 4(a – c): XRD of pulp obtained from banana stems, soya beans straw and pawpaw stems

Fourier Transform-Infrared analysis

All feedstocks showed almost similar functional groups (Fig. 5 a – c). In the case of feedstocks, a wide band was noticed at approximately 3402 cm^{-1} because of O–H stretching, which represents the existence of the OH group in cellulose, hemicellulose, and lignin [24]. The peak at 2860 cm^{-1} is associated with the antisymmetric -C-H-stretching vibrations of CH_3 groups in cellulose and similar result have been reported for cellulosic

materials (Azargohar et al., 2019; Huntley, Crews, & Curry, 2015; Wahyono, Astuti, Gede Wiryawan, Sugoro, & Jayanegara, 2019). The band at 1616 cm^{-1} shows the C=C stretching. The peak at 1360 cm^{-1} was assigned to O=S=O symmetric stretching vibration, likely resulting from the presence of SO_2 group from the Na_2S treatment. In addition, C=O stretching of the C–O group in cellulose, hemicellulose, and lignin can be detected at 1020 cm^{-1} (Asrofi et al., 2017).

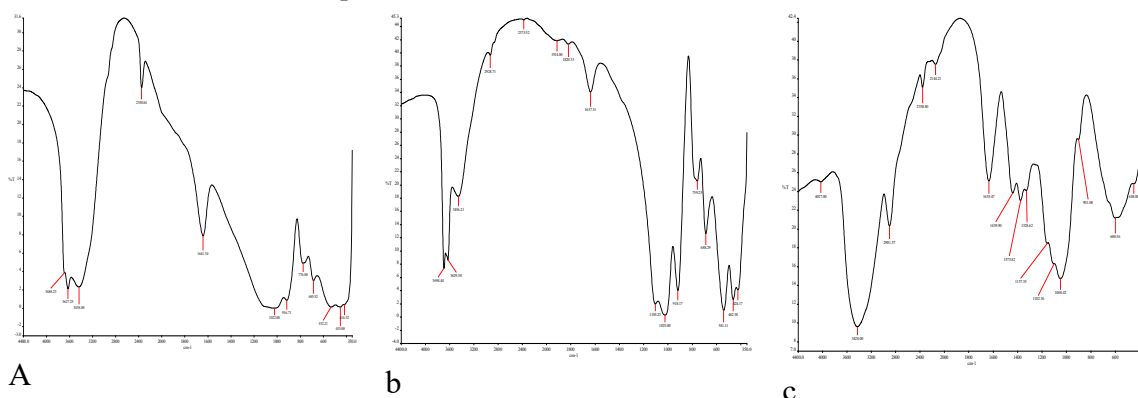


Fig. 5 (a – c): FTR spectra of pulp produced from Banana stems, pawpaw stems and soy beans straw.

3.3. Production of paper and particle board

The recovered cellulosic materials from banana/pawpaw stem and soybean straw were used to produce paper and particleboard respectively. Although the current study was a preliminary study to assess the remote possibility of using these materials for these purposes, the results obtained showed a lot of promise.

The papers produced were strong enough to withstand abrasion by blunt marker pen but ball pen bore through it. The low quality of the paper produced was because the production process was not optimized, especially with respect to the bonding material selected, starch. Therefore, it was indeed expected that the quality of the papers, given the conditions under which they were produced,

would not meet commercial standards. But with optimization, such a challenge can be addressed.

The particleboard produced also showed limited strength under pressure compared with commercially available particleboards. This is for the same reason as explained in the case of the papers produced.

4.0 CONCLUSIONS AND RECOMMENDATION

Three agricultural residues have been studied to assess their potential as substitute to wood for the production of pulp. Their physicochemical characteristics indicate that the materials have a lot of promise in the area of paper and particle board

production. Notwithstanding the positive results obtained in the current research, there is still much work to be done in the areas of characterizing the pulp and materials produced as well as optimization of the production process to achieve a more durable and competitive product.

5.0 REFERENCES

- Abd El-Sayed, E. S., El-Sakhawy, M., & El-Sakhawy, M. A.-M. (2020). Non-wood fibers as raw material for pulp and paper industry. *Nordic Pulp & Paper Research Journal*, 35(2), 215-230.
- Adel, A. M., El-Gendy, A. A., Diab, M. A., Abou-Zeid, R. E., El-Zawawy, W. K., & Dufresne, A. (2016). Microfibrillated cellulose from agricultural residues. Part I: Papermaking application. *Industrial Crops and Products*, 93, 161-174.
- Alam, M., Rikta, S. Y., Hasnine, M. T., & Ahmed, F. (2004). Production of Eco-friendly Handmade Paper from The Waste Paper Generated in Municipalities of Dhaka City, Bangladesh. *City*, 1, 1-3.
- Asrofi, M., Abral, H., Kasim, A., & Pratoto, A. (2017). XRD and FTIR studies of nanocrystalline cellulose from water hyacinth (*Eichornia crassipes*) fiber. *Journal of Metastable and Nanocrystalline Materials*, 29, 9-16.
- ATEŞ, S., Deniz, I., KIRCI, H., Atik, C., & Okan, O. T. (2015). Comparison of pulping and bleaching behaviors of some agricultural residues. *Turkish Journal of Agriculture and Forestry*, 39(1), 144-153.
- Azargohar, R., Nanda, S., Kang, K., Bond, T., Karunakaran, C., Dalai, A. K., & Kozinski, J. A. (2019). Effects of bio-additives on the physicochemical properties and mechanical behavior of canola hull fuel pellets. *Renewable Energy*, 132, 296-307.
- Fasoyiro, S., Ashaye, O., Adeola, A., & Samuel, F. (2005). Chemical and storability of fruit-flavoured (*Hibiscus sabdariffa*) drinks. *World J. Agric. Sci*, 1(2), 165-168.
- Ford, E. N. J., Mendon, S. K., Thames, S. F., & Rawlins, J. W. (2010). X-ray diffraction of cotton treated with neutralized vegetable oil-based macromolecular crosslinkers. *Journal of Engineered Fibers and Fabrics*, 5(1), 155892501000500102.
- Gonzalez, P. G. A., de Jesus Gariboti, J. C., Leal Silva, J. F., Lopes, E. S., Abaide, E. R., Lopes, M. S., . . . Tovar, L. P. (2023). Soybean straw as a feedstock for value-added chemicals and materials: recent trends and emerging prospects. *BioEnergy Research*, 16(2), 717-740.
- Gonzalo, A., Bimbela, F., Sánchez, J., Labidi, J., Marín, F., & Arauzo, J. (2017). Evaluation of different agricultural residues as raw materials for pulp and paper production using a semichemical process. *Journal of Cleaner Production*, 156, 184-193.
- Huntley, C. J., Crews, K. D., & Curry, M. L. (2015). Chemical functionalization and characterization of cellulose extracted from wheat straw using acid hydrolysis methodologies. *International Journal of Polymer Science*, 2015.
- Kadam, K. L., Forrest, L. H., & Jacobson, W. A. (2000). Rice straw as a lignocellulosic resource: collection, processing, transportation, and environmental aspects. *Biomass and Bioenergy*, 18(5), 369-389.
- Kashyap, B. K., Solanki, M. K., Kamboj, D. V., & Pandey, A. K. (2020). *Waste to Energy: Prospects and Applications*: Springer.
- Mousavi, S. M. M., Hosseini, S. Z., Resalati, H., Mahdavi, S., & Garmaroody, E. R. (2013). Papermaking potential of rapeseed straw, a new agricultural-based fiber source. *Journal of Cleaner Production*, 52, 420-424.
- Olejniak, K. (2013). Impact of pulp consistency on refining process conducted under constant intensity determined by SEL and SEC factors. *BioResources*, 8(3), 3212-3230.
- Omer, S. H., Khider, T. O., Elzaki, O. T., Mohieldin, S. D., & Shomeina, S. K. (2019). Application of soda-AQ pulping to agricultural waste (okra stalks) from Sudan. *BMC Chemical Engineering*, 1, 1-6.
- PAN, G. X., & LEARY, G. J. (2000). The bleachability of wheat straw alkaline

- peroxide mechanical pulp. *Cellulose chemistry and technology*, 34(5-6), 537-547.
- Plazonić, I., Barbarić-Mikočević, Ž., & Antonović, A. (2016). Chemical composition of straw as an alternative material to wood raw material in fibre isolation. *Drvna industrija*, 67(2), 119-125.
- Rousu, P., Rousu, P., & Anttila, J. (2002). Sustainable pulp production from agricultural waste. *Resources, Conservation and Recycling*, 35(1-2), 85-103.
- Saeed, H. A., Liu, Y., Chen, H., & Lucia, L. A. (2017). Suitable approach using agricultural residues for pulp and paper manufacturing. *Nordic Pulp & Paper Research Journal*, 32(4), 674-682.
- Salehi, K., Kordsachia, O., & Patt, R. (2014). Comparison of MEA/AQ, soda and soda/AQ pulping of wheat and rye straw. *Industrial Crops and Products*, 52, 603-610.
- Sarker, T. R., Azargohar, R., Dalai, A. K., & Venkatesh, M. (2020). Physicochemical and fuel characteristics of torrefied agricultural residues for sustainable fuel production. *Energy & Fuels*, 34(11), 14169-14181.
- Wahyono, T., Astuti, D. A., Gede Wiryawan, I. K., Sugoro, I., & Jayanegara, A. (2019). *Fourier transform mid-infrared (FTIR) spectroscopy to identify tannin compounds in the panicle of sorghum mutant lines*. Paper presented at the IOP Conference Series: Materials Science and Engineering.
- Worku, L. A., Bachheti, A., Bachheti, R. K., Rodrigues Reis, C. E., & Chandel, A. K. (2023). Agricultural residues as raw materials for pulp and paper production: Overview and applications on membrane fabrication. *Membranes*, 13(2), 228.

6.0 ACKNOWLEDGEMENTS

The authors appreciate the funding provided by the Royal Society of Chemistry, United Kingdom and the Centre for Food technology & Research, Benue State University Makurdi.

P007 - EVALUATION OF SORGHUM AND MILLET KUNUN-ZAKI ICE CREAM ENRICHED WITH FRESH MANGO AND BANANA FRUITS

Bai E.N^{*1}, Otor M.E², Otache E.A¹, Matthew A.O³, and Fakunle R.T³

¹Centre for Food Technology and Research, Benue State University, Makurdi, Benue State, Nigeria ²National Veterinary Research Institute, Jos, Plateau State, Nigeria, ³Department of Chemistry, Faculty of Physical Sciences, University of Ilorin, Kwara State, Nigeria

Corresponding author email: ellangbai@gmail.com

ABSTRACT

This study was designed to contribute to value addition by nutritionally evaluating ice cream formulated from kunun-zaki and soymilk incorporated with mango and banana fruits and comparing it with conventional ice creams. Two variants of ice cream were produced using a modified method for making ice cream designated as B (40% kunun-zaki, 40% banana pulp and 20% soymilk); C (40% kunun-zaki, 40% mango pulp and 20% soymilk), while the commercial dairy-based ice cream was served as the control (sample A). Proximate analysis, vitamins and mineral compositions were carried out on the samples using standard procedures. The results showed that all the formulated samples had lower fat content, ranging from 0.60 - 0.96 g/100g in comparison to the control sample with fat content of 8.15 g/100g. Similarly, Samples B and C reportedly contained higher vitamin B6, vitamin C, calcium and sodium content in comparison to sample A. Sensory evaluation showed the most acceptable variants in comparison to the control sample to be samples B and sample C. These findings further lend credence to the importance of value addition as a good strategy for providing healthier food alternatives while contributing to reduction of post-harvest losses of fruits.

KEYWORDS

Food production, Fruits, Ice Cream, Natural products, Post-Harvest losses

1.0 INTRODUCTION

Ice cream is a frozen dessert which has over the years been produced mainly from dairy products. These dairy products used in the production of ice cream are known to be milk and cream that also determines its nutrient and shelf life (1). Ice creams are expensive owing to the high economic costs associated with the use of dairy milk (1) and the health hazards (lactose intolerance, hypercholesterolemia) which have been reported to be associated with the consumption of dairy ice cream coupled with poor milk production in Nigeria. Consequently, attempts to obtain and utilize cheaper and safer substitutes with no chemical additives and comparative or even higher nutritional quality, particularly, in terms of improved protein, vitamin, and mineral contents have been canvassed as replacement of dairy base for value addition (2) to address malnutrition and contribute to control of post-harvest losses of crops and fruits (3).

Kunun-zaki is a popular cereal based non-alcoholic beverage drink (4) that can be used in the production of Ice creams. It originates from the

northern Nigeria where sorghum, millet or maize could be used for its preparation (5). Owing to nutrient losses during the various stages of production such as steeping, milling and sieving (6), its nutritional value can be boosted with addition of soybean (*Glycine max L.*), which has been shown to be loaded with essential amino acids (7). Hence, the formulation of ice cream from cereal based kunun-zaki supplemented with soybean milk, banana, mango and avocado fruits become important vehicles for delivering a variety of vitamins and minerals (8) that can contribute to addressing malnutrition and improving health trends, whose menace is on the increase particularly in developing societies (9). This study therefore evaluates a plant-based ice cream product enriched with fruits with the aim of improving its nutritional value while also contributing through value addition by post-harvest utilization of food crops and fruits.

2.0 MATERIAL AND METHODS

2.1 Sample collection

Seeds (Sorghum, millet, soybean) and fruits (Mango, Banana) for the preparation of kunun-zaki were all purchased from markets in Makurdi metropolis of Benue State, Nigeria.

2.2 Sample preparation

2.2.1 Preparation of “kunun-zaki”

Sorghum grains (2 kg) and millet (2 kg) were weighed and sorted by hand to remove foreign substances and dirt. They were then washed separately under running water to ensure it was clean before being steeped in water for 12 h, drained and grounded. Ginger was also washed along with the other ingredients and then ground into paste separately from the grains using a wet milling machine (disc attrition). To the paste, 4 L of boiling water was added to the large portion containing the composite paste to gelatinize the starch. The smaller portion containing the ingredients was then added to the larger portion immediately and stirred to mix properly and left overnight for saccharification/liquefaction or fermentation which is carried out by *Lactobacillus* among the wide range of microflora present in the soak grains which broke down shorter glucose chains (dextrins) into fermentable sugars according to previous method

(10). The mixture was sieved the next day using a muslin cloth and stored for further use.

2.2.2 Preparation of soybean milk

Sand and solid impurities were hand-picked before washing the soybean seeds. The seeds were then soaked in water for 12 h and the husks were removed by rubbing with hands. It was then drained out and blended using a wet milling machine (disc attrition). The slurry was then filtered using a double layered muslin cloth. Ginger was added and boiled for about 10 min while stirring constantly according to boiling extraction technique previously used (7).

2.2.3 Preparation of ice cream variants

Different ice cream samples were prepared using the standardized ice cream preparation method (11). Kunun-zaki ice cream variants were prepared by a combination of kunun-zaki and soymilk as base with banana and mango as fortificants. The fruits were first washed and frozen in an airtight Ziploc bag for 8 h before been used to process kunun-zaki with soymilk blends in the selected ratios determined from preliminary trials as indicated in the table below:

Ice cream samples	Composition in %			
	Kunun-zaki	Soymilk	Banana	Mango
A (Commercial Ice cream)	-	-	-	-
B	40	20	40	-
C	40	20	-	40

Sample A= commercial ice cream, Sample B= 40% kunun-zaki + 40% Banana + 20% Soymilk,

Sample C= 40% kunun-Zaki + 40% Mango+ 20% soymilk

2.3 Proximate Analysis

The proximate analyses of samples were carried out according to AOAC 2007 approved procedures. Moisture content was determined in a hot-air circulating oven (Gallenkamp, UK). For total ash content, samples of known weights were incinerated at 550 °C in a muffle furnace (Gallenkamp, UK). Crude fat determination was done by completely extracting a known weight sample in petroleum ether using hot extraction method while protein content was determined using the micro Kjeldahl method. Carbohydrate content was measured by difference approach.

2.3.1 Determination of physicochemical properties

The pH was determined directly using a digital pH meter (Jenway, England). Total titrable acidity and total solid contents was carried according to AOAC 2007 official method.

2.3.2 Determination of amino acid profile

The Amino acid profile was determined according to methods described by Benitez, 1989 (12) using an Applied Biosystems PTH Amino Acid Analyzer (MODEL: 120A). Tryptophan was determined separately due to its susceptibility to acid hydrolysis by using thioglycolic acid with 6N hydrochloric acid to preserve it according to (13).

2.3.3 Sensory evaluation

Sensory evaluation of the four ice cream samples was conducted by a 10-member panel of trained individual. The descriptive 9-point Hedonic scale with 9 -like extremely to 1– dislike extremely as described by Iwe, 2007 (14) was used for the evaluation. Ice cream quality was judged in terms of appearance/colour, taste, flavour, mouth feel (texture) and overall acceptability.

2.3.4 Statistical analysis

Measurements of each parameter were carried out in duplicates for all determinations. Data were analysed using Statistical Package for the Social Sciences (SPSS version 16.0). Similarities and differences amongst data sets were subjected to analysis of variance (ANOVA) with the New Duncan Multiple Range Test (NDMRT) employed to separate the means expressed as mean \pm standard deviation at 95 % confidence level ($p < 0.05$).

3.0 RESULTS AND DISCUSSION



Fig. 1: A-commercial ice cream, B-Kunun-zaki banana ice cream, C-Kunun-zaki mango ice cream

Table 2: Proximate Composition of the Ice Cream Samples

	Moisture (%)	Fat (%)	Protein (%)	Ash (%)	Carbohydrate (%)	Fibre
A	63.73 \pm 0.134 ^a	8.145 \pm 0.162 ^c	2.550 \pm 0.014 ^b	1.19 \pm 0.028 ^c	21.57 \pm 0.226 ^c	2.610 \pm 0.141 ^{bc}
B	72.01 \pm 0.056 ^b	0.600 \pm 0.014 ^a	2.190 \pm 0.056 ^a	0.014 \pm 0.003 ^a	23.42 \pm 0.190 ^c	1.770 \pm 0.282 ^a
C	75.27 \pm 0.353 ^b	0.850 \pm 0.028 ^b	2.160 \pm 0.014 ^a	1.010 \pm 0.127 ^c	17.650 \pm 0.353 ^a	2.950 \pm 0.042 ^c
p-value	0.001	0.001	0.001	0.001	0.001	0.012

Values are Mean \pm Standard deviation for two independent determinations

Values with same superscript down are not statistically significant (Duncan Multiple range test) at $p \leq 0.05$.

Table 3: Vitamin C and B₆ Content of the Ice cream Samples

	Vitamin (mg/100g)	B₆	Vitamin C (mg/100g)	Ca (ppm)	Na (ppm)
A	0.31±0.077 ^c		21.385±0.544 ^c	0.001±0.000 ^a	0.023±0.001 ^b
B	0.498±0.021 ^a		8.79±0.049 ^b	0.006±0.000 ^c	0.003±0.000 ^a
C	31.28±0.233 ^b		38.42±0.063 ^a	0.018±0.000 ^d	0.136±0.006 ^c
p-value	0.001		0.001	0.001	0.001

Values are Mean ± Standard deviation for two independent determinations

Values with same superscript down are not statistically significant (Duncan Multiple range test) at p≤0.05.

Table 3: Physico-Chemical parameters of the ice cream samples

	pH	TTA (%)	TS (%)
A	6.485±0.007 ^d	0.017±0.007 ^c	34.490±0.353 ^d
B	4.475±0.007 ^a	0.028±0.001 ^a	26.250±0.042 ^c
C	4.975±0.021 ^c	0.024±0.002 ^b	21.565±0.035 ^b
D	4.740±0.014 ^b	0.028±0.001 ^a	18.670±0.282 ^a

Total Titrable Acid-TTA, Total Solid -TS

Values are Mean ± Standard deviation for two independent determinations. Values with different superscript down the column differ significantly at p < 0.05 (Duncan Multiple range test).

Table 4: Amino Acid content of the ice cream samples

Amino acid	A	B	C	p-value
Leucine	3.505±0.007 ^c	2.505±0.007 ^b	0.870±0.000 ^a	0.001
Lysine	2.065±0.007 ^c	1.585±0.007 ^b	0.640±0.000 ^a	0.001
Isoleucine	2.22±0.014 ^c	0.980±0.000 ^b	0.385±0.007 ^a	0.001
Phenylalanine	1.050±0.014 ^b	1.055±0.007 ^b	0.705±0.007 ^a	0.001
Tryptophan	0.460±0.014 ^c	0.420±0.000 ^b	0.305±0.007 ^a	0.001
Valine	0.820±0.000 ^c	0.645±0.007 ^b	0.520±0.014 ^a	0.001
Methionine	0.745±0.007 ^b	0.810±0.014 ^c	0.550±0.014 ^a	0.001
Histidine	0.950±0.014 ^b	1.080±0.014 ^c	0.380±0.000 ^a	0.001
Threonine	1.655±0.007 ^c	0.990±0.014 ^b	0.440±0.000 ^a	0.0011
Proline	1.010±0.000 ^b	1.005±0.007 ^b	0.405±0.007 ^a	0.001
Tyrosine	0.515±0.007 ^b	0.685±0.007 ^c	0.345±0.007 ^a	0.001
Arginine	2.580±0.000 ^c	1.200±0.000 ^a	2.410±0.000 ^b	0.001
Cysteine	0.305±0.007 ^a	0.480±0.000 ^c	0.725±0.007 ^d	0.001
Alanine	0.990±0.000 ^c	0.835±0.007 ^b	0.760±0.000 ^a	0.001
Glutamic acid	3.165±0.021 ^a	4.345±0.007 ^c	3.635±0.007 ^b	0.001
Glycine	0.950±0.000 ^a	2.085±0.007 ^c	1.005±0.007 ^b	0.001
Serine	1.215±0.007 ^b	1.560±0.014 ^c	0.860±0.000 ^a	0.001
Aspartic acid	2.475±0.007 ^b	4.275±0.007 ^c	1.355±0.007 ^a	0.001
TEAA	13.47	10.07	4.795	
TNEAA	13.205	16.47	11.5	
TAA	26.675	26.54	26.295	

Data are presented as mean ± standard deviation. Values with different superscript down the column are statistically significant (Duncan Multiple range test) at $p < 0.05$.

Table 5: Sensory Evaluation of the Ice Cream Samples

	Colour	Flavour	Taste	Mouthfeel	Consistency	After taste	Overall acceptability
A	7.90±1.00 ^a	8.00±0.71 ^{bc}	7.55±1.34 ^b	7.67±0.69 ^b	8.00±0.55 ^c	7.70±0.55 ^b	8.00±0.55 ^c
B	7.89±0.84 ^a	8.20±0.70 ^c	7.53±0.89 ^b	7.40±0.71 ^b	7.98±0.89 ^b	7.75±0.55 ^{bc}	7.95±0.71 ^b
C	7.93±0.71 ^a	7.90±0.55 ^b	7.12±1.14 ^a	7.23±1.00 ^a	7.95±0.84 ^b	7.67±0.45 ^b	7.90±1.22 ^b
p-value	0.043	0.043	0.280	0.019	0.006	0.003	0.006

Data are presented as mean ± standard deviation. Values with different superscript down the column are statistically significant (Duncan Multiple range test) at $p < 0.05$.

3.1 Proximate composition

In Table 1, the moisture content of the value-added ice creams (B – C) varied from 72.01% to 78.08% comparable to the commercial sample, which recorded 63.73% which showed a significance difference between the value added ice cream and the commercial ice cream. The slight difference in values of experimental samples and the control may be due the presence of fruits, which naturally contain significant amount of water. However, the result of moisture contents is similar to those reported for formulated ice creams fortified with guava pulp (1) as well as calcium and vitamin D. Ash content was not significantly different from sample A which did not agree with the findings of Gita *et al.*, 2012 (15). The higher value observed in the control may be as a result of inclusion of chemical compounds such as magnesium hydroxide, potassium sorbate and polysorbate 80 in commercial ice cream products. The observed low percentage ash in the formulated ice cream samples may be attributed to the processing techniques for both kunun-zaki and soymilk (5) which might have resulted in some micronutrients leaching out through the sieved water. The fat content in all the formulated ice cream samples, which varied from 0.6 to 0.9 % are significantly lower than the control sample recording above 8 %. This could be attributed to the low-fat content of kunun-zaki and the fruits as noted by other researchers (16). The fat contents are consistent with the recommendation of consumption of food items with low fat

composition for healthier nutrition. Crude protein content of the samples ranged from 2.19 to 3.6 g/100 g. Although samples B and C contained lower amounts of protein compared to sample A, the values fall below standard range of 3.45 g/100 to 7.38 g/100 (2, 3, 15). Given that protein-energy malnutrition is a public health concern, consumption of value-added ice cream may be helpful in supplementing protein nutrition. The carbohydrate content of the formulated ice cream samples ranged from 23.4 to 15.8 % and were all significantly different ($p < 0.05$). The carbohydrate content of the control sample was 21.6 % which agreed with the findings of Hemali *et al.*, 2015 (1) who both observed in their separate works that dairy ice cream is high in carbohydrates and sugar. Crude fibre content of formulated ice cream sample C was higher than the control sample. This according to O'Neil *et al.*, 2013 (17) is from the soluble dietary fibre contained in mango which contributes in lowering cholesterol levels. The crude fibre content observed in sample A may be as a result of the emulsifiers and stabilizers used in production of commercial ice cream because standard dairy ice cream is reported to be low in crude fibre (3).

3.2 Vitamin and Mineral contents

Table 2 results showed that the formulated ice cream compared with the control sample contained reasonable amounts of vitamin C ranging from 18 – 38 mg/100 g. Sample C fortified with mango had the highest value which is consistent with established knowledge of high vitamin C content of

this fruit (17). Consumption of food items with vitamin C as natural antioxidant is encouraged owing to its ability to neutralize reactive oxygen species, which if unchecked could potentiate the growth of cancerous cells. This is further supported by the report that inclusion of synthetic ascorbic acid in food preparation may be deleterious in the sense that the artificial form can react with sodium benzoate to form benzene ring, which has been reported to be a potent carcinogen (18). In similar vein, the vitamin B6 content of sample C was found to be significantly ($p < 0.05$) higher than the control sample A, consistent with previous finding (19). Vitamin B6 plays an important role in protein and glucose metabolism as well as synthesis of haemoglobin. The calcium contents of our products were all significantly different ($p < 0.05$) from that in sample A. Although the value found here are lower than those reported for standard dairy milk which may be due to the different brand of dairy product used. The values recorded for sodium are low, the amount contained in sample C is significantly higher than the control sample. The claim that frozen dessert products are potential carriers of functional health-benefitting ingredients and thus can be useful for both dietetic and therapeutic purposes, is supported by the results of enhanced micronutrient composition of our value-added product where sample C contain higher amounts of vitamin C and Ca compared to the control.

3.3 Physicochemical Properties

In Table 3, the pH of sample A was near neutral which was in agreement with Mortensen 2017 (20) while those of the formulated ice cream samples had lower pH values similar to earlier findings, which suggest that slight lactic acid fermentation takes place during production of kunun-zaki (10)[10]. Since lower pH in foods helps to reduce the activity of spoilage microorganism, it implies that ice cream samples B and C may have higher shelf stability than sample A. The percentage total titrable acidity (TTA) for the formulated ice cream samples followed the expected trend of the higher the pH the lower the total acidity as seen in samples B, C, and vice versa as reported by others (21). However, sample A (control) had higher TTA than expected and did not agree with results of many such as (3).

3.4 Amino-acid Profile

Total amino acid content of the formulated ice cream samples as presented in Table 4 were similar to the control sample. The amounts of essential amino acid such as glutamic acid, glycine, aspartic acid, tyrosine, histidine, methionine which have a huge role in muscle growth and function was higher in the formulated ice cream sample C, suggesting a good driver for these essential nutrients and improvement on nutritive value of ice cream (19).

3.5 Sensory attributes of the ice cream samples

In Table 5, the results show that all samples including the control have similar rating by the panel members in terms of colour, flavour, taste, mouthfeel, consistency, after taste and overall acceptability as the values on the 9 – hedonic scale only vary slightly (22). However, the control sample which was a popular supreme ice cream vanilla flavour brand had a marginally higher rate value of overall acceptability. This may not be unconnected with the inclusion of additives such as colouring agents and sweeteners which may have positively impacted on the general sensory attributes.

4.0 CONCLUSION

This study established that value addition of “kunun-zaki” through formulation of novel ice cream products fortified with fruit pulp are capable of supplying essential nutrients to supplement the daily requirements. In addition, these plant-based substitutes for dairy ice cream will be a more affordable since all the raw materials are locally available in comparison to the dairy ice cream which Nigeria still largely depends on importation of about 70 per cent of its milk needs. This will also contribute to curbing the huge post-harvest loss of fruits experienced in Nigeria. Furthermore, the formulated ice cream has comparable sensory attributes that can even be further improved upon since they are healthier alternatives to the former. However, there is need to improve the percentage of soymilk to make up for the low protein content of kunun-zaki, which is the focus of our future work.

5.0 REFERENCES

1. H. H. Patel, B. K. Amin, Formulation and standardization of different milk ice-cream fortified with pink guava pulp. *International Journal of Dairy Science* **10**, 219-227 (2015).
2. K. Jyoti, R. P. Dubey, Development of nutritious ice-creams from soymilk and pumpkin seed milk and evaluation of their acceptability. *Food Science Research Journal* **7**, 96-100 (2016).
3. M. Umelo *et al.*, Proximate, physicochemical and sensory evaluation of ice cream from blends of cow milk and tigernut (*Cyperus esculentus*) milk. *Int. J. Sci. Res. Innov. Technol* **1**, 63-76 (2014).
4. M. J. Messina, Legumes and soybeans: overview of their nutritional profiles and health effects. *The American journal of clinical nutrition* **70**, 439s-450s (1999).
5. T. Gaffa, I. Jideani, I. Nkama, Traditional production, consumption and storage of Kunu—a non alcoholic cereal beverage. *Plant foods for human nutrition* **57**, 73-81 (2002).
6. N. Amusa, O. Ashaye, Effect of processing on nutritional, microbiological and sensory properties of kunun-zaki (a sorghum based non-alcoholic beverage) widely consumed in Nigeria. *Pakistan Journal of Nutrition* **8**, 288-292 (2009).
7. A. Ogo, E. O. Amali, E. Efiog, A. Gbaa, D. Enenche, Optimising Soymilk Protein Nutriture through Selection of Appropriate Processing Technique. *NIGERIAN ANNALS OF PURE AND APPLIED SCIENCES* **1**, 61-67 (2018).
8. J. L. Slavin, B. Lloyd, Health benefits of fruits and vegetables. *Advances in nutrition* **3**, 506-516 (2012).
9. A. Konstantas, L. Stamford, A. Azapagic, Environmental impacts of ice cream. *Journal of Cleaner Production* **209**, 259-272 (2019).
10. G. Terna, I. Jideani, I. Nkama, Nutrient and sensory qualities of kunun zaki from different saccharification agents. *International journal of food sciences and nutrition* **53**, 109-115 (2002).
11. A. Bear, Ice cream making, Wisconsin, Agric. Expt. Sta. *Bulletin* **4**, 38 (1993).
12. L. V. Benitez, Amino acid and fatty acid profiles in aquaculture nutrition studies. *Fish nutrition research in asia*, 23-35 (1989).
13. W. Horowitz, *Aoac. Method* **47**, (1975).
14. M. Iwe, Current trends in sensory evaluation of foods. *Re-joint Communication Service Limited. Enugu, Nigeria* **138**, (2007).
15. G. Bisla, P. V. Archana, S. Sharma, Development of ice creams from Soybean milk & Watermelon seeds milk and Evaluation of their acceptability and Nourishing potential. *Adv Appl Sci Res* **3**, 371-376 (2012).
16. T. Kasa, G. Fistum, Y. Madda, Chemical composition and nutritional effect of pineapple, mango, banana, avocado and orange: A review article. *Chem Proc Eng Res* **54**, 1-6 (2017).
17. C. O'Neil, T. Nicklas, V. Fulgoni, Mangoes are associated with better nutrient intake, diet quality, and levels of some cardiovascular risk factors: National Health and Nutrition Examination Survey. *J. Nutr. Food Sci* **3**, (2013).
18. M. Shahmohammadi, M. Javadi, M. Nassiri-Asl, An overview on the effects of sodium benzoate as a preservative in food products. *Biotechnology and Health Sciences* **3**, 7-11 (2016).
19. H. H. Salama, S. Sayed, A. Abdalla, Enhancing the nutritive values of ice milk based on dry leaves and oil of *Moringa oleifera*. *American Journal of Food Technology* **12**, 86-95 (2017).
20. M. Mortensen, *Classification of ice cream and related frozen products*. (Agricultural Experiment Station, Iowa State College of Agriculture and ..., 1911).
21. R. Kanwal, T. Ahmed, B. Mirza, Comparative analysis of quality of milk collected from buffalo, cow, goat and sheep of Rawalpindi/Islamabad region in

Pakistan. *Asian Journal of Plant Sciences* **3**, 300-305 (2004).

22. S. El-Samahy, K. M. Youssef, T. Moussa-Ayoub, Producing ice cream with

concentrated cactus pear pulp: A preliminary study. *Journal of the Professional Association for Cactus Development* **11**, 1-12 (2009).

P008 - PROXIMATE ANALYSIS OF SOME PROCESSED CASSAVA PRODUCTS OBTAINED WITHIN LAFIA METROPOLIS OF NASARAWA STATE

Idongesit V. Edet^{1*}, Igbum G. Gillian², Aondo T. Terungwa³, Utange P. Iorhemba², Saater J. Msurshima⁴

¹*Department of Chemistry, Faculty of Science, Federal University of Lafia, Nassarawa State*

²*Department of Chemistry, Benue State University, Makurdi, Benue State*

³*Federal Polytechnic Wannune, Benue State, Nigeria*

⁴*Chukwuemeka Odumegwu Ojukwu University Uli, Anambra state, Nigeria*

Corresponding author email: edetvalentine15@gmail.com

ABSTRACT

The widespread adoption of cassava and its derivatives across diverse industries in Nigeria has been a remarkable trend. As these applications continue to expand, understanding the nutritional value of these products becomes crucial. This study investigated and compared the proximate composition of five samples of processed cassava products (Niji® Foods Cassava Flour, IFGREEN® Odourless Fufu Flour, Aiteefills® Fufu Flour, Niji® Foods Garri and a local brand cassava starch) sourced from both supermarkets and local markets in Lafia town between February and May, 2023 using standard official methods for proximate analysis. The results were analyzed by Minitab version 20.0 by one way ANOVA and pair-wise comparison was made post hoc using Tukey t-tests. The moisture, ash, crude protein, crude fibre, crude fats and carbohydrate ranged from 4.34 – 12.70 %, 0.34 – 1.39 %, 1.30 – 10.06 %, 0.02 – 0.53 %, 5.82 – 12.53 % and 70.83 – 81.93 %. The study revealed that the results of the proximate composition in all the samples varied significantly ($P \leq .05$) indicating a diverse array of nutritional profiles in these cassava-based products.

KEYWORDS

Cassava, proximate composition, processed, nutritional value

1.0 INTRODUCTION

Cassava, scientifically known as *Manihot esculanta* has established itself as a prominent domesticated plant in the Pacific region. Originating from the Genus *Manihot* within the Euphorbiaceae family (1), this versatile plant finds utility in its storage root (tuber) and leaves. Notably, two distinct types of cassava plants exist: the erect type, with or without branching at the top, and the spreading type (2). Distinguished by its palmate lobed leaves, inconspicuous flowers, and large starchy tuberous root wrapped in a tough papery brown bark with white to yellow flesh (3), cassava presents itself as a botanical wonder. However, its perishable nature poses significant postharvest challenges, leading to considerable losses (4, 5).

In the pursuit of achieving food sufficiency and combating food crises in Africa, the invaluable contribution of cassava emerges as a game-changer (6). Recognized as Africa's food security crop, cassava plays a vital role in addressing the region's nutritional needs. Its processed forms have garnered

widespread application, serving not only as a staple food but also as a source of essential industrial products. Tapioca, farina, garri, fufu, starch, and more are among the diverse range of products derived from locally processed cassava tubers, with Nigeria standing out as a prime example of high domestic consumption despite substantial cassava production (7, 8). By understanding the factors that influence the chemical composition of processed cassava products, such as cultivar, geographical location, maturity stage, environmental conditions, and processing methods (9, 10), we can explore innovative approaches to enhance cassava cultivation, processing, and utilization. Embracing cassava's versatility holds the promise of fostering sustainable agricultural practices and bolstering food security in Nigeria. While various studies (11-13) have focused on the proximate composition of fresh cassava roots, there remains a significant knowledge gap regarding the different processed cassava products available in local markets and supermarkets within the city of Lafia, Nasarawa State, Nigeria. In light of this, the present research seeks to fill this void by delving into the proximate

composition of five distinct processed cassava products sourced exclusively from local markets in Lafia town. The focus of this investigation is to conduct a comprehensive comparative analysis on the proximate composition to shed light on the nutritional aspects of these products, providing valuable insights for consumers and policymakers alike.

2. MATERIAL AND METHODS

2.1 Sample collection

Samples consisting of products containing cassava as primary ingredients were randomly obtained directly from supermarkets and local markets in Lafia town from February to May, 2023. The five samples of processed cassava products were divided into four groups based on the method of processing: garri sample, fufu flour, high quality cassava flour and locally processed starch. The samples include Niji® Foods Cassava Flour, IFGREEN® Odourless Fufu Flour, Aitefills® Fufu Flour, Niji® Foods Garri and local brand cassava starch. They were designated as NFCF, IGFF, ATFF, NFG and LBCS respectively. The samples were obtained randomly and transported directly to the Chemistry laboratory, Faculty of Agriculture, Nassarawa State University, Shabu Campus, for analysis.

2.2 Preparation of samples

100g of each processed cassava product sample was put in tightly sealed envelopes and kept in field cellophane bags before analysis to prevent environmental contamination.

2.3 Proximate analysis

Proximate composition, namely, moisture, crude protein, crude fibre, crude fats, ash and nitrogen free extract (carbohydrate contents) in portions of the various samples were measured according to the standard methods as described in AOAC (14) and other standard techniques obtained from the literature.

2.3.1. Moisture Determination (% MD)

The moisture content was determined according to AOAC (14) method 925.10. 2 g of the samples was accurately weighed into a pre-labelled, pre-weighed beaker and transferred to a vacuum dry oven to dry at a temperature of 130 °C. The samples were heated within a time range of 1 h, 1 h -30 min, 2 h, 2 h -30 min, and 3 h respectively, and weighed till constant weight was achieved. All sampling and

analysis were done in triplicate (10). The formula used for the calculation of moisture content and dry matter can be seen below:

Sample weight – moisture content = dry matter

$$\% \text{ moisture content} = \frac{\text{drymatter}}{\text{weightofsample}} \times 100 \quad 2.1$$

2.3.2. Ash (% Ash)

The ash content was determined according to AOAC (14) method 923.03. Prepared samples were weighed into pre-weighed, porcelain crucibles. The samples were transferred to a muffle furnace (J M Ney furnace, model 2-525) and ashed at 550°C for 8 h. The crucibles were allowed to cool in desiccators and then weighed [13]. The formula that was used for the calculation of ash content can be seen below:

$$\% \text{ Ash} = \frac{W\text{tofAsh}}{\text{weightofsample}} \quad 2.2$$

2.3.3. Fat (% Fat)

The fat content in the samples were determined according to 920.39 of AOAC (11) by dissolving 8 g of the cassava samples in a 200 cm³ beaker containing 8.4 cm³ of hydrochloric acid and heated in a water bath for 1 h. After heating, the sample solutions were allowed to cool and then extracted with petroleum ether in a separating funnel. After extraction, the sample solution were heated to dryness and the weight collected after cooling (12). The formula that was used for the calculation of fat content can be seen below:

$$\% \text{ Fat} = \frac{\text{Weightlossofsample (extract)}}{\text{weightofsample}} \times 100 \quad 2.3$$

2.3.4. Crude Protein (% C.P)

The crude protein content was determined as described in Nuwamanya *et al.* (13) using Dumas combustion method of nitrogen content analysis (LecoTruspec Model FP-528, St Joseph Mi, USA) by taking about 0.3 g of sample and using the conversion factor:

$$\% \text{ protein} = \% \text{ N} \times 6.25 \dots\dots\dots 2.4$$

2.3.5. Crude fibre content (% C.F)

The crude fibre content was determined using the method 962.09 of AOAC (11). About 0.5 g of the sample was boiled in 50 mL of 0.3 M H₂SO₄ under reflux for 30 min, followed by filtering through a 75 mm sieve under suction pressure. The residue was washed with distilled water to remove the acid. The



residue was then boiled in 100 mL, 0.25 M sodium hydroxide under reflux for 30 min and filtered under suction. The insoluble portion was washed with hot distilled water to free the alkaline. The insoluble portion was dried to the constant weight in the oven at 100 °C, for 2 h, then cooled in the desiccator. The dried sample was ashed in a muffle furnace to subtract the mass of ash from the fibre after then the % of fibre was determined.

2.3.6. Nitrogen Free Extract (% NFE) as Carbohydrate content

NFE was determined by mathematical calculation. It was obtained by subtracting the sum of percentages of all the nutrients already determined from 100.

$$\% \text{ NFE} = 100 - (\% \text{ moisture} + \% \text{ CF} + \% \text{ CP} + \% \text{ EE} + \% \text{ Ash}) \quad \dots 2.5$$

% NFE represents soluble carbohydrates and other digestible and easily utilizable non-nitrogenous substances in the samples.

2.4 Data Analysis

Data was analyzed using a one-way analysis of variance (ANOVA). The mean differences were determined using the Tukey's Least Significance Difference test at 5% significant level. Values of $p \leq 0.05$ were considered statistically significant. All data were expressed as the mean \pm standard deviation (SD) of three observations. All calculations were done using the Minitab version 20 software.



3. RESULTS AND DISCUSSION

Table 1: Proximate composition of the processed cassava products

	Garri sample		Fufu flour sample			Composite flour sample			
	Standard	NFG	Standard	IGFF	ATFF	Standard	NFCF	Standard	LBCS
% MD	7.0 (max)	6.84d ± 0.02	10.0 (max)	4.34g ± 0.02	12.70a ± 0.01	12.0 (max)	9.07c ± 0.06	12.0 (max)	9.35b ± 0.02
% Ash	1.5 (max)	1.39c ± 0.01	0.6 (max)	0.34h ± 0.01	0.99e ± 0.01	0.7 (max)	1.05d ± 0.01	0.1 (max)	0.89f ± 0.01
% CP	1.0 (min)	3.50c ± 0.01	1.0 (min)	2.19d ± 0.01	1.30f ± 0.01	1.0 (min)	10.06a ± 0.02	0.5 (min)	2.18d ± 0.02
% Fat	-	5.82f ± 0.01	-	12.53a ± 0.01	6.61e ± 0.01	-	9.39d ± 0.01	-	9.43c ± 0.01
% CF	2.0 (max)	0.53c ± 0.01	2.0 (max)	0.02f ± 0.01	0.05e ± 0.01	1.5 (max)	0.06de ± 0.01	0.2 (max)	0.08d ± 0.01
% NFE	65 – 70 (min)	81.93c ± 0.03	65 – 70 (min)	80.59d ± 0.03	78.35e ± 0.02	65 – 70 (min)	70.38g ± 0.09	85 (min)	78.09f ± 0.02

3.1 Moisture Content (% MD)

The moisture content of the processed cassava samples displayed a range of 4.34% to 12.70% and exhibited significant variations ($P = .05$) among the products, as presented in Table 1. Notably, there were no significant differences ($P > .05$) between the moisture contents of LBCS and ATFF. However, ATFF, NFCF, and LBCS had relatively higher moisture content compared to NFG and IGFF. As anticipated, the garri sample (NFG) showed low moisture content due to the roasting process involved during its preparation. On the other hand, the moisture content in IGFF was lower than in AYFF. Among all the samples, Aitefills Fufu flour (ATFF) displayed the highest moisture content, which was significantly different ($P = .05$). Following this, LBCS, NFCF, NFG, and IGFF had progressively lower moisture content, with IGFF being the least. Comparable findings were reported by Manano *et al.* (15) in cassava varieties from

Uganda, with moisture contents falling in the average range of 5.43% to 10.87%, aligning with the results obtained in the current study.

The observed variations in moisture content could be attributed to differences in chemical constituents and processing methods employed for each product. Importantly, all the samples, except for ATFF, had moisture contents within the permissible limits set by the Standard Organization of Nigeria (SON) and FAO/WHO, ensuring the quality and safety of these cassava products.

3.2 Ash contents (% Ash)

The ash contents of the samples fell within an average range of 0.34% to 1.39% and exhibited significant variations ($P = .05$), as indicated in Table 1. Notably, NFG displayed the highest ash content at 1.39%, while IGFF had the lowest at 0.34%. Previous studies have suggested a relationship between higher dry matter contents and lower ash



contents (15, 16). In this context, fiber played a substantial role as a contributor to the ash contents in the samples. Similar findings have been reported in a related study where wheat flour varieties with higher fiber contents showed higher ash contents (17). The ash content in food products is of particular interest in the food industry, as it can influence flour quality. High ash contents might impact the whiteness of flours. Additionally, since ash content serves as an indicator of mineral contents, an increased mineral content may promote metal chelating activities, leading to the formation of metal-ion pigment complexes (18). These complexes can impart greenness, redness, or yellowness to the final product. Given the elevated ash contents in NFCF and LBCS, there is a plausible speculation that the possibility of forming metal ion-pigment complexes in these products is high. This observation provides valuable insights into the potential color characteristics of these products and their suitability for various applications in the food industry.

3.3 Crude Protein (% CP)

The protein contents of the samples displayed a wide range of 1.30% to 10.06%. Interestingly, IGFF and LBCS exhibited comparable protein levels ($P > .05$), while the protein content in the other samples showed significant differences ($P = .05$). Among the samples, NFCF, known for its high-quality cassava flour, had the highest protein content at 10.06%, which was significantly higher. Conversely, ATFF had the lowest protein content in this study. Comparing these findings with previous research, Manano *et al.* (15) reported protein content in the range of 0.74% to 1.52%. Additionally, other authors have reported even lower protein values, ranging from 0.3% to 0.6% protein (19, 20), and 0.72% protein (21). The observed variations in protein content can be attributed to environmental conditions, particularly soil fertility, from which the cassava tubers used to produce the products were sourced (9, 10). Notably, all the samples in this study surpassed the minimum protein values recommended by SON, which are 0.5% for starch and 1.0% for other cassava products. These results highlight the nutritional adequacy of the samples in terms of their protein content, which is vital information for assessing their potential dietary value.

3.4 Crude fats (% Fats)

The crude fat contents of the samples varied significantly ($P = .05$) and ranged from 5.82% to

12.53%, as indicated in Table 1. IGFF stood out with notably higher fat content compared to ATFF, while NFCF and LBCS also exhibited elevated fat levels. On the other hand, the garri sample (NFG) demonstrated relatively lower fat content. Interestingly, the fat contents reported in previous studies ranged from 0.1% to 0.3% (21, 22), 0.74% to 1.49%, and 0.41% (23), which were significantly lower than the results obtained in the current study. Fat serves as an important alternative energy source, and the variations observed in fat content among the samples may have implications for their nutritional and dietary significance.

3.5 Crude Fibre (% CF)

The fiber contents of the samples exhibited a range of 0.02% to 0.53%. Notably, NFCF, ATFF, and LBCS showed comparable fiber contents ($P > .05$), as shown in Table 1. As expected, the garri sample (NFG) had relatively higher fiber content compared to LBCS, NFCF, IGFF, and ATFF. Among the samples, NFCF and ATFF, as well as LBCS and NFCF, demonstrated relative comparability in their fiber content. The fibrous nature of cassava can influence its texture, with high-fiber varieties being coarser and low-fiber varieties being finer. Processing highly permeable fibers could result in an increased rate of nutrient release or loss (24). The variations in fiber content may be attributed to the different genetic varieties of cassava. However, it's important to be cautious about consuming excess fiber in the diet, as it can lead to increased faecal nitrogen, intestinal irritation, and reduced protein digestibility during production (25).

3.6 Total Carbohydrates (% NFE)

The percentage of total carbohydrates, represented as % NFE and determined by the difference method, varied across the samples, ranging from 70.38% to 81.93% (see Table 1). Surprisingly, the garri sample (NFG) exhibited the highest total carbohydrate content compared to the flour samples. Notably, the fufu flour sample IGFF showed a significantly high carbohydrate content of 80.59%, approaching the range observed in the garri sample. The differences among all samples were statistically significant ($P = .05$). Previous studies by Charles *et al.* (26) and (27) also reported similar results, with carbohydrate content in the range of 80.1% to 86.3% and 84.32% to 86.57%, respectively.

4. CONCLUSION



All samples exhibited favorable crude fiber levels, and their protein contents surpassed the recommended limits set by SON. Moisture contents were generally within the standard limits of both SON and FAO/WHO, except for ATFF, which showed a deviation. Interestingly, NFCF and LBCS demonstrated higher ash contents, raising the likelihood of metal ion-pigment complex formation. This observation might have implications for the primary quality of flours and starches (NFCF and LBCS) utilized in both the food and non-food industries. Additionally, IGFF, NFCF, and LBCS had notably higher fat contents compared to NFG, which presented relatively lower fat levels.

REFERENCES

1. C. A. Nyamekye, Norwegian University of Life Sciences, As, (2021).
2. D. B. Dhasan, K. Karthik, M. L. Reddy, M. G. S. Yadav, in *AIP Conference Proceedings*. (AIP Publishing, 2022), vol. 2519.
3. P. C. Kidasi, D. K. Chao, E. O. Obudho, A. W. Mwang'ombe, Farmers' sources and varieties of cassava planting materials in coastal Kenya. *Frontiers in Sustainable Food Systems* **5**, 611089 (2021).
4. S. Musah, E. Kwakye, S. Kudaddze, W. Adzawla, ANALYZING CASSAVA PROCESSORS' PREFERRED OUTPUT AND PROFITABILITY OF CASSAVA PROCESSING IN HOHOE MUNICIPALITY. *UDS International Journal of Development* **7**, 262-272 (2020).
5. L. P. Adjei *et al.*, Cyanide contamination assessment via target survey and physicochemical and bacteriological characterization: a case study of Akrofrom-Techiman cassava processing area in Ghana. *Environmental Monitoring and Assessment* **195**, 482 (2023).
6. E. O. Alamu, P. Ntawuruhunga, T. Chibwe, I. Mukuka, M. Chiona, Evaluation of cassava processing and utilization at household level in Zambia. *Food Security* **11**, 141-150 (2019).
7. Z. Isabirye, Makerere University, (2021).
8. J. Emurotu, U. Salehdeen, O. Ayeni, Assessment of heavy metals level in cassava flour sold in Anyigba Market Kogi State, Nigeria. *Advances in Applied Science Research* **3**, 2544-2548 (2012).
9. A. Agiriga, M. Iwe, Optimization of chemical properties of cassava varieties harvested at different times using response surface methodology. *American Journal of Advanced Food Science and Technology* **4**, 10-21 (2016).
10. A. E. Burns *et al.*, Variations in the chemical composition of cassava (*Manihot esculenta* Crantz) leaves and roots as affected by genotypic and environmental variation. *Journal of Agricultural and Food Chemistry* **60**, 4946-4956 (2012).
11. D. T. Do, J. Singh, I. Oey, H. Singh, Biomimetic plant foods: Structural design and functionality. *Trends in Food Science & Technology* **82**, 46-59 (2018).
12. I. Shadrach, A. Banji, O. Adebayo, Nutraceutical potential of ripe and unripe plantain peels: A comparative study. *Chem Int* **6**, 83-90 (2020).
13. C. Balagopalan, *Cassava in food, feed and industry*. (CRC press, 2018).
14. W. Horwitz, *Official methods of analysis of AOAC International. Volume I, agricultural chemicals, contaminants, drugs/edited by William Horwitz*. (Gaithersburg (Maryland): AOAC International, 1997., 2010).
15. J. Manano, P. Ogwok, G. W. Byarugaba-Bazirake, Chemical composition of major cassava varieties in Uganda, targeted for industrialisation. (2017).
16. T. Tadesse, A. Bekele, E. Tsegaye, W. Beshir, Performance of cassava clones under potential and low moisture stressed areas of Ethiopia. *Applied Science Reports* **13**, (2016).
17. E. Nuwamanya, Y. Baguma, M. N. Emmambux, J. R. N. Taylor, P. Rubaihayo, Physicochemical and functional characteristics of cassava starch in Ugandan varieties and their progenies. (2010).
18. E. R. Turner, Y. Luo, R. L. Buchanan, Microgreen nutrition, food safety, and shelf



- life: A review. *Journal of food science* **85**, 870-882 (2020).
19. C. Eleazu, K. Eleazu, Determination of the proximate composition, total carotenoid, reducing sugars and residual cyanide levels of flours of 6 new yellow and white cassava (*Manihot esculenta* Crantz) varieties. *American Journal of Food Technology* **7**, 642-649 (2012).
 20. A.-O. A. Omowonuola, E. M. Mary, A. F. Fidelis, A. S. A. Olalekan, A. A. Sunday, Quality Characteristics of Fermented Cassava Flour (Lafun) Produced Using Backslopping Method. *EC Nutrition* **7**, 52-57 (2017).
 21. A. Pavlovich-Abril, O. Rouzaud-Sández, A. L. Romero-Baranzini, R. L. Vidal-Quintanar, M. G. Salazar-García, Relationships between Chemical Composition and Quality-Related Characteristics in Bread Making with Wheat Flour–Fine Bran Blends. *Journal of Food Quality* **38**, 30-39 (2015).
 22. J. A. Montagnac, C. R. Davis, S. A. Tanumihardjo, Nutritional value of cassava for use as a staple food and recent advances for improvement. *Comprehensive reviews in food science and food safety* **8**, 181-194 (2009).
 23. L. Yu, A.-L. Nanguet, T. Beta, Comparison of antioxidant properties of refined and whole wheat flour and bread. *Antioxidants* **2**, 370-383 (2013).
 24. M. Somendrika, I. Wickramasinghe, M. Wansapala, S. Peiris, Analyzing Proximate Composition Of Macro Nutrients of Sri Lankan Cassava Variety" Kirikawadi". (2016).
 25. T. Shittu, A. Raji, L. Sanni, Bread from composite cassava-wheat flour: I. Effect of baking time and temperature on some physical properties of bread loaf. *Food Research International* **40**, 280-290 (2007).
 26. A. L. Charles, K. Sriroth, T.-c. Huang, Proximate composition, mineral contents, hydrogen cyanide and phytic acid of 5 cassava genotypes. *Food chemistry* **92**, 615-620 (2005).
 27. O. OLUWANÌYÌ, J. OLADÌPO, Comparative studies on the phytochemicals, nutrients and antinutrients content of cassava varieties. *Journal of the Turkish Chemical Society Section A: Chemistry* **4**, 661-674 (2017).



P009 - BIOACTIVE COMPONENTS AND ANTIOXIDANT ACTIVITIES OF TOASTED PEARL MILLET-AVOCADO SEEDS FLOUR BLENDS

F.Z.Igbua^{1*}, T.T. Iombor², F.S. Ameen-Olanrewaju³, J.O. Alechenu¹, A.A. Abdulquadri³,

¹Centre for Food Technology and Research, Benue State University, Makurdi, Nigeria

²Joseph Sarwuan Tarkaa University, Makurdi, Benue State, Nigeria

³Chemistry Department, University of Ilorin, Kwara State, Nigeria

Corresponding Author: E-mail address: igbuafrancis@gmail.com

ABSTRACT

In Nigeria, the seeds of avocado are under-utilized and considered as non-edible parts of the fruit, in spite of its nutritional and health benefit. The under-utilization of avocado seeds predisposes consumers to many degenerative diseases such as cancer, diabetes, cardiovascular diseases etc. In this study bioactive components and antioxidants activity of toasted pearl millet-avocado seed flour blends were evaluated. Pear Millet and Avocado seeds were processed into respective flours and blended on percentage (%) basis in the ratio of 100:0,90:10, 80:20, 70:30, 60:40,0: 100 (Pear Millet : avocado Seeds) which was labeled as sample EOE1(Control), EOE2, EOE3,EOE4, EOE5 and EOE6(Control) respectively. Saponin, carotenoids, flavonoids, phenolic DPPH, FRAP and metal chelating activities of pear millet and avocado seeds flour blends were determined using standard methods. The result revealed an increase in saponin (2.46-3.50 mg/g), carotenoids (2.44-17.53 µg/kg), flavonoids (7.82-34.71 mgQE/g), total phenolics (33.78-54.79 mgGAE/g) as well as DPPH (26.77-41.59%), FRAP (0.09-0.19 mMol) and Metal chelating (44.84-57.85%) with increasing levels of avocado.

KEYWORDS

Blends, Enrichment, Bioactive and Antioxidant

1.0 INTRODUCTION

Avocado (*Persea americana*) belongs to the family *Lauraceae*. The fruit is composed of carbohydrate, protein, fiber, vitamins C, E, K, B₁, B₂, B₆, B₉, as well as Fe and Zn (1). It is highly consumed in the world due to the presence of unsaturated lipids and its relevance in improving and maintaining healthy heart and circulatory system (1). Avocado has a seed which is encased in a soft pulp comprises 13-18% of the size of the whole fruit. The seed is one of the under-utilized non-edible parts of the fruit, which are usually discarded as residues. This seed is reported to have high levels of valuable bioactive compounds and natural antioxidants (1). Adeyemi (2) reported that avocado seed is used as food in the management of hypertension, diabetes, cancer and inflammation. Antioxidant constituents of the avocado seeds act as radical scavengers, which helps in converting the radicals to less reactive species (3). Millets are a group of highly variable small seeded grasses, widely grown around the world as cereal crops or grains for fodder and human food. Millet belongs to the family Poaceae (previously called Gramineae) and consists of

several varieties. They are the principal sources of energy, protein, vitamins and minerals (4). Millet contain phytic acid, tannins and phenols which can contribute to antioxidant activity, important in health, aging and metabolic disease (5). In spite the abundance of health benefits of millets; their antinutritional factor can reduce nutrient bioavailability thereby causing nutrient deficiency in the body. However, these antinutrients can be reduced by toasting, boiling fermentation etc.there by making nutrient bioavailable in the body.

2.0 MATERIALS AND METHODS

2.1 Source of Raw Materials

Raw pearl millet was purchased from Modern Market Makurdi while Avocado seeds were purchased from Railway Market Makurdi, Benue State. Some materials and equipment including digital weighing scale was obtained from the food processing laboratory of food technology and human ecology of federal university of agriculture, Makurdi.

Pear Millets

Fresh Avocado Seeds



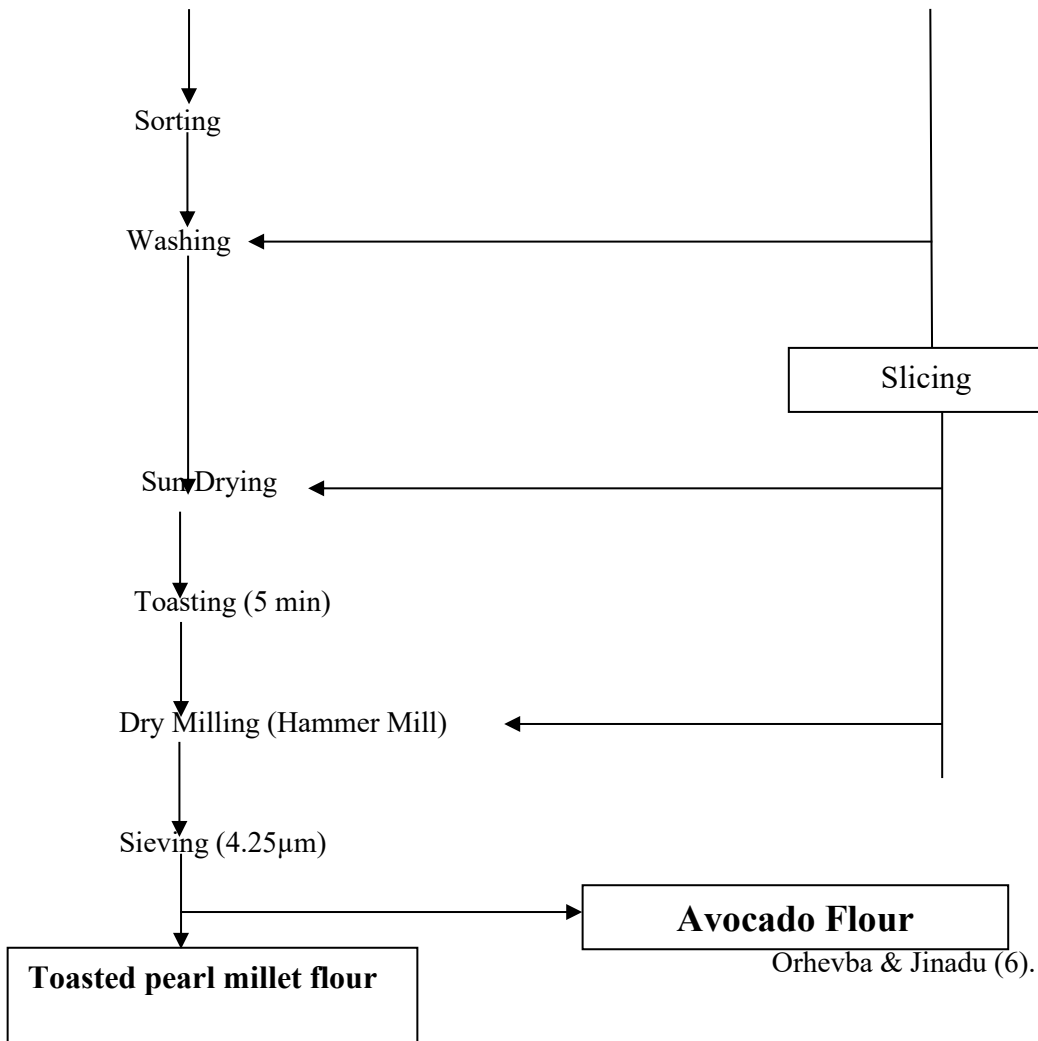


Fig 1: Flow chart for the Production of toasted pearl millet flour Mriddula, *et al.*(7).

Table 1: Blend formulation of toasted pearl millet-avocado seeds flour blends (%)

Sample	TMF	ASF
EOE1 (control)	100	0
EOE2	90	10
EOE3	80	20
EOE4	70	30
EOE5	60	40
EOE6 (control)	0	100

Key: TMF=Toasted millet flour, ASF= Avocado seed flour.



2.2. Determination Bioactive Compounds

Determination of Saponin

Saponin was determined according to the method described Uematsu *et al.*(8). One gram of sample was extracted with 20ml of ethanol for 10 min. The mixture was centrifuged (Gallenkamp, centrifuge England) at 3000 rpm for 10 min. Thereafter, 2 ml of the supernatant was placed in a test tube and evaporated over a boiling water bath. After cooling, 2 ml of ethyl acetate and 1 ml of anisaldehyde was added. Thereafter, 1 ml of a mixture of 50 ml concentrated H₂SO₄ and 50 ml ethyl acetate was added. After stirring, the test tube was placed in a water bath at 60 °C for 20 min and then allowed to cool for 10 min in a water bath maintained at room temperature. Absorbance was read with a spectrophotometer (Spectro21D, Pec Medicals, and USA) at 430 nm.

2.2.2 Determination of Total Carotenoids

The extractions of the pigment for carotenoid determination of the samples were carried out as described by AOAC (9). In to a conical flask containing 50ml of 95% ethanol, 10g of the milled sample was placed and maintained at a temperature of 80°C in a water bath for 20 minutes with periodic shaking. The supernatant was decanted, allowed to cool and its volume was measured by means of a measuring cylinder and recorded as initial volume. The ethanol concentration of the mixture was brought to 85% by adding 15 ml of distilled water and it was further cooled in a container of ice water for about 5minutes. The mixture was transferred into a separating funnel and 25ml of petroleum ether (pet-ether) was added and allowed to cool. The funnel was swirled gently to obtain a homogenous mixture and it was later allowed to stand until two separate layers were obtained. The bottom layer was run off into a beaker while the top layer was collected in to a 250ml conical flask. The bottom layer was transferred in to the funnel and re-extracted with 10ml pet-ether for 6 times until the extract became fairly yellow. The entire pet-ether was collected into 250 ml conical flask and transferred in to separating funnel for re-extraction with 50ml of 80% ethanol. The final extract was measured and poured in to sample bottles for further analysis.

2.2.3 Determination of Total Flavonoid

Total flavonoid contents were estimated according to the method of Ebrahimzadeh *et al.*(10). Briefly, 0.5 mL of extract sample (1 mg/mL) was mixed with 1.5 mL of methanol and then, 0.1 mL of 10% aluminum chloride was added, followed by 0.1 mL of 1 M potassium acetate and 2.8 mL of distilled water. The mixture was incubated at room temperature for 30 minutes. After 5 min, 0.3 ml 10 % AlCl₃ and 2 ml of 1M NaOH was added to the mixture. Immediately, the reaction flask was diluted to volume with the addition of 2.4 ml of double distilled H₂O and thoroughly mixed. Absorbance of the developed pink colour of the mixture was determined at 510 nm against a blank. Total flavonoid was expressed as catech in equivalent.

2.2.4 Determination of Total Phenolics

Total phenol contents in the extracts and fractions were determined by the method described by Kim *et al.*(11). The extract solution (0.5 mL) with a concentration of 1 mg/mL was added to 4.5 mL of deionized distilled water and 0.5 mL of Folin Ciocalteu's reagent (previously diluted with water 1:10, v/v) which was added to the solution. After mixing the tubes, they were maintained at room temperature for 5 minutes followed by the addition of 5 mL of 7% sodium carbonate and 2 mL of deionized distilled water. After mixing the samples, the samples were incubated for 90 minutes at room temperature. Standard curve was prepared by gallic acid in six different concentrations (12.5, 25, 50, 75, 100 and 150 mg/L). The absorbance was measured at 750nm wavelength using spectrophotometer. The total phenol content was expressed as milligram of gallic acid equivalents (GAE) per gram of extract (mg GAE/g extract).

2.3 Determination of Antioxidant Activity

2.3.1 Determination of DPPH Radical-Scavenging Activity

A DPPH radical scavenging activity was determined by method described by Pownall *et al.*(12). In the method, 1mL of the sample solution was mixed with 1 mL of 0.3 mM DPPH in methanol. The mixture was vortexed for 60 seconds



and incubated in the dark for 30 min. The change in colour from deep violet to light yellow was measured at wavelength of 517nm using a spectrophotometric. Methanol was used as blank. The free radical scavenging ability was calculated using the equation below.

$$\% \text{ DPPH} = \frac{\text{Absorbance of control} - \text{Absorbance of sample}}{\text{Absorbance of control}} \times 100 \quad \text{..... (1)}$$

2.3.2 Determination of Metal chelating Capacity

The metal chelating activity was measured described by Xie *et al.*(13). Five hundred microlitres (500 µL) of peptide sample solution was combined with 25 µL of 2 mM FeCl₂ and 925 µL double distilled water in a reaction tube. Fifty microlitre (50 µL) of ferrozine solution (5 mM) was added and mixed thoroughly. The mixture was then allowed to stand at room temperature for 10 min and an aliquot of 200 µL was pipetted into a clear bottom 96-well plate. A control was also conducted by replacing the sample with 500 µL of double distilled water. The absorbance of the samples was measured at wavelength of 562 nm using a spectrophotometer (Multiskan GO, Thermo Scientific). Percentage chelating effect (%) was calculated using the following equation:

$$\text{Metal ion chelating activity (\%)} = \frac{Ac - As}{Ac} \times 100 \quad \text{(2)}$$

Where: Ab = absorbance of the blank; As = sample absorbance

2.3.3 Ferric reducing antioxidant power (FRAP)

The ferric reducing antioxidant power of samples was measured according to a previously described method by Benzie and Strain (14) with some modifications for a microplate reader. Briefly, the FRAP reagent was freshly prepared by mixing 300 mM acetate buffer (sodium acetate buffer, pH 3.6), 10 mM 2,4,6-tripyridyl-s-triazine (TPTZ) in 40 mM HCl and 20 mM ferric chloride in a ratio 5:1:1 (v/v) before evaluation. Two hundred microlitres (200 µL) of FRAP reagent (preheated to 37°C) was added to 40 µL of sample or GSH in a 96 well microplate. Absorbance at 593 nm was measured relative to a reagent blank. Ferrous sulphate (conc: 0.0625-1 mM) was used to prepare a standard curve and the results of the samples was expressed as mmol Fe²⁺ reduced.

2.4. Statistical Analysis

Data were subjected to Analysis of Variance (ANOVA) using statistical package for social sciences (SPSS) version 17.0. Duncan's new multiple range test (DNMRT) was used to compare the treatment means. Statistical significance was accepted at p < 0.05

3.0 RESULTS AND DISCUSSION

3.1 Results

Table 2: Bioactive components of toasted pearl millet-avocado seeds flour blends

Sample	Saponin(mg/g)	Carotenoids(µg/kg)	Flavonoids (mgQE/g)	Phenolic(mgGAE/g)
EOE1	2.23 ^a ±0.07	0.58 ^a ±0.06	5.85 ^a ±0.11	23.85 ^a ±0.09
EOE2	2.46 ^b ±0.08	2.44 ^b ±0.11	7.82 ^b ±0.15	33.78 ^b ±0.15
EOE3	2.77 ^c ±0.17	12.37 ^c ±0.20	24.83 ^c ±0.22	39.78 ^c ±0.06
EOE4	3.07 ^d ±0.11	17.63 ^d ±0.21	33.18 ^d ±0.59	48.73 ^d ±0.17
EOE5	3.50 ^e ±0.05	17.53 ^d ±0.05	34.71 ^e ±0.22	54.79 ^e ±0.13
EOE6	3.60 ^e ±0.05	18.63 ^e ±0.15	35.78 ^f ±0.10	58.65 ^f ±0.19

Values are means ± standard deviations of triplicate determinations. Means in same column with same superscript are not significantly (p>0.05) different.

EOE1 = 100% Toasted millet flour; EOE2 = 90% Toasted millet flour + 10% Avocado pear seeds flour; EOE3 = 80% Toasted millet flour + 20% Avocado pear seeds flour; EOE4 = 70% Toasted millet flour + 30% Avocado pear seeds flour; EOE5 = 60% Toasted millet flour + 40% Avocado pear seeds flour and EOE6 =100% Avocado pear flour.

Table 3: Antioxidant Properties of toasted pearl millet-avocado seeds flour blends

Sample	DPPH (%)	FRAP (m Mol Fe ²⁺)	Metal chelating activities (%)
EOE1	24.02 ^a ±0.44	0.09 ^a ±0.00	44.11 ^a ±0.74



EOE2	26.77 ^b ±0.18	0.09 ^{ab} ±0.00	44.84 ^{ab} ±0.08
EOE3	35.82 ^c ±0.04	0.14 ^c ±0.02	44.97 ^b ±0.02
EOE4	37.71 ^d ±0.12	0.15 ^d ±0.00	48.55 ^c ±0.53
EOE5	41.59 ^e ±0.21	0.19 ^e ±0.02	53.75 ^d ±0.26
EOE6	48.92 ^f ±0.15	0.20 ^f ±0.00	64.72 ^e ±0.41

Values are means ± standard deviations of triplicate determinations. Means in same column with same superscript are not significantly ($p > 0.05$) different.

3.2 Discussion

3.2.1 Bioactive components of toasted pearl millet-avocado seeds flour blends

The result of the bioactive components of toasted pearl millet-avocado seeds flour blends is presented in Table 2. The saponin content ranged from 2.23 - 3.60 mg/g, carotenoids (0.58 - 35.78 µg/g), flavonoids (5.85 - 35.78 mg QE/g) and total phenolic (23.85 - 58.65 mg GAE/g). A significant ($p \leq 0.05$) increase in the bioactive constituents of toasted pearl millet-avocado seeds flour blends was observed with every 10% increase in the quantity of avocado seeds flour substitution. It was observed that 100 % avocado seeds flour had the highest content of saponins (3.60 mg/g), carotenoids (18.63 µg/g), flavonoids (35.78 mg QE/g) and total phenolic (58.65 mg GAE/g) than 100 % toasted pearl millet flour, thereby impacting positively on their content in the flour blends.

Studies have shown that saponins has the ability to lower blood cholesterol level; inhibit the growth of cancer cells, improved bone health and stimulation of the immune system (6).

Research has reported that consumption of carotenoids and flavonoid-rich foods protects humans against diseases associated with oxidative stress (15). Flavonoids are natural secondary metabolites of plants with rich antioxidant properties and are able to interact and scavenge the free radicals that can damage cell membranes and biological molecules. Most of the beneficial effects of flavonoids on health are related to their antioxidant and synergistic properties with other antioxidants. Avocado seed flour would serve as a good source of flavonoids (16).

Phenol content of fruits, vegetables and legumes has been harnessed therapeutically in the treatment/management/prevention of degenerative diseases associated free radicals (17).

3.2.2 Antioxidant Properties of toasted pearl millet-avocado seeds flour blends

The antioxidant property of toasted pearl millet-avocado seeds flour blends is presented in Table 3. The result ranged from 24.02 to 48.92 %, 0.09-0.20 mMol Fe²⁺ and 44.11-64.72 % for DPPH, FRAP and metal chelating actives respectively. The DPPH, FRAP and metal chelating activities ability of the flour blends were significantly ($p \leq 0.05$) elevated with every 10% substitution of toasted pearl millet flour with avocado seeds flour. The results of the antioxidants properties of the flours further indicated that avocado seeds flour (EOE6) had double the DPPH, FRAP and metal chelating power than toasted pearl millet flour (EOE1).

The toasted millet-avocado flour blends exerted a concentration-dependent manner on the DPPH scavenging activity which might indicate that there are some compounds being contributed on scavenging the DPPH radical. Increase in the level of substitution avocado seeds resulted in the increase of DPPH scavenging activity. These results indicated that the formulated flour blend with 60% toasted millet and 40% avocado seeds flour exhibited the best antioxidant activity amongst flour blends. Phytochemicals provide health benefits associated with their ability to prevent damage due to biological degeneration (18). Levels of individual antioxidants in food do not necessarily reflect their total antioxidant capacity, which could also depend on synergic and redox interactions among the different antioxidant molecules (phytochemicals, vitamins and minerals) present in foods. Among the phytochemicals, phenolic compounds are reported to be the main contributor of antioxidant activity in plant extracts due to their higher value in total content (their interaction and redox property (19) and their synergistic effectiveness as hydrogen donors, reducing agents and free radical scavengers (20).

4.0 CONCLUSION AND RECOMMENDATION

4.1 Conclusion



Substitution of toasted pearl millet to avocado seeds flour blends elevated total phenolic, flavonoids and carotenoids and saponin. The substitutions however, had greatest metal chelating activity, DPPH and FRAP antioxidant activity, indicating their biological potential in the treatment and prevention of different diseases.

4.2 Recommendations

Further studies should be carried out on the nutrients and antinutrients composition of the flour blends to enhance the commercialization flour.

5.0 REFERENCES

- 1 T.B. Bahru, Z. H.Tadele, E.G. Ajebe, Review on Avocado Seed: Functionality, Composition, Antioxidant and Antimicrobial Properties. *Chemical Science international journal* **27(2)**, 1-10(2019).
- 2 O.O. Adeyemi, S.O. Okpo, O.O. Ogunti, Analgesic and anti-inflammatory effects of the aqueous extract of leaves of *Persea americana* Mill (Lauraceae). *Fitoterapia* **73(5)**, 375-380 (2002).
- 3 A.Yadev, Antioxidants and its functions in human body. *Researches in Environmental and life science* **9(11)**, 1328- 1331(2016).
- 4 K.V.R.Rao, P. Mani, B. Satyanarayana, T.R.Rao, Purification and structural elucidation of three bioactive compounds isolated from *Streptomyces coelicoflavus* BC 01 and their biological activity. *Biotechnology* **7**, 24-29 (2017).
- 5 S. Pushparaj, A. Urooj, Antioxidant activity of two pearl millet (*pennisetum typhoideum*) cultivars as influenced by processing Antioxidants. *Journal of Food Science* **3**, 55-66(2014). DOI: 10:3390/ antiox 3310055.
- 6 B.A. Orhevba, A.O Jinadu, Determination of Physico-Chemical Properties and Nutritional Contents of Avocado Pear (*Persea Americana* M.). *Academic Research International* **1(3)**, 372-380(2011).
- 7 D. Mridula,R. Goyal and M. Manikantan, Effect of roasting on texture, colour and acceptability of pearl millet (*Pennisetum glaucum*) for making sattu. *International Journal of Agriculture Research*, **3(1)**, 61–68(2008). doi:10.3923/ijar.2008.61.68
- 8 Y. Uematsu, K. Hirata, K. Saito, Spectrophotometric determination of saponin in yucca extract used as food additive. *Journal of AOAC International* **83(6)**, 1451-1454 (2000)
- 9 Association of Analytical Chemists International, *Official Methods of Analysis of AOAC*, 17th ed.; AOAC international: Gaithersburg, MD, USA, 104(2012).
- 10 M.A. Ebrahimzadeh, S.J. Hosseinmehr,A. Hamidinia, M. Jafari, Antioxidant and radical scavenging activity of Feijoa sellowiana fruits peel and leaves. *Pharmacologyonline* **1**, 7-14(2008).
- 11 D.O. Kim, S. W. Jeong, C. Y. Lee, Antioxidant capacity of phenolic phytochemicals from various cultivars plums. *Food Chemistry* **81(3)**, 321-326(2003).



- 12 T.L.Pownall, C.C. Udenigwe, R.E. Aluko, Amino acid composition and antioxidant properties of pea seed (*Pisum sativum*L.) enzymatic protein hydrolysate fractions. *Journal of Agricultural Food Chemistry* **58**, 4712-4718(2010).
- 13 Z. Xie, J. Huang, X. Xu, Z. Jin, Antioxidant activity of peptides isolated from alfalfa leaf protein hydrolysate. *Food Chemistry* **111**, 370-376 (2008).
- 14 I.F.F. Benzie, J.J. Strain, The ferric reducing ability of plasma (FRAP) as a measure of antioxidant power: The FRAP assay. *Analytical Biochemistry* **239**, 70-76(1996). DOI: 10.1006/abio.1996.0292
- 15 G. Duthie, P. Morrice, Antioxidant capacity of flavonoids in hepatic microsomes is not reflected by antioxidant effects *in vivo*. *Oxidative Medical Cell Longevity* 1-6 (2012).
- 16 H. Annegowda, R. Bhat, L.M, Tze, A. Karim, S. Mansor, The free radical scavenging and antioxidant activities of pod and seed extract of *Clitoria fairchildiana* (Howard) - an underutilized legume. *Journal of Food Science and Technology* **50(3)**, 535-541 (2013).
- 17 Doss, M. Pugalenth, D. Rajendrakumaran and V. Vadivel, Phenols, flavonoids and antioxidant activity of underutilized legume seeds. *Asian Journal of Experimental Biological Science* **1(3)**, 700-705(2010).
- 18 V. Suryanti, S. D. Marliyana and H.E. Putri, Effect of germination on antioxidant activity, total phenolics, β -carotene, ascorbic acid and α -tocopherol contents of lead tree sprouts (*Leucaena leucocephala* (Imk.) de Wit). *International Food Research Journal* **23(1)**, 167-72(2016).
- 19 S.F. Sulaiman, A.A.B. Sajak, K.L. Ooi, E.M. Seow, Effect of solvents in extracting polyphenols and antioxidants of selected raw vegetables. *Journal of Food Composition and Analysis* **24(4-5)**, 506-515(2011).
- 20 S. Zhou, Z. Fang, Y. Lü, J. Chen, D. Liu, X.Ye, Phenolic and antioxidant properties of bayberry (*Myrica rubra* Siebet Zucc.) pomace. *Food Chemistry* **112(2)**, 394-99 (2009).

6.0 ACKNOWLEDGMENTS

We acknowledge the Royal Society of Chemistry, United Kingdom, for the award of a Researcher Development and Travel Grant of £ 474 to support the presentation of this article at the 2nd National Conference on Chemical Technology (NCCT 2023) scheduled for 14th to 17th November 2023 at Zaria, Kaduna State, Nigeria.



P010 - SYNTHESIS AND CHARACTERIZATION OF SILICA NANOPARTICLES FROM COCONUT HUSK

*¹Ikyenge B. A., ¹Ochohi S. O. and ²Samoh F. T

¹*Department of Chemistry, Benue State University, Makurdi, Benue State, Nigeria*

²*Department of Chemistry, University of Ilorin, Ilorin, Kwara State, Nigeria*

Corresponding author email: bkyenge@bsum.edu.ng

ABSTRACT

Silica Nanoparticles were synthesized using sol-gel method using coconut husk as the raw material. The Coconut husks were burned in an electric furnace to obtain coconut husk ash. The ash was treated using sol gel method to obtain Silica. Silica was obtained by mixing the coconut husk ash (CHA) in NaOH solution which was carefully titrated with HCl to form aqua gels which was washed, sieved and dried to get silica nano particles. The synthesized silica nano particles were characterized using SEM, UV-Vis, FTIR, XRD and EDX to determine the properties of the nano silica. SEM analysis showed the nanoparticles possessed flake-like structures and had irregular shapes. The functional groups were determined using FTIR, which showed the presence of Siloxane bands at 1170, 762 and 450 cm^{-1} . The optical properties of the nanoparticles studied using UV-Vis showed a wavelength of maximum absorbance at 287.42 nm. XRD showed that the nanoparticles obtained were in crystalline form due to the many diffraction peaks in SiO_2 , Fe_2O_3 and Al_2O_3 . EDX determined that the Silica nanoparticles contained 73.56 % Si and 15.37% O.

KEYWORDS

Coconut Husk Characterized, Nanoparticles, Sol-gel, XRD.

1.0 INTRODUCTION

Nanoparticles (NPs) and nanostructured materials represent an active area of research which makes them valuable in various fields. Nanoparticles and nanostructured materials have gained prominence in technological advancements due to their tunable physicochemical characteristics such as small size and large surface area, melting point, wettability, electrical and thermal conductivity, catalytic activity and light absorption (1).

Nanoparticles have been considered one of the most forefront materials in recent decades. They have been said to be the material of the next generation because of their unique designs and property combination compared with conventional materials (2). The properties of nanoparticles have been exploited in a wide range of applications such as in medicine, cosmetics, renewable energies, environmental remediation, water treatment and biomedical devices (3). Electronics, optics, organic catalysis, vector control, sensor, etc., have also drawn extensive attention to this field of study (4).

Since their discovery, silica nanoparticles have been broadly employed in many fields thanks to a very convenient and regular porosity showing high specific surface areas (5). The application of nano

technology in modern science has helped to synthesize large number of materials with different pore sizes and geometries (hexagonal, cubic, radial, etc.) and particle morphologies (spheres, rods, layered, etc.). Their applications are consequences of their porous nature and robust chemical composition, which permit their use in many applications: water treatment (6), gas processing (7), supported catalysis (8), and Nano-medicine, in which Mesoporous Silica Nanoparticles (MSNs) have demonstrated their capacity as drug delivery Nano-carriers (9, 10) and new-generation. In this work, silica nanoparticles are synthesized from coconut husk using sol-gel method.

2.0 EXPERIMENTAL

2.1 Sample Collection and preparation

Coconut husk samples used in this study were obtained from a coconut farmer in the North-Bank area of Makurdi, Benue State. The samples were cleaned and dried in an electric oven at temperature of 120 °C to remove most impurities and moisture.

2.2 Synthesis of Silica Nanoparticles



The clean coconut fibres were cut and placed in ceramic crucibles and then inserted into a furnace and heated at 700 °C for 2h to obtain the coconut husk ash (CHA). A known amount of CHA was added to a flask containing a 2.5 M Sodium hydroxide (NaOH) 40.00 g mol⁻¹ 98 % purity, Qualikems Laboratory Reagents, Qualikems Fine Chem PVT, Ltd, India) solution and then boiled at 100 °C for 1 h with constant stirring, thus producing a sodium silicate solution. The solution was filtered severally using No. 1 Whatman Filter papers to remove small quantities of metal and carbon residues and to obtain a clear solution. Nano silica was then produced by neutralizing sodium silicate with hydrochloric (HCl) 132.87 ml, 99.8 % purity, Guangdong Guanghua Sci-Tech Co., Ltd, China). The sodium silicate solution was allowed to cool and titrated slowly with 1.0 M HCl acid solution. To avoid local changes in pH during gel formation, the solution was stirred constantly. The solution was monitored with a pH meter (Eutech Instruments pH-700 meter), Silica gels started to form when change in PH was less than 10. The aqua gels formed were transferred into closed plastic vessels and allowed to age at 25 °C for 1–72 hrs. Deionised water was used to wash the gels. The gels were then filtered to remove excess impurities. The washing step was repeated, and the solids were collected and dried at 80 °C for 2 hrs. The solids were crushed and ground to powder using an agate mortar, and screened through a 200 mesh sieve to obtain the Nano silica grains.

2.3 Characterization of the Silica Nanoparticles

2.3.1 SEM Analysis

3.1 Scanning Electron Microscopy of SiNPs

Scanning electron microscopy (SEM) analysis was carried out using SEM machine to determine the morphological features of the synthesized Silica nanoparticles (SiNPs).

2.3.2. UV-Vis Analysis

UV-Vis analysis was carried out by scanning the solution containing the SiNPs at the wavelength from the range of 150 to 500nm using UV spectrophotometer UNICO 2800P.

Sample Preparation on solid sample- The solid sample should be coated on to a desired, transparent substrate. A blank sample of the transparent substrate should be brought for the Analysis.

2.3.3. FTIR Analysis

Fourier transform infrared spectroscopy (FT-IR) analysis was performed in all samples isolated. All spectra were recorded from 5000-400 cm⁻¹ using the Perkin Elmer 3000 MX spectrometer.

2.3.4. X-Ray Diffraction (XRD)

Inorganic geochemical analysis of silica nanoparticles was done using X-Ray Diffraction Spectrophotometer (Phillips-JEEB 4B) to determine the crystalline and amorphous nature of the synthesized nanoparticles.

2.3.5 Energy Dispersive X – ray Spectroscopy (EDX)

The energy dispersive x-ray analysis was carried out to determine the elemental composition of the silica nanoparticles.

3.0 RESULTS AND DISCUSSION:

The results of synthesis and characterization of the silica nanoparticles from coconut husk are presented as follows;



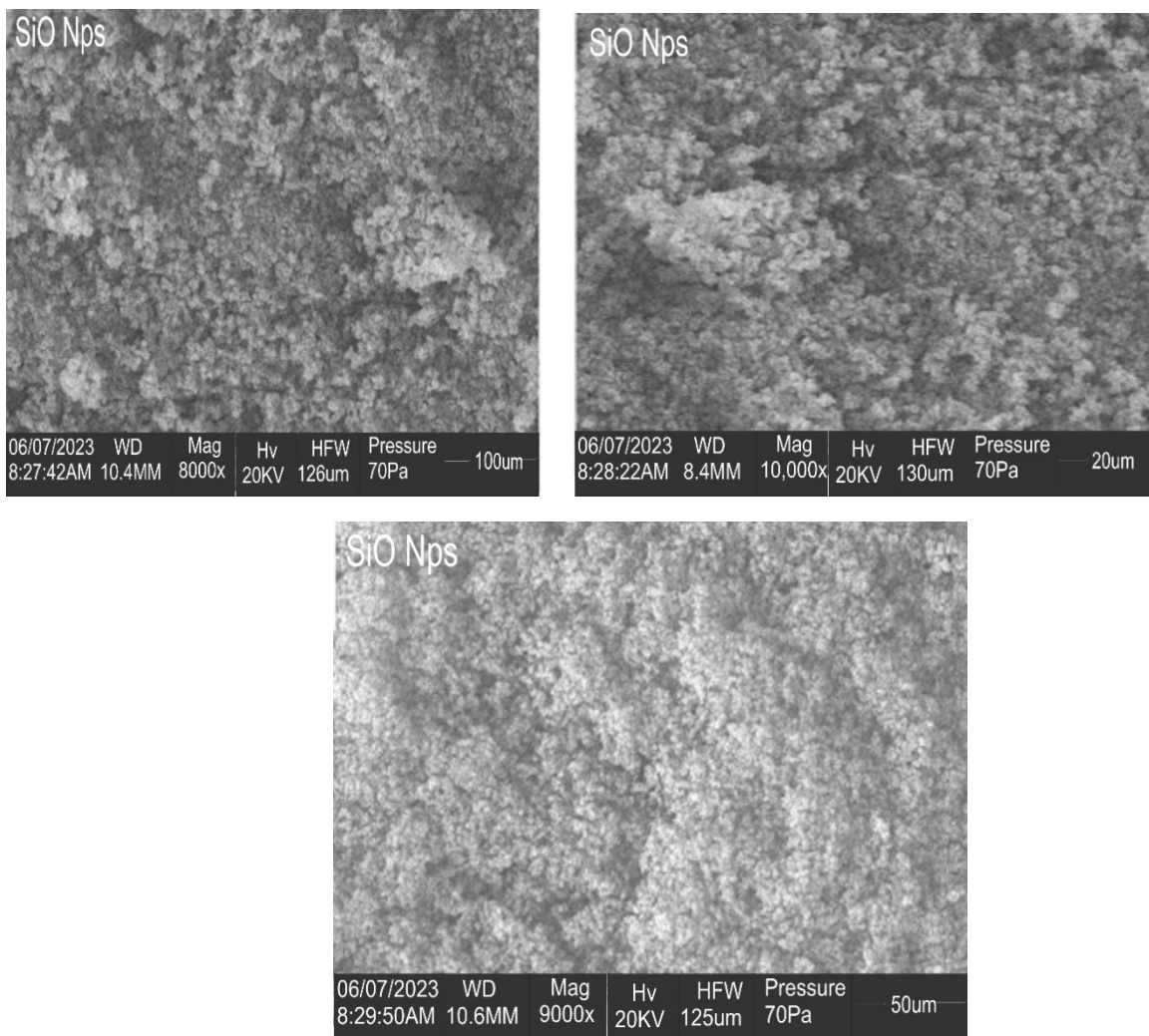


Fig. 1. Scanning Electron Microscopy of SiNPs

The morphological features of silica nanoparticles were studied using Scanning Electron Microscopy. The SEM images (Fig.1) showed that the nanoparticles decompose to smaller, finer particles and have irregular shapes. The nanoparticles can be

seen to be distributed randomly with little spaces between particles; the nanoparticles have no definite shape or form.

3.2 UV-Vis analysis of SiNPs

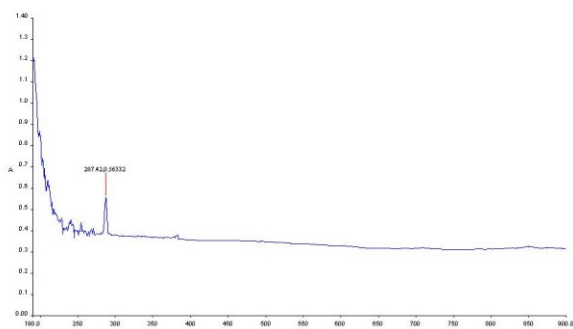


Fig. 2. UV-VIS spectra of SiNPs

The UV-Visible spectrum of SiNPs recorded maximum absorption band at 287.42 nm with absorbance of 0.56332 as shown in Fig.2. These optical features are similar to those obtained in previous reports and attributed to Si-O-Si bond confirming the presence of silica nanoparticles (11) also reported a strong absorbance at 311.35 nm for silica nanoparticles isolated from rice husk.

3.3 Fourier transform infrared spectroscopy (FT-IR)



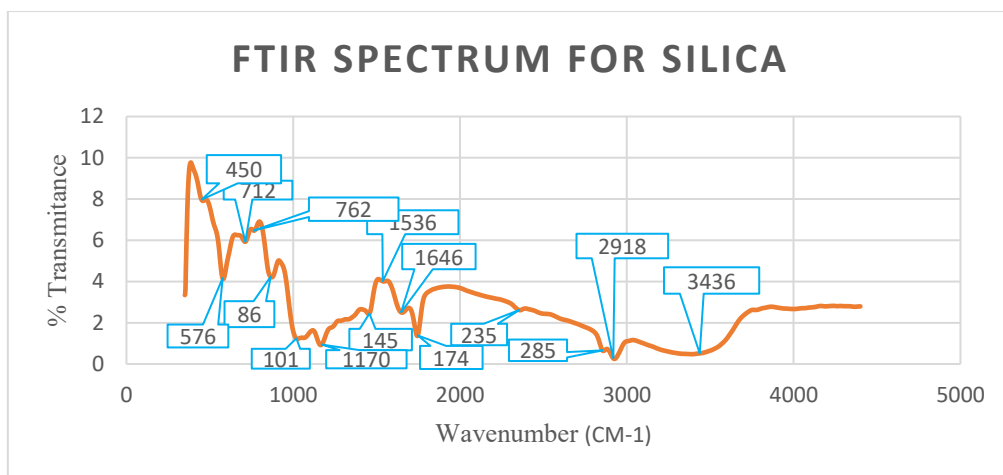


Fig. 3. Fourier Transform Infrared Spectroscopy (FT-IR) of SiNPs

Table 1: Absorption peaks of SiNPs

Wavenumber(cm^{-1})	Functional group
3436	Si-OH
2918	C-H
1646	C=O
1456	CH ₂ Strain
1170	Si-O-Si Stretching vibration
762	Si-O-Si Stretch vibration
450	Si-O-Si Bending vibration

The FTIR spectrum of silica nanoparticles derived from CHA carbonised at 700 °C for 2 h. A few crystals were mixed with KBr (Merck for spectroscopy) and pulverized in an agate mortar to form a homogenous powder, from which, under a pressure of 7 tons, the appropriate pellets was prepared and analysed. All spectra were recorded from 5000-400 cm^{-1} using the Perkin Elmer 3000 MX spectrometer. FTIR characterization is used to identify the molecules and their functional group present in the synthesized silica nanoparticles. As shown in Figure 3, the FTIR spectra of coconut husk ash displayed different absorption peaks at 3436, 2918, 1646, 1456, 1170, 762, and 450 cm^{-1} respectively. The band at 3436 cm^{-1} corresponded to the stretching vibration of the O-H bands from the silanol group (Si-OH). This is an indication that water molecules were absorbed on the silica surface. Marousek *et al.*, 2022 (12) reported that the FTIR analysis shows the formation of silica nanoparticles through the presence of asymmetric stretching vibration of Si-OH bond which absorbed at 3363 cm^{-1} due to water molecules. The band at 2918 cm^{-1} was assigned to the stretching vibration

of C-H bond. Then, a band located at 1646 cm^{-1} corresponding to the C=O stretching, which might be attributed to the hemicelluloses and lignin aromatic groups (13), and a band located at 1456 cm^{-1} , identified as the CH₂ strain of the cellulose in the CHA, were found (14). Furthermore, a strong band at 1170 cm^{-1} indicated Si-O-Si stretching vibration. Meanwhile, the band at the wavelength of 762 cm^{-1} was due to the Si-O-Si bond stretching, while at 450 cm^{-1} , it was due to the bending vibration of the same functional group. Hence, the presence of bands at 1170, 762 and 450 cm^{-1} confirmed the formation of silica following the acid treatment method (15).

3.4 X-ray diffraction analysis (XRD)



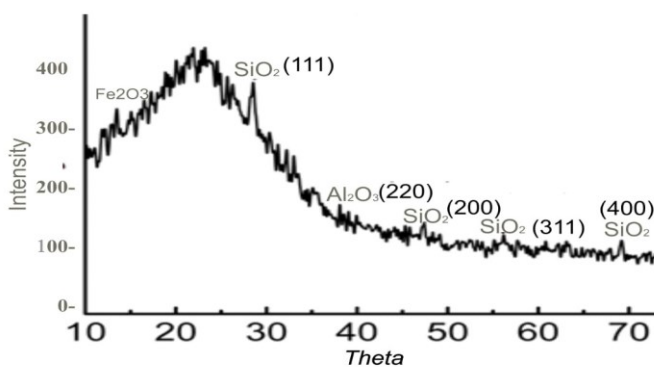


Fig. 4. XRD spectrum of Silica nanoparticles obtained from CHA.

XRD Analysis is used to determine the crystalline nature of silica nanoparticles. Figure 4 depicts the XRD spectra analysis of chemically synthesized silica at 700 °C for 2 h using the sol-gel method.

From the spectrum, the silica nanoparticles obtained was likely to be in a crystalline form. As a

result of the presence of many diffraction peaks aside silica (SiO_2), Ferric oxide (Fe_2O_3) and Aluminium oxide (Al_2O_3) were also present as impurities [16]. Many peaks corresponding to crystalline nature of SiO_2 were also found. However, the diffraction peaks of SiO_2 could be clearly observed at $2\theta = 27.65^\circ$, 46.39° , 55.98° and 69.50° , alongside a few peaks of Fe_2O_3 and Al_2O_3 at $2\theta = 15.35^\circ$, 38.61° , respectively. The silica became more apparent in the spectrum because of the other metallic oxides in the sample that dissolved upon reacting with the acid. It was also observed that, the most prominent peak at $2\theta = 27.65^\circ$ correspond to the (111) crystal plane. Therefore, the peaks observed indicates that the silica obtained by using sol-gel method is in crystalline form (16) also stated that, the peaks observed indicates that the silica obtained from coconut husk ash by using acid treatment method is crystalline in nature.



Table 2: The crystallite size of the silica nanoparticle was obtained by using the Debye Scherrer Equation ($d = \frac{\kappa\lambda}{\beta\cos\theta}$)

Peaks	θ (Brogs angle)	β (FWHM)	λ (wavelength)	diameter(nm)
1	27.65	30.0	1.546	2.86
2	46.39	15.5	1.546	5.84
3	55.98	12.5	1.546	7.54
4	69.50	19.5	1.546	5.20
Mean Diameter				5.36(nm)

3.5 Energy Dispersive X-ray Spectroscopy (EDX)

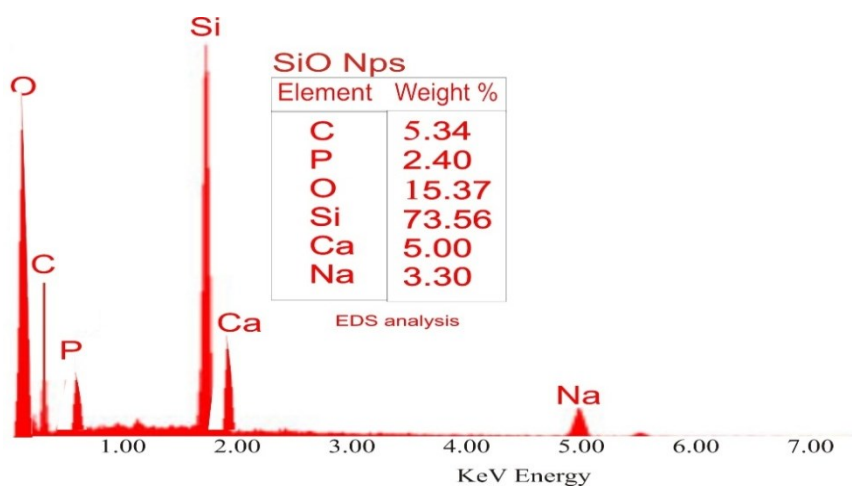


Fig. 5. EDX of SiNPs

The EDX of SiNPs is shown in figure 5. and the percentage composition of each element is indicated. The EDX result indicated the highest percent for Silicon (73.56 %), followed by Oxygen (15.37 %) which agrees with the fact that most of the impurities detected from the result of XRD were metallic oxides. Silica itself contains more than 50 % Oxygen (53.33 %). Phosphorous showed the least composition of 2.40 %.

4.0 CONCLUSIONS

Silica nanoparticles were successfully synthesized in this study using coconut husk. The nanoparticles were seen to possess crystalline structures. The functional groups and molecules were determined using FTIR, which shows the presence of Siloxane bands to confirm the formation of silica. The optical properties of the Nano silica were studied using UV-Vis spectrophotometer and showed a wavelength of maximum absorbance at 287.42 nm. The mean diameter of the silica nanoparticle from

the XRD analysis was at 5.36nm. Silica nanoparticles contained 73.56% Si and 15.37 O shown from the EDX analysis.

5.0 REFERENCES

1. J. Jeevanandam, A. Barhoum, Y. S. Chan, A. Dufresne, M. K. Danquah, Review on nanoparticles and nanostructured materials: history, sources, toxicity and regulations. *Beilstein journal of nanotechnology* **9**, 1050-1074 (2018).
2. M. Akter *et al.*, A systematic review on silver nanoparticles-induced cytotoxicity: Physicochemical properties and perspectives. *Journal of advanced research* **9**, 1-16 (2018).



3. M. Brust, C. J. Kiely, Some recent advances in nanostructure preparation from gold and silver particles: a short topical review. *Colloids and Surfaces A: Physicochemical and Engineering Aspects* **202**, 175-186 (2002).
4. C. Xu *et al.*, Nanotubular mesoporous bimetallic nanostructures with enhanced electrocatalytic performance. *Advanced Materials* **21**, 2165-2169 (2009).
5. P. Kumar, P. Tambe, K. M. Paknikar, V. Gajbhiye, Mesoporous silica nanoparticles as cutting-edge theranostics: Advancement from merely a carrier to tailor-made smart delivery platform. *Journal of Controlled Release* **287**, 35-57 (2018).
6. P. N. Diagboya, E. D. Dikio, Silica-based mesoporous materials; emerging designer adsorbents for aqueous pollutants removal and water treatment. *Microporous and Mesoporous Materials* **266**, 252-267 (2018).
7. B. Ghalei, A. Pournaghshband Isfahani, M. Sadeghi, E. Vakili, A. Jalili, Polyurethane-mesoporous silica gas separation membranes. *Polymers for Advanced Technologies* **29**, 874-883 (2018).
8. M. Davidson *et al.*, Hybrid mesoporous silica/noble-metal nanoparticle materials—synthesis and catalytic applications. *ACS Applied Nano Materials* **1**, 4386-4400 (2018).
9. M. Vallet-Regí, A. Rámila, R. Del Real, J. Pérez-Pariente, A new property of MCM-41: drug delivery system. *Chemistry of Materials* **13**, 308-311 (2001).
10. M. Vallet-Regí, F. Balas, D. Arcos, Mesoporous materials for drug delivery. *Angewandte Chemie International Edition* **46**, 7548-7558 (2007).
11. V. H. Le, C. N. H. Thuc, H. H. Thuc, Synthesis of silica nanoparticles from Vietnamese rice husk by sol-gel method. *Nanoscale research letters* **8**, 1-10 (2013).
12. J. Maroušek *et al.*, Silica nanoparticles from coir pith synthesized by acidic sol-gel method improve germination economics. *Polymers* **14**, 266 (2022).
13. M. Bansal, U. Garg, D. Singh, V. Garg, Removal of Cr (VI) from aqueous solutions using pre-consumer processing agricultural waste: A case study of rice husk. *Journal of hazardous materials* **162**, 312-320 (2009).
14. D. C. Marin *et al.*, Revalorization of rice husk waste as a source of cellulose and silica. *Fibers and Polymers* **16**, 285-293 (2015).
15. M. F. Anuar, Y. W. Fen, M. H. M. Zaid, K. A. Matori, R. E. M. Khaidir, The physical and optical studies of crystalline silica derived from the green synthesis of coconut husk ash. *Applied Sciences* **10**, 2128 (2020).
16. M. Mariana, F. Mulana, S. Sofyana, N. Dian, M. Lubis, in *IOP Conference Series: Materials Science and Engineering*. (IOP Publishing, 2019), vol. 523, pp. 012022.

6.0 ACKNOWLEDGEMENT

The authors would like to thank and acknowledge the Royal Society of Chemistry, United Kingdom, for the Researcher Development Grant awarded to support the presentation of this conference paper, at the 2nd National Conference on Chemical Technology, holding from 14th to 17th November 2023 in Zaria, Kaduna State, Nigeria.



P015 - OPTIMIZATION OF BIODIESEL PRODUCTION FROM BUSHEL KENTUCKY SEED OIL USING SULPHATED TIN OXIDE CATALYST

U. A. Ahmed^{*1}, I. A. Muhammed-Dabo¹ and H. Ibrahim².

¹Department of Chemical Engineering, Ahmadu Bello University, Zaria

²Department of Chemical Engineering Kaduna Polytechnic Kaduna

Corresponding author: uzausa200@gmail.com

ABSTRACT

An optimisation of heterogeneous reaction process for the transesterification of bushel Kentucky seed oil with methanol in the presence of sulphated tin oxide catalyst has been developed using response surface methodology (RSM). The effects of the main parameters, such as the amounts of $\text{SnO}_2/\text{SO}_4^{2-}$ (1.5 to 3.0), the molar ratio of methanol to oil (3:1 to 8:1) and the reaction temperature, on fatty acid methyl esters (FAME) yield were investigated. The optimal conditions were: molar ratio of methanol to oil of 5.50:1; catalyst concentration of 3.0 wt% in oil; and a reaction temperature of 52.50 °C. Under these conditions, the conversion of bushel Kentucky oil to FAME exceeded 94.9% after 1hour. GC-MS analysis revealed that the biodiesel contains 93.91% ester content and 6.09% non-ester composition. Response surface methodology (RSM) based on Central Composite Design (CCD) was employed to examine the reaction parameters (the weight of catalyst, molar ratio of methanol to oil and reaction temperature), and to optimize the reaction conditions for achieving the maximum yield of fatty acid methyl ester (FAME). Design Expert 6.06 software was used in the regression and graphical analyses of data. The statistical analysis of the model was performed to evaluate the analysis of variance (ANOVA).

KEYWORDS

Biodiesel, Optimization, Design of experiment, GC-MS, Bushel Kentucky seed oil

1.0 INTRODUCTION

In recent times, increasing demand for energy worldwide has resulted in faster rate of energy consumption generated from fossil fuel like crude oil, natural gas and coal. Most importantly, environmental concern has necessitated the diversification into various forms of renewable energy to meet the continuously growing demand with less harm to the environment (1).

The rising cost of petroleum products and climate change are some of the problems facing many developing countries. The solution to these problems can be found in the explorations of alternative energy resources. One of such alternative energy source for the transport sector is biodiesel, which can be produced from triglycerides (1, 2). Vegetable oils can also be used as fuel in diesel engines, but direct use of vegetable oils poses many problems in the long run, such as, injector chocking, ring sticking, wax formation, carbon deposits, misfire, ignition delay, and fuel atomization. These problems are attributed to high viscosity, low volatility, poly-unsaturation, high flash point, and low cetane number (3). The Flashpoint of the biodiesel is lowered than the raw oil and the cetane number is improved (4). The yield of biodiesel in the process of transesterification is

affected by several process parameters, which include; presence of moisture and free fatty acids (FFA), reaction time, reaction temperature, catalyst and molar ratio of alcohol and oil (5).

There is numerous feedstock that can be used to produce biodiesel. Amongst them; are Soybean, (6). Sunflower, (7). rapeseed and peanut oils (8). which have been considered in earlier times but their impact on food crisis have hindered their usage. The selection of raw materials mainly depends upon availability and cost (9). The feedstock for biodiesel production are animal fat and plant (vegetable) oil such as soybeans, rapeseed, jatropha, castor and Bushel Kentucky to mention a few. Calabash (*Bushel Kentucky*) seed is grown as a creepy like rope on floor or on threes and walls that is largely cultivated in Northern Nigeria. It is usually harvested between 90 to 120 days after planting. (10). Calabash fruit is majorly used in rural settlements as container and storage vessels. Its seed, which contains about 32.3% oil, which is non-edible, is currently of no significant economic use (11).

Optimization is the use of specific methods to determine the most cost-effective and efficient solution to a problem or design for a process. This technique is one of the major quantitative tools in



industrial decision making. A wide variety of problems in the design, construction, operation, and analysis of chemical plants (as well as many other industrial processes) can be resolved by optimization (12). This study aims to use the factorial design and response surface design to investigate the factors that affect the production of biodiesel from Bushel Kentucky seed oil using heterogeneous catalyst Sulphated Tin-Oxide ($\text{SnO}_2/\text{SO}_4^{2-}$)

Among the different types of metal oxides, tin oxide (SnO_2) has attracted immense interest. This is due to its dual valency and its ability to attain more than one oxidation state (13). Usually, SnO_2 prefers to possess the oxidation states of 2+ or 4+, which greatly promotes the variation in the composition of surface oxygen, and thus, the SnO_2 exhibits varied surface properties, which have a significant importance in catalysis (14).

Tin (IV) oxides loaded on the different oxides (TiO_2 , ZrO_2 , and Fe_2O_3) and activated at the same temperature can result in solid acid catalysts with different activities. For instance, over $\text{SnO}_2/\gamma\text{-Al}_2\text{O}_3$, a reasonable conversion of soybean oil into FAMES (ca. 68.5%) was obtained, whilst a conversion of 64.3% was reached using $\text{SnO}_2\text{-TiO}_2/\text{SiO}_2$ catalyst (15). Also, $\text{SnO}_2/\text{SiO}_2$ solid exhibited higher catalytic activity, giving a conversion of 81.6%. The sulphated tin (IV) oxide is one of the promising candidates for exhibiting the strongest acidity on the surface (14). The use of tin catalyst (i.e. metal oxide, anchored or supported metal compounds) has assumed higher position on

biodiesel production, because they are cheaper than zirconium catalyst and equally active in FFA esterification or TG transesterification reaction (16). In this study, Sulphated Tin Oxide was synthesized and used.

2.0 MATERIALS AND METHODS

2.1 Optimisation of biodiesel transesterification process variables

A central composite design is initially employed to determine which factors affect the biodiesel yield. Subsequent designs focus on determining the optimum conditions for producing biodiesel from this feedstock. Three factors are considered for the initial design and are listed below;

1. Temperature (A)
2. Methanol to Oil ratio (B)
3. catalyst loading (C)

A total of 20 experiments were designed using the central composite design (CCD), and a polynomial regression equation was developed, the Central Composite Design was used to analyse the factor interactions by identifying the significant factors contributing to the regression model. The yield was taken as the response, three parameters (temperature, methanol to oil ratio and catalyst loading) were used as variables for the design of the experimental matrix, and each of the variables was studied at two levels 'low' and 'high'. The statistical software (Design Expert 6.0.6) was used to design and analyse the biodiesel production process experiments. The levels and ranges of the studied factors are presented in Table 1.

Table 1: Experimental ranges and levels of the factors used in the design of the transesterification of Bushel Kentucky seed oil.

	Name of the parameter	Units	Low	High
A	Temperature	$^{\circ}\text{C}$	45	60
B	Methanol to oil ratio		3	8
C	Catalyst loading	wt%	1.5	3

Table 2. Factorial design matrix for the transesterification of bushel Kentucky calabash seed oil

Std	Run	Block	Temperature ($^{\circ}\text{C}$)	Methanol to Oil	Catalyst loading wt%	Yield (%)
5	1	Block 1	45.00	3.00	3.00	
19	2	Block1	52.50	5.50	2.25	
15	3	Block1	52.50	5.50	2.25	
10	4	Block1	65.11	5.50	2.25	



3	5	Block1	45.00	8.00	1.50
16	6	Block1	52.50	5.50	2.25
1	7	Block1	45.00	3.00	1.50
7	8	Block1	45.00	8.00	3.00
6	9	Block1	60.00	3.00	3.00
12	10	Block1	52.50	1.30	2.25
17	11	Block1	52.50	5.50	2.25
2	12	Block1	52.50	1.30	2.25
18	13	Block1	52.50	5.50	2.25
20	14	Block1	52.50	5.50	2.25
13	15	Block1	52.50	5.50	0.99
9	16	Block1	39.89	5.50	2.25
4	17	Block1	60.00	8.00	1.50
8	18	Block1	60.00	8.00	3.00
14	19	Block1	52.50	5.50	3.51
11	20	Block1	52.50	3.0	1.50

2.2 Ester Content Characterization

Upon establishing the optimum conditions, the oil produced at the optimum conditions was characterized for fatty acid methyl ester using GC-MS (Agilent 19091S-433UI) and other properties were also measured by the standard methods to confirm that the biodiesel produced had comparable properties with ASTM D 6751-02 standard B100.

3.0 RESULT AND DISCUSSION

Table 3. The optimum yield of fatty Acid methyl ester from the production



PEAK NO	NAME OF COMPOUND	MOLECULAR FORMULAR	PEAK AREA	%
1	Methyl 14 Methylpentadecanoate	C17H34O2	2.188	
2	Methyl decanoate	C11H22O2	1.094	
3	Methyl 15- methyl hexadecanoate	C18H36O2	2.248	
4	Methyl tridecanoate	C14H28O2	1.094	
6	Methyl trans,trans-9-octadecadienoate	C19H34O2	26.87	
7	Methyl heptacosanoate	C28H56O2	1.154	
8	Methyl eicosanoate	C21H42O2	1.154	
9	Methyl decosanoate	C23H46O2	1.154	
10	Methyl decanoate	C11H22O2	1.154	
11	Methyl (11E) -11- octadecenoate	C19H36O2	21.74	
12	Methyl (15E)-15- methyl tetracosonoate	C25H48O2	0.814	
13	Methyl 5-undecylcyclopropyl)pentanoate	C20H38O2	0.914	
14	Methyl(15Z)-15-tetracosenoate	C21H38O2	0.31	
15	Methyl 10- undecanoate	C12H22O2	20.616	
16	Methyl 8-(2-hexylcyclopropyl)octanoate	C20H38O2	10.308	
17	Methyl (7E) -7- nonenoate	C10H18O2	0.294	
18	Methyl (13E)-13- decosanoate	C23H44O2	0.604	
19	Methyl 13- teradecynoate	C15H26O2	0.10	
20	Methyl 12-(2-octylcyclopropyl)dodecanoate	C24H46O2	0.10	
FAME YIELD			93.91	

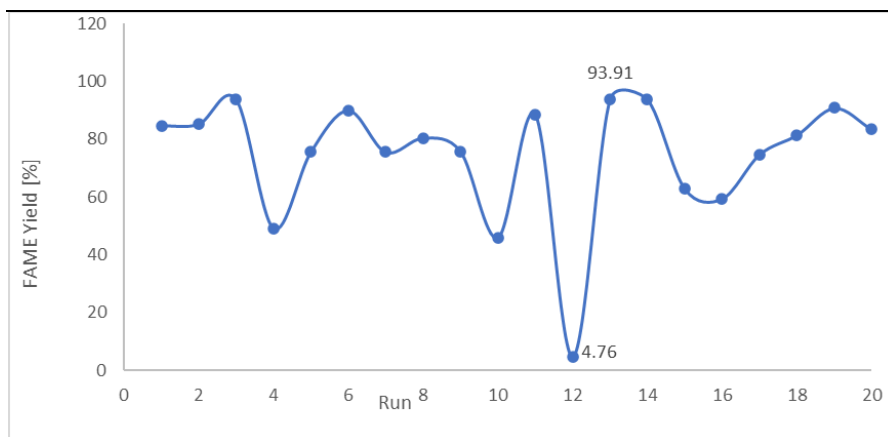


Fig. 1. A plot of FAME yield of each run for biodiesel produced from bushel Kentucky seed oil

3.1 Analysis of variance (ANOVA) for the yield of biodiesel

The ANOVA result (Table 3) shows that the biodiesel production parameters having a p-value less than 0.05 are considered significant for the percentage oil yield response factor. The insignificant factors were screened out from the model equation. Table 3 shows that the reaction

temperature (A), methanol to oil ratio (B) and catalyst concentration (C), also the interaction terms (AB, AC, BC) and the quadratic terms (A^2 , and C^2) are all signs that is they played a significant role on the yield of the biodiesel while B^2 is insignificant because they have p values greater than 0.05. The value of the square of the coefficient of regression (R^2) of the model as shown in Table 4 is 0.9897 suggesting the accuracy of the model



because the closer the value is to 1 the better the model.

Table 4 Analysis of variance (ANOVA) for the yield of biodiesel

Source	Sum of squares	DF	Mean square	F value	Pro>F	
Model	2308.67	9	256.52	107.17	<0.0001	Significant
A	370.40	1	370.49	154.79	<0.0001	
B	66.08	1	66.08	27.61	0.0004	
C	581.00	1	581.00	242.74	<0.0001	
A2	1073.15	1	1073.15	448.36	<0.0001	
B2	8.00	1	8.00	3.34	0.0974	
C2	191.39	1	191.39	79.96	<0.0001	
AB	21.13	1	21.13	8.83	0.0140	
AC	15.68	1	15.68	6.55	0.0284	
BC	66.13	1	66.13	27.63	0.0004	
Residual	23.93	10	2.39			
Lack of fit	19.35	5	3.87	4.23	0.0699	Not Significant
Pure error	4.58	5	0.92			
Cor total	2332.61	19				

Table 5. Model summary statistics for the oil yield

Std.Dev	1.55	R-Squared	0.9897
Mean	85.63	Adj.R-Squared	0.9805
C.V.	1.81	Pred.R.Squared	0.9338
PRESS	154.48	Adeq. Precision	31.774

Similarly, the Predicted R^2 of 0.9338 is in reasonable agreement with the Adjusted R^2 of 0.9805; i.e. the difference is less than 0.2. Adequate Precision measures the signal to noise ratio. A ratio greater than 4 is desirable. Hence the obtained ratio of 31.774 indicates an adequate signal. This model can be used to navigate the design space (Design-Expert version 6.0)

3.2 Predicted and actual plot for the oil yield optimization

A graph of the observed (actual) response values versus the predicted response values help to detect a value, or group of values, that are not easily

predicted by the model. The data points should be split evenly by the 45-degree line, according to design Expert version 6.0.

Figure 2 Diagnostic Plot of Predicted versus Actual Yield for RSC Model, selected Diagnostic test was being carried out from which figure 2 was been represent for the predicted values and actual (or experimental) values. This plot graphically shows that there is good agreement between predicted values and actual (or experimental) values which confirms the response surface cubic (RSC) model fit well.



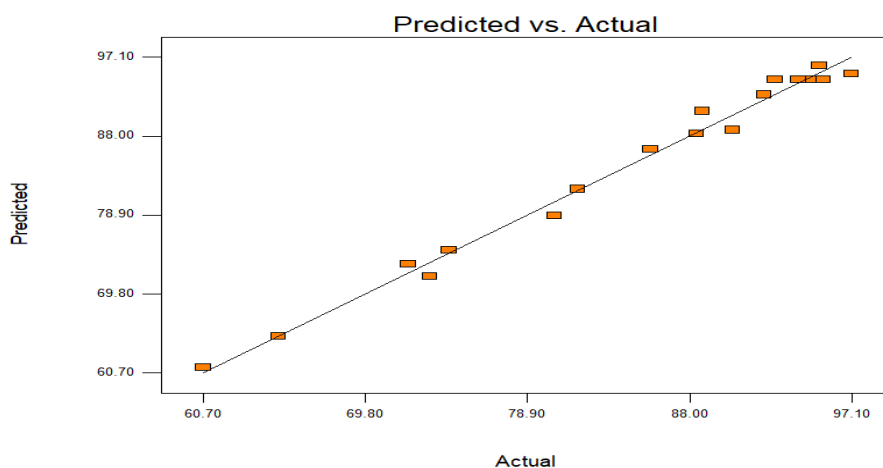


Fig. 2. Predicted vs. actual plot for biodiesel yield

Table 6. Optimization conditions

Name	Goal	Lower limit	Upper Limit
Temperature	Is in range	45	60
Methanol to Oil	Is in range	3	8
Catalyst	Is in range	1.5	3
Yield	Maximize	60.7	97.1

Table 7. The fifteen possible solutions found from the criteria set are presented.

Number	Temperature	Methanol to Oil	Catalyst	Yield	Desirability
1	50.47	7.60	2.88	97.5614	1.000
2	50.34	4.29	2.93	97.658	1.000
3	48.15	7.38	2.60	97.4483	1.000
4	49.51	7.07	2.41	97.4329	1.000
5	49.65	6.56	2.82	97.8362	1.000
6	48.98	7.46	2.34	97.3222	1.000
7	50.22	7.33	2.94	97.4587	1.000
8	50.41	7.20	2.97	97.428	0.999
9	48.38	7.85	2.47	97.6124	1.000
10	49.25	6.07	2.72	97.6502	1.000
11	51.59	5.01	2.78	97.6064	0.997
12	50.01	7.63	2.88	97.5558	0.989
13	50.20	6.33	2.73	97.9196	1.000
14	48.66	7.68	2.31	97.232	1.000
15	50.48	7.90	2.75	97.7823	1.000

The optimization results were randomly selected for verification in the laboratory and the result obtained is as shown in Table 8.

Table 8. Validation Table

Run	Yield %
-----	---------



	Temperature °C	Methanol to oil ratio	Catalyst concentration wt. %	Predicted	Actual
1	50.47	7.60	2.88	97.5614	97.5341
13	50.20	6.33	2.73	97.9196	97.908
4	49.51	7.07	2.41	97.4329	97.2319
5	49.65	6.56	2.82	97.8362	97.9132
2	50.34	4.29	2.93	97.658	97.5822

Therefore, from the result obtained as presented in Table 8. the optimized parameters are: reaction temperature (49.65 °C), Methanol: oil (6.56) and catalyst concentration (2.82wt.%).

4.0 CONCLUSION

The optimization was carried out using RSM in which statistical model equation was developed, which gives a binomial statistical model (BSM) to be:

$$\text{Yield} = +94.52 - 5.2 * A + 2.2 * B + 6.52 * C - 8.63 * A^2 - 3.64 * C^2 - 1.62 * A * B + 1.40 * A * C - 2.88 * B * C$$

The optimum solution obtained at the end of the numerical optimization for the biodiesel production was found to be temperature of 49.65 °C ratio (M/O) of 6.56 and catalyst of 2.82wt.%, which give us an optimum yield of 97.9132 % based on the constraints and the objective set for the optimization studies in which validation experiment confirms that the deduction obtained from numerical optimization studies for the yield as 97.9132 % was close to that which was obtained from the experiment as 97.1% given an error of 0.8132%.

The FAME was found to be temperature of 52.50°C ratio (M/O) of 5.50 and catalyst of 2.28wt.% which give us an optimum yield of FAME to be 93.91%.

REFERENCES

1. B. Garba, A. Bashir, Managing energy resources in Nigeria: studies on energy consumption pattern in selected rural areas in Sokoto state. *Nigerian Journal of Renewable Energy* **10**, 97-107 (2002).
2. N. K. Sahoo, A. Kumar, S. Sharma, S. Naik, in *Proceeding of International Conference on Energy and Environment*. ISSN. (2009), pp. 2070-3740.
3. F. Ma, M. A. Hanna, Biodiesel production: a review. *Bioresource technology* **70**, 1-15 (1999).
4. M. Agarwal, K. Singh, S. Upadhyaya, S. Chaurasia, in *Proceedings of the Chemeca*. (Citeseer, 2011).
5. D. K. Kuwornoo, J. C. Ahiekpor, Optimization of factors affecting the production of biodiesel from crude palm kernel oil and ethanol. *Journal homepage: www IJEE IEEFoundation org* **1**, 675-682 (2010).
6. I. Atadashi, M. K. Aroua, A. A. Aziz, N. Sulaiman, Production of biodiesel using high free fatty acid feedstocks. *Renewable and sustainable energy reviews* **16**, 3275-3285 (2012).
7. N. S. Talha, S. Sulaiman, Overview of catalysts in biodiesel production. *ARPN Journal of Engineering and Applied Sciences* **11**, 439-442 (2016).
8. R. Wang *et al.*, Biodiesel production from *Stauntonia chinensis* seed oil (waste from food processing): Heterogeneous catalysis by modified calcite, biodiesel purification, and fuel properties. *Industrial Crops and Products* **62**, 8-13 (2014).
9. P. Verma, M. Sharma, Performance and emission characteristics of biodiesel fuelled diesel engines. *International Journal of Renewable Energy Research* **5**, 245-250 (2015).
10. M. Mukhtar, C. Muhammad, M. U. Dabai, M. Mamuda, Ethanolysis of calabash (*Lageneria sinceraria*) seed oil for the production of biodiesel. *American Journal of Energy Engineering* **2**, 141-145 (2014).



11. H. Ibrahim *et al.*, Production of biodiesel from calabash seed oil. *American Chemical Science Journal* **14**, 1-8 (2016).
12. T. F. Edgar, D. M. Himmelblau, L. S. Lasdon, Optimization of chemical processes. (*No Title*), (2001).
13. A. A. Dabbawala, D. K. Mishra, J.-S. Hwang, Sulfated tin oxide as an efficient solid acid catalyst for liquid phase selective dehydration of sorbitol to isosorbide. *Catalysis Communications* **42**, 1-5 (2013).
14. R. Varala *et al.*, Sulfated tin oxide (STO)–Structural properties and application in catalysis: A review. *Arabian Journal of Chemistry* **9**, 550-573 (2016).
15. W. Xie, H. Wang, H. Li, Silica-supported tin oxides as heterogeneous acid catalysts for transesterification of soybean oil with methanol. *Industrial & Engineering Chemistry Research* **51**, 225-231 (2012).
16. M. K. Lam, K. T. Lee, A. R. Mohamed, Sulfated tin oxide as solid superacid catalyst for transesterification of waste cooking oil: an optimization study. *Applied Catalysis B: Environmental* **93**, 134-139 (2009).



P018 - PROCESSES OF ENERGY CONVERSION, TRANSFORMATION AND SOCIO-ECONOMIC UTILIZATION OF AGRO-WASTES TO BRIQUETTES: A COMPREHENSIVE REVIEW

Saidu Hassan Musa*¹, Nasir Fagge Isa¹, Haruna Musa¹, Adam Salihu Alhassan¹ and Umar Aliyu Ahmed¹

¹Center for Renewable Energy Research: Bayero University, Kano.

*Corresponding author: shmusa.crer@buk.edu.ng

ABSTRACT

Efficient utilization of enormous agro-residues resource is crucial for providing bioenergy, reducing environmental pollution, and increasing farmers' income. At present, direct combustion of agricultural residues for the purpose of biomass energy, particularly in rural areas, which leads higher pollution. Biomass can be relatively easily stored and transported compared with other types of renewable energy sources. Agricultural wastes can be converted into densified solid biofuel via briquette fuel technology to expand its possible applications and enhance its utilization efficiency as solid fuel. However, the potential economic, environmental and social impact of agricultural residues briquette fuel has been assessed for its large-scale use. This paper reviews the key aspects of the utilization of agricultural residues as important sources of renewable energy. The paper provides some essential background information on socio-economic utilization of agricultural residues. These wastes are commonly left piled in the field to decompose or burn in open fires which consequently provide risks to the environment as well as animal and human health. The bio-briquettes product is suitable as an energy source commonly used for electricity generation, heat, and cooking fuel. They are the perfect replacement for wood logs.

KEYWORDS

Agro-residues, solid biofuels, briquettes, renewable energy, biomass and bioenergy.

1.0 INTRODUCTION

The energy demand of developing countries is continuously increasing due to a variety of factors, such as population. The global and domestic energy sectors have both grown significantly in recent years. The energy consumption pattern of any country is an indicator of its socio-economic status (1). The generation of agro-waste for commercial, agricultural and industrial sectors is on the increase, especially with current population growth and industrialization (2). This waste is a source of biomass that can be used to produce various liquid and solid biofuels to address energy, environmental as well as socioeconomic challenges facing many communities in developing countries (3-5). Among the fuels that can be produced from agro-waste is briquette, whose energy is tapped through direct burning for cooking and other applications (6, 7). Clean and efficient energy derived from agricultural residues will improve access to energy for rural isolated households, improve indoor air quality, and contribute to rural development by increasing household income (8). This economic, environmental, and social context promotes the use of efficient and modern technologies for biomass

energy conversion of agricultural residues. One of the main technologies is biomass briquetting technology which converts loose agricultural residues to densified solid biofuel. The briquetting technology improves the characteristics of agro-residues for transportation, storage, feeding into furnaces, and combustion (9). More recently, and particularly in Africa, briquetting has been motivated by a desire to mitigate energy loss, air pollution and greenhouse gas emissions associated with inefficient burning or disposal of biomass residues. The growing interest in briquettes increasingly reflects concerns with the unsustainability of traditional, forest-based wood charcoal production systems and the imminent need for alternative fuels. However, the development of these technologies must be viable economically and environmentally to ensure sustainability. In this perspective therefore, the question lies on whether the technologies of briquetting are able to overcome economic challenges especially those affecting small-medium entrepreneurs (2). It is imperative to fulfil the growing energy requirements to meet the expected future global energy demand for economic development to drive the briquetting by SMEs to



create employment opportunities in Africa (10). However, at the same time, our society is currently facing the need to reduce its dependency on fossil fuels since there are recognized concerns regarding environmental and human health issues triggered by their excessive use, such as atmospheric pollution, respiratory disorders, and climate change driven by the release of greenhouse gases (GHG) (11). Briquette can be used especially in areas where modern cooking fuels for domestic and commercial applications are not readily available. Briquette comes in different forms, qualities and efficiency, depending on the source of biomass used and briquetting technology employed (12).

The issue of agro-waste generation has become an increasing concern in the recent years due to their significant role in causing various environmental problems (13). Agro-waste as the non-product outputs of production and processing of products such as fruits, vegetables, meat, poultry, dairy products and crops, whose value is less than the cost of collection, transportation and processing for beneficial use. Agro-waste is generated in huge amount, and millions of tons of this organic and biodegradable resource are wasted every year (14). The production of biofuels such as briquette from this abundant biomass is therefore an alternative approach towards sustainable management of this resource (5).

Briquetting is the process of converting low bulk density biomass into high density and energy-concentrated fuel. Literally, briquetting means biomass densification, in which a mechanical pressure is used to reduce the volume of agricultural residue and convert it to a solid form to make it easier for handling and storage. Historically, the rationale for producing briquettes was primarily economic, i.e., to reclaim unused waste and convert it to solid fuel that can be transported over long distances. The first known patents for briquetting technology were reported in the mid-1800s in USA, when the hike on the prices of coal required efficient use of waste products from mining. Briquettes have numerous applications ranging from domestic use for cooking and heating to space heating in the poultry industry. Briquette has been described to be one of the most efficient sources of energy (15). It can be produced from almost all agricultural waste, though the residues that are readily available with low moisture content (10 – 15%) are considered for use. Briquettes are produced using various technologies, including screw-press and piston-press methods. The

production process involves collection of feedstock, drying, grinding, sieving, compacting and cooling (16).

1.1 Agro-Waste as Feedstock for Briquette Production

Briquettes from banana waste and subjected them to thermogravimetric and combustion analyses and mechanical ability to determine the effects of mixing ratio. Briquette with higher banana leaves and banana pseudostem ratio was considered the best as it met all the standard values adhering to the characterization methods, thus describing it as competitive with other types of briquettes in terms of their strength and storage ability (17).

Analyzing the ability of the Spent Coffee Grounds (SCG) for briquettes production based on the use of xanthan gum as binder under low-pressure and low-temperature. Briquettes produced from the raw SCG showed low durability against handling, storage and feeding. However, the combinations containing 10% of xanthan gum produced briquettes that reached required commercial dry densities and showed low water absorption capacity and high durability (18).

Banana leaves, pseudo stem, and rice husk were prepared and characterized using proximate and ultimate chemical analyses, thermogravimetric analysis (TGA), high heating value (HHV) and differential scanning calorimetry (DSC). The waste was compacted into briquettes using hydraulic press and characterized again using the same analytical procedures. It was found that the briquettes exhibited the maximum energy release under combustion at temperatures that were lower than that of the waste (19).

The briquetting characteristics of woody and herbaceous biomass blends, including lodge pole pine, switch grass, and corn stover biomass. Briquette properties such as unit and bulk density, durability rating after 5 days of storage and the energy consumption of the process were determined. It was found that the blend moisture content affected the quality of the briquette produced; the durability of the briquettes increased with a corresponding increase in hammer mill screen size to 12.7 mm; energy consumption of the briquetting process was strongly dependent on hammer mill screen size and moisture contents of the blend; the chemical composition and energy properties of briquettes were improved after blending pine with switch grass and corn stover;



and the briquettes produced using lodge pole pine /switch grass / corn stover blends resulted in briquette quality that meets the CEN and ISO standards in terms of the physical properties (i.e., length, diameter, and durability rating values) and ash content (20).

The characterization of briquettes made from different residual concentrations of sugar bagasse and straw, where resistance and friability were determined. Lower ash and higher fixed carbon content in bagasse made it a suitable feedstock for briquette production. However, briquettes produced using both residues of sugar bagasse and straw showed feasible results, suggesting the use of blends as a viable alternative (21).

Assessing the use of agro-wastes in the production of charcoal briquette blend as source of clean energy by mixing varying compositions of carbonized biomass (cassava stem charcoal) and uncarbonized biomasses (pawpaw straw and cashew leaves) at the ratios of 0:100, 20:80, 80:20 and 100:0 using cassava starch as binder. The study found that the briquettes produced have desirable characteristics to produce fuel for cooking as they could easily be moulded, and were inflammable with low amount of smoke (22).

The used corn cobs, which is one of the most ubiquitous agro- waste, to produce briquette charcoal using locally fabricated metal kiln and locally sourced tapioca starch was used as binder at concentrations of 6.0, 10.0, 14.0 and 19.0 % w/w. The briquette charcoal was found to be a better fuel when compared to both sugarcane bagasse and wood charcoal, having a highest fixed carbon content and highest bulk density (23).

1.2 Briquetting Methods

Screw Extrusion Briquetting: This method involves forcing the raw material through a tapered die using a screw press, which generates heat and pressure, leading to the formation of briquettes and is widely used due to its simplicity, high production capacity and ability to handle various biomass feedstock (24).

Roller Press Briquetting: A roller press is used to compact the raw material into briquettes by applying high pressure between two rotating rolls. Binders can be added to improve briquette strength and it requires higher investment costs and expertise compared to other methods (25).

Piston Press Briquetting: In this method, a reciprocating piston compresses the raw material into a die to form briquettes. The pressure is applied by the movement of the piston thereby having slower production rate compared to screw extrusion method (26).

Binderless Briquetting: This approach involves compacting raw materials under high pressure without the use of binders. The inherent lignin content in some biomass materials acts as a natural binder, thus require higher pressure and specialized briquetting equipment (27).

Hydraulic Press Briquetting: Hydraulic presses are used to apply pressure on the raw material, typically with a hydraulic cylinder. This method is suitable for producing larger briquettes. Its low versatility, low energy consumption and minimal waste production makes it popular choice for industries and individuals looking for sustainable waste management solutions (28).

Pillow-shaped Briquetting: This technique forms briquettes with a distinctive pillow shape using a specially designed press. It is commonly used for producing charcoal briquettes. This method is easy handling, uniform size and lower production costs make it a popular choice for small scale producers and individuals.

1.3 Socio-economic Relevance of Briquettes

Briquettes, which are compacted and densified forms of biomass or other materials, have gained significant socio-economic importance due to their various benefits and applications. Here are some of the socio-economic advantages of briquettes.

Energy Access and Poverty Alleviation: Briquettes can serve as an affordable and accessible source of energy for communities that lack access to modern energy sources like electricity or clean cooking fuels. They can contribute to poverty alleviation by reducing the energy expenditures of households thereby improving their quality of life. Briquettes can provide an affordable and accessible energy source for communities with limited access to conventional fuels like coal or gas. This is particularly important in developing countries where energy poverty is prevalent. A study by Omer, (2005) (29) discusses the potential of briquettes to address energy poverty and enhance energy access.

Waste Management and Pollution Reduction: The use of briquettes encourages the collection and



utilization of agricultural waste materials that might otherwise be discarded or burned, causing pollution. By converting these waste materials into useful energy sources, briquettes help mitigate pollution and promote waste management. Briquettes offer an effective way to manage agricultural and forestry residues, converting them into a valuable energy resource. This helps reduce waste accumulation, mitigating environmental pollution and improving the overall cleanliness of rural areas. A study highlighted the potential of briquettes in waste management and resource utilization thereby reducing wastes in the environment (30).

Environmental Sustainability: Briquettes are often produced using biomass waste in order to reduce the burden on natural resources like forests and abstain from hazardous fossil fuels. This contributes to environmental sustainability by reducing deforestation, minimizing greenhouse gas emissions (GHG), and lowering the overall carbon footprint (31). Briquettes, when produced from sustainable biomass sources, can be considered a carbon-neutral energy source. They contribute to greenhouse gas emission reduction by replacing fossil fuels in various applications (32).

Rural Development and Employment Generation: The production and distribution of briquettes can create employment opportunities, particularly in rural areas where biomass resources are abundant. This can contribute to local economic development and improve livelihoods (33). The collection, processing, and manufacturing of briquettes involve various labour-intensive tasks, thereby contributing to employment generation. According to a study by Briquette production can provide employment opportunities for local communities and promote sustainable rural development (34). The production and distribution of briquettes can create employment opportunities, especially in rural areas. This boosts local economies and helps in poverty reduction by providing income-generating activities for communities (35).

Indoor Air Pollution Reduction: Briquettes, as an alternative energy source for clean cooking, can replace traditional solid fuels such as wood and dung, which are major contributors to indoor air pollution. This can lead to improved health outcomes, particularly for women and children who often spend significant time indoors. The use of briquettes produces less smoke and harmful emissions, thereby improving indoor air quality and public health (36).

1.4 Challenges and Future Prospects

Briquettes offer numerous environmental and economic benefits, including reduced greenhouse gas emissions and waste diversion. However, there are several challenges are availability and cost of raw materials, technical skills, equipment, market and government regulations associated with the production, adoption, and long-term viability. Briquettes offer promising benefits as an alternative fuel source, addressing challenges related to feedstock availability, technology, economics, and consumer acceptance will be crucial for their successful integration into the energy landscape. The future prospects of briquettes lie in technological advancements, policy support, and their role in contributing to sustainable development goals (37).

2.0 CONCLUSION

In conclusion this review lies in its comprehensiveness in the exploration of the technical, environmental, and socioeconomic aspects of converting agro-wastes into briquettes for energy generation. Briquettes as a cooking fuel can have several economic advantages over conventional fuels such as firewood, charcoal, or LPG (liquefied petroleum gas). Some economic arguments in favor of briquettes are cost effectiveness, efficiency, job security, energy security. Economic benefits of briquettes vary depending on local conditions, including the availability of raw materials, the efficiency of production processes, and market dynamics. Thus, it provides valuable insights into the viability and potential impact of this renewable energy solution.

3.0 REFERENCES

1. B. V. Bot, P. J. Axaopoulos, E. I. Sakellariou, O. T. Sosso, J. G. Tamba, Energetic and economic analysis of biomass briquettes production from agricultural residues. *Applied Energy* **321**, 119430 (2022).
2. T. H. Mwampamba, M. Owen, M. Pigaht, Opportunities, challenges and way forward for the charcoal briquette industry in Sub-Saharan Africa. *Energy for Sustainable Development* **17**, 158-170 (2013).



3. T. Bridgwater, Biomass for energy. *Journal of the Science of Food and Agriculture* **86**, 1755-1768 (2006).
4. I. E. Onukak, I. A. Mohammed-Dabo, A. O. Ameh, S. I. Okoduwa, O. O. Fasanya, Production and characterization of biomass briquettes from tannery solid waste. *Recycling* **2**, 17 (2017).
5. H. M. Marreiro *et al.*, Empirical studies on biomass briquette production: A literature review. *Energies* **14**, 8320 (2021).
6. S. Khlifi *et al.*, Briquettes production from olive mill waste under optimal temperature and pressure conditions: Physico-chemical and mechanical characterizations. *Energies* **13**, 1214 (2020).
7. M. O. Okwu, O. D. Samuel, Adapted hyacinth briquetting machine for mass production of briquettes. *Energy Sources, Part A: Recovery, Utilization, and Environmental Effects* **40**, 2853-2866 (2018).
8. A. K. Tripathi, P. Iyer, T. C. Kandpal, A techno-economic evaluation of biomass briquetting in India. *Biomass and bioenergy* **14**, 479-488 (1998).
9. J. Werther, M. Saenger, E.-U. Hartge, T. Ogada, Z. Siagi, Combustion of agricultural residues. *Progress in energy and combustion science* **26**, 1-27 (2000).
10. P. Nkala, University of Natural Resources and Life Sciences, (2011).
11. D. Soeder, S. Borglum, Part II the future of fossil fuels. *The Fossil Fuel Revolution: Shale Gas and Tight Oil*, 173-174 (2020).
12. B. Asamoah, J. Nikiema, S. Gebrezgabher, E. Odonkor, M. Njenga, A review on production, marketing and use of fuel briquettes. (2016).
13. Z. Zhang, A. M. Gonzalez, E. G. Davies, Y. Liu, Agricultural wastes. *Water Environment Research* **84**, 1386-1406 (2012).
14. F. Obi, B. Ugwuishiwu, J. Nwakaire, Agricultural waste concept, generation, utilization and management. *Nigerian Journal of Technology* **35**, 957-964-957-964 (2016).
15. U. Arachchige, Briquettes production as an alternative fuel. *Nature Environment and Pollution Technology* **20**, 1661-1668 (2021).
16. A. Hamzat, S. Y. Gombe, Y. Pindiga, Briquette from Agricultural Waste a Sustainable Domestic Cooking Energy. *Gombe Technical Education Journal* **12**, 63-69 (2019).
17. K. K. Ahmad, K. Sazali, A. Kamarolzaman, Characterization of fuel briquettes from banana tree waste. *Materials Today: Proceedings* **5**, 21744-21752 (2018).
18. A. Seco, S. Espuelas, S. Marcelino, A. Echeverría, E. Prieto, Characterization of biomass briquettes from spent coffee grounds and xanthan gum using low pressure and temperature. *BioEnergy research* **13**, 369-377 (2020).
19. B. G. de Oliveira Maia *et al.*, Characterization and production of banana crop and rice processing waste briquettes. *Environmental Progress & Sustainable Energy* **37**, 1266-1273 (2018).
20. J. S. Tumuluru, E. Fillerup, Briquetting characteristics of woody and herbaceous biomass blends: Impact on physical properties, chemical composition, and calorific value. *Biofuels, Bioproducts and Biorefining* **14**, 1105-1124 (2020).
21. L. S. Masullo *et al.*, Use of blends containing different proportions of straw and sugarcane bagasse for the production of briquettes. *REVISTA VIRTUAL DE QUIMICA* **10**, 641-654 (2018).
22. C. Nwankwo, T. Onuegbu, I. Okafor, P. Igwenagu, in *IOP Conference Series: Earth and Environmental Science*. (IOP Publishing, 2023), vol. 1178, pp. 012015.
23. A. Zubairu, S. A. Gana, Production and characterization of briquette charcoal by carbonization of agro-waste. *Energy Power* **4**, 41-47 (2014).
24. R. Saidur, E. Abdelaziz, A. Demirbas, M. Hossain, S. Mekhilef, A review on biomass as a fuel for boilers. *Renewable and*



- sustainable energy reviews* **15**, 2262-2289 (2011).
25. t. D. Taulbee, D. Patil, R. Q. Honaker, B. Parekh, Briquetting of coal fines and sawdust Part I: Binder and briquetting-parameters evaluations. *International journal of coal preparation and utilization* **29**, 1-22 (2009).
 26. S. Zinchik, Michigan Technological University, (2019).
 27. S. Yaman, Pyrolysis of biomass to produce fuels and chemical feedstocks. *Energy conversion and management* **45**, 651-671 (2004).
 28. N. Kaliyan, R. V. Morey, Factors affecting strength and durability of densified biomass products. *Biomass and bioenergy* **33**, 337-359 (2009).
 29. A. M. Omer, Biomass energy potential and future prospect in Sudan. *Renewable and Sustainable Energy Reviews* **9**, 1-27 (2005).
 30. J. Skvaril, K. G. Kyprianidis, E. Dahlquist, Applications of near-infrared spectroscopy (NIRS) in biomass energy conversion processes: A review. *Applied Spectroscopy Reviews* **52**, 675-728 (2017).
 31. R. Piloto-Rodríguez *et al.*, An approach to the use of *Jatropha curcas* by-products as energy source in agroindustry. *Energy Sources, Part A: Recovery, Utilization, and Environmental Effects*, 1-21 (2020).
 32. X. Zhu, Y. Zhang, W. Zhao, Differences in environmental information acquisition from urban green—a case study of qunli national wetland park in Harbin, China. *Sustainability* **12**, 8128 (2020).
 33. S. Y. Kpalo, M. F. Zainuddin, L. A. Manaf, A. M. Roslan, A review of technical and economic aspects of biomass briquetting. *Sustainability* **12**, 4609 (2020).
 34. A. Taghizadeh-Alisaraei, S. H. Hosseini, B. Ghobadian, A. Motevali, Biofuel production from citrus wastes: A feasibility study in Iran. *Renewable and Sustainable Energy Reviews* **69**, 1100-1112 (2017).
 35. B. V. Bot, J. G. Tamba, O. T. Sosso, Assessment of biomass briquette energy potential from agricultural residues in Cameroon. *Biomass Conversion and Biorefinery*, 1-13 (2022).
 36. J. J. Jetter, P. Kariher, Solid-fuel household cook stoves: Characterization of performance and emissions. *Biomass and bioenergy* **33**, 294-305 (2009).
 37. R. M. Singh, BIOBRIQUETTING IN NEPAL-SCOPE AND POTENTIALS: A.



P20 - EVALUATION OF BIOETHANOL PRODUCTION POTENTIAL FROM GUINEA CORN HUSK USING *SACCHAROMYCES CEREVISIAE* AND *SACCHAROMYCES CARLBERGENSIS*

Yahaya, U^{1*}., Jauro, A.G¹ ., Suleiman, R.A²., Hussaini, Y¹., Maina, M.A¹., and Khidir, H.Y².

¹Federal College of Forest Resources management, Maiduguri, Borno- Nigeria.

²Forestry Research Institute of Nigeria

Corresponding author: usmanyahayaks@yahoo.com, +2348062247888

ABSTRACT

Issue of global warming is undisputedly recognized globally. Among the reasons for this condition is the rise in greenhouse gases. The research was conducted to generate bioethanol from Guinea corn husks. Guinea corn husks were pretreated with HCl (3%) at 50 °C, 40 °C, and 30 °C for 30, 25, and 20 min before fermentation with *S. cerevisiae* and *S. carlbergensis*. The outcome revealed that 47.3 % of reducing sugar was achieved from Guinea corn husk sawdust pre-treated at 40 °C for 20 minutes as the highest yield, whereas the minimum yield of 34.5% was attained at 30 °C for 30 min. The peak bioethanol concentration of 1.70% was achieved after 25 minutes when the hydrolysate was fermented by *S. cerevisiae* and *S. carlbergensis* in synergy. At 30 minutes, *S. cerevisiae* produced a minimum bioethanol concentration of 0.59% after 7 days of fermentation. The research suggested that the synergy of *S. cerevisiae* and *S. carlbergensis* may be a good combination for bioethanol generation from Guinea corn husks pretreated with HCl (3%) at 40°C.

Keywords: *HCl, Guinea corn husk, Bioethanol, Fermentation, Reducing sugar.*

1.0 INTRODUCTION

Universal energy demands, uncertainty over petroleum resources and fear of global climate change have led to researchers to look for a substitute to liquid fuels sourced from crude oil. Ethanol has continuously remained as a good high-quality fuel because it decreases dependency on crude oil and possibilities of cleaner ignition, resulting in an improved atmosphere. The development of ethanol as a biofuel beyond its recent role as an oxygenated fuel would necessitate the use of lignocellulose as a raw material because it is renewable, abundant and inexpensive. The biological properties of the lignocellulosic constituents make them of vast biotechnological value for the generation of inexpensive bioethanol fuel. In terms of cost, lignocellulose biomass is cheaper than starch and sugar crops, it is renewable and obtainable in enormous quantities. Cellulose is the main polymer constituent of plant material and the richest polysaccharide in the world.

Bioethanol refers to alcohol generated by fermentation of sugar constituents of renewable biomass from plant. Bioethanol is measured as a vital renewable fuel that can partially substitute

fossil fuels. Universal yield of bioethanol improved from 50 million m³ in 2007 to more than 100 million m³ in the year 2012. U.S and Brazil represent about 80% of the universal supply of bioethanol, mostly from sugar cane and cone. In emerging countries, food raw materials are rather substituted by non-food like sorghum or cassava. The practice of common biomass might expressively raise bioethanol production. Ethanol is produced in the industries via the acid-catalyzed hydration of ethylene. Ethanol aimed for usage in alcoholic drinks and the one that is used as biofuel are produced through fermentation, in which some species of yeast such as *Saccharomyces cerevisiae* or bacteria such as *Zymomonas mobilis* digest sugar under low-oxygen environments to Sugars in order to generate ethanol and carbon dioxide. The key reasons for the increased expansion of bioethanol production is because it is a cheaper and almost carbon-neutral renewable fuel, dropping CO₂ discharges and related climate alteration. Bioethanol serves as an octane booster in unleaded fuel; and its serves as an oxygenated fuel blend for cleaner burning of fuel. This reduces exhaust emissions and improves air quality.



Due to reserve depletion and challenging industrial desires for petrochemical raw materials, the global focus is on ethanol yield through fermentation processes. Higher produce of ethanol yield rest on the usage of a good bacteriological strain, suitable fermentation substrate and appropriate development technology. Therefore, this current research was conducted to use Guinea corn husk for the production of bioethanol.

2.0 METHODOLOGY

2.1 Sample collection and handling

Guinea corn husk (1 kg) was collected in fresh polyethylene container from local milling centers. The waste was pulverized and filtered by a filter (2mm). The sample was then kept at room temperature.

2.2 Biomass Pretreatment

Guinea corn husk (100g) was placed in a 2 liter Erlenmeyer container. 1 liter of 3% HCl was added to the Erlenmeyer container. The containers were protected with cotton wool, covered in aluminum foil, heated in a water bath at 50°C, 40°C, and 30°C for 30, 25, and 20 min, and autoclaved (121°C) for about 15 min. The containers were filtered with filter paper (No.1) and the pH was attuned to 4.5 using 0.4 M NaOH.

2.3 Reducing Sugar Determination

The reducing sugar content was determined using the colorimetric dinitrosalicylic acid method. 3 ml of 3,5-dinitrosalicylic acid (DNS) was added to 3 ml of each of the hydrolyzate sample. The combination was placed in a hot water bath for 10 min and a reddish-brown color was detected. Then, 1 ml of 40% potassium sodium tartrate solution was added to the mixture to stabilize the color, and the combination was ventilated to room temperature using running water. The absorbance of all the samples was taken using a UV-Vis spectrophotometer (491 nm). The reducing sugar was then measured using a normal curve of known glucose concentration.

2.4 *S. cerevisiae* and *S. carlsbergensis* Inoculation and Bioconversion of the Fermentable Sugars to Ethanol

Peptone water was added to the earlier purified hydrolyzate and the pH was attuned to 5.6 by adding 10% sulfuric acid. It is then autoclaved for 15 min at 121 °C to sterilize the medium, then 1.2 g of *S. cerevisiae* and *S. carlsbergensis* were inoculated aseptically into the fermentation medium at a proportion of 1:1. The setup was raised at 30 °C for 3 weeks. The fermented medium was aliquoted and distilled after 7, 14 and 21 days to determine the ethanol content.

2.5 Determination of Bioethanol Concentration

Bioethanol concentration was measured using quantitative UV-Vis analysis of alcohols using chromium(vi) reagent. One ml of standard ethanol was dissolved with 99 ml of purified water to give a concentration of 1%. 8ml, 6 ml, 4ml, 2ml, and 0 ml of the 1% ethanol, respectively, were diluted to 10 ml with purified water to yield 0.8 %, 0.6%, 0.4%, 0.2% and 0 % of the ethanol. To all of the different ethanol concentrations, 2 ml of chromium mixture was added and kept for one hour for colour change. Absorbance of all the concentrations was taken at 588 nm with a UV-VIS spectrophotometer and the measurements were used to get an ethanol curve. 4 ml of each bioethanol sample was placed in investigation tubes and treated with 2 ml of the chromium reagent. The combination was allowed to stand for one hour and the absorbance was taken at 588 nm using the UV-VIS spectrophotometer.

3.0 RESULT

3.1 Reducing sugar

Reducing the sugar produce from the hydrolysates after hydrolysis with 3% HCl at 50 °C, 40 °C and 30 °C for 30, 25 and 20 min is shown below (Figure 3.1). In 3% HCl, the maximum yield of 47.3% was attained from Guinea corn husks at 40 °C for 20 min, while the minimum yield of 34.5% was obtained from Guinea corn husks sawdust at 30 °C for 30 minutes (Fig. 3.1).



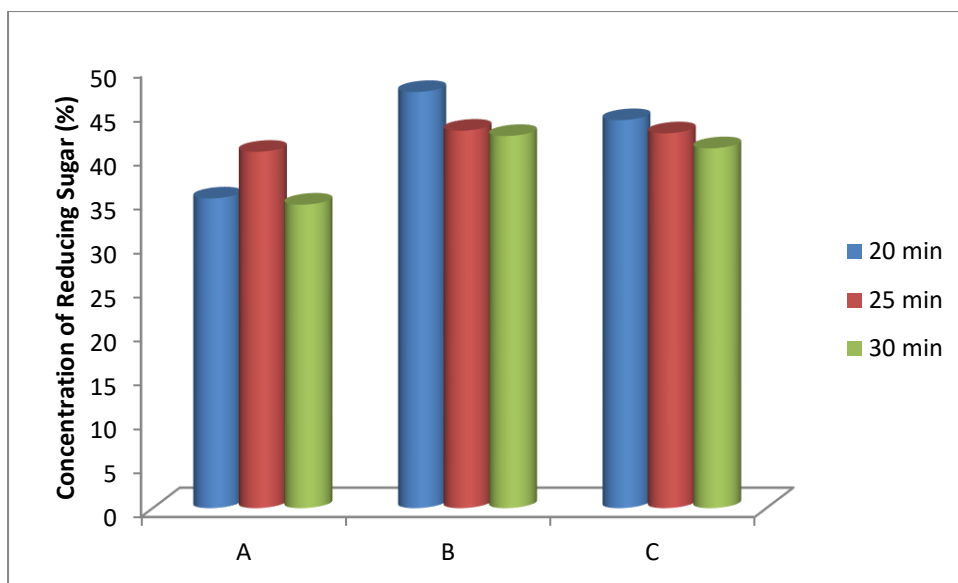


Figure 3.1: Reducing sugar produced from hydrolysates after hydrolysis with 3% HCl at 50 °C, 40 °C and 30 °C for 00, 25 and 20 min.

Key:

A: *Guinea corn husk* at 30°C

B: *Guinea corn husk* at 40°C

C: *Guinea corn husk* at 50°C

3.1 Concentration of bioethanol (%) from Guinea corn husks pretreated with 3% HCl at 40 °C for 00, 25 and 20 minutes using *S. cerevisiae*, *S. carlsbergensis* or consortium thereof.

Table 3.2 presents the concentration of bioethanol for a period of 3 weeks from Guinea corn husks pretreated with 3% HCl at 40 °C for 30, 25 and 20 min. using *S. cerevisiae* and *S. carlsbergensis*. The maximum bioethanol concentration (1.10%) was reached after 25 min. when the hydrolyzate of *S.*

cerevisiae and *S. carlsbergensis* was fermented after day 7, compared to other fermenting organisms. *S. cerevisiae* yielded the minimum concentration of 0.63% after 30 min. in day 7 of fermentation.

Table 3.1: Bioethanol Concentration (%) from Guinea corn husk pretreated with 3% HCl at 40°C for 30, 25 and 20 minutes using single and combined fermenting organism.

Organisms	Pretreatment time (min)	Fermentation days		
		7	14	21
<i>S. cerevisiae</i>	20	0.62 ^a ± 0.02	0.70 ^b ± 0.01	0.91 ^d ± 0.02
<i>S. carlsbergensis</i>	20	0.67 ^c ± 0.01	0.86 ^d ± 0.02	0.95 ^e ± 0.00
<i>S. cerevisiae</i> + <i>S. carlsbergensis</i>	20	1.03 ^f ± 0.00	0.91 ^f ± 0.03	0.85 ^c ± 0.03
<i>S. cerevisiae</i>	25	0.74 ^d ± 0.03	0.87 ^d ± 0.02	1.06 ^f ± 0.02
<i>S. carlsbergensis</i>	25	0.75 ^d ± 0.02	0.80 ^c ± 0.01	0.92 ^d ± 0.01
<i>S. cerevisiae</i> + <i>S. carlsbergensis</i>	25	1.70 ^g ± 0.00	0.90 ^e ± 0.01	0.83 ^b ± 0.02



<i>S. cerevisiae</i>	30	0.59 ^a ± 0.02	0.67 ^a ± 0.02	0.90 ^d ± 0.01
<i>S. carlsbergensis</i>	30	0.61 ^a ± 0.03	0.90 ^{ef} ± 0.01	0.93 ^c ± 0.02
<i>S. cerevisiae</i> + <i>S. carlsbergensis</i>	30	1.01 ^c ± 0.00	0.97 ^g ± 0.03	0.70 ^a ± 0.01

means in a column with different superscripts are significantly different ($p < 0.05$). Values are means ± standard deviation of three replicates.

4. DISCUSSION

As populace development increases, there is a consistent need aimed at energy resources, particularly from non-renewable forms. The prolong dependence on fossil fuel has led to the reduction of the reserve base and serious environmental dilapidation. This has led to the exploration for substitute and renewable energy sources. In this study, we investigated the production of bioethanol from Guinea corn husk waste. The hydrolysis results of the sawdust from Guinea corn husks pretreated with 3% HCl at 50 °C, 40 °C and 30 °C for 30, 25 and 20 min showed a maximum yield of reducing sugars, which is consistent with the results of Yahaya et al., 2017. These results showed a high occurrence of reducing sugars in Guinea corn husk when considering treatment time in relation to reducing sugar yield. Averagely, the maximum yield of 43.9% was achieved at 40 °C and a treatment time of 20 minutes. In order to guarantee effective biological conversion of lignocellulosic biomass, the collaboration among lignin and the polysaccharide constituents of the cell wall must be condensed via pretreatment, a procedure that is regarded as one of the vital steps in the process. Treating with dilute acid is among the most effective pretreatment means for lignocellulosic biomass. The treatment bids best performance in terms of recovery of hemicellulose sugars.

The maximum bioethanol concentration of 1.10% was reached after 25 min. when the hydrolyzate was fermented by *S. cerevisiae* and *S. carlsbergensis* in

REFERENCES

- i. B.C Saha. Dilute acid pretreatment, enzymatic saccharification and fermentation of wheat straw to ethanol. Process Biochemistry 40, 3693–3700 (2005)..
- ii. M.O Aiyejagbara. Production of bioethanol from elephant grass (*Pennisetum*

synergy. *S. cerevisiae* produced the minimum bioethanol concentration of 0.63% after 30 min. in 7 days of fermentation, which is greater than that of millet husk (0.11%) and bark of *E. tereticornis* (0.22%). The essential aspect of the fermentation is the choice of organism. The capacity to ferment pentoses together with hexoses is not widespread between organisms. *S. cerevisiae* is the best preferred organism for bioethanol production from hexoses owing to its great bioethanol tolerance, its ability to outcompete other yeasts, and its better resistance to contaminants and inhibitors from biomass.

5. CONCLUSION

This research was undertaken to investigate the ethanol yield of Guinea corn husks. The outcome reveals that dilute acid pretreatment can be used as a pretreatment alternative for liberating reducing sugar from lignocellulosic biomass such as guinea corn husk such as: B. Guinea corn husks could serve, which are abundant and do not compete with food materials. Bioconversion not only offers a cost-effective and safe method for disposing of agronomic and forestry remains, but similarly has the prospective to change lignocellulosic wastes into serviceable forms, like reducing sugars that can be used for ethanol production. Therefore, converting lignocellulosic waste

into biofuels (ethanol) can assist in the reduction of environmental contamination, contribute to mitigating greenhouse gas emissions, and help in sustainable waste management approach.

purpureum) stem. A thesis submitted to the school of postgraduate studies, Ahmadu Bello University, Zaria, Nigeria. (2015)

- iii. X. Liming, S. Xueling. (2004). High yield cellulose production by *Trichoderma reesei* Zu-on corn cob residue. Bioresour. Technol. 91, 259-262 (2004).



- the determination of reducing sugar, *Analytical Chem*, 31, 426 (1959).
- iv. Q. Kang, L. Appels, J. Baeyens, R. Dewil, T. Tan. "Energy efficient production of cassava-based bio-ethanol." *Advances in Bioscience and Biotechnology*, 5 (12), 925–939 (2014).
 - v. Q. Kang, L. Appels, J. Baeyens, R. Dewil, T. Tan. "Energy efficient production of cassava-based bio-ethanol." *Advances in Bioscience and Biotechnology*, 5 (12), 925–939 (2014).
 - vi. K. Qian, A. Lise, T. Tianwei, D. Raf. Bioethanol from Lignocellulosic Biomass: Current findings Determine Research Priorities. *The Scientific World Journal*, 10 (1155), 1-14 (2014).
 - vii. K. Qian, A. Lise, T. Tianwei, D. Raf. Bioethanol from Lignocellulosic Biomass: Current findings Determine Research Priorities. *The Scientific World Journal*, 10 (1155), 1-14 (2014).
 - viii. N. Ali, P. Ubhrani, M. Tagotra, M. Ahire . A Step Towards Environmental Waste Management And Sustainable Biofuel (Ethanol) Production From Waste Banana Peelings. *Ame. J. Eng. Res.* 3 (5), 110 – 116 (2014).
 - ix. M. Galbe, G. Zacchi. Pretreatment of lignocellulosic materials for efficient bioethanol production. *Adv. Biochem. Eng./Biotechnol.*, 108: 41–65 (2007).
 - x. C.N.Humphrey, U.O. Caritas. Optimization of ethanol production from *Garcinia kola* (bitter kola) pulp agro waste. *Afr. J. Biotechnol*, 6 (17), 2033-2037 (2007).
 - xi. G.L. Miller. Use of dinitrosalicylic acid reagent for the determination of reagent for
 - xii. A.A. Brooks. Ethanol production potential of local yeast strains isolated from ripe banana peels. *African journal of Biotechnology*, 7 (20), 3749-3752 (2008).
 - xiii. S.B. Oyeleke, N.M. Jibrin. Production of bioethanol from guinea corn husk and millet husk. *Afr. J. Microbiol. Res.* 3 (4), 147-152 (2009).
 - xiv. A.K. Agarwal. Biofuels: In wealth from waste; trends and technologies. (ed Lal and Reedy), 2nd Edition. The Energy and Resources Instituted (TERI) Press, ISBNSI-7993-067-X (2005).
 - xv. U. Yahaya, M.S. Abdulsalami, S.D. Denwe, J. Ibrahim. Evaluation of bioethanol production from *Gmelina aborea* sawdust using *saccharomyces cerevisiae* and *saccharomyces carlbergensis*. Proceedings of the 30th Annual International Conference of Biotechnology Society of Nigeria held on August, 27-30th at the Federal University of Technology, Minna, Niger State. Pp 366-371 (2017).
 - xvi. C.E. Wyman, B.E. Dale, R.T Elander, M. Holtzapple, M.R. Ladisch, Y.Y. Lee. Comparative sugar recovery data from laboratory scale application of leading pretreatment technologies to corn stover. *Bioresource Technology*, 96: 2026- 2032 (2005).
 - xvii. A.M.J. Kootstra, H.H. Beeftink, E.L. Scott, J.P.M. Sanders. Comparison of dilute mineral and organic acid pretreatment for enzymatic hydrolysis of wheat straw. *Biochemical Engineering Journal* 46 (2), 126 – 131 (2009).



- A. Rabah, S. Oyeleke, S. Manga, L. Hassan. Dilute acid pretreatment of millet and guinea corn husks for bioethanol production. International Research Journal of Microbiology, 2 (11),460-465 (2011).
- Escherichia coli Isolated from Soil in Afaka Forest Reserve, Kaduna State Nigeria. International Journal of Sustainable and Green Energy; 4 (2), 40-46 (2015).
- B. U. Yahaya, U.Y. Abdullahi, S.D. Denwe, N.M. Muktar, N.M . Bioethanol Production from Eucalytus camaldulensis Wood Waste Using Bacillus subtilis and
- xviii. T.W. Jeffries. Engineering yeasts for xylose metabolism. Current Opinion in Biotechnology 17, 320–326 (2006).



P025 - DEVELOPMENT OF DESKTOP TELEOPERATED MANIPULATOR: A NEW RESEARCH DIRECTION IN EXPERIMENTING IN A LABORATORY IN HAZARDOUS ENVIRONMENT- A REVIEW

Akang, I.V^{1*}, Afolayan, M.O², Yawas, D.S², Umoh, I.J², Alabi, A.A², Barminas, J.T¹, Iorpenda, M.J², Ugbo, O.T²

¹National Research Institute for Chemical Technology, Zaria, ²Ahmadu Bello University, Zaria

E-mail address: akangvictor2@gmail.com

ABSTRACT

The premium to be paid to life is ethically inadequate where it exists. Laboratory experimentation produces results sought. Technological advancement has attempted to eliminate accidental releases of chemicals in laboratory while experimenting, avoiding Health hazard. To actualize these, numerous approaches been adopted use personal protective equipment, creation of automated laboratory, these have not out-rightly stopped the perilous situations. This review discusses potentials of using (semi) humanoid robots in laboratory as alternative to humans, while accuracy and precision are not compromised, to achieve end-point. Incremental use of robots has urged the authors to search for optimal combination of software and hardware devices to improve output of laboratory experimentation. Humanoid robot are used in experimentations, which have been designed and built as desktop with a functional manipulator. A desktop manipulator which is of the size to be used on the bench of a laboratory is reviewed and studied, it is intended to succinctly analyse the progress of the development of robotics with respect to laboratory experimentation and adoption for hazardous environment. Some of these are found in some of the smart laboratories outside our shores. The results of the review highlight the potential being sought to be used to prevent the human person from direct contact with chemicals utilized during experimentation. Furthermore, their tele operational ability from their performance, facilitates its functionality and ingenious perfection and use of these teleoperated manipulator is a desideratum.

KEYWORDS

Trajectory, striction, simulation, virtual reality, dual quaternion.

1.0 INTRODUCTION

Experimental methods are commonly held up as the paradigm for testing hypotheses: the scientific method, widely disseminated in introductory science texts, is modeled upon them (1). The laboratory environment has been characterized by ongoing rapid and dramatic innovation since the 1980s. Laboratory technology is often at the forefront of medical advances. Information technology (IT) has revolutionized the transfer of data by decreasing the time it takes to order and receive test results and by creating opportunities for research on large datasets. Clinical laboratory technology will play a more important role in the future delivery of health care (2). A laboratory is a facility that provides controlled conditions in which scientific research, experiments are performed. Laboratory services are provided in a variety of settings: physicians' offices, clinics, hospitals and

regional and national referral centres (3). In such instances during the cause of experimentation, errors do occur which could be hazardous and/or fatal. The use of hazardous chemicals in work processes predates recorded history, industry became rapidly more complex and the use of sophisticated chemicals became increasingly widespread in the 20th century.

To alleviate researchers from the direct impact of hazardous chemicals or mitigating the perilous effect of these hazardous chemicals, reviews have taken place on several ways in which laboratory attendants, experimenters, researchers should comport themselves to carryout experiment in the laboratory to avoid accidents and achieve the set target which is the correct end-point. However, a few reviews have been dedicated to the use of personal protective equipment, use of smart or automatic laboratories and robots. In a bid to make the experimenter and/or researcher to operate naturally, the use of robots is offered.



1.1 Description of Desktop Robotics System

Robots are devices with assigned intelligence referred to as artificial intelligence and can be networked via remote control by human operators, these are playing increasingly important roles in hazardous environments where human lives are at risk (4). This review is intended to deal with the teleoperated desktop manipulator, which in certain instances is referred to as robot or robot arm. Roboticians would like to create robots with comparable versatility and skills with that of the humans. When automating a task that people perform, it is natural to consider the physical and intellectual mechanisms that enable a person to perform the task (5). Robots have been proven efficient workhorse for automotive and other manufacturing industries (6). In comparison, a robotic arm is a mechanical version of the human arm that is programmable and can perform functions that humans cannot achieve (7). Robotics is the science of perceiving and manipulating the physical world through computer-controlled mechanical devices (8). Robots, based on mode of operation are of two types, autonomous and teleoperated.

1.2 Usability and User Interface

Programmable manipulators have existed for close to thirty (30) years, since the advent of the microprocessor. Indeed, the microprocessor, introduced in 1976 by Intel, allowed a human master to *teach* the manipulator by actually driving the manipulator itself, or a replica thereof, through a desired task, while recording all motions undergone by the master. Thus, the manipulator would later repeat the identical task by mere playback. However, the capabilities of industrial robots are fully exploited only if the manipulator is programmed with a software, rather than actually driving it through its task trajectory, which many a time, requires separating the robot from the production line for more than a stipulated period of time. To achieve this feat, instructions are given via programs. This act of programming of the manipulator using set of instructions is referred to as algorithm.

The functionality of the manipulator can be assessed through kinematics and dynamics. Kinematics studies the motion of bodies without consideration of the forces or moments that cause the motion. Robot kinematics refers to the analytical study of the motion of a robot manipulator. Formulating the suitable kinematic

models for a robot mechanism is very crucial for analysing the behaviour of industrial manipulators. Robot dynamics provides the relationships between actuation and contact forces, and the acceleration and motion trajectories that result. The dynamic equations of motion provide the basis for a number of computational algorithms that are useful in mechanical design, control, and simulation. As a remote operation technology employing virtual reality (VR), in previous researches, the authors intend to improve the task efficiency of conventional teleoperated robotic system by using VR technology to give the operator a feeling of being at the actual work space in real-time.

Sanjay and Shweta (2012) (9) focused on the "Position Control of a Pick and Place Robotic Arm," specifically a 5-DOF articulated robot arm designed for real-time moulding machine operations.

Karl Bernorp *et al.* (2012) proposed the application of a mobile robot with kinematic redundancy for future pick and place operations in grocery stores. Though the desktop manipulator considered is not completely mobile as at the time of putting up this review.

Lian *et al.* (2012) (10) demonstrated how optimizing dimensional parameters of a 2-DOF parallel manipulator could enhance pick and place performance. Such dimensional parameters include the length of the arm w.r.t. the body size.

Altuzarra *et al.* (2011) (11) introduced two design methods for a mechanical drive to increase the end effector's angular range. The end effector is the arm which could be fingered hands or designed tool tip.

The purpose of the present review is to compare the previous works to that of the proposed desktop manipulator in alleviating the perilous challenges in experimentation in hazardous environments, while not leaving out accuracy and precision. In so doing, solve the problems of the previously-reported remote-operation of teleoperated robot system and enhance the improvement of its operability by incorporating modernized facilities which give the operator an effective visual sense, and taking advantage of the distinctive features of VR. New technologies have aided the incubation of these robotization, enhancing innovation in robotic technology. The usefulness of the system is also verified from the viewpoints of task efficiency and risk indexes. The development of this new technologies is a real industrial revolution, and it is called industry 4.0. According to Siciliano and



Oussama (2008) (5) of the Stanford team which was funded posited that, “The first truly functional arm from the group was designed by Victor Scheinman, who was a graduate student at the time. It was the very successful *Stanford Arm*, of which over ten copies were made as research tools to be used in various university, government, and industrial laboratories. The arm had six independently driven joints; all driven by computer-controlled servoed, DC electric motors. One joint was telescoping (prismatic) and the other five were rotary (revolute).” The arm was very fast. The first manipulator that we designed on our own was known simply as the *Hydraulic Arm*. As its name implies, it was powered by hydraulics.

1.3 Performance

Real time control robots with remote network control with human operators’ ability play an important part in hazardous and challenging environments where human life may be exposed to great dangers such as health issues (even death), assessing nuclear contaminated areas, assessing under water environment such as sea or flooded areas, putting out of fire and rescue operation in earthquake and/or disaster areas. One core technology of Industry 4.0 are creation of cobots, whose name comes from 'collaborative robot', precisely because the aim of this technology is to collaborate with the human worker to perform tasks. The main features that make cobots suited for production are flexibility and collaboration.

1.4 Application

The desktop manipulator is to be located in the Decontamination laboratory of the National Research Institute for Chemical Technology, Zaria, for use in carrying out experiments in hazardous situation. This would domicile the technology within the Institute, and that would facilitate the improvisation of the Technology within the Nigerian environment. An important amount of research has led to the development of different robots with sensing abilities, transport and manipulation of different applications.

Liao *et al.* (2013) (12) conducted optimal design work on a 3-DOF planar revolute chain parallel manipulator, aiming to improve its operational velocity and accuracy in pick and place tasks. The configuration of the Desktop Manipulator is not a parallel chain but serial.

Pedersen *et al.* (2016) (13) developed robot reconfiguration technologies for automating

production lines and introduced the concept of self-adjusting robot skills for production tasks. Kamali *et al.* (2016) (14) explored elastogeometric calibration methods to enhance the positioning accuracy of 6-DOF industrial robots. Pellegrinelli *et al.* (2017) (15) developed a methodology for planning and optimizing robot movements to minimize cycle time. Faulwasser *et al.* (2016) researched the control of trajectory accuracy in industrial robots, applying their findings to a KUKA LWR IV robot. Su *et al.*, (2018) (16) developed a wireless 3D manipulation system based on augmented reality for controlling robotic arms and also developed a wireless 3D manipulation system based on augmented reality for controlling robotic arms.

Considering safety, Quarta *et al.*, (2017) (17), worked on controller safety and software vulnerabilities. Guillo and Dubourg (2016) (18) developed an algorithm for real-time correction of welding paths in industrial robots. Kaltsoukalas *et al.*, (2015) (19) proposed an intelligent algorithm for trajectory planning in industrial manipulators, elucidating minimized operation time. Path planning and optimization were addressed by Fu *et al.*, (2018) (20), who proposed an improved A* algorithm for robot path planning, considering safety and path length reduction. Gao *et al.* (2018) presented a parameter identification method for reducing motion uncertainty in 6-DOF industrial robots based on the Denavit-Hartenberg model. Ding *et al.* (2018) (21) investigated dynamic identification for 6-DOF industrial robotic arms and introduced a procedure using a modified cuckoo search algorithm. Pan *et al.* (2018) (22) developed an adaptive robust controller for dynamic trajectory tracking in 6-DOF robots, resistant to parametric changes and uncertainties.

Wang *et al.* (2019) (23) proposed a smooth path planning method for industrial robots, optimizing joint movement for acceleration, deceleration, and constant speed segments. Pane *et al.* (2019) studied 6-DOF smart industrial manipulators and introduced compensation methods based on reinforced learning. Zhang *et al.* (2019) (24) improved the accuracy of robotic arm movement by using a hybrid whale optimization algorithm and genetic algorithm to determine dynamic parameters. Li *et al.* (2019b) (25) presented an error model for kinematic calibration of serial robots using double quaternions, allowing for more precise calibration.



In Liu *et al.*'s study (2018) (26), a trajectory planning method was introduced to minimize synthesis errors and achieve stable motion in industrial robots. Li *et al.* (2022) (27) combined arm motion detection, speech recognition, and pose recognition to design a teaching control system for manipulators, enabling accurate and rapid human-robot interaction. They highlighted the advantages of their system, including its simplicity, suitability for chemical operators, and use of a low-cost manipulator with advanced robot learning algorithms.

The field of teleoperated systems for object manipulation involves communication between a "master" operator and a "slave" robot, offering various levels of control and information exchange. Researchers have explored different aspects of this technology. Ni *et al.* (2018) (28) predicted object movements during teleoperated manipulation and corrected predictions in virtual reality. Bernardino *et al.* (2013) (29) used a teleoperated arm and gripper to mimic human precision grasps, creating synergies in the gripper. Li *et al.*, (30) introduced the ability to control the "slave" gripper using visual input commands from the "master."

2.0 WHY ROBOTS AND ROBOTICS

2.1 Integration with Other Equipment

In their respective studies, several researchers have made significant contributions to the field of robotics and automation. As previously highlighted, interaction with chemicals considered hazardous in a laboratory setting and/or environment could lead to perilous situation such as injury or loss of life. As a result, a number of innovative techniques have been carried out in the area of robotization to achieve the greatest safety while performing in the laboratory. These studies collectively contribute to the advancement of robotics and automation, addressing a wide range of challenges and opportunities in the field. The adoption of a multi-agent-based system for the humanoid in the 1990s for its ease of modular development and integration by adding more sensors and actuators and the need to integrate both the human and the robot in a unified human robot interaction framework (31). Robotics became available to everyone and is becoming a part of almost all aspects in our life (32). If earlier robotic complexes were produced mainly for industry and were expensive, large, and cumbersome to design and use, today a number of compact and inexpensive robots have been created. A desktop robot manipulator is a full-fledged

assistant for the simplification of the tasks of experimentation (32).

3.0 STANDOUT PERFORMANCE IN ROBOTICS USE

The term "robot" was introduced into our vocabulary by the Czech playwright Karel Capek in his satirical play *Rossum Universal Robots* (R. U. R.), in 1920, from the Czech (being his local dialect) word "robota" meaning work, where he depicted robots as machines which resembled human beings but worked tirelessly (33, 34).

How good is a robot? Three challenges arise from this question: first, defining performance from the robot's observable behaviour; second, quantifying performance with an index that is obtainable through direct measurement or computation, and representative of the measured quantity; and third, ensuring that this procedure is repeatable and general, to enable performance comparison, benchmarking, and an increase of safety and efficiency standards. However, the landscape of performance metrics for industrial manipulators is fragmented, and limited effort is being made toward a unified framework.

Telerobotic systems allow human operators to properly interact with a telerobot to telemanipulate objects located in a remote environment. This means that human actions are extended to remote locations allowing the execution of both simple and complex tasks and avoiding risky situations for the human operator(s). In other words, during the course of experimentation, the robot carries out the experiment just like the human would, in a precise and accurate manner, with the safety overtures not being overlooked.

In order to develop robot automation for new market sectors associated with short procedural maneuvers or variable manipulation lifetimes and frequent production change overs, the laboratory Desktop Manipulator exhibits a new level of flexibility and versatility. This was one of the reasons for the growing interest in making humans and robots share their working environments (when these are in the same environment) and sometimes even allowing direct physical contact between the two in order to make them work cooperatively on the same task by enabling human-industrial robot collaboration.

3.1 Robots used in place of the humans for carrying out experiment



Robotic systems specifically designed for automation of robotic tasks are rightly positioned for precision manipulation in carrying out experiments in the laboratory under hazardous situation (2). Such include humanoid robots which by virtue of their configuration resembles a human, and these selectively emulates the human in form and behaviour (5). These system(s) equipped with computer and its peripheral devices is capable of revolutionizing modern laboratory analysis (2). Historically, the human body and mind have actually intrigued researchers, designers and artists, focusing on the creation of robots with human capabilities, and their resemblance to humans share similar kinematics and dynamics as well as sensing and behavioural pattern (5).

The humanoid robotic system resembles the human through the 3H i.e. head, heart and hand. Though, the emphasis in this review is on the hand. Hands and arms are the main interfaces with which humans perform in the laboratory. Dexterity or manipulation with the hands illustrates the use of arms, hands via sensors to perform tasks performed by humans. Based on the configuration, some kinematic configurations will be easy to solve, while others are without closed form solution. In like manner, the complexity of the dynamic equations varies greatly with the kinematic configuration and the mass distribution of the links.

As for the teleoperated robot, the communication between the operator side i.e. human in the loop, for the multi-modal human system and the remote or slave of the teleoperated robot takes place over a network. Castellani *et al.*, (1986) (35) recently reported that a robot can perform preparative immunologic precipitations with final placements of the samples into a rotor for subsequent analysis. Although robots are nominally "universally programmable" machines capable of performing a wide variety of tasks, economies and practicalities dictate that different manipulators be designed for particular types of tasks. Researchers have approximated the human hand with varying levels of accuracy (5).

Artemiadis and. Kyriakopoulos (2005) (36) posited that there are two parts of the robotic manipulator is to be driven, some parts of the robotic system just like the elbow is being driven by EMG signals from biceps brachii, for an effective functioning.

A mathematical model of grasping must be capable of predicting the behaviour of the hand and object

under the various loading conditions that may arise during grasping. Generally, the most desirable behaviour is grasp maintenance in the face of unknown disturbing forces and moments applied to the object. Typically, these disturbances arise from inertia forces which become appreciable during high-speed manipulation or applied forces such as those due to gravity. Grasp maintenance means that the contact forces applied by the hand are such that they prevent contact separation and unwanted contact sliding. The special class of grasps that can be maintained for every possible disturbing load is known as closure grasps.

3.2 Contact Modelling

Three contact models useful for grasp analysis are reviewed here. The three models of greatest interest in grasp analysis are known as *point contact without friction*, *hard finger*, and *soft finger*. These models select components of the contact twists to transmit between the hand and the object. This is done by equating a subset of the components of the hand and object twist at each contact. The corresponding components of the contact force and moment are also equated, but without regard for the constraints imposed by contact unilaterality and friction models. For the Desktop Manipulator to be able to hold effectively, there must be points which must be in contact with the object to avoid slip.

3.2 Dynamic Model

At this stage, one determines the mathematical model which relates the input variables to the output variables. In general, such mathematical representation of the system is realized by ordinary differential equations. The system's mathematical model is obtained typically via one of the two following techniques.

- *Analytical*: this procedure is based on physical laws of the system's motion. This methodology has the advantage of yielding a mathematical model as precise as is wanted.
- *Experimental*: this procedure requires a certain amount of experimental data collected from the system itself. Typically, one examines the system's behaviour under specific input signals. The model so obtained is in general more imprecise than the analytic model since it largely depends on the inputs and the operating point.

3.3 Kinematic Modelling



In robot simulation, system analysis needs to be done, such as the kinematics analysis, its purpose is to carry through the study of the movements of each part of the robot mechanism and its relations between itself. The kinematics analysis is divided into forward and inverse analysis. The forward kinematics consists of finding the position of the end-effector in the space knowing the movements of its joints, and the inverse kinematics consists of the determination of the joint variables corresponding to a given end-effector position and orientation.

Any number of contacts may occur between any link and the object. The animated computer graphics (CG) image of the objects is generated by repeating the grasping technique of the human hand. The moment at which an object is grasped by the robot is detected from the relationship between the measured displacements of the robot arm and the size of the object. While the robot is holding the object, a CG image of the robot and the held object are generated by using the information on the moment at which it is grasped. After the robot releases the object, the object is recognized again by using the same process. In this review, the system is constructed using a 3-dimensional shape input device (stereo camera) to obtain information on the remote site and computer graphics (CG).

The most important property in a control system, in general, is stability. This fundamental concept from control theory basically consists in the property of a system to go on working at a regime or *closely* to it *forever*. Two techniques of analysis are typically used in the analytical study of the stability of controlled robots. The first is based on the *Lyapunov* stability theory. The second is the *input–output* stability theory. Both techniques are complementary in the sense that the interest in *Lyapunov* theory is the study of stability of the system using a *state* variables description, while in the second, interest is in the stability of the system from an input–output perspective.

The simplest way to specify the movement of a manipulator is the “point-to-point” method. This methodology consists in determining a series of points in the manipulator’s workspace, which the end-effector is required to pass through, compared to the continuous point method.

4.0 CONCLUSION

Robotics, sensors, actuators and controller technologies continue to improve and evolve at an amazing rate. Automation and robotics systems

today are performing motion control and real-time decision-making tasks that were considered impossible forty (40) years ago. It can truly be seen that this is a time where almost any form of physical work that the human person can do can be replicated or performed faster, more accurately, cheaper and more consistently using computer-controlled robots and mechanisms, and this provides the greatest safety. Human decision-making tasks are now being automated using advanced sensor technologies such as machine vision, 3D scanning and a large variety of non-contact proximity sensors. During the last thirty years, the fields of robotics, cognitive science and neuroscience made steady progress fairly independently with each other. This review has outlined the usefulness of the telerobot in the course of experimentation and its use to carryout experiment in a laboratory, to ensure the safety of man during the cause of the experimentation.

5.0 REFERENCES

1. C. E. Cleland, Historical science, experimental science, and the scientific method. *Geology* **29**, 987-990 (2001).
2. R. Felder, J. Boyd, K. Margrey, W. Holman, J. Savory, Robotics in the medical laboratory. *Clinical chemistry* **36**, 1534-1543 (1990).
3. A. Fritzsche, Corporate foresight in open laboratories—a translational approach. *Technology Analysis & Strategic Management* **30**, 646-657 (2018).
4. V. Vladareanu, R. I. Munteanu, A. Mumtaz, F. Smarandache, L. Vladareanu, The optimization of intelligent control interfaces using Versatile Intelligent Portable Robot Platform. *Procedia Computer Science* **65**, 225-232 (2015).
5. B. Siciliano, O. Khatib, T. Kröger, *Springer handbook of robotics*. (Springer, 2008), vol. 200.
6. M. Beetz, R. Chatila, J. Hertzberg, F. Pecora, AI reasoning methods for robotics. *Springer Handbook of Robotics*, 329-356 (2016).



7. M. T. Shaikh, M. A. Goodrich, in *2020 29th IEEE International Conference on Robot and Human Interactive Communication (RO-MAN)*. (IEEE, 2020), pp. 1033-1040.
8. S. Thrun, Probabilistic robotics. *Communications of the ACM* **45**, 52-57 (2002).
9. S. Patil, S. Lakshminarayan, Position Control of Pick and Place Robotic Arm. (2012).
10. B. Lian, Y. Song, G. Dong, T. Sun, Y. Qi, in *Intelligent Robotics and Applications: 5th International Conference, ICIRA 2012, Montreal, QC, Canada, October 3-5, 2012, Proceedings, Part I 5*. (Springer, 2012), pp. 261-270.
11. O. Altuzarra, B. Şandru, C. Pinto, V. Petuya, A symmetric parallel Schönflies-motion manipulator for pick-and-place operations. *Robotica* **29**, 853-862 (2011).
12. B. Liao, Y. Lou, Z. Li, Kinematics and optimal design of a novel 3-DoF parallel manipulator for pick-and-place applications. *International Journal of Mechatronics and Automation* **3**, 181-190 (2013).
13. M. R. Pedersen *et al.*, Robot skills for manufacturing: From concept to industrial deployment. *Robotics and Computer-Integrated Manufacturing* **37**, 282-291 (2016).
14. K. Kamali, A. Joubair, I. A. Bonev, P. Bigras, in *2016 IEEE International Conference on Robotics and Automation (ICRA)*. (IEEE, 2016), pp. 4320-4327.
15. S. Pellegrinelli, A. Orlandini, N. Pedrocchi, A. Umbrico, T. Tolio, Motion planning and scheduling for human and industrial-robot collaboration. *CIRP Annals* **66**, 1-4 (2017).
16. Y.-H. Su, C.-Y. Chen, S.-L. Cheng, C.-H. Ko, K.-Y. Young, in *2018 IEEE International Conference on Systems, Man, and Cybernetics (SMC)*. (IEEE, 2018), pp. 1809-1814.
17. D. Quarta *et al.*, in *2017 IEEE Symposium on Security and Privacy (SP)*. (IEEE, 2017), pp. 268-286.
18. M. Guillo, L. Dubourg, Impact & improvement of tool deviation in friction stir welding: Weld quality & real-time compensation on an industrial robot. *Robotics and Computer-Integrated Manufacturing* **39**, 22-31 (2016).
19. K. Kaltsoukalas, S. Makris, G. Chryssolouris, On generating the motion of industrial robot manipulators. *Robotics and Computer-Integrated Manufacturing* **32**, 65-71 (2015).
20. B. Fu *et al.*, An improved A* algorithm for the industrial robot path planning with high success rate and short length. *Robotics and Autonomous Systems* **106**, 26-37 (2018).
21. L. Ding, X. Li, Q. Li, Y. Chao, Nonlinear friction and dynamical identification for a robot manipulator with improved cuckoo search algorithm. *Journal of Robotics* **2018**, 1-10 (2018).
22. L. Pan, G. Bao, F. Xu, L. Zhang, Adaptive robust sliding mode trajectory tracking control for 6 degree-of-freedom industrial assembly robot with disturbances. *Assembly Automation* **38**, 259-267 (2018).
23. M. Wang, J. Xiao, F. Zeng, G. Wang, Research on optimized time-synchronous online trajectory generation method for a robot arm. *Robotics and Autonomous Systems* **126**, 103453 (2020).
24. L. Zhang *et al.*, Dynamic modeling for a 6-DOF robot manipulator based on a centrosymmetric static friction model and whale genetic optimization algorithm. *Advances in Engineering Software* **135**, 102684 (2019).
25. G. Li, F. Zhang, Y. Fu, S. Wang, Kinematic calibration of serial robot using dual quaternions. *Industrial Robot: the international journal of robotics research and application* **46**, 247-258 (2019).
26. Z. Liu *et al.*, Trajectory planning with minimum synthesis error for industrial robots using screw theory. *International Journal of Precision Engineering and Manufacturing* **19**, 183-193 (2018).
27. C. Li, A. Fahmy, J. Sienez, Development of a neural network-based control system for



- the DLR-HIT II robot hand using leap motion. *IEEE Access* **7**, 136914-136923 (2019).
28. D. Ni *et al.*, Point cloud augmented virtual reality environment with haptic constraints for teleoperation. *Transactions of the Institute of Measurement and Control* **40**, 4091-4104 (2018).
 29. A. Bernardino, M. Henriques, N. Hendrich, J. Zhang, in *2013 IEEE international conference on robotics and biomimetics (ROBIO)*. (IEEE, 2013), pp. 62-67.
 30. H. Sang *et al.*, Control design and implementation of a novel master–slave surgery robot system, MicroHand A. *The International Journal of Medical Robotics and Computer Assisted Surgery* **7**, 334-347 (2011).
 31. K. Kawamura, T. E. Rogers, X. Ao, in *Proceedings of the first international joint conference on Autonomous agents and multiagent systems: part 3*. (2002), pp. 1379-1386.
 32. E. Rubleva, A. Mudrich, in *Journal of Physics: Conference Series*. (IOP Publishing, 2021), vol. 2096, pp. 012178.
 33. P. I. Corke, W. Jachimczyk, R. Pillat, *Robotics, vision and control: fundamental algorithms in MATLAB*. (Springer, 2011), vol. 73.
 34. S. D. Kelly, R. M. Murray, Geometric phases and robotic locomotion. *Journal of Robotic Systems* **12**, 417-431 (1995).
 35. W. J. Castellani, F. Van Lente, D. Chou, Robotic sample preparation evaluated for the immunochemical determination of cardiac isoenzymes. *Clinical chemistry* **32**, 1672-1676 (1986).
 36. P. K. Artemiadis, K. J. Kyriakopoulos, in *2005 IEEE/RSJ International Conference on Intelligent Robots and Systems*. (IEEE, 2005), pp. 1003-1008.





P026 -WEIGHT LOSS AND ELECTROCHEMICAL TECHNIQUES TO ASSESS THE CORROSION INHIBITION POTENTIAL OF ETHANOL EXTRACT OF ACACIA NILOTICA POD ON MILD STEEL IN ACIDIC MEDIUM

*J. Ibrahim¹, B. Usman², Z. Suleiman³, R. Sabo⁴

¹Department of Chemistry, Faculty of Sciences, Confluence University of Science and Technology, Osara, P.M.B. 1040 Okene-Lokoja Road, Kogi State, Nigeria.

Corresponding Author's Email: ibrahimj@custech.edu.ng

GSM: +2347031297947

²Department of Pure and Industrial Chemistry, Faculty of Physical Sciences, College of Natural and Pharmaceutical Sciences, Bayero University Kano, P.M.B. 3011, Kano State, Nigeria

³Department of Applied Chemistry, School of Science and Information Technology, Federal University of Technology, Babura, Jigawa State, Nigeria.

⁴Department of Chemistry, Faculty of Sciences, Sule Lamido University, Kafin Hausa, P.M.B.048 Kafin Hausa, Jigawa State, Nigeria.

ABSTRACT

The corrosion inhibitory effect of ethanol extract of *Acacia nilotica* pod (ANP) on mild steel in 0.1M H₂SO₄ containing 0.1–0.5 g/L has been studied using weight loss, Fourier transform infrared (FTIR) spectroscopy, and scanning electron microscopy (SEM) methods. The results from weight loss show that the inhibition efficiency depends on the concentration of the plant extract as well as the time of exposure of the mild steel samples to H₂SO₄ solutions. The optimum inhibition efficiency of the extract obtained from weight loss measurements was found to be 87.57%. The surface morphology of mild steel, in the presence and absence of ANP, was studied using SEM. The FTIR spectroscopy analysis was used to confirm the adsorption process on the metal surface. Spectra analysis obtained from the FTIR study indicated that ANP was adsorbed onto the mild steel surface via the C-O and N=O functional groups. The results obtained revealed that ANP acts as a good inhibitor and could serve as an effective corrosion inhibitor of mild steel in a 0.1M H₂SO₄ solution.

KEYWORDS:

Acacia nilotica pod, corrosion, mild steel, tetraoxosulfate (VI) acid.

INTRODUCTION

Mild steel is widely used as a construction material in most of the major industries, particularly in food, petroleum, power production, chemical, and electrochemical industries, due to its versatile mechanical properties and low cost [21]. Corrosion of metals such as iron and steel due to exposure to the aggressive environment results in mechanical failure of equipment and causes dangerous and costly damages to oil, gas, and water pipelines, bridges, public buildings, vehicles, water and wastewater channels, and even home appliances [1, 2]. Therefore, corrosion protection processes for mild steel in aggressive acid and alkaline media are found to be important [3]. Several kinds of research have been carried out on the inhibition of the corrosion of mild steel due to its high technological value as well as a wide range of industrial applications. Generally, compounds

containing heteroatoms such as N, O, P, and S and a long carbon chain, as well as triple bonds or aromatic rings in their molecular structure, are used as inhibitors [4, 5]. These compounds are expensive, toxic, and non-eco-friendly. Plant materials are inexpensive, non-toxic, readily available, eco-friendly, and the richest source of heterocyclic compounds containing S and functional groups (such as -C=C-, -OR, -OH, -COOH, -NR₂, -NH₂, and -SR), which provide electrons that facilitate the adsorption of the inhibitor on the metal surface. Recent developments in the area of corrosion assessment have been the studies of various plant extracts as corrosion inhibitors [6–9]. It has been established that the inhibitory actions of plant extracts have been attributed to the presence of some organic compounds such as tannins, saponins, alkaloids, steroids, glycosides, and amino acids [9]. In view of this, this present study sought to investigate the



inhibitory effect of an ethanol extract of ANP on the corrosion of mild steel in an acidic medium using weight loss, FTIR spectroscopy,

2.0 MATERIALS AND METHODS

Material preparation

The mild steel used for this study was obtained from the department of mechanical engineering at Bayero University, Kano-New Campus. The mild steel sheets were of the following composition (wt%): Mn (0.27), Al (0.04), C (0.066), Ca (0.01), Cr (0.041), Cu (0.023), Te (0.17), I (0.25), Cl (0.21), Sc (0.03), Sb (0.20), Eu (0.10), Si (0.13), and the rest Fe (determined by ED-XRF). The sheet was mechanically pressed and cut into different coupons, each of dimensions 5cm x 4cm x 0.11 cm. Each coupon was degreased by washing with ethanol, rinsed with acetone, and allowed to dry in the air before being preserved in a desiccator. All reagents used for the study were analytical grade, and double-distilled water was used for their preparation.

Coupon preparation

The corrosion test was performed using coupons prepared from the mild steel, which were cut into 100 samples of dimensions 5cm x 4cm x 0.11 cm. Emery paper of different grades (240, 400, 800, and 1000 μ m) was used for polishing the samples, washing them in ethanol, degreasing them in acetone, drying them in air, weighing them, and storing them in desiccators prior to corrosion studies. The initial weight of each sample was taken and recorded.

Plant extract preparation

$$CR (g/h/cm^2) = \frac{\Delta W}{At} \quad (1)$$

$$\theta = 1 - \frac{W_1}{W_2} \quad (2)$$

$$\%I = \left(1 - \frac{W_1}{W_2}\right) \times 100 \quad (3)$$

Where W_1 and W_2 are the weight losses (in g/dm³) for mild steel coupons in the presence and absence of inhibitors in H₂SO₄ solutions, respectively. θ is the degree of surface coverage of the inhibitor, A is the area of the metal coupon (in cm²), t is the period of immersion (in hours), and W is the weight loss of the mild steel coupon (in grams) after time, t .

and scanning electron microscopy (SEM) methods of monitoring corrosion.

Samples of ANP were air dried, ground, and soaked in a solution of ethanol for 48 hours, after which the samples were cooled and filtered. The filtrates were further subjected to evaporation at 352 K in order to leave the sample free of ethanol. Stock solutions of the extract obtained were used in preparing different concentrations of the extract by dissolving 0.1, 0.2, 0.3, 0.4, or 0.5 g of the extract in 1 L of 0.1 M H₂SO₄ [9].

Acid Solution Preparation

A stock solution of 0.1 M H₂SO₄ was used as the corrodent for this study and was prepared from 98% H₂SO₄ (Merck) by diluting 5.40 mL of concentrated H₂SO₄ analar grade in a 1000 ml volumetric flask containing 150 mL distilled water and making it to the mark with distilled water, which was used throughout the experiments for the preparation of solutions. The concentration range of ANP ethanol extract employed varied from 0.1 to 0.5 g/L.

Weight loss measurement

Weight loss measurements were performed in a 250-mL beaker at 303 K. The solution volume used is 250 mL, and the mild steel was weighed and immersed in the solution for 1 hour after being retrieved, washed with distilled water, rinsed with ethanol and acetone, dried, and reweighed. From the initial and final weights of mild steel coupons, the weight loss (g), corrosion rate (g/h/cm²), inhibition efficiency (%I), and degree of surface coverage (θ) were calculated using equations 1–3, respectively.

Fourier Transform Infrared Spectrophotometry (FTIR)

FTIR analyses of the inhibitor and that of the corrosion products (in the presence and absence of the respective inhibitors) were carried out using an FTIR instrument, the 630 Cary series Agilent Technologies. Two coupons were separately dipped in 250 mL of 0.5 g/L inhibitor concentration for 2 days to form an adsorbed layer, after which they were retrieved, dried, and scraped with a sharp blade. The scraps were collected for analysis. The samples were prepared using KBr, and the analysis was done by scanning the sample through a wave number range of 400–4000 - 4000 cm⁻¹.



Surface analysis

The surface morphology of the mild steel coupons before and after inhibition was studied using an Inspect S50 scanning electron microscope. 5cm x 4cm x 0.1cm coupons were dipped in blank solution and 0.5 g/L inhibitor solution for 2 days. The coupons were then retrieved, rinsed with distilled water, and dried in the air. Each sample was mounted on a metal stub and sputtered with gold in order to make the sample conductive. Scanned images were taken at an accelerating voltage of 2.00 and 12.50 kV.

3.0 RESULTS AND DISCUSSION

Weight loss measurement:

Effect of inhibitor concentration

The effect of ANP extract concentration in relation to corrosion rate and inhibition efficiency at 303 K for the corrosion of mild steel in 0.1 M H₂SO₄ in the absence and presence of various concentrations of the plant pod extract are shown in figure. 1 and 2, respectively. From the plot (Fig. 1), it can be observed that the corrosion rate of mild steel coupons in 0.1 M H₂SO₄ decreased with an increase in the concentration of the plant extract.

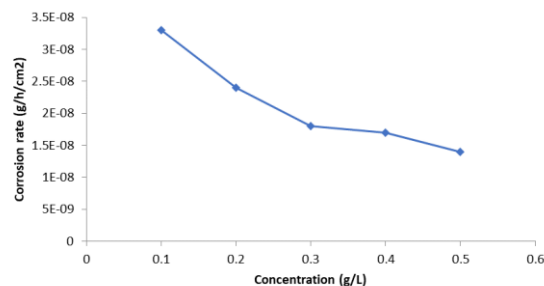


Figure 1. Variation of corrosion rate (g/h/cm²) of mild steel as a function of various concentration of ANP extract in 0.1M H₂SO₄ at 303K.

This is due to the fact that as the concentration of the plant extract increased, there was an increase in surface coverage of the adsorbed extract on the mild steel surface, which provided an impediment and consequently retarded metal dissolution [10]. This is in agreement with the findings of Niamien *et al.* [11] and Olasehinde *et al.* [12]. Furthermore, the inhibition efficiency (Figure. 2) of the extract was observed to increase with a rise in inhibitor concentrations. This may be due to an increment in the surface coverage, thus retarding metal corrosion [10].

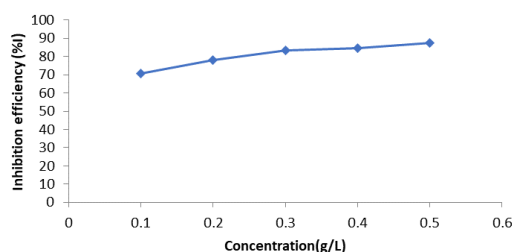


Figure 2: Variation of Inhibition Efficiency (%IE) against Various Concentrations of ANP Extract for Mild Steel Corrosion in 0.1 M H₂SO₄ at 303 K

Table 1. Inhibition efficiencies (%IE) and corrosion rates for corrosion of mild steel in the absence and presence of various concentrations of the extract in 0.1M H₂SO₄ at 303–333 K.

Conc.(g/L)	Corrosion Rate x10 ⁻⁴ (gh ⁻¹ cm ⁻²)				Inhibition efficiency (%)			
	303K	313K	323K	333K	303K	313K	323K	333K
Blank	1.11	3.45	5.79	7.93	-	-	-	-
0.1	0.33	1.19	2.30	3.86	70.54	65.45	60.23	51.34
0.2	0.24	0.93	2.05	3.42	78.04	72.95	64.61	56.90
0.3	0.18	0.75	1.53	2.88	83.40	78.31	73.59	63.73
0.4	0.17	0.58	1.39	2.54	84.68	83.27	76.07	67.99
0.5	0.14	0.52	1.10	2.32	87.57	84.92	80.98	70.69

Effect of immersion time



Figure 3 shows the weight loss-time curve for mild steel corrosion without and with varying concentrations of ANP extract in 0.1 M H₂SO₄ at 303 K. From the figure, it is evident that the weight loss of mild steel increases with an increase in the period of contact but drops in the presence of the inhibitor when compared to the blank solution.

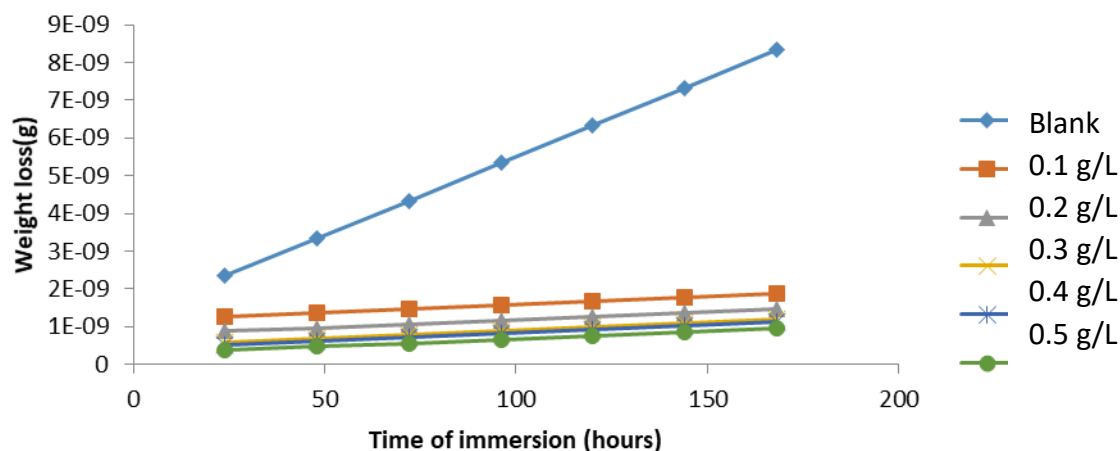


Figure 3: Effect of Immersion Time (hours) on Corrosion Rate of Mild Steel in 0.1 M H₂SO₄ in the Absence and Presence of ANP Extract at 303 K

It is also clear that weight loss reduces with a rise in inhibitor concentration, implying that the ethanol extract of ANP is an adsorption inhibitor for the corrosion of mild steel in H₂SO₄ and that the corrosion rates of mild steel and inhibition efficiency increase with a rise in the period of contact [13, 14].

Effect of temperature

The variation in corrosion rate of mild steel in 0.1M H₂SO₄ in the presence and absence of ANP extract inhibitor at different temperatures has been studied, and it is evident from Table 1 and the plot in figure 4 that the corrosion rate of

mild steel with or without extract increased with an increase in temperature. This finding is in agreement with the finding of E.E.Ebenso *et al.*(2010).

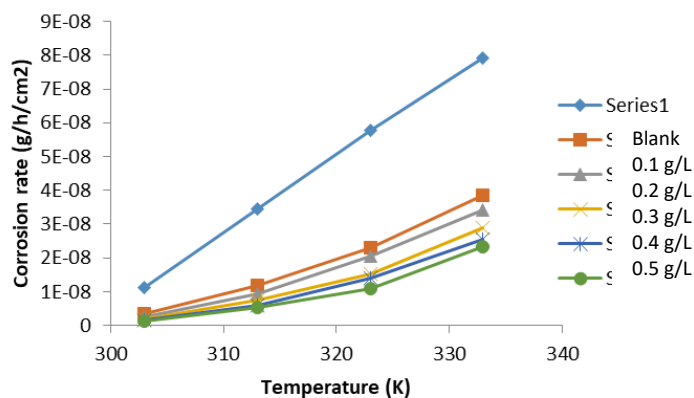


Figure 4: Variation of the corrosion rate of mild steel against temperature (303–333 K) in the absence and presence of different concentrations of ANP extract in 0.1 M H₂SO₄

This is due to the fact that as the temperature increased from 303 to 333 K, the rate of corrosion of the mild steel coupons also

increased as a result of the increasing average kinetic energy of the reacting molecules [15]. However, the corrosion rate is retarded in the



presence of the plant extract. The corrosion rate increases more rapidly with temperature in the absence of the extract. Two observations could be drawn from the result: (i) The mild steel surface is effectively damaged in the acidic medium [16], and (ii) ANP extract is a strong inhibitor for mild steel corrosion in 0.1M H₂SO₄ at a lower temperature. Furthermore, it is observed in Fig. 5 and Table 1 that the

inhibition efficiency of plant extract decreased with an increase in temperature for all concentrations of the inhibitor. This may be as a result of the increasing solubility of the adsorbed protective inhibitor barrier on the mild steel surface, thereby increasing the susceptibility of these coupons to dissolution in the acid media [12].

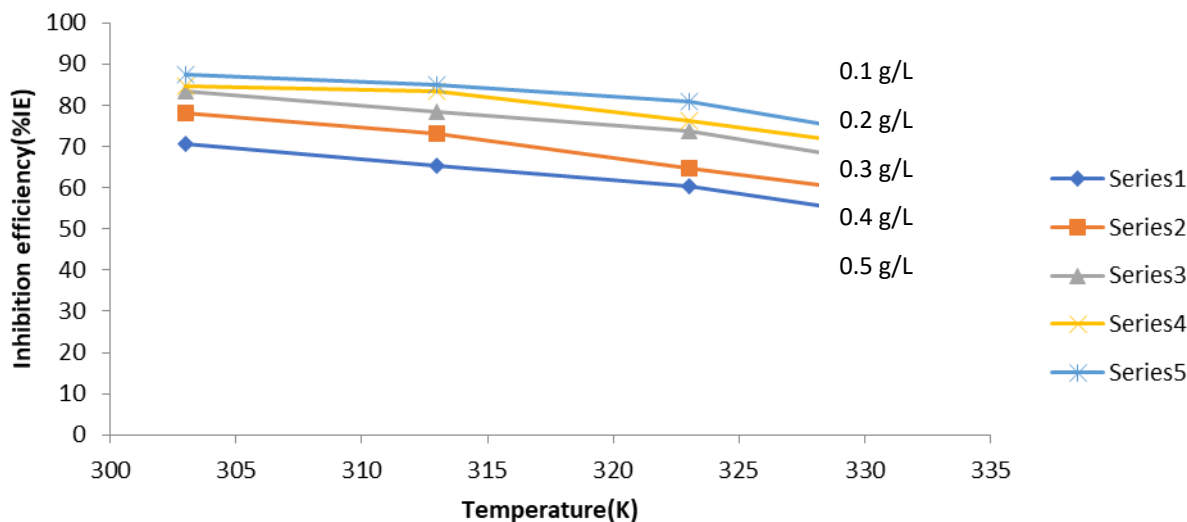


Figure 5: Variation of Inhibition Efficiency (%IE) Against Temperature for the Corrosion of Mild Steel in 0.1 M H₂SO₄ in the Presence and Absence of ANP Extract

Stability of the inhibitor

The stability of the ethanol extract of ANP for the corrosion of mild steel in H₂SO₄ (over a time range) was also studied by plotting values of inhibition efficiency versus the period of

contact, as shown in Figure 6. The plots indicate that at 303 K, the ethanol extract of ANP retained more than 87% of its inhibition efficiency even after 168 hours of immersion [9].



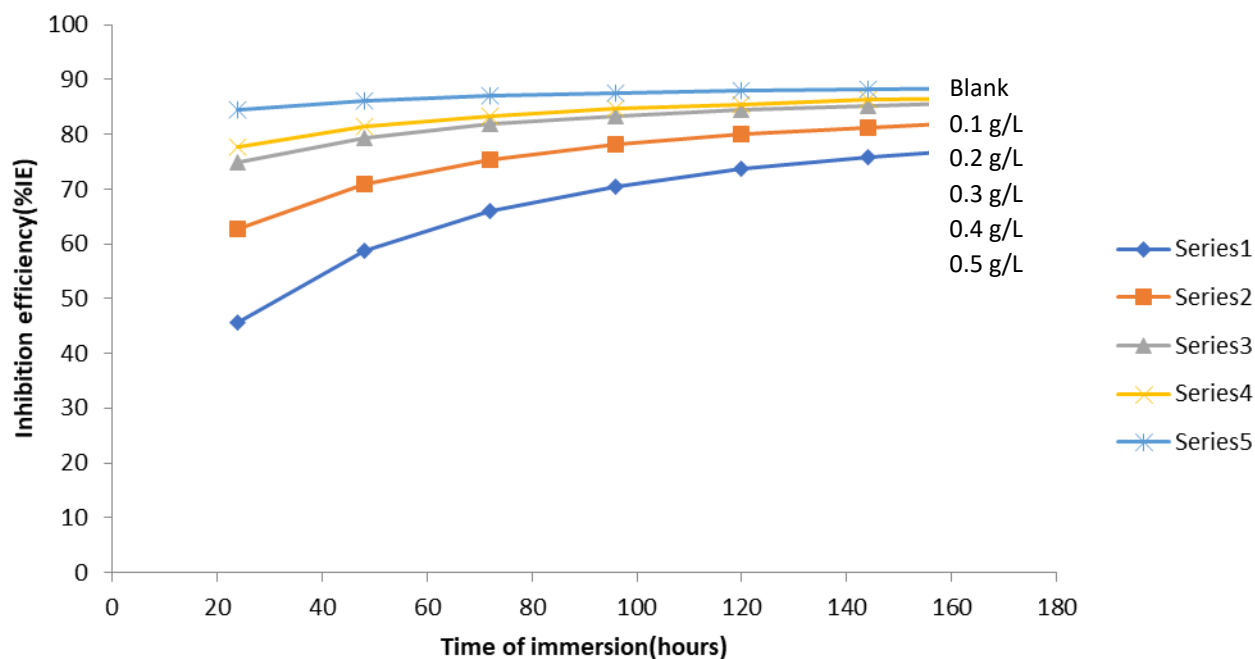


Figure 6: Effect of Immersion Time (hours) on Inhibition Efficiency (%IE) of ANP Extract on the Dissolution of Mild Steel in 0.1 M H₂SO₄ at 303 K

Surface Analysis

In Fig. 10b, the mild steel surface is highly damaged due to the effect of the acid on the surface, and in Fig. 10c, there is an improvement in the surface morphology, which shows a smooth surface when compared to the uninhibited surface.

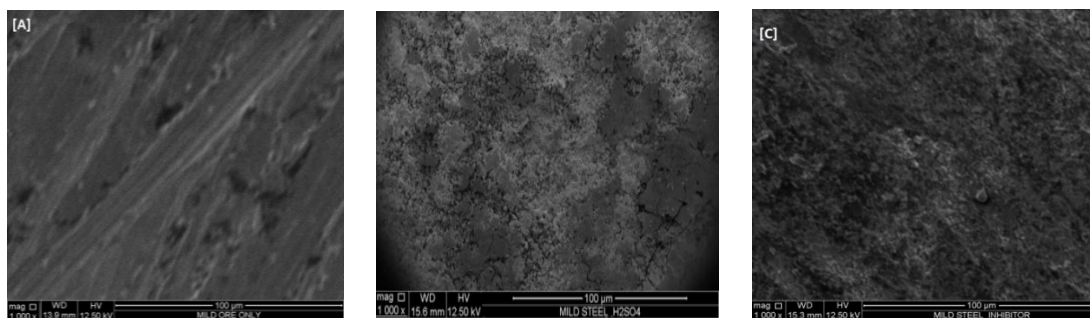


Figure 10: SEM micrographs of mild steel: (a) fresh mild steel; (b) without inhibitor; (c) with inhibitor

It is evident that the damaging effect of the acid on the mild steel is greatly reduced due to the protective layer of the adsorbed inhibitor that prevents corrosion caused by the acid attack on the mild steel surface. The smoothness of the mild steel surface in the presence of an inhibitor is due to the barrier of the protective film over the metal surface, which gives rise to more ordered corrosion products. This finding is in agreement with the finding of N.O.Eddy *et al.*(2009).

FTIR study

In order to further support the adsorption behavior of the inhibitor on the surface of mild steel, FTIR spectroscopy was employed. Fig. 11a shows the FTIR spectrum of the ethanol extract of ANP alone. Fig. 11b shows the FTIR spectrum of the corrosion product when an ethanol extract of ANP was used as an inhibitor.



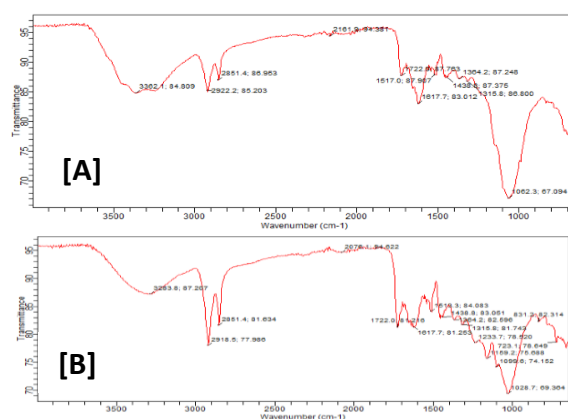


Figure 11: FTIR spectral of (a) ethanol extract of ANP and (b) corrosion product of mild steel in the presence of inhibitor.

Peaks and frequencies of FTIR adsorption for both spectra are presented in Table 6. From the results obtained, it is also evident that the C-O stretch at 1233.7 cm^{-1} was shifted to 1062.3 cm^{-1} , the -C=C- stretch at 1617.7 cm^{-1} was shifted to 1517.7 cm^{-1} , the C-H (Alkene stretch) was shifted from 2918.5 cm^{-1} to 2851.4 cm^{-1} , the aromatic C=O was shifted from 1722.0 cm^{-1} to 1722.8 cm^{-1} , the N=O (R-NO₂) was shifted from 1518.3 cm^{-1} to 1384.2 cm^{-1} and the phenolic-OH stretch was shifted from 3283.8 cm^{-1}

to 3362.1 cm^{-1} . These shifts in frequencies also indicate that there is an interaction between the inhibitor and the metal surface [17, 18, 19]. It is also evident from the data obtained that the C-O stretch at 1159.2 cm^{-1} as well as N=O (R-NO₂) at 1364.2 cm^{-1} were missing, suggesting that these bond frequencies might have been used for bonding between the vacant d-orbital of Fe and the inhibitor [16]. Therefore, ANLE was adsorbed onto the mild steel surface through these functional groups [20].

Table 6: Functional groups assigned to the adsorption of the ethanol extract of the pod and the corrosion product when the extract is used as an inhibitor

Ethanol extract			Corrosion product		
Wave No (cm ⁻¹)	Height	Assigned functional group	Wave No (cm ⁻¹)	Height	Assigned functional group
3283.8	87.207	O-H H-bonded	3362.1	84.809	O-H H-bonded
2918.5	77.986	C-H Alkene stretch	2851.4	86.953	C-H Alkane stretch
2851.4	81.634	C-H Alkene stretch	2922.2	85.203	C=O Aldehyde
1722.0	81.218	C=O Aldehyde	1722.8	87.783	C=O Aldehyde
1617.7	81.253	C=C Alkene	1517.7	83.012	C=C Alkene
1518.3	84.083	N=O Nitro (R-NO ₂)	1384.2	87.248	N=O Nitro (R-NO ₂)
1438.8	83.051	C-H -CH ₃ (bend)	1438.8	87.375	C-H -CH ₃ (bend)
1364.2	82.596	N=O Nitro (R-NO ₂)	-	-	-
1159.2	75.688	C-O stretch	-	-	-
1233.7	78.520	C-O stretch	1062.3	67.094	C-O stretch

4.0 CONCLUSION AND RECOMMENDATION

The results obtained from the study indicate that ANP extract effectively inhibited the corrosion of mild steel in 0.1 M H₂SO₄. Inhibition efficiency increases with increasing extract concentration and

immersion time and decreases with rising temperature. The inhibition potential of this inhibitor is attributed to the presence of phenol, tannin, alkaloids, and flavonoids in the extract. Hence, an increase in the reaction temperature of the medium will decrease the inhibition efficiency. In view of the above conclusion, the use of ethanol



extracts of ANP as green inhibitors is recommended.

5.0 REFERENCES

- [1] O.K. Abiola, N. C. Oforika, E. E. Ebenso, and N. M. Nwinuka (2007): Eco-Friendly Corrosion Inhibitors: Inhibitive Action of *Delonix Regia* Extract for the Corrosion of Aluminum in Acidic Medium *AntiCorrosion. Methods and Materials*. **54:4:219–224** (2007)
- [2] E. E. Ebenso, N. O. Eddy, and A. O. Odiongenyi (2008): Corrosion Inhibitive Properties and Adsorption Behavior of Ethanol Extract of *Piper Guinensis* as a Green Corrosion Inhibitor for Mild Steel in H₂SO₄. *African Journal of Pure and Applied Chemistry*, **2:11:107–115** (2008)
- [3] Bishir Usman, Hasmeriya Maarof, Hassan H. Abdallah, Rosmahida Jamaludin, Mohamed Noor Hasan, and Madzlan Aziz (2015): Theoretical and Experimental Studies of Corrosion Inhibition of Thiophen-2-Ethylamine on Mild Steel in Acid Media *Journal Teknologi (Science & Engineering)* **76:13:7–14** (2015)
- [4] E.E. Ebenso, D.A. Isabirye, and N.O. Eddy (2010): Adsorption and quantum chemical studies on the inhibition potentials of some thiosemicarbazides for the corrosion of mild steel in an acidic medium. *International Journal of Molecular Sciences*, **11: 24, 73–98** (2010)
- [5] I.B. Obot, S.A. Umoren, E.E. Ebenso, *et al.* (2009): The inhibition of aluminum corrosion in hydrochloric acid solution by exudate gum from *Raphia hookeri* *Desalination*, **250: 225–236** (2009)
- [6] E. E. Oguzie (2005): Inhibition of Acid Corrosion of Mild Steel by *Telfaria Occidentalis* Extract *Pigment and Resin Technology*, **34:6:321–326** (2005)
- [7] E. E. Oguzie, C. K. Enenebeaku, and C. O. Akalezi (2010): Adsorption and Corrosion-Inhibiting Effect of *Dacryodis Edulis* Extract on Low Carbon Steel Corrosion in Acidic Media. *Journal of Colloid Interface Sci.* 2010; **349: 283-292** (2010)
- [8] E.E. Oguzie (2006): Studies on the inhibition effect of *Occinum vivridis* extract on acid corrosion of mild steel *Materials Chemistry and Physics* **99:2–3: 441-446** (2006)
- [9] N.O. Eddy, S.A. Odoemelam, and A.O. Odiongenyi (2009): Inhibitive, Adsorption, and Synergistic Studies on Ethanol Extract of *Gnetum Africana* as Green Corrosion Inhibitor for Mild Steel in H₂SO₄. *Green Chemistry Letter Review*, **2:2:111–119** (2009)
- [10] I. B. Obot, N.O. Obi-Egbedi (2008): Fluconazole as an Inhibitor for Aluminum Corrosion in 0.1M HCl Colloids and Surfaces A: *Physicochem. Eng. Aspects*. **330: 207–212** (2008)
- [11] H. Momoh-Yahaya, N. O. Eddy, and E. E. Oguzie (2014): Inhibitive, Adsorptive, and Thermodynamic Study of Hypoxanthine Against the Corrosion of Aluminum and Mild Steel in Sulphuric Acid *Journal of Material and Environmental Science* **5:1: 237–244** (2014)
- [12] P.C. Okafor, E.E. Ebenso (2007): Inhibitive Action of *Carica Papaya* Extracts on the Corrosion of Mild Steel in Acidic Media and Their Adsorption Characteristics *Pigment Resin Technology*, **36 (3), 134–140** (2007)
- [13] P.M., Niamien H. A. Kouassi, A. Trokourey, F. K. Essy, and Odiongenyi (2009): & Y. Bokra (2011): *African Journal of Environmental STechnology*, **5:9:641 (2011)641(2011)**
- [14] N.O. Eddy, A. Steven, Odoemelam, O. Anduang, Odiongenyi.(2009): *Green Chemistry Letters and Reviews*,; **Vol.2** No.2, 111-119(2009)
- [15] Li X; S Deng; H Fu; and T Li (2009): *Electrochemical Acta*, **54, 4089** (2009)
- [16] M. A. Quraishi, A. K. Singh, and Piroxicam (2010): A Novel Corrosion Inhibitor for Mild Steel Corrosion in HCl Acid Solution *Journal of Material & Environmental Science* **1:2: 101–110** (2010)
- [17] N. O. Eddy, P. A. Ekwumengbo, and P. A. P. Mamza (2009a): Ethanol extract of *Terminalia catappa* as a green inhibitor for the corrosion of mild steel in H₂SO₄. *Green Chemistry Letters and Review*, **2:4:223-231 (2009a)**
- [18] N. O. Eddy, U. J. Ibok, and E. E. Ebenso (2009b): Adsorption, synergistic inhibitive effect, and quantum chemical studies on ampicillin and halides for the



corrosion of mild steel, *Journal of Applied Electrochemistry*, 2009b. DOI: 10.1007/s10800-009-0015-z

[19] E. S. Ferreira; C. Giancomelli; F.C. Giancomelli; and A. Spinelli (2004): Evaluation of the inhibitory effect of ascorbic acid on the corrosion of mild steel, *Materials Chemistry & Physics*, 83: 129–134 (2004)

[20] N.O. Eddy and A. Femi (2018): Experimental and Quantum Chemical Studies on Ethanol Extract of *Phyllanthus amarus* (EEPA) as a Green Corrosion Inhibitor for Aluminum in 1M HCl *Portugaliae electrochimica acta*.36:4:231-247 (2018)

[21] B. Usman, A.S. Mohammed, and A. B. Umar (2018): Quantum Chemical Evaluation on Corrosion Inhibition Performance of Balanitin-7 on Mild Steel in 1 M Hydrochloric Acid Solution *Appl. J. Envir. Eng. Sci. 4 N°3*. 380–386 (2018)

[22] Mohammed Shaib Auwal (2014): Preliminary phytochemical and elemental analysis of aqueous and fractionated pod extracts of *Acacia nilotica* (Thorn mimosa). *Vet.Res.Forum*.2014 Spring: 5(2):95-100.



P027 - EFFECT OF PROCESS VARIABLES ON METHYL ESTER PRODUCTION USING CHITOSAN AS HETEROGENEOUS CATALYST

*Akor, I. H.; *Adams P.O.; *Adekunle, I.J.

*Chemical Engineering Department, Confluence University of Science Technology, Osara, Nigeria
Contact: hillaryai@custech.edu.ng

ABSTRACT

Recently more attention has been channelled towards exploitation of Biodiesel owing to the world's crude oil reserve depletion coupled with the consumption rate, increase in greenhouse effect and its scarcities. This has lift-up issues related to its conservation and eco-friendly which brought about renewed interest in the use of bio-based substances. This research work was targeted at producing biodiesel using Chitosan as heterogeneous catalyst; this heterogeneous catalyst is promising for the Transesterification reactions of vegetable oils due to its economic benefits. More so, it is environmentally benign and could be operated in continuous processes (reused) unlike homogeneous catalysts. Chitosan was prepared from Deacetylation of chitin after which it was then used as a catalyst in the Transesterification reaction of melon seed oil with methanol. The effects of reaction time (45 to 105 min), methanol/fatty acid molar ratio (1.5:1 to 7.5:1), reaction temperature (55 to 70°C) and catalyst concentration (0.25 to 1.25 wt%) on the biodiesel production were studied. From the response surface model result, it was indicated that the highest yield (94%) was obtained at 60°C with 1 wt% catalyzed for 90 mins and molar ratio of 6:1 which was at a high concentration of catalyst (1% wt%), while the lowest result was obtained at lower concentration of the catalyst (0.25 wt%). Based on the results obtained from the characterization of this biodiesel and comparing with relevant standard, it proved that Chitosan maintained sustainable activity and shows a good quality of being used as a heterogeneous catalyst.

KEYWORDS

Biodiesel, Chitosan, Deacetylation, Transesterification.

1.0 INTRODUCTION

Power is the ability, strength or capacity to do work, where work is the vitality exacted within a specified direction. The desire of mankind to do work requires energy; this energy can exist in several forms: heat energy, mechanical energy, electrical energy and chemical energy, for where work is being done energy is being consumed or converted (Khurmi, 2011). To satisfy this craving of humanity, the quest for energy resources sets in, this led to the use of substances that has the potential of generating the required energy. Materials which have these properties that were found and used from time memorial are the mineral oil, vegetable oil and animal fats (Nie, 2012). Initially, pure vegetable oil was used to run the engine which had a major problem of high-fuel viscosity in compression ignition engines. Considering this problem attention was then channelled to those from the mineral oil (Diesel fuel), which were able to perform better than the pure vegetable oil (Udone, 2010).

Diesel fuel is thick oily fuel that is obtained from the distillation of petroleum. It has an ignition point of 540 and is ignited by the heat of compression. Globally, mineral oil has being of higher usage in

chemical industries to that of the vegetable oil and animal fats prior to its good burning properties of fuel viscosity, ignition temperature, cetane number and diesel index (Ejikeme *et al.*, 2011). This implies that more of it is consumed universally and it has also affected the biosphere (greenhouse effect) tremendously through the emission of harmful gases into the atmosphere mostly sulphur and carbon. Since more of it is being used, more of it is being released into the atmosphere, thereby creating public awareness for pollution free environment and also legislating of regulation guiding its disposal (Piyush *et al.*, 2006). Due to the increasing energy demand and a continual usage of mineral oil, an alternative source of this mineral oil has to be supplemented with similar properties as that of the mineral oil and biodegradable for easy disposal, meet its requirement. This calls for the production of biodiesel (Roknuzzaman, 2009).

Biodiesel are vegetable oil or animal fat-based diesel fuel consisting of long-chain alkyl substances which are both biodegradable and nontoxic for human/aquatic environment, associated with the use of vegetable oil and animal fats as its major feed stocks combing it with additives or through chemical modification like esterification, hydrogenation and Transesterification (Alamu *et*



al., 2009). This oil consists of a triglyceride which contains three fatty acids and a glycerol molecule. The instability and high-fuel viscosity of the oil can be significantly improved by converting natural fatty acyl ester into synthetic esters (Nie, 2012). The production of Biodiesel is seen as the Transesterification of the oil with alcohol, which requires the removal of the glycerol back bone from the oil and replacing it with ethyl group in the presence of a catalyst. The catalyst for this reaction are what categorises the reaction either acid or alkali homogenous catalyst. When acid catalyst is used it requires longer reaction time and also produces a lower yield of methyl ester (biodiesel) while when a base catalyst is used, it mostly reacts with the free fatty acid to form soap and in a two-step reaction process it incur more cost on production (Nie, 2012). More also using a homogenous catalyst creates the problem of catalyst recovery.

The best alternative in replacing the problem of these homogenous catalysts is the heterogeneous catalyst. Many types of heterogeneous solid catalysts such as metal oxides of MgO, CaO, SrO,

metal compounds supported on alumina or Zeolite, hydrotalcites, and unmodified egg shell have been studied (Olutoye *et al.*, 20011) and Chitosan also has been seen to have related properties as those of the heterogeneous catalyst by being biodegradable, non-toxic and catalyst recovery and also a renewable catalyst (Knorr, 2004). Chitosan is an organic natural polymer obtained by Deacetylation of chitin. After cellulose chitin is the second most abundant polysaccharide in nature. It is biologically safe, non-toxic, biocompatible and biodegradable polysaccharide; it is a major component of the shells of crustacean such as crab, shrimp, and crawfish. Chitosan has wide range of application in pharmaceutical, cosmetics, food preservatives, biocatalysts, waste water treatment processes and many others. Therefore, this present study focused on investigating the use Chitosan as heterogeneous catalyst in biodiesel production (No and Meyers, 1999).

The stoichiometry of the Transesterification reaction shows that one mole of triglyceride reacts with three moles of the alcohol and the reaction is reversible in the presence of the catalyst.

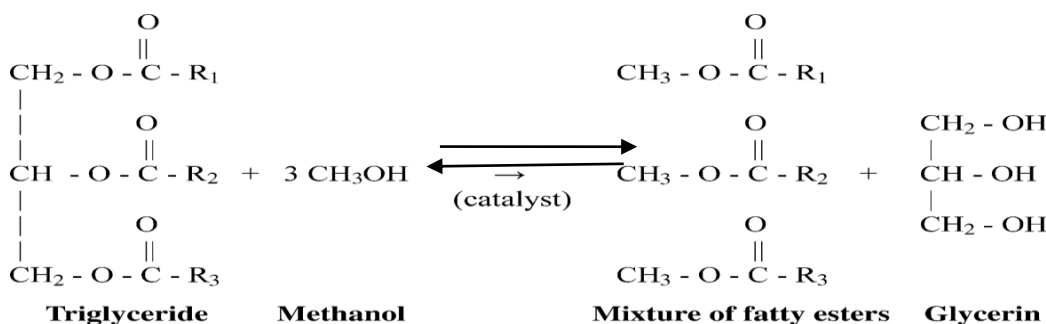


Fig. 1. The Transesterification reaction for biodiesel (Source: Jon, 2005)

The triglyceride is at first converted into diglyceride, then monoglyceride and finally glycerol in a stepwise manner.

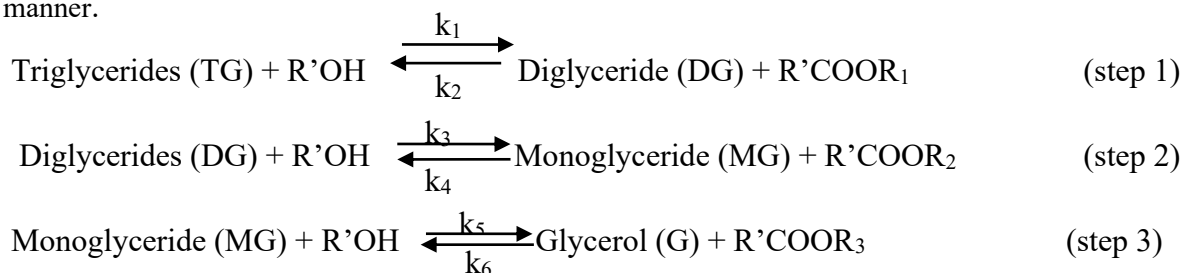


Fig. 2. The step wise process for Transesterification reactions for biodiesel

2.0 METHODOLOGY

Osteoglosid fish scales used in this study were obtained from Mobile fresh fish market, Minna Niger state. The pellet of NaOH was bought from

Minna Niger state and also the Hydrochloric acid (HCl) was given to me as gift from Mr Bullus of WAFT Department School of Agric. Federal university of technology, Minna. The Distilled water used was gotten from WAFT department as



well. Melon oil was purchased from Suleja Niger state while the methanol was obtained from Mobil chemical market, Niger state. Pellet of NH_3Cl was obtained from WAFT Dept. FUT Minna, and all other reagents used were of analytic purpose unless stated otherwise.

2.1 Synthesis of Chitosan

Chitosan is prepared by hydrolysis of acetamide groups of chitin. This is normally conducted by rigorous alkaline hydrolysis treatment due to the resistance of such groups imposed by the Trans arrangement of the C2-C3 substituent in the sugar ring. The block diagram below shows the step-by-step process involved in the process.

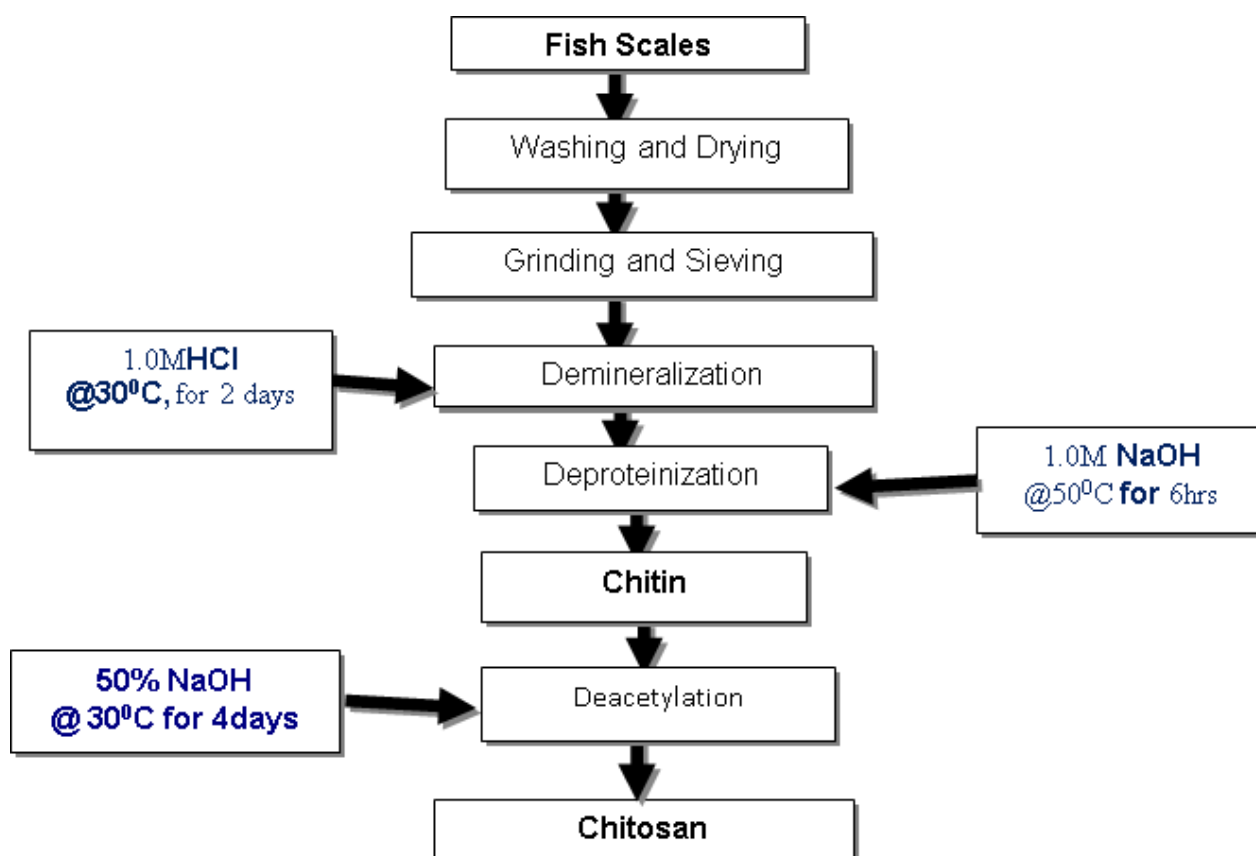


Fig. 3. Manufacturing process for Chitin and Chitosan

weighed into the beaker containing methanol and stirred in order to allow the activated Chitosan pellet to be absorbed into a solution. The solution was added to the oil and stirred with a Water bath (stirrer) for some period of time and temperature. The separation of the product was carried out with the aid of gravity settler (separating funnel) for few hours; this is clearly shown in figure 3.2. Two

2.2 Production of Methyl Ester

The presence of low content of free fatty acid in the crude melon seed oil makes the production of methyl ester undergo a single-step catalyzed Transesterification. The two-step catalyzed acid catalyzed Transesterification is meant for treatment process of content where the free fatty acid in the oil is high followed by the base catalyzed Transesterification which will then convert the oil to methyl esters of fatty acid. In the single-step catalyzed Transesterification, the catalyst is applied without pre-treating the oil. The oil was measured and poured into a flask, Methanol was also measured into a different beaker and certain percentage of the activated Chitosan catalyst as shown in table 3.3 was

layers were not clearly seen, like the case of homogenous catalyst but rather three different regions were formed; the MOME, the Glycerol and the Catalyst. Water at 45 °C was passed through the sample; this was done in order to allow excess catalyst, soluble material and other impurities to be separated from the MOME. The mixture of the MOME and water was separated into two beakers.



The separated MME was heated above 100 °C and it was held for 15 to 20 minutes so as to ensure the water evaporated.

Table 1. Variance of variable for response surface model

Factor	Lower axial level ($-\alpha$)	lower	Centre	Upper	Upper axial level ($+\alpha$)
Temperature($^{\circ}$ C)	55	60	65	70	75
Reaction time (Min)	45	60	75	90	105
Catalyst conc. (wt %)	0.25	0.5	0.75	1	1.25
Molar ratio	1.5	3	4.5	6	7.5

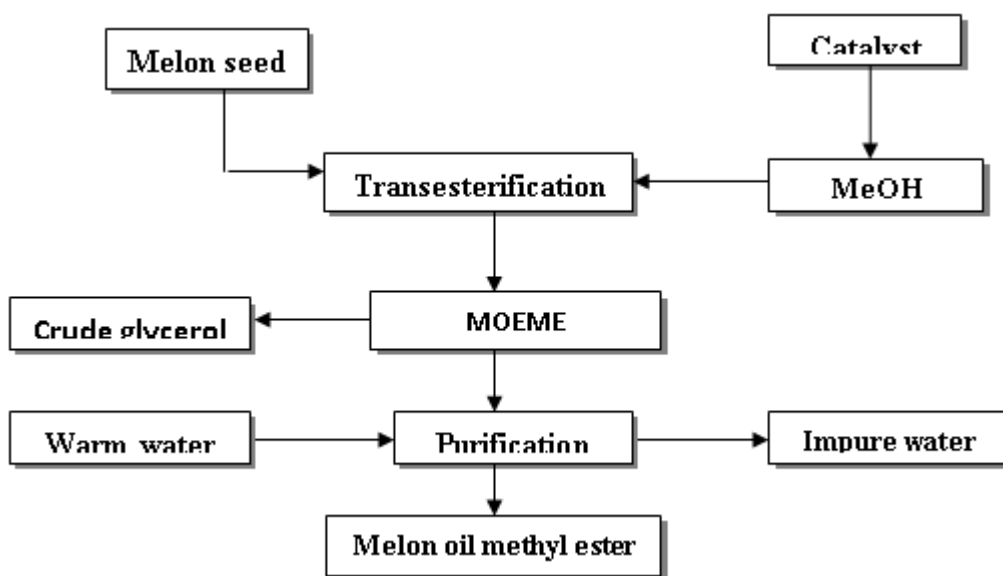


Fig.4. Flow diagrams illustrating the production of biodiesel from melon seed oil.



2.3 Analysis on melon oil and Methyl Ester

In this research several characteristic tests (Saponification value, specific gravity, ash content, moisture content, protein content, lipid content, crude fibre, carbohydrate content, Viscosity, pH) were performed on the adhesive extracted in accordance with Association of Official Analytical Chemistry method (AOAC, 1990) on the performance of an adhesive. More so, instrumental

analysis like Fourier transforms infrared (FTIR) was carried out to know the presences of functional groups in the samples at respective wave number using the Infrared Spectrophotometer,

3.0 RESULTS AND DISCUSSION

After the demineralization and the Deproteinization of the fish scales, the percentage composition of the scales was calculated as shown in Table 2 below.

Table 2. Chitin and Chitosan composition in fish Scales

Component	Experimental % Composition	Aguzue <i>et al.</i> , (2011) % Composition	Entsar <i>et al.</i> (2006) % Composition
Chitin	62.18	-	54.26
Chitosan	17.82	20.49	-

These results is seen to contain low amount of Chitosan compared to 20.49 % recorded by Aguzue *et al.*, 2011, and high amount of Chitin as compared to 54.26% recorded by Entsar *et al.*, 2006, this may

be attributed to the mineral composition of the area, as composition varies with the area of the retrieved source. This imply that, it is in different percentages depending on the place (Muzzarelli, 1997).

3.1 Analysis on Chitosan from fish scales

Table 3. Proximate analysis on Chitosan from fish scales

Parameters	Experimental Composition (%)
Moisture	6.40
Ash	5.42
D.D	51.34
Protein	3.07
Lipid	1.79
Carbon/nitrogen ratio	5.97
Carbohydrate	77.40

Table III shows the results obtained from this analysis. Moisture content is a measure of the amount of water molecule present in a sample at normal or atmospheric temperature and pressure. The mean moisture content of the Chitosan sample as shown in Table was 6.4%. According to Li (1992), it was stated that commercial Chitosan products contain <10% moisture content. This shows that the 6.4% obtained is still within the

range. As was earlier stated, Ash content measurement is an indicator of the effectiveness of the demineralization (DM) step (Bough *et al.*, 1978). The sample gave a rather high ash content of 5.4% which is still less than 31 – 36% for the case of absence of demineralization step. It was reported that values less than 10% of ash content are graded as good quality of Chitosan (No *et al.*, 1995).



Protein content of the Chitosan sample from the result was 3.07% and can be attributed to the low degree of Deacetylation of the chitin. Extended heating time and high alkali concentration can be applied to drastically improve the degree of Deacetylation hereby reducing the Protein content.

Degree of Deacetylation (DD) being one of the main parameters used in characterizing Chitosan, which shows the level of acetyl groups removed from the molecular chain of chitin, leaving behind the compound (Chitosan) with a high degree chemical reactive amino group (-NH₂). The result shows degree of Deacetylation of Chitosan to be

51.34% which lies within the range of 50% to 99% as recorded by Meyers, (1995).

3.2 Scanning Electron Microscopy of Chitosan sample

The surface morphology of Chitosan was observed using SEM, Figure V shows the scanning electron micrographs of Chitosan from fish scale source. As seen, the surface appearance depends on the type of crustacean concerned and also be attributed to the mineral composition of the area, as composition varies with the area of the retrieved source (Muzzarelli, 1997).

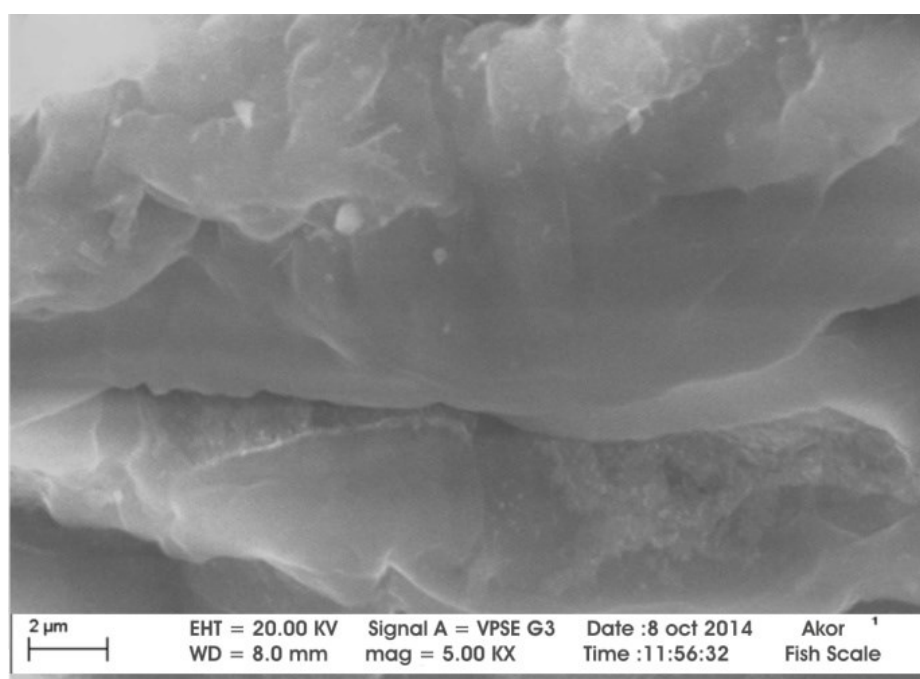


Fig. 5. SEM morphology of Chitosan from fish scale

The surface of Chitosan from scale in Figure V above shows scarcely fibril material and granular structure. A very uniform structure with a lamellar organization and less dense structure was observed clearly for this Chitosan, Which is similar to that reported by Aguzue *et al.*, (2011).

3.3 X- Ray Diffraction (XRD) analysis for Chitosan

The XRD pattern of the sample shows the Crystalline of Chitosan obtained from fish scale, which represents the structural arrangement of the samples. This is shown in Figure 6 below.



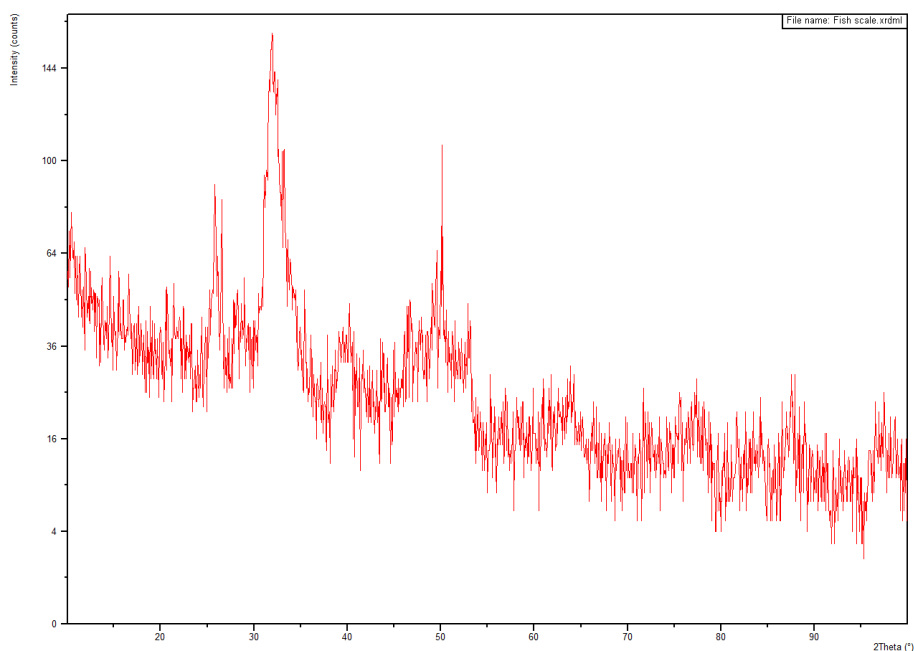


Fig. 6. X - ray diffraction (XRD) analyses for Chitosan from fish scale

The result pattern of the sample seen in figure VI shows that, five major crystalline reflections were observed in the 2θ range of 0 to 100° the peak intensities for the maximum and minimum peak are 42.57 and 150 respectively, at the position of 25.8534 and 31.8385 [$^\circ 2\theta$.], with weight of 0.3956 and 0.5274 [$^\circ 2\theta$.]. Aguzue *et al.*, (2011) reported that the XRD pattern of the fish scale sample used gave five crystalline reflections in the 2θ range of 10 to 60° and the peak intensities were 7.81, 50.95, 100.00, 98.52 and 21.22 at that 2θ range respectively while Zhang *et al.*, (2005) reported the

3.4 Properties of melon seed oil FAME

From the result obtained, it shows that the acid value of this melon seed oil is low and moderate with a value of 2.5245 mg/KOH, which is higher than the value reported by Giwa *et al.*, (2010). More so, Ejikeme *et al.*, (2010) reported 2.08 mg/KOH which is also slightly lower than the value obtained. This can be as a result of the fact that the oil were obtained from different source.

peak intensities as 16.775, 25.847, 31.772, 32.3102 and 34.1056 respectively.

The degree of Deacetylation been one of the major parameters which significantly influence the crystal structure of chitin and Chitosan (Kumirska, 2001); it has been reported by Wada and Saito that the level of treatment with HCl and NaOH also affects the rate of its crystalline. Figure V and VI shows that Chitosan has both crystalline and amorphous regions in the structure (Struszczyk, 1987).

Since the acid value of this melon seed oil was low the free fatty acid was also obtained to be low owing to the fact that it is half of the acid value.

Table 4. Physiochemical properties of melon seed oil

Property	Experimental Value	Giwa <i>et al.</i> , 2010. Value	Ejikeme <i>et al.</i> , 2010. Value
----------	--------------------	----------------------------------	-------------------------------------



Pour point ($^{\circ}\text{C}$)	-5.0000	-	-
Iodine value ($\text{gI}_2/100\text{g}$)	118.8000	114.4600	121.80
Flash point ($^{\circ}\text{C}$)	155.0000	-	186
Density at 25°C (g/ml)	0.9224	0.905.3	-
Kinematic viscosity (Cp)	19.7100	31.52	33.29
Specific gravity	0.91840	-	0.9138
Saponification value (mg KOH/g)	164.0925	204.44	192.500
Acid value (mg KOH/g)	2.5245	0.98	2.080
Free fatty acid (%)	1.26225	0.49	1.040
Ester value (mg KOH/g)	162.8303	-	-
Molecular weight (g/mol)	869.2000	-	-

3.5 Response from melon seed oil FAME production

The tables V shows effectiveness of the Chitosan catalyst produced and other factors like temperature, time and molar ratio where varied to obtain a good yield. From the result, it was indicated Statistical that the highest yield (94%) was obtained at 60°C with 1% m/m catalysed for 90mins and molar ratio of 6:1 which was at a high concentration of catalyst (1% m/m), while the lowest result was obtained at lower concentration of the catalyst (0.25% m/m). Chitosan maintained sustainable activity and shows a good quality of being used as a heterogeneous catalyst.

3.5.1 Flash point

The flash point of a fuel is that minimum temperature at which it will ignite when exposed to an ignition source (Ejikeme *et al.*, 2010). It measures the flammability of a fuel or its tendency to form a flammable mixture with air. From the analysis on table 4.6, the flash point of the methyl ester produced was found to be 160°C which is greater than the minimum standard specified by

ASTM D6751 (130°C) and this is very close to the value reported by Giwa *et al.*, (2011).

3.5.2 Density

The density of a substance is the ratio of its mass to volume at a given temperature condition. From the result obtained, the density was found to be 0.8540g/ml which is slightly lower than the limit specified by EN14214 as 0.86 g/ml . But Ejikeme *et al.*, (2010) reported a value of 0.8329 g/ml , which appears to be closer to the experimental value. The slight difference can be as a result of catalyst variation.

3.5.3 Kinematic Viscosity

Kinematic Viscosity is an important property that determines the flow property of fuel. The viscosity of biodiesel is normally lower than the viscosity of its raw vegetable oil or animal fat, and for this very reason it is considered an alternative fuel instead of animal or vegetable oil. The viscosity of the methyl ester produced here was found to be 5.97 cp and is slightly higher than the limit specified by EN14214 as 5.0cp . Aransiola *et al.*, (2013) reported 6.10 cp which is even higher than the specified value by EN14214.

Table 5. Response from melon seed oil FAME production

Run No.	Factor1: Temperature ($^{\circ}\text{C}$)	Factor 2: Reaction Time(Min)	Factor3: Catalyst Conc. (wt %)	Factor4: Molar Ratio	Response (wt %)
1	-1	-1	-1	-1	60
2	+1	-1	-1	-1	72
3	-1	+1	-1	-1	76
4	+1	+1	-1	-1	74
5	-1	-1	+1	-1	78



6	+1	-1	+1	-1	79
7	-1	+1	+1	-1	84
8	+1	+1	+1	-1	80
9	-1	-1	-1	+1	89
10	+1	-1	-1	+1	81
11	-1	+1	-1	+1	88
12	+1	+1	-1	+1	82
13	-1	-1	+1	+1	87
14	+1	-1	+1	+1	89
15	-1	+1	+1	+1	94
16	+1	+1	+1	+1	90
17	- α	0	0	0	68
18	+ α	0	0	0	74
19	0	- α	0	0	69
20	0	+ α	0	0	72
21	0	0	- α	0	0
22	0	0	+ α	0	86
23	0	0	0	- α	52
24	0	0	0	+ α	89
25	0	0	0	0	70
26	0	0	0	0	74
27	0	0	0	0	69
28	0	0	0	0	70
29	0	0	0	0	72
30	0	0	0	0	68

Table 6. Physiochemical properties of MSOFAME

Property	Experimental Value	Giwa <i>et al.</i> , 2010. Value	Ejikeme <i>et al.</i> , 2010. Value	Aransiola <i>et al.</i> , 2013). Value
Pour point ($^{\circ}$ C)	-5.0000	-	-	-
Iodine value (gI ₂ /100g)	118.8000	-	115.5	119.0
Flash point ($^{\circ}$ C)	160.0000	156	167	145
Density at 25 $^{\circ}$ C (g/ml)	0.8540	-	0.8329	0.8900
Kinematic viscosity (Cp)	5.97	6.24	-	6.10
Specific gravity	0.8559	-	0.8347	0.892
Saponification Value	169.056	192.450	-	180
Colour	Clear yellow	-	Clear yellow	Clear yellow

3.5.4 Heat of combustion

The heat of combustion was computed from the correlation given by Demirbas, (1998). The iodine

value and the saponification value were substituted into equation 3.11 to obtain the empirical value.



$$\begin{aligned} \text{HC} \\ = 10049.43 - 0.015IV \\ - 0.041SV \end{aligned} \quad (3.11)$$

3.6 Performance

Biodiesel rating is based upon engine performance which is a function of certain parameter like higher cetane number, higher combustion efficiency, higher lubricity, lower sulfur and aromatic content. Cetane number as high as 74.5 and above is obtainable with biodiesel and this means good ignition quality (Knothe, 2005). Other merits of biodiesel are its portability (ease of transportation and storage), ready availability and its potential for reducing petroleum dependency and energy security (NBB, 2009; Giwa *et al.*, 2010; Garpen, 2004).

4.0 CONCLUSION

In the study, the following conclusions were drawn: The Adhesive was successfully extracted from

REFERENCES

Acharya, S. K., Mishra, P., & Mehar, S. K. (2011). Effect of surface treatment on the mechanical properties of bagasse fiber reinforced polymer composite. *BioResources*, 6(3), 3155–3165.

Anbu, C. J., Dato, Y. B., & Nordin, B. Y. (2009). Particleboards from Rice Husk. *A Brief Introduction to Renewable Materials of Construction*.

ANSI. (2009). *American National Standards Institute, A208.1-2009, Composite Panel Association, 19465 Deerfield Avenue, Suite 306, Leesburg, VA 20176, USA*.

AOAC. (1990). *Association of Official Analytical Chemistry. Official Methods of AOAC International, 14th Edition, Gaithersberg, MD, USA*.

Azumah, O. K. (2014). Production of Particleboard Using Sawdust and Plastic

Cissus populnea plant studying the effect of process parameters via RSM and the optimum yield (84%) was obtained at 75°C with 40g sample dosage at 90mins for fresh sample, while the lowest yield (60%) was obtained at 85°C with 50g sample dosage at 30mins from dried sample using Ethyl acetate as extraction solvent respectively. Comparative study on the yield of the Adhesive obtained from different Samples (fresh and dried) shows higher percentage of adhesive in fresh sample to dried sample. From the Characterization of the Adhesive using Fourier Transform Infrared Spectroscopy (FT-IR), shows the presence of carboxylic group in the substance at similar stretching with literature. From the Characterization of Particleboard, it was indicated that sample J has the best MOE of 410 N/mm², MOR of 19.04 N/mm², with an average density of 1013kg/m³ respectively. Hence, the particleboard produced shows similar mechanical and physiochemical properties with the conventional boards and its mechanical properties met the LD-1 requirement of ANSI A208.1 Standards.

Waste. *Kwame Nkrumah University of Science and Technology College of Agriculture and Natural Resources Faculty of Renewable Natural Resources, Department of Wood Science and Technology*.

Chen, H. C., Chen, T. Y., & Hsu, C. H. (2006). Effects of wood particle size and mixing ratios of HDPE on the properties of the composites. *Holz Roh Werkst*, 64, 172–177.

Cuthbert, M. F. (2014). Analysis of energy characteristics of rice and coffee husks blends. *International Scholarly Research Notices*.

DIN EN 312. (2010). *German Institute for Standardization. Particleboards and fibreboards Specifications*.

Hanninen, T., Rautkari, L., Hautamaki, L., & Altgen, M. (2020). The effect of diammonium phosphate and sodium silicate on the adhesion and fire properties of birch veneer. *Holzforschung*, 74(4), 372–381.



Huang, J., & Li, K. (2016). Development and characterization of a formaldehyde-free adhesive from lupine flour, glycerol, and a novel curing agent for particleboard (PB) production. *Holzforschung*, 70(10), 927–935.

Indah, R., Nurfika, R., Karim, A., & Musrizal, M. (2018). Modifying Of Particle Boards From Rice Husk and Pinus Merkusii Sawdust And Using Soybean Waste Waters Based Adhesive. *2nd International Conference on Science (ICOS), Makassar, Indonesia*, 279.

Iwe, M. O., Obaje, P. O., & Akpapunam, M. A. (2004). Physicochemical Properties of Cissus Gum Powder extracted with the aid of Edible Starches. *Plant Foods for Human Nutrition*, 59, 161–168.

Jamaludin, K., Jalil, H. A., Jalaludin, H., Zaidon, A. A., Latif, M. M., & Nor, M. Y. (2001). Properties of Particleboard Manufactured from Commonly Utilized Malaysian Bamboo. *Pertanika J. Trop. Agric. Sci*, 24(2), 151–157.

Li, X., Cai, Z., Winandy, J. E., & Basta, A. H. (2010). Selected properties of particleboard panels manufactured from rice straws of different geometries. *Bioresource Technology*, 101(12), 4662–4666.

Loh, Y. W., H'ng, P. S., Lee, S. H., Lum, W. C., & Tan, C. K. (2010). Properties of Particleboard Produced from Admixture of Rubberwood and Mahang Species. *Asian Journal of Applied Sciences*, 3, 310–316.

Mohanty, B. N., Sujatha, D., & Uday, D. N. (2015). *Bamboo Composite material: Game -*

changer for developing economies. 10th World Bamboo Congress, Korea 2015.

Olutayo, A. A., Mbang, N. F., Michael, A. O., & Tolulope, O. A. (2019). Evaluation of Cissus populnea gum as a directly compressible matrix system for tramadol hydrochloride extended-release tablet. *Department of Pharmaceutics and Pharmaceutical Technology, Olabisi Onabanjo University, Ago Iwoye, Nigeria*.

Owofadeju, F. K., & Alawode, A. O. (2016). Evaluation of Vetiver (*Vetiveria nigriflora*) plant extract as eco-friendly wood preservative. *Arid Zone Journal of Engineering, Technology and Environment*, 12, 49–57.

Oyedemi, T. I. (2012). Characterization of Fuel Briquettes from Gmelina Arborea (Roxb) Sawdust and Maize Cob Particles Using Cissus Populnea Gum as Binder. *Department of Agricultural and Environmental Engineering, University of Ibadan*.

Pike, R. (2013). Adhesive. *Encyclopædia Britannica Online*. Encyclopædia Britannica Inc. Retrieved 9 April.

Topbaşı, B. (2013). *The examination of mechanical and physical properties of particleboard produced from waste banana peel*. Institute of Science, Süleyman Demirel University, Isparta, Turkey.

Yang, T. H., Lin, C. J., wang, S. Y., & Tsai, M. J. (2007). Characteristics of particleboard made from recycled wood-waste chips impregnated with phenol formaldehyde resin. *Building and Environment*, 42(1), 189–195.



P028 - BIOGENIC SYNTHESIS AND CHARACTERIZATION OF SULPHUR NANOPARTICLES FROM SULPHUR-RICH AGRORESIDUES (ONION AND CABBAGE PEELS)

Hauwa Salisu Usman*, Ibrahim Yusuf Sani, Aliyu Salihu, Abdullahi Balarabe Sallau

1. Department of Biochemistry, Ahmadu Bello University, Zaria, Nigeria.

*Corresponding Author's E-mail: ummisa71@gmail.com

ABSTRACT

Biogenic synthesis of sulphur nanoparticles (SNPs) is an efficient, one pot synthesis and eco-accommodating approach, discarding the need for intervention of noxious and perilous additives. In the present study, SNPs were synthesized in a single step process adopting a green method using onion peels. Biosynthesized SNPs were characterized using UV/Visible Spectroscopy and Fourier Transform Infrared Spectroscopy (FTIR) while Dynamic Light Scattering (DLS) Spectroscopy revealed the size and intensity of the nanoparticles. Results obtained from this study revealed an absorption spectrum at 267 nm by onion peels; a characteristic of SNPs formation. However, there was no clear distinct peak indicating formation of SNPs using cabbage peels. FTIR spectra of SNPs and control (onion peel extract) exhibited broad intense peaks at 1028.1 cm^{-1} and 1005.7 cm^{-1} , respectively, indicating a marginal shift and presence of flavanones (polyphenols) adsorbed on the surface of the nanoparticles. DLS Spectroscopy results showed dimension of nanoparticles within the range of 40 to 100nm. Onion peel nanoparticles have the potential for bulk synthesis of SNPs for wide range application in biomedical, cosmetics and environmental sectors.

KEYWORDS

Biogenic-synthesis, Sulphur-nanoparticles, Agro-residues, Onion-peels, Characterization.

1.0 INTRODUCTION

In recent years, nanoparticles synthesis using biological systems aimed at improving various biomimetic engineering methodologies has attracted huge interest in the scientific community. Materials are defined as nanomaterials if their size or one of their dimensions is in the range of 1 to 100 nm. The history of nanomaterial utilization is ancient, and human beings used these materials a long time ago for various applications, unknowingly. About 4500 years ago, humans exploited asbestos nanofibers to reinforce ceramic mixtures (1).

The ancient Egyptians were familiar with PbS nanoparticles about 4000 years ago and used them in an ancient hair-dyeing formula (2, 3).

The research and development of nanoparticles (NPs) have been explosive in growth and have achieved remarkable results in a variety of synthetic methods and promising unique applications. The remarkable properties of NPs are mainly due to their peculiar quantum-size, high specific surface

areas, and superior reactivity over their bulk counterparts (4).

As one of such reactive nanomaterials, sulfur has drawn attention recently due to its abundance and variety of functionalities which includes application as antibacterial agents, anti-cancer agent, catalysis, as gas sensors among others. Sulphur has been widely used industrially for the production of sulfuric acid, fertilizers, antimicrobial agents, pulp and paper, vulcanization of rubber, rechargeable batteries, and other petrochemicals (5). Sulfur has also been used as a component of formulations for various skin disorders such as dandruff shampoos and acne ointments and has been used as an antidote for acute exposure to radioactive materials (6).

Green synthesis approach utilizing biological specimens such as plants, yeasts, algae and fungus has emerged as a facile, affordable and eco-benevolent route as they are reliable, cost-effective, capable, straightforward and readily accessible when compared with known physical and chemical approaches (7).



(8)Awwad *et al.* (2015a) reported the rapid, cost-effective, and environmentally friendly biosynthesis of SNP using *Sophora japonica* pods extract as a capping, dispersing, and stabilizing agent. They obtained high crystalline and homogeneous spherical SNP in sizes ranging from 5 to 100 nm.

Awwad *et al.* (2015b) also synthesized environmentally friendly, high-efficiency monoclinic spherical SNP using *Albizia julibrissin* fruits extract with an average crystallite size of about 20 nm.

Araj *et al.* (2015) applied the biological approach to synthesis of SNPs using aqueous leaf extracts of citrus fruits acidified with dilute HCl and sodium thiosulfate solution. Kouzegaran and Farhadi (2017) synthesized SNP using a green surfactant (saponin) extracted from the plant *Acanthephylum bracteatum*.

Agricultural residue or agro-residue describes all organic material produced as by-products after harvesting and processing of agricultural crops. Agro-residues are non-wood ligno-cellulosic materials which includes onion peels, garlic peels, orange peels, cabbage peels, cane, bagasse, pea peels, wheat and rice straw e.t.c. Agro-residues are annually renewable and a low-cost source for natural cellulosic fibers. There are regions where these abundant agro-residues are still a waste, one of which is Nigeria. These valuable agricultural residuals lack any alternative commercial use as such they are discarded or incinerated. Hence, exploring a feasible application of agro-residues will lead to environmental as well as socio-economic benefits (9).

In lieu of this, our research focus was a preliminary design based on extraction and characterization of underutilized sulphur-rich agroresidues like onion and cabbage peels for green synthesis of sulphur nanoparticles (SNPs), adopting 'conversion of waste to wealth' concept.

2.0 METHODS

2.1. Preparation of Plant Extract

Allium cepa and *Brassica oleracea* were procured from Samaru in Sabon Gari Local Government Area of Kaduna State. The leaves were then identified and authenticated at the Herbarium Unit, department of Botany, Ahmadu Bello University Zaria, where voucher specimen numbers

ABU012068 (*Allium cepa*) and ABU06821 (*Brassica oleracea*) was deposited. They were carefully washed under running water and subsequently washed with deionized water to remove dust and debris. Agroresidue was obtained by peeling, followed by shade-drying at room temperature for a period of three (3) weeks and subsequent grinding using a blender. Each plant material (20 g) was dispersed into 100 ml deionized water in 200ml Erlenmeyer flask. The mixture was boiled at 100 degree celsius for 2 hours and then filtered using muslin cloth. The filtrate solution was used as the desired plant extract (10).

2.2. Synthesis of Sulphur Nanoparticles (SNPs)

Prior to synthesis of sulphur nanoparticles, all glassware were rinsed using an aqua regia solution 3:1(nitric acid: hydrochloric acid) to remove potential nucleation sites on the surface of the glassware. Sodium thiosulfate pentahydrate (0.078g) was dissolved in 50ml deionized water until complete dissolution. Then, 20ml of each plant extract was added to the aqua regia solution (3:1-nitric acid and hydrochloric acid). After 5 minutes of continuous stirring, 25ml of 20% citric acid was added to the preceding reaction mixture. The mixture was kept for 1 hour with continuous stirring, occasionally, after which a precipitate was observed. The precipitate was collected after washing with distilled water through centrifugation at 1000 rpm (10).

2.3. Characterization of Sulphur nanoparticles (SNPs)

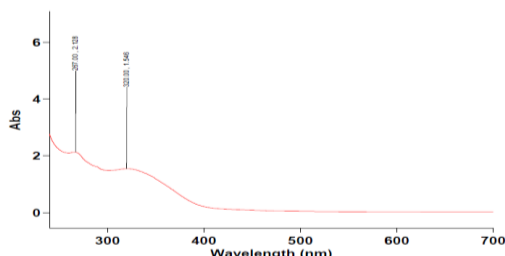
UV-Vis spectroscopy (UV-1601 PC, Shimadzu, Japan) was used for the preliminary characterization of as-synthesized SNPs with the scanning range of 200–700 nm. The functional groups present on the SNPs were analyzed by Fourier transform infrared spectroscopy (FTIR, 1750, Perkin- Elmer, USA). For FTIR measurements, the colloidal suspension of SNPs was centrifuged at 3000 rpm for 15 min and the pellet was washed four times to remove impurities. The spectra were recorded in the range of 600–4000 cm^{-1} . SNPs were also analyzed using Dynamic Light Scattering Spectroscopy (DLS) to identify possible size and range of the synthesized nanomaterial.

3.0 RESULTS AND DISCUSSION



3.1 Sulfur nanoparticles (SNPs)

Figure 1 shows the UV-Vis spectrum of SNPs. It is well known that α -sulfur exhibits an optical absorption maximum (λ_{Max}) in the range of 260–280nm (11). The peak at 267 nm in Figure 1 indicates the successful formation of SNPs. A



secondary peak at 320 nm in figure 1 corresponds to the b2-e3 transition (12), however, there was no clear distinct peak indicating formation of sulphur nanoparticles for cabbage peels within the range of 260-280nm; as depicted in figure 2; for this reason, only onion peels was adopted for the rest of the study.

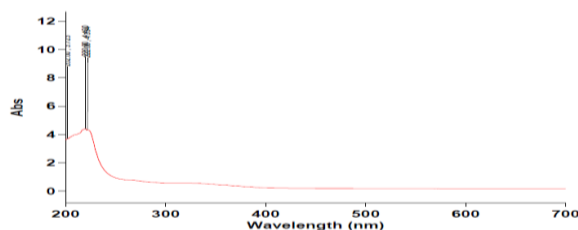


Figure 1 and 2: UV-Vis absorption spectrum of biosynthesized SNPs by onion peels at 267nm (left) and cabbage peels at 228nm (right).

The synthesized sulphur-nanoparticles were scanned by Fourier transform infrared (FTIR) spectroscopy in the range of 600–4000 cm^{-1} (Figure 3 and 4). The FTIR spectrum of the control (onion peel filtrate) exhibited a prominent peak at 2847.7 cm^{-1} , whereas in the spectrum of the SNPs, this peak shifted to 2851.4 cm^{-1} , indicating $-\text{OH}$ stretching (13). The peak at 2,918.2 cm^{-1} in both SNPs and control spectrum corresponds to the C-H stretching of CH_2 and CH_3 . A peak was observed at 1,796.6 cm^{-1} , corresponding to C=O stretching of the aldehyde group (14).

The control spectrum exhibited a peak at 1524.5 cm^{-1} , corresponding to the N-H stretching vibration in the amide linkages of the protein; this peak was not observed in the control spectrum. The band at 1259.0 cm^{-1} for the control extract was similar to that at 1226.3 cm^{-1} for SNPs, which corresponds to the S=O stretching of organic sulphate present in sulfones, sulfonyl chloride and sulfonamide (15). The spectra of the SNPs and control extract exhibited broad intense peaks at 1028.1 and 1005.7 cm^{-1} , respectively, indicating a marginal shift. These peaks were similar to that at 1,074 cm^{-1} and indicate the presence of flavanones adsorbed on the surface of the nanoparticles (16).

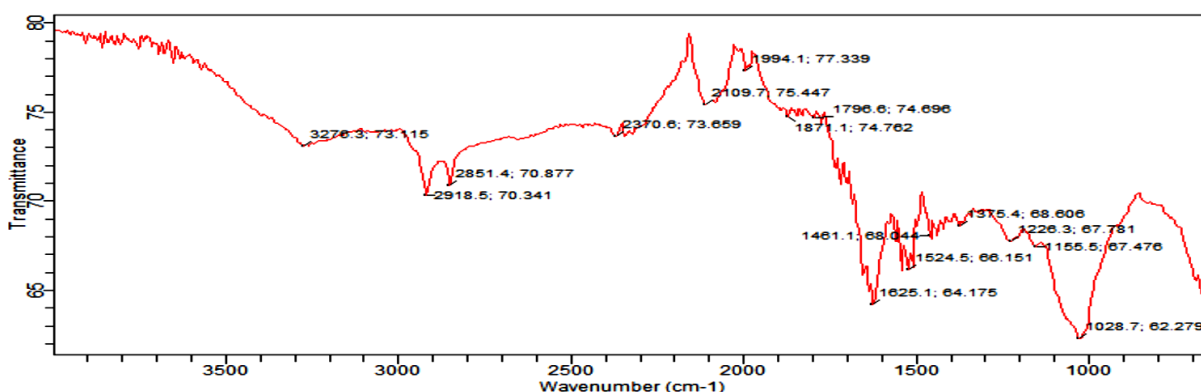


Figure 3: FTIR spectrum of biosynthesized Sulphur-Nanoparticles using onion peels.



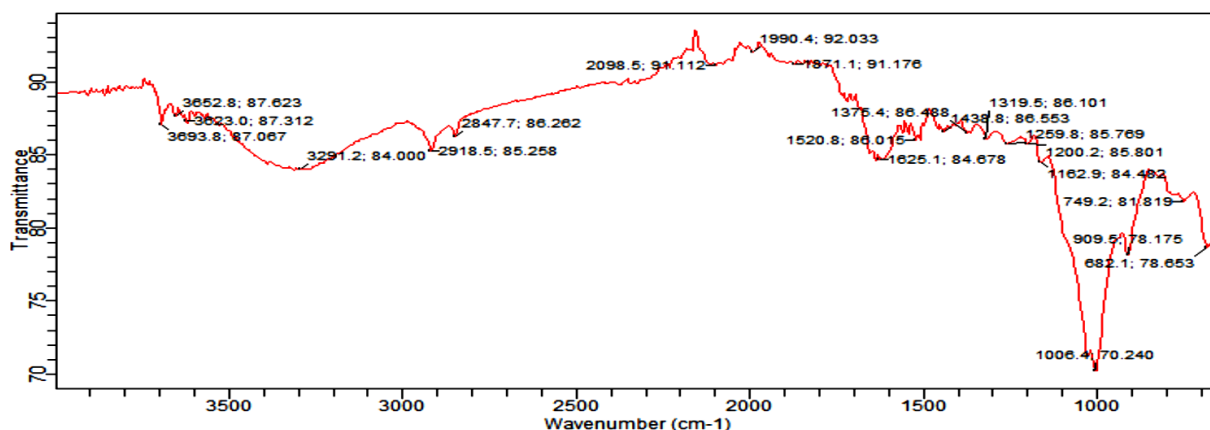


Figure 4: FTIR spectrum of biosynthesized Particles using onion peels filtrate (control)

Figure 5 and 6 shows the DLS (dynamic light scattering) spectra of the as-synthesized SNPs. Results obtained showed that bulk of the synthesized particles were within the range of 40nm- 100nm on the nanoscale (Figure 5); this is in line with the study of Awwad and Abdeen, (2015) who characterized SNPs with 60nm using leaves of *Sophora japonica*. Leaves of *Acanthephylum bracteatum* also revealed SNPs with dimension of 40nm (17) and 20nm for *Rosmarinus officinalis* leaves (18). However, larger sized SNPs were also reported at 89nm for *Azadirachta indica*, 95nm for *Mangifera indica*, 86nm for *Catharanthus roseus*

(19). Moreover, synthesis of SNPs using citric acid alone revealed nanoparticles with dimension within the range of 1-3nm; this implies the suitability of citric acid alone as a degrading agent in biogenic synthesis of sulphur-nanoparticles. Previous researches have also reported SNPs with a narrow size range of 2-15nm for *Ficus benghalensis* leaves (13). In the present study, disproportionation reaction was achieved using citric acid alone, without the use of sodium thiosulphide. This presents a more cost effective, rapid and ecofriendly method for the synthesis of sulphur nanoparticles using onion peels.

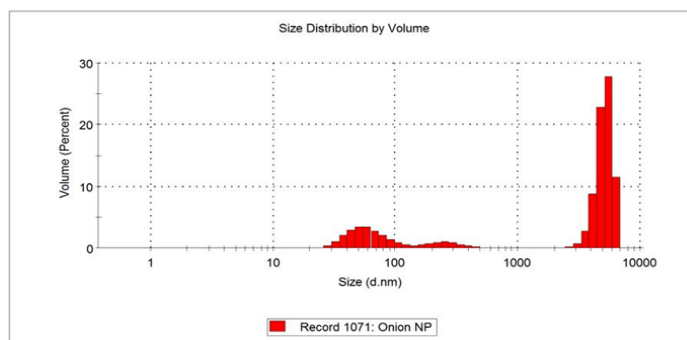


Figure 5: Dynamic light scattering spectra of SNPs synthesized using onion peels.

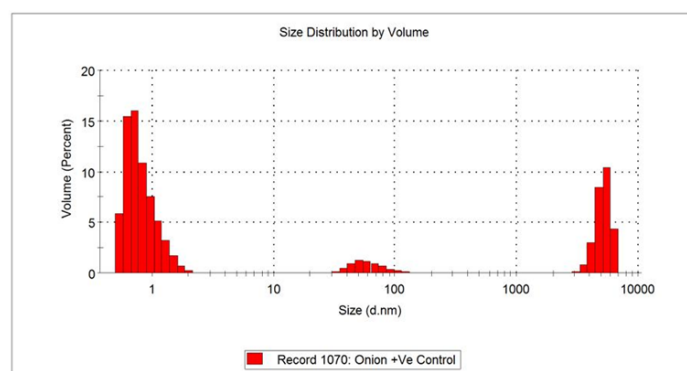


Figure 6: Dynamic light scattering spectra of SNPs synthesized from onion peels using citric acid as the degrading agent (control).

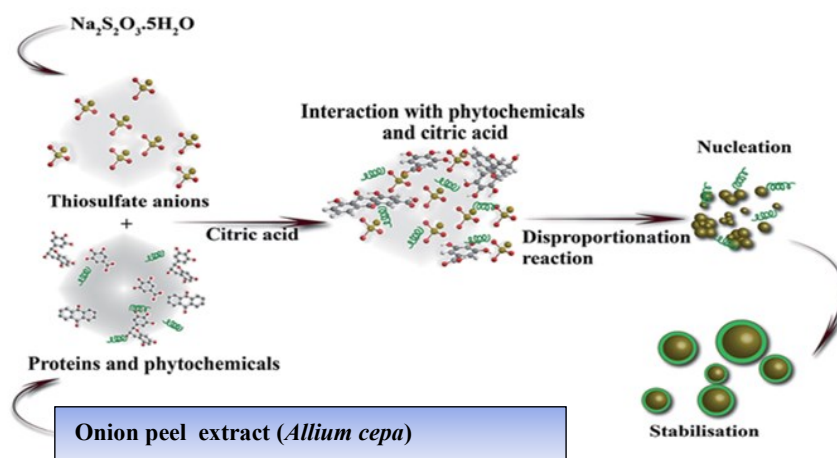


Figure 7: Mechanistic representation of biosynthesis of SNPs from onion peel extract (adopted from (10))

3.2. Biosynthesis mechanism

The possible mechanism of biosynthesis of SNPs is described in Figure 7. Polyphenolic compounds, which exist abundantly in all parts of the plants such as leaves, fruits, peels, seeds and flowers, are effective reducing agents to restrain reactive oxygen species (Tripathi *et al.*, 2018). Onion peels have a prominent amount of polyphenolic compounds. When these phytochemicals and citric acids are mixed with thiosulfate solutions, instantaneous reduction of S^{6+} to S^0 by phytochemicals and oxidation of S^{2-} to S^0 by citric acid occur simultaneously through the disproportionation process. Then S^0 undergoes a nucleation process to reach its optimum size and shape that are influenced by various parameters such as the nature of reducing and capping agent, temperature and pH (13, 15).

4.0 CONCLUSION

Sulphur nanoparticles were successfully synthesized from onion peels and characterized. The dimension of the particles were within the range of 40-100nm. The present study has revealed a rapid and ecofriendly approach for biogenic synthesis of sulphur nanoparticles using citric acid alone as the degrading agent. However, cabbage peels did not reveal a distinct peak showing a successful synthesis of sulphur nanoparticles at the preliminary characterization stage. Hence, it can be concluded that onion peel nanoparticles have the potential for bulk synthesis of sulphur nanoparticles in subsequent studies. Future research will focus more on practical application of SNPs, utilizing more imaging techniques for characterization and optimization of reaction conditions.

5.0 REFERENCES

1. F. J. Heiligtag, M. Niederberger, The fascinating world of nanoparticle research. *Materials today* 16, 262-271 (2013).



2. P. Walter et al., Early use of PbS nanotechnology for an ancient hair dyeing formula. *Nano letters* 6, 2215-2219 (2006).
3. J. Jeevanandam, A. Barhoum, Y. S. Chan, A. Dufresne, M. K. Danquah, Review on nanoparticles and nanostructured materials: history, sources, toxicity and regulations. *Beilstein journal of nanotechnology* 9, 1050-1074 (2018).
4. S. R. Vijayan et al., Seaweeds: A resource for marine bionanotechnology. *Enzyme and microbial technology* 95, 45-57 (2016).
5. D. A. Boyd, Sulfur and its role in modern materials science. *Angewandte Chemie International Edition* 55, 15486-15502 (2016).
6. S. Parcell, Sulfur in human nutrition and applications in medicine. *Alternative Medicine Review* 7, 22-44 (2002).
7. S. Matussin, M. H. Harunsani, A. L. Tan, M. M. Khan, Plant-extract-mediated SnO₂ nanoparticles: synthesis and applications. *ACS Sustainable Chemistry & Engineering* 8, 3040-3054 (2020).
8. A. M. Awwad, N. M. Salem, A. O. Abdeen, Phytochemical and spectral studies of synthesis sulfur nanoparticles using *Sophora japonica* pods extract. *Journal: Journal of Advances in Chemistry* 11, 3427-3432 (2015).
9. B. Chanana, M. S. Parmar, P. K. Sachdeva, Agro-residues: Beyond waste, potential fibres for textile industry. *FIBRE2FASHION.COM*, (2016).
10. R. Tripathi, R. P. Rao, T. Tsuzuki, Green synthesis of sulfur nanoparticles and evaluation of their catalytic detoxification of hexavalent chromium in water. *RSC advances* 8, 36345-36352 (2018).
11. N. Heatley, E. J. Page, Estimation of elemental sulfur by ultraviolet absorption. *Analytical Chemistry* 24, 1854-1854 (1952).
12. N. Richardson, P. J. Weinberger, *Electron Spectrosc. Relat. Phenom.* 6, 109-116. (1975).
13. R. Tripathi, S. J. Chung, Biogenic nanomaterials: Synthesis, characterization, growth mechanism, and biomedical applications. *Journal of microbiological methods* 157, 65-80 (2019).
14. N. Mehrotra, R. M. Tripathi, F. Zafar, M. P. Singh, Catalytic degradation of dichlorvos using biosynthesized zero valent iron nanoparticles. *IEEE transactions on nanobioscience* 16, 280-286 (2017).
15. R. Tripathi et al., Metal-induced redshift of optical spectra of gold nanoparticles: An instant, sensitive, and selective visual detection of lead ions. *International Biodeterioration & Biodegradation* 144, 104740 (2019).
16. S. S. Shankar, A. Rai, A. Ahmad, M. Sastry, Rapid synthesis of Au, Ag, and bimetallic Au core-Ag shell nanoparticles using *Neem* (*Azadirachta indica*) leaf broth. *Journal of colloid and interface science* 275, 496-502 (2004).
17. V. Javan Kouzegaran, K. Farhadi, Green synthesis of Sulphur Nanoparticles assisted by a herbal surfactant in aqueous solutions. *Micro & Nano Letters* 12, 329-334 (2017).
18. L. S. Albanna, N. M. Salem, A. M. Awwad, Seed germination and growth of cucumber (*Cucumis sativus*): effect of nano-crystalline sulfur. *J Agric Sci* 8, 219 (2016).
19. P. Paralikar, M. Rai, Bio-inspired synthesis of sulphur nanoparticles using leaf extract of four medicinal plants with special reference to their antibacterial activity. *IET Nanobiotechnology* 12, 25-31 (2018).



P029 - *TERMINALIA CATAPPA* AS INHIBITOR AGAINST IMPROVISED FERROUS IMPLANT IN CORROSIVE MEDIA VIA EXPERIMENTAL APPROACH

Uba Sani^{1*}, Idowu Elijah Agbele¹, Nsidibeabasi Calvin Nwokem¹, Israel Kehinde Omoniyi¹, Gaba Echiobi Emmanuel², Owolabi A Awwal³

¹Department of Chemistry, Ahmadu Bello University, Zaria, ²Department of Veterinary Medicine, Ahmadu Bello University, ³Department of Chemistry, 61455 Western Illinois University.

*Corresponding Author E-mail: agbeleid2022@gmail.com

ABSTRACT

Weight loss has been employed to evaluate the inhibition efficiency of Terminalia catappa against improvised ferric implant in acid medium. However, the effects of corrosion against metals are not disputable, as a result of aggressive media that are unavoidably employed in industries. Surface morphology revealed that the presence of the inhibitor reduced corrosion rate, since surface appearance of corrosion product is more ordered. Corrosion monitoring methods revealed that corrosion rates are depending on pH of corrosion system, concentration of inhibitors, temperature and type of inhibitor. The maximum inhibition efficiency of TC is 91.73% at temperature of 303K when inhibitor concentration was 0.5g/l. Thermodynamic parameter revealed the corrosion process is an endothermic reaction and TC extract acting as a mixed type inhibitor.

KEYWORDS:

corrosion, Terminalia catappa; Improvised ferrous implant; thermodynamic parameters.

1.0 INTRODUCTION

Ferric steel is widely utilized in a variety of industries because of its stability, high strength, workability, and weldability, including desalination plants, construction materials, the pharmaceutical industry, and thermal power plants (1-3). The unique characteristic of diver metallic materials are adjusted and optimized for suitable applications resulting to additional value and cost effectiveness of the metals (4). Improvised ferrous implant is iron-containing alloy recognized for its heat and corrosion resistances (5). Like some steels, improvised ferrous implant primarily contained carbon and iron, with the addition of other elements such as nickel, magnesium, molybdenum, and nitrogen in trace amount to increase their corrosion resistance (6).

2.0 LITERATURE REVIEW

Corrosion is a thermodynamic favorable and viable process that causes an adverse effect of deterioration and degeneration on metallic surface (7). Deterioration of metal as a result of corrosion has generated great issue for the manufacturing, mining, oil refinery, chemical plant and among others metal-based industries (8). The economic effect of corrosion of metals costs United State great amount of \$300 billion per annual at present prices (9).

However, researchers have struggled with the negative effects of corrosion on metals over the years. There are corrosion control methods such as electroplating, paint, plastic, powder, galvanization, cathodic protection, and grease among others (7, 10, 11). There are synthetic inorganic compounds that show excellent inhibitory and resistance corrosion activities, however adverse effect of poison generate enhance danger to the surrounding and system when employed (12). As a result, scientists are seeking corrosion inhibition methods that are animal or plant-sourced, natural products, inexpensive and eco-friendly corrosion inhibitors (13). Therefore, green corrosion inhibitors are plant-based molecules that are heavy metal-free, poison-free, and biodegradable. The leaves, bark, fruit, and roots have all been used in plants as inhibitors (14). The following researcher reported inhibition of metallic materials using green inhibitors (10, 15-19).

3.0 MATERIALS AND METHODS

3.1 Plant Collection, Extraction and Corrosion Medium Preparation

The collection of exudate of *Terminalia catappa* from whole plant stems in Ahmadu Bello University Teaching Hospital (ABUTH) premises Shika-Zaria, Nigeria. The extraction was carried out using alcohol, the extract is subjected to the rotatory evaporator at 340K to prevent ethanol contaminants



and finally concentrated the extract (10). The plant of *Terminalia catappa* is recognised in the field using conventional key and certified at the herbarium unit of the Biological Sciences Nigeria Police Academy Wudil, Kano State, Nigeria

3.2 The chemical composition of the metallic specimen

Table 1: Chemical composition of the improvised ferrous implant

Element	Si	Mn	P	C	Al	S	Cr	Cu	Fe
Quantity wt%	0.18	0.25	0.02	0.37	0.06	0.25	0.08	0.04	98.75

3.3 Scanning Electron Microscopy

Surface appearances of improvised ferrous implant were studied using scanning electron microscopy (SEM; JEOL JSM-5500, Japan). Scanned images were taken at an accelerating voltage of 2.00 and 15.00 kV at capture images specimen of 1cm x 0.03cm, after immersion time of 7days in 1MHCl alone and in the presence of 0.5g/l inhibitor concentration (21).

3.4 Corrosion Monitoring Procedures

3.4.1 Weight loss

The stainless-steel was pre-weighed and immersed in 200 ml of 1.0 M HCl in a beaker; placed on thermostat water bath at temperatures varied from 303 to 313K, for different time intervals in the presence and absence of the inhibitor (22). After 24 hours, the corrosion product was removed, rinsed in ethanol and dried in acetone and finally deepen in zinc dusts to prevent the further oxidation of metal before been re-weighed. The weight loss was measured three times to have reproducible results.

Weight loss determination

The weight loss (WL) was computed using the following formula:

$$WL = W_1 - W_2 \quad \text{Eq.1}$$

where W1 is the coupon's initial weight in grams before immersion, and W2 is the coupon's final weight in grams after immersion.

Evaluation of corrosion rate

The rate of corrosion (R) was computed using the following formula

The chemical composition of improvised ferrous implant was determines using Handheld NITON Metal Analyzer Model: XL2800 X-ray Fluorescence Spectrometers (XRF) at Department Mechanical Engineering in Ahmadu Bello University Zaria, Nigeria (20).

$$C_R, \text{mmyear}^{-1} = \frac{87.6WL}{ADT} \quad \text{Eq.2}$$

where WL is the weight loss in g, D is density in g cm-3, A is the area of specimen in cm2 and T is time of immersion in hours.

Calculation of Inhibition efficiency employing the following formula

$$IE, \% = \frac{C_{r1} - C_{r2}}{C_{r1}} \times 100$$

Eq.3

Where Cr1 is corrosion rate in the absence of inhibitor, while Cr2 is corrosion rate in the presence of inhibitor and IE is inhibition efficiency.

Surface coverage determination

The surface coverage (θ) was calculated using the following formula:

$$\theta = \frac{W_1 - W_2}{W_1} \quad \text{Eq.4}$$

Where W1 is the weight loss in absence of inhibitor, while W2 is the weight loss in presence of inhibitor

3.4.2 Effect of temperature

The effect of temperature on the corrosion of improvised ferrous implant in the absence and presence of inhibitor concentrations were evaluated using the Arrhenius transition state equations represented as follows.

$$\log CR = \log A - \frac{E_a}{2.303RT} \quad \text{Eq.5}$$



$$\log\left(\frac{CR}{T}\right) = \left\{ \log\left(\frac{R}{NAh}\right) + \frac{\Delta Sa}{2.303R} \right\} - \frac{\Delta Ha}{2.303RT}$$

Eq.6

The plots of log CR versus reciprocal of absolute temperature (1/T), with slope equal to -Ea/R, from which the activation energy for the corrosion process can be calculated. A is the

Arrhenius or pre-exponential factor, Ea is the activation energy, R is the universal gas constant, T is the temperature of the system, NA is the Avogadro gas constant, h is the plank constant (23), where ΔSa is the entropy of activation and ΔHa is the enthalpy of activation, CR is the corrosion rate of the metal.

4.0 RESULTS AND DISCUSSIONS

4.1 Scanning Electron Microscopy

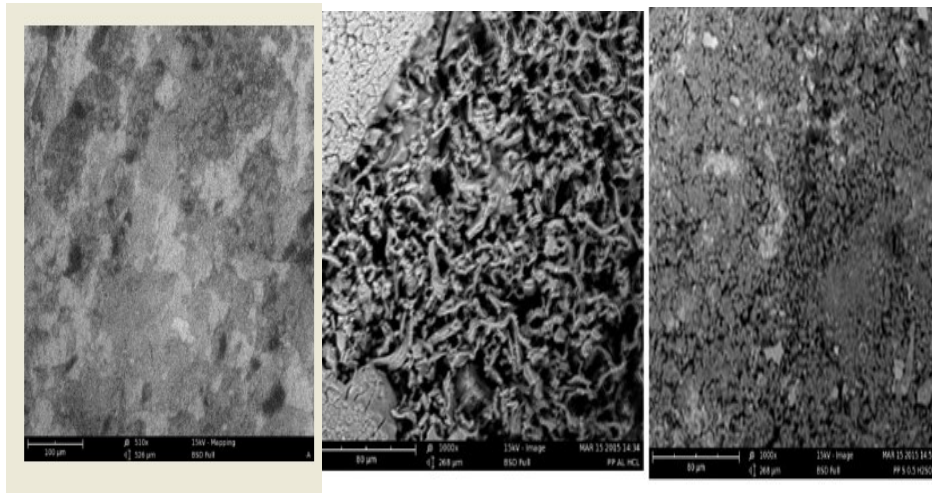


Figure 1. a: SEM micrograph of pure steel, b: SEM micrograph of steel corrode in 1.0 M HCl solution after 7days while c:SEM micrographs of steel corroded in the presence of 0.5g/l inhibitor concentration at x 5000 magnification

The surface morphology of the pure, corrode improvised ferrous implants in the absence and presence of *Terminalia catappa* inhibitor in Figure 1a, 1b and 1c showed the scanning electron micrographs (at x5000 magnification) respectively. Figure 1b indicated that the surface was deformed and greatly damaged in the acid medium that is without inhibitor and leading to lattice deformation. The deformation effect occurred as a result of corroding impact of the acid on the metal surface, while in the presence of the inhibitor the rate and effect of corrosion were reduced as seen in Figure 1c, therefore the metal surface is more ordered in corrosion product containing inhibitor, because the inhibitor served as surface coating and retard the corrosion and damage effects of the acid (24, 25).

4.2 Weight Loss and Corrosion Consideration Result

Variation of temperature effect on corrosion rate as seen Table 3 revealed that the inhibition efficiency decreases with increase in temperature of corrosion system, because at higher temperature the rate of

corrosion increase, because the kinetic energy of the reaction is greatly high. As a result larger surface area available for metal surface to expose to acid, but lesser chance for the inhibitor to adsorbed on the surface of the metal (26, 27).

Figure 3 revealed that the rate of corrosion has highest value in the acid medium, since the presence of acid accelerate corrosion by supplying hydrogen ions to the corrosion reaction system (28). Because corrosion is pH dependent, the rate of corrosion tends to reduce with respect to pH; therefore acid enhance the conductivity of moisture on the metal surface, allowing corrosion to happen faster (29). Figure 3 showed that the weight loss of improvised ferrous implant are affected by acid solution; there is increase in weight loss in acid medium, because the surface of metal is totally expose to the attack of acid thereby enhance release of metallic ion under corrosion viable condition (30). But as inhibitors are added and extract concentrations are increased, increase in the concentration of TC extract reduced weight loss and corrosion rate of steel through adsorption of the



inhibitor on the metal surface, therefore reduced the surface area for the attacked of the acid (31). Advance still, Figure 4 displayed the relationship between the inhibition efficiency and concentration of ethanolic extract of *Terminalia catappa* at 303 K and 313 K, there is corresponding decrease in corrosion rate as extract concentrations increase over the range of the temperatures of the system, simply because at a given temperature there is sufficient amount of extract (high concentration) in the corrosion medium that adsorbed on the metal surface thereby retard the rate of corrosion, because the inhibitor protect the metal surface by formation of a thin preventive oxide layer thereby reducing the surface area for corrosion reaction, but at the same time larger surface area for the inhibitors to adsorbed on the metal surface which eventually result to lower corrosion rate (10, 32).

Table 2 revealed that the variation of inhibitor concentrations from 0.1 to 0.5 g/l that lead to increase in activation energy, implies that inhibitor concentration has direct relationship with activation energy of the system; therefore mechanism of adsorption of the inhibitor on the metal surface is physisorption (33, 34). At higher inhibitor concentrations, there are plenty inhibitor samples to form chemically stable complex between metal interface and the inhibitor moieties, thereby foster the adsorption of the inhibitor on the surface of metal, while the surface area available for corrosion gradually reduced (22, 35, 36).



Table 2: Corrosion rate, surface coverage (θ) and percentage inhibition efficiency (% IE) of various concentrations of *Terminalia catappa* from gravimetric measurement

Temperature	C (g/L)	Corrosion rate (mm/yr)	Inhibition Efficiency(% IE)	Surface Coverage (θ)
303 K	Blank	0.309191		
	0.1	0.117787	65.22	0.6522
	0.2	0.103064	69.57	0.6957
	0.3	0.073617	78.26	0.7826
	0.4	0.049471	84.00	0.8000
	0.5	0.025570	91.73	0.9173
313K	Blank	0.338638		
	0.1	0.147234	52.38	0.5238
	0.2	0.125598	62.91	0.6291
	0.3	0.079506	74.29	0.7429
	0.4	0.070438	79.20	0.7920
	0.5	0.050593	85.06	0.8506

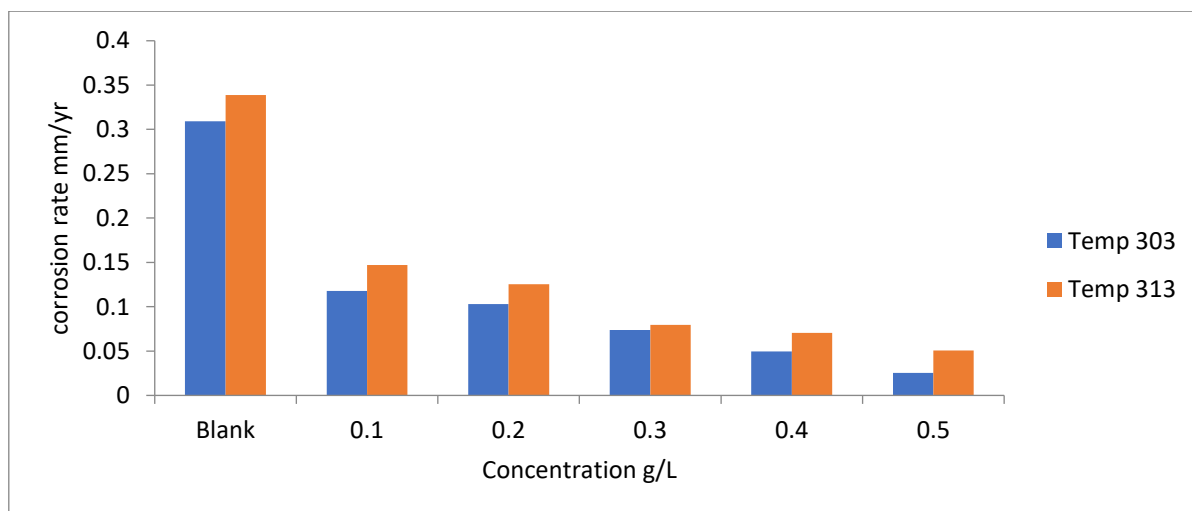


Figure 2 : Relationship between corrosion rate and concentration of TC extract at 303 K and 313 K.



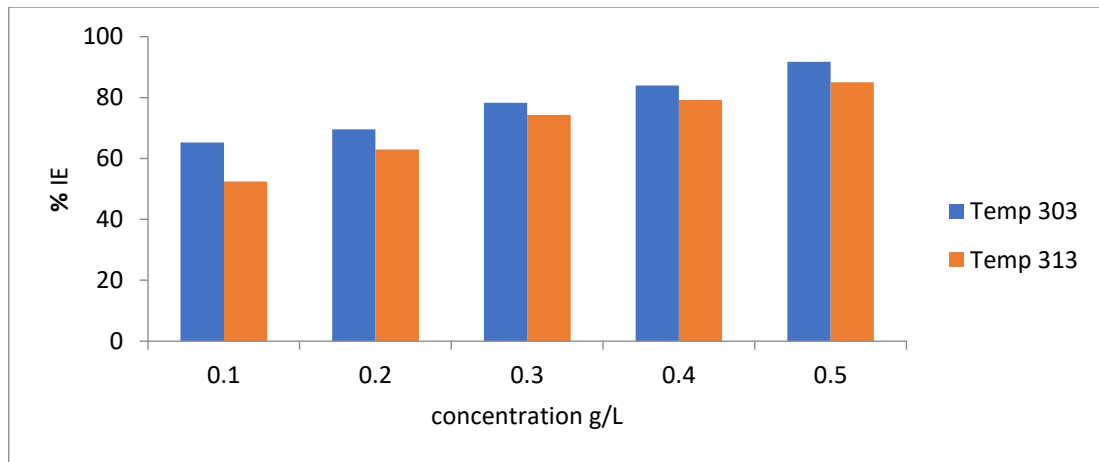


Figure 3: Relationship between the inhibition efficiency and concentration of ethanol extract of *Terminalia catappa* at 303 K and 313 K.

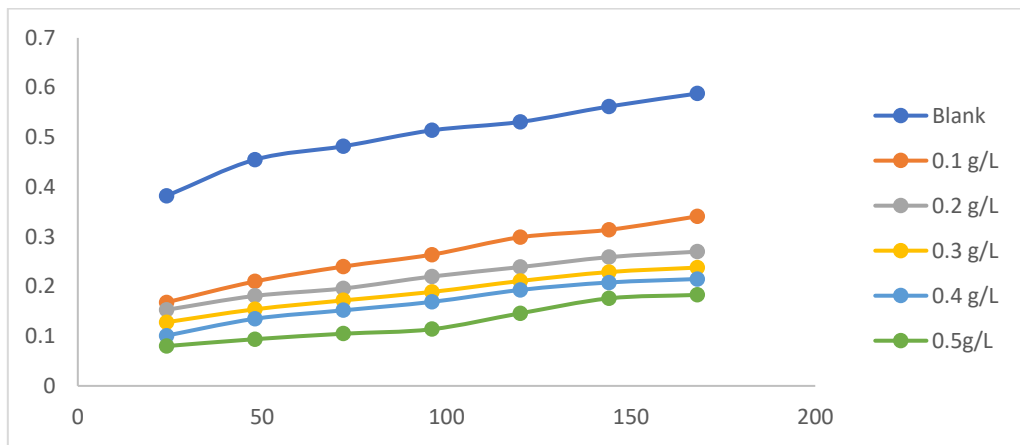


Figure 4: Variation of weight loss with time for the corrosion of the improvised ferrous implant in 1.0M HCl containing (0.1 to 0.5 g/L) *Terminalia catappa* (TC) at 303 K.

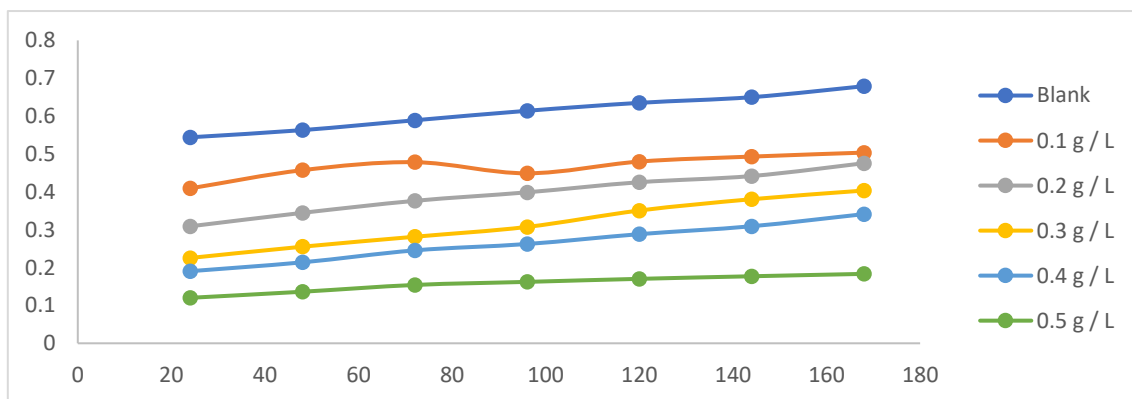


Figure 5: Variation of weight loss with time for the corrosion of the improvised ferrous implant in 1.0M HCl containing (0.1 to 0.5 g/L) *Terminalia catappa* (TC) at 313 K.



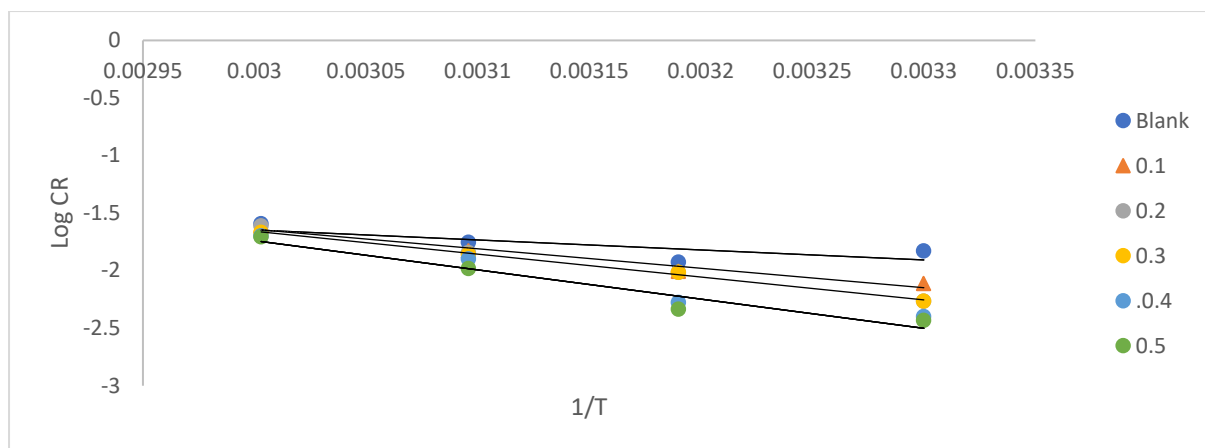


Figure 6: Variation of corrosion rate of improvised ferrous implant with inverse temperature in 1.0 M HCl containing various concentration of Terminalia catappa (TC) at 303 to 333K.

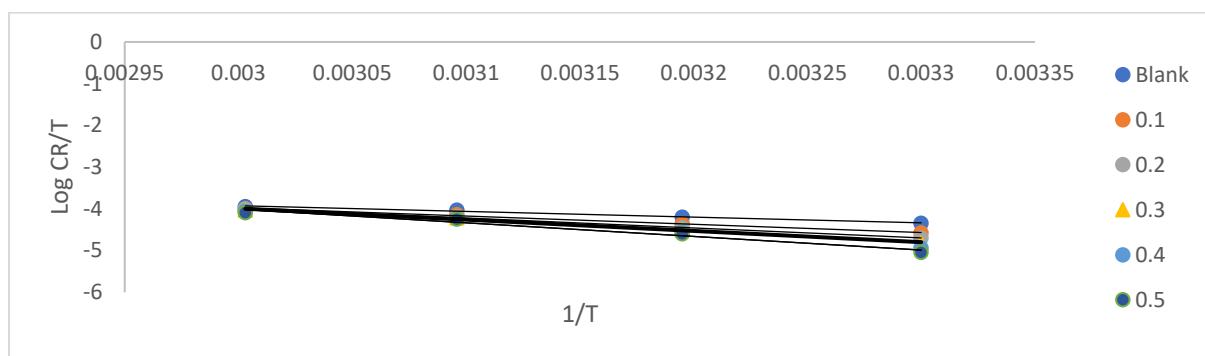


Figure 7: Variation of log CR/T of improvised ferrous implant with inverse temperature in 1.0M HCl containing various concentration of Terminalia catappa TC at 303 to 333K.

Table 3: Thermodynamic parameters of inhibitory capacity of TC

System	Ea (Kjmol ⁻¹)	ΔH (Kjmol ⁻¹)	ΔS (Kjmol ⁻¹ K ⁻¹)	R ²
Blank	0.8678	-	-	0.9892
0.1g/l	1.6921	26.39	-0.21	0.9945
0.2g/l	1.9885	22.76	-0.19	0.9231
0.3g/l	2.1345	42.17	-0.15	0.9671
0.4g/l	2.4970	43.94	-0.15	0.9921
0.5g/l	2.5381	46.55	-0.14	0.9687



4.3 Thermodynamic Properties and Consequences

Equation (5) was employed to determine the activation energy of the metal releasing system. Figures 6 displayed the plot of log CR as a function of $1/T$ without and with inhibitor. Table 3 revealed the amounts of entropy change ΔS , enthalpy change (ΔH), and activation energy (E_a) for the different concentration derived from Fig. 6. R^2 that is the linear regression coefficients obtained range from 0.9231 to 0.9945, which implies excellent correlation among the experimental information (37), therefore the Arrhenius equation is sufficient to evaluate the corrosion inhibitory capacity of improvised ferrous implant in 1M HCl (38). The activation energy determined for the blank is lower than the inhibitor containing solutions suggests that the adsorption mechanism is physisorption (17, 39). As the concentration of inhibitors increase from 0.1 to 0.5 g/l the value of activation energy increase, this could be ascribed to increase in energy barrier, which leads to complex formation between the improvised ferrous implant and inhibitor compound (40). The establishment of protective layer on the metal surface acts as a barrier to energy and mass transfer, therefore resulting to increase in activation energy of reaction condition in the presence of inhibitor (41). Equation 6 was used to derive the entropy and enthalpy changes of the reaction system. Figure 7 displayed the variation of log CR/T against inverse temperature in 1 M HCl containing various concentration of Guaiacum officinal at 303 to 333K. The values of enthalpy change generated are positive values, which are referred to as endothermic process. Corrosion process is normally identified to be an endothermic reaction (42). That is not all; ΔH is proportionally related to concentration of the inhibitors and the system temperature, while the sign of entropy change determined were negative. The increase in the value of ΔS with concentration indicates that reduction in orderliness occurred in TCing from reactants to the activated complex (43).

5.0 CONCLUSIONS AND RECOMMENDATION

The following conclusions may be derived from the study:

The use of *Terminalia catappa* [as an inhibitor for the corrosion of improvised ferrous implant in HCl is advocated in this research work.](#) Weight loss and

electrochemical tests confirmed that *Terminalia catappa* [indicates > 90.39% of corrosion mitigation efficiency at 0.5g/L.SEM result confirmed the surface adsorption of Terminalia catappa on the improvised ferrous implant.](#) Phenomenon of adsorption is proposed from the value of thermodynamic parameters.

Conflict of Interests

The authors declare that they have no conflict of interests regarding the publication of this paper.

6.0 REFERENCES

1. S. Z. Salleh et al., Plant extracts as green corrosion inhibitor for ferrous metal alloys: A review. *Journal of Cleaner Production* 304, 127030 (2021).
2. J. C. Souza, K. Apaza-Bedoya, C. A. Benfatti, F. S. Silva, B. Henriques, A comprehensive review on the corrosion pathways of titanium dental implants and their biological adverse effects. *Metals* 10, 1272 (2020).
3. M. Talebian et al., Pitting corrosion inhibition of 304 stainless steel in NaCl solution by three newly synthesized carboxylic Schiff bases. *Corrosion Science* 160, 108130 (2019).
4. C. Prakash et al., Multi-objective parametric appraisal of pulsed current gas tungsten arc welding process by using hybrid optimization algorithms. *The International Journal of Advanced Manufacturing Technology* 101, 1107-1123 (2019).
5. H. M. Cobb, *The history of stainless steel.* (ASM International, 2010).
6. A. Fahim, A. E. Dean, M. D. Thomas, E. G. Moffatt, Corrosion resistance of chromium-steel and stainless steel reinforcement in concrete. *Materials and Corrosion* 70, 328-344 (2019).
7. P. O. Ameh, Electrochemical and computational study of gum exudates from *Canarium schweinfurthii* as green corrosion inhibitor for mild steel in HCl solution. *Journal of Taibah University for Science* 12, 783-795 (2018).
8. A. M. Hasan, M. E. Abdel-Raouf, Applications of guar gum and its derivatives in



petroleum industry: A review. *Egyptian journal of petroleum* 27, 1043-1050 (2018).

9. G. Koch, Cost of corrosion. *Trends in oil and gas corrosion research and technologies*, 3-30 (2017).

10. F. Awe, Adsorptive studies of the inhibitive properties of ethanolic extracts of *Parinari polyandra* on mild steel in acidic media. *Communication in Physical Sciences* 4, (2019).

11. N. O. Eddy, F. E. Awe, C. E. Gimba, N. O. Ibisi, E. E. Ebenso, QSAR, experimental and computational chemistry simulation studies on the inhibition potentials of some amino acids for the corrosion of mild steel in 0.1 M HCl. *International Journal of Electrochemical Science* 6, 931-957 (2011).

12. C. Verma, E. E. Ebenso, M. Quraishi, C. M. Hussain, Recent developments in sustainable corrosion inhibitors: design, performance and industrial scale applications. *Materials Advances* 2, 3806-3850 (2021).

13. F. Ortega, F. Versino, O. V. López, M. A. García, Biobased composites from agro-industrial wastes and by-products. *Emergent Materials* 5, 873-921 (2022).

14. C. Verma, E. E. Ebenso, I. Bahadur, M. Quraishi, An overview on plant extracts as environmental sustainable and green corrosion inhibitors for metals and alloys in aggressive corrosive media. *Journal of molecular liquids* 266, 577-590 (2018).

15. O. A. Akinbulumo, O. J. Odejobi, E. L. Odekanle, Thermodynamics and adsorption study of the corrosion inhibition of mild steel by *Euphorbia heterophylla* L. extract in 1.5 M HCl. *Results in Materials* 5, 100074 (2020).

16. Sheetal, B. Chugh, S. Thakur, B. Pani, A. K. Singh, in *Sustainable Corrosion Inhibitors I: Fundamentals, Methodologies, and Industrial Applications*. (ACS Publications, 2021), pp. 21-36.

17. U. Eduok, E. Ohaeri, J. Szpunar, Electrochemical and surface analyses of X70 steel corrosion in simulated acid pickling medium: Effect

of poly (N-vinyl imidazole) grafted carboxymethyl chitosan additive. *Electrochimica Acta* 278, 302-312 (2018).

18. A. Hamilton-Amachree, N. B. Iroha, Corrosion inhibition of API 5L X80 pipeline steel in acidic environment using aqueous extract of *Thevetia peruviana*. *Chem. Int* 6, 110 (2020).

19. H.-Y. Lin et al., Entropy-driven binding of gut bacterial β -glucuronidase inhibitors ameliorates irinotecan-induced toxicity. *Communications Biology* 4, 280 (2021).

20. E. Obeng-Gyasi, J. Roostaei, J. M. Gibson, Lead distribution in urban soil in a medium-sized city: household-scale analysis. *Environmental science & technology* 55, 3696-3705 (2021).

21. M. Rbaa et al., Synthesis and characterization of novel Cu (II) and Zn (II) complexes of 5-[(2-Hydroxyethyl) sulfanyl] methyl}-8-hydroxyquinoline as effective acid corrosion inhibitor by experimental and computational testings. *Chemical Physics Letters* 754, 137771 (2020).

22. J. A. Aigbogun, M. A. Adebayo, Green inhibitor from *Thaumatococcus daniellii* Benn for corrosion mitigation of mild steel in 1M HCl. *Current Research in Green and Sustainable Chemistry* 4, 100201 (2021).

23. L. T. Popoola, Organic green corrosion inhibitors (OGCIs): a critical review. *Corrosion Reviews* 37, 71-102 (2019).

24. N. Farabi, D. Chen, J. Li, Y. Zhou, S. Dong, Microstructure and mechanical properties of laser welded DP600 steel joints. *Materials Science and Engineering: A* 527, 1215-1222 (2010).

25. W. Zhang et al., Performance and mechanism of a composite scaling-corrosion inhibitor used in seawater: 10-Methylacridinium iodide and sodium citrate. *Desalination* 486, 114482 (2020).

26. N. O. Eddy, P. O. Ameh, N. B. Essien, Experimental and computational chemistry studies on the inhibition of aluminium and mild steel in 0.1



M HCl by 3-nitrobenzoic acid. *Journal of Taibah University for Science* 12, 545-556 (2018).

27. M. Srivastava et al., Low cost aqueous extract of *Pisum sativum* peels for inhibition of mild steel corrosion. *Journal of Molecular Liquids* 254, 357-368 (2018).

28. A. El-Meligi, Hydrogen production by aluminum corrosion in hydrochloric acid and using inhibitors to control hydrogen evolution. *International Journal of Hydrogen Energy* 36, 10600-10607 (2011).

29. B. R. Smith, M. J. Conger, J. S. McMullen, M. J. Neubert, Why believe? The promise of research on the role of religion in entrepreneurial action. *Journal of Business Venturing Insights* 11, e00119 (2019).

30. N. J. Ostrowski, B. Lee, A. Roy, M. Ramanathan, P. N. Kumta, Biodegradable poly (lactide-co-glycolide) coatings on magnesium alloys for orthopedic applications. *Journal of Materials Science: Materials in Medicine* 24, 85-96 (2013).

31. M. H. Hussin, M. J. Kassim, The corrosion inhibition and adsorption behavior of *Uncaria gambir* extract on mild steel in 1 M HCl. *Materials Chemistry and Physics* 125, 461-468 (2011).

32. E. Oguzie, M. Chidiebere, K. Oguzie, C. Adindu, H. Momoh-Yahaya, Biomass extracts for materials protection: corrosion inhibition of mild steel in acidic media by *Terminalia chebula* extracts. *Chemical engineering communications* 201, 790-803 (2014).

33. R. Haldhar, D. Prasad, N. Bhardwaj, Surface adsorption and corrosion resistance performance of *Acacia concinna* pod extract: An efficient inhibitor for mild steel in acidic environment. *Arabian Journal for Science and Engineering* 45, 131-141 (2020).

34. I. Obot, S. Umoren, N. Obi-Egbedi, Corrosion inhibition and adsorption behaviour for aluminum by extract of *Aningeria robusta* in HCl solution: Synergistic effect of iodide ions. *Journal*

of Materials and Environmental Science 2, 60-71 (2011).

35. D. E. Arthur, A. Jonathan, P. O. Ameh, C. Anya, A review on the assessment of polymeric materials used as corrosion inhibitor of metals and alloys. *International Journal of Industrial Chemistry* 4, 1-9 (2013).

36. B. E. Brycki, I. H. Kowalczyk, A. Szulc, O. Kaczerewska, M. Pakiet, Organic corrosion inhibitors. *Corrosion inhibitors, principles and recent applications* 3, 33 (2018).

37. B. El Ibrahim, A. Jmiai, L. Bazzi, S. El Issami, Amino acids and their derivatives as corrosion inhibitors for metals and alloys. *Arabian Journal of Chemistry* 13, 740-771 (2020).

38. M. V. Fiori-Bimbi, P. E. Alvarez, H. Vaca, C. A. Gervasi, Corrosion inhibition of mild steel in HCL solution by pectin. *Corrosion Science* 92, 192-199 (2015).

39. A. Zarrouk et al., A theoretical investigation on the corrosion inhibition of copper by quinoxaline derivatives in nitric acid solution. *International Journal of Electrochemical Science* 7, 6353-6364 (2012).

40. S. Umoren, I. Obot, N. Obi-Egbedi, *Raphia hookeri* gum as a potential eco-friendly inhibitor for mild steel in sulfuric acid. *Journal of materials science* 44, 274-279 (2009).

41. O. Sanni, A. Popoola, O. Fayomi, Temperature effect, activation energies and adsorption studies of waste material as stainless steel corrosion inhibitor in sulphuric acid 0.5 M. *Journal of Bio-and Tribo-Corrosion* 5, 1-8 (2019).

42. Y. Zhao, H. Ren, H. Dai, W. Jin, Composition and expansion coefficient of rust based on X-ray diffraction and thermal analysis. *Corrosion Science* 53, 1646-1658 (2011).

43. N. Raghavendra, J. Ishwara Bhat, Green approach to inhibition of corrosion of aluminum in 0.5 M HCl medium by tender arecanut seed extract: insight from gravimetric and electrochemical studies. *Research on Chemical Intermediates* 42, 6351-6372 (2016).





P030 - PHYTOCHEMICAL AND ELEMENTAL ASSESSMENT OF SOME SELECTED HERBAL MIXTURES USED IN TREATING GASTRIC ULCER IN KADUNA METROPOLIS

Rifore, B.S., Jerome, P.I., Iorver P. D., Mathew, J., Abubakar, N.I

^{#1, 3, 4} Department of Chemistry, Nigerian Defense Academy, Kaduna

^{#2} Department of Chemical Engineering, Federal University of Technology, Minna

^{#5} Department of Biology, Ahmadu Bello University, Zaria

*Corresponding Author: rifore.belief@gmail.com

ABSTRACT

The phytochemical and elemental analysis of some selected herbal mixtures used for treating gastric ulcer was researched. The herbal mixtures were obtained from specific areas of Kaduna Metropolis which includes; Panteka (PA), Sabon Tasha (SA), Kano Road (KA), Kabala West (KAW) and Narayi (NA). Hot water extraction was used to extract the plant mixtures for phytochemical analysis. Phytochemical qualitative tests were carried for anthraquinones, saponins, flavonoids, cardia glycosides, terpenoids, steroids, carbohydrates, phenols and alkaloids, while AAS was used to conduct elemental analysis for the determination of Cu, Zn, Fe, Ca, Mg, Ni, Pb, Cd and Cr. The phytochemical screening revealed the presence of all the aforementioned phytochemicals except anthraquinones. PA and KA had more saponin presence while only PA had more tannin presence. The duplicate elemental analysis showed that the concentrations of Cu, Zn, Fe, Ca and Mg were significantly present in all samples within the range of 3.00 ± 0.07 Mg/Kg to 21.52 ± 0.021 Mg/Kg. Heavy metals like Ni, Pb, Cd and Cr were below detection limit (BDL) samples. All elements were within the WHO permissible limits in all the samples and all samples contained vital elements.

KEYWORDS

Phytochemicals; Natural Products; Heavy Metals; Medicinal Plants

1.0 INTRODUCTION

Natural products such as medicinal plants are very significant part of our ecosystem since they provide us with substances that treats various kinds of diseases (1). Medicinal plants contain phytochemicals such as alkaloids, flavonoids, saponins, tannins, and glycosides. These phytochemicals are secondary metabolites found in medicinal plants that are used to cure illnesses and relieve pain (2, 3). Several studies have also shown that these phytochemicals contained in medicinal plants also have therapeutic potential (4, 5). The ethnomedicinal qualities of the plants have been reported in numerous manuals (6, 7). As gastric ulcer treatment research advances, medicinal plant phytochemicals are building the framework for novel therapeutics (8, 9). Traditional treatments made from plants or herbs are frequently utilized in developing countries because they are simple to obtain, safe, affordable, and have little negative effects. However, doctors are cautious of recommending its use to patients due to misuse (10, 11).

Nigeria has over 7000 species of plants. These plant species are easy to access since they grow naturally. The knowledge of these plants by people of the past have fostered the use of the plants to treat illnesses like gastric ulcer (12). In Kaduna, various herbal treatment for gastric ulcer are sold in different locations. These herbs contain various kinds of plants which are obtained from different locations, and are prepared from different sources such as well water, borehole water and river water (13).

About 80% of the world's population relies on plant-based medicines and historically used herbs as their primary health care. Herbal medicines are well known for their therapeutic benefits. Nutritionally important mineral elements build up in the plants used as herbs and food supplements. Nonetheless, elements like lead, cobalt, chromium, cadmium, etc., can be harmful if they build up to certain concentrations in plants (12).

Lead, mercury, arsenic, and cadmium are the most frequent heavy metals that are hazardous to people, while cobalt and aluminum can also do so. The World Health Organization advises that medicinal plants, which serve as the basis for the majority of



herbal treatments, be examined for the presence of heavy metals (12). Most articles have assessed individual plants; however, in this research, our aim is to assess the phytochemicals and elements contained in the herbal mixtures used for the treatment of gastric ulcer in Kaduna Metropolis.

2.0 MATERIALS AND METHODS

2.1 Sample Collection

Samples of herbal plant mixtures used for treatment of gastric ulcer were collected from Narayi (NA), Panteka (PA), Kabala West (KAW), Kano Road (KA) and Sabon Tasha (SA) regions of Kaduna metropolis. The liquid samples were stored in bottles, labeled and kept in a cool dry environment prior to further analysis.



Fig 2.1: Herbal Mixture Samples Used for Gastric Ulcer Treatment

2.2 Preparation of Plant Extract for Phytochemical Analysis

The extraction of plant material was done by hot water extraction method. This was carried out by taking 250ml of the sample into a beaker. The mixture was heated in a water bath at 30°C-40°C and stirred continuously for 30 minutes. The crude

plant extract was filtered using filter paper and further dried in an oven for 15 minutes. The resulting extract was stored in sterile sample containers. The phytochemical screening was carried out in ABU Zaria, while the AAS analysis was carried out at the Federal Ministry of Agriculture and Food Security, Kaduna.



Fig 2.2: Crude Plant Extract from Herbal Mixture

2.3 Phytochemical Analysis

The preliminary qualitative phytochemical screening of the various plants extract was carried out using the methods reported by Yadav and Agarwala (14);

2.3.1 Test for Anthraquinones

Bontragers test: 10ml of benzene was added in 6.0g of the powdered sample in a conical flask and soaked for 10minutes and the filtered. Further 10ml of 1% ammonia solution was added to the filtrate

and shaken vigorously for 30 seconds and pink, violet or red color indicated the presence of anthraquinones in the ammonia phase.

2.3.2 Test for Tannins

Bromine water test: 10ml of bromine was added to the 0.5g aqueous extract. Discoloration of bromine water showed the presence of tannins.

Ferric Chloride test: about 0.5g each portion of aqueous extract was stirred with about 10ml of distilled water and then filtered. Few drops of 1% ferric chloride solution were added to 2ml of the



filtrate. Occurrence of a blue black, green or blue green precipitate indicates the presence of tannins.

2.3.3 Test for Saponins

Frothing test: 5.0ml of distilled water was mixed with aqueous crude plant extract in a test tube and it was mixed vigorously. The frothing was mixed with few drops olive oil and shaken vigorously and the foam appearance shows the presence of saponins.

2.3.4 Test for Flavonoids

Shinoda test: pieces of magnesium ribbon and concentrated HCl were mixed with aqueous crude plant extract after few minutes and pink color showed the presence of flavonoids.

Alkaline reagent test: 2ml of NaOH mixture was mixed with aqueous plant crude extract; concentrated yellow colour was produced which became colourless when added two drops of diluted acid to mixture. This result showed the presence of flavonoids.

2.3.5 Test for Cardiac Glycosides

Keller-Kiliani test: a solution of glacial acetic acid (4.0ml) with 1 drop of 2.0% FeCl₃ mixture was mixed with the 1.0ml aqueous plant extract and 1ml H₂SO₄ concentrated. A brown ring formed in between the layers showed the entity of cardiac glycosides.

2.3.6 Test for Terpenoids

Liebermann's test: 2ml of acetic acid and 2ml of chloroform with whole aqueous plant crude extract were mixed. The mixture was then cooled and concentrated H₂SO₄ was added. Green color showed the entity of aglycone, steroidal part of glycosides.

2.3.7 Test for Steroids

Salkowski's test: 2ml of concentrated H₂SO₄ was added to the whole aqueous plant crude extract. A reddish-brown colour was formed which indicated the presence of steroidal aglycone part of the glucoside.

2.3.8 Test for Carbohydrates

Molisch test: few drops of Molisch reagent was added to the solution of the extract followed by addition of concentrated H₂SO₄ from the side to form a lower layer. Violet ring at interface indicates the presence of carbohydrates.

2.3.9 Test for Phenols

Lead acetate test: few drops of lead acetate solution was added to the solution of the extract. Yellow color ppt indicates the presence of phenol.

2.3.10 Test for Alkaloids

Mayers test: few drops of Mayers, Wagners or Dragendorff reagent was added to the solution of the extract. Mayers reagent gives cream ppt, Wagner gives whitish ppt, Dragendorff gives orange ppt.

2.4 Elemental Analysis of Crude Plant Extract

The grounded vegetable matters were each taken in a porcelain crucible and ashed in a muffle furnace at 500°C until all the vegetable matter turned to a white ash. 0.5g of the ash was then treated with digestion mixture in the ratio (1:4:33) of (HClO₄:H₂SO₄:HNO₃) and the beaker placed in a fume cupboard. The mixture was gently heated at 150°C until it boiled. Heating continued until brown fumes disappeared leaving white dense fumes and the content reduced to 5ml. This was then cooled and made up to 50ml using distilled water. This was then used for heavy metal analysis using AAS (15).

3.0 RESULTS AND DISCUSSION

Table 3.1: Qualitative Phytochemical Screening of Crude Plant Extracts

S/N	Phyto. constituents	Test	PA	KA	NA	SA	KAW
1	Alkaloids	Dragendorff test	+	+	+	+	+
2	Cardiac glycosides	Keller kiliani test	+	+	+	+	+
3	Saponins	Frothing test	++	++	+	+	+
4	Phenolic compounds	Lead acetate test	+	+	+	+	+



5	Tannins	Ferric chloride test	++	+	+	+	+
6	Steroids	Salkowski test	+	+	+	+	+
7	Carbohydrates	Molisch test	+	+	+	+	+
8	Flavonoids	Shinoda test	+	+	+	+	+
9	Terpenoids	Libermann Burchard test	+	+	+	+	+
10	Anthraquinones	Bontragers test	-	-	-	-	-

Note: + present, ++ present, - absent.

Table 3.2 AAS Elemental Analysis for Plants Extracts (Mg/Kg) (mean±standard deviation)

	<i>Cu</i>	<i>Zn</i>	<i>Ni</i>	<i>Pb</i>	<i>Cd</i>	<i>Cr</i>	<i>Fe</i>	<i>Ca</i>	<i>Mg</i>
<i>NA</i>	9.32±0.1 27	3.75±0.0 07	0.005±0. 007	0.005±0. 007	0.04±0.0 1	0.16±0.0 2	3.925±0. 02	11.06±0. 03	18.07±0.02 8
<i>SA</i>	5.80±0.0 35	3.92±0.0 1	BDL	BDL	BDL	0.015±0. 007	7.46±0.0 1	13.31±0. 007	14.98±0.00 7
<i>PA</i>	11.10±0. 007	4.10±0.0 07	BDL	0.07±0	0.06±0.0 1	0.01±0.0 1	12.78±0. 05	9.80±0.0 1	21.52±0.02 1
<i>KA</i> <i>W</i>	6.77±0.0 78	3.00±0.0 07	BDL	BDL	0.005±0. 007	0.125±0. 021	4.59±0.0 1	14.07±0. 035	18.49±0.02 8
<i>KA</i>	8.41±0.0 28	3.01±0.0 1	BDL	0.02±0.0 1	0.08±0.0 1	0.08±0.0 1	9.415±0. 03	14.72±0. 007	15.09±0

Note: Results obtained above are mean ± standard deviation from duplicate analysis.

BDL= Below Detection Limit

The phytochemical analysis is of great importance as it provides us with the understanding of the therapeutic properties of herbal mixtures. In this study, the herbal samples contained phytochemicals as revealed by the phytochemical qualitative tests.

According to table 3.1, all samples contained alkaloids, cardiac glycosides, saponins, phenolic compounds, tannins, steroids, carbohydrates, flavonoids, and terpenoids did not contain anthraquinones. PA and KA contained more saponins than other plant extracts. Also, PA had the highest concentration of tannins. These differences can be attributed to the various plants mixed in the herbal mixture.

Futhermore, these phytochemicals have antioxidant, cytoprotective and antisecretory

properties. Alkaloids and phenolic compounds also exhibit anti-inflammatory, antimicrobial and antioxidant effects. Plants that contain alkaloids are efficient for treating headache, fever, and also possess antibacterial and analgesic properties (16). Cardiac glycosides have been reported to treat heart diseases and improve the pumping action of the heart especially in ulcer patients (17).

From Table 3.2, elemental analysis was carried to determine the quantitative concentrations of various elements in the herbal mixtures. Elements were obtained in the range of 0.00 mg/kg to 21.52 mg/kg. The concentrations of Cu, Fe, Mg, Zn and Ca were the highest, while those of Ni, Cr, Pb and Cd were the lowest. Ni was below detection limit in SA, PA, KA, and KAW.



From the mean values of the elemental analysis, it can be observed that Mg has the highest concentration in all of the samples followed by Ca, Cu, Fe and Zn, respectively. A high concentration of Mg, Zn, and Fe were obtained in PA. Other toxic elements such as Cd and Pb had little or no significant concentrations in all of the samples. Furthermore, all samples contained essential elements such as Ca, Fe, Mg, Cr, Cu and Zn, which play a vital role in biochemical/enzymatic processes and participate as constituents of different antioxidant compounds. Additionally, some of the elements have gastroprotective action (15).

The observed variations in the elemental concentrations of the extracts can be attributed to

differences in the botanical structures of the various plants, different compositions of the soil from which they were collected, the preferential absorbance of each plant species, the irrigation water and the climatic conditions (18).

Among the detected elements; Ca, Fe, Mg, Cu and Zn are considered essential elements for plant growth because they are directly involved in nutrition, and their absence in plants hinders appropriate life cycles (18). Although not considered essential elements, Cr, Ni and Cd show positive effects on plant growth below a certain limit.

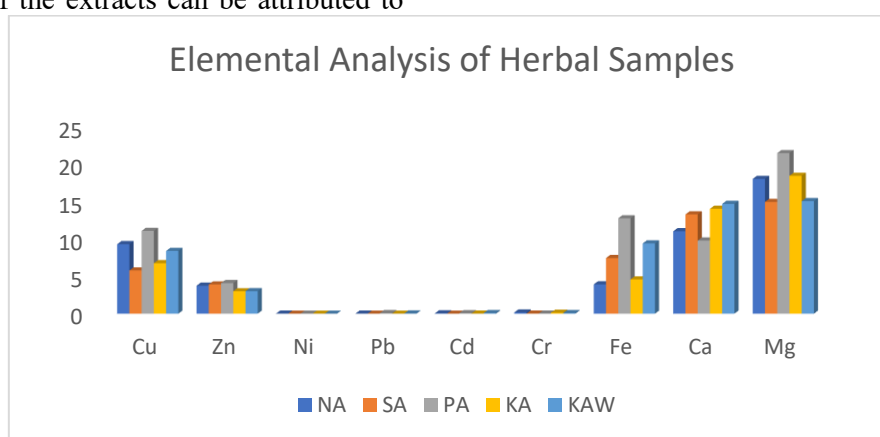


Fig 3.1: Graph of Elemental Analysis of Extracts from Herbal Mixtures

After their incorporation, the elements can be classified as essential elements (Mg and Ca from the detected elements) and trace elements (Cr, Ni, Pb, Fe, Cu, Zn and Cd from the detected elements). Although not all of the chemical elements possess biological activities that are fully described, most of them have functions directly related to the maintenance of health and the proper functioning of the body (15).

A large number of important physiological and biochemical processes in plants require Mg and Ca, which are essential nutrients. They primarily help in the manufacture of chlorophyll, the transport and use of photoassimilates, the activation of enzymes, and the synthesis of proteins. Cu is often regarded as the third most prevalent trace element in the body, behind zinc and iron. Additionally, it is a crucial catalyst for iron absorption, according to reports. It's lack could increase the risk of cardiovascular disease. Symptoms like neuropenia, heart problems, osteoporosis, and anemia may appear when there is a clear copper deficit (19).

Manganese-holding enzymes include pyruvate carboxylase and superoxide dismutase.

More than 200 enzymes, including alcohol dehydrogenase, ribonucleic polymerases, alkaline phosphatase, and carbonic anhydrase, are thought to contain zinc as one of their primary building blocks. Pb, Cd, and Ni are thought to be harmful substances by nature, and their presence in trace amounts in the samples of medicinal plants examined may be the result of pollution from vehicles and industrial operations. A high concentration of cadmium in plants is regarded as being extremely dangerous when ingested by humans. Additionally, it harms the liver and kidneys and raises blood pressure (18).

Cr is a necessary element that enhances the effectiveness of insulin and thus affects the metabolism of carbohydrates, lipids, and proteins. The use of beneficial copper oxides and fungaceous insecticides may be to blame for its high level. The availability of outlining elements in herbal mixtures is frequently strongly connected with the concentration of these components in plants. The



primary source of trace elements for plants, both as micronutrients and contaminants, is soil (15).

4.0 CONCLUSION

The result obtained from this experiment have validated that some of the herbal mixtures used for treating gastric ulcer in Kaduna Metropolis contain phytochemicals that have therapeutic effects. Furthermore, vital elements were confirmed in these mixtures at various concentrations Ca, Mg, Fe, Cu, and Zn were detected within the permissible limits while Cd, Pb, Ni, and Cr were detected below the permissible limits recommended by WHO. Special concentration should be given to various form of metals distributed within the plants in the herbal mixture, because metals in plants seems to have a decisive role in metal transfer to other organisms. Our examination revealed that heavy metals and trace elements present in the analyzed medicinal plants were within permissible limits of WHO (20).

5.0 REFERENCES

1. R. S. Bhat, S. Al-Daihan, Antimicrobial activity of *Garcinia mangostana* using different solvents extracts. *International Journal of Biosciences* **3**, 267-272 (2013).
2. S. K. Jain, *Manual of ethnobotany*. (Scientific publishers, 2010).
3. M. Ahmad *et al.*, Quality assurance of herbal drug valerian by chemotaxonomic markers. *African Journal of Biotechnology* **8**, (2009).
4. P. Sheng-Ji, Ethnobotanical approaches of traditional medicine studies: some experiences from Asia. *Pharmaceutical biology* **39**, 74-79 (2001).
5. M. Sarfaraj, M. A. Rahman, I. Ahmad, M. Saeed, Current approaches toward production of secondary plant metabolites. *J Pharm Bioallied Sci* **4**: 10-20. *Journal of Pharmacy and Bioallied Sciences* **4**, (2012).
6. M. Wink, Medicinal plants: a source of anti-parasitic secondary metabolites. *Molecules* **17**, 12771-12791 (2012).
7. M. Ahmad *et al.*, Use of chemotaxonomic markers for misidentified medicinal plants used in traditional medicines. *J Med Plant Res* **4**, 1244-1252 (2010).
8. R. Khan *et al.*, Antimicrobial activity of five herbal extracts against multi drug resistant (MDR) strains of bacteria and fungus of clinical origin. *Molecules* **14**, 586-597 (2009).
9. S. Acharyya, G. K. Dash, S. Mondal, S. K. Dash, Antioxidative and antimicrobial study of *Spondias mangifera* willd root. *Int. J. Pharm. Pharm. Sci* **2**, 68-71 (2010).
10. J. Hussain *et al.*, Assessment of herbal products and their composite medicinal plants through proximate and micronutrients analysis. *Journal of Medicinal Plants Research* **3**, 1072-1077 (2009).
11. A. Altemimi, D. G. Watson, M. Kinsel, D. A. Lightfoot, Simultaneous extraction, optimization, and analysis of flavonoids and polyphenols from peach and pumpkin extracts using a TLC-densitometric method. *Chemistry Central Journal* **9**, 1-15 (2015).
12. M. Osawaru, M. Ogwu, C. Ahana, Current status of plant diversity and conservation in Nigeria. *Nigerian J Life Sci* **3**, 168-178 (2013).
13. A. Kayode, B. Lawal, A. Abdullahi, M. Sonibare, J. Moody, Medicinal plants used in the treatment of gastric ulcer in southwestern and north central Nigeria. *Research Journal of Medicinal Plant* **13**, 119-128 (2019).
14. R. Yadav, M. Agarwala, Phytochemical analysis of some medicinal plants. *Journal of phytology* **3**, (2011).
15. P. C. ALIKWE, O. Owen, Evaluation of the chemical and phytochemical constituents of *Alchornea cordifolia*



- leaf meal as potential feed for monogastric livestock. *International Journal of Pharmaceutics and Drug Analysis* **2**, 360-368 (2014).
16. A. W. Al-Shahwany, Alkaloids and phenolic compound activity of *Piper nigrum* against some human pathogenic bacteria. *Biomed. Biotechnol* **2**, 20-28 (2014).
 17. D. K. Sharma, K. Shah, R. Dave, Phytochemicals: Promising potential uses in pharmacology. *Recent trends in Pharmaceutical Sciences*, 84 (2019).
 18. S. Gunavathy, H. B. Sherine, Determination of heavy metals and phytochemical analysis of some selected medicinal plants. *Int. J. Sci. Res. in Biological Sciences Vol* **6**, 3 (2019).
 19. E. Piccolo, C. Ceccanti, L. Guidi, M. Landi, Role of beneficial elements in plants: implications for the photosynthetic process. *Photosynthetica* **59**, 349-360 (2021).
 20. World Health Organization, Traditional Medicines. (2008).



P031 - THE IMPACT OF ARTIFICIAL INTELLIGENCE ON RESEARCH INNOVATION: NIGERIAN PERSPECTIVE

Philips Ifeanyi Eze*, Theophilus Aniemeka Enem**, Kenneth Osita Nwanya*

National Research Institute for Chemical Technology, Zaria, Department of Cyber Security, Air Force Institute of Technology, NAF Base, Kaduna***

Corresponding author email: ifeanynig@gmail.com

ABSTRACT

The emergence of Artificial Intelligence in today's cyberspace, is it just a hype or an agent of transformation? It is redefining innovation and has brought a paradigm shift on how researches are conducted. Artificial intelligence is an evolving technological field with great transformative potentials. It is not only coming to contribute to new product development but also as originator and facilitator. Nigerian researchers are informed of the dominance and opportunities provided by AI, but many are yet to be actively involved in its utilization. This paper tries to explore through literature and questionnaire on the awareness, acceptability and effect of this new technological trend. The outcome reveals that Nigerian researchers are aware and willing to accept and upgrade to this new model of innovative research. Most researchers are optimistic that innovation and modern research would be redefined by Artificial Intelligence.

KEYWORD

Artificial Intelligence, Innovation, Research, Technology, Nigeria

1.0 INTRODUCTION

An artificial intelligence model is an algorithm or a tool which takes decision based on certain data sets without human intervention. These data sets allow it to reach a conclusion or make predictions or forecast when adequate information is processed. This is highly suitable for solving complex problems (1, 2) It can also be described as a computer program that can learn and use data to achieve goals.(3)

Artificial intelligence is the science and engineering of making intelligent machines, using computers to solve tasks intelligently as if it is a human. This allows for perception, reason and action. Artificial intelligence obviously will aid in complex computations, accelerating research and handling of quantum data generated globally by both humans and machines(4)

Research and Development in the 21st century would be greatly affected by the introduction of artificial intelligence into the scene. Innovation processes would not be left out because artificial intelligence will enhance the efficiency of research processes and research outcomes. Cockburn *et al* (2018) in their working paper suggested that the introduction of artificial intelligence would lead to

a significant switch from labour-intensive research to passively generated large datasets and enhanced prediction algorithm. The researchers should take advantage of the interplay between the two research paradigms. They further stated that this would avail both private and public actors in research the tools for stimulating research productivity and innovation-oriented competitions. (5)

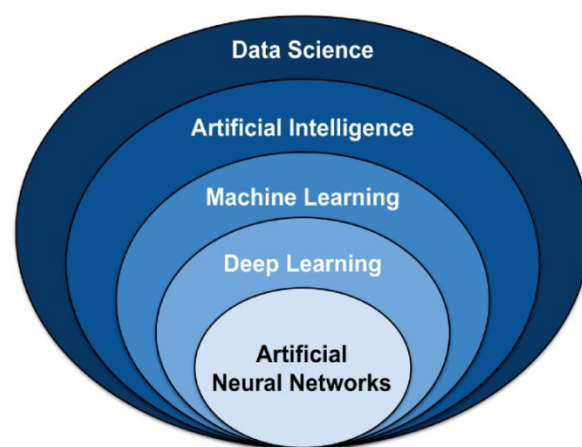


Fig. 1: Artificial Intelligence (AI) includes the sub-fields of Machine Learning



(ML) and Deep Learning (DL)

Source: <https://viso.ai/deep-learning/ml-aimodels/>

Artificial Intelligence may prominently upturn the efficiency of the existing economy. AI are reshaping the method of invention and innovation process as well as the organisation of Research and Development. Iain *et al* reiterated that Artificial Intelligence will lead to a substitution of labour-intensive research by passively generated large datasets and enhanced prediction algorithms. Hence policies should be made to encourage transparency and sharing of core datasets across private and public sector actors. They noted that it may be critical to stimulating research productivity and innovation oriented competitions.(5)

In April 2018, the founder of Facebook Mark Zuckerberg briefed the United States senate that AI tools could be used to identify hate speech and terrorist propaganda. Researchers would describe such classification tasks within the field of supervised machine learning.(6)

Artificial Intelligence is gradually being embraced by organizations to innovate and this is ever more revealed in scholarly works. Some works have been done on economic, technological and social factors of adoption of AI in firms willing to innovate. This is setting a research agenda for other companies and organization to consider the adoption of artificial intelligence as a new frontier for innovation.(7)

“We’ve never seen a technology move as fast as AI has to impact society and technology. This is by far the fastest moving technology that we’ve ever tracked in terms of its impact and we’re just getting started.” Paul Daugherty, Chief Technology and Innovation Officer, Accenture.

It has been claimed that Artificial Intelligence carries enormous potential for service and product innovation. Policy makers worldwide nowadays are strategizing on ways to foster environment conducive for Artificial Intelligence-based innovation. Broad based innovative solutions are being developed. These policies should focus on human resources development to have experts in AI technologies.(8)

The implications of innovation and design theory for scholars are also substantial. Novel theoretical questions arise and new frameworks are required. How can we define and conceptualize innovation,

in a context where change is never over and a solution is never obsolete? It is conspicuous that in Artificial Intelligence factories solutions are created, enhanced, and customized by machines which operate through loops that scale up rapidly, with the possibility of creating unintended outcomes.(9)

The data collected from experts’ interviews concerning Artificial Intelligence based innovation identifies key challenges for innovation management. Therefore significant emphasis should be on human factors and the need to address the availability of large volumes of good quality data from SMEs.(8)

Marcello *et al* performed a systematic literature review of over one thousand four hundred and forty-eight articles on the intersection between Artificial Intelligence and innovation. They discovered or identified three major factors for AI adoption in organisations and they include economic, technological and social factors. They developed an agenda for future research on adoption of AI by organisations as a vehicle for innovation. (7)

Swift advances in artificial intelligence have notable implications for the economy and society in general. These implications will affect productivity, employment and competition amongst organisations. The introduction of AI could dominate how organizations innovate to remain afloat. The broad applicability of deep learning and AI across many sectors would likely engender a race of proprietary advantage that leverages these new approaches. Effective policies to protect new entries and ensure data accessibility is of primary importance to avoid monopoly and anticompetitive practices. (5)

As organizations evolve to clinch a progressively AI-centric operating model, several vital business processes are being digitized hence reducing human labour and management. AI will change the practice of research by deviating from the normal traditional way of problem solving. New technologies bring great promise but also great challenges.(9)

Artificial Generative Intelligence will aid in various automations hence taking up responsibilities that will allow man have more time for other things. Data collection, pre-processing, topic modelling, analysis and visualization would require minimal manual efforts.(10)



AI in the 4th industrial revolution is delivering real value necessitated by the availability of relevant data, computational ability and algorithms. Studies conducted on AI influence on attaining Sustainable Development Goals reveals that AI is making poverty reduction achievable by providing relevant data and maps used to revolutionize agriculture, education and financial institution. The need to invest more in AIs was emphasized for emerging economies in achieving Sustainable Development Goals.(11)

In China a study was conducted on the impact of AI on technological innovation through logic reasoning and empirical modelling in manufacturing sectors within a period of 2008 to 2017. The result shows that AI affected technological Innovation by accelerating knowledge creation, technology spill over, improve learning and absorptive capacities. It also increases Research and Development and talent investment hence more foreign direct investment.(12)

The infusion of AI into different aspects o fundamental sciences such as information science, mathematics, medical science, physics and chemistry has helped to motivate researchers to deeply understand the state of the art applications of Artificial Intelligence.(13)

Succinctly stated, coupling capabilities of cognitive systems and humans allows enterprises to attain competitiveness in a hybrid society. Even though integrating AI into business systems and processes is a journey unlike any other digital technology application, its use is about the backing of humans and not the dominance of technology over humans. On this note, further research work should be carried out on the methodology for the identification of application potentials of artificial intelligence and the establishment of new forms of human-machine interaction for the design of enhanced innovation processes.(14)

Establishments globally must evaluate their vision and transform their workforce, processes, technology and data readiness in order to unleash the power of AI and survive in this digital age(15).

Artificial Intelligence is different from other digital technologies given its capabilities to evolve into both general-purpose technology and a method of inventing and several organisations are embracing it into their innovation strategies. Self-innovating

AIs is about to change how innovations are created and several organisations should leverage on this to develop more complex products and services.(16)

Sergey in his paper titled Multidimensional Data-Driven Artificial Intelligence Innovation by Sergey A. Yablonsky, the author considered some emerging issues that will require action in the nearest future. The evaluation logic presents a tool that managers, investors and company owners could use to identify and manage multi-dimensional big data-driven Artificial Intelligence innovation framework. In our present digital age, when intangible assets are fast becoming more critical for an organisation's performance, new big data driven AI value dimensions can support business leaders to provide more effective measurement and management of their intellectual and informational capital assets. (17)

One of the grand challenges of our time is the fostering of suitable AI that is not harmful but beneficial to human lives. The crucial link of civic conversation and public debate has been problematized in relation to the inability of marginalized communities to shape public debate, hence the need for accountable and responsible AI. (18)

A global survey conducted in 2016 of managers, health and life sciences, manufacturing, retailers and financial organisations indicates that one third of these institutions are involved in testing the waters of AI as a tool for transforming businesses and organize innovation activities.(19)

2.0 METHODOLOGY

This research explored through literature on the impact of AI on innovative research. We went further to narrow it down through a questionnaire deployed to respondents mainly researchers within Zaria as a sample of Nigerian researchers on their awareness, acceptability, utilization and approval of using AI as an innovative tool for research. More than 70 questionnaires were specifically deployed to mainly researchers and 85% were filled and returned.

3.0 RESULT AND DISCUSSION

The diagrams below show the results from the questionnaires distributed to various researchers of different ages and fields in Nigeria. This is to ascertain the effect of AI in research activities.



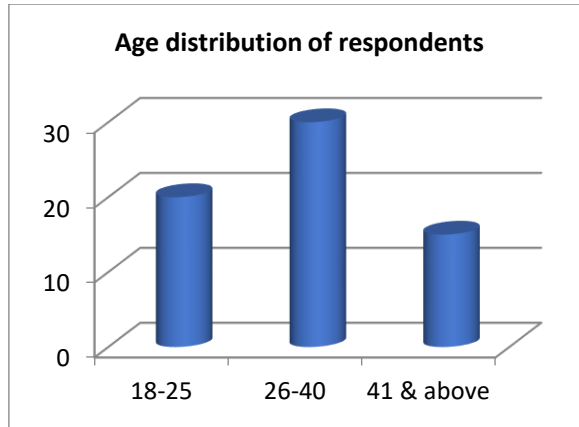


Fig. 2: Age distribution of respondents

Figure. 2 above shows the age distributions of various respondents. It was distributed into three groups, (18–25, 26-40, 41& above)

The above distribution reveals that larger numbers of the researchers are young and vibrant. This portends hope for the Nigerian research sector with young energetic group involved in research.

Moreover the younger ones are more receptive to technological change and innovations. *“AI has been rising as a powerful general-purpose technology that promises to lower uncertainty with more accurate predictions and to reduce the cost of labourous tasks.”* (20)

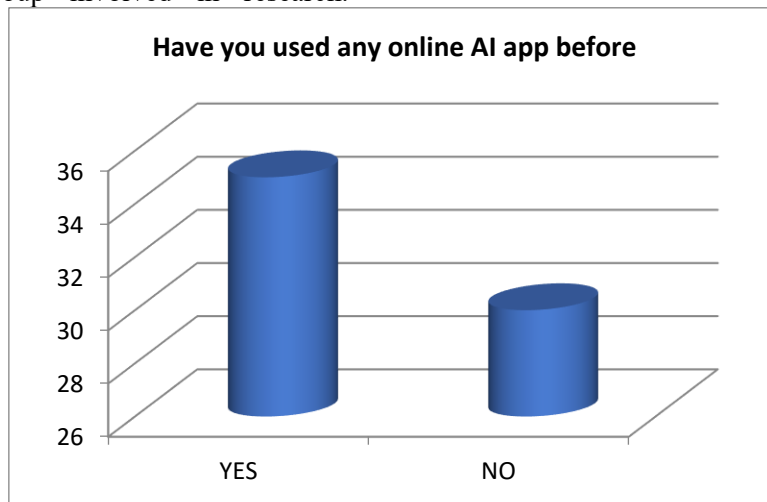


Fig. 3: Researchers and Online AI App

In figure 3 above most of the younger researchers acknowledged that they have used one or more AI applications online. Hence one can deduce that the

younger generation would be more open and receptive to innovation and innovative research.



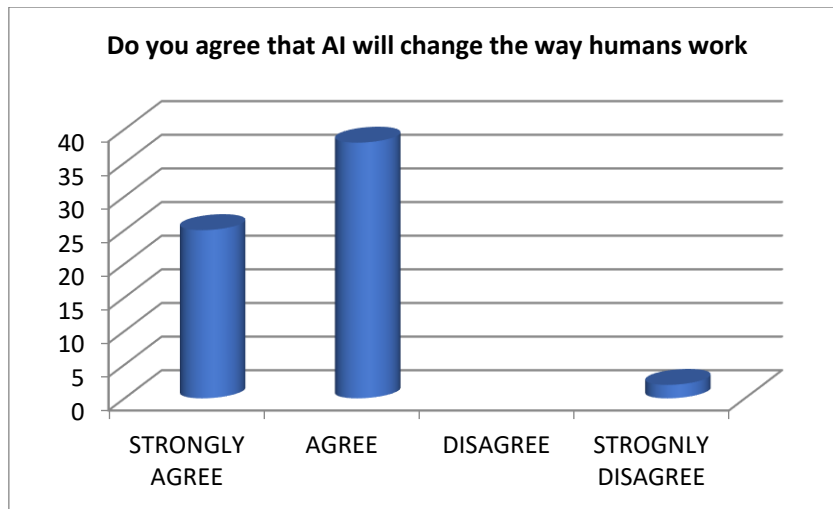


Fig. 4: AI and Human Activities

One key factor that makes a product or service marketable is novelty. AI may be the desired tool that will drive this change considering the amount of data in the cyber space. AIs would play a key role to mine these data for prospective and transformative innovations.

Most researchers agree on the affirmative that AI would change the way humans work. AI may be the new technological revolution that has come for the rescue. So many jobs done by humans may be phased out since AI would dominate such jobs for better efficiency.

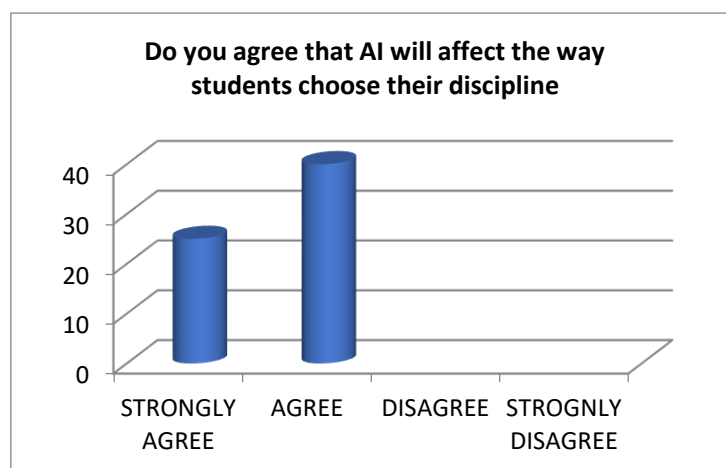


Fig. 5: AI and students' choice of careers

This trend will affect the educational curriculum. To conform to the best global practices, some school syllabus will be changed. Many courses offered by our institutions will be redesigned.

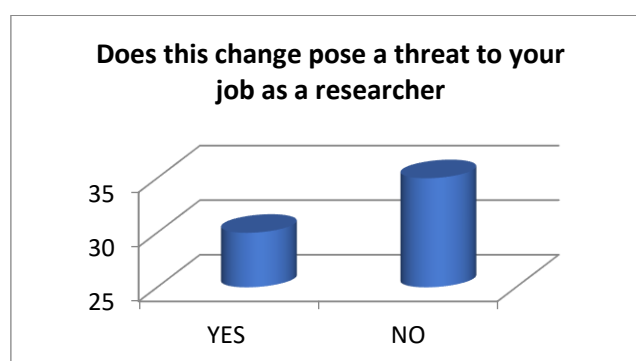


Fig. 6.0: AI and Job loss

Some researchers expressed fear that AIs pose threat to their jobs. The implication is that most researchers should upgrade their technological skills to be more digitally compliant.

The other respondents may be expressing their willingness to upgrade and become digitally updated. The 'No' responders may be aware that the best global practice to research is through machine learning and artificial intelligence.

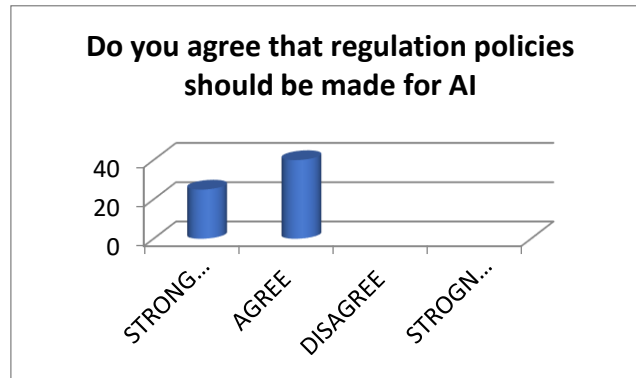


Fig. 7: AI and the need for regulation policy

The issue of governance of autonomous intelligence systems, responsibility, accountability, privacy and safety issues must be legally addressed. Acts and policies should be properly spelt out to address issues that may arise due to the deployment of AI systems. Patents, copyrights, and rights should not make the deployment of AIs a litigious technological advancement.

Global AI regulations should be enacted to prohibit the use Artificial intelligence on critical services that may threaten livelihoods.

4.0 CONCLUSION

Artificial Intelligence has come to stay and will boost productivity in our workplaces, culture and environment. Humans should leverage on the introduction of AI to focus more on jobs that need creativity and empathy. AI will make us feel life is moving fast and hence affect human behaviours. The emergence of AI would doubtless bring a change in research and development. The new norm would transform technological involvements in our daily lives. Government, researchers and the citizenry should live up to their expectations. The fields of neural networks, data science, data mining, expert systems, robotics will gain more relevance in the educational landscapes of many nations and school curriculum.

Many researchers acknowledged that they are aware of the new model and that the Nigerian Government and Institutions should adopt this model to catch up with the global best practice in

modern research. The school curriculum of most developing countries should also be updated to incorporate technology more deeply into our learning culture. For research and development institutions the time to implement and leverage on this new technology is now.

5.0 REFERENCES

1. K. Nico, The Ultimate Guide to Understanding and Using AI Models. *viso.ai*: <https://viso.ai/deep-learning/ml-ai-models/>, (2023).
2. K. Nico, in *viso.ai*. (2023).
3. E. Liu, M. S. Bhutani, S. Sun, Artificial Intelligence: The new wave of innovation in EUS. *Endoscopic Ultrasound*, 10(2), 79 (2021).
4. N. Saini, RESEARCH PAPER ON ARTIFICIAL INTELLIGENCE & ITS APPLICATIONS. *International Journal for Research Trends and Innovation (IJRTI)*, Vol. 8, Issue 4, 356-360 (2023).
5. I. M. Cockburn, R. Henderson , S. Stern, "The Impact of Artificial Intelligence on Innovation: An exploratory analysis," (In the



- Economics of artificial intelligence: An agenda, University of Chicago Press, 2018).
6. K. Niklas, G. Marc, H. Robin, S. Gerhard Satzger, "Machine Learning in Artificial Intelligence: Towards a Common Understanding," (Proceedings of the 52nd Hawaii International Conference on System Sciences, HICSS, Hawaii, 2019).
 7. M. M. Mariani, I. Machado, V. Margrelli, Y. K. Dwivedi, Artificial intelligence in innovation research: A systematic review, conceptual framework, and future research directions. *Technovation*, Vol 122, 102623 (2023,).
 8. P. Erich, Artificial intelligence for innovation in Austria. *Technology Innovation Management Review*,. *Technology Innovation Management Review*, Vol. 9, 12, 5-14 (2019).
 9. V. Roberto, L. Marco, V. Luca Innovation and Design in the Age of Artificial Intelligence. *Wiley Online Library*, Vol. 37, Issue 3, 212-227 (March 2020).
 10. M. C., G. M., Artificial Intelligence in Innovation: How to Spot Emerging Trends and Technologies. *IEEE Transactions on Engineering Management*, Vol. 69, no.2, pp493-510 (April 2022).
 11. M. David, Artificial Intelligence in the Industry 4.0, and Its Impact on Poverty, Innovation, Infrastructure Development, and the Sustainable Development Goals: Lessons from Emerging Economies? *MDPI*, Vol 13(11), 5788 (May 2021).
 12. J. Liu, H. Chang, J. Y. L. Forrest , B. Yang, Influence of artificial intelligence on technological innovation: Evidence from the panel data of china's manufacturing sectors. *Technological Forecasting and Social Change*, Vol 158, 120142 (2020).
 13. Y. Xu *et al.*, Artificial intelligence: A powerful paradigm for scientific research. *The Innovation*, 2, (4), (2021).
 14. C. Vocke, C. Constantinescu, D. Popescu, Application potentials of artificial intelligence for the design of innovation processes. *Procedia CIRP*, 84, 810 - 813 (2019).
 15. R. Iyoti, N. Ward-Dutton, P. Carnelly, S. Findling, Marshall, Artificial Intelligence 1.0. *IDC MaturityScope Doc#US44119919*, (2019).
 16. H. Philip, Reinventing Innovation Management: The Impact of Self-Innovating Artificial Intelligence. *IEEEExplore Vol 68, issue 2*, 628-639 (2020).
 17. A. Y. Sergey, Multidimensional Data-Driven Artificial Intelligence Innovation. *Technology Innovation Management Review*, 16 - 28 (Dec, 2019).
 18. A. Buhmann, C. Fieseler, Towards a deliberative framework for responsible innovation in artificial intelligence. *Technology in Society*, Vol 64, , 101475 (2021).
 19. A. Sudhir, The Impact of Artificial Intelligence on Innovation -An Exploratory Analysis. *International Journal of Creative Research Thoughts (IJCRT)*, Vol 4, Issue 4, pp.810-814 (2016).
 20. Y. Truong, S. Papagiannidis, Artificial intelligence as an enabler for innovation: A review and future research agenda. *Technological Forecasting and Social Change*, 183, 121852 (2022).





P032 - GASIFICATION OF MAIZE COBS AND ITS CHARACTERIZATION FOR ENERGY GENERATION

¹Philip, A.J., ²Jerome, P.I., ³Rifore, B.S., ⁴Fasanya, O., ⁵Isa, R.O, ¹Olutoye M.A

^{1, 2, 5}*Department of Chemical Engineering, Federal University of Technology, Minna,* ³*Department of Chemistry, Nigerian Defense Academy, Kaduna,* ⁴*Industrial and Environmental Pollution Department, National Research Institute for Chemical Technology.*

Corresponding Author: philipjerome93@gmail.com

ABSTRACT

The gasification of maize cobs and its characterization for its energy potential was carried out. The proximate analysis of the maize cob gave 17.5% moisture content, 1.5% ash content, 73.0% volatile matter, and 8.0% fixed carbon content. A high calculated calorific value of 14.71 MJ/kg was gotten. The exit gas from pyrolysis at 5500C consists of CO, CO₂, H₂, H₂O, CH₄, N₂, and C₂H₆ with percentage composition 7.3%, 11.49%, 0.52%, 4.7%, 4.18%, 3.66%, and, 7.83% respectively. At 700 °C, the compositions were found to be 8.4%, 13.2%, 0.6%, 5.4%, 4.8%, 4.2%, and 9.0% respectively while 9.49%, 14.91%, 0.68%, 6.1%, 5.42%, 4.74% and 10.17% respectively was obtained for pyrolysis 850°C. The gasification process revealed that as the temperature was increased more of the biomass was converted to gas leading to less char generation. The result also showed increase in hydrogen, methane, carbon monoxide as well as less desirable carbon dioxide with increase in pyrolysis temperature. The elemental analysis for percentage of carbon, hydrogen, oxygen, nitrogen and sulfur emitted during gasification at 700 °C for 15 minutes revealed C-78.43%, H-0.64%, O-19.98%, N-0.66%, and S-0.29%. The low amount of sulfur and nitrogen emitted concludes that maize cob can be tapped as a source for energy application. Optimization can be carried out to determine the optimal temperature for high calorific value gas yield.

KEYWORDS

Gasification; Maize Cob; Biomass; Proximate Analysis; Bio-fuel, Syngas

1.0 INTRODUCTION

Despite the advent of renewable energy, a huge amount of man's activities that provide global energy are heavily dependent on fossil fuels, to the degree of 85%. Due to the increase in population, urbanization, and economic growth, the demand for fuel is likely to increase by 50% in 2025 (1). The combustion of fossil fuels has led to an ever deterioration of climate due to the increase in greenhouse gases (GHG) which causes global warming and climate change (2). Thus, there is a fast-growing emphasis on energy transition and the adoption of renewable energy from biowaste resources which has the prospect of making waste management more efficient and also increasing energy resources in a country like Nigeria (3). Therefore, the transition from fossils to other energy sources is increasing renewable energy uptake across the globe. This transition also involves the conversion of waste materials into renewable energy.

The development of alternative recycling facilities, composting, and waste-to-energy in recent years has changed the final destination of these wastes, which is our main concern. Despite this, a sizable portion of the waste produced is still dumped in landfills, where it builds up and negatively impacts the ecosystem. Countries that adopt this policy aim to lessen the environmental issues connected to landfills, such as soil pollution and usage (4), leachate contamination of groundwater resources, greenhouse gas emissions from landfill gases, and so on. The production of biomaterials; such as the fractionation of lignocellulosic biomass from forestry and agricultural activities, as well as incineration, anaerobic digestion, pyrolysis, and thermal gasification using wastes as feedstock, have all been explored as alternatives to valorize the wastes produced (5-7).

Nigeria has a large quantity of biomass waste generated each year. The effect this waste has on humans and the environment poses a serious threat



(8). Biomass such as corn cobs is discarded after the kernel is removed. These widely available corn cobs in Nigeria can be characterized and evaluated for potential energy generation (8). Open burning of organics has been widely used in most communities in Nigeria which contributes to the greenhouse effect. (9), Hence the purpose of this study is to tap the potential of energy generation of biomasses. Thermal gasification has been employed among all the methods used in WtE facilities to valorize solid wastes, generating heat and syngas. Carbon monoxide (CO), hydrogen (H₂), nitrogen (N₂), carbon dioxide (CO₂), and light hydrocarbons (such as CH₄, C₂H₄, and C₂H₆) are the major components of syngas, a gaseous product that can be used as fuel.

Gasification has utilized a variety of raw materials over the years, including coal and biomass, which are generally feedstocks with a homogeneous composition. Due to their heterogeneous composition, using valorizing wastes, especially industrial wastes, in gasification might be difficult (10). This is why in this study, we have focused on biomass (maize cobs) with the aim of pyrolyzing and characterizing them, for energy generation.

This research aims to evaluate the potential of the biomass (maize cobs) for energy conversion; this will be achieved by determining the proximate analysis, ultimate analysis and the calorific value of the maize cob.

2.0 MATERIALS AND METHODS

2.1 Materials

Miller (Thomas Wiley Mill-Model ED5), 2mm stainless steel sieve, Triple beam weigh balance, Gallenkamp oven and furnace, desiccator, crucible, spatula, and corn hub. All analyses were conducted at the National Cereals Research Institute (NCRI) in Badeggi, Niger State.

2.2 Methods

2.2.1 Pretreatment and Gasification of Maize Cob

The corn cob used as biomass was obtained from Gidan Kwanu in Minna, Niger State. Initial size reduction was carried out on the corn cobs using a mortar and pestle. After preliminary size reduction, the corn cob was fed into the miller where it was ground and sieved to a mesh size of 2mm. 2 grams of ground maize cobs were loaded into the furnace.

Before pyrolysis, the reactor was purged with inert nitrogen gas to remove any residual air and create an oxygen-free environment.

The temperature of the furnace was raised gradually at a rate of 200C/min from ambient temperature. The maize cob samples were subjected to pyrolysis using ASTM standard method. Evolved gasses (syngas and volatiles) were analyzed for characterization.

2.2.2 Proximate Analysis

This analysis involved the determination of moisture content, fixed carbon, volatile matter and Ash content.

2.2.2.1 Moisture Content

The moisture content of a biomass is the quantity of water per unit mass of a dry biomass. It was done experimentally using the ASTM method of determining the moisture content of the biomass (8). The experiment was carried out by weighing an empty crucible, after which 2g of corn cob was added and distributed evenly by tapping the crucible lightly. The crucible containing the corn cobs was then placed in an oven at a temperature (of 105 °C) for one hour. On cooling, the crucible was weighed, together with the sample. The percentage moisture content was calculated:

$$\text{Moisture content (\%)} = 100 \frac{(B-C)-(C-A)}{(B-A)} \dots \dots \dots (1)$$

Where: A = weight of crucible (g), B = weight crucible + wet sample (g), C = weight of crucible + dry sample (g).

2.2.2.2 Ash Content Analysis

Ash content indicates the amount of inorganic matter or components left in the corn cob biomass after combustion. The determination of ash content in the corn cob was carried out using ASTM standard procedure by adding 2 g of corn cob after which the crucible was reweighed again with the sample in it. The crucible was placed in a furnace and allowed to heat at a temperature of 550°C with the sample in it, for one hour. This was to allow the combustible material not to burn completely. At room temperature, the crucible containing the sample was removed and reweighed.

The percentage was calculated according to the following equation:



$$\text{Ash content (\%)} = 100 \frac{A-B}{C} \quad \dots \dots (2)$$

Where:

A = weight of crucible with sample (g) B = weight of crucible with ash (g)

C = weight of sample (g)

2.2.2.3 Volatile Matter Content Analysis

The essence of volatile analysis is to give a measure of the gasses that were emitted during the thermal decomposition of the biomass in an inert

The fixed carbon of the biomass was computed using the relationship below (Jigisha et al, 2006):

$$FC = 100 - \%ASH - \%VM - \%MC. \quad \dots \dots (3)$$

Where

FC=fixed carbon; %Ash=% ash content and %VM=% volatile matter; % MC= percentage moisture content.

2.3 Ultimate Analysis

The ultimate analysis was carried out to know the elemental composition of the biomass. These elements present in biomass include carbon (C), hydrogen (H), oxygen (O), nitrogen (N) and sulfur (S). The elemental analysis of the maize cob was carried out using the ASTM standard procedure.

3.0 RESULTS AND DISCUSSION

3.1 Proximate Analysis of Maize Cob Biomass

Table 3.1: The Proximate Analysis (%) and Calorific Values (MJ/Kg) of Maize Cobs

EXPERIMENTAL VALUES (%)	
ANALYSIS	MAIZE COBS
Moisture Content	17.5
Ash Content	1.5
Volatile Content	73.0
Fixed Carbon	8.0
Calorific Value	14.7

3.2 Ultimate Analysis of Biomass

environment. The crucible was weighed and 2 g of corn cob was added, then the new weight of the crucible was measured. The corn cob was spread evenly in the crucible, which was then covered and placed in a furnace that was preheated already to a temperature of 950 °C for about seven minutes (11). The crucible was removed and cooled in a desiccator, then reweighed. The percentage volatile can also be calculated using the equation (12).

$$\%VM = [(initial\ weight - final\ weight)] \times 100$$

2.2.2.4 Fixed Carbon

The Carbon and hydrogen percentage was determined using the ASTM E777 procedure while the Nitrogen and Sulfur was determined using ASTM E778 and 775 respectively.

The Oxygen composition was obtained from the percentage difference of other elements using the equation below [19].

$$\text{Oxygen composition} = 100 - (\%S + \%N + \%H + \%O) \quad \dots \dots (4)$$

2.3.1 Heating (Calorific) Value

The net calorific value was determined by using the relationship below:

$$CV = 18.7 (1.0 - AC - MC) - (2.5MC) \quad \dots \dots (5)$$

Where: CV= lower calorific value; MC = moisture content; AC= ash content



Table 3.2: The Composition of Different Samples after Complete Combustion

SAMPLES	CARBON	NITROGEN	HYDROGEN	SULFUR	OXYGEN
Maize cobs	78.43	0.64	19.98	0.66	0.29

3.3 Analysis of Exit Gas of Maize Cobs

Table 3.3: The percentage composition of compounds in the gas stream at 550°C

COMPOUND	%VALUE
CO	7.33
CO ₂	11.49
H ₂	0.52
H ₂ O	4.70
CH ₄	4.18
N ₂	3.66
C ₂ H ₆	7.83

3.4 DISCUSSION OF RESULTS

The moisture content was calculated to be 17.5%. This is not high, since standards revealed that the suitable moisture content for biomass for biofuels should be less than 20%. The result is higher than those obtained by Ayodele (13), and those reported by Maj et al. (14). The difference in these values could be due to many reasons; including the source of Maize Cob and processing conditions. A higher moisture content is not desirable due to corrosion concerns. Ash content was determined to be 1.5 %, which is relatively low. The ash content of Maize Cob describes the inorganic matter that is left after the complete combustion of the biomass. This ash contains several elements which may not completely undergo combustion.

Maize Cob was also characterized by a volatile matter content of 73%, which was anticipated because of the organic nature of the material. Volatile matter contents in biomass are usually high because it indicates its potential to create huge amounts of inorganic vapours when used as feedstock in a gasification process. The higher the volatile matter content, the better its combustion and gasification rates because of the biomass yield upon carbonization (14). The fixed carbon content was determined to be 8.0 % which represents the percentage of carbon available for char combustion. This low fixed carbon-releasing content causes the biomass to have a prolonged heating time. The solid combustible residue that had its volatiles given off was observed to be low due to its low fixed carbon.

The calorific value obtained was 14.7 MJ/Kg which is slightly less than most values obtained from literature. Those obtained by Maj et al. (14) fell between 9.69MJ/Kg to 14.94 MJ/Kg. Our result obtained was also less than those obtained for agro-biomass obtained by Kang et al. (15).

Table 3.2 presents the results obtained from the ultimate analysis of maize cob. This analysis is very important because the chemical characteristics of Maize Cobs can also influence the biomass fuel and the operating conditions of the gasifier. The percentage compositions were observed to be 78.4% carbon, 19.98% hydrogen, 0.66% sulfur, 0.64% nitrogen and 0.29% oxygen. The carbon content was observed to be very high due to the cellulosic nature of the maize cobs. Biomass material contains hydrogen in the form of water, and the low hydrogen content was a result of the biomass being dried and stored well before use. The hydrogen content was also low due to the hydrocarbons emitted during combustion. The low oxygen content is due to the presence of oxygen in the form of moisture in the biomass; however, the biomass was combusted in the absence of oxygen and oxygen is contained in the water molecules of the biomass alone. Maize cob was observed to contain low sulfur and nitrogen percentage from the result of analysis carried out which is an advantage for the biomass. These elements are potential pollutants and have the tendency to contaminate the environment and are hazardous to living things in the environment when combusted. This low sulfur and nitrogen is an advantage that maize cob could



be blended with other potential solid fuels to reduce the sulfur content of those fuels (13).

According to Table 3.3, our major concerns were in the amount of CO and CO₂ released by the biomass. CO and CO₂ values of 7.33% and 11.49% were observed respectively. High composition of

CO and CO₂ can cause harm to the environment during combustion; thus, it is important to seek a suitable technology that would optimize this process. These potential pollutants can be reduced by blending maize cob with other fuels like coal with a lower percentage of carbon dioxide and nitrogen emissions.

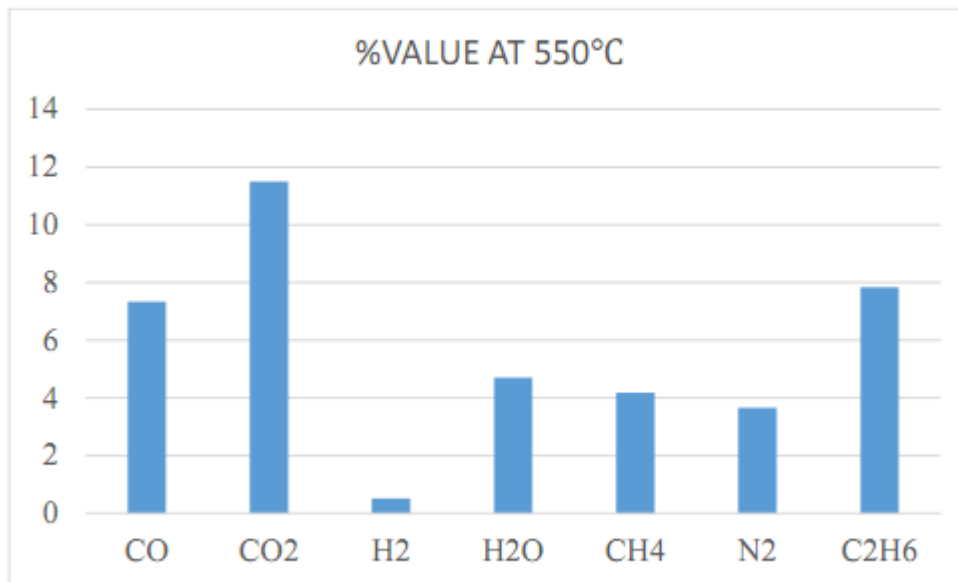


Figure 1: Chart for the percentage composition of compounds

4.0 CONCLUSION

From the above results and discussions, we can thus infer that the use of more optimized technologies for gasification can yield accurate results which will be useful for application in energy generation. The pyrolysis of maize cob has a great tendency to greatly improve the heating value for effective utilization of their biomass in energy conversions. The exit gas from the furnace was characterized by the compositions present in the stream. This is because most of the biomass is volatilized and produces gasses which are essential in power generation. Hence, this biomass can be used as a source of fuel and power generation.

5.0 REFERENCES

1. A. A. Sokan-Adeaga, G. R. Ana, A comprehensive review of biomass resources and biofuel production in Nigeria: potential and prospects. *Reviews on Environmental Health* **30**, 143-162 (2015).
2. Z. A. Elum, D. M. Modise, G. Nhamo, Climate change mitigation: the potential of agriculture as a renewable energy source in Nigeria. *Environmental Science and Pollution Research* **24**, 3260-3273 (2017).
3. R. Ibikunle, I. Titiladunayo, S. Dahunsi, E. Akeju, C. Osueke, Characterization and projection of dry season municipal solid waste for energy production in Ilorin metropolis, Nigeria. *Waste Management & Research* **39**, 1048-1057 (2021).



4. Y. Van Fan, J. J. Klemeš, C. T. Lee, S. Perry, Anaerobic digestion of municipal solid waste: Energy and carbon emission footprint. *Journal of environmental management* **223**, 888-897 (2018).
5. H. Mahmudul, M. Rasul, D. Akbar, R. Narayanan, M. Mofijur, Food waste as a source of sustainable energy: Technical, economical, environmental and regulatory feasibility analysis. *Renewable and Sustainable Energy Reviews* **166**, 112577 (2022).
6. H. K. Jeswani, A. Azapagic, Assessing the environmental sustainability of energy recovery from municipal solid waste in the UK. *Waste Management* **50**, 346-363 (2016).
7. M. Ram, J. C. Osorio-Aravena, A. Aghahosseini, D. Bogdanov, C. Breyer, Job creation during a climate compliant global energy transition across the power, heat, transport, and desalination sectors by 2050. *Energy* **238**, 121690 (2022).
8. C. Ibeto, J. Ayodele, C. Anyanwu, Evaluation of pollution potentials and fuel properties of nigerian sub-bituminous coal and its blends with biomass. *J. Mater. Environ. Sci* **7**, 2929-2937 (2016).
9. O. S. Anuge, A. Ghosh, K. T. W. Ng, in *Canadian Society of Civil Engineering Annual Conference*. (Springer, 2021), pp. 163-171.
10. O. Alves *et al.*, Techno-economic study for a gasification plant processing residues of sewage sludge and solid recovered fuels. *Waste Management* **131**, 148-162 (2021).
11. A. Kwaghger, L. Enyejoh, H. Iortyer, The development of equations for estimating high heating values from proximate and ultimate analysis for some selected indigenous fuel woods. *European Journal of Engineering and Technology Vol 5*, (2017).
12. Marquez-Montesino *et al.*, Study of the energetic potential of pine biomass Caribea *Revista Chapingo Cien-Cias Foreatale y dei ambient* **7(1)**, 83-89 (2001).
13. J. A. Ayodele, Evaluation of the fuel properties and thermal efficiency of sub-bituminous coal-biomass blend. *Researchgate*, (2014).
14. G. Maj *et al.*, Energy and emission characteristics of biowaste from the corn grain drying process. *Energies* **12**, 4383 (2019).
15. S. B. Kang, H. Y. Oh, J. J. Kim, K. S. Choi, Characteristics of spent coffee ground as a fuel and combustion test in a small boiler (6.5 kW). *Renewable Energy* **113**, 1208-1214 (2017).



P033 - PRODUCTION AND ASSESSMENT OF ALUMINUM SULPHATE CRYSTALS (ALUM) FROM RECYCLED ALUMINUM FOILS AS COAGULANT IN WATER TREATMENT

Olabimtan Olabode. H*¹, Ochigbo Victor¹, Latayo Musa.B¹, Adegboro Narcillina.N², Egwu Obilove. J³

¹National Research Institute for Chemical Technology, Department of Industrial and Environmental Pollution, Zaria Kaduna State, Nigeria, ³National Research Institute for Chemical Technology, Department of Scientific and industrial Research, Zaria Kaduna State, Nigeria, ⁴Nigerian Institute of Leather and Science Technology, Department of Polymer Technology, Zaria, Kaduna State, Nigeria, ⁵Federal University of Technology, School of Infrastructure, Process, Engineering and Technology, Chemical Engineering, Minna, Niger State, Nigeria.

Corresponding author's e-mail*: Olabode4angel@gmail.com

ABSTRACT

Water borne diseases and health implications resulting from poor water quality are significant concerns in many regions. In the absence of adequate water treatment facilities and resources, finding affordable and eco-friendly solutions becomes imperative. Turbidity in water, caused by suspended particles and impurities, is a common challenge in regions with limited resources and contaminated water sources. This approach endeavours to provide a sustainable solution by synthesizing aluminium sulphate crystals (alum) from discarded aluminium foils and evaluating their effectiveness as a coagulant in water treatment.

Aluminium sulphate (alum) is a well-known coagulant used in water treatment due to its ability to remove turbidity effectively. However, its production often relies on bauxite mining, which is resource-intensive and environmentally impactful.

The synthetic process was actualized through controlled precipitation and crystallization techniques using standard sulfuric acid and sodium hydroxide respectively. The synthesized crystals were physically evaluated with dosages from 10 to 100mg/L on the prepared turbid water samples, having established an optimum dosage of 100mg/L with 98% turbidity removal after 1 hour.

This study presents a significant step towards achieving the United Nations Sustainable Development Goal of ensuring clean water and sanitation for all.

KEYWORDS

Alum crystals, Waste aluminium foils, Turbid water treatment, precipitation and crystallization.

1.0 INTRODUCTION

Access to clean and safe water is a fundamental human right, recognized by the United Nations as an essential component of achieving sustainable development and ensuring the well-being of all (1). However, this right remains elusive for a significant portion of the global population, primarily in regions where water sources are contaminated and access to treatment facilities is limited (2). The quality of available water is often compromised by turbidity, a condition characterized by the presence of suspended particles and impurities, rendering it

unsuitable for consumption or domestic use (3). Addressing turbidity and ensuring the provision of safe water is a pressing global challenge.

Turbidity is not merely an aesthetic concern; it is closely linked to public health (4). High levels of turbidity in water are associated with an increased risk of waterborne diseases, which can have severe consequences, particularly in vulnerable communities with limited access to healthcare (5). Contaminants, including bacteria, viruses, and other pathogens, can hide within suspended particles, making effective removal of turbidity a crucial step in water treatment.



One of the established methods for reducing turbidity in water is coagulation (6). Coagulation involves the addition of a coagulant that destabilizes and aggregates suspended particles, allowing them to settle and be removed (7). Aluminum sulphate, commonly known as alum, is a widely recognized coagulant due to its effectiveness in water treatment (8). However, the conventional production of alum often relies on bauxite mining, an industry associated with high energy consumption, environmental degradation, and negative social impacts (9). This raises concerns about the sustainability of alum production and its long-term viability as a water treatment solution.

This research takes a novel approach to tackle both the issue of water turbidity and aluminium waste by synthesizing aluminium sulphate crystals (alum) from recycled aluminium foils and assessing their coagulation efficiency in water treatment. Recycling aluminium foils as a source of alum has the potential to address two significant challenges simultaneously: water turbidity and aluminium waste (10). Aluminium foils are commonly used in households and generate a substantial amount of waste. By converting this waste into a valuable resource for water treatment, this research offers a sustainable and environmentally friendly alternative to conventional alum production.

The significance of this research is underscored by the United Nations Sustainable Development Goals (SDGs), particularly Goal 6, which aims to ensure clean water and sanitation for all (11). Achieving this goal is not only a matter of meeting basic human needs but also a key driver of social and economic development.

Furthermore, this study aligns with Goal 12, which calls for responsible consumption and production, and Goal 15, which addresses life on land, considering the environmental impact of bauxite mining and the potential for resource conservation through recycling (12).

The introduction of this research sets the stage for the exploration of a sustainable and innovative solution to turbidity in water, grounded in the principles of recycling, environmental responsibility, and improved access to safe water. This study's contribution extends beyond the laboratory, offering practical implications for water treatment practices, resource conservation, and sustainable development, ultimately serving as a model for addressing critical global challenges.

2.0 MATERIALS AND METHODS

Recycled Aluminium Foils: Aluminium foils, collected from household waste, were utilized as the primary source material for the synthesis of aluminium sulphate (alum) crystals. These foils were selected as a sustainable alternative to conventional bauxite-based alum production due to their widespread availability and potential for resource conservation (12).

Sulfuric Acid (H_2SO_4): Laboratory-grade sulfuric acid was used as the source of sulphate ions in the synthesis process. It was procured from a reputable chemical supplier and utilized without further purification.

Sodium Hydroxide (NaOH): Sodium hydroxide, commonly known as caustic soda, served as the precipitant in the synthesis of alum crystals. It was obtained in a solid form and dissolved in distilled water to create a standardized sodium hydroxide solution (10M).

Distilled Water: Distilled water, free of impurities and ions, was used in various stages of the synthesis process to ensure accurate and reproducible results.

Turbid Water Samples: Turbid water samples were prepared using a suspension of fine soil particles in distilled water. The turbidity of these samples was controlled by adjusting the concentration of suspended particles. This approach allowed for the evaluation of the coagulation efficiency of the synthesized alum crystals.

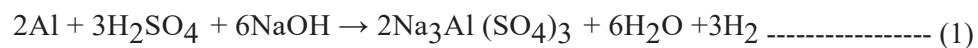
2.1 Synthesis of Aluminum Sulphate (Alum) Crystals

The synthesis of alum crystals was achieved through controlled precipitation and crystallization techniques with the waste aluminum foils that were initially cleaned and cut into small pieces. These foil pieces were then subjected to a controlled reaction with concentrated sulfuric acid, resulting in the formation of aluminum sulphate in solution. Sodium hydroxide was subsequently added to the aluminum sulphate solution, initiating the precipitation of aluminum sulphate crystals.

The resulting crystals were allowed to settle, and the supernatant solution was decanted. The crystals were then subjected to a series of washes with distilled water to remove any residual impurities. Following thorough washing, the alum crystals



were dried at a controlled temperature and stored for further analysis.



This equation represents the reaction between aluminum (Al) and sulfuric acid (H₂SO₄), which produces aluminum sulphate Na₃Al (SO₄)₃ and hydrogen gas (H₂). The addition of sodium hydroxide (NaOH) to the filtered solution results in

the precipitation of aluminum hydroxide (Al (OH)₃), which then converts to alum KAl (SO₄)₂•12H₂O upon drying in the oven. The overall reaction can be summarized as follows:

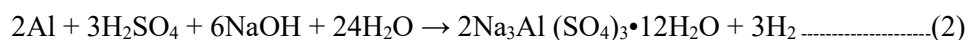


Figure 1: Crushed aluminium foils



Figure 2: Synthesized alum crystals



2.2 Evaluation of Coagulation Efficiency

A simulated water sample was prepared by adding 100 g of clay sand to 1 L of deionized water, with the mixture stirred with a magnetic stirrer for 30 minutes. Subsequently, various quantities of the

2.3 Qualitative Chemical Tests for Aluminum ion (Al^{3+})

Two drops of a diluted 1.4M potassium hydroxide (KOH) solution were introduced into the dissolved alum solution. Subsequently, sulfuric acid was incrementally added to the alum solution, first in drops and then in excess (13).

2.4 Qualitative Test for Potassium ions (K^+)

To further confirm the existence of potassium ions (K^+) in the synthesized alum crystals, a flame test

synthesized alum (ranging from 10 to 100 mg) were introduced separately into constant volume (100ml) of the polluted water samples (10). The mixtures were stirred for 1 minute and allowed to settle for 30 minutes. Afterwards the turbidities of the water mixtures were measured using a turbidity meter.

was conducted. The synthesized alum crystal was exposed to an open flame for approximately 20 seconds (14).

2.5 Confirmation for sulphate ion (SO_4^{2-})

A portion of finely ground alum crystal was introduced into a test tube containing distilled water, and the solution was stirred until the crystal completely dissolved. Subsequently, two drops of an aqueous solution of barium chloride ($BaCl_2$) were introduced into the mixture (15).

3.0 RESULTS AND DISCUSSION

Table 1: Qualitative analysis of ions present in the synthesized alum crystal

Test	Observation	Inference
Alum solution + $BaCl_2$ (aq) solution	White Precipitate formed, and insoluble	SO_4^{2-} Confirmed
Solid alum crystal+ heat (10 minutes)	Red flame turned to Pale purple flame color	K^+ Confirmed
Alum solution + H_2SO_4 (aq) in drop and in excess	Thick, white gelatinous precipitate formed insoluble in drop but soluble in excess	Al^{3+} Confirmed

The Tables above provides the results of different chemical tests conducted on alum solution and solid alum crystals to validate the activities of different ions in the compound according to the standard method. The first test involved adding an aqueous

$BaCl_2$ solution to the alum solution (2 g/50 ml), which developed a white precipitate that is insoluble after 20 hours. This confirms the availability of sulphate ions (SO_4^{2-}) in the



compound as BaSO₄, an insoluble white precipitate, is formed (13).

The second test involved heating solid alum crystals, which resulted in a pale purple flame color. This confirms the presence of aluminum ions confirms the presence of potassium ions (K⁺) as the (Al³⁺) in the compound as Al (SO) is formed due to the heat causes the alum crystals to decompose and release potassium ions, which produce a pale purple flame color (14).

The table shows the turbidity removal (in NTU - Nephelometric Turbidity Units) for different alum dosages, ranging from 0 mg/100ml to 100 mg/100ml. Turbidity removal refers to the reduction in cloudiness or haziness in the water and is a key parameter in water treatment. As the alum dosage increases, the turbidity removal percentage also increases.

The data clearly indicates a dosage-response relationship. As the dosage of alum increases, the percentage of turbidity removal also increases. This

The third test involved adding H₂SO₄ (aq) to the alum solution in drops and excess. This resulted in a thick, white gelatinous precipitate that is insoluble in the drop but soluble in reaction between H₂SO₄ and Al³⁺ (15).

Hence, the results provide important information for identifying and characterizing the compound, as well as for assessing its purity and quality. This is an indication that the synthesized alum crystal possesses all the necessary chemical properties expected of any alum crystal.

is a crucial finding as it helps determine the optimal alum dosage required for effective water treatment.

To achieve an optimum balance between efficient turbidity removal and cost-effectiveness, it is important to consider the diminishing returns observed at higher alum dosages. This means that beyond a certain point, increasing the alum dosage does not lead to a significant increase in turbidity removal. In this outcome, the optimum dose appears to be between 40 mg/100ml and 50 mg/100ml, where the percentage of turbidity removal is around 94-95%.

Table 2: Turbidity removal efficiency of synthesized alum at varying dosages

Alum dosage (mg/100ml)	Turbidity removal (NTU)			Actual Turbidity (NTU)	% Turbidity Removal
	1-hour sedimentation				
	1st Trial	2nd Trial	3rd Trial		
0	155	155	155	155	0
10	31.50	31.45	31.51	31.49 ± 0.03	79.68387
20	21.00	21.00	20.00	20.67 ± 0.58	86.66452
30	16.51	16.51	16.50	16.51 ± 0.01	89.34839
40	11.50	11.52	11.50	11.51 ± 0.01	92.57419
50	8.03	8.01	8.02	8.02 ± 0.01	94.82581
60	6.50	6.50	6.51	6.50 ± 0.01	95.80645
70	4.52	4.50	4.51	4.51 ± 0.01	97.09032
80	3.51	3.51	3.50	3.51 ± 0.01	97.73548
90	2.50	2.52	2.51	2.51 ± 0.01	98.38065



100	2.01	2.00	2.02	2.01 ± 0.01	98.70323
-----	------	------	------	-------------	----------

The turbidity removal efficiency was calculated using the following formula:

$$\% \text{ Turbidity removal} = \frac{(\text{Initial turbidity} - \text{Final turbidity})}{\text{Initial turbidity}} \times 100\%$$

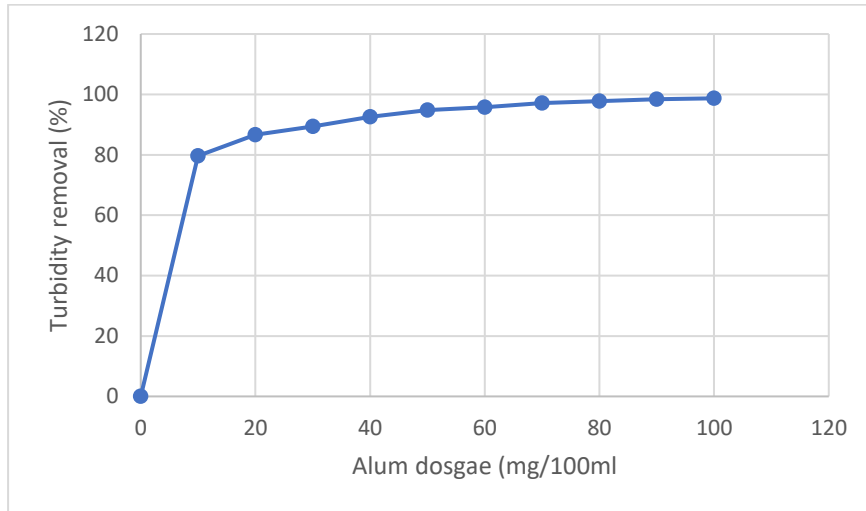


Figure 7. Percentage Turbidity removal by various alum crystal dosages

The dataset consists of multiple trials (1st, 2nd, 3rd trials) for each alum dosage.

The minimal variation in turbidity removal among trials indicates good reproducibility of the results.

The results provide for 1-hour sedimentation, which is a common practice in water treatment. Sedimentation allows suspended particles to settle at the bottom, resulting in clearer water. This suggests that alum dosages significantly accelerate the sedimentation process and improve water clarity.

This process demonstrates the effectiveness of alum as a coagulant in reducing turbidity as water

treatment facilities can use this information to optimize their alum dosage and improve the efficiency of the treatment process.

The consistent results with minimal variation indicate the reliability of the experimental methods and suggest that quality control measures were in place during the trials.

However, it is important to consider the environmental impact of residual aluminum in treated water as balancing effective treatment with environmental concerns is a key consideration in water treatment practices.



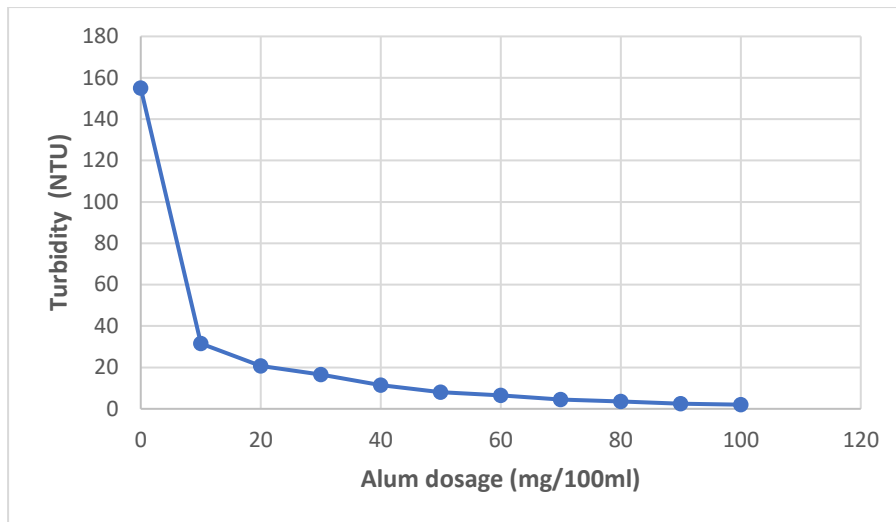


Figure 6. Turbidity removal by various alum crystals dosages

The results (Figure 6) reveal a clear and consistent trend as the alum dosage increases, turbidity removal also increases. This relationship is highly significant because it provides a quantitative understanding of the coagulation process. Coagulants like alum neutralize the negative charges on suspended particles, causing them to clump together and settle out of the water. The formation of larger flocs makes it easier to remove these particles, thereby reducing turbidity.

The research identified an optimal alum dosage range where the removal of turbidity is maximized, demonstrating that there is a point beyond which adding more alum does not significantly improve turbidity removal. This information is valuable for

water treatment facilities, as it allows for the cost-effective use of alum while achieving the desired water quality standards.

These findings have practical implications for water treatment processes. By understanding the relationship between alum dosage and turbidity removal, water treatment plants can fine-tune their coagulant dosing strategies. This not only improves the efficiency of the treatment process but also ensures that resources are used effectively. Additionally, the use of alum, which can be synthesized from recycled aluminum foil, presents an eco-friendly and cost-effective solution for turbidity removal.

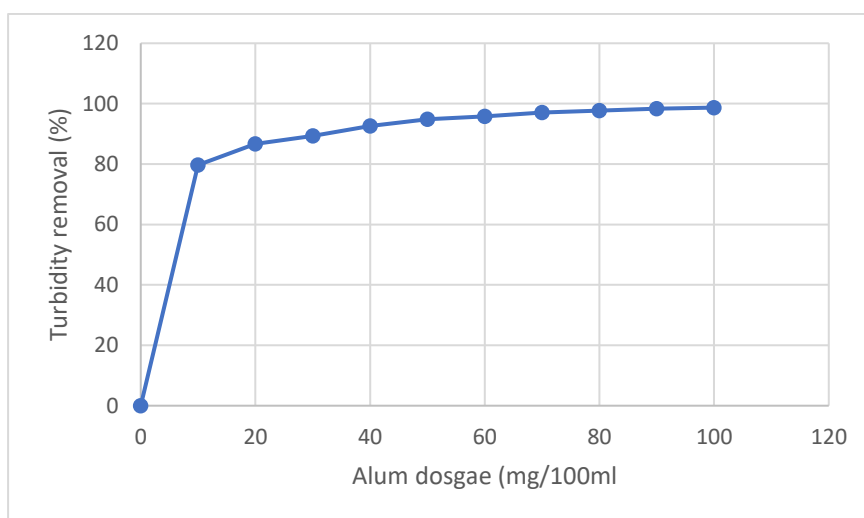


Figure 7. Percentage Turbidity removal by various alum crystal dosages



The alum crystal dosage increases, the percentage of turbidity removal also increases. This relationship is fundamental because it demonstrates the effectiveness of alum in coagulating and removing suspended particles from water. The mechanism involves the neutralization of the negative charges on the particles, leading to their aggregation and settling.

The data presented in the results show a remarkable decrease in turbidity as the alum dosage is increased from 0 mg/L to 100 mg/L. This decline in turbidity reflects the success of alum in clarifying the water. It is evident that alum, synthesized from recycled aluminum foil, can significantly contribute to water treatment processes by effectively reducing turbidity.

The findings not only emphasize the importance of the alum dosage but also reveal an optimal range where turbidity removal is maximized. This optimization is crucial for water treatment facilities as it helps them achieve the desired water quality standards while minimizing the cost of alum usage.

Furthermore, the results illustrate the cost-effectiveness and efficiency of using alum for turbidity removal. Alum, which can be derived

from waste aluminum foil, not only provides a sustainable solution for water treatment but also ensures that resources are utilized effectively.

4.0 CONCLUSION

This study demonstrates that alum is a highly effective coagulant in water treatment, and its usage can lead to significant improvements in water quality. This knowledge contributes to the development of more sustainable and environmentally friendly practices in water treatment, which is essential for providing clean and safe drinking water to communities around the world.

Similarly, the study showcases the potential of repurposing Aluminum waste to create an effective coagulant for water treatment and quality, providing a practical, sustainable, environmentally friendly solution to underscore the significance of adopting eco-friendly practices in addressing water treatment challenges and furthering the goals of environmental conservation and resource optimization.

5.0 REFERENCES

1. K. Meehan, J. R. Jurjevich, N. M. Chun, J. Sherrill, Geographies of insecure water access and the housing–water nexus in US cities. *Proceedings of the National Academy of Sciences* **117**, 28700-28707 (2020).
2. P. M. Bradley *et al.*, Public and private tapwater: Comparative analysis of contaminant exposure and potential risk, Cape Cod, Massachusetts, USA. *Environment international* **152**, 106487 (2021).
3. B. G. Kitchener, J. Wainwright, A. J. Parsons, A review of the principles of turbidity measurement. *Progress in Physical Geography* **41**, 620-642 (2017).
4. A. G. Mann, C. C. Tam, C. D. Higgins, L. C. Rodrigues, The association between drinking water turbidity and gastrointestinal illness: a systematic review. *BMC public health* **7**, 1-7 (2007).
5. A. J. De Roos *et al.*, Review of epidemiological studies of drinking-water turbidity in relation to acute gastrointestinal illness. *Environmental health perspectives* **125**, 086003 (2017).
6. Y. Sohrabi *et al.*, Chemical coagulation efficiency in removal of water turbidity. *International Journal of Pharmaceutical Research* **10**, 188-194 (2018).
7. P. Moussas, A. Zouboulis, Synthesis, characterization and coagulation behavior of a composite coagulation reagent by the combination of polyferric sulphate (PFS) and cationic polyelectrolyte. *Separation and purification technology* **96**, 263-273 (2012).
8. Y. Kong *et al.*, Coagulation behaviors of aluminum salts towards humic acid: detailed analysis of aluminum



- speciation and transformation. *Separation and Purification Technology* **259**, 118137 (2021).
9. A. Ruud, Can transnational aluminium producers be ecologically sustainable? A case study of Jamaica's bauxite/alumina industry. *Business Strategy and the Environment* **3**, 82-91 (1994).
 10. E. David, J. Kopac, Aluminum recovery as a product with high added value using aluminum hazardous waste. *Journal of hazardous materials* **261**, 316-324 (2013).
 11. T. T. Bui, D. C. Nguyen, M. Han, M. Kim, H. Park, Rainwater as a source of drinking water: A resource recovery case study from Vietnam. *Journal of Water Process Engineering* **39**, 101740 (2021).
 12. N. Voulvoulis, J. W. Skolout, C. J. Oates, J. A. Plant, From chemical risk assessment to environmental resources management: the challenge for mining. *Environmental Science and Pollution Research* **20**, 7815-7826 (2013).
 13. Y. Kim, Mineral phases and mobility of trace metals in white aluminum precipitates found in acid mine drainage. *Chemosphere* **119**, 803-811 (2015).
 14. G. Zeng, S. Xiong, Y. Qian, L. Ci, J. Feng, Non-flammable phosphate electrolyte with high salt-to-solvent ratios for safe potassium-ion battery. *Journal of The Electrochemical Society* **166**, A1217-A1222 (2019).
 15. J. G. Bell, M. Dao, J. Wang, Qualitative dependence of the electro-oxidation behavior of sulfite on solution pH. *Journal of Electroanalytical Chemistry* **816**, 1-6 (2018).



P35 - SARGASSUM SEaweEDS IN THE BLUE ECONOMY: A MINI REVIEW OF THEIR POTENTIAL AND APPLICATIONS IN CHEMICAL INDUSTRIES

Olabimtan Olabode.H^{1*}, Aronimo Samuel. B², Akinlotan Oluyinka.O³, Dadah Jummai.S⁴ and Yekeen Bayo.H⁵

¹ National Research Institute for Chemical Technology,

Department of Industrial and Environmental Pollution, Zaria Kaduna State, Nigeria, ² Kogi State College of Education (Technical), Department of Chemistry, Kabba, Kogi State, Nigeria, ³ Kogi State College of Education (Technical), Department of Integrated Science, Kabba, Kogi State, Nigeria, ⁴ Nigerian Institute of Leather and Science Technology, Department of Research and Development, Zaria Kaduna State, Nigeria, ⁵ The Oke Ogun Polytechnic, Department of Science Laboratory Technology, Saki, Oyo State, Nigeria.

Corresponding author's e-mail: **Olabode4angel@gmail.com**

ABSTRACT

The concept of the blue economy has gained considerable traction in recent years as a framework for sustainable development and economic growth, particularly in coastal regions and island nations. Central to this paradigm is the responsible utilization of marine resources to foster prosperity while preserving the delicate balance of ocean ecosystems. Among the myriad of marine resources, *sargassum* seaweeds have emerged as an intriguing subject of study and exploration. *Sargassum*, a genus of brown macroalgae, is known for its unique floating habitat in the Sargasso Sea and its wide distribution across the world's oceans. Beyond its ecological significance, *sargassum* seaweeds have garnered attention for their rich chemical composition.

This review delves into the intricate chemical constituents of *sargassum* species, elucidating the diversity of bioactive compounds, polysaccharides, pigments, and minerals they harbor. Through a thorough examination of scientific literature, we explore the potential applications of these chemical components in various industrial sectors. A particular emphasis is placed on the chemical industry, where *sargassum* seaweeds show promise as a valuable resource. While the opportunities presented by *sargassum* seaweeds in the chemical sector are substantial, this paper also addresses the complexities surrounding their utilization.

Environmental considerations, sustainable harvesting practices, and economic implications are carefully examined with the importance of responsible resource management and the need for interdisciplinary collaboration to harness the full potential of *sargassum* seaweeds within the blue economy context.

KEYWORDS

Blue economy, Sargassum seaweeds, Sustainable development, Marine resources and Chemical composition.

1.0 INTRODUCTION

The blue economy, a visionary concept born out of the growing imperative for sustainable development in coastal regions and island nations, is reshaping the way we perceive and utilize our planet's marine resources. This paradigm emphasizes the potential of oceans and seas not merely as vast expanses of water but as sources of boundless opportunities for economic growth, innovation, and ecological stewardship.

Central to the blue economy's success is the responsible exploitation of marine resources, and

among these resources, *sargassum* seaweeds have emerged as a topic of profound interest and intrigue.

Sargassum, a genus of brown macroalgae, commands a distinctive presence in the world's oceans. Its unique floating habitats, notably the Sargasso Sea in the North Atlantic, have captured the imagination of scientists, environmentalists, and policymakers alike (1). However, beyond its ecological importance as a refuge for marine life, *sargassum* seaweeds possess a remarkable reservoir of chemical compounds that hold significant promise for advancing the objectives of the blue economy.



This research paper embarks on a comprehensive exploration of the potential and applications of *sargassum* seaweeds in the chemical industries, thereby contributing to a deeper understanding of their role within the broader context of the blue economy. By delving into the intricate chemical composition of *sargassum* species, we aim to unravel the diversity of bioactive compounds, polysaccharides, pigments, and minerals that make these seaweeds a veritable treasure trove of natural resources. Within the chemical industry, *sargassum* seaweeds offer a spectrum of opportunities that span multiple sectors (2).

Their bioactive compounds hold the potential for breakthroughs in pharmaceuticals (3) and nutraceuticals (4), while their utility in biofuel production presents a pathway towards reducing our reliance on fossil fuels (5). Furthermore, the application of *sargassum*-derived materials in agrochemicals (6), bioplastics (7), and specialty chemicals opens new horizons for sustainable practices and innovative product development (8).

It is through the lens of these opportunities that we explore the transformative potential of *sargassum* seaweeds in chemical industries.

However, the utilization of *sargassum* seaweeds is not without its challenges. Environmental sustainability (9), responsible harvesting practices (10), and economic implications are integral aspects that demand careful consideration (9). As we venture into this exploration, we recognize the need for a holistic approach that seeks to balance economic prosperity with ecological preservation and societal well-being.

Hence, this paper serves as a beacon to guide through the intricate landscape of *sargassum* seaweeds in the blue economy. It aspires to stimulate interdisciplinary dialogue, drive innovation, and inform policy, ultimately fostering a harmonious relationship between humanity's quest for progress and the conservation of our invaluable marine ecosystems. As we navigate this promising yet complex terrain, it should be reminded that the blue economy's success lies not only in the opportunities it unveils but in our collective commitment to stewarding the oceans with wisdom and responsibility.

2.0 LITERATURE REVIEW

2.1 The Blue Economy and Its Significance

The concept of the blue economy has gained prominence as a holistic framework for sustainable development, particularly in regions closely tied to the oceans and seas. Emerging as a response to the growing recognition of the oceans' critical role in the global economy, the blue economy emphasizes responsible resource management and innovative approaches to harness the potential of marine ecosystems (11).

In essence, it seeks to balance economic growth with environmental conservation and social equity, ushering in a new era of prosperity that respects the boundaries of the planet (12).

The relevance of the blue economy extends far beyond its economic dimensions. It encompasses various sectors, from fisheries and tourism to renewable energy and biotechnology, all of which are intricately interconnected (13). As coastal and island communities increasingly turn to the ocean for livelihoods and sustenance, the blue economy serves as a guiding philosophy for inclusive and sustainable development (14).

2.2 *Sargassum* Seaweeds: Ecological Significance and Distribution

Sargassum seaweeds, a distinctive genus of brown macroalgae, have drawn considerable scientific attention due to their unique ecological attributes. The floating *sargassum* mats in regions such as the Sargasso Sea provide essential habitat for a diverse array of marine species, offering refuge, spawning grounds, and foraging opportunities (15). This ecological importance underscores the need for the conservation of *sargassum* habitats.

Sargassum species exhibit a wide distribution, with varying degrees of dominance in different oceanic regions. They are found in the Atlantic, Indian, and Pacific Oceans, making them a global resource of interest (16).

The distribution patterns are influenced by oceanic currents, temperature, and nutrient availability, with some species thriving in subtropical and tropical waters (1). Understanding the distribution and abundance of *sargassum* seaweeds is crucial for assessing their potential contributions to the blue economy.

2.3 Chemical Composition of *Sargassum* Seaweeds

One of the key facets of *sargassum* seaweeds that has garnered attention is their rich and diverse



chemical composition. These seaweeds are known to contain a multitude of bioactive compounds, polysaccharides, pigments, and minerals (4). The chemical profile of *sargassum* varies among species, geographical locations, and seasonal changes (17). This variation presents opportunities for tailored utilization in different industries.

Bioactive compounds found in *sargassum* seaweeds include phenolic compounds, terpenoids, and alkaloids, many of which exhibit significant antioxidant, anti-inflammatory, and antimicrobial properties (18). Polysaccharides extracted from *sargassum*, such as alginate and fucoidan, have diverse industrial applications, including in pharmaceuticals, food, and biotechnology (19). Additionally, the pigments found in *sargassum*, such as fucoxanthin, hold promise in nutraceuticals and as natural colorants (20).

2.4 Potential Applications in Chemical Industries

The chemical industry stands as one of the primary sectors poised to benefit from the unique chemical composition of *sargassum* seaweeds. Biofuel production, an urgent need in the face of climate change and dwindling fossil fuel reserves, is an area where *sargassum* holds significant promise. The high carbohydrate content in some *sargassum*



species can be converted into bioethanol and biogas (9).

Pharmaceutical and nutraceutical industries are increasingly exploring *sargassum*-derived bioactive compounds for drug development and dietary supplements. These compounds have shown potential in treating various health conditions, including cancer and cardiovascular diseases (7). Furthermore, the use of *sargassum*-derived materials in agrochemicals, bioplastics, and specialty chemicals presents novel opportunities for sustainable practices and the development of eco-friendly products.

2.5 Challenges and Considerations

Despite the promising applications, the utilization of *sargassum* seaweeds in the chemical sector is not without challenges. Environmental sustainability is a critical concern, given the potential impacts of large-scale harvesting on marine ecosystems. Responsible harvesting practices and strategies to mitigate these impacts are essential. Additionally, economic implications, regulatory frameworks, and the socio-economic effects on local communities are integral aspects that require careful consideration.

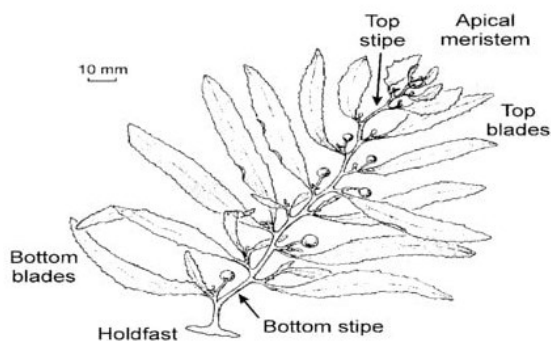


Figure 1. *Sargassum* seaweeds

3.0 METHODOLOGY

3.1 Data Collection and Source Selection

The methodology for this research involves a systematic review of the existing literature to gather comprehensive insights into the potential and applications of *sargassum* seaweeds in chemical industries within the context of the blue economy.

To ensure the rigor and relevance of the review, the following steps were taken:

3.2 Defining Inclusion Criteria

A set of inclusion criteria was established to identify relevant sources. These criteria included the publication date (2020-2023), language (English), and focus on *sargassum* seaweeds'



chemical composition, potential applications, and relevance to the blue economy.

3.3 Database Search

Several academic databases, including PubMed, Scopus, Web of Science, and Google Scholar, were systematically searched using relevant keywords. These keywords included "*Sargassum* seaweeds," "chemical composition," "industrial applications," "blue economy," and related terms.

3.4 Data Screening and Selection

(a) Initial Screening: The initial screening involved reviewing titles and abstracts of the retrieved articles to assess their relevance to the research objectives. Articles that did not meet the inclusion criteria were excluded.

(b) Full-Text Review: Full-text versions of potentially relevant articles were obtained and thoroughly reviewed. During this stage, articles were assessed for their quality, relevance, and the depth of information they provided regarding *sargassum* seaweeds' chemical composition and their potential applications in chemical industries within the blue economy context.

3.5 Data Extraction and Synthesis

(a) Data Extraction: Information pertinent to *sargassum* seaweeds, including their chemical constituents, variations among species, and industrial applications, was extracted from the selected sources.

Additionally, information on environmental impacts, sustainability, and economic implications was collected.

(b) Data Synthesis: The gathered data were synthesized and organized thematically to create a coherent narrative in the literature review. Key findings, trends, and gaps in the existing literature were identified and analysed.

3.6 Analysis and Interpretation

(a) Thematic Analysis: A thematic analysis approach was employed to categorize and analyze the extracted information. Themes were established based on the chemical composition, industrial applications, environmental considerations, and economic aspects of *Sargassum* seaweeds.

(b) Critical Evaluation: The literature was critically evaluated to identify strengths and limitations in the current body of knowledge. Emphasis was placed on the scientific rigor, diversity of sources, and the relevance of findings to the research objectives.

3.7 Ethical Considerations

Citation and Attribution: Proper citation and attribution were ensured throughout the literature review process to give due credit to the original authors and sources.

3.8 Reporting

Structured Presentation: The findings of the literature review were organized and presented in a structured manner, following the sections and themes outlined in the research paper, including the Introduction, Methodology, Results, Discussion, and Conclusion.

3.9 Limitations

It is important to note that the methodology for this literature review is based on existing published sources.

As such, the quality and depth of information are dependent on the available literature. Additionally, the research paper's knowledge cut-off date is September 2023, meaning that more recent developments or research may not be included in this review. Nonetheless, this methodology provides a systematic and comprehensive approach to examining the potential and applications of *sargassum* seaweeds in chemical industries within the context of the blue economy.

4.0 CHEMICAL COMPOSITION OF SARGASSUM SEaweeds

The chemical composition of *sargassum* seaweeds exhibits variability among species, geographical locations, and environmental conditions, leading to a wide spectrum of potential applications in diverse industries (4). The presence of bioactive compounds, polysaccharides, pigments, minerals, and lipids underscores their significance in pharmaceuticals, nutraceuticals, biotechnology, food, and various other sectors. These unique chemical attributes position *sargassum* seaweeds as a valuable resource with the potential to contribute to the sustainable development goals of the blue economy while addressing health and environmental challenges (21).



Table 1. Chemical details of *sargassum* Seaweeds

Chemical Component	Function/Potential Applications
Bioactive Compounds	Phenolic compounds: Antioxidants, anti-inflammatory agents Terpenoids and alkaloids: Antimicrobial, anticancer properties
Polysaccharides	Alginate: Gelling and thickening agent in food and pharmaceuticals Fucoidan: Anticoagulant, antitumor, immunomodulatory effects
Pigments	Fucoxanthin: Antioxidant, potential nutraceutical applications Chlorophylls: Natural colorants, health-promoting agents
Minerals	Iodine: Used in iodized salt and dietary supplements Calcium, magnesium, trace elements: Nutritional supplements, biofortification
Lipids	Fatty acids (including omega-3 and omega-6): Functional foods, dietary supplements

Table 2. Industrial Applications in the Chemical Sector

Industrial Application	Function/Potential Applications
Biofuel Production	Bioethanol: Renewable fuel production Biogas: Renewable energy generation
Pharmaceuticals & Nutraceuticals	Bioactive compounds: Drug development, dietary supplements Fucoidan: Potential in cancer therapies and dietary supplements
Agrochemicals	Bio stimulants: Enhancing plant growth, nutrient uptake, and stress tolerance
Bioplastics and Polymers	Alginate-based materials: Biodegradable films, coatings, bioplastics
Specialty Chemicals	Chlorophyll derivatives: Colorants, antioxidants, health-promoting agents Various compounds: Innovative product development in various industries

5.0 ENVIRONMENTAL AND ECONOMIC IMPACTS

The utilization of *sargassum* seaweeds in various industrial applications within the chemical sector offers promising opportunities, but it also entails significant environmental and economic considerations. This section examines the potential environmental impacts, sustainability challenges, and economic implications associated with harnessing *Sargassum* seaweeds as a resource.

5.1 Environmental Impacts

Ecosystem Disruption: Large-scale harvesting of *sargassum* seaweeds can disrupt marine ecosystems, particularly in regions where they serve as critical habitat and nurseries for various marine species. The removal of *Sargassum* mats may affect the reproductive and foraging patterns of marine organisms that rely on these floating habitats (22).

5.2 Biodiversity Concerns

The extraction of *sargassum* seaweeds may inadvertently capture and harm non-target species, including fish and invertebrates. Bycatch and unintended ecological consequences must be carefully managed to minimize adverse effects on marine biodiversity (23).

5.3 Nutrient Cycling

Sargassum plays a crucial role in nutrient cycling in marine ecosystems, acting as a natural nutrient sink. Harvesting may disrupt this process, potentially affecting nutrient availability and overall ecosystem health (24).

5.4 Invasive Species

The transport of *sargassum* seaweeds between regions, whether naturally or through human activities, raises concerns about potential invasions



by non-native species. Such invasions could alter local ecosystems and impact native species (25).

6.0 SUSTAINABILITY CONSIDERATIONS

6.1 Harvesting Practices

Sustainable harvesting practices must be developed and adhered to in order to minimize the environmental impacts of *sargassum* extraction. These practices may include selective harvesting, seasonal restrictions, and spatial management to protect critical habitats (26).

6.2 Resource Management

Effective resource management strategies are necessary to ensure the long-term sustainability of *sargassum* seaweeds as a resource. Monitoring of harvesting levels, population dynamics, and ecological health is crucial to prevent overexploitation (27).

6.3 Environmental Assessments

Prior to initiating large-scale harvesting operations, comprehensive environmental impact assessments (EIAs) should be conducted to evaluate the potential consequences on marine ecosystems. EIAs can help identify mitigation measures and inform responsible decision-making (28).

Table 3. Economic Implications

Economic Implication	Function/Potential Impact
Local Economies	Job creation in harvesting, processing, and related industries Community development in regions with abundant <i>sargassum</i> resources
Value Chains	Creation of value chains around <i>sargassum</i> -based products Diversification of revenue streams for industries and governments
Export Potential	Potential for foreign exchange earnings through exports of <i>sargassum</i> -based products Contribution to trade balances and national economic growth
Economic Viability	Economic analysis to assess the viability of <i>sargassum</i> -based industries Identification of market niches and investment opportunities

Balancing the environmental and economic aspects of *sargassum* seaweed utilization is essential for realizing its potential within the blue economy. Responsible resource management, sustainable harvesting practices, and environmental protection measures are paramount to mitigate adverse impacts on marine ecosystems. Simultaneously, the economic benefits, job creation, and export potential must be harnessed to support local communities and promote sustainable development. Effective governance, interdisciplinary collaboration, and adaptive management approaches are critical for ensuring that the utilization of *sargassum* seaweeds aligns with the principles of the blue economy and

contributes to a harmonious coexistence between human activities and the marine environment.

7.0 FUTURE DIRECTIONS AND CHALLENGES

As the exploration of *sargassum* seaweeds' potential and applications within the blue economy and chemical industries continues to evolve, several future directions and challenges emerge. This section outlines key areas for further research and development while addressing the complex challenges that must be navigated to maximize the benefits of *sargassum* utilization.



Table 4. Future Directions

Future Directions	Focus/Potential Areas of Development
Sustainable Harvesting	Develop sustainable harvesting practices to minimize environmental impact
Biotechnology and Bioprocessing	Advance biotechnology for efficient compound extraction Explore biorefinery approaches to optimize resource utilization
Environmental Monitoring and Assessment	Conduct comprehensive environmental impact assessments Establish long-term monitoring programs and predictive models
Innovation in Product Development	Explore novel products and applications in pharmaceuticals, bioplastics, and specialty chemicals

8.0 CHALLENGES

8.1 Environmental Sustainability

Balancing the economic potential of *sargassum* utilization with environmental sustainability remains a critical challenge. Careful resource management, adherence to harvesting regulations, and effective conservation strategies are necessary to prevent overexploitation and ecosystem disruption (29).

8.2 Regulatory Frameworks

The development of clear and adaptive regulatory frameworks for *sargassum* seaweed utilization is challenging due to the complexity of international waters and varying legal jurisdictions. Harmonizing regulations at regional and global levels is essential for responsible resource management (30).

8.3 Resource Variability

Sargassum seaweeds exhibit variability in their chemical composition and distribution, posing challenges for consistent resource availability. Understanding this variability and its implications for industrial applications is crucial for market stability (1).

8.4 Invasive Species Control

The potential for invasive *sargassum* species to disrupt local ecosystems requires proactive monitoring and management efforts. Strategies for preventing the spread of non-native species and minimizing ecological impacts need to be developed (31).

8.5 Competing Interests

Sargassum-rich regions often face competing interests, such as tourism and fisheries, which may conflict with seaweed harvesting activities. Balancing these interests and establishing collaborative approaches that consider all stakeholders are paramount (32).

9.0 CONCLUSION

The exploration of *sargassum* seaweeds in the context of the blue economy and their applications within the chemical sector unveils a world of promise and complexity. These remarkable brown macroalgae, found floating in oceanic realms, present a rich and diverse chemical composition that opens doors to a multitude of industrial opportunities. From biofuel production to pharmaceuticals, bioplastics, and specialty chemicals, *sargassum* seaweeds hold the potential to catalyze sustainable development and innovative product development.

However, this journey into *sargassum*'s potential is not without its challenges. Environmental considerations loom large, demanding the delicate balance between resource utilization and ecological preservation. Sustainable harvesting practices, conservation measures, and rigorous environmental assessments are essential to ensure that the exploitation of *sargassum* seaweeds aligns with the principles of the blue economy, preserving vital marine habitats and biodiversity.

The economic implications of *sargassum* utilization are equally compelling. Local economies stand to benefit from employment opportunities and economic diversification, while value chains offer avenues for revenue generation and export potential. Yet, the economic viability of *sargassum*-



based industries requires thorough analysis, market development, and effective governance to thrive.

The path forward is characterized by innovation, sustainable practices, and collaborative efforts. Sustainable harvesting, biotechnology advancements, and responsible resource management must underpin these ideas. Likewise,

REFERENCES

1. L. Berline *et al.*, Hindcasting the 2017 dispersal of Sargassum algae in the Tropical North Atlantic. *Marine Pollution Bulletin* **158**, 111431 (2020).
2. M. F. Nazarudin *et al.*, Metabolic variations in seaweed, Sargassum polycystum samples subjected to different drying methods via 1H NMR-based metabolomics and their bioactivity in diverse solvent extracts. *Arabian Journal of Chemistry* **13**, 7652-7664 (2020).
3. J. Liu *et al.*, Therapeutic and nutraceutical potentials of a brown seaweed Sargassum fusiforme. *Food Science & Nutrition* **8**, 5195-5205 (2020).
4. F. Santos *et al.*, Unraveling the lipidome and antioxidant activity of native Bifurcaria bifurcata and invasive Sargassum muticum seaweeds: A lipid perspective on how systemic intrusion may present an opportunity. *Antioxidants* **9**, 642 (2020).
5. R. Dickson, J. J. Liu, A strategy for advanced biofuel production and emission utilization from macroalgal biorefinery using superstructure optimization. *Energy* **221**, 119883 (2021).
6. T. Thompson, B. Young, S. Baroutian, Pelagic Sargassum for energy and fertiliser production in the Caribbean: A case study on Barbados. *Renewable and Sustainable Energy Reviews* **118**, 109564 (2020).
7. J. Liu *et al.*, Pharmaceutical and nutraceutical potential applications of Sargassum fulvellum. *BioMed Research International* **2020**, (2020).
8. J. J. Milledge, S. Maneein, E. Arribas López, D. Bartlett, Sargassum inundations in Turks and Caicos: Methane potential and proximate, ultimate, lipid, amino acid, metal and metalloid analyses. *Energies* **13**, 1523 (2020).
9. T. M. Thompson *et al.*, Techno-economic and environmental impact assessment of biogas production and fertiliser recovery from pelagic Sargassum: A biorefinery concept for Barbados. *Energy Conversion and Management* **245**, 114605 (2021).
10. D. Bartlett, F. Elmer, The impact of Sargassum inundations on the Turks and Caicos islands. *Phycology* **1**, 83-104 (2021).
11. M. Kabil, S. Priatmoko, R. Magda, L. D. Dávid, Blue economy and coastal tourism: A comprehensive visualization bibliometric analysis. *Sustainability* **13**, 3650 (2021).
12. Y. Song, Y. Wei, J. Zhu, J. Liu, M. Zhang, Environmental regulation and economic growth: A new perspective based on technical level and healthy human capital. *Journal of Cleaner Production* **318**, 128520 (2021).
13. R. M. Bădîrcea *et al.*, Connecting Blue Economy and Economic Growth to Climate Change: Evidence from European Union Countries. *Energies* **14**, 4600 (2021).
14. N. Shiiba, H. H. Wu, M. C. Huang, H. Tanaka, How blue financing can sustain ocean conservation and development: A proposed conceptual framework for blue financing mechanism. *Marine Policy* **139**, 104575 (2022).
15. S. K. Choi *et al.*, Population dynamics of the 'golden tides' seaweed, Sargassum horneri, on the southwestern coast of



- Korea: The extent and formation of golden tides. *Sustainability* **12**, 2903 (2020).
16. J. Gower, S. King, The distribution of pelagic Sargassum observed with OLCI. *International Journal of Remote Sensing* **41**, 5669-5679 (2020).
 17. A. Dewinta, I. Susetya, M. Suriani, in *Journal of Physics: Conference Series*. (IOP Publishing, 2020), vol. 1542, pp. 012040.
 18. M. K. A. Sobuj *et al.*, Effect of solvents on bioactive compounds and antioxidant activity of *Padina tetrastromatica* and *Gracilaria tenuistipitata* seaweeds collected from Bangladesh. *Scientific Reports* **11**, 19082 (2021).
 19. X. Chen *et al.*, Degradation of polysaccharides from *Sargassum fusiforme* using UV/H₂O₂ and its effects on structural characteristics. *Carbohydrate polymers* **230**, 115647 (2020).
 20. D. Nuraini, M. A. Alamsjah, E. Saputra, Application of Fucoxanthin Pigment Extract from *Sargassum* sp. on the Physical Quality of Blusher Preparation. *Journal of Marine and Coastal Science* **10**, 74-84 (2021).
 21. A. T. Mansour *et al.*, Dried brown seaweed's phytoremediation potential for methylene blue dye removal from aquatic environments. *Polymers* **14**, 1375 (2022).
 22. A. C. Graba-Landry, Z. Loffler, E. C. McClure, M. S. Pratchett, A. S. Hoey, Impaired growth and survival of tropical macroalgae (*Sargassum* spp.) at elevated temperatures. *Coral Reefs* **39**, 475-486 (2020).
 23. S. M. Hassan *et al.*, The potential of a new commercial seaweed extract in stimulating morpho-agronomic and bioactive properties of *Eruca vesicaria* (L.) Cav. *Sustainability* **13**, 4485 (2021).
 24. B. Lapointe *et al.*, Nutrient content and stoichiometry of pelagic *Sargassum* reflects increasing nitrogen availability in the Atlantic Basin. *Nature Communications* **12**, 3060 (2021).
 25. L. M. Marks, D. C. Reed, S. J. Holbrook, Niche complementarity and resistance to grazing promote the invasion success of *Sargassum horneri* in North America. *Diversity* **12**, 54 (2020).
 26. F.-L. Liu *et al.*, A concise review of the brown seaweed *Sargassum thunbergii*—a knowledge base to inform large-scale cultivation efforts. *Journal of Applied Phycology* **33**, 3469-3482 (2021).
 27. F. Amador-Castro, T. García-Cayuela, H. S. Alper, V. Rodriguez-Martinez, D. Carrillo-Nieves, Valorization of pelagic *Sargassum* biomass into sustainable applications: Current trends and challenges. *Journal of Environmental Management* **283**, 112013 (2021).
 28. A. Bond, J. Pope, A. Morrison-Saunders, F. Retief, Taking an environmental ethics perspective to understand what we should expect from EIA in terms of biodiversity protection. *Environmental Impact Assessment Review* **86**, 106508 (2021).
 29. L. E. Valentine *et al.*, Novel resources: opportunities for and risks to species conservation. *Frontiers in Ecology and the Environment* **18**, 558-566 (2020).
 30. J. Banach, E. Hoek-van den Hil, H. van der Fels-Klerx, Food safety hazards in the European seaweed chain. *Comprehensive reviews in food science and food safety* **19**, 332-364 (2020).
 31. Y. A. Fidai, J. Dash, E. Tompkins, T. Tonon, A systematic review of floating and beach landing records of *Sargassum* beyond the Sargasso Sea. *Environmental Research Communications* **2**, 122001 (2020).
 32. D. Britton *et al.*, Seasonal and site-specific variation in the nutritional quality of temperate seaweed assemblages: Implications for grazing invertebrates and the commercial exploitation of seaweeds. *Journal of Applied Phycology* **33**, 603-616 (2021).





P036 - MECHANOCHEMISTRY: A GREEN CHEMISTRY FOR GREEN TECHNOLOGY

Mohammed, Jibrin*

Nasarawa State University Keffi

Corresponding author email: jibrinmohammed@nsuk.edu.ng*

ABSTRACT

Mechanochemistry involves the chemical transformation of materials or substances induced by external mechanical energy or forces. In recent years, mechanochemistry has gained significant interest as green synthetic method to prepare new functional materials. This paper reviewed the relationship between mechanochemistry and the principles of green chemistry, mechanochemistry as green technology, mechanochemical reactions, peculiarities of mechanochemical reactions, applications, and the challenges of mechanochemistry. However, based on the review, with improved or new technologies, mechanochemistry is probably going to be one of the most efficient way to improve greenness in chemical industries and beyond.

KEYWORDS

Mechanochemistry; Green Chemistry; Green Technology; Mechanochemical Reaction

1.0 INTRODUCTION

An ideal chemical reaction should be simple, safe, effective, economical and free or have less hazardous byproducts among others (1). However, the concept of green chemistry was introduced to achieve these attributes. Thus, green chemistry can be described as the practice of chemical science and production in a way that is sustainable, safe and non-polluting, consuming small amounts of substances and energy while producing little or no waste (2). Furthermore, green chemistry is a multidisciplinary field, which is applicable to all branches of chemistry (physical, organic, inorganic, nanochemistry, mechanochemistry, and pharmaceutical chemistry), chemical industry and materials science (1).

However, the concept of mechanochemistry which is the main subject matter, can be described as the aspect of chemistry in which chemical reaction involving two or more substances are induced by external mechanical energy or force at room temperatures (3). In the laboratory, most mechanochemical reactions that involve solid reactants are carried out by a simple manual grinding of the reactants in a mortar with a pestle while shakers or ball mills are used for liquids or gaseous reactants. However, in order to gain control of the reaction conditions and to obtain reproducible results, various types of ball mills, or alternatively single- or twin-screw extruder have been used (4). In addition, scientific studies revealed that due to the application of mechanical force, the efficient energy dispersion and mass transportation have facilitated the elimination of

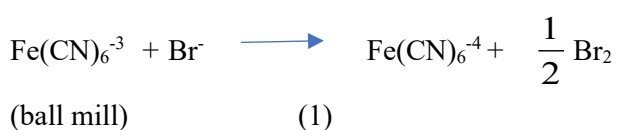
solvents and warranted greener, faster, and more straightforward chemical syntheses than conventional solvent-based reactions (5, 6). Moreover, mechanochemistry has gained significant interest as a powerful, more sustainable, time saving, environmentally friendly, and more economical synthetic method to prepare new functional materials (7).

Furthermore, the applications of mechanochemistry as green synthetic technique in various field of sciences such as pharmaceuticals, fertilizers, catalysis, nanotechnology, ceramics, waste management and metallurgy have been reported (4, 8, 9). In pharmaceuticals for instance, the manufacture of active pharmaceutical ingredients consumes large amounts of energy due to multi-stages involve which are associated with the use of large volume of solvents (10). Unused reaction products enter the soil via wastewater and pollute the environment. The intensive use of solvents, which is one of the major key players in the pharmaceutical industry during the synthesis, is of great concern as it affects the production cost and the environment (8). Interestingly, these challenges have been addressed to some extent by mechanochemistry through applying solvent-free synthesis for the manufacture of active pharmaceutical ingredients which eliminate or reduces the use of solvent to a large extent (5). Therefore, this paper reviewed the concept of mechanochemistry in relation to green chemistry for green technology.

1.1 Mechanochemical Reactions



According to literature survey, mechanochemical reactions can be carried out in any state of matter (solid, liquid or gas) [(11), (Silvina, 2023)]. However, a large number of mechanochemical reactions have been demonstrated and published globally. Lapshin *et al.*, 2021 (6) reported that mechanochemistry began with the grinding of mercuric sulfide from the mineral cinnabar (HgS) and copper metal (Cu) which react to produce mercury and copper sulfide (Cu₂S) in a Cu mortar with a Cu pestle in the presence of vinegar. Furthermore, mechanochemical reactions of inorganic materials of the main group elements (s- and p-blocks) have been recently reviewed (Silvina, 2023). These studies include simple oxides, sulfides and selenides, and their phase transformations; chalcogenides, nitrides, hydrides, and materials for hydrogen production and storage. The facile mechanochemical syntheses of coordination complexes of transition metals with organic ligands which led to mononuclear complexes and coordination clusters, cages, and other one-, two-, and three-dimensional architectures have been achieved (Silvina, 2023). Equation 1 shows the reduction of ferricyanide to ferrocyanide in a ball mill.



1.1.1 Peculiarities of Mechanochemical Reactions

Studies revealed that there are a growing number of chemical transformations that take place by mechanochemistry but very difficult to occur or not at all in solutions (6, 7, 12). This was attributed to their unique reaction mechanisms. Silvina (2023) reported that in the synthesis of functionalized fullerenes, mechanochemical nucleophilic behavior of CN⁻ was different from its behavior in

solutions, leading to a new compound, C₁₂₀ (18% yield). Mechanochemistry was used to identify and develop a novel C–N coupling of arylsulfonamides and carbodiimides, which readily took place by liquid assisted solvent (LAG), but in solution either failed or gave poor conversions (7, 12) reported the synthesis of a tris(allyl)aluminum complex based on the sterically hindered bis(trimethylsilyl)allyl ligand. Solution synthesis of such complex immediately dissociate upon dissolution. Other mechanochemical products that cannot be synthesized using solvents are various Iptycenes synthesized using double Diels Alder cycloadditions, and several cyclooctatetraene derivatives prepared from ethyl propiolate (an alkyne) using a Ni vial and Ni pellets as catalysts (Silvina, 2023).

1.1.2 Mechanochemistry as Green Technology

According to Lapshin *et al.*, 2021 (6), the major inspiration behind the rediscovery of mechanochemistry is green chemistry, specifically the need of pharmaceutical and chemical industries for cleaner, safer, and more efficient transformations. Mechanochemistry affords versatile chemical processes that do not require the use of reaction solvents, significantly reducing the generation of waste and pollution while simultaneously cutting down economic costs (7). Mechanochemical processes often give rise to larger yields than the analogous reactions in solution, and typically involve considerably reduced reaction times, good stoichiometry control, and enhanced product selectivity (6).

Silvina (2023) reported that all the twelve principles of green chemistry can be related in one way or the other to mechanochemistry. These principles and how they are supported through mechanochemistry with examples, are described in Table 1.

Table 1: The twelve principles of green chemistry and how they can be fulfilled through mechanochemistry.

Green Chemistry Principles	Outcome
<i>Waste prevention</i>	Largely reduced use of solvents and water. Reduced need of isolation and purification processes.
<i>Atom economy</i>	Avoid use of reactants in large excess. Typical high chemical selectivity and high yields. Example: Syntheses of MOFs directly from metal oxides instead of metal salts.
<i>Less hazardous syntheses</i>	Highly reactive species can be produced and immediately reacted, without using controlled atmospheres. Example: Mechanochemical activation of CaC ₂ avoiding the use of gaseous acetylene replacement of aqua regia with safer oxidants such as oxone



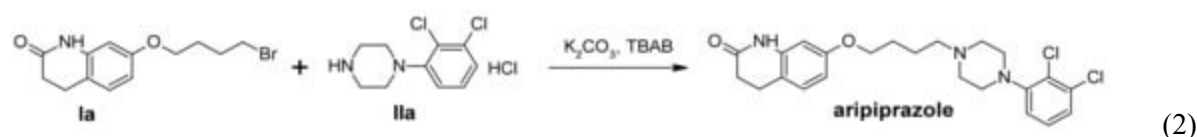
<i>Design of safer chemicals</i>	Alternative synthetic routes to active pharmaceutical ingredients and new solid-state forms (cocrystals, polymorphs). Example: Syntheses of new metallodrugs with reduced toxicity
<i>Safer solvents and auxiliaries</i>	Reactant solubility considerations are unnecessary. New potential reactants (less toxic, cheaper, safer to use) become available. Reactivity tunability using LAG selectively leading to different polymorphs, MOF topologies, etc.
<i>Design for energy efficiency</i>	Scalability for industrial production and continuous flow processes using reactive extrusion. Typical fast reaction rates and high yields, often at room temperature and ambient pressure. potentially leading to lower fossil fuel consumption
<i>Renewable feedstock use</i>	Biomass valorization reactions of cellulose, charcoal, lignin, chitin, and eggshell renewable feedstocks.
<i>Reduced derivatives</i>	Affords important synthetic processes in less steps and “one pot” syntheses. Example: Highly processed salts used as catalysts have been replaced with less costly mineral ores.
<i>Catalysis</i>	Milling media/vessels can be used as catalysts. Many enzymes remain active in ball milling and reactive extrusion.
<i>Design for Reactors degradation</i>	Affords the synthesis of biodegradable polymers and the efficient degradation of waste polymers such as polyethylene terephthalate.
<i>Real-time analysis</i>	Raman spectroscopy affords in situ monitoring of product formation.
<i>Accident prevention</i>	Automation of chemical processes in flow reactors is possible. A reduced exposure of humans and the environment to hazardous chemicals can be achieved.

1.2 Applications of Mechanochemistry

The applications of mechanochemistry as green technology in selected areas of focus include pharmaceuticals, fertilizers, catalysis, waste management and metallurgy are discussed below.

1.2.1 Pharmaceutical

In this era, where sustainability is a paramount concern, mechanochemistry shines as a green and sustainable approach to drug synthesis [(10), (Ying *et al.*, 2020)]. Thus, by eliminating the need for large volumes of solvents and reducing waste production, mechanochemistry significantly reduces the environmental impact associated with drug manufacturing [(13), (Schultheiss and Newman, 2009)]. This technique promotes the



1.2.2 Fertilizer

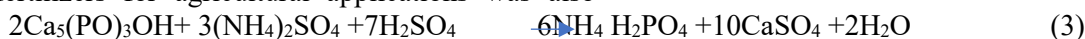
Application of mechanochemistry in the synthesis of fertilizer as green alternative to conventional methods which involve the use solvents depending on the type of fertilizer has been reported by many

principles of green chemistry by minimizing the use of hazardous chemicals and maximizing atom economy. Furthermore, these economical and environmentally friendly aspects of mechanochemistry align with the growing demand for sustainable practices in the pharmaceutical industry (5). However, a lot drugs have been synthesized using this technique. Examples, mechanochemical synthesis of Isoniazid and Pyrazinamide co-crystals with glutaric acid using solid state grinding and liquid assisted grinding by Ngilirabanga *et al.* (2020) (5), synthesis of Trazodone in a mortar and Aripiprazole in a ball mill (14), mechanochemical synthesis of Flucytosine and acetylsalicylic acid in a ball mill (15) have been achieved. Equation 2 shows the mechanochemical synthesis of Aripiprazole in the presence of potassium carbonate and catalysts PTC.

researchers (4, 16, 17). Thus, a recent study was carried out on mechanochemical preparation of a novel slow-release fertilizer based on K_2SO_4 -kaolinite by Ehab *et al.*, 2022 (17). Chen *et al.*, 2018 (4) reported the mechanochemical transformation of apatite to phosphoric slow-release fertilizer and



soluble phosphate. Mechanochemical preparation, properties and kinetic study of kaolin-N, P fertilizers for agricultural applications was also



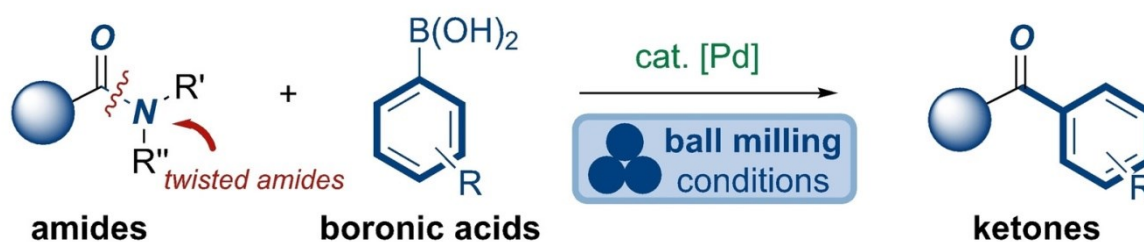
1. 2. 3 Catalysis

According to Amrute *et al.*, 2021 (18), mechanochemistry enables the synthesis of different forms of catalysts in a more sustainable and convenient way than conventional methods. However, in the case of nanostructured systems for instance, the mechanochemical synthesis of different metal nanoparticles used as catalysts

reported by Mohammad *et al.*, 2021 (16). Equation 3 shows the equation for the reaction,

including iron, copper, nickel, silver gold, and palladium has been demonstrated (18). Mechanochemistry is also a versatile platform for organocatalytic and metal-catalyzed transformations, such as the Suzuki–Miyaura coupling as illustrated in equation 4, Huisgen cycloaddition and olefin metathesis [(12, 19), (Thorwirth *et al.*, 2011)].

Solid-state Solvent-less Mechanochemical N–C(O) Activation of Amides



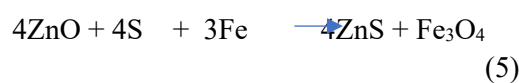
- solid-state N–C activation
- solvent-free
- fast, scalable
- operationally simple
- late-stage functionalization
- dual orthogonal solid-state solventless coupling

(4)

1.2. 4 Waste Management

Mechanochemistry has found application in solid waste management and it has been demonstrated to have many advantages over other conventional chemical methods of solid waste disposal, that include metal oxide waste, fly ash modification, rubber and plastic recycling (20). Thus, in China, Zhang *et al.*, 2007 (21) studied the devulcanisation of natural rubber vulcanizate with self-designed mechanochemical reactor of pan mill type. The study revealed that solid state mechanochemical milling primarily resulted in the devulcanisation through the scission of cross-linking bond rather than the natural rubber main chain. Jana and Das (2005) applied the mechanochemical devulcanization process to treat the waste generated from scrap tyres. Furthermore, Jana and Das, 2005 (22) have reported that a mechanochemical technique based on stress induced chemical reactions and structure changes of materials has shown a potential application in devulcanisation of cross-linked rubber. Zhang *et al.*, 2007 (23) developed a novel metal recycling process using two kinds of waste containing nonferrous metals (in oxide or metal) and iron/aluminium metals and ground them with sulphur sample to mechanically

induce solid-state reaction to form nonferrous metal sulfides and iron/aluminium oxides, which allows the use of the current mineral processing technologies to recover metals from various kinds of wastes. Equation 5 shows mechanically induced solid state reaction using zinc oxide as the metallic oxide and iron reducing agent

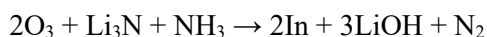


1.2. 5 Metallurgy

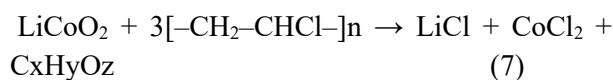
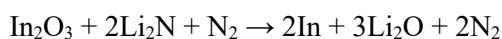
The extraction of metals from various ores or minerals such as magnetite, haematite, limonite, tungsten concentrate, molybdenite, monazite, rutile among others or recovery of metal from second-hand resources via mechanochemical technique has been demonstrated over the years (9, 24). McDonald and Muir, 2007 (25) reported that one of the keys to obtaining high and fast kinetics recovery of copper from chalcopyrite has been ultrafine grinding (mechanical activation) with particle sizes (80 mm) down to 5–15 μm. In a study carried out by Kano *et al.*, 2009 (24), it was observed that indium oxide could be reduced to metal in a non-thermal



process utilizing mechanochemistry. In the process, which was carried out in a planetary ball mill, lithium nitride was used as reductant and either ammonia or nitrogen gas was used to have a shielding atmosphere. The proposed mechanism for the process is illustrated in equation 6. A novel process was developed by Saito and co-workers where they milled lithium batteries (LIBs) electrodes together with polyvinyl (PVC) in a planetary ball mill (21, 26). It was observed that the recovery of Li and Co was dependent of grinding time and recoveries of Li and Co reached 100% and 90%, respectively after 30 h of grinding. Equation 7 also shows the mechanical milling of lithium batteries with PVC.



(6)



1.3 Challenges of Mechanochemistry

Currently, the study of mechanochemistry is still at infancy especially on commercial scale (Silvina, 2023). However, the fundamental physicochemical knowledge of mechanochemical processes in relation to thermodynamics, reaction mechanism and kinetics, is yet to be fully demonstrated in the literature. Additionally, the energetics of mechanochemical reactions, that is the mechanism of the energy flow in mechanochemical processes, starting from the energy of the reactants, the activation energy, how it flows through the chemical reaction to form products, and the energy require to form a product, and why particular products are formed (chemical selectivity), remain a challenge (Silvina, 2023). Furthermore, in most commercially available ball mills, the thermodynamic variables used to study and control chemical reactions, such as temperature and pressure remains a challenge (18).

2.0 CONCLUSION

The study of mechanochemistry can be described as inherently interdisciplinary involving multiple scientific disciplines. However, from the review, mechanochemistry is found to be sustainable, feasible, economical and technologically green with vast potential applications in chemical industries and other science related disciplines, but it also has some challenges that need further researches to be addressed.

3.0 REFERENCES

1. P. Anastas, I. Horvath, Innovations and green chemistry. *Chemical Reviews-Columbus* **107**, 2169-2173 (2007).
2. R. Khare, A. Kulshrestha, J. Pandey, N. Singh, Importance of Green chemistry in oxidation and reduction. *International Journal of Engineering and Technical Research* **7**, 264972 (2017).
3. R. T. O'Neill, R. Boulatov, The many flavours of mechanochemistry and its plausible conceptual underpinnings. *Nature Reviews Chemistry* **5**, 148-167 (2021).
4. M. Chen *et al.*, Mechanochemical transformation of apatite to phosphoric slow-release fertilizer and soluble phosphate. *Process Safety and Environmental Protection* **114**, 91-96 (2018).
5. J. B. Ngilirabanga, M. Aucamp, P. Pires Rosa, H. Samsodien, Mechanochemical synthesis and physicochemical characterization of isoniazid and pyrazinamide co-crystals with glutaric acid. *Frontiers in Chemistry* **8**, 595908 (2020).
6. O. Lapshin, E. Boldyreva, V. Boldyrev, Role of mixing and milling in mechanochemical synthesis. *Russian Journal of Inorganic Chemistry* **66**, 433-453 (2021).



7. A. R. Katritzky *et al.*, Benzotriazole-assisted thioacylation. *The Journal of organic chemistry* **70**, 7866-7881 (2005).
8. D. Tan, C. Mottillo, A. D. Katsenis, V. Štrukil, T. Friščić, Development of C–N Coupling Using Mechanochemistry: Catalytic Coupling of Arylsulfonamides and Carbodiimides. *Angewandte Chemie International Edition* **53**, 9321-9324 (2014).
9. Z. Ou, J. Li, Z. Wang, Application of mechanochemistry to metal recovery from second-hand resources: a technical overview. *Environmental Science: Processes & Impacts* **17**, 1522-1530 (2015).
10. A. S. McCalmont, A. Ruiz, M. C. Lagunas, W. T. Al-Jamal, D. E. Crawford, Cytotoxicity of Mechanochemically Prepared Cu (II) Complexes. *ACS Sustainable Chemistry & Engineering* **8**, 15243-15249 (2020).
11. C. Bolm, J. G. Hernández, Mechanochemistry of gaseous reactants. *Angewandte Chemie International Edition* **58**, 3285-3299 (2019).
12. J.-L. Do, C. Mottillo, D. Tan, V. Strukil, T. Friscic, Mechanochemical ruthenium-catalyzed olefin metathesis. *Journal of the American Chemical Society* **137**, 2476-2479 (2015).
13. M. Solares-Briones *et al.*, Mechanochemistry: A green approach in the preparation of pharmaceutical cocrystals. *Pharmaceutics* **13**, 790 (2021).
14. J. Jaškowska *et al.*, Mechanochemical synthesis method for drugs used in the treatment of CNS diseases under PTC conditions. *Catalysts* **12**, 464 (2022).
15. R. L. Carneiro *et al.*, Mechanochemical synthesis and characterization of a novel AAs–Flucytosine drug–drug cocrystal: A versatile model system for green approaches. *Journal of Molecular Structure* **1251**, 132052 (2022).
16. M. R. Alrbaihat, A. E. Al-Rawajfeh, E. AlShamaileh, A mechanochemical preparation, properties and kinetic study of kaolin–N, P fertilizers for agricultural applications. *Journal of the Mechanical Behavior of Materials* **30**, 265-271 (2021).
17. E. AlShamaileh *et al.*, Mechanochemical Preparation of a Novel Slow-Release Fertilizer Based on K₂SO₄-kaolinite. *Agronomy* **12**, 3016 (2022).
18. A. P. Amrute, J. De Bellis, M. Felderhoff, F. Schüth, Mechanochemical synthesis of catalytic materials. *Chemistry–A European Journal* **27**, 6819-6847 (2021).
19. F. Schneider, T. Szuppa, A. Stolle, B. Ondruschka, H. Hopf, Energetic assessment of the Suzuki–Miyaura reaction: a curtate life cycle assessment as an easily understandable and applicable tool for reaction optimization. *Green Chemistry* **11**, 1894-1899 (2009).
20. X. Guo, D. Xiang, G. Duan, P. Mou, A review of mechanochemistry applications in waste management. *Waste management* **30**, 4-10 (2010).
21. X. Zhang, C. Lu, M. Liang, Devulcanisation of natural rubber vulcanisate through solid state mechanochemical milling at ambient temperature. *Plastics, Rubber and Composites* **36**, 370-376 (2007).
22. G. Jana, C. Das, Devulcanization of automobile scrap tyres by a mechanochemical process. *Progress in*



- Rubber Plastics and Recycling Technology* **21**, 319-331 (2005).
23. Q. Zhang, S. Saeki, Y. Tanaka, J. Kano, F. Saito, A soft-solution process for recovering rare metals from metal/alloy-wastes by grinding and washing with water. *Journal of hazardous materials* **139**, 438-442 (2007).
24. J. Kano, E. Kobayashi, W. Tongamp, S. Miyagi, F. Saito, Non-thermal reduction of indium oxide and indium tin oxide by mechanochemical method. *Journal of Alloys and Compounds* **484**, 422-425 (2009).
25. R. McDonald, D. Muir, Pressure oxidation leaching of chalcopyrite. Part I. Comparison of high and low temperature reaction kinetics and products. *Hydrometallurgy* **86**, 191-205 (2007).
26. S. Saeki, J. Lee, Q. Zhang, F. Saito, Co-grinding LiCoO₂ with PVC and water leaching of metal chlorides formed in ground product. *International Journal of Mineral Processing* **74**, S373-S378 (2004).

P038 - A COMPARATIVE PROXIMATE AND MINERAL ANALYSIS OF BRANDED YOGHURTS AND NONO (LOCAL FULANI) YOGHURT SOLD IN ZARIA, KADUNA STATE, NIGERIA

Zaharaddeen N. Garba, Fatima Yahaya

Department of Chemistry, Ahmadu Bello University, Zaria, Nigeria

E-mail address: dinigetso2000@gmail.com

ABSTRACT

The purpose of this study was to carry out a comparative proximate and mineral analysis between branded yoghurts and local fulani yoghurt sold in Zaria, Kaduna State, Nigeria. Ten different samples (five branded, packaged yoghurts & five local fresh yoghurts) were picked at random from different areas which include: Samaru, Kwangila, Tudun Wada, Sabon Gari and Hanwa Maqera. The samples were labelled A-J. The analyses were conducted using the standard methods of the AOAC International. The results of the proximate composition showed that, there is no significant difference ($P < 0.05$) between the two groups with regards to the Proximate parameters analyzed. From the elemental analysis results, there is no significant difference ($P < 0.05$) between the two groups with regards to the Elements analyzed. The overall result revealed both groups of yoghurts to be very nourishing for the health, with the Fulani yoghurts having a slightly higher nutritional value than the branded yoghurts.

KEYWORDS

Zaria, Fulani, Yogurt, Nono, Proximate

1.0 INTRODUCTION

Yoghurt is a coagulated semi-solid milk product produced by souring or fermenting milk using pure starter cultures of *Lactobacillus bulgaricus* and *Streptococcus thermophiles* (1, 2). The characteristic taste of yoghurt is determined by its smooth, yet viscous with a subtle flavour that resembles a walnut (3). The gel-like texture is the primary characteristic. When added with thickening agent such as gelatine or other hydrocolloids, the

yoghurt texture is shown to stabilize, leading to an effective resistance against syneresis which produces a smooth sensation in the mouth when consumed (4). Nono (the Fulani word for cow's milk) is produced by obtaining the fresh raw cow milk, sieving it, and allowing it to ferment for 48 hours, then churning it to remove the fat and whey. It is sold by the Fulani women in Nigeria.

The vast array of yoghurt products available in the market makes it challenging for consumers to make



informed decisions about which yoghurt products are the most nutritious and beneficial for their health. While yoghurt is generally considered a healthy food, there can be significant variations in the nutritional content of different yoghurt products. The lack of information about the proximate composition of different yoghurt products makes it difficult for consumers to make informed choices about which products align with their dietary requirements. As such, there is the need to compare the proximate composition of various yoghurt products, including their protein, fat, carbohydrate, and mineral content, to determine the nutritional content of each product of the branded yoghurts and local Fulani yoghurts and identify which products are the most nutrient-dense and best for specific dietary needs.

Thus, the aim of this study is to carry out a comparative proximate analysis and mineral composition of branded yoghurts and nono (local fulani) yoghurt with the view of knowing the health effects associated with the consumption of these products.

2.0 EXPERIMENTAL

2.1 Study Area

Zaria is a metropolitan city in Kaduna State, Nigeria with a total area of 563 square kilometers and a population of about 736,000 people. Zaria has a tropical savanna climate with warm weather all year round, a wet season lasting from April to September, and a dry season from October.

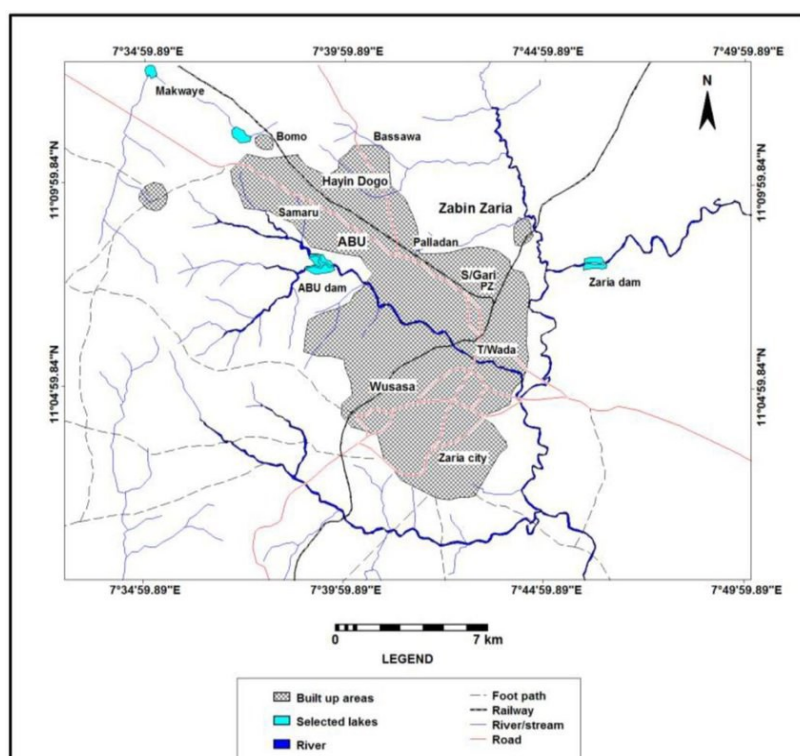


Fig. 1: A map of Zaria showing the sample area

2.2 Sample Collection

Ten different samples (five branded yoghurts and five local fresh yoghurts) were picked at random from different areas in Zaria city, which include Samaru, Kwangila, Tudun Wada, Sabon Gari and Hanwa Maqera. They were then taken to the National Animal Production Research Institute, Ahmadu Bello University, Zaria, Kaduna State, Nigeria for the analyses.

2.3 Sample Preparation

Exactly 10 ml of each sample was transferred into individual plastic sample bottles, and they were lettered A-J. The first five samples (A-E) are the branded yoghurt samples, while samples F-J are the local unbranded samples. They were stored in the refrigerator to prevent them from fermenting further, as that would affect the acidity levels.



2.4 Procedure for Proximate Analysis by AOAC (Association of Analytical Chemists)

2.3.1 Moisture Content

Exactly 5ml each of the local and branded yoghurt samples was placed into different crucibles that had already been weighed. The crucibles containing the samples were dried in an oven for 24hrs at 105°C, cooled in a desiccator and weighed.

$$\% \text{ Moisture} = \frac{W_1 - W_2}{W} \times 100 \quad (1)$$

W_1 = the weight in grams of empty crucible, W_2 = the weight in grams of crucible + residue and W = the weight in grams of the sample used

2.3.2 Ash Content

The residue that was obtained from the total solid analysis for each of the samples was used for this analysis. The crucibles containing the residues were placed in the furnace to be turned to ashes at 550 – 600°C for 3 hours, the crucibles containing the ash residue were cooled in a desiccator and weighed.

$$\% \text{ Ash} = \frac{W_1 - W_2}{W} \times 100 \quad (2)$$

W_1 = the weight in grams of empty crucible, W_2 = the weight in grams of crucible + ash, and W = the weight in grams of the sample.

2.3.3 Crude Protein Content

Exactly 5ml each of the local and branded yoghurt samples were placed into different digestion tubes, 5g of catalyst (mixture of NaSO₄ and CuSO₄ in ratio 5:1) was added to each of the flasks followed by the addition of 25cm³ concentrated H₂SO₄. The digestion tubes containing the mixtures were placed on digestion apparatus and heat was supplied below the boiling point of the acid until frothing ceased.

The mixtures were allowed to boil vigorously until the mixtures became clear. The digests were allowed to cool and diluted with distilled water to avoid caking down of the digest. The digests were made up to a known volume in different volumetric flasks with distilled water, the flasks were properly labelled. An aliquot from the digest was placed in the distillation apparatus and 20cm³ of NaOH solution (40%) was added. The mixture was heated

up as a result of the heat generated from the boiling water in the tank. The liberated ammonia was collected in a boric acid containing few drops of methyl red indicator which changed to a yellow color when ammonia came in contact with it.

The distillation was continued until twice the initial volume of the boric acid was collected. The distillation was discontinued, the distillate collected was titrated against standard hydrochloric acid solution (0.02M) and corresponding titre values were recorded.

Calculation

Total nitrogen, per cent by weight (on moisture – free basis)

$$\% \text{ Nitrogen} = \frac{14.01 \times \text{molarity} \times \text{extraction vol.} \times \text{titer value}}{\text{Aliquots} \times 1000 \times \text{sample weight}} \times 100 \quad (3)$$

Where;

Relative molecular weight = 14.01, Molarity = concentration HCl solution (0.0183M), Extraction volume = the total volume of the digest. (100cm³), Titer value = the total volume of acid used on titration, Aliquot = the volume of digest that was distilled [10cm³], and the Sample weight = the weight in gram of the material used.

Percentage conversion factor = 100

$$\% \text{ Crude Protein} = \% \text{ nitrogen} \times 6.38 \quad (4)$$

Where;

Nitrogen conversion factor = 6.38

2.3.4 Fat Content

10ml of 90% H₂SO₄ was placed into different butyrometers, 11ml each of the yoghurt samples was added to the acid in the butyrometers. 1ml of n-amyl alcohol was equally added to each of the sample in the butyrometer, the butyrometers were corked and mixed thoroughly by inverting the butyrometers several times until the mixture mixed well. The butyrometers containing the mixtures were centrifuged at 3000 rpm for fat separation. The butyrometers were placed in a water bath containing a very hot water for proper separation of



the fat, and the separated fat was read from the graduated part of the butyrometers.

Total Solids

$$\% \text{Total Solids} = 100\% - \% \text{moisture} \quad (5)$$

Solid Non-Fats

$$\% \text{Solid Non-Fats} = \% \text{total solids} - \% \text{fat} \quad (6)$$

Carbohydrates (CHO)

$$\% \text{CHO} = 100 - (\% \text{moisture} + \% \text{ crude protein} + \% \text{ash} + \% \text{fat}) \quad (7)$$

2.3.5 Lactic Acid

Exactly 10ml each of the local yoghurt sample was placed in different 250ml conical flasks, 10ml of distilled water was added to each flask containing the yoghurt sample, and 3 drops of phenolphthalein indicator was equally added to the mixture in the conical flasks, the mixtures were mixed thoroughly until the curd were no longer visible. The mixtures were titrated against 0.1m NaOH solution until pink color that persisted for 30seconds appeared and the titer values were recorded. The percentage of lactic acid was calculated using the formula below:

$$\% \text{ Lactic Acid} = \frac{0.009 \times \text{titer value}}{\text{sample weight} \times \text{density}} \times 100 \quad (8)$$

2.5 Statistical Analysis

The Statistical Analysis results were expressed as mean and standard deviation. Student's t-Test was used to compare the means at the significant level $P < 0.05$. All analyses were performed using Statistical Package for Social Sciences (SPSS).

3.0 RESULTS AND DISCUSSION

3.1 Proximate Composition

The proximate composition of the five branded yoghurts and the five unbranded yoghurts is shown in Table 1, revealing a significant difference in only the %Moisture ($P < 0.05$) between the two groups.

From the table, there is no significant difference ($P < 0.05$) between the two groups with regards to the % Total Solids, %Ash, %Carbohydrate, %Solid Non-Fat, %Crude Protein, %Fat, and %Lactic acid. However, there is a slight difference between their percent compositions.

From the results, the moisture content of the branded yoghurts (83.86%) is slightly lower than that of the Fulani Yoghurts (89.23%). The moisture content should be less than 84% (5). The high moisture content of the Fulani Yoghurt might be due to the reconstitution of the milk before fermentation (6).

Table 1: Proximate Analysis of Branded and Fulani Yoghurt. Values are means \pm standard deviation (SD) of determinations

	Branded Yoghurt	Fulani Yoghurt	p-value
%TS	16.54 \pm 4.38	10.75 \pm 0.77	0.085



%ASH	0.41 ± 0.012	0.45 ± 0.14	0.82
%FAT	1.21 ± 1.12	3.55 ± 1.01	0.81
%CP	2.16 ± 0.75	2.32 ± 0.34	0.10
%SNF	15.32 ± 5.29	7.89 ± 1.34	0.15
%LA	1.30 ± 0.45	1.95 ± 0.79	0.40
%MOISTURE	83.86 ± 4.46	89.23 ± 0.80	0.04
%CHO	12.80 ± 5.26	4.50 ± 1.34	0.12

In the Ash content determination, there was no significant difference ($P < 0.05$) between the two groups. But the Fulani Yoghurt (0.45%) has slightly more Ash than the branded yoghurts (0.41%). The higher Ash content of the Fulani Yoghurt might result from higher mineral content (6). Thus, this shows that Fulani Yoghurt can serve as a better source of minerals than the branded yoghurts.

For the crude protein determination, there was no significant difference ($P < 0.05$) between the two groups. The branded yoghurts had a slightly lower crude protein (2.16%) than that of the local yoghurts (2.32%). According to Codex standards, the yoghurt sample should contain not less than 2.70% protein content. Both sample groups were below that standard. Feeding from a perennial pasture resulted in higher concentration of fat, protein, casein, and whey than milk from cows fed with formulated feed (7). The higher protein content of Fulani yoghurt might be due to the pastoral practice by the herders.

For the Fat content determination, there was no significant difference ($P < 0.05$) between the branded and Fulani yoghurts. But the branded yoghurts (1.21%) had lesser fat than the Fulani yoghurts (3.55%). According to USDA, 2001 (8), yoghurts with more 3.25% of fat content should be labelled yoghurt, and yoghurt with fat content with 0.5- 2.0% should low-fat yoghurt and yoghurt with

less than 0.5% fat content should be labelled as Non-Fat yoghurt. Thus, this shows that the above analyzed yoghurts could be identified as low-fat yoghurts. Fats are good for the body system and increases the transport of vitamins (9). Fats play an important role in improving the consistency of yoghurt and also provide twice as much energy as same quantity of carbohydrate and protein (10). Therefore, this shows that the Fulani yoghurts will aid in the transport of vitamins faster than the branded yoghurts.

There was no significant difference ($P < 0.05$) for carbohydrates between the two groups, the Fulani yoghurts (4.5%) had lesser value than the branded yoghurts (12.80%). According to The Dairy Council, 2013 (11), yoghurt should contain carbohydrate content 13.7- 17.7%. The low carbohydrate value in the Fulani yogurts can be attributed to the process of fermentation which could make it ideal for lactose intolerant individuals.

In the lactic acid examination, there was no significant difference ($P < 0.05$) between the two groups. But the branded yoghurts had a lesser value (1.30%) than the Fulani yoghurts (1.95%). The low lactic acid in the branded yoghurts could be due to the duration of incubation (12).

Table 2: Elemental analysis of the branded and the Fulani yoghurts. Values are means ± standard deviation (SD) of determination

	Branded Yoghurt	Fulani Yoghurt	p-value
%Na	0.04 ± 0.01	0.04 ± 0.01	1.00
%K	0.04 ± 0.01	0.05 ± 0.01	0.46



%P	0.03 ± 0.02	0.02 ± 0.01	0.36
%Ca	0.28 ± 0.27	0.17 ± 0.06	0.08

3.2 Mineral (Elemental) Composition

In the table, there is no significant difference ($P < 0.05$) between the two groups with regards to the %Sodium, %Potassium, %Phosphorous and %Calcium. However, there is a slight difference between their percent compositions.

The sodium concentration of the branded yoghurts (0.04%) is similar to that of the Fulani Yoghurts (0.04%).

The potassium concentration of the Fulani yoghurts (0.05%) is slightly higher than that of the branded yoghurts (0.04%). Also, the phosphorous concentration of the branded yoghurts (0.03%) is slightly higher than the Fulani yoghurts (0.02%).

For the Calcium concentration, the value for the branded yoghurts (0.28%) was higher than that of the Fulani yoghurts (0.17%).

In summary, the results provide useful information about the nutritional and mineral content of two groups of yoghurts, which can be important for individuals who are seeking to incorporate a balanced and nutrient-rich diet. However, it is important to note that the results may vary depending on factors such as the location and conditions, incubation period, fermentation time, preservatives, and feeding of the cows, as well as the methods used for analysis. Both groups of yoghurts are very nourishing for the health, with the Fulani yoghurts having a slightly higher nutritional value than the branded yoghurts.

4.0 CONCLUSION

The concentration of the proximate analysis parameters (crude protein, carbohydrate, fat) is similar in both groups of yoghurts analyzed, except for the moisture, in which the Fulani yoghurt is higher. Also, the concentration is similar for both groups of yoghurts, with only minor variations between them. However, the branded yoghurts had a higher concentration of P and Ca than the Fulani yoghurts.

5.0 REFERENCES

1. U. G. Akpan, A. D. Mohammed, I. Aminu, Effect of preservative on the shelf life of yoghurt produced from soya beans milk. *Leonardo Electronic Journal of Practices and Technologies* **11**, 131-142 (2007).
2. M. Balogun, A. Arise, F. Kolawole, M. Ijadinboyo, Effect of partial substitution of cow milk with Bambara milk on the chemical composition, acceptability and shelf life of yoghurt. (2017).
3. J. W. Fuquay, P. F. Fox, P. L. McSweeney, Encyclopedia of dairy sciences. (*No Title*), (2011).
4. I. Sodini, J. Montella, P. S. Tong, Physical properties of yogurt fortified with various commercial whey protein concentrates. *Journal of the Science of Food and Agriculture* **85**, 853-859 (2005).
5. K. S. Matela, M. K. Pillai, P. Matebesi-Ranthimo, M. Ntakatsane, Analysis of proximate compositions and physiochemical properties of some yoghurt samples from Maseru, Lesotho. *Journal of Food Science and Nutrition Research* **2**, 245-252 (2019).
6. M. M. Dahiru, M. B. Hamid, N. Musa, Comparative proximate analysis and calcium composition between admiral yoghurt and local (fulani) yoghurt sold at Mayo-Belwa town, Adamawa state, Nigeria. *Science Letters (ScL)* **16**, 1-10 (2022).
7. T. F. O'Callaghan *et al.*, Effect of pasture versus indoor feeding systems



- on raw milk composition and quality over an entire lactation. *Journal of Dairy Science* **99**, 9424-9440 (2016).
8. USDA, Specifications for yoghurt, non-fat yoghurt and low-fat yoghurt. *United States Department of Agriculture (USDA)*, 200-203 (2001).
 9. S. Modu, H. Laminu, F. Sanda, Evaluation of the nutritional value of a composite meal prepared from pearl millet (*pennisetum typhoideum*) and cowpea (*vigna unguiculata*). *Bayero Journal of Pure and Applied Sciences* **3**, (2010).
 10. F. Ehirim, E. Onyeneke, Physico-chemical and organoleptic properties of yoghurt manufactured with cow milk and goat milk. *Academic Research International* **4**, 245 (2013).
 11. London, The nutritional composition of dairy products. *The Dairy Council*, (2013).
 12. V. Obatolu, E. Adebawale, F. Omidokun, E. Farinde, Comparative evaluation of yoghurt samples from goats and cows milk and commercial retail outlet. *Nigerian Journal of Animal Production* **34**, 163 171-163 171 (2007).



P039 - NUTRACEUTICALS AND NATURAL PRODUCTS IN THE LIGHT OF METABOLOMICS TECHNOLOGIES- A CUTTING-EDGES APPROACH TO DRUG DISCOVERY AND REPOSITIONING.

Saifullah Abubakar

Zamfara State College of Education.

Corresponding author email: bukarsaif@gmail.com

ABSTRACT

The evidence based therapeutic claims of the nutraceutical and natural products derivatives as the most promising and prolific resources in drug discovery are receiving increasing attention which paved their way toward the new frontiers and opportunities in chemical industries. Although, in the past few decades, pharmaceutical companies demonstrated insignificant attention towards natural products drug discovery, mainly due to its intrinsic complexity and rediscovery rates that become increasingly demotivating. Recently, technological advancements greatly helped to address the challenges and resulted in the revived scientific interest in drug discovery from natural sources. Thus, the emerging discipline of metabolomics technologies which comprehensively measured and characterized metabolites in biological samples contributed significantly in basic drug discovery and facilitate the exploration of drug repurposing strategy. Herein, we briefly summaries the latest advances in metabolomics technologies and update our knowledge of the application of metabolomics in drug discovery and repositioning.

KEY WORDS

Metabolomics technology, natural products, drug discover, drug repositioning

1.0 INTRODUCTION

Advance in technological developments have allowed the investigation of complex mixture in nutraceuticals and natural products, leading to the isolation and characterization of a number of successful novel compounds that provide a core scaffold for future drugs (1). Nutraceuticals comprise any non-toxic food extract supplement that has scientifically proven health benefits for both disease treatment and prevention. It includes bioactive ingredients extractable from food sources (plants and animals) whose intake could be through medicinal forms as supplement or drugs-like (2). Nutraceuticals are promising agents for the prevention and treatment of various disorder. Such as neurodegenerative disease, cancer, inflammation, obesity as well as the regulation of immune system function. Therefore, they have attracted substantial interest which offers novel opportunities for development of innovative products that will cover consumer needs for health-enhancing foods (3). Natural products represent most productive source of new lead compounds for drug discovery, due to their ability to cover a wider area of chemical space compared to the synthetic analogue (4). Several drugs currently used as therapeutic agents have been developed from

natural sources. Although, natural products also present challenges in drug discovery, such as technical barriers to screening, isolation, characterization and optimization, which contributed to a decline in their pursuit by the pharmaceutical industry. In recent years, several technological and scientific developments including improved analytical tools, metabolomics, genome mining and engineering strategies, and microbial culturing advances are addressing such challenges and opening up new opportunities. Currently, there is renew scientific keenness toward natural products in drug discovery program (5).

Current approached in drug discovery from natural sources requires a multidisciplinary approach utilizing available and innovative technologies to package such natural product compounds for medical practice and drug development (6). Technological development enabled the exploration of profiles of complex constituents from (plant and animal) leading to the isolation of a number of successful therapeutics drugs and novel lead compounds that can provide a core scaffold for future drugs.

In this context, metabolomics offers an invaluable tool to the study of nutraceutical/natural products.



Metabolomics is indeed applied as potential tool in drug discovery and repositioning aims at comprehensive analysis of small molecules or metabolites within biological system under a specific set of conditions assisted by technological developments in chromatography and spectrometry (4, 7, 8). Those techniques have been greatly improved by coupling mass spectrometers (MS) to chromatography, such as gas chromatography (GC) liquid chromatography (LC) and capillary electrophoresis (CE), and many types of mass analyser including magnetic or electric sector, time-of-flight (TOP), quadrupole (Q), ion trap (IT) and Fourier transform ion cyclotron resonance (FTICT) mass spectrometers and NMR spectroscopy (9).

The emerging discipline of metabolomics seeks to accomplish what was once thought to be science fiction by providing a snapshot of animal, plant, or microbial metabolism. metabolomics is simply a more comprehensive, more technologically advanced extension of both ancient and current medical practices. As a result of metabolomics research, scientists now understand, better than ever, how little we know about the importance of the presence, concentration, and flux of metabolites in health and disease. Metabolomics improves the understanding of the physiological and pathophysiological process (10). In this regards, metabolomics enables the identification of disease biomarkers and provides new insight into diseases mechanisms (11). Metabolomics helps advance the field of drug discovery by facilitating the understanding of the mechanism of diseases, identification of drug targets and elucidation of the mode of action of drugs. Previous studies have shown the applications of metabolomics in unveiling disease mechanism and facilitating early drug discovery (12).

1.1 Metabolomics technologies

The advanced technologies mainly NMR and MS greatly propelled the metabolite measurement (13). The major techniques in metabolomics involve experimental design, sample collection, sample processing, sample preparation, data acquisition and data analysis and metabolic pathway analysis (11, 14). The future of metabolomics is promising with ongoing advancements in technology, data integration and multi-omics approach, innovative

strategies and technologies that identify drug candidate.

1.2 Metabolites separation techniques

Chromatographic methods such as LC and GC improve the separation and quantification of metabolites which is achieved by column packed with diverse materials. LC-MS is the preferred method for analysing semi-polar metabolites when a soft ionization technique (e.g., electrospray ionization, atmospheric pressure chemical ionization) is employed. More polar solvents are often employed for the extraction of metabolites from samples to be analyzed with LC-MS (15). An advantage of LC-MS compared to GC-MS is that samples can more easily be recovered after fractionation and that sample derivatization is not required.

1.3 Metabolites detection techniques

1.3.1 NMR spectroscopy

Nuclear Magnetic resonance spectroscopy (NMR) is used to identify and quantify metabolites based on their unique chemical shifts. It is a powerful technique applied in elucidating the structure of organic compounds. NMR analysis is simple and reproducible, and provides direct quantitative information and detailed structural information, although it has relatively low sensitivity, meaning that it generally enables profiling only of major constituents(16). NMR has easy and rapid sample preparation, a fast and non-destructive analysis. This feature makes it a high-throughput, reproducible and relatively inexpensive technique (2). The NMR techniques mostly used is ¹H-NMR and 2-D NMR experiments usually coupled with multivariate data analysis. Furthermore, solid state NMR utilises High-Resolution-Magic Angle Spinning-NMR (HR-MAS-NMR) to analysis sample at the solid state without prior extraction (17). NMR based metabolomics approach was utilized to simultaneously monitor different level of possible variation in nutraceutical composition and natural products.

1.3.2 Mass spectrometry (MS)

Mass spectrometry (MS) is a technique used to detect and quantifying metabolites based on their molecular weight and fragmentation patterns. MS has become the workhorse in metabolic drug research. The efficacy of MS in the study metabolites stem from its proven success in disease



studies, pharmacokinetics and drug metabolite analysis. Various MS approaches such as LC-MS or GC-MS can be employed depending on the chemical properties of the targeted metabolites.

1.4 Drug Repositioning

Drug repositioning or repurposing is a drug discovery strategy in which an existing drug approved by regulatory agencies such as Food and Drug Administration (FDA), the European Medicines Agency (EMA) the Medicine & Health Care Products Regulatory Agency (MHRA) among others is employed as a therapeutic agent for a different disease. As information regarding the safety, pharmacokinetics, and formulation of existing drugs is already available, the cost and time required for drug development is reduced. The advantage of this strategy is that a few necessary steps in drug development are eliminated, thereby reducing the time required for clinical trials as well as the risk of failure due to adverse events (18). These techniques have been successful in identifying new drug candidates for several diseases and reduce failures typically associated with drug discovery (19) and may be a valuable strategy for finding therapeutics against rare diseases where there are little financial incentives for drug development (20). Owing to immense promise of a shortened development cycle many pharmaceutical companies are currently adopting drug repositioning to develop some of their FDA-approved and previously unsuccessful pipeline molecule as novel therapies for diverse disease condition (21).

Metabolomics analysis appears to be an excellent choice for large screening campaigns in this field, allowing the biochemical characterization of registered drugs and extrapolation of data obtained to known and relevant disease-specific pathophysiological consideration (12). Examples of drug repositioning include thalidomide, once used as a sedative, is now used to treat multiple myeloma, and Viagra, which is currently used as an erectile dysfunctions drug (22).

2.0 CONCLUSION

Natural Products remain a promising pool for the discovery of scaffolds with high structural diversity and various bioactivities that can be directly developed or used as starting points for optimization into novel drugs. Metabolomics is an innovative tool that is now emerging in drug discovery process by simultaneous investigation of

multiple metabolites in biological samples enabled by technological developments in chromatography and spectrometry. It has the potential to monitor the success of drug discovery and disease treatments. Moreover, it can detect differences between metabolites composition in various physiological states in organisms.

3.0 REFERENCES

1. A. Najmi, S. A. Javed, M. Al Bratty, H. A. Alhazmi, Modern Approaches in the Discovery and Development of Plant-Based Natural Products and Their Analogues as Potential Therapeutic Agents. *Molecules* 27, 349 (2022).
2. G. Valentino *et al.*, NMR-based plant metabolomics in nutraceutical research: an overview. *Molecules* 25, 1444 (2020).
3. T. Tsiaka *et al.*, Design and development of novel nutraceuticals: Current trends and methodologies. *Nutraceuticals* 2, 71-90 (2022).
4. H. Lachance, S. Wetzel, K. Kumar, H. Waldmann, Charting, navigating, and populating natural product chemical space for drug discovery. *Journal of medicinal chemistry* 55, 5989-6001 (2012).
5. A. G. Atanasov, S. B. Zotchev, V. M. Dirsch, C. T. Supuran, Natural products in drug discovery: Advances and opportunities. *Nature reviews Drug discovery* 20, 200-216 (2021).
6. P. S. Tresina, M. S. Selvam, A. Rajesh, A. Doss, V. R. Mohan, Natural products in drug discovery: Approaches and development. *Journal of Pharmaceutical Research International* 33, 93-110 (2021).
7. C. Wu, H. K. Kim, G. P. Van Wezel, Y. H. Choi, Metabolomics in the natural products field—a gateway to novel antibiotics. *Drug Discovery Today: Technologies* 13, 11-17 (2015).
8. R. Verpoorte, Y. Choi, H. Kim, NMR-based metabolomics at work in phytochemistry. *Phytochemistry reviews* 6, 3-14 (2007).
9. Q. Song, A.-h. Zhang, G.-l. Yan, L. Liu, X.-j. Wang, Technological advances in current



metabolomics and its application in tradition Chinese medicine. *RSC advances* 7, 53516-53524 (2017).

10. D. S. Wishart, Metabolomics for investigating physiological and pathophysiological processes. *Physiological reviews* 99, 1819-1875 (2019).

11. H. Pang, Z. Hu, Metabolomics in drug research and development: The recent advances in technologies and applications. *Acta Pharmaceutica Sinica B* 13, 3238-3251 (2023).

12. J. C. Alarcon-Barrera, S. Kostidis, A. Ondo-Mendez, M. Giera, Recent advances in metabolomics analysis for early drug development. *Drug discovery today* 27, 1763-1773 (2022).

13. Y. Xia, Advancements in metabolomics: from biomarker discovery to precision medicine *Journal of bioengineering and Biomedical Science* 13, 2 (2023).

14. Q. Xiao *et al.*, Plant metabolomics: A new strategy and tool for quality evaluation of Chinese medicinal materials. *Chinese Medicine* 17, 45 (2022).

15. H. K. Kim, Y. H. Choi, R. Verpoorte, NMR-based plant metabolomics: where do we stand, where do we go? *Trends in biotechnology* 29, 267-275 (2011).

16. J.-L. Wolfender, G. Marti, A. Thomas, S. Bertrand, Current approaches and challenges for the metabolite profiling of complex natural extracts. *Journal of Chromatography A* 1382, 136-164 (2015).

17. A. H. Emwas *et al.*, NMR Spectroscopy for Metabolomics Research. *Metabolites* 9, (2019).

18. Y. Zamami *et al.*, Drug-repositioning approaches based on medical and life science databases. *Frontiers in Pharmacology* 12, 752174 (2021).

19. G. L. Law, J. Tisoncik-Go, M. J. Korth, M. G. Katze, Drug repurposing: a better approach for infectious disease drug discovery? *Current opinion in immunology* 25, 588-592 (2013).

20. H. Mei *et al.*, Opportunities in systems biology to discover mechanisms and repurpose drugs for CNS diseases. *Drug discovery today* 17, 1208-1216 (2012).

21. V. Parvathaneni, N. S. Kulkarni, A. Muth, V. Gupta, Drug repurposing: a promising tool to accelerate the drug discovery process. *Drug discovery today* 24, 2076-2085 (2019).

22. J. S. Shim, J. O. Liu, Recent advances in drug repositioning for the discovery of new anticancer drugs. *International journal of biological sciences* 10, 654 (2014).



P040 - MODIFICATION OF UREA FORMALDEHYDE RESIN ADHESIVE USING NANO BIOCHAR DERIVED FROM BAMBOO WASTE AND IT'S APPLICATION IN PARTICLE BOARD PRODUCTION

A. I. Isah*, M.S. Abdulkadir, U. A. Paki and M. Hussein

Department of Mechanical Engineering, Nuhu Bamalli Polytechnic, PMB 1061 Zaria, Kaduna State
email: abufaseehah@gmail.com

ABSTRACT

This paper investigates the modification of urea-formaldehyde resin adhesive for particle board production using nanoparticles derived from bamboo waste. The objective is to enhance the adhesive performance of the urea-formaldehyde resin, reduce its environmental impact, and utilize bamboo waste as a valuable resource. Bamboo waste was processed to obtain bamboo nano-biochar which was incorporated into urea-formaldehyde resin adhesive. The modified adhesive was tested for its water absorption properties, Fourier Infrared transform (FTIR) and the Thermogravimetric analysis (TGA). Particle boards were then produced using the modified adhesive, and their mechanical and physical properties were evaluated. The results demonstrate the feasibility and potential of utilizing bamboo nano-biochar to improve the adhesive characteristics of urea-formaldehyde resin adhesive and produce high-quality particle boards with reduced formaldehyde emission.

KEYWORDS:

urea-formaldehyde resin, nano-biochar, bamboo waste, particle board, adhesive modification, formaldehyde emission

1.0

2.0 Introduction

Biochar simply refers to a by-product of biomass cellulose material developed by various thermo-chemical processes. Biochar can be converted into nano size material known as nano-biochar by reducing its particle size (1). Nano-biochar possesses a more suitable physio-chemical behaviour when compared to macro-biochar material, its more stable, has a different nanostructure, higher surface area and a unique catalytic ability. Among these physicochemical properties, the biodegradable ability plays a major role especially in agricultural applications. The incorporation of nano-biochar into UF resin adhesive led to a significant improvement in adhesive properties, including reduced viscosity, faster curing time, increased strength of bonding, and reduced formaldehyde emission (2).

Adhesives are materials that are used to glue two or more pieces of substrates together. Urea formaldehyde resin is an adhesive formed by the reaction of Urea and Formaldehyde (3). Urea formaldehyde resin is one of the most preferred adhesives in wood composite board's production (4). This is due to its low price, good

technological properties, and absence of colors in cured polymer and easy to of apply for a variety of curing conditions (5).

Particle boards are an essential material in the construction industry due to their versatility, cost-effectiveness, and sustainable attributes. Urea-formaldehyde (UF) resin adhesive is widely used for particle board production owing to its excellent bonding properties. However, limitations such as high formaldehyde emission and reduced water resistance have prompted the need for adhesive modifications.

Nanoparticles derived from bamboo waste offer a promising solution to overcome these challenges while adding value to bamboo waste as a renewable resource.

2.0 Materials and Method

2.1 Materials

Bamboo waste materials was obtained from Panteka market in Kaduna, Formaldehyde aqueous solution (HCHO, 37%), Urea (CH₄N₂O) and Sodium hydroxide (NaOH, 95%) were purchased



from Aladdin Industrial Corporation (Kaduna, Nigeria).

2.2 Sample collection and preparation

Bamboo waste was collected, washed, cleaned and dried for 24 hours. The bamboo material was then cut into smaller pieces and then grinded to powdered form. The powdered material is further processed to obtain bamboo cellulose nanoparticles using ball mill. The extracted nanoparticles were characterized for size, morphology, and chemical composition.

2.3 Preparation of Biochar and Nano biochar

Bamboo stalks were cut into smaller pieces. The pieces were placed in a well ventilate area for 7 days to dry them completely. The dried bamboo pieces were then placed in a kiln and slowly heat to 450 °C, the process is known as carbonization converts the bamboo into biochar by removing volatile compounds and leaving behind a carbon-rich material. The biochar was grind to fine powder through a sieve to obtain a uniform particle size. The nano-sized biochar particles were obtained by the use of a ball mill which helps break down the biochar particles into nano scale dimension.

2.3.1 Proximate analysis of Bamboo nano biochar

Proximate analysis is a method of partitioning of the compounds in the fibre (6). This system consists of the analysis of water content, ash content, volatile content and fixed carbon content. The methods of the analysis are thus:

2.3.1.1 Moisture content

Each sample of mass 10 g were measured and placed in the porcelain separately. The porcelain and its content were then dried in an oven at 110 °C to a constant weight for 3 h. Equation 1 was used to evaluate moisture content

$$\% \text{ Moisture content} = \frac{(g-x)}{g} \times 100 \quad (1)$$

Where,

g = weight of sample
x = weight of dry matter
(g - x) = loss in weight

2.3.1.2 Ash content

The total ash content equals the weight of the ash divided by the weight of the original sample multiplied by 100 %. The formula is given in equation 2

$$\% \text{ Ash} = \left(\frac{x}{g}\right) \times 100 \quad (2)$$

Where,

g = weight of sample
x = weight of ash

2.3.1.3 Volatile matter

The volatile matter of the fibre is calculated using Equation 3

$$\% \text{ Volatile matter} = \left(\frac{x-y}{g}\right) \times 100 \quad (3)$$

Where,

x = weight of sample
y = weight of dry matter
g = weight of residue

2.3.1.4 Fixed carbon

The percentage of fixed carbon was determined using Equation 4

$$\% \text{ fixed carbon} = 100 - (\text{VM} + \text{Ash} + \text{MC}) \quad (4)$$

Where,

VM = Volatile matter
Ash = Ash content
MC = Moisture content

2.3.2 Ultimate Analysis of Bamboo Nano-biochar

The elemental analysis simply refers to the chemical contents of the fibre; it gives the hydrogen content, nitrogen content, oxygen content and carbon content. The relationship used for analysing the constituent of the ultimate analysis is according to (Jenkins *et al.*, 2008)

2.3.2.1 Carbon content



The non aqueous titration method was used for this analysis. The carbon content was determined using Equation 5

$$\% \text{Carbon} = \frac{(B-T) \times M \times 0.003 \times 100 \times 1.33}{g} \quad (5)$$

Where,

B = Blank titre
T = Sample titre
M = Molarity of the acid used
g = weight of sample

2.3.2.2 Hydrogen content

The non aqueous titration method was used for analyzing hydrogen content of the fibre sample. The hydrogen content was determined using Equation 6

$$\% \text{ Hydrogen} = \frac{\text{wt of } H_2O \times 0.1119 \times 100}{\text{wt of pellet}} \quad (6)$$

2.3.2.3 Nitrogen content

The non aqueous titration method was also used for this analysis. The Nitrogen content was determined using Equation 7

$$\% \text{ Nitrogen} = \frac{T \times M \times 0.014 \times DF}{g} \times 100 \quad (7)$$

Where,

M = Molarity of the acid used
g = Weight of sample
T = Titre value
DF = Dilution factor diluted

2.3.2.4 Oxygen content

The total amount of all substances including ash content subtracted from 100% gives the percentage of Oxygen present in the sample. The Oxygen content was determined using Equation 8

$$\% \text{ Oxygen} = 100 - (C + H + N + S + \% \text{Ash}) \quad (8)$$

2.4 Synthesis of Urea-Formaldehyde Resin

The traditional alkali-acid alkali method was adopted for the preparation of the urea-formaldehyde resins. 200g of formaldehyde solution was measured and poured into a constant stirred tank reactor. 36 % aqueous NaOH solution was used to adjust the Ph of the solution to 8.0, 100 g of Urea was then added into the reactor and the mixture was slowly heated to 80 °C and the temperature was maintained for 40 min. Further 20 g of urea was added until the mixture reaches the target viscosity. The temperature was then allowed to drop to 70 °C, and another 7 g of urea was added to the solution again. When the temperature further drops to 40 °C, the pH of the solution was adjusted to alkaline conditions again and the urea formaldehyde resin was obtained.

2.5 Modification of UF Resins using Nano-biochar

The obtained nano-biochar was incorporated into UF resin adhesive through a simple blending process. Different loading levels of nano-biochar were evaluated to optimize the adhesive formulation and achieve desirable properties.

2.6 Characterization of the unmodified (neat) and modified UF Resins

2.6.1 Water Absorption Analysis of Unmodified (neat) and Modified UF Resins

The purpose of this test was to determine the water absorption capacity of dry Baobab pod fibres when immersed in water. ASTM D5229 was used, baobab pod fibres were dried in the sun for three days and the weight was determined using a weighing scale, the fibres were then immersed in distilled water at room temperature for 4 h and weighed immediately recorded. The water content of the fibres (in wt. %) was computed using Equation 9

$$\% \text{ absorption} = \frac{W_2 - W_1}{W_1} \times 100 \quad (9)$$

W_1 = weight of dried Baobab pod fibres
 W_2 = weight of Baobab pod fibres immersed in distilled water



2.6.2 FTIR Analysis of Unmodified (neat) and Modified UF Resins

The modified adhesives were characterized for their functional groups using the FTIR analysis. The changes in the features of the modified adhesives were analysed and compared with that of the standard neat UF resin adhesive.

2.6.3 TGA Analysis of Unmodified (neat) and Modified UF Resins

This is a thermal analysis technique used to determine changes in the material weight as a function of temperature or time. Its commonly use to study decomposition, oxidation and other thermal behaviours. The TGA instruments includes a balance (for measuring sample weight), a furnace (for heating the sample) and a sensitive detector (for measuring weight changes)

2.7 Preparation of Particle Board from Modified UF Resins

Particle boards were produced using the modified adhesive, and their mechanical properties (bending strength, internal strength) and other physical properties (thickness swelling, water absorption,) were analysed according to relevant standards.

3.0 Results and Discussion

3.1. Proximate characteristics of nano-biochar

The moisture content of the biochar has a great effect on performance of modified material, the higher the moisture content, the more detrimental it is to the performance of composites, it reduces stiffness and flexural strength. The result for the proximate analysis of bamboo nano-biochar is shown in Table 1. The proximate analysis of the Bamboo nano-biochar shows that, the fixed carbon 45 - 46 % which is the major constituent and the remaining constituent is ash amounting and volatile content which amounts to about 19 - 20 %.

Table 1: Proximate Analysis of Bamboo nano biochar

Temp °C	Moisture content (%)	Ash content (%)	Volatile Matter (%)	Fixed Carbon (%)
400	1.9	3.05	19.4	45.65
450	1.54	3.26	19.3	45.6
500	1.38	3.56	19.1	46.96

The flexural properties of the material have direct correlation with the ash content, volatile matter and fixed carbon which shows the amount of inorganic substituent in the carbon. When ash content is on the high side, the absorption capacity of the fibre will be reduced.

3.2. Ultimate characteristics of nano-biochar

Table 2 present the summary of results for the ultimate analysis of the nano-biochar. It can be seen that the sample consist predominantly of carbon greater than 60 % which indicates a good percentage of cellulose present in the fibre. Baobab fibres constitute elements that make it an excellent candidate for composite production.

Table 2: Ultimate analysis of Bamboo nano Biochar

Temp. °C	C (%)	H (%)	N (%)	O (%)
400	54.82	6.18	0.24	15.06



450	55.62	5.03	0.25	10.45
500	56.48	3.88	0.22	6.37

3.3. Water absorption characteristics of UF Resins

The water absorption capacity of the fibres increased with increasing nano-biochar loading. Natural fibres are hydrophilic in nature

and have that natural capacity to absorb water content which can make them to swell and deteriorate at a faster rate. Figure 4 shows the results of water absorption properties of unmodified and modified UF Resins.

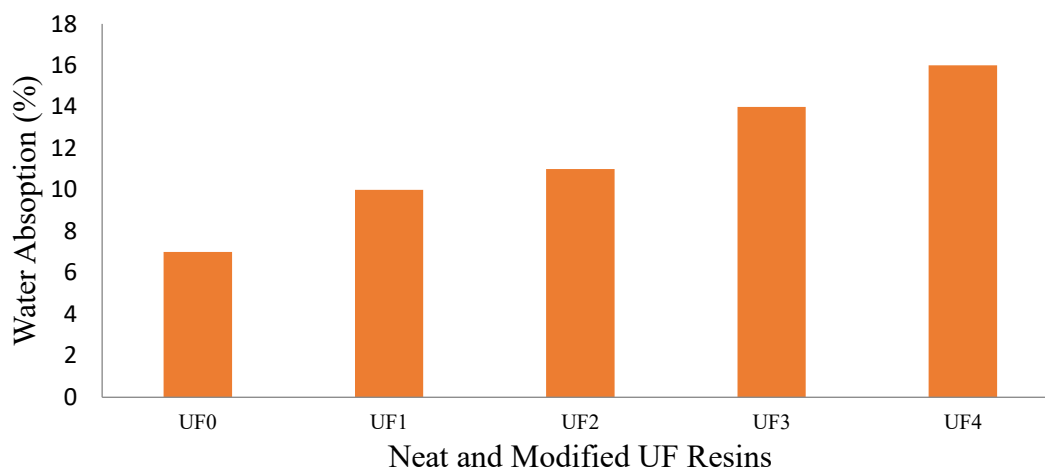


Figure 4: Water absorption properties of neat and modified UF Resins

3.4. FTIR characteristics of UF Resins

The frequencies and assignments of the FTIR absorption bands were summarized in Table 2.

Table 2: Assignments of Main Infrared Absorption of UF Resins

Wavenumber (cm ⁻¹)	Functional group	Class of compound
3332	O-H	Carboxylic acids
1625	C=O	Amides
1461	C-H	Alkanes and Alkynes
1114	C-O-C	Ethers

The band 3332 cm⁻¹ is related to stretching vibrations of O-H group. In the spectrum of the modified, a very intensive band was observed at 1625 cm⁻¹ due to stretching vibration of C=O groups. The bands located at 1461 and 1114 are as a result of presence of Alkanes and Ethers. It can be

seen from the bands in the modified spectrum that the bands appear simultaneously.

The FTIR Spectrum of the neat and modified UF Resins were shown in Figure 5,

3.4. TGA characteristics of UF Resins
The main decomposition temperature for the neat urea formaldehyde resin (UF₀) was observed at 402 °C while that of the modified was observed to be higher than that of the modified 459 °C, 487 °C, 489 °C and 512 °C for UF₁, UF₂, UF₃ and UF₄ respectively. The thermal degradation of the

modified UF Resins appears to be a cumulative phenomenon which shifted to a higher temperature indicating the modified samples to be thermally more stable than that of the unmodified. The modified UF has a much higher decomposition temperature than that reported for Pineapple leaf fibre composite (Threepopnatkul et al., 2009) which



is approximately 270 °C and 316 °C as peak degradation temperature for bamboo reinforced with hydroxybutyrate -co-valerate (4).

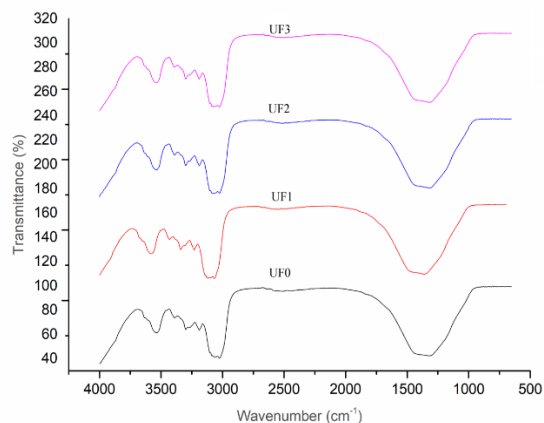


Figure 5: FTIR Spectra for neat (UF0) and modified UF resins (UF1, UF2 & UF3)

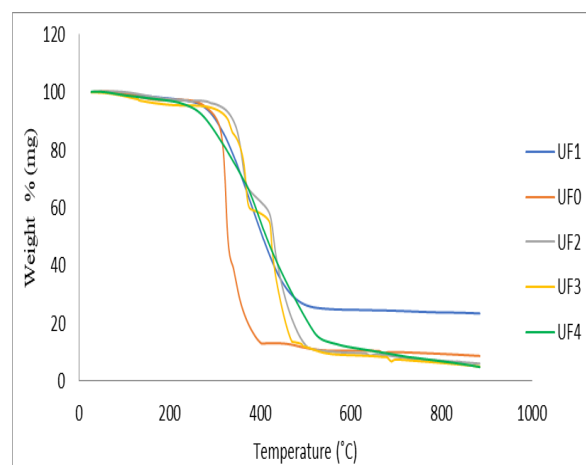


Figure 6: TGA spectrum of neat and modified UF Resins

4.0 Conclusion

This study demonstrates that the modification of UF resin adhesive using nanoparticles derived from bamboo waste offers a viable approach to enhance adhesive performance and produce high-quality particle boards with reduced formaldehyde emission. The aim was achieved through preparation and characterization of biochar and nano biochar produced from waste bamboo. The utilization of nano-biochar enables the valorisation of bamboo waste as a valuable resource, contributing to sustainable and eco-friendly particle board production. Further research is recommended to optimize the nano-biochar loading levels, explore different combinations of nanoparticles, and study the long-term performance and durability of the modified adhesive and particle boards.

References

1. S. Gao *et al.*, Unexpected role of amphiphilic lignosulfonate to improve the

storage stability of urea formaldehyde resin and its application as adhesives. *International Journal of Biological Macromolecules* **161**, 755-762 (2020).

2. P. Bekhta *et al.*, Properties of eco-friendly particleboards bonded with lignosulfonate-urea-formaldehyde adhesives and PMDI as a crosslinker. *Materials* **14**, 4875 (2021).
3. X. Wang, K. J. Cheng, Effect of glow-discharge plasma treatment on contact angle and micromorphology of bamboo green surface. *Forests* **11**, 1293 (2020).
4. H. Khanjanzadeh, R. Behrooz, N. Bahramifar, S. Pinkl, W. Gindl-Altmutter, Application of surface chemical functionalized cellulose nanocrystals to improve the performance of UF adhesives used in wood based composites-MDF type. *Carbohydrate polymers* **206**, 11-20 (2019).
5. F. Chang *et al.*, Factors affecting the temperature increasing rate in arc-shaped bamboo pieces during high-frequency heating. *BioResources* **15**, 2656-2667 (2020).
6. P. Yang *et al.*, Developing carbon dots as green modifiers for improving the bonding performance of low-molar-ratio urea-formaldehyde resin. *International Journal of Adhesion and Adhesives* **125**, 103416 (2023).





P041 - SORPTION STUDIES, OPTIMIZATION AND EFFECT OF REUSABILITY ON THE USE OF WASTE POLYPROPYLENE PLASTICS AS SORBENTS FOR OIL SPILL CLEAN UP

*Okpanachi, Clifford Baba.¹, Usman, Salifu, Oma.¹, Ekwoba, Lucky¹, Ocheme, Wilson¹. Agbogo, Victor.²

¹Department of Pure and Industrial Chemistry, Prince Abubakar Audu University, Anyigba

²Department of Chemistry, Nigerian Army University, Bui, Maiduguri

cliffordokpanachi@yahoo.com

ABSTRACT

This study aimed to use waste polypropylene plastics (WPP) as a sorbent for crude oil removal and to identify the optimum conditions of the oil removal. The application of response surface methodology (RSM) via central composite design (CCD) was used to analyse the effect of the four factor processes. Results from the RSM showed that the responses of oil sorption were significantly affected by the interaction of the factors. The fit summary from the WPP sorbents proved to be a good fit to the quadratic model while the diagnostics indicated good correlation of parameters. Numerical optimization applying desirability function was used to identify the optimum conditions for maximum oil sorption capacity. The optimum conditions were found to be at sorbent dosage = 3.38 g, contact time = 27 mins, initial oil concentration = 73 g/L and temperature = 28.00 °C. A confirmatory experiment which was performed to evaluate the accuracy of the optimization procedure resulted in an oil sorption capacity of 17.23 g/g when analysed under the optimized conditions. The effect of reusability of the WPP sorbents showed that it could be reused for 8 cycles after recovery suggesting high reusability thus adding one more step towards sustainability.

KEYWORDS:

Central composite design, Crude oil, Diagnostics, Optimization, Polypropylene, Reusability, Sorption.

1.0 INTRODUCTION

Products made from petroleum or crude oil products are still widely utilized due to their numerous advantages such as their ability to decrease friction, protect against corrosion, transfer heat under mechanical friction and to be used as fuels in combustion engines and spark ignition engines (1). In addition, petroleum and its derivatives are used in the manufacture of fertilizers, plastic wares, building materials, paints, clothing and to generate electrical power (2). Crude oil is a major driver of businesses, manufacturing, transportation as well as maritime trade at the national, regional and global levels. During the process of the off-shore production of crude oil and its transportation, a large number of oil spills occur. The oil spills occur very often due to the escape of crude oil from its confinements, offshore platforms and drilling rigs, and tends to cause harm to aquatic life and the environment (3). It also has an adverse effect on the economy, disrupting mainly the recreation and tourism activities.

Due to this, several efforts aimed at oil spill recovery have been done in the past years to identify the optimal cleaning-up technologies by means of physical, chemical, and biological methods (4). Among these techniques, the physical approach

through the application of sorbent materials is considered one of the most efficient and high-performing methods (5). It is a highly favoured procedure for cleaning oil-spill owing to its low cost, high efficiency and environmental friendliness.

Waste plastics such as polypropylene could be used as sorbents as they possess not only much higher sorption capacities but also have recyclability potential that many sorbents do not possess, hence they can be regenerated using various post treatment strategies for reuse (6). Also, robustness of these sorbents renders them useful in harsh environments typical of oil spills (7). One of the most attractive properties of these types of sorbents is that they are manufactured from waste plastics as well, hence they help to combat environmental problems of oils spills and waste pollution simultaneously (8).

Response surface methodology (RSM) is an effective statistical technique for optimizing complex processes. It can reduce the number of experimental trials needed to evaluate multiple parameters and their interactions (9). It is a very effective technique for this study because it presents statistical models which can be used to show the



relationship between the parameters that have been optimized (10). Moreover, central composite design (CCD) as a type of response surface design is also widely used in research works (11, 12). It (CCD) allows the simultaneous study of different experimental factors, their investigative interactions and optimization, and to quantify their influences on one or more properties of interest to multivariate models (13).

Hence, the goal of this study is to utilize waste polypropylene plastics (WPP) as a sorbent for oil removal, to apply CCD in order to identify the optimum conditions of oil removal and the effect of reusability of the WPP sorbents under the optimized conditions.

2.0 MATERIALS AND METHODS

Waste plastics made from commercial polypropylene (PP) was collected from refuse dumps and plastic waste collection centre in Tipper garage, Lokoja, Kogi State, Nigeria. The samples were thoroughly washed with water, dried,

shredded into particles of smaller sizes and sieved with laboratory sieves to obtain homogenous particle size of 300 μm .

2.1 Central Composite Design

A face-centred central composite design (CCD) which is appropriate for fitting second degree polynomial equations was applied to study the factors for the oil sorption capacity by the WPP. Four factors which are important variables in the oil sorption process were selected for the study. The factors are sorbent dosage, contact time, initial oil concentration and temperature. For a design of four independent factors ($K=4$), each with two different levels, the total number of experiments (N) was calculated using:

$$N = 4^2 + (2 \times 4) + 6 = 30 \quad (1)$$

Having specified the range of each of the process factors, they were coded to lie at ± 1 for the factorial points, 0 for the center points and \pm for the axial points (14). The chosen process factors with their limits, units and notations are presented in Table 1.

Table 1: Process factors and levels considered for the oil sorption

Factors	Units	Symbol	Levels				
			$-\alpha$	Low (-1)	Center (0)	High (+1)	$+\alpha$
Sorbent dosage	g	A	1.5	1.5	2.5	3.5	3.5
Contact time	min	B	10	10	20	30	30
Initial oil concentration	g/L	C	25	25	50	75	75
Temperature	$^{\circ}\text{C}$	D	25	25	35	45	45

The design had 30 experimental runs which comprised of 24 non-center points and 6 center points. Interactions between these factors were studied using the two variable interaction and the cube plots. Design expert software version 6.0 was used to generate the experimental runs and for the statistical analysis of the oil sorption process.

2.2. Oil sorption capacity

The waste polypropylene plastics (WPP) were subjected to crude oil sorption test, and in order to

To 1 liter of distilled water, a known concentration of crude oil was added. A known mass of the sorbent was added into the mixture in the beaker and left unperturbed at a known contact time in a water bath at a known temperature. After the contact time had elapsed, the sorbent was removed using sieving net and left to drain by hanging the

simulate the situation of oil spill and minimize experimental variation, the crude oil sample was held in beakers for 1 day in open air to release volatile hydrocarbon contents. The experiments were carried out with variations of the four process factors including sorbent dosage (1.5 – 3.5 g), contact time (10 – 30 min), initial oil concentration (25 – 75 g/L) and temperature (25 – 45 $^{\circ}\text{C}$) and were analyzed using the central composite design (CCD). The 30 experimental runs with the various combinations of the different factors were randomly performed according to Table 2.

net over the beaker in an oven for 4 hrs at 60 $^{\circ}\text{C}$ (15). The sorption capacity of the sorbent samples was calculated using the expression

$$\text{Oil sorption capacity} = \frac{\text{New Weight Gained (g)}}{\text{Original weight (g)}}$$

3.1. Fit Summary

3. RESULTS AND DISCUSSIONS



Results for Tables 2 and 3 showed the model summary statistics and analysis of variance for WPP respectively. Results Table 2 showed that the quadratic model was selected by the software for the sorbents which meant that it could be best used to explore the design space, to find optimal conditions of the process and also best used to explain the mathematical relationship between the independent variables and the dependent response (16).

For the model summary statistics which focuses on the model maximizing the "Adjusted R-squared" and the "Predicted R-squared" values, the adjusted R^2 and predicted R^2 should be within ≈ 0.20 of each other to be in reasonable agreement, if they are not there may be a problem with either the data or the model. The quadratic model for the WPP had adjusted R-squared values of 0.9644 and predicted values of 0.9184. These further confirm the better fitness of the quadratic model to the WPP sorbents.

Presented in table 3 was the analysis of variance (ANOVA) for the oil sorption capacity by WPP. Results indicated that its R^2 value was 0.9824. With the R^2 value above 0.75, it indicated adequate fitting of the WPP sorbents to the data. Results also revealed high F-values of 57.11 for the WPP sorbents indicating a high significance and very good fit to the model.

The WPP sorbents had Adequate precision (AP) values of 32.14. With the AP values greater than 4, it meant that the model gave an adequate signal and a very good prediction to the response. The coefficient of variation (CV) value of the sorbents was 1.47 which was lower than the standard value of 10, indicating a very good precision and reliability.

Table 2: Model Summary Statistics for the Oil Sorption Capacity by WPP Sorbents

Source	Standard Dev.	R-Squared	Adjusted R-Squared	Predicted R-Squared	PRESS	
Linear	0.49	0.8452	0.8205	0.7883	8.37	
2FI	0.52	0.8687	0.7996	0.6737	12.90	
<u>Quadratic</u>	<u>0.22</u>	<u>0.9816</u>	<u>0.9644</u>	<u>0.9184</u>	<u>3.23</u>	<u>Suggested</u>
Cubic	0.22	0.9915	0.9646	-0.1700	46.25	Aliased



Table 3: ANOVA for the Oil Sorption Capacity by Waste Polypropylene Plastics (WPP)

Source	Sum of Squares	DF	Mean Square	F Value	Prob > F	
Model	38.81	14	2.77	57.11	< 0.0001	Significant
A	13.71	1	13.71	282.51	< 0.0001	
B	0.72	1	0.72	14.83	0.0016	
C	12.72	1	12.72	262.03	< 0.0001	
D	6.27	1	6.27	129.10	< 0.0001	
A²	0.55	1	0.55	11.40	0.0042	
B²	0.17	1	0.17	3.41	0.0845	
C²	0.37	1	0.37	7.62	0.0146	
D²	1.77	1	1.77	36.52	< 0.0001	
AB	1.225E-003	1	1.225E-003	0.025	0.8759	
AC	0.29	1	0.29	6.01	0.0270	
AD	2.025E-003	1	2.025E-003	0.042	0.8409	
BC	0.053	1	0.053	1.09	0.3130	
BD	0.076	1	0.076	1.56	0.2311	
CD	0.50	1	0.50	10.39	0.0057	
Residual	0.73	15	0.049			
Lack of Fit	0.73	10	0.073	752.62	< 0.0001	Significant
Pure Error	4.833E-004	5	9.667E-005			
Cor Total	39.53	29				
Std. Dev.	0.22			R-Squared	0.9816	
Mean	14.98			Adj.R-Squared	0.9644	
C.V.	1.47			Pred.R-Squared	0.9184	
PRESS	3.23			Adeq. Precision	32.14	

3.2 CCD Response

Results for the CCD response of the oil sorption capacity are presented in Table 4. Results showed that the highest oil sorption capacity for the WPP sorbents was obtained at the 9th experimental run with a high level of sorbent dosage (3.5 g), high level of contact time (30 mins), high level of initial oil concentration (75 g/L) and a low level of temperature (25 °C), while the lowest oil sorption capacity for the WPP sorbents was obtained at the 23rd experimental run with a low level of adsorbent dosage (1.5 g), low level of contact time (10 mins), low level of initial oil concentration (25 g/L) and a high level of temperature (45 °C).

3.3 Effect of Interaction of two Variables on the Oil Sorption Capacity

3.3.1 Effect of the Interaction of Sorbent Dosage and Contact Time

The interaction plot of sorbent dosage and time on the oil sorption capacity by WPP sorbents is presented in Figure 1. It could be observed that increasing both the contact time and sorbent dosage at both levels resulted in the increase in the oil sorption capacity. This could be due to the fact that an increase in sorbent dosage results in more hydrophobic binding sites of the WPP available for the oil molecules to be sorbed, whereas an increased contact time provides enough time for the molecules to bind on the sorbent sites. Hence, at higher dosage the oil sorbed are higher due to the availability of more binding sites as compared to lower dosages which has fewer binding sites to sorb the same amount of oil in the adsorbate solution (17).



Table 4: Design Matrix and Response for the Oil Sorption Capacity by WPP Sorbents

Run	Dosage (g)	Time (min)	Conc. (g/L)	Temp (°C)	OSC WPP (g/g)
1	3.50	10.00	75.00	25.00	17.02
2	3.50	30.00	25.00	45.00	14.68
3	2.50	20.00	75.00	35.00	16.51
4	2.50	10.00	50.00	35.00	15.27
5	1.50	10.00	75.00	45.00	13.89
6	2.50	20.00	25.00	35.00	14.72
7	3.50	30.00	75.00	45.00	15.89
8	1.50	20.00	50.00	35.00	13.56
9	3.50	30.00	75.00	25.00	17.13
10	2.50	30.00	50.00	35.00	15.71
11	2.50	20.00	50.00	35.00	15.53
12	3.50	10.00	25.00	25.00	15.06
13	1.50	30.00	25.00	45.00	12.68
14	1.50	30.00	75.00	25.00	15.81
15	3.50	30.00	25.00	25.00	15.40
16	1.50	30.00	75.00	45.00	14.48
17	2.50	20.00	50.00	35.00	15.53
18	1.50	10.00	25.00	25.00	13.32
19	1.50	30.00	25.00	25.00	13.42
20	2.50	20.00	50.00	35.00	15.53
21	2.50	20.00	50.00	35.00	15.52
22	3.50	10.00	75.00	45.00	15.03
23	1.50	10.00	25.00	45.00	12.34
24	2.50	20.00	50.00	25.00	15.14
25	3.50	20.00	50.00	35.00	15.99
26	2.50	20.00	50.00	45.00	13.68
27	2.50	20.00	50.00	35.00	15.51
28	3.50	10.00	25.00	45.00	14.34
29	1.50	10.00	75.00	25.00	15.33
30	2.50	20.00	50.00	35.00	15.51

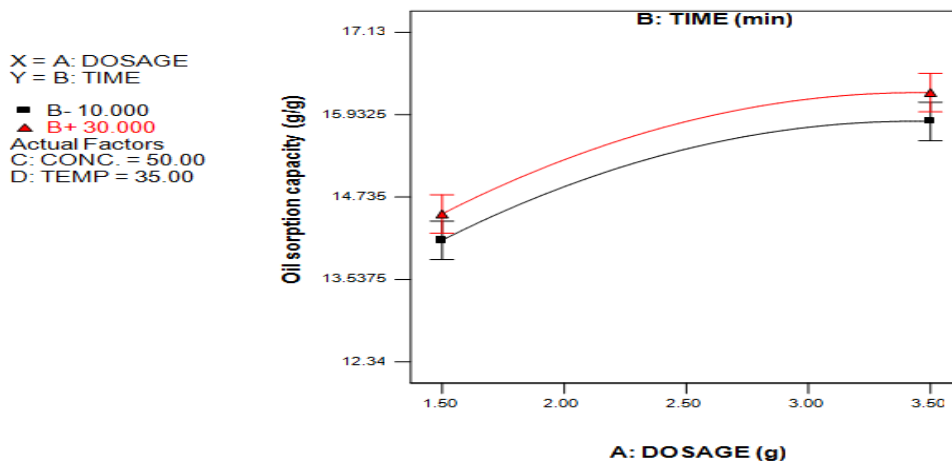


Figure 1: Interaction plot of Sorbent dosage and Contact time for the oil sorption capacity by WPP sorbents



3.3.2 Effect of the Interaction of Sorbent dosage and Temperature

The interaction plot of sorbent dosage and temperature on the oil sorption capacity by WPP sorbents is presented in figure 2. Results showed that the low temperature level gave higher sorption capacities than the high temperature level at the high- and low-level ends of the sorbent dosage. The plot further showed that the oil sorption capacity

was highest in the interaction effect at low temperature and high sorbent dosage. This probably could be due to the fact that at low temperature the crude oil will be more viscous making it less easy for it to drain off from the sorbents surface (3), and with the sorbent weights increasing, it meant that there were more available sites for sorption at that temperature.

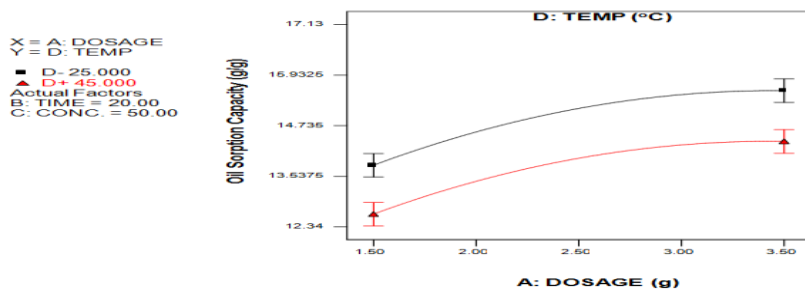


Figure 2: Interaction plot of Sorbent dosage and Temperature for the oil sorption capacity by WPP sorbents

3.3.3 Effect of the Interaction of Contact Time and Initial Oil Concentration

Presented in figure 3 is the interaction plot of the contact time and initial oil concentration on the oil sorption capacity by WPP sorbents. Results showed that increasing the contact time between the WPP sorbent and crude oil significantly increased the oil sorption capacity. It can be concluded that the contact time had a positive effect on oil sorption capacity, with the highest oil sorption capacity occurring at the levels of high contact time and

initial oil concentration. This is probably due to the fact that increasing the contact time increased the effective collisions between oil and sorbent probably by agitation leading to more sorption. At longer time intervals, the breakage of the oil droplets could be enhanced as a result of the interactions between the oil and the sorbents thus reducing the diameter of the oil droplets (emulsification) which leads to more interfacial area for sorption to occur.

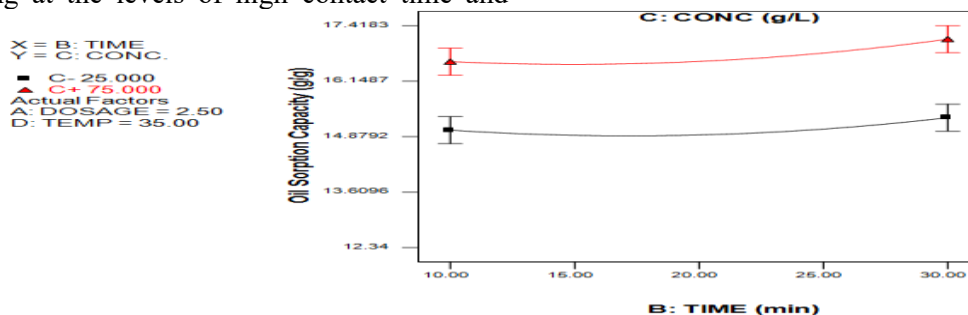


Figure 3: Interaction plot of Contact time and Temperature for the oil sorption capacity by WPP sorbents

3.4 Diagnostics

3.4.1 Normal probability plot

The normal probability plot for the oil sorption capacity by the WPP sorbents was presented in figure 4. A normal probability plot indicates that if the residuals follow a normal distribution, the points

will be scattered following a straight line for each of the responses (18).

From the plot of the WPP sorbents, it is evident from the figures that the residual points were reasonably aligned giving rise to a straight line plot suggesting normal distribution, further confirming the reliability and accuracy of the model terms.



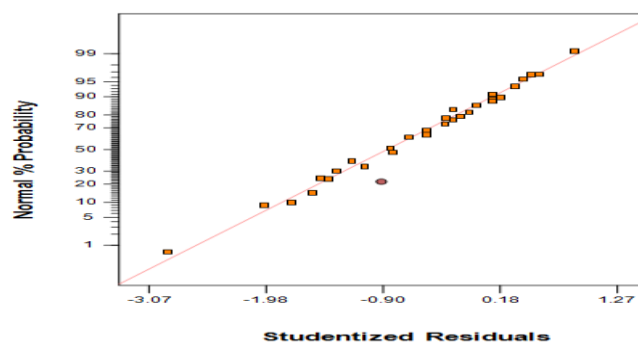


Figure 4: Normal Probability Plot for the Oil Sorption Capacity by WPP sorbents

3.4.2 Predicted values vs Actual values

The diagnostic case statistic results showed that the predicted values were very close to the actual values. As can be seen, the data points were well distributed close to a straight line which suggested an excellent relationship between the experimental

and predicted values of the response, and that the underlying assumptions of the above analysis were appropriate (19). This meant that it gave a good accuracy and representation and a very satisfactory fitting precision of the models.

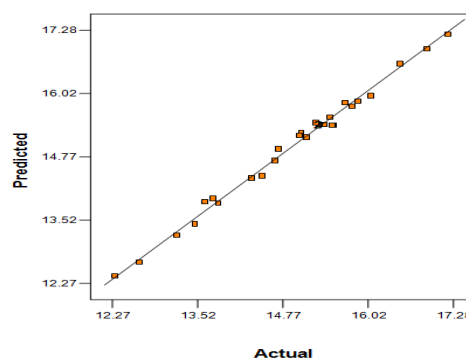


Figure 5: Predicted vs Actual values for the Oil Sorption Capacity by WPP sorbents

3.5 Optimization

In numerical optimization, we chose the desired goal for each factor and response. The possible goals were: to maximize, minimize, target or set within range. The desirability procedure involves finding the levels of the independent variables that simultaneously produce the most desirable predicted responses on the dependent variables and maximizing the overall desirability with respect to the controllable factors (20).

A multiple response method was applied for optimization of the factor processes with the combination of any four factors, namely; sorbent dosage, contact time, initial oil concentration, temperature and a response which was the oil sorption capacity. The criterion was set “in range” for sorbent dosage (1.5 – 3.5 g), “in range” for contact time (10 – 30 mins), “maximum” for initial

oil concentration (g L^{-1}) and “minimum” for temperature in order to analyses economically viable optimal conditions. The objective of this process was to find the maximum removal efficiency by maximizing the initial oil concentration with the sorbent dosage in range, with the response for the oil sorption capacity being set at maximum values with the upper and lower limits at 10.0 g/g and 20.0 g/g respectively. By seeking from 10 starting points in the response changes, the best local maximum for the optimized factor processes was found at sorbent dosage of 3.38 g, contact time of 27 mins, initial oil concentration of 73.00 g/L and a temperature of 28.00 °C. At this condition the response (oil sorption capacity) was 17.29 g/g with a desirability value of 0.900 for the WPP sorbents. These optimum values were checked experimentally which resulted in an oil sorption capacity of 17.23 g/g.



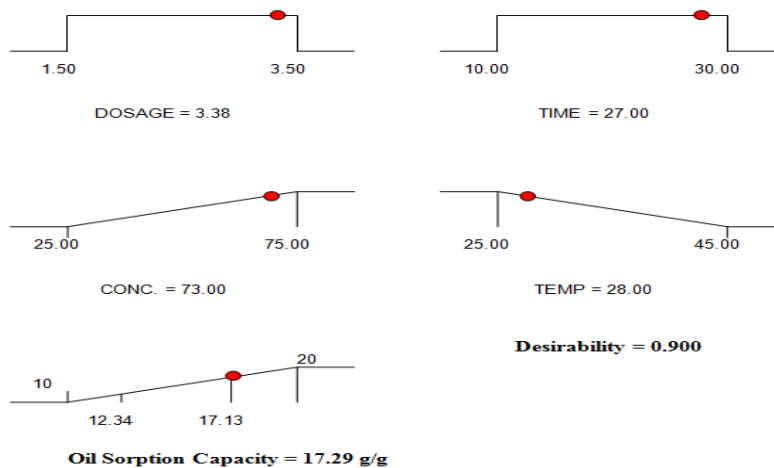


Figure 6: Ramp Function Graph for the Optimized conditions on the Oil Sorption Capacity by the WPP Sorbents

3.6 Effect of Reusability

The effect of reusability was analyzed for the WPP at the optimized conditions. Results revealed that the oil sorption capacity decreases with repeated use and that the WPP were used at least four times before they reached 50% of their original sorption capacity. This shows that the WPP sorbents samples are very good sorbents for oil spillage treatments.

Results showed that for the WPP sorbents, the oil sorption value which was initially 17.23 g/g decreased to 15.63 g/g in the first use, 13.77 g/g in the second use, 11.54 g/g in the third use, 9.46 g/g in the fourth use, 7.83 g/g in the fifth use, 6.04 g/g in the sixth use, 4.72 g/g in the seventh use and finally 3.48 g/g. These results showed that the WPP is a good sorbent with efficient reusable properties and good retaining ability.

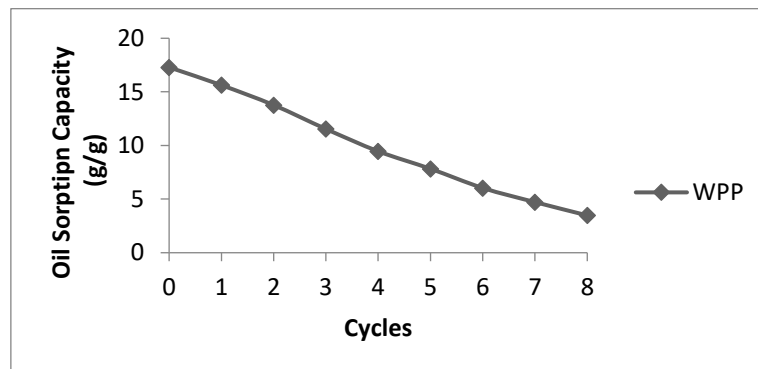


Figure 7: Effect of Reusability on the Oil Sorption Capacity by WPP sorbents

4.0 CONCLUSION

The optimized conditions of WPP as oil sorbent were obtained as follows; sorbent dosage 3.38 g, contact time 27.00 mins, initial oil concentration 73 g/L and temperature 28.02 °C. Under these optimum conditions, the predicted value from the model is 17.29 g/g and the obtained result was 17.23 g/g and this indicates the successful development model. It was important to note that the sorbents could be reused 4 times before it reached 50% of its sorption value, with maximum reusability occurring at 8 cycles. In the past years, most research on plastic has focused more on its elimination and disposal rather than its beneficial,

value-added reuse. This up-cycling of polypropylene waste to sorb crude oil provides a useful alternative to existing plastic recycling technologies and also put forward a facile sustainable approach in remediating environment pollution. The use of waste polypropylene plastics as sorbents would contribute to the sustainability of the environment and offer promising benefits for the commercial purpose in a future.

REFERENCES.

1. S. Ben Jmaa, A. Kallel, Assessment of performance of *Posidona oceanica* (L.) as biosorbent for crude oil-spill cleanup in



- seawater. *BioMed Research International* **2019**, (2019).
2. D. P. Nolan, *Handbook of fire and explosion protection engineering principles: for oil, gas, chemical and related facilities*. (William Andrew, 2014).
 3. G. A. El-Din, A. Amer, G. Malsh, M. Hussein, Study on the use of banana peels for oil spill removal. *Alexandria engineering journal* **57**, 2061-2068 (2018).
 4. V. Fiore, E. Piperopoulos, L. Calabrese, Assessment of *Arundo donax* fibers for oil spill recovery applications. *Fibers* **7**, 75 (2019).
 5. D. Ceylan *et al.*, Evaluation of butyl rubber as sorbent material for the removal of oil and polycyclic aromatic hydrocarbons from seawater. *Environmental science & technology* **43**, 3846-3852 (2009).
 6. A. O. Odeh, L. Okpaire, Modelling and optimizing the application of waste TYRE powder (WTP) as oil sorbent, using response surface methodology (RSM). *African Journal of Health, Safety and Environment* **1**, 1-12 (2020).
 7. J. Saleem, M. A. Riaz, M. Gordon, Oil sorbents from plastic wastes and polymers: A review. *Journal of hazardous materials* **341**, 424-437 (2018).
 8. J. Saleem, G. McKay, Waste HDPE bottles for selective oil sorption. *Asia-Pacific Journal of Chemical Engineering* **11**, 642-645 (2016).
 9. S. Arhin, N. Banadda, A. Komakech, W. Pronk, S. Marks, Optimization of hybrid coagulation-ultrafiltration process for potable water treatment using response surface methodology. *Water Science and Technology: Water Supply* **18**, 862-874 (2018).
 10. S. K. Behera, H. Meena, S. Chakraborty, B. Meikap, Application of response surface methodology (RSM) for optimization of leaching parameters for ash reduction from low-grade coal. *International Journal of Mining Science and Technology* **28**, 621-629 (2018).
 11. Y.-H. Huang, L.-C. Chen, H.-M. Chou, Optimization of process parameters for anti-glare spray coating by pressure-feed type automatic air spray gun using response surface methodology. *Materials* **12**, 751 (2019).
 12. B. Sadhukhan, N. K. Mondal, S. Chatteraj, Optimisation using central composite design (CCD) and the desirability function for sorption of methylene blue from aqueous solution onto *Lemna major*. *Karbala International Journal of Modern Science* **2**, 145-155 (2016).
 13. A. Asfaram, M. Ghaedi, K. Dashtian, G. R. Ghezelbash, Preparation and characterization of MnO. 4ZnO. 6Fe₂O₄ nanoparticles supported on dead cells of *Yarrowia lipolytica* as a novel and efficient adsorbent/biosorbent composite for the removal of azo food dyes: central composite design optimization study. *ACS Sustainable Chemistry & Engineering* **6**, 4549-4563 (2018).
 14. N. S. Muluh, Central composite design analysis and optimization of cadmium adsorption from synthetic wastewater by avocado seed activated carbon. *Int. J. Adv. Res. Dev* **5**, 652-661 (2017).
 15. J. C. Onwuka, E. B. Agbaji, V. O. Ajibola, F. G. Okibe, Kinetic studies of surface modification of lignocellulosic *Delonix regia* pods as sorbent for crude oil spill in water. *Journal of applied research and technology* **14**, 415-424 (2016).
 16. S. Ahmadi, L. Mohammadi, C. A. Igwegbe, S. Rahdar, A. M. Banach, Application of response surface methodology in the degradation of Reactive Blue 19 using H₂O₂/MgO nanoparticles advanced oxidation process. *International Journal of Industrial Chemistry* **9**, 241-253 (2018).
 17. N. T. Abdel-Ghani, G. A. El-Chaghaby, Biosorption for metal ions removal from aqueous solutions: a review of recent studies. *Int. J. Latest Res. Sci. Technol* **3**, 24-42 (2014).
 18. J. Martin, D. D. R. De Adana, A. G. Asuero, Fitting models to data: residual analysis, a primer. *Uncertainty quantification and model calibration* **133**, (2017).
 19. Y. Bai, G. Saren, W. Huo, Response surface methodology (RSM) in evaluation of the vitamin C concentrations in microwave treated milk. *Journal of food science and technology* **52**, 4647-4651 (2015).
 20. S. Chatteraj, N. K. Mondal, B. Das, P. Roy, B. Sadhukhan, Biosorption of carbaryl from aqueous solution onto *Pistia stratiotes* biomass. *Applied Water Science* **4**, 79-88 (2014).



P043 - EMISSIONS BASED ENVIRONMENTAL IMPACT ANALYSIS FROM A POWER-COOLING ORGANIC RANKINE CYCLE WITH EJECTOR SYSTEM

^{1,*}Kenneth O. Enebe ^{2,*}Ekwe B. Ekwe, ³Ene E. Bassey

¹Scientific Equipment Development Institute (SEDI) Enugu

²Department of Mechanical Engineering, Covenant University, Ota, Ogun State.

³Department of Mechanical Engineering, Cross River University of Technology, Calabar

*Corresponding authors: enebekenneth@gmail.com; ekwe.ekwe@covenantuniversity.edu.ng

ABSTRACT

Although Organic Rankine cycles does not require the combustion of its working fluid, the choice of operating refrigerants pose significant environmental impact from construction, operation and decommissioning phases. This research work focused on the evaluation of possible environmental impacts of an adapted power-cooling organic Rankine cycle using six different refrigerants with respect to the power generation potential within the system's operational phase. A simplified life cycle model was used for quantifying the related emissions subject to the thermodynamic operation of the cycle for each refrigerant. The analysis was done using the Engineering Equation Solver. The results reveal R114 and R600a as the refrigerants with the highest emissions of greenhouse gases amongst all others when all refrigerants are operating under the same conditions, but with the potential to generate the highest power from the system. Within the estimated 20 years system life cycle, the system can emit as much as 6.5 tons of carbon dioxide equivalent, while generating 66 kW of turbine power with R113 as the working fluid. The results can assist in the optimal refrigerant choice with regards to environmental sustainability, operating cost, and performance efficiency in the adapted power-cooling system.

KEYWORDS

Environmental impact, organic Rankine cycle, Power-cooling, refrigerants

1. Introduction

The organic Rankine cycle (ORC) is recognized as a highly developed means for harnessing the waste heat from industrial processes and other low-temperature heat sources in the conversion of thermal power to electrical energy (Mondejar et al., 2018). It offers the flexibility of a bottoming cycle to various low grade energy sources for additional power generation, and also other products like refrigeration and district water heating (Yu et al., 2013; Guzović et al., 2014; Ayub et al., 2015). The ORC derives its driving energy via a heat exchange between an evaporator and the low-grade heat flare gas. Although the ORC system does not require the combustion of its working fluid during operation, organic refrigerants used as its working fluid are susceptible to non-direct emissions of greenhouse gasses (GHGs) including carbon dioxide during either the production, operation and decommissioning phases. Therefore, the

choice of eco-friendly refrigerants are a necessity during the design process.

ORC refrigerants, based on their classification, possess negative environmental impacts linked to their global warming potential (GWP) and human toxicity potential (HTP). Amongst some considered environmental impacts, the most serious one is the GWP, followed by the HTP (Liu et al., 2013). In reference to the GWP of refrigerants, GHGs dominate as a cause of global warming, including residual heat and waste heat (Bian, 2020). As for HTP, the major pollutants that give rise to it are CO, NO_x, and SO_x (Li et al., 2012). There is therefore a need for the evolution of these gases and by-products (residual/waste heat) of industrial processes to be minimized or utilized respectively. This can be done by performing a greenhouse gas emissions evaluation to ascertain gases (and in what quantity) are released by various organic working fluids in ORCs especially with respect to leakages.



Furthermore, the GHG emissions evaluation in ORCs assists in identifying the impact they have on the environment and to make a decision to utilize the most effective and safest options. Research and development can even lead to the synthesis of new working fluids that meet the acceptable standards. Studies on the environmental impact of ORCs and their working fluid are already in the public domain, but relatively few (Park et al., 2019; Liu et al., 2013). For example, Liu et al., (2013) evaluated the environmental impact) of an organic Rankine cycle power-plant for waste-heat-recovery using life cycle analysis methodology during the construction, operation and decommissioning phases of the plant. They listed the inventory of environmental emissions for the plant using 7 different working fluids. Wang et al., (2019) evaluated a carbon footprint for an ORC using zeotropic mixture and concluded that the primary source of CO2 emissions emanate from ORC heat exchangers and also during leak process. Further studies also indicates indirect methods for reduction of emissions in ORC by optimization of component performance. Thus, Mohammadzadeh et al., (2017) showed that

installing an internal heat exchanger in an ORC system can bring about 3.6 % reduction in carbon dioxide emissions than conventional ORC. Due to the potential for environmental impact from ORC systems, the quantification of these emissions are pertinent, based on the structure and size of the operating cycle, as well as the working refrigerants, especially throughout the system life cycle. Accordingly, the research is focused on the evaluation of possible environmental impacts of an adapted power-cooling organic Rankine cycle using six different refrigerants with respect to the power generation potential within the system's operational phase. A simplified life cycle model was used for quantifying the related emissions subject to the thermodynamic operation of the cycle for each refrigerant.

2.0 Materials

The adapted ORC for cooling and power generation is shown in Fig. 1. The system is made up of various components including a vapour generator, an expander (or turbine), an ejector, a pump, throttling valve, evaporator, and a condenser.

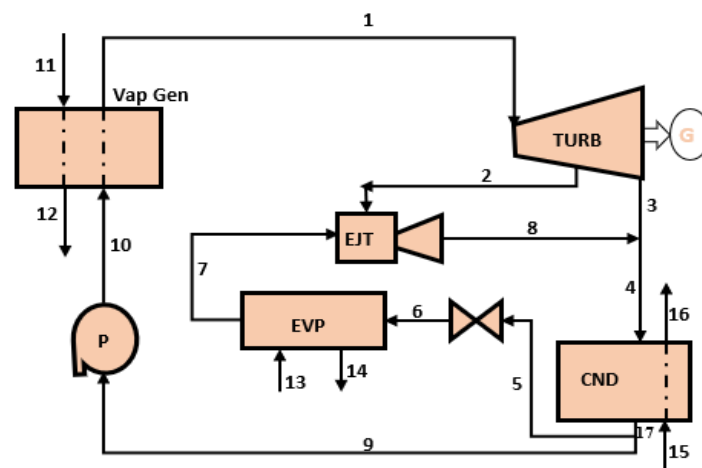


Figure 1: Schematic Diagram of the ORC for power and cooling (Abam et al., 2022)

The series of steps through which the system performs its functions are described as follows: Power is provided to the system by low-grade waste heat from any industrial process providing low grade heat. The heat is used to

increase the energy level of the circulating refrigerants via a heat exchanger herein referred to a vapour generator. The refrigerant gets vaporized to a super-heated vapour at state 1 before it is directed and passed through a



turbine to expand, thus, producing work and driving a generator to produce power. However, before the vaporized refrigerant is fully expanded, it is bled out of the turbine at state 2 to pass through the ejector nozzle. Upon exiting the ejector nozzle, the vaporized refrigerant has a high velocity, and this spurs the creation of a vacuum at the entrance into the mixing chamber. The created vacuum in the ejector mixing chamber at state 2 causes an inflow of secondary vapour (state 7) out of the evaporator to the mixing chamber and the exit stream (state 8) gets mixed with the expanded refrigerant vapour coming out of the turbine (state 3) at state 4. The mixture at state 4 passes to the condenser, inside which it gets water-cooled and condenses to a saturated liquid. On exiting the condenser at state 17, the liquid refrigerant gets split along two routes (states 5 and 9). The route through state 5 takes it into an expansion/throttling valve to reduce both its temperature and pressure so it can be evaporated to produce cooling in the evaporator at state 6. The evaporation happens because the refrigerant absorbs the heat from the substance placed in the evaporator; this is how the cooling effect is made on the substance. The second path out of the condenser through state 9 leads the saturated liquid to a pump where it is pressurized and sent to the vapour generator to start the cycle again. The working fluids (refrigerants) used in the operation of the ORC power/cooling system are R113, R114, R123, R141b, R245fa, and R600a. The operating thermodynamic assumptions adopted for the analysis are summarised as follows (Abam et al., 2022):

In all components, there is a steady flow condition for the refrigerant. Losses due to

friction, heat, and pressure in the components are negligible. Adiabatic system boundaries, thus, heat loss to the environment is negligible. Heat is provided from a modular turbine's exhaust gas estimated at 623 K, and the mass flux for the heat source was taken as 20 kg/s. The isentropic efficiencies of the pump and turbine are 70 % and 85 %, respectively. The pinch point temperature difference for the evaporator is kept at 278 K while that of the condenser is kept at 283 K. The ambient temperature was referenced at 293.17 K. The efficiencies of the nozzle, diffuser, and mixer unit in the ejector are 85 %, 85 %, and 95 %, respectively. There is an isobaric mixture process inside of the ejector mixing chamber. The nozzle exit pressure equals the inlet secondary pressure (Abam et al., 2022; Manente et al., 2017).

3.0 Thermodynamic modelling

The system's operating parameters were evaluated at component level based on the first law of thermodynamics. Using the steady flow energy equation, and neglecting all potential and kinetic energy interaction in the system, the general energy balance for the k^{th} component is expressed as (Bronicki, 2017; Cao et al., 2017):

$$\sum \dot{W}_k - \sum \dot{Q}_k = \sum_{i,e}^{m,n} |\dot{m}_i \dot{h}_i - \dot{m}_e \dot{h}_e| \quad 1$$

Where, the work and heat requirements in the k^{th} component are denoted with \dot{W}_k and \dot{Q}_k , respectively, while the mass and enthalpy are represented with \dot{m} and \dot{h} . The subscripts, i and e , are for flow inlet and outlet, respectively. The energy balance for the components is shown in Table 1.

Table 1: Process energy balance for each component

Component	Energy balance
Vapor generator	$\dot{m}_{11}h_{11} + \dot{m}_{10}h_{10} = \dot{m}_1h_1 + \dot{m}_2h_2$
Turbine	$\dot{m}_1h_1 + \dot{W}_{turb} = \dot{m}_2h_2 + (1-x)(h_2 - h_3) \times \eta_{isen, turb}$



Throttling valve	$\dot{m}_5 h_5 = \dot{m}_6 h_6$
Condenser	$\dot{m}_4 h_4 - \dot{m}_{17} h_{17} = \dot{m}_{16} h_{16} - \dot{m}_{15} h_{15}$
Ejector	$\dot{m}_2 h_2 + \dot{m}_7 h_7 = \dot{m}_8 h_8$
Pump	$\dot{W}_{pump} = \dot{m}_{10} (h_{10} - h_9) \times \eta_{isen, pump}$
Evaporator	$\dot{m}_6 h_6 + \dot{m}_{13} h_{13} = \dot{m}_7 h_7 + \dot{m}_{14} h_{14}$

3.1 Modelling of the ejector

The data used to model the ejector was acquired from (Haghparast et al., 2019; Mondal and De, 2017). With respect to the schematic of Fig. 1, the entrainment ratio for the secondary flow can be expressed as:

$$\omega = \frac{\dot{m}_7}{\dot{m}_2} \quad 2$$

The primary flow $V_{pf, n1}$ has a negligible inlet velocity at the nozzle. Thus, the primary flow outlet velocity, outlet enthalpy, and the efficiency of the nozzle, are denoted with the expressions (Haghparast et al., 2019).

$$V_{pf, n2} = \sqrt{2\eta_{Noz}(h_{pf, n1} - h_{pf, n2, s})} \quad 3$$

$$\eta_{Noz} = \frac{h_{pf, n1} - h_{pf, n2, s}}{h_{pf, n1} - h_{pf, n2, s}} \quad 4$$

Where: $h_{pf, n1}$ = enthalpy at point 7; $h_{pf, n2, s}$ = exit enthalpy of the primary flow under isentropic expansion; and η_{Noz} = nozzle efficiency. The mixing chamber area has an equation for the conservation of momentum that is given by:

$$\dot{m}_2 V_{pf, n2} + \dot{m}_7 V_{sf, n2} = (\dot{m}_2 \dot{m}_7) V_{mf, m, s} \quad 5$$

In comparison with the primary flow velocity $V_{pf, n2}$ if the secondary flow velocity $V_{sf, n2}$ were neglected, then the outlet velocity of mixed flow $V_{mf, m, s}$ will be:

$$V_{mf, m, s} = \frac{V_{pf, n2}}{1+\omega} \quad 6$$

The mixing chamber efficiency is given as:

$$\eta_{Mix} = \frac{V_{mf, m}^2}{V_{mf, ms}^2} \quad 7$$

Thus, the velocity of the mixed flow can be given by:

$$V_{mf, m, s} = \frac{V_{pf, n2} \sqrt{\eta_{Mix}}}{V_{mf, ms}} \quad 8$$

The mixing chamber energy equation gives the equation:

$$\dot{m}_2 \left(h_{pf, n2} + \frac{V_{pf, n2}^2}{2} \right) + \dot{m}_7 \left(h_{sf, n2} + \frac{V_{sf, n2}^2}{2} \right) = \dot{m}_8 \left(h_{mf, m} + \frac{V_{mf, m}^2}{2} \right) \quad 9$$

Equations (8) and (9) are simplified to give the mixed flow enthalpy as:

$$h_{mf, m} = \frac{h_{pf, n1} + \omega h_{sf, n2}}{1+\omega} - \frac{V_{mf, m}^2}{2} \quad 10$$

At the diffuser of the ejector, the velocity of the mixed flow is converted to an increase in pressure. Taking the efficiency of the diffuser into account, and upon the assumption that the outlet velocity of the mixed fluid is negligible, the actual diffuser efficiency and outlet enthalpy of the mixed flow are expressed as:

$$h_8 = h_{mf, m} + \frac{(h_{mf, ds} - h_{mf, m})}{\eta_{Dif}} \quad 11$$

$$\eta_{Dif} = \frac{h_{mf, ds} - h_{mf, m}}{h_{mf, d} - h_{mf, m}} \quad 12$$

Where:

$h_{mf, ds}$ = ideal outlet enthalpy of the mixed flow with isentropic compression; and η_{Dif} = diffuser efficiency



The entrainment ratio can be computed using Equation 13 (Haghparast et al., 2019).

$$\omega = \sqrt{\eta_{Noz}\eta_{Mix}\eta_{Dif} \left(\frac{h_2-h_a}{h_3-h_b} \right)} - 1 \quad 13$$

With the nozzle efficiency denoted with, nozzle mixing chamber efficiency, and diffuser efficiency, respectively represented with the terms η_{Noz} , η_{Mix} , and η_{Dif} in that order.

3.2 System environmental impact modeling

The environmental impact estimation is done using the relationship (Liu et al., 2013):

$$E_p(j) = \sum E_p(j)_i = \sum [Q(j)_i \cdot E_f(j)_i]$$

14

In equation 14, the relative contribution of the j^{th} phase (capturing the construction, operation and decommissioning phases) to the environmental impact of the system is denoted

Table 2: System operating enthalpies

State point	Operating enthalpies (kJ/kg)					
	R113	R114	R123	R141b	R245fa	R600a
1	462.6	273.5	524.5	429.5	487.9	812.5
2	430.7	224	432	355	473.2	714.2
3	447.1	256.4	501.9	400.8	460.5	760.2
4	430.3	229	457.9	364.6	455.9	696.4
5	312.9	103	298.9	159.2	274.9	317.5
6	312.9	103	298.9	159.2	274.9	317.5
7	399.5	185.9	410	311.1	426.8	560.4
8	416.6	206.7	422	335.1	452.1	644.3
9	312.9	103	298.9	159.2	274.9	317.5
10	313.8	103.9	299.8	160.2	276	319.7
11	631.6	631.6	631.6	631.6	631.5	631.6
12	424.6	424.6	424.6	424.6	424.6	424.6
13	300.4	300.4	300.4	300.4	300.4	300.4
14	274.3	274.3	274.3	274.3	274.3	274.3
15	83.38	83.38	83.38	83.38	83.3	83.38
16	146.1	146.1	146.1	146.1	146	146.1
17	312.9	103	298.9	159.2	274.9	317.5

with $E_p(j)$, while the contribution of the i^{th} element of impact to the j^{th} phase is labelled as $E_p(j)_i$. Similarly, the size of emissions and the equivalent emissions factor from the i^{th} element are represented as $Q(j)_i$ and $E_f(j)_i$, respectively. The environmental impacts were computed only for the operational phase of the plant using R113, R114, R123, R141b, R245fa, and R600a refrigerants.

4.0 Results and discussion

The simulation results were performed using the Engineering Equation Solver (EES) based on component energy balance and the initial operating data in section 2.0. A detailed quantification of the operating system properties with R113, R114, R123, R141b, R245fa, and R600a refrigerants is shown in Tables 2 for enthalpy. These properties aided the computations of environmental impacts based on the methodology provided with respect to the system's power output as obtained in Lie et al., (2013).

4.1 Results from emissions

The results of the GHG emissions profile of the power-cooling cycle is shown for R113, R114, R123, R141b, R245fa, and R600a. The system



was modelled with a yearly operation time of 7,000 hours and a lifetime of 20 years. These parameters, along with the environmental emissions inventory of the system in operation phase were used to model the emissions profile of the system. The system was simulated with the same inlet heat source parameters for each

refrigerant; however, the turbine inlet temperature (TIT) and pressure (TIP) were varied based on the thermal properties of each refrigerant. The turbine output power for each refrigerant under these conditions is shown in *Table 3*.

Table 3: Turbine Output Power for each Refrigerant at Turbine Inlet of 450 K and 18 bar

Refrigerant	Turbine output power (kW)	Turbine output power (kWh)
R113	65.95	0.018319444
R114	123	0.034166667
R123	121	0.033611111
R141b	107.8	0.029944444
R245fa	155.1	0.043083333
R600a	297.5	0.082638889

4.2 Evaluation of the GHG emissions profile of the plant

The environmental impact from each refrigerant is presented with respect to the quantity of respective harmful gasses per power of turbine output in the cycle. In the operation

phase of the plant, the indicators are presented in *Table 4* for all considered refrigerants.

Table 4: Environmental emissions inventory of the power-cooling cycle in operation phase (Liu et al., 2013)

Refrigerants	Emissions factor (kg/kWh)			
	CO ₂ ($\times 10^{-2}$)	CH ₄ ($\times 10^{-5}$)	NO _x ($\times 10^{-4}$)	CO ($\times 10^{-5}$)
R113	1.11	3.36	0.804	1.59
R114	5.20	15.7	3.76	7.42
R123	1.71	5.17	1.24	2.44
R141b	1.50	4.52	1.08	2.13
R245fa	3.43	10.4	2.48	4.89
R600a	1.81	5.47	1.31	2.58

Corresponding to the turbine output power obtained (*Table 5*) and the environmental emission inventory in *Table 6*, the GHG emissions pattern is shown in *Fig. 2* for throughout the 20-year life cycle. Based on the power output from the system, and the GWP of the refrigerants, the emissions profile vary accordingly. Carbon dioxide is the predominant

GHG followed by sulphur dioxide and nitrogen oxide. The refrigerant R114 possess the highest environmental impact, as well as R600a. R113 possessed the least environmental impact when used as the working fluid. However, the highest power output from the system results from the utilization of R600a, but with very high environmental impact.



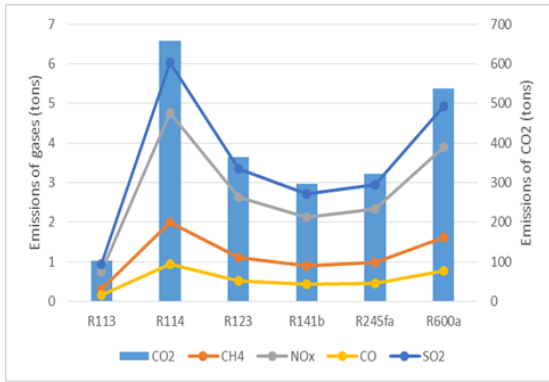


Fig. 2: Lifetime emissions of power-cooling cycle for different refrigerants at turbine inlet of 450 K and 18 bar

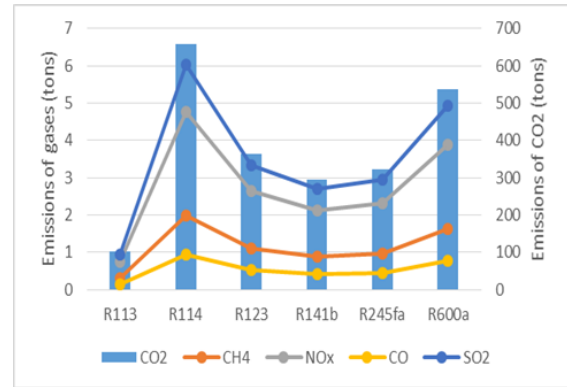


Fig. 3: Lifetime emissions of power-cooling system for different refrigerants at optimized turbine inlet temperatures

Across all the refrigerants, the results show that CO₂ is the gas that is produced/evolved the most, with it being evolved at least 108.8 times more than the next gas (SO₂). Following down the line is NO_x, before CH₄ (methane) and lastly CO (carbon monoxide). Most amount of emissions is produced by the refrigerants in the order: R114, R600a, R245fa, R123, R141b and R113. These results hold true when all refrigerants operate at the same

turbine inlet temperature (TIT) and turbine inlet pressure of 450 K and 18 bar respectively. Furthermore, at the same pressure of 18 bar, the TIT is altered to suit each refrigerant based on their thermodynamic properties, and the resulting output power in Table 5 and the emissions from each refrigerant in Fig. 3. The emissions pattern in Fig. 3 has a direct bearing with same operating conditions in Fig. 2.

Table 5: Turbine Output Power for each refrigerant at optimized turbine inlet temperatures

Refrigerant	Turbine Inlet Temperature (K)	Turbine output power (kW)	Turbine output power (kWh)
R113	450	65.95	0.018319444
R114	423	90.39	0.025108333
R123	473	151.9	0.042194444
R141b	473	141	0.039166667
R245fa	393	66.98	0.018605556
R600a	423	212	0.058888889

With the adjustment to the TIT, R245fa produced 56.8% less emissions. Conversely, R123 and R141b produced 25.5% and 30.8% more emissions respectively; the two highest increases.

4.3 Comparative evaluation of the system's thermodynamic performance and emissions generated with different refrigerants

For a better expression of the effects of each gas emitted, it is necessary to effectively express the emissions of the various gases as one Considering the lifetime of the power-cooling cycle, the emissions produced by the system for

common parameter referred to as the CO₂ equivalent of the gases. The CO₂ equivalent for each gas represents the number of units of CO₂ gas that would be equal to one unit of the evolved gas. It is obtained by multiplying the amount of gas evolved by the global warming potential (GWP) of that gas. Because the CO₂ equivalent is measured in units of CO₂ gas, the GWP of CO₂ is 1. The GWP is only expressed for gases that are considered as greenhouse gases. For this reason, SO₂ is excluded from this conversion since it is not a greenhouse gas.

each refrigerant based on the output power produced by the turbine is presented in Fig. 4.



The power-cooling cycle will pose less environmental impact when R113 is used as the

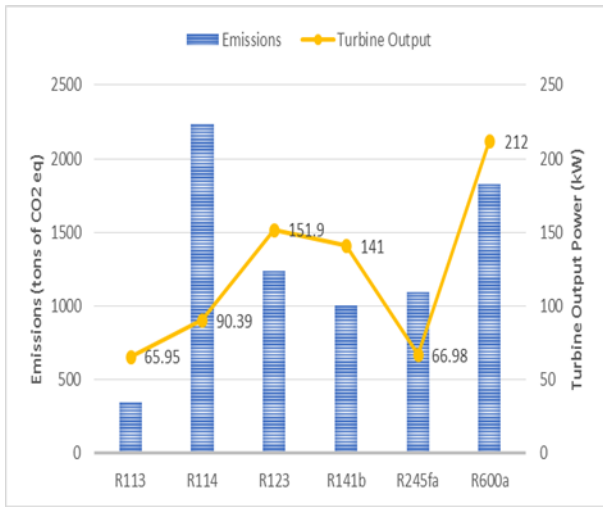


Fig. 4: Lifetime CO₂-eq emissions of power-cooling cycle by output power

4.4 Sensitivity analysis of the operating parameters on the performance of the system Sensitivity analysis was performed on the power-cooling cycle system to evaluate variables that considerably influence the system’s performance.

i. Effect of turbine inlet temperature on emissions (CO₂ eq) produced

To carry out a test on the effect of variations in turbine inlet temperature on the emissions produced, the turbine inlet pressure for the power-cooling cycle was kept constant at 18 bar. The results of the variation of turbine inlet temperature (TIT) on the emissions produced is shown in Fig. 5.

Across the board, the emissions produced increases with an increase in the turbine inlet temperature. Within the range that was worked with (i.e., 400 K to 475 K), the highest amount of emissions produced by each refrigerant was obtained at 475 K but the trend signifies that the increase in emissions will indefinitely get higher as long as the temperature is increased; perhaps until it the refrigerant no longer becomes useable in the power-cooling cycle at a particular temperature (which was not attained in this particular sensitivity analysis).

working fluid but with a 27 % reduction in estimated net turbine output compared to R114.

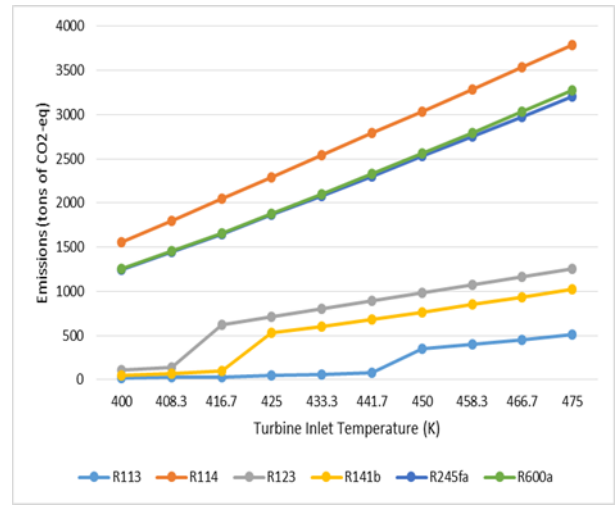


Fig. 5: Effect of turbine inlet temperature on emissions produced

In the graph for some refrigerants, we see “spikes” in the amount of emissions produced by the system. These spikes occur due to a change of state of the refrigerant from a subcooled liquid to a superheated gas. As the refrigerants change their state, they get more energy to drive the turbine in order to produce a greater output power from the turbine. The amount of power produced by the turbine is directly proportional to the emissions evolved, thus, this increase.

The result of this analysis infers that along an isobaric line (considering a refrigerant in its superheated gas phase), the output from the turbine, and thus the emissions produced by the system, would be the lowest possible at the temperature where the working fluid is just superheated.

ii. Effect of turbine inlet pressure on turbine output power (kW) and emissions produced (CO₂ eq)

To obtain the effect that a change in turbine inlet pressure would have on the emissions produced from the power-cooling cycle, the turbine inlet temperature of the system is kept constant at 450 K while the pressure is varied between 13 bar and 23 bar.



We immediately note that pressure variation at constant temperature does not cause as great a change in emissions produced as like temperature variation at constant pressure. The trend across all refrigerants is not uniform at every point, but it can be deciphered that the effect of pressure increases at constant temperature on the amount of power, and thus the emissions, produced is subject to the law of diminishing effect as the power produced increases at a diminishing rate with equal increases in turbine inlet pressure. In some cases, (i.e., for R113, R114, R123, and R141b) the power produced is seen to flat-line, or begin decreasing, within the pressure range that the sensitivity analysis was conducted.

For R113, we see the diminishing effect occur early on after 15.22 bar before a drastic drop in output power, but this significant drop happens as a result of a change in state of R113 from a superheated gas to a subcooled liquid.

5.0 Conclusion

The GHG emissions potential of an adapted power-cooling cycle was analyzed using for R113, R114, R123, R141b, R245fa, and R600a. The focus was on the operation phase of the plant which is known to contribute more to GHG emissions than the manufacturing and decommissioning phases in the system's life cycle. The following major conclusions are made:

- With similar turbine inlet operating pressure and temperature of 18 bar and 450 K, respectively, the refrigerants decreasing emissions profile were the order: R114, R600a, R245fa, R123, R141b and R113.
- Carbon dioxide had the higher emission potential in the system for all considered refrigerants, about 108.8 times than SO₂, NO_x, and CH₄.
- The power-cooling cycle will pose less environmental impact when R113 is used as the working fluid but with a 27 % reduction in estimated net turbine output compared to R114.
- The emissions produced increases with an increase in the turbine inlet temperature.

References

- Abam, F. I., Okon, B. B., B Ekwe, E., Isaac, J., O Effiom, S., C Ndukwu, M., Inah, O. I., A Ubi, P., Oyedepo, S., & S Ohunakin, O. (2022). Thermoeconomic and exergoenvironmental sustainability of a power-cooling organic Rankine cycle with ejector system. *E-Prime - Advances in Electrical Engineering, Electronics and Energy*, 2, 100064. <https://doi.org/10.1016/J.PRIME.2022.100064>
- Ayub, M., A. Mitsos, and H. Ghasemi, Thermo-economic analysis of a hybrid solar-binary geothermal power plant. *Energy*, 2015. 87: p. 326-335 DOI: <http://dx.doi.org/10.1016/j.energy.2015.04.106>.
- Bian, Q. (2020). Waste heat: the dominating root cause of current global warming. *Environmental Systems Research* 2020 9:1, 9(1), 1–11. <https://doi.org/10.1186/S40068-020-00169-2>
- Bronicki, L. (2017). History of Organic Rankine Cycle systems. In *Organic Rankine Cycle (ORC) Power Systems: Technologies and Applications* (pp. 25–66). <https://doi.org/10.1016/B978-0-08-100510-1.00002-8>
- Cao, L., Wang, J., Wang, H., Zhao, P., & Dai, Y. (2017). Thermodynamic analysis of a Kalina-based combined cooling and power cycle driven by low-grade heat source. *Applied Thermal Engineering*, 111, 8–19. <https://doi.org/https://doi.org/10.1016/j.applthermaleng.2016.09.088>.
- Guzović, Z., P. Rašković, and Z. Blatarić, The comparison of a basic and a dual-pressure ORC (Organic Rankine Cycle): Geothermal Power Plant Velika Ciglena case study. *Energy*, 2014. 76: p. 175-186 DOI: <http://dx.doi.org/10.1016/j.energy.2014.06.005>.
- Hagharast, P., Sorin, M. V, Richard, M. A., & Nesreddine, H. (2019). Analysis and design optimization of an ejector integrated into an organic Rankine cycle. *Applied Thermal Engineering*,



- 159, 113979.
<https://doi.org/https://doi.org/10.1016/j.applthermaleng.2019.113979>.
- Li, H., Yang, S., & Qian, Y. (2012). Life cycle assessment of coal-based methanol. *Computer Aided Chemical Engineering*, 31, 530–534.
<https://doi.org/10.1016/B978-0-444-59507-2.50098-6>
- Liu, C., He, C., Gao, H., Xie, H., Li, Y., Wu, S., & Xu, J. (2013). The environmental impact of organic Rankine cycle for waste heat recovery through life-cycle assessment. *Energy*, 56, 144–154.
<https://doi.org/10.1016/J.ENERGY.2013.04.045>.
- Manente, G., Lazzaretto, A., & Bonamico, E. (2017). Design guidelines for the choice between single and dual pressure layouts in organic Rankine cycle (ORC) systems. *Energy*, 123, 413–431.
<https://doi.org/https://doi.org/10.1016/j.energy.2017.01.151>
- Mohammadzadeh Bina, S., Jalilinasrabady, S., & Fujii, H. (2017). Energy, economic and environmental (3E) aspects of internal heat exchanger for ORC geothermal power plants. *Energy*, 140, 1096–1106.
[doi:10.1016/j.energy.2017.09.045](https://doi.org/10.1016/j.energy.2017.09.045).
- Mondal, S., & De, S. (2017). Ejector based organic flash combined power and refrigeration cycle (EBOFCP&RC) – A scheme for low grade waste heat recovery. *Energy*, 134, 638–648.
<https://doi.org/https://doi.org/10.1016/j.energy.2017.06.071>
- Mondejar, M. E., Andreasen, J. G., Pierobon, L., Larsen, U., Thern, M., & Haglind, F. (2018). A review of the use of organic Rankine cycle power systems for maritime applications. *Renewable and Sustainable Energy Reviews*, 91, 126–151.
<https://doi.org/10.1016/J.RSER.2018.03.074>.
- Park, J., Jung, I., Choi, W., Choi, S. O., & Han, S. W. (2019). Greenhouse gas emission offsetting by refrigerant recovery from WEEE: A case study on a WEEE recycling plant in Korea. *Resources, Conservation and Recycling*, 142, 167–176.
<https://doi.org/10.1016/J.RESCONRE.2018.12.003>
- Wang, S., Liu, C., Ren, J., Liu, L., Li, Q., & Huo, E. (2019). Carbon footprint analysis of organic Rankine cycle system using zeotropic mixtures considering leak of fluid. *Journal of Cleaner Production*, 118095.
[doi:10.1016/j.jclepro.2019.118095](https://doi.org/10.1016/j.jclepro.2019.118095).
- Yu, G., et al., Simulation and thermodynamic analysis of a bottoming Organic Rankine Cycle (ORC) of diesel engine (DE). *Energy*, 2013. 51: p. 281-290
 DOI:
<http://dx.doi.org/10.1016/j.energy.2012.10.054>.



P044 - PHYTOCHEMICAL, ANTIOXIDANT AND ANTIMICROBIAL POTENTIALS OF METHANOLIC AND HEXANE EXTRACTS OF *TERMINALIA CATAPPA*, *POLYANTHA LONGIFOLIA* AND *EUCALYPTUS CITODORA* PLANT LEAVES

Jibrin Isa*, Mohammed Jibril, Mahmud Fatima

Department of Chemistry, Faculty of Natural and Applied Sciences, Nasarawa State University, Keffi, Nigeria.

Corresponding author email: *jibrinisahyahaya@gmail.com

ABSTRACT

The leaves of *Terminalia catappa*, *Polyantha longifolia* and *Eucalyptus citodora* are indigenous to Nigerians as traditional remedies for certain illnesses such as fever, typhoid and respiratory tract infections. The methanol and hexane extracts of the plant leaves were subjected to preliminary phytochemical screening using standard methods. The phytochemicals contents were quantified using the methods described by AOAC (2006). The antioxidant and antimicrobial activity of the three plants' leaves extracts were evaluated. The results revealed that the leaves extracts were rich in secondary metabolites such as phenols, flavonoids, alkaloids, saponins, steroids and terpenoids. *T. catappa* has the highest phenolic and tannins contents of 2.224 ± 0.001 mg/g, *P. longifolia* has the highest alkaloid content (433 ± 0.671 mg/g) and also the highest flavonoid content (418 ± 4.359 mg/g). The high percentage inhibition, which is an indication of the free radical scavenging potentials of the extracts was observed in the methanolic extracts (66.988 ± 0.113 to 73.253 ± 0.045 %) which is higher when compared to hexane extracts (37.831 ± 1.989 to 54.940 ± 4.123 %). The hexane and methanolic extracts showed considerable activity against pure microbial isolates such as *S. aureus* and *E. coli*, with zones of inhibition within the range 9-12 mm.

KEYWORDS:

Phytochemical, Antioxidant, Antimicrobial, methanol, hexane.

1.0 INTRODUCTION

1.1 Medicinal Plants

Plants have been used for the treatment of diseases all over the world before the advent of modern clinical drugs and are known to contain substances that can be used for therapeutic purposes or as precursors for the synthesis of useful drugs [1]. Natural products have been the source of most of the active ingredients of medicines. This is widely accepted to be true when applied to drug discovery in 'olden times' before the advent of high-throughput screening and the post genomic era: more than 80 % of drug substances were natural products or were inspired by a natural compound [2]. From time immemorial, man depended on plants as medicine. From a historical perspective, it is evident that the fascination for plants is old as mankind itself. The plant kingdom represents a rich store house of organic compounds, many of which

have been used for medicinal purposes and efficacy in various pathological disorders [3]. Medicinal plants have been the mainstay of traditional herbal medicine among rural dwellers worldwide since antiquity to date [4].

1.1.1 Almond (*Terminalia catappa*)

Almond also known as tropical almond (*Terminalia catappa* or Durumi in Hausa), is among one of the most common trees seen throughout Nigeria and many other parts of south-eastern regions of Africa. *Terminalia catappa* is cultivated in some places for its striking features as well as its tasty nut. It is a large tropical tree belonging to Leadwood family, Combretaceae that grows mainly in the tropical region of the world. It is commonly used as a shady tree in Nigeria due to its shape with long horizontal branches and large leaves [5].

The leaves, stem/bark and roots of *Terminalia catappa* have been investigated for its medicinal



activities. These include the in vitro antimetastatic effects [6], anti-diabetic activities [7]; [8] and anti-bacterial activities [9]; [10]; [11]. The leaves of *Terminalia catappa* have been used in folk medicine for treating dermatitis and hepatitis. The extract of the leaves shows anti-oxidative, anti-inflammatory and hepata-protective properties [12].

1.1.2 *Eucalyptus citodora*

Eucalyptus citodora is an important ethnomedicinal plant belonging to the family Myrtaceae. It is used as a remedy for sore throat and other bacterial infection of the respiratory and urinary tracts. Essential oils of the leaves are used in the treatment of lung diseases while the feedstock oils are used as expectorants [13]. Topical ointments containing eucalyptus oil have also been used in traditional Aboriginal medicines to heal wounds and fungal infections. Eucalyptus oil obtained by steam distillation and rectification of the fresh leaves has Eucalyptol (1, 8-cineole) as its active ingredient and this is responsible for its various pharmacological actions [14].

1.1.3 *Polyantha longifolia* (Masquerade Tree)

Polyantha longifolia, the false Ashoka, also commonly known by its synonym *Polyalthia longifolia*, is an Asian small tree species in the family Annonaceae. It is native to southern India and Sri Lanka, but has been widely introduced elsewhere in tropical Asia. This evergreen tree is known to grow over 20 metre in height and is commonly planted due to its effectiveness in alleviating noise pollution. It exhibits symmetrical pyramidal growth with willowy weeping pendulous branches and long narrow lanceolate leaves with undulate margins [15]; [16]

1.1.4 Phytochemicals

Phytochemicals are bioactive nutrient chemicals in fruits, vegetables, grains, and other plant foods that may provide desirable health benefits beyond basic nutrition to lower the risk of major chronic diseases [17]. Phytochemicals are simply plant-derived chemicals. The word “phyto” comes from the Greek word plant. It is used to describe the secondary metabolites produced by plants. These metabolites are usually synthesized as a measure for self-defense against insects, pests, pathogens and herbivores. Phytochemicals differ from the essential nutrients (primary metabolites) such as the carbohydrates, proteins, fats, minerals, and vitamins that are needed for day-to-day

maintenance of the plants. Sometimes, phytochemicals are used to refer to functional foods with antioxidant properties, nutraceuticals, phytonutrients, anti-nutrients, phytotoxins, and so forth [18].

1.1.5 Antioxidants

Antioxidants are substances that can prevent or slow damage to cells caused by free radicals which are unstable molecules that the body produces as a reaction to environmental and other pressures. They are sometimes called “free-radical scavengers.” The sources of antioxidants can be natural or artificial. Antioxidants are molecules that fight free radicals in your body. Free radicals are compounds that can cause harm if their levels become too high in your body [19]. They are linked to multiple illnesses, including diabetes, heart disease, and cancer.

The body has its own antioxidant defences to keep free radicals in check. However, antioxidants are also found in food, especially in fruits, vegetables, and other plant-based, whole foods. Several vitamins, such as vitamins E and C, are effective antioxidants. Antioxidant preservatives also play a crucial role in food production by increasing shelf life [20]. Free radicals are constantly being formed in your body.

Without antioxidants, free radicals would cause serious harm very quickly, eventually resulting in death. However, free radicals also serve important functions that are essential for health. For example, the immune cells use free radicals to fight infections. As a result, the human body needs to maintain a certain balance of free radicals and antioxidants [21].

1.1.6 Antimicrobials

An antimicrobial is an agent that kills microorganisms or inhibits their growth. Antimicrobial medicines can be grouped according to the microorganisms they act primarily against. For example, antibiotics are used against bacteria and antifungal are used against fungi. They can also be classified according to their function. Agents that kill microbes are called microbial, while those that merely inhibit their growth are called biostatic. In recent years, there has been a growing interest in researching and developing new antimicrobial agents from various sources to combat microbial resistance [22].



1.1.7 Aim and objectives of the study

The aim of this study is to investigate the phytochemical, antioxidant and antimicrobial potentials of methanol and hexane extracts of *Terminalia catappa* (almond) leaves, *Polyantha longifolia* (Masquerade Tree) leaves and *Eucalyptus citodora* leaves.

The objectives of this study include:

- i. To obtain methanolic and hexane extracts of Almond, Eucalyptus and Masquerade tree leaves respectively via cold extraction process.
- ii. To subject the extracts to qualitative phytochemical screening.
- iii. To subject the extracts to quantitative phytochemical screening.
- iv. To subject the extracts to antioxidant screening.
- v. To subject the extracts to antimicrobial screening.

2.0 MATERIALS AND METHODS

2.1 Materials

All the reagents used were of analytical grade and were used without further purification. The reagents were purchased from Petsin Laboratory Keffi, Nasarawa state. The glass wares were washed thoroughly with detergent using tap water, rinsed with distilled water and dried in an oven at 80 °C for two (2) hours, then cooled in a desiccator prior to use. Analytical balance of model; AS 120.R1 PLUS, was used. Water bath of model HH-4-CHINA WATER, SOPTOP, single beam UV-Visible spectrophotometer of model 720C-, Zenithlab incubator of model (IB-9025A) and high pressure electric autoclave of model Yx280A were all used in the analysis.

2.2 Methods

2.2.1 Sample identification

The fresh leaves samples were collected from Nasarawa State University Keffi, some portion of each of the samples were neatly placed in a sample bag, labelled as A, B, and C. The labelled samples were sent to the Plant Identification and Taxonomy Laboratory, Ahmadu Bello University, Zaria, for identification, by taxonomist Mr. Namadi Sunusi. ABU0591, ABU01193 and ABU08421 were the

voucher numbers for *Terminalia catappa*, *Eucalyptus citodora* and *Polyantha longifolia* respectively.

2.2.2 Sample collection and preparation

The leaves samples were washed under a running tap water thrice for five (5) minutes. The samples were placed into a sieve to allow the water drain out, then spread over a clean table and allowed to dry at room temperature for two (2) weeks.

2.2.3 Sample extraction

The dried leaves were pulverized and sieved, then the powdered samples were stored in a polyethylene bag. About 400g (each) of the samples was weighed and subjected to maceration with methanol and n-hexane as extraction solvents respectively. The extracts were filtered and allowed to evaporate to dryness. Each extract was transferred into a sterile bottle and kept in the refrigerator at a temperature of 4°C.

2.2.4 Qualitative Phytochemical Screening

Qualitative phytochemical screening was carried out on methanol and hexane extracts of leaves of *Terminalia catappa* (Almond), *Eucalyptus citodora* and *Polyantha longifolia* (Masquerade tree) as described by [23] and [24].

2.2.4.1 Test for flavonoids

Sodium Hydroxide test: 2 g of sample extract was boiled with distilled water and then filtered using Whatman No. 1 filter paper. 2cm³ of the filtrate was dissolved in 20cm³ of 10 % aqueous Sodium Hydroxide to give a yellow coloration. A change in color from yellow to colorless on addition of dilute Hydrochloric acid indicated the presence of Flavonoids [24].

2.2.4.2 Test for saponins

About 0.5 g of the sample extracts was added to 10cm³ of distilled water in a test tube. The test tube was corked and shaken vigorously. Production of frothing which persisted on heating indicated the presence of saponins [24].

2.2.4.3 Test for steroids

Lieberman Burchard test: about 2cm³ of acetic anhydride was added to 2 cm³ of sample extract, followed by careful addition of 2cm³ concentrated sulfuric acid (H₂SO₄). A color change from violet to blue on standing, and then to bluish-green indicated the presence of steroids [25].



2.2.4.4 Test for tannins

One (1) g of extracts was boiled in 20cm³ of distilled water in a test tube and then filtered. A few drops of 0.1 % Ferric Chloride was added, a blue-black coloration was observed, which confirmed the presence of Tannins [26].

2.2.4.5 Test for alkaloids

One (1) cm³ of the plant extract was dissolved in 5cm³ of 1 % aqueous Hydrochloric acid on a steam bath and filtered while hot. Distilled water was added to the residue and further filtered. The filtrate was divided into three equal portions. The first portion was treated with few drops of Mayer's reagent (Potassium mercuric iodide solution), the second portion was treated with Wagner's reagent (solution of iodine in potassium iodide) and the last portion was treated with Dragendroff's reagent (Potassium bismuth solution). The formation of a cream color precipitate with Mayer's reagent, reddish-brown precipitate with Wagner's reagent and Dragendroff's reagent gave an orange-brown precipitate indicated a positive test for alkaloids [26].

2.2.4.6 Test for glycosides

About 5cm³ of sample extract was treated with 2cm³ of glacial acetic acid containing one drop of ferric chloride solution. This was underplayed with 1 cm³ of concentrate sulfuric acid. A brown ring at the interface indicates a deoxysugar. A violet-green ring appearing below the brown ring indicated a positive presence of glycosides [25].

2.2.4.7 Test for anthraquinones

Borntrager's test: 5cm³ of extract was mixed with 10cm³ of benzene and filtered. 5cm³ of 10 % ammonia solution was added to the filtrate and shaken. The presence of pink, red or violet color in the ammoniac (lower) phases indicated the presence of anthraquinones [25].

2.2.4.8 Test for terpenoids

Salkowski's test: 5cm³ of extract was mixed with 2cm³ of chloroform, and 3 cm³ concentrated sulfuric acid was carefully added to form a layer. A reddish-brown coloration of the interface was formed indicating the presence of terpenoids [25].

2.2.5 Quantitative Phytochemical Screening

Quantitative phytochemical screening was carried out on methanol and n-hexane extracts of leaves of *Terminalia catappa* (Almond), *Eucalyptus citodora* and *Polyantha longifolia* (Masquerade tree) using

standard procedures to quantify the phytochemical constituents as described by [27] and [28].

2.2.5.1 Test for alkaloids

Five (5) g of the plant sample were prepared in a beaker and 200cm³ of 10% acetic acid in ethanol was added to the plant sample. The mixture was covered and allowed to stand for 4 hours. The mixture was filtered and the extract was allowed to become concentrated in a water bath till it reaches a quarter (1/4) of the original volume. Concentrated ammonium hydroxide was added until the precipitation was complete. The whole solution was allowed to settle and the precipitate was collected and washed with dilute ammonium hydroxide and then filtered. The residue is alkaloid, which was then dried and weighed [28].

2.2.5.2 Test for tannins

The quantity of tannins was determined by using the spectrophotometer method. 0.5g of plant sample was weighed into a 50cm³ plastic bottle. 50cm³ of distilled was added and stirred for 1 hour. The sample was filtered into a 50 cm³ volumetric flask and made up to mark. 5cm³ of the filtered sample was then pipette out into test tube and mixed with 2cm³ of 0.1 M ferric chloride in 0.1M hydrochloric acid and 0.008 M potassium ferrocyanide. The absorbance of the sample was measured with a spectrophotometer at 395 nm wavelength within 10 minutes [28].

2.2.5.3 Test for saponins

The plant samples were ground and 20g of each plant sample was put into a conical flask and 100 cm³ of 20% ethyl alcohol was added to the plant sample. The sample was heated over a hot water bath for 4 hours with continuous stirring at about 55 °C. The mixture was then filtered and the residue re-extracted with another 200 cm³ of 20% ethyl alcohol. The combined extracts was reduced to 40 cm³ over a water bath at about 90 °C. The concentrated extract was then transferred into a 250 cm³ separating funnel and 20 cm³ of diethyl ether was added to the extract and vigorously shaken. The aqueous layer was recovered while the diethyl ether layer was discarded and the purification process was repeated. 60 cm³ of n-butyl alcohol was added and the combined extracts was washed twice with 10 cm³ of 5% sodium chloride. The remaining



solution was then heated to evaporation in a water bath; the samples were dried in the oven to a constant weight, the resulting weight is the saponins content in the sample [28].

2.2.5.4 Test for flavonoids

Ten (10) g of plant sample is repeatedly extracted with 100 cm³ of 80% aqueous methanol at room temperature. The whole solution was then filtered through filter paper and the filtrate was evaporated to dryness in a water bath. The sample was then weighed until a constant weight [28].

2.2.5.5 Test for steroids

One (1) cm³ of Methanolic extract of steroid solution was transferred into 10 cm³ volumetric flasks. 2 cm³ of 4N sulfuric acid and iron (III) chloride (0.5% w/v, 2cm³), were added, followed by potassium hexacyanoferrate (III) solution (0.5%w/v, 0.5 cm³). The mixture was heated in a water-bath maintained at 70±20 °C for 30 minutes with occasional shaking and diluted to the mark with distilled water. The absorbance was measured at 780 nm against the reagent blank [28].

2.2.5.6 Test for terpenoids

About 2 g of the plant powder was weighed and soaked in 50cm³ of 95 % ethanol for 24 hours. The extract was filtered and extracted with petroleum ether (60 °C) then concentrated to dryness. The dried extract was treated as total terpenoids [28].

2.2.5.7 Test for anthraquinones

Borntrager's reaction was used to detect anthraquinone aglycones in the extract. About 2 cm³ of 2 M hydrochloric acid was added to 8 cm³ of the sample, and the mixture was heated on a hot water bath for 15 minutes, then cooled and filtered. The filtrate was then extracted with chloroform. The chloroform layer was separated and shaken with 10% potassium hydroxide solution. The total anthraquinone content was analyzed by UV spectrophotometer at an absorbance of 515 nm [28].

2.2.5.8 Test for cardiac glycosides

Cardiac glycoside content in the sample was evaluated using Buljet's reagent as described by [29]. 1 g of ground sample was soaked in 10 cm³ of 70 % methanol for 2 hours, and then filtered. The extract obtained was purified using lead acetate and sodium dihydrogen phosphate solution before the

addition of freshly prepared Buljet's reagent (containing 95 cm³ aqueous picric acid and 10 % sodium hydroxide). The difference between the intensity of colors of the experimental and blank (distilled water and Buljet's reagent) samples gives the absorbance and is proportional to the concentration of the glycosides.

2.2.6 Antioxidant Analysis

The free-radical scavenging activity of the plant extracts were evaluated by accessing its discoloration of 2,2-diphenyl-1-picrylhydrazyl radical (DPPH) in methanol by a slightly modified method of [20]. The following concentrations of the extract were tested (0.1, 0.3 0.5, 0.7, 0.9, 1.0 mg/cm³). The decrease in absorbance was monitored at 517 nm. Vitamin C was used as a standard at concentrations (0.1, 0.3, 0.5, 0.7, 0.9, 1.0 mg/cm³). For a concentration of 0.1 cm³, 0.2 cm³ of the extract was placed in a test-tube and 1.8 cm³ of ethanol was added followed by an addition of 0.5 cm³ of 1mM of DPPH in methanol. The same was repeated for the other concentrations using the dilution formula $C_1V_1 = C_2V_2$. Where C_1 the concentration of the stock (plant extract) = 1 mg/cm³ and V_2 the volume of the dilute solution = 2 cm³ in all cases. A blank solution was prepared containing 2 cm³ of methanol and 0.5 cm³ of DPPH. Optical absorbance of the sample and blank solutions were determined using the UV- Visible spectrophotometer at a wavelength of 517 nm [20].

2.2.7 Antimicrobial Activity

The antimicrobial activity was studied by determining the zones of inhibitions using the Agar well diffusion method for the methanolic and hexane extracts of the plant samples. The molten Mueller Hinton agar was inoculated with 100 µL of inoculum (1×10^8 cfu/ml) and poured into the petri plate. A well was prepared in the plate with the help of a cork borer (0.85 cm). 100 µL of the test compound at varying concentrations were introduced into the well. The plates were incubated overnight at 37°C. Microbial growth was determined by measuring the diameter of zones of inhibition. The experiment was done three times and the mean value were presented [30].

The antifungal activity of the plants extracts was determined using standard methods as described by [30].

2.3 Statistical Analysis



The triplicate data values of percentage inhibition for antioxidants in methanolic and hexane extracts, were analysed using Statistical Packages for Social Sciences (SPSS) software, Window version 22 according to CLSI. Each experimental value was expressed in terms of mean \pm SD (mean and

standard deviation). Significance in the difference between the two groups was tested by Student t-test, assessed by comparing the corresponding P-value of the test. The P-value $<$ 0.05 was considered significant for the study.

a. RESULTS AND DISCUSSION

Table 1: Qualitative phytochemical screening

Phytochemical	TM	TH	PM	PH	EM	EH
Phenols	+++	++	+++	+	+++	+
Alkaloids	+	+	+	+	+	+
Steroids	+	+	++	-	+++	+
Tannins	++	+	+	-	+++	+
Saponins	+	+	+	+	++	++
Flavonoids	-	+	+	+	-	+
Terpenoids	+	+	+	+	+	+

Legend:

+ = present, - = absent, **TM** = methanolic extracts of *Terminalia catappa*, **TH** = hexane extracts of *Polyantha longifolia*, **PM** = methanolic extracts of *Eucalyptus citodora*, **PH** = hexane extract of *Polyantha longifolia*, **EM** = methanolic extract of *Eucalyptus citodora*, **EH** = hexane extract of *Eucalyptus citodora*

Table 2: Quantitative phytochemical screening

Parameters	<i>T. catappa</i> (mg/g)	<i>P. longifolia</i> (mg/g)	<i>E. citodora</i> (mg/g)
Phenol	2.2240.001	1.3480.022	1.4580.002
Alkaloids	2000.776	4330.671	269.50.781
Saponins	15.650.880	6.500.173	15.050.017
Flavonoids	1190.866	4184.359	391.50.849
Tannins	2.2240.001	1.3480.022	1.4580.002
Steroids	0.0010.000	0.0420.000	0.0010.000
Terpenoids	52.20.624	77.20.767	45.20.823

Each value is a mean of three determinations \pm standard deviation

a. Discussion

The results obtained from the phytochemical screening, antioxidant and antimicrobial activity of methanolic and hexane extracts of *T.catappa*, *P.*

longifolia and *E. citodora* leaves are presented in table 1 to 4. Table 1 shows the qualitative phytochemical screening for methanolic and hexane extracts of *T. catappa*,



Table 3: Antioxidant activity of methanolic and hexane extracts

Plant Extract	Conc (mg/cm ³)	% Inhibition (methanolic)	% Inhibition (hexane)
<i>T. catappa</i>	0.10	72.449±2.158	37.831±1.989
<i>T. catappa</i>	0.30	69.317±1.249	43.775±1.230
<i>T. catappa</i>	0.50	70.442±1.307	44.337±2.608
<i>T. catappa</i>	0.70	67.912±3.385	52.530±0.000
<i>T. catappa</i>	0.90	68.353±2.499	52.048±0.590
<i>P. longifolia</i>	0.10	73.253±0.454	43.855±2.351
<i>P. longifolia</i>	0.30	70.000±2.329	45.863±8.953
<i>P. longifolia</i>	0.50	69.600±0.398	51.647±4.942
<i>P. longifolia</i>	0.70	67.350±1.705	53.333±2.715
<i>P. longifolia</i>	0.90	66.988±0.113	54.940±4.123
<i>E. citodora</i>	0.10	72.691±1.136	41.044±0.910
<i>E. citodora</i>	0.30	72.129±0.718	43.052±2.783
<i>E. citodora</i>	0.50	71.486±0.000	44.498±0.839
<i>E. citodora</i>	0.70	71.567±1.590	49.639±2.095
<i>E. citodora</i>	0.90	69.880±0.455	52.450±0.046

Table 4: Antibacterial and Antifungal Activity of the Methanolic Extracts

Test organism	Plant extracts	Zone of inhibition (mm)			Control (mg/cm ³)	Zone of inhibition (mm)			Control (mg/cm ³)
		Conc. (mg/cm ³)				Conc. (mg/cm ³)			
		(methanolic)				(hexane)			
		200	100	50		200	100	50	
<i>E. coli</i>	<i>P. longifolia</i>	18	11	9	23	21	15	11	23
<i>Salmonella spp.</i>	<i>P. longifolia</i>	14	10	9	26	13	10	6	26
<i>S. aureus</i>	<i>P. longifolia</i>	16	11	8	22	15	12	10	19
<i>E. coli</i>	<i>E. citodora</i>	17	15	11	26	19	15	12	23



<i>Salmonella spp.</i>	<i>E. citodora</i>	11	10	9.5	26	19	15	13	26
<i>S. aureus</i>	<i>E. citodora</i>	15	12	11	23	21	19	16	20
<i>E. coli</i>	<i>T. catappa</i>	25	23	19	23	18	13	10	23
<i>Salmonella spp.</i>	<i>T. catappa</i>	22	15	14	26	20	15	14	26
<i>S. aureus</i>	<i>T. catappa</i>	22	20	20	24	20	10	12	24
<i>A. niger</i>	<i>P. longifolia</i>	-	-	4.5	7	4	3.5	9.5	11
<i>A. niger</i>	<i>E. citodora</i>	-	2	-	10	-	6	3	9
<i>A. niger</i>	<i>T. catappa</i>	8	3	2	12	-	6	-	5

Key: Reference drug = Gentamycin as control for bacteria and Ketoconazole as control for fungus

P. longifolia and *E. citodora*. The methanolic extract of *T. catappa* contained a wide range of secondary metabolites such as tannins, flavonoids, phenols, saponins, alkaloids, steroids and terpenoids. The hexane extract of *T. catappa* also showed very similar presence of secondary metabolites, in smaller amounts compared to the methanolic extracts. Although flavonoid was absent in the methanolic extract of *T. catappa*, it was present in the hexane extract in low concentrations. Methanolic and hexane extracts of *P. longifolia* showed considerable presence of secondary metabolites too, with the methanolic extract containing phenols, tannins and steroids in moderate to high concentrations and the hexane extract showing moderate to low concentrations of these phytochemicals. Though, terpenoids were absent in the methanolic extracts, but was present in the hexane extract. The methanolic and hexane extracts of *E. citodora* gave moderate to high concentrations of the presence of phytochemicals with the presence of tannins, phenols, saponins, steroids and terpenoids being more abundant in the methanolic extracts than in the hexane extract.

The presence of these phytochemicals in the extracts could be explained by the fact that during their growth, plant synthesize aromatic compound or secondary metabolites that are involved in many physiological processes of the plant such as cell growth, seed germination, fruit ripening, and defense against external aggression. The absence of some phytochemicals in the hexane extracts may be as a result of the non-polar nature of hexane and its inability to effectively extract polar phytochemical compounds [31].

Table 2 shows the results for the quantitative phytochemical screening of *T. catappa*, *P. longifolia* and *E. citodora*, and they were seen to contain moderate amounts of phenols and tannins, with *T. catappa* containing 2.224 ± 0.001 , *P.*

longifolia containing 1.348 ± 0.002 and *E. citodora* containing 1.458 ± 0.002 mg/g respectively. The alkaloid content for the three plants was high within the range of 200 ± 0.76 to 433 ± 0.671 mg/g. Saponin content for the sample was within 6.5 ± 0.173 to 15.650 ± 0.880 mg/g. The steroid content was 0.001 ± 0.000 for *T. catappa* and *E. citodora* and 0.042 ± 0.000 for *P. longifolia* respectively. *T. catappa* has high content of flavonoids of about 119 ± 0.866 mg/g, *E. citodora* has a higher value of 391.500 ± 0.017 mg/g and *P. longifolia* has the highest flavonoid content with value of 418 ± 4.359 mg/g. The terpenoids content of the plant are within the range of 45.200 ± 0.823 to 77.200 ± 0.767 mg/g which is in agreement with that of [32].

Table 3 shows result for antioxidant activity for the methanolic and hexane extracts of *T. catappa*, *P. longifolia* and *E. citodora*, with percentage inhibition ranging from 66.988 to 73.253 for the methanolic extracts, and 37.831 to 52.450 for the hexane extracts. A student t-test with P-value < 0.05 implies there is a significant variation in the percentage inhibition of the methanolic and hexane extracts of the plants.

Tables 4 shows the antimicrobial activities of methanolic and hexane extracts of the plants leaves against four pure isolates (*S. aureus*, *Salmonella spp.*, *E. coli* and *A. niger*). The zones of inhibition were seen to be within 9-21 mm at concentrations of 50-200 mg/cm³ against control drug (Gentamycin 500 mg) for anti-bacterial activities and 2-9 mm with ketoconazole 500 mg as antifungal control drug.

4.0 CONCLUSION

This research has revealed the efficacies of methanolic and hexane extract of the plant leaves,



T. catappa studied as potential antimicrobial agents at zones of inhibition ranges from 10 -20mm when compared to others. Results of the antifungal activity of the plants' extracts against *A. niger* fungus revealed moderate activity observed in both methanolic and hexane extracts at zones of inhibition between 2 – 8 mm. However, it can be concluded that there is sequential relationship between phytochemicals, antioxidants and antimicrobial activities as exhibited by the plants' extracts, thus observed that whatever antioxidant and antimicrobial behaviors exhibited by the extracts are as a result of the presence of certain phytochemicals (secondary metabolites). Phytochemicals that could be responsible for antioxidant activities of the extracts are phenols, terpenoids and flavonoids respectively, while those responsible for antimicrobial activity are basically steroids and saponins. These findings would add to the global natural database, and justifies the ethnobotany use of the plants leaves to cure some illnesses.

5.0 REFERENCES

1. Sofowora, A., (1982). Medicinal Plants and Traditional Medicine in Africa. 2nd ed., John Willey and Sons Limited, Ibadan, 8-14.
2. Sneader, W. (1996). Drug Prototypes and Their Exploitation. Wiley, UK.
3. Hammer, K. A., Carson, C. F., and Riley, T. V. (1999). Antimicrobial Activity of Essential Oils and Other Plants.
4. Sarker, S. D., Nahar, L. and Kumarasamy, Y. (2007). Assessment of Phytochemical, Antioxidants and Antimicrobial Activities of Some Medicinal Plants of Kaski District of Nepal. *American Journal of Plant Sciences*. 11(9).
5. Mohammed, A. S. I. and Kaitu, A. H. (2007). Phytochemical screening of the leaves Of *Lohpira lanceolata* (Ochanaceae). *Life Science Journal*, 4 (4): 76-79.
6. Chen, C. S., Fa, Y. S., Jung, L.S., Hsien, K.W., Zin, C.Y. and Shou, H.Y. (2007). In vitro and in vivo anti-metastatic effects of *Terminalia catappa* L. *Food and Chemical Toxicology*, 45(7): 1194 – 1201.
7. Rao, N.K. and Nammi, S. (2006). Antidiabetic and Renoprotective Effects of the Chloroform Extract of *Terminalia chebularetz*, Seeds in Streptozotocin Induced Diabetic Rats. *MBC: CAM*, 6; 17-17.
8. Nagappa, A. N., Thakurdesa, P. A., Venkat, R. N. and Singh, J. (2003). Antidiabetic activity of *Terminalia catappa* Linn Fruits. *Journal of Ethnopharmacology*. 88: 45-50.
9. Elizabeth, K.M. (2005). Antimicrobial Activity of *Terminalia Bellerica*. *Indian Journal of Clinical Biochemistry*, 20 (2): 150-153
10. Rajarajan, S., Asthana, M. and Shanthi, G. (2010). The in vitro Bactericidal Activity of Lyophilized Ethanolic Extract of Indian Almond (*Terminalia catappa* Linn) Fruit Pulp on Two Pathogenic Bacteria From Sub gingival Plaques. *Indian Journal of Natural Products and Resources*, 1(14): 466-469.
11. Kinoshita, S., Inoue, Y., Nakama, S., Ichiba, T., and Aniya, Y. (2007). Antioxidant and Hepatoprotective Actions of Medicinal Herb, *Terminalia catappa*L. from Okinawa Island and its Tannin corilagin. *Phytomedicine*, 4(11): 755-765.
12. Neeru, V and Sharma, S. K. (2008). Biologically Active Compounds from The Genus *Hibiscus*. *Journal of Pharmaceutical Biology* 46(3), Pp 145-153.
13. Adeniyi, B.A., Lawal, T.O. and Olaleye, S.B.(2006).Antimicrobial and Gastroprotective activities of *Eucalyptus camaldulensis*(Myrtaceae) crude extracts. *Journal of Biochemical Sciences*, 6(6): 1141-1145.
14. Trivedi, N.A and Hotchandani, S.C. (2004). A study of the Antimicrobial Activity of the Oil of Eucalyptus. *Indian Journal of Pharmacology*, 36: 93-94.
15. Plants of the World Online (POWO): *Polyantha longifolia* (retrieved 30 August 2020) (<http://www.plantsoftheworldonline.org/taxon/urn:lsid:ipni.org:names:77123022-1>)
16. Dkhil, M. A., Al-Quraishy, S., Al-Shaebi, E. M., Abdel-Gaber, R., Thagfan, F., Abdullah, Q. and Mahmood, A.A. (2021). "Medicinal plants as a fight against murine blood-stage malaria". *Saudi Journal*



- of Biological Sciences. *Saudi Biological Society (Elsevier)*.28(3): 1723–1738.
17. Liu, R. H. (2004) Potential Synergy of Phytochemicals in Cancer Prevention: Mechanism of Action. *Journal of Nutrition*, 134, 3479S-33485S.
 18. Fatoba P.O., Omojasola, P.F., Awe, S. and Ahmed, F. G. (2003). “Phytochemical screening of some selected tropical African Mosses”. *Nigerian Society for Experimental Biology (NISEB) Journal* 3(2): 49–52.
 19. Escott-Stump, S. and Lippincott, W. (2008). Nutrition and Diagnosis-related care. Philadelphia. *American Journal of Clinical Nutrition*. (6), 112-116.
 20. Brand-Williams, W., M. E. Cuvelier, and C. Berset. (1995). “Use of Free Radical Method to Evaluate Antioxidant Activity,” *Lebensmittel Wissenschaft and Technologies*, vol. 28, Pp. 25–30.
 21. Okegbile, G., and Taiwo, Y. (1999). Official Methods of analysis in Association of Official Analytical Chemists, 15th. ed., Washington D.C.
 22. Rios, J. L. and Recio, M.C. (2005). Medicinal plants and antimicrobial activity. *Journal of Ethno-pharmacology*, 100, Pp: 80-84
 23. Fausat, K. O., Arogundade, A., Moshood, I. A., and Efere, M. O. (2018). Comparative Evaluation of Antioxidant Properties of Methanol Extracts of *Allium cepa* Bulb, *Allium cepa* Bulb Peels and *Allium fistulosum*, *Kragujevac Journal of Science*.40(2018) 131-141.
 24. Ajiboye, B., Emmanuel, I., Genevieve, E., and Oluwafemi, A. O. (2013). Qualitative and Quantitative Analysis Phytochemicals in *Senecio biafrae* Leaves. *International Journal of innovative Pharmaceutical Science*, 1(5)2013;428-432
 25. Sofowora, A. (1982). *Medicinal Plants and Traditional Medicine in Africa*. 2nd edition, John Willey and Sons Limited., Ibadan, 8-14.
 26. Trease, G. E., and Evans, W. C. (1989). *Pharmacognosy* 13th edition, English Language Book Society, Bailliere Tindall, Britian, 376-480.
 27. Odebiyi, A. and Sofowora, A. E. (1990). Phytochemical Screening of Nigerian Medicinal Plants. Part III. *Lloydia*, 41, 234-246.
 28. Harborne, J.B. (1998). *Phytochemical Methods - A Guide to Modern Techniques of Plant Analysis*. Chapman and Hall, London. Pp. 182-190.
 29. El-Olemy, M. M., Farid, J. A. and Abdel-Fattah, A. A. (1994). Ethanol Extract of *P. stratiotes*; *NISEB Journal* 1(1) 51-59.
 30. Jigna, P. and Chandra, S. (2007) In vitro Antimicrobial Activity and Phytochemical Analysis of Some Indian Medicinal Plants, *Turkish Journal of Biology* 31(1)9
 31. Mahama, A., Saidou, C., Kamga, T. F. R., Nodem, S. F. S., Mohammadou, B. A. and Ali, A. (2019). Phytochemical Screening, DPPH Scavenging and Antimicrobial Activities of Leaves of *Eucalyptus camaldulensis*, *Cassia mimosoides* and *Verpis heterophylla* from Northern Cameroon.
 32. Soetan, K.O. (2008). “Pharmacological and Other Beneficial Effects of Anti Nutritional Factors in Plants – A review”. *African Journal of Biotechnology*. 7(25):4713–4721.
 33. Lopez, L. M., Grimes, D. A., Shulz, K. F. and Curtis, K. M. (2006). *Cochrane Database of systematic Reviews* 2: 7.



P045 - ZEOLITE (ZSM-5) DOPED HYDROXYAPATITE BIO-COMPOSITES DERIVED FROM CATFISH SKELETONS FOR BONE REPAIRS; SYNTHESIS AND BIOMECHANICAL CHARACTERIZATION

E. S. Akpan^{a,c*}, M. Dauda^a, L. S. Kuburi^a, D. O. Obada^{a,b}, E. G. Emmanuel^d A.Y Atta^e

^aDepartment of Mechanical Engineering, Ahmadu Bello University, Zaria, Nigeria

^bAfrica Center of Excellence on New Pedagogies in Engineering Education, Ahmadu Bello University, Zaria

^cNational Research Institute for Chemical Technology, Basawa, Zaria, Nigeria

^dVeterinary Teaching Hospital, Ahmadu Bello University, Zaria, Nigeria

^eDepartment of Chemical Engineering, Ahmadu Bello University, Zaria, Nigeria

Corresponding author: onefryo@gmail.com

ABSTRACT

Catfish bones-derived hydroxyapatite (HAp) and varying weights of 3, 5, & 7 (wt.%) of zeolite (ZSM-5) respectively were synthesized by means of sol-gel route with the zeolite serving as reinforcing material. The bio-composite scaffolds were consolidated by a compaction protocol and solid-state sintering. Afterward, FT-IR analyses showed functional groups of the pure and reinforced variants, while the mechanical properties of the bio-composites were elucidated through micro-hardness, wear rate and compressive strength measurements. Also, the bioactivity profiles of the scaffolds *in-vitro* analyses in a simulated body fluid (SBF) and phosphate buffered saline solution (PBS) were both conducted for a period of 7 & 14 days respectively. The FT-IR analyses showed that HAp and reinforced variants exhibited phosphate and hydroxyl peaks with characteristic lower bands for the reinforced variants. Some typical vibrations of ZSM-5, evident at 1094 and 963 cm^{-1} . Hardness properties reduced with increasing weight percent of ZSM-5 but were within the range of hardness values for aged human cortical bones. Wear rate under dynamic load, was seen to be far lower for pure HAp with a corresponding increase with lower zeolite content. Compressive strength results of pure HAp was >16MPa but that of the doped Z-HAp scaffolds were found to be within the range of 3.33 – 5.33 MPa. The produced scaffolds showed good bioactivity profile from Optical Microscopy examinations through the formation of apatite layer on the HAp matrix after immersion in SBF and increased with increase in zeolite content, while biodegradable showed slow bio-resorbability due to their stable matrixes. Altogether, the zeolite reinforced HAp can be considered useful for clinical trials on bone repair.

KEYWORDS:

Catfish bones, hydroxyapatite, ZSM-5, in-vitro, apatite formation, Mechanical measurements; Biodegradability

INTRODUCTION

The bones in the human body are crucial for providing structural support and serves as a source of calcium phosphate for blood cell formation. Unfortunately, the bone is liable to fracture when their biological systems decline [1]. Typically, a compatible bioactive material should be non-toxic, and stable in the living body [2,3]. In this way, the state-of-the-art is to fabricate clinically useful biomaterials for bone tissue applications [4-6]. Amongst all the bio-ceramics, hydroxyapatite (HAp), has been widely employed as implants and bone fillers because it has chemical similarities with the inorganic component of human bones and teeth and shows good compatibility with the human body [1,2,7].

Unfortunately, the mechanical integrity of natural hydroxyapatite is low [8,9] which makes it prone to mechanical failure when implanted. Therefore, it is imperative to enhance the mechanical integrity of HAp. This can be achieved by using silica-based materials like zeolite because of their suitable properties [10]. In this way, the reinforcement method needs to be carefully optimized by controlling the sintering temperature and atmosphere and introducing reinforcements into HAp matrix [11]. Fabricating HAp with some reinforcements has been conducted by chemical processes and extraction from natural sources such as bovine [12] etc. It is noteworthy that HAp gotten from natural raw materials has distinct properties with trace minerals desirable for healthy bones as compared to the synthetic type.



Therefore, this work reports the production of low-cost hydroxyapatite from catfish bones and its subsequent reinforcement with varying weight composition of zeolite (ZSM-5). The work concluded by evaluating the chemical, mechanical, and bioactivity characteristics of the catfish bones/zeolite bio-composites for bone repairs and/or restoration.

MATERIALS AND METHODS

Materials

The natural HAp was prepared from waste catfish bones. First, the bones were collected from local restaurants and washed with tap water. Next, the bones were immersed in boiling water for 4 hours and oven dried at 150 °C for 8 hours in order to rid them of fatty and surface proteins. Further treatment of the bones was conducted in open air burning to deprotenize the bones. Direct conversion to HAp was carried out in a muffle furnace at 900 °C and a holding time of 2 hours, and at a ramp rate of 5 °C/min. The calcined bone samples were ground to powder and sieved through a standard 100 µm mesh sieve to obtain a fine powder. Pure HAp scaffolds were initially obtained by cold compaction pressure of 1MPa and sintered at 900°C with a dwelling time of 2hrs.

Preparation of ZSM-5/Hydroxyapatite (Z-HAp) and their representative scaffolds

Laboratory grade normal cation form of ZSM-5 (Si/Al=80), was obtained from Zeolyst, International, U.S.A. The zeolite-reinforced hydroxyapatite was then synthesized by the sol-gel method using 3, 5, and 7 wt.% of zeolite powders according to the procedure by Iqbal et al., [13, 14]. The products (Z-HAp powders) was dried at 60 °C for 24 h, formed into scaffolds (Ø25 mm and 10 mm height) by a low compaction pressure of 1 MPa in order to conduct hardness, compressive and wear tests singly. Sintering of the scaffolds was conducted at 900 °C for 2 h.

Mechanical Properties Evaluation

Hardness testing

Micro Hardness (Hv) values of sintered samples were empirically derived using a Vickers indentation machine with a micro hardness tester as outlined in ASTM standard E384, 1999. The produced scaffolds were subjected to an applied load of 300 g for a dwelling period of 10 secs after calibration. A total of 3 indentations were made on each scaffold, and the obtained hardness values was averaged. The working mechanism of the indenter

and the accuracy of the applied load were carefully controlled to ensure that the results were reliable.

Compressive strength testing

The compressive modulus of the prepared scaffolds was carried out according to ASTM standard E9-89a, (1994) using a universal testing machine (UTM), which was fitted with a 2 kN load cell after calibration.

Wear rate measurement

The wear rate was measured according to ASTM 1994 Annual Book of ASTM Standards: Section

2-Metals Test Methods and Analytical Procedures. Vol. 03.01 - Metals-Mechanical Testing; Elevated and low temperature Test for each of the developed HAp and bio-ceramics (ZSM-5 zeolite doped HAp) scaffolds using the expression in equation 1;

$$K = \frac{\text{wear rate, } \Delta m}{\rho \times F \times S} \dots(1)$$

Where, Δm is change in mass (g)

ρ is the density of the Z-HAp scaffolds (g/cm³)

F is the applied normal force (N)

S is the total sliding distance (m)

Tests for bioactivity

5 g each of varying compositions of the Z-HAp composites were formed by uni-axial compaction at a pressure of 1MPa into circular shaped scaffolds (Ø25 mm and 5 mm height) using a UTM (Micro Vision industries). Sample compositions and the pure CB were initially sterilized in an autoclave at a pressure of 1bar for 30mins, they were then placed in an air-tight polyethylene container containing 50 mL SBF solution, and carefully positioned in an incubator using a water bath for a period of 7 days and 14 days respectively at 37°C as described by [15]. The SBF solution was replaced each day according to the protocol of [16, 17]. The retrieved samples were thoroughly rinsed with distilled water and dried at 60 °C before carrying out various characterization studies. The morphology of the composites was then revealed by an optical microscope (LEICA ICC50W).

Biodegradability assessment of bio-composites

Biodegradability studies were conducted to assess the gradual weight loss of composites in a PBS solution for 14 days by dissolving a PBS tablet in 100 mL of deionized water to obtain a pH of 7.4.



Each sample of the bio-composite, as described above was placed in 50 mL of the PBS solution and carefully kept in an incubator. Readings were taken for the pH variation and weight loss of each respective bio-composite sample before and after the incubation using a pH meter and an analytical balance (accuracy: 0.001g). The percentage of weight decrease (W_d) was calculated using the equation 2.

$$W_d = \frac{W_a - W_b}{W_a} \times 100\% \text{ ----- (2)}$$

Where, W_a and W_b are the respective weights of samples before and after soaking in the biological fluid

Chemical Characterization of the bio-powders using FTIR

Fourier transform infrared spectrophotometer (FTIR), Shimadzu, FTIR-8400s, with a spectra range of 4000– 400 cm^{-1} was used to analyze the functional groups of the powder samples.

DISCUSSION OF RESULTS

Functional group identification and Structural Patterns of ZSM-5, HAp and Doped HAp

Fourier transform infrared spectrophotometer (FT-IR), Shimadzu, FT-IR-8400s, with a spectra range of 4000– 400 cm^{-1} was used to analyse the functional groups of the powder samples. The FT-IR spectra of pure ZSM-5, ZSM-5 doped HAp and pure HAp is shown in Figure 1. The bands near 542, 790 and 1080 cm^{-1} are typical of ZSM-5 and represents double ring vibration, and internal and external asymmetric stretch, respectively which is due to the formation of ZSM-5 phase only [18]. The FT-IR of the ZSM-5-HAp samples (3, 5 and 7 wt.%) showed that the band at 3573 cm^{-1} is ascribed to the stretching of the vibration band of OH^- in HAp. The typical asymmetric stretching of PO_4^{3-} was noticeable at 1047 cm^{-1} and 1092 cm^{-1} . It was also observed that with 3wt.% ZSM-5, there was a negligible change in the FT-IR spectrum of the HAp structure. Nonetheless, with an increase in ZSM-5 content from 5 to 7%, the intensity of the hydroxyl mode decreased at 630 cm^{-1} and a broadening of the stretching vibration of OH^- was noticed. Some typical vibrations of ZSM-5, evident at 1094 and 963 cm^{-1} and ascribed to Si-O stretch and Si-O symmetric stretch were not noticed as a result of some overlapping of the phosphate bands [19]. Table 1 gives the characteristic properties of ZSM-5, ZSM-5 doped HAp (3, 5 and 7 wt.%) and pure HAp.

Table 1: Characteristic properties of ZSM-5, ZSM-5 doped HAp (3, 5 and 7 wt.%) and pure HAp.

Material	Grain Size (nm)	Ca/P ratio	Lattice Parameters
3Z-HAp	25.53	1.95	a = b= 9.4166 A, c = 6.8745 A Card No.: 96-900-1234
5Z-HAp	22.19	1.74	
7Z-HAp	19.21	1.79	
HAp-CB2	41.05	1.79	
ZSM-5	9.5		a = 20.58 A, b= 19.600 A, c = 13.74 A Card No.: 96-155-2089



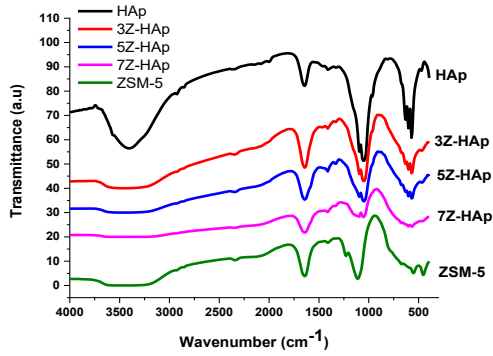


Fig. 1: FT-IR Spectra of powders

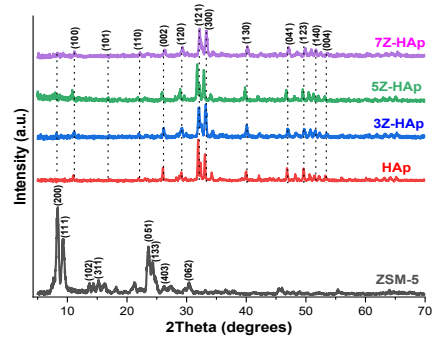


Fig. 2: XRD Patterns of powders

The XRD patterns of the as-received ZSM-5, and zeolite/HAp samples at the optimum processing parameters are seen in Figure 2. Diffraction peaks of ZSM-5, HAp and Z-HAp were found to be in accordance with the structure of the crystalline materials. The similarity of the XRD signatures of HAp and the corresponding doped samples showed that the sol-gel method was efficient in synthesizing the biomaterials. Broadening of the 3Z-HAp reflections corresponded to its relative improved hardness. Hydroxyapatite was still a predominant phase for all the doped materials, and the reflections were matched with hydroxyapatite card number of 96-900-1234.

Mechanical Measurements of derived pure HAp and Doped Z-HAps

The mechanical measurement results for the pure HAp and its corresponding zeolite doped scaffolds is shown in Figure 3. Hardness was seen to decrease with increased zeolite content which could be attributed to the reduced chemical interaction

between the zeolite and the HAp matrix. It is noteworthy that the hardness values of 0.65, 0.62 and 0.50 GPa for 3, 5 and 7 wt.% ZSM-5 doped samples, respectively, are lower than the micro-hardness values (0.69 GPa) obtained for the pure optimal HAp (CB2), however the micro-hardness results still fall within the range of the hardness of cortical bones, (0.3-0.6 GPa) of humans aged between 46-99 years [19]. Compressive strength results of the doped Z-HAp scaffolds were found to be within the range of 3.33 MPa – 5.33 MPa. These values fall within the mid-range values for compressive strength of trabecular bones which are in the range 2.00 – 5.00 MPa [20]. However, that of CB2 proved the highest (>16MPa) thereby surpassing the ultimate compressive strength of the trabecular bone in the mandibular bone region which ranges from 0.22 to 10.44 MPa [20].

Pure hydroxyapatite scaffolds have been seen to have a wear rate of between $8 \times 10^{-6} \text{ mm}^3/\text{Nm}$ [21] while coefficient of friction (COF) is said to be in a range of 0.7 & 0.8 [22, 23]. The wear rate results for the pure HAp and zeolite doped HAp scaffolds are as seen also in Figure 3. Wear rate under dynamic load, was seen to be far lower for the pure HAp with a corresponding increase in lower zeolite content.



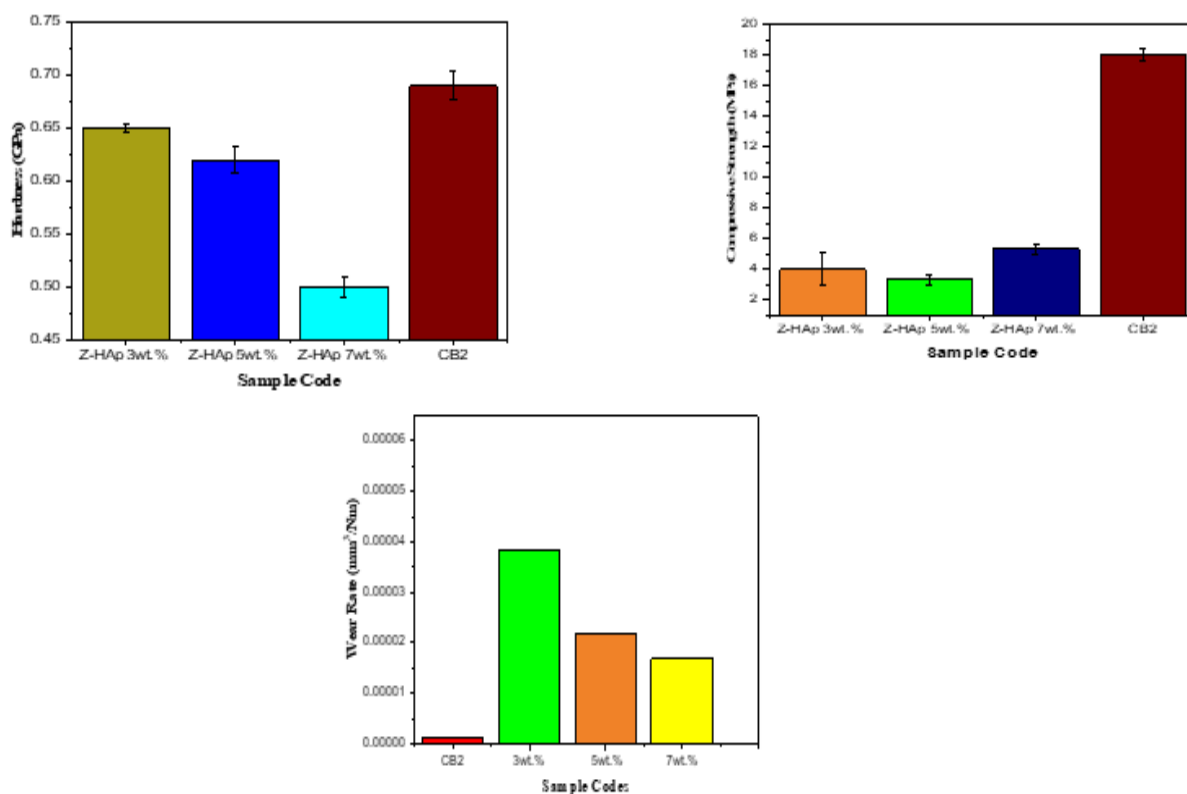


Fig.3: Mechanical Measurements of CB2 HAp and Doped Z-HAp scaffolds

The morphology of the samples (zeolite reinforced composite scaffolds) before and post immersion in the simulated SBF for 7 days is presented in Figure 3. From the optical microscope- derived images, it is evident that the sample surfaces were covered by an apatite layer owing to the change in contrast observed before and post immersion. The extent of the formation of apatite layers is evident with continuous change in contrast, post immersion, with increasing ZSM content from 3 to 7 wt.%. These results are significant as it shows that bioactivity of the developed scaffolds is affected by the ZSM content. This increasing bioactivity vis-à-vis the ZSM-5 content can be ascribed to presence of the silanol group (Si–OH) on the surface of HAp [24]. The mechanism involves the exchange of calcium ions (Ca^{2+}) from the surface of the scaffolds and protons from the simulated body fluid with a consequent formation of silanol groups. The calcium ions combine with the silanol group as it disintegrates into negatively charged species to produce amorphous calcium silicate. This calcium silicate gradually takes up the positive ions an interaction with the phosphate ions is triggered in the SBF to eventually produce an amorphous

calcium phosphate layer which is regarded as the apatite layer crystalline in nature.

pH and Biodegradability Weight Loss Profile

Figure 4 shows both graphs of pH variations and biodegradability of HAp and varying wt.% Z-HAp scaffolds over a period of 14 days. pH initially increased for all the samples with CB2 showing the highest trend and afterwards reduced to almost at constant values. This is an indication of slow solubility or bio-resorbability of the developed HAp. The recorded high alkalinity of the SBF solution for CB2 during immersion could be attributed to the release of more PO_4^{3-} ions more than that of Ca^{2+} ions. Biodegradability graph confirmed that the biodegradability weight loss profile agrees with the pH variation graph. CB2 HAp was seen to have the least decrease in weight owing to a more stable bond within its matrix system. This



phenomenon is desirable in bone treatments or implants [25].

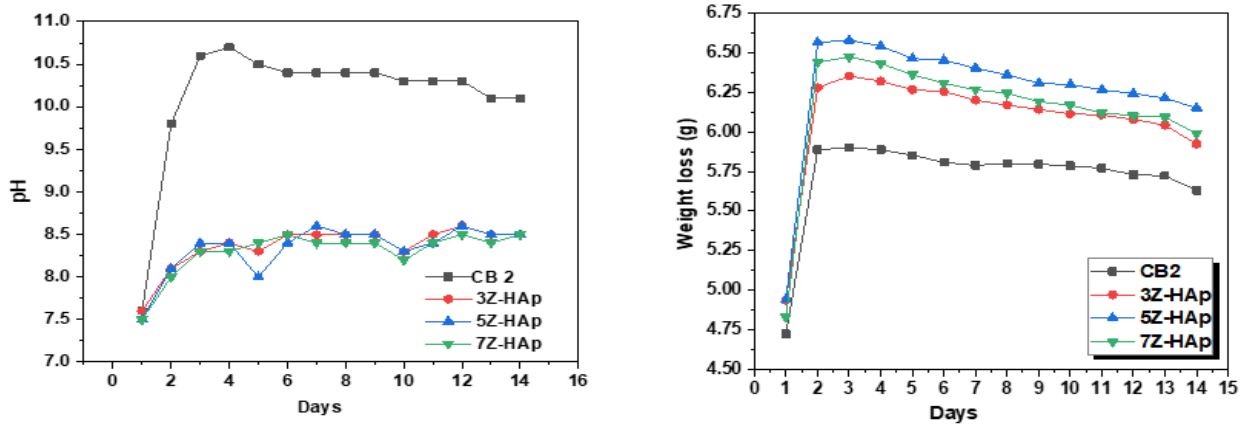


Fig. 4: *In vitro* Biodegradability profile of CB2 HAp and Doped Z-HAp

***In vitro* Experiment for HAp and Doped Z-HAp in Simulated Body Fluid (SBF)**

Naturally, *in vitro* bioactivity vis-à-vis the zeolite doped HAp is enhanced by the formation of silanol group (Si-OH) on the surface of the HAp [26]. The mechanism usually involves an exchange of calcium ions (Ca^{2+}) from the surface of the scaffolds and protons from the simulated body fluid which leads to a consequential formation of silanol groups. Invariably, the calcium ions then combine with the silanol group as it steadily disintegrates into

negatively charged species to produce amorphous calcium silicate. This calcium silicate then takes up the positive ions gradually. Consequently, an interaction with phosphate ions is triggered in the SBF that eventually produces an amorphous calcium phosphate layer which is regarded as the apatite layer and are crystalline in nature. Optical and SEM images as seen in Figure 5, substantiates the increase in apatite formation in the sample matrixes following an equivalent increase in submerged period in the SBF as illustrated in the respective circled regions.

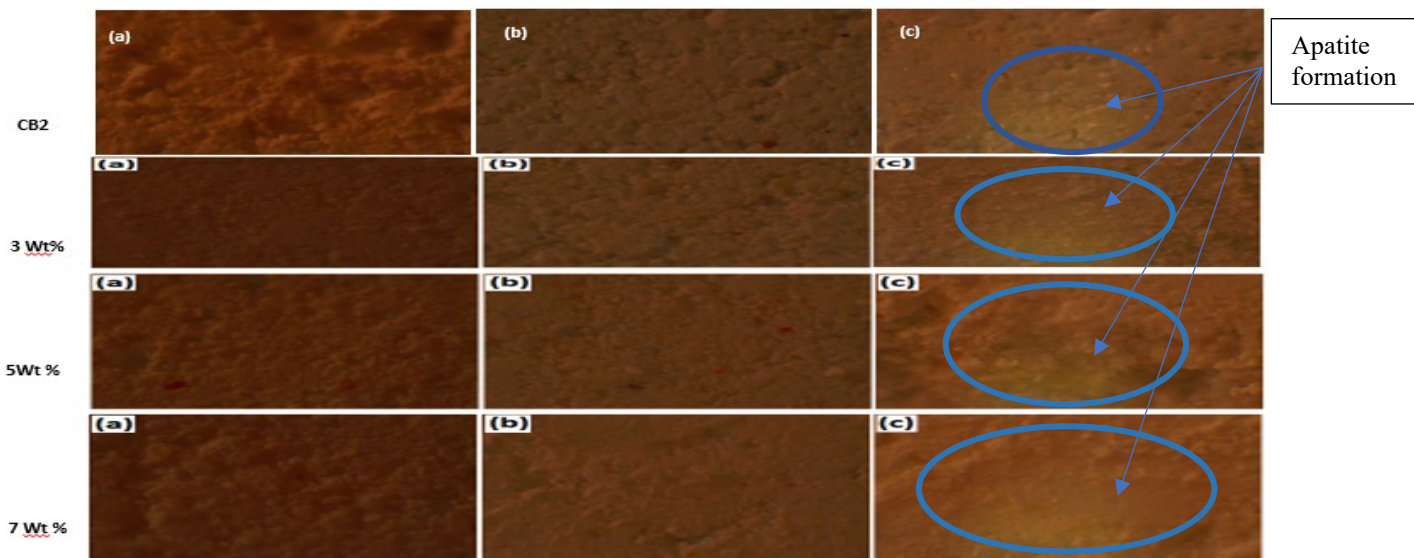


Fig. 5: Shows OM images (at 400x) of bio-composites submerged in SBF for 0, 7 & 14 days revealing apatite formation on surfaces



CONCLUSION

This study on the Zeolite doped hydroxyapatite derived from catfish skeletons for bone repairs; reveals the presence of zeolite and hydroxyapatite, through functional group identification, in the zeolite HAp composites. The mechanical measurements showed hardness values of the Zeolite reinforced HAp to be within the hardness range for cortical bones (0.3-0.6 GPa) of humans aged between 46-99 years, while compressive strength results of the doped Z-HAp scaffolds were found to be within the range of 3.33 MPa – 5.33 MPa slightly exceeding mid-range values for compressive strength of trabecular bones which are in the range 2.00 – 5.00 MPa [20].

However, pure HAp (CB2) had its value falling within (>16MPa), thus surpassing the ultimate compressive strength of the trabecular bone in the human mandibular region (0.22 to 10.44 MPa). Subsequently, wear rate under dynamic load, showed values of $3.85 \times 10^{-5} \text{ mm}^3/\text{Nm}$, $2.18 \times 10^{-5} \text{ mm}^3/\text{Nm}$, and $1.69 \times 10^{-5} \text{ mm}^3/\text{Nm}$ for 3, 5 and 7 wt.% ZSM-5 doped samples, respectively, while CB2 showed a value of $1.058 \times 10^{-6} \text{ mm}^3/\text{Nm}$ thus surpassing the value of that of pure HAp being $8 \times 10^{-6} \text{ mm}^3/\text{Nm}$ [21]. These values points to the promises that the scaffolds can be said to be clinically useful.

The biodegradability graph (figure 4) confirmed that the bio-resorbability weight loss profile strongly agrees with the pH variation graph, while the morphology of the scaffolds post immersion in simulated body fluid (SBF) verified the suitability of the bio-composites to accelerate the growth of hydroxyapatite during tissue/bone repair applications. Overall, this study suggests that HAp-ZSM-5 composite can be considered suitable for clinical trials on bone repair.

References

- [1] Best, S. M., Porter, A. E., Thian, E. S., & Huang, J. (2008). Bioceramics: past, present and for the future. *Journal of the European Ceramic Society*, 28(7), 1319-1327.
- [2] Suchanek, W., & Yoshimura, M. (1998). Processing and properties of hydroxyapatite-based biomaterials for use as hard tissue replacement implants. *Journal of Materials Research*, 13(1), 94-117.
- [3] Williams, D. F. (2008). On the mechanisms of biocompatibility. *Biomaterials*, 29(20), 2941-2953.
- [4] Katti, K. S. (2004). Biomaterials in total joint replacement. *Colloids and surfaces B: Biointerfaces*, 39(3), 133-142.
- [5] Fathi, M. H., & Zahrani, E. M. (2009). Mechanical alloying synthesis and bioactivity evaluation of nanocrystalline fluoridated hydroxyapatite. *Journal of Crystal Growth*, 311(5), 1392-1403.
- [6] Obada, D. O., Dauda, E. T., Abifarin, J. K., Dodoo-Arhin, D., & Bansod, N. D. (2019). Mechanical properties of natural hydroxyapatite using low cold compaction pressure: Effect of sintering temperature. *Materials Chemistry and Physics*, 122099.
- [7] Liu, H. S., Chin, T. S., Lai, L. S., Chiu, S. Y., Chung, K. H., Chang, C. S., & Lui, M. T. (1997). Hydroxyapatite synthesized by a simplified hydrothermal method. *Ceramics International*, 23(1), 19-25.
- [8] Hench, L. L. (1991). Bioceramics: from concept to clinic. *Journal of the American Ceramic Society*, 74(7), 1487-1510.
- [9] Aoki, H. (1991). Science and medical applications of hydroxyapatite. *JAAS*, 1991, 123-134.
- [10] Arcos, D., & Vallet-Regí, M. (2010). Sol-gel silica-based biomaterials and bone tissue regeneration. *Acta Biomaterialia*, 6(8), 2874-2888.
- [11] Adeogun, A. I., Ofudje, A. E., Idowu, M. A., & Kareem, S. O., 2018. Facile Development of Nano Size Calcium Hydroxyapatite Based Ceramic from Eggshells: Synthesis and Characterization. *Waste and biomass valorization*, 9(8), 1469-1473



- [12] Obada, D. O., Dauda, E. T., Abifarin, J. K., Bansod, N. D., & Dodoo-Arhin, D. (2020). Mechanical measurements of pure and kaolin reinforced hydroxyapatite-derived scaffolds: A comparative study. *Materials Today: Proceedings*.
- [13] Iqbal, N., Kadir, M. A., Iqbal, S., Razak, S. I. A., Rafique, M. S., Bakhsheshi-Rad, H. R., Abbas, A. A. (2016). Nano-hydroxyapatite reinforced zeolite ZSM composites: A comprehensive study on the structural and in vitro biological properties. *Ceramics International*, 42(6), 71757182.
- [14] Ozturk, S., and Yetmez M. (2016). Studies on Characterization of Bovine Hydroxyapatite/CaTiO₃ Biocomposites. *Hindawi Publishing Corporation Advances in Materials Science and Engineering* Volume 2016, Article ID 6987218, <http://dx.doi.org/10.1155/2016/6987218>
- [15] Kokubo, T., Kushitani, H., Sakka, S., Kitsugi, T., and Yamamuro, T. (1990). Solutions able to reproduce in vivo surface-structure changes in bioactive glass-ceramic A-W", *J. Biomed. Mater. Res.*, 24, 721-734 (1990).
- [16] Fan, Y., & Lu, X. (2008). A study of apatite formation on natural nano-hydroxyapatite/chitosan composite in simulated body fluid. *Mater. Sci. China* 2008, 2(1): 91–94 DOI 10.1007/s11706-008-0016-6
- [17] Engstrand, J., Unosson, E., Engqvist, H. (2012). Hydroxyapatite formation on a novel dental cementing human saliva. *International Scholarly Research Network ISRN Dentistry Volume* 2012, Article ID 624056, 7 pages doi:10.5402/2012/624056.
- [18] Khatamian M., & Irani M (2009). Preparation and characterization of nanosized ZSM-5 zeolite using kaolin and investigation of kaolin content, crystallization time and temperature changes on the size and crystallinity of products. *Journal of the Iranian Chemical Society* 6(1): 187-194 DOI: 10.1007/BF03246519
- [19] Saika, B., and Parthasarathy, G. (2010). Fourier transform infrared spectroscopic characterization of kaolinite from Assam and Meeghalaya, Northeastern India. *Journal of Modern Physics* 1(4), 206-210. Doi:10.4236/jmp.2010.14031
- [20] Mirzaali, M. J., Schwiedrzik, J.J., Thaiwichai, S., Best, J.P., Michler, J., Zysset, P.K., et al., (2016). Mechanical properties of cortical bone and their relationships with age, gender, composition and microindentation properties in the elderly. *Bone* 2016; 93:196–211.
- [21] Athanasiou, K. A., Zhu, C. F., Lanctot, D. R., Agrawal, C. M., & Wang, X. (2000). Fundamentals of biomechanics in tissue engineering of bone. *Tissue Engineering Volume 6, Number 4, 2000 Mary Ann Liebert, Inc.*
- [22] Misch, C. E., Qu, Z., & Bidez, M. W. (1999). Mechanical properties of trabecular bone in the human mandible: implications for dental implant treatment planning and surgical placement. *Journal of oral and maxillofacial surgery*, 57(6), 700-706.
- [23] Mishra, A., Khobragade, N., Sikdar, K., Chakraborty, S., Kumar, S. B., Roy, D. (2017). Study of mechanical and tribological properties of nanomica dispersed hydroxyapatite-based composites for biomedical applications. *Hindawi Advances in Materials Science and Engineering* Vol. 2017, Article ID 9814624 <https://doi.org/10.1155/2017/9814624>.
- [24] Fu, Y., Batchelor, A. W., Wang, Y., and Khor, K. A. (1998). Fretting wear behaviours of



thermal sprayed hydroxyapatite (HA) coating under unlubricated conditions. *Wear*, vol. 217,

no. 1, pp. 132–139, 1998

[25] Rajkumar, M., Meenakshi S. N., Rajendran, V. (2011). Preparation of size controlled, Stoichiometric and bioresorbable hydroxyapatite nanorod by varying initial pH, Ca/P ratio

and sintering temperature. *Digest Journal of Nanomaterials and Biostructures* Vol. 6, No 1,

January-March 2011, p. 169 – 179

[26] Sánchez-Robles, M. J., Gamero-Melo, P., & Cortés-Hernández, D. A. (2013). In vitro hydroxyapatite formation on the Ca doped surface of ZSM-5 [Ga] type zeolite. *Ceramics International*, 39(7), 7387-7390



P046 - ADSORPTIVE APTITUDES OF TWO (2) NIGERIAN CLAYS FOR AQUEOUS CU, PB AND ZN METALS

E. S. Akpan^{1*}, A. S. Akuso¹, O. O. Fasanya¹, O. U. Ahmed², J. O. Otsai¹, V. Ochigbo¹, O. M. Lawal¹, M. L. Batari¹, A. R. Isa¹, K. Muazu¹, J. T. Barminas¹, L. Z. Clement¹, B. M. Musa³

¹National Research Institute for Chemical Technology (NARICT), Zaria, Kaduna State, Nigeria

²Chemical Engineering Department, Bayero University, Kano, Kano State, Nigeria

³Chemical Engineering Department, Ahmadu Bello University, Zaria, Kaduna State, Nigeria

*Corresponding Author onefryo@gmail.com

ABSTRACT

This work reports the synthesis of environmentally friendly water filtration membranes being Bauchi clay from Bauchi State, and Ant-Hill clays from NARICT environment singly, for the treatment of heavy metals in polluted water. The raw clays were initially characterized to determine their respective chemical compositions via EDXRF, and were then sintered at 500°C for 2 hours at a ramp rate of 5 °C/min after initial sieving and cold compaction. Other constituents used included deionized water and heavy metal precursors such as lead (II) nitrate (Pb(NO₃)₂), copper (II) sulphate pentahydrate (CuSO₄.5H₂O), and zinc acetate di-hydrate ((CH₃COO)₂.Zn.2H₂O). The micro filtration performances of the membranes were assessed using 50ml of simulated polluted water containing heavy metals. The filtrates were analysed for the concentration of heavy metals remaining in the solution after micro filtration using AAS machine. Results obtained showed that membranes synthesized from Bauchi clay was more effective in the removal of heavy metal ions than the Ant-Hill clay given their initial concentrations of 100ppm before dilution. Bauchi clay membrane exhibited percentage removal of 97.63%, 99.45% and 73.08% for Cu²⁺, Pb²⁺ and Zn²⁺ respectively. However, both Bauchi clay and Ant-hill clay as base materials for developing ceramic membranes were very promising.

KEYWORDS:

Bauchi clay, Ant-Hill clay, Membrane, Heavy metals, Adsorption, Concentrations

INTRODUCTION

Industrial wastewater often contains reasonable concentration of heavy metals. The concentration of these heavy metals is largely dependent on the processes from which these effluents are generated. Untreated wastewater is toxic and poses an environmental challenge. This has led to the imposition of regulations by numerous environmental protection agencies to govern the quality of effluent discharge. Consequently, the development of efficient effluent treatment systems has become a matter of great importance.

Membrane separation technologies have been considered as an effective means of separation of many dissolved chemicals inclusive of heavy metals and suspended solids from the waste streams. Efforts have been focused on the development of functional materials to achieve low-cost processing of industrial separation schemes. Most membranes are mainly fabricated using

ceramics or polymers. Polymeric membranes are widely used for wastewater, desalination and gas separation applications. They are much cheaper than inorganic ceramic membranes but are characterized by ease of fouling and poor long-time stability(1, 2).

Despite being more expensive, inorganic membranes, which consist of ceramics and carbon-based membranes are still in high demand. They possess good thermal, mechanical and chemical strength as well as reusability and high tubing propensity, making them more suitable for industrial processes(3-5). Ceramic membranes are produced from either alumina, silica, titania and/or zirconia. These membranes are however expensive because of the high cost of materials and high sintering temperatures; ranging from 1300-1500 °C (2). The use of natural clays for membrane development is a viable alternative especially in developing nations (4, 5). Studies have been carried out on the use of clays for removal of dyes and other



organic pollutants (6) as well as heavy metals such as Cd, Pb, Mn and Zn amongst others(7, 8).

Clays from different locations tend to have differing properties which range from metal content, morphology, colour, porosity and texture amongst others (9). This tends to affect the behaviour of clay when utilized in one form or the other. Clays infested by ants are a popular occurrence in Africa and Australia. Ants tend to form mounds out of clays often referred to as anthills. These have been used as catalyst support in transesterification reactions, lining for furnaces(10) and removal of dyes and some heavy metals from wastewater (11, 12). Anthills, depending on location have high silica and alumina content with intrinsic pore structure (11).

Based on the potential benefits of membranes produced from low-cost materials, clay from two local sources were explored and an investigation of their effectiveness in heavy metals polluted water treatment.

For the purpose of this work, locally available clay materials from Bauchi State and Ant-Hill clay from within the premises of National Research Institute for Chemical Technology (NARICT), Zaria, Kaduna State, Nigeria were used.

MATERIALS AND METHODS

Raw Materials Sourcing

Analytical grades of lead (II) nitrate ($\text{Pb}(\text{NO}_3)_2$), copper (II) sulphate pentahydrate ($\text{CuSO}_4 \cdot 5\text{H}_2\text{O}$), and zinc acetate ($(\text{CH}_3\text{COO})_2 \cdot \text{Zn} \cdot 2\text{H}_2\text{O}$) were used

without further purification in preparation of solutions. The clay materials were obtained from Darazo Local Government Area (10.9965°N , 10.4088°E) in Bauchi State, Nigeria whilst the Ant-Hill clay was obtained in Sabon Gari local government (11.1167°N , 7.7333°E) of Kaduna State, both in Northern Nigeria.

Characterization of Raw Materials

Pristine samples from Anthill clay (AHC) and Bauchi clay (BC) were collected, and carefully dried in an oven at 105°C for 1 hour. They were pulverized manually using laboratory ceramic mortar and pestle, and then sieved with $100 \mu\text{m}$ mesh to obtain fine uniform powders. Each sample was then characterized using EDXRF Analyzer for metals to determine their elemental and oxide properties. Next, Fourier Transform infrared (FT-IR) spectroscopy analyses was employed to show the functional groups present in the clay materials.

Elaboration of Membranes

Typically, 50 g each of the clay samples were each thoroughly mixed with 5 wt.% of cold-water starch as pore formers. Deionized water (4 ml) was then added to each mixture as a binder, before being compacted with a compaction pressure of 13.79 MPa using a hydraulic press. This led to the formation of circular scaffolds with diameter of 50mm and 10 mm height. This process was replicated to acquire a total of 5 scaffolds from each clay source as shown in Figures 1 and 2 respectively. The produced membranes were air-dried at room temperature for 48 h. Then further dried in an oven at temperature of 250°C for 4 h to decompose the starch used in pore formation. The membranes were further sintered in a muffle furnace at a temperature of 500°C at a ramp rate of $5^\circ \text{C}/\text{min}$ and held for two hours. The sintered membranes were allowed to cool for 24 h before being removed from the furnace.





Figure 1: Bauchi clay membrane



Figure 2: NARICT Ant Hill membrane

Simulation of Heavy Metals Solutions

Solutions of zinc acetate, lead (II) nitrate and copper (II) sulphate pentahydrate were prepared by dissolving 1.6730g, 0.7992g and 1.9645g respectively of each salt in 1000 ml of deionized water to obtain 500 ppm concentration of the ions respectively. From this stock solution, 100, 200, 300 and 400 ppm solutions of each metal ion were prepared.

Application of Membranes Produced from Bauchi and NARICT Ant-Hill Clay Samples

To evaluate the efficiency of the fabricated membranes, filtration experiments were conducted with each of the clay membranes. Pristine clay membranes were used to filter 50 ml of each of the prepared solutions. The filtrates were then collected and analysed using atomic absorption spectrum (AAS).

RESULTS & DISCUSSION

Elemental analysis of Bauchi and Ant-Hill clays

The chemical composition of each clay sample was determined using X-ray Fluorescence (XRF) and is

presented in Table 1. The predominant elemental components of both clay material sources were observed to be SiO_2 , Al_2O_3 , Fe_2O_3 and MgO while the other portions of the clay were a mix of diverse alkali earth metals. AHC contained 10% more silica than BC, while BC contained more alumina and iron oxide than AHC. Both clays had approximately the same amount of MgO within their matrix.

The high concentration of silica in both clay samples suggests that they may have high tendency to be chemically inert. This means that removal of metal ion from solution may be strictly by physio-adsorption.

The FTIR spectra shown in Figure 3 for both sets of clay shows bands corresponding to Al-Al-OH, bending vibrations are observed at 913 cm^{-1} . The very strong band at 1000 cm^{-1} showed vibration of Si-O which is typically observed in kaolinite minerals. Stretching vibrations of the tetrahedral layer (13). Peaks in the region of 1637 cm^{-1} and 1982 cm^{-1} are as a result of -OH buckling vibration trapped with the crystal lattice of the samples(14).

Table 1: Chemical composition of clay samples

S/N	Component	Weight, wt.%	
		Bauchi Clay	Ant-Hill Clay
1	SiO_2	41.866	50.546



2	Al ₂ O ₃	20.866	15.704
3	Fe ₂ O ₃	10.866	4.5951
4	MgO	3.940	3.75
5	TiO ₂	1.6591	0.7405
6	K ₂ O	1.233	2.1733
7	SrO	0.609	0.1682
8	ZrO ₂	0.4216	0.4313
9	CaO	0.3297	0.2274
10	P ₂ O ₅	0.2359	0.3157
11	SO ₃	0.1782	0.1589
12	Cl	0.141	0.1056
13	MnO	0.0885	0.03432
14	Others	0.0810	0.30942

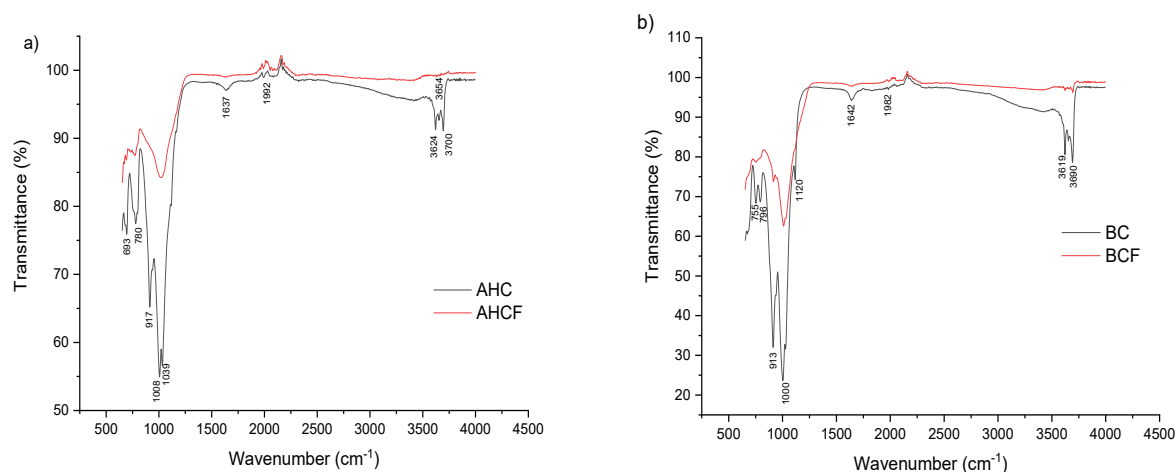


Fig 3: FTIR spectra of raw clay samples and fired clay membrane for a) Ant hill clay and b) Bauchi clay

In both fired clays, the peak between 900-1000 cm⁻¹ can be attributed to the presence of Si-O-Al which is important in adsorption of metal ions. Likewise in the fired clays, intensities of peaks observed at 3620 cm⁻¹, 3653 cm⁻¹ and 3696 cm⁻¹ which are attributed to stretching and bending vibrations of OH group are reduced suggesting partial metakaolin formation (15). The hydroxyl and Si-O sites are important sites for adsorption (16). However, the intensities of these peaks appeared more pronounced in the Fired Bauchi clay than the anthill clay.

Performance Tests

The performance of each membrane produced was appraised in duplicate by comparing the concentrations of lead, copper and zinc before and after filtration. The absorbance of the metals in solution after filtration were obtained via AAS of

which the results were utilized in determining the concentrations of each metal from the calibration plots as prepared from the standard solutions.

The performances of the membranes were determined by colour and concentrations of the metals in solution at atmospheric pressure after micro filtration. Generally, Bauchi clay membrane was seen to be more efficient than Ant-Hill clay membrane from the experiment at 100 ppm concentrations as depicted in Figure 4, were percentage removal of Cu²⁺, Pb²⁺ and Zn²⁺ were seen to be 97.63%, 99.45% and 73.08% respectively as against initial diluted samples. These results therefore implied that Bauchi clay presents a more promising material source for the production of ceramic membranes for heavy metals removal and by extension pollution control. The presence of iron in clay has been associated with



increase in adsorptive properties (17). This is as a result of ease of formation of iron complexes with adsorbed ions. However, it is clearly noted that this may not be the only reason for the improved

performance of the Bauchi clay. Future studies will endeavour to include particle and pore analysis of the clay.

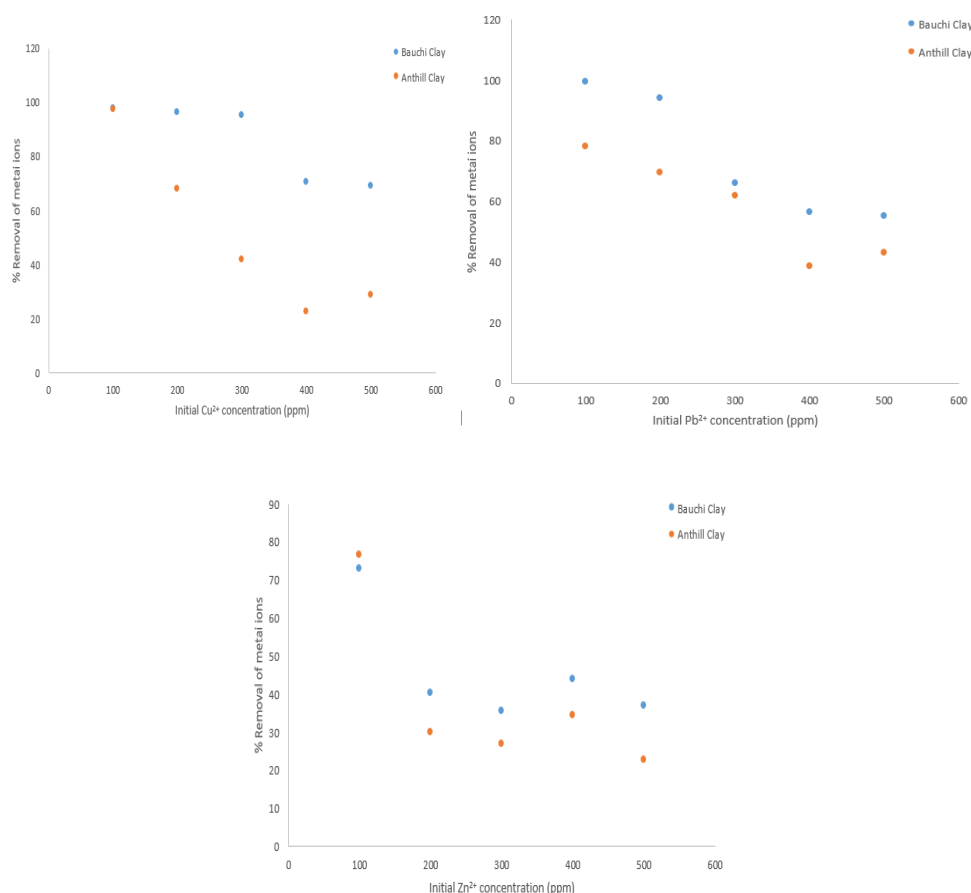


Fig 4: AAS absorptive characteristics of Ant hill clay and Bauchi clay of the metals in solution after filtration

CONCLUSION

The clay membranes from Bauchi and Ant-Hill from NARICT were successfully synthesized for the adsorption of metal ions simulated as wastewater effluent is eco-friendly. From the EDXRF result, it shows that the clay materials have high propensities of chemical inertness and thermal stability thus making them versatile in applications of wastewater treatments. The simulated wastewater was prepared by dissolving 1.6730g, 0.7992g, and 1.9645g of the salt containing the heavy metals (copper, lead and zinc). The results obtained from the analysis of AAS after micro filtration revealed that membranes synthesized from both Bauchi clay and Ant-hill clay can be said to be effective overall for the removal of heavy metal ions in polluted or produced water as shown in Figure 4 above, by significantly reducing their percentage concentrations respectively. Therefore, this work offers new insights into the exploitation of local clays as an environmentally friendly and

cheap source of raw materials for the syntheses of efficient and effective micro filtration membranes for the treatment of heavy metals polluted water.

REFERENCES

1. Z. He, Z. Lyu, Q. Gu, L. Zhang, J. Wang, Ceramic-based membranes for water and wastewater treatment. *Colloids and Surfaces A: Physicochemical and Engineering Aspects* **578**, 123513 (2019).
2. S. L. Sandhya Rani, R. V. Kumar, Insights on applications of low-cost ceramic membranes in wastewater treatment: A mini-review. *Case Studies in Chemical and Environmental Engineering* **4**, 100149 (2021).
3. M. Mouiya *et al.*, Fabrication and characterization of a ceramic membrane from clay and banana peel powder: Application to industrial wastewater



- treatment. *Materials Chemistry and Physics* **227**, 291-301 (2019).
4. M. Mohamed Bazin, N. Ahmad, Y. Nakamura, Preparation of porous ceramic membranes from Sayong ball clay. *Journal of Asian Ceramic Societies* **7**, 417-425 (2019).
 5. M. Amin, M. Subri, Preparation and Characterization of Porous Ceramic Membranes for Micro-Filtration from Clay/CuZn Using Extrusion Methods. *MATEC Web Conf.* **156**, 08015 (2018).
 6. M. A. S. A. F. Anwar Ma'ruf, Agus Mulyadi Purnawanto and Rina Asih Kusumajati, Development of Hybrid Membrane from Clay/TiO₂-PVA for Batik Wastewater Treatment. v. **18**, (2019-12-01).
 7. J. A. Alexander, M. A. A. Zaini, S. Abdulsalam, U. Aliyu El-Nafaty, U. O. Aroke, Isotherm studies of lead(II), manganese(II), and cadmium(II) adsorption by Nigerian bentonite clay in single and multimetal solutions. *Particulate Science and Technology* **37**, 403-413 (2019).
 8. K. C. Khulbe, T. Matsuura, Removal of heavy metals and pollutants by membrane adsorption techniques. *Applied Water Science* **8**, 19 (2018).
 9. G. O. Ihekweme *et al.*, Characterization of certain Nigerian clay minerals for water purification and other industrial applications. *Heliyon* **6**, e03783 (2020).
 10. E. K. Arthur, E. Gikunoo, Property analysis of thermal insulating materials made from Ghanaian anthill clay deposits. *Cogent Engineering* **7**, 1827493 (2020).
 11. A. S. Yusuff, O. A. Adesina, Characterization and adsorption behaviour of anthill for the removal of anionic dye from aqueous solution. *International Journal of Environmental Science and Technology* **16**, 3419-3428 (2019).
 12. A. S. Yusuff, I. I. Olateju, Experimental investigation of adsorption capacity of anthill in the removal of heavy metals from aqueous solution. *Environmental Quality Management* **27**, 53-59 (2018).
 13. R. Chihi, I. Blidi, M. Trabelsi-Ayadi, F. Ayari, Elaboration and characterization of a low-cost porous ceramic support from natural Tunisian bentonite clay. *Comptes Rendus Chimie* **22**, 188-197 (2019).
 14. R. Dewi, H. Agusnar, Z. Alfian, Tamrin, Characterization of technical kaolin using XRF, SEM, XRD, FTIR and its potentials as industrial raw materials. *Journal of Physics: Conference Series* **1116**, 042010 (2018).
 15. M. H. Abd Aziz, M. H. D. Othman, N. A. Hashim, M. R. Adam, A. Mustafa, Fabrication and characterization of mullite ceramic hollow fiber membrane from natural occurring ball clay. *Applied Clay Science* **177**, 51-62 (2019).
 16. T. K. Sen, D. Gomez, Adsorption of zinc (Zn²⁺) from aqueous solution on natural bentonite. *Desalination* **267**, 286-294 (2011).
 17. U. Ifeoma Mary, I. Onyedikachi Anthony, in *Advanced Sorption Process Applications*, E. Serpil, Ed. (IntechOpen, Rijeka, 2019), pp. Ch. 7.



P048 - EFFECT OF ABSTRACTION TEMPERATURE AND TIME ON THE PERCENTAGE YIELD OF OIL EXTRACTED FROM LEMON PEELS VIA HYDRO-DISTILLATION TECHNIQUE

*¹Samuel, Alkali, Akuso; ¹Kabiru, Mu'azu; ¹Etukessien, S. Akpan; ¹Joseph, O. Otsai; ¹Ganiyu, Abubakar; ¹Batari, Musa. Latayo; ²Samson, Olorunbi; Joshua; ¹Lois, Zinas Clement.

¹National Research Institute for Chemical Technology (NARICT), Zaria, Kaduna State, Nigeria

²Chemical Engineering Department, Ahmadu Bello University, Zaria, Kaduna State, Nigeria

*Corresponding Author: alkaliakuso@gmail.com

ABSTRACT

Essential oils extracted from lemon peels have extensive applications in the food industries, flavouring agents, medicines, pharmaceuticals, cosmetics and domestic household products etc. Citrus is commonly grown worldwide and generates a lot of waste peels that are disposed after processing. Utilizing and/or adapting these waste peels into value added products can be economically beneficial by boosting the national economy and thus improving on its growth domestic product (GDP). In this work, effect of extraction temperature and time on lemon peels was investigated using hydro-distillation technique to mine essential oil (EO) from lemon peels. The optimum extraction temperature and time, the weight and percent EOs yield by hydro-distillation obtained were 96°C and 60 minutes, 2.27g and 0.38% and 2.22g and 0.37%, respectively.

KEYWORDS

Lemon peels, temperature, time, hydro-distillation, essential oil, optimum, citrus fruits

INTRODUCTION

Essential oils are fatty liquids that comprises of esters and other aromatic compounds that make up the distinct scent of a plant [1,2]. Essential oils are concentrated majorly in glands scattered throughout the fruit peels and leaf of the plant [2]. Most essential oils that are extracted from citrus fruits are usually rich in the other parts of the plant. Citrus fruits have relatively high amounts of essential oils when compared to non-citrus fruits, which makes them one of the rich fruits to extract oil from.

Citrus fruits cultivation is an important economic activity in some parts of the world because of its health benefits, and thrives in all seasons particularly during spring [3]. Citrus fruits require sunlight during the ripening stage. The fruits take between 6-8 months to ripen after fertilization. Citrus fruits include grapefruit, lemon and lime, oranges, and tangerine among other fruits [3,4]. Therefore, the cultivation of citrus fruit is common and is grown particularly in countries around the Mediterranean [3]. Today, Nigeria extensively grows citrus fruits from moderate to tropical zones within the northern and southern parts of the country. Plate 1 shows image of lemon citrus fruit.



Plate 1: Lemon citrus fruit

In the processing of citrus juice, the peels are generally considered as waste which litters the environment and causes environmental pollution [5]. One of the products from citrus peels is essential oils which is an aromatic liquid characterized by the scent it produces.

Globally, citrus output was seen to have increased from 115.18 million tons to 178.48 million tons from 2010 to 2015 which amounted to 25%–40% of the total fruit weight [6]. The global production of oranges as at 2018 was 49.3 million tons [5]. Amongst world leading producer of citrus fruits, Nigeria is positioned ninth and first in Africa producing 3.33 million tons of citrus fruits [5]. In spite of Nigeria being the leading producer of citrus fruits in Africa, production of essential oils is very low, as virtually all the essential oils utilized by various industries are imported. Such importations unnecessarily increase the demand on US dollar and the devaluation of Nigerian Naira with unwanted



consequences that have been bedeviling the national economy.

The presence of the essential substance of limonene in citrus peels has drawn the attention of industries or essential oil producers to this product, which has anti-cancer and aromatherapy significances, biological, antioxidant, antimicrobial properties and herbal fragrance [7]. They also exhibit antibacterial, antifungal, and insecticidal properties [5].

The main constituent of citrus essential oil is limonene [7]. Limonene concentration in citrus essential oils varies between 30% and 99% depending on the species of the plant, 30–40% in bergamot, 40–75% in lemon and 68–98% in sweet orange [5, 7]. The range of oil yield from citrus peels is said to be between 0.5 - 5.0% (w/v) [5].

Globally the estimated world's citrus production to about 161.8 million tons in 2021 [3]. Lemon is one of the most generally used or consumed fruits globally due to its health and nutritional benefits to mankind.

Essential oils are concentrated mainly in secretory cavities scattered throughout the fruit peels, accounting for about 1–3% fresh weight on the average which are release when rubbed with hand, heated or otherwise stimulated [1, 7]. Quality and quantity of essential oils extracted from citrus peels are affected by several factors such as nature of the fruit, origin, genotype, soil condition, age, climate, plant organ, vegetative cycle, and the extraction process [5].

There are various techniques for the extraction of essential oils from citrus plants, such as cold press, steam distillation, solvent extraction, water, and hydro-distillation [5] as well as organic solvent extraction and supercritical CO₂ [7].

Essential oils extracted from citrus has different recipe of natural constituents and has substantial applications in the manufacturing of pharmaceutical and food industries, flavouring agents, medicines, pharmaceuticals, food flavour additives and natural antimicrobials [5], as well as cosmetics, and domestic household products [7]. The residue of the Lemon peels after oil extraction can be used to improve soil fertility since they are rich in nitrogen, phosphorus and potassium [7].

Therefore, the general objective of this study was to investigate the effect of extraction temperature and

time on the percentage yield of essential oil from lemon peels using hydro-distillation technique.

MATERIALS AND METHODS

Material Sourcing and Preparation

Wholly ripened fresh lemon fruits were purchased from the commercial orchard in Samaru market, Zaria, Kaduna State, Nigeria. The lemon fruits were washed to remove dirt, peeled manually, then shredded to sizeable pieces using citrus peel shredder and dried for 2 hours at 45°C in an oven and then stored at room temperature for further use. The research was carried out at the National Research Institute for Chemical Technology (NARICT), Zaria, Kaduna State, Nigeria.

Extraction of Essential Oil

Hydro-distillation is a modification of steam distillation technology, for the extraction of essential oil from lemon peels. The method of hydro-distillation of essential oil extraction employed by [6] was adopted for this work. Therefore, the primary advantage of adopting hydro-distillation is its ability to isolate the oil from plant materials below 100°C to avoid overheating [8]. About 600g of lemon peels was rinsed with distilled water and oven dried at 45°C for 2 hours, then immersed in 2000ml of distilled water in a distillation flask, heat was supplied to the flask using a temperature-controlled heating mantle. The experiment was carried out at a temperature of 88°C for 60 minutes. The distillation time, solid to solvent ratio (lemon peels and distilled water) were kept constant throughout the experiment, while varying the temperature of distillation at an interval of 2°C from 88°C to 98°C. In the second phase of the experiment, the distillation temperature and solid to solvent ratio (lemon peels and water) were kept constant and varying the distillation time at an interval of 15 minutes from 15 to 75 minutes. The steam generated ruptured the lemon peels oil glands and on passing through the condenser, was condensed as a result of counter flow of oil-steam and cooling water. The condensate, which is a mixture of oil and water, were collected in a conical flask. The mixture formed two distinct layers of oil and water. The oil which is less dense than water float at the top, and was easily separated using a separating funnel. Figure 1, shows hydro-distillation set-up for essential oils extraction from lemon peels.



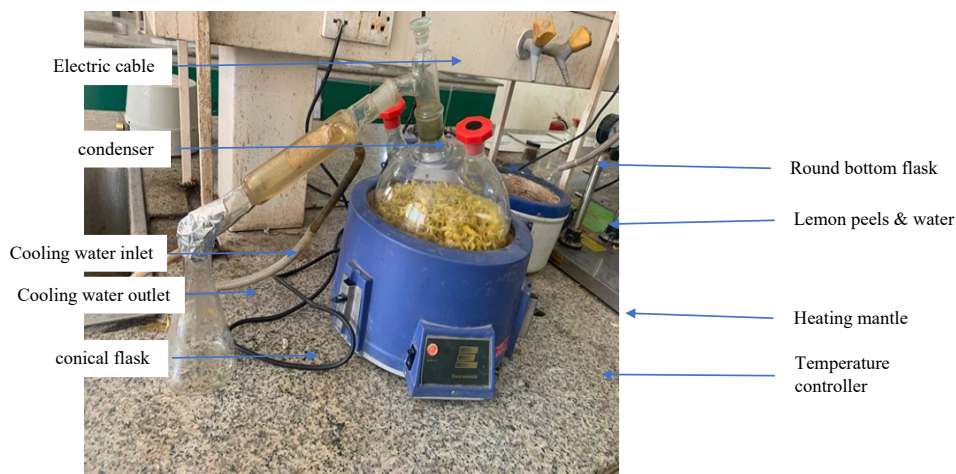


Figure 1: Hydro-distillation set-up for lemon peels extraction of essential oil

Figure 2 shows process flow diagram of essential oil extraction from lemon peels.

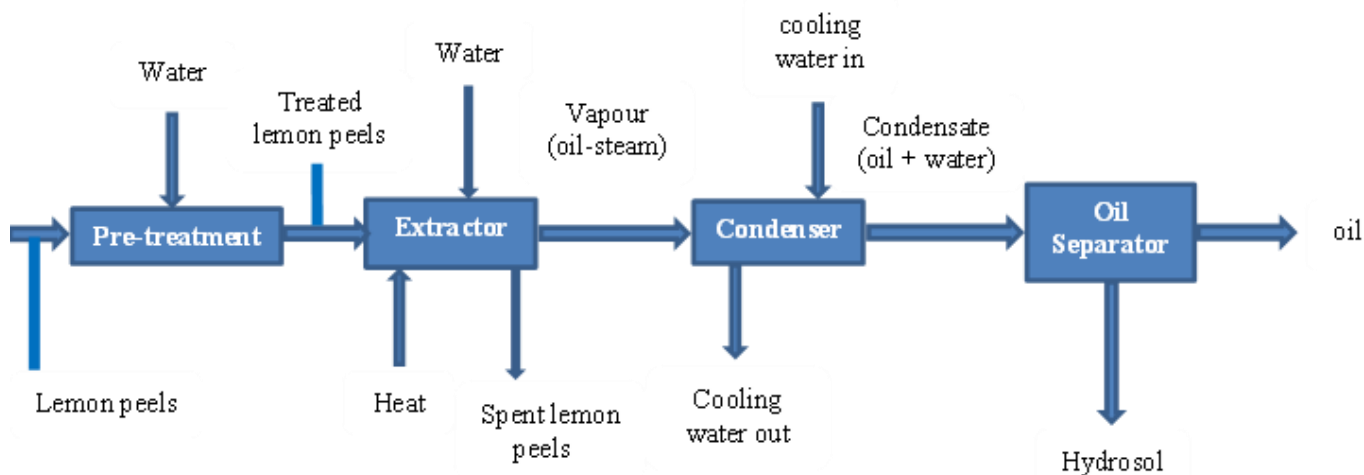


Figure 2: Process flow diagram of hydro-distillation of essential oil extraction from lemon peels

RESULTS AND DISCUSSION

The effect of temperature on percentage yield of the extracted essential oil from lemon peels was studied at different temperatures of 88, 90, 92, 94, 96, and 98°C per batch operation, while other parameters, time and solid to solvent (lemon peels: water) ratio, were held constant until equilibrium was attained. The results obtained were represented graphically as shown in Figure 3.

Figure 3 shows that as temperature increases the amount of the oil extracted increases proportionally to temperature of 96°C. On further increase in temperature to 98°C, the quantity of oil extracted was insignificant compared to the previous temperatures. Also, after extrapolation of the values of temperatures of 100, 102, and 104°C, the difference in quantity of oil obtained remained constant (0.05ml). Equation 1 is the extrapolation formula used to extrapolate the two endpoints (x_1, y_1) and (x_2, y_2) temperatures.

$$y_3 = y_1 + \frac{(x_3 - x_1)}{(x_2 - x_1)} * (y_2 - y_1) \quad 1$$

where, y_1, y_2 and y_3 are oil yield, while x_1, x_2 and x_3 are temperature values.



It can be inferred that the optimal temperature for the extraction was 96 °C. Any further increased in temperature beyond 96 °C has no significant effect on the oil yield. The results obtained from this work were in agreement with the findings [7].

Effect of Hydro-Distillation Time on Yield of Lemon Peels Essential Oil Extraction

From the analysis done, it indicated that, hydro-distillation time is an important factor which has the tendency to affect the yield of oil extracted from lemon peels. Hence, the effect of hydro-distillation time on the oil yield was investigated. The extraction time was studied from 15 minutes to 75 minutes, while the hydro-distillation temperature and solid to solvent (lemon peels and water) ratio were kept constant throughout the extraction process.

Figure 4 shows the effect of hydro-distillation time against oil yield.

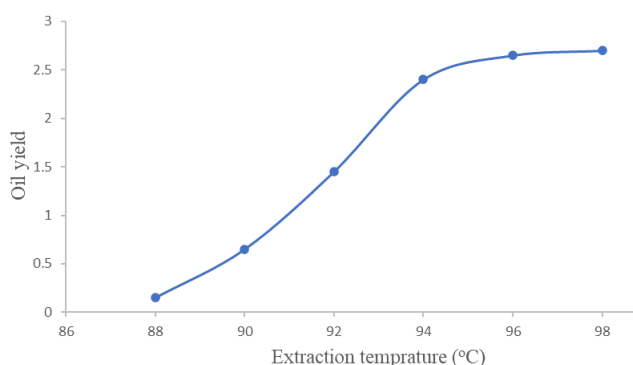


Figure 3: Effect of hydro-distillation temperature on the yield of lemon peels essential oil extraction

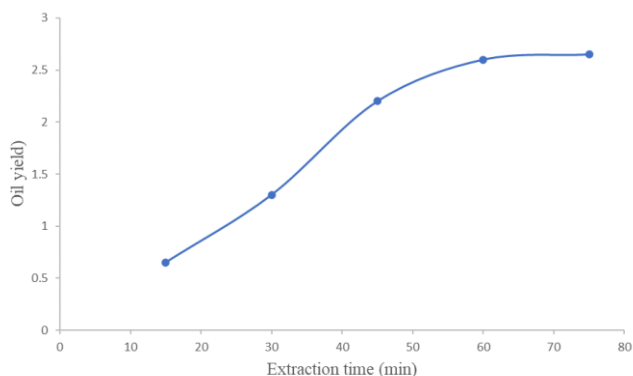


Figure 4: Effect of hydro-distillation time on the yield of lemon peels essential oil extraction

It was also observed from Figure 4, as extraction time increases the oil yield also increased significantly from 15 minutes to 60 minutes. On further increase in extraction time from 60 minutes to 75 minutes, the increase in the oil yield was insignificant. This implied that, extending extraction time beyond 60 minutes has less significant effect in the yield of the oil. Using Equation 1, extrapolating the extraction time of 90 and 105 minutes, the difference in the oil yield remained constant (0.10ml). Any further increase in time beyond 75 minutes had no significant effect on the oil yield. The results obtained from this work agreed with other previous findings [6, 7].

CONCLUSION

The optimum amount of oil obtained were at 96°C and 60 minutes. It was also observed that, beyond the optimum temperature of 96°C and extraction time of 60 minutes the oil yield was not significant. As such, extraction of the oil should not exceed the optimum parameters of 96°C and 60 minutes. The weight and percentage yield of essential oils mined from lemon peels at an extraction temperature of 96°C was 2.27g and 0.38% and for an extraction time of 60 minutes was 2.22g and 0.37%, respectively.

Essential oils extracted from lemon peels using hydro-distillation technique has been successfully studied. Lemon peels are supposedly waste products generated in the processing of citrus fruits and often constitute solid waste environmental pollution. These wastes contain value added constituents and have substantial applications in the health sector, perfumery, cosmetics, food, pharmaceutical industries and the likes. The spent peels from the extraction of essential oil from lemon fruits, when properly decomposed can add value to the soil by enriching its fertility.

REFERENCES

1. Andrews, A. J. (2018). How to Extract Oil from the Skin of Oranges. <https://healthyeating.sfgate.com/healing-benefits-cinnamon-oil-7738.html>
2. Muhammad, M. A., Salim, U. R., Faqir, M. A. & Ehsan E. B. (2006). Comparative Physical Examination of Various Citrus Peel Essential Oils. *International Journal of Agriculture and Biology*, 8(2), 186-190.



3. John Misachi (2017). The World's Top Citrus Producing Countries. *worldAtlas.com*
4. Narmin Baazova (2017). Top 10 Citrus Fruit Producing Countries in the World. <https://www.linkedin.com/pulse/top-10-citrus-fruit-producing-countries-world-narmin->
5. Olugbenga, A. F. & Kingsley, E. A. (2018). Optimization of Oil and Pectin Extraction from Orange (Citrus Sinensis) Peels: A Response Surface Approach. *Journal of Analytical Science and Technology*, 9(20), 1-59.
6. He-Shuai, H., Emmanuel, M. B., Rong, Z., Rong, Z., Ya-Li, H., Zhong-Hua, Y., & Can. Q. (2019). Extraction of Essential Oil from Citrus Reticulate Blanco Peel and its Antibacterial Activity Against Cutibacterium Acnes (formerly *Propionibacterium acnes*). <https://www.ncbi.nlm.nih.gov/pmc/articles/PMC6909146/>
7. Mansour, G., Alimohammad, B., Ali, Z., Nariman, A. & Mohammad, J. T. (2018). Optimization of essential oil extraction from orange peels using steam explosion. <https://www.sciencedirect.com/science/article/pii/S2405844018330901>
8. Zarith A. A., Akil A., Siti, H. M. S., Alptug, K., Muhammad, M. A., David, L. Mohd, R., Magdah, G., Mohammad, A., Kamal and Ghulam, Md. A. (2018). Essential Oils: Extraction Techniques, Pharmaceutical and Therapeutic Potential - A Review. *ResearchGate: Current Drug Metabolism*, 19(00), pp. 1 – 11.



P049 - APPLICATION OF CHEMICAL TECHNOLOGY IN FOOD PRODUCTION, PROCESSING, AND PRESERVATION IN NIGERIA: CHALLENGES AND CONCERNS

Aliyu M.K¹, Adamu.H², Owigho, O³; Faruk.A.U¹, Umar. R⁴, Ibrahim. A¹ and Adamu.M.E⁵,

Department of Agricultural Extension and Economics¹, Food Technology and Home Economics Department², Delta State University of Science and Technology, Ozoro. Delta State³.Department of Livestock and Fishery⁴

kabiramhammad41@gmail.com

ABSTRACT

The application of chemical technology in food production, processing, and preservation has the potential to significantly impact the food industry in Nigeria. This paper explores the prospects and issues associated with the utilization of chemical technology in various aspects of the Nigerian food sector. It highlights the role of chemical technology in improving food safety, extending shelf life, and enhancing the nutritional value of food products. Additionally, the paper discusses the environmental and health concerns that may arise from the use of certain chemicals in food processing. The study emphasizes the need for a balanced approach that considers both the benefits and risks associated with chemical technology in food production. Through a comprehensive review of the existing literature, this paper aims to provide insights into the current state of chemical technology in the Nigerian food industry and its potential for future growth. It thus concludes with some recommendations on safety measures on the adoption of chemical technology processing and preservation in the Nigerian food system.

KEYWORDS

Application, Chemical Technology, Food Production, Processing, and Preservation.

INTRODUCTION

Food is a fundamental component of human existence, providing sustenance, nourishment, and cultural significance to societies across the globe. In Nigeria, a nation characterized by its rich and diverse culinary traditions, ensuring the availability of safe, nutritious, and high-quality food is of paramount importance (FAO,2019). However, this goal is not without its challenges. Nigeria, with its burgeoning population and dynamic food industry, must grapple with the dual mandate of meeting the nutritional needs of its food products in the global market place. In this context, the application of chemical technology in food production, processing, and preservation has emerged as a crucial force driving change and transformation within the Nigerian food sector. Chemical technology encompasses a spectrum of practices, from the use of additives and preservatives to enhance food safety and shelf life to the incorporation of innovative techniques for improving food quality. As Nigeria strives to address the complex web of issues surrounding food security, food safety, and food quality, the role of chemical technology becomes both pertinent and contentious. With rising consumer awareness, there

is a greater emphasis on food safety in Nigeria. This paper embarks on a comprehensive exploration of the prospects and issues associated with the application of chemical technology in food production, processing, and preservation within the Nigerian context. It delves into the multifaceted facets of chemical technology, examining its potential to revolutionize the nation's food landscape while simultaneously navigating the challenges it presents. Through an in-depth analysis, this paper aims to shed light on the current state of chemical technology in Nigeria's food industry, the opportunities it holds, and the critical considerations it demands. As we embark on this exploration of chemical technology in the Nigerian food landscape, it is imperative to acknowledge that the prospects and issues surrounding its application are not confined solely to the realm of science and technology. Rather, they intersect with socioeconomic, environmental, and cultural dimensions, creating a complex tapestry that necessitates careful analysis and informed decision-making. In the following sections, we will dissect these intricacies, aiming to provide valuable insights for policymakers, food industry stakeholders, researchers, and consumers alike. In



essence, the journey ahead is one of discovery, challenge, and opportunity, as we navigate the multifaceted landscape of chemical technology in the context of Nigeria's food production, processing, and preservation.

Application of Chemical Technology in the Nigerian Food System: An overview

The hasty urbanization of the world has created new challenges for the modern food industry. Trends for more frequent food consumption outside the home and fast preparation of ready-to-eat meals has led to growing numbers of produced foods and ingredients. Consequently, this has resulted in the growing industrialization of food production, globalization and trade of food supply and a growing number of food recalls. The industrialized production of foods has to guarantee retailers and consumers enhanced food safety and nutritional quality of locally grown products. In addition, it must satisfy consumer desires of additional health benefits as well as retailers demands for longer shelf-lives (Tatiana and Hamid,2021)

Nigeria, with its vast and diverse agricultural landscape, is home to a rich tapestry of food traditions and a burgeoning population. Ensuring a consistent and safe food supply for its citizens while navigating the complexities of the global food market is a multifaceted challenge. Within this context, the application of chemical technology has emerged as a critical factor in shaping the trajectory of food production, preservation, and processing in Nigeria. Food processing in Nigeria has seen advancements in technology and equipment. The adoption of modern food processing techniques, including drying, milling, and extrusion, has improved the value addition of agricultural products (Odunfa, 2016). With rising consumer awareness, there is a greater emphasis on food safety in Nigeria. Food producers and processors are increasingly adhering to food safety standards and quality control measures (Bolarinwa, 2018).

1. Food Production and Crop Protection:

- **Chemical Pesticides and Herbicides:** Chemical pesticides and herbicides are widely used in Nigerian agriculture to protect crops from pests, diseases, and weeds. These chemical technologies, while improving crop yield and quality, also raise concerns about environmental impact and pesticide residues (Ewuola and Oyewole, 2016).

- **Fertilizers:** Chemical fertilizers are instrumental in enhancing soil fertility and promoting crop growth. Their judicious use contributes to increased agricultural productivity, although excessive application can lead to soil degradation (Ogunlela *et al.*, 2017).

2. Food Preservation:

- **Chemical Preservatives:** The use of chemical preservatives, such as sodium benzoate and sorbic acid, is prevalent in the Nigerian food processing industry. These additives inhibit microbial growth and extend the shelf life of products, particularly in fruit juices, canned foods, and bakery items (Adepoju *et al.*, 2019).
- **Natural Antimicrobials:** In response to concerns about synthetic preservatives, research efforts are exploring natural antimicrobial compounds derived from plants, herbs, and spices as alternatives for food preservation (Olurin *et al.*, 2020).

3. Food Processing:

- **Flavor Enhancers and Food Additives:** Chemical flavor enhancers and food additives are used to improve the sensory attributes of processed foods. Monosodium glutamate (MSG) and various food colorants are commonly employed (Maga, 1982).
- **Texture Modifiers:** Emulsifiers, stabilizers, and thickeners are used to maintain desired textures in processed foods, contributing to their palatability and consistency (McClements, 2015).

4. Food Quality Enhancement:

- **Fortification:** Chemical technology facilitates the fortification of foods with essential vitamins and minerals to address nutritional deficiencies (Mannar & Hurrell, 2017). This practice is particularly significant in combating malnutrition.
- **Quality Control and Analysis:** Chemical analysis techniques, such as chromatography and spectroscopy, play a pivotal role in ensuring the quality and safety of food products (Bolton, 2015).

5. Consumer Awareness and Preferences:

Consumer awareness about the presence of chemical preservatives in food products has been



increasing. Many consumers are seeking natural and minimally processed food options. The food industry is responding to changing consumer preferences by exploring alternative preservation methods, such as high-pressure processing and natural antimicrobial agents (Oluwole et al., 2017). This shift reflects the ongoing dialogue between producers and consumers regarding food safety and quality.

6. Regulatory Framework:

Nigeria, like many countries, has regulations in place to control the use of chemical preservatives in food. However, the enforcement and monitoring of these regulations can be challenging. Stakeholders, including government agencies and industry associations, are discussing the need for stricter enforcement of regulations and the establishment of clear guidelines for the use of chemical preservatives (Ojo et al., 2020). This is essential to ensure food safety and protect consumer interests.

7. Impact on Export Market:

The use of chemical preservatives can affect Nigeria's export potential, as some international markets have stricter regulations on allowable preservatives. The Nigerian food industry is exploring methods to reduce or eliminate the use of chemical preservatives in export-oriented products to meet international standards and access global markets (Ijabadeniyi et al., 2018). This discussion emphasizes the importance of balancing local and international food safety requirements.

8. Research and Innovation:

Research efforts in Nigeria are focused on developing safer and more sustainable food preservation methods. Researchers are actively working on finding natural alternatives to chemical preservatives, as well as improving packaging and storage technologies to reduce the need for preservatives (Adepoju et al., 2020). Collaborative efforts among academia, government, and industry are driving innovation in food preservation.

Food Safety and Quality Enhancement through the Application of Chemical Technology in Food Processing.

Food safety and quality are paramount in the food processing industry, and chemical technology plays a vital role in ensuring both. Below are discussions on how chemical technology is used to enhance

food safety and quality in food processing, along with relevant citations and references:

1. Food Preservation and Safety:

Chemical preservatives, such as antimicrobial agents and antioxidants, are widely used in food processing to extend shelf life and prevent spoilage (Jay *et al.*, 2005). These additives inhibit the growth of harmful microorganisms, reducing the risk of foodborne illnesses. The use of chemical preservatives has raised concerns about their potential health risks, including allergic reactions and long-term health effects (Adepoju et al., 2019). There is ongoing debate regarding the safety and regulation of these preservatives in the Nigerian food industry.

2. Flavor Enhancement:

Chemical flavor enhancers, like monosodium glutamate (MSG), are used to improve the sensory attributes of food products (Maga, 1982). Proper use of these additives can enhance the overall taste and palatability of processed foods.

3. Texture and Appearance Improvement:

Chemical additives like emulsifiers, stabilizers, and thickeners are employed to maintain desired textures and appearances in food products (McClements, 2015). They contribute to the uniformity and attractiveness of processed foods.

4. Nutritional Enhancement:

Fortification of foods with vitamins and minerals is a common practice in food processing (Mannar & Hurrell, 2017). Chemical technology enables the addition of essential nutrients to processed foods, addressing nutritional deficiencies.

5. Food Safety Testing:

Chemical analysis techniques, including chromatography and spectroscopy, are used for quality control and the detection of contaminants in food products (Bolton, 2015). These methods ensure that processed foods meet safety standards.

6. Preserving Freshness in Produce:

Ethylene absorbers and controlled atmosphere storage systems use chemical technology to extend the shelf life of fresh fruits and vegetables (Kader, 2002). This contributes to food safety by reducing waste and enhancing quality.



Challenges and Concerns

While chemical technology offers numerous benefits, there are several challenges and concerns associated with its application in the Nigerian food industry. They include:

- **Health Concerns:** The use of chemical additives and preservatives has raised concerns about potential health risks, allergenicity, and long-term effects on consumers (Magnuson et al., 2013).
- **Environmental Impact:** The overuse of chemical pesticides and fertilizers can lead to environmental degradation, including soil and water pollution (Ewuola & Oyewole, 2016).
- **Regulation and Oversight:** The Nigerian government has established regulations governing the use of chemical technologies in food production and processing. However, challenges remain in enforcing and monitoring these regulations (Ojo et al., 2020).
- **Consumer Preferences:** Changing consumer preferences for natural and minimally processed foods pose challenges for the food industry, leading to a shift toward cleaner labels and natural ingredients (Oluwole et al., 2017).

Conclusion and Recommendation

The paper therefore posits that the application of chemical technology in the Nigerian food system is a dynamic and evolving process. The prospects are promising, offering solutions to critical issues of food security and nutrition. Yet, the issues are real and multifaceted, calling for responsible and forward-looking actions. As Nigeria navigates the path forward, the key lies in harnessing the potential of chemical technology while safeguarding the health and well-being of its people, its environment, and its future generations. Ultimately, the success of this journey will be measured by the ability to strike a harmonious balance between progress and responsibility in shaping the future of food in Nigeria. It therefore recommends the following; Strengthen Regulatory Oversight, Promote Research and Innovation, Consumer Education, Sustainable Agriculture Practices, Diversify Food Preservation Techniques, Strengthen Food Safety Testing, Promote Natural Alternatives, Collaborative Initiatives. International Standards Compliance: and Continuous Monitoring and Evaluation:

REFERENCES

1. Adegbaaju, A. S., (2020). Innovative approaches to food preservation in Nigeria: A
2. Adepoju, O. T., et al. (2019). Emerging food safety issues in Nigeria: A review. *Food Control*, 100, 1-8.
3. Bolarinwa, O. (2018). Enhancing Food Safety in Nigeria: Current Trends and Challenges. *Journal of Food Quality*, 2018, 1-8.
4. Bolton, J. R. (2015). Analytical techniques in food safety: Review of current issues and future perspectives. *TrAC Trends in Analytical Chemistry*, 67, 87-98.
5. Eboh, E. C., & Okoruwa, V. O. (2018). Commercialization of Agriculture in Nigeria: A Synthesis of Findings from the Nigeria Strategy Support Program (NSSP). International Food Policy Research Institute.
6. Eneji, R. E., et al. (2020). Challenges and Opportunities for Sustainable Food Production and Food Security in Nigeria. *Sustainable Agriculture Research*, 9(2), 11-21.
7. FAO. (2019). Food Security and Agriculture in Nigeria: A Situation Analysis. Food and Agriculture Organization of the United Nations.
8. Idowu, M. O. (2019). Small and Medium Enterprises (SMEs) in Food Processing in Nigeria: Challenges and Prospects. *Journal of Agriculture and Food Research*, 1, 100003.
9. Ijabadeniyi, O. A., et al. (2018). Chemical preservation and food safety in Nigeria: A review. *Journal of Food Safety*, 38(6), e12512.
10. Jay, J. M., Loessner, M. J., & Golden, D. A. (2005). *Modern Food Microbiology* (7th ed.). Springer.
11. Kader, A. A. (2002). *Postharvest Technology of Horticultural Crops* (3rd ed.). University of California, Division of Agriculture and Natural Resources.
12. Maga, J. A. (1982). Monosodium Glutamate. In R. L. Ory & J. W. Bier



- (Eds.), Handbook of Food Additives (pp. 203-255). CRC Press.
13. Magnuson, B. A., et al. (2013). Aspartame: A Safety Evaluation Based on Current Use Levels, Regulations, and Toxicological and Epidemiological Studies. *Critical Reviews in Toxicology*, 43(8), 1-41.
 14. Mannar, M. G. V., & Hurrell, R. F. (2017). Food Fortification in a Globalized World. *Food and Nutrition Bulletin*, 38(2_suppl), S1-S3.
 15. McClements, D. J. (2015). *Food Emulsions: Principles, Practices, and Techniques* (3rd ed.). CRC Press.
 16. Odunfa, S. A. (2016). Food Processing Technology in Nigeria: Status, Challenges, and Opportunities. In T. Adedeji (Ed.), *Handbook of Food Engineering* (pp. 123-146). CRC Press.
 17. Ojo, M. O. (2017). Diversification of the Nigerian Economy Through Agriculture: An Assessment of Cocoa Production. *International Journal of Agriculture and Biology*, 19(5), 1057-1062.
 18. Ojo, M. O., et al. (2020). Regulatory framework for food preservatives in Nigeria: Challenges and prospects. *Food Control*, 107, 106787.
 19. Oluwole, O. B., et al. (2020). Application of chemical analysis techniques in food quality control: A review. *Food Science & Nutrition*, 8(3), 1210-1221.
 20. Oyewole, O. B., et al. (2017). Food additives in Nigeria: Types, health effects, and regulatory issues. *Food Control*, 72, 367-374.
 21. Tatiana . K and Hamid .E (2021). *Frontiers: Current Challenges in Food Process Design and Engineering. Specialty Grand Challenge*. Published: 04 November 2021 doi: 10.3389/frfst.2021.780013

P050 -THERMAL ANALYSIS OF A DEVELOPED NANO CUO BASED-NEEM OIL CUTTING FLUID FOR MACHINING Ti-6Al-4V

T. S. Abdulrahman^{1*}, M. Dauda², M. Sumaila³ and L.S. Kuburi⁴

Department of Mechanical Engineering Technology, Federal Polytechnic Nasarawa
Department of Mechanical Engineering, Ahmadu Bello University, Zaria, Kaduna.
yatahir2301@gmail.com, [+2348051632954](tel:+2348051632954)

ABSTRACT

This study investigated the thermal and thermophysical properties of a developed nanoCuO-based neem oil cutting fluid for machining Ti-6Al-4V. The thermogravimetric analysis (TGA) of the cutting fluid revealed that the nano CuO-based neem oil cutting fluid exhibited a remarkable improvement of 88.75% in thermal stability compared to its neem oil-based cutting fluid counterpart. Similarly, the Differential Thermal Analysis (DTA) demonstrated a significant 24.24% enhancement in the melting temperature of the cutting fluid. Additionally, substantial improvements have been revealed with a 5.74% increase in specific heat, a 3.4% reduction in viscosity, a 1.84% increase in density, a 19.7% decrease in surface tension, and a notable 34.5% increase in thermal conductivity. These findings underscore the potential of the nano CuO-based neem oil cutting fluid as a superior choice for machining Ti-6Al-4V, offering enhanced thermal stability and improved thermophysical properties, thus contributing to more efficient and sustainable machining of Ti-6Al-4V.

KEYWORDS:

nano CuO, neem oil cutting fluid, thermal stability, thermophysical properties, Ti-6Al-4V, machining.

1.0 INTRODUCTION

Thermogravimetric Analysis (TGA) and Differential Thermal Analysis (DTA) are crucial techniques in the realm of material science and

engineering which are employed to investigate the thermal behaviors and transformations of materials (Haines, 2013). These methods are indispensable for evaluating the thermal stability and decomposition processes of diverse substances.



In recent years, researchers have focused on the development of advanced cutting fluids to enhance machining processes. Cutting fluids play a pivotal role in metalworking by lubricating, cooling, and enhancing overall machining performance. The nano CuO-based neem oil cutting fluid combines the advantages of nanotechnology (utilizing green chemistry synthesis approach) and sustainability offered by neem oil.

Thermal stability is a critical attribute of cutting fluids, especially given the high temperatures generated during machining of difficult-to cut materials like Ti-6Al-4V. Similarly, the Differential Thermal Analysis (DTA) of the nano CuO-based neem oil cutting fluid has unveiled a substantial enhancement in its melting temperature. These findings suggest that this cutting fluid can endure higher temperatures during machining processes, thereby enhancing tool longevity and machining efficiency.

Beyond thermal stability and melting behavior, the thermophysical properties of the nano CuO based neem oil cutting fluid at a concentration of 0.05% CuO nanoparticles, the cutting fluid exhibited significant enhancements in the thermophysical properties. These improvements in thermophysical

properties result in efficient dissipation of heat generated during machining, better chip evacuation, enhanced lubrication, improved wetting and cooling capabilities, efficient heat transfer, reduction of tool wear, enhanced lubrication and overall enhancement of machining precision.

2.0 MATERIALS AND METHODS

2.1 Materials

The materials used for phytochemical synthesis of copper oxide nanoparticles and formulation of the nano CuO based neem oil cutting fluid include: neem leaves (500g), neem oil (4 litres), Copper II chloride pentahydrate ($\text{CuCl}_2 \cdot 5\text{H}_2\text{O}$) powder (2500g), Di-ionized (DI) water (4 litres), Distilled water (10 litres), Oxalic acid (500ml), Triethanol amine (500g), Sodium citrate (500g), Copper oxide nanoparticles (10g), Hydrochloric acid (10ml, 0.1M) and Sodium Hydroxide (10 ml, 0.1M). The equipment used in the present study are listed in Table 1.

2.2 Equipment

Equipment used are listed in Table 1

Table 1: Equipment

S/N	Equipment	Specification
1	PerkinElmer Thermal Analyser	STA 600
2	Digital Viscometer	RVDV-1
3	Thermal conductivity apparatus	H470
4	Copper calorimeter and stirrer	PH 20152
5	A set of capillary tubes	
6	Beam balance	
7	Insulating jacket	
8	Test tube	
9	Beaker	

2.3 Thermal Analyses of the nano CuO based neem oil cutting fluid

Thermogravimetric analysis (TGA) and Differential thermal analysis (DTA) were conducted on the formulated and developed cutting fluids as reported below.

2.3.1 Thermo Gravimetric Analysis (TGA)

The STA 6000 simultaneous thermal analyzer was used to analyze liquid sample in compliance with ASTM E1131: Standard Test Method for Thermogravimetric (TG) Analysis of Solids and

Liquids. The sample was weighed (12mg) and placed in a clean and dry ceramic crucible along with a blank reference material. The sample and reference pans were inserted into the instrument and heated at a constant rate with continuous measurement of thermal properties.

2.3.2 Differential Thermal Analysis (DTA)

In the DTA experiment, the sample and reference materials were subjected to the same temperature program, and the temperature difference between the sample and reference was recorded as a function of temperature. The procedure is in line with ASTM



E1356: Standard Test Method for Differential Thermal Analysis (DTA) of Solids and Liquids

2.3.3 Measurement of the thermophysical properties of the cutting fluids

The thermophysical properties of the cutting fluids were measured in the Department of Physics at Ahmadu Bello University, Zaria. The equations utilized for calculations are given as follows.

2.3.3.1 Density

The density of the sample was calculated using equation 1 from Halliday *et. al.* (2013). The

The relation for viscosity has been adapted from Poggio *et. al.* (2015) and it is given by:

$$\frac{\eta_{\text{nanofluid}}}{\eta_{\text{water}}} = \frac{(d_{\text{nanofluid}} \times t_{\text{nanofluid}})}{d_{\text{water}} \times t_{\text{water}}} \quad 2$$

Where

$\eta_{\text{nanofluid}}$ is the viscosity of water

η_{water} is viscosity of nanofluid

$d_{\text{nanofluid}}$ is density of nanofluid

d_{water} is density of water

$t_{\text{nanofluid}}$ is timing of run off of nanofluid

t_{water} is timing of run off of water

2.3.3.3 Surface tension

Surface tension of the sample was determined using capillary method. The surface tension was calculated using Hagen-Poiseuille's equation for capillary flow (Cengel and Cimbala, 2013).

$$\eta = \frac{\rho g h r}{2} \quad 3$$

Where, ρ = density of the sample, r = radius of the tube, g = acceleration due gravity and h = height of sample rise in the capillary tube.

2.3.3.4 Specific heat

The specific heat capacity of the liquid sample (nanofluid) was determined using the mixture method. By applying the principle of heat conservation, the specific heat capacity of the liquid sample (nanofluid) can be calculated using the formula:

$$c = \frac{M_1 \times c_1 \times (\theta_3 - \theta_1)}{M_2 \times (\theta_3 - \theta_2)} \quad 4$$

2.3.3.5 Thermal Conductivity of the cutting fluid samples

Thermal conductivity of the cutting fluid samples was measured using an H470 thermal conductivity apparatus. The heat transfers originating from elements within the plug, other than conduction through the fluid under test, were assessed before thermal conductivity tests.

same procedure was followed for both nano CuO based cutting fluid and neem oil-based cutting fluid.

Density of sample = (mass of sample)/ (volume of sample) 1

2.3.3.2 Viscosity

The viscosity of the cutting fluid was measured using a digital viscometer. The digital viscometer measured time taken for the fluid to flow through the capillary tube and the viscosity was calculated from the resulting flow rate.

The rate of heat transfer was calculated using the relation:

$$Q_c = \frac{K \pi d_m L \Delta t}{\Delta r} \quad 5$$

$$Q_e, \text{ Heat input} = \frac{V^2}{\text{Resistance}} \quad 6$$

The incidental heat transfer, Q_i is the difference between the heat input and heat conducted through sample. The thermal conductivities of air, nano CuO based neem oil cutting fluid, neem oil-based cutting fluid and mineral oil-based cutting fluid are each denoted by K.

$\pi d_m L$ is the heat transfer area.

Δt is the change in temperature = plug temperature-jacket temperature

Δr is the radial clearance

V is the voltage applied to the heater

3.0 RESULTS AND DISCUSSION

The TGA, DTA and thermophysical properties of the developed cutting fluids are presented in this section.

3.1 Thermogravimetric Analysis (TGA) of the formulated Cutting fluids

In Figures 1 to 5, M_i represents the initial mass of the sample while M_f stands for the final mass of the sample. T_i and T_f represent the initial and final



temperatures of the sample. The temperatures have been determined for both TGA and DTA curves using the tangent method which is based on the principle that the heat capacity of a material is

proportional to the slope of the curve relating the temperature of the material to the amount of heat that is added to it (Brezina,1999).

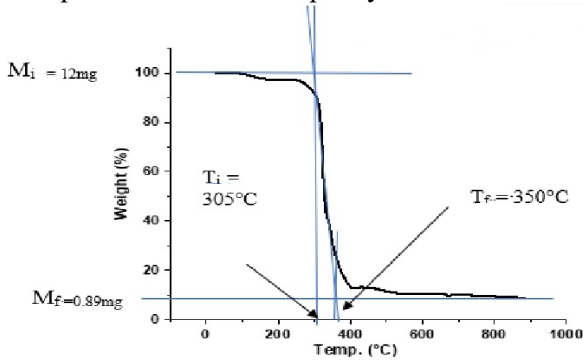


Figure 1: Variation of Weight with Temperature of neem oil-based cutting fluid

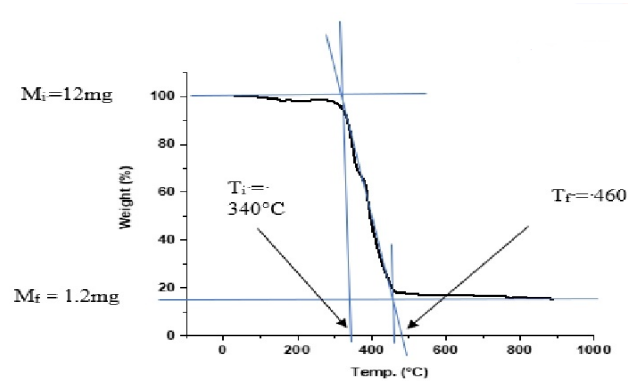


Figure 2: Variation of Weight with Temperature of nano CuO based neem oil cutting fluid (0.008% by volume of CuO nano particles).

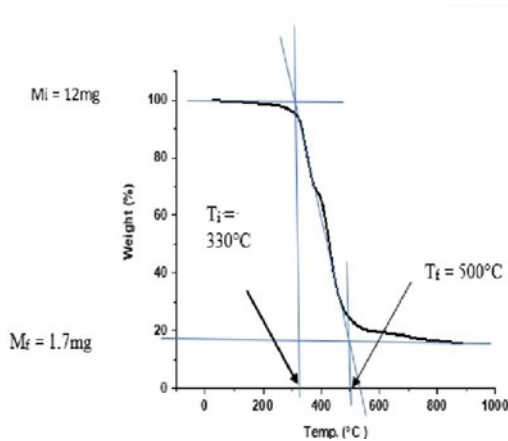


Figure 3: Variation of Weight with Temperature of nano CuO based neem oil cutting fluid (0.016% by volume of CuO nano particles).

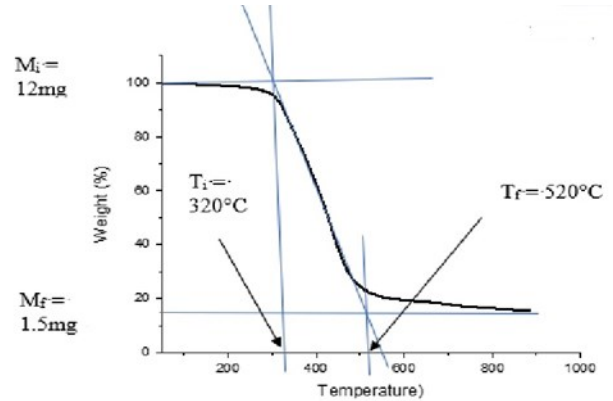


Figure 4: Variation of Weight with Temperature of nano CuO based neem oil cutting fluid (0.025% by volume of CuO nanoparticles).

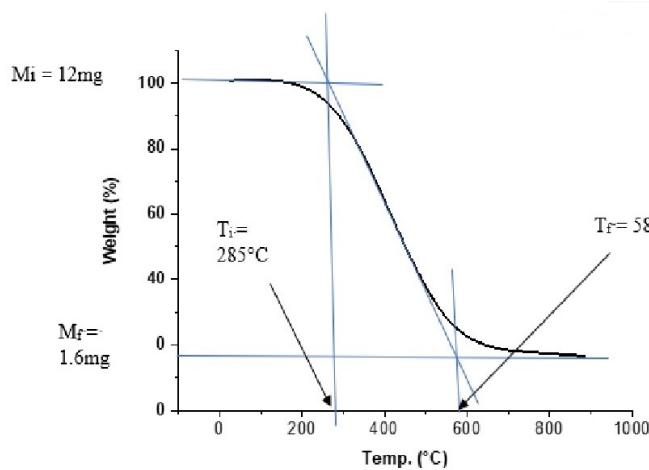


Figure 5: Variation of Weight with Temperature of nano CuO based neem oil cutting fluid (0.05% by volume of CuO nano particles)

Table 2: Evaluation of thermal stability of the cutting fluids

Cutting Fluid	Initial Decomposition Temperature (°C)	Final Decomposition Temperature (°C)	Percentage Increase in thermal stability (%)
Neem oil-based Cutting Fluid	305	350	14.75
Nano CuO based-neem oil cutting fluid (at 0.05% nano CuO addition)	285	580	103.5
Percentage Difference between the cutting fluids	$\frac{(103.5-14.75)}{14.75} \times 100$		88.75

3.2 Differential Thermal Analysis (DTA) of the formulated Cutting fluids

In Figures 6 to 10, T_i , T_p and T_f represent initial or starting temperature of the experiment, peak

temperature and final temperature or ending temperature of the experiment respectively. The peak melting temperature in this case refers to the melting temperature.

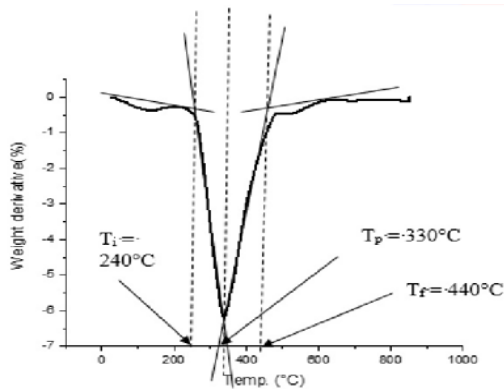


Figure 6: Variation of Weight derivative with Temperature of neem oil-based cutting fluid

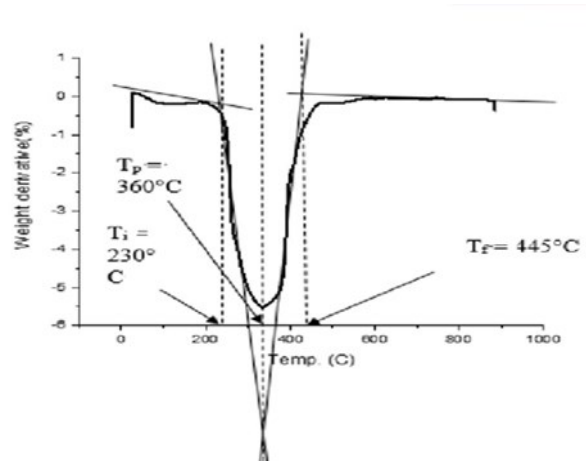


Figure 7: Variation of Weight derivative with Temperature of nano CuO based neem oil cutting fluid (0.008% by volume of CuO nano particles).



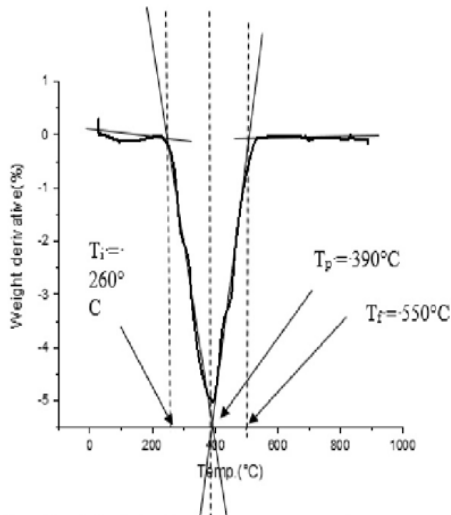


Figure 8: Variation of Weight derivative with Temperature of nano CuO based neem oil cutting fluid (0.016% by volume of CuO nano particles).

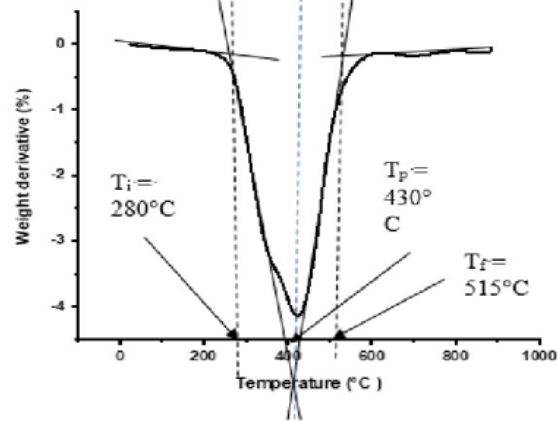


Figure 9: Variation of Weight derivative with Temperature of nano CuO based neem oil cutting fluid (0.025% by volume of CuO nano particles).

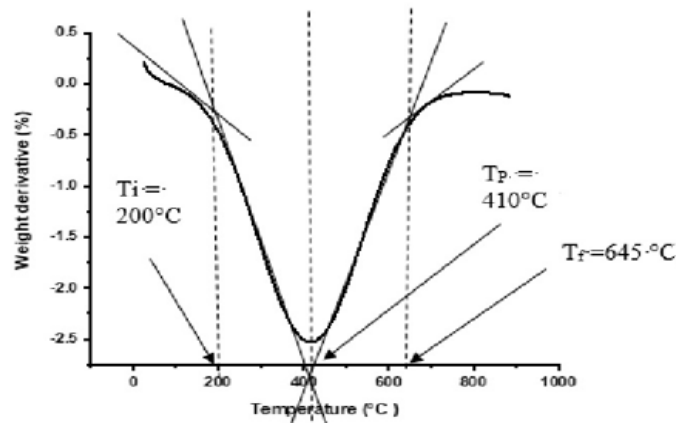


Figure 10: Variation of Weight derivative with Temperature of nano CuO based neem oil cutting fluid (at 0.05% by volume of CuO nano particles).

Table 3: Evaluation of Melting Temperatures of the cutting Fluids

Cutting Fluid	Initial Temperature	Melting Temperature	Percentage increase
Neem oil-based cutting fluid	240	330	37.5
Nano CuO based-neem oil cutting fluid	200	410	105
Percentage difference		$\frac{(410-330)}{330} \times 100$	24.24

The evaluated thermophysical properties of the cutting fluid are given in Table 4.



Table 4: Thermophysical properties of the cutting fluids

Thermophysical property	Neem oil-based cutting fluid	Nano CuO based Neem oil cutting fluid	Percentage enhancement (%)
Specific heat(J/kgK)	4067.2	4300.676	5.74%
Viscosity (MPa. S)	17.384	16.753	-3.4%
Density (kg/m ³)	15.9	16.2	1.84
Surface tension (N/m)	0.006247244	0.005058948	-19.7
Thermal conductivity (W/mK)	0.1109	0.1492	34.5%

The addition of CuO nano particles increased the specific heat capacity of the neem oil-based cutting fluid by 5.74% indicating its ability to absorb more heat before its temperature rises. This leads to better thermal stability and reduced thermal damage to the workpiece and tool as posited by El-Sherbini *et. al.* (2019).

At the addition of 0.05% nano CuO, the viscosity of the neem oil-based cutting fluid was reduced by 3.4%. Decreased viscosity of the cutting fluid allows it to flow more easily, leading to better chip evacuation in machining context. This finding is supported by Katpatal *et. al.* (2019) and El-Sherbini *et. al.* (2019)

The addition of CuO nano particles has led to a 19.7 % decrease in the surface tension of the neem oil-based cutting fluid. This improves the wettability of the cutting fluid, allowing it to spread more easily over the workpiece surface (Wang *et. al.* 2019). Improved wetting leads to better lubrication and reduced chip adhesion, resulting in improved surface finish and dimensional accuracy. This finding has been buttressed by Reddy and RaO (2019) and Agarwal *et. al.* (2016).

The addition of 0.05% of nano CuO has significantly enhanced the thermal conductivity of the neem oil cutting fluid by 34.5%. By implication, the cutting fluid can conduct 34.5% times more heat per unit time and per unit temperature difference than the neem oil-based cutting fluid. This leads to improved machining performance. This finding is supported by Gupta and Srivastava (2021), El-Sherbini *et. al.* (2020) and Katpatal *et. al.* (2020).

The increased density of the cutting fluid by 1.84% can help to improve chip control, which can lead to a smoother machining operation and a better surface finish, reduced tool wear, which can extend the life of the tools and improved cooling as found by Suresh *et. al.* (2019).

4.0 CONCLUSIONS AND RECOMMENDATIONS

4.1 CONCLUSIONS

In terms of thermal stability, the nano CuO-based neem oil cutting fluid exhibited approximately 88.75% improvement compared to the neem oil-based cutting fluid, as observed through Thermogravimetric Analysis (TGA) and a 24.24% enhancement in melting temperature through Differential Thermal Analysis (DTA). Additionally, at a concentration of 0.05% CuO nanoparticles, the cutting fluid demonstrated notable improvements in thermophysical properties. The specific heat increased by 5.74%, viscosity decreased by 3.4%, density increased by 1.84%, surface tension decreased by 19.7%, and thermal conductivity significantly increased by 34.5%.

4.2 RECOMMENDATION

Further studies should be conducted on the biodegradability and toxicity of the cutting fluid to aquatic and terrestrial organisms and their effects on soil, air, and water quality

5.0 REFERENCES

- Adhikari, B., Adhikari, L., & Poudel, P. (2021). Effect of copper oxide nanoparticles on the stability and tribological performance of vegetable oil-based cutting fluid. *Surface and Coatings Technology*, 387, 125836. doi:10.1016/j.surfcoat.2021.125836.
- Agarwal, V., and Tiwari, A. K. (2016). Effect of nano-CuO on the thermal conductivity, specific heat capacity, viscosity, and



surface tension of vegetable oil-based cutting fluid *International Journal of Engineering Science and Technology*, 8 (12), 3587–3592.

ASTM E1131 (2018): Standard Test Method for Thermogravimetric (TG) Analysis of Solids and Liquids. *ASTM International*. doi:10.1520/E1131-18.

ASTM E1356 (2017): Standard Test Method for Differential Thermal Analysis (DTA) of Solids and Liquids. *ASTM International*. doi:10.1520/E1356-17.

Brezina, O. (1999). Thermal analysis. In: Encyclopedia of Analytical Chemistry, 2nd ed.; Meyers, R. A., Ed.; John Wiley and Sons, Ltd.: Chichester, West Sussex, England; New York, NY, USA, 1999; Vol. 10, pp. 11069–11080.

Cengel, Y. A., and Cimbala, J. M. (2013). Fluid mechanics: fundamentals and applications McGraw-Hill Higher Education.

El-Sherbini, A., El-Khodary, A., and Abd-El-Aziz, A. (2019). Effect of nano-CuO on the performance of vegetable oil-based cutting fluid. *Journal of Materials Processing Technology*, 268, 310-317.

El-Sherbini, A., Abd-El-Aziz, A., and El-Khodary, A. (2020). Effect of nano-CuO on the performance of vegetable oil-based cutting fluid. *Journal of Materials Processing Technology*, 280, 116746.

Gupta, V., and Srivastava, R. (2023). Synthesis of titanium dioxide nanoparticles using pomegranate peel extract: effects of time, pH, and temperature. *Nanomaterials*, 13(1), 306.

Halliday, D., Resnick, R., and Walker, J. (2013). Principles of Physics (10th Edition) Wiley.

Haines, P. J. (2013) Principles of Thermal Analysis and Calorimetry Royal Society of Chemistry.

Katpatal, D. C., Andhare, A. B., and Padole, P. M. (2020). Effect of nano-CuO on the machinability of mild steel. *Materials Today: Proceedings*, 27, 1864–1869.

Khan, M. I., Khan, M. A., & Khan, M. S. (2022). Effect of copper oxide nanoparticles on the tribological and thermal characteristics of vegetable oil-based cutting fluid *Tribology Letters*, 68, 11. doi:10.1007/s11249-022-02033-8.

Kumar, S., and Tiwari, A. (2020). Performance evaluation of nano-CuO-based neem oil cutting fluid. *Journal of Industrial Lubrication and Tribology*, 42(3), 252-257.

Poggio, Claudio; Ceci, Matteo; Beltrami, Riccardo; Colombo, Marco; and Dagna, Alberto (2015). Viscosity of endodontic irrigants: influence of temperature. *Dental research journal*, 12. 425–30. 10.4103/1735–3327.166189.

Reddy, M., and Rao, P. V. (2019). Thermal conductivity of neem oil and its blends with vegetable oils. *Energy Conversion and Management*, 51(1), 316–320.

Selvi, S., Vijayakumar, R., and Balasubramanian, P. (2021). Preparation and characterization of nanofluids of copper oxide and neem oil for machining applications *Materials Today*:

Suresh, K., Kumar, S., & Dhinakaran, S. (2019). Effect of nano CuO addition on the performance of neem oil-based cutting fluid in the machining of AISI 1045 steel. *Surface and Coatings Technology*, 373, 125223. <https://doi.org/10.1016/j.surfcoat.2019.125223>.

Wang, X., Wei, X., Liu, S., Chen, Y. and Zhang, J. (2019). Effects of copper oxide-based cutting fluids on surface finish, tool life, and cutting temperature in drilling operations. *Journal of Cleaner Production*, 235, 992–1022. <https://doi.org/10.1016/j.jclepro.2019.06.047>





P051 - ANTIFUNGAL COMPOUNDS PRODUCED BY LACTIC ACID BACTERIA: LANTIPLANTIBACILLUS PLANTARUM OQ224994.1 FROM SOIL SAMPLES OF NATURE GARDEN AHMADU BELLO UNIVERSITY ZARIA.

J. S. Obidah^{1*}, C. M. Z. Whong², I. O. Abdullahi³, J. Kabir⁴, F. F. Umaru⁵, M.M. Fathuddin⁶

Department of Microbiology, Modibbo Adama University Yola, Adamawa State, Nigeria 1, Department of Microbiology, Ahmadu Bello University Zaria, Kaduna State, Nigeria. 2, 3& 6, Department of Veterinary Public Health and Preventive Medicine, Ahmadu Bello University Zaria, Kaduna State, Nigeria 4, Department of Biological Sciences, Faculty of Science, Taraba State University, Jalingo Taraba State, Nigeria. 5.

¹Corresponding author email: sjobidah@mau.edu.ng

ABSTRACT

Lactic Acid Bacteria (LAB) can produce a wide variety of secondary metabolites, with many having antifungal properties. In this study, 5 strains of LAB were isolated from soil samples collected from Nature Garden of Ahmadu Bello University Zaria, Nigeria and were screened for antifungal activity against *Aspergillus flavus*, *A. fumigatus*, *A. brasiliensis*, *Talaromyces purpureogenus*, *Penicillium notatum* and *Fusarium oxysporum* using overlay method. All isolates demonstrated strong activity with a range of 30.2±0.1 - 45.3±0.3 mm inhibition diameter. The identity of isolates was confirmed by comparing BLAST nucleotide sequences with those of Biological sequences within National Centre for Biotechnology Information (NCBI) database. The percentage of similarities between the 5 isolates and those available in GenBank ranged from 99.74 % for *Lactiplantibacillus plantarum* (KR816154.1), 99.80% *L. pentosus* (AB362757.1), 99.10%, *Levilactobacillus brevis* (CP031208.1), 99.26% *Lactiplantibacillus plantarum* (OQ224994.1) and lastly 99.85% *Lactiplantibacillus plantarum* (KY203913.1). *Lactiplantibacillus plantarum* OQ224994.1 cell-free extracts were obtained using solvent extraction with ethyl acetate, while column and thin-layer chromatography were used to purify constituent compounds. Antifungal compounds; Cyclopentadecane, Propionic Acid, 3-Iodo-, Heptadecyl Ester, Octacosane, Methanamine, N-(Phenyl Methylene)-, N-Oxide, Bis-(2-Ethylhexyl) Phthalate, Octadecanamide, 1,6-Octadiene, 5,7-Dimethyl-, (R) And Z-(13,14-Epoxy) Tetradec-11-En-1-Ol Acetate were identified based on Gas Chromatography Mass Spectrophotometry (GC-MS).

KEYWORDS

Antifungal, compounds, Lactic Acid Bacteria, *Lactiplantibacillus plantarum*, Soil.

1.0 INTRODUCTION

Lactiplantibacillus plantarum belongs to the family Lactobacillaceae of the larger group known as LAB which have been defined as a group of bacteria that produce large amount of lactic acid as a major end product of their carbohydrate fermentation (Karakas and Karakas, 2018). LAB are Gram positive, non-spore forming, catalase negative bacteria and comprises the following genera: *Aerococcus*, *Alloiococcus*, *Carnobacterium*, *Enterococcus*, *Lactobacillus*, *Lactococcus*, *Leuconostoc*, *Oenococcus*, *Pediococcus*, *Streptococcus*, *Symbiobacterium*, *Tetragenococcus*, *Vagococcus* and *Weissella* (Horvath *et al.*, 2009). LAB are found in many nutrient rich

environments and occur naturally in various food products such as dairy and meat products, and vegetables (Chen *et al.*, 2017).

Many moulds and yeast species are considered as common contaminants of foods and feed, because of their ubiquitous nature and the ability to thrive in a wide range of environmental conditions. Studies on fungal inhibition by lactic acid bacteria and the compounds produced by these bacteria is still novel. While a number of publications regarding antibacterial activity of LAB is large, our knowledge of the antifungal activities of these bacteria is still limited. Furthermore, it is a well-known fact that increasing amounts of microorganisms are becoming resistant to antibiotics. Fungi are no exceptions, and more species which are human pathogens and spoilage moulds in food and feed systems are becoming



resistant. However, yeasts and moulds are not only becoming resistant to antibiotics, but also to preservatives such as sorbic and benzoic acids, as well as chemical treatment with cleaning compounds (Perczak *et al.*, 2018)

LAB are widespread in nature, and are well known for their ability to produce lactic acid and a wide range of beneficial secondary metabolites. Majority of reports on antimicrobial activity of LAB have focused on antibacterial effects, while those on antifungal effects are few. In addition, using microorganisms to prevent fungal pollution has been sparking and gaining interest in recent years due to consumers' demand for reducing potential negative effects of chemical fungicides on the environment. The age-long tradition of using lactic acid bacteria in food and feed processing, in combination with recent knowledge on positive health benefits of ingestion of probiotic LAB, makes them a promising alternative (Aspri *et al.*, 2017).

2.0 LITERATURE REVIEW

The genus *Lactobacillus* is Gram-positive, homofermentative, thermophilic and non-spore forming rods. Most *Lactobacillus* species do not ferment pentoses and none of the organisms encodes genes for the pentose phosphate pathway or pyruvate formate lyase. They comprise 262 species that are extremely diverse at phenotypic, ecological and genotypic levels. (Zheng *et al.*, 2020). Based on the polyphasic approach, a proposed reclassification of the genus *Lactobacillus* into 25 genera including the emended genus *Lactobacillus*.

2.1 *Lactiplantibacillus plantarum*

Lactobacillus plantarum previously designated as *Streptobacterium plantarum* are non-motile rods occurring singly, in pairs, or in short chains. Some strains reduce nitrate in limited glucose concentration and pH 6.0 or higher. Some strains exhibit pseudo-catalase activity or true catalase when haeme is present. The species has a nomadic lifestyle; it is a dominant member of the microbiota in spontaneous vegetable and olive fermentations and also occurs in sourdough, dairy fermentations, and fermented meats (Gänzle, 2019; Hutkin, 2019). *L. plantarum* contributes to spoilage of beer and wine. *L. plantarum* also is part of the microbiota of insects and is isolated from the human intestinal tract, particularly the oral cavity. Two subspecies are recognized: *Lactiplantibacillus plantarum* subsp. *plantarum* and *Lactiplantibacillus*

plantarum subsp. *argenteratensis* (Storelli, *et al.*, 2018)

2.2 Antifungal Compounds Produced by *Lactobacillus*

Many *Lactobacillus* strains have been reported to produce antifungal molecules, including:

2.2.1 Organic Acids: LAB produce a large array of organic acids namely: lactic acid, acetic acid, propionic acid, citric acid, phenyllactic acid, benzoic acid, and other organic acids. A good number of these acids have demonstrated antifungal abilities; however, the mechanisms of action of some organic acids are still not clearly understood (Jin *et al.*, 2021). The ability of acetic acid to inhibit the growth of pathogenic fungi can be attributed to its low negative (-10) logarithm of acid (pKa). The higher concentration of undissociated acids can traverse the cell membrane, then dissociate in the cell, resulting in acid stress (Jin *et al.*, 2021). Other organic acids, lactic acid demonstrated weaker inhibitory effects (Crowley *et al.*, 2013). However, it is believed that lactic acid demonstrates a synergistic effect in association with other organic acids to ultimately enhance antifungal activity (Russo *et al.*, 2017).

2.2.2 Hydrogen Peroxide (H₂O₂): Some LAB produce H₂O₂, which has been shown to affectively hinder the growth and metabolism of foodborne pathogenic bacteria and fungi. As a strong oxidizer, H₂O₂ plunders electrons and molecules of nearby microorganisms and thus exerts its killing effect by destroying proteins molecular structure. Since LAB do not produce catalase, H₂O₂ cannot be decomposed, and therefore accumulates in the cell, preventing fungal growth. Martin and Maris (2012), reported that 3% H₂O₂ solution exhibited low antifungal activity against *Penicillium*, *Cladosporium*, *Scopulariopsis*, *Aspergillus*, and *Eurotium* but damaged conidia of seven fungal species.

2.2.3 Antifungal Peptides: Antifungal peptides are the main antifungal compounds produced by LAB. Arulrajah *et al.* (2021), used *Lactobacillus pentosus* RK3 to ferment kenaf seeds to produce antifungal peptides, where eight cationic peptides were identified in the fermentation mixture, which showed inhibitory effects on *Fusarium* and *Aspergillus brasiliensis*. Four of the peptides were shown to be similar to *Gossypium mustelinum* (cotton), two peptides corresponded to *Gossypium barbadense* (Sea-island cotton), and two were novel cationic *de novo* peptides. Similarly, Nionelli *et al.*



(2020), identified nine peptides from bread hydrolysates fermented by *Lactobacillus brevis*, and these peptides prevented growth of *Penicillium roqueforti*. The inhibitory effect of antifungal peptides on fungi is mainly due to the interaction between negatively charged molecules of the fungal membrane and positively charged polypeptides, which destroys the membrane structure resulting in cell death (Rai *et al.*, 2016).

3.0 MATERIALS AND METHODS

3.1 Isolation of Lactic Acid Bacteria

One (1 g) each of soil samples were taken and placed into 9 ml of sterile distilled water. Ten- fold serial dilutions were made from the mixture and 1 ml from the last 3 dilutions (10^{-7} , 10^{-8} and 10^{-9}) were pipetted and plated on De Man Rogosa and Sharpe (MRS) molten agar plates supplemented with 0.7% precipitated calcium carbonate obtained from National Institute for Chemical Research Technology Zaria, Nigeria. The plates were incubated anaerobically at 37 °C for 48 hours. Colonies with clear distinct zones around them were picked and transferred to new MRS agar plates by streaking to obtain pure colonies (Awan and Rahman, 2005).

3.2 Screening of Lactobacilli for Antifungal activity

The antifungal activity of LAB was investigated using an overlay assay. Bacteria were inoculated in 2 cm lines on MRS agar plates and allowed to grow at 30 °C under anaerobic condition for 48 hrs. Ten millilitre of soft molten potato dextrose agar containing 1 ml of (120×10^4 spores/ml) inoculum of mould spores were then poured onto the agar plates and incubated at room temperature for 3-5 days followed by measurement of zones of inhibition zone around the colonies (Lind *et al.*, 2005).

3.3 Molecular Characterization of Lactic Acid Bacteria Isolates

Molecular characterization was carried out to confirm the identity of LAB isolates by first extracting genomic DNA, followed by DNA quantification, PCR amplification of 16s RNA, Gel electrophoreses, Post-PCR purification and Sequencing carried out at Inqaba Biotech. West Africa Ltd, Ibadan, Nigeria.

3.4 Solvent Extraction and Purification of Antifungal Compounds

Twenty-four hour-old cells of LAB were used to inoculate a sterile MRS broth medium containing 5 % glucose in an Erlenmeyer flask. The pH of the medium was adjusted to 4.8 and incubated at 30 °C for 3 days. At the end of the fermentation cycle, the culture broth was filtered and the supernatants were separated by centrifugation at 8,000 rpm for 15 min. Antifungal compounds were extracted with ethyl acetate (99.5% purity LOVA CHEM. PVT. Ltd. India) (1:3 ratios) in a separation funnel. The Mixture were mixed properly and allowed to stand for 1hr. Solvent phase was collected and allowed to air dry at room temperature to obtain the crude bacterial cell free extracts (BCF) (Maraidhas *et al.*, 2014).

The Method of Talwinder *et al.* (2016), was adopted with slight modification. Dried Bacterial cell free extracts were mixed with 2 g of silica gel. On the other hand, slurry for column chromatography was prepared by adding 20 ml of Chloroform (99.5% purity LOVA CHEM. PVT. Ltd. India). The mixture was subjected to column chromatography using silica gel (60–120 mesh size; column, 1.5 cm \times 15 cm) packed and pre-equilibrated with chloroform. The column was then eluted step-wise with linear gradients of: chloroform/methanol (100:0, 90:10 and 80:20) at a flow rate of 2 ml/min. One hundred (100) ml of each gradient were used for elution, and a fraction of 25 ml each were collected and evaporated at room temperature. Final purification of the active compounds was achieved by preparative Thin Layer Chromatography (18 \times 20 cm plate).

3.5 Identification of the antifungal compounds using Chromatography/Mass Spectrometry (GC-MS).

Samples were analysed with a GC (7890B GC System) Mass spectroscopy detector (5977A MSD). (Agilent Technologies, Palo Alto, CA, USA). One microliter of each sample was injected with 1 min of split flow delay and resolved on a 30 m \times 0.25 mm -0.25 μ m DB- 5MS column (Agilent Technologies, Palo Alto, CA, USA). Inlet, interface, and ion source temperatures were 250, 250 and 230 °C, respectively. Oven starting and final temperatures were set at 50 and 230 °C, respectively, with a rate of 5 °C/min for 36 min and then for 2 min at a constant temperature. Electron impact mass spectra were recorded from m/z 50 to 550 at 70 eV. Metabolite annotation was achieved by mass spectra comparison with analytical standards, in house library and the NIST14 database



(National Institute of Standards and Technology, Gaithersburg, MD, USA) (Sacano *et al.*, 2021).

4.0 RESULTS AND DISCUSSION

4.1 Isolation of *Lactobacillus* from Soil Samples

Table 1: Number of *Lactobacillus* species isolated from soil samples in various location of Nature Garden of Ahmadu Bello University, Zaria.

Location	Number of Soil samples collected	Number <i>Lactobacillus</i> species Isolated
North	2	5
South	2	4
East	2	4
West	2	3
Central	2	5
Total	10	23

Lactic acid bacteria are mostly used as starter culture for the production of fermented dairy products, and they occur naturally as indigenous microbiota of the raw milk (Aspri *et al.*, 2017). However, these organisms are also ubiquitous and are widely spread in various niches such as; dairy, meat, vegetables, the gastrointestinal and urogenital tracts of humans and animals, soil and water (Liu *et al.*, 2014). The isolation of *Lactobacillus* was made easier by supplementing De Mann Rogosa and Sharpe (MRS) medium with 0.7% precipitated calcium carbonate (CaCO₃). Supplementing MRS medium has transformed the medium into a differential medium where *Lactobacillus* colonies growing on the medium were easily identified due to the formation of clear zones around them. *Lactobacillus* produces organic acids such as lactic acid and acetic acid as the main products of fermentation. These acids react with CaCO₃ to produce calcium lactate, which forms the clear zone around the *Lactobacillus* colonies. As described by Yusmarini *et al.* (2019), the function of adding CaCO₃ is to distinguish *Lactobacillus* from bacteria that are not acid producing, which is indicated by the presence of a clear zone in the media. CaCO₃ in the media will react with acids produced by lactic acid bacteria and form calcium lactate, which is soluble in the media and is visible by the formation of clear zones around the colonies.

Screening for Antifungal Activities of *Lactobacillus* species

A total number of 10 soil samples were collected, 2 each from the five cardinal points (North, South, East, West and Central) location within the Nature garden. Twenty-three (23) *Lactobacillus* species were isolated from the soil samples obtained (Table 1).

The twenty-three (23) *Lactobacillus* species isolated, were subjected to antifungal testing against test fungi namely; *Aspergillus flavus*, *A. fumigatus*, *A. brasiliensis*, *Talaromyces purpureogenus*, *Penicillium notatum*, and *Fusarium oxysporum* (Table 2). From the result, 6 *Lactobacillus* isolates designated by the codes (N1, N2, S2, S3, W4 and C4) demonstrated antifungal properties against the test fungi. The highest antifungal activity was recorded by isolates W4 with an inhibition diameter of 45.3±0.3 mm against *Aspergillus flavus*, whereas, the lowest activity of 30.2±0.1 mm inhibition diameter was demonstrated by isolate C2 against *Fusarium oxysporum*. Other isolates (N1, N2, S2, and S3) also produced antifungal activities with inhibition diameters ranging from (31.3±0.5- 41.4±0.4 mm) against all test fungi.

Lactobacilli have been reported to induce rapid acidification of raw materials during fermentation, producing a wide array of metabolites that have antifungal activities. These primarily include; organic acids, CO₂, H₂O₂, fatty acids, antifungal peptides, volatile compounds, and other antifungal compounds that inhibit fungal growth (Sadeghi *et al.*, 2019). They also produce large and varying quantity of proteolytic enzymes, comprising: cell-wall proteinases, peptide transporters, and ample intracellular peptidases, which are responsible for the biodegradation of mycotoxins and other cellular components produced by fungi into less toxic and less harmful/toxic compounds (Bangar *et al.*, 2021).



Table 2: Antifungal activity of *Lactobacillus* species against test fungi

L.B isolates	Zone of inhibition (mm)					
	A.f	A.fu	A.b	T. p	P. n	F.o
N1	31.3±0.5	-	35.0±0.8	-	40.3±0.5	-
N2	-	-	-	35.1±0.1	32.7±0.2	31.0±0.0
S3	-	40.5±0.2	-	31.7±0.5	-	-
S2	32.2±0.4	-	30.6±0.7	-	-	-
W4	45.3±0.3	-	36.0±0.8	-	41.4±0.4	-
C2	-	30.5±0.3	-	-	-	30.2±0.1

Key: **N1:** *Lactobacillus* species isolate North 1. **N2:** *Lactobacillus* species isolate North 2 **S2:** *Lactobacillus* species isolate South 2. **S3:** *Lactobacillus* species isolate South 3. **W4:** *Lactobacillus* species isolate West 4. **C2:** *Lactobacillus* species isolate Central 2. **A.f:** *Aspergillus flavus* **A.fu:** *Aspergillus fumigatus*. **A.b:** *Aspergillus brasiliensis*. **T.p:** *Talaromyces purpureogenus*. **P.n:** *Penicillium notatum*. **F.o:** *Fusarium oxysporum*

Molecular Confirmation of LAB Isolates

Polymerase Chain Reaction (PCR) amplification of 16S target region of isolates using 16S-27F and 16S-1492R primers were carried out and compared with the FASTA DNA ladder which contains varying fragment of DNA sizes. Figure 1 results of PCR amplification shows that five (5) isolates 16S RNAs were amplified and they all align with the 1Kb of the fast DNA ladder. Bacterial species have at least one copy of 16S rDNA gene containing highly conserved regions together with variable regions, which is used for identification of new strains. Variation can occur between species in both length and sequence of the 16S rDNA and its region therefore its useful for characterization of bacterial species (Todd, 2012). Results from this study is in

agreement with those carried out by Adeyemo and Onilude, (2014) and Gbemisola *et al.* (2020), which isolated and identified *L. plantarum* from fermenting cereals as well as molecular study of the Phytase Gene in Lactic Acid Bacteria isolated from *Ogi* and *Kunun-Zaki*, African fermented cereal gruel and beverage using 16S rDNA. Isolate (C2) designated as KMU-2 failed to amplify. No amplification of PCR fragment can be attributed to varying factors such as; use of wrong primer sequence or error in PCR primers, incorrect annealing and extension temperatures, incorrect primer concentration and template might be damaged or degraded or contain inhibitors, inadequate concentration of template in reaction (Todd, 2012).

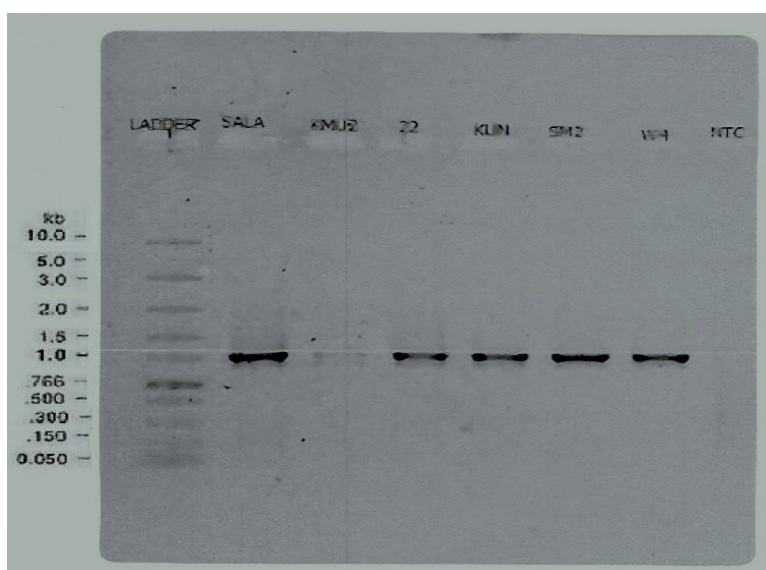


Figure 1: Gel electrophoresis of Amplicons of 16S rRNA of *Lactobacillus* species with size of 1kb.



Key: LADDER: DNA ladder indicating various DNA fragment sizes. **SALA:** Well for third isolate from Southern part of the garden (S3). **KMU-2:** well containing Isolate from central part of the garden. No band was detected. **22:** well for Second Isolate from the Northern part of the Garden (N2). **KUN:** well for first isolate from Northern part of the garden (N1). **SM2:** well for second isolate from southern part of the garden (S2). **W4:** well for the fourth isolate from the western part of the garden (W4). **NTC:** well containing Nuclease free water as negative control.

The percentage of similarities between the isolates and those available in GenBank ranged from 99.74 % for isolate N1 and is similar to *L. plantarum* (KR816154.1) 99.80% for isolate N2 which correspond to *L. pentosus* (AB362757.1), 99.10% for S2 correspond to *Levilactobacillus brevis* (CP031208.1). 99.26% for S3 isolate which is similar to *L. plantarum* (OQ224994.1) and lastly 99.85% for W4, corresponding to *L. plantarum* (KY203913.1). Table: 3. *L. plantarum* has the highest occurring organism. *L. plantarum* exhibits ecological and metabolic adaptability and is capable of inhabiting a range of ecological niches including fermented foods, meats, plants, and the mammalian gastro-

intestinal tract (Filannino *et al.*, 2018). Often, the ability of various bacterial strains to adapt to specific environment was proposed to be accomplished by genome specialization that facilitates niche-specific phenotypic fitness. This typically occurs via a process of genome decay in unutilized genes and enrichment of those that impart habitat specific fitness. This adaptive process generally ensures that individual bacterial strains isolated from the same ecological niche cluster genetically and carry similar niche specific genetic signatures. This has been demonstrated to be the case for *L. gasseri* and *L. jensenii* isolated from human vaginal environments and *L. reuteri* strains isolated from different vertebrate intestinal tracts (Mendes-Soares *et al.*, 2014).

Table 3: Results of Isolates and the similarities between Sequences queried and the Biologic sequences within National Centre for Biotechnology Information (NCBI) data base.

S/N	Isolate	Prediction (%)	GenBank Accession Number	BLAST Predicted Organism
1	N1	99.74	KR816164.1	<i>L. plantarum</i>
2	N2	99.80	AB362757.1	<i>Lactobacillus pentosus</i>
3	S2	99.10	CP031208.1	<i>Levilactobacillus brevis</i>
4	S3	99.26	OQ224994.1	<i>L. plantarum</i>
5	W4	99.85	KY203913.1	<i>L. plantarum</i>

Solvent Purification of Antifungal Compounds using Column Chromatography

Cell-free extracts of *L. plantarum* (OQ224994.1) were extracted using 99% ethyl acetate and were subjected to purification by column chromatography using Chloroform/methanol solvent systems in the following ratios: 100:0, 90:10, 80:20 and 70:30. 5ml fractions from each solvent systems were collected, given total 20 fractions. From these, the mass of antifungal compounds recovered after evaporation was 119 mg.

Gas Chromatography-Mass Spectrophotometry (GC-MS) of Antifungal Compounds from *L. plantarum* OQ224994.1

The highest area percent of 41.048% Cyclopentadecane, followed by Propionic acid, 3-iodo-, heptadecyl ester with 39.0599%, octacosane (4.1478%), Methanamine, N-(phenylmethylene)-, N-oxide (3.4085%), Bis(2-ethylhexyl) phthalate (2.8601%), octadecanamide (2.4989%), 1,6-Octadiene, 5,7-dimethyl-, (R)- (1.9323%) and Z-(13,14-Epoxy) tetradec-11-en-1-ol acetate (1.7149%). Other parameters such as peak number (PK), Retention Time (R.T), Chemical Abstract Service number (CAS) and Percentage quality are as shown from Table 4.



Our findings differ with the works of Chella *et al.* (2014), who reported lower area percentages of cyclopentadecane (1.13%), propionic acid (3.87%) and octacosane (1.82%). However, our results were in agreement with the work of Gamal (2020), who reported similar percentages of 40.34% cyclopentadecane (38.57%), propionic acid and (4.024%) for octacosane. Cyclopentadecane is a cyclic molecule with chemical formula C₁₅H₂₆. It has an average mass of 246.38 g/mol. It is used in the synthesis of many organic compounds, particularly-oxides, which are important for production of pharmaceuticals and agrochemicals. Cyclopentadecane is also found in plants and animals as a natural compound and act as an antioxidant to inhibit lipid peroxidation or as an anti-inflammatory agent (NIST, 2023). Cyclopentadecane is considered a volatile organic compound. These compounds have been implicated with various antifungal activities. The mechanism of antifungal activity of volatile organic compounds (VOCs) include; damage to the integrity of cell membranes, leading to the leakage of cell components and oxidative stress (Di Francesco *et al.*, 2016).

Propanoic acid-3-iodoheptadecylester belongs to the fatty acid family of antifungal compounds produced by *Lactobacillus* and other bacteria. Just

like other fatty acids, antifungal activity linked to cell membrane disruption. Propionic acid (PPA) and its derivatives also triggers a novel apoptotic cell death mechanism known as “mitochondria mediated apoptosis signalling” through the accumulation of ROS and activation of metacaspase. Several apoptotic markers, including; PS exposure (an early apoptosis marker) and DNA and nuclear fragmentation (late apoptosis markers), were observed in PPA-treated cells. An altered MMP and mitochondrial calcium uptake induced by PPA caused mitochondrial dysfunction. Because of this damage, cytochrome *c* was released from mitochondria into the cytosol, and apoptosis signalling was actively promoted (Jieun and Dong 2016).

N-(phenylmethylene)-, N-oxide is a hydroxyl group containing compound. The isoxalidine ring can react as a ligand for copper as well as many metals and the resulting compounds indicated strong antimicrobial activities (Faiz *et al.*, 2016). TPPO exhibited potential antifungal activities due to mitochondrial dysfunction in *Candida albicans* as TPP⁺-conjugates can bypass active expulsion by efflux pumps and accumulate in the fungal mitochondria to exert fungicidal activity (Chang *et al.*, 2018).

Table 4: Antifungal compounds from *L. plantarum* OQ224994.1

S/N0	PK	RT	Area (%)	Library/ID	Ref	CAS	Qual (%)
1	10	31.536 2	41.048	Cyclopentadecane	74571	000295-48-7	53
2	11	31.803 5	39.0599	Propionic acid, 3-iodo-, heptadecyl ester	253017	1000406-24-8	90
3	13	34.512 6	4.1478	Octacosane	235614	000630-02-4	96
4	4	26.354	3.4085	Methanamine, N-(phenylmethylene)-, N-oxide	15911	003376-23-6	38
5	15	35.402 3	2.8601	Bis(2-ethylhexyl) phthalate	233372	000117-81-7	87
6	12	33.584 7	2.4989	Octadecanamide	143048	000124-26-5	91
7	9	29.567 7	1.9323	1,6-Octadiene, 5,7-dimethyl-, (R)-	17356	085006-04-8	46
8	6	28.024	1.7149	Z-(13,14-Epoxy)tetradec-11-en-1-ol acetate	128537	1000131-33-2	41

Key: PK: Peak number. RT: Retention time. Ref: Reference number CAS: Chemical Abstract Service number. Qual: Quality.



Conclusion

In conclusion, this study isolated 5 *Lactobacillus* species namely; *L. plantarum* KR816164.1, *L. plantarum* OQ224994.1, *Lactobacillus pentosus* AB362757.1, *Levilactobacillus brevis* CP031208.1 and *Lactiplantibacillus plantarum* KY203913.1 from soil samples of the Nature garden of Ahmadu Bello University Zaria, Kaduna State. The *Lactobacillus* species demonstrated strong antifungal activities against the test fungi; *A. flavus*, *A. fumigatus*, *A. brasiliensis*, *T. purpureogenus*, *P. notatum* and *F. oxysporum*. It went further to identify various antifungal compounds produced in the cell-free extract of *L. plantarum* OQ224994.1 which comprises Cyclopentadecane, Propionic acid, 3-iodo-, heptadecyl ester, octacosane, Methanamine, N-(phenyl methylene)-, N-oxide, Bis-(2-ethylhexyl) phthalate, octadecanamide, 1,6-Octadiene, 5,7-dimethyl-, (R) and Z-(13,14-Epoxy) tetradec-11-en-1-ol acetate.



References

- S. M. Adeyemo, A. A. Onilude, Molecular identification of *Lactobacillus plantarum* from Fermenting cereals. *International Journal of Biotechnology and Molecular Biology Research*. 5(6), 59-67 (2014).
- B. Arulrajah, B. J. Muhiadin, M. S. Qoms, M. Zarei, A. S. M. Hussin, H. Hasan, Production of cationic antifungal peptides from kenaf seed protein as natural bio-preservatives to prolong the shelf-life of tomato puree. *International Journal of Food Microbiology*. 359, 109418, (2021).
- M. Aspri, D. Bozoudi, D. Tsaltas, C. Hill, P. Papademas, Raw donkey milk as a source of *Enterococcus* diversity: Assessment of their technological properties and safety characteristics. *Food Control*. 73, 81–90. (2017).
- J. A. Awan, S. U. Rahman, *Microbiology Manual*. Unitech Communications, Faisalabad, Pakistan. 49-51 (2005).
- S. R. Bangar, N. Sharma, M. Kumar, F. Ozogul, S. S. Purewal, M. Trif, Recent developments in applications of lactic acid bacteria against mycotoxin production and fungal contamination. *Food Bioscience*. 44:101444 (2021).
- W. Chang, J. Liu, M. Zhang, H. Shi, S. Zheng, X. Jin, Efflux pump-mediated resistance to Antifungal compounds can be prevented by conjugation with triphenylphosphonium cation. *National Communication*. 9, 5102 (2018).
- P. P. Chella, S. Sowmya, P. Prabhakaran, V. Balasubramanian, A. Palanirajan, S. Thangaraja
- V. D. Ramasamy, S. S. Jeya, K. G. Velliyur, Identification of novel PPAR γ agonist from GC-MS analysis of ethanolic extract of *Cayratia trifolia* (L.): a computational molecular simulation studies. *Journal of Applied Pharmaceutical Science*. 4 (09), 006-011 (2014).
- A. Perczak, P. Golinski, M. Bryla, A. Waskiewicz, The efficiency of lactic acid bacteria against Pathogenic fungi and mycotoxins. *Arhiv Za Higijenu RadaI Toksikologiju*, 69(1):32–45(2018).
- Y. Chen, Y. Liao, Y. Lan, H. Wu, F. Yanagida, Diversity of Lactic Acid Bacteria Associated with Banana Fruits in Taiwan. *Current Microbiology*. 74(4), 484–490 (2017).
- S. Crowley, J. Mahony, D. van Sinderen, Current perspectives on antifungal lactic acid bacteria as natural bio-preservatives. *Trends Food Science Technology*. 33, 93–109 (2013).
- Y. Faiz, W. Zhao, J. Feng, C. Sun, H. He, J. Zhu, Occurrence of triphenylphosphine oxide and other organo-phosphorus compounds in indoor air and settled dust of an institute building. *Build Environment*. 106, 196–204 (2016).
- A. Di-Francesco, M. Di Foggia, E. Baraldi, *Aureobasidium pullulans* volatile organic compounds as alternative postharvest method to control brown rot of stone fruits. *Food Microbiology*. 87, 103395 (2020).
- P. Filannino, M. De Angelis, R. Di Cagno, G. Gozzi, Y. Riciputi, M. Gobbetti, How *Lactobacillus plantarum* shapes its transcriptome in response to contrasting habitats. *Environmental Microbiology* 20, 3700–3716 (2018).
- A. I. Gamal, M. Osama, M. S. Sharaf, A. M. Al-Gamal, N. M. Youssef, M. Dabiza, F. El Ssayad, Extraction, Evaluation and Structure Elucidation of Bioactive Metabolites of *Lactobacillus helveticus* CNRZ 32. *Bio interface Research in Applied Chemistry*. 11 (1): 7677 – 7688 (2021).
- P. Horvath, A. C. Coûté-monvoisin, A. D. Romero, P. Boyaval, C. Fremaux, R. Barrangou, Comparative analysis of CRISPR loci in lactic acid bacteria genomes. *International Journal of*



- Food Microbiology, 131, 15th Meeting of the Club des Bacteries Lactiques, 62–70 (2009).
- R. W. Hutkins, *Lactobacillus*. Microbiology and technology of fermented foods, 2nd. IFT Press, Chigaco, Illinois (2019).
- Y. Jieun, G. L. Dong, A novel fungal killing mechanism of propionic acid. FEMS Yeast Research. 16(7): 1-9 (2016).
- H. Martin, P. Maris, Synergism between hydrogen peroxide and seventeen acids against five Agri-food-borne fungi and one yeast strain. Journal of Applied Microbiology. 113, 1451–1460 (2012).
- (NIST) National Institute of Standard and Technology. Top, Mass spectrum. Gas Chromatography. NIST Chemistry webbook 69, 2-3 (2023).
- L. Nionelli, Y. Wang, E. Pontonio, M. Immonen, C. G. Rizzello, H. N. Maina, Antifungal Effects of bioprocessed surplus bread as ingredient for bread-making: identification of active Compounds and impact on shelf-life. Food Control. 118, 107437 (2020).
- J. Jin, T. T. H. Nguyen, S. Humayun, S. Park, H. Oh, S. Lim, Characteristics of sourdough Bread fermented with *Pediococcus pentosaceus* and *Saccharomyces cerevisiae* and its bio-Preservative effect against *Aspergillus flavus*. Food Chemistry 345, 128787 (2021).
- E. Karakas, A. Karakas. Isolation, identification and technological properties of lactic acid Bacteria from raw cow milk. Bioscience Journal 34(2): 385-399. (2018).
- H. Lind, H. Jonsson, J. Schnürer, Antifungal effect of dairy propionibacteria contribution of organic acids. International Journal of Food Microbiology 98, 157-165 (2005).
- W. Liu, H. Pang, H. Zhang, Y. “Biodiversity of lactic acid bacteria,” in *Lactic Acid Bacteria*, eds H. Zhang and Y. Cai . Dordrecht: Springer, 103–203 Cai, (2014).
- V. A. Mariadhas, K. Da Hye, K. Pyoung, J. Min Woong, I. Soundarrajan, J. Mariamichael, D. L. Kyung, A. A. Naif, C. Ki Choon, In vitro antifungal, probiotic and antioxidant properties of novel *Lactobacillus plantarum* K46 isolated from fermented sesame leaf. Annals of Microbiology.64, 1333–1346 (2014).
- H. Mendes-Soares, H. Suzuki, R. J. Hickey, L. J. Forney, Comparative functional genomics of *Lactobacillus* spp. reveals possible mechanisms for specialization of vaginal lactobacilli to their environment. Journal of Bacteriology 196, 1458–1470 (2014).
- K. S. Talwinder, J. A. Roberto, C. Mei-Chen, Sensory evaluation of gluten-free quinoa whole grain snacks. Heliyon 2(12), 35-55 (2016).
- C. L. Todd, Polymerase Chain Reaction: Basic Protocol plus Troubleshooting and Optimization Strategies. Journal of Visualized Experiment 63: 3998 (2012).
- F. L. Tulini, N. Hymery, T. Haertlé, G. Blay, E. C. Le-Martinis, Screening for antimicrobial and proteolytic activities of lactic acid bacteria isolated from cow, buffalo and goat milk and cheeses marketed in the southeast region of Brazil. The Journal of Dairy Research, 83 (1), 115 124. (2016).
- M. Rai, R. Pandit, S. Gaikwad, G. Kovics, Antimicrobial peptides as natural bio-preservative to enhance the shelf-life of food. Journal Food Science and Technology 53, 3381–3394 (2016).
- P. Russo, M. P. Arena, D. Fiocco, V. Capozzi, D. Drider, G. Spano, *Lactobacillus plantarum* with broad antifungal activity: a promising approach to increase safety and shelf-life of cereal based products. *International Journal of Food Microbiology*. 247, 48–54 (2017).



- A. Sadeghi, M. Ebrahimi, S. A. Mortazavi, A. Abedfar, Application of the selected antifungal LAB isolate as a protective starter culture in pan whole-wheat sourdough bread. *Food Control* 95, 298–307 (2019).
- P. Scano, M. B. Pisano, A. Murgia, S. Cosentino, P. Caboni, GC-MS Metabolomics and Antifungal Characteristics of Autochthonous *Lactobacillus* Strains. *Dairy*. 2, 326–335 (2021).
- G. Storelli, M. Strigini, T. Grenier, L. Bozonnet, M. Schwarzer, C. Daniel, R. Matos, F. Leulier, *Drosophila* perpetuates nutritional mutualism by promoting the fitness of its intestinal symbiont *Lactobacillus plantarum*. *Journal of Cell Metabolism* 27, 362-377 (2018).
- J. V. S. Yusmarini, S. Fitriani, S. Rahmayuni, V. F. Artanti, U. Pato, Characteristics of probiotic tapai made by the addition of *Lactobacillus plantarum* 1. *International Journal of Agricultural Technology*. 15(1), 195-206 (2019).
- J. Zheng, W. Stijn, S. Elisa, M. A. Charles, P. Franz, H. Harris, M. B. Paola, M. Paul, W. O’Toole, B. P. Peter, V. Jens, W., Koichi, W. Sander, W. Giovanna, G.G Michael, A taxonomic note on the genus *Lactobacillus*: Description of 23 novel genera, emended description of the genus *Lactobacillus* Beijerinck 1901, and union of *Lactobacillaceae* and *Leuconostocaceae*. *International Journal of Systematic and Evolutionary Microbiology*. 1-75(2020).
- M. G. Gänzle, Fermented Foods. In: *Food Microbiology. Fundamentals. Frontiers*. Doyle MP, Diez- Gonzalez F, Hill C (eds) ASM Press, pp 855–900. (2019).



P052 - RESISTOTYPING OF ESCHERICHIA COLI AND LISTERIA SPP. ISOLATED FROM MILK AND MILK PRODUCTS SOLD AROUND ZARIA

M. M. Fathuddin^{1*}, S. A. Ado², M. B. Tijjani³, H. M. Kazeem⁴, J. S. Obidah⁵, L. E. O. Ameh⁶

Department of Microbiology, Ahmadu Bello University Zaria, Kaduna State, Nigeria.1, 2, 3 & 6, Department of Veterinary Microbiology, Ahmadu Bello University Zaria, Kaduna State, Nigeria 4, Department of Microbiology, Modibbo Adama University Yola, Adamawa State, Nigeria 5.

Corresponding author email: muhsinfathuddin@gmail.com

ABSTRACT

The World Health Organisation (WHO) has identified *Escherichia coli* and *Listeria* spp. as major causes of foodborne bacterial gastrointestinal infections worldwide, with dairy products being the most common source. A total of 66 isolates *E. coli* (44) and *Listeria* spp. (22) were isolated from 400 milk product samples subjected to Antimicrobial Susceptibility Testing (AST) via Disc Diffusion and E-Test Methods. The Disc Diffusion Method showed that 11 (17.19%) isolates were sensitive to all tested antibiotics, while 16 (25.01%) were resistant to a single antibiotic. Thirty-one (54.69%) were resistant to two antibiotics, and two (03.13%) showed resistance to at least three antibiotics. Only two (03.13%) showed resistance to all four antibiotics. Resistance was most frequently observed to Tetracycline (20.83%), followed by Ampicillin (13.26%), Gentamicin (02.65), and Ciprofloxacin (01.14%). On the E-Test, for *E. coli*, the resistance rate for Ampicillin (60%) Gentamicin, and Ciprofloxacin at 00% and TET (100%). *Listeria* spp. had Ampicillin 60% susceptibility and were indeterminate to Ciprofloxacin, Gentamicin and Tetracycline due to no breakpoint available. Based on these findings, it is clear that urgent action is required to address the growing problem of Antimicrobial Resistance (AMR) and prevent the spread of antibiotic-resistant pathogens.

KEYWORDS

Resistotyping, Escherichia coli, Listeria spp., Antibiotics, Milk, Milk-products

1.0 INTRODUCTION

Cattle, in particular, are critical to sub-Saharan Africa's industries, providing meat, milk, by-products, draught power, and income generation (Umaru *et al.*, 2016). In 2020, it was estimated that 20.7 million cattle were reared in Nigeria, primarily in small and medium-scale units owned by the Fulani (Ajayi *et al.*, 2023). Diseases that limit cattle production, on the other hand, hurt socioeconomic aspects such as poor growth, abortion, and decreased milk yield (Kikwai *et al.*, 2022; Avila-Granados *et al.*, 2019). Milk is locally processed by the Fulanis and consumed in many African countries, including Nigeria (Aboki *et al.*, 2019). Milk and its products, on the other hand, can harbour microorganisms that can cause diseases such as *Brucellosis*, *Cholera*, *Colibacillosis*, *Listeriosis*, *Salmonellosis*, *Shigellosis*, *Staphylococcosis*, *Tuberculosis*, and others. (Aworh *et al.*, 2021; Rahman, *et al.*, 2019). Although the presence of *Escherichia (E.) coli* and *Listeria* spp., including antibiotic-resistant strains, in raw milk, fermented milk, and other milk products has been studied and documented around

the world (Ababu *et al.*, 2020; Praça *et al.*, 2023), including Nigeria (Kayode and Okoh, *et al.*, 2022; Okon *et al.*, 2022). Current information on the safety of raw cow milk and fermented milk products in Zaria along with the occurrence of *E. coli* and *Listeria* spp., as well as antibiotic resistance patterns are limited. The goal of this research was to determine the resistance pattern of *E. coli* and *Listeria* spp. found in cow milk and fermented milk in Zaria, Nigeria.

2.0 LITERATURE REVIEW

2.1. Fermented Dairy Products

Traditional fermented dairy products are crucial for food security and diet in Africa, as they contain high nutrients which include; amino acids, lipids, and vitamins (Noah and Salam, 2020). Milk, a highly perishable product, is used in fermentation to increase shelf life (Obioha *et al.*, 2023). Raw cow



milk is known as 'Madara' and its products such as skimmed milk is 'Nunu/Nono', local yoghurt is 'Kindirimo', and milk fat is 'Mai-shanu' (Agu *et al.*, 2015; Makut and Ishaya 2012). These products are versatile and used to create various commercial products like Cheese, Yoghurt, Nono, and Kindirimo (Noah and Salam, *et al.*, 2020). Kindirimo is popular among Hausas in northern Nigeria, while Nono is skimmed or partially cultured skimmed milk (Oyeyinka *et al.*, 2023). Yoghurt, a sour custard-like food made from milk curdled by bacteria like *Lactobacillus bulgaricus* and *Streptococcus thermophilus*, has been around for a long time and has a similar texture and flavour to fruit. (Keta *et al.*, 2020). These products are consumed without further heat treatment and are becoming increasingly popular due to their perceived health benefits (Obioha *et al.*, 2023). However, the crude nature of the production process has raised food safety concerns, as it has been found to contain potentially pathogenic microorganisms such as *Escherichia coli*, *Salmonella*, *Shigella*, *Staphylococcus aureus*, and *Bacillus cereus* (Fagbemigun, *et al.*, 2021; Obioha *et al.*, 2023).

2.2. Organisms

Gram-negative bacteria, particularly Enterobacteria, are common in dairy foods. These bacteria can be found in milk, introduced during the manufacturing process, or as part of starter or adjunct cultures. Pathogens can also contaminate fermented dairy products, potentially causing rare cases or outbreaks of disease if multiplication occurs during manufacturing or storage (Fernández *et al.*, 2015). *E. coli* is a versatile bacterium that belongs to the *Proteobacteria* phylum and the genus *Escherichia* and is noted for its genetic and phenotypic variety (Petitjean *et al.*, 2021; Pitout and Finn, 2020; Yu *et al.*, 2021). *E. coli* is a well-studied model organism with a high level of genetic diversity and adaptation to different environments and hosts (Koteswar *et al.*, 2017; Mailyan, 2016; Sonowal, and Shariff, 2019). **Murray and colleagues initially identified *Listeria* in rabbit fatalities in 1924. Pirie called *Listeria hepatolytica***

in 1927 **after Sir Joseph Lister, was a pioneer in antiseptics.** In 1929, three patients in Denmark were diagnosed with *Listeria*-induced infectious mononucleosis. **To standardise the bacterium's naming, the name *Listeria monocytogenes* was selected in 1940** (Kaptchouang Tchatchouang *et al.*, 2020). *Listeria monocytogenes*, *Listeria innocua*, *Listeria seeligeri*, *Listeria welshimeri*, *Listeria ivanovii*, *Listeria grayi*, and *Listeria murrayi* are among the species in the phylum *Firmicutes* (Nwaiwu, 2020).

3.0 MATERIALS AND METHODS

3.1 STUDY AREA:

The study area included two (2) local government areas (Soba-gari and Zaria) in Kaduna state, see Figure 1.

3.2 ISOLATED ORGANISMS: Between October 2022 and March 2023, a total of 66 isolates [*Escherichia coli* (44 isolates) and *Listeria* spp. (22 isolates)] were isolated from 400 samples [100 each] of milk and milk products (*Kindirimo*, *Nono*, and Yoghurt) sold in the Zaria and Sabon-gari.

3.3 ANTIMICROBIAL SUSCEPTIBILITY TEST (AST)/RESISTOTYPING: The AST for Ampicillin (AMP), Ciprofloxacin (CIP), Gentamicin (GEN), and Tetracycline (TET) were performed concurrently with Disc Diffusion Test (Bioanalyse, Turkey) using AM30µg, CIP05µg, GM10µg and TE10µg respectively and E-Test (HiMedia, India) per the Clinical and Laboratory Standards Institute (CLSI) and The European Committee on Antimicrobial Susceptibility Testing (EUCAST) reference methods. Mueller-Hinton Agar (HiMedia, India) plates were produced fresh for each test. The Minimum Inhibitory Concentration (MIC) and Zone of Inhibition (ZOI) values of AMP, CIP, GEN, and TET are interpreted as S (Susceptible), I (Intermediate), or R (Resistant) using the criteria indicated at <http://em100.edaptivedocs.net> (CLSI) and <http://www.eucast.org> (EUCAST) (Han *et al.*, 2022).



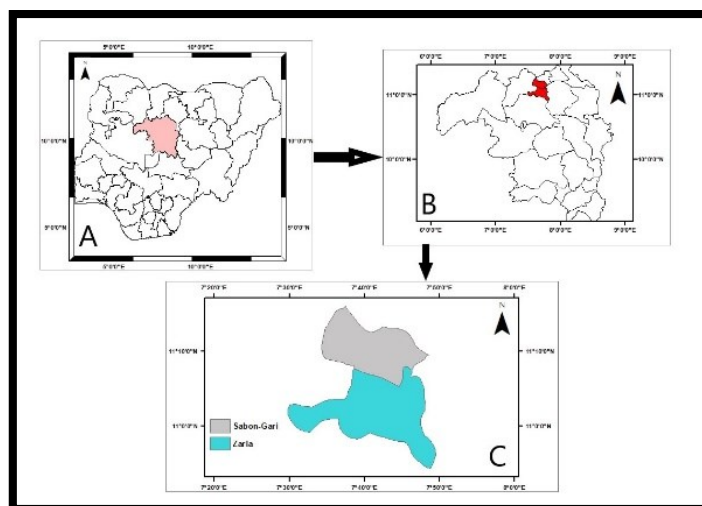


Figure 01: Map of Zaria and Sabon-gari

4.0 RESULTS AND DISCUSSION

Figure 2 shows the ZOI results for the antibiotic AMP against *E. coli* with the CLSI breakpoints (Resistance (R) <13, Intermediate (I) 14-16-, Susceptible (S) ≥17), and the EUCAST breakpoints (R<14, S≥14). According to CLSI, 34 (77.27%) of the isolates were resistant, with 00 (00.00%) intermediate and 10 (22.73%) susceptible. In the case of EUCAST, 34 (77.27%) were resistant, while 10 (22.73%) were susceptible.

From Figure 3, the CLSI breakpoints for ZOI (CIP) on *E. coli* are R<21, I 22-25, and S≥26; while the EUCAST breakpoints are R<22, I 22-25, and S≥25. A total of 16 Isolates were resistant (36.36%), with 14 (31.82%) intermediate and 14 (31.82%) susceptible according to both CLSI and EUCAST.

Figure 4 depicts the ZOI (GEN) on *E. coli* with CLSI breakpoints R<14, I 15-17, S≥18; and EUCAST breakpoints R<17, S≥17. On CLSI, 07 Isolates (15.91%) were resistant, with 02 (04.55%) intermediate and 35 (79.55%) susceptible, whereas on EUCAST, 09 (20.45%) resistant and 36 (81.82) susceptible.

Figure 5 depicts the ZOI (TET) with a CLSI breakpoint of R<11, I 12-14, S≥15; however, the EUCAST has no breakpoint for the tetracycline as it is not recommended for AST. According to CLSI, there were 42 resistant (95.45%), 01 intermediate (02.27%), and 01 susceptible (02.27%).

In a study by Igbinsosa, and Chiadika, (2021) on *E. coli* O157:H7 isolated from raw and

fermented (*Nono*) milk in Benin City, Nigeria, their resistance rates findings are in contrast with ours as our AMP (77.27%) against their 100%. And our CIP and GEN findings had a resistance rate of 36.36% and 15.91% respectively, in contrast to theirs (*E. coli* O157:H7 0% both, *E. coli* 02.4% and 14.5%). According to our TET resistant rate of 95.45% in contrast to theirs of *E. coli* O157:H7 36.8% and *E. coli* 51.2%, It was found that they is a progressive decrease in resistance to the antibiotics AMP, TET, CIP, GEN as shown by the percentages (100/100%-51.2/36.8%-0/14.5%-0/02.4%) respectively, and in our study TET, AMP, CIP, GEN i.e., (95.45%-77.27%-36.36%-15.91%) respectively.

Figure 6-9 depicts the ZOI on *Listeria* spp. for the selected drugs. However, AMP cannot be compared due to the difference in drug concentration recommended by EUCAST i.e., 2µg/ml and CLSI (CLSI M45, 2016) does not have breakpoints for disk diffusion method but only for MIC. To this end, the results were not classified due to the absence of available breakpoints for CIP, GEN, and TET on CLSI or EUCAST for *Listeria* spp.

However, considering R=5, 22 cases of resistance were observed to these drugs, the highest resistance was recorded with TET (14, 63.64%), then AMP (04, 18.18%), GEN (03, 13.64%) and the least in CIP (01, 04.55%). In our study, most resistance was found with TET, AMP, GEN, CIP (63.64%-18.18%-13.64%-04.55%) respectively.



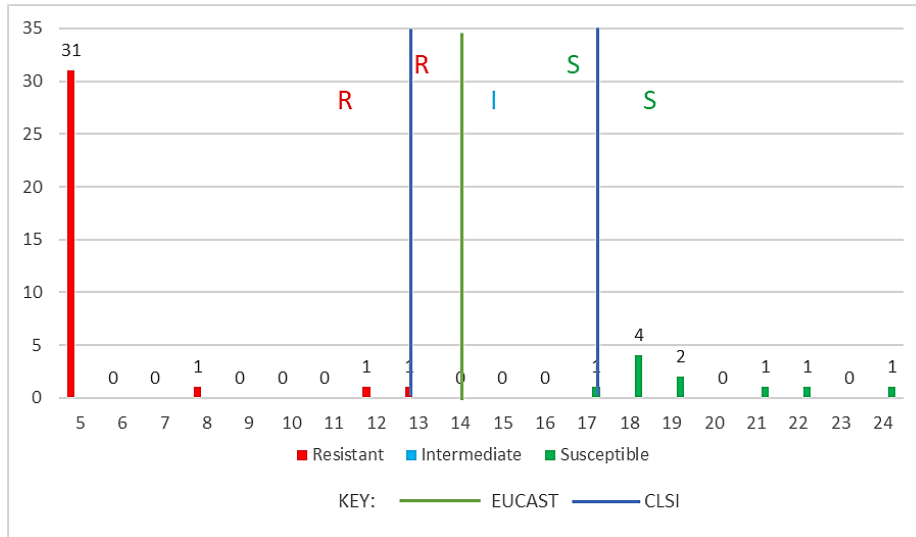


Figure 02: AST Using Ampicillin (AM30µg) on *E. coli*

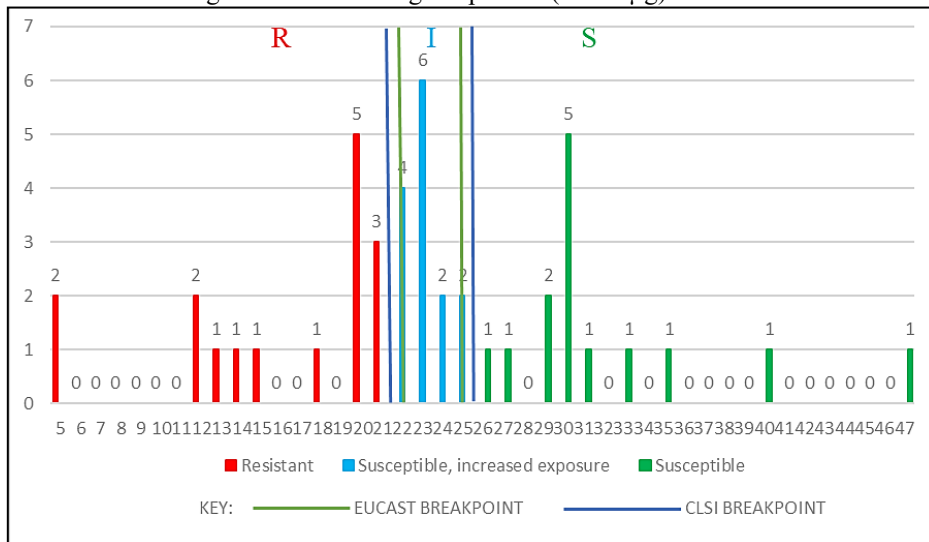


Figure 03: AST Using Ciprofloxacin (CIP05µg) on *E. coli*

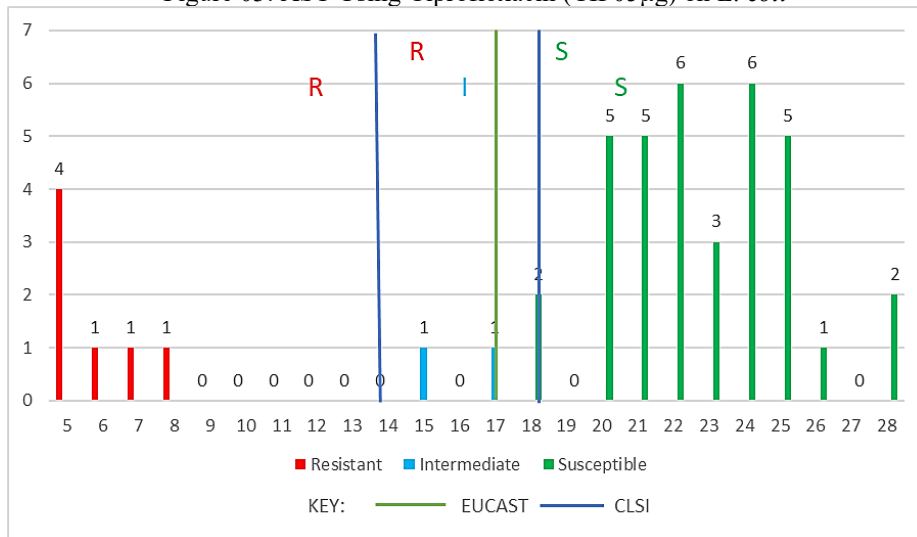


Figure 04: AST Using Gentamicin (GM10µg) on *E. coli*



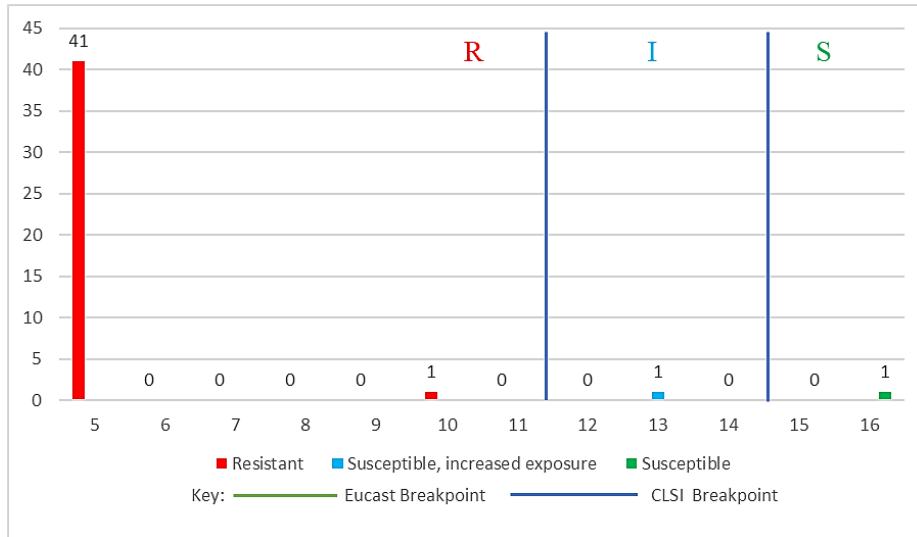


Figure 05: AST Using Tetracycline (TE10µg) on *E. coli*

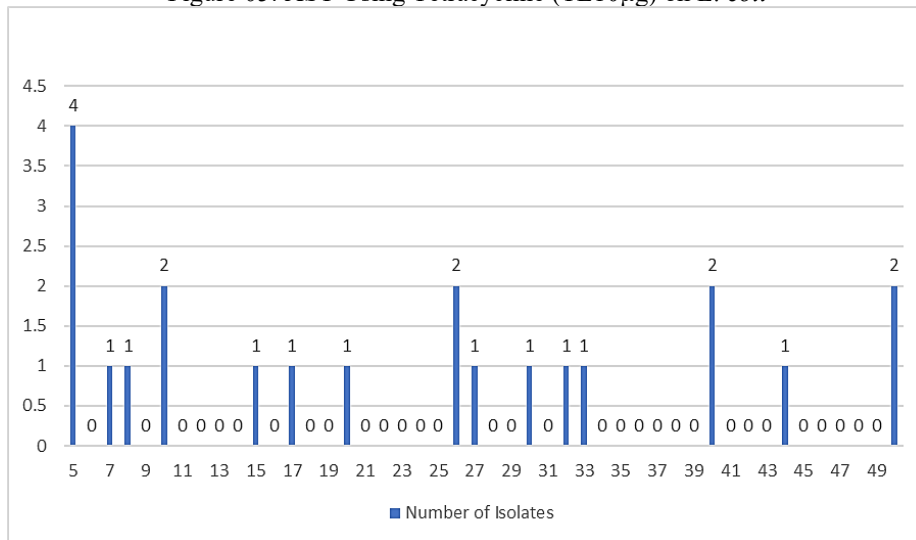


Figure 06: AST Using Ampicillin (AM30µg) on *Listeria* spp.

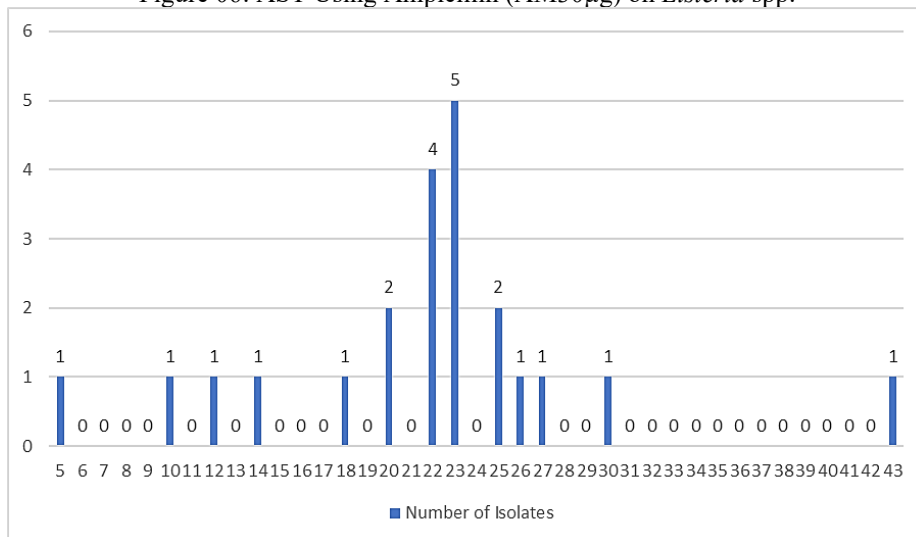


Figure 07: AST Using Ciprofloxacin (CIP05µg) on *Listeria* spp.



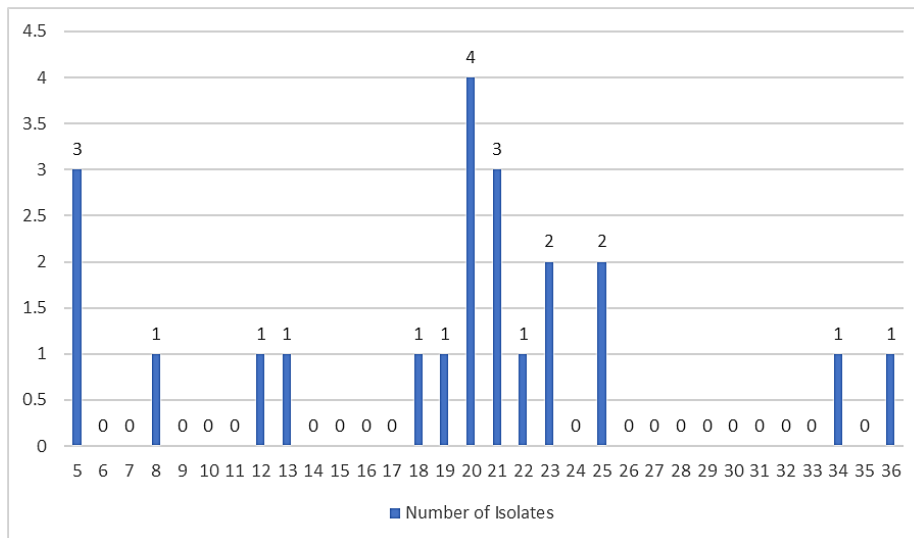


Figure 08: AST Using Gentamicin (GM10µg) on *Listeria* spp.

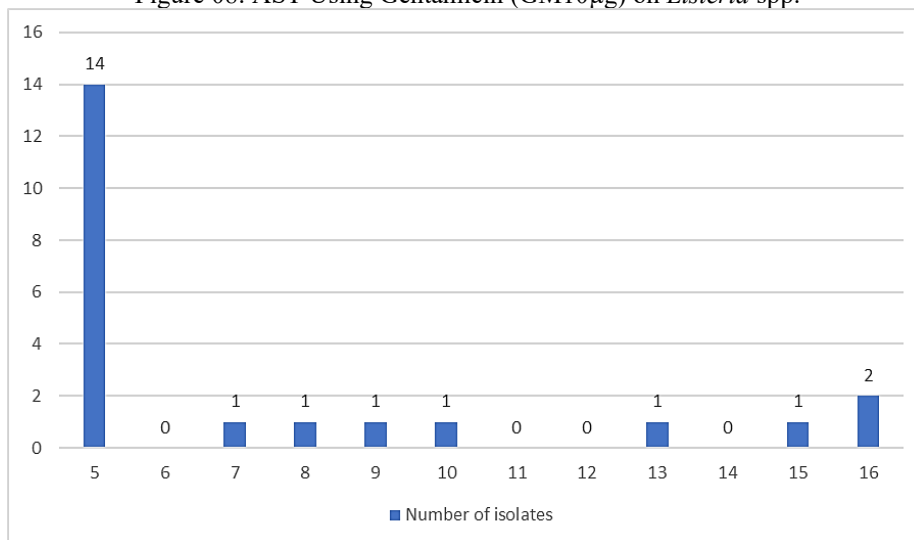


Figure 09: AST Using Tetracycline (TE10µg) on *Listeria* spp.

The data presented in Table 1 clearly shows that *E. coli* displayed 5 distinct Antimicrobial Resistance Patterns (ARPs) across Groups A, B, H, N and P, meanwhile *Listeria* spp. exhibited 4 ARPs in Groups A, B, H, and K. The largest resistant population of 31 (48.44%) is in Group H with primary resistance to AMP and TET. From these nine (9) groups, representatives were selected for the E-test MIC i.e., 2 per group, total of 18 organisms.

Table 2 highlights the E-Test pattern. The MIC breakpoints for *E. coli*, CLSI (AMP S≤08 I16 R≥32; CIP S≤0.25 I0.5 R≥01; GEN S≤02 I04 R≥08, TET S≤04 I08 R≥16). However, EUCAST

does not have a breakpoint for E-Test, as such the micro-dilution method for MIC is most preferred. A variation was specifically observed for *E. coli*, selected isolates from Groups A and B were susceptible to AMP while the other groups were resistant, the selected organisms were susceptible to CIP and GEN even Group P isolates, also all isolates were resistant to TET. The resistance rate observed of 60% in AMP, 0 for both CIP and GEN while 100% for TET. When compared with Ayaz *et al.*, (2015) out of the 102 *E. coli*, the resistance rate was observed for AMP at 14.7%, CIP at 00% and TET at 24.5%. In another study by Šiugždaitė *et al.*, (2018) out of the 48 *E. coli* tested, resistance rates were observed to AMP (77.1%), TET (64.6%) GEN (41.7%) and enrofloxacin (27.1%) similar drug to CIP. Malekzadegan *et al.*, (2018) out of the 126 *E. coli* isolates, had the resistance rate observed against AMP (88.9%), GEN (19.8%), and CIP (15.1%).



While for *Listeria* spp., CLSI (AMP S≤02 I- R-, CIP S- I- R-, GEN S- I- R-, TET S- I- R-). A variation was also specifically observed for *Listeria* spp., selected isolates from Groups A, H and K were susceptible to AMP while Group B was resistant when it should be resistant to only TET. Unfortunately, the selected organisms were indeterminable to CIP, GEN and TET due to no breakpoint available for both CLSI and EUCAST. Only AMP had a susceptible rate of 60%.

5.0 CONCLUSIONS

According to this study, antibiotic resistance among pathogenic bacterial strains in milk and milk products is emerging in Zaria, Nigeria. This is

corroborated by antibiotic susceptibility tests on isolated *E. coli* and *Listeria* spp. Furthermore, according to CLSI, TET had the highest resistance among *E. coli* (95.45%), while EUCAST had AMP (77.27%). TET (95.45%), AMP (77.27%), CIP (36.36%), and GEN (15.91%) showed the overall resistance. *Listeria* spp., showed a resistance pattern of TET (63.64%), AMP (18.18%), GEN (13.64%), and CIP (04.55%). Group H had the most resistant population, with predominant resistance to AMP and TET. According to the E-Test, both CIP and GEN were most effective across all groups for *E. coli*, TET was completely resistant, and AMP was 60% resistant among tested isolates. We are unable to identify the level of resistotyping/antimicrobial susceptibility testing for *Listeria* spp. due to absence of defined breakpoint.

Table 1: AST Summary

Group	Antimicrobial Resistance Pattern (Resistotyping)	Number Of Antibiotics	MAR Index	Number Of Isolates	Percent	Organism (Percent)
A	AM-CIP-GM-TE	0	0.00	011	017.19	<i>Listeria</i> spp. (12.5), <i>E. coli</i> (04.7),
B	AM-CIP-GM-TE	1	0.25	016	025.01	<i>E. coli</i> (15.6), <i>Listeria</i> spp. (09.4),
C	AM-CIP-GM-TE	1	0.25	000	000.00	-
D	AM-CIP-GM-TE	1	0.25	000	000.00	-
E	AM-CIP-GM-TE	1	0.25	000	000.00	-
F	AM-CIP-GM-TE	1	0.50	000	000.00	-
G	AM-CIP-GM-TE	2	0.50	000	000.00	-
H	AM-CIP-GM-TE	2	0.50	031	048.44	<i>E. coli</i> (42.2), <i>Listeria</i> spp. (06.3),
I	AM-CIP-GM-TE	2	0.50	000	000.00	-
J	AM-CIP-GM-TE	2	0.50	000	000.00	-
K	AM-CIP-GM-TE	2	0.50	004	006.25	<i>Listeria</i> spp. (06.3)
L	AM-CIP-GM-TE	3	0.75	000	000.00	-
M	AM-CIP-GM-TE	3	0.75	000	000.00	-



N	AM-CIP-GM-TE	3	0.75	002	003.13	<i>E. coli</i> (03.1),
O	AM-CIP-GM-TE	3	0.75	000	000.00	-
P	AM-CIP-GM-TE	4	1.00	002	003.13	<i>E. coli</i> (03.1)
Total	031-036-058-011			066	100.00	100.0

Key: Green – Susceptible, Red – Resistance

Table 2: E-Test Summary

Organism	Antibiotic strip (Abb.)	Concentration [$\mu\text{g/ml}$]	CLSI breakpoints (MIC) [$\mu\text{g/ml}$]			Number of isolates*		
			S	I	R	S	I	R
<i>Escherichia coli</i>	Ampicillin (AMP)	0.016-256	≤ 08	16	≥ 32	04	-	06
	Ciprofloxacin (CIP)	0.016-256	≤ 0.25	0.5	≥ 01	10	-	-
	Gentamicin (GEN)	0.016-256	≤ 02	04	≥ 08	10	-	-
	Tetracycline (TET)	0.016-256	≤ 04	08	≥ 16	-	-	10
<i>Listeria</i> spp.	Ampicillin (AMP)	0.016-256	≤ 02	-	-	06	-	-
	Ciprofloxacin (CIP)	0.016-256	-	-	-	-	-	-
	Gentamicin (GEN)	0.016-256	-	-	-	-	-	-
	Tetracycline (TET)	0.016-256	-	-	-	-	-	-

6.0 REFERENCES

G. A. Umaru, J. K. P. Kwaga, M. Bello, M. A. Raji, Y. S. Maitala, Antibiotic resistance of *Staphylococcus aureus* isolated from fresh cow milk in settled Fulani herds in Kaduna State, Nigeria. *Bulletin of Animal Health and Production in Africa*, 64(1), 173-182 (2016).

M. O. Ajayi, E. B. Herbert, A. Imosemi, N. Nyekwere, D. T. Eyongndi, O. O. Oladele, Legal Implications of Free-Range System of Rearing Cattle in Nigeria: A Review. In IOP Conference Series: Earth and Environmental Science (Vol. 1219, No. 1). (IOP Publishing, 2023). p. 012013

C. Kikwai, M. Ngeiywa. Review on the Socio-Economic Impacts of Trypanosomiasis. *Africa Environmental Review Journal*, 5(2), 89-100 (2022).

L. M. Avila-Granados, D. G. Garcia-Gonzalez, J. L. Zambrano-Varon, A. M. Arenas-Gamboa.

Brucellosis in Colombia: Current status and challenges in the control of an endemic disease. *Frontiers in veterinary science*, 6, 321. (2019)

E. I. Aboki, I. I. Umar, M. O. Akintunde, E. D. Mashikan, Economics of cow milk production in Yola South local government area of Adamawa State, Nigeria. *South Asian Research Journal of Agriculture and Fisheries*, 1(2), 44-49 (2019).

O. C. Aworh, Food safety issues in fresh produce supply chain with particular reference to sub-Saharan Africa. *Food Control*, 123, 107737 (2021).

M. T. Rahman, M. A. Sobur, M. S. Islam, S. Ievy, M. J. Hossain, M. E. El Zowalaty, H. M. Ashour. Zoonotic Diseases: Etiology, Impact, And Control. *Microorganisms*, 8(9), 1405. (2020).



- A. Ababu, D. Endashaw, H. Fesseha. Isolation and antimicrobial susceptibility profile of *Escherichia coli* O157: H7 from raw milk of dairy cattle in Holeta district, Central Ethiopia. *International Journal of Microbiology*, 2020, 1-8. (2020).
- F. Akrami-Mohajeri, Z. Derakhshan, M. Ferrante, N. Hamidiyan, M. Soleymani, G. O. Conti, R. D. Tafti. The prevalence and antimicrobial resistance of *Listeria* spp in raw milk and traditional dairy products delivered in Yazd, central Iran (2016). *Food and Chemical Toxicology*, 114, 141-144. (2018).
- J. Praça, R. Furtado, A. Coelho, C. B. Correia, V. Borges, J. P. Gomes, A. Pista, R. Batista, *Listeria monocytogenes*, *Escherichia coli* and Coagulase Positive Staphylococci in Cured Raw Milk Cheese from Alentejo Region, Portugal. *Microorganisms*, 11(2), 322. (2023).
- R. Ranjbar, F. Safarpour Dehkordi, M. H. Sakhaei Shahreza, E. Rahimi, Prevalence, identification of virulence factors, O-serogroups and antibiotic resistance properties of Shiga-toxin producing *Escherichia coli* strains isolated from raw milk and traditional dairy products. *Antimicrobial Resistance and Infection Control*, 7(1), 1-11. (2018).
- A. J. Kayode, A. I. Okoh, Assessment of multidrug-resistant *Listeria monocytogenes* in milk and milk product and One Health perspective. *PLoS One*, 17(7), e0270993. (2022).
- I. J. Okon, B. B. Adamu, R. I. Joseph, L. C. Ogbu, J. N. Emelogu, K. N. Akubue, C. S. Egbulefu, Isolation of *Salmonella* Sp. and *E. coli* from Fermented Milk Product (Nono) in Kuje Area Council (FCT, Abuja, Nigeria) and their Antimicrobial Resistant Status. *International Journal of Pharmaceutical and Bio Medical Science*, 2(10), 435-441. (2022).
- A. A. Noah, N. O. Salam. Effect of Lactic Acid Bacteria on Microbial, Proximate and Sensory Qualities of Nono (A Nigerian Fermented Milk Product). *International Journal of Microbiology and Application*, 7(1), 1-5. (2020).
- P. I. Obioha, A. Anyogu, B. Awamaria, H. B. Ghoddusi, L. I. I. Ouoba, Antimicrobial resistance of lactic acid bacteria from Nono, a naturally fermented milk product. *Antibiotics*, 12(5), 843. (2023).
- H. O. Agu, M. H. Badau, U. M. Abubakar, V. A. Jideani. A survey on existing practices adopted in Dambu production and utilization in some northern states of Nigeria. *African Journal of Food Science* Vol. 9(3) pp. 142-154, (2015) DOI: 10.5897/AJFS2014.1135 (2015).
- M. D. Makut, J. Ishaya. An Assessment of The Bacteriological Quality of Cow Milk Products Sold in Keffi Metropolis, Nasarawa. *NSUK Journal of Science and Technology*, Vol. 2, No. 1and2, ISSN: 1597 – 5527 (2012)
- A. T. Oyeyinka, R. Makhuvele, K. K. Olatoye, S. A. Oyeyinka. African fermented dairy-based products. In *Indigenous Fermented Foods for the Tropics*. Academic Press. (pp. 169-188). (2023)
- J. N. Keta, S. Hadi, A. A. Aliero, M. N. Keta, A. Hamisu. Evaluation of Fungi Species from Commercial Yoghurt in Birnin Kebbi, Kebbi State Nigeria. *Equity Journal of Science and Technology*, 6(1), 72-72. (2020).
- O. Fagbemigun, G. S. Cho, N. Rösch, E. Brinks, K. Schrader, W. Bockelmann, F. S. Oguntoyinbo, C. M. Franz. Isolation and characterization of potential starter cultures from the Nigerian fermented milk product nono. *Microorganisms*, 9(3), 640. (2021).
- M. Fernández, J. A. Hudson, R. Korpela, C. G. de los Reyes-Gavilán. Impact on human health of microorganisms present in fermented dairy products: an overview. *BioMed research international*, 2015. (2015).
- M. Petitjean, B. Condamine, C. Burdet, E. Denamur, E. Ruppé, Phylum barrier and *Escherichia coli* intra-species phylogeny drive



the acquisition of antibiotic-resistance genes. *Microbial Genomics*, 7(8). doi: 10.1101/2020.10.26.345488 (2021).

J. D. Pitout, T. J. Finn. The evolutionary puzzle of *Escherichia coli* ST131. *Infection, Genetics and Evolution*, 81, 104265. (2020).

D. Yu, G. Banting, N. F. Neumann. A review of the taxonomy, genetics, and biology of the genus *Escherichia* and the type species *Escherichia coli*. *Canadian Journal of Microbiology*, 67(8), 553-571. doi: 10.1139/CJM-2020-0508. (2021).

B., Koteswar, A., Devivaraprasad, Reddy., G., Ravi, I., Karunasagar. Occurrence of Pathotypes of *Escherichia coli* in Aquatic Environment. *International Journal of Current Microbiology and Applied Sciences*, (2017). doi: 10.20546/IJCMAS.2017.609.402

E.S. Mailyan. (2016). *Escherichia Coli*: An Infectious or a Factorial Pathogen? *Journal of Dairy, Veterinary and Animal Research*, (2016) doi: 10.15406/JDVAR.2016.03.00096

T. Sonowal, M. Shariff. A typical *Escherichia coli*: A Dilemma of a Clinical Diagnostic Laboratory. *Indian Journal of Medical Microbiology*, 37(2), 287-288. (2019). doi: 10.4103/IJMM.IJMM_19_60

C. D. Kaptchouang Tchatchouang, J. Fri, M. De Santi, G. Brandi, G. F. Schiavano, G. Amagliani, and C. N. Ateba. Listeriosis outbreak in South Africa: a comparative analysis with previously reported cases worldwide. *Microorganisms*, 8(1), 135. (2020).

O. Nwaiwu. What are the recognized species of the genus *Listeria*? *Access Microbiology*, 2(9). (2020). doi: 10.1099/ACMI.0.000153

R. Han, X. Yang, Y. Yang, Y. Guo, D. Yin, L. Ding, S. Wu, D. Zhu, F. Hu. Assessment of ceftazidime-avibactam 30/20- μ g disk, Etest versus broth microdilution results when tested against enterobacterales clinical isolates. *Microbiology Spectrum*, 10(1), e01092-21. (2022).

I. H. Igbinosa, C. Chiadika, Prevalence, characteristics and antibiogram profile of *Escherichia coli* O157: H7 isolated from raw and fermented (nono) milk in Benin City, Nigeria. *African Journal of Clinical and Experimental Microbiology*, 22(2), 223-233. (2021).

N. D. Ayaz, Y. E. Gencay, I. Erol. Phenotypic and genotypic antibiotic resistance profiles of *Escherichia coli* O157 from cattle and slaughterhouse wastewater isolates. *Annals of Microbiology*, 65(2), 1137-1144. (2015).

J. Šiugždaitė, A. Gabinaitienė, R. Šiugžda. Antimicrobial resistance of pathogens from ewes subclinical mastitis. *Veterinarija ir Zootechnika*, 73(095). (2016).

Y. Malekzadegan, R. Khashei, H. Sedigh Ebrahim-Saraie, Z. Jahanabadi. Distribution of virulence genes and their association with antimicrobial resistance among uropathogenic *Escherichia coli* isolates from Iranian patients. *BMC Infectious Diseases*, 18(1), 1-9. (2018).



P053 - EVALUATION OF BIOGAS PRODUCTION FROM THE DIGESTION & CO-DIGESTION OF POULTRY DROPPINGS, PIG MANURE, AND BREWERY-SPENT GRAIN USING ENZYMES AMYLASE.

Ogbobe, P.O.¹, Onyiah, M.I. ^{2*}, Ude, M.U.³

^{1,2,3}Projects Development Institute, (PRODA), P. M. B. 01609 Emene, Enugu State, Nigeria

Corresponding author email: ugwuayi@yahoo.com.

ABSTRACT

This study investigated the oxygen-independent fermentation of three lignocellulosic biomasses and their co-digestion to produce biogas using the enzyme amylase. Two experiments were conducted as part of the investigation, one using a water displacement setup in a lab and the other using a 10-liter biogas tank for each waste substrate. Standard procedures were used to determine the physico-chemical characteristics. The study's residence time, reaction temperature, enzyme concentration, and pH are the variables that were investigated. 1 kg of each substrate was mixed with water in a ratio of 1:1 *v/v* to form a slurry and fermented for 50 days.

The biogas yield from the digestion of poultry manure, pig manure, and spent grains individually using the enzyme amylase was 34 mL, 29 mL, and 33 mL, respectively, while the co-fermented substrates yielded (36 mL) at a reaction temperature of 50 °C residence time (20 days) and p^H 8. Gas analysis was carried out to determine the profile of the gas generated from the single and co-fermented substrates, The investigation reveals that the co-fermented substrates had a greater methane content than poultry dung, brewery leftover grain, and lastly pig manure, with a methane level of 63.28% and CO_2 (29.47%).

KEYWORDS

Biogas, Co-fermentation, Poultry dropping, Enzyme Amylase, Oxygen-Deprived Fermentation, pig manure, Brewery Spent Grain.

1.0 INTRODUCTION

Previous research has indicated that global energy requirements have risen in recent years due to expanding population, civilization, and economic activities of developed and developing countries worldwide. The rapid dwindling of these conventional energy sources like fossil fuels, coal, and gasoline, combined with growing environmental concerns related to their use, has necessitated the search for an alternative, environmentally friendly renewable energy source capable of fostering sustainable development (1). Plant and animal material waste are classified as biological or inorganic based on their composition, with most of them causing environmental problems due to improper waste disposal practices. Achieving optimal energy utilization, particularly for biogas, is feasible by employing relevant energy conversion and recovery technologies such as pyrolysis, torrefaction, and oxygen-deprived digestion. Therefore, it is proposed to recover energy from plant and animal waste material without causing harm to the environment (2). Biogas is a mixture of gases derived from

decomposing substrates such as plant and animal waste, household wastes, crops, and industrial waste carried out by a syntrophic and collaborative bacteriological association and consists of four stages: chemical reaction, acidogenesis, acetogenesis, and biomethanation. (3). Biogas production technology has the potential to alleviate energy insecurity, which is a significant impediment to Africa's economic progress. The methane and energy content of the generated gas often varies and is determined by the physical and chemical parameters of the substrate used (4). Oxygen-deprived fermentation (OdF) is a complicated procedure with various restricting constraints limiting the efficacy of the process such as ammonium build-up, poor feedstock modification, and protracted lag phases (5). Furthermore, oxygen independent fermentation of mono substrates poses significant difficulties due to substrate peculiarities (6). For example, the airtight decomposition of lignin-rich plant & animal materials may lack the essential nitrogen (N) content, resulting in poorer alkalinity capacity and undesirable circumstances, as well as volatile fatty acid suppression (6). Oxygen-Deprived co-



fermentation has gained popularity recently since it offers a viable replacement to mono digestion for overcoming difficulties and increasing the efficacy of the process (5). Although OdF offers an inexpensive way to reduce pH variation, ammonium build-up, year-round availability, and low energy yields, it faces also numerous difficulties that have hampered its advancement. The ability of microorganisms to acclimatize, digester stability, and the elimination of toxic compounds due to toxicity from various feedstocks are additional minor difficulties related with co-digestion (7). These have prompted investigators to look for alternate strategies for reducing the problems caused by oxygen-independent co-fermentation, such as addition of enzymes during the OdF process. Numerous studies have investigated the decomposition of poultry droppings when combined with other organic wastes but none of them focused on the co-fermentation of poultry droppings, pig manure and brewery spent grain with the influence of enzymes amylase & carboxymethyl-cellulase. Co-fermentation of poultry droppings with metropolitan garbage slurry was a project undertaken by Borowski & Weatherly (8). According to the experiment, adding 30% more poultry manure to sewage sludge did not boost specific gas yield ($376\text{dm}^3/\text{kg VS}$ versus $384\text{dm}^3/\text{kg VS}$), and the gas production rate as calculated per unit volume was 1.5 higher for sludge, and manure mixture. Longer SRT favoured the phenomenon where nutrients were released into the supernatant during the digestive processes. The liquor that resulted from the decomposition of just the sludge was very high in natural soot (COD of $2705\text{-}6034\text{ gO}_2/\text{m}^3$) and abundant in orthophosphates ($348\text{-}358\text{ gP}/\text{m}^3$). In contrast, following co-digesting sludge with manure, greater ammonium nitrogen was discovered in the supernatant ($2094\text{-}2221\text{gN}/\text{m}^3$). However, no indication of ammonia inhibition was present. In order to establish which of the two garbage materials generates better biogas production, Evangeline et al. (9) compared the biogas yields of cow manure and poultry manure. The research was divided into two studies, each using a 30 L fixed dome fermentor and a water displacement setup similar to that seen in a lab. Waste substrates were combined 1:1 with water in both tests, which were carried out at mesophilic temperatures. The day-to-day gas output of each substrate was calculated in milliliters, and it was found that cow manure yielded an average of 29.9 ml per day and poultry

waste produced 60.7 ml per day of biogas. According to analysis, the weight proportion of methane and carbon (IV) oxide in cow manure was roughly 92% and 6.68% by weight, respectively, while poultry manure contained about 90% methane and 6.56% by weight. According to the completed research, there is no information or published literature on the production of biogas from the co-digestion of spent grains from breweries, pig manure, and poultry droppings under the effect of the enzyme's amylase. Hence it is necessary to close this knowledge gaps.

2.0 MATERIALS AND METHODS

2.1.1. Collection of materials

The Poultry and pig leftovers used for this research were purchased at Anyalogu farms in Ngwo, Enugu State. A vendor in Ngwo, Enugu State, sold dehydrated brewery residual grain. Other materials for this experimental investigation, which include a thermometer for measuring temperature, a balance scale, a distillation flask, a gas extraction hose for transferring the gas produced, a CHNSO elemental analyzer, and four 10-liter containers for preparing the slurry, were sourced from the Biochemical Analytical Laboratory in Kenyatta, Enugu. The collected pig and poultry leftovers were air-dried and pulverized into a powder for consistency.

2.1.2. Sample preparation & experimental procedure

Poultry droppings, brewery spent grain, and pig manure were sun-dried to reduce moisture and then macerated to increase the contact surface. Samples were sieved to remove contaminants such as pebbles, food waste, grasses, and plastics. The dried, macerated, and sieved samples were finely ground with a laboratory blender and sieved through a sieve ($500\text{ }\mu\text{m}$) to obtain uniform sizes. The experiment was conducted between the mesophilic and thermophilic temperature range of $27.5\text{ - }57.5^\circ\text{C}$ with the influence of enzyme amylase. The mode of feeding into the digester was the batch method which means loading the digester and maintaining air-tight surrounding as depicted in Table 1. The four reactors labeled samples A (poultry droppings), B (pig manure), C (brewery spent grain), and D (co-digested substrates). Digester (A) comprised poultry droppings & water mixed in the ratio of 1000g of PD & 1.0 liters of H_2O , Digester B constitutes 1000g of pig manure &



1.0 liters of H_2O , (C) constitutes 1000g of brewery spent grain & 1.0 liters of H_2O , while Digester (D) which contains the co-digested substrates, constitutes 333g of poultry droppings, 333g of pig manure, 333g of brewery spent grain and 1.0 liters of H_2O .

2.1.3. Measurement of Biogas Production

When biogas production started in the digester, the gas was transferred to a chamber containing an acidified brine while biogas production started in the reactors. The same drops of tetraoxsulphate (VI) acid were combined with a saturated sodium chloride solution to produce the acidified brine. Since the biogas could not dissolve in the acidified brine solution, the pressure build-up was the reason for the displacement of the solution. Subsequently, the liquid displacement method used by (10) was used to measure the amount of biogas.

2.1.4. Analytical methods

The standard method of ASTM (11) was used to determine the moisture content (MC), ash content (AC), volatile matter (VM), crude fibre and energy content (calorific value) of the biomass feedstocks. Based on the methodology described by (12), the final examination of the feedstocks, which included carbon, hydrogen, nitrogen, sulphur, and oxygen, was carried out. The compositional analysis of the feedstock which includes hemicellulose content, lignin, and cellulose content was achieved based on the method reported by (12).

3. Results and Discussion

3.1. Characterization of the substrates

The chosen feedstock materials used in this experiment, which included residual grains from breweries, pig manure, and poultry leftovers, were analyzed proximally, chemically, and compositionally, as depicted in Table 2. These substrates often have considerable disaccharide contents, showing their viability for possible uses in biogas production despite modest variations for each type of biomass. The disaccharide concentration of the co-digested substrate was the greatest (24.33%), followed by that of brewery spent grain (17.20%), pig manure (15.62%), and poultry droppings (14.55%). Pectin accumulation in lignocellulose material is an impediment to the overall procedure because it inhibits pathogenic decomposition, though it may be appropriate for other determinations. A biomass with a high pectin

and/or ash composition is unsuitable for biofuel generation. It was observed from this investigation that brewery spent grain had the highest pectin content (14.35%), followed by the co-digested substrates (9.48%), poultry droppings (9.77%), and the least pig manure (9.11%). This information is similar to the study reported by (13). However, it was discovered that co-digested substrates had the highest polyose content (20.23%), followed by pig manure (21.33%), poultry droppings (23.47%), and brewery leftover grain (29.55%). The outcomes are consistent with those mentioned in (14). The contents of humidity, volatile matter, ash, and fixed carbon were also calculated and listed in Table 2 below. The moisture content, which is calculated as a proportion of the mass of the raw material, is used to reflect how much usable material is present in the raw material. According to Onochie et al.'s research (15), successful and sustained combustion requires between 8 and 12 percent moisture content, whereas a high moisture content has an extraordinarily high carbon depletion rate. Only the humidity level of the spent grain from the brewery is a little bit above the suggested 12% standard. Ash is the formal name for the solid biomass residue that results after thermochemical conversion at $575 \pm 10^\circ\text{C}$ for 3 hours. Comparatively, Table 2 shows that the ash contents of the various biomass wastes are rather similar to one another. Pig dung (11.18%) produced the least amount of content, followed by brewery leftover grain (12.86%), poultry droppings (12.52%), and co-digested substrates (13.10%). Volatile matter is the portion of the feedstock that is released after being heated for precisely seven minutes at $500^\circ\text{C} \pm 10^\circ\text{C}$ in a muffle furnace. The reactivity of the fuel is influenced by the volatile stuff in the biomass (12). High levels of volatile materials, however, guarantee quick ignition. As a result, it would be simpler to light the gas made from the decomposition of the combined substrates with (77.08%) volatile matter than it would be from either of the individual substrates made from pig dung, brewery leftover grain, or poultry droppings. The produced volatile material is comparable to that described by [16]. The quantity of biomass that is left over after non-volatile matter has been released, excluding ash and moisture content, is known as the non-volatile carbon content. It can be observed that the non-volatile carbon of the substrates is relatively close, with the co-digested substrate having the highest value of (18.11%) while the least is poultry droppings with (15.72%). The suitability and quality of biogas to be produced by any selected biomass could be informed by ultimate analysis; hence, other macronutrient components (C, H, N,



O, and S) in the substrate being used will aid in sufficient microbial growth. More well-balanced macronutrients have been shown to boost buffering capacity and are sufficient to support a stable digestive process in oxygen-deprived co-fermentation processes (10). In comparison, Table 2 shows that spent grains had the highest carbon content of (57.30%), followed by pig manure (40.18%), co-fermented waste (40.06%) and

poultry manure (39.18%). The nitrogen content for the selected biomass waste ranges from (3.41 to 3.82%), which are relatively close: hydrogen (5.08-5.72%), oxygen (33.68-49.11%) and sulfur (0.08-0.15%). Due to their high carbon content and low nitrogen and sulfur content (Table 2), poultry manure, pig manure and brewer's grains are considered plausible biomass for green energy production.

Table 1. Proportion of biomass waste and water used

Biomass waste	Weight of waste g	Vol. of water used litres
Poultry droppings	1000	1.0
Pig manure	1000	1.0
Brewery spent grain	1000	1.0
Co-digestion		
PD +PM +BSG	333g each	1.0

PD = Poultry droppings, PM = Pig manure, BSG = Brewery spent grain

Table 2. Characterization of poultry droppings, pig manure & brewery spent grain

Parameter	Poultry droppings	Pig manure	Brewery spent grain	Co-digested substrate 1 : 1 : 1
Particle size (μm)	500	500	500	500
Carbon content (%)	39.18	40.18	57.30	40.06
Nitrogen cont. (%)	3.59	3.82	3.65	3.41
C : N	10.91	10.51	15.69	11.75
Fixed carbon (%)	15.72	16.42	17.36	18.11
Ash content (%)	12.52	11.18	12.86	13.10
Volatile matter (%)	70.34	69.17	71.26	77.08
Moisture cont. (%)	10.26	9.51	12.65	8.33
Polyose (%)	23.47	21.33	29.55	20.23
Disaccharide (%)	14.55	15.62	17.20	24.33
Pectin (%)	9.77	9.11	14.35	9.48
Hydrogen (%)	5.71	5.72	5.41	5.08
Oxygen (%)	37.16	33.68	41.67	49.11
Sulphur (%)	0.15	0.14	0.11	0.08

Poultry droppings (PD), Pig manure (PM), Brewery spent grain (BSG)

3.2. Fourier transform infra-red analysis

The FTIR spectra of poultry dropping are shown in Figure 1a. The strength of the vibration at $3430\text{--}3300\text{cm}^{-1}$ is attributed to the *O – H* stretches of



the hydroxyl groups of phenols, alcohols, and carboxylic acids. Similarly the area between 2100 and 1650cm^{-1} were associated to the $C-H$ bonding in cellulose and hemicellulose. The carbonyl bands in the region 1990cm^{-1} were attributed to the hydroxyl $C=O$ stretching vibration, which belonged to the ester functional groups with the function of linking celluloses and hemicelluloses related to carboxylic compounds and ketones. The strength of the vibrations at 1641cm^{-1} and 1600cm^{-1} is attributed to the $C=C$ stretching of the aromatic ring and the $C=C$ aromatic backbone vibration of lignin. However, the intensity of the vibration at 1035cm^{-1} is attributed to the $C-O$ stretching vibration in cellulose and hemicellulose. There was no significant difference in the size of the peaks at 872cm^{-1} – 679cm^{-1} representing the $C-H$ bending vibration in the cellulose plane. This is similar to the investigation reported by [20]. Figure 1b show the spectra of pig manure. The absorption band of the single bond region ($2500 - 4000\text{cm}^{-1}$) is attributed to methylene groups of aliphatics. $C-H$ stretch of the alkyne group, normal “polymeric” “dimeric” and internally bonded OH bond stretching vibration of alcohol and hydroxyl compound and). $N-H$ vibrations from amides and amines. The triple bond region ($2000 - 2500\text{cm}^{-1}$) from the IR spectra is attributed to the presence of carbonyl compounds like transition metal carbonyls and some common inorganic ion like cyanide ion, thiocyanate and other related ions. Within the double bond region of this spectrum ($1500 - 2000\text{cm}^{-1}$) a lot of functional groups were discovered such as $C=C$ stretching vibration of the aromatic rings of lignin. $C=C$ stretch of alkene, $N-H$ in plane bending of amides and amines, $C=O$ stretch of amides. Aromatic combination bands and $N-O$ symmetric & asymmetric stretch of nitro compounds. The finger print region of the mid IR spectra ranging from ($600 - 1500\text{cm}^{-1}$) is attributed to $C-H$ bending patterns of aromatic rings and meta di-substituted compounds. $C-Cl$ & $C-Br$ stretch of aliphatic chloro and bromo compounds. OH out of plane

bend of alcohol and hydroxyl compound, $C-S$ stretch of thio-substituted compound. The above report is similar to that of [21] & [22]. The FTIR spectra of brewery spent grain is displayed in Figure 1c. The absorption band of the single bond region ($2500 - 4000\text{cm}^{-1}$) is attributed to $O-H$ vibrations of the hydroxyl groups of phenols, alcohols and carboxyl, $N-H$ vibrations from amides and amines (Padmavathy et al. 2003). $C-H$ stretching of the lignocellulose component, Methylene groups of aliphatics, $H-C-H$ asymmetric and symmetric stretch of alkanes or primary amines. The triple bond region ranging from ($2000 - 2500\text{cm}^{-1}$) is attributed to the presence of carbonyl compounds like transition metal carbonyls and some common inorganic ion like cyanide ion, thiocyanate and other related ions. Aliphatic and aromatic cyanide nitriles, $C\equiv C$ terminal and medial acetylenic group. The double bond region ($1500 - 2000\text{cm}^{-1}$) is attributed to $N-H$ in plane bending of the amide II, Compounds derived from Maillard reactions & $C=O$ stretching of hemicellulose. $C=C$ stretching vibrations of the aromatic rings of lignin, $C=N$ stretching vibrations attributed to Maillard reaction, $C=O$ stretching in quinones, ketonic acids and primary amides, $C=O$ stretch of aldehydes, ketones, acid carboxylic and esters, $C=O$ stretch of acyl chlorides and symmetric of anhydrides. From the finger print region, it was observed that the spectra below is filled with a lot of peaks ranging from ($600 - 1500\text{cm}^{-1}$). This region is attributed to $C-F$ stretch of alkyl halides, CN stretch of primary, secondary and tertiary amines, $C-OH$ stretching vibration of cellulose and hemicelluloses, $C-H$ bend of aromatic compound, $C-H$ bend of m-disubstituted aromatic compound, $C-H$ bend of alkenes, $C-Cl$ and $C-F$ stretch of aliphatic chloro and fluoro compounds. $C-O$ stretch of primary, secondary and tertiary alcohol, $C-O$ stretch of alkyl-substituted ether, $C-S$ vibration of thio-substituted compounds. Presence of common inorganic ions like phosphate ion and silicate ion and CN stretch of primary amine. This is similar to the investigation reported by (16).

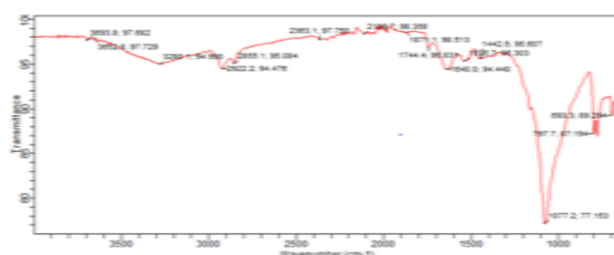
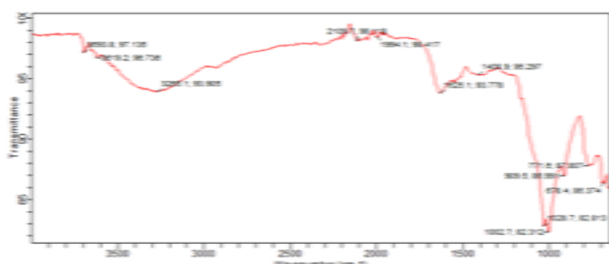


Fig. 1a. FTIR spectra of poultry dropping

Fig. 1b. FTIR spectra of pig manure

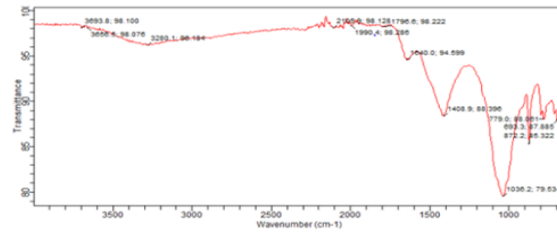


Fig. 1c. FTIR spectra of brewery spent grain

3.3. Biogas composition and analysis using enzyme amylase

Table 3 shows the composition of biogas produced from poultry dropping, pig manure, brewery spent grain and its co-digestion using enzyme amylase. The methane content produced from the co-digested

substrates was higher than the composition of the individual substrates. The co-fermented substrates has a methane and carbon concentration of 63.28% and 29.47% followed by poultry droppings, brewery spent grain and finally pig manure. The results obtained show that the biomass substrates are good source of material for producing biogas with the influence of enzyme amylase.

Table 3: Composition of biogas produced from the three substrates using enzyme amylase

Gas composition (%)	Feedstocks			
	PD	PM	BSG	PD +PM +BSG
CH_4	60.23	57.75	59.11	63.28
CO_2	31.16	33.48	32.41	29.47
H_2O	2.77	2.81	2.98	2.44
O_2	0.91	1.08	1.01	1.03
N_2	2.98	2.67	2.43	2.19
NH_3	0.83	0.92	0.71	0.57
H_2	0.78	0.82	0.94	0.41
H_2S	0.34	0.47	0.41	0.61

4. Conclusion

In this work a study on the evaluation of biogas production from the fermentation and co-fermentation of poultry dropping, pig manure and brewery spent grain using enzyme amylase was carried out. The process parameters for the co-fermentation such as: residence time, reaction temperature, enzyme concentration and p^H was

investigated. The experimental results suggested the optimal conditions as follows: reaction temperature of 50°C, residence time (20days), enzyme concentration of 6µmol/l and p^H 8. It was established that by co-digesting the biomass substrates in various proportions, a stable oxygen-deprived fermentation can be achieved.



References

1. Anthony, N.M., Mohamed, B., Tumisang, S., and Catherine, J.N. “Modelling the kinetics of biogas production from co-digestion of pig waste and grass clippings”, **Proceedings of the World Congress on Engineering**, Vol. II, 2016.
2. Moses, O.F., Olumuyiwa, A.L., Adekunle, A.A., Peter, P.I., Ayokunle, O.B., & Prabhu, P. “Prediction of Biogas Yield from Codigestion of Lignocellulosic Biomass Using Adaptive Neuro-Fuzzy Inference System (ANFIS) Model”, **Journal of Engineering**, Vol. 2023, pp. 1-16. (<https://doi.org/10.1155/2023/9335814>).
3. Dinova, N., Belouhova, M., Schneider, I., Rangelov, J., & Topalova, Y. “Control of biogas production process by enzymatic and fluorescent image analysis”, **Biotechnology & Biotechnological Equipment**, 32(2), (2018), pp.1-10. (<https://doi.org/10.1080/13102818.2018.1425637>).
4. Alfa, I. M., Dahunsi, S. O., Iorhemen, O. T., Okafor, C. C., & Ajayi, S. A. “Comparative evaluation of biogas production from Poultry droppings, Cow dung and Lemon grass”, **Bioresource Technology**, 157, (2014), pp. 270–277. (<https://doi.org/10.1016/j.biortech.2014.01.108>).
5. Slobodkina, I.A., & Azizov, A.A. “Anaerobic co-digestion of food wastes and chicken dung in lab-scale two stage system”, **Issues in Biological Sciences and Pharmaceutical Research**, Vol. 9(1), 2021, 12-18. (<https://doi.org/10.15739/ibspr.21.002>).
6. Callaghan, F.J., Wase, D.A.J., Thayanithy, K., Forster, C.F., “Continuous codigestion of cattle slurry with fruit and vegetable wastes and chicken manure”, **Biomass and Bioenergy** 27, (2002) pp. 71–77. ([https://doi.org/10.1016/s0961-9534\(01\)00057-5](https://doi.org/10.1016/s0961-9534(01)00057-5)).
7. Mumme, J., Srocke, F., Heeg, K., & Werner, M. “Use of biochars in anaerobic digestion”, **Bioresource Technology**, Vol. 164, (2014), pp. 189-197. (<https://doi.org/10.1016/j.biortech.2014.05.008>).
8. Borowski, S., & Weatherly, L. “Co-digestion of solid poultry manure with municipal sewage sludge”, **Bioresource Technology**, Vol. 142, (2013), pp. 345-352. (<https://doi.org/10.1016/j.biortech.2013.05.047>).
9. Evangeline, A.D., Marvel, L.A., Moses, E.E., Iyanuoluwa, E.O., & Amanda, O.N. “Comparative analysis of biogas produced from cow dung and poultry droppings”, **International Conference on Energy & Sustainability Environment**, 331, (2019), pp. 1-9. (<https://doi.org/10.1018/1755-1315/1/012064>).
10. Samuel, O., Michael, O., Raphael, O., & Joseph, O. “Co-digestion of livestock wastes for Biogas production. Bioengineering and Bioscience, Vol. 4(3), (2016), pp. 42-49. (<https://doi.org/10.13189/bb.2016.040303>).
11. American Society for Testing and Materials. Standard test methods for moisture in activated carbon. Philadelphia: ASTM Committee on Standards; 1991.



12. Fajobi, M.O., Lasode, O.A., & Adeleke, A.A. (2022), “Investigation of physicochemical characteristics of selected lignocellulose biomass”, *Sci. Rep.* 12, 2918. (<https://doi.org/10.1038/s41598-022-07061-2>).
13. Ude, M.U., & Oluka I.S. (2021). “Optimization of production and characterization of Biofuel produced from cassava and potato peels”, *The Proceedings of the Nigerian Academy of Science*, Vol. 14, No 1, pp. 66-81.
14. Akindele, O.O., & Olusola, A.A. “Evaluation of biogas production from co digestion of pig dung, water hyacinth and poultry droppings”, *Waste Disposal & Sustainable Energy*, Vol. 1, (2019), pp. 271-277.
15. Onochie, U.P., Obanor, A.I., Aliu, S.A., & Ighodaro, O.O. “Proximate and ultimate analysis of fuel pellets from oil palm residues”, *Nigerian Journal of Technology (NIJOTECH)*, Vol.36, No. 3, (2017), pp. 987-990. (<http://dx.doi.org/10.4314/njt.v36i3.44>).
16. Pauly, M., and Keegstra, K. “Cell-wall carbohydrates and their modification as a Resource for Biofuels. *Plant Journal*, Vol. 54, (2008), pp. 559-568. (<http://dx.doi.org/10.1111/j.1365-313X.2008.03463.x>).



P054 - PARTICLE SIZE AND SIZE DISTRIBUTION OPTIMIZATION OF PALLADIUM NANOPARTICLES BIOSYNTHESED USING SIDA ACUTA LEAF EXTRACT AS REDUCTANT: TAGUCHI-GREY RELATIONAL APPROACH

M. A. Abdulrahman^{1*}, M. Sumaila¹, M. Dauda¹, O. K. Abubakre,^{2,3}

Department of Mechanical Engineering, Ahmadu Bello University, Zaria, Kaduna State, Nigeria¹

Department of Metallurgical and Materials Engineering, Federal University of Technology, Minna, Nigeria²

Nanotechnology Research Group, Centre for Genetic Engineering and Biotechnology (CGEB), Federal University of Technology, PMB 65, Bosso Minna, Niger State, Nigeria³

Corresponding author email: send2mamudhmalik@yahoo.com

ABSTRACT

This study investigated effect of processing parameters on the hydrodynamic diameter and polydispersity index (PDI) of Sida Acuta (SA) plant extract assisted fabricated-Pd NPs using Taguchi-Grey Relational Analysis. L9 Taguchi orthogonal array was adopted for the experimentation and grey relational grades for the process optimization. The percentage contribution of each factor was evaluated using ANOVA at 95% confidence level. Pd NPs production was virtually confirmed by the change in colour of the reaction mixture and disappearance of the UV-visible absorption spectrum band of Pd²⁺ after the reaction. FTIR analysis of the SA-Pd NPs indicates the presence of O-H band of hydroxyl and carboxylic acid, and C=C stretch of aromatic compounds around the Pd NPs. SEM and XRD analyses revealed agglomerated nearly spherical shaped face centered cubic structure with average crystallite size of ~12nm. The Taguchi-grey relational analysis obtained the optimum hydrodynamic diameter of 62.5 nm and PDI of 0.232 at the process parameters of 10mg/ml extract concentration, 30mins reaction time and 60oC reaction temperature. The result of ANOVA showed that extract concentration has the highest contribution while time displayed the lowest contribution.

1.0 INTRODUCTION

Palladium nanoparticles (Pd NPs) among other metal nanoparticles, have received considerable attention due to their unique characteristics, such as excellent chemical stability, high photocatalytic performance, good thermal stability, and optical and electronic properties, which make them suitable for use as catalysts in organic reactions and fuel cells, element in gas sensor and hydrogen storage materials, drug delivery carrier and surface coatings (1-4). Metal NPs can now be produced through three broadly classified methods, namely chemical, physical, and biological methods (5). The chemical methods involve the use of toxic and hazardous chemicals that are harmful to the environment. Chemically synthesized NPs, because of the toxic chemicals used in their production, even after several washes, can be harmful when used for biomedical applications (6). The physical methods involve the use of expensive equipment, and NP production using these methods is usually done at

high temperature and pressure (7). Biological methods are regarded as facile, cheap, eco-friendly, and simple one-step methods for production of NPs. This approach utilizes plants and microorganisms to reduce metal ions from metal salts to metal atoms, which further coalesce and grow to form metal NPs (2,8). The use of extract from the fruit, leaf, root, and bark of plants have captured the interest of researcher due to its simplicity and potential for NP feature control. Numerous plants including, *Padina boryana*, *Origanum vulgare L.*, *Chrysophyllum cainito*, *Anogeissus latifolia*, and guar gum have been employed to biosynthesize different sizes of Pd NPs (2,9,10,11). They all ascertain that the primary metabolites, such as alkaloids, flavonoids, polyphenols, saponins, and tannins, in the plant extracts were responsible for the reduction of metal ions to zero-valent metal (12). Sida Acuta (SA) is a common weed that grows in cultivated land, pastures, lawns, and roadsides. It's traditionally utilized to treat malaria, ulcer, fever and gonorrhoea, which suggest that SA possess antioxidant, antimicrobial, cytotoxic, and other properties (13).



Phytochemical analysis of the SA leaf extract confirmed the presence of alkaloids, steroids, saponins, tannins, Flavonoids, Oxalate, Polyphenols, and glycosides, making it a suitable bioreductant for the production of metal NPs (14, 15). Recently, researchers have explored the use of SA extract as a reducing agent for production of Ag and ZnO NPs (16,17). However, there is no literature report on the production of Pd NPs using the most readily available and inexpensive weed (SA). Moreover, the size and size distribution shape and morphology of Pd NPs can be altered, by adjusting the process parameters (3). Studies have shown that smaller particle sizes with narrow size distributions measured by the value of their polydispersity index (PDI) have a great influence on the performance of NPs (10). It is, however, important to determine process parameters that produce Pd NPs with optimum size and PDI.

Taguchi Orthogonal array is one of the optimization methods that have been widely adopted by researchers, to determine process parameters with the best characteristics. However, the Taguchi method can only optimize one quality characteristic at a time. But Taguchi method can be utilized with other statistical and mathematical models, such as Grey Relational Analysis, Particle swarm optimization, and grey fuzzy Taguchi for multi-objectives optimization (18). To the best of the authors' knowledge, there is no literature report on the bio-fabrication and process optimization of Pd NPs synthesized using SA plant extract as a reducing agent. Hence, this work aimed to optimize the particle size and PDI of Pd NPs synthesized through the reaction between PdCl₂ and aqueous leaf extract of SA using Taguchi-grey relational analysis.

2.0 MATERIALS AND METHODS

2.1 Materials

Palladium Chloride (PdCl₂), produced by BUH Chemical Limited Poole, London, was purchased from Steve Moore chemical store, Zaria. The deionized water used was obtained from the Pharmaceutical laboratory at Ahmadu Bello

University, Zaria, and the SA leaf was collected from Dogarawa, Zaria. All chemicals used in this work are of analytical grade.

2.2 Methods

2.2.1 Collection and preparation of SA leaf extract

Fresh plant of matured SA was collected from an open field around Dogarawa, Zaria. The leaves were manually stripped off their stems and the SA leaf extract was prepared according to the methods prescribed by Hazarika *et al.* (19). The SA leaf was washed thoroughly with running tap water, after which it was washed with de-ionized water to make it free from dust. The leaf was shade-dried at room temperature for 28 days and then pulverized using a mechanical blender. The SA leaf powder was sieved using a 75µm-mesh sieve. The leaf powder was macerated by dissolving 100g leaf powder in 500 ml distilled water and was allowed to stand for 24 hours with intermittent stirring. The precipitate was removed by filtration using a sieve and Whatman no.1 filter paper. The filtrate was concentrated using a rotary evaporator (Model BUCHI, Model Number R110, England) and was evaporated to dryness on a water bath (Model BATH, Model Number B11, China) at 60°C. The extract was collected in a container and stored in a freezer for later use.

2.2.2 Green synthesis of Pd NPs

The Pd NPs were synthesized according to the method described by Majumdar *et al.* (9). 6.25ml of SA leaf extract (12.8mg/ml) was added to 43.75ml of 3mM aqueous PdCl₂ solution in a 50ml conical flask. A magnetic stirrer was applied to stir the mixture at 60°C for 30 minutes. The mixture was allowed to cool and then centrifuged at 3000r.p.m. for 15 minutes to separate and collect the produced Pd NPs. The influence of the process parameters such as, stirring temperature, extract concentration, and reaction time at different levels (as presented in Table 1), on the hydrodynamic size and polydispersity index of Pd NPs were studied using Taguchi Grey Relational Analysis.

Table 1: Factors and levels for the optimization of size and polydispersity of Pd NPs

Factor	Levels		
Synthesis parameter	-1	0	1
Extract concentration (mg/ml)	10	20	30
Stirring Time (mins)	30	60	90
Stirring Temperature (°C)	60	70	80

Table 2: L9 Taguchi orthogonal array for the experimental runs

Run order		Factors and their levels			Response	
S/No	Run	Extract conc.(mg/ml)	Stirring Time(min)	Stirring Temp.(°C)	Hydrodynamic Diameter (nm)	PDI
1	9	10	30	60		
2	2	10	60	70		
3	7	10	90	80		
4	3	20	30	70		
5	4	20	60	80		
6	8	20	90	60		
7	5	30	30	70		
8	6	30	60	80		
9	1	30	90	60		



2.2.3 Optimization process for Taguchi-grey relation analysis

2.2.3.1 Taguchi orthogonal array.

In this study, three factors with three levels as shown in Table 1, were considered, as such L9 Taguchi orthogonal array was adopted and the experimental design is shown in Table 2.

As highlighted in Table 2, the experimental design aimed to maximize two responses, namely hydrodynamic diameter and PDI, and to avoid the limitation of the Taguchi method, grey relational analysis was used for the multiple response optimization process.

2.2.3.2 Procedure for grey relation analysis

Grey relation analysis involves selecting an objective function that suits the target goal of each response during the pre-processing of the experimental data. Grey relational grades for individual responses were determined by separately normalizing each responses (experimental data) using the appropriate objective function. In this study, both the hydrodynamic diameter and PDI have the same objective function which is, the smaller the better, and the normalization values were computed using equation (1).

$$x_i^*(k) = \frac{\min. x_i^{(0)}(k) - x_i^{(0)}(k)}{\max. x_i^{(0)}(k) - \min. x_i^{(0)}(k)} \quad (1)$$

Where; $x_i^*(k)$ = Grey relational generated value, $\min. x_i^{(0)}(k)$ = Smallest value for $x_i^{(0)}(k)$ in the k^{th} response, $\max. x_i^{(0)}(k)$ = largest value for $x_i^{(0)}(k)$ in the k^{th} response.

The normalized experimental data were used to calculate the grey relational coefficient using equation (2). The calculated grey relational coefficient, $\varepsilon_i(k)$, expresses the relationship between the desired and the actual experimental data.

$$\varepsilon_i(k) = \frac{\Delta_{\min} - \zeta \times \Delta_{\max}}{\Delta_{0i}(k) - \zeta \times \Delta_{\max}} \quad (2)$$

Where; $\Delta_{0i}(k) = |x_0^*(k) - x_i^*(k)|$ is the absolute value of the difference between the reference sequence $x_0^*(k)$ and the comparable sequence $x_i^*(k)$; ζ = Distinguishing coefficient (0-1); Δ_{\min} = Smallest value of $\Delta_{0i}(k)$; Δ_{\max} = Largest value of $\Delta_{0i}(k)$.

The grey relational grades were obtained by averaging the grey relational coefficient of the individual responses corresponding to each experimental runs using equation (3).

$$Y_i = \frac{1}{n} \sum_{k=1}^n \varepsilon_i(k) \quad (3)$$

The values of the grey relational grades were used to analyze the optimal processing parameters that yielded the best quality characteristics. The average grey relational grades were ranked from the highest to the lowest values, and the highest value corresponds to the experimental parameters that provide the quality characteristics close to the desired quality. The optimum factors levels that gave the desired quality characteristics were determined by mean grey relational grades (MGRGs) which involve averaging the grey relational grades corresponding to each of the factors at each of their levels. The levels with the highest MGRGs were selected as the optimum process parameters. The difference of the highest and lowest values of MGRGs for each factor was computed and ranked. The ranked depict the level of contributions of the each factor on the optimum characteristics.

2.2.3.3 Prediction and validation of the optimum process parameters

The GRGs of the optimum experimental parameters obtained from the MGRGs was estimated using equation (4) and was compared with the GRGs obtained by evaluating the responses measured from Pd NPs produced using the optimal experimental parameters.

$$\hat{\gamma} = \gamma_m + \sum_{i=1}^q (\bar{\gamma}_i - \gamma_m) \quad (4)$$

Where $\hat{\gamma}$ is the estimated grey relational grade using the optimal factors level, γ_m is the total mean of the grey relational grade, $\bar{\gamma}_i$ is the mean of the grey relational grade at the optimal level and q is the number of factors that significantly affect the performance characteristics.

The quantitative percentage contributions and the significance of the factors on the target characteristics were analyzed using ANOVA.

2.2.4 Characterization of bio-synthesized Pd NPs

The produced Pd NPs was characterized using UV-visible spectrophotometer (UV-1800,



manufactured by SHIMADZU, Japan), dynamic light scattering analysis (Malvern Nanozetasizer Nano-S equipment, Worcestershire, UK), FTIR analysis (Shimadzu Irtfinity-1), XRD analysis (Rigaku, Smartlab) and SEM micrograph (TESCAN, MAIA3 XM).

3.0 RESULTS AND DISCUSSION

3.1 Production of Pd NPs

The solution mixtures containing the PdCl₂, aqueous leaf extract of SA, and deionized water before and after stirring at 60 °C for 30 minutes were shown in plate I. The change in colour of the mixture from brown to darkish brown suggested the reduction of Pd²⁺ to Pd NPs through the reaction between PdCl₂ and the metabolites in the SA leaf extract. This colour change was consistent with those observed by Vinodhini *et al.*, (20), Kora and Rostogi (10), Hazarika *et al.*, (19), and Shaik *et al.*, (3), who separately synthesized Pd NPs using extracts of *Allium fistulosum*, *Basella alba* and *Tabernaemontana divaricate*,

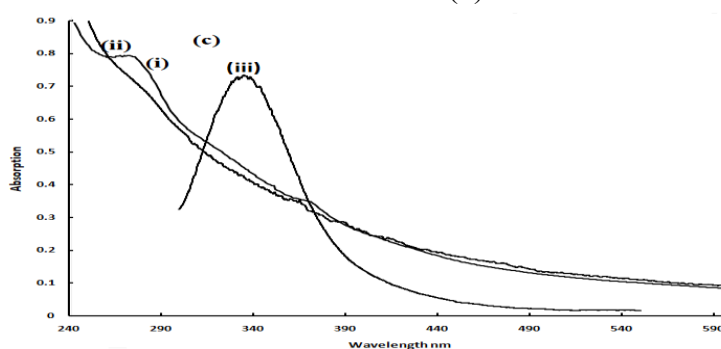
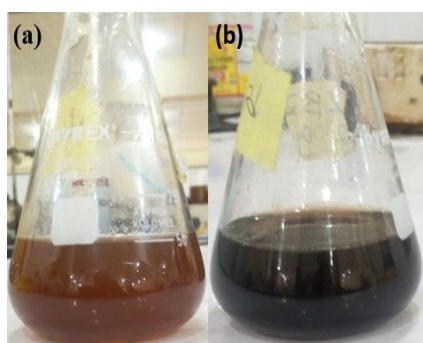


Figure 1: mixture of SA leaf extract with (a) PdCl₂ before reaction (b) Pd NPs after reaction and (c) UV-vis spectra of aqueous solutions of (i) SA leaf extract, (ii) Pd NPs and (iii) PdCl₂

3.2.2 Ftir analysis

FTIR analysis was performed on the SA leaf extract and the synthesized Pd NPs at the scanning range of 4000-650cm⁻¹ wavenumber to identify the functional groups in the SA leaf extract and those responsible for the reduction, capping, and stabilization of the Pd NPs. As presented in Figure 2(a), the FTIR spectrum of the SA leaf extract (i) shows some peaks at the wavenumber of about 3350, 2920, 1610, 1390, 1032, and 890 cm⁻¹. The band between 3500-3350cm⁻¹ indicated the

GarciniapedunculataRoxb, gum ghatti and *Origanum vulgare L.* respectively.

3.2 Characterization of the Pd NPs Produced

3.2.1 Ultraviolet visible spectroscopy

UV-visible spectrophotometer analysis conducted on the SA extract, Pd salts as well as the reaction mixtures confirmed the production of Pd NPs. The surface plasmon resonance of the PdCl₂ solution presented in Figure 1(iii), shows a discrete absorption peak at the wavelength of 335nm, signifying the presence of Pd²⁺ ion (10), however, after the synthesis as shown in Figure 4.1a (ii), Pd²⁺ absorption peak changed to a broad continuous absorption spectrum, indicating the presence of zero-valent Pd NPs (9).

presence of the O-H of the hydroxyl group, while the band with a peak centred at 2895cm⁻¹ corresponds to C-H stretch of aldehydes. The peaks at 1610cm⁻¹and 1390 cm⁻¹ belong to the C=C stretch of alkenes and NO₂ stretch of aromatic nitro compounds respectively. The existence of a C-F stretch of alkyl and aryl halides was observed in the fingerprint region with a peak at 1033.5cm⁻¹. These analyses are consistent with the FTIR spectrum interpretations of SA leaf extract given by Ramraj *et al.*, (21), Ramesh *et al.*, (20) and Idrees *et al.*, (17)



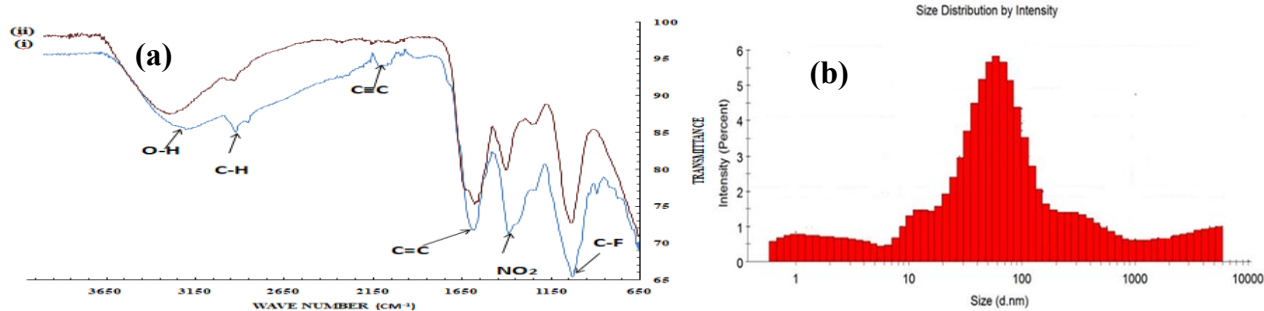


Figure 2: (a) FTIR spectra of (i) SA leaf extract and (ii) Pd NPs, (b) DLS size analyses of Pd NPs

FTIR spectrophotometer analysis was performed on the SA leaf extract synthesized Pd NPs (Figure 2a(ii)), and it was found to possess some of the peaks observed in the SA leaf extract spectrum. The functional groups with peaks at 3224.1, 2926, 1625.1, 1370.1, and 1036.2 cm^{-1} found in the Pd NPs spectrum (i) were slightly shifted from their initial positions when compared with the FTIR spectrum of the SA leaf extract (see Figure 2), this The hydrodynamic diameter and the PDI of the produced Pd NPs was analysed using dynamic Light scattering spectroscopy. As shown in Figure 2b, the hydrodynamic diameter and PDI of the Pd NPs were 45.62 nm and 0.519, respectively. The Pd NPs size of 45.62nm obtained from the DLS analysis was lower than the optimum hydrodynamic diameter of 74.5nm as reported in the work Kora and Rastogi (10), however, the PDI value of 0.3 recorded in their report was less than the 0.519 measured in this study. This implied (as seen in Figure 3) that even though the mean hydrodynamic diameter is comparatively smaller, the particles contain a good percentage of smaller and larger particles which account for the wide particle size variation. In another study, the mean diameter of 5.5nm for biosynthesized Pd NPs using *glacosimine* as a reducing and capping agent was reported (22).

The overall properties of NPs are effect by both their particle size and size distributions, as such, the particle size and size distribution of the SA leaf extract synthesized Pd NPs was optimized by adjusting some process parameters, such as extract concentration, reaction temperature, and reaction time, using the Taguchi L9 orthogonal array in conjunction with Grey Relational Analysis.

is an indication that these functional groups not only acted as a reducing agent but also contributed in capping and stability of the Pd NPs (22). Furthermore, the peak at 1370.1 cm^{-1} was broadened and its intensity decreased, suggesting the increased contribution of the nitro compound in the conversion process (3).

3.2.3 Dynamic light scattering spectroscopy

3.3 Particle Size and Polydispersity Index Optimization

Taguchi orthogonal array was adopted for the experimental design, while the responses were analyzed using grey relation analysis as the Taguchi method does not accurately optimize more than one response (18). Table 3 present the responses which are the intensity-weighted hydrodynamic diameter (nm) and the PDI of the NPs in aqueous solutions as obtained from the DLS analysis. As can be seen in Table 3, experimental conditions number eight (8) gave the lowest value of hydrodynamic diameter for the Pd NPs production, however, the PDI at that run was the highest for all the runs. The least PDI and the highest hydrodynamic diameter were observed with the experiment number one (1). Grey relational analysis was used (as seen in Table 4) to combine the effect of these responses to a single value based on the desired targeted characteristics. This single value was used as basis for the optimization.



Table 3: Factors, levels and response for the biosynthesis of Pd NPs

Factors and their levels				Response	
Experiment No	Extract conc.(mg/ml)	Stiring Time(min)	Stiring Temp.(°C)	Hydrodynamic Diameter (nm)	PDI
1	10	30	60	107.5	0.194
2	10	60	70	59.46	0.232
3	10	90	80	77.03	0.218
4	20	30	70	66.4	0.41
5	20	60	80	74.2	0.197
6	20	90	60	94.59	0.204
7	30	30	80	93.8	0.275
8	30	60	60	47.62	0.519
9	30	90	70	73.35	0.404

Based on the grey relational grades for the biosynthesis of Pd, as seen in Table 4, the experiment number two (2) in Table 4, has the best ranking with the highest grey relation grade (GRGs) value of 0.763542. However, the optimal combination of experimental conditions may not necessarily be included in the Taguchi orthogonal arrays used for the experiments. The experimental characteristics. Factor levels with the highest MGRGs (see bold values) correspond to the optimum levels for that factor. From this analysis, the combination of experiment parameters for the

Table 4: Grey relation analysis and ranking for production of Pd NPs

Exp. No	Grey relation generation		Grey relation coefficient		Grey relation grade	Rank
	Hydrodynamic diameter	PDI	Hydrodynamic diameter	PDI		
1	0	1	0.333333333	1	0.666667	4
2	0.802271209	0.883077	0.716610819	0.810474	0.763542	1
3	0.508851035	0.926154	0.504465038	0.871314	0.687889	3
4	0.686372745	0.335385	0.61453202	0.429326	0.521929	8
5	0.556112224	0.990769	0.529723992	0.981873	0.755799	2
6	0.215597862	0.969231	0.389286179	0.942029	0.665658	6
7	0.228790915	0.750769	0.393326327	0.667351	0.530339	7
8	1	0	1	0.333333	0.666667	4
9	0.570307281	0.353846	0.537812107	0.436242	0.487027	9

settings that have the best rankings are only closer to the optimum parameters that would offer the desired characteristics (23). Mean grey relation grades (MGRGs) generated from Table 4 as shown in Table 5, provided the optimum combination of experimental settings with potentials for best performance

size and size distribution of SA leaf extract produced Pd NPs were found to be extract at level 1 (10mg/ml), temperature at level 2 (70°C) and time at level 1(60minutes).

Table 5: MGRGs for Pd NPs production

Factor	Average Grey Relation Grading by factor levels			Delta	Rank
	Level 1	Level 2	Level 3		
Extract (mg/ml)	0.70603	0.6478	0.56134	0.14470	1
Time (mins)	0.63650	0.67318	0.62550	0.02768	3
Temp (°C)	0.6663	0.59083	0.65801	0.07550	2
Mean of the grey relation grading = 0.638391					

Table 6: Comparative results of Pd NPs produced with experimental runs and the optimize conditions

Level	Initial Condition	Best Experimental condition	Optimal Condition		
	E ₃ ,t ₁ ,T ₁	E ₁ ,t ₂ ,T ₂	Predicted	experimented	%Error
Hydrodynamic diameter (nm)	47.62	59.46		61.25	3.00
PDI	0.519	0.232		0.22	5.17
GRGs	0.666667	0.763542	0.748761	0.766911	0.44
% improvement (GRGs)			1.94	0.44	

Table 7: ANOVA for GRAs of the process parameter of Pd NPs

Source	DF	Adj. SS	Adj. MS	Ft	P	% Contribution
Regression	5	0.080833	0.016167	30.07	0.009	
Extract	1	0.031402	0.031402	58.40	0.005	24.64
Temperature	1	0.037316	0.037316	69.40	0.004	29.28
Time	1	0.010323	0.010323	19.20	0.022	08.10
Temp.*Temp.	1	0.036585	0.036585	68.04	0.004	28.70
Time*Time	1	0.010226	0.010226	19.02	0.022	08.02
Residue Error	3	0.001613	0.000538			01.27
Total	8	0.127465				

Note: sources with P> 0.05 are insignificant

$$\text{Grey} = -5.658 - 0.007234 \text{ Extract} + 0.1916 \text{ Temperature} - 0.00965 \text{ Time} - 0.001354 \text{ Temperature} \times \text{Temperature} + 0.000079 \text{ Time} \times \text{Time} \quad (5)$$

The optimum process parameters obtained from Tables 5 was used to synthesize Pd NPs and its particle size and PDI were evaluated using DLS analysis. Initially, the GRGs of the selected optimal conditions in Table 5 was estimated using equation

4, and was compared with the GRG obtained from experiment conducted using the optimum process parameters for the Pd NPs Production. The estimated GRG value (see Table 6) of 0.748761 was computed for the selected optimum levels, while the



GRG value of 0.766911 was obtained for the Pd NP sample synthesized with the optimum processing parameters. The hydrodynamic diameter and the PDI of the Pd NPs produced with the optimum parameters were 62.25nm and 0.22 respectively. The mean hydrodynamic diameter of the particles increased from 59.64nm obtained from the best-ranked production settings in Table 3 to 62.25nm measured from Pd NPs synthesized using the optimum processing parameters. This difference in the particle size can be attributed to the higher rate of reduction reaction between the PdCl₂ and the SA leaf extract as a result of the increase in the production temperature, leading to multiple nucleation and fast coalescence of the adjacent smaller NPs to stable Pd NPs (24). The SA leaf extract concentration promotes the production of smaller NPs by encapsulating the NPs and preventing it from further growth. It is believed that binding energy between the Pd atoms at lower extract concentrations prevailed over the capping ability of the plant extract (25). Even though there was a 3.0% increase in the hydrodynamic diameter of the Pd NPs with the optimum process parameters, the PDI of the Pd NPs was reduced by about 5%. This slight increase in the PDI value seen from the best experimental conditions can be ascribed to the presence of much smaller particles, which also agglomerate to form larger particles thereby widening the particle size variation.

3.6 Analysis of Variance (ANOVA)

The analyses of variance (ANOVA) for the data were performed at a 95% confidence level to identify the significant factors and the level of their contribution to the production process. Table 4.10 showed that all factors and interactions considered in ANOVA for the production of Pd NPs were significant as their corresponding P values were less than 0.05. Additionally, the temperature had the highest contribution of 29.28%, followed by extract concentration with 24.64%, then time with 08.10%

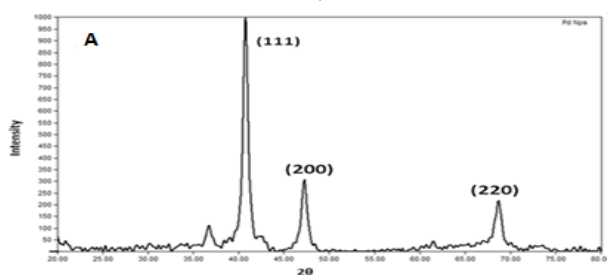


Figure 4: (A) X-Ray diffraction pattern and (B) SEM image of SA assisted biosynthesis of Pd NPs

3.8 SEM Analysis of the Produced NPs

contribution. And because the difference between the R square value of 98.04% and the R square adjusted of 94.78% was small (3.26%), the model generated in equation (5) was considered to have good predictive ability (26). A similar trend was observed for the ANOVA analysis of the response data for the production of Ni NPs. As seen in Table 4.11, all the factors which include the extract, temperature and time were significant with P values lower than 0.05. Temperature was detected to have the highest contribution (64.20%), while 08.07% and 20.60% contributions were recorded for time and extract concentration respectively. About 4.39% was computed as the difference between the R square (92.68%) and R square adjusted (88.29%). Generally, as posited by Lundstedt *et al.*, (26), if the difference in the R squares is less than 20%, then the model is deemed acceptable.

3.7 XRD Analysis of the Biosynthesized Pd NPs

The spectrum of the Pd NPs synthesized using SA extract as a reducing and capping agent, as seen in Figure 4(A), showed a typical reflection of crystalline Pd NPs with 2θ diffraction peaks at 36.72°, 40.72°, 47.28° and 68.74° that correspond to the crystallographic planes indexed as (101), (111), (200) and (220) respectively. These 2θ positions of the diffraction peaks are a reflection from the planes of faced centred cubic crystal structure of Pd NPs and matches with the diffraction peaks of standard Pd NPs with JCPDS PDF card number: 46-1043 (22). The average crystalline size of 9.67nm was calculated using Scherrer's formula and data from the XRD analysis. This average crystallite size was smaller than the 21.1nm calculated by Mallikarjuna *et al.*, (27), similar to about ~11nm observed by Sonbol *et al.*, (2), but larger than the 4.8nm reported by Kora and Rastogi (10) who separately fabricated Pd NPs using different plant extracts.

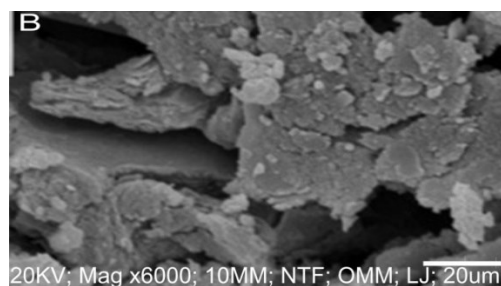


Figure 4(B) showed the SEM micrograph of the SA leaf extract synthesized Pd NPs at 6000



magnifications. As with the nature of green route nanometal synthesis, the image revealed NPs of Pd that are spherical and loosely aggregated in to lumps (28).

4.0 CONCLUSIONS

SA leaf extract was successfully used as reducing and capping agent for the production of Pd NPs from its salt PdCl₂ as confirmed by the visual colour changes from brown to dark brown for Pd NPs. The synthesis was further confirmed by the disappearance of Surface Plasmon Resonance of Pd²⁺ at an absorption peak of 424nm for Pd NPs. Particle size and PDI optimization of the produced NPs based on the smaller the better objective function was conducted by varying the synthesis parameters. The outcome revealed that Pd NPs of 61.25nm at the PDI of 0.22 was produced with extract concentration at level 1, reaction temperature at level 1 and reaction time at level 2. This implies an increase in the hydrodynamic diameter by about 3% and a decrease in the PDI by about 5% as compared to the best experimental runs. Analysis of variance indicated that all the synthesis parameters are significant at 95% level of confidence, however, the reaction temperature made the highest percentage contribution for the Pd NPs synthesis. The average crystallite size of Pd NPs from the XRD data was ~12nm.

REFERENCE

1. M. A. Ehsan, A. M. Kumar, R. K. Suleiman, A. S. Hakeema, A. Fabrication of thickness-controlled NiPd nano-alloy thin films as anticorrosive coatings on 316L SS substrates for application in marine environment. *Surface & Coatings Technology*. 418, 127253.(2021)
2. H. Sonbol, F. Ameen, S. Alyahya, A. Almansob, S. Alwakeel, Padina boryana mediated green synthesis of crystalline palladium nanoparticles as potential nanodrug against multidrug resistant bacteria and cancer cell. *Scientific Reports* 11:5444 (2021).
3. M. R. Shaik, Z. J. Q. Ali, M. Khan, M. Kinyil, M. E. Assal, H. Z. Alkathlan, Green Synthesis and Characterization of Palladium Nanoparticles Using Origanum vulgare L. Extract and Their Catalytic Activity. *Molecules* 22:165 (2017).
4. J. Kong, M. G. Chapline, H. J. Dai, Functionalized carbon nanotubes for molecular hydrogen sensors, *Adv. Mater.* 13(18)1384–1386 (2001).
5. R. K. Das, V. L. Pachapur, L. Lonappan, M. Naghdi, R. Pulicharla, S. Maiti, et al. Biological synthesis of metallic nanoparticles: plants, animals and microbial aspects. *Nanotechnol. Environ. Eng.* 2:18 (2017).
6. S. Hua, M. B. C. de Matos, J. M. Metselaar, G. Storm, Current trends and challenges in the clinical translation of nanoparticulate nanomedicines: pathways for translational development and commercialization. *Front. Pharmacol. Pharmacol.* 9:790 (2018).
7. K. N. Thakkar, S. S. Mhatre, R. Y. Parikh, Biological synthesis of metallic nanoparticles. *Nanomed. Nanotechnol. Biol. Med.* 6, 257–262 (2010).
8. S. M. Mousavi, S. A. Hashemi, G. Younes, A. Atapour, A. Amani, A. Savardashtaki, et al. Green synthesis of silver nanoparticles toward bio and medical applications: review study. *Artif. Cells* 46, S855–72 (2018).
9. R. Majumdar, S. Tantayanon, B. G. Bag, Synthesis of palladium nanoparticles with leaf extract of *Chrysophyllumcainito* (Star apple) and their applications as efficient catalyst for C – C coupling and reduction reactions *Int Nano Lett* 7:267–274 (2017).
10. A. J. Kora, L. Rastogi, Green synthesis of palladium nanoparticles using gum ghatti (*Anogeissus latifolia*) and its application as an antioxidant and catalyst. *Arab J Chem.* <https://doi.org/10.1016/j.arabjarabj.c.2015.06.024>
11. F. Anjum, S. Gul, M. I. Khan, M. A. Khan, Efficient synthesis of palladium nanoparticles using guar gum as stabilizer



- and their applications as catalyst in reduction reactions and degradation of azo dyes. *Green process synthesis*. 9: 63-76 (2020).
12. D. Khwannimit, R. Maungchang, P. Rattanakit, Green synthesis of silver nanoparticles using *Clitoria ternatea* flower: an efficient catalyst for removal of methyl orange, *Int. J. Environ. Anal. Chem.* 1–17 (2020).
 13. D. K. Simplicio, M. N. Wendyam, P. I. Denise, O. Djeneba, G. Messanvi, D. S. Comlan DS, et al, *Sida acuta* Burm. f.: a medicinal plant with numerous potencies. *Afr J Biotechnol* 6(25):2953–59 (2007).
 14. M. Hassan, F. M. Musa, A. Adamu, B. Gabi, Phytochemical analysis and antibacterial activity of fractions of *Sida acuta* against some reference isolates of bacteria. *Science World Journal* 17(1) 26-29 (2022).
 15. P. Nwankpa, O. G. Chukwuemeka, G. C. Uloneme, C. C. Etteh, P. Ugwuezumba, Phyto-nutrient composition and oxidative potential of ethanolic leaf extracts of *Sida Acuta* in wista albino rats. *Journal of Biotechnology*. 14(49):3264-3269 (2015).
 16. A. M. Ramesh, K. Pal, A. Kodandaram, B. L. Manjula, D. K. Ravishankar, H. G. Gowtham, M. Murali, A. Rahdar, G. Z. Kyzas, Antioxidant and photocatalytic properties of zinc oxide nanoparticles phyto-fabricated using the aqueous leaf extract of *Sida acuta*. *Green Processing and Synthesis*. 11: 857–867 (2022).
 17. M. Idrees, S. Batoool, T. Kalsoom, S. Raina, M. A. Sharif, S. Yasmeen, microbial actions and corrosion inhibition potential Biosynthesis of silver nanoparticles using *Sida acuta* extract for antimicrobial actions and corrosion inhibition potential. *Environmental Technology*. <https://doi.org/10.1080/09593330.2018.1435738> (2018).
 18. A. Das, A. Majumder, P. Kr, Detection of Apposite PSO Parameters Using Taguchi Based Grey Relational Analysis: Optimization and Implementation Aspects on Manufacturing Detection of Apposite PSO Parameters using Taguchi Based Grey Relational Analysis: Optimization and Implementation Aspects on Manufacturing Related Problem. *Procedia Materials Science*. 3rd International Conference on Materials Processing and Characterisation (ICMPC 2014) 6: 597 – 604 (2014).
 19. M. Hazarika, D. Borah, P. Bora, A. R. Silva, P. Das, Biogenic synthesis of palladium nanoparticles and their applications as catalyst and antimicrobial agent. *PLoS ONE* 12(9):1-19 e0184936 (2017).
 20. S. Vinodhini, B. S. Mary, T. A. Arul, Green synthesis of palladium nanoparticles using aqueous plant extracts and its biomedical applications. *Journal of King Saud University – Science* 34, 102017 (2022).
 21. S. M. Ramraj, A. Kubaib, P. M. Imran, M. K. Thirupathy, Utilizing *Sida Acuta* leaves for low-cost adsorption of chromium (VI) heavy metal with activated charcoal. *Journal of Hazardous Materials Advances* 11, 100338 (2023).
 22. S. Ullah, A. Ahmad, A. Khan, J. Zhang, M. Raza, A. U. Rahman, M. Tariq, U. Ali Khan, S. Zada, Q. Yuan, Palladium nanoparticles synthesis, characterization using glucosamine as the reductant and stabilizing agent to explore their antibacterial & catalytic applications. *Microb. Pathog.* 125, 150–157 (2018).
 23. M. I. Equbal, R. M. Shamim, R. K. Ohdar, A grey-based Taguchi method to optimize hot forging process. 3rd International Conference on Materials Processing and Characterisation (ICMPC 2014) *Procedia Materials Science* 6: 1495 – 1504(2014).



24. M. I. Din, A. Rani, Recent Advances in the Synthesis and Stabilization of Nickel and Nickel Oxide Nanoparticles: A Green Adeptness. *International Journal of Analytical Chemistry*. 1-14 (2016).
25. N. Kazem, S. Elias, R. Khadijeh, M. M. Y. Wan, Influence of dose on particle size of colloidal silver nanoparticles synthesized by gamma radiation. *Radiat. Phys. Chem.*, 79, 1203–1208 (21010).
26. T. Lundstedt, E. Seifert, L. Abramo, B. Thelin, A. Nystrom, J. Pettersen, R. Bergman, Experimental design and optimization. *Chemometrics and Intelligent Laboratory Systems*. 42: 3–40 Ž (1998).
27. K. Mallikarjuna, L. V. Reddy, S. Al-rasheed, A. Mohammed, S. Gedi, W. K. Kim, Green Synthesis of Reduced Graphene Oxide- Supported Palladium Nanoparticles by *Coleus amboinicus* and Its Enhanced Catalytic Efficiency and Antibacterial Activity. *Crystals*. 11, 134 (2021).
28. J. Kanda, S. Madiwale, B. Bashte, S. DindorKar, P. Dhawal. P. More, Green mediated synthesis of palladium nanoparticles using aqueous leaf extract of *Gymnema synvestre* for catalytic reduction of Cr (VI). *Applied sciences*. 2:1854 (2020).

P055 - THE ROLE OF NATURAL COAGULANT IN WASTE WATER TREATMENT

Yahaya, U^{1*}., Suleiman, R.A²., Maina, M.A¹and Odey, B.O².

¹*Federal College of Forest Resources management, Maiduguri, Borno- Nigeria.*

²*Forestry Research Institute of Nigeria*

Corresponding author: usmanyahayaks@yahoo.com, +2348062247888

ABSTRACT

This paper focus on the use of different natural coagulant in wastewater treatment. A total of 23 plants species belonging to 11 families were recorded. Majority of the plant coagulants cited in this review are legumes under Fabaceae family, with approximate percentage occurrence of 41%, followed by *malvaceae* family with approximately 14%, and *curcubitaceae* family with approximately 9%, while the rest showed low percentage occurrences. Many of the researchers observed highest percentage turbidity removal when using *Moringa oleifera* seed compared with other natural plants coagulant. Therefore, Potentiality of natural or plant base coagulants are providing good evidence of substituting the long use chemical coagulants due to their accessibility, nontoxic, cost effectiveness and biodegradable natures. Thus, there is need for many researchers to embark on many researches in order to standardize and quantify the usage of natural coagulants.

KEY WORDS

Coagulant, Natural, Wastewater, Treatment, Fabaceae.

INTRODUCTION

Living on earth largely depends on water for their survival in one way or the other,

developing countries and third world countries are facing potable water supply problem due to in adequate financial resources. UN reported



that 1.1 billion people in the world do not have access to an adequate supply of drinking water and these people are among the world's poorest. The two major sources of water are underground and surface water. These water sources can easily be contaminated with pathogenic microorganisms, colour, suspended solids, odour-causing particles which may change the safety of the water. These problems are commonly solved through the conventional technology used in the water treatment which includes coagulation, flocculation, sedimentation, filtration and disinfection. For the treatment of wastewater if the particles are non-settling or too slow to settle then addition of coagulants and or flocculants is required. Coagulants are chemical use in water treatment to withdraw the forces that stabilizes the colloidal particles which lead to particle suspension on to the water. Several coagulants and flocculants have been used in conventional water treatment process. These materials are classified into inorganic coagulants (e.g. aluminium and ferric salts) and synthetic organic polymers (e.g. polyacryl amide derivatives and polyethylene imine). But, the most common chemical coagulant used were alum, iron and other synthetic chemicals.

However, aluminium has different effects on to the human health, such as memory loss, abdomen colic, intestinal constipation, spasms, difficulty of learn and loss of energy when utilized as a coagulant in the treatment of wastewater. Recent studies have proven a number of serious problem associated to the use of aluminium salts which include Alzheimer's disease correlated with high aluminium residuals in treated water, extreme sludge production during water treatment and extensive changes in water chemistry owing to reactions with the OH⁻ and alkalinity of water. Thus there is need to replace the conventional coagulant with the natural one. These natural coagulants can be extracted or produced from plant, animal or microorganisms. Recently, potentiality of natural or plant base coagulants was reported to include their accessibility, nontoxic, cost effectiveness and biodegradable natures. Natural coagulants are not only water clarifying agents, but they also have certain activity such as antimicrobial and removal of heavy metals among others. Hence it is highly

attractive in the conversion of raw surface water into potable drinking water. The objective of the current study was to explore the potentiality of using natural coagulants as a substitute to the commercial synthetic coagulant used (e.g. Aluminium and iron).

Coagulation Mechanisms

Coagulation has long been practiced, and the key objective is to remove colloidal impurities as well as removing turbidity from the water. Coagulants are mainly chemicals added to the water to withdraw the forces that stabilizes the colloidal particles and caused the particles to be suspended in the water. By application of the coagulant the individual colloids aggregates and grow bigger and eventually settled the impurities at the bottom of the container.

Turbidity Causes

Turbid water simply refers to the murky or cloudy in appearance which caused by impurities imparts leading to unpleasant taste to the water. Turbidity is always caused from the suspended negatively charged particles or natural organic matter found in the water. On account of the surface electrical charge, these particles commonly repel each other, making it difficult for them to aggregate and settle. Thus, to keep away from the repulsive charge and destabilize the suspension, a coagulant with the opposite charge is supplemented to the water. According to the report given by turbidity removal efficiencies were proven to be significantly affected by pH variations and the quantity of natural coagulants used. Turbidity can be measured using an instrument called turbidimeter, which measure the relative clarity of a liquid and the optical character of water and subsequently express the amount of light that is scattered by some materials in the water when a light is projected through the water sample. Thus, the higher the intensity of scattered light, the higher the turbidity. The turbidity values of the water sample can be express as (± 0.01 NTU) Nephelometric Turbidity Units. In drinking water treatment, the coagulation process is used to destabilize suspended particles and to react with organic materials in the raw water. Proper coagulation is essential



for good filtration performance and for disinfection by product (DBP)

RESULTS

A total of 23 plants species belonging to 11 families were recorded, Fabaceae had the highest number of occurrences with

approximately 41%, follow by *malvaceae* family with approximately 14%, and *curcubitaceae* family with approximately 9%, while the rest showed low percentage occurrence (Figure 1). It is revealed that in almost all plant cited the part of the plant used was seed, while some uses flowers and or seed but only few uses leaf part (Table 1).

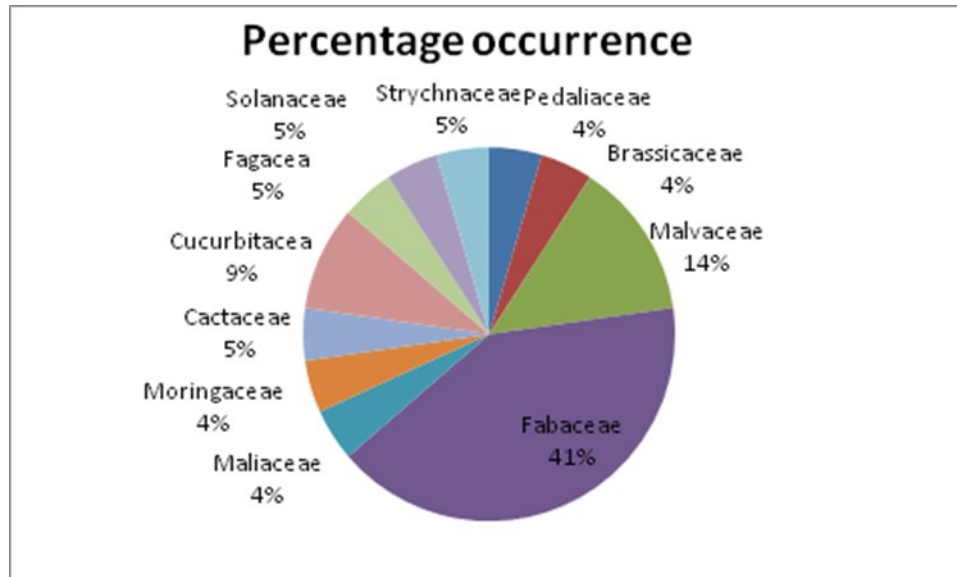


Figure 1 Percentage occurrences of different plant families

DISCUSSION

From the result obtained Fabaceae revealed highest number of occurrences with 41%, follow by *malvaceae* and *curcubitaceae* family with 14%, and 9% respectively. Many of the researchers observed highest percentage turbidity removal from *Moringa oleifera* when compared with other natural plants coagulant. This contrasts the finding of Saravanan *et al.*, (2017) who obtained highest coagulation and turbidity removal from *Azadirachta Indica* when compared with *Dolichas lablab*, *Moringa Oleifera* and *Hibiscus Rosa sinensis*. Nevertheless, Vijayaraghavan *et al.*, (2011) reported that *Moringa oleifera* seed has

recently received the greatest degree of attention in the water treatment. Abood *et al.*, (2017) compared sesame seeds and peanut seeds, thus discovered that peanut seeds are more effective than sesame seeds as far as turbidity is concern because the peanut seeds revealed higher percentage removal of 88.3% compared to sesame seed with 79.7%. Despite, the highest removal efficiency of roselle seeds was found to be lower than that of the synthetic coagulant at pH 4 with 81.2 to 93.13% for roselle seeds and aluminium sulphate respectively. The activities of these natural coagulant may be attributed to the presence of many bioactive compounds especially polyphenolics, vitamins and minerals.



Table 1 Plants with potentiality in waste water treatment and the part used

Botanical name	English name	Family	Part used
<i>Raphanus Raphanistrum</i>	Radish	Brassicaceae	Seed
<i>Sesamum indicum</i>	Sesame	Pedaliaceae	Seed
<i>Hibiscus sabdariffa</i>	Roselle	Malvaceae	Seed
<i>Dolichas lablab,</i>	Lablab bean	Fabaceae	seeds and flowers
<i>Azadirachta Indica,</i>	Neem tree	Maliaceae	seeds and flowers
<i>Moringa Oleifera,</i>	Horseradish, bean oil tree	Moringaceae	Seeds
<i>Hibiscus Rosa Sinensis</i>	China rose	Malvaceae	seeds and flowers
<i>Luffa cylindric</i>	Smooth Luffa,	Cucurbitacea	
<i>Hibiscus Esculentu</i>	Okra,	Malvaceae	
<i>Glycine max</i>	Soya bean	Fabaceae	
<i>Cicer arietinum</i>	hick Pea,	Fabaceae	Seed
<i>Coccinia indica</i>	Small Gourd,	Cucurbitacea	
<i>Phaseolus Angularis</i>	Red Bean	Fabaceae	Seed
<i>Guar gum</i>	Guar Bean,	Fabaceae	
<i>Dolichos biflorus</i>	Horsegram	Fabaceae	
<i>Arachis Hypogea</i>	Ground nut	Fabaceae	Seed
<i>Vigna Unguiculat</i>	cow Pea	Fabaceae	
<i>Pisum Sativum</i>	Green pea	Fabaceae	
<i>Quercus spp</i>	Acorn	Fagacea	Leaves
<i>Solanum Melongena</i>	Eggplant	Solanaceae	Seed
<i>Strychnos potatorum</i>	Clearing-nut	Strychnaceae	Seed
<i>Hylocereus Undatus</i>	Dragon fruit	Cactaceae	Leaf
<i>Citrullus lanatus</i>	Water melon	Cucurbitaceae	Seed

CONCLUSION

From the result obtained it demonstrate potentiality of plant base coagulants, and its good evidence of substituting commercial coagulants due to their accessibility, nontoxic, cost effectiveness and biodegradable natures. Thus, there is need for many researchers to

embark on researches in order to standardize and quantify the usage of natural coagulants. Hence, more studies are needed to determine, isolate and characterize each active constituent with coagulation effect. Natural coagulant can serve as an environmentally friendly in the treatment of high turbid water.



REFERENCES

- i. I.M, Muhammad, S, Abdulsalam, A, Abdulkarim, A.A, Bello. Water Melon Seed as a Potential Coagulant for Water Treatment. *Global Journal of Researches in Engineering: Chemical Engineering*.15(1):17-25 (2015).
- ii. M.M. Abood, N.N. Azhari, A.O. Abdelmoneim,. The use of peanut and sesame seeds as natural coagulant in the water treatment. *Infrastructure University Kuala Lumpur Research Journal* 5 (1):1-10 (2017).
- iii. S.Y. Choy, K.M.N. Prasad, T.Y. Wu. A review on common vegetables and legumes as promising plant-based natural coagulants in water clarification. *Int. J. Environ. Sci. Technol.* 12:367–390 (2013).
- iv. N.F.A. Saharudin, R. Nithyanandam. Wastewater Treatment by using Natural Coagulant. 2nd eureka 2014 – Wastewater Treatment by using Natural Coagulant (2014).
- v. G. Vijayaraghavan, T. Sivakumar, K.A. Vimal. Application of plant based coagulants for waste water treatment. *International Journal of Advanced Engineering Research and Studies*. 1(1):88- 92 (2011).
- vi. E.H. Khader, T.H.J. Mohammed, N. Mirghaffari. Use of Natural Coagulants for Removal of COD, Oil and Turbidity from Produced Waters in the Petroleum Industry. *Journal of Petroleum & Environmental Biotechnology*. 9 (3):1-7 (2018).
- vii. I.M, Muhammad, S, Abdulsalam, A, Abdulkarim, A.A, Bello. Water Melon Seed as a Potential Coagulant for Water Treatment. *Global Journal of Researches in Engineering: Chemical Engineering*.15(1):17-25 (2015).
- viii. M.M. Abood, N.N. Azhari, A.O. Abdelmoneim,. The use of peanut and sesame seeds as natural coagulant in the water treatment. *Infrastructure University Kuala Lumpur Research Journal* 5 (1):1-10 (2017).
- ix. S.Y. Choy, K.M.N. Prasad, T.Y. Wu. A review on common vegetables and legumes as promising plant-based natural coagulants in water clarification. *Int. J. Environ. Sci. Technol.* 12:367–390 (2013).
- x. N.F.A. Saharudin, R. Nithyanandam. Wastewater Treatment by using Natural Coagulant. 2nd eureka 2014 – Wastewater Treatment by using Natural Coagulant (2014).
- xi. I.R.K. Sain, I. Sivanesan, Y. Keum. Phytochemicals of *Moringa oleifera*: a review of their nutritional, therapeutic and industrial significance. *3 Biotech*. 6(203): 1-14 (2016).
- xii. S.Y. Choy, K.M.N. Prasad, T.Y. Wu. A review on common vegetables and legumes as promising plant-based natural coagulants in water clarification. *Int. J. Environ. Sci. Technol.* 12:367–390 (2013).
- xiii. J. Saravanan, D. Priyadarshini, A. Soundammal, G. Sudha, I. Sur, K. yakala. Wastewater Treatment using Natural Coagulants. *SSRG International Journal of Civil Engineering (SSRG - IJCE)* 4 (3):40-42 (2017).
- xiv. G. Vijayaraghavan, T. Sivakumar, K.A. Vimal. Application of plant based coagulants for waste water treatment. *International Journal of Advanced Engineering Research and Studies*. 1(1):88- 92 (2011).
- xv. M.M. Abood, N.N. Azhari, A.O. Abdelmoneim,. The use of peanut and sesame seeds as natural coagulant in the water treatment. *Infrastructure University Kuala Lumpur Research Journal* 5 (1):1-10 (2017).



P056 - SUSTAINABLE HYDROGEN PRODUCTION USING CERIUM-ENHANCED COPPER-ZINC-MCM41 CATALYSTS

Ahmad Muhammad Abiso^{1*}, Opeoluwa O Fasanya², Sharafadeen Gbadamasi², Abdulazeez Y Atta¹, Baba Jibril El-yakubu¹

¹Ahmadu Bello University Zaria,

²National Research Institute of Chemical Technology

Corresponding author email: ahmadabiso@gmail.com

ABSTRACT

This study investigates the influence of cerium on the performance of copper-zinc-MCM41 catalysts in the production of hydrogen through methanol steam reforming. Copper-based catalysts supported on mesoporous materials have shown potential in this reaction. Copper-cerium-zinc-MCM41 and copper-zinc-MCM41 catalysts were synthesised and characterised using various techniques. The findings demonstrate that the addition of cerium enhances catalyst stability, increases active sites, and improves resistance to deactivation. The modified catalysts exhibit enhanced methanol conversion rates and selectivity for hydrogen production. This improvement is attributed to effective CO formation suppression and enhanced redox properties. The study highlights the potential for cerium incorporation to optimise copper-based catalysts for methanol steam reforming, advancing clean energy technologies and sustainable hydrogen production.

KEYWORDS

Methanol Steam Reforming, Copper Catalysts, Cerium, Zinc, MCM41 Support, Sustainable Hydrogen Production, Clean Energy, Catalyst Modification.

1.0 INTRODUCTION

The quest for sustainable and clean energy sources has driven extensive research into catalytic processes that facilitate the conversion of readily available feedstocks into hydrogen—a versatile and clean energy carrier (1). Among these processes, methanol steam reforming (MSR) has emerged as a promising route for hydrogen production (2). In the context of MSR, copper-based catalysts have garnered significant attention due to their ability to promote the reaction kinetics effectively (3). These catalysts are frequently supported on various materials to enhance their stability and reactivity.

Mesoporous materials, such as MCM41, have demonstrated excellent potential as catalyst supports for MSR, owing to their high surface area, tunable pore structure, and thermal stability (3–5). However, challenges persist in optimising the catalytic performance of copper-MCM41 catalysts, including the control of CO formation, maintenance of active sites, and resistance to deactivation. To address these issues, researchers have explored the incorporation of additives or promoters into the catalyst composition.

Among the numerous additives investigated, cerium and zinc have shown particular promise in enhancing the catalytic properties of copper-based materials. Cerium is known for its oxygen storage and release capacity, redox properties, and ability to suppress coke formation. At the same time, zinc has been found to influence the dispersion of copper species and improve the catalyst's redox behaviour (6). These characteristics suggest that cerium and zinc could effectively modify the surface properties and redox behaviour of copper-MCM41 catalysts, thereby impacting their catalytic performance in MSR.

In this context, this study focuses on elucidating the impact of cerium incorporation into copper-zinc-MCM41 catalysts for MSR. Through comprehensive characterisation and catalytic evaluation, we aim to provide valuable insights into the design and optimisation of catalysts for efficient and sustainable hydrogen production, contributing to the advancement of clean energy technologies.

2.0 MATERIALS AND METHODS

2.1 Materials



Cetyl TrimethylAmmonium Bromide (BDH), Zinc Nitrate (BDH), Copper Nitrate (BDH), Cerium Nitrate, tetraethyl-orthosilicate (Sigma Aldrich) and ammonium hydroxide (BDH) were used for the synthesis of CuZn/MCM-41 catalysts. Methanol (Fischer) and distilled deionized water were used for methanol steam reforming reactions.

2.2 Catalyst Synthesis

MCM-41 is prepared using hydrothermal synthesis which involves crystallising substances from high-temperature aqueous solutions at high vapour pressures. The molar composition ratios of the reagents used were SiO: 0.14CTAB: 114H₂O: 8NH₄OH. 2.2g of CTAB which serves as a surfactant was first weighed and dissolved in de-ionised water at room temperature and stirred to get a colourless solution. 8.66g of Tetraethyl-orthosilicate was then added drop-wise to the mixture while stirring for 30 minutes. And 11.6g ammonium hydroxide was added drop-wise to ensure the environment was basic. The solution was then stirred for another 3 hours and then aged in an oven at 110°C for 18 hours. The obtained precipitate was filtered and washed thoroughly with de-ionised water. The filtered material was air dried for 24 hours, followed by oven drying at 110°C for 24 hours.

The metal precursors were deposited onto MCM41 through the co-impregnation method. For the co-impregnation the required concentration of copper nitrate (9wt%) solution, zinc nitrate (1.5wt% and 3wt%,) solution and cerium nitrate (1.5wt%) solution were simultaneously added to a solution of MCM-41 at 70 °C to yield the Cu-Zn-Ce-MCM-41 catalyst. The solutions were heated till all the water evaporated. The catalysts were calcined at 550°C for 6 hours at a heating rate of 1°C/min to remove the surfactant (CTAB). The target amount was 9% of Cu and 3% of Zn in Cu-Zn-MCM41 and 9% of Cu, 1.5% of Zn and 1.5% of Ce in Cu-Zn-Ce-MCM41.

2.3 Catalyst Characterisation

Fourier Transform Infrared Spectroscopy (FTIR) was carried out to obtain a molecular fingerprint of the samples. This was carried out using Spectrum One of Perkin Elmer. The samples were mixed with 99% potassium bromide before the analysis. Infrared radiations were passed through the samples and a spectrum representing the molecular transmission was recorded for each sample.

X-ray diffraction is used to determine the atomic and molecular structure of the catalyst by bombarding a sample with incident rays and monitoring the interaction between the sample and the incident ray. Powder X-ray diffraction (XRD) patterns were recorded on a Rigaku Mini Flex Focus diffractometer instrument operating at 30 kV and 10 mA with Cu target K α -ray ($\lambda = 0.154056$ nm) irradiation. Diffraction data (2θ) was collected between 5° and 90° with a scanning rate of 10°/min.

To determine the surface area, pore size and pore volume of the catalysts, N₂ adsorption-desorption analysis was conducted using ASAP2460 version 3.01 Micrometrics Instrument. Brunauer, Emmet Teller's (BET) kinetic theory is used to calculate the surface area of the catalyst after degassing for about 5 hours.

2.4 Performance Evaluation of the Catalysts

The performance of the synthesized catalysts for methanol steam reforming was evaluated using a Finetec 4100 fixed bed reactor whose setup is illustrated in Figure 1. The system contains a 60 cm-long cylindrical reactor with an internal diameter of 9mm. Prior to charging the catalysts in the reactor, they were mixed with glass beads in a ratio of 1:5. The catalysts were then reduced in 10% hydrogen for 2 hours at 300 °C before the commencement of the reaction.



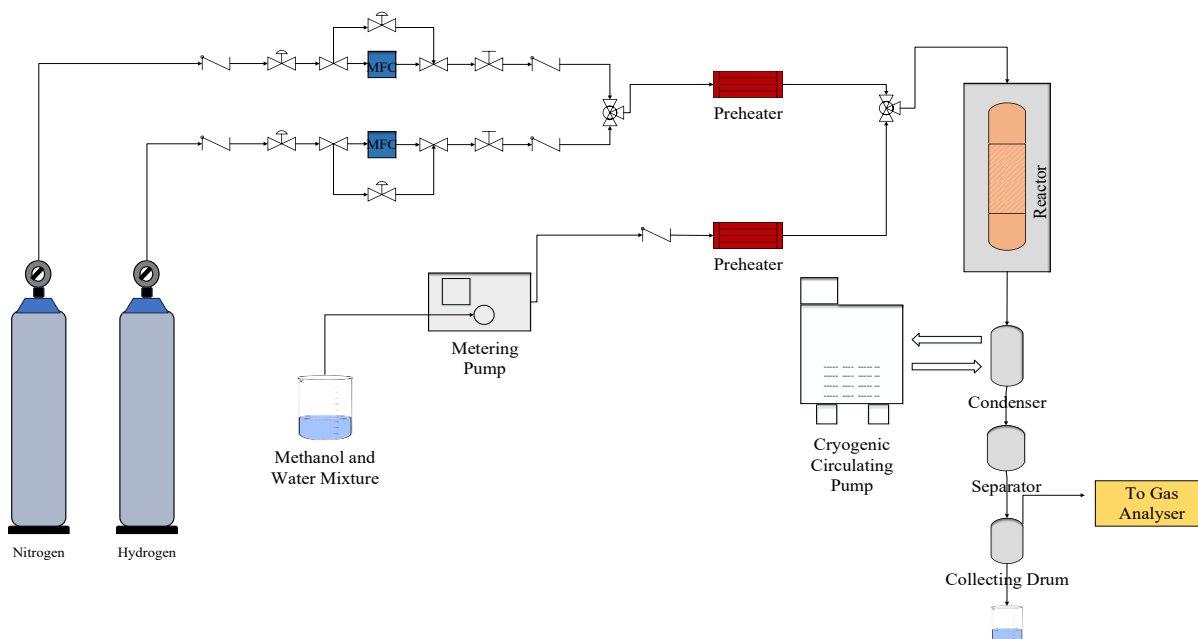


Figure 1: The process flow diagram of the methanol steam reforming experimental setup

Methanol and water were charged into the reactor in a 1:3 ratio, with nitrogen gas acting as the carrier and flowing at 40 ml/min. It should be noted that before being charged into the reactor, the feed and the nitrogen gas carrier are preheated to 120 °C. The methanol and water mixture were fed to the reactor at a rate of 2 ml per hour. The product stream was analysed using a Wuhan Cubic Gasboard 3100P gas analyser equipped with a

$$X_{MeOH}(\%) = \frac{n_{CO} + n_{CO_2} + n_{CH_4}}{n_M} \times 100 \quad 1$$

$$S_{CO}(\%) = \frac{n_{CO}}{n_{CO} + n_{CO_2} + n_{CH_4}} \times 100 \quad 2$$

$$S_{CO_2}(\%) = \frac{n_{CO_2}}{n_{CO} + n_{CO_2} + n_{CH_4}} \times 100 \quad 3$$

$$Y_{H_2}(\%) = 100 \times \frac{X_{MeOH}}{100} \times \frac{S_{H_2}}{100} \quad 6$$

Where n_{CO} , n_{CH_4} and n_{H_2} are the molar flow rates of CO, CO₂, CH₄ and H₂ in the dry reformat (mol/min) respectively, n_M is the molar flow rate of methanol in the mixture feed (mol/min). X_{MeOH} is the methanol conversion, S_{CO} , S_{CO_2} , S_{CH_4} and S_{H_2} are product selectivity for carbon monoxide, carbon dioxide, methane, and hydrogen respectively and Y_{H_2} is the hydrogen yield in the product stream.

thermal conductivity detector (TCD) for H₂ detection and an electron capture detector (ECD) for CO, CO₂ and CH₄ measurements. The system was allowed for 2 hours to attain a steady state before readings were obtained.

The methanol conversion, CO selectivity, CO₂ selectivity, CH₄ selectivity and H₂ selectivity are defined as follows:

$$S_{CH_4}(\%) = \frac{n_{CH_4}}{n_{CO} + n_{CO_2} + n_{CH_4}} \times 100 \quad 4$$

$$S_{H_2}(\%) = \frac{n_{H_2}}{n_{H_2} + 2n_{CH_4}} \times 100 \quad 5$$

3.0 RESULTS AND DISCUSSION

3.1 X-ray Diffraction

X-ray diffraction is one of the most crucial methods for characterising ordered mesoporous materials. In contrast to crystalline materials, where it is caused by local order in the atomic range, the XRD peaks in ordered mesoporous materials appear because of the ordered array of parallel pore walls. XRD was employed to identify the structural phases present, calculate lattice parameters including crystallite dimensions, and assess alterations in the configurations and dimensions of the well-ordered



mesopores. Figure 2 below shows the XRD patterns of the pristine MCM41 and the as-synthesised catalysts. The X-ray diffraction of the pristine MCM41 shows an intense 100 peak around 5° which can be attributed to the interplanar spacing between the mesoporous channels within the material. The small 110 peak next to it relates to the

ordering of the pores within the hexagonal lattice. The broad peak appearing between 20° and 30° is typical of amorphous silica which is the fundamental component of MCM-41. The peaks seen at 35, 38, 58, 61, 66, and 68 in the XRD patterns of impregnated catalyst samples correspond to the CuO crystals.

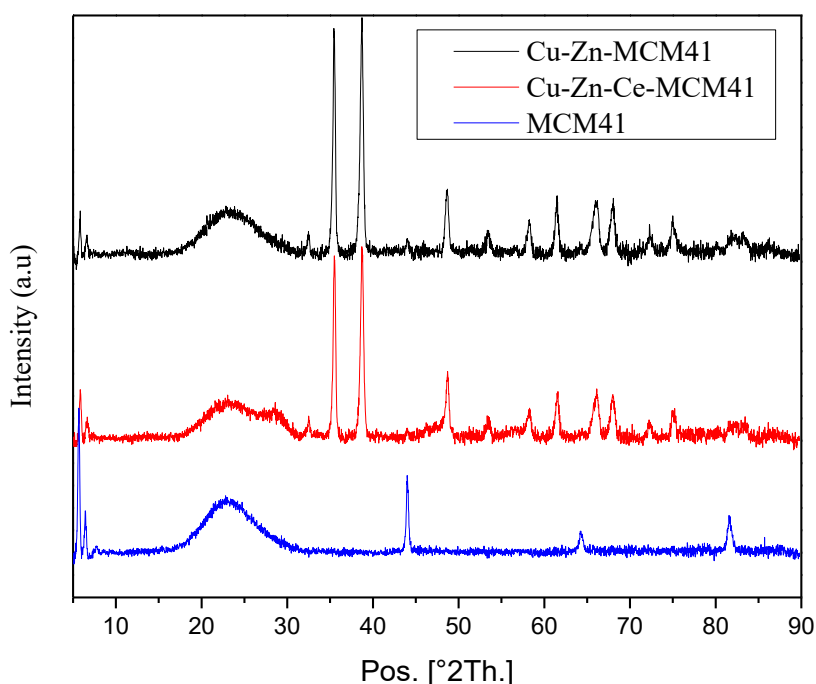


Figure 2: X-ray diffraction patterns of MCM41 and MCM41-supported catalysts

3.2 Fourier Transform Infrared Spectroscopy

FTIR spectroscopy was carried out to monitor the changes in bonding properties caused by metal incorporation in the mesoporous MCM-41 matrix and determine the presence of any unwanted molecule in the structure of the catalysts. The spectra of the parent MCM-41 and the four synthesised catalysts containing Cu, Zn and Ce in different ratios are shown in Figure 3.

One of the primary characteristics of MCM41 spectra is the prominent peak at 1046 cm⁻¹ which is attributed to Si-O-Si group asymmetric stretching vibrations. It is possible to trace the band at 795 cm-

1 to the normal symmetric stretching of Si-O-Si. This is consistent with what Piskin et al. (7) reported on the FTIR study of MCM-41. The peak at 1624 cm⁻¹ is a representation of the bending vibrations of O-H attributed to adsorbed water molecules trapped inside the MCM-41 matrix. A large band extending about 3,391 cm⁻¹, caused by stretching vibrations of structural -OH groups or physically adsorbed water, is one of the primary characteristics of MCM-41 spectra (7). The absence of a peak in the 2500–2800 cm⁻¹ range indicates that the surfactant (CTAB) has been eliminated, as peaks in that range can be attributable to the surfactant's aliphatic C–H stretching vibrations (4).



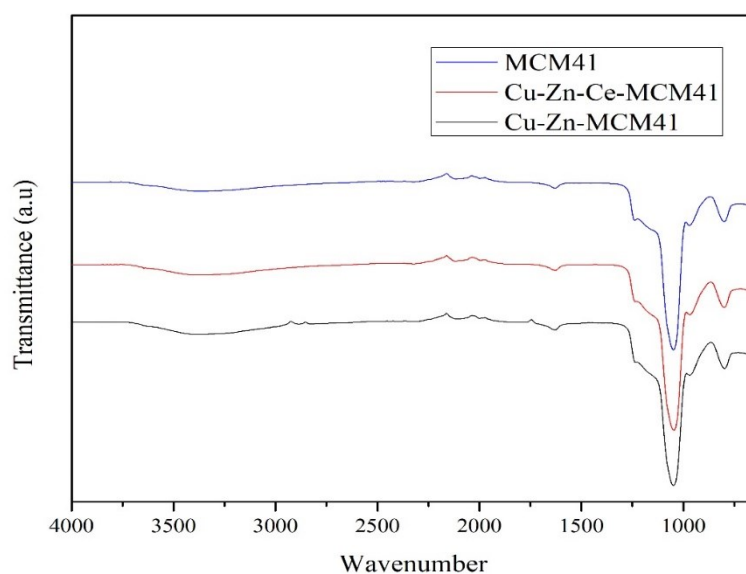


Figure 3 FT-IR spectra of the parent MCM-41 and the four synthesised catalysts

3.3 Nitrogen Adsorption- Desorption

Nitrogen physio-sorption was carried out to determine the textural properties of the pristine MCM41 and MCM41-supported catalysts. Figure 4 depicts the MCM-41 and MCM-41 supported catalysts' N₂ adsorption-desorption isotherms. According to the empirical IUPAC classification, all samples show a typical type IV isotherm with H1 hysteresis loops, a characteristic of mesoporous materials. The isotherms also show a linear increase in nitrogen intake at lower relative pressures, which can be attributed to monolayer nitrogen adsorption on the pore walls, and a sudden increase at intermediate relative pressures ($P/P_0 = 0.3 - 0.4$). This observation suggests the occurrence of

capillary condensation in the mesopores of MCM-41 (8). Additionally, multilayer adsorption onto the outer surface of catalysts can be seen as a lengthy plateau at high relative pressures ($P/P_0 = 0.4 - 1$). Incorporating metals into the MCM-41 has not significantly changed the 2D mesopores architectures, as evidenced by the fact that the general characteristics of the MCM-41 isotherm are likewise observed for the supported catalysts. The area of the N₂ adsorption-desorption curves, compared to that of MCM-41, has been reduced by adding metals to the support. As a result, the curves in Figure 4 show that the doped metals cover the pores in MCM-41, decreasing its accessible surface area, and nitrogen adsorption (5).



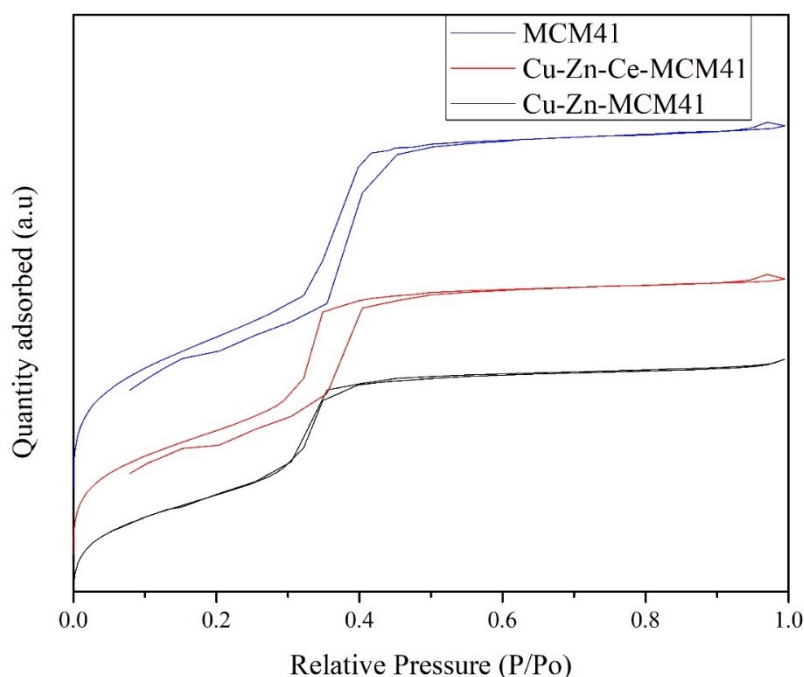


Figure 4: N₂ Adsorption-Desorption Isotherms of MCM41 and MCM41 supported catalysts

Table 1 presents the synthesized samples' specific surface area, pore volume and mean pore size. The highest pore volume (0.785 cm³/g) and specific surface area (871.45 m²/g) belong to pristine MCM-41. The lowest surface area was observed in Cu-Zn-MCM41 which is 640 m²/g. Ce addition to Cu-Zn-MCM41 results in a reduction in the mean pore size

and volume while marginally increasing the surface area by improving surface roughness. Furthermore, according to Table 1, Cu and Zn impregnation reduces the surface area, pore size, and pore volume of MCM-41 by blocking a portion of the mesopores.

Table 1: BET Surface area, pore size and pore volumes of different Cu-MCM-41 catalyst samples.

	BET Surface Area (m ² /g)	Pore Size (nm)	Pore Volume (cm ³ /g)
MCM41	871.4506	3.61	0.785574
Cu-Zn-MCM41	640.0272	3.28	0.524347
Cu-Zn-Ce-MCM41	713.5776	3.39	0.604230

3.4 Performance Tests

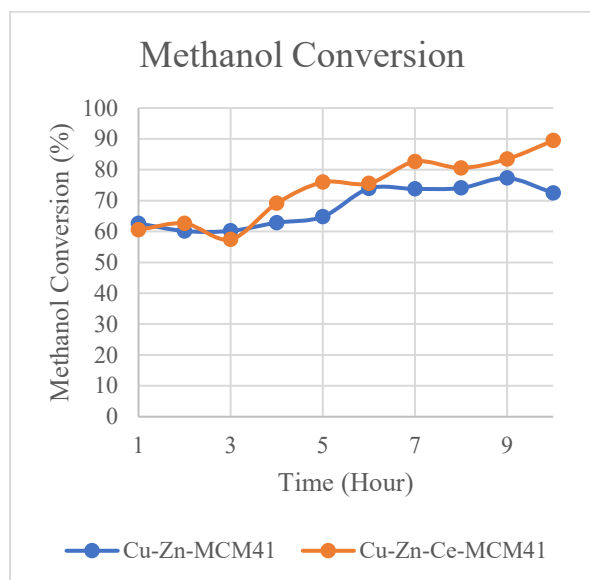
In order to evaluate the catalytic performance of the synthesised catalysts for MSR, a 10-hour time on-stream experiment was conducted on each of the synthesized catalysts. Figure 5 illustrating methanol conversion and hydrogen yield in methanol steam reforming (MSR) over Copper-Zinc (Cu-Zn) catalysts and Copper-Zinc-Cerium (Cu-Zn-Ce) catalysts reveals an intriguing trend. Notably, the

Cu-Zn-Ce-MCM41 catalyst consistently exhibits higher methanol conversion in the long run compared to the Cu-Zn catalyst. This observation can be attributed to several key factors. Cerium, serving as a promoter in the Cu-Zn-Ce catalyst, contributes significantly to its enhanced performance. Cerium possesses unique redox properties that facilitate the activation of reactants and the regeneration of active sites on the catalyst's surface (9, 10). This property allows the Cu-Zn-Ce



catalyst to sustain its catalytic activity over an extended period, ultimately leading to higher methanol conversion rates (6).

Furthermore, cerium acts as a stabilising agent for copper species on the catalyst surface. This stabilisation prevents the agglomeration of copper species, which can lead to deactivation. Consequently, more active sites remain accessible



for the MSR reaction, resulting in increased methanol conversion(11).

The observed superior performance of Cu-Zn-Ce catalysts may also be attributed to the synergistic effects arising from the combination of cerium and zinc. These promoters may work together to enhance the overall catalytic performance, further boosting methanol conversion rates.

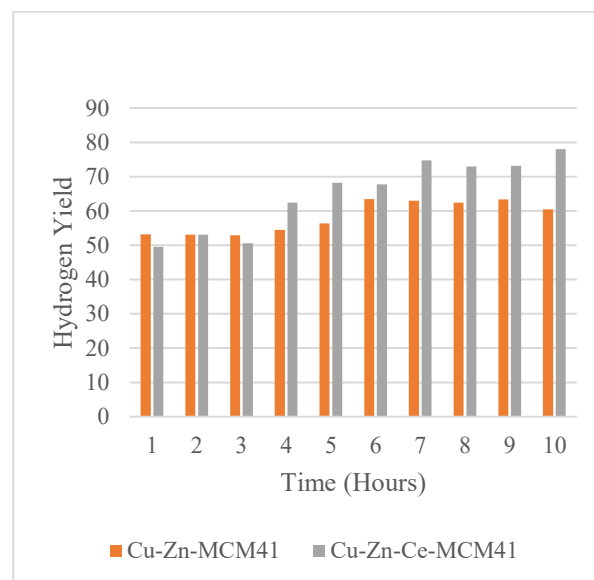


Figure 5 Methanol Conversion and Hydrogen yield profiles for the as-synthesised catalysts at 300°C

Figure 6 depicts product distribution in methanol steam reforming (MSR) over Copper-Zinc (Cu-Zn) catalysts and Copper-Zinc-Cerium (Cu-Zn-Ce) catalysts and offers intriguing insights into the influence of cerium on the reaction outcomes. Notably, the Cu-Zn-Ce catalyst exhibits a distinct advantage over the Cu-Zn catalyst, with slightly

Zn-Ce catalyst plays a pivotal role in enhancing the activation of methanol molecules. Cerium possesses unique redox properties that aid in the more efficient breakdown of methanol into its constituent hydrogen and carbon dioxide. This enhanced methanol activation results in a cleaner product stream, as less methanol is diverted towards CO and CH₄ formation (6).

Furthermore, the stability of the catalyst is a crucial factor in maintaining the selectivity for desired products, namely hydrogen and carbon dioxide, while minimising the production of undesired by-products such as CO and CH₄. Cerium contributes significantly to the overall stability of the Cu-Zn-Ce catalyst, ensuring that it remains selective for the desired reactions (12).

lower carbon monoxide (CO) and methane (CH₄) levels in its product distribution.

This disparity in product distribution can be attributed to several key factors, each of which underscores the pivotal role of cerium as a promoter in catalysis. First and foremost, cerium's presence in the Cu-

Cerium's ability to suppress methanation reactions is another vital aspect. These methanation reactions lead to CH₄ formation and can be less favoured in the presence of cerium. This suppression ensures that a higher fraction of carbon atoms end up as carbon dioxide, rather than CH₄, in the product distribution of the Cu-Zn-Ce catalyst (13).

Additionally, cerium's unique redox behaviour plays a role in efficient oxygen species removal from the catalyst's surface. This is essential for preventing the conversion of hydrogen into water through the water-gas shift reaction, which can lead to CO formation. By maintaining a low oxygen content on the catalyst surface, cerium helps minimise CO production, contributing to the observed differences in product distribution (14).



Practically, the implications of this graph are significant for MSR applications, especially in the quest for clean hydrogen production. The Cu-Zn-Ce catalyst's ability to yield a product stream with reduced CO and CH₄ content aligns perfectly to

produce clean hydrogen, a valuable energy carrier. Simultaneously, this minimises the formation of greenhouse gases and undesired by-products, aligning the process with environmental and sustainability objectives.

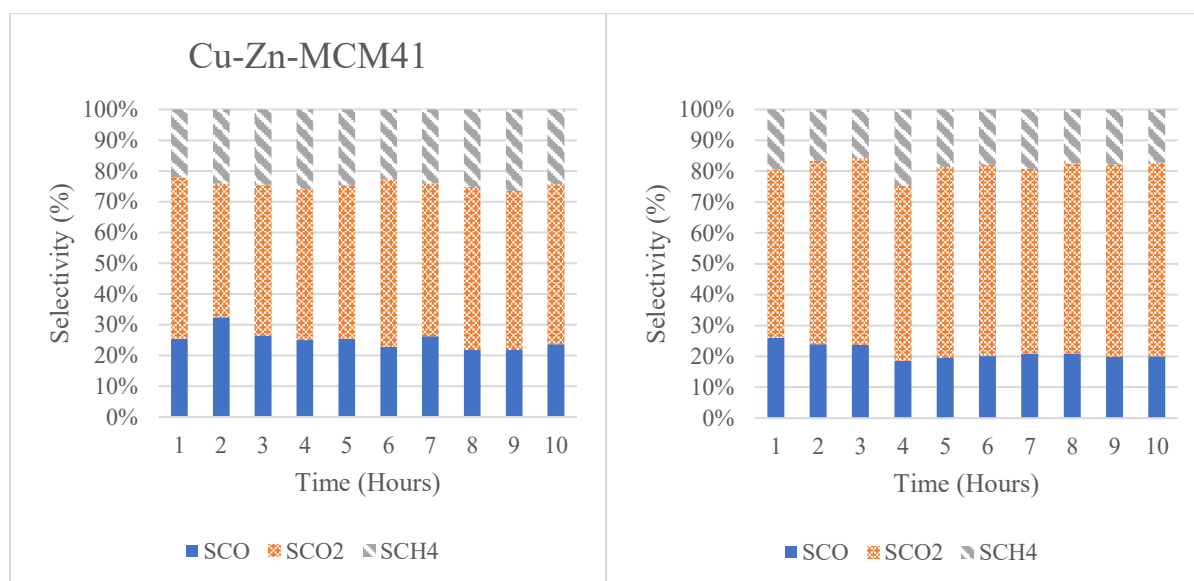


Figure 6: Product Distribution of the MSR reaction with the two catalysts.

4.0 CONCLUSIONS

In this study, we have investigated the impact of cerium incorporation into copper-zinc-MCM41 catalysts for methanol steam reforming (MSR). Our findings have shed light on the potential of cerium as an effective promoter in enhancing the catalytic performance of copper-based catalysts for hydrogen production.

The characterisation results have confirmed that the addition of cerium and zinc leads to modifications in the catalyst structure and redox behaviour. These modifications, including improved redox properties, and effective suppression of CO formation, collectively contribute to improved catalyst stability and activity in MSR. Specifically, the modified catalysts exhibited enhanced methanol conversion rates and selectivity for hydrogen production.

5.0 REFERENCES

1. P. Nikolaidis, A. Poullikkas, A comparative overview of hydrogen production processes. *Renew. Sustain. Energy Rev.* **67**, 597–611 (2017).
2. M. Byun, H. Lee, C. Choe, S. Cheon, H. Lim, Machine learning based predictive model for methanol steam reforming with technical, environmental, and economic perspectives. *Chem. Eng. J.* **426**, 131639 (2021).
3. V. G. Deshmane, R. Y. Abrokwah, D. Kuila, Synthesis of stable Cu-MCM-41 nanocatalysts for H₂ production with high selectivity via steam reforming of methanol. *Int. J. Hydrogen Energy.* **40**, 10439–10452 (2015).
4. R. Y. Abrokwah, thesis, North Carolina A&T State University (2016).
5. O. O. Fasanya, A. Y. Atta, M. T. Z. Myint, J. Dutta, B. Y. Jibril, Effects of synthesis methods on performance of CuZn/MCM-41 catalysts in methanol steam reforming. *Int. J. Hydrogen Energy.* **46**, 3539–3553 (2021).
6. S. Bepari, M. Khan, X. Li, N. Mohammad, D. Kuila, Effect of Ce and



- Zn on Cu-Based Mesoporous Carbon Catalyst for Methanol Steam Reforming. *Top. Catal.* **66**, 375–392 (2023).
7. S. Piskin, M. S. Yilmaz, O. D. Ozdemir, Synthesis and characterization of MCM-41 with different methods and adsorption of Sr²⁺ on MCM-41. *Res Chem Intermed* (2013), doi:10.1007/s11164-013-1182-4.
 8. S. Sohrabnezhad, A. Jafarzadeh, Synthesis and characterization of MCM-41 ropes. *Mater. Lett.* (2017), doi:10.1016/j.matlet.2017.10.059.
 9. J. F. Brazdil, The Emergence of the Ubiquity of Cerium in Heterogeneous Oxidation Catalysis Science and Technology. *Catalysts.* **12**, 959 (2022).
 10. S. Gao, D. Yu, S. Zhou, C. Zhang, L. Wang, X. Fan, X. Yu, Z. Zhao, Construction of cerium-based oxide catalysts with abundant defects/vacancies and their application to catalytic elimination of air pollutants. *J. Mater. Chem. A.* **11**, 19210–19243 (2023).
 11. Y. Chen, Y. Huang, Influence of ceria existence form on deactivation behaviour of Cu-Ce/SBA-15 catalysts for methanol steam reforming. *Int. J. Hydrogen Energy.* **48**, 1323–1336 (2023).
 12. M. Hosseini Abbandanak, M. Taghizadeh, N. Fallah, High-purity hydrogen production by sorption-enhanced methanol steam reforming over a combination of Cu–Zn–CeO₂–ZrO₂/MCM-41 catalyst and (Li–Na–K) NO₃·MgO adsorbent. *Int. J. Hydrogen Energy.* **46**, 7099–7112 (2021).
 13. H. Shahsavar, M. Taghizadeh, A. D. Kiadehi, Effects of catalyst preparation route and promoters (Ce and Zr) on catalytic activity of CuZn/CNTs catalysts for hydrogen production from methanol steam reforming. *Int. J. Hydrogen Energy.* **46**, 8906–8921 (2021).
 14. C. Yu, S. Sakthinathan, B. Hwang, S.-Y. Lin, T.-W. Chiu, B.-S. Yu, Y.-J. Fan, C. Chuang, CuFeO₂–CeO₂ nanopowder catalyst prepared by self-combustion glycine nitrate process and applied for hydrogen production from methanol steam reforming. *Int. J. Hydrogen Energy.* **45**, 15752–15762 (2020).



P057 - MENTHOL-BASED HYDROPHOBIC DEEP EUTECTIC SOLVENT FOR THE DEGRADATION OF PHENOLIC POLLUTANTS IN REFINERY EFFLUENT

Deborah Oluwatomilola Adeoye^{a, c*}, Zaharaddeen Sani Gano^b, Omar Umar Ahmed^d, Suleiman Mohammed Shuwa^a, Abdulazeez Yusuf Atta^a, Baba Yakubu Jubril^a

a – Department of Chemical Engineering, Ahmadu Bello University, Zaria, Kaduna State, Nigeria.

b – National Research Institute for Chemical Technology, Zaria, Kaduna State, Nigeria.

c – Nigerian Institute of Leather and Science Technology, Zaria, Kaduna State, Nigeria.

d – Department of Chemical and Petroleum Engineering, Bayero University, Kano, Nigeria.

*Corresponding Author: yawehst2006@gmail.com

ABSTRACT

Phenol is a dangerous recalcitrant organic micro-pollutant present in industrial wastewater. Even in low concentrations, it is highly poisonous. Because of phenol's plethora of applications, it constitutes health hazards to the entire ecosystem when wastewater containing this pollutant is not adequately treated. In this study, two long-chain organic acid-based hydrophobic deep eutectic solvents were prepared and characterized for the treatment of phenol in wastewater. These HDESs are Menthol-Decanoic acid (MC₁₀) and Menthol-Dodecanoic acid (MC₁₂). The HDESs were used in synergy with hydrogen peroxide to generate peroxy acids for the degradation of pollutants in refinery wastewater. The degradation of two pollutants (phenol and 4-nitrophenol) was investigated. The percentage of total organic compounds reduction was 88.75% and 67.08% for MC₁₀ and MC₁₂ respectively. The recyclability of each HDES was also investigated for three runs. The percentage of total organic compounds reduced from 88.75% to 33.33% for MC₁₀, while it reduced from 67.08% to 11.25% for MC₁₂.

KEYWORDS

Phenol, Nitrophenol, Menthol, Decanoic acid, Dodecanoic acid, Hydrophobic Deep Eutectic Solvent, Ultrasonication.

1.0 INTRODUCTION

Phenol is a precursor for numerous products such as herbicides, drugs, paints, cosmetics, and lubricants, with its primary use as an intermediate in the production of phenolic resins (e.g. phenol-formaldehyde resins). It is also converted to a precursor of plastics via condensation with acetone which results in bisphenol-A (BPA) for the manufacture of polycarbonates and epoxide resins, forming its other major use. Phenolic pollutants are well-known recalcitrant organic contaminants that are generated from numerous industrial processes which include wood preservation, pharmaceutical production, textile dyeing, plastic and resin production, metal coating, coal conversion, and petroleum refining (6, 4, 16). They normally exist in the effluents of the numerous relevant industries such as refineries (6–500 mg/L), coking operations (28–3,900 mg/L), coal processing (9–6,800 mg/L), petrochemical plants (2.8–1,220 mg/L), and others sources such as pharmaceuticals, plastics, wood

products, paint, pulp, and paper industries containing about 0.1–1,600 mg/L phenols (12, 17, 14, 1, 18).

Phenolics can cause loss of consciousness or outrightly collapse the central nervous system. Some of the dangerous effects of inhaling phenolic vapours are dyspnea, coughing, cyanosis, and lung oedema. Phenol poisoning can greatly damage inner organs including kidneys, liver, spleen, lungs, and heart. In the event of serious phenolic poisoning, neuropsychiatric problems are inevitable. As stated by the Occupational Safety and Health Administration, the limits of phenolic skin contact should be less than 5 mg/L, and it is considered that the ingestion of 1g of phenol is fatal for humans (17, 1, 18).

The need for the elimination of phenol and its derivatives from wastewater before such is released into the environment is paramount because exposure to these pollutants results in a consequential threat to human health and the entire



ecological community (4). For safety, and to forestall environmental issues, it is very imperative to eliminate phenolics from the wastes of different production units before they're discharged into the biosphere. Conventional techniques for the elimination of phenol in industrial wastewaters are membrane filtration; coagulation/flocculation; ion exchange; electrolysis, adsorption on activated carbon; chemical reduction, and advanced oxidation processes (such as chlorination, ozonation, Fenton oxidation, photocatalytic oxidation).

Advanced Oxidation Processes (AOPs) among others have gained more popularity due to their ability to extensively eliminate these pollutants (11, 10). AOPs refer to the procedures that largely use *non-selective* hydroxyl radicals for eliminating organic pollutants in wastewater. In the conventional Fenton process, non-selective hydroxyl radicals are generated by reacting hydrogen peroxide and iron (II) salt, and then the produced radicals are used for the degradation of phenolic pollutants in industrial wastewater. These are methods capable of speeding up the oxidation of pollutants. They can work in synergy with other substances and techniques to provide a robust remediation of wastewater. When in synergy with other substances and techniques, they are referred to as Integrated Advanced Oxidation Processes (I-AOPs).

Numerous factors are capable of interfering with and limiting the efficiency of I-AOPs, and these include water chemistry, the molecular structure of organic pollutants, and ions co-occurring in water. For instance, when organic matter (humic acid and fulvic acid) and inorganic ions (halide, carbonate, and nitrate ions) are present in water, they can affect the degradation efficiency. These ions (organic and inorganic) are usually either converted to high redox potential radicals when they collide with reactive species to increase the reaction rates, or

they act as radical scavengers which results in a decrease of the process efficiency (15).

Due to the non-selective nature of hydroxyl radical generated from hydrogen peroxide and the presence of organic and inorganic ions that cumulatively reduce the efficiency of AOPs, alternative oxidizing agents are been researched into that will generate selective/target-oriented radicals that will improve the efficiency of wastewater treatment. Peroxy acids (peracids) are peroxides produced by reacting carboxylic acids with hydrogen peroxide in the presence of a strong acid. They are strong oxidants and are more reactive than hydrogen peroxide. The oxidation capability of peroxides is connected to the substituent's electronegativity. Electrophilic peroxides are known to be stronger oxygen-atom transfer agents because their tendency to donate oxygen-atom corresponds with the acidity of the O-H bond.

This research was to investigate the use of hydrophobic DES-based peracids to treat phenol-contaminated wastewater. These DESs were prepared from monoterpene and long-chain saturated organic acids. The DES components selected are all-natural, rich in sources, and widely used in human life.

2.0 MATERIALS AND METHODS

2.1 Hydrophobic Deep Eutectic Solvent Synthesis

Menthol (99% assay) was purchased from Molychem, Decanoic acid (98% assay), and Dodecanoic acid (99% assay) from Loba Chemie. In this work, binary mixtures of monoterpene (menthol) and carboxylic acids (decanoic acid, and dodecanoic acid) were prepared by adding the components into glass vessels (at the molar ratios as contained in table 1). The solid mixtures were melted under stirring on a magnetic stirrer hot plate at 80°C until a homogeneous liquid mixture was obtained and cooled to room temperature.

Table 1: Composition of different Hydrophobic Deep Eutectic Solvents

HBA	HBD	Abbreviation	Mole Ratio	Physical Appearance
Menthol	Decanoic acid	MC ₁₀	1:1	Colourless liquid
	Dodecanoic acid	MC ₁₂	1:1	Colourless liquid

2.3 Degradation Process

Simulated wastewater was prepared by dissolving 30mg of analytical-grade phenol crystals in 1 litre

of distilled water. 3g of ferrous sulphate was dissolved in the contaminated wastewater to catalyze the homolysis of the DES-peracid. The pH



of the wastewater was adjusted using 0.1M NaOH or 0.1M H₂SO₄. 20ml of contaminated wastewater was introduced into sample bottles and DES-peracid was added. These samples were placed inside an ultrasonicator with 60 kHz sonication speed at 30°C for 60 minutes. The samples were removed and left for phase separation between the DES-peracid and treated water. The water phase was taken for analysis to determine the phenol concentration.

2.4 Analysis

i. FTIR for HDES

The spectrum of each sample was determined by a Cary 630 FTIR spectrometer (Agilent Technologies). A small quantity of each sample was scooped with a spatula and placed on the spectrometer sampling surface. With the aid of an in-built interferometer, the spectrometer measures the energy transmitted to the sample. Emitted infrared radiation from the black body (furnace) hits the interferometer, where spectral encoding occurs. The resultant signal is then transmitted through the sample surface, in which specific energy wavelengths are absorbed. The beam finally proceeds through the detector and is passed to the

iv. Total Organic Compounds Analysis (Titration method)

4 ml of sample was transferred into a digestion tube, and 1 ml of 0.0667M potassium dichromate was added. 5 ml of concentrated sulphuric acid was added while mixing constantly. Two blank tubes were prepared (i.e. with reagents but without sample). The sample tubes and 1 blank were placed in a pre-heated block at 150°C for 30 minutes and later removed to cool. The other blank is left unheated. The contents of the tube were quantitatively transferred to labelled 100ml conical flasks, and 0.3 ml (3 – 4 drops) indicator solution was added. While using a magnetic stirrer to ensure good mixing, all samples and blanks were titrated with acidified ferrous ammonium sulphate solution. The endpoint is a colour change from green/violet to red. The titres values were recorded for each sample, the heated blank, and the unheated blank (8, 9).

3.0 RESULTS AND DISCUSSION

processing computer for the Fourier transform of energy signals.

ii. Moisture Content (Hydrophobicity)

10 ml of the prepared HDES was introduced into six sample bottles, and 10 ml of distilled water was added to each of them. There was proper agitation of the mixture, and the samples were left for 24 hours. It was observed after 24-hour intervals that there was distinctive phase separation in the sample bottles, giving an upper phase consisting of HDES and a bottom phase consisting of water. The HDES phases were then removed from the sample mixture using a syringe and set aside for moisture content analysis using a Karl Fischer Moisture Analyser. The moisture content of each sample was determined by a Metrohm 756 Karl Fischer Coulometer Analyser.

iii. Phenol and 4-Nitrophenol concentration

An ultraviolet-visible spectrophotometer was used to determine the initial phenol, 4-nitrophenol concentration (before treatment) and the final concentration (after treatment) at 270nm and 320nm after scanning and plotting the calibration curve.

3.1 HDES FTIR Spectra

Fourier Transform Infrared (FTIR) spectra of the different terpenes and organic acids and the resultant HDES from their combinations were determined to investigate and ascertain this interaction. Figure 1 presents the cascaded spectra of menthol, decanoic acid (C₁₀) and MC₁₀ HDES. C₁₀ being the HBD, showed a characteristic carbonyl stretching band (C=O) at 1692.2 cm⁻¹, while MC₁₀ showed a shift in the OH band in menthol to 3406.8 cm⁻¹ and a corresponding shift in the C=O band to 1710.8 cm⁻¹. The alkane C-H stretching bands reflecting in the HBD and HBA were maintained in the resulting HDES (MC₁₀). In Figure 2, the HBD for MC₁₂ was dodecanoic acid (C₁₂) with an initial C=O band at 1692.2 cm⁻¹. The menthol OH band shifted from its initial wavelength to 3410.5 cm⁻¹, while the C=O band in C₁₂ experienced a slight backward shift to 1710.8 cm⁻¹ as reflected in MC₁₂.



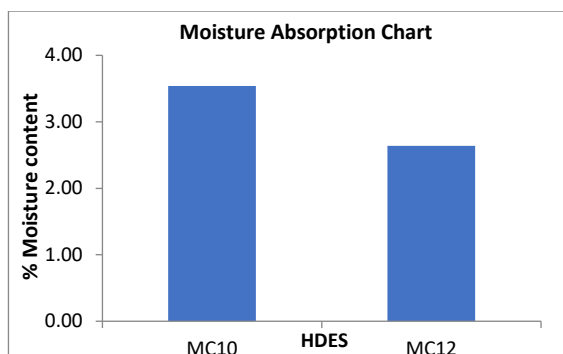


Figure 5: Percentage Moisture Content for HDESs (test for hydrophobicity)

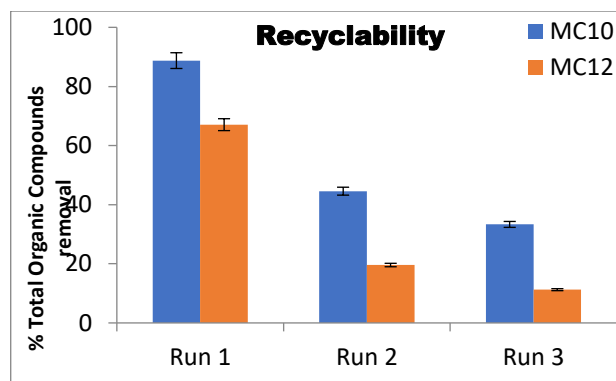


Figure 6: Recyclability using HDESs

4.0 CONCLUSION

Two (2) menthol-based hydrophobic deep eutectic solvents from long-chain organic acids were successfully prepared, all in a ratio of 1:1. Both were liquids at room temperature. The prepared HDESs were characterized using FTIR, and the spectra revealed remarkable shifts in the O-H stretching bands and C=O stretching bands of the HDESs when compared with their precursors. The changes in the OH stretching bands and C=O stretching bands resulted from the intermolecular hydrogen bond formed between the starting materials to give HDES. Also, the extent of moisture absorption into the matrix of the HDESs was determined. It was observed that the degree of hydrophobicity increased with an increase in the alkyl chain of the organic acids.

Both HDESs were then used in synergy with H_2O_2 to degrade Phenol and 4-nitrophenol micro-pollutants from simulated wastewater. These best process parameters were thereafter used to treat refinery wastewater in which the efficiency of phenol degradation was 76% for MC₁₀ and 59% for MC₁₂. The recyclability of the spent HDESs was also studied for three runs by determining the Total Organic Compound (TOC) in the raw and treated refinery effluents. For MC₁₀, the percentage reduction of total organic compounds from the wastewater was from 88.75 to 33.33 % for the three runs while for MC₁₂, it reduced from 67.08 to 11.25 %.

REFERENCES

1. Ahmed, S., Rasul, M. G., Martens, W. N., Brown, R., & Hashib, M. A. (2010). Heterogeneous photocatalytic degradation

of phenols in wastewater: A review on current status and developments.

Desalination, 261(1–2), 3–18.
<https://doi.org/10.1016/j.desal.2010.04.062>

2. Ali, H. H., Ghareeb, M. M., Al-Remawi, M., & T. Al-Akayleh, F. (2020). New insight into single phase formation of capric acid/menthol eutectic mixtures by Fourier-transform infrared spectroscopy and differential scanning calorimetry. *Tropical Journal of Pharmaceutical Research*, 19(2), 361–369.

<https://doi.org/10.4314/tjpr.v19i2.19>

3. Florindo, C., Branco, L. C., & Marrucho, I. M. (2019). Quest for Green-Solvent Design: From Hydrophilic to Hydrophobic (Deep) Eutectic Solvents. *ChemSusChem*, 12(8), 1549–1559.

<https://doi.org/10.1002/cssc.201900147>

4. Hamid, M., & Khalil-ur-Rehman. (2009). Potential applications of peroxidases. *Food Chemistry*, 115(4), 1177–1186.
<https://doi.org/10.1016/j.foodchem.2009.02.035>

5. Ibrahim, R. K., Hayyan, M., AlSaadi, M. A., Ibrahim, S., Hayyan, A., & Hashim, M. A. (2019). Physical properties of ethylene glycol-based deep eutectic solvents. *Journal of Molecular Liquids*, 276, 794–800.
<https://doi.org/10.1016/j.molliq.2018.12.032>



6. Michałowicz, J., & Duda, W. (2007). Phenols - Sources and toxicity. *Polish Journal of Environmental Studies*, 16(3), 347–362.
7. Mjalli, F. S., Murshid, G., Al-Zakwani, S., & Hayyan, A. (2017). Monoethanolamine-based deep eutectic solvents, their synthesis and characterization. *Fluid Phase Equilibria*, 448, 30–40. <https://doi.org/10.1016/j.fluid.2017.03.008>
8. Nelson, D. A. and Sommers, L. E. (1996). *Total carbon, organic carbon, and organic matter. Methods of soil analysis: Part 3 Chemical methods*.
9. Nelson, D. A. and Sommers, S. (1983). *Total carbon, organic carbon, and organic matter. Methods of soil analysis: Part 2 chemical and microbiological properties*.
10. Qayyum, H., Maroof, H., & Yasha, K. (2009). Remediation and treatment of organopollutants mediated by peroxidases: A review. *Critical Reviews in Biotechnology*, 29(2), 94–119. <https://doi.org/10.1080/07388550802685306>
11. Radushev, A. V., Plotnikov, A. V., & Tyryshkina, V. N. (2008). Regeneration methods of decontamination of phenol-containing waste waters. *Theoretical Foundations of Chemical Engineering*, 42(5), 781–794. <https://doi.org/10.1134/S0040579508050527>
12. Rappoport, Z. (2004). *The Chemistry of Phenols*. John Wiley and Sons.
13. Santana, A. P. R., Mora-Vargas, J. A., Guimarães, T. G. S., Amaral, C. D. B., Oliveira, A., & Gonzalez, M. H. (2019). Sustainable synthesis of natural deep eutectic solvents (NADES) by different methods. *Journal of Molecular Liquids*, 293, 111452. <https://doi.org/10.1016/j.molliq.2019.111452>
14. Takht Ravanchi, M., Kaghazchi, T., & Kargari, A. (2009). Application of membrane separation processes in petrochemical industry: a review. *Desalination*, 235(1–3), 199–244. <https://doi.org/10.1016/j.desal.2007.10.042>
15. Tufail, A., Price, W. E., & Hai, F. I. (2020). A critical review on advanced oxidation processes for the removal of trace organic contaminants: A voyage from individual to integrated processes. *Chemosphere*, 260, 127460. <https://doi.org/10.1016/j.chemosphere.2020.127460>
16. Varsha, Y. ., Deepthi CH, N., & Chenna, S. (2011). An Emphasis on Xenobiotic Degradation in Environmental Clean up. *Journal of Bioremediation & Biodegradation*, 02(04), 1–10. <https://doi.org/10.4172/2155-6199.s11-001>
17. Veeresh, G. S., Kumar, P., & Mehrotra, I. (2005). Treatment of phenol and cresols in upflow anaerobic sludge blanket (UASB) process: A review. *Water Research*, 39(1), 154–170. <https://doi.org/10.1016/j.watres.2004.07.028>
18. Zhang, Q., De Oliveira Vigier, K., Royer, S., & Jérôme, F. (2012). Deep eutectic solvents: Syntheses, properties and applications. *Chemical Society Reviews*, 41(21), 7108–7146. <https://doi.org/10.1039/c2cs35178a>



P059 - HIERARCHICAL ZSM-5 AS A POTENTIAL CATALYST FOR ENHANCED PERFORMANCE

S. S. Salisu^{1,2*}, W. C. Okafor^{1,2}, A. Aliyu¹, A. Y. Atta¹, B. J. El-Yakubu¹

¹Department of Chemical Engineering, Ahmadu Bello University, Zaria, P.M.B 1045, Nigeria

²Research and Development Centre, Dangote Petroleum Refinery and Petrochemicals, FZE, Union Marble House, Ikoyi, Lagos Nigeria

Corresponding author email: shafasanda1@gmail.com

ABSTRACT

The microporous nature of the conventional ZSM-5 catalyst has limited mass transfer potential and as such prevents proper diffusion of molecules through the micropores. In this study, Hierarchical ZSM-5 (Hi ZSM-5) was synthesised by creating mesopores in the ZSM-5 via desilication. Detailed characterization was carried out using X-ray diffractometer (XRD), X-ray fluorescence (XRF), Fourier transform infrared (FTIR) Spectroscopy and the acid site distribution was quantified using NH₃-TPD. Results show that the relative crystallinity (RC) of ZSM-5 reduced from 100% to 85.6% due to desilication. The reduction in Silica-to-Alumina (Si/Al) ratio of ZSM-5 from 46.90 to 25.93 was observed, while the percentage mesoporosity and pore width of ZSM-5 increased from 15 to 44% and 2.0 to 3.9nm respectively. The increase in mesoporosity and decrease in Si/Al ratio implies more active sites and accessibility for better yield of product.

KEYWORDS

Desilication, Diffusion, Hierarchical ZSM-5, Mesopores, ZSM-5

1.0 INTRODUCTION

The ZSM-5 zeolite catalyst is well known for being efficient in the conversion of hydrocarbons by isomerisation, aromatisation and cracking reactions. The crystallinity, large surface area, well-defined micropores, interconnected network of pathways, strong acidity, and high resistance to deactivation are inherent properties advantageous to ZSM-5 (1). Due to the presence of the Aluminium in the framework, their distinctive microporous structure made up of 10-membered ring channels results in significant Bronsted acidity. For reactions initiated by the formation of carbonium ion, Bronsted acid sites (BAS) are required which is largely dependent on the Silica-to-Alumina ratio of the catalyst. Reactions such as cracking and isomerisation, the reactants and products must easily diffuse through pores of the catalyst to avoid prolonged residence time leading to coking and formation of undesired products. However, diffusion restrictions can occur in the

2.0 MATERIALS AND METHODS

2.1 Desilication of ZSM-5

small micropores that obstruct access to active sites and reduce catalytic efficiency. Mesopores can be included in the ZSM-5 structure to improve mass transfer, ease diffusion restrictions, and provide better access to active areas by desilication or dealumination (2–5).

While dealumination is attractive, the framework structure of the zeolite is easily destroyed leading to reduction in the catalytic properties of the catalyst (6). Desilication is one of the most widely used processes for creating secondary porosity in ZSM-5. This technique relies on preferentially removing silicon from the ZSM-5 structure in an alkaline environment. The concentration of the alkaline solution affects the Si/Al ratio during desilication of ZSM-5 and needs to be monitored so as not to exceed the optimal range required to maintain the integrity of the zeolite framework (7). It is against this backdrop that this research seeks to investigate the hierarchical ZSM-5 for enhanced mass transfer.

Commercial ZSM-5 catalyst (Si/Al ratio of 50, Zeolyst International) was employed in this research. NH₄-ZSM-5 with Si/Al of 50 was Calcined at 550°C for 5hr at a rate of 30°C/min to



transform it to Hydrogen form (HZSM-5). 16.6g of HZSM-5 was put in 500 ml of 0.3M Sodium hydroxide solution and stirred at 65°C for one hour (Dauda et al., 2020). The residue was filtered using a vacuum system. Deionised water was used to wash the solid until a neutral pH was observed. It was then dried at 90°C for an hour to remove moisture. The dried sample was ion-exchanged with 1M Ammonium chloride at 70°C for 3 hours to remove adherent Sodium. The resultant mixture was washed to dissolve the residual Sodium chloride, followed by filtration, drying and calcination at 550°C for 5hr to convert it to HZSM-5.

2.2 Catalyst Characterisations

ZSM-5 and Hi-ZSM-5 were characterized to determine the extent at Hi ZSM-5 was synthesised and catalytic properties required for effective molecular mass transfer. Structural analysis was conducted via X-ray diffraction (XRD) and energy dispersive X-ray fluorescence spectroscopy (EDXRF). The XRD patterns were collected using a Cu K α radiation source operating at 45 kV and 40 mA. Each sample was scanned from 4 to 80 degrees 2 θ at a step size of 0.026261 degrees. High Score Plus software was used for analysing the XRD patterns to determine crystallite size and phase composition. EDXRF analysis revealed the elemental composition of the catalysts.

Fourier transform infrared (FTIR) spectroscopy was performed on a THERMO SCIENTIFIC NICOLET Is10. The spectra were recorded in transmittance mode with Potassium Bromide (KBr) pellets and Nujol (Organic paraffin) at a resolution of 4cm⁻¹ from 450 cm⁻¹ to 4000 cm⁻¹.

intensities in the 5°-10° and 20°-25° ranges were significantly reduced after desilication, revealing a reduction in relative crystallinity of ZSM-5 from 100 to 85.6% and a partial breakdown of the ZSM-5 framework. This shows that, the ZSM-5 framework partially disintegrated following desilication and decreased crystallinity (Silaghi et

al., 2014). These results align with previous studies by (Monama et al., 2020; Qiao et al., 2017; Yusuf et al., 2023) which revealed that ZSM-5's light desilication had little impact on crystallinity, while (Dauda et al., 2020) stated that higher NaOH concentrations over the range of 0.3M causes observable decrease.

FTIR spectrum of ZSM-5 and hierarchical ZSM-5 (Hi ZSM-5) is presented in Figure 2, revealing distinct structural characteristics. The FTIR spectra provide valuable insights into lattice vibrations, fingerprint regions, and functional groups, shedding

light on the composition and structural changes of the catalysts. Within the FTIR spectrum, strong and sharp absorption bands are observed in the 450-1500 cm⁻¹ range, indicating the presence of Si-O and Al-O bonds within the ZSM-5 framework.

Nitrogen adsorption-desorption isotherms were obtained at -196°C using a V-Sorb 2800P analyser to characterise the textural properties. Prior to analysis, the samples were outgassed at 300°C for 4 hours to remove moisture and contaminants. Specific surface area, mesopore volume and pore size distribution were calculated from the isotherms using the Brunauer-Emmett-Teller (BET) model.

NH₃-TPD experiment was performed with Micrometrics, Auto-Chem II 2920 instrument connected with thermal conductivity detector (TCD). 50mg of the sample was heated to 200°C in an Argon (Ar) flow of 20ml/min, which was maintained for 30mins before the sample was cooled to room temperature (still in Ar atmosphere), and then the sample was exposed to stream of 10% NH₃ balanced Helium (20ml/min) for 30mins. The sample was further exposed to an Ar flow for 30mins to clear the residual NH₃ until the baseline reached zero. After that the sample was heated to 850°C in Ar atmosphere at 10°C/min and spectra was recorded using TCD.

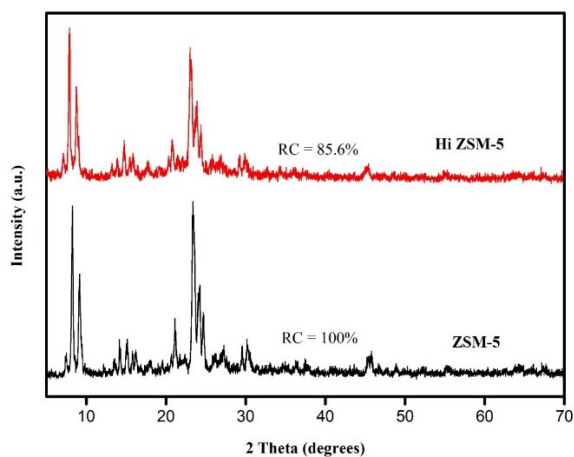
3.0 RESULTS AND DISCUSSION

The X-ray diffraction (XRD) patterns obtained from the analysis using an XRD diffractometer provided valuable insights into the structural characteristics of the synthesised catalysts, specifically ZSM-5 and hierarchical ZSM-5 (Figure 1). The XRD patterns of both the ZSM-5 and hierarchical ZSM-5 catalyst samples exhibited distinct peaks corresponding to the ZSM-5 zeolite structure. These peaks were observed at 2 θ angles of 6.00°, 8.00°, 9.00°, 23.00°, 24.00°, 30.00°, and 46°. This suggests that the parent ZSM-5 structure was retained even after the desilication. However, upon closer examination, it was noticed that the peak

light on the composition and structural changes of the catalysts. Within the FTIR spectrum, strong and sharp absorption bands are observed in the 450-1500 cm⁻¹ range, indicating the presence of Si-O and Al-O bonds within the ZSM-5 framework.



These bonds correspond to the five-membered ring pentasil units and indicate zeolite crystallinity. In the case of ZSM-5, the FTIR spectra show intense absorption bands associated with these bonds, confirming the crystalline nature of the catalyst. Changes in the strength of specific bands in the FTIR spectra of Hi ZSM-5 point to variations in the zeolite crystallinity. Noticeable reductions in the intensity of certain bands are observed, indicating alterations in the structural integrity induced by the effect of desilication which further supports XRD. The band at 3423 cm^{-1} indicates the stretching of the internal tetrahedral Si-OH-Al hydroxyl bridges attributable to Bronsted acid sites which broadens upon desilication. The band at 1632 cm^{-1} , which indicates the existence of hydroxyl (OH^-) of absorbed water on the surface of the ZSM-5 (7).



Desilication of reference catalysts increased mesoporosity from 15 to 44%, evidenced by higher BET surface areas compared to the parent ZSM-5. The Si/Al ratio decreased after alkaline treatment to 25.93 at 0.3M NaOH as seen previously (7). The parent ZSM-5 zeolite has a pore size of 2.0nm, while hierarchical ZSM-5 zeolite has a pore size of 3.90nm. This significant difference in pore size provides compelling evidence for categorising the new catalyst as hierarchical. In this case, the presence of mesopores in the hierarchical structure

Figure 1: XRD Patterns of the Reference ZSM-5 Catalyst and the Hierarchical ZSM-5 Catalysts.

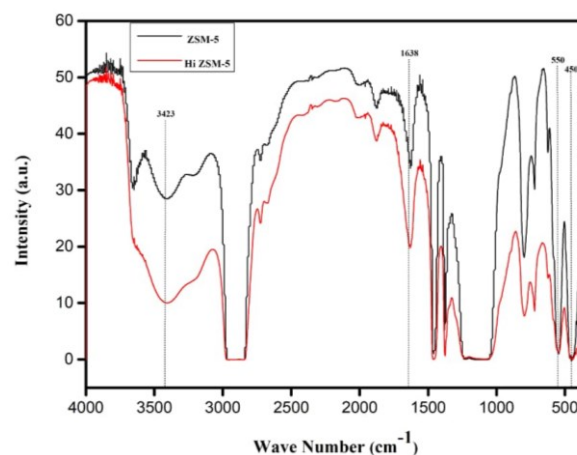


Figure 2: FTIR Spectra of the ZSM-5 and Hierarchical ZSM-5 Catalysts

is indicated by the larger pore size of the hierarchical ZSM-5 zeolite (3.90) compared to the conventional ZSM-5 zeolite (2.0). The larger pore size suggests that the hierarchical ZSM-5 catalyst has more mesopores, which can aid in reactant molecule diffusion and provide greater access to active sites within the catalyst. The mesopores also enhance better interaction of infrared radiation with the sample during FTIR analysis as seen in Figure 2, the intensity is more compared to ZSM-5.

Table 1: Physico-chemical Properties of ZSM-5 and Hierarchical ZSM-5

Catalyst(s)	Si/Al ^a Ratio	S _{BET} ^b (m ² /g)	S _{micro} ^c (m ² /g)	S _{meso} ^c (m ² /g)	S _{meso} ^c (%)	V _{total} ^d (cm ³ /g)	V _{micro} ^e (cm ³ /g)	V _{meso} ^f (cm ³ /g)	V _{meso} ^f (%)	Pore width(nm)
ZSM-5	46.90	456.20	388.40	67.80	15	0.25	0.16	0.075	30.59	2.00



Hi ZSM-5* 25.93 488.60 273.10 215.50 44 0.46 0.12 0.34 74.51 3.90

*Hierarchical ZSM-5, a XRF analysis. b From N₂ adsorption measurement (BET method). c From N₂ adsorption measurement (t-plot). d From N₂ adsorption measurement at P/P₀ = 0.9956. e From N₂ adsorption measurement (t-plot). F V_{meso} = (V_{total} - V_{micro}).

The N₂ adsorption-desorption isotherms of ZSM-5 and hierarchical ZSM-5 are shown in Figure 3. It shows that the modified molecular sieves are all typical of microporous structure and the adsorption occurred at a low relative pressure of $0.4 < P/P_0 < 0.98$. Nitrogen adsorption-desorption analysis was performed to characterise the textural properties of the parent and desilicated ZSM-5 (Hi ZSM-5). The parent ZSM-5 isotherm showed less hysteresis loop size than Hi ZSM-5, confirming the dominance of

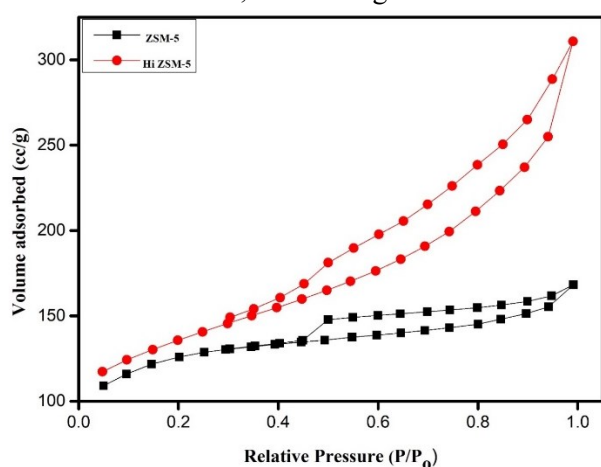


Figure 3: Nitrogen Adsorption-Desorption Isotherms of ZSM-5 and Hierarchical ZSM-5 Catalyst

The concentration and strength of acid sites play a critical role in the performance of zeolite catalysts. The acidity of the parent ZSM-5 and Hi ZSM-5 was assessed in this study using temperature-programmed desorption of ammonia (NH₃-TPD). This was done by taking measurements of the desorption profile of NH₃ during controlled heating. The NH₃-TPD profiles are classified as a low-**5.0 CONCLUSION**

This study investigates hierarchical ZSM-5 for improved mass transfer. ZSM-5 was desilicated for the experiment using an alkaline (NaOH) procedure. The parent and desilicated ZSM-5's crystallinity, elemental content, acidity, surface area, and pore size were investigated. Desilication caused ZSM-5's relative crystallinity to drop from 100 to 85.6 %. The desilicated ZSM-5, however, kept the traits and pattern of the parent ZSM-5. XRF

micropores in the parent ZSM-5. Upon desilication, the Hi ZSM-5 isotherm hysteresis loop size increased. NaOH modification's increased hysteresis loop size correlates to greater mesopore volume as the capillary condensation regions expand. Ultimately, the desilication process generated hierarchical porosity in the ZSM-5 by selectively extracting micropore walls to create mesopores.

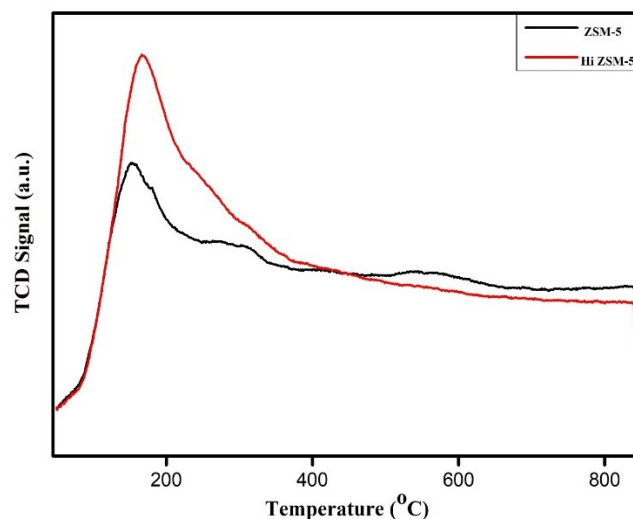


Figure 4: Acidity of ZSM-5 and Hierarchical ZSM-5 Catalysts

temperature peak below 200°C, an intermediate-temperature peak at 250 -350°C and a high-temperature peak at 400-500°C (8). Figure 4 shows the NH₃-TPD profiles of ZSM-5 and Hi ZSM-5. Both catalysts exhibited one notable peak, with the low-temperature peak at around 170°C corresponding to weak acid sites.

further confirmed desilication when the Si/Al ratio of ZSM-5 dropped from 46.90 to 25.93. BET proved the creation of mesopores with the percentage mesoporosity and pore width of ZSM-5 increase from 15 to 44% and 2.00 to 3.90nm, respectively. NH₃TPD revealed that Hi ZSM-5 has more of the weak acid sites compared to ZSM-5. In general, the characterisation of ZSM-5 and desilicated ZSM-5 improved our knowledge of the structural and acidic features of catalyst, particularly concerning the impact of desilication



on crystallinity, surface area, and pore characteristics. It is necessary to examine the two catalysts' performance tests to fully understand the

6.0 REFERENCES

1. J. A. Botas, D. P. Serrano, A. García, J. De Vicente, R. Ramos, Catalytic conversion of rapeseed oil into raw chemicals and fuels over Ni- and Mo-modified nanocrystalline ZSM-5 zeolite. *Catal. Today* **195**, 59–70 (2012).
2. H. Chen, M. Yang, W. Shang, Y. Tong, B. Liu, X. Han, J. Zhang, Q. Hao, M. Sun, X. Ma, Organosilane Surfactant-Directed Synthesis of Hierarchical ZSM-5 Zeolites with Improved Catalytic Performance in Methanol-to-Propylene Reaction. *Ind. Eng. Chem. Res.* **57**, 10956–10966 (2018).
3. I. B. Dauda, M. Yusuf, S. Gbadamasi, M. Bello, A. Y. Atta, B. O. Aderemi, B. Y. Jibril, Highly Selective Hierarchical ZnO/ZSM-5 Catalysts for Propane Aromatization. *ACS Omega* **5**, 2725–2733 (2020).
4. D. Liu, L. Cao, G. Zhang, L. Zhao, J. Gao, C. Xu, Catalytic conversion of light alkanes to aromatics by metal-containing HZSM-5 zeolite catalysts—A review. *Fuel Process. Technol.* **216**, 106770 (2021).
5. G. G. Oseke, A. Y. Atta, B. Mukhtar, B. J. El-Yakubu, B. O. Aderemi, “Synergistic differences between the structural alterations of ZSM-5 and Hi ZSM-5.

Effect of Zn with Ni on ZSM-5 as Propane Aromatization Catalyst: Effect of Temperature and Feed flowrate” (preprint, In Review, 2022); <https://doi.org/10.21203/rs.3.rs-1637890/v1>.

6. M. Ghazimoradi, N. Safari, S. Soltanali, H. Ghassabzadeh, Effect of simultaneous dealumination and metal incorporation of zeolite ZSM-5 on the catalytic performance in HTO process. *Microporous Mesoporous Mater.* **351**, 112486 (2023).

7. I. B. Dauda, M. Yusuf, S. Gbadamasi, M. Bello, A. Y. Atta, B. O. Aderemi, B. Y. Jibril, Highly Selective Hierarchical ZnO/ZSM-5 Catalysts for Propane Aromatization. *ACS Omega* **5**, 2725–2733 (2020).

8. L. Chen, T. V. W. Janssens, M. Skoglundh, H. Grönbeck, Interpretation of NH₃-TPD Profiles from Cu-CHA Using First-Principles Calculations. *Top. Catal.* **62**, 93–99 (2019).



P060 - TREATMENT OF PHENOLIC WASTEWATER WITH ZERO-VALENT IRON IMMOBILIZED ON POWDERED ACTIVATED CARBON COATED WITH CHITOSAN

Muhammad Yusuf Suleiman^{1*}, Opeoluwa O. Fasanya², Sharafadeen Gbadamasi², Abdulazeez Yusuf Atta¹, Baba Jibril El-Yakubu¹

Ahmadu Bello University Zaria, National Research Institute for Chemical Technology Zaria
Corresponding author email: yusufmuhammad554@gmail.com

ABSTRACT

Industrial effluent discharge into water bodies poses significant environmental challenges. This is often inadequately addressed by traditional wastewater treatment methods, leading to secondary pollution. Advanced oxidation processes (AOPs), such as the Fenton process, offer promise for eliminating non-biodegradable industrial contaminants. This study focuses on enhancing the Fenton process's efficiency using nano zero-valent iron (ZVI) immobilized on powdered activated carbon (PAC) coated with chitosan (CH) as a catalyst. Characterization techniques, including Fourier transform infrared spectroscopy (FTIR), X-ray diffraction (XRD), Brunauer-Emmett-Teller surface area determination (BET), and energy dispersive X-ray fluorescence spectroscopy (EDXRF), confirmed successful ZVI incorporation onto chitosan-coated activated carbon, resulting in a catalyst with 16.23 wt% iron loading and a specific surface area of approximately 152.26 m²/g. Catalytic tests evaluated the PAC-CH-ZVI catalyst's performance in degrading phenol in wastewater. Optimal conditions for phenol removal were identified as pH 3.0, 70 mM H₂O₂ concentration, and a 40°C reaction temperature achieving up to 85% phenol degradation. Comparative tests with other catalysts (PAC and PAC-CH) highlighted the superior performance of PAC-CH-ZVI, underscoring the role of ZVI in enhancing phenol degradation. This research highlights the potential of the Fenton catalyst comprising ZVI immobilized on chitosan-coated powdered activated carbon for efficiently removing persistent industrial pollutants like phenol from wastewater.

KEYWORDS

Phenol degradation, Nano zero-valent iron, Chitosan-coated activated carbon, Advanced oxidation processes, Wastewater treatment

1.0 INTRODUCTION

Considering the discharge of substantial industrial effluents into water bodies and the environment, water and environmental pollution have become a paramount concern over decades, including issues related to water quality degradation, threats to ecosystems, human health risks, biodiversity loss, secondary pollution generation, regulatory and legal challenges. Petroleum refining processes produce a significant amount of wastewater, which contains various kinds of pollutants, including biological materials, phenols, oils, organics, phosphate, nitrates and highly persistent metals. Large amounts of water are consumed in oil refineries for cooling systems, crude desalting, distillation, hydro-treating and during maintenance and shutdown. According to Abdulredha et

al.(2021), processing a barrel of crude oil consumes about 300 litres of water on average (1).

Phenol is a recalcitrant organic compound found in the effluent of petroleum refineries, phenolic resin manufacturing, petrochemicals and herbicide manufacturing industries. Because of its refractory and biotoxicity nature, it requires specific treatment to remove or partly minimize its concentration to allowed levels permissible for direct discharge (2).

Different technologies are available for the treatment of industrial effluents. The traditional treatment technologies such as coagulation, flocculation, membrane separation, activated carbon adsorption, biological, chemical, physicochemical, electrochemical and photochemical approaches cannot eradicate the recalcitrant compounds found in the industrial



effluents and involve the transfer of the non-biodegradable waste into sludge, giving rise to secondary pollution. Therefore, further treatment is essential for safe disposal (3). Advanced oxidation processes (AOPs) such as the Fenton process, ultrasonic and microwave irradiation, using heterogeneous catalysts, serve as potential alternative technologies for breaking down this non-biodegradable portion of the waste. They involve *in situ* generation of highly reactive species, such as hydroxyl radical, hydrogen peroxide, ozone and sulfate radical, characterized by low selectivity of attack. They can oxidize most of the organic contaminants found in effluents. AOPs offer the promising ability to degrade recalcitrant organic compounds and other pollutants. Among the AOPs mentioned earlier, the Fenton process has been observed to exhibit high reactivity and efficient remediation of contaminants due to its high efficiency, feasible control, low cost and eco-friendly nature (4).

The high reactivity and large specific surface area of zero-valent iron, coupled with nano-particle size and high reactivity, has attracted the attention of numerous researchers for its application in wastewater treatment.

Lütke et al. (2019) demonstrated that activated carbon derived from black wattle bark waste exhibited a remarkable removal efficiency of 95.89% for phenolic compounds in a simulated industrial effluent (5). Agarwal et al., (2013) investigated the co-adsorptive removal of phenol and cyanide using chitosan and achieved removal percentages of 60.97 and 90.86%, respectively, at a 30 g/L adsorbent dose (6). It was noted that using activated carbon or chitosan for adsorption may lead to secondary pollution, and modifications can potentially enhance phenol removal. Yehia et al. (2015) utilized the ultrasound-assisted advanced Fenton process and achieved 75% phenol removal after 60 minutes using nano zero-valent iron (ZVI) and hydrogen peroxide (7). However, issues such as ZVI aggregation and leaching were observed. Dong et al., (2019) investigated the enhancing effects of activated carbon-supported ZVI on anaerobic digestion of phenol-containing organic wastewater, achieving an 81.32% removal of phenol due to the micro-electrolytic effect of ZVI (8). Messele et al., (2016) reported greater than 90% conversion of phenol using nanoscale zero-valent iron supported on activated carbon, with satisfactory stability and reutilization of the catalyst. Still, residual phenol concentrations remained above 1 ppm (2).

Furthermore, Raji et al., (2021) employed chitosan-coated activated carbon cloth-supported ZVI as a Fenton catalyst, achieving significant colour (84.7%) and chemical oxygen demand (COD) removal (76.2%) from melanoidin wastewater, with less than 2% iron leaching after five treatment cycles. The chitosan coating contributed to reduced leaching and highlighted the potential of the Fenton catalyst for removing other recalcitrant compounds in industrial effluents (4). In this paper, the efficiency of ZVI immobilized on chitosan-coated powdered activated carbon catalyst was further evaluated in treating phenol-containing wastewater by considering the optimal conditions to achieve high phenol removal via the Fenton reaction.

2.0 MATERIALS AND METHODS

2.1 Materials and Chemicals

Activated charcoal powder and glacial acetic acid were purchased from BDH laboratory reagents UK, phenol crystals (Molychem, Mumbai, India), medium molecular weight chitosan, Sodium borohydride, hydrogen peroxide (Sigma-Aldrich), Ferrous sulphate (Winlab Laboratories).

2.2 Methods

2.2.1 Synthesis and characterization of Fenton catalyst

Powdered activated carbon (PAC, 500 mg) was initially treated with 1.5 M hydrochloric acid for four hours, then washed, filtered and dried in an oven. The treated activated carbon was then immersed in 40 ml of 2% chitosan solution (prepared by dissolving chitosan in 2% v/v acetic acid) for 1.5 h under shaking. The chitosan-adsorbed activated carbon was rinsed with deionized water, filtered and dried in an oven at 40 °C overnight. The prepared dry-based chitosan-coated powdered (PAC-CH) activated carbon was kept in aqueous solutions of 0.2M FeSO₄ for 3 h under N₂ bubbling for the chelation of ferrous iron ions with chitosan. The slurry was diluted five times using a mixture of ethanol and deionized water (v/v 1:1) to flush out excess ions, then filtered and dried. It was then added to 100 mL of 0.2M NaBH₄ with magnetic stirring and N₂ bubbling to reduce ferrous iron (Fe²⁺) entirely to ZVI. After agitation for 30 min, the chitosan-coated activated carbon impregnated with ZVI was separated from the mixture and subjected to another Fe²⁺ chelation and reduction process to increase the amount of ZVI



loading. It was then washed with acetone three times before vacuum drying at 40 °C.

2.2.2 Catalyst characterization

The interaction within chitosan-coated powdered activated carbon catalyst and that with ZVI impregnation (PAC-CH-ZVI) was examined by Fourier Transform Infrared Spectroscopy (FTIR). BET surface area and total pore volume were obtained by N₂ adsorption at 77K on the Brunauer–Emmett–Teller (BET) Analyzer. Energy Dispersive X-ray Fluorescence spectroscopy (EDXRF) was used to determine the iron content on the synthesized catalyst.

2.2.3 Catalytic activity tests

A stock solution of 1000 mg/L phenol was prepared with distilled water and stored in a refrigerator. Working solutions of 200 mg/L were prepared by diluting the stock solution with distilled water just before use.

The prepared catalyst's performance was evaluated by degrading 10 ml of 200 mg/L phenol-containing wastewater stirred at 200 rpm in a 50 ml beaker through a Fenton reaction using 150 mg of the prepared catalyst. H₂O₂ concentration of 30 mM was used initially for the experiment. The pH of the solution was adjusted to 3.0, 4.0, 5.0 and 6.0 using H₂SO₄ or NaOH, and the reaction temperature was set initially to 30 °C for 90 mins. For each cycle, the level of phenol removal was evaluated using a UV-Vis spectrophotometer (752N SearchTech) by recording the changes in optical absorbance at 275 nm. The pH value that gave the highest percentage of phenol removal was used in subsequent treatments. H₂O₂ concentration of 30, 50 and 70 mM was then varied, and the optimal concentration was used in subsequent steps. The reaction

temperature was also varied to determine the best temperature for the degradation process. The removal efficiency was tested at 30, 35 and 40°C for 90 minutes. The optimum reaction temperature was recorded and used in subsequent analyses.

3.0 RESULTS AND DISCUSSION

3.1 Characterization of Fenton Catalyst

The FTIR spectra in Figure 1 shows the functional groups and the interaction within powdered activated carbon coated with chitosan (PAC-CH) and powdered activated carbon coated with chitosan with ZVI loading (PAC-CH-ZVI) catalysts. The presence of peaks in all catalysts around 3600 cm⁻¹ is due to OH stretching vibrations in activated carbon. N-H stretching of primary aliphatic amine was observed around 3400 cm⁻¹ for both PAC-CH and PAC-CH-ZVI. Peaks at 2952 cm⁻¹ for PAC-CH and 2907 cm⁻¹ for PAC-CH-ZVI are due to C-H stretching vibration of the chitosan backbone due to the addition of chitosan on activated carbon (4). Broad peaks observed at 2326 cm⁻¹ for PAC and PAC-CH and at 2322 cm⁻¹ for PAC-CH-ZVI are assigned to -COOH broadening due to the presence of a carboxylic group. The broad peak between 2160 and 2000 cm⁻¹ (peak at 2083 cm⁻¹) for PAC-CH-ZVI is assigned to C=N broadening in all three catalysts. N-H bending of primary amines was observed at 1543.1 cm⁻¹ in both PAC-CH and PAC-CH-ZVI. The relative intensity of the peaks assigned to COOH broadening, C=N broadening, NH bending and C=O stretching in PAC-CH-ZVI are weaker compared to that in PAC-CH confirming the loading of ZVI onto PAC-CH. This was further confirmed by the EDXRF analysis for PAC-CH-ZVI in Table 1. From the results, it can be observed that 16.23 wt% Fe was immobilized on PAC-CH-ZVI.



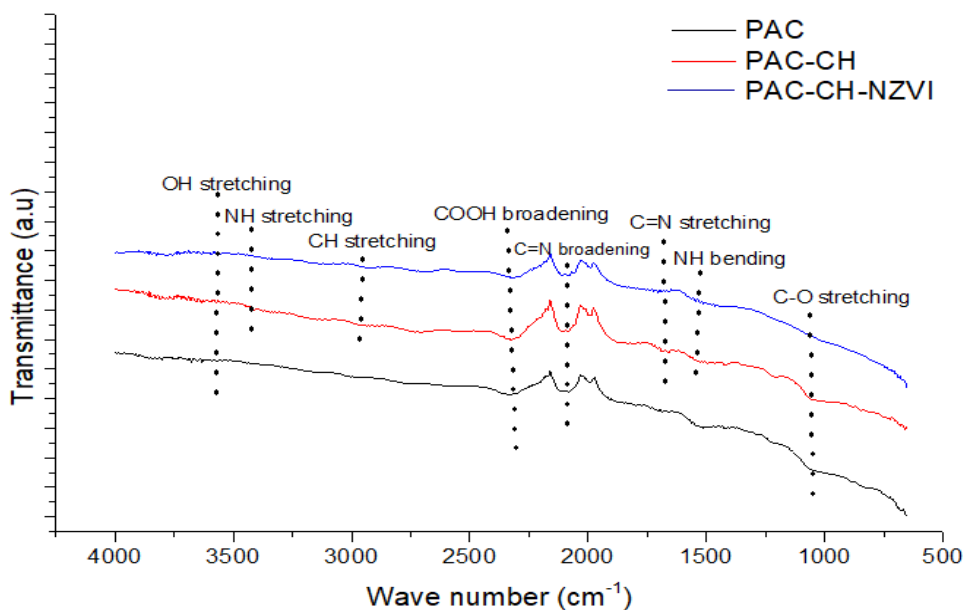


Figure 1: FTIR spectra for PAC, PAC-CH and PAC-CH-ZVI

Table 1: XRF analysis for PAC-CH-ZVI

Compound	Weight %
Fe	16.23
Zn	2.31
SiO ₂	10.20
SO ₃	4.51

Table 2 shows the specific surface area of the synthesized catalysts. The specific surface area of PAC was calculated to be approximately 184.16 m²/g. There was a slight decrease in the surface area to approximately 123.85 m²/g when chitosan was

coated on PAC indicating the formation of composite and loading of chitosan on the porous framework of the powdered activated carbon (Nandanwar et al., 2023). The surface area increases to 152.26 m²/g upon loading ZVI onto PAC-CH support.

Table 2: Specific surface area of catalysts

Catalysts	BET surface area (m ² /g)	Pore volume (cm ³ /g)
PAC	184.16	0.437



PAC-CH	123.85	0.380
PAC-CH-ZVI	152.26	0.325

3.2 Catalyst Activity Testing

Figure 2 shows the effect of different pH values on Fenton degradation of 200 mg/L phenol at 30 mM H₂O₂ concentration and 30 °C using PAC-CH-ZVI catalyst. The phenol degradation rate decreases with an increase in the working pH of the solution. At a pH of 3.0, 67% phenol removal was achieved. This is due to more available H⁺ in the solution to oxidize ZVI to Fe²⁺, which further oxidizes to Fe³⁺

on reaction with H₂O₂ and generates the [•]OH radicals that degrade the phenol (9). As the pH increases to 6.0, a decrease in the rate of degradation to 51% was observed mainly due to a decrease in the amount of H⁺ which limits the production of Fe²⁺. At pH values lower than 3.0, excess H⁺ will lead to the scavenging of [•]OH radicals, inhibiting their production. Excessive leaching of iron also occurs at very acidic pH, which will affect the catalyst's reusability (10).

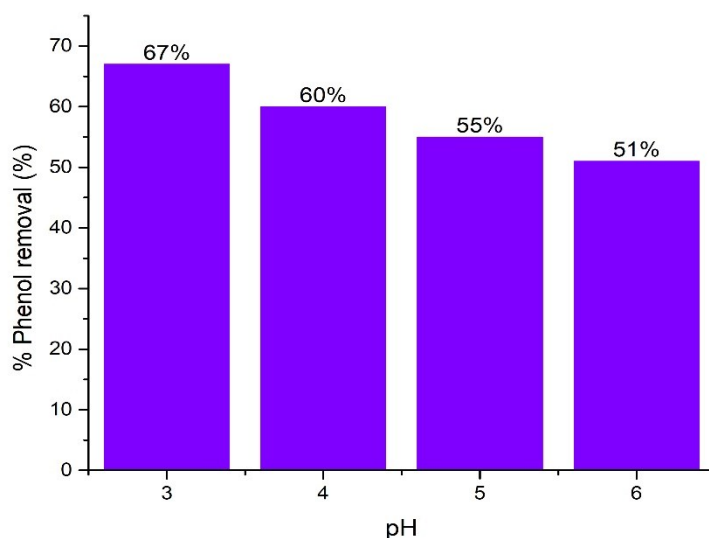


Figure 2: Effect of pH on phenol removal using PAC-CH-ZVI at 30 mM H₂O₂, 30°C

Figure 3 shows the effect of hydrogen peroxide concentration on Fenton degradation of phenol. It can be observed that an increase in the concentration of the oxidant from 30 mM to 70 mM increases the degradation of phenol from 67% to about 79%. This shows that the hydroxyl radicals

generated from the reaction of Fe²⁺ and H₂O₂ perform the role of degrading phenol into simpler compounds. Too much concentration of H₂O₂ may lead to the scavenging effect of the generated hydroxyl radicals, which may decrease catalyst performance (11).



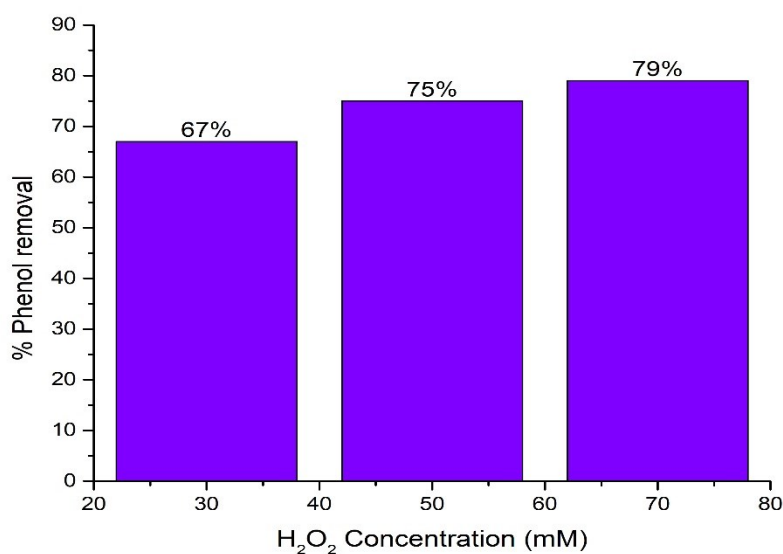


Figure 3: Effect of H₂O₂ concentration on phenol removal using PAC-CH-ZVI at pH of 3.0 and 30 °C

In order to enhance the production of hydroxyl radicals leading to more efficient degradation of phenol, the reaction temperature was increased from 30°C to 40°C. From Figure 4, the percentage of phenol removal increases appreciably from 79% at 30°C to 83% at 35°C, and to 85% when the temperature was raised to 40°C. At higher

temperatures, hydrogen peroxide (H₂O₂) decomposes more rapidly, leading to more hydroxyl radicals (12). However, excessive decomposition of H₂O₂ at much higher temperatures can potentially reduce their availability for phenol degradation due to the formation of scavengers (13).

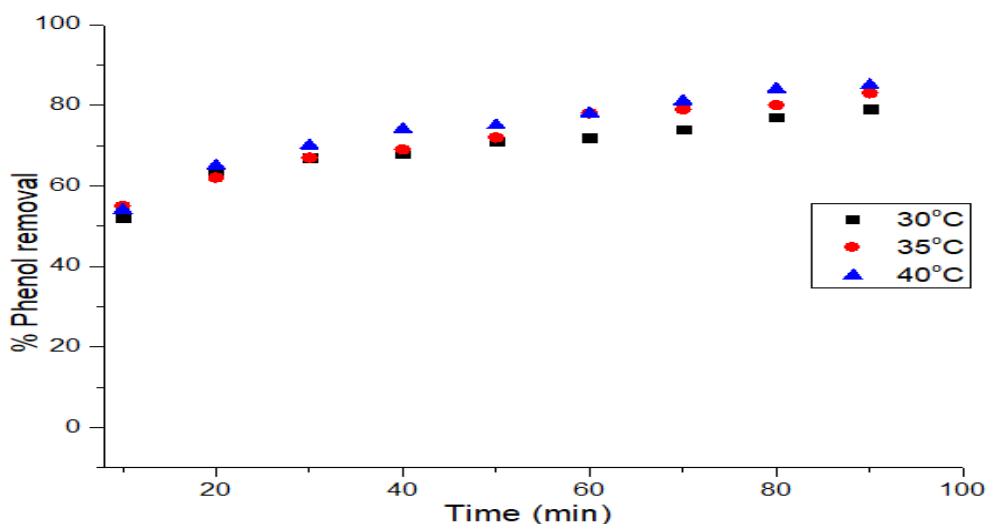


Figure 4: Effect of temperature on phenol degradation using PAC-CH-ZVI at pH of 3.0 and H₂O₂ concentration of 70 mM

To evaluate the role of ZVI in contaminants degradation, the phenol removal process was tested with the other two prepared catalysts. As can be seen from Figure 5, both PAC and PAC-CH removal rate is less than that of PAC-CH-ZVI. The

higher phenol removal of 53% by PAC than 46% by PAC-CH may be due to the higher surface area of PAC for adsorption than that of PAC-CH, as shown in Table 2.



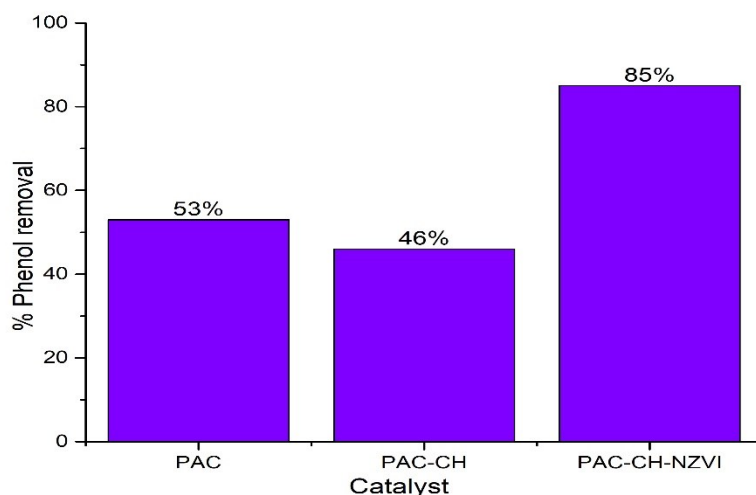


Figure 5: Comparison of PAC, PAC-CH, and PAC-CH-ZVI performance for phenol removal

4.0 CONCLUSIONS AND RECOMMENDATION

In this study, zero-valent iron immobilized on powdered activated carbon support coated with chitosan was synthesized and applied in the treatment of phenol containing wastewater. Comprehensive characterization techniques confirmed the successful incorporation of ZVI onto the catalyst, with substantial iron loading (16.23 wt%) and a specific surface area of approximately 152.26 m²/g. Optimal operational conditions was found to be pH of 3.0, hydrogen peroxide (H₂O₂) concentration of 70 mM, and reaction temperature of 40°C, resulting in phenol removal rates of up to 85%. Comparative tests underscored the superior performance of PAC-CH-ZVI compared to other catalysts (PAC and PAC-CH), highlighting the pivotal role of ZVI in enhancing phenol degradation. These findings hold significant promise for addressing environmental challenges posed by recalcitrant industrial pollutants like phenol. The PAC-CH-ZVI catalyst offers an environmentally friendly and cost-effective solution for removing persistent contaminants from wastewater. By advancing the understanding of optimal conditions and catalyst performance, this research contributes to the broader goal of sustainable industrial wastewater treatment. Future work should focus on further optimization, scale-up, regeneration strategies, and comprehensive environmental assessments to ensure this catalytic system's practical applicability and environmental benefits.

5.0 REFERENCES

1. M. Abdulredha, A. H. Khalil, S. A. Ali, I. Idowu, J. Amoako-Attah, Elimination of phenol from refineries effluents using electrocoagulation method. *IOP Conf. Ser. Earth Environ. Sci.* **877**, 012053 (2021).
2. S. A. Messele, C. Bengoa, F. Stüber, A. Fortuny, A. Fabregat, J. Font, Catalytic wet peroxide oxidation of phenol using nanoscale zero-valent iron supported on activated carbon. *Desalination Water Treat.* **57**, 5155–5164 (2016).
3. R. L. Singh, R. P. Singh, Eds., *Advances in Biological Treatment of Industrial Waste Water and their Recycling for a Sustainable Future* (Springer Singapore, Singapore, 2019; <http://link.springer.com/10.1007/978-981-13-1468-1>), *Applied Environmental Science and Engineering for a Sustainable Future*.



4. M. Raji, S. A. Mirbagheri, F. Ye, J. Dutta, Nano zero-valent iron on activated carbon cloth support as Fenton-like catalyst for efficient color and COD removal from melanoidin wastewater. *Chemosphere*. **263**, 127945 (2021).
5. Preparation of activated carbon from black wattle bark waste and its application for phenol adsorption - ScienceDirect, (available at <https://www.sciencedirect.com/science/article/abs/pii/S2213343719305196>).
6. B. Agarwal, C. Balomajumder, P. K. Thakur, Simultaneous co-adsorptive removal of phenol and cyanide from binary solution using granular activated carbon. *Chem. Eng. J.* **228**, 655–664 (2013).
7. F. Z. Yehia, Gh. Eshaq, A. M. Rabie, A. H. Mady, A. E. ElMetwally, Phenol degradation by advanced Fenton process in combination with ultrasonic irradiation. *Egypt. J. Pet.* **24**, 13–18 (2015).
8. D. Dong, R. Wang, P. Geng, C. Li, Z. Zhao, Enhancing effects of activated carbon supported nano zero-valent iron on anaerobic digestion of phenol-containing organic wastewater. *J. Environ. Manage.* **244**, 1–12 (2019).
9. N. Zhang, J. Chen, Z. Fang, E. P. Tsang, Ceria accelerated nanoscale zerovalent iron assisted heterogenous Fenton oxidation of tetracycline. *Chem. Eng. J.* **369**, 588–599 (2019).
10. Q. Chen, P. Wu, Y. Li, N. Zhu, Z. Dang, Heterogeneous photo-Fenton photodegradation of reactive brilliant orange X-GN over iron-pillared montmorillonite under visible irradiation. *J. Hazard. Mater.* **168**, 901–908 (2009).
11. S. M. Kumar, Degradation and mineralization of organic contaminants by Fenton and photo-Fenton processes : Review of mechanisms and effects of organic and inorganic additives *D e g r a d a t i o n a n d m i n e r a l i z a t i o n o f o r g a n i c c o n t a m i n a* (2017).
12. J. Farias, E. D. Albizzati, O. M. Alfano, Kinetic study of the photo-Fenton degradation of formic acid. Combined effects of temperature and iron concentration. *Catal. Today.* **144**, 117–123 (2009).
13. R. Vasquez-Medrano, D. Prato-Garcia, M. Vedrenne, Ferrioxalate-Mediated Processes. *Adv. Oxid. Process. Wastewater Treat. Emerg. Green Chem. Technol.*, 89–113 (2018).



P062 - DETERMINATION OF ACTIVITY CONCENTRATION, HAZARD INDICES AND ABSORBED DOSE RATES OF SOME RADIONUCLIDES FOUND IN SELECTED FERTILIZERS USED IN YOLA

Elvanus, E.M^{1*}., Tukki O.H¹, Jochthan M.G²., Bernard M.², Mohammed A.², Timtere P.²

¹National Research Institute for Chemical Technology, Zaria Nigeria

²Department of Physics Modibbo Adama University, Yola Nigeria

Correspondent author email: ewarammagaji@gmail.com

ABSTRACT

Fertilization increases efficiency and improves product quality recovery in agricultural activities. However, the major routes through which humans are exposed to ionizing radiation are via the food chain which results in absorption of radionuclides. This research work was carried out to determine the radioactivity concentration, hazard indices, and absorbed dose rate of some fertilizers used in Adamawa State, Nigeria. Six different fertilizer samples (Cow dung, Chicken dung, NPK 20:10:10, Urea, NPK 15:15:15 and NARICT Minero-organic NPK 7:7:7) were used for the study and a NaI (TI) gamma – ray spectrometer was used to determine the activity concentrations. The results showed that ²²⁶Ra concentration was lower than the recommended threshold of 35Bq/kg in all the samples. Except for urea and cow dung, the concentration of ⁴⁰K for all other fertilizer samples was above UNSCEAR recommended threshold of 420 Bq/kg. Also, the fertilizer samples were all above the recommended threshold of 45Bq/kg for ²³²Th. Internal and external hazard indices were lower than recommended limits of ≤ 1 respectively, except for NPK 15:15:15, while the gamma index and dose rates were higher than the UNSCEAR recommended threshold of ≤ 1 , 60nGy/hr, 84nGy/hr respectively for all samples.

KEYWORDS

Dose Rate, Radioactivity Concentration, Radionuclide, Fertilizers, Hazard Indices.

1.0 INTRODUCTION

Fertilization increases efficiency and enhances better quality of product recovery in agricultural activities, and it is one of the most important ways of adding nutrients to the soil (1). Fertilizer is considered to be source of natural radionuclides and a potential source of heavy metals. It contains heavy metals like Hg, Cd, As, Pb, Cu, and Ni; and natural radionuclides such as ²³⁸U, ²³²Th, ⁴⁰K and ²¹⁰Po (1). However, in recent years, fertilizer usage has increased exponentially throughout the world, and this may result in serious health and environmental problems, arising from accumulation of radionuclides in soil and plant systems (1). Plants absorb nutrients from fertilizers within the soil, and then pass it on to human beings through the food chain. Thus, fertilization leads to water, soil, and air pollution (1).

Estimating the levels of radiation in the environment is crucial in implementing appropriate controls for the sake of radiological protection since the constituents that make up the environment contains various number of radionuclides and their

decay products. The major ways by which humans become exposed to these radiations are radiation from sources outside the body (external exposure), radionuclides that are ingested through consumption of food and water or as inhaled radioactive gases (internal exposure) (2).

Investigation of gamma activity in the chemical fertilizers, has been performed to determine the effect of the use of chemical fertilizers on human health. A possible negative effect of chemical fertilizers is contaminating the cultivated lands by trace metals and some naturally occurring radioactive materials (NORM) (3). Radionuclides present in phosphate fertilizers affect the common people and farmers immensely (4). Large concentration of natural radionuclides in the fertilizers contaminates the environment and agricultural field (4). Direct inhalation of dust of phosphate fertilizers could affect the farmers on agricultural land (5, 6). Exposure of workers and the public to radiation from fertilizers is, therefore, not unlikely (7). Higher radiation levels are associated with the chemical fertilizers, therefore, the study of natural activity in artificial fertilizers are of a great interest in environmental pollution field (6).



Based on the research conducted by (8), fertilizer samples (Urea, ZA, KCL, NPK, TSP, and Phosphate) contained ^{238}U , ^{232}Th , ^{226}Ra , and ^{40}K , elements in each sample. The elements found in the samples had different values. The highest activity of ^{238}U ($558.66 \pm 5.64\text{Bq/Kg}$) is in TSP fertilizer sample. The highest activity of ^{232}Th ($2925.05 \pm 84.25\text{Bq/Kg}$) is found in NPK fertilizer sample. The highest activity of ^{226}Ra ($69.77 \pm 0.94\text{Bq/Kg}$) is in TSP fertilizer sample, and the highest activity of ^{40}K ($17.87 \pm 6.31\text{Bq/Kg}$) is found in sample KCL fertilizer (8). Radium equivalent activity in the sample was highest on the fertilizer samples KCL (835.31525 Bq/kg); followed by Phosphate fertilizers (495.331 Bq/kg); then NPK, TSP, ZA and Urea that are 325.886, 82.003, 1.978, and 1.183 Bq/kg, respectively. Radium equivalent activity at KCL and Phosphate fertilizer samples exceed 370 Bq/kg, which is the maximum permissible dose of radiation (9). The minimum and maximum values of absorbed dose in the samples studied in the work, where found to vary from 0.58 to 452.37 nGy/hr. The absorbed doses are 452.37, 268.16, 167.25, 38.16, 0.92, and 0.58 nGy/hr for the KCL, phosphate, NPK, TSP, ZA, and Urea fertilizers, respectively (8). The index of gamma radiation risks is highest for the KCL at 7.27 followed by Phosphate (4.31), NPK (2.64), TSP (0.56), ZA (0.014) and Urea (0.009) (8).

Ilori & Alausa (2019) studies showed also that, the activity concentration of ^{40}K , ^{238}U and ^{232}Th in the

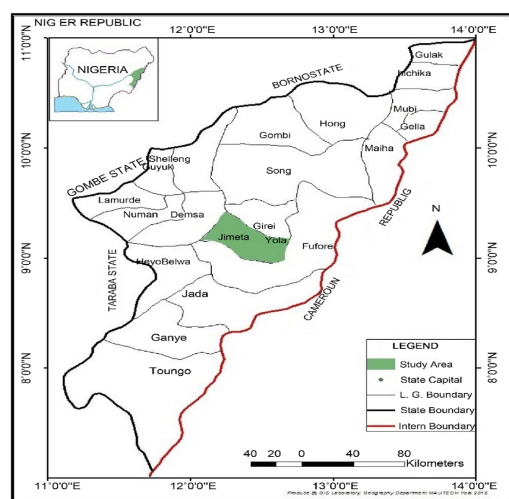


Fig. 1 Map of Adamawa State, Nigeria (<https://www.googlemaps.com>).

2.2 Sample Collection: Six different fertilizer samples (NPK 20:10:10, NPK 15:15:15, NARIC Minero-organic NPK 7:7:7, Urea, Chicken dung and Cow dung) were collected from agro-chemical

cow dung samples range from 115.21 to 225.44 Bq/kg with a mean value of $184.90 \pm 40.92\text{ Bq/kg}$ for ^{40}K ; 10.13 to 13.17 Bq/kg with a mean value of $11.50 \pm 0.78\text{ Bq/kg}$ for ^{238}U and 8.12 to 11.28 Bq/kg with a mean value of $10.20 \pm 0.71\text{ Bq/kg}$ for ^{232}Th (10). The activity concentrations in cattle dung samples were higher than the corresponding values in the grass from the study area. This may be attributed to the ingestion of other sources of radionuclides such as the drinking water available to the cattle grazing in the study area (11). The ^{40}K value of $218.6 \pm 66.0\text{ Bq/kg}$ obtained in Abeokuta was higher than that of the present study (12). However, the ^{238}U and ^{232}Th activity concentration values of 10.5 ± 1.1 and $8.3 \pm 1.9\text{ Bq/kg}$ obtained in Abeokuta were lower when compared to that obtained in the present study.

This research study aims at determining the activity concentrations, hazard risk indices, and dose rates of radionuclides found in some fertilizers used in Yola, Nigeria. This is done to ascertain the possible risk they may pose by the continuous application of these fertilizers to the same piece of land for cultivation over a long period.

2.0 Materials and Methods

2.1 Sample Area:

The study area was Adamawa, Nigeria, a state sharing boundary with Taraba, Borno, Gombe states, Cameroon, and Niger Republic.

stores in Jimeta modern market, Cattle range at Kasuwan Shanaye along bypass road Jimeta, NARICT Yola office and Flova poultry farm along army barracks road Jimeta, Yola North, Nigeria,

2.3 Sample Preparation and Analysis: Sample preparation and analysis were carried out as described by CERT (13). 1 Kg of each sample collected were crushed to a powdered form using Vitamix A3500 ascent series smart blender, and sieved through a 1 mm mesh screen to remove the larger grain sizes. The ground samples were then air dried in a temperature-controlled room ($21\text{ }^{\circ}\text{C}$) for 24 hours so that moisture is removed from the different fertilizers. After moisture removal, the samples were ready and packaged in 1 Kg Ziploc bags for radionuclides analysis.

2.3.1 Evaluation of Radioactivity of Samples:

The sealing process included smearing of the inner rim of each container lid with Vaseline petroleum jelly, filling the lid assembly gap with candle wax to block the gaps between lid and container, and tight-sealing lid-container with masking adhesive



tape. Radon and its short-lived progenies were allowed to reach secular radioactive equilibrium by storing the samples for 30 days prior to gamma spectroscopy measurements (13). The data acquisition software used was Maestro by Canberra Nuclear Products. Each sample was measured for a period of 29000 seconds. The peak area of each energy in the spectrum was used to compute the activity concentrations in each sample using equation (1):

$$C (Bq.kg^{-1}) = C_n / C_f \quad (1)$$

with the amplifier gain that gives 72% energy resolution for the 661.7KeV of Cs-137 and counted for 30minutes. The standards used to check for the calibration are the IAEA gamma Spectrometric

Table 1. Spectral Energy windows used in the Analysis.

Isotope	Gamma Energy (KeV)	Energy Window (KeV)
R-226	1764.0	1620 – 1820
Th-232	2614.5	2480 – 2820
K-40	1460.0	1380 – 1550

Table 2. Energy Calibration for quantitatively Spectral Analysis

Isotope	Calibration Factors		Activity Concentration Conversion Factors	Detection Limits	
	10^{-3} (cps/ppm)	10^{-4} (cps/ppm)		Ppm	Bq/Kg
^{40}K	0.0260	6.4310	0.0320	454.5400	14.5400
^{226}Ra	10.5000	8.6320	12.2000	0.3200	3.8400
^{232}Th	3.6120	8.7680	4.1200	2.2700	9.0800

2.4 Theoretical Framework

2.4.1 Risk Index Gamma Radiation

In determining the gamma radiation risk index ($I_{\gamma r}$), (IARC. 2012). The equation used is:

$$I_{\gamma r} = 0.0067 A_{Ra} + 0.01 A_{Th} + 0.00067 A_K \leq 1 \quad (2)$$

where A_{Ra} , A_{Th} , A_K is the activity of ^{226}Ra , ^{232}Th dan ^{40}K .

2.4.2 External and Internal Hazard

The external and internal radiation exposure of a sample is defined in relation to an external and

Where, C is activity concentration of the radionuclides in the sample measured in Bq.kg^{-1} , C_n is count rate (counts per second). Count per second (cps) = $\text{Net Count} / \text{Live Count}$, C_{yfc} is Calibration factor of the detecting system (13).

2.3.2 Calibration and Efficiency Determinations

Calibration of the system for energy and efficiency were done with two calibration point sources: Cs-137 and Co-60. These were done

reference materials RGK-1 for ^{40}K , RGU-1 for ^{226}Ra (Bi-214 peak) and RTG-1 for ^{232}Th (Ti-208), the background count rate done for 29000sec (13).

internal hazard called external and Internal Hazard index, H_{ex} , H_{in} , and are expressed as

$$H_{in} = A \frac{^{238}\text{u}}{185} + A \frac{^{232}\text{Th}}{256} + A \frac{^{40}\text{K}}{4810} \leq 1 \quad (3)$$

where A is still the specific activity concentration and H_{in} is the internal hazard index (14).

$$H_{ex} = A \frac{^{238}\text{u}}{370} + A \frac{^{232}\text{Th}}{259} + A \frac{^{40}\text{K}}{4810} \leq 1 \quad (4)$$

where A is the specific activity concentration and H_{ex} is the external hazard index (14).



2.4.3 Absorbed Dose

Absorbed dose (D) is a gamma radiation in the air at a height of 1 m from the surface to equalize the distribution of naturally radioactive materials or commonly abbreviated as NORM i.e., ^{226}Ra , ^{232}Th and ^{40}K . The equation used to determine D are; (UNSCEAR 2000)

$$D(\text{out})\text{Bq/kg} = 0.427 A_{\text{Ra}} + 0.662 A_{\text{Th}} + 0.043 A_{\text{K}} \quad (5)$$

$$D(\text{in})\text{Bq/kg} = 0.92 A_{\text{Ra}} + 1.1 A_{\text{Th}} + 0.081 A_{\text{K}} \quad (6)$$

where A_{Ra} , A_{Th} , A_{K} are the activities of ^{226}Ra , ^{232}Th and ^{40}K respectively (14).

3.0 Results and Discussion

3.1 Activity Concentrations of ^{40}K , ^{226}Ra , and ^{232}Th in the Samples.

The results of the activity concentration of the radionuclides (^{40}K , ^{226}Ra , and ^{232}Th) in each of the different samples are presented in the Table 3.

Table 3. Activity Concentration of ^{40}K , ^{226}Ra , and ^{232}Th in the Samples measured in Bq/Kg

	K-40 (Bq/Kg)	Ra-226 (Bq/Kg)	Th-232 (Bq/Kg)
NPK 20:10:10	2012.60±4.34	4.38±0.15	83.36±1.33
NPK 15:15:15	2116.26±3.53	5.99±0.14	152.52±1.08
NARICT NPK 7:7:7	1207.65±3.72	4.80±0.20	143.20±1.48
Urea	227.65±2.78	4.24±0.17	125.94±1.26
Chicken Dung	434.55±3.52	4.33±0.14	111.08±1.26
Cow Dung	306.16±3.49	2.71±0.13	108.76±3.93
Permissible limits (UNSCEAR, 2010)	420.00Bq/Kg	35.00Bq/Kg	45.00Bq/Kg

From Table 3, the concentration of ^{40}K in inorganic fertilizers ranges from 2116.27±3.53Bq/kg to 227.65±2.78 Bqkg⁻¹, NPK 15:15:15 with the highest value and urea having the lowest value respectively. These value of ^{40}K are contrary with what was obtained by (15, 16); where concentration of ^{40}K ranged from 199.20±41.03 - 212.32±32.90Bq/kg, 8-12628Bq/kg, 12-2276Bq/kg, and 80.85-5000Bq/kg. Except for urea, other inorganic fertilizers are above UNSCEAR (2010) world recommended limit value of 420Bq/kg. While the organic fertilizer ranges from 306.16±3.49Bq/kg to 434.55±3.52Bq/kg, cow dung having the lowest value while chicken dung having the highest respectively. Cow dung is within UNSCEAR (2010) world recommended value of 420 Bqkg⁻¹ while is for chicken dung, it is above the world recommended value of 420Bqkg⁻¹ (9).

The activity concentration of ^{226}Ra in inorganic fertilizers ranges from 5.99±0.14Bq/kg to 4.24±0.17Bq/kg, NPK 15:15:15 having the highest value while urea has the lowest. These values of ^{226}Ra are contrary with what was obtained by (15, 16); where concentrations were higher and ranged from 5-329Bq/kg, 12-244Bq/kg, 10.97±0.57-13.17±0.44Bq/kg, and 0.50±0.20-134.00±6.00Bq/kg. Therefore, this shows that most of the concentrations from the study were less than reviewed study, possibly due to the differences in products from different manufacturers. That of organic fertilizers ranges from 4.33±0.14Bq/kg to 2.71±0.13Bq/kg, cow dung having the lowest value and chicken dung having the highest value. All the different fertilizer samples (inorganic, organic, and minero-organic fertilizers) had ^{226}Ra concentration lower than the recommended value of 35Bqk⁻¹ set by (9).



Concentration of ^{232}Th in inorganic fertilizers ranges from $83.36 \pm 1.33 \text{Bq/kg}$ to $152.52 \pm 1.08 \text{Bq/kg}$, NPK 20:10:10 having the lowest value while NPK 15:15:15 has the highest value respectively. Values of ^{232}Th contrast that obtained by (15, 16) where concentration ranged from $3-22 \text{Bq/kg}$, $1-27 \text{Bq/kg}$, $0.20 \pm 0.04-69.77 \pm 1.23 \text{Bq/kg}$, $5-39 \text{Bq/kg}$, $8.12 \pm 1.41-10.36 \pm 0.60 \text{Bq/kg}$. Results of the organic fertilizer ranges from $108.76 \pm 3.93 \text{Bq/kg}$ to $111.08 \pm 1.26 \text{Bq/kg}$, cow dung having the lowest value while chicken dung has the highest value. All the different fertilizer samples were all above the recommended value of 45Bqkg^{-1} set by (9).

Results from all samples showed consistently high concentration of ^{40}K , ^{226}Ra , and ^{232}Th in NPK fertilizers and less in the Nitrogen and organic fertilizers. NPK 15:15:15 had the highest concentrations of ^{40}K , ^{226}Ra , and ^{232}Th as compared to NPK 20:10:10 and NARICT NPK 7:7:7. This may possibly be as a result of the percentage composition of phosphorous and potassium, since nitrogen posed less significant effect as seen in the pure nitrogen (urea) fertilizer. The study also showed a high concentration of ^{40}K , ^{226}Ra , and ^{232}Th in chicken dung than the cow dung and urea, possibly due to the chemical composition of the chicken dung.

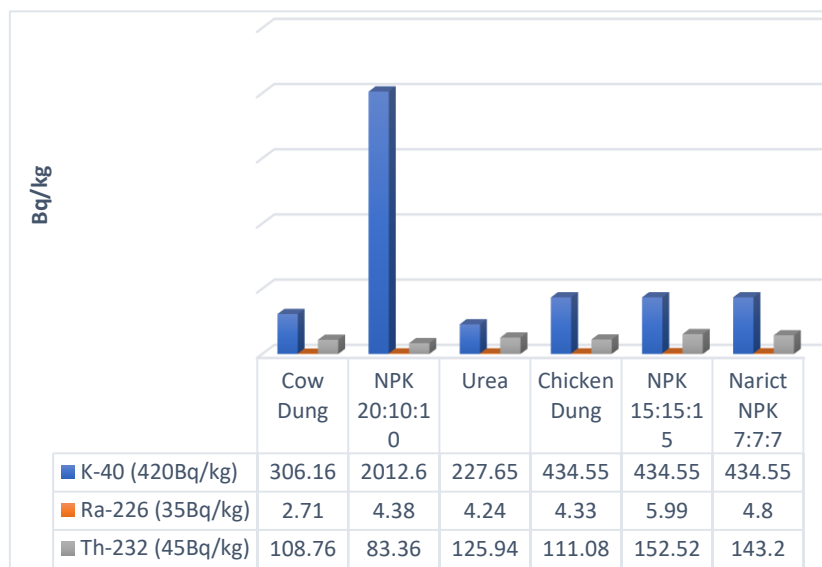


Figure 2: Activity Concentration of ^{40}K , ^{226}Ra , and ^{232}Th of all the samples.

3.2 Result of Radiological Hazard index in the Samples

Table 4. Values of Radiological Hazard indices for the Samples

	$I_{\gamma T}$	H_{in}	H_{ex}
NPK 20:10:10	2.21	0.77	0.75
NPK 15:15:15	2.98	1.07	1.05
NARICT NPK 7:7:7	2.27	0.84	0.82
Urea	2.81	0.56	0.55
Chicken Dung	1.43	0.55	0.53
Cow Dung	1.31	0.50	0.49



From Table 4, the gamma hazard risk index for inorganic fertilizers ranges from 2.21 to 2.98, with NPK 20:10:10 having the lowest value while NPK15:15:15 has the highest value. These values are significantly contrary with those obtained by (3, 17); which showed that fertilizer samples in India, Indonesia, Egypt, Saudi Arabia, and Brazil ranged from 0.009 – 7.27. showing that gamma risk index in other countries are significantly higher than that of the present studies. That of organic fertilizers ranges from 1.31 to 1.43, cow dung having the lowest value while chicken dung has the highest value. Implying that all the index are greater than unity (9), thus the fertilizers requires radiological attention for monitoring and protection.

All fertilizer samples had internal and external hazard index less than unity except for NPK 15:15:15 which had values of 1.07 and 1.05 for internal and external hazard index respectively. These values are also contrary with that obtained by (3, 17) which showed that fertilizer samples in India, Indonesia, Egypt, Saudi Arabia, and Brazil had internal and external index ranging from 0.198 – 3.218 and 0.118 – 2.170 respectively. Therefore, proper monitoring and protection is required in the application of NPK 15:15:15 fertilizers as it is above the recommended value of ≤ 1 set by (9).

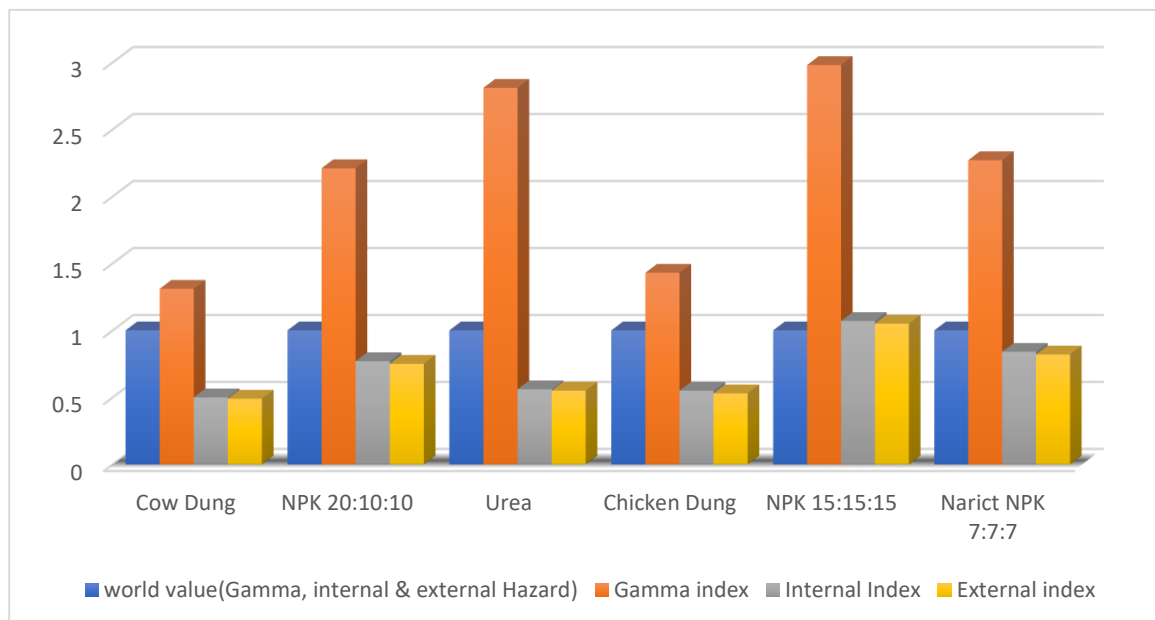


Figure 3: Comparison of gamma hazard index, internal and external hazard index with world recommended value of ≤ 1 (9).



3.3 Result of Outdoor and Indoor Absorbed Dose

Table 5. Outdoor and Indoor Absorbed Dose Rates (nGy/hr) of the Samples

	D_{Outdoor} (nGy/hr)	D_{Indoor} (nGy/hr)
NPK 20:10:10	143.59	258.74
NPK 15:15:15	194.52	344.70
NARICT NPK 7:7:7	148.78	259.76
Urea	94.97	160.87
Chicken Dung	94.07	161.36
Cow Dung	86.32	146.93
Permissible limits (UNSCEAR, 2000)	60nGy/hr	84nGy/hr

The outdoor absorbed dose rate of the inorganic fertilizers ranged from 94.97nGy/hr to 194.52nGy/hr, NPK 15:15:15 having the highest value, while urea has the lowest value. The values were to the values obtained by (3, 17), which showed the values ranging from 32 – 241nGy/hr, 31 – 230nGy/hr, and 30 – 225nGy/hr. Even though the results from present studies were all above the recommended value of 60nGy/hr (18), it still showed that outdoor absorbed dose rate were higher in the NPK fertilizers than in the pure nitrogen and organic fertilizers, with NPK 15:15:15 as the highest. The organic fertilizers ranges from 94.07nGy/hr to 86.32nGy/hr for chicken dung and cow dung respectively. All the inorganic, organic, and mineroorganic fertilizers sampled were above 60nGy/hr, which is the world recommended value by UNSCEAR (2000). This means that individuals using all the sampled fertilizers could be exposed to hazard risks through the food chain and therefore

need to carefully use protective measures during application.

The indoor absorbed dose rate for the inorganic fertilizers ranges also from 160.87nGy/hr to 344.70nGy/hr, NPK 15:15:15 having the highest value and urea having the lowest value. These values are also contrary to 40 – 340nGy/hr, and 41.074 – 58.481nGy/hr, obtained in separate studies conducted by (3, 17). Both indoor and outdoor adsorbed dose rates were higher than recommended value for all the different fertilizers. The indoor absorbed dose of organic fertilizer ranges from 146.93nGy/hr to 161.36nGy/hr for cow dung and chicken dung respectively. The inorganic and organic fertilizers were above the recommended value of 84nGy/hr by (18), which also showed persistent use pose risk to individuals through the food chain and application.



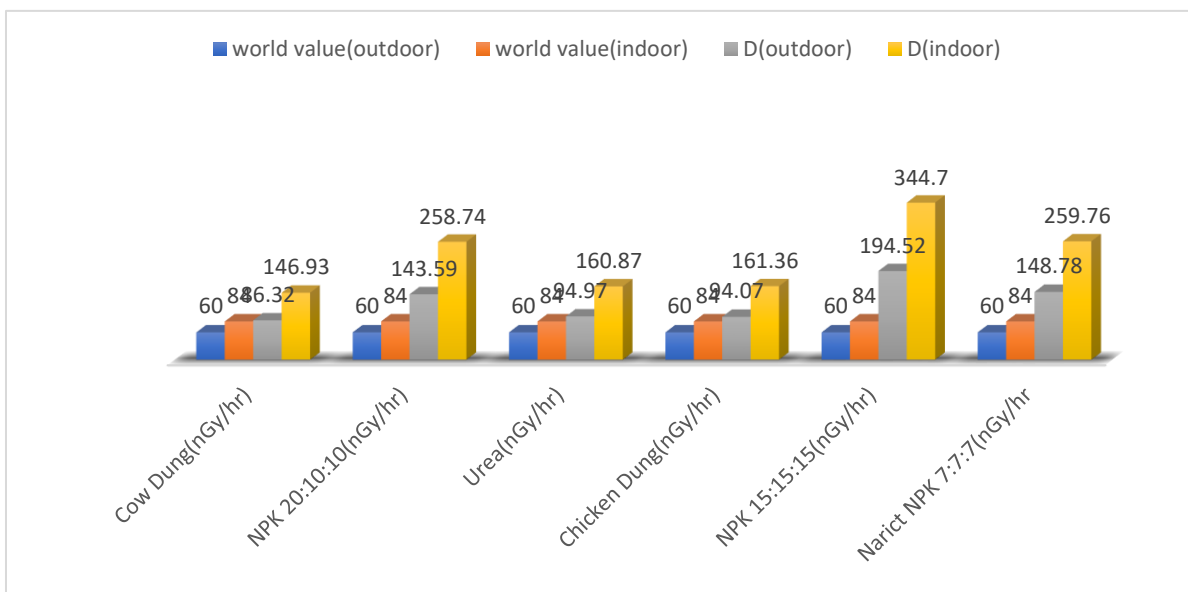


Figure 4.3: Comparison of Absorbed Dose with the world recommended values.

4.0 Conclusion

Among the six different fertilizer samples discussed, the radionuclide activity concentration, maximum and minimum values varied across the three radionuclides examined (^{226}Ra , ^{232}Th and ^{40}K), except for NPK 20:10:10, 15:15:15, and 7:7:7 all others were less than 420Bq/kg recommended value for ^{40}K (18), all fertilizer samples had values for ^{226}Ra less than the recommended value of 35Bq/kg (18), while all the values for ^{232}Th of the different fertilizer samples were above the recommended value of 45Bq/kg (18).

The Internal and external indices were all below unity, which is the recommended maximum value by (18), except for the internal and external index of NPK 15:15:15 which were all above unity. This suggests adequate monitoring, protection, and safety measures to ensure safety of individuals using such fertilizers. The gamma hazard index for all the different fertilizer samples were all above unity which shows and recommends attention to gamma hazards on all the fertilizers. Therefore, soil analysis should be performed carefully, before fertilizer application to soil, to minimize radiation hazard as low as reasonably achievable.

References

1. Gonen, E, Master Thesis, Namık Kemal University Institute of Science (2012).

2. UNSCEAR, Effects of Ionizing Radiation on Immune System (2008).

3. R. Lambert, C. Grant, S. Sauve, Cadmium and zinc in soil solution extracts following the application of phosphate fertilizers. *Sci. Total Environ.* **378**, 293–305 (2007).

4. D. Ghosh, A. Deb, S. Bera, R. Sengupta, K. K. Patra, Measurement of natural radioactivity in chemical fertilizer and agricultural soil: evidence of high alpha activity. *Environ. Geochem. Health* **30**, 79–86 (2008).

5. H. Pfister, G. Philipp, H. Pauly, Population dose from natural radionuclides in phosphate fertilizers. *Radiat. Environ. Biophys.* **13**, 247–261 (1976).

6. L. C. Scholten, C. W. M. Timmermans, Natural radioactivity in phosphate fertilizers. *Fertil. Res.* **43**, 103–107 (1996).

7. P. S. Hameed, G. S. Pillai, R. Mathiyarasu, A study on the impact of phosphate fertilizers on the radioactivity profile of cultivated soils in Srirangam (Tamil Nadu, India). *J. Radiat. Res. Appl. Sci.* **7**, 463–471 (2014).

8. R. Hatika, P. Subekti, Determination of Risk of Radioactive in Chemical Fertilizer Using



Gamma Ray Spectrometry. *Mater. Sci. Forum* **948**, 20–25 (2019).

9. UNSCEAR, United Nations Scientific Committee on the Effects of Atomic Radiation (2010).

10. A. Ilori, S. Alausa, Estimation of Natural Radionuclides in Grasses, Soils and Cattle-dung from a Cattle Rearing-field at Mangoro-Agege, Lagos State, Nigeria. **4**, 018–024 (2019).

11. Ojo, T. J., Afolayan, B. O., Distribution of Radionuclide Concentration with Proximity to the Lagoon in Lagos State, Southwestern Nigeria. *Int. Inst. Sci. Technol. Educ. IISTE E-J.* **15**, 1–5 (2013).

12. Alausa, S. K., Olabamiji, A. O., Odunaike, Kola, Estimation of natural radionuclides in cattle from a rearing-field at Alabata, Abeokuta, Ogun State Southwestern Nigeria. *J. Niger. Assoc. Math. Phys.* **29**, 353–362 (2015).

13. Centre for Energy, Research and Training (CERT), Analysis Procedure Manual for NaI(Tl) Gamma Spectroscopy, (2022).

14. IARC, Agents classified by the IARC monographs, Volumes 1-111 (2012). monographs.iarc.fr/ENG/Classification Alpha order.

15. M. N. Alam, M. I. Chowdhury, M. Kamal, S. Chose, H. Banu, D. Chakraborty, Radioactivity in Chemical Fertilizers Used in Bangladesh. *Appl. Radiat. Isol.* **48**, 1165–1168 (1997).

16. R. O. Hussain, H. H. Hussain, Investigation the natural radioactivity in local and imported chemical fertilizers. *Braz. Arch. Biol. Technol.* **54**, 777–782 (2011).

17. D. K. Gupta, S. Chatterjee, S. Datta, V. Veer, C. Walther, Role of phosphate fertilizers in heavy metal uptake and detoxification of toxic metals. *Chemosphere* **108**, 134–144 (2014).

18. UNSCEAR, United Scientific Committee on the Effect of Atomic Radiation (2000).



P064 - GAS DYNAMICS THROUGH METAL FOAM: INNOVATIVE EXPERIMENTAL SETUP AND INSIGHTS

Muhammad Baba Hassan^{1*}, Taofeek Onimisi Adam², Abdulrazak Jinadu Oturu³, Olalekan David Adeniyi⁴

Federal University of Technology Minna 1, Federal University of Technology Minna 2, King Faisal University 3,

Federal University of Technology Minna 4

Corresponding author email: engrmbhassan001@gmail.com

ABSTRACT

This paper presents an innovative experimental setup designed for the investigation of gas dynamics through metal foam structures. The research rigorously details the fabrication of an experiment rig capable of accurately measuring gas flow rates and pressure differentials, allowing for a comprehensive understanding of gas behaviour within these materials. The experiment rig's successful construction and calibration of the 0-5 V Transducer have established a reliable relationship between pressure and voltage readings, enabling precise data conversion. Subsequently, a test pressure drop experiment was conducted to explore the correlation between gas flow rates, pressure drop, and voltage readings. The key findings from this study provide valuable insights into gas dynamics through metal foam, with implications for applications in gas filtration, heat exchange, and energy storage. The experiment rig's adaptability to handle compressed gases enhances its utility in various research and practical scenarios. This research encourages further experimentation, application exploration, collaborative efforts, and educational outreach, aiming to advance our understanding of gas dynamics through metal foam structures and foster knowledge sharing in the scientific community.

KEYWORDS

Gas dynamics, metal foam, experiment rig, pressure drop, gas behaviour.

1.0 INTRODUCTION

1.1 Background and Motivation

The investigation of gas dynamics through metal foam structures is a topic of paramount significance in contemporary science and engineering. Metal foams have garnered substantial attention in these domains due to their unique physical and thermal properties, which offer considerable promise in an array of applications (1). Their porous structure, characterized by an intricate network of interconnected pores and channels, provides a platform for numerous technological advancements. The central motivation behind this study is rooted in the need to gain a profound comprehension of how gases traverse these complex metal foam structures and to harness this knowledge for optimizing various processes (2, 3).

One critical realm in which this research holds substantial importance is filtration. Metal foam, with its intricate porosity, exhibits exceptional potential for enhancing gas-solid separation processes (4). By studying gas dynamics within metal foam, it becomes possible to understand how gases move through these porous structures, influencing filtration efficiency, particulate matter capture, and overall system performance. This

knowledge has far-reaching implications in diverse industries, including environmental engineering, where efficient gas filtration is imperative for maintaining air quality and mitigating pollution. Furthermore, in industrial settings, filtration processes are integral to the production of high-purity gases and materials, making the optimization of metal foam-based filtration systems a significant industrial objective (5).

Beyond filtration, the investigation of gas dynamics in metal foam structures has extensive ramifications in the field of heat exchange. Effective heat transfer is pivotal in industries spanning from electronics cooling to aerospace applications. The ability to predict and control gas behaviour within metal foam materials plays a pivotal role in enhancing the efficiency of heat exchangers and, consequently, improving energy efficiency (6, 7). With an understanding of how gases circulate within metal foam, researchers can optimize the design of heat exchangers, promoting more effective and sustainable thermal management solutions.

Energy storage systems represent yet another domain where comprehending gas dynamics through metal foam is imperative. With the advent of sustainable energy sources such as solar and wind power, efficient energy storage is crucial (8).



Metal foam's capacity to act as a medium for gas storage holds immense promise in this context. The research in this area seeks to uncover the nuances of gas behavior within metal foam structures, thereby enabling the development of high-performance gas-based energy storage systems (9). Such systems can contribute significantly to mitigating energy imbalances and supporting the transition to renewable energy sources, a fundamental objective in the quest for sustainable energy solutions.

Furthermore, the investigation into gas dynamics within metal foam structures arises from a

recognition of the critical role metal foams play in a myriad of applications. From filtration systems that protect environmental and industrial ecosystems to heat exchangers that drive energy efficiency and storage systems that facilitate the transition to clean energy sources, the potential of metal foams is vast. By delving into the intricacies of gas dynamics within metal foam, this study is motivated by the pursuit of knowledge that can transform science and engineering, forging the path to enhanced technological solutions in a wide array of sectors (10).



Figure 1: Open cell metal foams

2.0 MATERIALS AND METHODS

2.1 Fabrication of the Experiment Rig

The experiment rig was constructed for the precise measurement of gas flow rates and pressure differentials. It was designed to handle up to two simultaneous compressed gases flows for various research applications. The following materials and steps were employed.

2.1.1 Equipment Used

- i. 1.6m long NNW-PVC-119 Acrylic pipe (NuoNuoWell)
- ii. Two 10LPM Gas flowmeters (Shunhuanliu Liangibiao)
- iii. Two 20LPM Gas flowmeters (Shunhuanliu Liangibiao)
- iv. Two 1 1/2" Slip x 1 1/2" Slip Plumbing PPR Plastic Ball Valve
- v. 0-5 V Transducer (Piezoelectric)
- vi. Plastic divider
- vii. JS-0006 PVC Glue (SgooHan)
- viii. Flexible rubber pipe

- ix. Air compressor (1PH, 50Hz, Zhuhai Landa Compressor Co. Ltd.)
- x. 28 Kg CO₂ cylinder (Norris Cylinder Company) filled with CO₂ gas
- xi. 2.52 Kg Air cylinder (Norris Cylinder Company) for compressed air storage

2.1.2 Procedure

Two 0.2m long NNW-PVC-119 Acrylic pipes were cut to serve as gas inlets. A 1 1/2" Slip x 1 1/2" Slip Plumbing PPR Plastic Ball Valve was attached at the end of each pipe using JS-0006 PVC Glue.

For the assembly of the air flow measurement system, a 10LPM Gas flowmeter was attached to the top of each 0.2m PVC pipe. All two 10LPM Gas flowmeters were connected to the end of the 1.6m NNW-PVC-119 Acrylic pipe using PVC glue.

To measure pressure differentials, the 1.6m Acrylic pipe was sealed at the 0.4m mark using a plastic divider. The inlet of a 20LPM Gas flowmeter was connected to the section where the gas mixture flows from, and the outlet was connected to the section after the plastic divider.



The 0-5 V Transducer was inserted into the Acrylic pipe at the 0.5m mark, ensuring proper positioning for accurate readings. A small hole was drilled to allow the transducer's connecting wire to pass through, and it was sealed airtight.

A sample holder was created using a white NNW-PVC-119 Acrylic pipe, 5cm long. A plastic divider was placed a few centimeters after the end of the sample holder. The inlet and outlet of the 20LPM Gas flowmeter were connected to opposite sides of the plastic divider for gas flow control during sample experimentation.

The exhaust connection involved connecting one end of the 1.6m Acrylic pipe to the outside of the laboratory using a flexible rubber pipe for the safe release of gases after experimentation.

The successful completion of the experiment rig's fabrication provides a versatile setup for accurate gas flow rate measurements and pressure differentials, enabling a wide range of experimental applications. The rig's capability to handle up to two simultaneous compressed gas flow enhances its utility across diverse research scenarios.

2.2 Calibration of the Transducer

The objective of this laboratory activity was to calibrate the 0-5 V Transducer (Piezoelectric) to establish the relationship between pressure and voltage readings. This calibration process is essential for accurate data conversion during subsequent experiments where the transducer will be used for pressure measurements.

2.2.1 Equipment Used

- i. T-joint pipe
- ii. 0-4 bar Analog pressure gauge (SKM)
- iii. 0-5 V Transducer (Piezoelectric)
- iv. Transparent plastic sheet
- v. Drill
- vi. Wires for the 0-5 V Transducer connection
- vii. 4 Minutes Epoxy Glue

2.2.2 Procedure

In the calibration procedure, a T-joint pipe assembly was acquired for the setup. This T-joint pipe facilitated the simultaneous placement of both the pressure gauge and the transducer within the same pipeline.

Subsequently, at one end of the T-joint pipe, a 4 bar analog pressure gauge with its dial oriented outward was affixed. This pressure gauge was employed as a reference instrument for measuring pressure.

Furthermore, within the T-joint pipe, positioned at the terminus of the pressure gauge, was the 0-5 V Transducer of the same model. The transducer's role entailed the conversion of applied pressure into an electrical voltage signal.

To ensure the integrity of the transducer compartment, the opening above the transducer was sealed by means of a transparent plastic sheet. A meticulous procedure involved drilling a hole through this plastic sheet to facilitate the extension of wires connected to the transducer, which was subsequently sealed in an airtight manner using 4 Minutes Epoxy Glue. This airtight sealing was crucial to prevent any gas leakage during the calibration process.

Simultaneously, the opening situated directly opposite the transducer within the T-joint pipe was also sealed. To achieve this, a flat transparent plastic sheet was employed. A hole was carefully drilled through this plastic sheet to enable the insertion of a pipe through which air would be introduced into the confined compartment. This meticulous sealing process was executed to ensure the precision and accuracy of pressure measurements during calibration.

2.2.3 Data Collection

With the setup complete, air was introduced into the confined compartment through the pipe. At regular intervals, pressure readings from the analog pressure gauge and the corresponding voltage readings from the transducer were taken.

2.2.3.1 Tabulation and Plotting of Data

The data obtained from the pressure gauge and transducer were meticulously tabulated, including pressure and voltage readings at each interval. The calibration data was then plotted on a graph to establish the relationship between pressure and voltage. This relationship is essential for converting future voltage readings from the transducer into accurate pressure measurements.

2.3 Test Experiment Using Air

Firstly, the task of connecting the air cylinder to the designated gas inlets within the flow rig was undertaken. It was of utmost importance to ensure the secure attachment of the cylinder, guaranteeing that all connections remained devoid of gas leakages throughout the process.



The next phase involved the compression of air. The Air compressor (1PH, 50Hz, Zhuhai Landa Compressor Co. Ltd.) was employed for this purpose, allowing for the controlled compression and storage of air into a 2.52 Kg Air cylinder designated for compressed air storage. This facilitated the creation of a stable and controlled air flow environment required for the experiment's accuracy.

Subsequently, the flow rig was meticulously set up for experimentation. This entailed the full opening of all flowmeters and valves within the flow rig, thus ensuring the unhindered flow of air during the course of the experiment.

To accurately measure the electrical voltage output of the transducer, the wires of the transducer were correctly connected to the designated terminals of a UT-3360 Multimeter.

The introduction of air into the flow rig commenced in a systematic and planned manner. Initially, air was introduced into the flow rig, with its flow rate set to 0 liters per minute (LPM). Concurrently, voltage readings from the 0-5 V Transducer (Piezoelectric) was recorded. This initial step established a baseline voltage reading for air in a static state.

Subsequently, the introduction of air was initiated. The flow rate of air was systematically increased

from 0 to 5 LPM, with increments of 1 LPM at a time. Voltage readings from the 0-5 V Transducer (Piezoelectric) were recorded at each air flow rate. For each flowrate, the experiment was conducted three times, and the average of the three voltage readings was duly recorded.

3.0 RESULTS AND DISCUSSION

3.1 Experimental flow rig

The fabrication of the experimental flow rig yielded successful results, culminating in a functional setup for gas dynamics analysis. The schematic diagram of the flow rig is meticulously illustrated in Figure 1, providing a visual representation of the experimental apparatus. To facilitate a comprehensive understanding of the rig's components, the associated symbols are elucidated in Table 1, ensuring clarity in its operation. For a more vivid depiction, Figure 2 offers a pictorial view of the flow rig, allowing to visually grasp its design and arrangement. Furthermore, Figure 3 presents the calibration setup, providing valuable insights into the precise instrumentation used to measure and analyze gas behavior within the experimental system. These visual aids serve to enhance the comprehension of the experimental setup and its components.

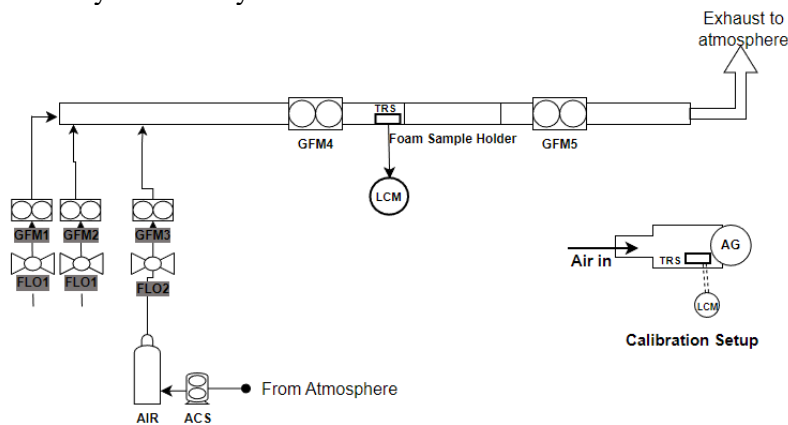


Figure 2: Process Flow diagram of the experimental Rig

Table 1: Symbols And Meaning For The Flow Rig

SYMBOLS AND MEANING			
Symbols	Meaning	Manufacturer	Capacity/Range
AIR	Air Cylinder	Norris Cylinder Company	2.52 kg
ACS	Air Compressor	Zhuhai Landa Compressor Co. Ltd.	1PH, 50Hz



GFM	Gas Flowmeter	Shunhuanliu Liangibiao	0 - 10 LPM (1&2) 0 - 20 LPM (3&4)
AG	Analog Pressure Guage	SKM	0 – 4 bar
TRS	Transducer	Piezoelectric	0 - 5 V
LCM	LCD Multimeter	UNI-T	UT890C
	Acrylic pipe	NuoNuoWell	NNW-PVC-119
FLO	Ball valve	Aquazen	15mm To 80mm



Figure 3: Experimental Rig



Figure 4: The Calibration Setup

3.2 Calibration Plot

Through a comprehensive regression analysis, the plot in Figure 5 facilitated the creation of a robust equation that unequivocally reveals the relationship between pressure and voltage. The resulting equation, represented as $\text{Pressure}(\text{bar}) = 1.4969\Delta V^2 + 2.7956\Delta V$, encapsulates the precise mathematical model that underpins this relationship. This equation serves as a powerful tool for accurately converting voltage readings into corresponding pressure values, enhancing the accuracy and reliability of pressure measurements in subsequent experiments.

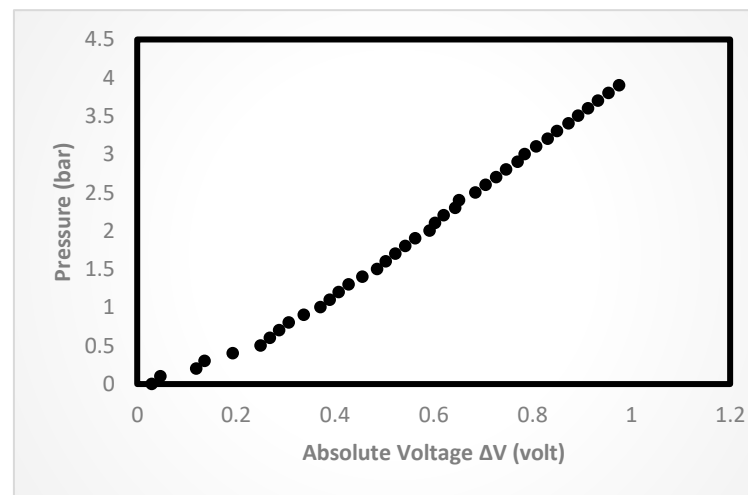


Figure 5: Pressure vs Voltage Plot

3.3 Test Experiment

In the provided Table 2, several parameters are recorded during the test experiment, including U1 (LPM), U3 (LPM), and V (Volt). Notably, we can examine the relationship between U3 and P4, focusing on how changes in U3 impact the P4 values.



As U3, representing the flow rate in Liters Per Minute (LPM), increases from 0 to 4.5 LPM, there is a clear and consistent pattern in the corresponding P4 values. P4 also exhibits a gradual increase, with values rising from 0.00000 to 0.00014. This relationship suggests a correlation between the flow rate (U3) and the pressure measurement (P4). Specifically, as the flow rate through the system (U3) increases, the pressure (P4) also rises in a linear fashion. This relationship is expected in fluid

dynamics, where an increase in the flow rate typically results in higher pressure.

Summarily, the data clearly demonstrates a positive relationship between U3 and P4, with an increase in flow rate leading to a corresponding increase in pressure, indicating the influence of flow dynamics on the pressure measurements in the experimental setup.

Table 2: Experimental Data

U1 (LPM)	U3 (LPM)	V (Volt)	ΔV	P4
0	0	0.00007	0.00000	0.00000
1	0.5	0.00008	0.00001	0.00003
2	1.5	0.00009	0.00002	0.00006
3	2.5	0.0001	0.00003	0.00008
4	3.5	0.00011	0.00004	0.00011
5	4.5	0.00012	0.00005	0.00014

4.0 CONCLUSIONS AND RECOMMENDATION

The research focused on investigating gas dynamics through metal foam structures using an innovative experiment rig. The following key conclusions have been drawn from the study:

1. The fabrication of the experiment rig was successfully completed, providing a versatile setup for accurate gas flow rate measurements and pressure differentials.
2. The experiment rig can effectively handle CO2 gas and compressed air, making it suitable for a wide range of research and experimentation applications.
1. Further Experimentation: Continuing to use the experiment rig for in-depth studies on gas dynamics through different types of metal foam structures and various gas compositions.

3. Calibration of the 0-5 V Transducer was successfully achieved, establishing a reliable relationship between pressure and voltage readings for accurate data conversion.
4. The pressure drop experiment conducted using the rig provided essential insights into the relationship between gas flow rates, pressure drop, and voltage readings. This data will serve as a valuable resource for further research and applications in the field of gas dynamics and metal foam

Based on the findings and the overall research process, the following recommendations are made:

- This will expand our understanding of gas behavior within these materials.
2. Exploration of Applications: Explore practical applications for the experimental setup, such as gas filtration, heat exchange, and energy



storage systems. Collaborate with industry partners to implement these findings in real-world scenarios.

3. Enhanced Monitoring: Consider adding additional sensors and data collection systems to the experiment rig to gather more comprehensive data, including temperature and humidity measurements, which may influence gas behavior.
4. Data Analysis Tools: Invest in data analysis tools and software to more effectively process and interpret the data collected, enabling researchers to gain deeper insights into the observed phenomena.
5. Collaborative Research: Foster collaboration with other research institutions and experts in the field of gas dynamics and metal foam to share knowledge and leverage collective expertise for broader advancements.
6. Educational Outreach: Use the experiment rig and research findings for educational purposes, providing hands-on training for students and researchers interested in gas dynamics and experimental setup.

These recommendations will contribute to the continued advancement of our understanding of gas dynamics through metal foam structures and promote the practical use of this knowledge in various applications.

5.0 REFERENCES

1. N. Iqbal, A. Akgül, R. Shah, A. Bariq, M. M. Al-Sawalha, A. Ali, On solutions of Fractional-Order gas dynamics equation by effective techniques. *Journal of Function Spaces*. 2022, 1–14 (2022).
2. C. Wang, J. Li, S. Guo, Retracted Article: The influence of gradient and porous configurations on the microwave absorbing performance of multilayered graphene/thermoplastic polyurethane composite foams. *RSC Advances*. 9, 21859–21872 (2019).
3. J. Wu, Z. Wu, H. Ding, Y. Wei, W. Huang, Y. Xing, Z. Li, L. Qiu, X. Wang, Three-Dimensional Graphene Hydrogel Decorated with SnO₂ for High-Performance NO₂ Sensing with Enhanced Immunity to Humidity. *ACS Applied Materials & Interfaces*. 12, 2634–2643 (2020).
4. H. Wu, S. Kitipornchai, J. Yang, Free Vibration and Buckling Analysis of Sandwich Beams with Functionally Graded Carbon Nanotube-Reinforced Composite Face Sheets. *International Journal of Structural Stability and Dynamics*. 15, 1540011 (2015).
5. H. M. T. Al-Najjar, J. M. Mahdi, D. O. Bokov, N. B. Khedher, N. Alshammari, M. J. C. Oplencia, M. A. Fagiry, W. Yaïci, P. Talebizadehsardari, Improving the Melting Duration of a PV/PCM System Integrated with Different Metal Foam Configurations for Thermal Energy Management. *Nanomaterials*. 12, 423 (2022).
6. S. Liao, G. Li, X. Wang, Y. Wan, P. Zhu, Y. Hu, T. Zhao, C. Wong, Metallized skeleton of polymer foam based on Metal–Organic decomposition for High-Performance EMI shielding. *ACS Applied Materials & Interfaces*. 14, 3302–3314 (2022).
7. M. Esapour, A. Hamzehnezhad, A. A. R. Darzi, M. Jourabian, Melting and solidification of PCM embedded in porous metal foam in horizontal multi-tube heat storage system. *Energy Conversion and Management*. 171, 398–410 (2018).
8. J. Mitali, S. Dhinakaran, A. A. Mohamad, Energy storage systems: a review. *Energy Storage and Saving*. 1, 166–216 (2022).
9. J. Guo, Z. Du, G. Liu, X. Yang, Q. Sun, Compression effect of metal foam on melting phase change in a shell-and-tube unit. *Applied Thermal Engineering*. 206, 118124 (2022).
10. N. Iqbal, A. Akgül, R. Shah, A. Bariq, M. M. Al-Sawalha, A. Ali, On solutions of Fractional-Order gas dynamics equation by



effective techniques. Journal of Function Spaces. 2022, 1–14 (2022).

P065 - METAL FOAMS AND AIR FLOW: EXPERIMENTAL FINDINGS AND INSIGHTS

Taofeek Onimisi Adam^{1*}, Muhammad Baba Hassan², Abdulrazak Jinadu Oturu³, Olalekan David Adeniyi⁴

Federal University of Technology Minna ¹, Federal University of Technology Minna ², King Faisal University ³, Federal University of Technology Minna ⁴

Corresponding author email: adam.taofeek@gmail.com

ABSTRACT

Metal foams, with their remarkable properties, have found diverse applications across various industries. This paper explores the critical aspect of fluid flow through Alantum foam, focusing on the pressure drop behavior. Through systematic experimental investigation, a clear and consistent positive correlation between air velocity (U_4) and pressure gradient (∇P_4) is observed. As air velocities increase within the experimental setup, the resultant surge in pressure gradient aligns with fundamental fluid dynamics principles, reflecting the dynamic nature of fluid behavior in response to changing flow rates. These findings are invaluable for applications ranging from filtration systems to aerospace technologies, as they provide insights into system optimization.

KEYWORDS

Metal foams, Alantum foam, pressure drop, fluid dynamics, experimental investigation.

1.0 INTRODUCTION

Metal foams, characterized by their cellular structure composed of a solid metal matrix with interconnected voids, have gained significant attention and recognition in recent years. Their remarkable properties and versatility have propelled them into various industries, offering potential solutions to long-standing engineering challenges (1). Their unique attributes include an exceptional strength-to-weight ratio, the capability to absorb energy efficiently, superior thermal insulation properties, and excellent sound damping characteristics. These features render metal foams particularly appealing for applications spanning automotive, aerospace, construction, and beyond (2,3).

As the appeal of metal foams has grown, researchers have diligently explored these materials to comprehend their mechanical, thermal, and acoustic properties. Various manufacturing techniques have evolved, such as powder metallurgy, melt infiltration, and gas injection methods, which allow tailoring the foam's microstructure, pore size distribution, and overall attributes (4,5). These developments aim to maximize their performance in diverse applications by optimizing the manufacturing processes.

The intricate structures of metal foams possess intriguing characteristics, but the fluid flow behavior within these materials remains an area of keen interest. In applications like heat exchangers, filters, and energy absorption devices, understanding the pressure drop dynamics and fluid flow patterns within metal foams is paramount (6). The pressure drop characteristics, governed by the porous structure's properties, such as pore morphology, pore size, and foam density, are of particular significance (2).

Research efforts have been devoted to investigating pressure drop across metal foams and developing models for predicting their behavior. These studies are vital due to the complexity of metal foams and the diverse range of operating conditions they encounter. Existing correlations, while valuable, often lack the accuracy and comprehensiveness necessary to grasp the intricate physics governing fluid flow in these materials (7). Consequently, further research is crucial to advance our understanding of fluid flow through metal foams and to refine predictive models for practical applications.



The multifaceted nature of metal foams necessitates an in-depth examination of their behavior in varying operational scenarios. This study focuses on addressing a fundamental aspect of their performance – the pressure drop characteristics. By conducting experimental investigations and analyzing the resulting data, we aim to enhance our understanding of how gas flow rates influence pressure drop in Alantum foam, a novel porous material (8,9). As a building block in this area of research, this study contributes to the growing body of knowledge in fluid dynamics, porous materials, and their applications. Through this research, we endeavor to bridge existing knowledge gaps and offer insights into the practical implications of pressure drop characteristics in Alantum foam.

2.0 MATERIALS AND METHODS

2.1 Equipment Used

For the systematic investigation of pressure drop characteristics in Alantum foam, a range of essential equipment and materials were employed.

- i. Air gas cylinder
- ii. Air
- iii. Alantum 450 μm
- iv. Flow rig with gas inlets
- v. Air compressor (1PH, 50Hz, Zhuhai Landa Compressor Co. Ltd.)
- vi. UT-3360 Multimeter

The Schematic and pictorial diagram of the flow rig used are as shown in Figure 1 and 2 while Table 1 explains the components of the flowrig.

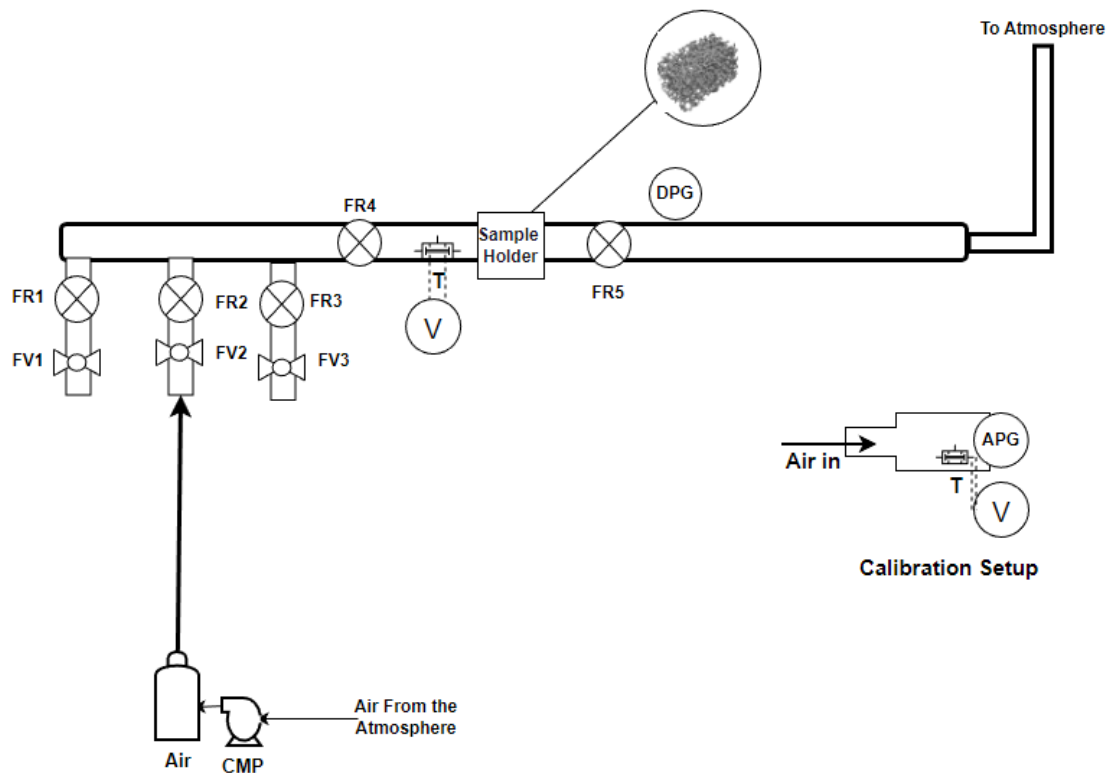


Figure 1: Schematic diagram of the flow rig.





Figure 2: The flow rig.

Table 1: Specifications of the flow rig parts.

SYMBOLS AND MEANING			
Symbols	Meaning	Manufacturer	Capacity/Range
Air	Air Cylinder	Norris Cylinder Company	2.52 kg
CMP	Air Compressor	Zhuhai Landa Compressor Co. Ltd.	1PH, 50Hz
FR	Gas Flowmeter	Shunhuanliu Liangibiao	0 - 10 LPM (1,2&3) 0 - 20 LPM (4&5)
DPG	Digital Pressure Guage	VOKTTA	0 – 200 PSI
APG	Analog Pressure Guage	SKM	0 – 4 bar
T	Transducer	Piezoelectric	0 - 5 V
V	LCD Multimeter	UNI-T	UT890C
	Acrylic pipe	NuoNuoWell	NNW-PVC-119
FV	Ball valve	Aquazen	15mm To 80mm

2.2 Procedure

The air gas cylinder was securely connected to its designated gas inlet on the flow rig, ensuring that



all connections were leak-free. Air compression and storage were skillfully executed, channeling the air into a 2.52 Kg Air cylinder from Norris Cylinder Company. This process was accomplished using an Air compressor (1PH, 50Hz, Zhuhai Landa Compressor Co. Ltd.), guaranteeing a controlled and steady airflow for the experiment.

The flow rig was meticulously prepared for the experiment. All flowmeters and valves within the flow rig were fully opened to ensure the unimpeded flow of air during the study. The transducer's wiring was properly handled, with the wires being precisely connected to the designated terminals of a UT-3360 Multimeter. This multimeter plays a crucial role in measuring the electrical voltage output of the transducer. The metal was securely placed in the sample holder and tightened back in place.

The experimental sequence commenced with the systematic introduction of air into the flow rig. Initially, air flowed through the rig at a rate of 0 liters per minute (LPM), allowing for the recording of voltage readings from the 0-5 V Transducer (Piezoelectric), thus establishing a baseline voltage reading for air at rest.

Subsequently, the introduction of air continued, with airflow being gradually increased from 0 to 10 LPM in 1 LPM increments. Voltage readings from the 0-5 V Transducer were diligently recorded at each combination of air flow rates. The experiment was systematically repeated three times for each flowrate, with the average of the three voltage readings being meticulously documented.

The precise measurement of flow rates was carried out for the gas stream created from the air flow rates. These measurements were taken just before the sample holder, denoted as U4 on the flowmeter, ensuring the availability of accurate flow rate data for correlation with voltage readings.

The experiment yielded a comprehensive dataset that included all voltage readings and flow rate data, each of which was diligently recorded and methodically organized. This data set will be subject to thorough analysis to uncover the precise relationship between air flow rates, pressure drop, and voltage readings.

3.0 RESULTS AND DISCUSSION

3.1 Experimental Findings

The data collected during the experiment revealed significant insights into the pressure drop characteristics of Alantum foam. The voltage readings from the piezoelectric transducer, combined with flow rate measurements, provided a comprehensive view of how pressure drop behaves in this unique material.

The table presents data obtained from the experimental test, which displays the relationship between the air velocity, denoted as U4 (m/s), and the corresponding pressure gradient, $\nabla P4$ (Pa). The data points reveal an intriguing connection between the velocity of air flow and the resulting pressure gradient.

U1 (LPM)	U2 (LPM)	U4 (LPM)	U4 (m3/s)	U4 (m/s)	Volt	ΔV	P4	$\nabla P4$ (Pa)
0	0	0	0.00000	0.00000	0.00000	0.00000	0.00000	0.0000000
	1	0.5	0.00001	0.01645	0.00002	0.00002	0.00005	4.5977779
	2	1.5	0.00003	0.04934	0.00005	0.00005	0.00014	13.7942025
	3	2.5	0.00004	0.08223	0.00008	0.00008	0.00023	22.9917856
	4	3.5	0.00006	0.11512	0.00012	0.00012	0.00032	32.1905273
	5	4.5	0.00008	0.14801	0.00015	0.00015	0.00041	41.3904277
	6	5.5	0.00009	0.18091	0.00018	0.00018	0.00051	50.5914868
	7	6.5	0.00011	0.21380	0.00021	0.00021	0.00060	59.7937048
	8	7.5	0.00013	0.24669	0.00025	0.00025	0.00069	68.9970817



	9	8.5	0.00014	0.27958	0.00028	0.00028	0.00078	78.20161762
	10	9.5	0.00016	0.31247	0.00031	0.00031	0.00087	87.4073127

3.2 Analysis of Results

The results presented in Table 3.2 reveal a compelling and coherent trend that underscores the fundamental principles of fluid dynamics. As the air velocity (U_4) within the experimental setup steadily increases, a proportional surge in the pressure gradient (∇P_4) is observed, as explicitly shown in Figure 3. This observed relationship serves as a tangible representation of the positive correlation between air velocity and pressure gradient. In simpler terms, it elucidates that as air flows at swifter velocities through the test rig, it inherently generates a progressively higher-pressure gradient across the entire system (10).

This phenomenon aligns seamlessly with the bedrock principles of fluid dynamics, where the velocity of a fluid is intrinsically tied to the generation of pressure differentials. When air moves at elevated speeds, it imparts greater kinetic energy to the system, leading to a heightened impact on its surroundings (11). Consequently, this increased kinetic energy translates into a greater force per unit area, which is the very essence of pressure gradient. Therefore, the observed upward trend in pressure gradient with increasing air velocity not only confirms established fluid dynamics principles but also underscores the dynamic nature of fluid behaviour in response to changing flow rates.

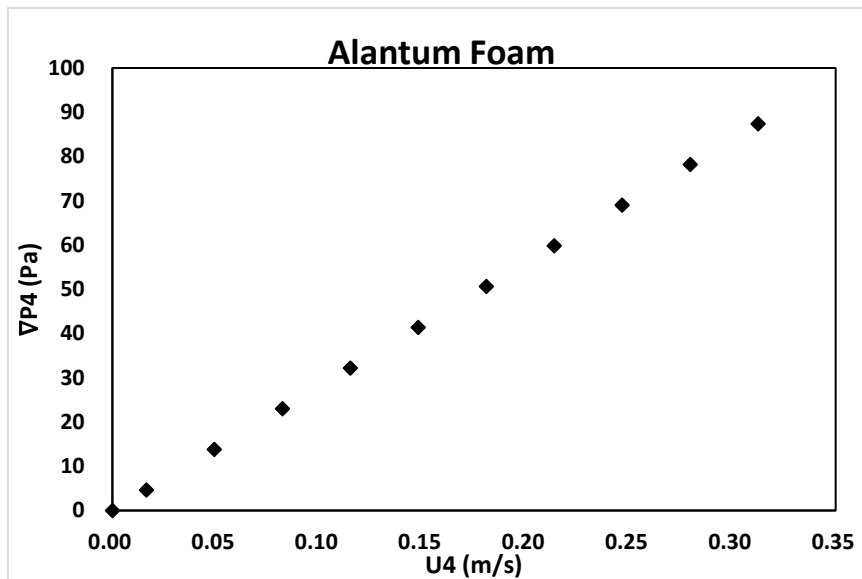


Figure 3: Pressure gradients as a function of velocity plot

4.0 CONCLUSIONS AND RECOMMENDATION

The experimental investigation into pressure drop characteristics in Alantum foam revealed notable trends and insights. As gas flow rates increased, a corresponding rise in pressure drop across the Alantum foam samples was observed, which aligns with expectations and indicates the foam's inherent resistance to gas flow. The porous structure of Alantum foam played a significant role in shaping this pressure drop dynamics, emphasizing the material's suitability for various applications. The precise measurement of flow rates contributed to

the accuracy of the correlation between gas flow rates and pressure drop, underscoring the importance of meticulous data collection in understanding this phenomenon. The experiment's high degree of repeatability, with three repetitions for each combination of flow rates, lends robustness and reliability to the results.

These findings have far-reaching implications for the diverse applications of Alantum foam, such as its use in filtration systems, heat exchangers, and aerospace applications. A comprehensive comprehension of pressure drop characteristics is essential for optimizing these applications, offering engineers and researchers valuable insights into the



behavior of Alantum foam under varying gas flow conditions. Moreover, the observed positive correlation between air velocity and pressure gradient reinforces fundamental fluid dynamics principles, which can be applied in designing systems involving fluid flow. This knowledge advances our understanding of Alantum foam's behavior and its potential for enhancing a wide array of industrial processes and applications, paving the way for innovative solutions in fluid dynamics and material science.

While this study has undeniably delivered valuable insights into the intricate world of pressure drop characteristics within Alantum foam, it is imperative to recognize and address its inherent limitations. The complex nature of porous materials, coupled with the multitude of potential influencing factors, underscores the need for further in-depth research to attain a more holistic understanding of the subject. Future endeavors can expand upon the foundations laid in this research by delving into the following crucial areas:

1. **Development of Quantitative Predictive Models:** Creating predictive models that quantitatively capture the pressure drop phenomenon in Alantum foam is a promising avenue for future research. These models can offer engineers and researchers valuable tools for accurately predicting pressure drop under various conditions.
2. **Impact of Foam Parameters:** Investigating the effects of foam parameters, such as foam density and pore size, on pressure drop, will provide a more nuanced understanding of the foam's behavior. This knowledge is fundamental for tailoring Alantum foam to specific applications.
3. **Exploring Different Gases:** Extending the scope of study to encompass different gases and gas mixtures within Alantum foam is a natural progression. Such investigations can shed light on the foam's versatility in accommodating diverse applications.
4. **Foam Degradation Analysis:** Examining the implications of foam degradation over time on pressure drop characteristics is a critical aspect of future research. This analysis will ensure the

longevity and sustainability of systems incorporating Alantum foam.

In closing, this research represents a significant leap in the quest to unravel the enigmatic world of pressure drop within Alantum foam. The exceptional properties of this material hold the potential to revolutionize an array of industries, with its pressure drop behaviour standing as a pivotal factor in unlocking its full potential. As technology advances and applications evolve, the insights derived from this study will undoubtedly contribute to the refinement and optimization of systems employing Alantum foam, propelling further progress in the ever-evolving field of fluid dynamics.

5.0 REFERENCES

1. B. Parveez, N. A. Jamal, H. Anuar, Y. Ahmad, A. Aabid, M. Baig, Microstructure and mechanical properties of metal foams fabricated via melt foaming and powder metallurgy technique: a review. *Materials*. 15, 5302 (2022).
2. A. Garg, H. D. Chalak, L. Li, M. Belarbi, R. Sahoo, T. Mukhopadhyay, Vibration and buckling analyses of sandwich plates containing functionally graded metal foam core. *Acta Mechanica Solida Sinica*. 35, 1–16 (2022).
3. M. Iasiello, M. Mameli, S. Filippeschi, N. Bianco, Metal foam/PCM melting evolution analysis: Orientation and morphology effects. *Applied Thermal Engineering*. 187, 116572 (2021).
4. R. Kumar, M. Kumar, J. S. Chohan, Material-specific properties and applications of additive manufacturing techniques: a comprehensive review. *Bulletin of Materials Science*. 44 (2021), doi:10.1007/s12034-021-02364-y.
5. M. Kumar, V. Sharma, Additive manufacturing techniques for the fabrication of tissue engineering scaffolds:



- a review. *Rapid Prototyping Journal*. 27, 1230–1272 (2021).
6. S. U. Nisa, S. Pandey, P. Pandey, A review of the compressive properties of closed-cell aluminum metal foams. *Proceedings of the Institution of Mechanical Engineers, Part E: Journal of Process Mechanical Engineering*. 237, 531–545 (2022).
 7. X. Han, Q. Wang, Y. G. Park, C. T'Joen, A. D. Sommers, A. M. Jacobi, A review of metal foam and metal matrix composites for heat exchangers and heat sinks. *Heat Transfer Engineering*. 33, 991–1009 (2012).
 8. M. Awais, N. Ullah, J. Ahmad, F. Sikandar, M. M. Ehsan, S. Salehin, A. A. Bhuiyan, Heat transfer and pressure drop performance of Nanofluid: A state-of-the-art review. *International Journal of Thermofluids*. 9, 100065 (2021).
 9. M. S. Shadloo, A. Rahmat, A. Karimipour, S. Wongwises, Estimation of pressure drop of Two-Phase flow in horizontal long pipes using artificial neural networks. *Journal of Energy Resources Technology-transactions of the Asme*. 142 (2020), doi:10.1115/1.4047593.
 10. M. Ali, M. H. Iqbal, N. A. Sheikh, H. M. Ali, M. Manzoor, M. M. Khan, K. F. Tamrin, Performance Investigation of Air Velocity Effects on PV Modules under Controlled Conditions. *International Journal of Photoenergy*. 2017, 1–10 (2017).
 11. G. K. Batchelor, *An introduction to fluid dynamics* (2000; <https://doi.org/10.1017/cbo9780511800955>).
- 12.



P066 - INVESTIGATION ON THE EFFECT OF IRON OXIDE (FeO_3) PIGMENT ON THE PRODUCTION OF COLOURED CEMENT FOR CONCRETE WORKS

J.S. Okoh*, A.S. Kovo, P.E. Dim

Federal University of Technology, Minna.

Email: spensoitodo@gmail.com

ABSTRACT

Coloured concrete has gained significant popularity in Engineering and decorative applications due to its aesthetic appeal. Iron oxide (FeO_3) pigments are widely used to impart color to cement-based materials. This research work investigates the effect of FeO_3 pigment on the production of colored cement for concrete works. It explores the influence of FeO_3 pigment on concrete properties, such as compressive strength, durability, absorption rate and color stability. The effects of these pigments were studied on Portland cement, the strengths studied by compressive strength test with an average strength of 5.8% for 3days, and the durability studied through water absorption with an average of 6.96%, as well as concrete setting time, and 100% colour retention which is imbedded in the concrete material. It is found from this research that colored pigments does not affect concrete works when applied but enhance compressive strength, inbuilt colour that is not just on the peripheral but imbedded inside the concrete.

Keywords: Cement, Pigments, Iron oxide (FeO_3), Colour retention

1.0 INTRODUCTION

Cement is the most widely used and adaptable material in the construction industry for its properties and cost (6). Despite its numerous qualities, the production of cement contributes largely to the release of carbon dioxide (CO_2) in the atmosphere and, its structures have a dull grey appearance (2). Concrete appearance is affected by many factors, including the ingredients in the mix, mix design, handling and placing procedures, forming and curing methods, surface finishes and textures, environmental conditions, and craftsmanship (8). Concrete used to be grey, it used to be ALL GRAY (4). But, of recent, Engineers, Architects and designers use coloured cement as a tool to incorporate an element of innovation, differentiation and exclusivity to their projects (9). Thanks to colour the possibilities in architecture design have been expanded (3). Furthermore, cementitious products manufacturers are aware of the importance of adding colour to cement, as it makes it possible to give an added value to their products and have a degree of differentiation from their competition (4, 5). This increase in the use of coloured construction materials has been possible thanks to new developments in the incorporation and handling of pigments in recent years (1).

A Pigment is a matter that alters or enhances the colour of any object as an outcome of absorption. Pigmentation in bricks is very vital in the sense that it changes dull objects into eye catching marketable product (7). Iron Oxides pigment are matters that are non-toxic and can resist harsh weather (10), there are two types of iron oxides pigment which have been used for concrete colouration, they are Natural and Synthetic Iron Oxide.

Key components that every manufacturer should have in mind when using iron oxide pigments to colour concrete:

- i. The quality of the Pigment
- ii. Water to Cement Ratio
- iii. Cement Content
- iv. Aggregate colour.

This research work is carried out to produce pigmented colour cement using Iron Oxide (FeO_3) as the pigment, for direct production of coloured cement and reduce cost of purchasing different materials for the same purpose.

2.0 Materials and Methods

2.1 Materials: Chemicals used for this research were of analytical grade. The solvent used for this



research was distilled water obtained from Panlac Chemical Ltd. Sodium Hydroxide (NaOH) was used as the precipitate. Iron Oxide (Fe_2O_3) pigments and Dangote Cement of 42.5R grade was obtained from Dei Dei International building market Abuja, Nigeria.

2.2 Production of Red Pigment: Iron Oxide (Fe_2O_3) pigments were used for the production process, it was chosen because of its chemical composition and deliquesce in nature to adapt to cement mixtures. Ferrous Sulphate was crushed and purified to remove impurities and to achieve consistent composition. A solution of the iron salt is prepared and reacted with a precipitating agent Sodium Hydroxide (NaOH) in the presence of an oxidizing agent, such as hydrogen peroxide or sodium chlorate. This causes the iron to form a solid precipitate of ferric hydroxide. The ferric hydroxide precipitate is allowed to age, typically for several days, to allow the particles to grow in size and develop the desired red colour. The aged precipitate is then washed several times with water to remove any impurities or remaining precipitating agent. The washed precipitate is dried, either by air-drying or by heating in an oven. The dried precipitate is then calcined at a temperature, between 800-900 °C, to convert the ferric hydroxide to red iron oxide. The calcined red iron oxide is ground into a fine powder.

2.3 Production of Pigmented Colour Cement:

3kg of iron Oxide was measured, weighed in a scale and mixed with 50kg of Dangote Blocmaster cement in a pre-blending concrete mixer and allowed to mix thoroughly.

2.4 Inter-lock/Kerbs Production Using the New Product (Pigmented Cement):

Two-and-a-half-wheel barrow of stone dust to 50kg of pigmented cement for each sample, thorough hand mixing was done and water added to the continuous process until required mold is achieved, surfacing of the mould was achieved with the aid of a cube box and allowed to dry for 72hrs. The interlocks produced

3.0 Results and Discussions

In FTIR spectroscopy, the wavenumber and intensity of the peaks can provide information about the chemical bonds present in the sample. The wavenumber corresponds to the energy of the light absorbed, which is characteristic of a specific type of bond. The intensity of the peak can give an indication of the amount of that bond present.

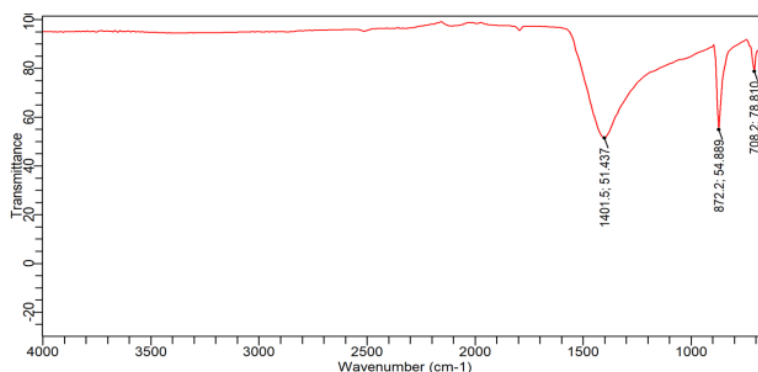


Figure 1: FTIR Spectrum Of Raw Red Pigment

- Peak 1 at $708.19419 \text{ cm}^{-1}$ could correspond to the Fe-O stretching vibrations in iron oxide.
- Peak 2 at $872.19705 \text{ cm}^{-1}$ might be related to the bending modes of water (H_2O) or hydroxyl groups (OH^-) present in the sample.
- Peak 3 at $1401.47903 \text{ cm}^{-1}$ could be associated with carbonate (CO_3^{2-}) groups, indicating the presence of carbonates in the sample.



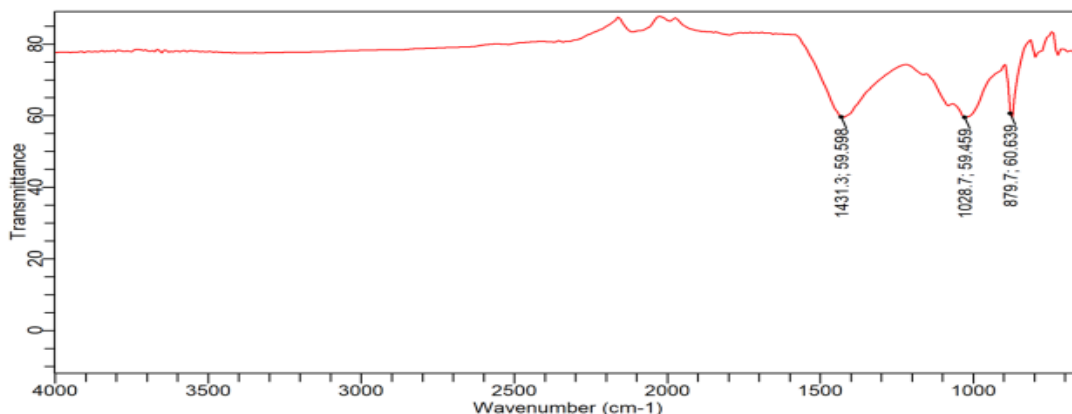


Figure 2: FTIR Spectrum Of Raw Produced Red Pigment

- Peak 1 at $879.65173 \text{ cm}^{-1}$: This could be associated with the C-H bending vibrations in organic compounds. If the iron oxide powder is organic or has organic additives, this peak could be related to those components.
- Peak 2 at $1028.74524 \text{ cm}^{-1}$: This wavenumber is often associated with C-O stretching vibrations in ethers and alcohol groups. If the iron oxide powder contains these functional groups, this peak could be indicative of them.
- Peak 3 at $1431.29773 \text{ cm}^{-1}$: This could be associated with C-H bending vibrations in the plane of the molecule, often seen in alkenes and aromatics.

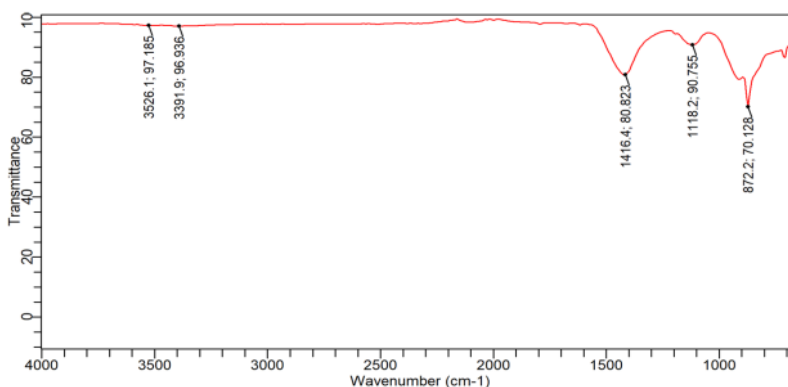


Figure 3: FTIR Spectrum Of Portland Cement

- Peak 1 at $872.19705 \text{ cm}^{-1}$: This could be associated with the bending modes of water (H_2O) or hydroxyl groups (OH^-) present in the sample.
- Peak 2 at $1118.20135 \text{ cm}^{-1}$: This wavenumber is often associated with Si-O stretching vibrations in silicates, which are a major component of Portland cement.
- Peak 3 at $1416.38838 \text{ cm}^{-1}$: This could be associated with carbonate (CO_3^{2-}) groups, indicating the presence of carbonates in the cement.
- Peak 4 at $3391.81143 \text{ cm}^{-1}$ and Peak 5 at $3526.06159 \text{ cm}^{-1}$: These peaks in the high wavenumber region are typically due to O-H stretching vibrations, indicating the



presence of hydroxyl groups or water in the sample.

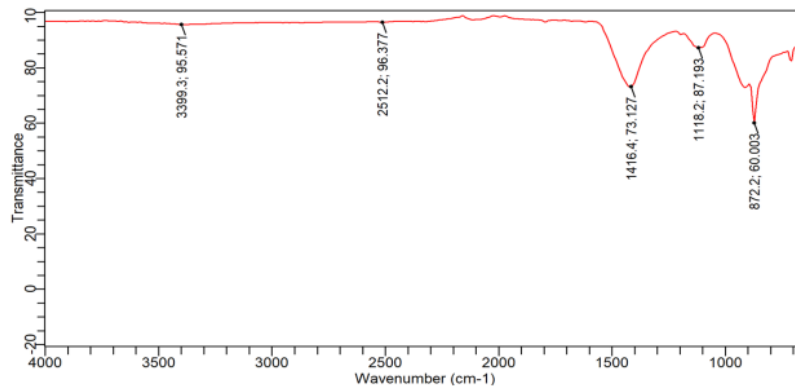


Figure 4: FTIR Spectrum Of Red Pigment Cement

- Peak 1 at 872.19705 cm^{-1} : This could be associated with the bending modes of water (H_2O) or hydroxyl groups (OH^-) present in the sample.
- Peak 2 at 1118.20135 cm^{-1} : This wavenumber is often associated with Si-O stretching vibrations in silicates, which are a major component of Portland cement.
- Peak 3 at 1416.38838 cm^{-1} : This could be associated with carbonate (CO_3^{2-}) groups, indicating the presence of carbonates in the cement.
- Peak 4 at 2512.22570 cm^{-1} : This peak is associated with the combined iron oxide groups.
- Peak 5 at 3399.33211 cm^{-1} : This peak in the high wavenumber region is typically due to O-H stretching vibrations, indicating the presence of hydroxyl groups or water in the sample.

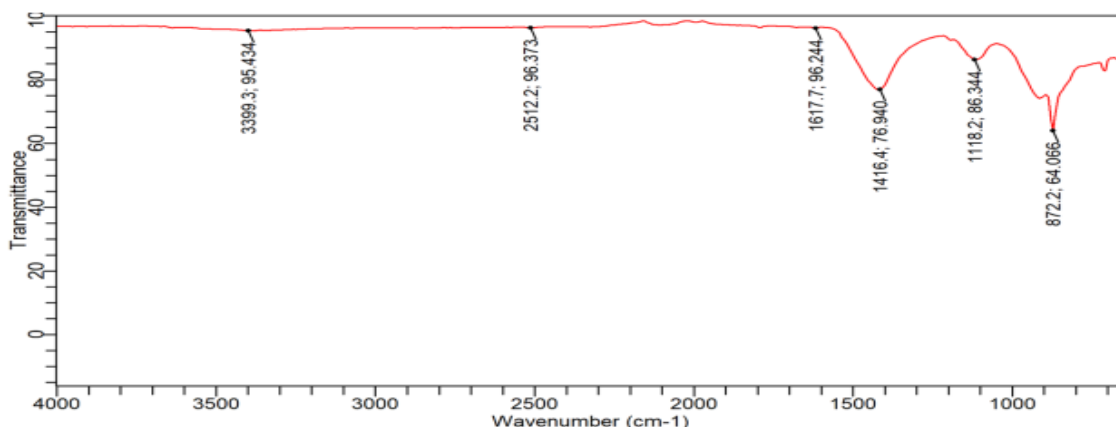


Figure 5: FTIR spectrum of produced red pigment cement

- Peak 1 at 872.19705 cm^{-1} : This could be associated with the bending modes of water (H_2O) or hydroxyl groups (OH^-) present in the sample.



- Peak 2 at 1118.20135 cm^{-1} : This wavenumber is often associated with Si-O stretching vibrations in silicates, which could be present in the sample.
- Peak 3 at 1416.38838 cm^{-1} : This could be associated with carbonate (CO_3^{2-}) groups, indicating the presence of carbonates in the sample.
- Peak 4 at 1617.66462 cm^{-1} : This peak could be associated with C=O stretching

vibrations, indicating the presence of carbonyl groups in the sample.

- Peak 5 at 2512.22570 cm^{-1} : This peak is colored iron pigment group.

The FTIR analysis carried out confirmed that the introduction of colour pigment was successful and no significant chemical changes were occurred when added to already existing Portland cement, and also the production of the produced red pigment had no changes as compared to the purchased pigments.

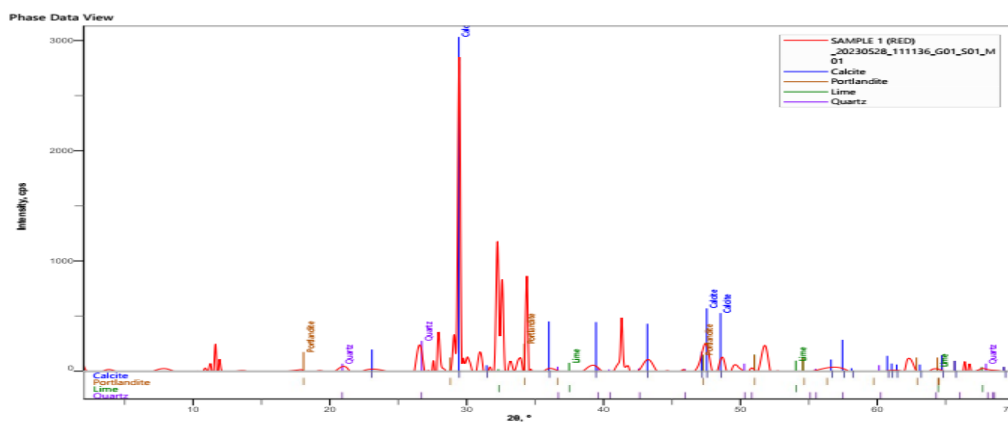
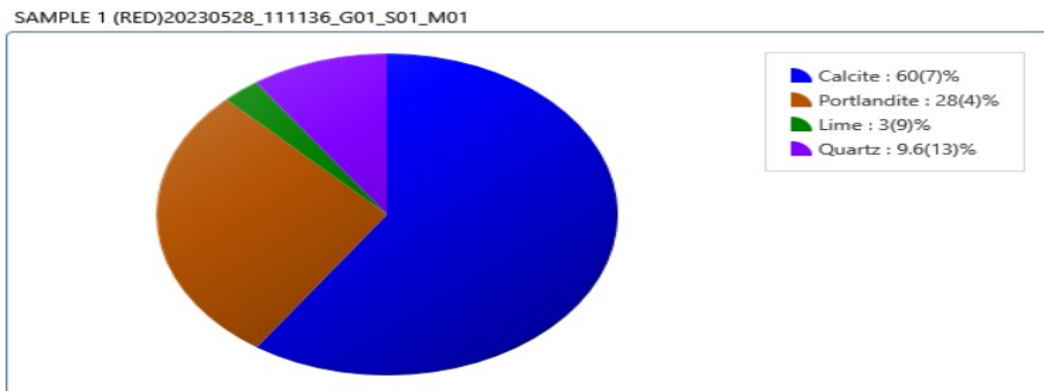


Figure 6: XRD PATTERN OF RED PIGMENTED CEMENT



PIE REPRESENTATION OF COMPONENTS FOR RED PIGMENT CEMENT.



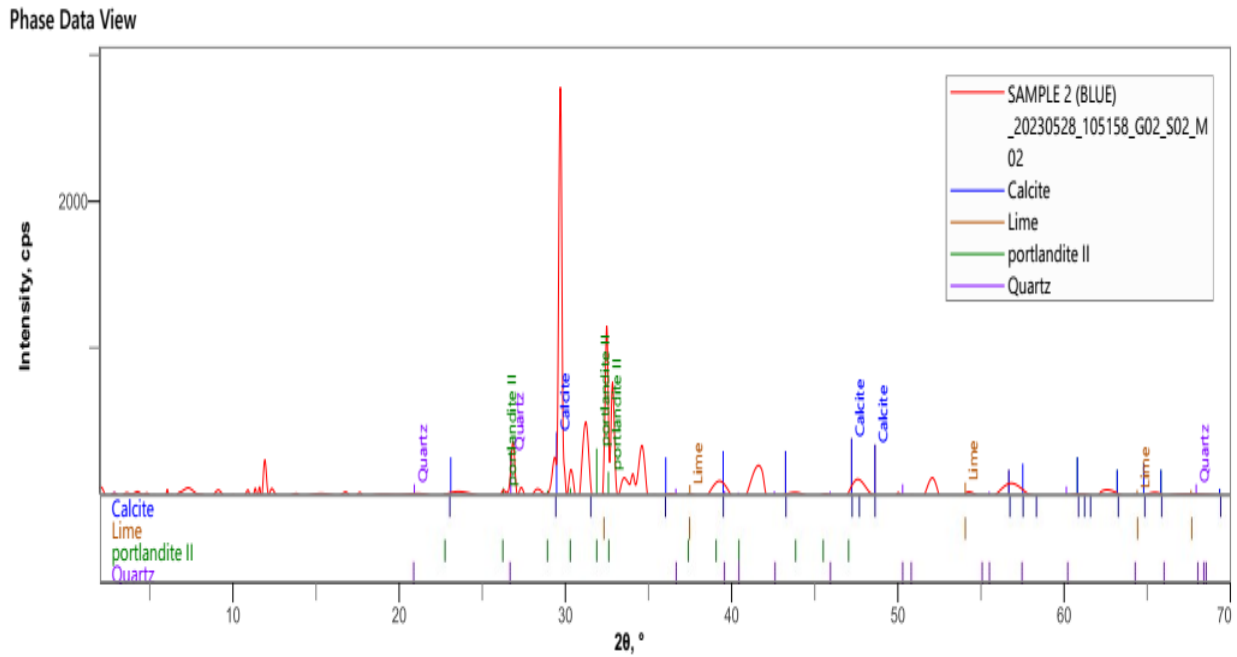
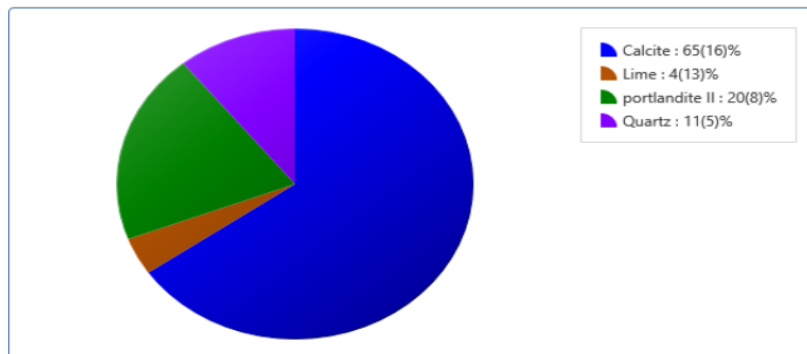


Figure 7: XRD PATTERN OF PRODUCED RED PIGMENTED CEMENT



PIE REPRESENTATION OF COMPONENTS FOR RED PIGMENT CEMENT.

The results obtained from the red pigmented cement and the produced red pigment cement after the age of 3 days curing. The X-ray diffraction (XRD) pattern provides the chemical composition and crystalline structure of

the mixes at the time of testing. So, results are directly related to the content of the hydration phases. The main components identified are: Calcite, Lime, Portlandite and Quartz which are shared in their various proportions in the pie chart results.

Table 1: COMPRESSIVE STRENGTH TEST FOR 3 DAYS AGING FOR PRODUCED RED PIGMENT KERB.



S/No	Sample ID	Concrete Age	Weight in Air (kg)	Volume m ³	Density (kg/m ³)	Load (kN)	Compressive Strength N/mm ²	Av. Compressive Strength N/mm ²
1	A	3 Days	3.560	0.001728	2060	174.078	6.063	5.885
2	B		3.545	0.001728	2052	172.051	5.992	
3	C		3.640	0.001728	2106	162.544	5.601	

Table 2: COMPRESSIVE STRENGTH TEST FOR 3 DAYS AGING FOR RED PIGMENT KERB

S/No	Sample ID	Concrete Age	Weight in Air (kg)	Volume m ³	Density (kg/m ³)	Load (kN)	Compressive Strength N/mm ²	Av. Compressive Strength N/mm ²
1	A	3 Days	3.815	0.001728	2208	174.539	6.079	5.878
2	B		3.440	0.001728	1991	159.567	5.557	
3	C		3.675	0.001728	2127	172.252	5.999	

The compressive strength is determined in accordance with the EN 196-1:2016. Prismatic specimens (195 × 195 × 98 mm) were cast, compacted and cured in a control chamber at a temperature of 20 ± 2°C and humidity of 98 ± 1 % until the age of testing (3 days). At each age, the compressive strength achieved are the average of 3 days tests, respectively.

4.0 Conclusions and Recommendations

In conclusion, the addition of FeO₃ pigment to cement has been found to have a positive effect on the properties of coloured cement for concrete works. The study has reported improved compressive strength, durability, color stability, and workability when FeO₃ pigment is added to cement. The optimal dosage of FeO₃ pigment ranges from 4% to 6% by weight of cement, depending on the specific application.

Further research can be studied in the dosage of FeO₃ pigments should be optimized for different shades while making sure that the pigment's incorporation does not affect the concrete's chemical and physical properties. Particle size and distribution should be taken into account during this optimization, carrying out long-term performance studies, particularly for colour stability and durability, working with standardization bodies to develop guidelines for pigment incorporation,

assessing the environmental impact of pigment use, and developing educational materials for construction professionals.

5.0 References

1. Gholampour, T. Ozbakkaloglu (2017), Performance of sustainable concretes containing very high-volume class-F fly ash and ground granulated blast furnace slag, *J. Clean. Prod.* 162 pp.1407–1417.
2. H.-D. Yun, J.-W. Lee, Y.-I. Jang, S.-J. Jang, W. Choi (2019), Microstructure and mechanical properties of cement



mortar containing phase change materials, *Appl. Sci.* 9

3. I. Belykh, V. Sopov, L. Butska, L. Pershina, O. Makarenko (2018), Predicting the strength and maturity of hardening concrete, in: *MATEC Web of Conferences*.
4. L.F. de Magalhaes, S. França, M.D.S. Oliveira, R.A.F. Peixoto, S.A.L. Bessa, A.C.D.S. Bezerra (2020), Iron ore tailings as a supplementary cementitious material in the production of pigmented cements, *J. Clean. Prod.*
5. L. Hatami, M. Jamshidi (2021), Effects of type and duration of pigment milling on mechanical and colorimetric properties of coloured self-compacting mortars, *J. Build.Eng.* 35
6. Mehreen Z. Heerah, Isaac Galobardes, Graham Dawson (2020), Characterisation and control of cementitious mixes with colour pigment admixtures, Elsevier Ltd. 10.1016/j.cscm.2021.e0057. PP 1-18.
7. R. Christie, *Colour Chemistry*, Royal Society of Chemistry, Cambridge, (2015).
8. Viola Hospodarova, Jozef Junak, Nadezda Stevulova (2016), *Color Pigments in Concrete and their Properties*, An International Journal for Engineering and Information Sciences, Vol. 10, No. 3, pp. 143–151.
9. V. Hospodarova, J. Junak, N. Stevulova (2016), Color pigments in concrete and their properties, *Int. J. Eng. Inf. Sci.* 10 (no. 3) pp.143–151.
10. X. Deng, J. Li, Z. Lu, J. Chen, K. Luo, Y. Nui, (2020) Effect of hydrated lime on structures and properties of decorative rendering mortar, *Constr. Build. Mater.*



P067 - PREPARATION OF HIERARCHICAL FE-ZSM-5 FOR THE SELECTIVE CATALYTIC CRACKING OF CRUDE OIL

Hassana G. A^{1*}, Osigbesan A. A², Zanna U.A. S³, Bala U⁴, Oladipo M. O⁵, ADO A. D⁶, Atta A. Y⁷

Chemical Engineering Department, Ahmadu Bello University, Zaria.

Corresponding author email: hassana2014.ha@gmail.com

ABSTRACT

The use of zeolites for the cracking of heavy hydrocarbons in petroleum and petrochemical industries cannot be overemphasized. In this study, iron oxide impregnated hierarchical ZSM-5 was prepared and its performance was tested on the cracking of 50 ml of crude oil and compared to the thermal cracking of the same quantity of crude oil. The catalyst was characterized by FTIR, XRD, XRF and BET techniques; FTIR showed the functional groups that are peculiar to the frame work of ZSM-5, the XRD pattern also showed the characteristic peaks of ZSM-5 indicating the crystallinity of the catalyst while the BET analysis illustrated the surface area and pore size distribution of the catalyst which indicates that the catalyst possessed the properties needed for its catalytic performance. XRF analysis displayed the elemental and oxide composition of the catalyst, in which iron was confirmed to have been doped in the ZSM-5 for enhanced catalytic performance in the cracking of crude oil sample. The cracked crude oil using the catalyst was analysed using GC-MS technique in which aromatic compounds had increased significantly compared to ordinary thermally cracked crude oil and the crude oil samples. Hence, the Fe-Hi-ZSM-5 was suitable for the catalytic cracking of crude oil.

Keywords:

Crude oil, hierarchical zsm-5, characterization, cracking, catalytic

1.0 INTRODUCTION

Zeolites are frequently used in the petrochemical applications because they have a framework structure, excellent hydrothermal stability and a lot of catalytic active sites. Yet the zeolites' microporous structure which has pores smaller than 2nm, causes slow bulk molecular transport and quick deactivation (1). Molecular confinement can be a blessing or a curse in catalyst. One example of zeolites, which are crystalline aluminosilicate materials with inherent acidity and distinct pore windows. Only molecules that can fit in the pores during catalytic cycle can develop, and only molecules that can pass through the pore windows are permitted to leave the catalytic reaction site. However, confinement is a problem for molecular diffusion. Such diffusional restrictions, a well-known issue in industrial catalysis, could leave a significant portion of acid sites in a zeolite crystal unoccupied (2). Low overall efficiencies and undesirable secondary reactions, including coking, cause the conversion rate to decrease and the catalyst to quickly lose its activation, having devastating effects on overall performance (3).

Fluid catalytic cracking (FCC) unit is one of the most important refinery technologies, while the heavy or extra heavy oils molecules are much larger

than the micropores of the traditional catalysts such as Y or ZSM-5 zeolites (4), which are usually used as the main active components in FCC unit. The acid sites in zeolites, which perform the vital cracking function, mainly exist in the micropores of the zeolite and are mostly inaccessible for the heavy and extra-heavy oils molecules (5). Hence, it is very difficult to directly crack the heavy and extra-heavy oils into the target products such as gasoline, diesel oil, light olefin, and the chemical intermediates for the creation of desired product. While this is happening, the strong diffusion limitation also has some unfavourable effects such as the side reaction or excessive carbon deposition. Therefore, this has led to an increase in interest in the effective converting of the heavy or extra-heavy oils with bulky molecules into the target products (1).

Particularly in the production of petrochemicals, which include aromatic hydrocarbons like gasoline, ethylbenzene, and cumene, these zeolites have been used. Although, they each have unique physical and chemical characteristics, they all have several desirable traits, such as high density due to the strong oxygen connection between Si and Al and the temperature stability up to 800⁰C (5).

Hierarchical zeolites have the potential to provide a breakthrough in transport limitation, which hinders



pristine microporous zeolites and thus may broaden their range of applications. In this study, iron oxide (FeO) doped Hierarchical ZSM-5 (Fe-HZSM-5) would be synthesized for the cracking of crude oil to obtain lighter hydrocarbon compounds.

2.0 METHODOLOGY

2.1 Materials, Equipment and Reagents

2.1.1 Reagents:

Commercial ZSM – 5, Sodium Hydroxide, Ammonium Nitrate, and Iron Nitrate Nonahydrate were collected from the store of Prof. Atta's Laboratory, Chemical Engineering Department, Ahmadu Bello University, Zaria. While deionized water was obtained from National Research Institute for Chemical Engineering, NARICT, Basawa.

2.1.2 Materials and Equipment:

Glass wares such as beakers, volumetric flask, conical flask, crucibles, hotplate with magnetic stirrer, stirring bar, drying oven, muffle furnace, litmus paper, general laboratory centrifuge.

2.2 Catalyst Preparation

Steps in the formation of iron modified hierarchical ZSM-5:

The preparation of hierarchical ZSM-5 was carried out by calcining the commercial ZSM-5 in a muffle furnace at 550 °C for 5 h. Alkaline treatment was followed on the calcined commercial ZSM-5 in a mixture of 0.5 M NaOH solution at 65 °C for 1 h. The zeolite is then filtered, centrifuged and washed using deionized water several times while monitoring the pH until it comes below 8. The zeolite was further acidified or converted to H-type by ion exchange process using the aqueous 0.5 M ammonium nitrate solution. The zeolite was then labelled H-ZSM-5. The acidified zeolite was dried at 100 °C for 12 h and subsequently calcined at 550 °C for 5h. Iron oxide doping on the H-ZSM-5 was carried out by the incipient wetness impregnation method on wt/wt % basis. At 3 wt/wt %, iron loading was done and the resulting iron modified hierarchical ZSM-5 (Fe-Hi-ZSM-5) was dried in oven at 120 °C for 12 h and calcined in a muffle furnace at 550 °C for 5 hours (1).

2.3 Catalyst Characterization

The properties of the prepared catalyst were characterised using FTIR, XRD and XRF. The presence of the required functional groups was determined using the Shimadzu 8400S Fourier Transform Infrared spectrophotometer (FT-IR), the crystallinity of the catalyst frame work was ascertained by obtaining the X-ray diffraction patterns using powder X-Ray Diffraction technique, Shimadzu 6000 with Cu-K radiation ($\lambda=1.54184 \text{ \AA}$) and $2\theta = 4-70^\circ$ and operated on 40 kV and 30 mA. N₂ adsorption-desorption technique was employed to obtain the specific surface area as well as the pore analysis of the catalysts. XRF analysis was carried out to determine and confirm the percentage (%) loading of the metal impregnation into the prepared hierarchical ZSM-5 (Hi-ZSM-5).

2.4 Characterization of Feed Stock and Products

Physicochemical properties analysis of the feed stock will be carried out. The physical properties will include the API density, viscosity and specific gravity. FT-IR analysis will be carried out on both the feed stock and the products to obtain the existing functional groups in the feed stock and products; while Gas Chromatography – Mass Spectrophotometry (GC-MS) analysis will be carried out to obtain the chemical compositions of the feed stock and products.

2.5 Experimental Procedure:

The reaction was carried out *in situ* in a batch reactor as adapted from (6). The operating conditions are for the feedstock to catalyst ratio was 50 ml: 1 g, the operating temperature was 350 °C at heating rate of 5 °C per minute from the ambient. The residence or reaction time was 1 hour, while the pressure was monitored and maintained within acceptable limit.

3.0 RESULTS AND DISCUSSION

3.1 Catalyst Characterization:

Typical powder XRD patterns of the prepared Fe-Hi-ZSM-5 as shown in figure 3.12, the sample showed a characteristic diffraction pattern of ZSM-5 with typical peaks at 2θ of $7-10^\circ$ and $22-25^\circ$ (7). The characteristic peaks of iron oxide were expected at 2θ of 30, 42 and 64 (8), but they were not so prominent. This is probably due to the fact that iron oxide particles sizes are below the visible range of the XRD equipment. However, This XRD result is also in conformity with the



International Zeolite Association Online Structure database (9).

FTIR spectrum of the Fe-Hi-ZSM-5 is displayed in Figure 1. The figure shows that there are prominent peaks along wavebands from 750 – 4000 cm^{-1} . The peaks at 3036.06 to 3905.98 cm^{-1} can be assigned to the stretching and bending vibrations of the adsorbed water molecules in the sample. The peak at 1217.12 cm^{-1} can be assigned to the asymmetric vibration of the external T-O while that at 1080.17 cm^{-1} is assigned to the asymmetric stretching of the internal T-O. The peak around 782.77 cm^{-1} belonged to the symmetrical stretching of T-O where T is either Al, Si or Fe. The FTIR spectrum therefore, showed the necessary functional group available in the prepared Fe-Hi-ZSM-5, and thus in line with the XRD patterns obtained of the sample.

Elemental and oxide compositions obtained from XRF data are displayed in Table 1. Some oxides and elements such as magnesium (Mg), calcium (Ca),

were seen in trace concentrations. While oxides of silicon (S), aluminium (Al) and iron (Fe) were found to be 85.807, 6.655 and 5.813 mg/cm^2 or 91.272, 4.171 and 2.326 mol %, the silicon, aluminium and iron elements were 40.110, 3.522 and 4.066 mg/cm^2 . The results from the analysis, indicated the Si / Al ratio of the Fe-Hi-ZSM-5 was to 11.39, and the percentage loading of Iron III oxide calculated was 2.80 wt % is approximately 3 wt % that was loaded during the impregnation process.

From the XRD, FTIR and chemical composition analysis results, the sample prepared was iron-containing hierarchical ZSM-5 zeolite. However, the Fe-Hi-ZSM-5 did not show any pronounced XRD peaks to indicate the iron oxide species but the generic name ORTHOCLASE indicates the presence of the iron oxide in the framework of the zeolite. Therefore, the iron oxide was well dispersed in the framework of the hierarchical ZSM-5.

Figure 1: FTIR spectrum of the Fe-Hi-ZSM-5

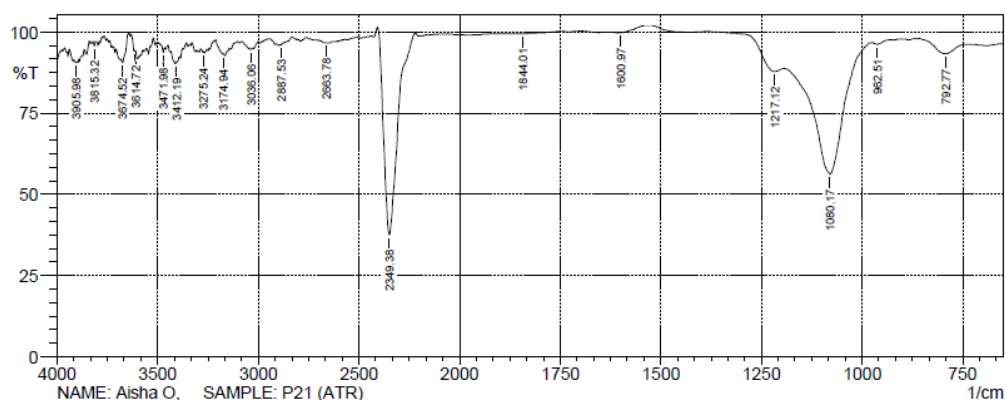


Table 1: Elemental and Oxide Composition of the Fe-Hi-ZSM-5

Elements	Concentration	Oxides	Concentration	Moles %
O	50.774	SiO	85.807	91.272
Al	3.5222	Fe ₂ O ₃	5.813	2.236
Si	40.110	CaO	0.158	0.180
Cl	0.891	K ₂ O	0.368	0.250
K	0.305	Al ₂ O ₃	6.655	4.171
Ca	0.113			
Fe	4.066			



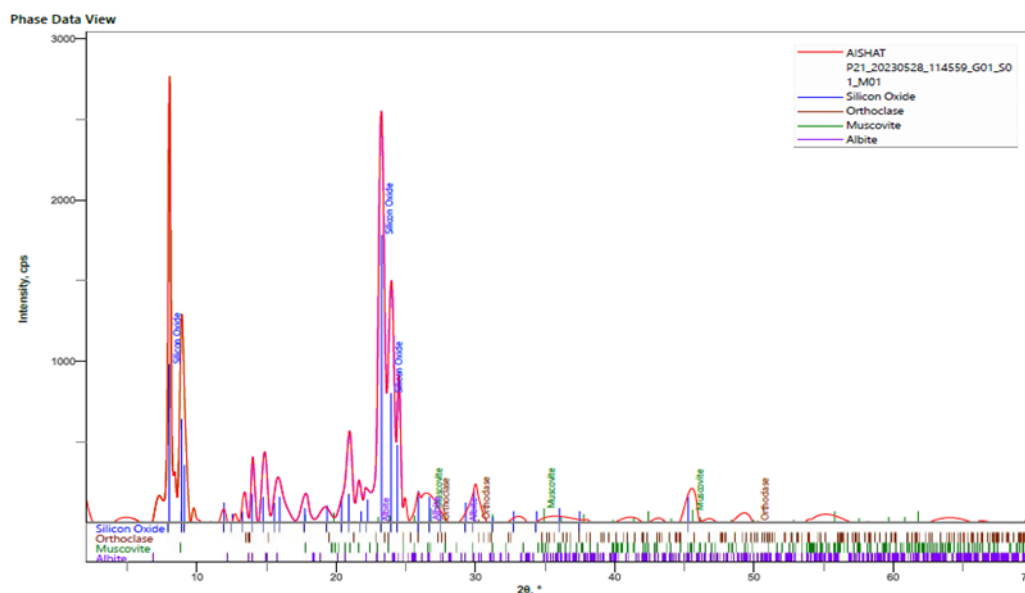


Figure 2: XRD crystallography of the Fe-Hi-ZSM-5

Table 2: Surface area and pore size distribution of the Fe-Hi-ZSM-5 catalyst.

BET surface area (m ² /g)	External surface area (m ² /g)	Micropore surface area (m ² /g)	Pore volume (cm ³ /g)	Micropore volume (cm ³ /g)	Pore size (nm)
269.3	269.3	326.3	0.162	0.01616	5.848

Table 2 presents the surface area and pore size distribution of the catalyst; the surface areas presented as calculated by the various models and methods were within the range of areas possessed by hierarchical ZSM-5 as reported by (10). The catalyst possesses excellent micropore volumes (0.016 cm³/g) which commensurate with the pore diameter of 5.85 nm. The analysis of the catalyst shows that the catalyst prepared is hierarchical in nature with the ability to perform expectedly in the cracking of crude oil molecules.

3.2 Product Analysis:

The chemical compositions of the crude oil and the cracked oil from the uncatalyzed and catalyzed runs using the prepared hierarchical ZSM-5 were analyzed by the GC-MS technique. Figure 3 a, b and c show the chromatographs comprising of the retention time of about 45 minutes and abundance of the compounds detected in the samples; and the peaks were identified using the National Institute of Standards and Technology (NIST) reference database (Library) of the GC-MS. The compositions were grouped into classes of prominent hydrocarbons including Paraffins, Olefins and Aromatics.



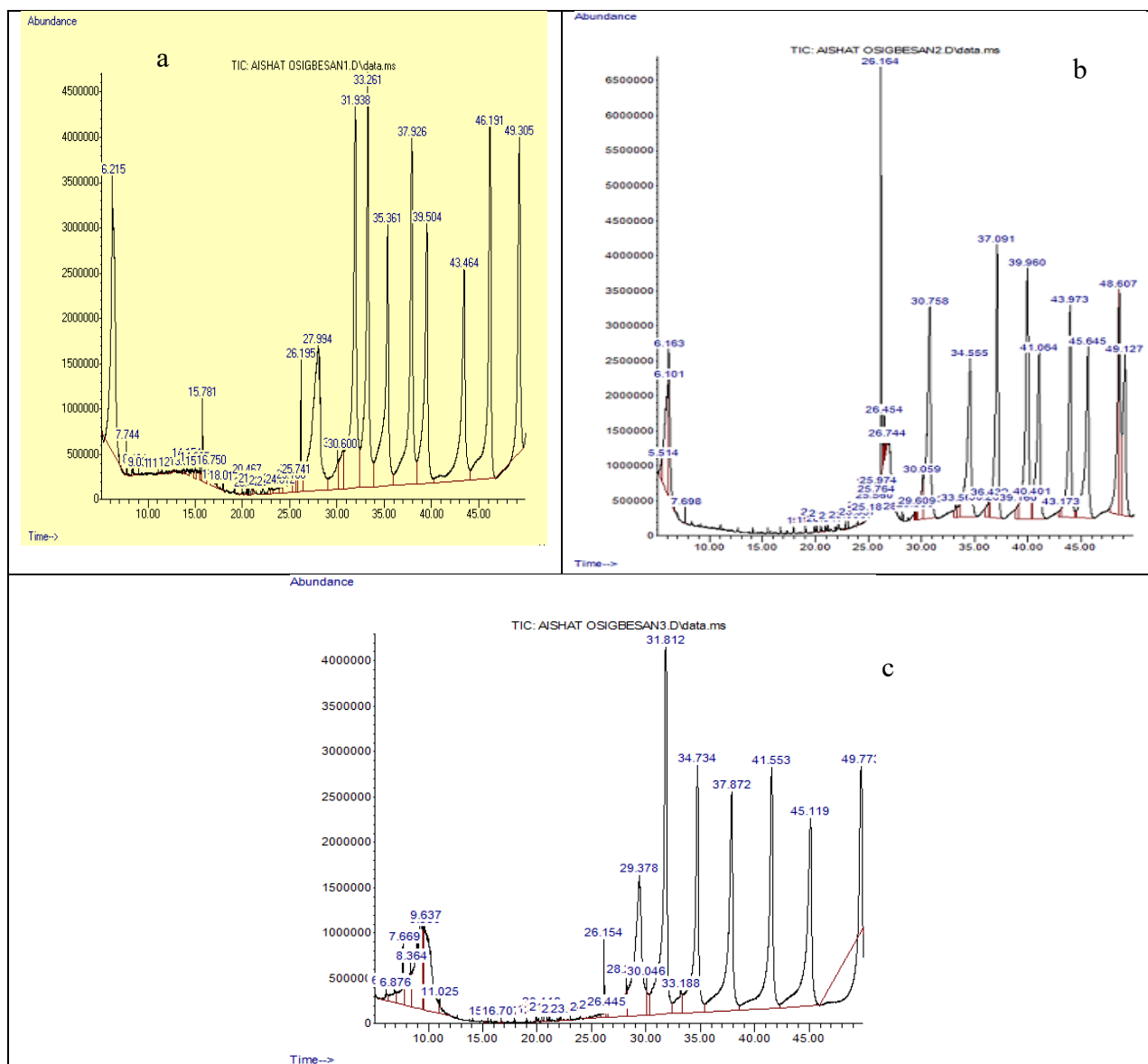


Figure 3: Chromatographs of the GC-MS analysis of the crude oil (a), thermally cracked oil at 350 °C (b) and catalytically cracked oil at 350 °C (c).

Table 3: Chemical composition of the crude oil, thermally cracked oil at 350 °C and catalytically cracked oil at 350 °C obtained from the GC-MS analysis.

Method	Class of Compounds	Range of Hydrocarbon	Relative Area %
Crude	Paraffins	C ₂₀ – C ₄₂	3.69
	Olefins	C ₂₅ - C ₃₀	0.99
	Esters		77.84



	Aromatic	C ₆ – C ₉	10.67
Thermal cracking	Paraffins	C ₁₀ – C ₂₂	0.34
	Olefins	C ₆ – C ₁₀	0.09
	Aromatic	C ₆ - C ₉	8.59
Catalytic cracking	Paraffins	C ₁₁ – C ₂₀	2.67
	Olefins	C ₆ – C ₁₀	0.11
	Aromatics	C ₆ – C ₉	19.46

It was observed from the chromatographs that the retention time for all components in each sample was maintained at 45 minutes, however, the peaks found in sample (a) presented in Figure 3a belonged to the hydrocarbon classes including paraffins, olefins, esters and aromatics with relative area (%) illustrated in Table 3; the result for the esters indicated highest relative area of about 77 %. The composition of the thermally cracked oil improved significantly to obtaining paraffins (C₁₀-C₂₂) with reduced relative area of 0.34 %, olefins (C₆-C₁₀) of relative area of 0.09 % and aromatics (C₆-C₉) with relative area of 8.59 % with acid compounds discovered in the samples. The catalytic cracking improved the quality of the oil composition following the composition of the sample presented in the chromatograph and illustrated in the table. The aromatic compounds increased substantially to 19.46 % in relative area compared to that present in the crude oil and thermally cracked crude oil samples.

The GC-MS analysis of the samples, therefore, showed the effect of using the prepared hierarchical ZSM-5 impregnated with iron oxide on the catalytic cracking of crude oil. The result is in conformity with the works of (1).

4.0 CONCLUSION

In conclusion, the hierarchical ZSM-5 zeolite was successfully impregnated with iron oxide to obtain Fe-Hi-ZSM-5 as catalyst. The catalyst has remarkable mesoporosity of 5.848 nm, excellent micropore volume and large surface area required to enhance cracking of heavy crude oil molecules. The diffractogram presented in the XRD analysis confirmed the presence of the characteristic peaks of ZSM – 5 which were not distorted by the impregnation of the iron oxide, an indication of the crystallinity of the catalyst. The FTIR analysis presented also was appropriate showing the required functional groups necessary for the best performance of the catalyst in the cracking of the crude oil sample.

The catalyst was used for the cracking of 50ml crude oil at 350 °C for 1 h; its performance was compared to thermal cracking of the crude oil samples. The catalytically cracked crude oil yielded the best quality in terms of the relative area of aromatics occupied in the chromatograms presented by the GC-MS analysis. Hence, the Fe-Hi-ZSM-5 prepared exhibited a good performance in the cracking of crude oil sample.

5.0 REFERENCES

1. D. Wang, H. Sun, W. Liu, Z. Shen, W. Yang, Hierarchical ZSM-5 zeolite with radial mesopores: Preparation, formation mechanism and application for benzene alkylation. *Frontiers of Chemical Science and Engineering* **14**, 248-257 (2020).
2. M. E. Potter *et al.*, Understanding the Role of Molecular Diffusion and Catalytic Selectivity in Liquid-Phase Beckmann Rearrangement. *ACS Catalysis* **7**, 2926-2934 (2017).
3. L. Meng, B. Mezari, M. G. Goesten, E. J. M. Hensen, One-Step Synthesis of Hierarchical ZSM-5 Using Cetyltrimethylammonium as Mesopore and Structure-Directing Agent. *Chemistry of Materials* **29**, 4091-4096 (2017).
4. M. S. Rigutto, R. van Veen, L. Huve, in *Studies in Surface Science and Catalysis*, J. Čejka, H. van Bekkum, A. Corma, F. Schüth, Eds. (Elsevier, 2007), vol. 168, pp. 855-XXVI.
5. B. Peng *et al.*, Fluid catalytic cracking technology: current status and recent



- discoveries on catalyst contamination. *Catalysis Reviews* **61**, 1-73 (2018).
6. D. V. Pham, N. T. Nguyen, K. H. Kang, P. W. Seo, S. Park, Study into the effects of the feedstock properties and stability on the catalytic hydrocracking of heavy oil. *Fuel* **339**, 127427 (2023).
 7. W. Rao *et al.*, Iron-doped hierarchically porous Fe-ZSM-5 zeolite with 3D continuous pore architecture for catalytical degradations. *Materials Chemistry and Physics* **271**, 124704 (2021).
 8. Y. M. Mos, A. C. Vermeulen, C. J. N. Buisman, J. Weijma, X-Ray Diffraction of Iron Containing Samples: The Importance of a Suitable Configuration. *Geomicrobiology Journal* **35**, 511-517 (2018).
 9. N. Syuhadah, N. Japri, Z. Ramli, N. Mahat, Reactivity of mesoporous ZSM-5 zeolite towards Friedel-Crafts acylation of anisole and propionic anhydride. *Malaysian Journal of Catalysis* **2**, 62-66 (2017).
 10. G. Song *et al.*, Synthesis and Characterization of Hierarchical ZSM-5 Zeolites with Outstanding Mesoporosity and Excellent Catalytic Properties. *Nanoscale Research Letters* **13**, 364 (2018).



P068 - ANALYSIS OF ACID OPTIONS IN THE PURIFICATION OF SPENT MOTOR ENGINE OIL USING ACIDIFIED CLAY

Jibril, A. A.^{1*} & Aboje, A. A.²

Department of Chemical Engineering, Federal University of Technology Minna

*Corresponding author email: Chemab08.aa@gmail.com

ABSTRACT

This study focuses on the purification of spent Shell Helix lubricating oil to promote environmental sustainability and economic viability. The purification process involves the use of acidified clay treatment, utilizing three different acid options: mineral sulfuric acid, organic acetic acid, and organic citric acid (a novel washing agent). Various physicochemical properties of the clay mineral, spent lubricating oil, purified oil, and fresh lubricating oil were examined. These properties included the kinematic viscosities at 40°C and 100°C, pour point, flash point, and metal content determined through Atomic Absorption Spectrometry (AAS). The clay mineral's surface area was notably enhanced from 53.308 m²/g to 89.513 m²/g after acidification, which facilitated the purification process. The results demonstrated that certain properties of the spent lubricating oil, such as kinematic viscosities, pour point, and flash point reduced due to the presence of contaminants from prior use, while metal content increased. However, the acidified clay treatment successfully purified the spent oil, bringing its physicochemical properties closer to those of the fresh oil sample after treatment. The extent of purification, however, varied depending on the type of acid used. This research underscores the potential for sustainable management of spent lubricating oils through acidified clay treatment.

KEYWORDS

Spent oil, purification, shell helix, acidified clay, kinematic viscosity

1.0 INTRODUCTION

Engine oil, a crucial component derived from crude oil, plays a multifaceted role in the functioning of internal combustion engines. Apart from lubrication, it also contributes to cleaning, corrosion prevention, sealing improvement, and engine cooling by dissipating heat (1). Lubricating oils, being a vital fraction of crude oil, find application in diverse engines and machinery, from automobiles to industrial equipment (1). These oils serve the purpose of reducing friction and wear in moving parts within combustion engines and various machines (2).

The disposal of used lubricating oils is an environmental and economic concern. Impurities introduced during use, such as dirt, metal debris, water, or chemicals, render the oil less effective over time. Disposing of used oil inappropriately, whether in drains or rivers, can lead to serious pollution issues, releasing harmful substances into the environment (3). Therefore, sustainable disposal methods, like purification, have gained importance in addressing the environmental challenges arising from the indiscriminate disposal of used engine oil (4). Recycling and re-refining of used engine oil can offer environmental benefits by reducing pollution and conserving resources (5). While re-refining is well-established in developed

countries, it is yet to gain widespread traction in certain developing nations (6).

The ever-growing demand for fossil fuels, particularly in the transportation sector, highlights the need for recycling plants to mitigate the environmental hazards associated with improper disposal of spent oil (7). In this study, the purification of spent Shell Helix engine oils was conducted using acidified clay with three acid options as washing agents. The extent of purification using different acids was assessed, and the physicochemical properties of the purified Shell Helix oils were compared to fresh oil samples to determine the most effective washing agent.

2.0 MATERIALS AND METHODS

2.1 Materials

The materials used for this research work were all sourced locally, they include the used (Shell Helix 20W-50) Crankcase oil from Honda civic 2008 model, Clay from the back of Talba market in Minna, Niger State, At a depth of about 30cm, Conventional laboratory reagents from Panlac Chemicals along Keteren Gwari Road, Minna Niger State. Apparatus and Equipments from Technology Incubation Centre David Mark Road, Minna Niger State



2.2 Methods

2.2.1 Sampling of clay

Clay sample was collected at the back of building material market along Talba farm in Minna Niger State, North Central Nigeria as-mined in lump form, crushed to suitable sizes and then sun dried (8). The Characterization of the clay was then carried out using Brunauer–Emmett–Teller (BET) analysis.

2.2.2 Used Oil Sampling Process

Spent engine oil (Shell Helix 20W-50) was used as the test sample, about 4 litres of used engine oil was collected from a Honda civic 2008 model in a plastic gallon after 2 months and 2 weeks of using the car over a distance of 3500 km using the Drain Stream Method as reported by (3). The equivalent fresh engine oil was purchased from Total filling station at Federal housing authority Lugbe FCT Abuja.

2.2.3 Preparation of The Clay Sample

A 200g sample of Untreated clay was crushed and combined with 500cm³ of distilled water to create a suspension. Impurities like solid materials, stones and other particles settled at the bottom of the container and were separated by carefully decanting off the clay particles at the top of the container. The remaining mixture was then placed in a Binatone oven (specifically the Binatone TTO 5001 laboratory oven) to remove moisture using a temperature of 1050c for a duration of 6 hours. Once dried, the clay was grounded into a powder form and sieved through a very fine mesh of 74µm. (9).

2.2.4 Acidification of clay

A round bottom flask with a capacity of 1000cm³ was used to mix thoroughly 200g of clay particles with a size of 74µm with 400cm³ of 1M H₂SO₄. The resulting mixture was heated on a magnetically stirred hot plate at a temperature of 2000C for a duration of 3 hours (9). Afterwards, the clay was washed carefully with distilled water to further remove precipitates, stones and impurities until a neutral pH was reached as indicated by a PH indicator. The clay was then filtered and baked for about 6 hours at 200 °C to remove water and stored in dry place so that it can be used later in the purification process. The obtained dry and clean clay is called activated clay because it is active chemically and electrostatically as reported by (10).

2.2.5 Pre-treatment of Used/Spent lubricating oil

To eliminate contaminants like sand, metal chips and micro impurities from the used lubricating oil, a filtration process was carried out. The filtration process involved the use of a Buckner funnel and filter paper. The filter paper was fitted into the Buckner funnel and the used oil was then filtered by passing it through the set-up. The resulting lubricating oil was allowed to settle for 24hours after which it was preheated at 450 C for 30 minutes to degrade some additives and reduce the workload of the acid (11).

2.2.6 Treatment of Spent Lubricating Oil using Acid Technique

Three separate beakers were used to accurately measure three samples of pre-treated engine oil each measuring 300cm³. Then 30cm³ of each acid was poured separately into a 50cm³ beaker. The regulator hot plate was switched on and the 300cm³ of used engine oil in the beaker was placed on top. The used engine oil was then heated for about 5 minutes until temperature of 450C was attained; after which each acid was gently poured into the three separate beakers. The first beaker 1M H₂SO₄, Second beaker 1M CH₃COOH and third beaker 1M C₆H₈O₇. and the whole mixture was stirred continuously for 10 minutes.

At the end of the acid treatment step, the acid treated oils were allowed to settle for 24 hours to form sediments at the bottom of the beakers. After which the acidic-oil mixtures were properly decanted into separate 500 ml beakers using mesh clothes while the residue (acidic sludge) at the bottom of the beakers were carefully discarded (2).

2.2.7 Acidified Clay Treatment Procedure

The process involves packing the acidified clay (30g) after grinding it to a particle size of 74µm into a buckner funnel, with a filter paper inserted in it. Then the funnel was connected to a vacuum pump which allowed the sulphuric acid treated oil to pass through the clay bed. This procedure was repeated for all the acids (12).

2.2.8 Neutralization Procedure

To neutralize the acid in the three oil samples, 100cm³ of 10% NaoH was added. After which the oil was left to settle for 24 hours and then decanted into a beaker while the residue at the bottom was discarded. Also, the pH of the decanted oil was



recorded and noted to check if neutralization was completed (2). Finally, the resulting purified lubricating oil was obtained and ready for analysis as reported by (9).

3.0 RESULTS AND DISCUSSION

The clay mineral was characterized using BET analysis to determine the change in the surface area, pore volume and pore diameter between the untreated clay and treated clay mineral similarly the used and purified engine oil samples were characterized to determine the changes in their physiochemical properties when compared to the corresponding fresh oil. The result obtained is discussed below: -

3.1 Characterization Of Clay Sample Using Brunauer-Emmett-Teller (BET)

The Brunauer-Emmett-Teller theory (BET) is commonly used to estimate specific surface area (SSA) of solid materials, extending the Langmuir monolayer adsorption model to multilayer adsorption. SSA is a crucial morphological characteristic in applications involving porous structures, like industrial adsorbents, catalysts, and

polymers. Pores are classified based on their size: micropores ($d_{pore} < 2$ nm), mesopores (2 to 50 nm), and macropores (> 50 nm), with further divisions into ultra-micropores, medium-sized micropores, and super-micropores (13).

The results in Table 1 shows a significant increase in the surface area of clay after acidification, increasing from 53.308 m^2/g for untreated clay to 89.513 m^2/g for acidified clay. This increase in porosity is attributed to the acidification process at high temperatures, which partially dissolves exchangeable cations, creating more surface area for adsorption (14). This aligns with previous research, which noted that the adsorptive capacity of an adsorbent is directly linked to its surface area. The pore volume also increases, from 0.025 cm^3/g for untreated clay to 0.211 cm^3/g for acidified clay, in line with similar studies (14). Additionally, the pore diameter decreases from 160.253 nm for untreated clay to 153.720 nm for acidified clay, as the activation process involves breaking up agglomerates, allowing plate separation (14). These findings are consistent with previous research (14, 15), albeit partially agreeing with others (4, 16) that reported a significant increase in surface area of activated clay.

Table 1: Result of the Characterization of Clay Mineral

	SURFACE AREA((m2g-1)	PORE VOLUME((cm3g-1)	PORE DIAMETER((nm))
UNTREATED CLAY	53.308	0.025	160.253
ACIDIFIED CLAY	89.513	0.211	153.720

3.2 Characterization of Fresh, Used and Purified Engine oils using Quality test procedures

3.2.1 Kinematic viscosity:

Viscosity, the measure of a fluid's resistance to flow, serves as a crucial indicator of spent engine oil quality, allowing the detection of contaminants and oxidation products. Contaminants like soot, dirt, glycol, and water, as well as fuel dilution and

shearing of viscosity index improvers, can influence viscosity. A higher viscosity reflects a stronger oil film, which is essential for effective lubrication (2). The study tested the kinematic viscosities of spent, purified, and fresh oil samples at 40°C and 100°C and found that the type of acid and clay used in the treatment of used engine oil significantly impacts viscosity. Spent oil had kinematic viscosities of 118.9 cSt and 13.9 cSt, in agreement with previous findings (17), while the



purified oil samples showed higher viscosities than spent oil and were closer to fresh oil as shown in Figure 1. This increase in viscosity in purified oil is attributed to the conversion and removal of impurities by acids and filtration. Notably, the

results suggest that the purification of spent engine oil using organic acetic acid and mineral sulfuric acid with acidified clay is effective in removing contaminants, with sulfuric acid showing advantages over other methods (2).

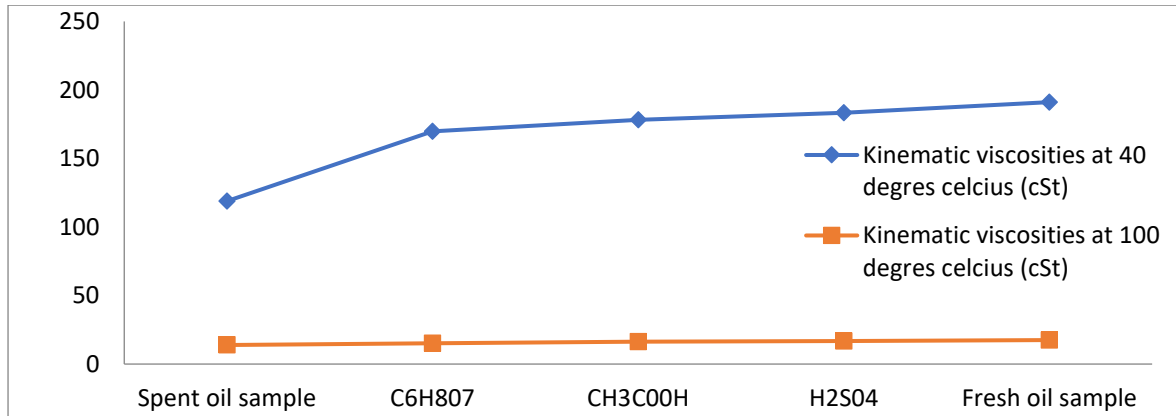


Figure 1: Kinematic Viscosities of Spent, Purified and Fresh Engine oil samples at 40 °C and 100 °C

3.2.2 Flash point:

The flash point, indicating the lowest temperature at which air vapors from a substance will briefly ignite upon exposure to flame or spark, serves as a significant marker of a lubricating oil's quality. A lower flash point often signals contamination with volatile substances like gasoline, making it a reliable indicator of oil condition (18). Figure 2 illustrates the flash point results for spent engine oil, purified oil samples, and fresh engine oil. The flash point of spent engine oil is 106°C, while purified oil samples exhibit values within the range of 133°C to 189°C. This increase in flash point is attributed to

the reduction of contaminants through the purification process, in line with prior research (4). Fresh engine oil, with a flash point of 201°C, surpasses that of spent oil, a decrease in flash point attributed to dilution by unburned fuel during engine operation (3). The flash points of the purified engine oil and fresh engine oil samples consistently exceed that of spent engine oil, aligning with earlier studies (3, 11, 17). Furthermore, the flash points achieved through purification with organic acetic acid and mineral sulfuric acid closely resemble those of fresh engine oil, highlighting their effectiveness in purifying contaminated engine oil.

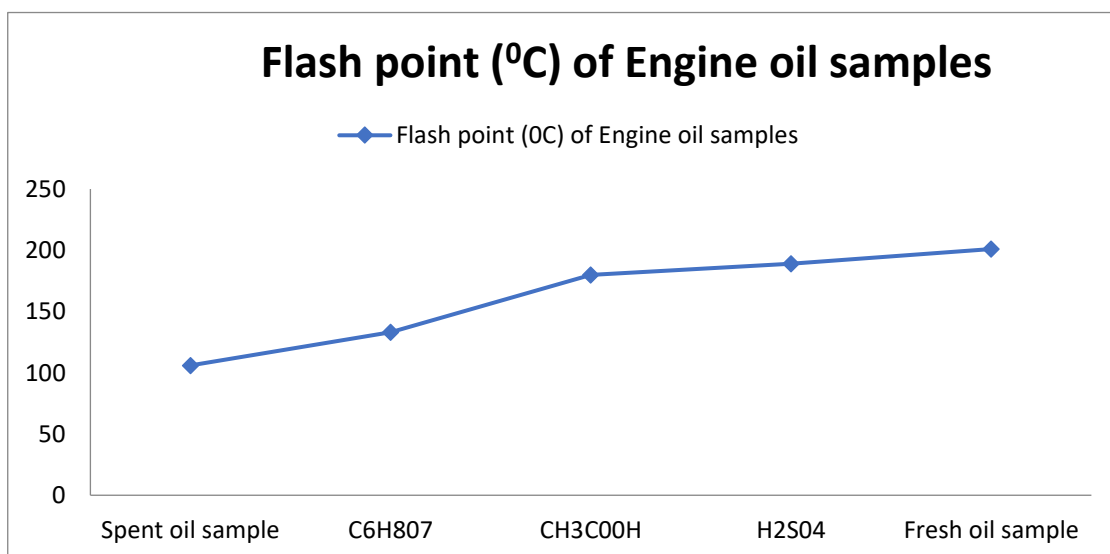


Figure 2: Flash Point (°C) of Spent, Purified and Fresh Engine oil Samples

3.2.3 Pour point



The pour point, a critical parameter, signifies the lowest temperature at which lubricating oils remain functional for specific applications, with significant implications for their flow characteristics, especially in cold conditions. Engine base oils often contain waxes and paraffins that solidify at low temperatures, leading to higher pour points, particularly in oils with high wax and paraffin content. The study's results, as depicted in Figure 3, reveal that purified oil samples exhibit pour point

values ranging from -11°C to -9°C , surpassing the -15°C pour point of spent engine oil, aligning with previous research (12, 19). Notably, when the acidified clay treatment employs organic acetic acid and mineral sulfuric acid as washing agents, the resulting pour point values closely match those of fresh engine oil, highlighting the efficacy of these agents in purifying spent or contaminated engine oil.

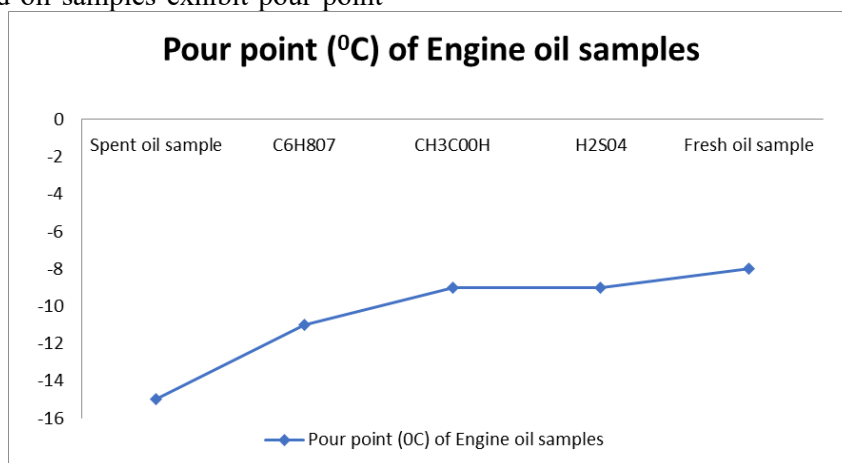


Figure 3: Pour point ($^{\circ}\text{C}$) of Spent, Purified and Fresh Engine oil Samples

3.3 Metal Content Determination Using Atomic Absorption Spectrometry (AAS)

3.3.1 Determination of Iron (Fe):

The most common wear metal in a car's engine that is introduced into the engine oil after a period of use is iron. Iron comes from many various places in the engine such as liners, camshafts and crank shaft, pistons, gears, rings, and oil pump (3). Figure 3 shows that the Iron concentration for the spent

engine oil is high while that of the purified engine oil samples have lower iron concentrations. The purified oil sample using acidified clay with organic acetic acid gives the lowest iron concentration of 0.851ppm which can be compared to the iron concentration of the fresh engine oil sample. Fe concentration in used oil sample should fall within 100-200ppm range reported by (9), very high iron amounts indicate excessive wear of engine parts. The result obtained is in agreement with the result of (3, 11, 20)



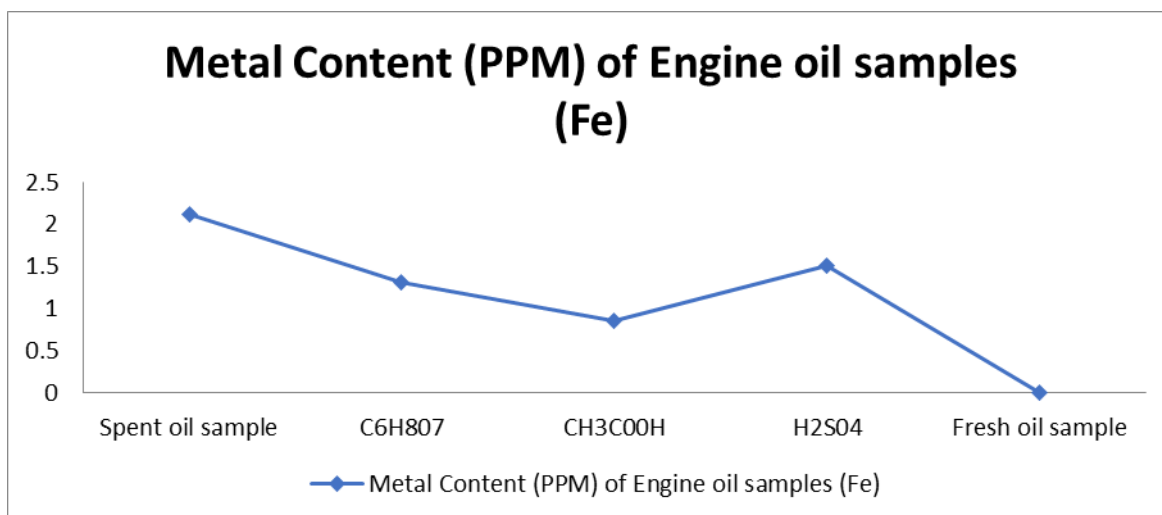


Figure 3:Iron (Fe) Content (PPM) of Spent, Purified and Fresh Engine oil Samples

3.3.2 Determination of Manganese (Mn):

Manganese is a rear metal that is usually introduced into the spent engine oil in small amounts. Manganese (Mn) is introduced from wear of cylinder liners, valves, and shafts (3). Figure 4 shows that the purification process was able to reduce the manganese concentration of spent engine oil however the purified engine oil using acidified

clay with organic citric acid and acetic acid gives a manganese concentration of 1.764ppm and 1.941ppm respectively. Which are lower than the values obtained for Mineral sulphuric acid acidified clay treatment. Therefore, purification with organic citric and acetic acid proves to be more effective for the removal of manganese in spent engine oil. The result obtained is in agreement with the result reported by (3).

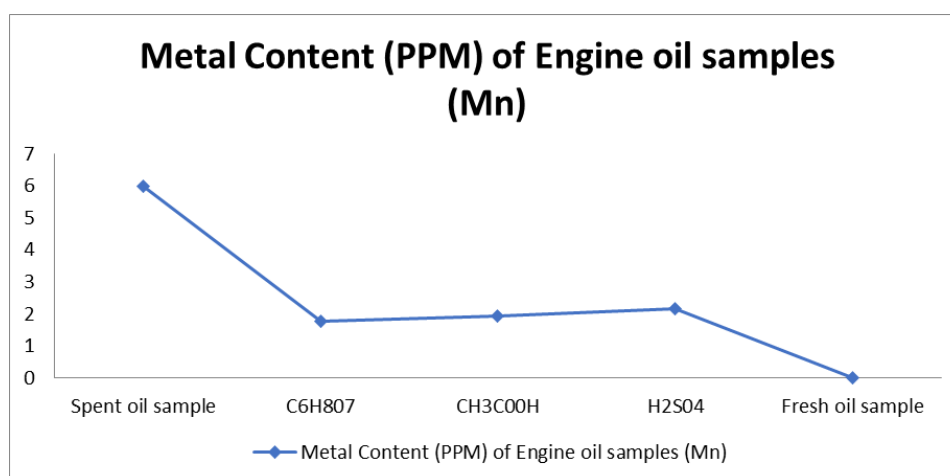


Figure 4:- Manganese (Mn) Content (PPM) of Spent, Purified and Fresh Engine oil Samples

4.0 CONCLUSIONS AND RECOMMENDATION

The study explored the efficacy of 1M acidified clay, using mineral sulfuric acid, organic acetic acid, and organic citric acid as a novel washing agent, for the purification of spent Shell Helix(20W-50) engine oil. A comprehensive characterization, encompassing kinematic viscosities at 40°C and 100°C, pour point, flash point, and metal content analysis via AAS, was

conducted to assess the effectiveness of these acids in the purification process. Additionally, the porosity of the acidified bentonite clay used in the process was characterized using BET analysis, revealing its high porosity, falling within the macropores category with a diameter exceeding 50 nm.

The findings indicate that acidified clay treatment with mineral sulfuric and organic acetic acids yielded results comparable to fresh engine oil in the



purification process, significantly enhancing the quality of the spent engine oil. However, the use of acidified clay with organic citric acid showed less effectiveness in the quality improvement of the purified oil. The AAS analysis demonstrated a measurable reduction in metal content after purification, with acetic acid being particularly effective in decreasing iron (Fe) concentration, and organic citric acid proving the most efficient in reducing manganese (Mn) content.

This study therefore recommends the use of mineral sulphuric acid and organic acetic acid in the purification of spent engine oil using acidified clay treatment technique.

5.0 REFERENCES

1. D. I. Osman, S. K. Attia, A. R. Taman, Recycling of used engine oil by different solvent. *Egyptian Journal of Petroleum* **27**, 221-225 (2018).
2. F. UGWELE, T. CHIME, Comparative study of the different methods of purifying used mobil oil using different acids as washing agents.
3. I. Hamawand, T. Yusaf, S. Rafat, Recycling of waste engine oils using a new washing agent. *Energies* **6**, 1023-1049 (2013).
4. E. A. Afolabi *et al.*, Optimization of the recycle used oil and its fuel quality characterization. (2016).
5. S. Widodo, D. Ariono, K. Khoiruddin, A. N. Hakim, I. G. Wenten, Recent advances in waste lube oils processing technologies. *Environmental Progress & Sustainable Energy* **37**, 1867-1881 (2018).
6. M. A. Dos Reis, M. S. Jeronimo, Waste lubricating oil rerefining by extraction-flocculation. 1. A scientific basis to design efficient solvents. *Industrial & engineering chemistry research* **27**, 1222-1228 (1988).
7. H. Mahmudul *et al.*, Production, characterization and performance of biodiesel as an alternative fuel in diesel engines—A review. *Renewable and Sustainable Energy Reviews* **72**, 497-509 (2017).
8. S. Olukotun *et al.*, Investigation of gamma radiation shielding capability of two clay materials. *Nuclear Engineering and Technology* **50**, 957-962 (2018).
9. M. Dabai, N. Bello, Comparative study of regeneration of used lubricating oil using sulphuric and oxalic acids/clay treatment process. *Int. J. Innov. Sci. Eng. Technol* **6**, 13-23 (2019).
10. F. C. Akilimali, Feasibility study of recycling used lubricating oil. *A project work submitted to the department of Petroleum Engineering, The University of Dodoma*, (2017).
11. J. Udonne, V. Efeovbokhan, A. Ayoola, D. Babatunde, Recycling used lubricating oil using untreated, activated and calcined clay methods. *J. Eng. Appl. Sci* **11**, 1396-1401 (2016).
12. J. D. Udonne, A comparative study of recycling of used lubrication oils using distillation, acid and activated charcoal with clay methods. *Journal of Petroleum and Gas Engineering* **2**, 12-19 (2011).
13. K. C. Kim, T.-U. Yoon, Y.-S. Bae, Applicability of using CO₂ adsorption isotherms to determine BET surface areas of microporous materials. *Microporous and Mesoporous Materials* **224**, 294-301 (2016).
14. H. Shabanzade, A. Salem, S. Salem, Management of adsorbent content in waste motor oil regeneration by spectrophotometrical study and effective acidification in production of nano-porous clay. *Spectrochimica Acta*



- Part A: Molecular and Biomolecular Spectroscopy* **202**, 214-221 (2018).
15. S. Salem, A. Salem, A. A. Babaei, Preparation and characterization of nano porous bentonite for regeneration of semi-treated waste engine oil: Applied aspects for enhanced recovery. *Chemical engineering journal* **260**, 368-376 (2015).
 16. B. K. Aziz, M. A. Abdullah, S. Kaufhold, Kinetics of oil extraction from clay used in the lubricating oil re-refining processes and re-activation of the spent bleaching clay. *Reaction Kinetics, Mechanisms and Catalysis* **132**, 347-357 (2021).
 17. M. H. Mintesinot, (2021).
 18. R. Abu-Ellella, M. Ossman, R. Farouq, M. Abd-Elfatah, Used motor oil treatment: turning waste oil into valuable products. *International journal of chemical and biochemical sciences* **7**, 57-67 (2015).
 19. E. Kwao-Boateng, T. Anokye-Poku, A. N. Agyemang, M. K. Fokuo, Re-Refining used engine oil in Ghana using solvent extraction and acid-clay treatment. *International Journal of Chemical Engineering* **2022**, (2022).
 20. H. Mensah-Brown, Re-refining and recycling of used lubricating oil: An option for foreign exchange and natural resource conservation in Ghana. *ARPJN Journal of Engineering and Applied Sciences* **10**, 797-801 (2015).



P070 - BATCH ADSORPTION OF HEAVY METAL IONS FROM PHARMACEUTICAL WASTEWATER USING COCONUT SHELL AND GROUNDNUT HULL ACTIVATED CARBON

ADENLE Nafisat Adebola ^{1*}, AKANIMO Emene Amba ², ABDULRAZAK Jinadu Otaru ³

¹Federal University of Technology Minna

²Federal University of Technology Minna

³King Faisal University

*Corresponding author email: adenle.adebola@gmail.com

ABSTRACT

Water, an essential natural resource for life, faces contamination from various sources, threatening ecosystems. To combat this, the study explores the potential of activated carbon from coconut shells and groundnut hulls to remove heavy metals from pharmaceutical wastewater. Proximate and ultimate analyses reveal the effectiveness of these materials, with coconut shell-based activated carbon showing remarkable promise due to its high fixed carbon content. The results also highlight the enhanced adsorption capacity of activated carbon, notably the mesoporous nature of coconut shell activated carbon. The findings suggest that such adsorbents can efficiently bind metal ions, making them suitable for heavy metal removal from wastewater. This study underscores the importance of utilizing cost-effective and eco-friendly adsorbents for water pollution mitigation, potentially promoting sustainable agricultural practices through the use of residual ash content.

KEYWORDS

Water Pollution, Heavy Metals, Activated Carbon, Agricultural By-products.

1.0 INTRODUCTION

Water is a vital natural resource essential for both plant and animal life, and it plays a fundamental role in maintaining a safe and sustainable environment for future generations. It possesses unique properties, being the only substance that exists in all three physical states on Earth's surface, and is primarily sourced from lakes, rivers, and groundwater (1, 2). However, the contamination of water resources with organic and inorganic substances is a major concern, with pollutants originating from various sources, including industries, agriculture, and urban areas, posing a severe threat to human, plant, and animal ecosystems (3, 4).

Wastewater, laden with organic and inorganic contaminants, is a significant contributor to pollution and requires effective management strategies. Recycling and reusing industrial wastewater have gained attention, especially in agriculture, due to its nutrient-rich composition. Various sources of water pollution, including natural runoff, mineral deposits, and human activities such as electronics manufacturing, mining, and textile dyes, contribute to the contamination of water bodies (5, 6). Anthropogenic activities like electronics production, refineries, plastics, textiles, and mining release heavy metals

into the environment, causing health problems and disrupting the food chain for aquatic, human, and plant life (7, 8).

The presence of pharmaceutical contaminants, including painkillers, birth control hormones, and other medicines, in water bodies is a growing concern. These contaminants interact and are absorbed by living organisms, posing potential hazards to the environment. Sources of pharmaceutical contamination range from hospital effluents to industrial discharges, agricultural run-offs, and human and animal excreta, all of which have adverse effects on ecosystems (9). Different methods, such as ion exchange, membrane filtration, adsorption, and chemical precipitation, are employed to remove toxic pollutants from wastewater, but adsorption is widely favoured due to its efficiency and reduced chemical usage. Developing cost-effective adsorbents using readily available industrial and agricultural by-products has the potential to address the challenge of heavy metal removal from wastewater, ultimately contributing to cleaner and safer water resources (10). The research objective is to assess the removal efficiency of activated carbon derived from coconut shell and groundnut hull in eliminating Cr^{6+} , Pb^{2+} , and Fe^{2+} from pharmaceutical wastewater.



2.0 MATERIALS AND METHODS

2.1 Materials

The feedstocks used in this research work are coconut shell and groundnut hull which was collected from Kasuwan Gwari Market, Minna, Niger State, Nigeria. Also, pharmaceutical wastewater was collected from Dana pharmaceuticals, Maitumbi, Minna, Niger State.

2.2 Research Methodology

Figure 3.1 summarizes the experimental procedure used in the production of activated carbon from coconut shell and groundnut hull and for the removal of heavy metals from pharmaceutical wastewater.

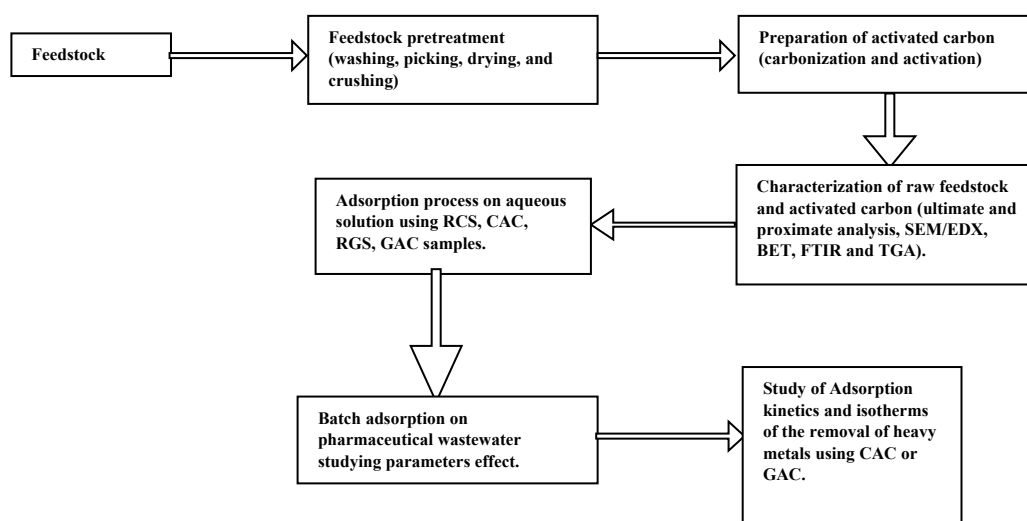


Figure 1: Block flow diagram of the methodology

2.2.1 Samples Collection and Preparation

Coconut shell and groundnut hull were collected from Kasuwan Gwari Market, Minna, Niger State, Nigeria, and transported to the Technology Incubation Laboratory, Tunga, Minna. To ensure sample purity, foreign objects were meticulously removed, and the materials were thoroughly washed with deionized water to eliminate dirt and surface impurities. Following this, the coconut shell and groundnut hull were sun-dried for two days, followed by an oven-drying process at 105 °C for 3 h. The dried samples were then grounded and sieved to achieve particle sizes ranging from 500 to 1000 µm.

2.2.2 Activated Char Production

The study aimed to produce activated char with both high yield and a large surface area. To achieve this, a chemical activation synthesis method was employed. The prepared coconut shell and groundnut hull samples were carbonized at 400 °C

for 1 h using a Muffle Furnace, followed by cooling in a desiccator. This carbonization process enhanced the carbon content of the adsorbent through dehydration and devolatilization. Subsequently, both samples were impregnated with 1M Sulfuric acid (H₂SO₄) at a ratio of 1:10 (adsorbent to H₂SO₄ solution) at 70 °C for 12 h separately. The resulting slurry was separated to remove excess liquid, and the residue was calcined at 500 °C for 2 h. The activated char was collected, washed with distilled water to eliminate residual acids and inorganic materials until a neutral pH was reached, and then dried in an electric oven at 80 °C for 2 h(11).

2.2.3 Proximate and Ultimate Analysis

The proximate analysis of the samples, Raw coconut shell (RCS), Coconut shell activated carbon (CAC), Raw groundnut shell (RGS) and Groundnut shell activated carbon (GAC) was performed to determine moisture content, volatile matter, ash content, and fixed carbon content. This



was carried out in accordance with standardized methods, including ASTM D2079 for moisture content, ASTM E1755 for ash content, and ASTM E872 for volatile matter. Fixed carbon content was determined by subtracting the sum of the moisture content, volatile matter, and ash content from 100(12).

The ultimate analysis of carbon, hydrogen, nitrogen, sulfur, and oxygen (CHNS) content in the samples was conducted by placing 1 gram of the samples in a muffle furnace operating at temperatures ranging from 900°C to 1050°C. During the high-temperature combustion process in the presence of oxygen gas, carbon, hydrogen, and nitrogen values were converted into their corresponding gases (CO₂, H₂O, and NO_x). Oxygen

content was indirectly determined based on the difference between carbon, hydrogen, nitrogen, sulfur, and ash content.

3.0 RESULTS AND DISCUSSION

3.1 Collection and Analysis of pharmaceutical Wastewater

The pharmaceutical waste water was collected from Dana Pharmaceutical Limited, Maitumbi, Minna, Niger State and was analyzed at Sheda Science and Technology Complex (SHETSCO), Abuja, in order to determine the concentrations of heavy metals present in the wastewater. The analysis result is as presented in Table 3.

Table 3: Analysis of wastewater collected from Dana Pharmaceuticals

Heavy Metal Ion	Concentration (mg/L)	WHO permissible limit in
	Drinking water (mg/L)	
Lead (Pb ²⁺)	2.8728	0.01
Cadmium (Cd ²⁺)	0.012	0.003
Iron (Fe ²⁺)	13.1586	0.3
Chromium (Cr ⁶⁺)	12.2171	0.05
Copper (Cu ²⁺)	0.2516	2

3.2 Proximate and Ultimate Analysis.

The proximate compositions of the raw and activated samples is as shown in Table 4.

Property	RGS in wt%	GAC in wt%	RCS in wt%	CAC in wt%
Moisture content	3.30	1.48	7.91	7.58
Volatile matter	76.29	6.55	82.33	28.07
Fixed Carbon	4.55	82.22	2.62	59.53



Ash content 15.86 9.75 7.14 4.82

Table 4:

Proximate Analysis result of RCS, CAC, RGS, GAC

The proximate and ultimate analysis of the feed samples (coconut shell and groundnut hull) revealed significant differences in volatile matter, fixed carbon, and ash content due to the materials physiochemical structure. Carbonization and subsequent chemical activation led to a notable increase in fixed carbon content (57-78% for both coconut shell and groundnut hull) and a decrease in volatile matter (54-70%) in the resulting activated carbons. Activated carbon from coconut shell exhibited a high fixed carbon content of 82.22 wt%, making it a suitable adsorbent for various applications. The reduction in ash content, attributed to sulfuric acid treatment, was significant, with coconut shell activated carbon having 9.75 wt% ash content, down from 15.86 wt% in the precursor feed. The process selectively removed mineral matter while preserving the organic structure. The low moisture and ash content in both activated carbons confirm their suitability as effective adsorbents, enhancing their efficiency in adsorption processes. Additionally, the presence of a quantifiable amount of ash content suggests the potential use of the activated carbons as organic fertilizers. Ultimate analysis of the samples was also conducted, providing insights into the carbon, hydrogen, nitrogen, sulfur, and oxygen content of the materials.

Table 5 presents the ultimate analysis of the feed samples and the resulting activated carbons. The feedstocks are rich in organic matter, mainly composed of carbon, hydrogen, oxygen, and traces of nitrogen. These elements originate from lignocellulose and fiber components, with nitrogen content primarily coming from protein and plant-based extractives. Following carbonization and activation, the activated carbon products exhibit significantly reduced hydrogen and oxygen content due to the thermal decomposition of volatile matter. The carbon content in the activated carbons substantially increased, reaching 76.53 wt% for coconut shell and 55.16 wt% for groundnut hull, as compared to their initial values. This increase in carbon content aligns with the higher fixed carbon content observed in the proximate analysis, suggesting that coconut shell is a more suitable feedstock for activated char production due to its lignin content. In contrast, groundnut hull contains highly thermally volatile components and fewer recalcitrant organic components. The differences in ultimate and proximate compositions of the activated products from the two materials highlight the variations in their physiochemical, biochemical, and structural properties, consistent with previous studies on feedstock-dependent variations in activated carbon composition under similar processing conditions.

Table 5: Ultimate Analysis Result of RCS, CAC, RGS, GAC

Property	RCS in wt%	CAC in wt%	RGS in wt%	GAC in wt%
----------	------------	------------	------------	------------



Carbon	54.91	76.53	39.05	55.16
Hydrogen	14.62	5.69	22.55	15.32
Nitrogen	0.14	0.213	0.22	0.30
Oxygen	30.33	17.57	38.18	29.22

3.3 Brunauer, Emmet and Teller (BET)

Elevating the pyrolysis temperature has a significant impact on the thermal degradation and volatilization processes of biomass, leading to increased surface area and pore volume development, subsequently enhancing its adsorption capacity(13). Notably, the coconut shell activated carbon exhibits significantly higher surface area and pore volume values in comparison to the raw coconut shell, with the surface area surging from 2.160 m²/g to 307.4 m²/g and the pore volume expanding from 0.0082 cm³/g to 0.061 cm³/g. This indicates a mesoporous nature for the coconut shell activated carbon, characterized by a

high surface density attributable to its surface area. According to IUPAC classifications, pore structures fall into three categories: microporous for pore diameters < 2 nm, mesoporous for diameters between 2 nm and 50 nm, and macroporous for diameters exceeding 50nm. Consequently, the raw coconut shell's 65.086 nm pores are macroporous, while its activated carbon of 3.423 nm pores are mesoporous. The presence of mesoporous structures in activated carbon facilitates the movement of adsorbates to the micropores, thus enhancing adsorption processes. The porosity on the surface of coconut shell activated carbon further fosters efficient binding of metal ions to active sites, making it an effective adsorbent.

Table 6: BET data for RCS and CAC

Parameters	RCS	CAC
BET Surface area (m ² /g)	2.160	307.4
Pore Volume (cm ³ /g)	0.0082	0.061
Pore Size (nm)	65.086	3.423

4.0 CONCLUSIONS AND RECOMMENDATION

This study addressed the critical issue of heavy metal contamination in pharmaceutical wastewater

by employing activated carbon derived from coconut shells and groundnut hulls. The materials were meticulously collected and processed, leading to a significant increase in fixed carbon content and



reduction in volatile matter, thus enhancing their suitability for adsorption. The ultimate analysis revealed differences in composition between the two feedstocks, with coconut shells exhibiting higher carbon content, making it a preferred choice for activated char production. The activated carbon demonstrated excellent adsorption properties, marked by its increased surface area and mesoporous nature, which enhances its capacity to effectively bind metal ions and remove contaminants from wastewater. The reduction in ash content due to sulfuric acid treatment further supports its potential application as an organic fertilizer. With these results, the study recommends the utilization of coconut shell and groundnut hull-based activated carbon for the removal of heavy metals from pharmaceutical wastewater, contributing to cleaner and safer water resources. This research highlights the significance of utilizing cost-effective, eco-friendly adsorbents for addressing water pollution challenges while simultaneously offering the potential for sustainable agricultural practices through the use of residual ash content.

5.0 REFERENCES

1. M. Ahmed, B. Hameed, E. Hummadi, Insight into the chemically modified crop straw adsorbents for the enhanced removal of water contaminants: A review. *Journal of Molecular Liquids* **330**, 115616 (2021).
2. N. H. Solangi *et al.*, Development of fruit waste derived bio-adsorbents for wastewater treatment: A review. *Journal of Hazardous Materials* **416**, 125848 (2021).
3. W. He *et al.*, Innovative technology of municipal wastewater treatment for rapid sludge sedimentation and enhancing pollutants removal with nano-material. *Bioresource Technology* **324**, 124675 (2021).
4. S. S. Gharbia *et al.*, Evaluation of wastewater post-treatment options for reuse purposes in the agricultural sector under rural development conditions. *Journal of Water Process Engineering* **9**, 111-122 (2016).
5. S. Sarkar, S. Chakraborty, Nanocomposite polymeric membrane a new trend of water and wastewater treatment: A short review. *Groundwater for Sustainable Development* **12**, 100533 (2021).
6. Y. L. Cheng *et al.*, Occurrence and removal of microplastics in wastewater treatment plants and drinking water purification facilities: A review. *Chemical Engineering Journal* **410**, 128381 (2021).
7. Z. Yu *et al.*, Comprehensive assessment of heavy metal pollution and ecological risk in lake sediment by combining total concentration and chemical partitioning. *Environmental Pollution* **269**, 116212 (2021).
8. A. Saravanan *et al.*, Effective water/wastewater treatment methodologies for toxic pollutants removal: Processes and applications towards sustainable development. *Chemosphere* **280**, 130595 (2021).
9. B. Feier, I. Ionel, C. Cristea, R. Săndulescu, Electrochemical behaviour of several penicillins at high potential. *New Journal of Chemistry* **41**, 12947-12955 (2017).
10. M. Imran-Shaukat, R. Wahid, N. Rosli, S. Aziz, Z. Ngaini, in *IOP Conference Series: Earth and Environmental Science*. (IOP Publishing, 2021), vol. 765, pp. 012019.
11. A. T. Ojedokun, O. S. Bello, Liquid phase adsorption of Congo red dye on functionalized corn cobs. *Journal of Dispersion Science and Technology* **38**, 1285-1294 (2017).
12. A. Agarwal, U. Upadhyay, I. Sreedhar, S. A. Singh, C. M. Patel, A review on valorization of biomass in heavy metal removal from wastewater. *Journal of Water Process Engineering* **38**, 101602 (2020).
13. A. Kumar, H. M. Jena, High surface area microporous activated carbons prepared from Fox nut (*Euryale ferox*) shell by zinc chloride activation. *Applied Surface Science* **356**, 753-761 (2015).





P071 - INSIGHT INTO THE DEACTIVATION OF FRESH FCC CATALYST FROM A TYPICAL FCC UNIT OF A PETROLEUM REFINERY

W.C. Okafor^{1,2*}, S. S. Salisu^{1,2}, A.Y. Atta¹, A. Aliyu¹ and B. J. El-Yakub¹

¹Department of Chemical Engineering, Ahmadu Bello University, Zaria, P.M.B 1045, Nigeria

²Research and Development Centre, Dangote Petroleum Refinery and Petrochemicals, FZE, Union Marble House, Ikoyi, Lagos Nigeria

*Corresponding author's email – okaforwinston1@gmail.com

ABSTRACT

The fluid catalytic cracking unit (FCCU) is the highest consumer of catalysts in the petroleum refinery and congruently generates a tremendous quantity of spent catalysts due to rapid deactivation by coke, metal poisons, and thermal changes after several cycles. In this study, the deactivation of fresh FCC catalyst (FFCCC) by way of characterization is discussed. Spent and fresh FCC catalyst samples were obtained from a complex refinery in Nigeria, and an in-depth characterization was done to ascertain the extent of deactivation using Breneur-Emmet-Teller (BET), X-ray fluorescence (XRF) and X-ray diffraction (XRD) analyses. Results show that FFCCC deactivation crystallinity by 53.22% and total specific surface area by 27.85%. Loss in Alumina, La₂O₃, TiO₂, and P₂O₅ were 3.27%, 3.18%, 16.25%, and 24.00% respectively. The loss in structural and compositional properties of SFCCC shows great potential for its regeneration and rejuvenation towards sustainable reuse in other industrial processes.

Keywords:

Coke, Deactivation, FCC, Fresh catalyst, Spent catalyst, Refinery

1.0 INTRODUCTION

The fluid catalytic cracking unit (FCCU) is one of the key secondary processing units in the petroleum refinery, which converts atmospheric residue/waxy distillate (lower value products) to more economical and valuable products such as high-octane gasoline, liquefied petroleum gas (LPG) and light olefins which serves as useful petrochemical feedstock(1-3). In a typical FCCU, the hot catalyst from the regenerator interacts with the feed (Vacuum gas oil or Atmospheric residue) in the riser within a contact time of 2-3 seconds at about 550 °C where the cracking reaction occurs. Hydrocarbon vapour products formed are disengaged from the catalyst to avoid further cracking. At this point, becomes deactivated by coke and metals from the feedstock and is referred to as a spent FCC catalyst (SFCCC). The spent catalyst is regenerated in the regenerator by burning off coke deposits and then re-contacted with the feedstock to continue the cycle(4, 5).

The FCC conversion process employs a mesoporous, highly selective, and stable Zeolite-Y-based catalyst in addition to ZSM-5 (Olefin enhancer) to achieve maximum selectivity, activity and stability(6). Due to the contaminated nature of feedstocks, metals like Vanadium, Nickel, Iron, and Sodium in the form of porphyrin complexes,

naphthenates, or inorganic compounds are adsorbed on active sites of the catalyst which promotes decelerated conversion to desired products and leads to the formation of light gases(7). Vanadium, the most deleterious metal poison, reacts with steam under the regenerator condition to form Vanadic acid, which induces the dealumination of the zeolite structure(4, 8). The dealumination increases the silica-alumina ratio and reduces the acidity, which in turn reduces the rate of hydrogen transfer reactions. Nickel poison on catalyst a major cause of uncontrolled dehydrogenation reactions, which produces lighter incondensable hydrocarbons and hydrogen-rich gas - a major bottleneck to the unsaturated gas concentration unit of the FCC. SFCCCs are often regenerated in-situ by the combustion of coke in the regenerator to improve the catalyst activity for a sustained cycle of cracking reactions. The regeneration process, which occurs in an air atmosphere at temperatures above 700 °C within a very short contact time, affects the structure and function of the catalyst. At temperatures above 500 °C, the catalyst's Bronsted acid sites (BAS) are lost, and the structure of the catalyst may collapse due to sintering, resulting in the loss of micropore, mesopore and total surface area of the catalyst. These shortcomings of in-situ regeneration are disadvantageous to refiners since the regeneration time is crucial to ensure continuous



circulation of regenerated catalyst to the riser of the reactor. Against this backdrop, ex-situ regeneration becomes necessary, as coke can be burned off at a relatively lower temperature for a prolonged time.

Ex-situ regeneration requires understanding the extent to which spent catalysts are damaged or deactivated and then devising means of regeneration and rejuvenation for the intended use. For the case of continuous use in cracking reactions, (9) have identified various routes, such as calcination, oxychlorination, and acid treatment, for the removal of coke and metal impurities by dissolution/leaching. Bronsted acid sites recovery of the catalyst becomes vital for cases where the reaction initiation stage follows the formation of carbonium ions. Recently, (10, 11) enhanced BAS of spent RFCC catalyst using a 3M mix of Citric and Sulphuric acid and recorded increased conversion of palm oil to kerosine and diesel fractions.

(12) have demonstrated the potential of SFCCC as a pyrolytic catalyst in the thermal treatment of refinery waste-activated sludge, favouring the yield of hydrogen-rich gas and saturated hydrocarbon. For the case of pyrolysis, little or no modification to the structure and function of the catalyst is important since the residual activity of the catalyst is harnessed at higher severity/condition.

SFCCC is rich in rare earth metals such as Lanthanum and Cerium as well as heavy metal impurities such as Vanadium and Nickel, which could act as potential ore for their extraction. In a recent study by (13, 14) over 80% of Lanthanum and Cerium were recovered using Sulphuric acid. The process, however, resulted in the dealumination of the resultant zeolite structure, which is a major drawback to the catalytic property of the catalyst. In research conducted by (15), SFCCC was treated using 9.0m/l of HCl at a solvent-to-liquid ratio (S/L) of 0.005g/L and a temperature of 293K for 30 minutes, about 91% of Lanthanum and 92.2% of Cerium were recovered. The composition of SFCCC, therefore, creates a huge potential for the recovery of rare earth metals, which presents a potential investment opportunity, since these resources are costly and concentrated in minimal quantities across Asia and Latin America.

The potential of SFCCC as base materials for most industrial processes cannot be overlooked, and the need for extensive research on its alternative uses cannot be underscored. Against this backdrop, this research seeks to study the extent of the

deactivation of SFCCC from a commercial refinery towards finding an alternative application for its reuse.

2.0 MATERIALS AND METHODS

Fresh and Spent FCC catalysts were collected respectively from the hopper and regenerator of the FCC Unit of the FCC - Kellog Brown and Roots (KBR) technology in Nigeria. They were containerised in an airtight vessel to avoid water ingress. The fresh catalyst is a Rare Earth Exchanged Zeolite-Y Catalyst (REY), a proprietary product of ALBERMARLE Incorporated Limited.

2.1 X-Ray Diffraction (XRD)

Catalysts crystallinity was determined using the XRD patterns obtained from Rigaku MiniFlexII X-ray diffractometer using Cu K α radiation (operated at 40 kilovolts and 40 mili ampere, K $_{\alpha 1}$ = 1.540598, K $_{\alpha 2}$ = 1.544426 and K $_{\beta}$ = 1.392218, 2 θ from 3 $^{\circ}$ – 70 $^{\circ}$ at scanning speed of 12 $^{\circ}$ per minutes. The percentage relative crystallinity indices of the catalyst samples were calculated from the equation below

$$\% \text{ Relative Crystallinity Index} = \frac{\text{Area of crystal peaks of unknown sample}}{\text{Area of Crystal peaks of reference sample}} \times 100$$

Equation 1

2.2 X-Ray Fluorescence (XRF)

The elemental composition of the metal oxides of fresh and spent FCC catalysts was determined using the XRF equipment at atmospheric conditions. A hand-held Thermofisher scientific NITON XL3t (Waltham, Massachusetts, USA) XRF machine was used to analyze the chemical composition of the catalyst samples. Results obtained were recorded as a percentage of metal oxides in the samples.

2.3 Surface Area and Micropore Analyses

Desorption using Nitrogen gas was conducted at 77K using the micrometrics ASAP-2020 model. Catalyst vacuum-degassing was conducted at 573K for 10hrs. Catalyst specific surface areas were calculated using nitrogen adsorption isotherm data using the BET model. Analysis from the t-plot was used to measure the micropore volumes and area

3.0 RESULTS AND DISCUSSION



3.1 Elemental Composition of Fresh and Spent FCC Catalysts

The elemental compositions of the fresh and spent FCC catalyst samples were determined using the XRF, as shown in Table 1. Dealumination of fresh FCC catalyst (3.27%) could be associated with the deactivation, probably by steam in the regenerator, steam reacts with Vanadium in the regenerator to form Vanadic acid which has potential to weaken the Al-Si bond thereby causing ease of removal of Alumina from the zeolite matrix(4, 5). The Silica-to-Alumina (Si/Al) ratio thus increased by 10.30% which is likely to reduce the BAS of the spent FCC

catalyst. Additive such as Phosphorus Pentoxide (P_2O_5) was also reduced by 24.00%, possibly due to thermal degradation in the reactor and regenerator sections operating at 520 and 730°C, respectively which are far above its Sublimation temperature range of 350 to 420°C. The deactivation by metal impurities such as Nickel oxide indicated a 60% increase due to the nature of the feedstock. In contrast, the rare earth metal component (Lanthanum oxide) of the catalyst remained almost unchanged indicating the possibility of concentrated adjacent acid sites for hydrogen transfer reactions.

Table 1.0 Elemental compositions of Fresh and Spent FCC catalysts

S/N	Metal oxides (wt %)	FFCCC	SFCCC	% Change
1	Al_2O_3	34.60	33.47	-3.27
2	SiO_2	47.83	51.02	+6.67
3	NiO	0.05	0.08	+60.00
4	La_2O_3	9.12	8.83	-3.18
5	TiO_2	2.83	2.37	-16.25
6	P_2O_5	1.25	0.95	-24.00
7	SO_3	0.91	0.56	-38.46
Si/Al ratio		2.350	2.592	10.30

3.2 Crystallinity of Fresh and Spent FCC Catalysts

XRD analysis was performed on fresh, spent, and regenerated catalysts. The percentage relative crystallinity indices (RCI) were determined according to equation 1. This reduction in the RCI

of the spent catalyst by 11.38% could be associated with coke's presence during deactivation in the regenerator of the FCC unit(11). Metal poisons from FCC feedstock, such as Nickel and Iron, are adsorbed on active sites of catalysts and contributed to the reduction in the RCI and activity of the fresh catalyst(11)



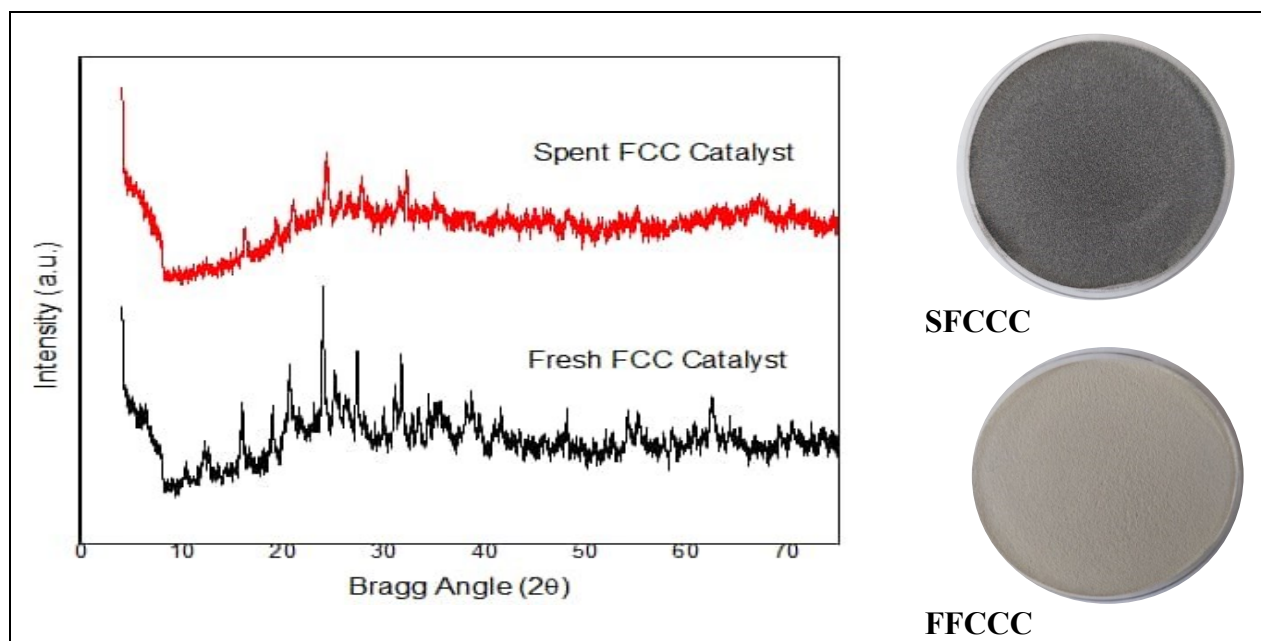


Figure 1: XRD spectra of fresh and spent FCC catalysts

3.3 Structural and Physicochemical Properties of Fresh and Spent FCC Catalysts

The structural properties of the fresh and spent FCC catalysts were analyzed, and the total surface area, pore volume, and average pore diameter were determined using the BET method, as shown in Table 2. The reduction in total surface area from 207.123 to 149.24m²/g for the case of fresh FCC catalyst could be attributed to the presence of coke, metal poisons and sintering of the catalyst during the deactivation process.

The reduction in the microporous surface area (Mi-SA) compared to the mesoporous surface area (Me-SA) can be attributed to the rapid deactivation by coke suspected to be aliphatic in nature(16). At the same time, the loss in the micropore volume (MPV) could be due to the collapse of pore structures as a result of the severity of regeneration of the SFCCC and prolonged cyclic cracking reactions. The increase in apparent pore diameter (APD) of the

SFCCC could be attributed to the loss of active components of the catalyst, such as P₂O₅, due to sublimation. Moreover, at higher temperatures, above 500°C, it is shown that the catalyst's Bronsted acid sites (BAS) could be lost, especially in an Oxygen environment in the regenerator of the FCC unit.

The isotherm plots of the FFCCC and SFCCC are shown in Figure 2. The hysteresis loop is characterized by the type iv isotherm plot depicting a mesoporous material based on IUPAC classification. The adsorption volume by FFCCC at the initial pressure is relatively higher than that for SFCCC due to more surface area available for molecular interaction. The clearer separation of the hysteresis loop for SFCCC beginning at relative pressure above 0.4 indicates more mesoporosity (17). It is highly suggested, therefore, that deactivation by coke occurs predominantly in the micropore of the catalyst while the regeneration only burns off mesoporous coke since the technology of partial burn applies in the FCC unit.

S/N	Properties	Unit	FFCCC	SFCCC	% Change
1	BET -SA	(m ² /g)	207.1230	149.4780	-27.83
2	Mi SA	(m ² /g)	180.9260	113.4440	-37.30
3	Me-SA	(m ² /g)	26.1970	36.0340	+37.55
4	MPV	(cc/g)	0.07538	0.04738	-37.15



5	DFT APD	(nm)	2.8018	2.9640	+5.79
---	---------	------	--------	--------	-------

Table 2: Textural properties of the catalyst samples

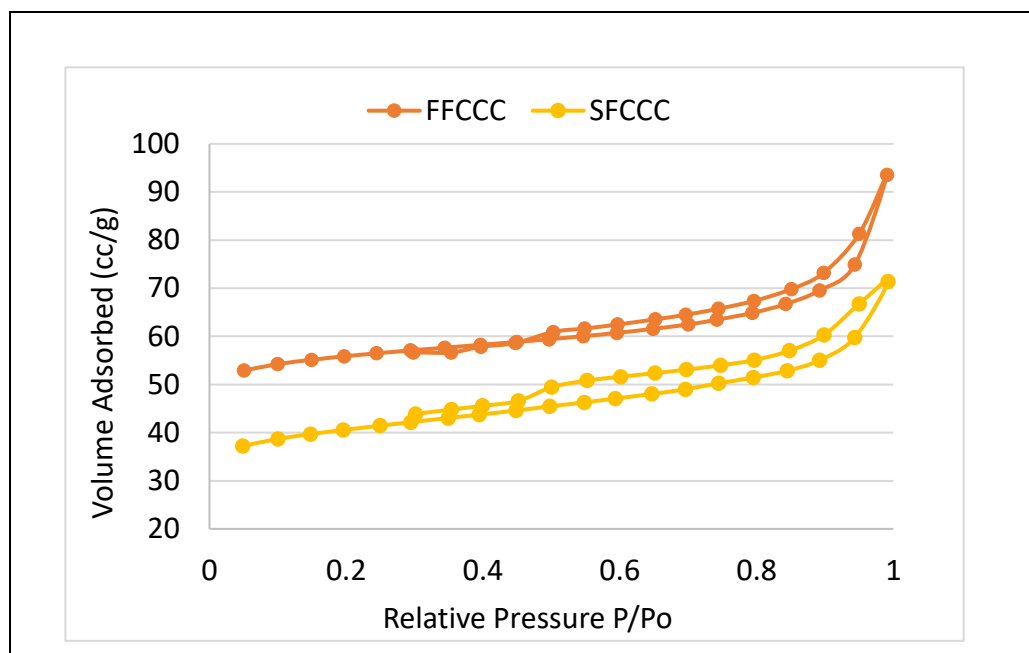


Figure 2: Isotherm plots of FFCCC and SFCCC

4.0 CONCLUSION

The deactivation of the fresh FCC catalyst by coke predominantly takes place in the micropores of the catalyst, accounting for the reduction in the surface area and crystallinity and during the regeneration, only a fraction of the coke is burned off in the micropore compared to the mesopores of the catalyst. The analyses of fresh FCC catalyst deactivation after several cycles of cracking and regeneration show that Fresh FCC catalyst deactivation reduces the relative crystallinity index by 53.22% and total specific surface area by 27.85%. while the loss in Alumina, La₂O₃, TiO₂ and

P₂O₅ were 3.27%, 3.18%, 16.25%, and 24.00% respectively

6.0 REFERENCES

1. T. Gameiro, C. Costa, J. Labrincha, R. Novais, Reusing spent fluid catalytic cracking catalyst as an adsorbent in wastewater treatment applications. *Materials Today Sustainability* **24**, 100555 (2023).

5.0 ACKNOWLEDGEMENT

The authors wish to acknowledge the support of the Dangote Petroleum and Petrochemicals FZE, Lagos, Nigeria for the research funding and the Nigerian Content Development and Monitoring Board (NCDMB) for their technical support.

2. A. Pathak, R. Kothari, M. Vinoba, N. Habibi, V. Tyagi, Fungal bioleaching of metals from refinery spent catalysts: A critical review of current research, challenges, and future directions. *Journal of Environmental Management* **280**, 111789 (2021).
3. T. Wang *et al.*, Enhanced regeneration of spent FCC catalyst by using oxalic acid-sulfuric acid mixture under



- ultrasonic irradiation. *Journal of Materials Research and Technology* **15**, 7085-7099 (2021).
4. P. Bai *et al.*, Fluid catalytic cracking technology: current status and recent discoveries on catalyst contamination. *Catalysis Reviews*, (2018).
 5. E. T. Vogt, B. M. Weckhuysen, Fluid catalytic cracking: recent developments on the grand old lady of zeolite catalysis. *Chemical Society Reviews* **44**, 7342-7370 (2015).
 6. A. Lappas *et al.*, in *Studies in Surface Science and Catalysis*. (Elsevier, 2002), vol. 142, pp. 807-814.
 7. Y. Liao, T. Liu, X. Du, X. Gao, Distribution of Iron on FCC catalyst and Its effect on catalyst performance. *Frontiers in Chemistry* **9**, 640413 (2021).
 8. M. H. Muddanna, S. S. Baral, Leaching of nickel and vanadium from the spent fluid catalytic cracking catalyst by reconnoitering the potential of *Aspergillus niger* associating with chemical leaching. *Journal of Environmental Chemical Engineering* **7**, 103025 (2019).
 9. S. I. Cho, K. S. Jung, S. I. Woo, Regeneration of spent RFCC catalyst irreversibly deactivated by Ni, Fe, and V contained in heavy oil. *Applied Catalysis B: Environmental* **33**, 249-261 (2001).
 10. I. Istadi *et al.*, Enhancing Brønsted and Lewis acid sites of the utilized spent RFCC catalyst waste for the continuous cracking process of palm oil to biofuels. *Industrial & Engineering Chemistry Research* **59**, 9459-9468 (2020).
 11. I. Istadi *et al.*, Acids treatment for improving catalytic properties and activity of the spent RFCC catalyst for cracking of palm oil to kerosene-diesel fraction fuels. *Molecular Catalysis* **527**, 112420 (2022).
 12. Q. Wang *et al.*, Spent fluid catalytic cracking (FCC) catalyst enhances pyrolysis of refinery waste activated sludge. *Journal of Cleaner Production* **295**, 126382 (2021).
 13. F. Ferella *et al.*, Spent FCC E-Cat: towards a circular approach in the oil refining industry. *Sustainability* **11**, 113 (2018).
 14. G. Lu, X. Lu, P. Liu, Recovery of rare earth elements from spent fluid catalytic cracking catalyst using hydrogen peroxide as a reductant. *Minerals Engineering* **145**, 106104 (2020).
 15. J. Wang *et al.*, Kinetics study on the leaching of rare earth and aluminum from FCC catalyst waste slag using hydrochloric acid. *Hydrometallurgy* **171**, 312-319 (2017).
 16. S. Li *et al.*, Non-Destructive characterisation of coke deposit on FCC catalyst and its transient evolution upon Air-Firing and Oxy-Fuel regeneration. *Chemical Engineering Journal* **430**, 132998 (2022).
 17. J. Xu, T. Zhang, Fabrication of spent FCC catalyst composites by loaded V₂O₅ and TiO₂ and their comparative photocatalytic activities. *Scientific Reports* **9**, 11099 (2019).



P072 - BIOGAS SYNTHESIS FROM HUMAN EXCRETA USING ZIRCONIA DOPED SILICA CATALYST

Sunday Essien^{1*}, Elizabeth Eterigho²

*Department of Chemical Engineering, Federal University of Technology,
Minna, Niger State*

*Corresponding Author Email: sundayessien86@gmail.com.

ABSTRACT

Open defecation is an enormous environmental hazard that plagues the ecosystem. A laboratory scale batch biogas digestion using human excreta was undertaken with Zirconia doped silica catalyst (ZrO_2/SiO_2). The mass of gas produced, methane content were measured by electronic weighing balance and Mestek CGA02A methane detector respectively. The effect of catalyst doping and catalyst loading on yield were studied. The catalyst increased the yield of biogas from 7.22 L/KgVS (Litres per kilogram volatile solid) to 19.02L/KgVS and methane content from 14.00% LEL (lower explosive limit) to 97.00% LEL. This equals the purity level of externally purified biogas and meets the energy (Calorie value) need for domestic and industrial applications. This result of the biogas yield shows a remarkable 163.90% efficiency in yield of catalyzed digestion over un-catalyzed and 592.80% increase in methane content over the un-catalyzed system using the same substrate.

KEYWORDS

Open defecation, Biogas, Catalyst loading, Catalyst doping, Human excreta

1.0 INTRODUCTION

In recent years Biogas has gained much attention in energy application both in domestic and industrial settings, in areas such as; powering of cars, trains, electricity generation, as well as in cooking (1). The limitation of Biogas as low-calorie value product in relation to Liquefied Petroleum Gas (LPG) and Compressed Natural Gas (CNG) tend to limit its application. The most critical task in this regard, is to produce Biogas of higher methane content with little or no impurities, in order to enable its use without conversion to Bio-methane by purification, thereby increasing its calorie value, and the removal of moisture that accompanies its production, making it liquefiable without purification (2). Prominently, the number of impurities present in the Biogas determines in usage both in the domestic and industrial applications. Unpurified Biogas presents engineering problems such as; fouling of engine tappet, rusting of cylinder bore and emission of obnoxious gases from car exhaust and during combustion. The production of Biogas from sewage and kitchen waste by designing a sewage and kitchen waste bio digester to replace the present soak away system and kitchen waste disposal in waste dumps, will go a long way in enforcing the recently enacted federal legislation against open defecation and by extension reduction, if not

elimination of deforestation. Open defecation and deforestation are of common knowledge in our society, and these have impacted negatively in the life of the inhabitant of the area, as water bodies and environment have been polluted by human faeces and forest depleted and land exposal to erosion with resultant loss of nutrients, leading to breeding of diseases vectors, diseases and even death. The recent enactment of a law against open defecation and the subsisting law on deforestation necessitate a need to develop an efficient sewage-based digester system for converting human waste into renewable energy fuel for use in cooking and electricity generator, thereby reducing deforestation and open defecation; making open defecation unattractive since it could serve as a source of fuel for cooking. This work explores the possibility of developing a novel catalyst blend for biogas production. The research targets the improvement of the Biogas yield of Zirconia-Silica Catalyzed Biogas digester using human excreta as substrate.

1.1 DIGESTION OF HUMAN EXCRETA WITH AND WITHOUT CATALYST

Biogas has been produced with various compositions of catalyst, water and substrate. Biogas yield, methane content was used to evaluate



the effect of catalyst on the digestion efficiency. It was observed that catalyst when used in the right proportion to feedstock can enhance yield and methane content instead of inhibiting the anaerobic digestion. Biogas can be formed in nature from refuse dumps and rumen of ruminant animals in mild acidic environment, naturally occurring biogas, and results from anaerobic digestion of organic matter by (6). The substrates utilized also include agricultural waste and other activities that generate organic waste as by products. For example, rice straw, pruning, beet, beer and Alcohol production, grass clippings and other agricultural processing activities.

Synthetic biogas, unlike natural biogas, are synthesized either from organic fraction of municipal solid waste, sewage sludge, food waste, fish waste, animal manure, in artificial digesters. (3).

(4) used human faeces as substrate for biogas synthesis. In his work, the key result showed that specific biogas (SBP) of about $0.15\text{m}^3/\text{m}^3/\text{kg}/\text{sv}$ (in normal condition) with an organic loading rate (OLR) of about $0.417\text{kgsv}/\text{m}^3/\text{day}$ were obtained. However, longer digestion time, slurry composition variation, and environmental conditions were not considered without any use of catalyst.

(5) in their work examined the effect of metal addition (ions), such as trace metals in the anaerobic fermentation process, especially on the activities of the enzyme, hydrogenase. The result of their study shows that metal ion addition facilitates the intracellular electron transportation and the provision of essential nutrition for microbial growth, thereby increasing the production of biological hydrogen from anaerobic fermentation.

(6) in their study assessed the effect of different supports materials (expanded clay and activated carbon, Mutag Biochip) on microbial production of hydrogen in an anaerobic packed bed reactor (APBR), using synthetic waste water at low pH as main source of carbon. The result shows that the amount of hydrogen was highest in Mutag Biochip ($R_{1, 1.80\text{molH}_2/\text{mol glucose}}$) followed by clay ($R_{2, 1.74\text{molH}_2/\text{molglucose}}$) and activated carbon ($R_{3, 1.46\text{molH}_2/\text{molglucose}}$). These prove that the reactor with the highest yields (R_{1} and R_{2}) had the lowest acetate/butyrate ratios of 1.7 and 1.6 respectively, while those with the

lowest hydrogen yield ($R_{3,}$) had the highest acetate/butyrate ratio of 4.8. This indicates that hydrogen is produced from the acetate and butyrate by the microbes under the influence of the support materials which has some immobility effect on the gas production.

(7) evaluated HRT and Solid Retention Time (SRT) effect on hydrogen production from organic solid waste using a sequencing batch reactor (SBR) under mesophilic conditions. The result obtained shows that a short SRT of 20h decreased the hydrogen production by up to 90%, and that, optimal hydrogen can be produced at an HRT of 16h and SRT of 55h, showing that HRT is the main parameter that determines the microbial community composition. The result showed that *Olsenella* genus was predominant at HRT less than 8h, *Clostridium* at an HRT of 16h when the slurry was analyzed for microbe composition.

(8) studied biogas production using Silica gel as catalyst. A fictitious laboratory scale digester was used to synthesize biogas from poultry farm and domestic kitchen waste at a digestion temperature of between 26°C to 3°C . The result shows that $7921\text{ml}/\text{kg}$ ($7921\text{L}/\text{kg}$) was obtained without silica gel and $10545\text{ml}/\text{kg}$ ($10.545\text{L}/\text{kg}$) with catalyst, an improvement of 33.12% over digestion without catalyst.

(9) in their study investigated the effect of iron oxide nanoparticles (IONPs) on the anaerobic co-digestion in which olive mill wastewater and chicken manure were used as substrate under mesophilic conditions. Biogas yield, methane (CH_4) content, the removal efficiency of TS, VS., acidification and hydrolysis percentage were also investigated. Their result showed 1.3% to 4.2% enhancement in methane generation yield over the control.

2.0 MATERIAL AND METHODS

2.1 Materials

The materials used for this research include Zirconia, Silica, Distilled water and human excreta. The human excreta were collected from Kure village opposite Kure market in Minna, Nigeria. The substrate was reduced to 2mm grain size in a mortar. The water used was obtained from a local chemical store, Panlac Nigeria Limited. Zirconia and silica were also obtained from the store. The Mestek CGA02A Methane gas analyzer used in analyzing the produced biogas was obtained online as shown in plate 1.0.



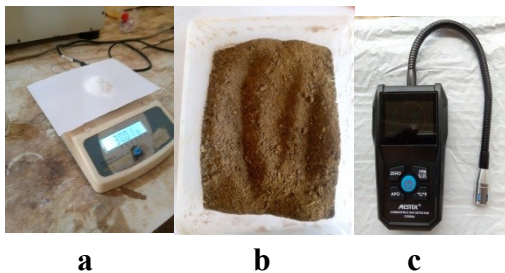


Plate 1.0: (a) Zirconiumdioxide (b) Human excreta (c) Mestek CGA02A Methane Gas Analyzer

2.2 Methods

The dried sample of the substrate underwent physicochemical analysis in order to determine its moisture content, volatile solid and total solid (10). This analysis was carried out in the Unit Operations Laboratory, Department of Chemical Engineering, Federal University of Technology, Minna, Nigeria. Thermogravimetric analysis was also conducted on the catalyst sample developed. The catalyst samples were calcinated at 500 °C for about an hour and twenty minutes.

The catalyst were developed using the method specified by (11) in their work on the structural characterization of Ni/ZrO₂/SiO₂ nanocomposites prepared by wet impregnation method. Alternate quantities of ZrO₂ was mixed with SiO₂ in various proportions of 10g, 20g, and 30g in the ratio of 3:7, 7:3 and 1:1 respectively. This resulted in three different catalysts doping of ZrO₂/SiO₂. The ZrO₂/SiO₂ mixed oxide was calcined at 500° c in an inert furnace atmosphere in order to prevent any oxidation reaction on the composite when heated.

The calcined catalyst was then added to the substrate at 10%, 20%, 30% catalyst loading and digested with 660g of distilled water in ten 3.5×10⁽⁻³⁾ m³ mini digesters, of which one digester without catalyst added, served as the control. The digestion was carried out for 35 days in the Unit Operation Laboratory, Chemical Engineering Department, Federal University of Technology, Minna, Niger State, Nigeria.

3.0 RESULT AND DISCUSSION

The Digestion result is presented herewith and hereby discussed

3.1 Effect of catalyst doping

The result of Balanced Design Analysis of Variance (BD-ANOVA) means plot of gas produced by catalyst doping (figure1.0) showed a large difference among the mean of gas produced between the three levels of catalyst doping when catalyst loading is at smallest index level. Also, at catalyst doping levels of 1 and 3, the mass of gas produced mean increases between catalyst loading levels, 10% and 20% while decreasing for level 2. When catalyst loading is at level 20% the curves start to parallel, indicating that there is not interaction effect between catalyst doping and catalyst loading of levels 10% and 30%. Therefore, the main effect of both factors (catalyst loading and catalyst doping) is zero at this level. However, the two effects are additive and the main effect of catalyst doping does not depend on (or interact with) the levels of catalyst loading of Levels 20% and 30%. Figure 1.0 depicts the effect on biogas production.



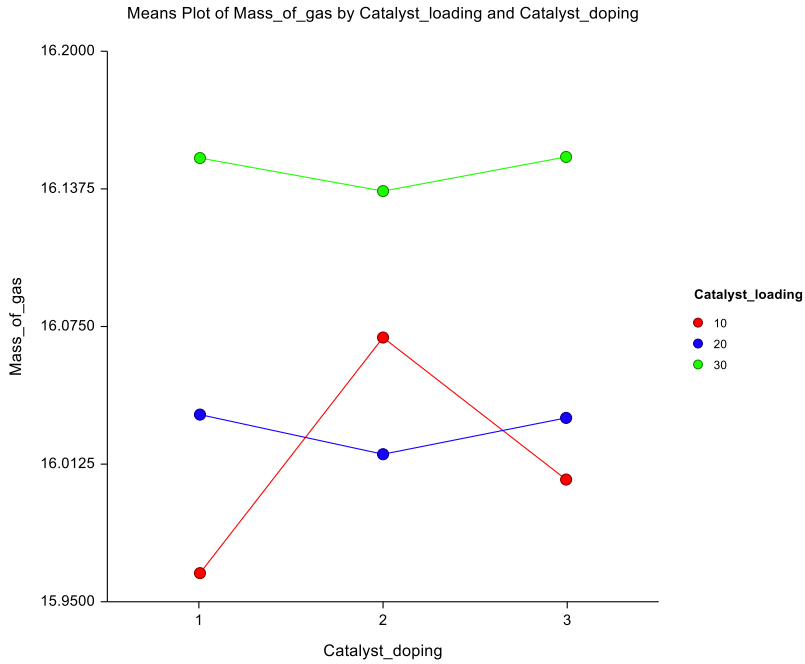


Figure 1.0 Mean plot of biogas production by catalyst doping

3.2 Effect of catalyst loading

The result of the BD-ANOVA means plot of biogas production by catalyst loading (Figure 2.0) showed that catalyst doping has not effect, since catalyst loading levels 20% and 10% overlaps with one another. Moreover, as catalyst loading level of 30%

and 20% are parallel to one another, it therefore means that, the effects of catalyst loading levels 30% does not depend on (interacts with) the levels of catalyst doping.

Figure 2.0 shows the mean plot of biogas production by catalyst loading.

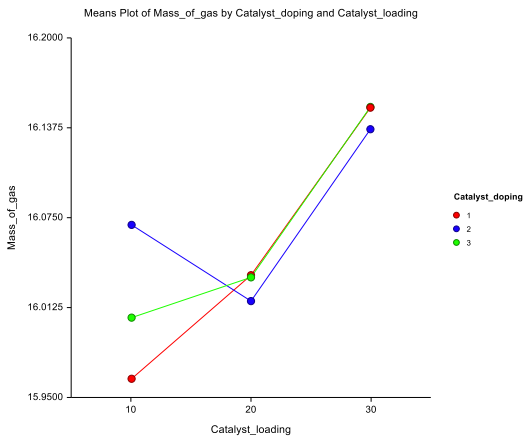


Figure 2.0 Mean plot of biogas production by catalyst loading

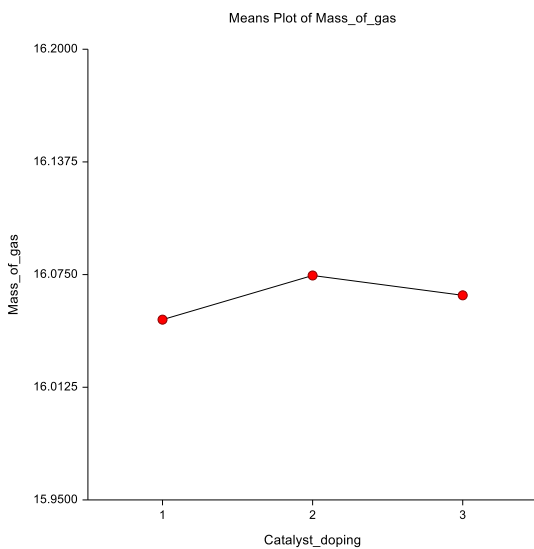
3.3 Effect of catalyst loading and doping on gas production

Table 1.0 Summary of Balanced Design Analysis of Variance (BD-ANOVA) showing the effect of catalyst loading and catalyst doping on gas production

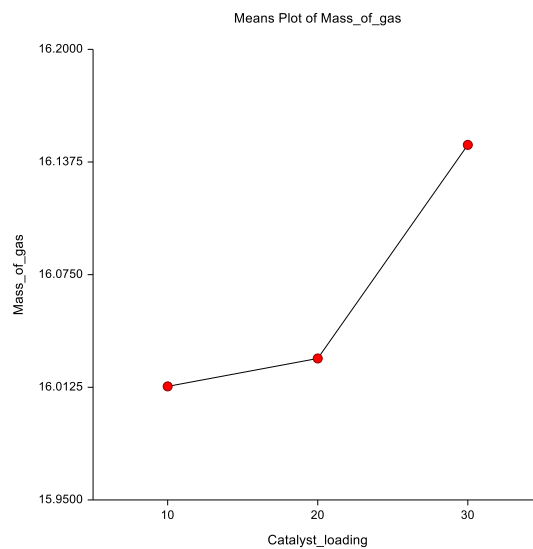


Model	DF	P-Value
A: Catalyst doping	2	0.88872
B: Catalyst loading	2	0.01961*
AB	4	0.85491
S	153	
Total Adjusted	161	
Total	162	

The Result of the BD- ANOVA (Table4.3) showed that catalyst loading had significant ($P \leq 0.05$) effect on biogas production while catalyst doping had not different significantly ($P > 0.05$).



(a)



(b)

Figure3.0 (a) Mean plot of mass biogas produced against catalyst doping, (b) Mean plot of mass of biogas produced against catalyst loading\

Table 2.0 Summary of yield of biogas produced

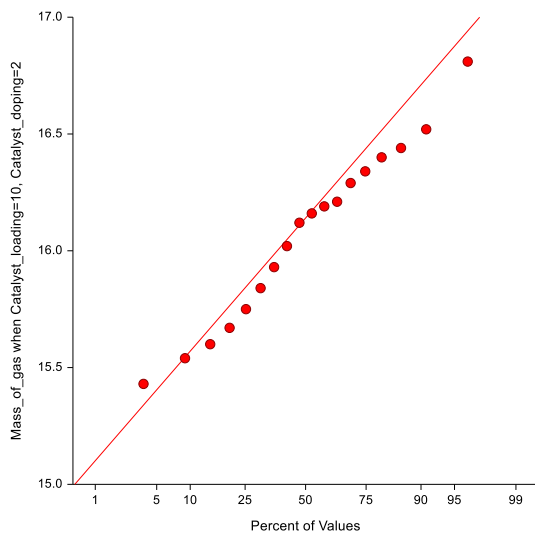


S/N	Experimental Setup	Yield(L/kgV S)
1	Control	7.22
2	Catalystdoping1loading10	10.77
3	Catalystdoping1loading20	11.30
4	Catalystdoping1loading30	12.75
5	Catalystdoping2loading10	19.05
6	Catalystdoping2loading20	13.30
7	Catalystdoping2loading30	12.48
8	Catalystdoping3loading10	13.30
9	Catalystdoping3loading20	11.17
10	Catalystdoping3loading30	12.75

The result of the mean plot of mass of biogas produced indicates that catalyst loading at level 10% produces the highest biogas yield at a catalyst doping of level 2, as shown in figure 3.0(a). While Figure 3.0(b) shows that the catalyst loading of 30% produces the highest cumulative mass of biogas in

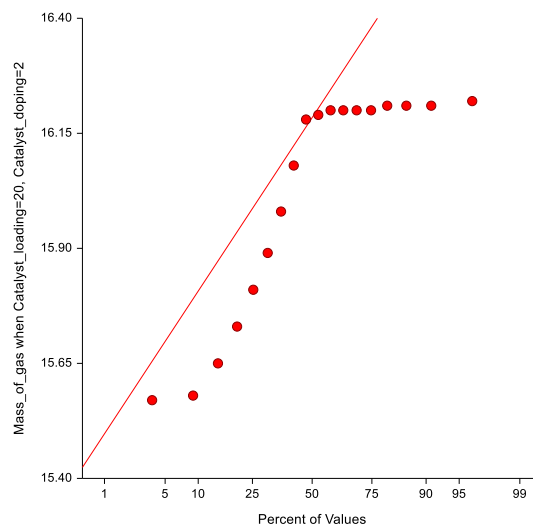
the first eighteen (18) days of digestion. Table 1.0 shows the BD-ANOVA result of the effect of catalyst loading and doping on mass of biogas produced.

Normal Probability Plot of Mass_of_gas when Catalyst_loading=10, Catalyst_doping



(a)

Normal Probability Plot of Mass_of_gas when Catalyst_loading=20, Catalyst_doping=



(b)

Figure 4.0 (a) Normal probability plot of mass of biogas at catalyst loading=10, catalyst doping=2, (b) Normal probability plot of mass of biogas at catalyst loading=20, catalyst doping=2

3.4 Methane content

The digested biogas was analysed *in situ* with a hand-held combustible gas detector model CGD02A, calibrated in lower explosive limit (LEL) and part per minute of resolution 1%LEL and 1PPM and detection flow of 1L/min. The gases detected

are Natural gas, coal gas and liquefied petroleum gas with a response time of 2 seconds, measurement range of 1% to 100%LEL and 50ppm to 50000ppm and measurement accuracy of + or -5%FS

The result of the measurement is shown in table 3.0



Table 3.0 Summary of amount of methane gas (CH₄) in generated biogas measured with Mestek CGD02A

Digester	Amount of Methane present(%LEL)	Measurement Temperature	Remark
Control	14.0	31.4	
Catalystdoping1, loading 10	0.0	31.4	
Catalystdoping1, loading 20	0.0	31.4	
Catalystdoping1, loading 30	0.0	31.4	
Catalystdoping2, loading 10	88.0	31.4	
Catalystdoping2, loading 20	97.0	31.4	
Catalystdoping2, loading 30	Gas bag spill	31.4	Digestesd spill into gas bag
Catalystdoping3, loading 10	62.0	31.4	
Catalystdoping3,loading 20	Gas bag Spill	31.4	Digestesd spill into gas bag
Catalystdoping3, loading 30	0.0	31.4	

The tabulated result of the methane content measurement shows that the digester of catalystloading=20doping=2 generate the highest amount of methane (97%LEL) followed by the digester catalyzed with catalystloading=10doping=2 (88%) and thirdly by catalystloading=30catalyst doping=3 (62%). While the control yielded only 14%LEL. The result, therefore, prove that biochemical reactions can be catalyzed with inorganic heterogeneous catalyst together with enzymatic catalysis.

4.0 CONCLUSION AND RECOMMENDATION

4.1 Conclusion

From the experiment conducted and the analysis undertaken, the following facts can be drawn: The human excreta are a viable substrate for biogas synthesis, which has a yield of both biogas and bio-methane content. The BD-ANOVA analysis of the mass of gas produced revealed that catalyst loading

have significant effect on the yield, with a probability of 0.01961 which is less than significant level of $\alpha=0.05$ while catalyst doping hat not effect. Therefore, catalyst loading had significant effect on the process yield. To further investigate and established the actual catalyst doping combination that has the highest effect on yield, the Two-Sample T- Test was conducted. This revealed that catalyst doping of 10% (Catalyst doping=2, loading=10) gave the highest yield as depicted in figure 4.0(a). The highest yield of biogas produced was 19.02L/KgVS which is 163.9% over the control of 7.22L/KgVS. The methane content obtained for the catalyzed doping of 20% (Catalyst doping=2, loading=20) gave the highest methane content of 97%LEL), while the control had only 14%LEL. The biogas produced from catalyzed digestion (Catalyst doping=2, loading= 20) can be used as bio-methane to power generators, cars and cooking meals drive turbines without necessarily purifying it.



4.2 Recommendation

From the foregoing further research should be undertaken to ascertain the optimum parameters that would give the highest yield of biogas and methane content from a single catalyst loading and doping combination.

5.0 REFERENCES

1. R. Mudasar, M.-H. Kim, Experimental study of power generation utilizing human excreta. *Energy Conversion and Management* **147**, 86-99 (2017).
2. A. Aprilianty *et al.*, in *E3S Web of Conferences*. (EDP Sciences, 2022), vol. 335, pp. 00052.
3. O. G. Igbum, A. C. Eloka-Eboka, S. Adoga, Feasibility study of biogas energy generation from refuse dump in a community-based distribution in Nigeria. *International Journal of Low-Carbon Technologies* **14**, 227-233 (2019).
4. A. Pudi *et al.*, Hydrogen sulfide capture and removal technologies: A comprehensive review of recent developments and emerging trends. *Separation and Purification Technology* **298**, 121448 (2022).
5. N. Sawyerr, C. Trois, T. Workneh, V. I. Okudoh, An overview of biogas production: Fundamentals, applications and future research. *International Journal of Energy Economics and Policy*, (2019).
6. P. Muri, R. Marinšek-Logar, P. Djinović, A. Pintar, Influence of support materials on continuous hydrogen production in anaerobic packed-bed reactor with immobilized hydrogen producing bacteria at acidic conditions. *Enzyme and microbial technology* **111**, 87-96 (2018).
7. Y. Reygadas, S. A. Spera, D. S. Salisbury, Effects of deforestation and forest degradation on ecosystem service indicators across the Southwestern Amazon. *Ecological Indicators* **147**, 109996 (2023).
8. A. Johnny, Y. T. Kumar, A. Rao, Investigation study of biogas production using catalyst. *International Journal of Pure and Applied Mathematics* **119**, 15829-15839 (2018).
9. K. Al Bkoo Alrawashdeh *et al.*, Impact of Iron oxide nanoparticles on sustainable production of biogas through anaerobic co-digestion of chicken waste and wastewater. *Frontiers in Chemical Engineering* **4**, 974546 (2022).
10. F. Inegbedion, Estimation of the moisture content, volatile matter, ash content, fixed carbon and calorific values of saw dust briquettes. *MANAS Journal of Engineering* **10**, 17-20 (2022).
11. S. M. Ulfa, D. Prihartini, A. Taufiq, in *IOP Conference Series: Materials Science and Engineering*. (IOP Publishing, 2019), vol. 515, pp. 012014.

1. R. Mudasar, M.-H. Kim, Experimental study of power generation utilizing human excreta. *Energy Conversion and Management* **147**, 86-99 (2017).
2. A. Aprilianty *et al.*, in *E3S Web of Conferences*. (EDP Sciences, 2022), vol. 335, pp. 00052.
3. O. G. Igbum, A. C. Eloka-Eboka, S. Adoga, Feasibility study of biogas energy generation from refuse dump in a community-based distribution in Nigeria. *International Journal of Low-Carbon Technologies* **14**, 227-233 (2019).
4. A. Pudi *et al.*, Hydrogen sulfide capture and removal technologies: A comprehensive review of recent developments and emerging trends. *Separation and Purification Technology* **298**, 121448 (2022).
5. N. Sawyerr, C. Trois, T. Workneh, V. I. Okudoh, An overview of biogas production: Fundamentals, applications and future research. *International Journal of Energy Economics and Policy*, (2019).
6. P. Muri, R. Marinšek-Logar, P. Djinović, A. Pintar, Influence of support materials on continuous hydrogen production in anaerobic packed-bed reactor with



- immobilized hydrogen producing bacteria at acidic conditions. *Enzyme and microbial technology* **111**, 87-96 (2018).
7. Y. Reygadas, S. A. Spera, D. S. Salisbury, Effects of deforestation and forest degradation on ecosystem service indicators across the Southwestern Amazon. *Ecological Indicators* **147**, 109996 (2023).
 8. A. Johnny, Y. T. Kumar, A. Rao, Investigation study of biogas production using catalyst. *International Journal of Pure and Applied Mathematics* **119**, 15829-15839 (2018).
 9. K. Al Bkoor Alrawashdeh *et al.*, Impact of Iron oxide nanoparticles on sustainable production of biogas through anaerobic co-digestion of chicken waste and wastewater. *Frontiers in Chemical Engineering* **4**, 974546 (2022).
 10. F. Inegbedion, Estimation of the moisture content, volatile matter, ash content, fixed carbon and calorific values of saw dust briquettes. *MANAS Journal of Engineering* **10**, 17-20 (2022).
 11. S. M. Ulfa, D. Prihartini, A. Taufiq, in *IOP Conference Series: Materials Science and Engineering*. (IOP Publishing, 2019), vol. 515, pp. 012014.



P074 - DETERMINATION OF BIOMASS AND LIPID PRODUCTIVITY OF *CHLORELLA VULGARIS* FOR BIODIESEL PRODUCTION

Okibe P.O^{1*}, Ayilara I.S¹, Anyim-Patrick B.¹, Salami V.U¹

¹National Research Institute for Chemical Technology, Zaria P.M.B 1052 Basawa Zaria, Kaduna State Nigeria.

*Corresponding author email: orachuks2008@yahoo.com, oradelight@gmail.com

ABSTRACT

This study aims at exploring the potential of *Chlorella vulgaris* as a bio-fuel source. *Chlorella vulgaris* (stock culture UTEX 259) was sub-cultured at a laboratory scale. The cells were kept in 250ml, 500ml, and 1000ml Erlenmeyer flasks with 200ml, 300ml, and 600ml of medium respectively, and shaken occasionally in Bold Basal Medium with initial pH value 7 at the temperature of $22 \pm 3^{\circ}\text{C}$ with constant light intensity for the culture which was not more than 2500 lux on a 16:8 light to dark cycle for 7 weeks. The biomass productivity was estimated by collecting 20ml inoculums (algae cells) and analyzed at 3-day intervals to estimate the biomass concentration (% by dry weight) which was put into an equation to calculate the biomass productivity. UV-Spectrophotometer was also used to determine the cell density by measuring the optical density at 512nm. The results showed a range of 1.52-151.51mg/L/day. The optimum biomass productivity was observed at weeks 3 & 4 while weeks 1(log phase) and weeks 6& 7 (death phase) had the least biomass productivity. The lipid productivity was determined by harvesting and extracting lipids from the microalgae. The weight of the lipid was used to calculate the lipid productivity which was 3.75mg/L/day. This study concludes that *Chlorella vulgaris* is a potential source of biofuel because of its ability to accumulate biomass.

Keywords:

Chlorella vulgaris, bio-fuel, biomass, algae, lipid.

1.0 INTRODUCTION

Fossil fuels are widely used in the world, but there are a number of serious problems with burning these fuels to provide energy. Fossil fuels have fueled U.S. and global economic development over the past century. Yet fossil fuels are finite resources and they can also irreparably harm the environment. According to the Environmental Protection Agency, the burning of fossil fuels was responsible for 79 percent of U.S. greenhouse gas emissions in 2010. They can cause significant damage to the natural and built environments, and to the health of the people who are exposed to the chemicals that are released when these fuels are burned. It is these types of problems that have made alternative, renewable sources of energy a more attractive option since they do not produce the same kinds of pollution and problems.

Biodiesel is a clean burning fuel derived from a renewable feedstock such as vegetable oil or animal fat, it is biodegradable, less toxic, and produces lesser CO_2 , sulfur dioxide, and unburned hydrocarbons than petroleum-based fuel. Biodiesel molecules are mixtures of fatty acids methyl esters

(FAMES) produced usually from transesterification reaction between triglycerides esters (vegetable oil or animal fat) and alcohol (methanol) in the presence of alkalis such as potassium hydroxide or sodium hydroxide as catalyst. Algal biodiesel is made from lipids extracted from algae cells. The transesterification process replaces glycerol with methanol, forming fatty acid methyl esters, which are the major constituent of biodiesel. Solvent extraction is the most widely used method for extracting lipids from microalgae and hexane is one of the most widely used solvents in extraction based on its high extraction capability and low cost. Algae are eukaryotic organisms that grow quickly and take carbon dioxide out of the atmosphere, they can potentially serve as a great home-grown source of renewable, sustainable fuel for our nation's transportation fleet. Algae fuel (algal biofuel) is an alternative to fossil fuel that uses algae as its source of natural deposits (1). Microalgae have been reported as a potential source of many different renewable biofuels such as methane (2), biohydrogen, and biodiesel produced from the microalgal oil (3). Algal oil and biodiesel have been considered promising alternative fuel sources for the future. Since mass culture was first scaled up (4)



at the Massachusetts Institute of Technology (MIT), various studies were designed to determine different aspects of algae and biodiesel production, including methane production, algae characterization, genomics, and comparison between species, among other characteristics. Microalgae cultivation then became an option to optimize oil production in a more efficient and environmentally friendly way. *Chlorella vulgaris* is a single-celled green algae belonging to the class Chlorophyceae. (*microbe.wiki*)

2.0 MATERIALS AND METHODS

2.1 MICROALGAE STRAIN AND MEDIUM

The stock culture of *Chlorella vulgaris* UTEX 259 was obtained from the National Research institute for chemical technology (NARICT) Zaria, Kaduna

The Bold Basal Medium was used and the stock solutions were prepared from the chemicals presented below.

2.2 Components of the Bold Basal medium.

Stock solutions Concentration per liter of distilled water (g·L⁻¹) 10ml 25g/l NaNO₃, 10ml 2.5g/l CaCl₂, 2H₂O, 10ml 7.5g/l MgSO₄·7H₂O, 10ml 7.5g/l K₂HPO₄, 10ml 17.5KH₂PO₄, 10ml 2.5NaCl, 1ml 50.0 EDTA, 1ml 31.0 KOH, 1ml 4.98, 10ml CaCO₃ FeSO₄·7H₂O, 1 drop H₂SO₄, 1ml 11.42 H₃BO₃, 1ml 8.82 ZnSO₄·7H₂O, 1ml 1.44 MnCl₂·4H₂O, 1ml 0.71MnO₃, 10ml NaHCO₃

To prepare MBL medium, one mL of each stock solution (1–11) was added to one litre of Milli-Q water. The pH was adjusted to 7.0 using hydrochloric acid. The media was autoclaved at 121 °C (15 PSI) for 15 min.

2.3 Culture Conditions

The *Chlorella vulgaris* was grown at the Algae laboratory in National Research institute for chemical technology, Zaria Kaduna state using sterilized Bold Basal Medium under aseptic conditions. The culture temperature was fixed at 22 ± 3 °C. Fluorescent light was used to supply constant light intensity for the culture which was not less than 2500 lux on a 16:8 light to dark cycle. Cells were kept in 250ml, 500ml, 1000ml Erlenmeyer flasks with 200ml, 300ml, 600ml of medium respectively and shaken occasionally. In order to obtain larger quantities of biomass, cells were transferred into 1500ml Erlenmeyer with 1000ml of medium.

2.4 Growth Monitoring

The growth of the culture was measured using two different methods. The first method was using a UV/Vis spectrophotometer (JENWAY 6705, Staffordshire, UK) to monitor the growth curve by measuring the optical density (OD) of the culture at 512 nm. The second method was by dry weight after collecting 20 milliliter of culture media is collected, the algae cell was harvested by centrifugation, dried using an oven and the dry weight calculated.

2.5 Microalgae Harvesting

The microalgae cells were harvested using a Beckman Avanti J-251 high-speed centrifuge (Beckman Coulter, 2.4 Chaska, MN, USA) at 4000 rpm for 10 min. The samples were then transferred to pre-weighed Petri dishes. In order to determine the dry weight of the *Chlorella vulgaris* cells the resulting biomasses were oven-dried. The optical density (@512nm) was measured using a UV Spectrophotometer to determine the biomass concentration.

2.6 Lipid productivity

Daily lipid productivity was calculated using the equation:

$$\text{Daily lipid production (mg lipid l}^{-1}\text{ day}^{-1}) = \text{DW} \times (\text{lipid} / 100 / \text{day}) \times 1,000$$

Where, DW = algal dry weight (g l⁻¹), lipid = g 100 g⁻¹ DW, and day = growth period.

2.7 Biomass productivity

Daily biomass productivity was calculated using the equation

$$\text{Daily biomass production (mg biomass l}^{-1}\text{ day}^{-1}) = \text{DW} / \text{SV} / \text{day}$$

Where DW=dry weight (g l⁻¹), SV= sample volume, day=growth period

2.8 Biomass determination by dry weight of algae

The algae cells were harvested using a centrifuge and collected in pre-weighed Petri- dishes, dried in an oven at 105°C for some minutes, and removed and allowed to cool then weighed and the biomass (% by dry weight) was calculated.

2.9 Lipid Content

Lipid Content (% by weight of algae) = Weight of lipid plus flask- Weight of flask/Weight of algae input.

2.10 Soxhlet Extraction of Total Lipids



0.035g of algae was placed in a soxhlet and extracted for about 3 hours using 205 milliliter of chloroform methanol 2:1(v/v). After the extraction was completed, the solvent was recovered and the oil was weighed. The weight of the oil was calculated.

3.0 RESULTS AND DISCUSSION

3.1 suitable growth condition for optimum biomass yield

Table 1: Effects of culture duration on biomass concentration (mg/L) of *Chlorella vulgaris* grown in four culture media.

	1	2	3	4	5	6	7
A	300	1400	1800	2600	500	300	300
B	700	1700	2500	2000	500	400	400
C	400	2000	2500	1900	800	600	500
D	600	2400	1800	3000	900	600	600

Table 1 shows the result of the effects of culture duration on biomass concentration over time in four culture media. A-D represents four culture media, and 1-7 represents time in weeks. The statistical

analysis (ANOVA, $P < 0.05$, $P (0.00)$) shows that there is a significant difference in the biomass concentration over time.

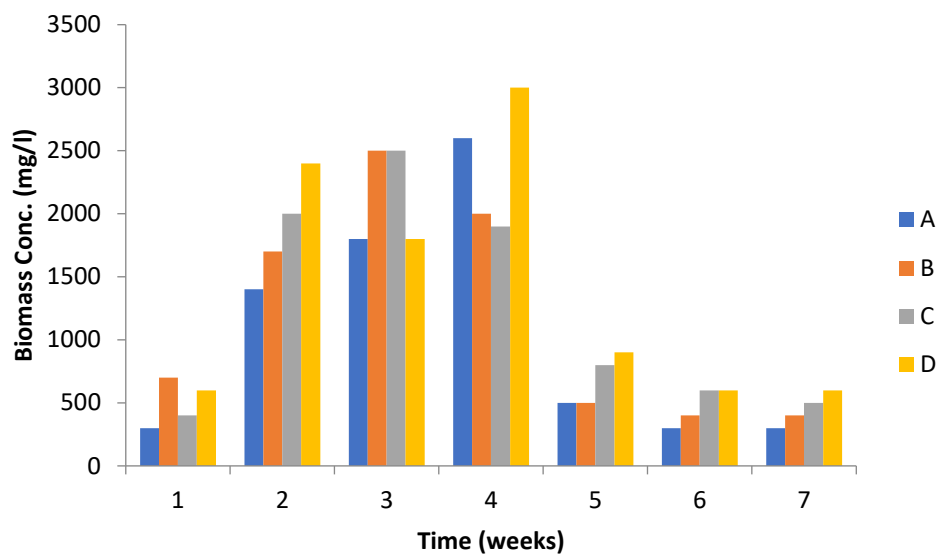
Table 2. Effects of culture duration on biomass concentration (mg/L) of *Chlorella vulgaris* grown in four culture media.

	1	2	3	4	5	6	7
A	300	1400	1800	2600	500	300	300
B	700	1700	2500	2000	500	400	400
C	400	2000	2500	1900	800	600	500
D	600	2400	1800	3000	900	600	600

Table 2 shows the result of the effects of culture duration on biomass concentration over time in four culture media. A-D represents four culture media, and 1-7 represents time in weeks. The statistical

analysis (ANOVA, $P < 0.05$, $P (0.00)$) shows that there is a significant difference in the biomass concentration over time.





(A, B, C, D) represent different culture media.

Fig.1: Biomass concentration versus time

Table 3: Biomass productivity (mg/L/day) of *Chlorella vulgaris* grown in four culture media.

	1	2	3	4	5	6	7
A	1.52	70.71	90.91	131.31	25.25	1.52	1.52
B	35.40	85.86	126.23	101.01	25.25	20.20	20.20
C	20.20	101.10	126.23	95.96	40.40	30.30	25.25
D	30.30	121.21	90.10	151.51	45.45	30.30	30.30

Table 3 shows the biomass productivities of *Chlorella vulgaris* grown in four culture media (A-D) in 7 weeks (1-7) culture duration.

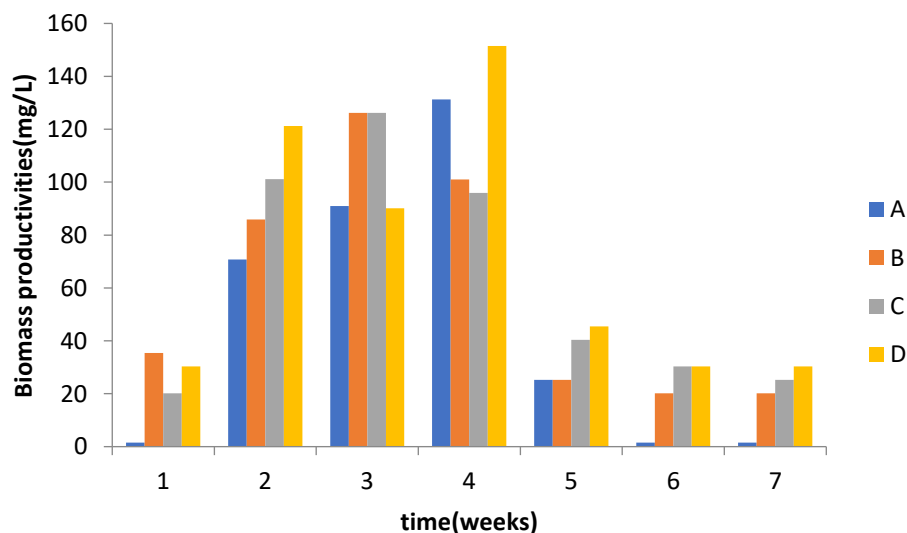


FIG 2: Biomass productivities of *Chlorella vulgaris* cells grown in four culture media over the period of 7 weeks.

3.2 DISCUSSION

As shown in Fig 2 biomass productivity was slow in week 1, increased progressively in week 2 and was at optimum in weeks 3 & 4, and began to decline in week 5 with a further decline in weeks 6 & 7. The biomass concentration over time as well as the biomass productivity was optimum in weeks 3 & 4. (5) reported biomass productivity of 0.28g/L/day (growth rate 0.58). (6) reported biomass productivity of 141.8mg/L/d($\times 10N$) and 63.1mg/L/d and lipid productivity of 47.4mg/L/d($\times 10N$) and 33.2mg/L/d($\times 10N$) and 13.3mg/L/d($\times 1N$) & 5.3mg/L/d($\times 1N$). Ignacio et al.,2015 reported biomass concentration of 0.0854g/L/d (cell density= 8.83×10^{-1}) and lipid productivity (2 – 18 mg/L/d). The lipid content result from the soxhlet extraction showed that the lipid percentage is 25%. (7) reported a lipid content of 24.85 – 36.45%. Ignacio et al.,2015 reported 52 – 58%. (8) reported 38% lipid content. Teresa et al.,2013 reported a lipid content of 33.5%. as shown in Fig 1 the growth curve of algae cells in BBM for 67 days shows that the cell density in the first week is relatively slow due to the low inoculation ratio and as it is known the log phase has lower cell density. In the next (2nd) week, the cell density or the growth curve becomes exponential. The growth curve attained a stationary phase in week 3 to week 4. Afterwards (week 5-7) the death set in with a resultant lower cell density. This result shows that this study's optimum culture duration for *Chlorella vulgaris* is weeks 3 and 4. The statistical analysis shows that there is a significant difference (ANOVA, $P=0.00$, $P<0.05$) in the biomass concentration of *C.vulgaris* during the 7-week culture duration

The biomass productivities are shown in Table 2 above. The minimum biomass productivity was 1.52 mg/L while the maximum was 151.51mg/L.

4.0 CONCLUSIONS AND RECOMMENDATION

The biomass productivity over time as well as the lipid productivity of *Chlorella vulgaris* brings this research work to the conclusion that *Chlorella vulgaris* is a potential as well as promising source of renewable biodiesel because of the amounts of biomass and lipids produced during the study period. Further study should be done with varying factors to enhance biomass and lipid productively

because the factors that enhance biomass productivity do not favor lipid productivity, so it is recommended that studies should be carried out to determine the factors as well as the most suitable culture media for optimum biomass and lipid productivity.

5.0 REFERENCES

1. S. A. Scott *et al.*, Biodiesel from algae: challenges and prospects. *Current opinion in biotechnology* **21**, 277-286 (2010).
2. P. Spolaore, C. Joannis-Cassan, E. Duran, A. Isambert, Commercial applications of microalgae. *Journal of bioscience and bioengineering* **101**, 87-96 (2006).
3. A. Banerjee, R. Sharma, Y. Chisti, U. Banerjee, Botryococcus braunii: a renewable source of hydrocarbons and other chemicals. *Critical reviews in biotechnology* **22**, 245-279 (2002).
4. J. S. Burlew, Algal culture from laboratory to pilot plant. *Algal culture from laboratory to pilot plant.*, (1953).
5. W. Kim *et al.*, Optimization of culture conditions and comparison of biomass productivity of three green algae. *Bioprocess and biosystems engineering* **35**, 19-27 (2012).
6. T. M. Mata, R. Almeida, N. S. Caetano, Effect of the culture nutrients on the biomass and lipid productivities of microalgae *Dunaliella tertiolecta*. *Chem Eng* **32**, 973 (2013).
7. L. B. Bruno, R. Udhaya, S. Sandhya, Biomass and lipid productivity by four fresh water microalgae in photoreactor. *Journal of Modern Biotechnology* **2**, 82-88 (2013).
8. Y. Liang, N. Sarkany, Y. Cui, Biomass and lipid productivities of *Chlorella vulgaris* under autotrophic, heterotrophic and mixotrophic growth conditions. *Biotechnology letters* **31**, 1043-1049 (2009).





P075 - PREVALENCE OF URINARY SCHISTOSOMIASIS AMONG PUPILS OF SELECTED PRIMARY SCHOOLS IN JOS SOUTH LOCAL GOVERNMENT AREA, PLATEAU STATE

JABBA Joshua Ruth¹, GODIYA Salu Karnilus², MOSES Nanbol Chirdan³, TIMOTHY Yamma Obidah⁴, MUSA Muhammed Auwal⁵, SARAH Tissereh Yohanna⁶

National Research Institute for Chemical Technology, Lantang Outstation, Plateau State

*Corresponding Author: Jabba Joshua Ruth: ruthjabba@gmail.com

ABSTRACT

It has been estimated that more than 97% of all schistosomiasis cases occur in Africa. Nigeria is one of the countries known to be highly endemic for urinary schistosomiasis with more than 100 million people at risk and about 25million already infected. Urinary schistosomiasis is caused by *Schistosoma haematobium*, transmission occurs via exposure to open bodies of water where the infective stage known as the cerceria penetrates the human skin leading to acute and chronic symptoms such as fever, abdominal discomfort, blood in urine, hepatomegaly, and bladder cirrhosis. The aim of this study was the determining of prevalence and identification of risk factors among schoolchildren A cross-sectional school-based study was conducted among primary school pupils in Jos South Local Government Area, Plateau State Nigeria between February to March 2020, and February, 2021. A total of 264 urine samples was collected from the school children, using a 50ml sterile container, Swe-Care Uric 9V Urinalysis Reagent Strip was used to detect the presence of haemoglobin in the urine, 49 of 264 (18.6%) were positive for hematuria, 43 of 264 (16.3%) were positive for eggs, Data on Sociodemographic, Socioeconomic, and environmental factors were obtained using a pretested questionnaire. results obtained were computed using SPSS version 22, pupils who swim in river/stream/pond/dam had higher prevalence (68.3%) compared with those who did not swim in river/stream/pond/dam (1.0%). This difference was statistically significant ($\chi^2=154.254$, $p=0.001$). Swimming in open freshwater bodies was the main risk factor for *S. haematobium* infection. Preventive chemotherapy using praziquantel should be combined with certain specific information, education, and communication strategies in order to change children's behaviour, thus avoiding contact with unprotected open freshwater.

Keywords:

Schistosoma haematobium, Polymerase Chain Reaction, Cerceria, Praziquantel

1.0 INTRODUCTION:

Schistosomiasis is a parasitic disease caused by the blood fluke of the genus *Schistosoma*(1). Five major species are known to infect humans: *Schistosoma haematobium*, *S. mansoni*, *S. japonicum*, *S. mekongi* and *S. interculatum*(2). The difference between the *Schistosoma* species is principally related to the different intermediate and definitive hosts they infect, their morphology, and their final location within the human host(3). Urinary schistosomiasis is caused by *Schistosoma haematobium* and is diagnosed as haematuria or blood in urine(4). Urinary schistosomiasis progressively causes damage to the bladder, ureters, and kidneys(5). As part of the transmission cycle, *Schistosoma* must infect very specific intermediate snail host species, and then undergo a process of extensive asexual multiplication within the snail's

body to create the free-swimming cercariae that will infect the next round of human hosts(6). Schoolchildren, adolescents and young adults have been found to have the highest prevalence and morbidity rate due to Schistosomiasis. Thus, the negative impacts caused by untreated infections demoralize both social and economic development on school performance among infected children in endemic areas(7). It causes growth retardation, anaemia, Vitamin-A deficiency as well as possible cognitive and memory impairment, which limits their potential in learning(8).

2.0 METHOD

A cross-sectional school-based study was conducted among primary school pupils in Jos South Local Government Area of Plateau State. 264 urine samples were collected from pupils between 7 to 15 years from the participating schools, using a



50ml labelled, sterile, wide-mouth screw-capped plastic containers distributed to the selected pupils with the name, age, sex and school noted on the bottle and the instruction on how to collect midstream urine.

Samples were preserved in the cooler using ice packs and transported to the laboratory within 10 minutes and was used for Urinalysis reagent strips test, and microscopy

2.1 Microscopy:

The sedimentation method described by Olusegun et al., (2011) (9) was used. 30 ml urine samples received from the subjects were thoroughly mixed, after which a 10 ml aliquot was transferred into a centrifuge tube and spun at 5000 rpm for 5 minutes, the supernatant was decanted, while a drop of the sediment was placed on a clean grease-free slide and covered with a coverslip. It was examined under the microscope using the x 10 and x 40 objectives.(9). The number of eggs were counted and recorded as eggs/10ml urine, categorised into light intensity (< 50 eggs/10 ml of urine) and heavy (\geq 50 eggs/10 ml of urine) infections(10).(WHO, 2007)(WHO, 2002).

2.2 Statistical Analysis:

The data obtained was analysed using Statistical Package for Social Sciences (SPSS version 22). Chi-square test was used to determine the relationship between the prevalence of *S. haematobium* and other categorical variables.

3.0 RESULT:

The study revealed that 43(16.3%) pupils out of the 264 examined had urinary Schistosomiasis with Gyel LEA having the highest prevalence rate (30.8%), followed by GJSS Angulu (27.3%), Kufang LEA (12.0%) and Jovad School International (10.0%). Hwolshe LEA (7.1%) had the least number of cases (Table 4.1). This was not statistically significant at $p = 0.98$

Table 4.2 shows the relationship between prevalence of urinary schistosomiasis and socio-demographic characteristics of subjects which revealed that more Male pupils (17.7%) than Female (14.0%) were positive to urinary schistosomiasis. However, this difference was not statistically significant ($\chi^2=0.618$, $p=0.432$).

Assessing the various risk factors associated with urinary schistosomiasis,. Relationship between prevalence and awareness about schistosomiasis revealed that pupils who were not aware about the disease had higher prevalence (16.6%) compared to those who are aware (13.0%). However, this difference was not statistically significant ($\chi^2=0.195$, $p=0.659$). Similarly, pupils who swim in river/stream/pond/dam had higher prevalence (68.3%) compared with those who did not swim in river/stream/pond/dam (1.0%). This difference was statistically significant ($\chi^2=154.254$, $p=0.001$). More prevalence (26.8%) was seen among pupils who washed their cloths at stream/rivers compared to those who washed their cloths at home (11.5%). This difference was statistically significant ($\chi^2=9.694$, $p=0.002$). Relating source of water at home with prevalence, the study revealed that more prevalence (23.4%) was seen among pupils who uses stream/river water compared with well (13.7%) and borehole/tap (12.5%) respectively. This difference was however, not statistically different ($\chi^2=4.042$, $p=0.133$). Table 4.5 Shows Symptoms associated with Urinary Schistosomiasis among study population which revealed that 56 pupils representing 21.2% experienced pain during urination, while 25.0% had frequent urination and 29.5% observed blood at the end of urination, 29.5% observes drop of blood at the end of urination, 5.3% took prophylactic treatment against intestinal and or urinary parasites, 4.2% have ever been given tablet (praziquantel) in school, while 47.3% had abdominal pain (Table 4.3).

Relating the symptoms with the prevalence of the disease, the study revealed that most pupils who experienced pain during urination (30.4%) had Schistosomiasis. The difference was statistically significant ($\chi^2=10.319$, $p=0.001$). This implies that pain during urination is associated with urinary schistosomiasis. The study further revealed that terminal haematuria was strongly significant with urinary schistosomiasis ($\chi^2=31.223$, $p=0.000$). This was evident as more who had drop of blood at the end of urination had higher prevalence (35.9%) compare to those who did not (8.1%). There was no significant association between abdominal pain and urinary schistosomiasis ($\chi^2=0.300$, $p=0.584$). Pupils who took prophylactic treatment against intestinal and or urinary parasites had higher prevalence (28.6%) compare with those who were not on drugs or had never take the drugs (15.6%). However, this difference was not statistically significant ($\chi^2=1.636$, $p=0.201$). Similarly, pupils who had ever been given tablet (praziquantel) in



school had higher prevalence (36.4%). However, the difference was not statistically significant ($\chi^2=3.393$, $p=0.065$) (Table 4.4)

at least 50eggs/10ml while majority 35(81.4%) had less than 50eggs/10ml of urine. This implies that the overall intensity of Schistosomiasis among the study population was 18.6% (Table 4.5).

The study revealed that out of the 43 participants who had Schistosomiasis, 8 representing 18.6% had

Table 1: Prevalence and Intensity of Urinary Schistosomiasis in the selected schools in Jos South Local Government Area Plateau State.

Schools	No. of sample	No. positive	Intensity	χ^2	p-value
A	55	15(27.3)	2 (13.0)	0.4278	0.9801
B	39	12(30.8)	3(25.0)		
C	70	5(7.1)	1(20.0)		
D	50	6(12.0)	1(16.7)		
E	50	5(10.0)	1(20.0)		
Total	264	43(16.3)	8(18.6)		

Table 2: Relationship between prevalence of urinary schistosomiasis and socio-demographic characteristics of subjects (n=264)

Variables	Positive f(%)	Negative f(%)	Total f(%)	χ^2	p-value
Sex					
Female	14(14.0)	86(86.0)	100(100.0)	0.618	0.432
Male	29(17.7)	135(82.3)	164(100.0)		
Age (years)					
5-7	6(12.2)	43(87.8)	49(100.0)	3.234	0.357
8-10	6(14.3)	36(85.7)	42(100.0)		
11-13	19(22.1)	67(77.9)	86(100.0)		
14+	12(13.8)	75(86.2)	87(100.0)		
School level					
Nursery	8(14.8)	46(85.2)	54(100.0)	0.108	0.742
Primary	35(16.7)	175(83.3)	210(100.0)		
Parent's occupation					
Farming	17(15.9)	90(84.1)	107(100.0)	0.879	0.830



Laundry	5(21.7)	18(78.3)	23(100.0)
Others	16(16.8)	79(83.2)	95(100.0)

Table 3: Relationship between risk factors and prevalence of urinary Schistosomiasis (n=264)

Risk factors	Positive f(%)	Negative f(%)	Total f(%)	χ^2	p-value
Awareness about Schistosomiasis					
Yes	3(13.0)	20(87.0)	23(100.0)	0.195	0.659
No	40(16.6)	201(83.4)	241(100.0)		
Do you swim in river/stream/pond/dam					
Yes	41(68.3)	19(31.7)	60(100.0)	154.254	0.001
No	2(1.0)	202(99.0)	204(100.0)		
Where do you wash your cloths					
At home	21(11.5)	161(88.5)	182(100.0)	9.694	0.002
At stream/river	22(26.8)	60(73.2)	82(100.0)		
What is your source of water at home					
Well	19(13.7)	120(86.3)	139(100.0)	4.042	0.133
Stream/River	18(23.4)	59(76.6)	77(100.0)		
Borehole/Tap	6(12.5)	42(87.5)	48(100.0)		
What toilet facilities do you use at home					
Water system	23(15.5)	125(84.5)	148(100.0)	2.601	0.457
Pit toilet	19(19.6)	78(80.4)	97(100.0)		
None	1(6.3)	15(93.8)	16(100.0)		
Others	0(0.0)	3(100.0)	3(100.0)		

Table 4: Relationship between symptoms and prevalence of Urinary Schistosomiasis among study population (n=264)

Risk factors	Prevalence			χ^2	p-value
	Positive f(%)	Negative f(%)	Total f(%)		
Do you experience pain during urination					
Yes	17(30.4)	39(69.6)	56(100.0)	10.319	0.001
No	26(12.5)	182(87.5)	208(100.0)		
Are you having frequent urination					
Yes	11(16.7)	55(83.3)	66(100.0)	0.009	0.923
No	32(16.2)	166(83.8)	166(83.8)		
Do you observe drop of blood at the end of urination					
Yes	28(35.9)	50(64.1)	78(100.0)	31.223	0.000
No	15(8.1)	171(91.9)	186(100.0)		
Are you having an abdominal pain					
Yes	22(17.6)	103(82.4)	125(100.0)	0.300	0.584



No	21(15.1)	118(84.9)	139(100.0)		
Have you taken prophylactic treatment against intestinal and or urinary parasites					
Yes	4(28.6)	10(71.4)	14(100.0)	1.636	0.201
No	39(15.6)	211(84.4)	250(100.0)		
Have you ever been given tablet (praziquante) in school					
Yes	4(36.4)	7(63.6)	11(100.0)	3.393	0.065
No	39(15.4)	214(84.6)	253(100.0)		

Table 5: Relationship between Intensity of Schistosomiasis and Demographic variables

Demographic variables	≥ 50 eggs/10ml f(%)	< 50eggs/10ml f(%)	Total (%)	χ^2	P
Sex				4.013	0.045*
Female	5(62.5)	9(25.7)	14(32.6)		
Male	3(37.5)	26(74.3)	29(67.4)		

f = Fisher's Exact Test,

* = statistically significant

3.1: Discussion

In this study the prevalence of Urinary Schistosomiasis is 16.3% among pupils of selected schools in Jos South Local Government Area, Plateau State, with Gyel LEA (30.8%) having the highest cases followed by GJSS Angulu (27.3%), Kufang LEA (12.0), and Jovad School International (10.0). hwolshe LEA (7.1%) had the least number of cases. Comparatively, the result of this study revealed lower prevalence rate than 18.7% previously reported by co-workers among irrigation farmers in Jos South Local Government Area(11). Other studies outside Jos had consistently reported higher prevalence of urinary Schistosomiasis such as prevalence rate of 58.54% among children in Ardo-Kola Local Government Area, Taraba State, Nigeria(12), and 31.8% among school children in Yemen(13). The low prevalence of the disease, recorded in the inhabitants from the study area may probably be due to the fact that some of the Schools are located in areas that are not close to open bodies of water, and most of them have good source of water and toilet facilities also, the nationwide deworming program using praziquantel that targeted school children is a systemic approach that might have helped in reducing the transmission rate of the parasite.

However, findings from this study still revealed a level of endemicity of the infection among the population in the study area. A recent survey of a

50 year prevalence of urinary Schistosomiasis in Nigeria, ranked Plateau State among highly endemic ($> 50\%$) areas in terms of Schistosomiasis burden.¹⁴ The study revealed a relatively high prevalence of Schistosomiasis in Plateau State, and falls into the ≥ 10 but $< 50\%$ moderate risk community category(14).

Gender difference in infection rate of Schistosomiasis among the study population reveals higher risk of Schistosomiasis in male (17.7%) than the female (14.0%) this could be due to the fact that they are more involved in farm work than the females and various outdoor activities such as the social habit of bathing, fishing, and swimming in infested water bodies while females do not participate in these activities due to socio-cultural grounds. For instance, the development of secondary sexual characters which prevents females from visiting streams unlike their male counterparts. This finding is in consonant with the work of other research fellows such as (15-22).

In this study, individuals within the age range of 11-14 years were found to be more infected by the disease, Schistosomiasis than individuals in other age groups(15, 21, 23-25). The possible reason for these findings may be probably because they spent more time in infested streams for contact activities, such as bathing, playing, swimming or washing clothes, as a result, they get infected by the infective stage of the parasite, cercariae. This group also



contaminates the streams with their urine and faeces which may contain the eggs of the parasites. So, they act as sources of transmission of the disease.

Occupation of father is associated with urinary Schistosomiasis where children whose fathers are farmers were more infected (15.9%). This result agrees with studies from Ghana and Nigeria (26, 27), where children participated in field activities with their fathers. This shows lack of awareness towards risk of urinary schistosomiasis among fathers to make their children aware of the risk of urinary schistosomiasis, as reported from an earlier study in South-western Nigeria(28).

Relating prevalence and risk factors of Schistosomiasis, this study identified lack of knowledge as a significant predictor of Schistosomiasis among the children studied. Therefore, health education regarding good personal hygiene, sanitary practices, and awareness about Schistosomiasis can help curtail the transmission of Schistosomiasis(29).

Data collected on water contact activities such as swimming, washing at river/stream, and source of water for home provide a platform for exposure to cercaria, which is the infective stage of the parasite. Thus, most suggestions are centred on protection from water contact activities. (30) the study reveals that common symptoms of pain during urination, and hematuria which are associated with Schistosomiasis are statistically significant.

4.0 CONCLUSION

Findings from this study reveal the prevalence of *S. hematobium* infection (16.3%) among pupils of selected primary schools in Jos south local government area, plateau state. It is also affected by the socio-cultural characteristics and accounts for the obvious difference in the distribution of the disease between age, sex, and other socio-demographic factors. Increased water contact activities such as swimming, washing near open water bodies and farming were correlated with increased risk of infection. Lack of knowledge also plays an important role in the prevalence of the disease.

4.1 Recommendation

1. Health education is a very effective means of improving knowledge about urinary schistosomiasis and has the potential to reduce the prevalence of the disease

2. Mass administration of praziquantel should be integrated into the ongoing school feeding programme of primary schools in the country.

3. Government should ensure supply clean and safe water to all households within the country especially study areas to avoid use of river water which poses risk of infection

4. Students should be educated on the importance of water, sanitation and hygiene (WASH) and the danger of open defecation.

5. Vector control, detection and treatment of animal reservoirs for the sustained control and elimination.

5.0 REFERENCES

1. M. Viana, C. L. Faust, D. T. Haydon, J. P. Webster, P. H. Lamberton, The effects of subcurative praziquantel treatment on life-history traits and trade-offs in drug-resistant *Schistosoma mansoni*. *Evolutionary applications* **11**, 488-500 (2018).
2. B. Ukoroije, J. Abowei, Some occupational diseases in culture fisheries management and practices. Part two: Schistosomiasis and Filariasis. *Int J Fish Aquat Sci* **1**, 64-71 (2012).
3. W. H. Organization, *The social context of schistosomiasis and its control: an introduction and annotated bibliography*. (World Health Organization, 2008).
4. E. Nkegbe, Sex prevalence of schistosomiasis among school children in five communities in the lower river Volta basin of South Eastern Ghana. *African Journal of Biomedical Research* **13**, 87-88 (2010).
5. K. Karunamoorthi, M. J. Almalki, K. Y. Ghailan, Schistosomiasis: A neglected tropical disease of poverty: A call for intersectoral mitigation strategies for better health. *Journal of Health Research and Reviews (In Developing Countries)* **5**, 1-12 (2018).
6. R. Sturrock, Schistosomiasis epidemiology and control: how did we get here and where



- should we go? *Memórias do Instituto Oswaldo Cruz* **96**, 17-27 (2001).
7. M. J. Van der Werf *et al.*, Quantification of clinical morbidity associated with schistosome infection in sub-Saharan Africa. *Acta tropica* **86**, 125-139 (2003).
 8. D. P. McManus *et al.*, Schistosomiasis in the People's Republic of China: the era of the Three Gorges Dam. *Clinical microbiology reviews* **23**, 442-466 (2010).
 9. A. F. Olusegun, O. C. Ehis, O. Richard, Proportion of urinary schistosomiasis among HIV-infected subjects in Benin city, Nigeria. *Oman Medical Journal* **26**, 175 (2011).
 10. J. U. N. P. o. HIV/AIDS, World Health Organisation. *AIDS epidemic update: December 2006*, (2007).
 11. J. Damen, E. Kopkuk, M. Lugos, Prevalence of urinary schistosomiasis among irrigation farmers in North Central Nigeria. (2018).
 12. R. S. Houmsou *et al.*, Cross-sectional study and spatial distribution of schistosomiasis among children in Northeastern Nigeria. *Asian Pacific Journal of Tropical Biomedicine* **6**, 477-484 (2016).
 13. H. Sady *et al.*, Detection of *Schistosoma mansoni* and *Schistosoma haematobium* by real-time PCR with high resolution melting analysis. *International journal of molecular sciences* **16**, 16085-16103 (2015).
 14. C. O. Ezeh, K. C. Onyekwelu, O. P. Akinwale, L. Shan, H. Wei, Urinary schistosomiasis in Nigeria: a 50 year review of prevalence, distribution and disease burden. *Parasite* **26**, (2019).
 15. S. Umar *et al.*, Prevalence and molecular characterisation of *Schistosoma haematobium* among primary school children in Kebbi State, Nigeria. *Annals of parasitology* **63**, 133-139 (2017).
 16. H. Omenesa, H. Bishop, H. Raji, Prevalence of urinary schistosomiasis among pupils attending primary schools in Bomo Village, Zaria-Nigeria. *International Journal of Research in Engineering and Science* **3**, 14-19 (2015).
 17. I. A. Muhammad, K. Abdullahi, A. Y. Bala, S. a. A. Shinkafi, Prevalence of urinary schistosomiasis among primary school pupils in Wamakko Local Government, Sokoto State, Nigeria. *The Journal of Basic and Applied Zoology* **80**, 1-6 (2019).
 18. H. A. H. A. Ismail *et al.*, Prevalence, risk factors, and clinical manifestations of schistosomiasis among school children in the White Nile River basin, Sudan. *Parasites & vectors* **7**, 1-11 (2014).
 19. M. A. Shehata, M. F. Chama, E. Funjika, Prevalence and intensity of *Schistosoma haematobium* infection among schoolchildren in central Zambia before and after mass treatment with a single dose of praziquantel. *Tropical parasitology* **8**, 12 (2018).
 20. E. Angora *et al.*
 21. K. Mohammed *et al.*, Prevalence of urinary schistosomiasis among primary school children in Kwalkwalawa area, Sokoto state, north-western Nigeria. *Asian Journal of Research in Medical and Pharmaceutical Sciences* **3**, 1-10 (2018).
 22. K. Mohammed *et al.*, A multivariate analysis on the assessment of risk factors associated with infections and transmission of schistosomiasis haematobium in some selected areas of North-Western, Nigeria. *J Med Bioeng* **4**, (2015).
 23. H. Okpala *et al.*, A survey of the prevalence of Schistosomiasis among pupils in Apata and Laranto areas in Jos, Plateau State. *OJHAS* **1**, (2004).
 24. A. Dawet, Prevalence and intensity of *Schistosoma haematobium* among residents of Gwong and Kabong in Jos north local government area, Plateau State, Nigeria. *International Journal of Biological and Chemical Sciences* **6**, 1557-1565 (2012).
 25. E. E. Ekanem, F. M. Akapan, M. E. Eyong, Urinary schistosomiasis in school children of a southern Nigerian community 8 years after the provision of potable water.



- Nigerian Postgraduate Medical Journal* **24**, 201-204 (2017).
26. O. Akogun, S. Obadiah, History of haematuria among school-aged children for rapid community diagnosis of urinary schistosomiasis. *Nig J Parasitol* **17**, 11-16 (1996).
 27. B. Ayele, B. Erko, M. Legesse, A. Hailu, G. Medhin, Evaluation of circulating cathodic antigen (CCA) strip for diagnosis of urinary schistosomiasis in Hassoba school children, Afar, Ethiopia. *Parasite* **15**, 69-75 (2008).
 28. S. A. Risikat, A. A. Ayoade, Correlation analysis between the prevalence of *Schistosoma haematobium* and water conditions: A Case Study among the School Pupils in Southwestern Nigeria. *IJRRAS* **13**, 160-165 (2012).
 29. W. A. Istifanus, A. F. Chinedu, S. M. Panda, S. L. Kela, A. B. Samaila, in *Science Forum (Journal of Pure and Applied Sciences)*. (Faculty of Science, Abubakar Tafawa Balewa University Bauchi, 2018), vol. 15, pp. 40-40.
 30. M. Kabiru *et al.*, Prevalence and intensity of *Schistosoma haematobium* infections: a community based survey among school children and adults in Wamakko town, Sokoto State Nigeria. *Int J Trop Med Public Health* **2**, 12-21 (2013).

P076 - PRODUCTION OF HYDROCHAR AS ADSORBENTS FOR REMOVAL OF HEAVY METALS FROM PHARMACEUTICAL WASTEWATER

A. M. Abdulrahman*, M. U. Garba, A. S. Muhammed

Federal Univeristy of Technology Minna,

*Corresponding author email: adammohammed42463@gmail.com

ABSTRACT

Water pollution is a growing global crisis, endangering ecosystems and human health through the contamination of water sources, particularly from sewage and industrial wastewater. This study explores the application of liquid-solid adsorption, with a specific focus on heavy metals and pharmaceutical waste removal from water. These pollutants, such as heavy metals, pharmaceuticals, phenols, dyes, and pesticides, often coexist in wastewater, making treatment a complex challenge. Adsorption, especially using "green" materials like hydrochar derived from biomass through hydrothermal carbonization (HTC), is a promising solution. The pharmaceutical industry, known for employing heavy metals and various chemicals, is closely scrutinized for its wastewater's environmental impact. The study highlights the removal of heavy metals and pollutants and reviews various techniques employed for water treatment. It emphasizes the role of rice husk (RH) hydrochar in adsorption, discussing its properties and production via HTC. Results revealed the high potential of RH hydrochar for heavy metal removal and changes in material characteristics. This study underscores the significance of efficient water treatment strategies in combating water pollution challenges.

KEYWORDS

Water pollution, Hydrochar, Heavy metal removal, Pharmaceutical wastewater, Hydrothermal carbonization

1.0 INTRODUCTION

Water pollution, a growing global crisis, endangers ecosystems and human health by contaminating water sources with pollutants from sewage and industrial wastewater. The diverse nature of these pollutants, spanning organic and inorganic compounds, necessitates efficient removal methods (1, 2). Liquid-solid adsorption has emerged as a powerful technique for addressing various

pollutants, particularly heavy metals and pharmaceutical waste, which can have severe health implications if present in excessive quantities in drinking water. The simultaneous existence of diverse pollutants in wastewater, such as phenols, dyes, pesticides, heavy metals, and pharmaceuticals, presents a formidable challenge for wastewater treatment (3, 4). Adsorption has become a promising approach to tackle this complex web of contaminants.



The expansion of urbanization and industrialization has contributed to water resource degradation globally. Industrial wastewater effluents, laden with dyes and heavy metal ions, disrupt aquatic environments (5). The pharmaceutical industry, a major contributor to industrial wastewater, employs various chemicals and heavy metals in drug development and manufacturing, further straining wastewater treatment efforts. To combat this, researchers have turned to low-cost adsorbents, notably "green adsorption" materials derived from agricultural sources and residues. Hydrochar, produced through hydrothermal carbonization (HTC) of biomass, has emerged as a promising candidate for heavy metal removal from pharmaceutical wastewater due to its unique properties and eco-friendly nature (6).

The pharmaceutical industry employs heavy metals for multiple purposes, necessitating strict regulations. It also utilizes a wide range of chemicals and compounds in drug development and manufacturing, which can raise environmental concerns. These substances include Active Pharmaceutical Ingredients (APIs), excipients, solvents, and various other chemicals (7, 8). Understanding pharmaceutical wastewater and its components is vital to address the environmental challenges it poses.

Heavy metal pollution from industrial activities like textiles, metal plating, mining, and paint production remains a significant concern. The adsorption of heavy metals on biochar, particularly hydrochar produced through hydrothermal processes, involves various mechanisms like electrostatic attraction, ion-exchange, and surface complexation (9, 10). The presence of oxygen-containing and nitrogen-containing functional groups in hydrochar enhances its adsorption capacity, making it a promising option for heavy metal removal. (10, 11).

Multiple techniques, including membrane filtration, coagulation, flocculation, oxidation, and biological treatment, have been used for pollutant removal from water. Each method has advantages and limitations, making the choice of the most suitable

method crucial (12). Adsorption has gained popularity for its effectiveness, ease of use, and environmental friendliness. Researchers have explored various adsorbents, considering their physico-chemical characteristics and source materials.

Understanding the chemical and physical properties of biomass components, including cellulose, hemicellulose, and lignin, is essential for hydrochar production through hydrothermal carbonization (HTC). Thermochemical technologies, such as HTC, offer versatile means for converting biomass materials into valuable products with applications in environmental treatment and carbon sequestration. Factors like temperature, residence time, adsorbent dosage, and pH are critical in optimizing hydrochar's efficiency for pollutant removal, making it a promising solution for water pollution challenges (13).

2.0 MATERIALS AND METHODS

2.1 Materials And Chemicals

Rice husk (RH) was sourced from a local rice mill, meticulously cleaned by multiple washes with distilled water (DW), and subsequently subjected to oven drying for moisture content removal. The acquisition of sulphuric acid H_2SO_4 involved obtaining it from PANLAC CHEMICALS. Ltd. (Minna, Niger state). It is worth noting that all chemicals used throughout the study were of analytical purity and utilized in their as-received state, with the preparation of all solutions being carried out using distilled water. Comprehensive information about the reagents, including details on their source, purity, and nomenclature, can be found in Table 1. In addition, Table 2 offers an extensive list of the apparatus and equipment used in the experimental procedures, serving as a valuable reference for understanding the tools instrumental to the study's execution. Figure 1 provides a visual representation in the form of a Block diagram of the comprehensive Experimental Method, which encompassed various critical stages.

Table 1: Lists of reagents

S/N	REAGENTS	% PURITY	SOURCE
1	Sodium hydroxide pellet (NaOH)	>99	Sidmach Aldrich
2	Hydrochloric Acid (H_2SO_4)	>99	Panlac Chemical, Minna



3	Deionized Water	>99	Panlac Chemical, Minna
---	-----------------	-----	------------------------

Table 2: Lists of apparatus and equipment used

S/N	EQUIPMENT	MODEL TYPE	SOURCE
1	(PTFE) inner steel autoclave	50 ml	TIC LAB, Minna
2	Beakers	100 ml, 500 ml, 1000 ml	TIC LAB, Minna
3	Conical flask	1000 ml	TIC LAB, Minna
4	Measuring cylinder	100 ml	TIC LAB, Minna
5	Weighing balance	(Ohas)	TIC LAB, Minna
6	Filter paper		TIC LAB, Minna
7	pH paper		TIC LAB, Minna
8	Round bottom flask	500 ml	TIC LAB, Minna
9	Distillation apparatus		TIC LAB, Minna
10	Sample bottles	500 ml,	TIC LAB, Minna

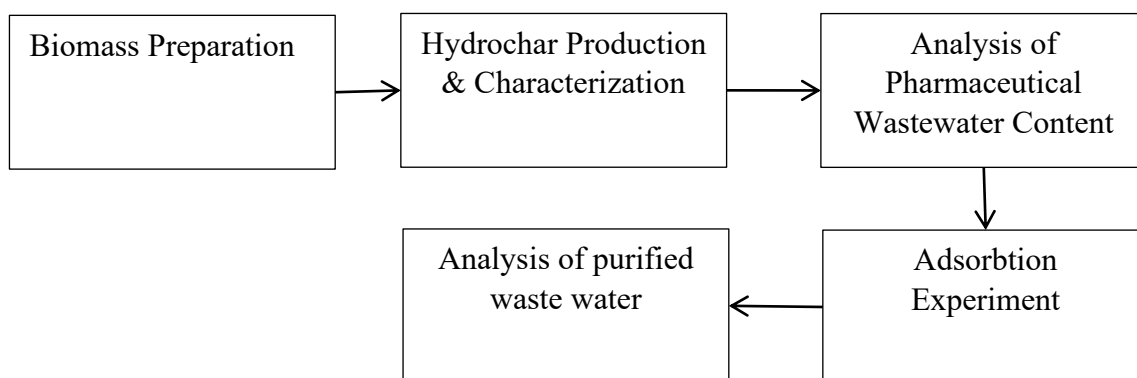


Figure 1: Block diagram of Experimental Method

3.0 RESULTS AND DISCUSSION

3.1 FAAS of Pharmaceutical Waste Water

The result of the analysis of Pharmaceutical waste water for Cu, Fe, Cd, Cr and Pb were 0.2516, 13.1586, -0.0112, 12.2171, 0.8728 respectively.

Table 3: Analysis of Pharmaceutical waste water

S/N	HEAVY METAL	CONCENTRATION	WHO PERMISSIBLE LIMIT (MG/L)
1	Cu	0.2516	0.20
2	Fe	13.1586	0.30
3	Cd	-0.0112	0.05



4	Cr	12.2171	0.003
5	Pb	0.8728	0.01

3.2 FTIR Of Raw Biomass And Hydrochar

The FTIR spectra of raw RH shows some dominant peaks at 2922.23286 cm^{-1} , 1640.02865 cm^{-1} , and 1013.83589 cm^{-1} , which represent O–H stretching, aliphatic C–H stretching and Si–O stretching, respectively. These peaks changed with the carbonized rice husk where the O–H stretches at

2922.23286 cm^{-1} aliphatic C–H stretching 1028.74524 cm^{-1} and Si–O stretching 790.19562 cm^{-1} . It can be seen that there was no much significant variation between the band peaks in the hydrochar to those observed in the raw biomass which conform to results reported by E. Danso-Boateng et al., 2021.

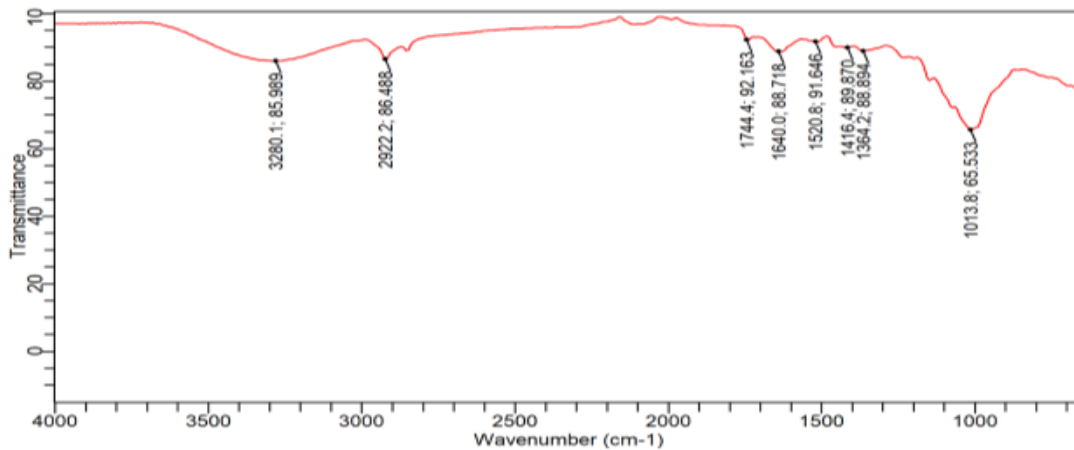
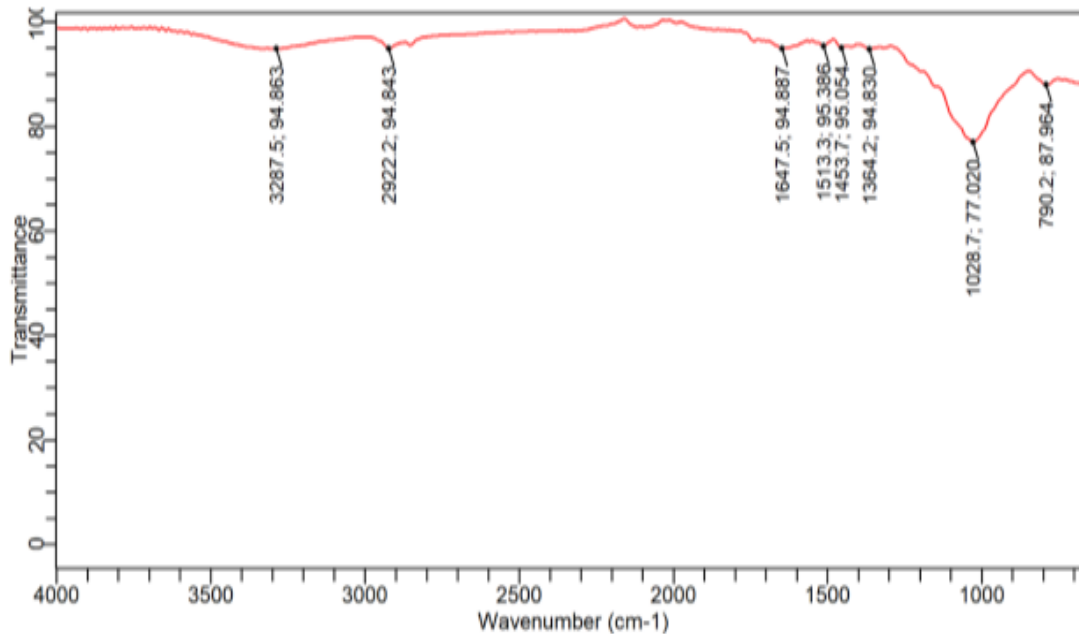


Figure 2: The FTIR spectra of raw RH Biomass

Figure 3: The FTIR spectra of RH Hydrochar



3.3 SEM Of Raw Rice Husk Biomass And Hydrochar

Structural plant organics such as hemicellulose, crystalline cellulose and lignin are contained in Rice husks. The husk total surface is affected by the presence of storage compounds such as starch



glucose and bio-oil. The SEM micrographs of the raw rice husk shown in Fig.5.0 (a) and (b) reveals regular symmetrical ridge-like strands of cells which conform to results reported by Kunal et al. and E. Danso-Boateng et al., 2021. The appearance of this waste differs from other biomass wastes as a result of the regular cellular structure observed on the exterior husk of the micrographs. However, heating at 250 °C for 2 h changed the organics to produce brittle and flaky hydrochar in Fig 5.1 (c) and (d) The surface area and porosity of the

hydrochar were increased compared to those of the raw husk. The study demonstrated that the hydrochars produced from these biomass wastes have the potential to be used as adsorbents. The SEM images showed that the hydrochars have porous structures, which resulted from denaturing of biomass structures. The surface area of the hydrochars were significantly higher than the corresponding raw biomass. The enhanced porosity and surface area of the hydrochars result in more characteristics active sites for sorption of pollutants.

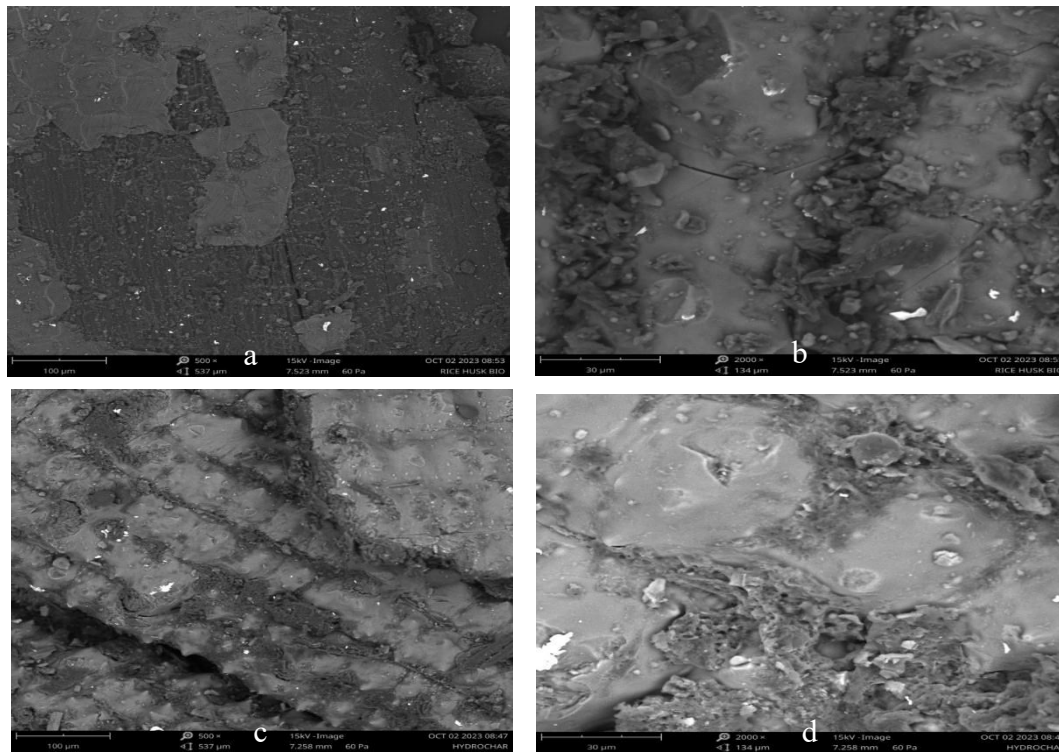


Figure 4: SEM images of RH at 1000× and 2000×: a and b raw rice husk; c and d hydrochar

3.4 XRD Of Raw Risk Husk Biomass

The highest intensity was observed at 1350 cps (count per seconds), while the weight fraction of Quartz (24%) Chabazite-Ca (42%), Urea (31%) and, syn Mellite (3%) for the Rice husk biomass.

Furthermore, the rice highest intensity was observed at 2200 cps (count per seconds) while the highest weight fractions percentage was Quartz (38%), Urea(35%), Chabazite-Ca (24%) and syn Mellite(4%).



Quantitative analysis report

General information

Analysis date	2023-10-02 10:06:58	Measurement start time	2023-10-02 09:56:11
Analyst	Administrator	Operator	Administrator
Sample name	RICE HUSK BIO	Comment	
Measured data name	C:\WallPaper\02-10-2023\RICE HUSK BIO_20231002_095112_...	Memo	

Multiple Profile

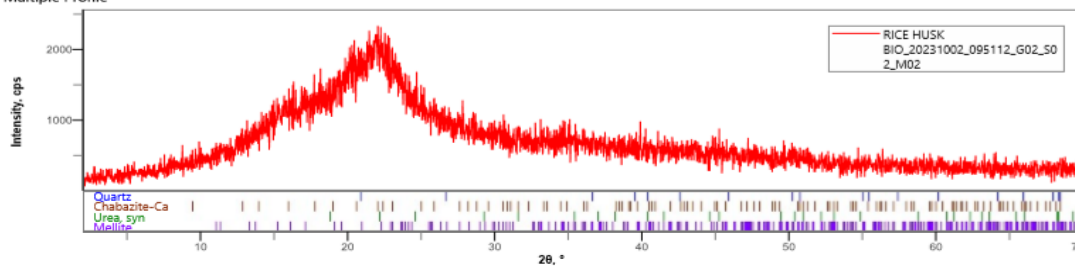


Figure 5:

Quantitative analysis report

General information

Analysis date	2023-10-02 10:09:58	Measurement start time	2023-10-02 10:00:01
Analyst	Administrator	Operator	Administrator
Sample name	HYDROCHAR	Comment	
Measured data name	C:\WallPaper\02-10-2023\HYDROCHAR_20231002_095112_G...	Memo	

Multiple Profile

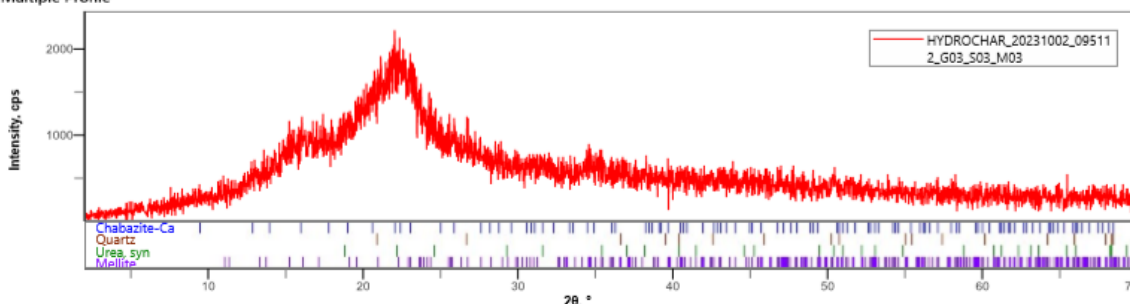


Figure 8: plots of XRD result for Raw Rice husk (a) and Hydrochar (b)

3.5 Resultant Mass Yield from the Hydrochar produced from Rice husk biomass

There was decrease in the mass of the rice husk biomass from 65 g To 58 g as the hydrochar is being produced while the dionized water of 250 ml increased to 2557.24 ml of aqueous solution while the remaing 0.76 for the gases.

4.0 CONCLUSIONS AND RECOMMENDATION

This study emphasizes the significance of efficient water treatment strategies to address the escalating global water pollution crisis. The contamination of water sources by diverse pollutants, including

heavy metals and pharmaceutical waste, poses serious threats to ecosystems and human health. Liquid-solid adsorption, particularly using hydrochar derived from biomass through hydrothermal carbonization (HTC), demonstrates promise in addressing this issue. The pharmaceutical industry, known for its utilization of heavy metals and various chemicals, presents a unique challenge in wastewater treatment. Various techniques have been employed for pollutant removal from water, each with its merits and limitations. The use of hydrochar as an adsorbent proves to be an effective and environmentally friendly solution.

Based on the findings of this study, it is recommended that further research and



development efforts be directed towards the practical implementation of hydrochar derived from hydrothermal carbonization in wastewater treatment processes. These efforts should focus on scaling up production and optimizing the efficiency of hydrochar as an adsorbent for heavy metal removal, especially in the context of pharmaceutical wastewater. Additionally, continued investigation into the influence of various factors, such as temperature, residence time, adsorbent dosage, and pH, on the performance of hydrochar is essential for fine-tuning its application in real-world scenarios. Collaboration between research institutions, environmental agencies, and industries, particularly the pharmaceutical sector, should be encouraged to promote the adoption of environmentally friendly adsorption methods to mitigate water pollution. Lastly, public awareness and policy initiatives should be advanced to address the broader issue of water pollution and its adverse effects on ecosystems and public health.

5.0 REFERENCES

1. H. Li, J. Lu, Can regional integration control transboundary water pollution? A test from the Yangtze River economic belt. *Environmental Science and Pollution Research* **27**, 28288-28305 (2020).
2. H. B. Quesada *et al.*, Surface water pollution by pharmaceuticals and an alternative of removal by low-cost adsorbents: A review. *Chemosphere* **222**, 766-780 (2019).
3. A. Bonilla-Petriciolet, D. I. Mendoza-Castillo, H. E. Reynel-Ávila, *Adsorption processes for water treatment and purification*. (Springer, 2017), vol. 256.
4. U. A. Edet, A. O. Ifelebuegu, Kinetics, isotherms, and thermodynamic modeling of the adsorption of phosphates from model wastewater using recycled brick waste. *Processes* **8**, 665 (2020).
5. T. S. Adebayo, A. A. Awosusi, I. Adeshola, Determinants of CO₂ emissions in emerging markets: an empirical evidence from MINT economies. *International Journal of Renewable Energy Development* **9**, 411 (2020).
6. R. V. P. Antero, A. C. F. Alves, S. B. de Oliveira, S. A. Ojala, S. S. Brum, Challenges and alternatives for the adequacy of hydrothermal carbonization of lignocellulosic biomass in cleaner production systems: a review. *Journal of cleaner production* **252**, 119899 (2020).
7. J. Magano, J. R. Dunetz, Large-scale carbonyl reductions in the pharmaceutical industry. *Organic Process Research & Development* **16**, 1156-1184 (2012).
8. A. Gičević, L. Hindija, A. Karačić, in *CMBEBIH 2019: Proceedings of the International Conference on Medical and Biological Engineering, 16–18 May 2019, Banja Luka, Bosnia and Herzegovina*. (Springer, 2020), pp. 581-587.
9. L. Zhang, G. Zhu, X. Ge, G. Xu, Y. Guan, Novel insights into heavy metal pollution of farmland based on reactive heavy metals (RHMs): Pollution characteristics, predictive models, and quantitative source apportionment. *Journal of hazardous materials* **360**, 32-42 (2018).
10. S. Cheng *et al.*, Application research of biochar for the remediation of soil heavy metals contamination: a review. *Molecules* **25**, 3167 (2020).
11. T. H. Tran *et al.*, Adsorption isotherms and kinetic modeling of methylene blue dye onto a carbonaceous hydrochar adsorbent derived from coffee husk waste. *Science of the Total Environment* **725**, 138325 (2020).
12. V. Gitis, N. Hankins, Water treatment chemicals: Trends and challenges. *Journal of Water Process Engineering* **25**, 34-38 (2018).
13. J. A. Okolie, S. Nanda, A. K. Dalai, J. A. Kozinski, Chemistry and specialty industrial applications of lignocellulosic biomass. *Waste and Biomass Valorization* **12**, 2145-2169 (2021).



P077 - PHYSICO-CHEMICAL AND FUNCTIONAL PROPERTIES OF TAMARIND (*TAMARINDUS INDICA*) SEED KERNEL STARCH

R.S.A Sangodare*, I. Abdulwaliyu., O. Esew, P.N. Okoro, I.I. Uduakobong, Sule, A.M., O. Olanipekun, S. Garba, I. Bello, S.A. Ibraheem

Scientific and Industrial Research Department, National Research Institute for Chemical Technology, Zaria, Nigeria.

*Corresponding author: sangodares@yahoo.com

ABSTRACT

Tamarind Seed Kernels are by-products of tamarind pulp industries and currently constitute a huge waste. This work is aimed at the production and investigation of the physical, chemical and the functional properties of tamarind starch from tamarind seed kernel obtained locally. Standard methods of analysis were employed for the various analyses. Result indicates that tamarind starch produced had low moisture content with relatively high carbohydrate content, it was found to have low lipid content, with reasonable protein content. The results of the Functional properties of the starch produced showed, 10.29 ± 0.012 g/100g, 20.01 ± 0.012 g/100g, 9.83 ± 0.005 g/100g, 23.00 ± 0.000 g/100g, 19.00 ± 0.000 g/100g, 262.5 ± 0.372 g/100g, 96.48 ± 0.026 g/100g, 26.00 ± 0.000 g/100g, 38.00 ± 0.000 (°C) and 0.76 ± 0.002 (g/cc), of swelling capacity, foam capacity, foam stability, emulsion activity, emulsion stability, water absorption capacity, oil absorption capacity, least gelation capacity, gelatinization temperature, and bulk density respectively. The result of this work suggests that tamarind seed kernel starch possesses qualities that make it excellent raw materials for the production of valuable food and pharmaceutical product.

Keywords: *Tamarind seed, Starch, Functional properties, By-product*

1.0 INTRODUCTION

Tamarind (*Tamarindus indica*) is a tropical tree native to Africa and widely cultivated in various parts of the world. While tamarind pulp and its culinary uses are well-known, the seeds of the tamarind fruit have been an underexplored source of a valuable biopolymer. Tamarind seed kernel starch (TSKS) are found to be rich in xyloglycan, amylose and amylopectin (Kumar *et al.*, 2008; Sudharsan *et al.*, 2016). Tamarind seeds are a by-product of the tamarind pulp industry and are often discarded as waste. However, tamarind seeds contain a high amount of starch (Shankaracharya, 1998). Tamarind starch can be extracted and used in a variety of food and for industrial applications. Total starch content

present in each tamarind seed is estimated to be around 65–70% and about 84.68% purified starch can be recovered from the tamarind seed (1).

Tamarind seed starch is a white, odorless, and tasteless powder. It has a granular structure and is insoluble in water and organic solvents. These starch molecules composed of (1–4)- β -d-glucan backbone substituted with side chains of α -d-xylopyranose and β -d-galactopyranosyl, (1,2)- α -d-xylopyranose linked (1–6) to glucose residues. The glucose, xylose and galactose units are present in the ratio of 2.8:2.25:1.0 (2). Tamarind seed starch has a high amylose content, which gives it good thickening and gelling properties. Defatted Tamarind seed starch has an amylose content of 27.55 wt.%



and 72.45 wt.% of amylopectin (3). It is also resistant to retrogradation, which means that it does not easily lose its thickening and gelling properties over time (4).

Tamarind seed starch can be used in a variety of food and industrial processes. In the food industry, tamarind seed starch has been used to develop biodegradable films, edible coatings, and food packaging materials (El-Siddig *et al.*, 2006). In the industrial sector, tamarind seed starch is used as an adhesive in the paper and

2.0 MATERIALS AND METHOD

2.1.0 Materials

Tamarind fruits, cheese cloth, hot air oven, Furnace,

2.1.1 Chemicals and Reagents

Chemicals and reagents used in this work were of analytical grade

2.2 Sample preparation

Tamarind seeds were procured from the local market of Sabon Gari in Sabon Gari local government, Zaria, Nigeria. Raw fruits were washed with water to remove dust and adhering pulp and sorted for infected seeds that float during washing. The cleansed seeds were dried at room temperature 72 hours, and subsequently oven dried at 65°C for 30 min to reduce moisture. The seeds were cooled then stored in clean bags at room temperature for analysis.

2.3 Method

2.3.1 Starch production

Starch was produced from tamarind seed kernel following the conventional method of starch production.

packaging industries, as sizing agent in the textile industry (Gunaseena *et al.*, 2014), and a filler and excipient used to develop new drug delivery systems and biomedical implants in pharmaceuticals (5). As a result of these wide arrays of tamarind seed starch usage, the aim of this study was to determine some functional properties of tamarind seed starch available locally.

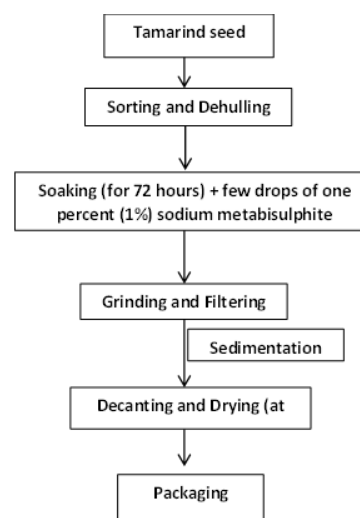


Figure 1: Stepwise traditional (conventional) wet method for the

2.4 Proximate determination

Proximate composition of the tamarind seed kernel starch was carried out using the method of AOAC 2003

2.5 Determination of functional properties

The functional properties of the tamarind seed starch were determined following the method as described in the work of Chandra and Samshe (2013).



3.0 RESULTS AND DISCUSSION

Table 1 depicts some chemical and physical characteristics of the tamarind seed kernel starch. It was observed in this study that *Tamarindus indica* kernel starch (TSKS) had moisture content of 0.069 g/100g, an indication that it was properly dried. The moisture content is considerably lower than the content (8

Table 1: Some chemical and physical characteristics of tamarind seed kernel starch

Chemical and physical characteristics	Composition
Moisture (g/100g)	0.06
Ash (g/100g)	3.01
Lipid (g/100g)	4.90
Protein (g/100g)	14.58
Total carbohydrate (g/100g)	77.45
Acidity (me/g)	5.00
pH	10.90
Solubility	0.80
Red (color measurement)	2.1
Yellow (color measurement)	2.5
Blue (color measurement)	1.5

The ash content of TSKS obtained in this study was 3.01%. Similarly, Kamla (2014) reported ash content of 3.2 g/100g, while ash contents of 4.55 g/100g, and 2.74 g/100g were reported for roasted tamarind seed, and the seed flour respectively (6). The crude lipid obtained was 4.9 g/100g, which is lower than 5.4 - 10.9 g/100g obtained in studies (8, 9). The crude protein content obtained in this study was 14.58 g/100g, while (10), revealed crude protein content within the range of 2.3 to 12.7 g/100g. The crude protein content observed in this study suggests that, the TSKS could be used as a component in baking flours and thickener in food industries and may contribute in parts to protein requirements of livestock rations. Most Colour measurement showed 2.1, 2.5, and 1.5 for red, yellow, and blue respectively. Generally, colour measurement of flour is important,

g/100g) reported in study (6). The relatively low moisture content could retard or makes the TSKS less prone to colonization by organism degradation, similar to observations reported for root, tuber and cereal starches (7).

importantly, if a starch is low in protein, it could affect the purity and crystal nature of the starch, as well as physicochemical properties of starches (11). This study therefore indicates that tamarind starch is stable in purity.

The acidity, pH, solubility of the TSKS were investigated and reported in this study. The pH value (10.9) obtained in this study falls within the acceptable range of pH for pharmaceutical grade starch. The solubility of TSKS was 0.8, which shows the magnitude of interaction between starch chains within the amorphous and crystalline domain, and is influenced by the ratio of amylose to amylopectin (12).

considering its application in food system, and sometimes, the colour of food is an important prerequisite for consumer acceptability.



Table 2: Some functional properties of tamarind seed starch

Functional Properties	
Swelling capacity (g/100g)	10.29±0.012
Foam capacity (g/100g)	20.01±0.012
Form stability (g/100g)	9.83±0.005
Emulsion activity (g/100g)	23.00±0.000
Emulsion stability (g/100g)	19.00±0.000
Water absorption capacity (g/100g)	262.05±0.372
Oil absorption capacity (g/100g)	96.48 ±0.026
Least gelation capacity (g/100g)	26.00±0.000
Gelatinization temperature (°C)	38.00±0.000
Bulk density (g/cc)	0.76±0.002

Functional properties of starch are the intrinsic physico-chemical properties that reflect the complex interaction between the composition, structure and the nature of the environment in which they are associated and measured. Table 2 highlights some of the functional properties of tamarind seed starch. The results showed 10.29±0.012 g/100g, 20.01±0.012 g/100g, 9.83±0.005 g/100g, 23.00±0.000 g/100g, 19.00±0.000 g/100g, 262.5±0.372 g/100g, 96.48 ±0.026 g/100g, 26.00±0.000 g/100g, 38.00±0.000 (°C) and 0.76±0.002 (g/cc), of swelling capacity, foam capacity, foam stability, emulsion activity, emulsion stability, water absorption capacity, oil absorption capacity, least gelation capacity, gelatinization temperature, and bulk density respectively.

The water absorption capacity (262.5±0.372 g/100g), and swelling capacity (20.01±0.012) of the starch obtained from tamarind seed kernel, is considerably lower than the water absorption capacity (1636 ± 1.33 g/100g), and swelling

capacity (20.92±0.52 g/100g) of the tamarind starch reported in the work of Singthong, (2011). High water absorption capacity of any food material strongly suggests that, it could be used in formulation of foods like dough, bakery products, cheese etc. (13). On the contrary, the oil absorption capacity (96.48 ±0.026 g/100g) obtained in this study is significantly higher than the capacity (3.35±0.03 g/100g) reported in study (Singthong, 2011). The ability of starch to absorb oil is a measure of the emulsifying potentials of the starch. The oil absorption capacity is also important as it improves the mouth feel and retains flavor (14).

Emulsion activity and stability as obtained in this study were considerable, and are key components of quality starches. Emulsion activity is related to the capacity of surface active molecules to cover oil-water interface created by mechanical homogenization, thus reducing the interfacial tension, and consequently, the more active the emulsifying starch is, the more the interfacial tension is lowered (15).

4.0 CONCLUSION AND RECOMMENDATION

Tamarind starch as investigated in this study reveal the applicability of the starch in many local and industrial processes, TSKS can be harnessed for its valuable properties either as raw material for the production of other valuable products or as an additive

5.0 REFERENCES

1. M. Chowdhury *et al.*, Biodegradable, physical and microbial analysis of tamarind seed starch infused eco-friendly bioplastics by different percentage of Arjuna powder. *Results in Engineering* **13**, 100387 (2022).
2. P. Goyal, V. Kumar, P. Sharma, Carboxymethylation of Tamarind kernel powder. *Carbohydrate Polymers* **69**, 251-255 (2007).



3. C. Chandra mohan *et al.*, Design and characterization of spice fused tamarind starch edible packaging films. *LWT - Food Science and Technology* **68**, 642-652 (2016).
 4. F. Xie, H. Zhang, Y. Wu, Y. Xia, L. Ai, Effects of tamarind seed polysaccharide on physicochemical properties of corn starch treated by high pressure homogenization. *LWT* **150**, 112010 (2021).
 5. N. Thombare, S. Srivastava, A. R. Chowdhury, Multipurpose applications of tamarind seed and kernel powder. (2014).
 6. L. O. Akajiaku, J. N. Nwosu, N. C. Onuegbu, N. E. Njoku, C. Egbeneke, Proximate, mineral and anti-nutrient composition of processed (soaked and roasted) Tamarind (*Tamarindus indica*) seed nut. *Current Research in Nutrition and Food Science Journal* **2**, 136-145 (2014).
 7. E. Nuwamanya, Y. Baguma, E. Wembabazi, P. Rubaihayo, A comparative study of the physicochemical properties of starches from root, tuber and cereal crops. *African Journal of Biotechnology* **10**, 12018-12030 (2011).
 8. E. De Caluwé, K. Halamouá, P. Van Damme, *Tamarindus indica* L.–A review of traditional uses, phytochemistry and pharmacology. *Afrika focus* **23**, 53-83 (2010).
 9. F. Khairunnuur *et al.*, Nutritional composition, in vitro antioxidant activity and *Artemia salina* L. lethality of pulp and seed of *Tamarindus indica* L. extracts. *Malaysian Journal of Nutrition* **15**, (2009).
 10. F. Makinde, T. Ayodele, Impact of Processing on Physical, Chemical and Pasting Properties of Tamarind (*T. indica*) Seed Flour. *Journal of Applied Sciences and Environmental Management* **26**, 1039-1047 (2022).
 11. R. F. Tester, W. R. Morrison, Swelling and gelatinization of cereal starches. I. Effects of amylopectin, amylose, and lipids. *Cereal chem* **67**, 551-557 (1990).
 12. J. Blazek, L. Copeland, Pasting and swelling properties of wheat flour and starch in relation to amylose content. *Carbohydrate polymers* **71**, 380-387 (2008).
 13. S. Chandra, S. Singh, D. Kumari, Evaluation of functional properties of composite flours and sensorial attributes of composite flour biscuits. *Journal of food science and technology* **52**, 3681-3688 (2015).
 14. B. I. Olu-Owolabi, T. A. Afolabi, K. O. Adebowale, Pasting, thermal, hydration, and functional properties of annealed and heat-moisture treated starch of sword bean (*Canavalia gladiata*). *International Journal of Food Properties* **14**, 157-174 (2011).
 15. Y. Wang *et al.*, Emulsion and its application in the food field: An update review. *eFood* **4**, e102 (2023).
- Chandra S and Samshe (2013). Assessment of functional properties of different flours.). *African Journal of Agricultural Research*, 8(38), 4849-4852. DOI:10.5897/AJAR2013.690.
- Singthong J (2011). Characterization of flour and starch from tamarind seed. *Starch Update 2011: The 6th International Conference on Starch Technology*, 172-178.



P078 - SILATION TECHNIQUES AS A VIABLE TECHNIQUE FOR THE DEVELOPMENT OF SUPER ADSORBENT FOR OIL SPILL CLEANUP: A REVIEW

Suleiman M.A.^{1*}, Salisu Z. M¹, Ishiaku U. S², Yakubu M.K², Elisha B.I², and Daniel D¹.

¹Textile Technology Department, National Research Institute for Chemical Technology, Zaria, Nigeria (NARICT)

²Department of Polymer and Textile Engineering, Ahmadu Bello University Zaria, Nigeria

*Corresponding Author email: mohammed_suleiman89@yahoo.com

ABSTRACT

Oil spill is a very topical issue as it causes catastrophic damage to the environment, to this effect it is imperative to develop efficient, cost effective techniques to tackle this menace. Sorbent materials especially those from natural sources in their natural state are plagued with inherent shortcomings as such modification techniques such as Silation, grafting, acetylation, etc. have been employed to achieve hydrophobicity to effect oil spill cleanup. Superhydrophobic sorbents have attracted remarkable attention especially in their tremendous capacity for efficient crude oil-water separation application in oil spill recovery. This paper provides an overview on Silation technique modifications of sorbents surface energy and chemistry to achieve super hydrophobicity thus providing a viable technique for the development of super hydrophobic sorbent. This technique influences vital sorbent properties such as sorbent density, pore volumes, specific surface, average pore sizes and porosity depending on the type of silating agents employed this in turn affect the absorption and adsorption capacities and capabilities of the resulting sorbent.

Keywords: Oil spill, Hydrophobicity, Sorbent, Superhydrophobic, Silation

1.0 INTRODUCTION

Oil spill has a catastrophic impact on the environment, (1-3) as such attracts immense attention of researchers around the globe to ameliorate this effect. Oil spill is the discharge of hydrocarbon into the environments due to human activities (4-6) resulting in pollution. Several methods have been employed to tackle this devastating oil pollution. Methods such as chemical, physical, biological have been employed. Each method / strategy has its comparative merit and demerit. In chemical methods, in-situ burning, dispersions are costly with high secondary pollution especially in the case of burning. Biological method is affected by numerous factors such as pH, temperature, organic species to mention but a few since microorganism is employed (5) however physical method booms and skimmer are employed to hold the oil. These method despite their merit have been reported to be limited (7) an efficient and economic method is the sorption technique which have attracted attention of researcher in recent times. This sorption technique is environmentally benign especially bio based sourced adsorbents as they create less secondary pollution (8). However, these adsorbent have shortcomings of low separation efficiency and recovery difficulty despite been abundant, cheap and easy to use (5). Researcher in their quest to improve the capacity of

sorbent resulted in modification of adsorbent to achieve hydrophobic or super hydrophobic sorbents, as adsorption is the process where pollutant is sorbed onto/into a solid surface by physical forces with high contact angles. Recent surface modification techniques include Grafting (9-11) Acetylation (12, 13) Silation (14) and so on. To achieve hydrophobicity. This hydrophobicity can be achieved by either modifying the surface chemistry or morphology to attain a contact angle of between 90° to 149°. These hydrophobic surfaces have low surface energy and surface roughness (15). Researchers in their quest to increase the capacity of the sorbent facilitated the development of super hydrophobic sorbent with contact angle above 150°.

Recent development in super hydrophobic adsorbent results in promising three-dimensional aerogel for oil spill treatment prepared from inorganic sources such as polypropylene fibres, graphene and have been reported to have secondary pollution due to its environmentally malignant. These necessitate the use of biodegradable sources such as cellulose which have advantages of being abundant and cheap which will enhance its disposability. Most natural based sorbent have inherent shortcomings of buoyancy, poor selectivity towards crude and high affinity towards water due to the presence of -OH groups in the fibre



structure. These inherent shortcomings provide a nexus that facilitates surface modification employing various techniques as earlier mentioned (16).

2.0 SURFACE WETTING PHENOMENA

Surface morphology and chemistry to a great extent determine the wettability of surfaces and contact angles. To achieve super hydrophobic surface certain parameters such as surface structure and energy have to be lowered by either coating, adhesion or modification of the surface structure or chemistry to emulate Cassie-Baxter or Wenzel effect (17). Examples that occur in nature include Lotus leaf (18), shark skin (19), rose petals (20), water strider legs (21) and butterfly wings. Surface wetting property of a surface is crucial in oil-water separation as it applies to crude oil in water. These properties (surface roughness and energy) enhance the crude oil absorption and adsorption on the surface of the adsorbent (22). Essentially, Superhydrophobic surfaces have the lowest free energy or associated high surface roughness with minimal interaction with water droplet and the corresponding surface (22). The state of wetting of a surface shown as the angle (θ) of a liquid in solid surface in the presence of a different fluid is shown below denoted as

$$\cos \theta = \frac{\gamma_{SG} - \gamma_{LS}}{\gamma_{LG}} \dots \dots \dots (a)$$

Where θ_Y denotes the equilibrium static contact angle of the liquid in the presence of the solid (adsorbent) and gas. γ_{SG} , γ_{LS} , γ_{LG} represent the

solid-gas, liquid-solid, and liquid-gas interfacial tension respectively the wettability of the flat surface is represented as the contact angle of water droplet and is given by the Young's equation (23) while the surface roughness is accounted for by Wenzel state given as

$$\cos \theta_{App} = r \cos \theta_Y \dots \dots \dots (b)$$

Where r is the ratio of the actual rough surface area to that of the horizontal projected area and is the apparent contact angle θ_{App} where $r=1$ gives a perfectly planar surface while when $r>1$ for a rough surface given in figure (b) and these Wenzel equation is only valid for homogeneous solid-liquid interfaces.

The Cassie-Baxter (θ_{CB}) model given by shown in figure (c) is for heterogeneous interfaces with equation expressed as (24) expanded the Wenzel equation to give:

$$\cos \theta_{CB} = f_1 \cos \theta_Y - f_2 \dots \dots \dots (c)$$

Where (θ_{CB}) is the contact angle on rough surface and f_1 , f_2 are the areas fraction of solid and vapour on the surface respectively which is the surface fraction and varies from 0-1. Where f is 0 the surface is super hydrophobic and when f is 1 there is complete wetted i.e., super hydrophilic. These extreme non-wetting state gives the super hydrophobicity. This non-wetting effect is regarded as the lotus effect (super non-wetting) also known as super hydrophobic effect

Table 1: Hydrophilic and hydrophobic surface properties retrieved from adapted from (17).

Properties	Hydrophilic surface	Hydrophobic surfaces	Super hydrophobic surfaces
Contact angle	Low (<90°)	High (>90°)	Very high (>150°)
Adhesiveness to water	Good	poor	non
Wettability	Good	Poor	very poor
Solid surface free energy	High	Low	lowest



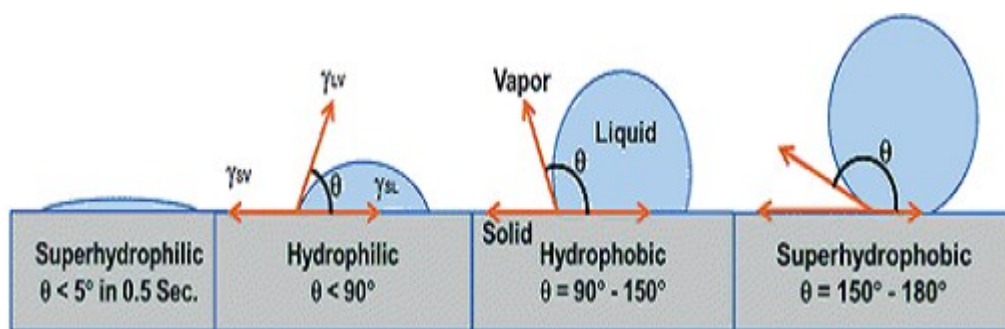


Figure 1: Various condition of contact angle of drop of liquid on the surface adopted from (17)

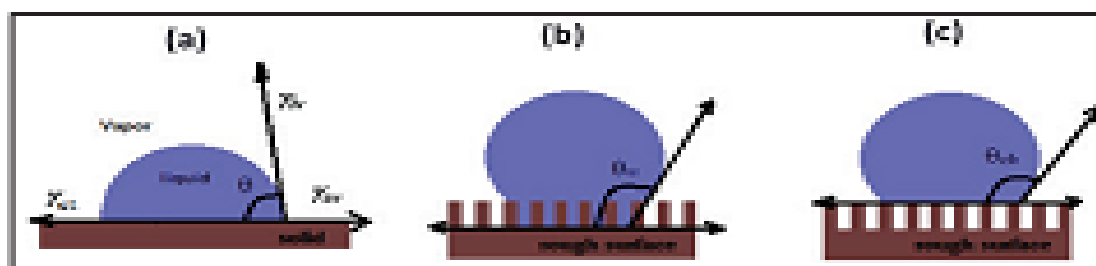


Figure 2: wetting behavior in different state (a) Young's model (b) Wenzel model and (c) Cassie-Baxter model also adopted from (17).

3.0 WETTING STATE AT MOLECULAR LEVEL

The presence of functional group influences the behavior of the surfaces. It affects the wettability especially at molecular level. Functional groups such as $-OH$, COO^- , $-COOH$, NH_2 , $-OSO_3^-$, presence at the surface affects the surface energy by increasing the surface energy resulting in hydrophilic surface with contact angle below 90° . However, Silation introduces $Si-O-Si(CH_3)$ functional group to the surface thereby reducing the surface energy resulting to a hydrophobic surface. Consequently, the presence of functional groups such as styrene monomer also introduce hydrophobicity to the surface.

Furthermore, functional groups such as carboxylate and sulfonate that ionize tends to produce hydrophilic surface. But aromatic chains with their steric hindrance property induce hydrophobic property and surfaces with low dielectric constant will not interact through Van der Waals or Hydrogen bonds with polar functional groups. Increasing the affinity of the surface which in turn increase the surface energy resulting in hydrophilicity of the surface (17).

4.0 SILATION TECHNIQUE TO PRODUCE SUPER HYDROPHOBIC SURFACES

Silation is one of the techniques to produce super hydrophobic surface of the sorbents. This simply entails the replacement of silanol polar group by non-polar functional radicals from silane. The effectiveness of silation depends on the type of silylating agents used for silation and the co-precursors (25). These also affect physicochemical properties of the sorbents such as specific area, pore volume, density and porosity. Silation by mono, di, tri alkyl or aryl silylating agents gives different contact angles (26). However Tri alkyl silanes such as trimethylchlorosilane (TMCS) and hexamethyldisilazane (HMDZ) gave contact angles of above 150° (162° and 165°) respectively with a porosity of about 96.9 %. These silation agents results to an increased surface roughness by the increased presence of $-Si-(CH_3)_3$ group on the surface which gives a contact angle of 0° to 165° which corresponds to superhydrophobic surface.

Since oil spill cleanup is of utmost importance, pores collapse control and capillary tension that develops during solvent evaporation and also to satisfy the super hydrophobic behaviour of the sorbent surface, modification should be by silation. The type of silylating agent especially those of trifunctional silanes have appeared to produce lower surface area and lower degree of hydrophobicity compared to that of mono-fuctional agents (27), (27) compared the performance



of aerogels silyated with mono Trimethylchlorosilane (TMCS), tri Methyltrimethoxysilane (MTMS), Methyltriethoxysilane (MTES) or organofunctional silanes Methacryloxypropyltrimethoxysilane (MEMO), 3-glycidyloxypropyltrimethoxysilane (GLYMO) for oil spill cleanup. It is evident that TMCS gave the highest specific area attributed to the formation of stable and efficient non-polar trimethylsilyl group of TMCS in the structure thus increasing the pore volume and average pore sizes however with a reduced density with a super hydrophobicity of 152° . Consequently, those of MTMS, MTES

which are tri- functional silane in their structure attaches with three hydroxyl groups on the surface but only one-polar group remains on the surface resulting to a reduced contact angle. However, having increased density of the sorbent as shown in figure 3. The branching structure of MTMS, MEMO, MTES and GLYMO with large acrylate and epoxy groups. These functional groups may decelerate the Silation reaction rate as a result of steric hindrance resulting in a reduced porosity and pore volume and increased density however gave contact angles of 142° , 120° , 98° , 42° respectively (27).

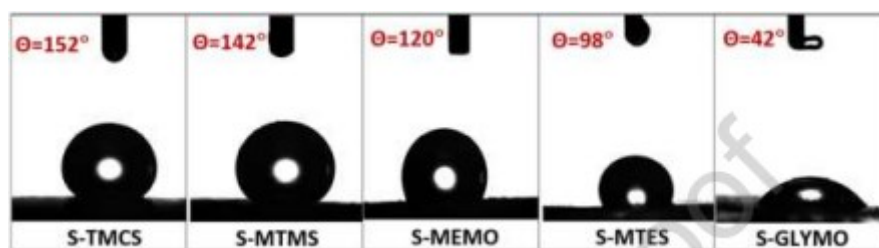


Figure 3: Contact angles images of sorbents surfaces modified with different silating agents adopted from (27).

5.0 CONCLUSION

In this paper, astonishing capacities of super hydrophobic sorbents in combating crude oil spill have been covered. Silation agents especially those of tri alkyl silane such as TCMS produce super hydrophobic sorbents with contact angel above 150° . These silation agents affects essential sorbent characteristics such as pore volume, density and porosity which affects the efficacy of the sorbent in crude oil cleanup.

6.0 REFERENCES

1. H. Bidgoli, Y. Mortazavi, A. A. Khodadadi, A functionalized nano-structured cellulosic sorbent aerogel for oil spill cleanup:

Synthesis and characterization. *Journal of hazardous materials* **366**, 229-239 (2019).

2. J. Yen Tan, S. Yan Low, Z. H. Ban, P. Siwayanan, A Review on Oil Spill Clean-up Using Bio-Sorbent Materials with Special Emphasis on Utilization of Kenaf Core Fibers. *BioResources* **16**, (2021).

3. J. Wang, S. Liu, Remodeling of raw cotton fiber into flexible, squeezing-resistant macroporous cellulose aerogel with high oil retention capability for oil/water separation. *Separation and Purification Technology* **221**, 303-310 (2019).

4. H. Cheng *et al.*, Cotton aerogels and cotton-cellulose aerogels from environmental waste for oil



spillage cleanup. *Materials & Design* **130**, 452-458 (2017).

5. M. Chhajed, C. Yadav, A. K. Agrawal, P. K. Maji, Esterified superhydrophobic nanofibrillated cellulose based aerogel for oil spill treatment. *Carbohydrate polymers* **226**, 115286 (2019).

6. M. A. Mahmoud, Oil spill cleanup by raw flax fiber: Modification effect, sorption isotherm, kinetics and thermodynamics. *Arabian Journal of Chemistry* **13**, 5553-5563 (2020).

7. F. Rafieian, M. Hosseini, M. Jonoobi, Q. Yu, Development of hydrophobic nanocellulose-based aerogel via chemical vapor deposition for oil separation for water treatment. *Cellulose* **25**, 4695-4710 (2018).

8. H. Maleki, Recent advances in aerogels for environmental remediation applications: A review. *Chemical Engineering Journal* **300**, 98-118 (2016).

9. K. Jarrah, S. Hisaindee, M. H. Al-Sayah, Preparation of oil sorbents by solvent-free grafting of cellulose cotton fibers. *Cellulose* **25**, 4093-4106 (2018).

10. Z. M. Salisu, I. S. Umaru, D. Abdullahi, M. K. Yakubu, Optimisation of crude oil adsorbent developed from a modified styrene kenaf shive. *Journal of Materials Science and Chemical Engineering* **7**, 38-51 (2019).

11. Y. Zuo, X. He, P. Li, W. Li, Y. Wu, Preparation and characterization of hydrophobically grafted starches by in situ solid phase polymerization. *Polymers* **11**, 72 (2019).

12. R. Asadpour, N. B. Sapari, M. H. Isa, S. Kakooei, Acetylation of oil palm empty fruit bunch fiber as an adsorbent for removal of crude oil. *Environmental Science and Pollution Research* **23**, 11740-11750 (2016).

13. W. Chai *et al.*, Pomelo peel modified with acetic anhydride and styrene as new sorbents for removal of oil pollution. *Carbohydrate polymers* **132**, 245-251 (2015).

14. Y. Li *et al.*, Preparation of corn straw based spongy aerogel for spillage oil capture. *Korean Journal of Chemical Engineering* **35**, 1119-1127 (2018).

15. S. Rasouli, N. Rezaei, H. Hamed, S. Zendejboudi, X. Duan, Superhydrophobic and superoleophilic membranes for oil-water separation application: A comprehensive review. *Materials & Design* **204**, 109599 (2021).

16. M. Zamparas, D. Tzivras, V. Dracopoulos, T. Ioannides, Application of sorbents for oil spill cleanup focusing on natural-based modified materials: A review. *Molecules* **25**, 4522 (2020).

17. K. Manoharan, S. Bhattacharya, Superhydrophobic surfaces review: Functional application, fabrication techniques and limitations. *Journal of Micromanufacturing* **2**, 59-78 (2019).

18. L. Feng *et al.*, Super-hydrophobic surfaces: from natural to artificial. *Advanced materials* **14**, 1857-1860 (2002).

19. Y. Liu, G. Li, A new method for producing "Lotus Effect" on a biomimetic shark skin. *Journal of colloid and interface science* **388**, 235-242 (2012).

20. Y. Zheng, X. Gao, L. Jiang, Directional adhesion of superhydrophobic butterfly wings. *Soft Matter* **3**, 178-182 (2007).

21. X. Gao, L. Jiang, Water-repellent legs of water striders. *nature* **432**, 36-36 (2004).

22. K. K. Chenab, B. Sohrabi, A. Rahmanzadeh, Superhydrophobicity: advanced biological and biomedical applications. *Biomaterials science* **7**, 3110-3137 (2019).

23. Y. Thomas, An essay on the cohesion of fluids. *Philos. Trans. R. Soc. London* **95**, 65-87 (1805).

24. A. Cassie, S. Baxter, Wettability of porous surfaces. *Transactions of the Faraday society* **40**, 546-551 (1944).

25. A. B. Gurav *et al.*, Porous water repellent silica coatings on glass by sol-gel method. *Journal of Porous Materials* **18**, 361-367 (2011).

26. A. P. Rao, A. V. Rao, G. Pajonk, Hydrophobic and physical properties of the ambient pressure dried silica aerogels with sodium silicate precursor using various surface modification agents. *Applied surface science* **253**, 6032-6040 (2007).

27. S. S. Çok, F. Koç, N. Gizli, Lightweight and highly hydrophobic silica aerogels dried in ambient pressure for an efficient oil/organic solvent adsorption. *Journal of Hazardous Materials* **408**, 124858 (2021).



P079 - DETERMINATION OF LD50, FECUNDITY AND LOCOMOTOR EFFECT OF AQUEOUS BEETROOT (*BETA VULGARIS*) PLANT EXTRACT IN THE PRODUCTION OF COLORANT FOR FOOD AND PHARMACEUTICAL INDUSTRY USING *DROSOPHILA MELANOGASTER*

Gero M., Salisu Z.M., Ukanah P.S., Barminas J.T. Chibuzo-Anakor N.C., Daniel D., Umar I.S and Oddy-Obi C.I.

Department of Textile Technology, National Research Institute for Chemical Technology, Zaria
Corresponding Author: geromohammed@yahoo.com

ABSTRACT

The study aimed at assessing the LD50, fecundity and locomotor effect of Beetroot (*Beta vulgaris*) in *Drosophila melanogaster*. To assess the lethal dose, or LD50, the experimental animals (1-4 days old) of both sexes were given oral exposure to a range of doses of the plant extract for seven days (1 mg, 10 mg, 50 mg, 100 mg, 200 mg, 250 mg, 300 mg, 350 mg, 400 mg, 450 mg). The fecundity test and locomotor effect in the fruit fly, a five-day treatment period using 50 mg, 100 mg, 200 mg, and 300 mg doses of the extract was conducted. Beetroot (*Beta vulgaris*) aqueous extract was shown to have a 295.3 mg LD50 in *D. melanogaster*, indicating that the plant extract is generally harmless. The outcome also demonstrated that there was no significant difference between the treated and untreated flies in terms of fecundity or locomotor behaviour ($P > 0.05$). The fruit fly's ability to reproduce as well as its ability to move is therefore not considerably impacted by the extract at the used concentrations. The tested concentrations used in this research are relatively safe (because of high LD50 295.3 mg) in the fruit fly and slightly increase the emergence of new fly with no observable negative effect in locomotor activity. This makes the plant sweet able material for colorant for food and pharmaceutical industry.

Keywords: Beetroot, locomotor, fecundity, *Drosophila melanogaster* and lethal dose

1.0 Introduction

Beetroot (*Beta vulgaris*) also known as the common beet, garden beet, red beet, or table beet is a root vegetable in the *Chenopodiaceae* family. Other vegetables in this family include spinach, chard, quinoa, and sugar beets [1]. It is noted that not all medicinal plants are safe for consumption in the crude form. Some level of toxicity may arise as a result of potential toxic compounds they contain and the application of pesticide during cultivation [2,3]. Beetroot is grown widely in Germany and France and in lesser amounts in other European countries, Africa, Asia and South America. It is now a popular salad vegetable. Beetroot is a true biennial that produces thickened root and a rosette of leaves during the first year followed by flowers and seeds during the second year. They are mainly grown for their swollen roots but the leaves can also be eaten as spinach. The flowers are very small with a diameter of 3 to 5 mm and are produced in dense spikes. They are

green or tinged reddish, with five petals. The fruit is a cluster of hard nut lets [4]. Besides other active chemicals, beetroots contain a unique class of water-soluble, non-phenolic antioxidants, the betalains, red betacyanins and yellow betaxanthines [5]. Beetroots have been shown to contain a variety of minerals: calcium, iron, magnesium, potassium, selenium, zinc) and vitamins (vitamin C, thiamin, vitamin B6, vitamin A, beta carotene, vitamin E, and vitamin K [6].

Studies have shown that many African countries still rely on traditional medicine to meet different health needs [7]. Extracts of plants are used for the treatment of various diseases which forms the basis for all traditional systems of medicine [8]. Recent reports indicate that *Beta vulgaris* extracts (root) possess antihypertensive, antioxidant [9], anti-inflammatory, and hepatoprotective activities [10, 11, 12, 13]. Previously, red beetroot extract has been demonstrated to be an effective multiorgan tumour suppressing agent in laboratory animals



[12,14,15].

One major and overriding criterion in the selection of herbal medicines for use in health services is safety. Plants extracts should not only be efficacious but safe for consumption [16]. To ensure the safety of these products given their rapidly increasing use, there is need to assess the risk associated with herbal medicine and products derived from them [17]. The toxic effects produced by the administration of drugs as derivatives of these plants are much more a serious problem than the disease itself [18]. Although *Beta vulgaris* is used worldwide in traditional medicine, toxicological data on the plant are scarce. This study was designed to assess the toxicity of the root aqueous extract in *Drosophila melanogaster*, with the purpose of providing information on the safe use of this plant.

2. MATERIALS AND METHODS

Plant

material

Beetroot was obtained from a local vendor at the vegetable market in zaria. The plant was identified by a Taxonomist at the Department of Bioresource centre at the National Research Institute for Chemical Technology Basawa Zaria, Kaduna State, Nigeria. A voucher number UBHB 374 was obtained and deposited in the Herbarium. The beetroots were washed thoroughly so as to remove any of the mud or impurities from the surfaces, peeled using a kitchen knife and chopped finely into small bits of about 2cm each. The chopped beetroot was blended using an electric Moulinex Blender LM 2411, Wanette, Oklahoma, USA. Distilled water (200-300 ml) was added to make it into a smooth consistent paste or juice, until no solid beetroot was visible. The juice was extracted using a muslin cloth and stored in a plastic container, rapped with black cellophane so as to prevent fermentation and auto-oxidation. The juice obtained was freeze dried [Armfield vacuum freeze dryer Model FT 33, Ringwood, England] and ready for use. The freeze dried sample of 10% beetroot juice was evaluated to contain 9808.0 mg GAE/100 ml polyphenols and 8334.0 mg QE/100 ml flavonoids [21].

2.2 *Drosophila* Stock

The animal stock (Harwich strain of both sexes) used in this work was obtained from the *Drosophila* Laboratory Africa Center of Excellence in Phytomedicine Research and Development (ACEPRD), University of Jos, Nigeria. The flies were maintained and rare using corn meal food. The

food contained, 100 gm of yellow-corn powder, 10 gm dry yeast (inactive and not hydrolyzed), 10 gm of agar-agar powder, 1 gm of methyl- parabin dissolve in 10 ml absolute ethanol and portable water adds to 1000 ml. All experiments were carried out using the same batch of corn powder, agar-agar powder, and Yeast. The fly's culture was maintained at 23 + 1°C, relative humidity ≈60% and 12 hours' dark and light cycle.

2.3 Equipment and Reagents

The equipment used in the work include; Eppendorf centrifuge 5427 R, Jenway 7315 UVSpectrophotometer, Metlar analytical balance MT-200B, glass stirring rod, beakers, plastic vails (50 cm height, 2 cm diameter), Rotary evaporator (RE-52A by PEC MEDICAL USA), hand magnifying lens, counting brushes, filter paper, cotton wool. Reagents used include; Analytical grade methanol (CAS: 67-56-1, Lot: 1214788) by Fisher scientific UK, 70% ethanol, phosphate buffer saline (PBS), distilled water. All other solutions, chemicals and buffers used were prepared fresh using glass wires.

2.4 Methods

2.4.1 Plant material extraction

400 gm of pulverized Beetroot (*Beta vulgaris*) root was macerated in 2 L of distil water by cool extraction for 72 hours in an Amber bottle with occasional shaking. After the extraction period, the mixture in the bottle was filtered using Whatman No 1 filter paper; the filtrate was concentrated in a rotary evaporator at 48°C and later dried using a freeze dryer. The root aqueous extract was used subsequently to determine the phytochemicals, lethal dose (LD50), fecundity and locomotor, reproductive, negative geotaxis effect using the *D. melanogaster* model.

2.4.2 Experimental design

Determination of LD50 and assessment of the effect of root aqueous extract of beet root on the reproductive capacity (fecundity) and climbing behaviour of *Drosophila* was done using a short-term dietary regimen. Newly eclosed flies (both sexes), 1-4 days old were randomly divided into 11 separate groups, each group houses 60 flies in a 50 ml plastic vails and each group has 4 replicates were exposed to graded concentrations (10 mg, 20 mg, 30 mg and 40 mg, 50mg, 60mg) of the plant extract or without extract (control) for 7 days. The concentrations of the extract and duration for



treatment employed in this work were predetermined from a pilot study (data not shown) and LD50 plot (Fig. 1). Newly emerged flies were used for this research work because it represents an important stage of organogenesis in animals. Therefore, the developing organism is more fragile and susceptible to toxicants due to low and unmaturing immunity and underdeveloped organ system compare to the adults, as such can easily be affected by any chemical change within its immediate surrounding environment [20].

- Group I - Flies fed with food + 0 mg Extract (control)
- Group II - Flies fed with food + 10 mg Extract (exposed)
- Group III - Flies fed with food + 20 mg Extract (exposed)
- Group IV – Flies fed with food + 30 mg Extract (exposed)
- Group V – Flies fed with food +40 mg Extract (exposed).
- Group VI – Flies fed with food +50 mg Extract (exposed).
- Group VII – Flies fed with food +60 mg extract (exposed).

2.4.3 Determination of 7 days LD50

The lethal dose (LD50) was determined using a protocol previously described by Iorji et al. [25]. Briefly, sixty (60) flies (both sexes) of 1-4day old were anesthetized under light ice, counted and exposed to 10 graded concentrations (100 mg, 200 mg, 300 mg, 400 mg, 500 mg, 600 mg, 700 mg, 800 mg, 900 mg, 1000 mg) of the plant extract and 1 ml distilled water (control) in 10 gm food for 7 days. Cumulative fly death was recorded every 24 hours for the duration of the treatment.

2.4.4 five-day treatment for fecundity and negative geotaxis

From a 14 days' survival curve (result not shown), 5 days' treatment was set-up with flies' survival above 70% to determine short time effects of the plant extract on the reproductive (fecundity) and locomotor capacities in the fruit fly. The protocol previously described by Abolaji et al. [20] was adopted. Briefly, sixty flies aged 1-4 days old were treated with 10 mg, 20 mg, 30 mg, and 50 mg and 60mg of the extract per 10 gm fly food respectively.

2.4.5 Reproductive effect

The fecundity of drosophila was studied after exposure of the flies to the test material according to the method previously described by Charpentier et al. [26] with slight adjustment. Briefly, 10 flies (10- males, 10- females) were sorted out from each 5 days' treatment group and control under ice anesthesia, the flies were allowed to recover fully for 20 mins and transferred into vials containing fresh fly food that has no treatment and allowed to mate and lay egg for 24 hours. After the allotted time (48 hours), the flies were removed. The experimental set up was observed every 24 hours for 14 days for the possible emergence of new flies. The average number of flies that emerged during the duration of the experiment (14 days) is a direct measure of the viable egg laid and hence, a measure of the effect of the plant extract in the fecundity of *Drosophila melanogaster* [19].

2.4.6 Negative geotaxis (Climbing) assay

The locomotor or climbing performance of *D. melanogaster* exposed to concentrations of Beetroot (*Beta vulgaris*) extract and control were investigated via negative geotaxis assay according to the protocol previously described by Abolaji et al. [20]. Briefly, 10 flies treated with the plant extract and untreated(control) were immobilized under light ice anesthesia and placed separately in vertical labeled glass vials (length, 15 cm; diameter, 1.5 cm) and allowed for 20 min to recover.

Thus, the flies were gently tapped to the bottom of the column. In 6 s, the number of flies that climbed up to the 6 cm mark of the column, as well as those that remained below this mark was scored. Data obtained were expressed as the percentage of flies that escaped beyond the 6 cm mark in 6 s. The score of each group was an average of three independent trials for each group of treated and control flies.

2.5 Statistical Analysis

The data were expressed as mean±SEM. The analysis was carried out using (ANOVA) followed by Tukey's posthoc test to identify statistically different test groups. The results were considered statistically significant at $P < 0.05$.



3. Results and Discussion

Table1: Phytochemical Constituents of Beetroot Extracts.

S/N	Parameters	Extract
1	Tannin	+ve
2	Saponin	+ve
3	Alkaloids	+ve
4	Anthroquinones	-ve
5	Flavonoid	+ve
6	Steroids	+ve
7	Terpenoids	+ve
8	Phenols	+ve

3.1 7 Days LD50

The lethal dose (LD50), defined as the concentration of test material in a normal fly food (media) that cause 50% of fly death in 7 days [27]. The concentration for use in the research was obtained from exposing the flies to ten staggered concentrations (stated above) of the plant extract for 7 days. Thereafter, the LD50 of the plant extract

was determined to be 295.3 mg. This value of LD50 shows that the extract is relatively safe.

3.2 Fecundity

The fecundity of the treated and untreated flies did not show any difference. This means that while taking this plant extract, patients' reproductive capacity is not affected negatively since both the exposed and unexposed groups were able to emerge appropriately.

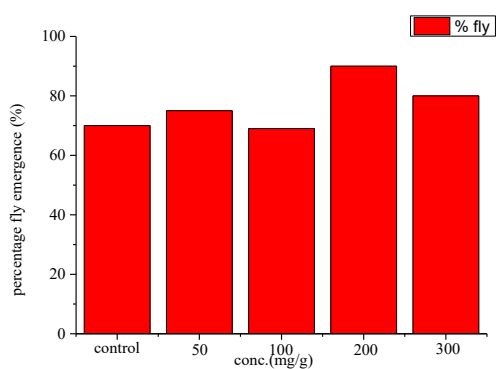


figure 1.0: percentage of fly emergence at different concentration

3.3 Locomotor Effect

The ability of the treated and untreated flies to climb against gravity was not altered by the

administration of the plant extract. This further demonstrated the safety of this plant material on motor co-ordination in *Drosophila melanogaster*.



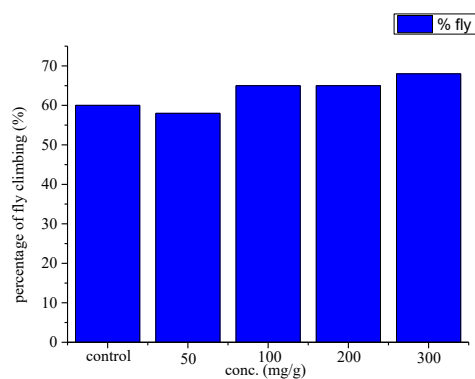


figure 1.2:percentage of fly climbing at different concentration

3.4 Discussion

The concentration of root aqueous extract of beetroot that is capable of killing 50% (LD50) of the population in *D. melanogaster* was found to be 295.3 mg/10 g fly medium. This value showed that the extract is relatively safe. This is a confirmation of the used of this plant material for different purposes [22, 28].

From the result, we discovered that the plant extract did not alter the reproductive capacity of the experimental animal. Hence, there was no significant difference ($P > 0.05$ vs control) between the treated groups as compared to the control. Though the result showed that at 600 mg concentration, demonstrated a slide increased in the percentage of flies that enclosed when compared to the control (and other concentrations). But the difference was not significant ($P > 0.05$). This observed increase in fertility in *D. melanogaster* by the plant extract may in part suggests why oil from this plant is used to improved fertility by local women in Ethiopia [21,23,24].

INTERESTS

Authors have declared that no competing interests exist.

References

- 1 Goldman IL, Navazio JP :Table beet. In: Prohens J, Nuez F (eds) Vegetables I Asteraceae, Brassicaceae, Chenopodiaceae, and Cucurbitaceae. Springer, New York, 219–238. 2008.
- 2 Annan K, Dickson RA, Amonsah IK, Nooni IK: The heavy metal contents of some selected medicinal plants sampled from different geographical locations. *Pharmacognosy Res* 5: 103-108. 2013.
- 3 Folashade KO, Omoregie EH, Ochogu AP: Standardization of herbal medicines- A review. *International Journal of Biodiversity and Conservation* 4: 101-112. 2012.
- 4 Kovacevic SZ, Tepic AN, Jevric LR, Kuzmanovic SOP, Vidovic SS, Sumin ZM, Ilin ZM: Chemometric guidelines for selection of cultivation conditions Influencing the antioxidant potential of beetroot extracts. *Journal Computers and Electronics in Agriculture* 118: 332-339. 2015.
- 5 Al-Aboud NM: Effect of red beetroot (*Beta vulgaris* L.) intake on the level of some haematological tests in a group of female volunteers. *ISABB J. Food Agric. Sci.* 8: 10-17. 2018.
- 6 U.S. Department of Agriculture. USDA National Nutrient Database for Standard Reference, Release 26. Available at: <http://ndb.nal.usda.gov>. 2011
- 7 Oyeboode O, Kandala N, Chilton PJ, Lilford RJ: Use of traditional medicine in middle-income countries a WHO-SAGE study. *Health Policy Plan* 31: 984-991. 2016.
- 8 Etuk EU, Agaie BM, Onyeyili PA, Ottah CU: Toxicological studies of aqueous stem bark extract of *Boswellia dalzielii* in albino rats. *Indian J. Pharmacol* 38: 359-360. 2006.
- 9 Ninfali P, Angelino D: Nutritional and functional potential of *Beta vulgaris* *cicla* and *rubra*. *Fitoterapia* 89: 188–199. 2013.



- 10 Singh B, Hathan BS: Chemical composition, functional properties and processing of Beetroot-a review. *International Journal of Scientific and Engineering Research* 5: 679-684. 2014.
- 11 Jain SGV, Sharma PK: Anti-inflammatory activity of aqueous extract of *Beta vulgaris* L. *Journal of Basic and Clinical Pharmacy* 2: 83–86. 2011.
- 12 Chakole R, Zade S, Charde M: Antioxidant and anti-inflammatory activity of ethanolic extract of *Beta vulgaris* Linn. roots. *International Journal of Biomedical and Advance Research* 2: 124–130. 2011.
- 13 Venugopal K, Arul T, Kavitha K, Moodley MK, Rajagopal K, Balabhaskar, Bhaskar M: The impact of anticancer activity upon *Beta vulgaris* extract mediated biosynthesized silver nanoparticles (ag-NPs) against human breast (MCF-7), lung (A549) and pharynx (Hep-2) cancer cell lines. *Journal of Phytochemistry and Phytobiology, B: Biology* 173: 99-107. 2017.
- 14 Kapadia GJ, Azuine MA, Rao GS, Arai T, Iida A, Tokuda H: Cytotoxic Effect of the Red Beetroot (*Beta vulgaris* L.) Extract compared to Doxorubicin (Adriamycin) in the Human Prostate (PC- 3) and Breast (MCF-7) Cancer Cell Lines. *Anti-Cancer Agents in Medicinal Chemistry* 11: 280-284. 2011.
- 15 Reddy MK, Alexander-Lindo RL, Nair MG: Relative inhibition of lipid peroxidation, cyclooxygenase enzymes, and human tumor cell proliferation by natural food colors. *Journal of Agricultural and Food Chemistry* 53: 9268–9273. 2005.
- 16 Bulus T, Atawodi SE, Mamman M: Acute toxicity effect of the aqueous extract of *Terminalia avicennioides* on white albino rats. *Science World Journal* 6: 1-4. 2011.
- 17 WHO: National Policy on traditional medicine and regulation of herbal medicine: Report of a WHO Global Survey. WHO, ISBN:9241593237, Geneva. 2005.
- 18 Siddique NA, Meyerb M, Najni AK, Akram M: Evaluation of antioxidants activity, quantitative estimation of phenols and flavonoids in different parts of *Aegle armelo*. *African Journal of Plant Science* 4: 1–5. 2010.
19. Hanson FB, Ferris FR. A quantitative study of fecundity in *Drosophila malenogaster*. *J. Exp. Zool.* 1929;54(3):485–506.
20. Abolaji AO, et al. Ovotoxicants 4-vinylcyclohexene 1,2-monoepoxide and 4-vinylcyclohexene diepoxide disrupt redox status and modify different electrophile sensitive target enzymes and genes in *Drosophila melanogaster*. *Redox Biol.* 2015;5:328–339.
21. Lorenzo DN, Li MG, Mische SE, Armbrust KR, Ronum LPW, Hays TS. Spectrin mutations that cause spinocerebellar ataxia type 5 impair axonal transport and induce neurodegeneration in *Drosophila*. *J. Cell Biol.* 2010;189(1):143–158.
22. Feyssa DH, Njoka JT, Asfaw Z, Nyagito MM. Uses and management of *Ximenia americana*, Olacaceae in semi-arid East Shewa, Ethiopia. *Pak. J. Bot.* 2012;44(4):1177–1184.
23. Abbink J. Plant use among the Suri people of Southern Ethiopia: A system of knowledge in danger? *AAP.* 2002;70:199–206.
24. Abbink J. Indigenous knowledge and development monitor. *PRELUDE HA* 37; 1995.
25. Iorjiim WM, Omale S, Etuh MA, Bagu GD, Ogwu SO, Gyang SS. EFV b-HAART Increases mortality, locomotor deficits and reduces reproductive capacity in *Drosophila melanogaster*. *J. Adv. Biol. Biotechnol.* 2020;23(1):26–38.
26. Charpentier G, et al. Lethal and sublethal effects of imidacloprid, after chronic exposure, on the insect model *Drosophila melanogaster*. *Environ. Sci. Technol.* 2014;48:4096–4102.
27. Mohammad F, Singh P, Sharma A. A *Drosophila* systems model of



pentylentetrazole induced locomotor plasticity responsive to antiepileptic drugs. *BCM Syst. Biol.* 2009;3(11):1–17.
J. Ethnopharmacol. 2008;116(2):370–376.

28. Jeruto P, Lukhoba C, Ouma G, Otieno D, Mutai C. An ethnobotanical study of medicinal plants used by the Nandi people in Kenya



P080 - ASSESSMENT OF THE EFFICACY OF SOME SELECTED PLANTS AS DERIVED BIO-PESTICIDES IN THE CONTROL OF COWPEA PESTS ON THE FIELD

Esew O*, Anchau H.G., Aribido O.S., Ochigbo M.E., Musa J.M and Ibraheem S. A

*¹ Scientific and Industrial Research Department, NARICT Zaria, Kaduna State.

corresponding author email: onyeesew@gmail.com

ABSTRACT

The efficacy of natural plant based biopesticides in controlling cowpea pest was evaluated in this study. The selected plants used include combined extract of neem leaves (*Azadirachta indica*), garlic (*Allium sativum*), baobab leaves (*Adansonia digitate*), chilli pepper (*Capsicum frutescens*) and ginger (*Zingiber officinale*). Cowpea pest including aphids, bean stem maggot, leaf miners and bruchids were the targeted insects for this assessment. Field trial was carried out on scientific and Industrial research farm, NARICT Zaria during the farming season of 2022. Thirty experimental plots were mapped out and arranged into ten different treatment plots of three groups. The bio-pesticide group, the synthetic group and the control group. Parameters such as pest population, pest mortality, seed produced per pod, yield and plant damage were measured in the study. Results obtained showed that the derived biopesticide exhibited significant efficacy in controlling cowpea pest when compared to the untreated group. In both biopesticide and synthetic groups there was an observation in pest mortality, pest reduction of cowpea pest but the synthetic group showed adverse effect on non-targeted insect. The biopesticide extract showed negligible negative effect on cowpea plants as observed from absence of plant damage. This present finding suggests that the derived biopesticide possess potential bio-pesticidal activity in controlling cowpea pest.

1.0 INTRODUCTION

Cowpea, popularly called beans is an important source of protein for people in sub-sahara Africa, where access to other sources of protein is often limited. Its high protein content, excellent amino acid profile and nutrient-rich composition makes it an ideal crop for addressing malnutrition. Additionally, its versatility and ease of cultivation makes it an attractive option for small scale farmers. Nigeria is the world's largest producer and consumer of cowpea. About more than 3.6 million tons of cowpea is consumed annually, but 500,000 tons of cowpea is imported annually to meet local demand (1). However, the cowpea plant suffers from insect pests that feed on it during planting and post harvesting period, which causes low yield. The devastating activities of these pests brought about different chemical pesticides in use, to control the pests. These pesticides resolved the problem to a reasonable extent. But the adverse effect of the chemical pesticides on humans and the environment is of great concern. Degraded soil, groundwater pollution and food safety have been a huge concern due to the over dependence (2). Studies indicate that some plants have pesticidal properties which show antifeedant, repellent and toxic effects on a wide range of insect pests and are easy and cheap to prepare (3 - 5). These brought about the choice of

using bio-pesticides as an alternative. Biopesticides are natural, biologically occurring compounds that are used to control agricultural pest infesting plants. Synthetic pesticides have been widely used for pest control in agriculture and public health since 1950s (6). However, the negative impacts of these synthetic pesticides on the environment, such as the pollution of water bodies, soil degradation and loss of biodiversity. Additionally, the prolonged exposure to synthetic pesticides on human health, including cancer, reproductive problems and respiratory diseases have raised concerns in recent years. Therefore, there is need to assess the effectiveness of alternative pest control measures, such as derived bio-pesticides as it is environmentally friendly. Synthetic insecticides such as carbamates, organo-phosphorous, organo-chlorines and temephos used in insect control are quite impactful (7); however, their drawback is that they are expensive, there is an emerging development of resistance in insect species which lead to increase use and negative effects on non-target organisms including humans and the environment in terms of pollution (8-11). Hence, the need to develop new biodegradable, eco-friendly, specific, effective and safe biopesticide which are toxic to insects but at the same time do not exhibit toxicity to mammals and humans is of paramount importance for future control measure



(12). The aim of this study is to formulate bio-pesticide from neem leaves (*Azadirachta indica*), garlic (*Allium sativum*), baobab leaves (*Adansonia digitate*), chilli pepper (*Capsicum frutescens*) and ginger (*Zingiber officinale*) and to evaluate its insecticidal activity on aphids, bean stem maggot, leaf miners and bruchids.

2.0 MATERIALS AND METHODS

The field trial was conducted at scientific and industrial research farm during the raining seasons of 2022. The seeds used for the trial were sourced from institute of Agricultural Research (IAR) Zaria, Kaduna state, Nigeria and the specie name is IAR-48. Thirty (30) experimental plots were demarcated and arranged into 10 treatment plots each with an average size of 5m x 5m. These 3 groups of 10 plots each were named group A which was treated with synthetic pesticide, group B was treated with the derived bio-pesticides and group C was left untreated. Each group was separated from the next group by 5 feet long to prevent transfer of pests from either of the groups.

2.1 Land Preparation, Sowing, Weeding.

The experimental field was ploughed, harrowed and ridged. Three seeds of beans were sown per hole to avoid germination failure. The intra-row spacing and inter-row spacing was 20cm and 75cm respectively. Pre-emergence herbicides (Galex^R) was applied after sowing in order to control the menace of weeds. Supplementary hoe weeding and other agronomics practices of raising good beans plants were equally observed (13).

2.1.1 Collection of Plant Sample

The plant sample of baobab leaves, neem leaves and ripe neem seeds were collected within NARICT premises, shade dried and then grinded into powder while ginger, garlic and red chilli were bought from Basawa market, shade dried and grinded into powder. The powdered sample of each plant will be stored in an air tight container until use

2.1.1.1 Biopesticide Constitution and Application.

The biopesticide was formulated with the indigenous plant parts by weighing garlic, ginger pepper, neem leaves, baobab in the ratios of 2:2:2:1:1 and mixed in 500mls of water and allowed to stand for 24hrs. The mixture was sieved using

muslin cloth, after which the supernatant was rinsed with 500mls of water, the filtrate was transferred into a knapsack sprayer and made 15 liters with water.

2.1.1.2 Application of Biopesticides and Synthetic Pesticides

Spraying of synthetic pesticides on group A, plant derived biopesticides on group B was done at three different intervals i.e., 3, 7, and 8 weeks after planting when the plants was at vegetative, flowering and pod growth stages, respectively using knapsack sprayer (13). All the spraying operations were conducted early in the morning when the target insect pest was available and less active.

2.1.1.3 Evaluation of the Efficacy of the Plant Derived Biopesticides

In order to evaluate the effectiveness of the plant derived biopesticides, the following parameters were assessed during the field study.

2.1.1.4 Assessment of Insect Pest Population

Five stands were selected randomly from the central middle row of each plot and tagged for recording observation on the insect pest. Pre-spray population of insects was taken and thereafter populations of insects were observed at 1, 3, 5 and 7 days after treatment application. The assessment of individual insect pests was done using plant infestation scale, which placed plants parts in different classes of infestation (14).

2.1.1.5 Assessment of Seeds Produced Per Pod

Assessment of seeds produced per pod were achieved by utilizing the earlier randomly selected plants. Five pods were picked from the five randomly selected plants and the total number of seeds per pod were counted and finally divided by the number of pods sampled to get the average.

2.1.1.6 Assessment of Yield

Harvesting commence when the plant leaves virtually turned yellow and almost all the pods were fully dried. During the harvesting, two middle rows were selected and pods were picked in each plot within 24hrs. All the pods were placed in a separate polythene bag. The bags were labeled according to



the groups and weight of the harvested pods were recorded accordingly. The pods from each plot were threshed separately, winnowed and grains weights

$$\text{Seed yield (kg/ha)} = \frac{a \times 10,000}{b \times 1000}$$

$$b \times 1000$$

where a = plot yield

b= net plot size

3.0 RESULTS AND DISCUSSIONS

In this study, the result showed that the derived biopesticide and the synthetic pesticide showed different degrees of efficacy against the insect pests assessed, but it is even more interesting to note that the biopesticide treatments exhibited a better efficacy in controlling the cowpea insect pest, than the synthetic pesticides and control. The results go further to reveal that the combined extracts of chilli pepper, ginger, neem leaves, baobab leaves and garlic have more damaging effect on the insect pest population than on cowpea plants. This agrees with the findings of (16,17) which reported that neem, garlic and ginger were effective against pod borer insects and also protect plants against insect infestation for at least two weeks. The severity of leave damage was more pronounced in the untreated group, compared to the synthetic group. (13) reported on the comparative efficacy of ginger, garlic, sour sop, tobacco, chilli pepper and neem in which the various plant part where used separately and all plant parts exhibited toxicity on cowpea pest. (18) also reported on the evaluation of freshly prepared juice from garlic (*Allium sativum* L.) as a biopesticide against the maize weevil, *Sitophilus zea-mais*. This is a confirmation that some plant materials have bio-pesticidal properties, as seen in the previous work reported by (19) that plant products usually act either through physical or biochemical processes thereby lowering the insect pest population. Previous studies have confirmed the insecticidal properties of ginger, garlic, neem, baobab and chilli pepper when carried out separately (13). Neem has an active ingredient called azadirachtin that acts on insects by repelling them, inhibit their feeding, disrupts their rothw, metamorphosis and reproduction. Garlic and chili pepper act as stomach poison and antifeedant against many cowpea pest (20). The spraying of both synthetic pesticide and the biopesticide was done at the onset of the flowers of the beans and pod

were recorded accordingly. The seed yield of all the harvested pods were calculated using the following formula (15).

formation, this was because the presence of flowers attracts the insects to the plant, plant extracts from garlic bulb have also been reported to be effective against post- flowering insect pests of cowpea (21). It was observed that throughout the planting period there was no presence of insect on the biopesticide group but there were insects observed in both synthetic pesticide and untreated group. This agrees with the findings of Amatobi (2000) which reported the use of crude extracts of chilli pepper fruit and tobacco leaves to control insect pests in a greenhouse study. Several authors have demonstrated the efficacy of different plant materials as biopesticides for the control of different pests species (21-23). Insect mortality was observed after the second spray in the synthetic group. The biopesticide group gave more yield 24.78g obtained from 5 pods selected randomly, the synthetic gave a yield of 20.89g and the untreated gave a yield of 10.45g. This result corresponds positively with the earlier work conducted (20) which showed that plant extracts increases the yield of vegetables and pea plants by protecting them from insect pest. (24) in a field trial found that *tephrosia volgelii* hook aqueous extracts not only reduced maize stalk borer numbers and damage symptom but improved grain yield as well. Previous studies have confirmed the insecticidal properties of ginger, garlic, neem, baobab and chilli pepper (13). Hence, the combination of this extracts gives a better result compared to only the application of individual extracts.

4.0 CONCLUSION

The results from the field trial conducted showed that plant derived biopesticide have the potential as an alternative biopesticide to synthetic pesticide offering a more sustainable and environmentally friendly approach in pest management because the where found effective in controlling the insect pest that infested cowpea on the field during the



different growth stages. Further research should be carried out in other to isolate, purify and characterize the active ingredients responsible for the potency of the derived biopesticide and its mode of action. There is also need to investigate the potency of the derived biopesticide on other crops that have similar pests as cowpea.

REFERENCES

1. <http://sciencenigeria.com>pbr-com>
2. S. Gupta, A.K. Dikshit. Biopesticides: An eco-friendly approach for pest control. *Journal of Biopesticides*. **3**(1):186-188 (2010).
3. E. A Shadia. Control Strategies of Stored Product Pest. *Journal of Entomology*, **8**: 101-122 (2011).
4. S. Karunakaran, R.F.Niranjana. Laboratory Evaluation of some Selected Indigenous Plant Leaf and Garlic Bulb Extracts against *Tribolium castaneum* (coleoptera: Tenebrionidae) in Chickpea. *ISA*, 196 (2019)
5. F.H. Fargalla, E.A. Mousa, A.E.Afsah. The Effect of Certain Pesticides on Some Pest Infesting Cowpea and the YieldCrop in Qalyobia governorate. *Egyptian Journal of Agricultural Research*. **91**(2), 471-480 (2013).
6. F.M. Onu, E. Ogu, M.E, Ikehi. Use of Neem and Garlic Dried Powdersfor Controlling some Stored Grains Pests. *Egyptian Journal of Biological Pest Control*, **25**(2): 507-512 (2015).
7. B. Ndakidemi, K. Mtei, P. Ndakidemi. Impacts of synthetic and botanical pesticide on beneficial insects **7**(6): 364-372 (2016).
8. N. Liu. Insecticide Resistance in Mosquitoes: Impact, Mechanisms, and Research Directions. *Annual Review of Entomology*, **60**:537-559 (2015).
9. Food and Agriculture Organization: Resistance Management guidelines 260-280 (2012).
10. P. Sola, B.M, Mvumi, J.O Ogendo. Botanical Pesticide Production, trade and regulatory mechanisms in sub-saharan Africa: making a case for plant-based pesticidal product. *Food Security*, **6**:369-384 (2014)
11. X. Zhang, Q. Xu, W. Lu. Sublethal effects of four synthetic insecticides on the generalist predators *Cryptorhinus lividipennis*. *Journal of Pest Science*. **88**: 383-392 (2015)
12. R. Jbilou, A. Ennabili, F. Sayah .Insecticidal Activity of Four Medicinal Plant Extracts against *Tribolium castaneum* (Herbst)(coleoptera: Tenebrionidae). *African Journal of Biotechnology*, **5**(10):936-940 (2016)
13. B.I, Ahmed, I. Onu, L. Mudi, Aliyu, M. Comparative Efficacy of some Selected Plant Derived Biopesticides for the Control of Insect Cowpea (*Vigna unguiculate* (L.) Walp.) in Katsina State, Nigeria. *Korean journal of crop science*. **52**(2) 183-197(2007)
14. S. Kumar. Biopesticides: A Need for Food and Environmental Safety. *Journal of Biofertilizer and Biopesticides* **3** (4): 1-3. (2012)
15. A.K Raheja. Assessment of Losses Caused by Insect Pest of Cowpea in Northern Nigeria. *Pesticides Action Network*. **22**: 299-333 (1976).
16. J. Kumar, A. Ramla, D. Malick. An Overview of some Biopesticides and their importance in Plant Protection for Commercial: Acceptance. *Plants*, **10**(6), 1185 (2021).



17. S.B . Panhwar. Farmer Adoption of Plant materials for Insect control. International Service for National Agricultural Research, *Haqye, Netherland*. 4:61-68(2002).
18. I.D. Nwachukwu, E.F. Asawalam. Evaluation of Freshly Prepared Juice from Garlic (*Allium sativum L.*) as a Biopesticide against the Maize Weevil, *Sitophilus zeamais* (Motsch.) (Coleoptera: Curculionidae). *Journal of Plant Protection Research* 54(2):132-138 (2014).
19. S.M. Dungum, M.C. Dike, S.A Adebitan. Efficacy of Plant Materials in the Control of Field Pests of Cowpea. *Nigerian Journal of Entomology*, 22:46-53 (2005).
20. PAN. Pesticides in Tropical Agriculture: Hazards and Alternative, Pesticides Action Network, Margraf Verlag 281(1995).
21. A.M. Oparaeke, M.C. Dike, C.I. Amatobi. Insecticidal Potential of Extracts of garlic, (*Allium sativum L.*) bulb and African Nutmeg for control of field Pest of Cowpea. *Esn Ocassional Publication* 32:90-99(2000)
22. C.I. Amatobi. Cashew Plant Crude Extracts as a Promising Aphicide in Cowpea Insect Pest Management. Abstracts of paper and poster presentations, World Cowpea Research Conference III, IITA-Ibadan, Nigeria, 4-7th September 11(2000).
23. S.Ekesi. Effects of Volatiles and Crude Extracts of different Plants Materials on Egg Viability of *Maruca vitrata* and *Clavigralla tomentosicollis*. *Hortscience*, 28:305-310 (2000).



P081 - STUDY OF THE EFFECTS OF PROCESS CONDITIONS ON BLEACHING OF PALM OIL USING ACTIVATED CLAY

Ihedioha, Onyedikachi Joseph ^{1*}, Onoh, Ikechukwu Maxwell ², Okeke, Chinedu Luke ¹

¹Projects Development Institute (PRODA), Emene Industrial Layout Enugu, Nigeria

²Department of Chemical Engineering, Enugu State University of Science & Technology, Enugu, Nigeria

*Corresponding author email: tility4u@gmail.com

ABSTRACT

The study of the effect of process conditions on bleaching of palm oil using activated clay was carried out. The acid and base used for the clay activation were HCl and NaOH respectively. Batch adsorption bleaching experiments were carried out to investigate the effects of temperature, clay dosage and contact time on the percentage bleaching of the palm oil using acid and base activated clay, and unactivated clay. The results of the One Factor At a Time (OFAT) experiments showed that HCl activated clay performed best, followed by the unactivated clay. The optimization of the bleaching of palm oil using differently activated clay samples (HCl activation, NaOH activation and Un-activated clay) was designed using the Latin Square design of experiment at four (4) experimental levels each. The ANOVA result indicated that temperature and dosage had significant effects on the palm oil bleaching, while the effect of time was not statistically significant at 0.05 level. Meanwhile, the acid activated clay gave the highest percentage bleaching of 58.97%, followed by the un-activated clay at 52.01%, and the alkaline activated clay at 38.09%. The bleached oils were characterized by measuring the saponification, iodine, and free fatty acid values. There were differences due to the clay activation method, and a one-way analysis of variance indicated that the differences in saponification and iodine values were statistically significant at 0.05 level. The acid activated clay bleached oil had the highest saponification and iodine value, implying that though the acid activation enhanced the percentage bleaching, it had a significant impact on the saponification and iodine values of the oil respectively.

KEYWORDS

Palm oil, activated clay, adsorption bleaching, HCl, NaOH

1.0 Introduction

Palm oil is an edible vegetable oil that is primarily produced by extracting its oil from the fresh fleshy fruits of oil palms which serves as an important ingredient for the food industry because of its superior characteristics and attributes [1, 2]. Palm oil in its raw form contains impurities such as organic pigments, oxidation metals, trace metals and trace soaps [1, 3]. For palm oil to be edible these impurities which negatively impact the taste and smell of the oil as well as its appearance and shelf life stability must be sponged out through the bleaching process [1]. The bleaching of the oil is accomplished via adsorption of the impurities onto a surface-active micro porous adsorbent material or

bleaching agent for a period of time by Vander Waal forces [4, 5].

The refining of palm oil through adsorptive bleaching remains inevitable in the palm oil refining industry. The major adsorbent used in the industry is bleaching earth, but it is expensive in terms of production cost. Bleaching is a process which involves the adsorption of unwanted components with the use of an adsorbent in the presence of heat [6]. Activated carbon, silica and acid activated clays are common adsorbents used in the industry for bleaching purposes [7]. Most of the adsorbents used in Nigeria are imported activated carbon and fuller earth but the enforcement by the Nigerian government to stop importation has led to the need to substitute these imported goods with locally sourced materials [6].



Clay is a highly abundant and substitutable material in Nigeria that can be used as an adsorbent [6]. The clays that can be used may be naturally active or activated clays. The adsorptive bleaching activity of naturally active clays are quite high due to their high surface area but activated clays applied for bleaching purposes show a much higher activity [8]. It has been proven that the adsorptive property of local clays can be improved by activating them with acidic or alkaline reagents [6]. Some advantages of acid-activated adsorbents include the dealumination of the structure, the removal of metal ions in the octahedral layer and opening of the platelets thereby increasing the pore diameters and surface areas [8]. Studies on the bleaching capacities of some Nigerian clays have been studied by some researchers [6, 8, 9]. This work sentenced on using activated clay (locally sourced material) as an alternative to activated carbon in bleaching of palm oil.

2.0 MATERIALS AND METHOD

2.1 Equipment and Raw Materials

Electric oven, 721S visible spectrophotometer, 80-2 centrifuge, heating furnace, beakers, volumetric flask, conical flask, pipette, test tube, Whatman no 1 filter paper, funnel, stirrer, bowls, stop watch, sieve, 100 ml measuring cylinder, electric weighing meter (s. mettle precision balance). The white-coloured purified Kaolin clay was obtained from the Ceramics Department of Projects Development Institute (PRODA), Enugu. The crude palm oil was purchased from Eke market in Enugu state Nigeria. And all the chemicals used for activation and others were of analytical grade from local markets.

2.2 Clay Activations

2.2.1 Acid Activation

About 50 ml of water was poured in the 250 ml volumetric flask before adding 109.85 ml of HCl. The volumetric flask was then topped up with water to make 5 M HCl. To activate the clay, about 100 g of the purified clay was weighed using the electric weighing meter into a 500 ml beaker. 250 ml of the 5 M HCl was added, and the mixture was stirred continuously for about 30 minutes using a stirrer. Thereafter, the mixture was allowed to stand at room temperature for 24 hours. The mixture was filtered, and the solid residue was washed repeatedly with water to achieve neutrality in pH. Then, the residue was recovered by centrifuging at

6000 rpm for 10 minutes. The solid was dried in electric oven at 100°C for 24 hours before being calcined in the furnace at 600°C for 4 hours. It was then sieved to 250 µm, properly labeled and stored in an air tight container for the bleaching process.

2.2.2 Alkaline Activation

For the alkaline activation, 5 M NaOH was prepared by weighing 50.2 g of solid NaOH weighed in a 100 ml beaker using an Electric weighing meter. The solid was dissolved with water in a 250 ml volumetric flask to get the 5 M concentration. 100 g of the purified clay was measured in an electric weighing meter and soaked with 250 ml of 5 M NaOH in a 500 ml beaker. The mixture was stirred for about 30 minutes and allowed to stand for 24 hours at room temperature. The mixture was filtered, and the residue was washed repeatedly with distilled water until the pH was 7.0. Meanwhile, the pH was monitored with a pH paper. The clay was recovered by centrifuging at 6000 rpm for 10 minutes. The solid was dried in oven at 100°C for 24 hours. The clay was finally calcined in the furnace at 600°C for 4 hours. It was also sieved to 250 micrometer and stored in an air tight container for further bleaching process.

2.3 Palm oil Bleaching

Exactly 10 ml of raw palm oil was measured into a 120 ml beaker attached with a thermometer. The beaker was placed on an electric hot plate at a temperature according to the design run. When the target temperature reached, 1 g of the clay sample was weighed into the beaker, and the mixture was stirred periodically until the desired time according the design run was achieved. The mixture was filtered with Whatman No 1 (16 mm) filter paper. The absorbance of the oil filtrate was measured using a spectrophotometer at a wavelength of 540 nm. The blank experiment was carried out the same way without the addition of any adsorbent. The percentage bleaching was calculated using Equation 1.

$$\begin{aligned} \% \text{ Bleaching} &= \frac{A_o - A}{A_o} \times 100 \end{aligned} \quad (1)$$

Where: A_o =
Absorbance of the blank oil sample; A =
The absorbance of the bleached oil sample



2.4 The Design of the Bleaching Experiment

The effects of the process parameters on the bleaching of palm oil using the differently activated clay samples were conducted using the Latin Square design. The temperature, clay dosage and time were varied at four levels from 40°C to 100°C, 1g/10 ml of oil to 4g/10 ml of oil, 5 min to 20 min. The design matrix outlined the order of the sixteen experimental runs.

$$\text{Variance} = \frac{1}{n} \left[\sum_1^n X_i^2 \right] - \frac{1}{N} T^2 \quad (2)$$

Where:

n = number of levels of each parameter; X_i = sum of values in each level;

T = sum of values in all the levels, N = the number of values in all the levels

NOTE: The total variation was calculated using Equation 3

$$\text{Total Variation} = \sum_1^N t^2 - \frac{1}{N} T^2 \quad (3)$$

Where: t = The value at each run

The variation due to random error was calculated by subtracting the variation due to the parameters from the total variation. The mean square values were calculated by dividing the variance with the degree of freedom in each parameter, and the F-value was calculated by dividing the mean square values by the error mean square. A parameter is significant if the F value is higher than the critical F-value.

The following are their equations:

$$\text{Saponification Value; SV} \left(\frac{\text{mg}}{\text{g}} \right) = C * V * M * \frac{1}{W} \quad (4)$$

Where:

$$V(\text{ml}) = V_{\text{Blank}} - V_{\text{Actual}}$$

C = Molarity of KOH; M = Molar weight of KOH; W = Weight of the oil sample

Note the V_{BLANK} is higher than the V_{ACTUAL}

$$\text{Acid value; AV} \left(\frac{\text{mg}}{\text{g}} \right) = C * V * M * \frac{1}{W} \quad (5)$$

Where:

$$V(\text{ml}) = V_{\text{Actual}} - V_{\text{Blank}}$$

C = Molarity of NaOH; M = Molar weight of NaOH; W = Weight of the oil sample

2.5 The Analysis of the Results

The results of the Effects of the process parameters on the bleaching of palm oil were analyzed using the Analysis of Variance (ANOVA) tool. The variance was calculated from the sum of the values in each parameter using Equation 2.

Meanwhile, the degree of freedom for each parameter was the number of levels minus 1.

2.6 Oil Characterization

The Association of Official Analytical Chemists (AOAC, 1990) method was used to measure the Saponification value, the Acid value, and the Iodine value.



$$\text{Iodine value; IV} \left[\frac{\text{g}}{100\text{g}} \right] = V * C * M * \frac{1}{W} * 100 \quad (6)$$

Where:

$$V(\text{ml}) = V_{\text{Blank}} - V_{\text{Actual}}$$

C = Molarity of sodium thiosulphate; M = Molar weight of iodine = 126.9

W = Weight of the oil sample.

3.0 RESULTS AND DISCUSSION

3.1 The Design Matrix with the percentage bleaching of oil

The Latin-Square Design with the experimental response, which is the percentage oil bleaching from the acid activated, alkaline activated and un-activated clay are shown in Tables 1. The percentage bleaching was calculated using the activities of the clay.

Equation 1, following the absorbance of the blank oil and the bleached oil at 540nm wavelength. The percentage bleaching was applied to calculate the effects of the process parameters using Analysis of Variance (ANOVA) calculations. The acid activated clay gave the highest percentage bleaching of 58.97. It was equally observed that the percentage bleaching values from the un-activated clay were higher than the values from the alkaline activated clay. In other words, the alkaline activation did not enhance the bleaching

Table 1: Latin Square Design Matrix with Percentage Oil Bleaching from HCl-Activated Clay, NaOH-Activated Clay and Un-activated Clay

Std	Dosage (g/10ml)	Temp (°C)	Time (min)	HCl-Clay % Bleaching	NaOH-Clay % Bleaching	Un-activated Clay % Bleaching
1	1	40	5	12.696	5.849	8.7019
2	2	40	10	14.158	7.601	10.5812
3	3	40	15	15.894	7.947	13.9073
4	4	40	20	15.806	8.387	14.1935
5	1	60	10	13.356	7.372	11.0147
6	2	60	15	18.263	8.084	12.2754
7	3	60	20	25.566	12.298	15.8576
8	4	60	5	26.603	14.103	20.5128
9	1	80	15	13.871	12.258	13.2258
10	2	80	20	28.947	15.789	19.4079
11	3	80	5	28.492	22.905	26.5363
12	4	80	10	30.394	24.094	27.2441
13	1	100	20	29.667	25.667	27.0000
14	2	100	5	51.917	27.382	48.4118
15	3	100	10	58.667	29.667	40.0000
16	4	100	15	58.974	38.095	52.0147

3.2 The Analysis of Variance (ANOVA) Tables

3.2.1 Analysis of Variance for oil bleaching using acid-activated clay, base-activated clay and Un-activated clay



The Latin-square design with the responses for each run is shown in Table 2. The summary of the data for HCl activated clay, NaOH activated clay and Un-activated clay is in Table 3, and the analysis of variance table in Table 4-6. The F-values for temperature and dosage were higher than the F-critical at 0.05 significant levels. This implies that temperature and dosage had significant impact or effect on the bleaching of palm oil using the acid activated clay. In other words, the hypothesis that the percentage bleaching of palm oil at different temperature and clay dosage were the same cannot be accepted at 0.05 significant levels. The effects of

temperature and dosage can also be seen from Figures 1 and 2 where the percentage bleaching increased with the increase in temperature and dosage, respectively.

On the other hand, the F-value for time was less than the F-critical, meaning that the bleaching time or contact time did not have a significant effect on the bleaching of palm oil. It implies that whether the contact time was 5, 10, or 15 minutes, the results were the almost the same. In Figure 3, the percentage bleaching was almost the same irrespective of the contact time.

Table 2: Latin square design with the values for HCl activated clay, NaOH activated clay and Un-activated clay

HCl activated clay	D1	D2	D3	D4
T1	t1(12.696)	t2(14.158)	t3(15.894)	t4(15.806)
T2	t2(13.356)	t3(18.263)	t4(25.566)	t1(26.603)
T3	t3(13.871)	t4(28.947)	t1(28.492)	t2(30.394)
T4	t4(29.667)	t1(51.917)	t2(58.667)	t3(58.974)
NaOH activated clay	D1	D2	D3	D4
T1	t1(5.849)	t2(7.601)	t3(7.947)	t4(8.387)
T2	t2(7.372)	t3(8.084)	t4(12.298)	t1(14.103)
T3	t3(12.258)	t4(15.789)	t1(22.905)	t2(24.094)
T4	t4(25.667)	t1(27.382)	t2(29.667)	t3(38.095)
Un-activated clay	D1	D2	D3	D4
T1	t1(8.702)	t2(10.581)	t3(13.907)	t4(14.194)
T2	t2(11.015)	t3(12.275)	t4(15.858)	t1(20.513)
T3	t3(13.226)	t4(19.408)	t1(26.536)	t2(27.244)
T4	t4(27.000)	t1(48.412)	t2(40.000)	t3(52.015)

Table 3: Summary of the data for HCl activated clay, NaOH activated clay and Un-activated clay

HCl activated clay	Level 1	Level 2	Level 3	Level 4	Variance
Temperature	58.555	83.789	101.704	199.224	2840.202



Dosage	69.590	113.286	128.619	131.777	615.4909
Time	119.707	116.575	107.003	99.987	61.0066
NaOH activated clay	Level 1	Level 2	Level 3	Level 4	Variance
Temperature	29.784	41.856	75.047	120.811	1244.394
Dosage	51.146	58.856	72.816	84.679	166.0033
Time	70.239	68.734	66.384	62.141	9.355306
Un-activated clay	Level 1	Level 2	Level 3	Level 4	Variance
Temperature	47.384	59.661	86.414	167.426	2186.033
Dosage	59.942	90.676	96.301	113.965	379.4381
Time	104.163	88.840	91.423	76.459	96.77946

Table 4: Analysis of Variance Table for HCl activated clay NaOH activated clay and Un-activated clay

Source of Variance	Variance	Degree of Freedom	Mean square	F-value	F-critical
Temperature	2840.202	3	946.7340608	28.23247	4.76
Dosage	615.4909	3	205.1636205	6.118165	
Time	61.0066	3	20.33553321	0.606424	
Error	201.2011	6	33.53352398		
Total	3717.901	15			

Table 5: Analysis of Variance Table for NaOH activated clay

Source of Variance	Variance	Degree of Freedom	Mean square	F-value	F-critical
Temperature	1244.394	3	414.798	51.82036	4.76
Dosage	166.0033	3	55.33443	6.912884	
Time	9.355306	3	3.118435	0.389584	
Error	48.02722	6	8.004536		
Total	1467.78	15			

Table 6: Analysis of Variance Table for Un-activated clay

Source of Variance	Variance	Degree of Freedom	Mean square	F-value	F-critical
Temperature	2186.033	3	728.6777	43.32687	4.76



Dosage	379.4381	3	126.4794	7.520412
Time	96.77946	3	32.25982	1.918156
Error	100.9089	6	16.81815	
T otal	2763.159	15		

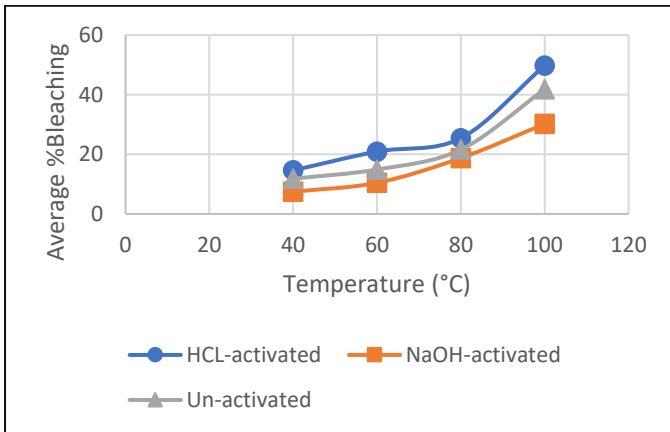


Figure 1: The effects of temperature on the bleaching of palm oil using differently activated clay.

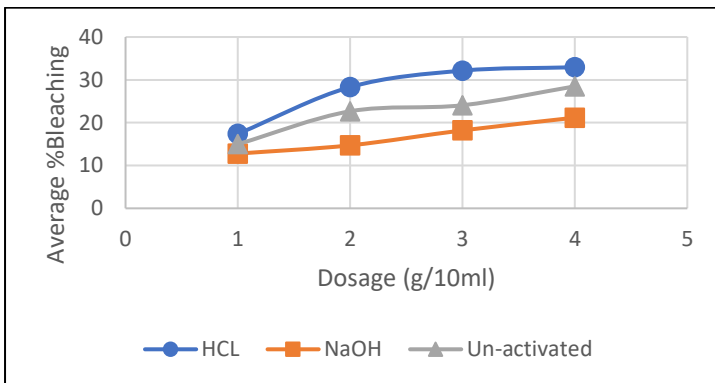


Figure 2: The effects of clay dosage on the bleaching of palm oil using differently activated clay.

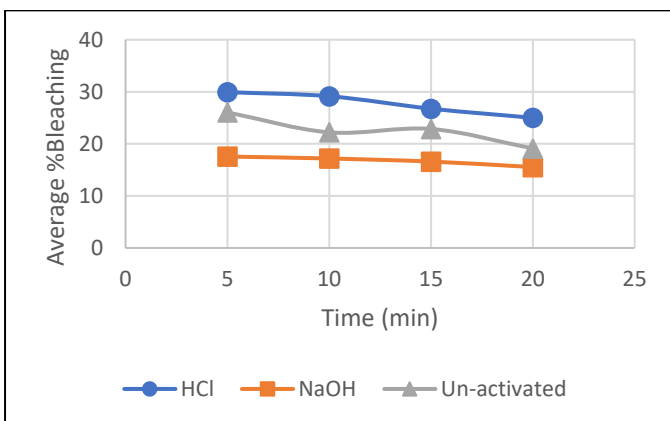


Figure 3: The effects of contact time on the bleaching of palm oil using differently activated clay.



3.3 Palm oil characterization

The results of the palm oil characterization before and after bleaching are shown below:

Table 7 Acid values, Saponification values and Iodine values of the bleached and the unbleached palm oil

	Run1	Run2	Average Acid Value(mg/g)
HCl Treated	11.7647	10.9804	11.373
NaOH Treated	11.7241	11.7241	11.724
Clay Treated	11.7241	11.7241	11.724
Non-Treated oil	10.5263	11.9298	11.228
	Run1	Run2	Average Saponification value(mg/g)
HCl Treated	241.569	248.889	245.229
NaOH Treated	214.118	225.098	219.608
Clay Treated	217.241	217.241	217.241
Non-Treated oil	216.140	207.742	211.941
	Run1	Run2	Average Iodine value (g/100g)
HCl Treated	26.048	26.048	26.048
NaOH Treated	25.161	25.825	25.493
Clay Treated	26.036	25.818	25.927
Non-Treated oil	26.716	26.966	26.841

One-Way Analysis of variance for the acid values of the oil

Using ANOVA tool of Microsoft Excel, the ANOVA was calculated as shown in Table 8. The F value was 0.392 and the F-critical was 6.59, so the differences in acid value due to the bleaching were not statistically significant at 0.05 significant levels.

For the saponification values, the F-value was 14.38 and the F-critical was 6.59. In other words, the

differences in saponification value due to the bleaching of the palm oil were statistically significant at 0.05 significant levels. The saponification value of the oil bleached by the HCl-activated clay was higher than the others and this could be attributed to the acidic nature of the HCl-activated clay.

For the iodine value, the F-value was 9.16 and the F-critical was 6.59. Oil bleaching had significant effect on the iodine value of the palm oil.



Table 8 ANOVA for Acid, Saponification and Iodine values of the bleached and unbleached palm oil

ANOVA (Acid value)						
<i>Source of Variation</i>	<i>SS</i>	<i>Df</i>	<i>MS</i>	<i>F</i>	<i>P-value</i>	<i>F critical</i>
Between Groups	0.380135	3	0.126712	0.392147	0.766073	6.591382
Within Groups	1.292492	4	0.323123			
Total	1.672627	7				
ANOVA (Saponification value)						
<i>Source of Variation</i>	<i>SS</i>	<i>Df</i>	<i>MS</i>	<i>F</i>	<i>P-value</i>	<i>F critical</i>
Between Groups	1320.13	3	440.0435	14.38705	0.013101	6.591382
Within Groups	122.3443	4	30.58608			
Total	1442.475	7				
ANOVA (Iodine value)						
<i>Source of Variation</i>	<i>SS</i>	<i>Df</i>	<i>MS</i>	<i>F</i>	<i>P-value</i>	<i>F critical</i>
Between Groups	1.895719	3	0.631906	9.165177	0.02893	6.591382
Within Groups	0.275786	4	0.068946			
Total	2.171505	7				

4.1 Conclusion

The main purpose of this research was to identify the effect of process parameters on bleaching of palm oil using activated clay. The adsorption of beta carotene from palm oil was successfully carried out through bleaching process using HCl and NaOH activated and unactivated kaolin clay. Based on the experiments and analysis conducted, it can be concluded that although there are multiple ways of bleaching palm oil to remove the impurities and improve their behaviours, activated bleaching earth remains a viable material for oil bleaching.

1. Raji, W., R. Azike, and F. Wirsiy, *Optimization of Bleaching Process of Crude Palm Oil by Activated Plantain (Musa paradisiaca) Peel Ash Using Response Surface Methodology*. Open Journal of Optimization, 2019. **08**: p. 38-46.
2. S, O. and C. Uzoh, *Experimental process Design of Sorption Capacity of Kogi and Ibusa Clay Activated with HNO₃ and H₂SO₄ acids in palm oil Bleaching*. 2014.

References



3. Usman, M.A., et al., *Characterization, Acid Activation, and Bleaching Performance of Ibeshe Clay, Lagos, Nigeria*. ISRN Ceramics, 2012. **2012**: p. 658508.
4. Ekwu, F.C. *Decolourization of Palm Oil by Nigerian Local Clay: A Study of Adsorption Isotherms and Bleaching Kinetics*. 2013.
5. Usman, M., O. Oribayo, and A. Adebayo, *Bleaching of Palm Oil by Activated Local Bentonite and Kaolin Clay from Afashio, Edo-Nigeria*. 2013.
6. Nwabanne, J.T., O. Elijah, and O. Nwankwoukwu, *Equilibrium, Kinetics and Thermodynamics of the Bleaching of Palm Oil Using Activated Nando Clay*. Journal of Engineering Research and Reports, 2018: p. 1-13.
7. Almeida, E.S., et al., *Elucidating how two different types of bleaching earths widely used in vegetable oils industry remove carotenes from palm oil: Equilibrium, kinetics and thermodynamic parameters*. Food Res Int, 2019. **121**: p. 785-797.
8. Bayram, H., et al., *Optimization of bleaching power by sulfuric acid activation of bentonite*. Clay Minerals, 2021. **56**: p. 1-22.
9. Ajemba, R., R. Igbokwe, and P. Onukwuli, *Kinetics, equilibrium, and thermodynamics studies of colour pigments removal from palm oil using activated ukpor clay*. Archives of Applied Science Research, 2012. **2012**: p. 1958-1966.



P082 - PHYSICO-CHEMICAL AND FUNCTIONAL PROPERTIES OF TAMARIND (*TAMARINDUS INDICA*) SEED KERNEL STARCH

R.S.A Sangodare¹, I. Abdulwaliyu¹, O. Esew¹, P.N. Okoro¹, I.I. Uduakobong¹, Sule, A.M, O. Olanipekun¹, S. Garba¹, I. Bello¹, I.A. Saheed¹

¹Scientific and Industrial Research Department, National Research Institute for Chemical Technology, Zaria, Nigeria.

*Corresponding author: sangodares@yahoo.com

ABSTRACT

Tamarind Seed Kernels are by-products of tamarind pulp industries and currently constitute a huge waste. This work is aimed at the production and investigation of the physical, chemical and the functional properties of tamarind starch from tamarind seed kernel obtained locally. Standard methods of analysis were employed for the various analyses. Result indicates that tamarind starch produced had low moisture content with relatively high carbohydrate content, it was found to have low lipid content, with reasonable protein content. The results of the Functional properties of the starch produced showed, 10.29±0.012 g/100g, 20.01±0.012 g/100g, 9.83±0.005 g/100g, 23.00±0.000 g/100g, 19.00±0.000 g/100g, 262.5±0.372 g/100g, 96.48 ±0.026 g/100g, 26.00±0.000 g/100g, 38.00±0.000 (°C) and 0.76±0.002 (g/cc), of swelling capacity, foam capacity, foam stability, emulsion activity, emulsion stability, water absorption capacity, oil absorption capacity, least gelation capacity, gelatinization temperature, and bulk density respectively. The result of this work suggests that tamarind seed kernel starch possesses qualities that make it excellent raw materials for the production of valuable food and pharmaceutical product.

KEYWORDS: Tamarind seed, Starch, Functional properties, By-product

1.0 INTRODUCTION

Tamarind (*Tamarindus indica*) is a tropical tree native to Africa and widely cultivated in various parts of the world. While tamarind pulp and its culinary uses are well-known, the seeds of the tamarind fruit have been an underexplored source of a valuable biopolymer. Tamarind seed kernel starch (TSKS) are found to be rich in xyloglycan, amylose and amylopectin [1,2].

Tamarind seeds are a by-product of the tamarind pulp industry and are often discarded as waste. However, tamarind seeds contain a high amount of starch [3]. Tamarind starch can be extracted and used in a variety of food and for industrial applications. Total starch content present in each tamarind seed is estimated to be around 65–70% and about 84.68% purified starch can be recovered from the tamarind seed [4].

Tamarind seed starch is a white, odorless, and tasteless powder. It has a granular structure and is insoluble in water and organic solvents. These starch molecules composed of (1–4)-β-d-glucan backbone substituted with side chains of α-d-xylopyranose and β-d-galactopyranosyl, (1,2)- α-d-xylopyranose linked (1–6) to glucose residues. The glucose, xylose and galactose units are present in

the ratio of 2.8:2.25:1.0 [5]. Tamarind seed starch has a high amylose content, which gives it good thickening and gelling properties. Defatted Tamarind seed starch has an amylose content of 27.55 wt.% and 72.45 wt.% of amylopectin [6]. It is also resistant to retrogradation, which means that it does not easily lose its thickening and gelling properties over time [7].

Tamarind seed starch can be used in a variety of food and industrial processes. In the food industry, tamarind seed starch has been used to develop biodegradable films, edible coatings, and food packaging materials [8]. In the industrial sector, tamarind seed starch is used as an adhesive in the paper and packaging industries, as sizing agent in the textile industry [9], and a filler and excipient used to develop new drug delivery systems and biomedical implants in pharmaceuticals [10]. As a result of these wide arrays of tamarind seed starch usage, the aim of this study was to determine some functional properties of tamarind seed starch available locally.

2.0 MATERIALS AND METHOD



2.1.0 Materials

Tamarind fruits, cheese cloth, hot air oven, Furnace,

2.1.1 Chemicals and Reagents

Chemicals and reagents used in this work were of analytical grade

2.2 Sample preparation

Tamarind seeds were procured from the local market of Sabon Gari in Sabon Gari local government, Zaria, Nigeria. Raw fruits were

washed with water to remove dust and adhering pulp and sorted for infected seeds that float during washing. The cleansed seeds were dried at room temperature 72 hours, and subsequently oven dried at 65°C for 30 min to reduce moisture. The seeds were cooled then stored in clean bags at room temperature for analysis.

2.3 Method

2.3.1 Starch production

Starch was produced from tamarind seed kernel following the conventional method of starch production.



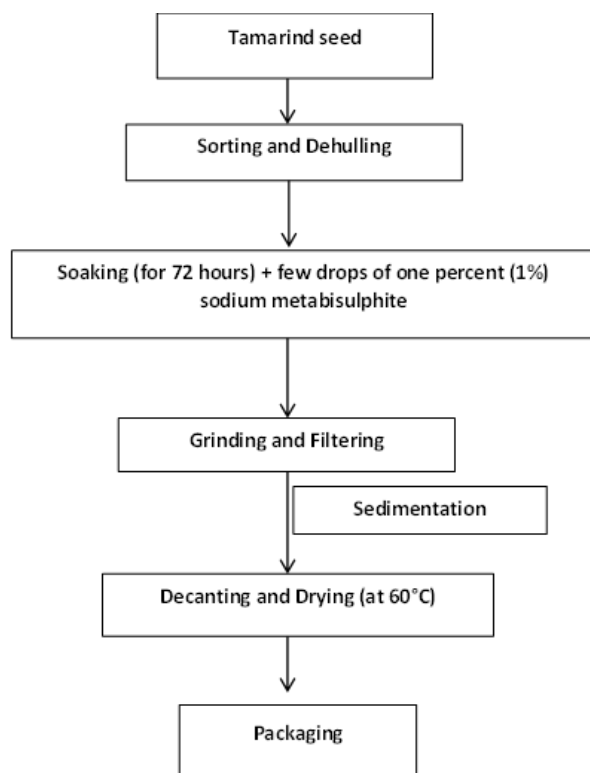


Figure 1: Stepwise traditional (conventional) wet method for the production of starch

2.4 Proximate determination

Proximate composition of the tamarind seed kernel starch was carried out using the method of AOAC 2003.

2.5 Determination of functional properties

The functional properties of the tamarind seed starch were determined following the method as described in the work of Chandra and Samshe [11].

3.0 RESULTS AND DISCUSSION

Table 1 depicts some chemical and physical characteristics of the tamarind seed kernel starch. It was observed in this study that *Tamarindus indica*

kernel starch (TSKS) had moisture content of 0.069 g/100g, an indication that it was properly dried. The moisture content is considerably lower than the content (8 g/100g) reported in study [12]. The relatively low moisture content could retard or makes the TSKS less prone to colonization by organism degradation, similar to observations reported for root, tuber and cereal starches [13].

Table 1: Some chemical and physical characteristics of tamarind seed kernel starch



Chemical and physical characteristics	Composition
Moisture (g/100g)	0.06
Ash (g/100g)	3.01
Lipid (g/100g)	4.90
Protein (g/100g)	14.58
Total carbohydrate (g/100g)	77.45
Acidity (me/g)	5.00
pH	10.90
Solubility	0.80
Red (color measurement)	2.1
Yellow (color measurement)	2.5
Blue (color measurement)	1.5

The ash content of TSKS obtained in this study was 3.01%. Similarly, Kamla [14] (2014) reported ash content of 3.2 g/100g, while ash contents of 4.55 g/100g, and 2.74 g/100g were reported for roasted tamarind seed, and the seed flour respectively [15]. The crude lipid obtained was 4.9 g/100g, which is lower than 5.4- 10.9 g/100g obtained in studies [16,17]. The crude protein content obtained in this study was 14.58 g/100g, while Makinde and Ayodele, [18] revealed crude protein content within the range of 2.3 to 12.7 g/100g. The crude protein content observed in this study suggests that, the TSKS could be used as a component in baking flours and thickener in food industries and may contribute in parts to protein requirements of livestock rations. Most importantly, if a starch is low in protein, it could affect the purity and crystal nature of the starch, as well as physicochemical properties of starches [19]. This study therefore indicates that tamarind starch is stable in purity.

The acidity, pH, solubility of the TSKS were investigated and reported in this study. The pH value (10.9) obtained in this study falls within the acceptable range of pH for pharmaceutical grade starch. The solubility of TSKS was 0.8, which shows the magnitude of interaction between starch chains within the amorphous and crystalline domain, and is influenced by the ratio of amylose to amylopectin [20].

Colour measurement showed 2.1, 2.5, and 1.5 for red, yellow, and blue respectively. Generally, colour measurement of flour is important, considering its application in food system, and sometimes, the colour of food is an important prerequisite for consumer acceptability.

Table 2: Some functional properties of tamarind seed starch

Functional Properties	
Swelling capacity (g/100g)	10.29±0.012
Foam capacity (g/100g)	20.01±0.012
Form stability (g/100g)	9.83±0.005
Emulsion activity (g/100g)	23.00±0.000
Emulsion stability (g/100g)	19.00±0.000
Water absorption capacity (g/100g)	262.05±0.372
Oil absorption capacity (g/100g)	96.48 ±0.026
Least gelation capacity (g/100g)	26.00±0.000
Gelatinization temperature (°C)	38.00±0.000



Functional properties of starch are the intrinsic physico-chemical properties that reflect the complex interaction between the composition, structure and the nature of the environment in which they are associated and measured. Table 2 highlights some of the functional properties of tamarind seed starch. The results showed 10.29±0.012 g/100g, 20.01±0.012 g/100g, 9.83±0.005 g/100g, 23.00±0.000 g/100g, 19.00±0.000 g/100g, 262.5±0.372 g/100g, 96.48 ±0.026 g/100g, 26.00±0.000 g/100g, 38.00±0.000 (°C) and 0.76±0.002 (g/cc), of swelling capacity, foam capacity, foam stability, emulsion activity, emulsion stability, water absorption capacity, oil absorption capacity, least gelation capacity, gelatinization temperature, and bulk density respectively.

The water absorption capacity (262.5±0.372 g/100g), and swelling capacity (20.01±0.012) of the starch obtained from tamarind seed kernel, is considerably lower than the water absorption capacity (1636 ± 1.33 g/100g), and swelling capacity (20.92±0.52 g/100g) of the tamarind starch reported in the work of Singthong, [21]. High water absorption capacity of any food material strongly suggests that, it could be used in formulation of foods like dough, bakery products, cheese etc. [6]. On the contrary, the oil absorption capacity (96.48 ±0.026 g/100g) obtained in this study is significantly higher than the capacity (3.35±0.03 g/100g) reported in study [21]. The ability of starch to absorb oil is a measure of the emulsifying potentials of the starch. The oil absorption capacity is also important as it improves the mouth feel and retains flavor [22].

Emulsion activity and stability as obtained in this study were considerable, and are key components of quality starches. Emulsion activity is related to the capacity of surface active molecules to cover oil-water interface created by mechanical homogenization, thus reducing the interfacial tension, and consequently, the more active the emulsifying starch is, the more the interfacial tension is lowered [23].

4.0 CONCLUSION AND RECOMMENDATION

Tamarind starch as investigated in this study reveal the applicability of the starch in many local and industrial processes, TSKS can be harnessed for its valuable properties either as raw material for the production of other valuable products or as an additive

REFERENCES

1. Kamla M. (2014). Physicochemical, Functional Properties and Proximate Composition of Tamarind Seed. *Journal of Agri Search*, 7(1):51-53.
2. Kumar, C. S., & Bhattacharya, S. (2008). Tamarind Seed: Properties, Processing and Utilization. *Critical Reviews in Food Science and Nutrition*, 48(1), 1–20.
<https://doi.org/10.1080/10408390600948600>
3. Sudharsan, K., Chandra Mohan, C., Azhagu Saravana Babu, P., Archana, G., Sabina, K., Sivarajan, M. and Sukumar, M. (2016). Production and characterization of cellulose reinforced starch (CRT) films. *International Journal of Biological Macromolecules*, 83, 385–395.
<https://doi.org/10.1016/j.ijbiomac.2015.11.037>
4. Chowdhury, M. A., Badrudduza, MD., Hossain, N., & Rana, Md. M. (2022). Development and characterization of natural sourced bioplastic synthesized from tamarind seeds, berry seeds and licorice root. *Applied Surface Science Advances*, 11, 100313.
<https://doi.org/10.1016/j.apsadv.2022.100313>



5. Ferrara, L. (2019). Nutritional and Pharmacological Properties of *Tamarindus Indica L.* *Journal of Nutrition and Food Science Forecast*, 2(2):1-5.
6. Chandra S., Singh S and Kumari D (2015). Evaluation of functional properties of composite flours and sensorial attributes of composite flour biscuits. *J Food SCiTechnol*, 52(6); 3681-3688. DOI: 10. 1007/S13197-014-1427-2.
7. Rodriguez-Amado, J.R., Lafourcade, P.A., Escalona, A.J.C., Perez, R.R., Morris, Q.H. and Keita, H. (2016). Antioxidant and Hepatoprotective Activity of a new Tablets Formulation from *Tamarindus indica L.* Evid Based Complement. *Alternat Med.*, 39(8):67-72. <https://doi.org/10.1155/2016/3918219>
8. El-Siddig, K., Gunasena, H.P.M., Prasa, B.A., Pushpakumara, D.K.N.G., Ramana, K.V.R., Vijayanand. P. and Williams, J.T. (2006). Tamarind – *Tamarindus indica L.* Fruits for the future 1. Southampton Centre for Underutilized Crops, Southampton, UK, p 188.
9. Xie, F., Ren, X., Zhu, Z., Luo, J., Zhang, H., Xiong, Z., Wu, Y., Song, Z., & Ai, L. (2023). Tamarind seed polysaccharide-assisted fabrication of stable emulsion-based oleogel structured with gelatin: Preparation, interaction, characterization, and application. *Food Hydrocolloids*, 142, 108761. <https://doi.org/10.1016/j.foodhyd.2023.108761>.
10. Van den Bilcke, N., Alaerts, K., Ghaffaripour, S., Simbo, D. J., & Samson, R. (2014). Physico-chemical properties of tamarind (*Tamarindus indica L.*) fruits from Mali: selection of elite trees for domestication. *Genetic Resources and Crop Evolution*, 61(2), 537–553. <https://doi.org/10.1007/s10722-014-0080-y>
11. Chandra S and Samshe (2013). Assessment of functional properties of different flours.). *African Journal of Agricultural Research*, 8(38), 4849-4852. DOI:10.5897/AJAR2013 .690.
12. Akajiaku L.O, Nwosu J.N, Onuegbu N.C, Njoku N.E and Egbeneke C.O.(2014). Proximate, Mineral and Anti-Nutrient Composition of Processed (Soaked and Roasted) Tamarind (*Tamarindus indica*) seed. *Current Research in Nutrition and Food Science* 2(3):136-145. DOI: <http://dx.doi.org/10.12944/CRNFSJ.2.3.05>.
13. Nuwamanya, E., Baguna, Y., Wembabazi, E., and Rubaihayo, P., (2011). A Comparative Study of the Physicochemical Properties of Starches from Root, Tuber, and Cereal Crops. *African Journal of Biotechnology*, Vol. 10(56), Pp 12018 – 12030.
14. Caluw, ED; Halamov, K; Damme, PV (2010). *Tamarindus indica L.*: A review of traditional uses, phytochemistry and pharmacology. *Afrika Focus* 23(1): 53-83. <https://doi.org/10.1163/2031356X-02301006>
15. Khairunnuur, F.A., Zulkhairi, A., Azrina, A., Moklas, M.A.M., Khairullizam, S., and Zamree, M.S. (2009). Nutritional composition, in vitro antioxidant activity and *Artemiasalina L.* Lethality of pulp and sed of *Tamarindus indica L.* Extracts



- Malaysia Journal of Nutrition*. 15 (1)65-75.
16. Makinde, F.M and Ayodele, T.I. (2022). Impact of Processing on Physical, Chemical and Pasting Properties of *Tamarindus indica* Seed Flour. *Journal of Applied Science and Environmental Management*. 26 (6) 1039-1047. <https://doi.org/10.4314/jasem.v26i6.7>
 17. Tester, R.F., and Morrison, W.R. (1990). Swelling and Gelatinization of Cereal Starches. Effect of Amylopectin. Amylose and Lipids. *Cereals Chemistry*. 67: 551 – 557.
 18. Blazek J and Copeland L (2008). Pasting and swelling properties of wheat flour and starch in relation to amylose content carbohydrate polymers. 71:380-387. <https://doi.org/10.1016/j.carbpol.2007.06.010>
 19. Komakech, R., Kim, Y., Matsabisa, G. M., & Kang, Y. (2019). Anti-inflammatory and analgesic potential of *Tamarindus indica* Linn. (Fabaceae): a narrative review. *Integrative Medicine Research*, 8(3), 181–186. <https://doi.org/10.1016/j.imr.2019.07.002>.
 20. Zizka, A., Thiombiano, A., Dressler, S., Nacoulma, B. M., Ouédraogo, A., Ouédraogo, I., Ouédraogo, O., Zizka, G., Hahn, K., & Schmidt, M. (2015). Traditional plant use in Burkina Faso (West Africa): a national-scale analysis with focus on traditional medicine. *Journal of Ethnobiology and Ethnomedicine*, 11(1). <https://doi.org/10.1186/1746-4269-11-9>
 21. Singthong J (2011). Characterization of flour and starch from tamarind seed. *Starch Update 2011: The 6th International Conference on Starch Technology*, 172-178.
 22. Olu-Owolabi B.I., Afolabi TA and Kayode O. Adebowale KO (2011) Pasting, Thermal, Hydration, and Functional Properties of Annealed and Heat-Moisture Treated Starch of Sword Bean (*Canavaliaglabadiata*), *International Journal of Food Properties*, 14:1, 157-174, DOI: 10.1080/10942910903160331
 23. Wang Y., Ai C., Wang H., Chen C., Teng H., Xiao J and Chen L (2023). Emulsion and its application in the food field: an update review. *Food*, 4(2); 102. <https://doi.org/10.1002/efd2.102>.



P083 - SLAUGHTERHOUSE EFFLUENT: ENVIRONMENTAL IMPACTS, PRE-TREATMENTS, AND APPLICATIONS

Ridiwanulai O. JIMOH^{1*}, Amina G. MUSA¹, Sumaiya I. ABUBAKAR², Zainab MUHAMMAD¹, Jibrin ABDULKADIR³, Elizabeth WINFUL³, Victor OCHIGBO³, Bridget E. NWOBI³, Mahmood ABDULLAHI³

¹Department of Microbiology, Ahmadu Bello University Zaria.

²Department of Biochemistry, Ahmadu Bello University Zaria.

³Industrial and Environmental Pollution Department, National Research Institute for Chemical Technology Zaria.

*Corresponding author's email: ridwanullahijimoh7@gmail.com

ABSTRACT

Meat and other animal products are important dietary sources of protein for ages contributing to the prevalence of slaughterhouses globally. Although the activities of these slaughterhouses are important for the production of meat and other animal products for human consumption, the inappropriate disposal of slaughterhouse wastes has led to a great deal of environmental pollution. The effects of these wastes range from malodorous discharges to the spread of highly resistant pathogens which are harmful to man and animals. This review article focuses on the generation of wastes from slaughterhouses, their environmental impacts as well as the possible pretreatment methods for the production of valuable products from the wastes which can be used for diverse applications.

Keywords: Slaughterhouse, Environmental pollution, Environmental impacts, Pretreatment, Valuable products.

1.0 Introduction

The increasing global population has placed a great deal of demand on meat production as a dietary source of protein to feed the growing world population (1, 2). This increasing demand has contributed immensely to the prevalence of slaughterhouses (otherwise known as **abattoirs**) all over the world consequently increasing the volume of waste (both solid and liquid) generated from these sources. Slaughterhouse wastes or effluents refer to the residual animal byproducts left unused following the slaughter of animals (3). The Food and Agriculture Organization (FAO) under the United Nations (UN) reported that global meat consumption has been increased by 100% in the last decade and estimates a double fold increase by the year 2050 (1).

The global livestock population is around **4.89 billion** including bovines, caprines, ovines, and swine species with around **27.88 billion** poultry species (4). Some underutilized remnants, including offals, bones, tendons, and blood, are edible and enjoyed as delicacies in certain countries. Nevertheless, approximately 60% of these remnants which become wastes that must be discarded or recycled contribute about a few million

metric tons of waste in the environment without any scientific intervention, producing socio-economic and -environmental concerns (5, 6).

In many developing countries like Nigeria, these wastes are inappropriately disposed into the environment with little or no treatment leading to further environmental problems. Increase in meat production for the increasing Nigerian population has resulted in upsurge in the number of slaughterhouses springing up in major cities in Nigeria (4, 7-9). It has been reported that Nigeria Produces about **227,500** tons of fresh animal wastes on daily basis with a typical abattoir slaughtering about ten cows daily and generating about **3,880 kg** of solid wastes on a daily basis (9).

The activities of these abattoirs are not regulated by the authorities thereby leading to the indiscriminate disposal of these wastes into the environment (8). These indiscriminate refuse dumping do not only constitute a menace to effective environmental management but are also associated with reduction in air quality of the environment, potential transferable antimicrobial resistance patterns, and many infectious organisms which can be pathogenic to human (9).



These wastes pose a great environmental threat to the people living close to abattoirs as well as those living far from it, since the wastewater emanating from these slaughterhouses can find their way into water bodies and move great distances to places far away from the slaughterhouses causing health risk and **pollution** challenges of varying severity. This review is aimed at studying the **environmental impacts** of slaughterhouse wastes in the Nigerian context suggesting possible ways of waste **pretreatment** and the applications of the treated wastes across various facets of life.

1.1 Characteristics of Slaughterhouse Effluents

It was reported by Loganath & Senophiyah-Mary (1) and Sandoval *et al.*, (10) that the production of meat and dairy products for human consumption utilizes about **24%** and **25%** of the total freshwater used by the food and beverage industry respectively. A slightly higher percentage of **29%** freshwater consumption yearly was reported by Bustillo-Lecompte *et al.*, (11).

The wastes generated from these slaughterhouses usually depend on the species of the slaughtered animal, the slaughtering method as well as the cleaning practices adopted and they are typically evaluated using bulk parameters because of the broad range of Slaughterhouse Wastewater (SWW) and pollutant loads (8, 11). SWW is characterized by high level of biochemical oxygen demand (BOD), chemical oxygen demand (COD), total organic carbon (TOC), total nitrogen (TN), total phosphorus (TP), and total suspended solids (TSS) (7, 10-13). However, the waste materials usually contain elevated amounts of nitrogen, phosphorus, hair, urine, dung, fur, fats, paunch contents, salts, putrescible materials and pathogenic microorganisms and so on (8, 9, 14-16).

1.2 Dangers of Slaughterhouse Effluents.

Slaughtering houses are known globally to contaminate the environment either directly or indirectly as a result of their activities which pose a great deal of threat to the environment and a host of other life forms because their activities contaminate both surface and subsurface waters as well as the surrounding air (8). Most slaughterhouses in Nigeria are typically sited near water bodies and residential areas leading to the indiscriminate disposal of effluents from these sources into gullies

and contaminating underground water and nearby streams (17, 18).

Observation showed that most slaughterhouses in Nigeria lack refrigeration, good sewage or waste disposal systems, adequate clean water sources, slaughtering and processing facilities (7, 19) leading to water pollution from abattoir effluents and other sources like dairy farms, pastures, and sewage. This pollution poses environmental and public health risks, exacerbated by the improper placement of abattoirs in residential areas alongside the fact that slaughtering is carried out by slaughter men and butchers who are ignorant of sanitary principles associated with effluents from abattoirs (7).

The increased amount of organic debris, nutrients, pathogens, detergents, antibiotics and heavy metals in slaughterhouse waste waters is hazardous to man and aquatic ecosystem with severe implications worldwide ranging from diseases and infections to deaths (20). Rahman *et al.*, (21) reported that the activities of slaughterhouses (such as freezing, smoking, cutting and scorching of bones and meat) generate some toxic gases such as CO₂, CO, CH₄, SO₂ and NO₂ which pollute the air and presents problems with varying severity such as global warming, ozone layer depletion, acid rain, malodorous discharge and other health risks.

Untreated slaughterhouse effluents is also implicated in the spread of diseases through pathogenic microorganisms which originates from animal carcasses and intestinal micro biota causing diseases such as cholera, dysentery, diarrhoea and typhoid. This issue is exacerbated by the high organic content and nutrients in the effluent, which can promote the rapid growth of microbial cells. Additionally, the presence of numerous colloidal particles leads to significant turbidity in this type of effluent, which is undesirable. This turbidity can provide surfaces for the attachment of microorganisms and undesirable chemicals while obstructing light penetration (18, 22).

The excessive input of nitrate, sulfates, phosphorus, and organic matter into the river leads to nutrient enrichment, promoting the stubborn proliferation of invasive species, particularly water



hyacinth (*Eichhornia crassipes*) (18). Some other notable problems associated with waste materials emanating from slaughterhouses include, clogging of irrigation pipes, production of malodorous discharge, sludge flotation and waste adherence to microbial cells which in turn reduces the ability of the microorganisms to degrade the organic matter present in the waste (23).

1.3 Pretreatment of Slaughterhouse Effluents

Due to the detrimental impacts of slaughterhouse effluents on the environment, it is imperative that this waste be adequately treated prior to disposal in order to mitigate the effects of such wastes (8). Mozhiarasi & Natarajan (3) highlighted some of the most common methods of disposing slaughterhouse wastes in developing countries such as: Composting, Open dumping/Landfilling, incineration etc. These methods however present some challenges such as generation of secondary contamination, greenhouse gas (GHG) emissions, air pollution among others. Some current methods of pretreatments include:

1.3.1 Enzymatic Pretreatment of Slaughterhouse Effluents.

This method of effluent pretreatment uses lipases to reduce the oil and grease contents of the effluents due to their environmentally friendliness and effectiveness under mild reaction conditions (13). It was reported that lipases from microbial sources are preferable to those from plants and animal origins due to the ease of genetic manipulation, stability, selectivity, broad substrate specificity and rapid growth (24). Solid state fermentation of slaughterhouse wastes using *Penicillium spp* produced lipase enzyme which aided the removal of organic matter in effluents and led to the production of biogas which can be trapped and used in other fields (13).

1.3.2 Effluent treatment with Bio-nanoparticles (BioNPs)

A research by Antunes *et al.*, (22) reported that utilizing *Moringa oleifera* (MO) protein extracts in combination with magnetic nanoparticles (such as iron) for wastewater treatment can enhance performance, leading to improved sedimentation, reduced sludge volume, and the possibility of reuse. This is because the introduction of Bio-nanoparticles (BioNPs) (MO-functionalized nanoparticles) enhanced the efficiency of the coagulation/flocculation/sedimentation (C/F/S) process thereby reducing turbidity and the Chemical Oxygen Demand (COD). This resulted in quicker contaminant removal and higher removal rates compared to treatments using only MO at equivalent coagulant concentrations.

1.3.3 Anaerobic digestion of slaughterhouse effluents.

Among the various types of treatments, anaerobic processes are the best selection of biological treatment for slaughterhouse wastewater treatment due to high concentration of organic matter and nutrients (9, 25). Up-flow Anaerobic Sludge Blanket reactor (UASB) represents a reliable method for treatment of different industrial wastewater. The popularity of UASB reactor stems from low sludge generation, low capital investment and maintenance cost, less land and energy requirements and biogas production (1, 25)

To achieve this, the waste slurry should first undergo characterization to measure its essential properties, following standard methods such as those outlined in American Public Health Association (APHA 2012). Parameters to be monitored include: temperature, pH, dissolved oxygen (DO), salinity, oxidation-reduction potential (ORP), conductivity, total dissolved solids (TDS), and turbidity. Analyses encompass Polycyclic Aromatic



Hydrocarbons (PAHs), acidity, alkalinity, biochemical oxygen demand (BOD), nitrate, and phosphate (1, 2, 9, 18, 23).

Methane (CH₄), the most valuable component, is produced through the anaerobic process of “methanogenesis or bio-methanation”. This process involves multiple microbial steps. Firstly, breaking down polymeric biomass (e.g., proteins, polysaccharides, cellulose) into smaller molecules (e.g., amino acids, monosaccharides, acetate) by bacteria or fungi. Intermediary reactions can either promote (CO₂, H₂) or inhibit (NH₃) the process. Finally, archaea, comprising over 80 species, synthesize Methane (CH₄) by reducing CO₂ or acetoacetic compounds (1, 26).

As reported by Odekanle *et al.*, (9), after the anaerobic digestion of slaughterhouse effluents, biogas production commenced on the sixth day which increased steadily till the fifteenth day before production declined. The study yielded a daily and cumulative biogas volumes of 0.00103m³/kg VS (1.03L) and 0.0309m³/kg VS (30.90L) respectively. Another report explains the production of bio-methane through anaerobic codigestion (Co-DA) of avian feathers with diluted swine manure in a ratio of 1:10. CH₄ production increased significantly over 146 days, with an appreciable rise in proteolytic organisms (26).

The biogas produced during anaerobic digestion consists of about 60% methane, with the remaining 40% including CO₂, H₂S, and other gases. The sludge obtained at the end of the process is also a useful product that can be applied as a fertilizer, since it is rich in nutrients such as nitrogen, phosphorus, and potassium. Methane can be used directly as a fuel for heat and electricity generation (23).

1.3.4 Other Methods of Slaughterhouse effluents treatments

Membrane processes are becoming an alternative treatment method for meat processing effluents (11). Musa & Idrus (27) also noted that membrane technologies could be used in the treatment of water and slaughterhouse effluents by using different membrane processes, including microfiltration (MF), ultrafiltration (UF), nanofiltration (NF), and reverse osmosis (RO) with overall efficiencies of up to 90%. Another method for effluents pretreatment is the Coagulation process where colloidal particles in the Slaughterhouse wastewater (SWW) are grouped into larger particles, called flocs. The colloidal particles in SWW are nearly negatively charged which make them stable and resistant to aggregation. For this reason, coagulants with positively charged ions are added to destabilize the colloidal particles to form flocs and facilitate the sedimentation process. Various coagulant types can be found in the market, and the most widely used are inorganic metal based-coagulants such as aluminum sulfate, aluminum chlorohydrate, ferric chloride, ferric sulfate, and poly-aluminum chloride with removal efficiencies of up to 80% for BOD, COD, and TSS (11, 27). Advanced Oxidation Processes (AOPs) work by producing reactive species such hydroxyl radicals (OH⁻), which can break down even the most resistant organic contaminants and boost biodegradability. AOPs refer to a variety of techniques, and combining many processes to achieve synergistic effects is a typical practice (28).

Purple nonsulfur bacteria (PNSB) can be used to treat sewerage because of the features of the wastewater. PNSB may grow in wastewater through a variety of metabolic routes, which offers a number of benefits. PNSB under light circumstances has shown to decrease the rotten-egg smell from H₂S and also created single cell protein (SCP) biomass. PNSB biomass has a high protein content as well as vitamins, photopigments, and vital amino acids. The presence of these elements suggested that PNSB biomass had a high potential for SCP (29).

1.4 Applications of Treated Slaughterhouse Effluents.

Regardless of its toxicity, slaughterhouse effluents are a valuable resource that can be used in various facets of human life. This application of slaughterhouse effluents is a waste to wealth approach which is aimed at reducing the generation of organic wastes from slaughterhouses and



utilizing the slaughterhouse wastes after treatments for a wide range of applications such as the production of animal feeds, biogas, enzyme manufacturing, wood glue, fertilizer, etc (16).

1.4.1 Irrigation for Agricultural Purposes

Menegassi et al., (8) demonstrated how the use of wastewater to cultivate Hay resulted in elevated levels of sodium within the top 0.20 meters of the tropical soil used thereby confirming an earlier report by Pereira *et al.*, (2011) which showed an increased productivity and forage quality of Hay irrigated with anaerobically treated wastewater. This approach allows for the use of lower-quality water, contributing to water resource conservation, thus presenting slaughterhouse effluent as a good source of water for irrigation (10). This practice improves water management in irrigated systems, decrease the pressure on the water bodies and the cost compared to another source of water supply (8). Slaughterhouse wastes treated with Purple Non-Sulfur Bacteria (PNSB) contains high levels of Plant Growth Promoting Bacteria (PGPB) and Plant Growth Promoting Substances (PGPS) which can be used in agriculture (Bio fertilizer) for promoting plant development and yield while reducing CH₄ and CO₂ levels (17).

1.4.2 Microbial Cultivation and Production of Enzymes.

Effluent from slaughterhouses contains nutrients that foster the growth of microorganisms (mainly bacterial growth). This was confirmed by filtering slaughterhouse wastes and adding granulated agar to the filtrate as a solidifying agent. Then the mixture was sterilized with the autoclave. Upon inoculation of microbial colonies on the prepared agar plates and incubation at 37^oC for 24 hours, luxuriant bacterial growth was observed on the plates indicating bacterial growth. With this result, Ramakodi *et al.*, (16) concluded that effluents from slaughterhouses contain the necessary nutrients favoring the growth of bacteria and can be implemented for use as a basic microbiological culture medium for bacterial growth. Similarly, enzymatic pretreatment of slaughterhouse wastes has been shown to produce large amount of bio-methane (13). The microorganisms present in slaughterhouse wastes were also reported to produce some bioactive compounds of industrial importance. An example of such important

enzymes is Protease which was produced by a bacterium called *Chromobacterium violaceum* (16).

1.4.3 Alternative Source of Electricity.

The globally calculated energy requirement is 13 Terawatts with over 80% coming from fossils (1). Due to the Nigeria's dependence on fossil fuels for provision of sustainable power supply, there is urgent need for alternative energy source especially renewable energy such as those from slaughterhouses which have high potential for biogas production due to their high organic matter content, protein and lipid matter embedded there-in (1, 9, 23). Fat, oil and grease from slaughterhouse wastewater can be transformed into biodiesel, biogas and even bio-methane. The Co-digestion of Slaughterhouse Wastewater (SWW) with *Opuntia ficus-indica* (OFI) was reported by Panizio *et al.*, (30) to increase biogas yield by using 75% SWW and 25% OFI which can be used as an alternative source of energy (1, 10).

It was reported that Nigeria is capable of generating between 24.08Kwh to 38.52Kwh of electricity from anaerobic digestion of the 227,500 tons of slaughterhouse wastes generated daily by converting the bio-methane produced during the anaerobic digestion of slaughterhouse wastes using low end conversion efficiency and high-end conversion efficiency respectively (9).

1.4.4 Production of biomaterials from slaughterhouse wastes

Slaughterhouse waste consists of a blend of components like manure, urine, leftover feed, fodder, and carcass waste/offals. The composition of slaughterhouse waste varies based on the animal type and specific waste product. Nonetheless, it often contains valuable biomaterials like collagen, keratin, and hydroxyapatite, all of which find applications in the biomedical field as well as potential applications in the field of Xenotransplantation (26). Ayon *et al.*, (4) reported the production of important biomedical materials such as Biobran (a nylon material which can be used as wound dressings), **Hydroxyapatite**



generated from femur bone residues which when conjugated with 8-20nm size silver nanoparticles exhibits a good antibacterial activity against Methicillin Resistant *Staphylococcus aureus* (MRSA). Furthermore, the fermented hydrolysate exhibits antagonistic properties against *Salmonella typhi*, poultry waste holds promise as a source for producing biomaterials like keratinous proteins and biocomposites (4). Additionally, stem cells derived from urine, feces, and slaughterhouse wastewater can contribute to creating functional bioartificial structures. However, the extensive utilization of slaughterhouse wastes for biomedical applications still requires in-depth studies before full implementation (26).

2.0 Conclusion.

Generation of wastes from slaughterhouses pose a great deal of environmental hazard due to the components of the wastes coming from these sources. Regardless of their adverse impacts, these wastes sources contain important components such as collagen, keratin, and hydroxyapatite that can be used as a starting material in the production of other value-added products. The applications of Slaughterhouse wastes ranges from biomedical applications such as bio-composites used after surgery, to bio fertilizers as plant growth promoter down to the industrial sector for the generation of other products. An extensive review of existing works on the applications of slaughterhouse wastes shows the possibility of electric power generation (between 24.08Kwh to 38.52Kwh) providing a solution to the global energy crisis. It is imperative that the government formulates policies that will foster adequate disposal of wastes from slaughterhouses and the proper treatment of these wastes for the production of value-added products. This can be approached by implementing proper waste disposal and collection

practices, construction of modern treatment facilities and improvement of the existing ones for optimal utilization of these waste materials.

References.

1. R. Loganath, J. Senophiyah-Mary, Critical review on the necessity of bioelectricity generation from slaughterhouse industry waste and wastewater using different anaerobic digestion reactors. *Renewable and Sustainable Energy Reviews* **134**, 110360 (2020).
2. O. J. Odejobi, E. L. Odekanle, A. Bamimore, O. A. Falowo, F. Akeredolu, Anaerobic digestion of abattoir wastes for biogas production: optimization via performance evaluation comparison. *Cogent Engineering* **9**, 2122150 (2022).
3. V. Mozhiarasi, T. S. Natarajan, Slaughterhouse and poultry wastes: Management practices, feedstocks for renewable energy production, and recovery of value added products. *Biomass Conversion and Biorefinery*, 1-24 (2022).
4. A. Tarafdar *et al.*, Advances in biomaterial production from animal derived waste. *Bioengineered* **12**, 8247-8258 (2021).
5. B. B. Adhikari, M. Chae, D. C. Bressler, Utilization of slaughterhouse waste in value-added applications: Recent advances in the development of wood adhesives. *Polymers* **10**, 176 (2018).
6. R. L. Khan, A. A. Khraibi, L. F. Dumée, P. R. Corridon, From waste to wealth: Repurposing slaughterhouse waste for xenotransplantation. *Frontiers in Bioengineering and Biotechnology* **11**, 1091554 (2023).
7. O. T. Dada *et al.*, Environmental hazard and health risks associated with slaughterhouses in Ibadan, Nigeria. *Environmental Hazards* **20**, 146-162 (2021).
8. L. C. Menegassi *et al.*, Reuse in the agro-industrial: Irrigation with treated



- slaughterhouse effluent in grass. *Journal of Cleaner Production* **251**, 119698 (2020).
9. E. Odekanle, O. Odejobi, S. Dahunsi, F. Akeredolu, Potential for cleaner energy recovery and electricity generation from abattoir wastes in Nigeria. *Energy Reports* **6**, 1262-1267 (2020).
 10. M. A. Sandoval, R. Salazar, Electrochemical treatment of slaughterhouse and dairy wastewater: Toward making a sustainable process. *Current Opinion in Electrochemistry* **26**, 100662 (2021).
 11. C. Bustillo-Lecompte, M. Mehrvar, Slaughterhouse wastewater: treatment, management and resource recovery. *Physico-chemical wastewater treatment and resource recovery*, 153-174 (2017).
 12. W. G. Djonga, E. Noubissié, G. B. Noumi, Removal of nitrogen, phosphate and carbon loads from slaughterhouse effluent by adsorption on an adsorbent based on Ayous sawdust (*Triplochyton scleroxylon*). *Case Studies in Chemical and Environmental Engineering* **4**, 100120 (2021).
 13. K. J. Haselroth *et al.*, Effectiveness of *Aeromonas hydrophila* for the removal of oil and grease from cattle slaughterhouse effluent. *Journal of Cleaner Production* **287**, 125533 (2021).
 14. P. Jensen *et al.*, Anaerobic membrane bioreactors enable high rate treatment of slaughterhouse wastewater. *Biochemical Engineering Journal* **97**, 132-141 (2015).
 15. A. Mulu, T. Ayenew, S. Berhe, Impact of slaughterhouses effluent on water quality of Modjo and Akaki river in Central Ethiopia. *Int J Sci Res* **4**, 2319-7064 (2013).
 16. M. P. Ramakodi, N. Santhosh, T. Pragadeesh, S. V. Mohan, S. Basha, Production of protease enzyme from slaughterhouse effluent: an approach to generate value-added products from waste. *Bioresource Technology Reports* **12**, 100552 (2020).
 17. E. Chukwuma, A. Rashid, G. Okafor, A. Nwoke, Fuzzy based risk assessment of abattoir operations and treatment facilities: a case study of Onitsha North/South LGA of Anambra State of Nigeria. *Food and Bioproducts Processing* **119**, 88-97 (2020).
 18. E. I. Olaniran, T. O. Sogbanmu, J. K. Saliu, Biomonitoring, physico-chemical, and biomarker evaluations of abattoir effluent discharges into the Ogun River from Kara Market, Ogun State, Nigeria, using *Clarias gariepinus*. *Environmental monitoring and assessment* **191**, 1-17 (2019).
 19. O. M. Buraimoh *et al.*, Analysis of bacterial composition in slaughterhouse effluent from a major livestock market in Nigeria. *The Libyan Journal of Science* **26**, (2023).
 20. A. Aziz, F. Basheer, A. Sengar, S. U. Khan, I. H. Farooqi, Biological wastewater treatment (anaerobic-aerobic) technologies for safe discharge of treated slaughterhouse and meat processing wastewater. *Science of the total environment* **686**, 681-708 (2019).
 21. U. ur Rahman, A. Sahar, M. A. Khan, Recovery and utilization of effluents from meat processing industries. *Food Research International* **65**, 322-328 (2014).
 22. A. d. S. Antunes *et al.*, Influence of bionanoparticles to treat a slaughterhouse wastewater. *Environmental Technology* **43**, 4528-4544 (2022).
 23. A. J. Vilvert *et al.*, Minimization of energy demand in slaughterhouses: Estimated production of biogas generated from the effluent. *Renewable and Sustainable Energy Reviews* **120**, 109613 (2020).
 24. M. I. Saadatullah, M. Jan, M. N. Waheedullah, Z. Rehman, Isolation, identification and characterization of a lipase producing *Pseudomonas*. *J. Biomat* **2**, 51-57 (2018).
 25. M. Besharati Fard, S. A. Mirbagheri, A. Pendashteh, J. Alavi, Biological treatment of slaughterhouse wastewater: kinetic modeling and prediction of effluent. *Journal of Environmental Health Science and Engineering* **17**, 731-741 (2019).
 26. V. E. Broering *et al.*, Bioprocessing of broiler feathers to produce biomethane. *World's Poultry Science Journal* **79**, 331-350 (2023).



27. M. A. Musa, S. Idrus, Physical and biological treatment technologies of slaughterhouse wastewater: a review. *Sustainability* **13**, 4656 (2021).
28. P. Alfonso-Muniozguren, A. I. Gomes, D. Saroj, V. J. Vilar, J. Lee, The role of ozone combined with UVC/H₂O₂ process for the tertiary treatment of a real slaughterhouse wastewater. *Journal of Environmental Management* **289**, 112480 (2021).
29. T. Bunraksa, D. Kantachote, S. Chaiprapat, The potential use of purple nonsulfur bacteria to simultaneously treat chicken slaughterhouse wastewater and obtain valuable plant growth promoting effluent and their biomass for agricultural application. *Biocatalysis and Agricultural Biotechnology* **28**, 101721 (2020).
30. R. M. Panizio, L. F. d. C. Calado, G. Lourinho, P. S. D. de Brito, J. B. Mees, Potential of biogas production in anaerobic co-digestion of *Opuntia ficus-indica* and slaughterhouse wastes. *Waste and Biomass Valorization* **11**, 4639-4647 (2020).



P084 - PRODUCTION OF FIRE RETARDANT FROM KAOLIN AND INDUSTRIAL EFFLUENT FOR NIGERIAN BUILDING CONSTRUCTION INDUSTRY

Longtau Pirmak

Nigerian Building and Road Research Institute, Abuja
pirmaklongtau@gmail.com

ABSTRACT

In recent times, industries have been working to develop products, methods, and processes to limit hazards and threats from fire. The entire importance of fire retardant is to delay ignition, retard the burning process once it starts, and suppress the development of smoke. This project used Kaolin and recycled Ammonium Phosphate $(\text{NH}_4)_3\text{PO}_4$, from fertilizer industry effluent to produce fire retardant. $(\text{NH}_4)_3\text{PO}_4$ salt, which was separated from the solution using simple distillation process, was analyzed chemically to ascertain its chemical composition. Sieve size analysis was carried out on Kaolin and found to be suitable. Scanning Electron Microscopy (SEM), X-Ray Fluorescence (XRF), X-Ray Diffraction (XRD) and Refractive Index (RI) of kaolin was determined and found to fall within standards and regulations. Results revealed presence of $(\text{NH}_4)_3\text{PO}_4$ in the effluent. Fire retardant was produced varying percentage by volume of $(\text{NH}_4)_3\text{PO}_4$ in the mixture. Flammability test results showed that ignition time and smoke density of fire retardant produced was better than conventional fire retardant. This study concludes that Kaolin and $(\text{NH}_4)_3\text{PO}_4$ fertilizer from industrial effluent has potentials to be used for the production of alternative fire retardant.

Keyword: *Fire Retardant, Flash Point, Flame Spread Time, Smoke Density, Chemical Analysis*

INTRODUCTION

Fire is one of the most destructive forces in the world. Fire are hard to fight and often impossible to control, and the loss of human life, injury, and damage to property are staggering. Many industries have been working for a long time to develop products, methods, and processes to limit the hazards and threats from fire; sprinkler systems, fire extinction systems, and smoke and fire detection devices. Although these product and process have led to a significant reduction in loss of lives and damages to properties but the methods and process enumerated above are control measures. Flame retardants (FRs) are chemical compounds added to or otherwise incorporated into paints to provide varying

degrees of flammability protection. By delaying ignition, retarding the burning process once it starts, and/or suppressing the development of smoke, FRs give the victims of fire more time to escape, limit the loss of life and injury, and protect property. Chemical compounds that can be used as fire retardants are: Bromade, Polybrominated diphenyl, Polychlorinated biphenyls etc. according to National Institute of Environmental health report, 2017, these compounds are toxic and are environmentally unfriendly. Continues inhalation of these chemical compounds has adverse effect on human lives especially in infants. Fire retardant produce from these chemical compounds are effective but expensive. This project therefore, seek to provide solutions to the challenges that has bedevilled the existing fire retardant by using



local and recycled materials to produce fire retardants that are environmentally friendly and are less expensive. More than 175 different Fire Retardants exist which are made of different chemicals and compounds. (10). The annual global consumption of FRs is over 2.25 million tones. (1). Most commonly used FRs are brominated FRs, Halogenated FRs, Chlorinated FRs, FRs comprising of metal Hydroxides (Aluminium Hydroxides, magnesium Hydroxides etc.). (7) found out that Brominated FRs are more numerous than other FRs due to their efficiency and because at high temperatures, the decomposing product of Brominated compounds are less volatile. (6) conducted a study on Human health Effects of Brominated FRs and concluded that the primary health effects associated with Brominated FRs include: endocrine disruption, hepatotoxicity and neurotoxicity. The compounds of Brominated come in contact with humans and animals largely through inhalation. (1). Over the years, researchers have been researching into alternative and environmentally friendly FRs. It is against these backdrops that this study intends to find pragmatic solutions to environmental and health concerns of existing FRs using alternative and locally sourced materials and waste materials. (4) characterized the effluent from fertilizer industries in Southern Nigeria and concluded that, the waste consists of several chemical compounds with varied concentration depending on the source of the waste, time of the day and season of the year. In any case the percentage concentration of Ammonium Phosphate present in the waste ranges from 15 – 25% of the total waste. The chemical composition and particle size analysis of kaolin was investigated by (9), they reported

that the particle size distribution of kaolin particles are mainly in the range of 0.4 – 5 micros and the RI is greater than 1.36. The characterization of the effluent and kaolin (whose deposit is large in plateau state), would make it suitable for use in the production of cost effective and environmentally safe fire retardant. They are made up of the following components;

- i. **Binders;** which can be resins or oils but can be organic compounds. Its binds pigment fillers and additives together. E.g. alkyds, polyurethane, epoxy, etc.
- ii. **Pigments;** they are finely ground organic or inorganic powder of higher reflective index (RI) of >1.5, and has particles size of between 0.01 to 5 micros. Provide colour and adhesive. E.g., white lead, zinc oxide, Aluminum oxide, etc.
- iii. **Thinner;** used to dissolve the binder and to facilitate application, it can be liquid or water. E.g., Turpentine oil, Benzene, Mineral spirit, etc.
- iv. **Drier;** to accelerate drying process e.g., Zinc sulphate, Lead octate, Magnesium oxide etc.
- v. **Filler/Extenders;** it is a non-expensive commonly natural organic material added in order to increase its volume. E.g., ground silica, gypsum etc.
- vi. **Additive;** chemicals added to improve or modify the properties of the paints.

The percentage composition of each of the constituent is shown in the pie chart below.

1.0.1. Constituents of Fire Retardants



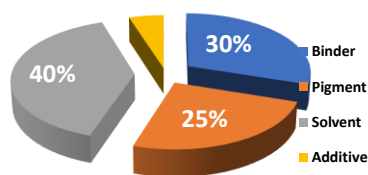


Figure 1: Composition and Constituent of Fire Retardant

1.1. STATEMENT OF THE PROBLEM

In recent times, researchers have raised health concerns over the usage of the existing FRs which are largely Brominated. The compounds used are toxic to human lives and are environmentally unfriendly. The continues inhalation of the chemical compounds used in the production of FRs has adverse effect on human health.

1.2. SIGNIFICANCE OF THE STUDY

This study would produce a cost effective FR that would be friendly environmentally and would have less toxic effect on human lives. It would enhance the use of locally sourced raw materials thereby reducing the importation of raw materials. It would also reduce the overdependence on foreign product. It would also reduce waste through recycling.

1.3. AIM AND OBJECTIVES

The aim of this study is to assess the potential of kaolin and fertilizer industry waste as alternative materials for the production of fire

Sample of fertilizer industrial waste was collected from Notore and Chasco fertilizer industries Kano State. Samples of kaolin have



Plate 1: KAOLIN (PIGMENT/FILLER)

Industrial effluent was subjected to simple distillation process to separation Amoninium Phosphate from other compounds in the waste. Kaolin was crushed to fine particles and refractive Index, Sieved size analysis, SEM, XRD and XRF was carried out on it.

retardant. This will be achieved through the following;

- i. Separation of $((\text{NH}_4)_3\text{PO}_4)$ from fertilizer industry waste.
- ii. Determination of the suitability of $((\text{NH}_4)_3\text{PO}_4)$ from fertilizer industry waste.
- iii. Determination of the suitability of kaolin and its characterization.
- iv. Determination of optimal mix ratio for the fire retardant mixture.
- v. Assessment of the flammability parameters of the fire retardant produced.

2.0. MATERIALS AND METHODS

2.1. Materials

- i. Kaolin
- ii. Conventional Fire retardant
- iii. Thermocouples
- iv. Epoxy resin
- v. Fire extinguisher
- vi. Fertilizer industry waste
- vii. Burners
- viii. Safety gears

2.2. Methods

been sourced for from Bokkos in Plateau state. The binder used was epoxy.



3.0. RESULTS AND DISCUSSION

3.1. CHEMICAL ANALYSIS OF RAW MATERIALS

Chemical analysis of Fertilizer industrial waste was carried out and their percentage concentration was also determined.

Table 2 showing elements present in fertilizer industry waste

No.	Element	Zn	Cu	Cr	Ni	Pb	Cd	Ca	Mg	k
	Unit	mg/kg s.m.	mg/kg s.m.	mg/kg s.m.	mg/kg s.m.	mg/kg s.m.	µg/kg s.m.	g/kg s.m.	mg/kg s.m.	g/kg s.m.
Sample 1 (Notore)		90	1.41	0.93	0.41	0.43	128.98	2.39	842.35	2.34
Sample 2 (Chasco)		55.21	5.53	1.88	1.03	0.69	163.47	7.92	900.48	2.60

Author's Laboratory Results, 2023

Table 3 showing compounds present in fertilizer industry effluent and their percentage contributions.

No.	Element	ZnO	NH ₃	NPO ₃	(NH ₄) ₃ PO ₄	PbO	KCO ₃	Ca ₂ CO ₃	Mg ₂ CO ₃	Others	Total
	Unit	Percentage (%)									
Sample 1		14.47	11.09	10.57	28.31	8.47	18.40	3.39	2.81	2.49	100
Sample 2		12.21	15.53	11.88	23.47	11.69	13.07	4.92	6.48	0.75	100

Author's Laboratory Results, 2023

3.2. Chemical Test on Kaolin

A. Scanning Electron Microscopy of Kaolin

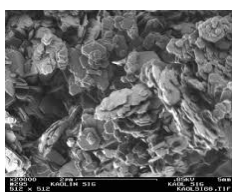


Plate 2: SEM of Kaolin Sample A

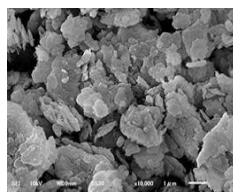


Plate 3: SEM of Kaolin Sample B

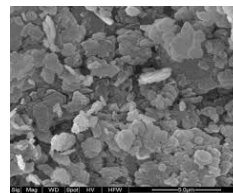


Plate 4: SEM of Kaolin Sample C

B. X-Ray Fluorescence of Kaolin

Table 4 showing XRF of Kaolin

Oxides	Percentage concentration (%)		
Al ₂ O ₃	43.30	41.10	41.70
SiO ₂	52.00	49.00	51.50
K ₂ O	0.041	ND	ND
CaO	0.214	0.28	0.353
TiO ₂	1.68	2.07	2.19
V ₂ O ₅	0.085	0.068	0.072
Cr ₂ O ₃	0.036	0.047	0.051
MnO	0.016	0.014	0.015
Fe ₂ O ₃	1.04	1.20	1.34
NiO	0.011	0.0091	0.0094
CuO	0.0071	0.01	0.0069
ZnO	0.068	0.011	0.007
Ga ₂ O ₃	0.018	0.019	0.024
Ag ₂ O	1.40	1.59	1.62
Re ₂ O ₇	0.055	0.073	0.13

Author's Laboratory Results, 2023

C. X-Ray Diffraction of Kaolin



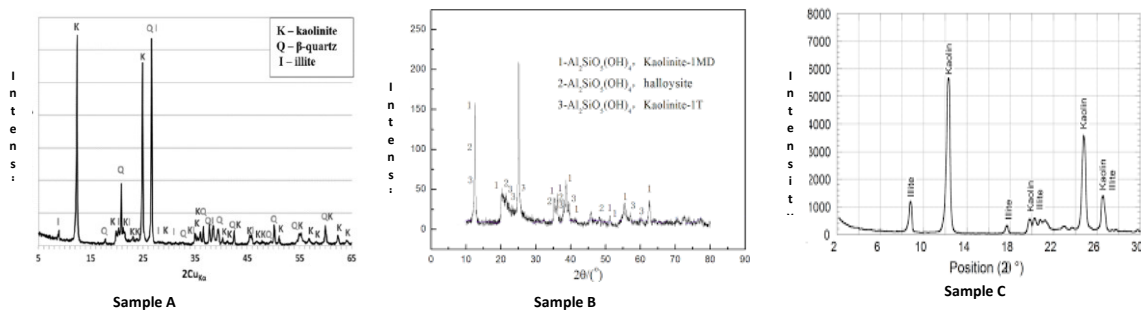


Figure 2: XRD of Kaolin Samples

D. Particle size Distribution

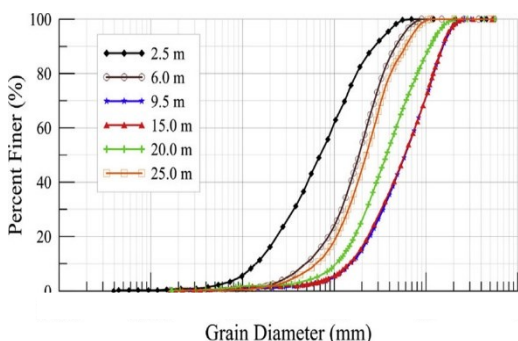


Figure 3: Particle Size Distribution of Kaolin

E. Refractive Index

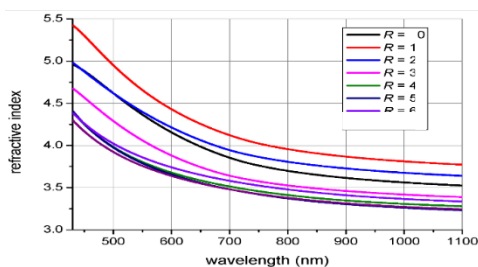


Figure 4: Refractive Index of Kaolin

Grain size distribution of kaolin soil was determined after the sample of kaolin was grinded using a grinding machine and was sieve using a sieve size. Test procedure was in accordance to (3). The Particle analysis revealed a range of between 0.15 to 0.70 micros. The Nigeria industrial standard for paint production (11) stipulates that any material to be sued as a filler or pigment should have a particle size of $0.4 \geq RI \geq 0.55 \mu\text{m}$. All the samples of kaolin above passed the stipulations as such can be used for the production of fire retardant.

The ratio of the velocity of light in a vacuum to its velocity in a specified medium (Kaolin) was tested using Methods include visual examination, study of the absorption spectrum, and measurement of refractive indices

3.3. Production of Test Samples

The materials needed for the production of flame retardant was measured in volume (M^3). Dry materials; kaolin and $(\text{NH}_4)_3\text{PO}_4$, was mixed in a container, Epoxy (a wet material) was added to the mixture and stirred using a stirrer, solvent was lastly added and the mixture was stirred until it is properly mixed.

The table below summarizes the experimental design that was used for this work.

Table 5 showing different percentages contribution by volume of raw materials for the production of fire retardant.

S/NO	MATERIALS (%)				Total volume (%)
	Kaolin (Pigment)	$(\text{NH}_4)_3\text{PO}_4$ (Additive)	Epoxy (Binder)	Solvent Turpentine oil /H ₂ (Solvent)	
1	27	2	30	41	100
2	26	4	30	40	100



3	25	6	30	39	100
4	24	8	30	38	100
5	23	10	30	37	100

Authors' Computation, 2023



Plate 9; Fire Retardant Produced

Poland ceiling materials were sourced from major building material markets in the Federal Capital Territory. The ceiling boards were measured using a tape, marked with a marker and cut using a hand saw, to a dimension of 600mm x 600mm. a circle of 250mm radius was inscribe on the samples using a compass. 1, 2 and 3 coats of the fire retardant produced was applied on the cut ceiling boards using different mix designs and allowed to dry for 24 hours. A circle of 250mm radius was inscribed on the ceiling boards using a compass. The fire resistance of the ceiling material was determined separately. This is to ascertain the effectiveness of the fire retardant produced and how long it can retard flame.

3.4. TESTING OF SAMPLI

3.4.1. Density

Table 6 Showing Densities of Samples

S/N		WEIGHT (KG)	LENGTH (M)	WIDTH (M)	THICKNESS (M)	VOLUME (M ³)	DENSITY (KGM ⁻³)
1	A	0.64	0.6	0.6	2.71E-03	9.76E-04	7.41E-04
2	A1	0.71	0.6	0.6	2.92E-03	1.05E-03	8.62E-04
3	A2	0.76	0.6	0.6	2.49E-03	8.96E-04	6.27E-04
4	A3	0.82	0.6	0.6	2.74E-03	9.86E-04	7.60E-04
5	B1	0.70	0.6	0.6	2.87E-03	1.03E-03	8.37E-04
6	B2	0.77	0.6	0.6	2.53E-03	9.11E-04	6.47E-04
7	B3	0.81	0.6	0.6	2.67E-03	9.61E-04	7.21E-04
8	C1	0.71	0.6	0.6	2.85E-03	1.03E-03	8.21E-04
9	C2	0.75	0.6	0.6	2.53E-03	9.11E-04	6.47E-04
10	C3	0.80	0.6	0.6	2.67E-03	9.61E-04	7.11E-04
11	D1	0.71	0.6	0.6	2.96E-03	1.07E-03	8.84E-04
12	D2	0.74	0.6	0.6	2.57E-03	9.25E-04	6.66E-04
13	D3	0.83	0.6	0.6	2.67E-03	9.61E-04	7.21E-04
14	E1	0.72	0.6	0.6	2.87E-03	1.03E-03	8.37E-04
15	E2	0.75	0.6	0.6	2.57E-03	9.25E-04	6.66E-04
16	E3	0.81	0.6	0.6	2.74E-03	9.86E-04	7.60E-04
17	F1	0.72	0.6	0.6	2.92E-03	1.05E-03	8.62E-04



18	F2	0.77	0.6	0.6	2.67E-03	9.61E-04	7.11E-04
19	F3	0.82	0.6	0.6	2.77E-03	9.97E-04	7.78E-04
20	H1	0.74	0.6	0.6	2.99E-03	1.08E-03	9.04E-04
21	H2	0.78	0.6	0.6	2.71E-03	9.76E-04	7.41E-04
22	H3	0.84	0.6	0.6	2.92E-03	1.05E-03	8.62E-04

Authors' Laboratory Results

Table 6 shows the density of the ceiling after the application of the alternative fire retardant produced. It was observed that the density of the boards increased with increase of the number of coats. The single coat boards appeared less denser

compared to the 2 and 3 coats boards (1), studied the influence of wood density to fire resistance of wood and concluded that, there is a direct relationship between the density and fire resistance of wood.

3.4.2. Ignition Time

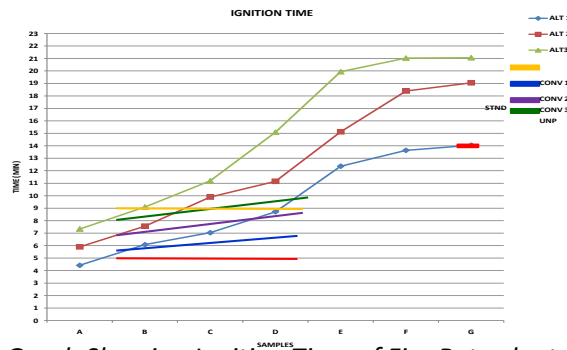


Figure 5. Graph Showing Ignition Time of Fire Retardants

The ignition time of a material is the time at which the material catches fire. The ignition time of a combustible material is key to the safety of occupants in times of fire emergency. Figure 3 show the flash point of ceiling boards painted with conventional and the alternative fire retardant produced. It was observed that the ignition time of the fire retardant produced increased with increase in number of coats. The results obtained was compared to conventional fire retardant and performed better. The conventional fire retardant ignited between 5.5mins and 8.3mins for 1 to 3 coats. The fire retardant produced had its flash point to be between 4mins and 21mins. Comparing these results with the average minimum flash point stipulated by the building g code and fire safety code (9mins), the fire retardant produced had prolonged ignition time. Ceiling boards with no

application of fire retardant had a flash point of 5 mins.

3.4.3. Ignition Temperature

The ignition temperature of a material is the temperature at the material ignites. The graph above shows the ignition temperature of Ceiling boards after the application of fire retardant produced and conventional fire retardant. It was observed that the ignition temperature of boards with 1 coat of fire retardant produced was between 208.55°C and 688.26°C, 2 coats had a flash point of between 223.44°C and 705.78°C, and 3 coats had an ignition temperature of between 243.05°C and 786.57°C. Fire retardant produced with the mix design of 18% kaolin and 12% (NH₄)₃PO₄,



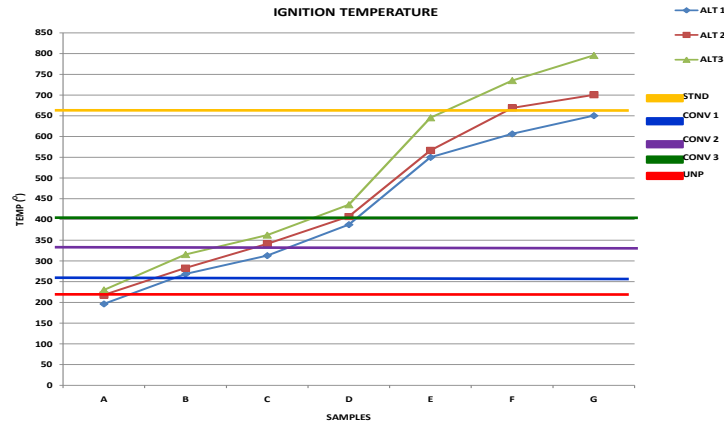


Figure 6. Ignition Temperature of Fire Retardants

performed better than other mixtures.[1 coat – 621.03°C, coat 2 – 705.78°C, coat 3 – 786.57°C]. The ignition temperature of conventional fire retardant was found to be between 261°C and 400°C. Fire retardant produced performed better in terms of the temperature it ignited compared to

conventional fire retardant. According to the Nigerian Building and national fire safety code, the ignition of any material to be used as fire retardant should not be less than 500°C. The ignition temperature for Ceiling board without fire retardant was 128.59°C.

3.4.4. Flame Spread Time

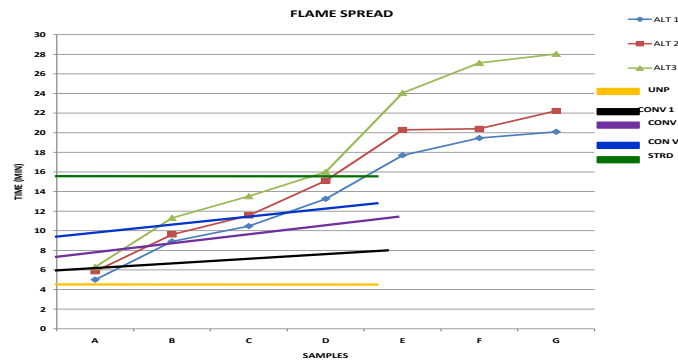


Figure 7. Graph Showing Flame Spread Time of Fire Retardants

The flame spread of a material is the time at which the material spread flame over a particular distance. Using a radius of 250mm, the flame spread of fire retardant was measured and compared. The flame spread time of 1 coat of the alternative fire retardant produced was found to be between 5.20mins and 16mins, 2 coats had a flame spread time of between 5.89mins and 18.39mins, the flame spread time for 3 coats was found to be between 5.89mins and 20mins. Again, alternative fire retardant produced with 18% kaolin and 12% $(NH_4)_3PO_4$, performed

better [16mins, 18.39mins and 20mins]. However, the result for conventional fire retardant shows that the flame spread time for 1 coat was between 6mins and 8mins, 2 coats was between 7mins and 11.5mins and 3 coats was found to be between 9mins and 13mins. The Nigerian Building code and the National Fire Safety Code stipulates that flame spread time of a fire retardant material less than 14mins shall not be used in buildings with occupants. The flame spread time of unpainted ceiling board was 4.59mins.

3.4.5. Smoke Density



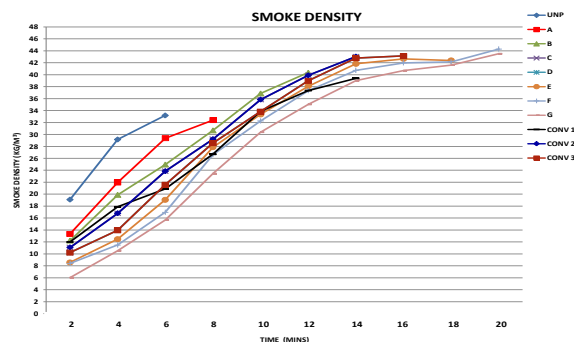


Figure 8. Graph Showing Smoke Density of Fire Retardants

Smoke Density is the measure of the concentration of smoke as the material combust. The smoke analysis of a material is of utmost importance as it could prevent or slow down rescue operations during fire emergency. The smoke density which was measured using a smoke meter, was measured at the flash point and flame spread time of the material. It was observed that conventional fire retardant produced denser smoke (10.80mg/m^3 to 44mg/m^3) compared to the alternative fire retardant produced (6.28mg/m^3 to 43.47mg/m^3). The rate of development of smoke for conventional fire retardant is greater than that of the fire retardant produced. Ceiling boards not painted with fire retardant had a smoke density of between 18mg/m^3 and 47mg/m^3 .

4.0.CONCLUSION AND RECOMMENDATION

4.1.CONCLUSION

- i. The density of a material is directly proportional to its flash point.
- ii. The alternative fire retardant produced had better performance in terms of flammability properties compared to conventional fire retardant.
- iii. Kaolin and $(\text{NH}_4)_3\text{PO}_4$ fertilizer from industrial effluent has potentials to be used in the production of alternative fire retardant.

4.2.RECOMMENDATION

- i. This study recommends the use of Kaolin and $(\text{NH}_4)_3\text{PO}_4$ fertilizer from industrial effluent as raw materials for the production of alternative and cost effective –fire retardant.

REFERENCES

1. Albrecht G.B. Andreas H. & Peer H. *The Velocity of Combustion in Relation to the Density of Wood*. Journal of Wood and Wood Products. (2010).
2. America Standard Tests Method E119 – 16a. *Standard Test Methods for Fire Tests of Building Construction and Materials*.
3. America Standard Tests Method D422. *Standard Test Method for Particle Size Analysis of Soil*.
4. Anna, M. & Wai, R.J. *The Significance of Brominated Flame Retardants in the Environment: Current Understanding, Issues and Challenges*. Chemosphere. **46** 579 – 58. (2017).
5. ISO 5660 – 1. *Reaction-to-fire tests — Heat release, smoke production and mass loss rate*. 2nd Edition.
6. Jan L., Carola R., Gunner B. & Anuschka P. *Human Health Risk Associated With Brominated Flame Retardants (BFRs)*. Environmental International pp. 170-180. (2015).
7. Kim Y.R., Harden F.A., Toms L.M. & Normans R.E. *Health and Consequences of Exposure to Brominated Flame Retardant: A Systematic Review*. Chemosphere PMID: 24529398, Doi: 10: 1019/j. (2014).



8. Osnat, S., Asher, B. & Ariel, K. *Environmental Impact of Flame Retardants (Persistence and Biodegradable)*. International Journal of Environmental Research and Public Health. **6(2)**:478 – 91. (2009).
9. Shehu Y., Suzi S., Jikan N. & Azman B. *Chemical Composition and Particle Size Analysis of Kaolin*. Traectoria Nanki – Part of Science. **Vol. 3, No. 10**, ISSN: 2413-9009. (2017).
10. Wikoff, D.S.& Birnbaum, L.S. *Human Health Effects of Brominated Flame Retardant. Brominated Flame Retardants. The Handbook of Environmental Chemistry. Vol.16*. (2011).
11. Nigerian Industrial Standards (NIS). *Standards for Paint and Varnishes, Specifications for Emulsion paints for decorative Purposes*.



P085 - ASSESSING THE ECOLOGICAL AND ENVIRONMENTAL IMPACTS OF OIL SPILLS FROM REFINERIES ON SOIL AND WATER – A MINI REVIEW

Sheriffdeen A. Jimoh^{a*}, Abdulquadri O. Isiaka^b, Elizabeth O. Paul^b, Benson Odah^c, Meshach John^d, Judith U. Okoduwa^e, Victor Ochigbo^e, Bridget E. Nwobi^e, Jeffery Tsware Barminas^f

^aDepartment of Biochemistry, Ahmadu Bello University Zaria.

^bDepartment of Microbiology, Ahmadu Bello University Zaria

^cDepartment of Environmental Chemistry, Benue State University, Benue

^dDepartment of Microbiology, Kaduna State University.

^{e,f}Industrial and Environmental Pollution Department, National Research Institute for Chemical Technology.

*Corresponding Author's email: Sheriffdeenjimoh431@gmail.com

ABSTRACT

Oil spills from refineries represent a serious environmental crisis with a far-reaching negative effect on soil, air, marine ecosystem, and human health and social economic wellbeing of the nation. The ecological effect of such oil spills on the environment cannot be over emphasized therefore there is need for the evaluation of the level of impact and proffer suitable solutions. In this review paper, we explore the various ways by which oil spill physically, biologically and chemically alter the environment, practices of remediation, challenges and limitations of remediation of crude oil spills in Nigeria.

Key Words: Oil Spills, Refineries, Remediation, Pollution, Niger Delta.

INTRODUCTION

The Oil and Gas industry is one of the world's leading industries that brings in wealth but also leaves behind negative effects affecting the entire ecosystem. Apart from greenhouse gases, refineries produce hazardous atmospheric contaminants and residual wastes that lead to some of the ecological problem of refinery operation. Oil is the one of the most used type of energy source which constitute about 31.8% of the global energy consumption (1), and constitute adverse ecological effect (for example climate change, ozone destruction, human toxicity and terrestrial eco toxicity) that is crucially affecting the environment.

The main source of energy for the entire world as well as the economic backbone of countries that produce oil is crude oil. However, as crude oil exploration and exploitation increases, so does the amount of environmental pollution caused by these activities. The usage and transportation of crude oil around the world continues to pose a threat to the environment, even incidences of oil spill during oil firm activities lead to large oil spill incidents offshore and onshore (2). These has left the environment in a polluted form as greenhouse gases are released during exploration and spills thereby affecting the ozone layer, water is contaminated as toxic contaminants are deposited such as benzene, toluene, ethyl benzene and xylene which adversely affect aquatic life, lead to loss of occupation for

fishermen, impacts negatively on the health of the inhabitants that derive their water for domestic use from such bodies and affects crop quality on polluted farmland.

There are no consistent figures on the amount of oil spills in Nigeria, but it is estimated that oil spill account for as many as 546 million gallons of oil into the Niger Delta environment over the last 5 decades, that account for about 11 million gallons annually (2). The United Nations Environmental Programme (UNEP) reports based on two years scientific research revealed unprecedented widespread oil contamination of soil and water bodies with severe consequences on health, agriculture, ecological and aquatic life especially in Ogoni Land who are living in chronic state of pollution (2).

In 2008/2009 two major spill events received world attention, because of the exceptionally large volume of oil released into the near sea level Ogoni land region from a 24-inch trans Niger Delta pipeline operated by shell petroleum development company (SPDC) Nigeria (3). The first spill was reported to have started on 28th August and stopped 7th November, while the second spill started 7th December and stopped on 7th November 2008, both spills had a duration of 149 days (3). This spill has led to widespread environmental destruction in the Ogoni land region which has left the inhabitants seriously improvised, sick (skin, ocular irritations,



birth defects), and in a state of hopelessness. The thickness of the oil is also a factor of oil spill toxicity, oil volatility increases with oil toxicity this toxicity of oil is a function of types of oil and its source region. All crude oils contain many compounds primarily volatile and semi volatile compounds as well as concentration of poly aromatic hydrocarbons (PAH), they are ubiquitous and are termed as potential environmental contaminants that is carcinogenic, mutagenic. [26] Heavy metals presenting extensive dangers to toxicity to humans and marine biota [19]. Some trace element also found in the soil are Nickel, aluminum, tin, chromium these metals have been reported to cause several health problems in minute amounts [22]

This PAH are group of organic compounds with multiple fused rings such as benzene which are formed by incomplete combustions of oil by the physical and chemical transformations which are very toxic to the aquatic ecosystem and pose a serious health issues to humans who are exposed to seafood and water which can later cause adverse effects such as DNA damage and cancer, tricky part of PAHs is that they can persist , bio accumulate (can accumulate in the tissue of aquatic organism which definitely affect the food chain and affect the trophic levels including human who consume sea food).

There are various causes of oil spills which include operational failure, third party damage, spills resulting from vandalism and terrorism [4]. In most part of the world accidental third-party damage of crude oil pipeline has become increasingly common especially during excavation, but recently pipeline interdiction and illegal bunkering has been reported in countries like Columbia, Canada, Iran, Iraq, Indonesia, U.S.A, U.K, Saudi Arabia, Middle east as well as Asia and Africa (4).

For example, the Bodo oil spills in the Niger Delta region in 2008 which was caused by operational problems recorded about 4,000 barrels of oil spill a day for 10 weeks. The Size of the spill is comparable to the Exxon Valdez 1989 disaster in Alaska, where 10 million gallons of oil destroyed the remote coastline and the explosion on the deep-water Horizon (DWH) drilling rig that took place on April 20th 2010, in the east Mississippi Canyon area (N 28.73667 W 88.38694) in the northern Gulf of Mexico, 66km off the coast of Louisiana (LA), when the wells were enclosed 87 days later, 3.19 million barrels of oil were released into the ocean during the spill (5, 6) .

Purpose and Scope of the review paper

The purpose of this review paper is to comprehensively evaluate the ecological and environmental consequences of oil spills originating from refineries. This will provide insight and create awareness of the ecological ramifications, methodology, and recommendation for mitigating and preventing the challenges of refinery related oil spills and the measures to curb them.

The scope of this review encompasses the following

- i. Causes and Occurrence of Refinery Oil Spills
- ii. Ecological Impacts on Water Ecosystem
- iii. Ecological Impacts on Soil Ecosystem
- iv. Human Health and Social Implication
- v. Mitigation and Cleanup Efforts
- vi. National and International Regulations Governing Refinery Operations and Spill Response, Specifically Related to Soil and Water

OIL REFINERIES AND OIL SPILLS

Oil refinery is an industrial process plant where crude oil is converted and refined into useful products such as the gasoline (petrol), diesel fuel, asphalt, heating oil, kerosene, liquefied petroleum naphtha and takes place in an oil refinery(7) . Oil refineries are typically large, extensive piping running throughout with a stream of fluid between large chemical processing units such as distillation columns

Basically, oil refineries operate to convert high molecular weight hydrocarbons into lower molecular weight compounds ready for consumer utilization for example petroleum burnt in internal combustion engines to provide power for ships, automobiles, aircraft engines.

Nigeria an oil producing country, have some refineries such as:



Overview of the causes and occurrence of oil spills from refineries

The production, exploration and consumption of oil and petroleum products are increasing worldwide, and the threat of oil pollution increases accordingly. The movements of petroleum from the oil fields to the consumer involves transfers between many different modes of transportation including pipelines tank trucks, tankers and rail cars. Accidents can happen during any of these production, exploration and transportation steps or storage times.

Legislation and stringent operating codes are used by governments and industry to reduce the use of oil spills. Many operating and maintenance procedures has been invoked by industries which can lead to oil spills (10).

Spills occurs frequently because of the extensive use of oil and petroleum particularly in our daily lives. About 450,000 tons of oil and petroleum products are used in Canada every day, the United States uses about 10 times this amount and worldwide about 20 million of oil is used per day. The consequences of oil spills on the ecosystem and natural resources are widespread and long term so there is need for logistic workforce who can take suitable response in short time (11).

Marine oil spills once occurs prevent light diffusion and oxygen penetration in the bottom layer of the sea (11).

ECOLOGICAL IMPACT ON WATER ECOSYSTEM

Oil spills in water bodies (seas, oceans, rivers, streams) refer to the release of crude oil and its constituents into these bodies as a result of man's activities which include but not limited to mechanical failure, pipeline vandalization and/or corrosion, exploration, extraction, transportation, storage, natural disasters such as earth quakes, and usage processes (12-14). These spills are further enhanced due to lack of or minimal environmental regulations /standards being followed to the latter.

These spills have caused untold losses to the inhabitants of the affected areas whose source of livelihood is from the water bodies. Fishing and farming being the predominant occupation of people living in such areas have been greatly affected as there is a very high level of hydrocarbon contamination in the water leading to destruction of fishing habitats in the mangroves as a result of the

presence of a persistent oil film on surface waters which prevents natural aeration and leads to death of fresh water organisms and marine life (15).

Major oil spills in marine environment such as the Exxon Valdez oil spill in 1989, and the recent deep-water horizon (DWH) causes large scale of environmental pollution. Such detrimental effect of oil spills in waterbodies depends on the volume, types and biota species affected with different levels of resistance, physical strength and toxicity [7].

Oil spills can affect wildlife both aquatic and terrestrial in many ways. The severity of damage will depend on the type of hydrocarbons involved, the quantity spilled, the temperature at the time of incident (oil spill), and the season. Dissolved or emulsified oil in the water column can contaminate plankton, algae, fish eggs and larvae which vary in terms of long- and short-term effect. Different species have shown different levels of biological resistance when they come in contact with spilled oil, these effects aggravate in higher altitude where species that experience seasonal reproductive events are likely to demonstrate long lasting effects as a results of spawning habitat alteration [7]. Oil spills affects marine invertebrate such as the coral reefs, there is extensive evidence of coral damage and death following contacts with oil as well as impacts on subtidal coral abundance, reproductive health. This effect of oiling on the corals is long termed as reproductive capability slows because of decreased quality of larval and coral gametes and because of contacts with hydrocarbons from sediments. Also, sea birds are also a victims of oil spills in terms of mortality they are particularly vulnerable as contact with oil inhibits both flight and insulation abilities, their ingestion processes as well as the feeding and consumption of contaminated food and inhalation of the oil water results in several internal poisoning and high mortality rates [7].

Oil spills also affect marine mammals such as the turtles, when they come in physical contacts with oil the breathing of air is saturated with petroleum vapors and the ingestion of food is contaminated with oil. Young and juvenile turtles have been found to starve to death when their esophagus has become blocked with petroleum residues. The primary dangers to marine mammals are their inability to detect presence of oil slicks, their consumption of contaminated food, accidental consumption of marine tar residuals, as well as



- UNEP report concludes that pollution of soil by petroleum hydrocarbons in Ogoniland is extensive in land areas, sediments and swampland. Most of the contamination is from crude oil although contamination by refined product was found at three locations.
- The assessment found there is no continuous clay layer across Ogoniland, exposing the groundwater to hydrocarbons spilled on the surface. In 49 cases, UNEP observed hydrocarbons in soil at depths of at least 5m. This finding has major implications for the type of remediation required.
- At two-thirds of the contaminated land sites close to oil industry facilities which were assessed in details, the soil contamination exceeds Nigerian national safety standards, as set out in the Environmental guidelines and Standards for the Petroleum Industries in Nigeria (EGASPIN).

Relationship between Soil and Water Contamination

Oil spills on land can seep into the soil, where it may persist and spread, potentially reaching groundwater. Contaminated groundwater can, in turn flow into nearby surface water bodies, such as rivers, streams, lakes, causing water contamination. Also contaminated water bodies when used for irrigation in farmlands can lead to the pollution of such farmlands. Contaminated surface water can lead to contamination of sediments, affecting benthic ecosystem and potentially re-releasing contaminants into the water column.

The combined impact of soil and water contamination can result in cumulative ecological effects, increasing the overall harm to affected ecosystem. This can make recovery and remediation efforts more challenging.

HUMAN HEALTH IMPLICATIONS

Petroleum Hydrocarbons from oil spills can enter human body either through direct or indirect

contact. Direct contact includes, breathing contaminated air, and direct contact with the skin while walking in contaminated areas. Indirect contact is due to bathing in contaminated water or ingesting of contaminated food. Crude oil contains many compounds which can be volatile and semi volatile organic] compounds including PAHs, as well as Nitrogen and Sulfur containing compounds and metals. These hydrocarbons have bad effect on people with regards to both extent of exposure and degree of toxicity is also a factor which affect how detrimental it is to humans (18)

Human health is badly affected by the oil spill contamination and the effect depends solely on the type of site (land, river and ocean). Other factors include the kind and extent of exposures for examples cleaning workers at the oil spills site are at greater risk, health disorders include skin and eye irritation, breathing and neurological problems. (18)

The exploitation and exploration of oil produces environmental risk and usually takes months to produces disease and, in some cases, it leads to deaths, some of the major health problems are psychological health, (such as stress, anxiety, and depression), blood disorders (exposure of crude oil can cause deterioration effects on many biological system including changes in hematogenic system. One of the hematogenic disorders that is evident in people exposed to hydrocarbons is leukemia). Reproductive health and developmental toxicity (Exposure to petroleum hydrocarbons can induce chromosomal aberration in humans which is a direct damage to DNA.) (19)

Socio-economic consequences Of Oil Spills

The discovery and exploration of natural resources including oil have several socio economic environmental implications on the citizens (20).

Oil spills have contaminated farmland and fishing waters, affecting agriculture and fishing, which are primary sources of livelihood and sustenance for the Ogoni people. This also leads to reduced agricultural productivity and fishery yields that leads to income loss and food insecurity. Also, they are many industries which are directly linked to the environment, such as boat manufacturing and repair, shipping, and equipment maintenance, may also suffer job losses. Additionally, businesses that provide goods and services to the affected communities may face reduced demand (21).



Clean Up and Mitigation Efforts

The principal approaches used for mitigation of oil spills is towards:

1. restricting the spread of spill to offshore areas and soil environment
2. enhancing the recovery of spilled oil,
3. increasing the degradation of unrecovered oil, and
4. curtailing the influence on marine ecosystem

Overview of Strategies and Technology for Oil Spill Responses in Water and Soil Environment

Oil spill remediation involves a complex approach that includes cutting edge technology, enacting cleanup techniques, and ecologically considerate methods. This method includes the following; Bioremediation, phytoremediation, along with the use of chemical dispersants, and physical techniques like skimming and vacuuming which are essential for containment and removal.

Several remediation techniques have been implemented in the Ogoniland of Niger delta to address hydrocarbons contamination with little or no success (9) UNEP reported the use of Remediation by Enhanced Natural Attenuation (RENA) has been inappropriate for the Niger delta environment [13]

Remediation Techniques for Oil Spill

Remediation is the process of returning soil, waterbodies, or air functionality to the state they were prior to contamination. Variety of techniques exist for remediation depending on the media (e.g., air, water, or soil) and contaminants, this could be mechanical or physical, chemical and biological methods (22).

Remediation techniques have been developed to clean up the marine and soil environments after oil spills incidents. These techniques have been adopted over the years as a means to reduce the toxic impacts of crude oil spillage on the environment. The most commonly used mechanical or physical techniques include collection and skimming, boomers, wiping, water flushing, tilling as

well as cutting vegetation and burning (23).

The physical or Mechanical removal of oil spills is usually utilized as an initial strategy for cleaning up in aquatic and terrestrial environments.

The most common chemical method of clean-up is the use of dispersants, solidifiers and the rest such as biosurfactants and soil oxidizers. The biological treatments are another clean up method developed in the 1980s which uses microorganisms or plants for removing oil pollutants such as bioremediation, phytoremediation (23).

Evaluating the Effectiveness of different Clean-up methods for both Water and Soil Contamination

The Niger Delta is low lying region with an extensive river network. Rivers therefore play an important role in the distribution of pollutants within the delta system (3). Therefore, there is need for remediation methods, such physical methods of oil spills cleanup are:

Booms: Since oil is less dense than water, they float on the surface of water bodies when oil spills. They act as a stationary physical barrier that enclose floating oil and prevent it from spreading. Booms are used for diverting oil from biological sensitive areas or to concentrate oil and maintain adequate thickness so the skimmers can be used for other cleanup methods, these processes facilitate oil recovery from spill sites. Most boom designs are categorized into curtain boom and fence boom, fire boom or fire-resistant boom (24, 25).

- Fire booms are specially constructed with fireproof metals that can withstand very high temperatures generated by burning oil. The fire boom can either fence or curtain design.

- The curtain boom consists of a subsurface skirt that remains under water to contain the oil and is supported by a large air or foamed-filled floatation chamber usually of circular cross section.

- Fence booms resembles floating fence-like structures that are composed of rigid and semi-rigid materials and having a flat cross-section which has a vertical position in



the water by means of integral or external buoyancy (24, 25).

Skimmers: They help in the recovery of spread oil with the help of boomers, skimmers trap the oil from the surface with the help of disks, belts, continuous chains of oleophilic materials and then oil is squeezed out in the recovery tank without changing its properties so it can be reprocessed or reused. Weir skimmers use a dam for trapping the oil and then it can be pumped out through a pipe or hose to a storage tank for recycling purposes. The type and thickness of oil spills and weather conditions generally determine the success of skimming. Skimmers are generally effective in calm waters and subject to clogging by floating debris. They are categorized into oleophilic, suction, and weir skimmers (25).

- Oleophilic skimmers have the ability to adhere to oil and then trap the oil from the surface and the oil is scraped or squeezed out into a collecting recovery tank, they are made up from oleophilic properties materials.
- Suction skimmers have the simplest design and are widely used for the recovery of oil from beaches, confined areas or land surfaces, they are made in such a way that they suck up oil
- Weir skimmers use gravity action to collect floating oil from the oil water. They act like dams to trap the oil, and the oil is pumped out of the weir central sink through a pipe.

In situ burning

This is a method used to control or mitigate oil spills on water surfaces; it involves the ignition and burning of the spilled oil while it's still on the water surface. It is usually considered the last resort in oil spill response

Soil Washing

Soil washing is mostly used as a pretreatment method for cleaning up soils. It is an ex-situ

treatment process that involves the use of liquid/water sometimes combined with chemical additives and a mechanical instrument to scrub soils (26). This process mechanically separates contaminated sand from uncontaminated soil.

Thermal Desorption

This method is also called thermal stripping, low temperature thermal volatilization, or soil roasting. It involves heating the contaminated soil to very low temperatures of about 200-1000 F to enhance the vaporization and physical separation of contaminants with low boiling points from the soil (26). Depending on the organics present and the temperature of the thermal desorption, this process can cause complete or partial decomposition of some organic contaminants.

Soil Vapor Extraction

Soil vapor extraction is the technique in which contaminants in the soil are allowed to vaporize at the soil temperature by applying vacuum in soil. This method can be done by putting perforated pipes into the contaminated soil and pulling air through the soil and into the pipes. This creates pore spaces and increases the air flow in soil. Contaminants are extracted in gaseous form through a vapor extraction well, which may then be treated before being released. That is why this process is also called vacuum extraction, or enhanced in situ volatilization (26). The soil is periodically sampled to see if it meets the cleanup level. This technique works well if the contaminant is a volatile compound like gasoline, which easily turns into a vapor.

Pump and Treat

Pump and treat system are a commonly adopted remediation technique. In this method, the contaminated water is pumped out of the ground to the surface and treated in surface water facilities. It could be passed through a filter or other treatment system to remove the contamination and the treated water can be reused. The treatment depends on the kind of contaminants present in the groundwater.

Physical method principally involves soil replacement and thermal decomposition; the method is labor intensive, expensive and suitable for contaminated sites. This implies it could be unsuitable for large scale contamination in the Niger delta region



Chemical means of remediating the marine environment do not only block the spreading of the oil spill, but also protect the shoreline and sensitive marine habitats. These methods are, therefore, among the best remediation techniques available for both onshore and offshore [16]. Dispersants and solidifiers are used together with physical methods to treat oil spill by changing the physical and chemical properties of the oil

Dispersants:

Dispersants have surface-active agents known as surfactants dissolved in one or more solvents and stabilizers. The main aim of dispersant application is to weather the oil slicks into small droplets, which submerge into the depth of the water column and become rapidly diluted and easily degraded [16]. Examples of concentrated types of dispersants include: SlickgoneNS, Neos AB3000, Corexit 9500, Corexit 8667, Corexit 9600, SPC 1000t, Finasol OSR 52, Nokomis3-AA, Nokomis 3-F4, SaffRon Gold, ZI-400, and Finasol OSR 528 (25).

Dispersant molecule contains both oleophilic (attracted by oil) and hydrophilic (attracted by water) parts. When applied on the oil spill site, the solvent transports the dispersants to the oil/water interface where the molecules rearrange so that the oleophilic part is in the oil and the hydrophilic part is in the water. This process reduces the surface tension of the oil/water interface, which together with wave energy, results in droplets separating from the oil slick. Dispersants also allow for rapid treatment of polluted water, slow down the formation of oil water emulsions, make the oil less likely to stick to surfaces (including animals such as sea birds), and accelerate the rate of natural biodegradation (25)

Solidifiers:

Solidifiers are those hydrophobic polymers enhanced by Van der Waals forces, which on reaction with oil, convert it into a solid rubber state that does not sink and can be easily removed by physical means. They are hydrophobic polymers (oleophilic) that can be applied as dry particulate or semisolid materials. There are three types of solidifiers, each having unique characteristics and properties: polymer sorbents, cross-linking agents, and polymers with cross-linking agents. Examples of solidifiers are Rawflex, Norsorex, Oil Bond, Molten wax, Elastol, Gelco 200, CI agent, Rubberizer, Jet Gell, SmartBond HO, etc. [16].

The chemical method has the potential to contaminate other environmental media including air and water bodies through the introduction of solvents and reagents during remediation. Specifically, the approach is fast at clean-up of contaminants, however, harmful wastes generated in the process include carbon dioxide and other greenhouse gases which are emitted into the surrounding environment and have a negative effect on human health (22).

Biological oil spill cleanup involves the use of plants and microorganisms to carry out remediation of polluted sites and particularly, the cleanup of crude oil spills. As a result, biological methods such as bioremediation and phytoremediation have been applied as biological techniques to achieve the cleanup of oil-polluted sites. Bioremediation is the use of microorganism to mitigate or eliminate environmental hazards and attempts to accelerate the natural biodegradation rates by modifying environmental factors. Bioremediation uses microorganisms and their yields to eliminate contaminants from the environment (22) whereas phytoremediation enhances this process in the presence of plants.

Bioremediation method is a very simple and cheap remediation technique. In this method, microorganisms degrade and metabolize any chemical substance and re-establish environmental quality. Microorganisms fasten the natural weakling process by assimilating organic molecules to cell biomass with carbon dioxide, water and heat as by products.

However, Bioaugmentation, bio stimulation and bio ventilation. Bioaugmentation is to enhance the performance of the microbial population through the addition of bacterial with specific catabolic activities, strains or enrichment consortia to increase the rate of contaminant degradation (22). This implies an import of some contaminant degrading microbes to the already existing microbial population at the intervention area to quicken the rate of contaminant degradation. One challenge of this approach that there is no single strain of bacteria that has the requisite metabolic capacity to degrade all oil components. Thus, studies recommend different types of bacteria strains and fungi for the remediation of hydrocarbon contaminants. The adjustment of environmental parameters such as nutrient introduction, biopolymers and biosurfactants is described as bio stimulation (27)



Bio ventilation on the other hand involves the addition of oxygen to the soil voids to stimulate the growth of microbes. Oxygen is a necessity and often the limiting factor in the process of biodegradation as it enhances microbial metabolism of organic matter and generate more energy [13]

Bioventing has been shown to be effective and efficient in the remediation of able end of diesel and biodiesel fuel with a higher remediation rate compared to natural attenuation.

Phytoremediation of crude oil spill in soil

Species of different plants have been identified due to their potential for phytoremediation of crude oil hydrocarbons of polluted soils. These plants are initially characterized with good tolerance to petroleum-contaminated soil. The four o'clock flower (*Mirabilis jalapa L.*) was successfully demonstrated as a phytoremediator due to having a particular tolerance to petroleum contamination. The removal efficiency of total petroleum hydrocarbons (TPHs) was doubled by *M. jalapa* over a 127-day period. Forest tree species such as teak (*Tectona grandis*) and gmelina (*Gmelina arborea*) have shown acceptable abilities to thrive well in a contaminated habitat having crude oil up to 10 % w/w of soil. However, biomass and height of the test plants were significantly affected at higher levels of oil treatments [14]. Branquillo (*Sebastiania commersoniana*), a Brazilian native tree, have been also proved to be tolerant to soil petroleum contamination. This tree decreased petroleum hydrocarbons up to 94 % in contaminated soil. Seed germination and early growth of seven plant species including corn (*Zea mays*), millet (*Panicum miliaceum*), sorghum (*Sorghum bicolor*), lettuce (*Lactuca sativa*), okra (*Abelmoschus esculents*), watermelon (*Citrullus lanatus*), and soybean (*Glycine max*) were evaluated in experimental systems contaminated with oil field produced water. Results indicated a high tolerance of sorghum, okra, millet, and corn to oil phytotoxicity compared to others. Two crop species, corn (*Z. mays*) and soybean (*G. max*), have also demonstrated tolerance to crude oil-contaminated soils [14].

Bioremediation Technique Using Plants:

Plants have different mechanism for the removal and/or degradation of organic hydrocarbons from impacted soils. Although only a few degradation processes occur directly in plant tissues, most degradation are the result of the complex

association of roots, root exudates, rhizosphere, and microbes, which is termed as rhizoremediation [14].

Phytoremediation of crude oil spills in aquatic ecosystems.

In aquatic ecosystems such as lakes, rivers, and wetlands, there are different types of plants termed macrophytes thriving in or near water that are emergent, submergent, or floating. They can be possibly used as oil hydrocarbon phytoremediators. One of the characteristics that make them suitable for phytoremediation is their ability to grow fast. They are invasive and rapidly become abundant. Thus, they can be replaced with new growth soon after the damage caused by oil pollution [14]. The fibrous roots of some aquatic plants can provide larger surface and denser rhizospheres for microbial colonization. (26) reported that water hyacinths' (*Eichhornia crassipes*) fibrous root systems are able to significantly remediate the floating petroleum hydrocarbons on surface waters. Biscuit grasses (*Paspalum vaginatum Sw.*) were also reported to be potential candidates for petroleum hydrocarbons phytoremediation.

According to UNEP (9) study in Ogoni land identified current technologies in contaminated land remediation. However, many of the remediation approaches such as the physical and chemical could leave behind environmental footprint deny access to land for agriculture and accelerate greenhouse gas emissions with caution secondary environmental impacts resulting from remediation technologies should be considered in order not to create more problems in the process of solving one.

Challenges and Limitations in Mitigating and Remediating Refinery Oil Spills in these Ecosystem

They are unique combination of challenges and limitations that can hinder the remediation processes of oil spill from refineries. Which may include frequency of spill, lack of data on the extent of oil spill and its impact on the environment, issues related to governance and enforcement, technical capacity for remediating oil spills and funding.

Here are some of the key challenges and limitations specific to Nigeria:

The nature of oil infrastructure and contextual issues within the Niger Delta encourages frequent spills to occur. These circumstances lead to



unpredictable and inevitable spills in the region causing re-impact of clean-up of areas [19]

Limitation: Frequent spills can strain resources and divert attention away from long-term prevention and remediation efforts.

Governance structure: Regulating contaminated land in the Niger Delta is a joint task between various organizations. Conflict and responsibility overlap have reportedly resulted from this. For instance, disputes regarding clean-up obligations have frequently arisen between the Department of Petroleum Resources (DPR) and the National Oil Spills Detection Agency (NOSDRA) (27). For example, in the event of an oil spill, the operator is required to notify DPR and NOSDRA, who will then each launch a separate risk assessment of the site (27). Conflict may therefore result from different evaluations.

Technical capacity: For efficient restoration, the region of the Niger Delta needs highly qualified professionals due to the intricate nature of the land contamination and the level of contamination. Given the extent of contamination, the region currently lacks the technical competence needed to conduct effective remediation techniques [13]. The regulators cannot identify the use of inappropriate remediation technology in the region; thus, operators continue to use substandard technologies for contaminated land clean-up in the region (9). This practice suggests that regulators require training in current science for effective contaminated land remediation.

Funding: In the Niger Delta, providing funds to remediate contaminated environment seems to be an ongoing issue. Nigeria's successive governments have pledged to remediate the Niger Delta region and set various timetables, but they have been unable to do so because they lack the funding. In response to the UNEP study, for instance, a USD 1 billion Trust Fund would have been established with donations from the Nigerian government and business owners for the clean-up of Ogoniland. However, as of right now, no attempts that are publishable have been done to create a trust fund for the remediation [13]. Past and ongoing spills have received little to no attention for remediation due to a lack of funding.

Current legislation: The lack of proper legislation for effective and efficient remediation in the area is a key obstacle to the clean-up of Ogoniland [13].

Policy framework and implementation in Nigeria is largely tenure-based. The implication is that a policy or commitment made by an administration might be neglected by succeeding administrations. Meanwhile restoration of degraded ecosystem most times takes decades of sustained scientific and financial commitment

Conclusion

Discussion on national and international regulations governing refinery operations and spill response, specifically related to soil and water

They should be national regulation where laws are made regarding spills prevention and response, like in the U.S clean water act regulation and clean Air act is significant, the international maritime organization sets global standards for shipping and spill response through conventions like MARPOL (Marine pollution).

In addition, they should be regulation where by refineries has detailed spill response plans including strategies for containing, cleaning and reporting spills to minimize their environmental impacts. Environmental impact assessment (EIA) should also be done when there is need for expansion or start new projects to evaluate potential harm to the soil or water environment.

Governments of various countries have shown interest to solve problems produce by oil spills. For this, governments have firming many polices which is mandatory for every company to adopt. Developed country like U.S.A has especially setup National Institute of Environmental Health Sciences under the department of Health and Human Services to handle the oil spillage problem. They are running regular educational courses and training programs of oil spill for their workers in coordination with Occupational Safety and Health Administration. They have also developed National Contingency Plan for responding to both hazardous substance and oil spill releases [18].

Sustainable development (SD) should be taken serious it has become ideology which builds a modern world, the 2030 Agenda for SD call all people, from individuals to crucial stakeholders, business persons and international organization to take action in solving current challenges and enhancing the quality of life also improving social, economic, and environment condition that oil spills has posed (15).



Developing country like India has also developed contingency plans like National Oil spill Disaster Contingency Plan under Ministry of Defense in cooperation with Directorate of Fisheries & Environment and Coast Guard. India is a part of United Nation Convention on the Law of the Sea and therefore has obligation to protect marine environment (28).

Contingency plan should be made in Nigeria such as:

- National oil spill disaster contingency plan
- Regional oil spill disaster contingency plan
- District oil spill disaster contingency plan
- State oil spill disaster contingency plan
- Lastly this plan should be facilitated. (28)

References

1. M. ABDELGADİR, G. YILAN, G. A. ÇİFTÇİOĞLU, The Assessment of Environmental Impacts: A Case Study of a Crude Oil Refinery in Sudan.
2. O. S. Ugwuoke, C. F. Oduoza, Framework for Assessment of Oil Spill Site Remediation options in Developing Countries a Life Cycle Perspective. *Procedia Manufacturing* **38**, 272-281 (2019).
3. C. B. Obida, G. A. Blackburn, J. D. Whyatt, K. T. Semple, Counting the cost of the Niger Delta's largest oil spills: Satellite remote sensing reveals extensive environmental damage with > 1million people in the impact zone. *Science of the Total Environment* **775**, 145854 (2021).
4. H. Umar, M. Khanan, A. Ahmad, M. Isma'il, Assessing The Economic Consequences of Pipeline Sabotage in The Niger Delta Area of Nigeria Using Geographic Information System.
5. A. Fentiman, N. Zabbey, Environmental degradation and cultural erosion in Ogoniland: a case study of the oil spills in Bodo. *The Extractive Industries and Society* **2**, 615-624 (2015).
6. J. Beyer, H. C. Trannum, T. Bakke, P. V. Hodson, T. K. Collier, Environmental effects of the Deepwater Horizon oil spill: a review. *Marine pollution bulletin* **110**, 28-51 (2016).
7. H. Shen, X. Wen, E. Trutnevyte, Accuracy assessment of energy projections for China by Energy Information Administration and International Energy Agency. *Energy and Climate Change* **4**, 100111 (2023).
8. A. S. Akinwumiju, A. A. Adelodun, S. E. Ogundeji, Geospatial assessment of oil spill pollution in the Niger Delta of Nigeria: an evidence-based evaluation of causes and potential remedies. *Environmental Pollution* **267**, 115545 (2020).
9. U. UNEP, Environmental assessment of Ogoniland. *Background to Environmental Degradation in Ogoni Land*, (2011).
10. J. Michel, M. Fingas, in *Fossil fuels: current status and future directions*. (World Scientific, 2016), pp. 159-201.
11. M. Baniasadi, S. M. Mousavi, A comprehensive review on the bioremediation of oil spills. *Microbial action on hydrocarbons*, 223-254 (2018).
12. B. Zhang *et al.*, in *World seas: an environmental evaluation*. (Elsevier, 2019), pp. 391-406.
13. E. Chinedu, C. K. Chukwuemeka, Oil spillage and heavy metals toxicity risk in the Niger Delta, Nigeria. *Journal of Health and Pollution* **8**, 180905 (2018).
14. K. E. Ukhurebor *et al.*, Environmental implications of petroleum spillages in the Niger Delta region of Nigeria: a review. *Journal of Environmental Management* **293**, 112872 (2021).
15. I. Radelyuk, K. Tussupova, J. J. Klemeš, K. M. Persson, Oil refinery and water pollution in the context of sustainable development: Developing and developed countries. *Journal of Cleaner Production* **302**, 126987 (2021).
16. M. M. Abarshi, E. O. Dantala, S. B. Mada, Bioaccumulation of heavy metals in some



- tissues of croaker fish from oil spilled rivers of Niger Delta region, Nigeria. *Asian Pacific Journal of Tropical Biomedicine* **7**, 563-568 (2017).
17. M. W. Hester, J. M. Willis, S. Rouhani, M. A. Steinhoff, M. C. Baker, Impacts of the Deepwater Horizon oil spill on the salt marsh vegetation of Louisiana. *Environmental Pollution* **216**, 361-370 (2016).
 18. S. Kuppusamy *et al.*, Impact of total petroleum hydrocarbons on human health. *Total Petroleum Hydrocarbons: Environmental Fate, Toxicity, and Remediation*, 139-165 (2020).
 19. M. I. Ramirez, A. P. Arevalo, S. Sotomayor, N. Bailon-Moscoco, Contamination by oil crude extraction–Refinement and their effects on human health. *Environmental Pollution* **231**, 415-425 (2017).
 20. A. O. Adeola *et al.*, Crude oil exploration in Africa: socio-economic implications, environmental impacts, and mitigation strategies. *Environment Systems and Decisions* **42**, 26-50 (2022).
 21. A. O. Babatunde, Oil pollution and water conflicts in the riverine communities in Nigeria’s Niger Delta region: challenges for and elements of problem-solving strategies. *Journal of Contemporary African Studies* **38**, 274-293 (2020).
 22. N. Zabbey, K. Sam, A. T. Onyebuchi, Remediation of contaminated lands in the Niger Delta, Nigeria: Prospects and challenges. *Science of the Total Environment* **586**, 952-965 (2017).
 23. S. Yavari, A. Malakahmad, N. B. Sapari, A review on phytoremediation of crude oil spills. *Water, Air, & Soil Pollution* **226**, 1-18 (2015).
 24. A. Dhaka, P. Chattopadhyay, A review on physical remediation techniques for treatment of marine oil spills. *Journal of Environmental Management* **288**, 112428 (2021).
 25. D. Dave, A. E. Ghaly, Remediation technologies for marine oil spills: A critical review and comparative analysis. *American Journal of Environmental Sciences* **7**, 423 (2011).
 26. P. E. Ndimele *et al.*, in *The political ecology of oil and gas activities in the Nigerian aquatic ecosystem*. (Elsevier, 2018), pp. 369-384.
 27. K. Sam, N. Zabbey, Contaminated land and wetland remediation in Nigeria: opportunities for sustainable livelihood creation. *Science of the Total Environment* **639**, 1560-1573 (2018).
 28. S. Tewari, A. Sirvaiya, Oil spill remediation and its regulation. *International Journal of Engineering Research and General Science* **1**, 1-7 (2015).



P86 - ENHANCING PALM OIL REFINING USING ACTIVATED CARBON DERIVED FROM A LOW-RANK COAL (LRC)

Ephraim Akuaden Audu^a, Jibrin Yusuf Yahaya*^a, Yusuf Ozovehe Usman^a, Musa Haladu^a, Jibrin Yalwa^a Zarumi Muhammad^a, Emmanuel Musa^a, Saheed Ademola Ibraheem^b

^a*Inorganic and Analytical Division, Scientific and Industrial Research Department, National Research Institute for Chemical Technology (NARICT), PMB 1052, Zaria, Nigeria.*

^b*Organic Division, Scientific and Industrial Research Department, National Research Institute for Chemical Technology (NARICT), PMB 1052, Zaria, Nigeria.*

*Corresponding author: yusufyahaya76@gmail.com, 08036486001

ABSTRACT

The palm oil industry is integral to global food production but faces significant challenges associated with low quality due to the presence of impurities. This study explores the refining of palm oil using activated carbon produced from low-rank coal (LRC). The activated carbon was synthesized using H₂SO₄ as activating agent followed by calcination at 500 °C for 3 hours. Characterization using XRF, XRD, FTIR and Ultimate analysis revealed the formation of activated carbon with improved attributes. The performance of the activated carbon for palm oil refining was evaluated by studying the physicochemical parameters and carotene content of the refined product. The results showed that the refining process led to a decrease in carotene, FFA, moisture, refractive index, Peroxide, iodine and acid values and from 756.43 mg/L, 8.42%, 0.7%, 1.46553, 6.8 meq/kg, 57.8 g/meq and 16.83 mgKOH/g respectively in the crude palm oil to 638.53 mg/L, 1.42%, 0.25%, 1.46524 6.2 meq/kg, 45.17 g/meq and 2.8 mgKOH/g in the refined palm oil. The reduction in these parameters indicates that the prepared activated carbon was successful in refining crude palm oil. This research suggests that activated carbon from LRC can be utilized for palm oil refining to improve the quality. Moreover, this study contributes to sustainability efforts by repurposing an otherwise underutilized resource.

KEYWORDS: *activated carbon, low-rank coal, palm oil refining, crude palm oil*

1.0 INTRODUCTION

Activated carbon has been known to be a resourceful material because of its properties such as high surface area, high porosity and chemical stability. Activated carbon has found applications in processes such as filtration of toxic gases, water treatment, supercapacitor electrodes and as catalyst support [1]. Activated carbon is a carbonaceous material with a large internal surface area and a highly developed porous structure resulting from the processing of different raw materials. It is composed mainly of carbon but also contains other elements depending on the processing methods and the raw materials used [2]. Activated carbon's porous structure allows it to adsorb materials from both liquids and gaseous phases.

Current research trends show that scientists are seeking economical materials suitable to be used as

activated carbon. The utilization of coal as activated carbon has been reviewed by many researchers [3, 4]. Coal is a fossil fuel, formed from vegetation that has been consolidated between other rock strata and altered by the combined effects of pressure and heat over millions of years. Coal is classified into four main types, or ranks: anthracite, bituminous, subbituminous, and lignite. According to the US Energy Information Administration (EIA), ranking depends on the amounts of carbon present in the coal and on the extent of heat energy generated by the coal. Most high-ranked coal is used to power steam engines because of its high calorific values. However, low-ranked coal has been underutilized by industries. Coal could be used for the preparation of activated carbon because of its characteristic microstructure and porosity [5]. Low Ranked Coal (LRC) from Mai Ganga coal deposit in Gombe, Gombe state, Nigeria is widely available and contains a substantial amount of carbon which can be used for the production of activated carbon.



Additionally, utilizing low-rank coal is a way to repurpose an otherwise underutilized resource in the country.

Edible oils are composed mainly of triglycerides which are from plant sources. Examples include palm oil, soy oil, olive oil, coconut oil, groundnut oil, etc. Vegetable edible oils offer a good source of omega-3, omega-6 fatty acids and fat-soluble vitamins A, E and K [6]. Consumption of low-quality oils poses health risks such as cancer, inflammation, risk of heart attack and diabetes due to the presence of oxidation products [7]. Contaminants such as pesticides, metals, mineral oil aromatic hydrocarbons (MOAH), aflatoxins, dioxins, and polycyclic aromatic hydrocarbons (PAH) may be present in edible oils due to the oil processing method, storage, transportation, or even from the soil which the crops are grown [8, 9]. This underscores the need for refining edible oil that will result in high oil quality.

Palm oil is the most consumed edible oil in the world, having surpassed all others [10]. Palm oil and palm kernel oil are extracted from the oil palm's fruit flesh and seed, respectively, providing ingredients for numerous edible and personal care products as well as feedstock for biofuels [11]. Crude palm oil (CPO) is a vegetable oil derived from the pulp of oil palm which consists of solid triglyceride with lipases, free fatty acid (FFA), pigments, phosphatides, coloring agents and carotene [12]. Refined palm oil (RPO) is produced by removing impurities, free fatty acids (FFA), etc. resulting in a clear, stable and odorless edible oil suitable for consumption.

Palm oil refining is a critical process in the food industry, aimed at purifying the oil for safe consumption. Methods used in palm oil refining include thermal, chemical and physical refining methods [13, 14]. The high-temperature processes involved in the thermal method of palm oil refining can lead to the partial hydrogenation of unsaturated fatty acids, resulting in the creation of trans fats which have several adverse health effects. Also, chemical refining processes often involve the use of significant quantities of chemicals. The disposal of these chemicals and the waste generated from the refining process can have negative environmental consequences. Palm oil refining using the adsorption process is used to overcome the challenges of the above methods. Refining of palm oils with activated carbon requires minimal use of chemicals, and lower temperature in the refining process [15].

Although Mai Ganga coal has been activated using KOH as reported by Umar et al., (2020) [16], however, acid activation using H₂SO₄ and H₃PO₄ has not been reported anywhere. Furthermore, multiple studies have reported the use of different adsorbents for palm oil refining. None have looked into refining palm oil using activated carbon derived from Mai Ganga coal. In this paper, low-ranked coal from Mai Ganga coal deposit was used to prepare an activated carbon using H₂SO₄, and applied in the refining of palm oil.

2.0 MATERIALS AND METHODS

Chemicals Reagents and Equipment

Low Ranked Coal (LRC) was collected from Mai Ganga coal deposit in Gombe, Gombe state, Nigeria. The crude palm oil (CPO) was procured from the local market in Basawa, Zaria, Kaduna state. H₂SO₄ (Merck), Isooctane (CDH), sodium hydroxide (LOBA CHEMIE), phenolphthalein and absolute ethanol (GHTECH). The chemical used are of analytical grade and was used as supplied.

2.1 Chemical activation of adsorbent

Raw coal was washed with distilled water several times, allowed to air dry under the sun and subsequently oven dried at 105 °C for 4 hours. Afterward, the coal was ground into powder and sieved using BSS 20 mesh size (841 microns). Activation of the coal was achieved using 0.5 M H₂SO₄ at a ratio of 10:1 v/w (volume to weight). The mixture was agitated for 24 hr on a magnetic stirrer and filtered followed by calcined at 500 °C for three hours. Subsequently, the sample was washed several times with distilled water until a stable pH was obtained and dried at 105 °C to constant weight.

2.2 Refining of crude palm oil

Degumming was carried out using the following procedure; 25 mL of the crude palm oil (CPO) was placed in a beaker on a hot plate magnetic stirrer. Two drops of 0.5 M H₂SO₄ were added at 90 °C and stirred for 10 minutes. After degumming, 0.25 g of the CAC was added to the CPO at a temperature of 105 °C, agitated for 1 hr then filtered to obtain the Refined palm oil (RPO).



2.3 Characterization Techniques

Infrared data was collected using a Shimadzu-8400S Fourier Transform Infrared Spectrometer (Kyoto, Japan) over the range of 4000–400 cm^{-1} . X-ray Diffraction (XRD) measurements were conducted to determine the crystallinity of the sample using an Empyrean Pan Analytical X-ray Diffractometer (Worcestershire, United Kingdom) with 2θ between 2-80°. Elemental composition was obtained using Phenom world XRF analyzer (Thermo Fischer, Waltham, U.S.).

2.4 CAC Performance Evaluation

Physicochemical parameters were determined using the Association of Official Analytical Chemists (AOAC, 2011), moisture content was determined using the oven drying method while carotene content was determined using a UV-2550 Shimadzu following the method of [17].

3.0 RESULTS AND DISCUSSION

3.1 Elemental Composition Analysis of RLC and CAC

The results obtained from XRF analysis of the Low Ranked Coal (LRC) and Coal derived Activated Carbons (CAC) are shown in Table 1. The result reveals that the raw coal contains Oxygen (42.543 wt%) Silicon (15.456 wt%), Aluminum (7.424 wt%), Iron (11.735 wt%) and Calcium (11.735) in appreciable amounts. On activation, the amount of Silicon and Aluminum increased to 16.472 wt% and 8.883 wt% respectively while the amount of other elements reduced signifying higher purity of the activated carbon. Silicon and Aluminum have been known to be good materials for the adsorption of contaminants. Furthermore, CAC has a higher percentage level of oxygen compared to that of the LRC as a result of the acid treatment as expected. This suggests the presence of more oxygen-containing functional groups which could increase its adsorption capacity for larger molecules as corroborated by the work of Wang et al., (2005) [18]

Table 1: Elemental composition of LRC and CAC

	Element	Symbol	Raw Coal	Acid Activated Coal
1	Oxygen	O	42.543	51.150
2	Magnesium	Mg	2.166	0.000
3	Aluminum	Al	7.424	8.883
4	Zinc	Zn	0.027	0.004
5	Sulphur	S	4.519	14.459
6	Chlorine	Cl	2.024	2.251
7	Potassium	K	0.326	0.227
8	Calcium	Ca	11.735	4.548
9	Titanium	Ti	1.695	0.661
10	Copper	Cu	0.209	0.031
11	Chromium	Cr	0.013	0.009
12	Manganese	Mn	0.305	0.123
13	Iron	Fe	11.735	1.015



14	Cobalt	Co	0.087	0.087
15	Nickel	Ni	0.012	0.002

3.2 Ultimate analysis of LRC and CAC

The ultimate analysis of LRC and CAC is presented in Table 2. Moisture content is an important parameter used to determine the quality of an activated carbon [19]. The result of moisture content of LRC and CAC were found to be 4.54% and 4.21% respectively signifying a reduction in the moisture content after activation. Additionally, the result indicated the CAC moisture content falls within the requirement of the National Industrial Standard 06-3730-1995 of a maximum of 15% (NIS, 1995). A higher percentage of ash could lead

to clogging of pores resulting in a reduction in the surface area which invariably affects the adsorption process of the activated carbon [20]. The result shows that there was a decrease in the ash content from 14.45% in LRC to 12.40% in CAC suggesting improvement in the absorption capability. Fixed carbon content increases from 29.16 in LRC to 33.60% in CAC. This implies a higher amount of carbon in CAC which correlates with greater volume activity and indicates better-quality activated carbon, enhancing its effectiveness in various applications.

S/N	Parameters (%)	LRC	CAC
1	Moisture content	4.54	4.21
2	Volatiles Content	51.85	49.79
3	Ash Content	14.45	12.40
4	Fixed Carbon	29.16	33.60
5	Sulphur Content	1.14	0.91

3.3 XRD Analysis of LRC and CAC

The XRD patterns of Raw Coal (RC) and Coal derived Activated Carbons (CAC) are shown in Figure 1. The diffraction pattern shows a low degree of structural order signifying that atoms are not arranged in a long-range periodic array. This type of pattern suggests that the material is amorphous. Activated carbon showed a disordered

microcrystalline structure in which graphitic microcrystals are randomly oriented [21]. The appearance of a broad peak between 27.115 and 27.20 in the XRD of the non-activated as well as in the activated carbon indicates the presence of carbon.

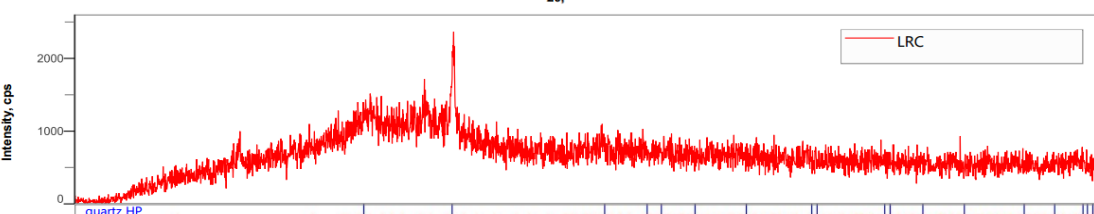
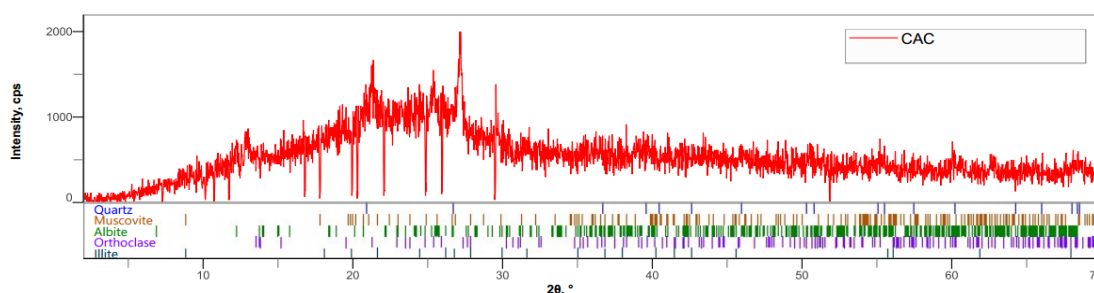


Figure 1. XRD pattern of CAC and LRC

3.4 Physicochemical and carotene analysis

The results of the physicochemical parameters of RPO and CPO are presented in Figure 2. The findings revealed a substantial enhancement in the quality of the refined palm oil, with notable improvements in several key parameters. Specifically, the activated carbon treatment led to a reduction in free fatty acids (FFA) from 8.42% to 1.42%, a decrease in moisture content from 0.7% to 0.25%, a minimal change in the refractive index (from 1.46553 to 1.46524), a decrease in peroxide value from 6.8 meq/kg to 6.2 meq/kg, a reduction in iodine value from 57.8 g/meq to 45.17 g/meq, and a substantial decrease in acid value from 16.83 mgKOH/g to 2.8 mgKOH/g. The low value of PV implies the RPO is less likely to go rancid, additionally, the obtained value falls within the SON permissible limits (<10 meq/kg). The IV

decreased from 57.8 in CPO to 45.17 g/meq suggesting an increase in saturation in the oil and a decrease in the possibility of oxidation. A lower value of moisture 0.25 as found in RPO shows an improvement in stability, lower rate of autooxidation and rancidity of the oil, moreover, the obtained value falls within limits of moisture content in palm oil allowed by SON (<1%). The refractive index, RI in RPO was found to be within the range set by (CODEX STAN 210-1999) 1.463-1.465. Lower values of FFA and AV suggest CAC was effective in improving the quality of the oil. This means a lower likelihood of oxidation, safer for consumption. Furthermore, the obtained values after refining fall within the permissible limits for FFA and AV set by SON (<5%). The activated carbon was able to reduce the carotene content from 756.43 to 638.53 mg/L.

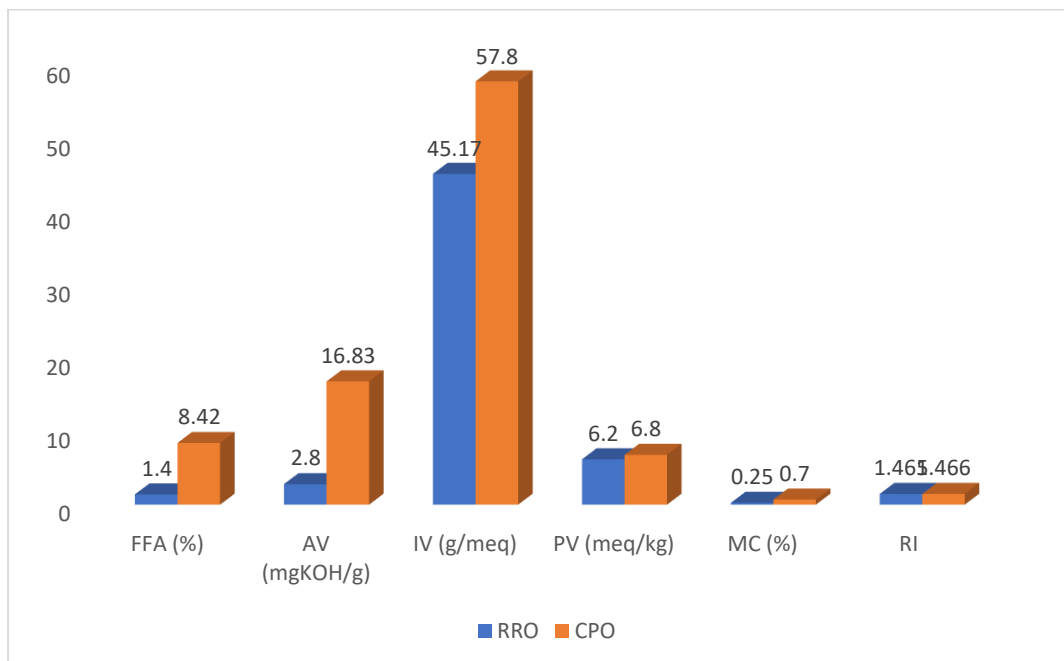


Figure 2. Physicochemical analysis of RPO and CPO



Key: FFA: free fatty acid, MC: moisture content, RI: refractive index, PV: Peroxide value, IV: iodine value and AV: acid values



Figure 3. Carotene content for RPO and CPO

CONCLUSION

This study offered insights into the application of Coal-Derived Activated Carbon (CAC) from LRC for palm oil refining. The characterization carried out on CAC confirmed its suitability to be used as a viable adsorbent. Furthermore, the research demonstrated the application of CAC as an

Reference

1. Sujiono, E., D. Zabrian, V. Zharvan, and N. Humairah, *Fabrication and characterization of coconut shell activated carbon using variation chemical activation for wastewater treatment application*. Results in Chemistry, 2022. **4**: p. 100291.
2. Kannan, N. and S. Devi, *Studies on removal of copper (II) and lead (II) ions by adsorption on commercial activated carbon*. Indian Journal of Environmental Protection, 2005. **25**(1): p. 28.
3. Chingombe, P., B. Saha, and R. Wakeman, *Surface modification and characterisation of a coal-based activated carbon*. Carbon, 2005. **43**(15): p. 3132-3143.
4. Cuhadaroglu, D. and O.A. Uygun, *Production and characterization of activated carbon from a bituminous coal by chemical activation*. African journal of Biotechnology, 2008. **7**(20).
5. Goel, J., K. Kadirvelu, C. Rajagopal, and V.K. Garg, *Removal of lead (II) by adsorption using treated granular activated carbon: batch and column studies*. Journal of hazardous materials, 2005. **125**(1-3): p. 211-220.
6. Zhou, Y., W. Zhao, Y. Lai, B. Zhang, and D. Zhang, *Edible plant oil: global status, health issues, and perspectives*. Frontiers in Plant Science, 2020. **11**: p. 1315.
7. Negash, Y.A., D.E. Amare, B.D. Bitew, and H. Dagne, *Assessment of quality of edible vegetable oils accessed in Gondar City, Northwest Ethiopia*.



- BMC research notes, 2019. **12**(1): p. 1-5.
8. Sánchez-Arévalo, C.M., L. Olmo-García, J.F. Fernández-Sánchez, and A. Carrasco-Pancorbo, *Polycyclic aromatic hydrocarbons in edible oils: An overview on sample preparation, determination strategies, and relative abundance of prevalent compounds*. *Comprehensive Reviews in Food Science and Food Safety*, 2020. **19**(6): p. 3528-3573.
 9. Zio, S., H. Cisse, O. Zongo, F. Guira, F. Tapsoba, N.S. Somda, . . . Y. Traore, *The oils refining process and contaminants in edible oils: A review*. *J. Food Technol. Res*, 2020. **7**: p. 9-47.
 10. Boyce, J., *The palm oil debate: What you need to know*. Nature's Path. <https://www.naturespath.com/en-us/blog/the-palm-oil-debate-what-you-need-to-know>, 2017.
 11. Cassiday, L., *Red palm oil*. Revista Palmas Bogota, 2017.
 12. Guliyev, N., H. Ibrahimov, J. Alekperov, F. Amirov, and Z. Ibrahimova, *Investigation of activated carbon obtained from the liquid products of pyrolysis in sunflower oil bleaching process*. *International Journal of Industrial Chemistry*, 2018. **9**(3): p. 277-284.
 13. Gharby, S., *Refining vegetable oils: Chemical and physical refining*. *The Scientific World Journal*, 2022. **2022**.
 14. Mba, O.I., M.-J. Dumont, and M. Ngadi, *Palm oil: Processing, characterization and utilization in the food industry—A review*. *Food bioscience*, 2015. **10**: p. 26-41.
 15. Gibon, V., *Palm oil and palm kernel oil refining and fractionation technology*, in *Palm oil*. 2012, Elsevier. p. 329-375.
 16. Umar, A., I. Muhammad, M. Funtua, and H. Mohammed, *ADSORPTION STUDY OF PARTICLE SIZES OF MAIGANGA COAL*. *African Journal of Engineering and Environment Research* Vol, 2020. **1**(2): p. 65-76.
 17. Silva, S.M., K.A. Sampaio, R. Ceriani, R. Verhe, C. Stevens, W. De Greyt, and A.J. Meirelles, *Effect of type of bleaching earth on the final color of refined palm oil*. *LWT-Food Science and Technology*, 2014. **59**(2): p. 1258-1264.
 18. Wang, S., Y. Boyjoo, A. Choueib, and Z. Zhu, *Removal of dyes from aqueous solution using fly ash and red mud*. *Water research*, 2005. **39**(1): p. 129-138.
 19. Pambayun, G.S., R.Y. Yulianto, M. Rachimoellah, and E.M. Putri, *Pembuatan karbon aktif dari arang tempurung kelapa dengan aktivator ZnCl₂ dan Na₂CO₃ sebagai adsorben untuk mengurangi kadar fenol dalam air limbah*. *Jurnal Teknik ITS*, 2013. **2**(1): p. F116-F120.
 20. Timur, S., I.C. Kantarli, S. Onenc, and J. Yanik, *Characterization and application of activated carbon produced from oak cups pulp*. *Journal of Analytical and Applied Pyrolysis*, 2010. **89**(1): p. 129-136.
 21. Qiu, T., J.-G. Yang, and X.-J. Bai, *Investigation on microstructural changes of Anthracite during Graphitization and effect of Silica content on product crystal structure*. *Energy Sources, Part A: Recovery, Utilization, and Environmental Effects*, 2021. **43**(7): p. 769-782.



P087 - CHEMICAL SAFETY MEASURES SURVEY ON HAZARDOUS CHEMICALS UTILIZED IN SMALL-SCALE BUSINESSES IN THE THREE MOST AGRARIAN STATES OF SOUTHWEST NIGERIA

Ashade Noah O.^{1*}, Oriah Vincent N.¹, Adamolekun Oluwakemi¹, Yusuf Habiba¹, Arala Raimi I.¹, Olabimtan Olabode H.² and Barminas Jeffrey T.³

¹Outstation Department, National Research Institute for Chemical Technology, Zaria

²Industrial and Environmental Pollution Department, National Research Institute for Chemical Technology, Zaria

³Scientific and Industrial Research Department, National Research Institute for Chemical Technology, Zaria

Corresponding Author: ashadenoah3@gmail.com

ABSTRACT

Chemicals play a fundamental role in contemporary society, serving as indispensable components in industrial processes, agriculture, healthcare, and daily household activities. Their significance is undeniable, yet the potential risks linked to their usage must not be overlooked. This study sought to assess the chemical safety measures within small-scale businesses across Ekiti, Ondo, and Osun States in Southwest Nigeria.

To achieve this objective, a structured survey questionnaire was deployed from September to November 2022 to sample small-scale business proprietors/entrepreneurs or key employees, targeting the three most agrarian states within the Southwest geopolitical zone of Nigeria. A total of one hundred and thirty-three completed questionnaires were collected, encompassing data on the gender distribution of business proprietors or key personnel, and type of business.

Findings unveiled that a substantial portion of small-scale enterprises within these three predominantly agrarian states in Southwest Nigeria belong to the micro and small-size businesses, categorizing them as micro (fewer than 10 employees), small (10 to 49 employees), and medium-sized businesses (50 to 149 employees). Moreover, a gender analysis of business proprietors was conducted.

The assessment of chemical safety measures among small-scale businesses in these agrarian states emphasizes the urgent need for heightened awareness and enhanced safety protocols, particularly among micro and small-scale enterprises. Ensuring the safe handling of hazardous chemicals is imperative for safeguarding the environment and the well-being of individuals engaged in small-scale businesses. Future endeavors should prioritize safety education and regulatory adherence to mitigate chemical-related risks and foster sustainable economic development.

Keywords: *Hazardous chemicals; chemical safety measures; Southwest Nigeria; Micro, Small and Medium-sized businesses.*

1.0 Introduction

From the substances that sustain life to those that propel technological advancements, chemicals occupy a pivotal role as they have woven themselves intricately into the fabric of our daily lives. As such, chemicals play a fundamental role in contemporary society, serving as indispensable components in industrial processes, agriculture, healthcare, and daily household activities where most small-scale businesses are paramount.

Chemicals are ubiquitous, playing a multifaceted role in areas ranging from agriculture to industry,

and from healthcare to household goods. They have become a critical aspect of contemporary living (1).

The importance of chemicals to man's daily existence cannot be overstated, as they serve as both the lifeblood of our flourishing global economy and the potential harbingers of peril when mishandled. Their significance to humanity can be perceived in their capacity to revolutionize modern life. These compounds underpin various sectors, including agriculture, manufacturing, and healthcare, contributing to increased crop yields, novel pharmaceuticals, durable materials, and an array of consumer products. They have allowed us to unlock the secrets of the universe through scientific exploration, enabling innovations in space



exploration, energy production, and information technology. The chemical industry has, undeniably, fostered economic growth and technological advancements on a global scale (2).

However, with this growing dependence on chemicals comes the perilous dimension of hazardous substances. The mismanagement of chemicals poses a threat to both human health and the environment. The improper handling, storage, and disposal of hazardous chemicals can lead to catastrophic accidents and long-term ecological damage. So, persons conducting a business or undertaking (PCBUs) as business owners/entrepreneurs /managers /personnel must comprehend the diverse types of chemical hazards, ranging from acute chemical spills to chronic exposure, to avert potential disasters (3); (4).

A hazardous chemical is any substance, mixture, or article that satisfies the criteria of one or more hazard classes in the “globally harmonized system of classification and labeling of chemicals (GHS). Examples of hazardous chemicals include acids, hydrocarbons, heavy metals, asbestos, and silica, and their potential harm ranges from respiratory illness or dermatitis to cancer. About chemicals, a hazard is a set of intrinsic properties of the substance, mixture, article, process, or protocol that may cause adverse effects to organisms or the environment. There are two broad types of hazards associated with hazardous chemicals that may present an immediate or long-term injury or illness to people. These are health hazards and physical hazards (1).

For hazardous chemicals, there are three major routes of entry into the human body: (a) inhalation, where hazardous chemicals are normally being inhaled in the form of gas, vapour, fumes, aerosol, airborne particles, or dust. (b) skin absorption, where chemicals can be absorbed through the skin directly or indirectly via contaminated media such as clothing. (c) ingestion, where there is indirect/direct swallow of the chemicals via contaminated media such as fingers (5).

Some chemicals may not be hazardous by nature. However, when they undergo physical or chemical changes during grinding, mixing, heating, dissolution, dilution, and other chemical reactions, the processes or the products/by-products may become hazardous. The hazards arise mainly from the formation of hazardous chemicals and, the evolution of large amounts of heat or gaseous products (5).

The chemical industry in Nigeria for instance, most especially large-scale industries such as petrochemical companies, is one of the largest industries involved in the production of ethylene, propylene, butadiene, and other petroleum-related products, which are used to manufacture secondary products such as plastics, soaps, detergents, and solvents for the general society. The operations of this type of industry as a large-scale industry involve the use of machinery and equipment to transform raw materials into finished products. Earlier studies have identified various kinds of hazards within the work environment in the chemical industry of Nigeria. Some of these include noise and vibration hazards, chemical hazards, falls from heights, biological hazards, electrical hazards, and fire and explosion hazards. The study reported a high rate of fatalities in factories in Nigeria with chemical-related activities being the highest of all (6). As such, small-scale businesses were put into consideration in this present survey to see if the trends are the same.

To safeguard humanity against the pernicious effects of hazardous chemicals, risk assessment has become a crucial practice. Risk assessment evaluates the potential dangers and uncertainties associated with the use of chemicals and aids in the formulation of preventive measures and regulations. It ensures that the benefits derived from chemical innovations far outweigh the risks posed, thereby making informed decisions on the utilization of these substances (4).

Also, the significance of chemicals reverberates in the context of Southwest agrarian states in Nigeria. Agriculture remains the backbone of Nigeria's economy, with Southwest agrarian regions playing a pivotal role in food production and economic sustenance. The cultivation of crops and the management of chemical inputs are inextricably linked, underscoring the importance of safe chemical use in agriculture (7).

Moreover, the synergy between agrarian communities and small-scale businesses in Nigeria is undeniable. Small-scale enterprises, often intertwined with agriculture, rely on the produce and raw materials supplied by agrarian communities. These businesses, including food processing units, artisan workshops, and agro-based industries, play an integral role in bolstering the national economy and providing employment opportunities in the region. The dynamics between agriculture and small-scale businesses are pivotal to



the sustenance of rural livelihoods and the overall economic well-being of Nigeria as a nation (8).

This survey study aims to assess the chemical safety measures in place for hazardous chemicals utilized in small-scale businesses operating in the three most agrarian states (Ekiti, Ondo, and Osun states) of Southwest Nigeria. By examining the existing safety protocols, identifying areas of improvement, and promoting best practices, this research seeks to enhance the safety and sustainability of these businesses, ensuring the continued economic growth of the region while safeguarding the well-being of its inhabitants. To achieve this, a well-structured survey questionnaire was deployed from September to November 2022 to sample small-scale business proprietors/entrepreneurs or key employees, targeting the three most agrarian states within the Southwest geopolitical zone of Nigeria.

2.0 Sampling and Data Collection

Preliminary information was first sought on the three most agrarian states with less prevalence of large-scale chemical industries amongst the states within the Southwest geopolitical zone of Nigeria. Having recognized Ekiti, Ondo, and Osun states, a purposive sampling method was adopted for the chemical safety measures survey on hazardous chemicals in small-scale businesses using a well-structured questionnaire (2).

Using the well-structured survey questionnaire, data was collected on the socio-demographic characteristics of the respondents, workplace or business, awareness of hazardous chemicals in their workplace or processes of production, and awareness of hazard control measures and safety protocols. Items in the questionnaire were sectioned for responses.

2.1 Methodology

The first step in this methodology is the creation of a well-structured survey questionnaire. The questionnaire was designed to cover aspects of chemical safety in the workplace, including safety guidelines such as those provided by the Occupational Safety and Health Administration (OSHA) in the United States or the European Chemicals Agency (ECHA) in Europe. Questions were clear, concise, and arranged logically to facilitate efficient data collection (4); (9).

Before distributing and/or administering the questionnaire, a crucial pilot test was conducted in the first week of September 2022 at the Ikare Akoko

area of Ondo State with a small group of representatives from the target small businesses. This helped to identify any ambiguities or issues with the questionnaire's wording or structure, and administering of the questionnaire.

To minimize selection bias, a purposive sampling method was employed for the survey based on the availability of small business owners, managers, and key employees in each state that are directly involved in chemical handling in the process of production or sales. Questionnaires were subsequently administered in person. After the data collection, descriptive statistics such as frequencies and percentages were used to present the general overview of the chemical safety measures adopted by small-scale businesses.

3.0 Findings

The use of a well-structured survey questionnaire provided an objective and systematic method of evaluating chemical safety measures in small businesses that allows evaluation across various businesses to seek their knowledge and awareness regarding chemical safety. Which information provided is valuable information and knowledge as the data collected through surveys can inform the development of policies and regulations that promote chemical safety in small businesses. The summary of the survey questionnaire is presented in Table 1.

Table 1 summarizes the gender distribution and types of businesses surveyed in the study across Ekiti, Ondo, and Osun States. It provides valuable insights into the diversity of small businesses in the region, which is essential for tailoring safety measures and policies to suit their specific needs. Findings unveiled that a substantial portion of small-scale businesses within these three predominantly agrarian states in Southwest Nigeria belong to the micro and small-size businesses, categorizing them as micro (fewer than 10 employees), small (10 to 49 employees), and medium-sized businesses (50 to 149 employees). Moreover, a gender analysis of business proprietors/owners/managers/employees was conducted (10).

4.0 Discussion

The utilization of hazardous chemicals in small-scale businesses is a subject of considerable concern, given the potential risks and the limited resources typically available to such enterprises. The study conducted in the Southwest region of Nigeria, focusing on Ekiti, Ondo, and Osun States,



offers insights into the state of chemical safety measures among these small businesses. The findings of the survey revealed that a significant portion of small-scale enterprises in these states can be categorized as micro, small, and medium-sized businesses. Micro and small businesses, defined by their employment size of fewer than 50 employees, dominate the landscape. This characterization aligns with the Federal Republic of Nigeria's National Policy on Micro, Small, and Medium Enterprises (10), which recognizes the prevalence of micro and small enterprises in the country.

Another notable aspect is the gender distribution among business proprietors and key personnel. In this study, gender diversity varied across different businesses and states, with no specific trend, although female gender was more prevalent in the

soap and detergent small businesses than male counterparts. However, recognizing the gender dynamics within these small businesses is essential for crafting effective policies and safety measures. Gender sensitivity and inclusivity are vital components in developing a holistic approach to chemical safety.

The primary objective of the study was to assess the chemical safety measures in place within these businesses. While the study does not provide a detailed account of the specific safety measures adopted, it underscores the importance of heightened awareness and enhanced safety protocols. Small-scale enterprises often lack the resources and knowledge needed to effectively manage and mitigate chemical-related risks (11).



Table 1: Summary of the survey questionnaire on gender dynamics and type of business

State	Business	T	M	F	Mi	Sm	Me
Ekiti	Liquid soap and soap chemicals	12	01	11	10	02	00
Ondo	Soap, cosmetics, disinfectant, and cleaning service	20	10	10	09	11	00
Osun	Soap/detergent, cosmetics, and cleaning service	06	05	01	03	03	00
Ekiti	Agrochemicals and rat poison	06	04	02	06	00	00
Ondo	Agrochemicals	03	02	01	03	00	00
Osun	Agrochemicals, rat poison, and mortuary	07	07	00	04	03	00
Ekiti	Printing and paints	08	07	01	08	00	00
Ondo	Paints	04	03	01	01	03	00
Osun	Paints, plastics, foam, and textile	05	04	01	00	05	00
Ekiti	Water: sachet and table	08	07	01	03	05	00
Ondo	Water: sachet and table	10	05	05	00	10	00
Osun	Water/solvent-based medicine	04	02	02	00	04	00
Ekiti	Photo printing lab	08	07	01	08	00	00
Ondo	Photo printing lab	ND	ND	ND	ND	ND	ND
Osun	Photo printing lab	03	02	01	02	02	00
Ekiti	Battery charging, and sales of acid	09	09	00	09	00	00
Ondo	Battery charging, and sales of acid	ND	ND	ND	ND	ND	ND
Osun	Battery charging, and sales of acid	ND	ND	ND	ND	ND	ND
Ekiti	Panel beating and welding	04	04	00	04	00	00
Ondo	Panel beating and welding	ND	ND	ND	ND	ND	ND
Osun	Panel beating and welding	ND	ND	ND	ND	ND	ND
Ekiti	Herbal remedies	ND	ND	ND	ND	ND	ND
Ondo	Herbal remedies	08	07	01	00	08	00
Osun	Herbal remedies	ND	ND	ND	ND	ND	ND

KEY

T= Total of the collected survey structured questionnaire

M Male personnel/entrepreneur/employee

F= Female personnel/entrepreneur/employee

Mi= Micro-sized business

Sm= Small-sized business

Me= Medium-sized business

ND= Not Determined



To foster chemical safety, regulatory adherence is crucial. The European Chemical and Health Agency (4) guides safety data sheets and underscores the significance of comprehensive data on hazardous chemicals. However, many small businesses may not be aware of or fully compliant with such regulations. This study's findings emphasize the need for regulatory authorities to ensure that small businesses have access to, and can comply with relevant safety guidelines and regulations.

Chemicals, in their broadest sense, encompass a vast array of substances. From the water we drink (thus, necessitating the chemical safety measures adopted in sachet and table water production as part of the area sought for in the present survey) to the plastics we use, chemicals are integral to the very fabric of our existence. These compounds, characterized by their distinctive properties and functions, serve as the fundamental building blocks for materials, fuels, medicines, and a myriad of consumer products that are important to agrarian communities. This foundational role makes chemicals indispensable agents of transformation, underpinning our remarkable achievements in various fields (2).

The small businesses were targeted to compare their safety measures against chemical industry best practices and benchmarks which can motivate businesses to enhance their chemical safety protocols. The range of hazards and exposures encountered in small businesses are reported to be extensive, although it was suggested that many of the hazards are similar across businesses and industries, regardless of size, yet others may be unique to small businesses that are predominated by a small number of employees (11).

In agriculture that is the key basis of agrarian communities, for instance, chemicals such as agrochemicals play an essential role as chemicals are instrumental in enhancing food production. Pesticides, herbicides, and fertilizers have revolutionized farming, ensuring higher crop yields and food security for growing populations. These chemical inputs enable us to harness the full potential of our arable lands from the agrarian states of the Southwest zone of Nigeria, making agriculture a linchpin of just not a national food security but a global sustenance. Meet with this, the agrochemical sale managers were often seen dispensing some of these agrochemicals to peasant farmers at a retail level, and this is a key reason that was part of the purposeful sampling for the

chemical safety measure survey embarked upon in these three states (8).

In the context of Southwest agrarian states in Nigeria, the significance of chemicals takes on added dimensions. Agriculture is the backbone of Nigeria's economy, with the Southwest region playing a crucial role in food production and economic sustenance. Chemical inputs, including fertilizers and pesticides, are essential for increasing agricultural productivity, underscoring the importance of responsible chemical usage in these states.

Moreover, the link between agrarian communities and small-scale businesses in Nigeria is undeniable. Small-scale enterprises, often intertwined with agriculture, rely on the produce and raw materials supplied by agrarian communities. These businesses play a vital role in boosting the national economy and providing employment opportunities in the region (8); (12).

Also, in the healthcare of the agrarian communities, for instance, chemicals do play a significant role. Pharmaceuticals and medical treatments are rooted in the principles of chemistry to alleviate ailments and save lives. So also, are the herbal remedies rooted in the principles of chemistry that back up chemicals? In recent times, efforts have been shifted to the area of herbal-based drug discovery (12).

5.0 Conclusion

As chemicals have become not only agents of transformation but also potential sources of vulnerability. Therefore, comprehending the multifaceted role of chemicals, the importance of safe chemical practices, and their influence on Nigeria's economy is imperative. By navigating this intricate landscape with vigilance and wisdom, we can harness the benefits of chemicals while mitigating the inherent risks, ensuring a brighter and safer future for all.

The safety of hazardous chemicals is not only about protecting the well-being of individuals but also has broader economic and environmental implications. Small businesses are often integral to local economies, and chemical safety incidents can disrupt their operations, leading to economic losses (12). Moreover, the improper handling of hazardous chemicals can lead to environmental contamination, which affects not only businesses but also the entire community.



The assessment of chemical safety measures in small-scale businesses in the Southwest region of Nigeria underscores the need for comprehensive efforts to enhance awareness, implement safety protocols, and ensure regulatory adherence, especially among micro and small-scale enterprises. Ensuring the safe handling of hazardous chemicals is imperative for safeguarding the environment and the well-being of individuals engaged in small-scale businesses.

Given the prevalence of micro and small enterprises in the region, targeted safety education and support programs are essential. Regulatory bodies and relevant agencies should focus on providing these businesses with accessible and understandable guidelines. By doing so, they can help mitigate chemical-related risks and foster sustainable economic development.

In conclusion, the study highlights the importance of chemical safety measures in small businesses, particularly those in developing regions like the Southwest of Nigeria. It provides a basis for future initiatives to prioritize chemical safety in these enterprises to protect the environment, the workforce, and local economies.

References

1. Managing risks of hazardous chemicals in the workplace Code of Practice. (2021).
2. G. C. Afube, I. L. Nwaogazie, J. N. Ugbebor, Identification of Industrial Hazards and Assessment of Safety Measures in the Chemical Industry , Nigeria Using Proportional Importance Index. **19**, 1–15 (2019).
3. A. F. Fatusin, OCCUPATIONAL HEALTH HAZARDS AMONG SMALL SCALE INDUSTRIES IN ONDO STATE NIGERIA. **6**, 25–31 (2020).
4. *Guidance on the Compilation of Safety Data Sheets* (2020).
5. G. Notes, Chemical Safety in the Workplace.
6. A. O. Ezenwa, A study of fatal injuries in Nigerian factories. **51**, 485–489 (2001).
7. 7, chukwu 2023 Impact of Agricultural Sector on Economic Growth in Nigeria.
8. C. Joy, IMPACT OF SMALL AND MEDIUM SCALE ENTREPRISES ON ECONOMIC. **2**, 97–108 (2020).
9. Job Hazard Analysis. **2002** (2002).
10. FEDERAL REPUBLIC OF NIGERIA NATIONAL POLICY ON.
11. I. Laird, K. Olsen, L. H. Stephen, L. Melissa, I. Laird, K. Olsen, L. H. Stephen, L. Melissa, Article information : To cite this document : (2011).
12. M. J. Oluseye, THE ROLE OF SMALL AND MEDIUM SCALE ENTERPRISES IN UNEMPLOYMENT REDUCTION IN NIGERIA. **9** (2023).



P088 - ASSESSMENT OF FIRE RETARDANCY PROPERTIES OF BIOLOGICALLY AND CHEMICALLY EXTRACTED JUTE FIBRES USING SURFACE EMBEDMENT

Salisu, Z.M, Ukpong M. K, *Lawal O.M, Umar S.M, Suleiman M. A, Oddy-Obi I. C, Ilyasu A, Sulaiman I.A, Barminas J.T.

National Research Institute for Chemical Technology, (NARICT), Zaria, Nigeria

***Corresponding Author's e-mail:** olamilekanlawal17@yahoo.com, [+2349036882222](tel:+2349036882222)

ABSTRACT

Growing environmental protection consciousness has revived the interest to develop eco-friendly fibres from bio-renewable resources due to their unique intrinsic properties and their wide applications. In recent times, attention of researchers has been shifted to methods of developing natural fibres capable of replacing synthetic counterpart in automobile and construction applications. However, natural fibres have some limitations that need to be addressed such as; mechanical properties, compatibility with resins, fire resistance and so on. In this present study, triammonium phosphate and pentaerythritol were used to impact fire resistance properties on biologically and chemically extracted jute fibres. Furthermore, tensile properties and flame resistance (such as vertical burn, char length, ignition time and after-flame time test) were investigated on the treated jute fibres. It was established that the fire-retardant treatment impacted flame resistance significantly on the extracted jute fibres.

Keywords: *Fire retardants, natural fibres, eco-friendly, triammonium phosphate, pentaerythritol.*

1.0 INTRODUCTION

Due to the increasing in global environmental protection awareness and information of health hazards associated with the manufacture and use of some synthetic fibres (1). There has been increasing demand for natural fibres in various applications such as building materials and automobile components due to its ecological and economic benefits (2). However, most of these natural fibres are sensitive to flame and as such; enhancement of fire resistance of these fibres becomes more and more important in order to comply with the safety requirement of the fibre composite products. Currently a limited amount of literature is available on the flammability characteristics of natural fibres. However, more research findings are needed in this field to extend their applications in

constituent which is liable for the strength of the plant fibres and variance in strength may be due to growth conditions of the plant and soil nature. Cellulose is a lined, semi-crystalline polysaccharide build-up of polymer links compromising the recurring modules of anhydroglucose grouped via

automobiles, marine, aerospace, mining and construction industries.

Among all the natural fibres, jute appears to be most useful, inexpensive and commercially available. Jute can be made into different complex-shaped components owing to its attractive reinforcing potential (3). Also, jute is among the few natural fibres that have mechanical, resistance and flexibility properties. The extracted fibres must be treated chemically or bacterially to separate it from the non-fibrous substances like wax, pectin, and other substances. These fibres can be converted into fine woven fabrics. Jute fibres are environmentally friendly as they are completely biodegradable (4). In plant based fibres, cellulose is the primary structural constituent and the cellulose portion influences the mechanical properties of the lignocellulose fibres. The cellulose is the fundamental

1,4- β -D-glucosidase. The recurring modules of the monomers are termed as degree of polymerization. The monomers of glucose in the chain of cellulose result in formation of the hydrogen bonds among the link forming fibres as well as associated chains. The binding of intramolecular and intermolecular



hydrogen regions results in development of linear crystalline structure called cellulose.

Various chemical treatments are being used to impact fire retardancy on natural fibres, compared with the FR treatment of cotton fibre, less research findings on the FR treatment of jute fibre have been reported (5). In previous reports, some simple inorganic and organic compounds like sodium metasilicate nonahydrate, ortho-phosphoric acid, diammonium hydrogen phosphate, ammonium sulfamate, borax, thiourea, and urea were used to treat jute fibre. In some other reports, organophosphorus flame retardants and tetrakis (hydroxymethyl) phosphonium chloride imparted durable FR

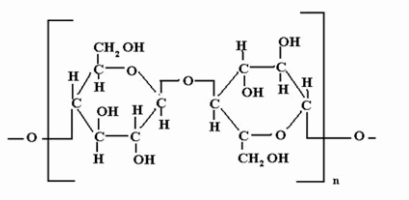


Figure 1: Chemical structure of cellulose

Some of the principal properties of these chemicals is that they have inherent flame resistant, cheap and commercially available.

Flammability is defined as how easily something will burn or ignite, causing fire or combustion. Natural fibres are very sensitive to flame; improvement of flame retardant property of the fibre is critical for use in the construction and other industries. Fire retardancy can be impacted chemically on natural fibres by treatment with flame retardant chemicals.

In this work ammonium tetraoxophosphate(V) and pentaerythritol were used as fire retardants, the resulted fibres were assessed for mechanical and flammability properties.

2.0 Materials and Method

2.1. Materials

The jute plants were sourced locally from Kogi State, Nigeria. Sodium hydroxide (NaOH), Ammonium phosphate $[(NH_4)_3PO_4]$ and pentaerythritol $[C_5H_{12}O_6]$ were purchased from DamaoChemical Reagent Co., Ltd.

property on jute fibre (Shi-Qiong L. *et al.*, 2022). Pentaerythritol (IUPAC: 2,2-Bis(hydroxymethyl)1,3-propanediol), $C_5H_{12}O_4$, is a crystalline polyhydric alcohol with a neopentane backbone. The water-soluble organic compound, used chiefly in the manufacture of alkyd resins, varnishes, plasticizers, and explosives is also a versatile building block for preparation of many poly-functionalized compounds. Its low volatility and high flash point make it excellent resistant to ignition in case of major electrical failure and transformer rupture. Another advantage of using pentaerythritol as intumescent flame retardant is its high thermal stability(6).

(Tianjin, China). All the above reagents are of analytical grade and used as purchased without further purification. Distilled water was employed in preparing the desired solutions.

2.2. Extraction process

2.2.1 Biological retting: The jute plant stalks were soaked in water for duration of three weeks to enable microorganisms feed on the lignin and pectin that bind the fibres together. After three (3) weeks of soaking the fibres were extracted, washed and air dried

2.2.2. Chemical retting: The barks of the jute plant were treated with 4 %w/v NaOH solution at temperature of 70 °C for 60 min to remove the lignin and pectin that bind the fibres together. Then the fibres were separated, washed and air dried.

2.3. Fire retardancy treatment process

15 g of $(NH_4)_3PO_4$ was dissolved in 250 ml of water to prepare an aqueous solution. Another solution was constituted using 3 g of (9-pentaerythritol) dissolved in 100 ml of water to prepare 3 wt% solution. The two solutions were increased proportionally to cater for the whole of the fibres



extracted. In the first treatment process, fibres were soaked in the $(\text{NH}_4)_3\text{PO}_4$ solution for period of 2 hours and transferred to the solution of 9-pentaerythritol for another 2 hours at liquor ratio of 1:20 i.e for every gram of the fibre 20 ml of the solution was used. After then the fibres were squeezed and air dried at room temperature.

2.4. Mechanical and fire retardancy test

2.4.1. Mechanical test

The mechanical test of the chemically treated jute fibres were carried out using a universal tester [Model: WDS-3 max] with a test force of 3KN. The Displacement (mm) and tensile strength of the fibres were determined at a maximum force of 779N and test speed of 50m/min. The results were recorded and calculated by the instrument software.

2.4.2. Fire retardancy test

Vertical Burn Test

The standard 20-mm Vertical Burn Test of the Underwriter's Laboratory of the United State (UL 94) was used to evaluate the flammability of the treated and control samples according Li *et al.* The fibre was burnt vertically on a Bunsen burner flame and the reaction of the fibre against flame was recorded.

Char Length Test

Maximum length of each sample fibre destroyed by combustion was determined according to the procedure of (Davisa *et al.*, 2012).

Burning Time Test

A Bunsen burner flame was applied at the bottom of each sample in a vertical position and the time taken to burn to 7.5 cm mark was recorded according to ASTM D 568 standard reported by Weil and Levchik.

Ignition Time

A Bunsen burner flame was applied to the lower edge of each sample in a vertical position and the time of the flame impingement that caused the sample to ignite was recorded according to ASTM D 3713 standard.

After-Flame Time Test

A Bunsen burner flame was applied at the lower edge of each sample in a vertical position. The flame was removed and the time taken for the burning sample to extinguish was noted according to ASTM D 3801 standard.

3.0 RESULT AND DISCUSSION

3.1 Mechanical Properties

The biological extracted fibre different significantly in appearance from the chemically extracted fibre. The appearance of the biological extracted fibre slightly green due to the presence of residual plant materials, while the chemical extracted fibre was cleaner and softer consistency. However, the tensile strength of chemically extracted fibre was significantly higher than the biological extracted fibre. Biological extraction yielded average tensile strength of 103.86MPa with 8.53mm, the chemical extracted fibre of comparable diameter showed a tensile strength of (87.28MPa) and 1.83mm displacement. This could be attributed to quality of the fibre which is dependent on the method of extraction. The trend observed is expected, due to the inevitable degrading effect of the chemicals applied on the raw plant materials.

Also, the result mechanical test of the biological and chemical extracted fibres treated with fire retardant chemicals (84.92MPa and 78.10MPa respectively) shows a drop-in value of the mechanical properties when compared to the first result. This revealed that treatment with fire retardant chemicals impacted negatively on the tensile strength of the fibres. However, a quick comparative look at the values suggests that the chemically extracted fibres treated with fire retardant chemicals had a better mechanical property compared to the biologically extracted ones with fire retardant chemicals. This could be due to interfacial bonding between the chemically extracted fibre with the fire-retardant chemicals which is stronger compared to the biologically extracted fibre with the same fire-retardant chemicals.

Table 1. Mechanical Properties of the untreated and treated fibres



Sample	Tensile Strength (MPa)	Displacement (mm)
Bio	103.82 ± 17.39	8.53 ± 1.34
Chem	87.28 ± 5.63	1.83 ± 0.53
Bio + F.R	84.92 ± 7.70	4.54 ± 1.00
Chem + F.R	78.10 ± 4.26	3.07 ± 0.23

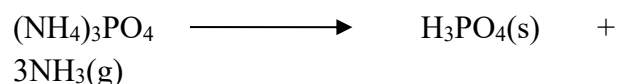
3.2 Fire Reterdancy Properties

Considering the combustion of triammonium phosphate used in the experiment which releases three mole of ammonia gas, when is subjected to flame could be said has potential of resisting flame burning to a significance extent. According to the work of (6) reported that when pentaerythritol was added to ammonium phosphate salts a significance improvement was observed in resistance to flame of the resulted products. In the light of the above triammonium phosphate and pentaerythritol were employed for treatment of the extracted jute fibres from two different extraction methods.

The role of the fire retardants on the burning of the jute fibres were studied. The burning properties of the fibres with and without fire retardant chemicals is presented in Table 2. The results show that Biological extracted fibre treated with fire retardants (Bio-FR) has 52.9 mm/min and chemical extracted fibre with fire retardants (Chem-FR) has 70.2 mm/min vertical burning rate respectively. This shows (Chem-FR) significantly burnt faster

than (Bio-FR). However, the incorporation of fire retardants had a progressive influence on the burning behaviour of the fibre. It also shows that (Bio-FR) has the best burning performance as compared to (Chem-FR). The results of other burning test such as char length, burning time ignition time and after flame were also in agreement with the trend initially established (i.e.

Equation showing combustion of the triammonium phosphate



Bio-FR > Chem-FR). Also, chemically extracted (Chem) fibre was subjected to all the flame tests to serve as control and it was observed that (Bio-FR) comparatively had best performance, followed by (Chem-FR) and (Chem).

Table 2. Flammability Properties of the untreated and treated fibres

Sample	Vertical Burn (mm/min)	Char Length (cm)	Burning Time (sec)	Ignition Time (sec)	After Flame Time (sec)
Chem-FR	70.2	7.0	6.10	2.19	9.24
Bio-FR	52.9	6.20	8.36	2.44	9.56
Chem	82.8	7.50	5.0	1.74	7.03

FTIR Test

Figure 2 shows super imposed FTIR spectral of the samples under investigation (Bio, Bio-FR, Chem and Chem-FR). The region of the broad absorption bands at 3414.12 to 3311.89 cm⁻¹ for the extracted fibres are characterized with O-H stretching and H-bend bond structure that mostly contains major

functional groups of phenols, alcohol and water. A small peak at



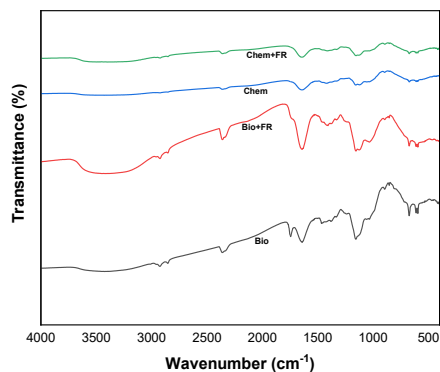


Figure 3. Showing superimposed spectral of the treated jute fibres

2926.18 cm^{-1} for (Bio), 2924.18 cm^{-1} for (Bio-FR), 2926.11 cm^{-1} and 2924.18 cm^{-1} was attributed to the C-H stretching and O-H stretching bond structure that contains a functional group of alkanes (cellulose and lignin) and carboxylic acids. For biological extracted (Bio), it shows a small peak band at 1745.64 cm^{-1} is characterized as the C=O stretching bond structure from functional group of carboxylic acids. The peaks found at 1647.88 cm^{-1} for Bio, 1641.48 for Bio-FR, 1631.83 cm^{-1} for Chem and 1643.41 cm^{-1} for Chem-FR is characterized as the C=C stretching bond structure from the functional group of alkanes (lignin), the peak at 1408.08 to 1456.30 cm^{-1} are characterized as C-H bending bond from the functional group of alkanes (cellulose, hemicellulose and lignin) and peak at 1155.40 cm^{-1} and 1157.33 cm^{-1} are characterized as the C-O stretching bond structure from the functional group of alcohol, (cellulose, hemicellulose and lignin), carboxylic acids, esters and ethers.

References

1. H. Bouguessir, H. Harkati, R. Mansour, G. Priniotakis, Physico-chemical and mechanical engineering applications unco rre ed pr oo f v. doi: 10.3233/JCM-180776 (2018).
2. M. Aravindh, S. Sathish, R. R. Raj, A. Karthick, V. Mohanavel, P. P. Patil, M. Muhibbullah, S. M. Osman, A Review on the Effect of Various Chemical Treatments on the Mechanical Properties of Renewable Fiber-Reinforced Composites. **2022** (2022).
3. S. Bhattacharjee, M. H. Sazzad, M. A. Islam, M. M. Ahtashom, M. Y. Miah, Effects of fire retardants on jute fiber reinforced polyvinyl chloride / polypropylene hybrid composites. **2**, 162–167 (2013).
4. Y. Gowda, T. Girijappa, S. M. Rangappa, Natural Fibers as Sustainable and Renewable Resource for Development of Eco-Friendly Composites : A Comprehensive

4.0 Conclusion

The overall result highlights the effects of the chemical composition to assist the improvement of fire retardancy performance of the fibre materials, offering technology toward another effective environmental safeguarding. The mechanical test carried out on the extracted jute fibres revealed the fibre from the biological extraction has the higher tensile strength as compared to the fibre from chemical extraction method. This observation is due to the fact that the biological extracted fibre was free from the degrading effect of chemicals and the better cross-sectional diameter of the fibre. The same trend was also observed when the samples from the two method of extraction with the fire retardant treatment were compared, which means the treatment did not alter the intermolecular bond that exist in the structure of the fibres. Although, a significance drop was observed in the values of tensile strength recorded.

Also from the results of the fire tests, it can be concluded that the flame resistance properties of the jute fibres treated with triammonium phosphate and pentaerythritol were improved and as such it has a potential to be incorporated as a reinforcement in places where materials that have flame resistance are needed. Still more work is to be done on the flammability of the treated fibres to fully characterize and optimize the effects of the chemicals and to ensure their successful application as well as to establish their commercial viability.



- Review. **6**, 1–14 (2019).
5. A. Ur, R. Shah, M. N. Prabhakar, J. Song, Current Advances in the Fire Retardancy of Natural Fiber and Bio-Based Composites – A Review. **4**, 40684 (2017).
6. H. Abba, H. Musa, A. A. Kogo, A. A. Salisu, Studies on the Effects of Ammonium Phosphates on the Flammability Properties of Poly(Vinyl Alcohol) Films. *Niger. J. Basic Appl. Sci.* **20**, 173–176 (2012).



P089 - ASSESSMENT OF FUNCTIONAL COTTON FABRIC PRODUCED USING CHEMICALLY SYNTHESIZED SILVER-NANO COATING

Ukpong M. K, Salisu, Z.M., Umar S.M, Lawal O.M, Suleiman M. A., Ilyasu A, Sulaiman I.A, Iroegbu U, Oneli I. C, Barminas J.T

National Institute for chemical technology,(NARICT), Zaria, Nigeria

Corresponding Author, E-mail:kokomartino29@gmail.com.Tel.: +2347033693392

ABSTRACT

High performance cotton fabric is gaining increasing awareness as a wearable fabric due to their attractive physical, chemical and antimicrobial properties. The current study elucidates a facile approach for the development of functional cotton fabric using environmentally benign chemicals. Silver Nano particles (AgNPs) were synthesized via chemical reduction method and coated on cotton fabric using dip and ultrasonication techniques. UV-Visible spectra analysis was used to identify the formation of the silver Nano particles. The successful deposition and morphology of AgNPs on cotton fabric were verified using FTIR and SEM. The FTIR spectra of the coated cotton fabrics showed changes in peak bands as a result of the deposition of the AgNPs. The SEM images showed uniform coating of silver nanoparticles on the surface of fabrics. The antibacterial activity of the functional Ag-cotton fabric was also investigated. This study may provide a simple strategy to manufacture Ag-based antibacterial cotton fabric for potential applications in medical and textile industry

Key words: *Silver Nano particles, cotton fabric, anti-bacterial activity, ultrasonication. UV-VIS spectra*

1.0 Introduction

The development of nanoscience and nanotechnology is an emerging area in the applications of nanoscale materials and structures in the range of 1-100nm. In the last few decades, nanoparticles have been employed in various applied fields of science [1–3]. Among various nano particles, silver nanoparticles (AgNPs) are of particular interest due to their remarkable antimicrobial and localized surface plasmon resonance properties, which render them unique properties such as broad-spectrum antimicrobial [4-6], Chemical /Biological sensors and biomedicine materials [7-9] and so on.

Presently, many methods and approaches have been reported for the synthesis of AgNPs by using chemical, physical, photochemical and biological routes. Each method has its setback with common problems being costs, scalability, particle sizes and size distribution and so on [16-17]. Among the existing methods, the chemical methods have been mostly used for production of AgNPs. It is well known that chemical method can successfully

produce pure, well-defined nano particles and is also the most common method because of its convenience and simple equipment. Furthermore, chemical methods provide an easy way to synthesize AgNPs in solution, because they can be implemented under simple and mild conditions

Natural textiles such as cotton fabric have widely been used as sportswear, healthcare and medical textiles due to its excellent properties including biodegradability, hygroscopicity, flexibility, breathability, good skin affinity and low cost. However, cotton provides an excellent environment for microbial growth under certain humidity and temperature, causing discoloration, mechanical strength loss and attendant health issues [10]. Currently, the modification of cotton fabrics to produce functional textiles has attracted significant attention and coating the cotton fabric with antimicrobial agents has become a popular way to produce high performance functional textiles [11,12].

The conventional antimicrobial agents used in textile industry such as metal salts, quaternary ammonium compounds and triclosan are being



replaced due to economic, health, environmental, and efficiency issues [13]. Nanotechnology has provided new insights into the development of functional nanomaterials. Due to their size, nanoparticles present unique and radically different physical, chemical, and biological properties compared to bulk materials; in addition to size, the properties also depend on their shapes, configurations, crystallinity, and structure [14]. Among these nanomaterials, silver nanoparticles (AgNPs) has been effectively incorporated into the cotton fabrics as the antimicrobial agents due to strong inhibitory and antimicrobial effects on a broad spectrum of bacteria, fungi and virus with low toxicity to human being [15].

Agglomeration (aggregation) is an important issue associated with the preparation and application of nanoparticles, since it is energetically favourable for nanoparticles to aggregate and/or fuse together in order to reduce the very large and active surface area [22]. In order to inhibit aggregation, dispersions of nanoparticles and nanoclusters are repeatedly stabilised using a wide variety of surface-active additives serving as a capping agent [22,23]. Capping agents are of utmost importance as stabilizers that inhibit the over-growth of nanoparticles and prevent their aggregation/coagulation in colloidal synthesis. Different types of capping agents have been used in nanoparticles' synthesis including surfactants, small ligands, polymers, dendrimers, cyclodextrins, and polysaccharides.

Polysaccharides have been widely employed as a suitable medium for reducing and stabilizing metal nanoparticles (MNPs) due to their environmentally benign properties [18]. Among these polysaccharides, carboxymethyl cellulose (CMC), has been successfully used to synthesize AgNPs. CMC is water soluble, presents chemical stability, and is not toxic and besides, being a reducing agent, it also can act as a particle stabilizer [19–21].

In this study, a facile method was developed to functionalize cotton fabric with AgNPs in the presence of CMC as a non-toxic stabilizing and reducing agent. The synthesized AgNPs were coated on cotton fabric using dip and ultrasonication techniques. The chemical composition and surface morphology of Ag-cotton fabrics were also examined using Fourier transform infrared spectrophotometer (FTIR) and scanning electron microscope (SEM). The antimicrobial activity of Ag-cotton fabrics was evaluated against *Staphylococcus aureus*.

2.0 Materials and Methods

2.1 Materials

Silver nitrate (AgNO_3), Carboxymethyl cellulose (CMC) and sodium hydroxide (NaOH) were purchased from Sigma Aldrich Co. (Germany). Sodium bicarbonate was purchased from Cardinal Chemicals and scientific supplies, Zaria, Nigeria. All the above reagents were of analytical grade and used as purchased without further purification. Cotton fabric (180 counts) was obtained from a local market.

2.2 Synthesis of silver nanoparticles

The silver nanoparticles were prepared according to the method described by Hebeishet *al.* [24] with little modifications. In the synthesis, the colloidal solution of silver nanoparticles was prepared by dissolving 2 g/l of CMC in 0.4N NaOH. The solution was stirred with its temperature raised to 70°C. A solution of 0.05 M AgNO_3 was added at one time to the mixture and stirred for 30 minutes to complete the process. The colloidal AgNPs solution kept for further use.

2.3 Coating of Silver nanoparticle on cotton fabric

The cotton fabric to be used was cleaned using solution made of 2 g/L sodium carbonate and 2 g/L commercial detergent at 60°C for 30 min with fabric-to-liquor ratio of 1:50. The fabrics were subsequently washed twice with deionized water and dried at room temperature. For the preparation of Ag-cotton fabric, a set of cotton fabrics were made into (4x4cm²) square pieces and immersed (dip) in the prepared colloidal AgNPs solution and kept for 24h at dark. In another study, ultrasonication was performed for the cotton fabric/AgNPs colloidal solution for 2h. The AgNPs deposited cotton fabrics were first washed thoroughly with water to remove traces of reducing and stabilizing agents. The fabrics were dried overnight at 60°C in the oven.

2.4 Characterization

The absorption spectra of the AgNPs solution was measured using UV-VIS (UV-2500PC series) spectrophotometer measured in the wavelength range of 250 to 600 nm. The chemical composition of the cotton/Ag fabrics were investigated using



FTIR (FTIR-8400S) spectrophotometer in the attenuated total reflection mode. Scanning electron microscopy (SEM,1034 Series) was applied to observe the surface morphology of the cotton and cotton/Ag fabrics, at 5Kv accelerating voltage.

2.5 Anti-bacteria assay of the Ag-cotton fabric

Antibacterial activity of silver nanoparticle-coated cotton fabric was studied by disk diffusion method (4,32). A Gram-positive bacterium, *Staphylococcus aureus* (*S. aureus*), was used as the testing organism. Pure cultures were sub-cultured in Muller-Hinton broth for 24 h at 37°C. The sub-cultured organism was swabbed uniformly on a plate using sterile cotton swabs. The Ag NP-coated and uncoated fabrics were gently placed on bacteria-inoculated solidified agar gel plates. The plate was incubated at 37°C for 24 h. The antibacterial activity was ensured by observing whether a zone of inhibition was produced around the samples or not. It was recorded by digital photography.

3.0 Result and Discussion

3.1 Formation of the AgNP

Silver nanoparticles were prepared using Carboxymethyl cellulose (CMC) as the reducing and

stabilizing agent. After adding AgNO_3 solution to the prepared CMC, a visible colour change was observed as the colourless solution changed to yellowish brown and then dark brown which indicated the formation of Ag NPs. The colour change is the most commonly used indicator for the formation of metal nanoparticles [24]. The intensity of colour increased with time indicating adequate growth of nanoparticles.

3.2 UV-VIS Spectra of the AgNPs

Description on the reaction mechanism for formation of silver nanoparticles (AgNPs) by carboxymethyl cellulose (CMC) macromolecules was reported in literature [24,25]. Where, CMC was concurrently used as reducing agent for silver ions (Ag^+) and stabilizer for the obtained silver nanoparticles (Ag^0). The presence of a reducing alcoholic and aldehyde groups in the CMC played a dual role for reduction and stabilization of the net produced AgNPs. Subsequently, the produced AgNPs were stabilized by the polymeric chains of CMC for preventing the aggregation of smaller particles which might result in enlarged clusters. The UV- VIS spectra showed a peak in the visible region around 427 nm indicating the maximum absorption, as shown in Fig. 1. This was due to surface plasmon excitation, and it confirmed the formation of Ag NP.

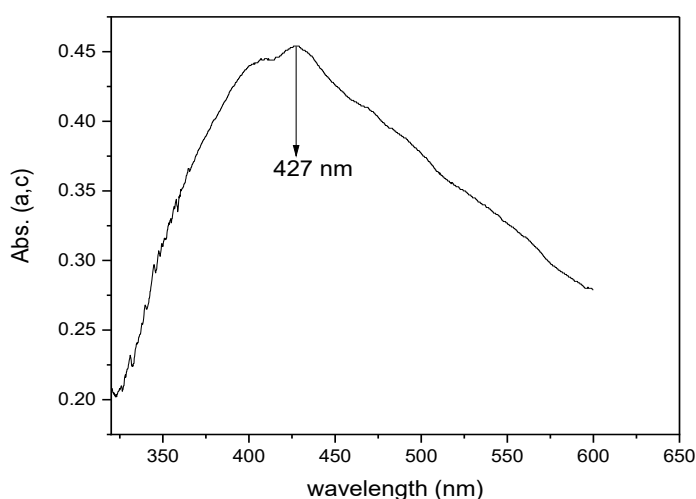


Fig 1:UV-VIS spectra of AgNPs



3.3 FTIR spectra of the uncoated and Ag-coated cotton fabric

Figure 2 displays the FTIR spectra of uncoated (Ao) and Ag-coated cotton fabrics (Ad) and (As) obtained via dip and ultrasonication method. The spectrum of the uncoated cotton fabrics shows broad peak between 3400 and 3200 cm^{-1} (A) which is assigned to stretching of hydrogen-bonded hydroxyl group in cellulose, while the absorbance

at 2970 and 2950 cm^{-1} (B) is due the symmetric C-H and C-H₂ stretching vibrations. However, new peaks were observed in the Ag-cotton coated fabrics. The notable broad bands between 3700 and 3400 cm^{-1} (a), 1700 and 1600 cm^{-1} (b) and 1150 and 1050 cm^{-1} (c) corresponds to O-H, C=O and C=O stretching vibrations. The peak at c indicates the formation of a new C=O group owing to the reduction of Ag by several hydroxyl groups (in the carboxylic group) which were oxidised at the expense of Ag when Ag was reduced [25].

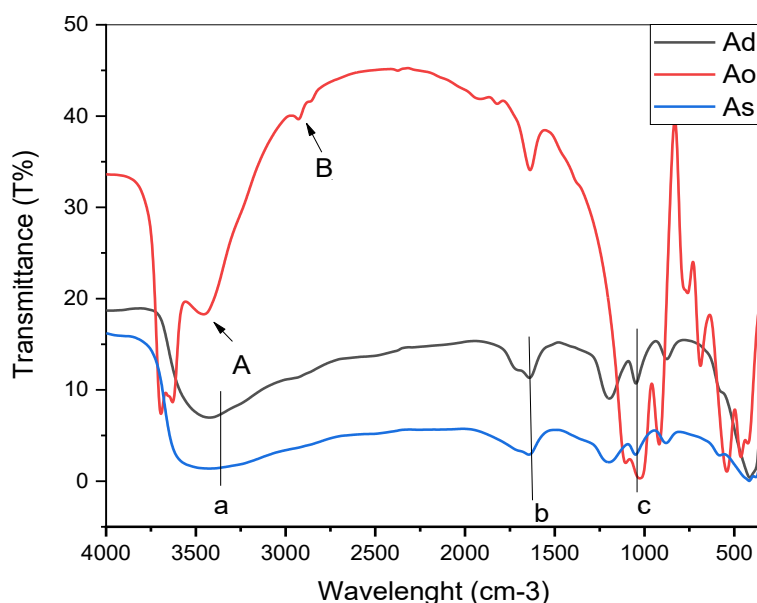


Figure 2: FTIR spectra of Uncoated cotton fabric (Ao), coated cotton fabric via Dip (Ad) and Ultrasonication (As) method

3.4 SEM Images of the uncoated and Ag-coated cotton fabric

The surface morphology of Ag-coated cotton fabrics were investigated by scanning electron microscope (SEM). Figure 3a, 3b and 3c shows the SEM images of the uncoated coated (Ao), Ag-coated fabric (Ad) and (As) obtained via dip and ultrasonication methods. In the Dip method (Fig. 3b), the SEM micrograph reveals that the AgNPs were not well spread over the cotton fabrics which could be due to the agglomeration of the particles on the surface of the cotton fabric, thereby

leading to the formation of micro-particles. However, in the Ultrasonication method (Fig. 3c), the SEM result showed a smooth uniform dispersion of the AgNPs on the cotton fabric which indicated that a high surface coverage was formed on the cotton fabric as a result of the ultrasonication treatment which helps to disperse the nano particle during the coating process. Furthermore, the result also indicated that the amount of AgNPs on the fabric is higher for Ao compared to Ad.



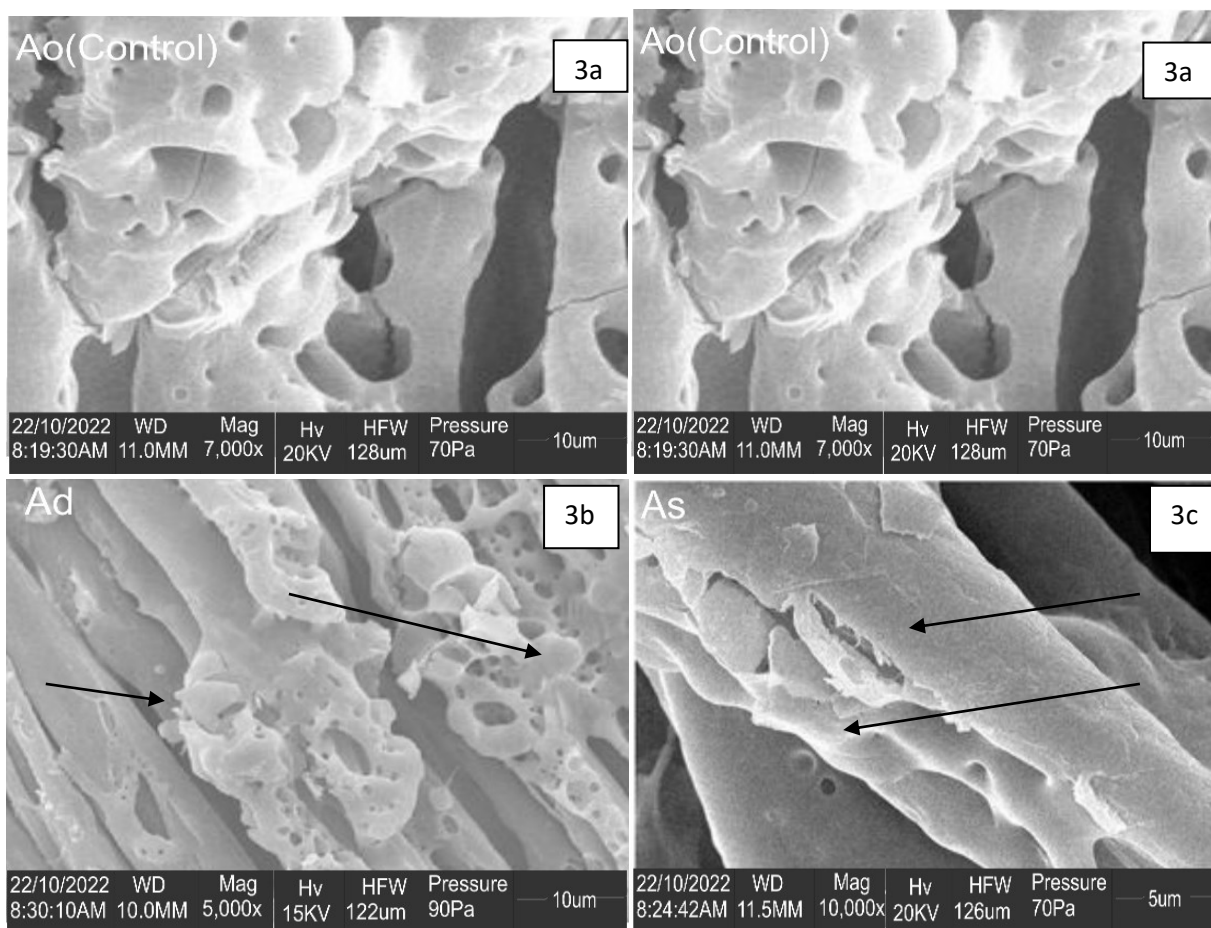


Fig3: SEM images of cotton fabrics: Uncoated cotton fabric (Ao), Dip (Ad) and ultra sonicated (As) coating with AgNPs

3.5 Antibacterial activity

The antibacterial properties of Ag NP-coated cotton fabric were evaluated against *S. Aureus* bacteria strain using the disk diffusion technique [26]. Fig 4 shows the antimicrobial activity of uncoated and Ag-coated fabric where the uncoated fabric was used as a reference. The zone of inhibition represents the antimicrobial activity of Ag NPs-coated fabric. The formation of inhibition zone clearly indicates that the Ag NPs-incorporated fabric possesses antimicrobial action due to the

action of Ag NPs on the organism's membrane. The Ag NPs-incorporated fabric showed an inhibition zone around the fabric for both dip and ultrasonicated specimens. The uncoated reference fabric did not show any antibacterial activity. The zone of inhibition was broader for ultrasonicated fabric than the dip-coated fabric. This may be due to the presence of higher amounts of Ag NPs in ultrasonicated coated fabric compared to the dip coated fabric. The higher diameter of inhibition zone around the sample shows that the Ag NPs-coated fabric has a better antibacterial effect against *S. aureus*.



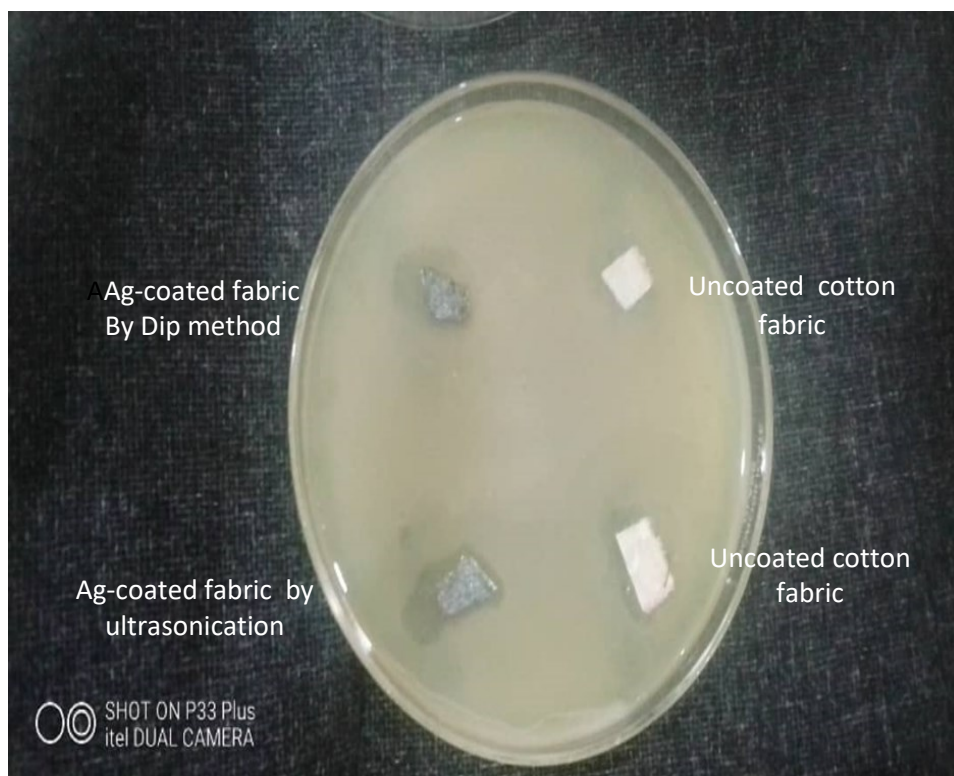


Fig4: Digital photograph image of antibacterial activity of uncoated, coated Ag-cotton fabrics against *Staphylococcus aureus*

4.0 Conclusion

Silver nano particles was successful synthesized via chemical method using carboxymethyl cellulose (CMC), as reducing and stabilizing agent. The synthesized AgNPs were coated on cotton fabric so as to enhance the functional properties of the fabric. The synthesized AgNPs were coated on the cotton fabrics using dip and ultrasonication techniques. The SEM result showed that the ultrasonication process was a better technique as it helped to disperse the nano particles uniformly to the fabric during the coating process. Due to physical and chemical interaction, the nanoparticles were bound uniformly on the fabric surface. The fabric coated with AgNP using ultrasonication technique exhibited better antibacterial activity against *S. aureus* bacterial strain compared to dip method. This was due higher deposit of AgNPs on the cotton fabric obtained through ultrasonication technique. The advantage of this process is its ease of operation and its efficiency. This study may provide a simple strategy to manufacture Ag-based antibacterial cotton fabric for potential applications in medical and textile industry.

References

- 1] G. Franci, A. Falanga, S. Galdiero, L. Palomba, M. Rai, G. Morelli, M. Galdiero (2015). "Silver nanoparticles as potential antibacterial agents", *Molecules*, vol.20, pp.8856-8874.
- [2] S. Jana & T. Pal (2007) "Synthesis, characterization and catalytic application of silver nanoshell coated functionalized polystyrene beads", *J. Nanosci. Nanotechnol.* vol.7, pp.2151- 2156.
- [3] R. Stiuftuc, C. Iacovita, C. M. Lucaciu, G. Stiuftuc, A. G. Dutu, C. Braescu, N. Leopold (2013) "SER-active silver colloids prepared by reduction of silver nitrate with short-chain polyethylene glycol", *Nanoscale Res. Lett.* vol.8, pp.47.



- [4] Z.-C. Xing, W.-P. Chae, J.-Y. Baek, M.-J. Choi, Y. Jung, and I.-K. Kang (2010). "In vitro assessment of antibacterial activity and cytocompatibility of silver-containing PHBV nanofibrous scaffolds for tissue engineering," *Biomacromolecules*, vol. 11, no. 5, pp.1248–1253.
- [5] E. Amato, Y. A. Diaz-Fernandez, A. Taglietti (2011). "Synthesis, characterization and antibacterial activity against gram positive and gram negative bacteria of biomimetically coated silver nanoparticles," *Langmuir*, vol. 27, no. 15, pp. 9165–9173.
- [6] I. Perelshtein, G. Apperlot, N. Perkas, G. Guibert, S Mikhailov, A. Gedanken, (2008) "Sonochemical Coating of Silver Nanoparticles on Textile Fabrics (Nylon, Polyester and Cotton) and Their Antibacterial Activity." *Nanotechnology*, 19 (24) 245705.
- [7] G. A. Evtugyn, R. V. Shamagsumova, P. V. Padnya, I. I. Stoikov, I. S. Antipin (2014) "Cholinesterase sensor based on glassy carbon electrode modified with Ag nanoparticles decorated with macrocyclic ligands", *Talanta*, vol.127, pp.9-17.
- [8] N. T. K. Thanha, & L. A. W. Green (2010). "Functionalisation of nanoparticles for biomedical applications", *Nano Today*, vol.5, pp.213-230.
- [9] N. Alon, Y. Miroshnikov, N. Perkas, I. Nissan, A. Gedanken, O. Shefi, (2014) "Substrates coated with silver nanoparticles as a neuronal regenerative material", *Int. J. Nanomed.* vol.9, pp.23-31.
- [10] M.E. El-Naggar, A.G. Hassabo, A.L. Mohamed, T.I. Shaheen (2017). Surface modification of SiO₂ coated ZnO nanoparticles for multifunctional cotton fabrics, *J. Colloid Interface Sci.* 498 413–422.
- [11] Nadi A, Boukhriss A, Bentis A, Jabrane E, Gmouh S (2018). Evolution in the surface modification of textile: a review. *Text Prog* 50:67–108. <https://doi.org/10.1080/00405167.2018.1533659>
- [12] D. S. Morais., R. M Guedes, M. A. Lopes (2016) Antimicrobial approaches for textiles: from research to market. *Materials* 9:498. <https://doi.org/10.3390/ma9060498>
- [13]., D.M. Mitrano ; E . Lombi;, Y.A.R Dasilva.; B Nowack (2016). Unraveling the complexity in the aging of nano enhanced textiles: A comprehensive sequential study on the effects of sunlight and washing on silver nanoparticles. *Environ. Sci. Technol.* 50, 5790–5799. [CrossRef]
- [14].K. M. M. Abou El-Nour, A. A. Eftaiha, A. Al-Warthan, and R. A. A. Ammar (2010), "Synthesis and applications of silver nanoparticles," *Arabian Journal of Chemistry*, vol. 3, no. 3, pp. 135–140..
- [15].I, Sondi,. & B. Salopek-Sondi (2004) . Silver nanoparticles as antimicrobial agent: A case study on E. coli as a model for Gram-negative bacteria. *J. Colloid Interface Sci.* 275, 177–182. [CrossRef] [PubMed]
- [16]. K. M. M. El-Nour, A. Eftaiha, A. Al-Reda, A. A. Ammar (2010). "Synthesis and applications of silver nanoparticles", *Arabian J. Chem.* vol.3, pp.135-140.
- [17] A. B. Smetana, K. J. Klabunde, C. M. Sorensen (2005). "Synthesis of spherical silver nanoparticles by digestive ripening, stabilization with various agents, and their 3-D and 2-D superlattice formation", *J. Colloid. Interface Sci.* vol.284, pp. 521-526..
- [18].Shams, R.; Rizvi, Q.E.H.; Dar, A.H.; Majid, I.; Khan, S.A.; Singh (2021). A. Polysaccharides: Promising Constituent for the Preparation of Nanomaterials. In



Polysaccharides: Properties and Applications; Scrivener Publishing: Beverly, MA, USA; pp. 441–457. [CrossRef]

[19] M. A. Garza-Navarro, J. A. Aguirre-Rosales, E. E. Llanas-Vázquez, I. E. Moreno-Cortez, A. Torres-Castro, and V. Gonzalez-Gonzalez (2013). “Totally ecofriendly synthesis of silver nanoparticles from aqueous dissolutions of polysaccharides,” *International Journal of Polymer Science*, vol. 2013, Article ID 436021, 8 pages, 2.

[20] M. N. Nadagouda & R. S. Varma (2007). “Synthesis of thermally stable carboxymethyl cellulose/metal biodegradable nanocomposites for potential biological applications,” *Biomacromolecules*, vol. 8, no. 9, pp. 2762–2767.

[21] A. A. Hebeish, M. H. El-Rafie, F. A. Abdel-Mohdy, E. S. AbdelHalim, and H. E. Emam (2010). “Carboxymethyl cellulose for green synthesis and stabilization of silver

nanoparticles,” *Carbohydrate Polymers*, vol. 82, no. 3, pp. 933–941.

[22] H. Lee & K. S. Chou (2005). “Inkjet Printing of Nanosized Silver Colloids”, *Nanotechnology*, vol.16, pp.2436-2441.

[23] Z. Anna, S. Ewa, Z. Adriana, G. Maria, H. Jan (2009). “Preparation of silver nanoparticles with controlled particle size”, *Procedia Chem.* vol.1, pp.1560-1566, 2009.

[24] A. A. Hebeish, M. H. El-Rafie, F. A. Abdel-Mohdy, E. S. Abdel-Halim, and H. E. Emam (2010). *Carbohydr. Polym.*, 82,933.

[25]. H. E. Emam & H. B. Ahmed (2016). *Carbohydr. Polym.*, 135,300

[26] M. Balamurugan, N. Kandasamy, S. Saravanan, N. Ohtani (2014). “Synthesis of Uniform and High-Density Silver Nanoparticles by Using *Peltophorumpterocarpum* Plant Extract”, *Jpn. J. Appl. Phys.* 53 (5S1) 05FB19 1–7.



P090 - DEVELOPMENT OF SELF IGNITED FIRE EXTINGUISHER BALL: A REVIEW

Suleiman, M. A^{1*}, Salisu, Z.M¹, Barminas, J.T¹, Ukpong M.K¹, Lawal, O.M¹, Ilyasu, A¹, Adams, A.A², Umar I. S¹, Sulaiman I. A¹, Oddy-Obi, I.C¹

National Research Institute for Chemical Technology, Zaria, Nigeria
Institute of Natural and Applied science, Necmettin Erbakan University, Konya, Türkiye
Corresponding Author: * mohammed_suleiman89@yahoo.com

ABSTRACT

Fire outbreak is one of the repeated devastating disasters that consumes many lives and properties. Techniques were invented to address this disaster and the most widely accepted is fire extinguisher. In 19th Century, new technology was developed to address the problem of traditional fire extinguisher, this method is the pull push release sway method and getting close to the fire is not required. The conventional fire extinguishing system found not enough to curb losses and not always possible to extinguish small fire. Later on, new method came up where the technical solution includes a simpler design of a fire extinguisher, and increase its utilization efficacy. In decade ago, another research was made, where the main objective was to easily control the small fire at the initial phase by using the traditional fire extinguisher. In this work, the dry powder in the fireball is a mixture of mono ammonium phosphate as active ingredient, ammonium sulphate, tri-calcium phosphate, polymeric compound, drying agent and pigment. Inside the ball there-in a fuse extending from the interior detonator, linkage to exterior surface that senses the fire and burst, follows by the dispersion of the extinguishing dry chemical powder to quench the fire.

Keywords: *Fire extinguisher, Innovative, Dry powder, Conventional, Detonator, Fuse.*

1.0 INTRODUCTION

Fire outbreak due to its devastating effect on lives and properties has attracted attention of researchers in recent times. These huge consequences of fire outbreak to lives and properties has necessitated interventions to mitigate these effects. The impact of these fire outbreak shown by the report of Centre for Fire Statistics (CFS) (2023) of fire incidents 57 countries around the globe including Nigeria; 2.5-4.5 million fires were recorded annually, in which 17-62 thousand people died. There were over 50 recorded fire outbreaks in different Nigerian markets within a year. The study found that substandard fire extinguishers and inadequate wall space fire protection devices contribute to rapid spread fires in Nigeria (8). This disastrous impact of fire to the environment, economy and human live has necessitate strategies to prevent, control or eliminate it when it occurs (7).

The invention of fire extinguisher has tremendously helped and saved countless lives and properties, which has gone through a variety of changes from its design to further increase its efficiency and ability to put out fire.

Fire extinguisher ball is a kind of revolutionary self-ignited solution for initial fire, wherever there is fire emergency. In fact, the use of fire extinguishing ball is one of the fastest and simplest ways of extinguishing fire. ABC dry powder extinguisher agent mainly extinguish fires by chemical inhibition, offering superior performance and environmental friendliness (6). It helps to minimize damage, reduce fire brigade actions and sometimes prevent the need for evacuation of people (12).

The first recorded fire extinguisher was patented in England in 1723 by Ambrose Godfrey. Godfrey was a great chemist who developed a liquid designed model to extinguish fires which contained a pewter chamber of gunpowder. A system of fuses would light up, exploding the gunpowder and scattering the solution around the fire (9)



In 1819 Captain George William Manby invented the first version of the modern fire extinguisher which was a copper vessel containing three gallons of pearl ash solution under compressed air pressure (11). Early in 1900s, carbon dioxide fire extinguishing systems have been in use, extinguishing fire relatively quickly and leaving no residue (3). In the 1960's major developments in dry chemical agents led to the introduction of potassium bicarbonate. Dry chemical powders are advisable for the highest efficiency of fire extinguishing system (5).

Dry chemicals can be found with particle size ranging from 10 to 75 microns. The relationship of particle size to extinguishing effectiveness implies that the surface area of dry chemical agents plays a key role in extinguishing a fire (4). The dry chemical extinguishers put out fire by coating the fuel with a thin layer of dust, separating the fuel from the oxygen in the air. Powder also works to interrupt the chemical reaction of the fire, so these extinguishers are extremely effective in putting out fire. These review entails brief classification, an overview of fire extinguisher ball.

2.0 FIRE EXTINGUISHER

A fire extinguisher are active fire protection devices used to extinguish or control fires in an emergency, preventing danger or threats (1). It is not intended for use on an out-of-control fire, such as one which has reached the ceiling, endangers the user (i.e., no escape route, smoke, explosion hazard, etc.), or otherwise requires the expertise of a fire brigade. Typically, a fire extinguisher consists of a hand-held cylindrical pressure vessel containing an agent which can be discharged to extinguish a fire. A cartridge base fire extinguishers are commonly used, but can become dangerous if not properly handled or maintained (10).

2.1 CLASSIFICATION OF FIRE EXTINGUISHER

Extinguisher can be classified by the type of extinguishing medium which they contain. At present, the main types of extinguishers are:

- i. Water based;
- ii. Foam based;
- iii. Powders – ABC/BC/D Type;
- iv. Carbon dioxide;

- v. Clean agents; and
- vi. Water mist type

3.0 EXTINGUISHING MEDIA, PROPELLANTS AND

3.1 FILLING REQUIREMENTS

D. Extinguishing Media

Water and water mist

Carbon dioxide: Carbon dioxide used in extinguisher shall conform to IS 15222.

Clean Agents: For clean agent, certificate of manufacturer/supplier shall be made available. Further name of clean agent shall be marked on the label of the extinguishers.

- a. Powders: Powders used in the extinguisher shall conform to IS 4308.
- b. Foam Concentrates: Foam concentrates used in the extinguisher shall conform to IS 4989.

B. Propellants

The propellants for stored pressure and cartridge operated extinguishers shall be air, carbon dioxide and nitrogen

C. Filling Requirements (Type Test)

Fill Density: The maximum fill density for carbon dioxide extinguishers shall not exceed 0.667kg/l. the fill density for clean agent fire extinguishers shall not exceed the values given by the supplier/manufacturer of the gas.

Filling Tolerance: the actual charge of an extinguisher shall be the nominal charge within the following limits:

Water based extinguisher: 0 percent to + 5 percent by volume;

- vii. Foam based extinguisher: 0 percent to + 5 percent by volume;
- viii. Powder extinguishers: + 2 percent by mass;
- ix. Carbon dioxide extinguishers: 0 percent to + 5 percent by mass;
- x. Clean-agent extinguishers: 0 percent to 5 + percent by mass; and



- xi. Water mist type: 0 percent to + 5 percent by volume.

3.2 FIRE EXTINGUISHING BALL

The modern form of the ball is a hard foam shell, wrapped in fuses that lead to an accelerator (pyrotechnic device) charge inside it. The ball bursts a few moments after contact with flame, thereby dispersing a cloud of ABC dry chemical powder which extinguishes the fire. The coverage area is about 5m² (54 sqft) (9). The ball could be placed in a fire-prone area. The automatic fire extinguishing system using ignition sensing fuse can operate without power supply and can detect and extinguish fire (2).

Fire Extinguisher Ball could be termed as a fully automatic type of fire extinguisher. When thrown or rolled into fire, it will burst and extinguish the fire instantly. It may be positioned where the hotspots are such as flammable objects, circuit breaker box, gas tank etc. An activation or trigger strip is implanted into the ball's outer casing. It firmly holds the dry fire extinguishing agent inside. When the activator or trigger is exposed to flames for more than a few seconds, the casing will burst open and disperse a cloud of chemical powder in the surroundings.

3.2.1 MATERIALS FOR FABRICATION OF FIRE EXTINGUISHER BALL

We use five raw materials to produce the fire extinguishing device. The five materials are as follows;

- EPS Box
- ABC dry powder
- Ammo
- Fuse
- Adhesive

1. EPS Box: Expanded Polystyrene (EPS) is a lightweight cellular plastic material consisting of small hollow spherical balls. It is this closed cellular construction that gives EPS its remarkable characteristics.

2. ABC dry powder: ABC Dry Chemical, ABE Powder, tri-class, or multi-purpose dry chemical is a dry chemical extinguishing agent used on class A, class B, and class C fires. It uses a specially fluidized and siliconized monoammonium

phosphate powder. ABC dry chemical is usually a mixture of monoammonium phosphate and ammonium sulfate, the former being the active one. The mix between the two agents is usually 40–60%, 60-40%, or 90-10% depending on local standards worldwide. The USGS uses a similar mixture, called Phos Chek G75F.

3. Ammo: Ammunition (informally ammo) is the material fired, scattered, dropped or detonated from any weapon. Ammunition is both expendable weapons (e.g., bombs, missiles, grenades, land mines) and the component parts of other weapons that create the effect on a target (e.g., bullets and warheads). Nearly all mechanical weapons require some form of ammunition to operate.

4. Fuse: In an explosive, pyrotechnic device, or military munition. A fuse is the part of the device that initiates function. In common usage, the word fuse is used indiscriminately. However, when being specific (and in particular in a military context), the term fuse describes a simple pyrotechnic initiating device, like the cord on a firecracker whereas the term fuse is sometimes used when referring to a more sophisticated ignition device incorporating mechanical and/or electronic components.

5. Adhesive: Adhesive, also known as glue, cement, mucilage, or paste, is any non-metallic substance applied to one or both surfaces of two separate items that binds them together and resists their separation.

3.3 TESTING OF THE DEVICE IN REAL LIFE SITUATION

The device can be tested in a real situation by a middle size of fire, after sometime the powder inside it spread into the area and will extinguished the fire successfully. The whole area covered with powder.

4.0 CONCLUSION

The self-ignited fire extinguisher ball is reliable fireball, more facile and robust. Development of such fire ball would curb immensely the incessant menace of fire outbreak as it devastated lives and properties in many places such as; markets, offices, worshiping places, residential houses, schools, health care centres, banks etc. The preeminent merit of this technology is its ability of putting out small fire before it lingered into a big fire. Its efficiency and functions cut across different fields of human endeavour. Therefore, for progress in the course of research, there is need for the researcher to looked into more modification on the chemical agent that



can sufficiently cover large perimeter to exit fire and coupling Artificial Intelligent (AI) technology.

REFERENCES

1. A., Fonsula, V., & Handoko, M. (2019). Crew Capability Assessment in using Portable Fire Extinguisher during Fire Drill Implementation on MV. Vinca. *KnE Social Sciences*, <https://doi.org/10.18502/kss.v3i23.515>
2. Choi, Y., Yoon, B., Kim, E., & Shin, M. (2011). Development of automatic extinguisher using ignition sensing tube for smart fire protection system. *International Journal of Precision Engineering and Manufacturing*, 12, 1015-1021. <https://doi.org/10.1007/S12541-011-0135-3>.
3. Harrington, J., & Senecal, J. (2016). Carbon Dioxide Systems., 1531-1586, <https://doi.org/10.1007/978-1-4939-2565-045>
4. Huang, D., Wang, X., & Yang, J. (2015). Influence of Particle Size and Heating Rate on Decomposition of BC Dry Chemical Fire Extinguishing Powders. *Particulate Science and Technology*, 33, 488 - 493. <https://doi.org/10.1080/02726351.2015.1013591>.
5. Kovalev, O., Kalinovsky, A., & Polivanov, O. (2019). DEVELOPMENT OF INDIVIDUAL ASPECTS OF CONTAINER METHOD OF FIRE EXTINGUISHING. *Fire Safety*. <https://doi.org/10.32447/10.32447/207>
6. Li, H., Hua, M., Pan, X., Li, S., Guo, X., Zhang, H., & Jiang, J. (2019). The reaction pathway analysis of phosphoric acid with the active radicals: a new insight of the fire-extinguishing mechanism of ABC dry powder. *Journal of Molecular Modeling*, 25, 1-12. <https://doi.org/10.1007/s00894-019-4136-y>.
7. Oloke, O. C. Oluwunmi, A. O. Oyeyemi, K. D, Ayedun, C. A & Peter, N. J. (2021). Fire risk exposure and preparedness of peri-urban neighbourhood in Ibadan, Oyo State Nigeria. 4th International Science & Sustainable Development: Advance in Science and Technology for Sustainable Development (ICSSD) 2020, volume 655, Issue 1.
8. Sunday, O., Zubairu, S., & Isah, A. (2019). Determination of Active Protection Measures against Fire in Wuse Market of the Federal Capital Territory of Nigeria. *American Journal of Civil Engineering and Architecture*. <https://doi.org/10.12691/AJCEA-7-2-3>.
9. The history of Fire Extinguishers. *Atwood Fire & Security*. [Online] [Cited: December 05, 2011]<http://www.atwoodsecurity.com/fire-extinguisher-products-and-service/fire-extinguisher-history.html>.
10. Tumram, N., Ambade, V., & Dixit, P. (2018). Fatality During Servicing of Fire Extinguisher. *Journal of Forensic Sciences*, 63. <https://doi.org/10.1111/1556-4029.13531>.
11. Yun, H., S., Kim, H., & Park, I. (2017). Development of Independent Sprinkler



for Fire Safety., 16, 124-128.
<http://doi.org/10.14775/ksmpe.2017.16>

12. (2021). Fire extinguishers and their purpose. *Okhrana truda i tekhnika bezopasnosti na promyshlennykh*

predpriyatiyakh (Labor protection and safety procedure at the industrial enterprises). <https://doi.org/10.33920/pro-4-2107-08>.



P091 - THE PRESENCE OF ALKALOIDS AND ANTI-MALARIAL ACTIVITY OF *P. GUAJAVA* LEAVES EXTRACT

*^{1,2}Isah, H. A. and ²Ahmad, D.

1. Department of Chemistry, Faculty of Science, Nigerian Defence Academy, Kaduna State.

2. Department of Pure and Industrial Chemistry, Faculty of Natural and Applied Sciences, Umaru Musa Yar'adua University, Katsina, Nigeria.

*Corresponding Author: hadizaaminu246@gmail.com, +2347047818643

ABSTRACT

The potential use of plants as nontoxic, safe and alternative sources for malaria management and treatment by pregnant women has been investigated. The extraction of these plants is essential in isolating antimalarial agents with the aim of understanding their role in the treatment of malaria. Therefore, this study was designed to identify the presence of alkaloid in relation to antimalarial activity present in *P. guajava* leaves against *P. falciparum*. All plant leaves tested positive for the presence of alkaloids. The antimalarial test was carried out at 24- and 48-hours incubation using a blood sample containing 5 % parasitaemia was used to determine the anti-plasmodial activity of the plant leaves extract. All the different concentrations of the plant leaves extracts; 10 mgml⁻¹, 5 mgml⁻¹, 2.5 mgml⁻¹ and 1.25 mgml⁻¹ tested positive for antimalarial activity when screened. The highest concentration 10 mgml⁻¹ showed the most elimination of the malaria parasite at both 24 and 48 hours. The leaf extract of *Psidium guajava* showed 58 % elimination of *Plasmodium falciparum*. The investigation results of the antimalarial activity is promising and shows that *Psidium guajava* could be used in the management of malaria by pregnant women during their first trimester.

KEYWORDS

Antimalarial, Alkaloids, *Psidium guajava* leaves, Antimalarial drugs.

INTRODUCTION

The use of natural products especially plants for the treatment of several ailments has been the longest medical practice globally (1, 2). With herbalists prescribing variety of plants to treat and manage diseases, the plants are either given whole or as concoctions (3, 4). Some plants such as *artemisia annua* were traditionally used as concoctions to treat as several ailments. In the 1990's researchers in China embarked on research to find antimalarial treatments for the soldiers and eventually isolated artemisinin as the active ingredient present in *Artemisia annua* to treat malaria (5, 6).

Malaria is a treatable and avoidable disease caused by five *Plasmodium* parasite species, two species *P. falciparum*, *P. vivax* pose the greatest treat (7). The most prevalent and deadliest *Plasmodium* parasite in the African continent is the *P. falciparum* which results in 96 % deaths of the 620,000 deaths caused by malaria globally in 2021 (7). Quinine originally discovered from *Cinchona* tree and its derivatives

were initially used in the treatment of malaria however, rise in antimalarial resistance resulted in the search for alternatives (8). The discovery and isolation of artemisinin as a potent antimalarial agent provided a solution for antimalarial resistance. In order to reduce cases of resistance, partial resistance and reduced efficacy; artemisinin are mainly used as a combination with other drugs (Artemisinin-based combination therapy (ACT)) (7, 9). Though ACTs are largely used to treat malaria these antimalarials cannot be administered to pregnant women within the first trimester of their pregnancy due to severe birth defects associated with ACTs (10).

Currently, the use oral quinine plus clindamycin is the recommended first line treatment administered to pregnant women during their first trimester (11). However, resistance and easy access to these medications restricts low-income families. *Psidium guajava* leaves have been used traditionally by pregnant women to aid with pregnancy, treat gastrointestinal, malaria and microbial infections (12).



Several phytochemicals such as quercetin, avicularin, apigenin, guaijaverin, kaempferol, hyperin, myricetin, gallic acid, catechin, epicatechin, chlorogenic acid, epigallocatechin gallate, and caffeic acid have all been identified and isolated from the plant(13). Therefore, the present study was designed to investigate the presence of alkaloid in *P. guajava* leaves relation to the antimalarial activity observed.

MATERIALS AND METHODS

Plant material identification

Leaves from *Psidium guajava* leaves were collected from Sabon-gari area in Daura, Katsina state. The leaves were then authenticated as *Psidium guajava* at the Biology Department of Umaru Musa Yar'adua University (UMYU), Katsina state, Nigeria.

Plant Preparation and Extraction

The leaves of *P. guajava* were washed with water then air-dried and pulverized to a powdered form. 50 g of ground guava leaves was macerated in 100 mL of ethanol for 72 h. The mixture was then filtered and concentrated under reduced pressure to yield 5.5 g crude extract. 100 mL of distilled water was added to the crude leaf extract to make a 100 mL crude mixture. The pH of the resulting mixture was adjusted from 3.2 to 11.2 by the addition of a few drops of concentrated sodium hydroxide. Liquid-liquid partitioning was carried out on the resulting mixture using 3 x 100 mL of dichloromethane (DCM) both layers were collected, the DCM solution was concentrated under reduced pressure to afford a brownish residue.

Alkaloid Screening of DCM Extract

The presence of the phytochemical alkaloid was tested in the crude *P. guajava* leaves DCM extract previously obtained. All procedures were developed at room temperature. The extract was used for the subsequent qualitative analysis of metabolites using the method described by Junaid RS and Patil MK in 2020 (14).

Antimalarial Screening of Crude DCM Extract

The antimalarial activity of the leaves extract of *P. guajava* was determined using blood sample with

5% parasitaemia collected from Bayero University Care Hospital Kano. Malaria parasite was identified by the ring shape of the immature trophozoites which retained blue colour of the stain. Parasitaemia levels and species parasites were recorded as described by Chotivanich *et al.* (15).

Separation of the Erythrocytes

Blood sample with 5% parasitaemia collected from Bayero University Care Hospital Kano was centrifuged at 2500 r/m for 15 mins. After centrifugation, the supernatant (plasma) was discarded while the sediments (erythrocytes) were further centrifuged with normal saline at 2500 r/m for 5 mins. The supernatant was then discarded and the erythrocytes were suspended in normal saline.

In vitro Anti-malarial Assay

Psidium guajava leaf extract was screened for antimalarial activity against the *P. falciparum* strain. The *P. falciparum* strain was cultivated by a modified method described by Trager and Jensen. The extracts were dissolved in DMSO. The final concentration of (Dimethyl sulfoxide (DMSO) used was not toxic and did not interfere with the assay. Stock solution was prepared by dissolving 1 g of the extract in 1ml of DMSO. Using serial doubling dilution, four different concentrations (10mg/ml, 5mg/ml, 2.5mg/ml and 1.25mg/ml) of the extract was prepared. The antiparasitic effect of the compounds was measured by growth inhibition percentage as described by Carvalho and Krettli(16). The culture media of 1 L of RPMI 1640 liquid media was prepared by dissolving 10.4 g of the powdered RPMI 1640 into 1 L of distilled water and the autoclaving at 121°C for 15 mins. 0.5 mL of the extract solutions (10 mgml⁻¹, 5 mgml⁻¹, 2.5 mgml⁻¹, 1.25 mgml⁻¹) and 0.5 mL RPMI 1640 media were each transferred into their clearly labelled test-tubes. To each concentration of the extract, 0.1 ml of the malaria positive erythrocytes was added and shaken gently to ensure even distribution of the erythrocytes. The test tubes were transferred into a bell jar containing a burning candle. The cover of the bell jar was then replaced until the flame of the candle stopped burning. This supplied about 95 % Nitrogen, 2 % Oxygen, and 3 % Carbon dioxide as described by Trager and Jensen, 1976. The whole set up was transferred into an incubator maintained at 35°C for 24hrs to 48hrs. A control group consisting of culture media and positive erythrocytes (negative control) and culture media positive erythrocytes and anti-malarial agent Artemether (positive control) was also incubated



along with the test concentrations. After 24 h of incubation, a thin smear from test tube was transferred onto clean glass slides and fixed in absolute methanol (CH₃OH) then stained with Giemsa's stain. Each smear was observed under microscope using oil immersion to count the number of infected erythrocytes (16-18).

RESULTS

Phytochemicals of the extracts of *P. guajava* leaves

The qualitative phytochemical analysis to test for the presence of alkaloid in the crude DCM extract showed the presence of alkaloids in the leaves of *P. guajava* plant. The pH of the crude extract which was initially 3.2 was adjusted to 11.2 to enable the efficient extraction of alkaloids.

In vitro anti-malarial assay

Psidium guajava leaves extract was screened for its *in vitro* antimalarial activity against the *P. falciparum* strain using artemether as control. The anti-malarial activity of the extracts was tested after 24 h and 48 h incubation respectively to determine growth inhibition of the parasite. At 24 h the death of some *P. falciparum* was observed at all concentrations of the crude extract with 10 mgml⁻¹ showing the highest death of 6 parasites and 1.25 mgml⁻¹ showing the lowest death 1 parasite. At 48 h the death rate at each concentration increased with 10 mgml⁻¹ still showing the highest death of 9 parasites and 1.25 mgml⁻¹ showing the lowest death of 2 parasites. On average after 48 h death of parasites were observed at all concentrations; 10, 5, 2.5 and 1.25 mgml⁻¹. Whereas, for the standard control (artemether) after 48 h the death of all the parasites were observed at the different concentrations 10, 5, 2.5 and 1.25 mgml⁻¹ (Table 1).

Table 1: Raw data analysis at each concentration activity of the extract and standard control (Artemether) after incubation.

Parasites dead after incubation period	Concentrations of DCM extract mgmL ⁻¹			
	10	5	2.5	1.25
24 h	6	4	3	1
48 h	9	6	5	2
Artemether (control)- All parasites were dead after 48 h at all concentrations				

The percentage elimination at the end of the incubation was determined for all the concentrations of the crude extract (Table 2). The results showed a 58 % elimination of the *P.*

falciparum parasite by the crude leave extract while the standard control (artemether) showed 2 % elimination at the end of the incubation.

Table 2: Anti-plasmodial activity of the extract and standard control (Artemether) against the malaria parasites

	Crude DCM Extract (at all concentrations)	Artemether (Control)
Average number of parasites before incubation	62	62
Average number of parasites after incubation	36	2



Total number of parasites dead after incubation	26	60
Percentage of elimination at the end of incubation. %= $N/N_x \times 100$	58 %	3 %

Where N is the total number of the parasites after incubation and N_x is the total number of the parasites before incubation.

DISCUSSION

The phytochemical analysis of *P. guajava* leaves extract showed the presence of alkaloids which is attributed with possessing some pharmacological activities traditionally observed from the plant. Organic extraction was also carried out based on the physicochemical properties of bioactive natural product(s) of interest by qualitative analysis and by adjusting the pH of the aqueous extract before partitioning with organic solvent. The phytochemical of interest being alkaloids was successfully tested and observed after the pH was adjusted to 11.2, alkaloids are basic in nature with a pH value of 10.5 that possesses high retention factors based on their polarity and mostly appear in the form of neutral molecules when isolated (19).

The crude DCM extract was then subjected to antimalarial screening against *P. falciparum* and artemether as the positive control (Table 1). The Table shows different concentrations of the leaves extract tested against *P. falciparum* at 24 and 48 h after incubation. At all the concentrations parasitic death was observed suggesting that bioactive compound(s) present in the crude extract are anti-malarial agents (20). At 1.25 mgmL⁻¹ the death of the parasites observed was very slow after both 24 and 48 h incubation. From 2.5 to 10 mgmL⁻¹ the number dead parasites gradually increase with their highest death observed after 48 h. From literature alkaloids such as quinines are good antimalarial agents we postulated that an alkaloid was the likely bioactive compound responsible(8).

When the percentage elimination of the extracts was compared with that of the artemether (control) (Table 2) a significant difference in their elimination was observed. Artemether is a potent antimalarial used to treat both complicated and uncomplicated malaria cases but are not recommended during the first trimester of pregnancy(21). Therefore, using artemether as a control was to access the level potency of our leaf extract in relationship to the artemether.

CONCLUSION

The qualitative analysis of *P. guajava* leaves extract showed the presence of the alkaloids. The antimalarial activity of the extract was screened at different concentrations against *P. falciparum* carried out. The results showed that the higher the concentration of the extract the more the antimalarial activity observed. The potency of the bioactive compound is much lower than that of the control (artemether) suggesting *P. guajava* leaves can be used as in the management of malaria and its possibility of it being used during the first trimester.

REFERENCES

1. D. J. Newman, G. M. Cragg, Natural Products as Sources of New Drugs over the Nearly Four Decades from 01/1981 to 09/2019. *Journal of Natural Products* **83**, 770-803 (2020).
2. A. G. Atanasov *et al.*, Natural products in drug discovery: advances and opportunities. *Nature Reviews Drug Discovery* **20**, 200-216 (2021).
3. S. Wachtel-Galor, I. F. F. Benzie, in *Herbal Medicine: Biomolecular and Clinical Aspects*, I. F. F. Benzie, S. Wachtel-Galor, Eds. (CRC Press/Taylor & Francis Copyright © 2011 by Taylor and Francis Group, LLC., Boca Raton (FL), 2011).
4. B. B. Mishra, V. K. Tiwari, Natural products: An evolving role in future drug discovery. *European Journal of Medicinal Chemistry* **46**, 4769-4807 (2011).
5. in *Artemisinin-Based and Other Antimalarials*, L. Guoqiao, L. Ying, L. Zelin, Z. Meiyi, Eds. (Academic Press, 2018), pp. 1-67.
6. Z. Guo, Artemisinin anti-malarial drugs in China. *Acta Pharmaceutica Sinica B* **6**, 115-124 (2016).



7. W. H. Organization, "Guidelines for Malaria 16 October 2023," (World Health Organization, Geneva, 2023).
8. J. Achan *et al.*, Quinine, an old anti-malarial drug in a modern world: role in the treatment of malaria. *Malar J* **10**, 144 (2011).
9. F. Nosten, N. J. White, Artemisinin-based combination treatment of falciparum malaria. *Am J Trop Med Hyg* **77**, 181-192 (2007).
10. S. J. Rogerson, Management of malaria in pregnancy. *Indian J Med Res* **146**, 328-333 (2017).
11. C. O. Obonyo, E. A. Juma, V. O. Were, B. R. Ogutu, Efficacy of 3-day low dose quinine plus clindamycin versus artemether-lumefantrine for the treatment of uncomplicated Plasmodium falciparum malaria in Kenyan children (CLINDAQUINE): an open-label randomized trial. *Malar J* **21**, 30 (2022).
12. P. G. Daswani, M. S. Gholkar, T. J. Birdi, Psidium guajava: A Single Plant for Multiple Health Problems of Rural Indian Population. *Pharmacogn Rev* **11**, 167-174 (2017).
13. A. Adamu, Phytochemical screening of guava leave extract. *International Journal of Pure and Applied Science Research* **12**, 89-95 (2021).
14. J. R. Shaikh, M. Patil, Qualitative tests for preliminary phytochemical screening: An overview. *International Journal of Chemical Studies* **8**, 603-608 (2020).
15. K. Chotivanich, K. Silamut, N. P. Day, Laboratory diagnosis of malaria infection. *Australian Journal of Medical Science* **27**, 11-15 (2006).
16. L. H. Carvalho, A. U. Krettli, Antimalarial chemotherapy with natural products and chemically defined molecules. *Memórias do Instituto Oswaldo Cruz* **86**, 181-184 (1991).
17. W. Trager, J. B. Jensen, Human Malaria Parasites in Continuous Culture. *Science* **193**, 673-675 (1976).
18. M. T. Makler *et al.*, Parasite lactate dehydrogenase as an assay for Plasmodium falciparum drug sensitivity. *Am J Trop Med Hyg* **48**, 739-741 (1993).
19. S. Qiu *et al.*, Natural alkaloids: basic aspects, biological roles, and future perspectives. *Chin J Nat Med* **12**, 401-406 (2014).
20. A. Yadav *et al.*, Antimalarial activity of Psidium guajava leaf extracts. *Int J Sci Res Chemi* **5**, 63-68 (2020).
21. L. Slutsker, R. G. F. Leke, First-trimester use of ACTs for malaria treatment in pregnancy. *The Lancet* **401**, 81-83 (2023).



P092 - CONFIGURATION OF SOLID OXIDE FUEL CELL USING BIOFUEL OBTAINED FROM SUGARCANE BAGGASSE

Audu, Maryam Oyiza^a Afolabi, Eyitayo Amos^{a*}

^a*Department of Chemical Engineering, Federal University of Technology Minna-Nigeria.*

*Corresponding author: E-mail: elizamos2001@yahoo.com Phone: +2348105262842

ABSTRACT

Process configurations for the simulation of Solid Oxide Fuel Cells (SOFCs) fuelled with rich hydrogen streams sourced from sugarcane bagasse was developed for simulation in Aspen Plus. The study determined the pathways for the generation of hydrogen from sugarcane bagasse bearing current advancements and technological enhancements. Pathway for hydrogen production using steam reforming of diluted bioethanol and that of generation of bio-syngas from sugarcane bagasse via gasification were explored. The sourced hydrogen was configured to fuel a solid oxide fuel cell which was informed by recent advancements that enable operation at intermediate temperatures (500 – 750 °C) so as to mitigate high-temperature related challenges that has ravaged the deployments of SOFCs systems for over a decade. Operating at intermediate temperature is preferred as it will result in relatively minor sealing problems, simplified thermal management, faster phases of startup and shutdown, achievement of a higher thermo-mechanical stability of the fuel cell and reduced degradation of both the fuel cell and the components of the system that contains it.

Keywords: *Hydrogen, Bagasse, Solid oxide fuel cell, Bioethanol, Steam reforming, Gasification*

1.0 Introduction

The demand for energy is growing as well as the world population but the fossil fuel consumption is increasing. In order to mitigate the emissions of greenhouse gases, researchers have focused their efforts on renewable energy sources (Yannay et al 2015).

Among agricultural wastes, sugarcane bagasse (SB) is abundant and has the potential to be transformed into energy and chemical feedstock. Bagasse is the fibrous residue obtained after sugarcane juice is extracted. Generally, 280 kg or 30–32% of wet bagasse is produced from 1 t of sugarcane (Rodrigues et al 2003). In many sugar mills, it is used as fuel to generate heat and power for the milling process. A significant amount of bagasse feedstock for biofuels production as it was successfully used to produce bio-ethanol, bio-methane, bio-hydrogen, and bio-butanol. Other bio-products from SB include Xylitol, Organic acids, Xylooligosaccharides, Enzymes etc. Furthermore, SB can be used as adsorbents, briquettes and

remains stockpiled, which is an environmental and socio-economic problem (Lavarack et al 2002).

The conversion of sugarcane to chemical and energy sources is a viable option to considerate for reducing environmental pollution and increasing the economic value of bagasse. SB can be converted in various ways to increase the economic value of sugarcane. These include pyrolysis and hydrothermal methods for producing energy, pulp and paper, chemicals and other products. Hydrothermal treatment is able to convert low-carbohydrate biomass into materials with high-energy content or directly into biofuel.

A recent and extensive review of the applications of SB revealed its suitability in light of the need for energy and environmental sustainability. This establishes SB can be regarded as a sustainable

ceramics, polymer composites, cement and ceramics (Ajala et al., 2021).

Bioethanol fuel has an important role in the field of environmental conservation by mitigating global warming and conserving fossil fuel. It is an alcohol made of carbohydrates through a fermentation process. The production of bioethanol from



biomass or waste is one way to reduce both the consumption of crude oil and environmental pollution (Ajala et. al, 2021).

Hydrogen is a candidate fuel considered as a gradual replacement for traditional fossil fuel with the aim of making energy systems more reliable, cleaner, and effective, thus in turn ensure energy security and environmental sustainability(1). High reactivity of hydrogen at the electrochemical anode triggers the oxidation reaction of hydrogen to yield water as a by-product, which is ecologically more suitable than carbon dioxide (2).

Hydrogen is generated from three main thermo-chemical reforming techniques used in the reformation of hydrocarbons namely partial oxidation, auto-thermal reforming and steam reforming(3). The possibility to exploit diluted bioethanol streams for hydrogen production by steam reforming is recently discussed (Antonio et al., 2017).

Fuel cells are electrochemical devices that efficiently and cleanly change the chemical energy of a fuel into electrical energy without going

through a combustion process with water yielded as the major by-product (4, 5). Fuel cells are grouped according to the operating temperature or the kind of electrolyte in use (6). At low temperature, fuel cells operate with hydrogen as its major fuel whereas at a high temperature range, it operates on carbon monoxide, methane, their mixtures as well as hydrogen. In comparison with conventional multi-step thermo-mechanical process, fuel cells involve a single energy conversion hence resulting into a greater efficiency(4). Recent advancement in research on renewable energy has enlisted fuel cell in the future to be a significant and prospective energy source (7). This is further strengthened by an observation that the utilization of biomass - derived fuel in a fuel cell result to lower cost of operation (8).

2.0 Methodology

This section describes the methods used in the process of data collection to inform the development of configurations of hydrogen fuelled solid oxide fuel cell. An illustration of the steps taken is shown in Figure 1.

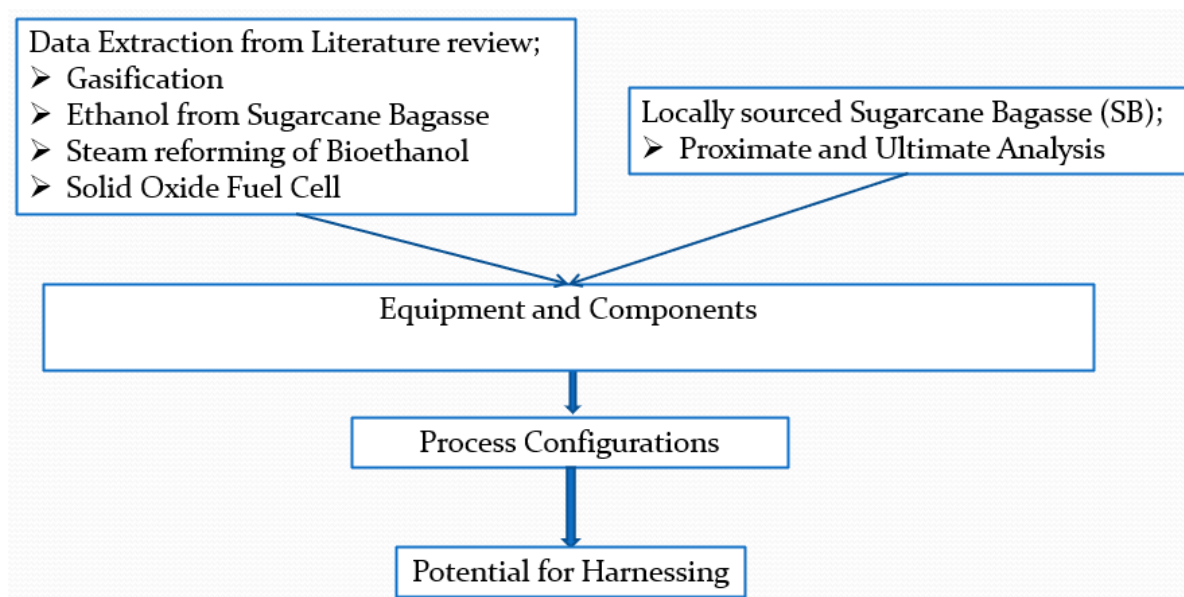


Figure 1: Study methodology

Data Extraction

Data was extracted from literature on advancements in the production of hydrogen from sugarcane bagasse. Also, recent findings on the design and operation of solid oxide fuel cell (SOFC) were

considered. The content analysis of the sugarcane bagasse which was obtained from locally produced brown sweet (Alewa) factory in Bida, Local Government Area of Niger State, Nigeria is presented in Table 1 below.



Table 1: Analysis of locally sourced sugarcane bagasse (Rabiu et al., 2017)

ANALYSIS	WT (%)
Proximate	
Moisture	13.21
Volatile Matter	7.26
Ash	4.80
Fixed Carbon	74.73
Ultimate	
Carbon	48.20
Hydrogen	5.40
Nitrogen	1.60
Sulphur	0.80
Oxygen	44.00
Fibre Content	
Lignin	26.40
Cellulose	33.30
Unicellulose	30.10
Extractives	10.20

The configurations were informed by the following findings from review of literature.

Gasification of bagasse

A circulating fluidized bed gasifier is the most appropriate for sugarcane bagasse since it has (Ku et., al, 2017);

- ❖ low tar content production
- ❖ high carbon and tar conversion rates
- ❖ high heat transfer rates between the fuel and bed material
- ❖ suitability for large capacity systems
- ❖ operating at reaction temperatures ranging between 973K and 1273K and
- ❖ handling outlet syngas temperatures ranging between 873K and 1073K

Ethanol production from sugarcane bagasse

Challenges exist during the critical step in bioethanol production, such as;

- ❖ physicochemical and biological pretreatment
- ❖ enzymatic saccharification.

Critical factors such as reaction temperature, pH, acid concentration are focused to ensure (Prasad et al. 2018);

- ❖ effective delignification
- ❖ inhibitory compound removal with low sugar loss; dilute acid method of pretreatment is the most preferred, and
- ❖ the utilization of simultaneous saccharification and fermentation (SScF)

Hydrogen production from ethanol

- ❖ Catalytic Ethanol Steam Reforming (ESR) is a promising reaction as a sustainable, carbon-neutral hydrogen production process (Ogo and Sekine, 2020).
- ❖ Co-based and Ni-based catalysts are suitable for industrial ESR processes but critical factors affecting its use include;
- ❖ The particle size and oxidation state of the active metal,
- ❖ acid–base and redox properties of the support, and
- ❖ appropriate promoter (such as CeO₂) selection are important factors to minimize coke and by-product formation.

Solid oxide fuel cell

- ❖ Solid Oxide Cell can produce alternatively electric energy in Fuel Cell mode (Afolabi et al., 2021).
- ❖ Advances in the chemistry and processing of materials are enabling a reduction in the



operating temperature of SOFCs in the so-called intermediate temperature region (IT) between 500 and 750°C (Guiseppe and Petronilla, 2018)

- ❖ The use of new materials, which work best at intermediate temperature, involves a series of advantages, such as;
- ❖ minor sealing problems
- ❖ smaller number for Balance of Plant components
- ❖ simplified thermal management
- ❖ faster phases of startup and shutdown
- ❖ achievement of a higher thermo-mechanical stability of the fuel cell and

- ❖ reduced degradation of both the fuel cell and the components of the system that contains it.

3.0 Results and Discussion

First configuration (Gasification)

The configuration presented in Figure 2 expresses the production of hydrogen from sugarcane bagasse through gasification and the resulting syngas was fed to SOFC.

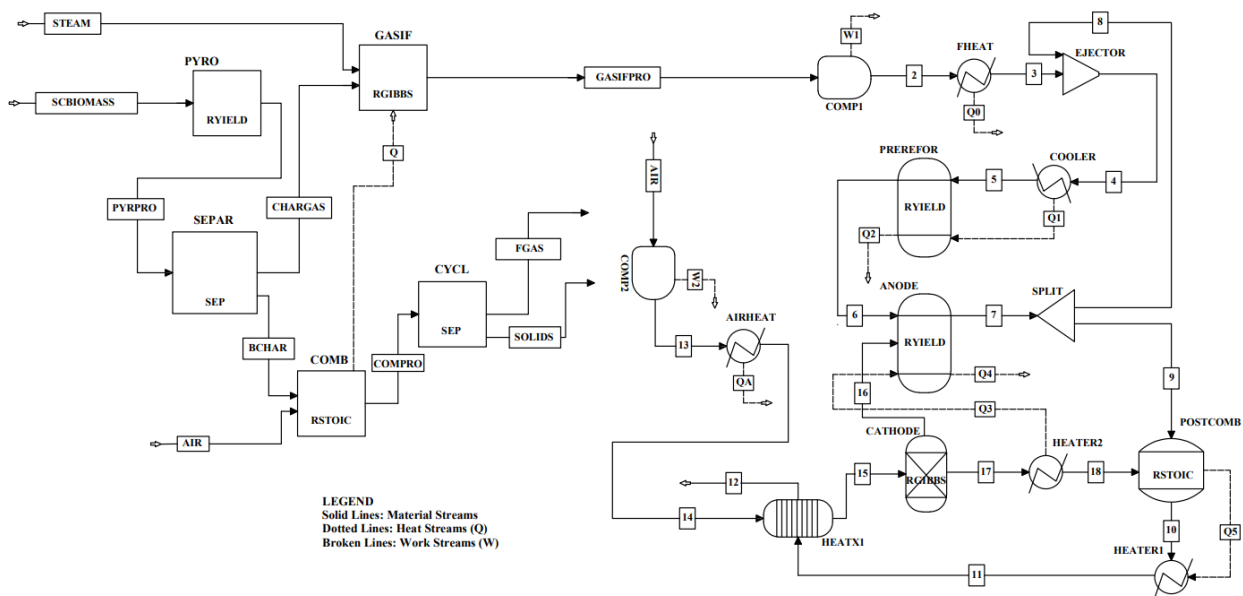


Figure 2: Configuration of syngas fed solid oxide fuel cell

The reactions taking place during the gasification process in a gasifier includes char gasification, Boudouard, methane decomposition, water gas shift reaction and steam reforming. The following assumptions were considered in configuring the gasification process:

- Process is steady state and isothermal
- H₂, CO, CO₂, CH₄, H₂O, tar and char are considered the product of devolatilization
- Spherical and uniform size particle of average diameter throughout the process;
- Char contains carbon and ash
- Pressure drops are neglected
- Heat loss from the reactors and Tar formation are not considered during the process

- Char is considered as impurity free as 100 % carbon and Ash from the biomass is considered as inert, it does not react with other components.

In this configuration, the zero-dimensional and time independent reactions were considered. Given thermodynamic equilibrium model was considered for the configuration, there was no need for reaction kinetics and the reactor hydrodynamics. The stoichiometric and nonstoichiometric methods were used. Minimization of the Gibbs free energy method was employed and the reaction zones were represented by a number of blocks.

The feed stream to the configuration was tagged “SCBIOMASS”, which will be an unconventional



stream requiring proximal and ultanal inputs. The next step was the devolatilization stage which was performed in the block PYR in which the RYield reactor was represented in the configuration. In PYR, the feedstock was transformed from a non-conventional solid into volatiles and char. The yield of volatiles was equal to the volatile content in the fuel according to the proximate analysis (Rabiu et al., 2017). The combustion and gasification of biomass were simulated by a block called GASIF in which the chemical equilibrium was determined by minimizing the Gibbs free energy. The product was passed as a feed to the SOFC section.

The syngas product from gasification process 'GASIFPRO' stream was fed to the 'COMP1' block, preheated in the block 'FHEAT' and its exit entered the 'EJECTOR', where it was mixed with the recycled depleted fuel and the outlet pressure (stream 4) was decreased to slightly above atmospheric pressure and is directed to 'COOLER1'. The two blocks 'COOLER1' and 'PREREFOR' represented the stack pre-reformers. 'COOLER1' sets the pre-reforming temperature, which is calculated by means of a design spec, which varies the temperature of 'COOLER1' until the net heat duty of 'PREREFOR' equals zero, i.e. adiabatic. The gas was cooled simulating the endothermicity of the steam reforming process. The equations configured in the represented stack reformers include steam reforming and water-gas shift reactions. The pre-reformed fuel (stream 6) enters 'ANODE', where the remaining CH_4 is reformed, CO is shifted and H_2 is oxidised.

The stream 'AIR' was fed to 'COMP2', the air compressor and its discharge was preheated in 'AIRHEAT' and its exit stream entered 'HEATX1' where it was heated further by the hot combustion

plenum products. Stream 15 enters the 'CATHODE' block, whose function is to separate out the O_2 required for the electrochemical reaction. The required O_2 was directed to the 'ANODE' block. The temperature of the depleted air (stream 17) is brought up to Top in 'HEATER2'. The heat is supplied by the electrochemical reaction, which was simulated by taking a heat stream (Q3) from 'HEATER2' to 'ANODE'. Stream 7 enters the block 'SPLIT', whose function is to split the stream into a recycle and a stream directed to the combustion plenum. The split fraction is determined by a specified STCR, defined as the molar ratio of steam to combustible carbon. Excess steam as well as increasing the concentration of H_2 and CO_2 inhibits the formation of carbon.

Carbon deposition not only represents a loss in the system but results in deactivation of catalysts and decreases the activity of the anode by clogging the active sites. The depleted fuel and oxidant are fed to 'POSTCOMB' where complete combustion of the remaining fuel occurs. The heat generated is represented by the heat stream Q5, which is fed to 'HEATER1', whose function is to set the combustion products temperature. Finally, the combustion products (stream 11) serve to preheat the incoming air in the 'HEATX1' block.

Second Configuration (Ethanol Steam Reforming)

The configuration in Figure 3 presents the production of ethanol from sugarcane bagasse, the steam reforming of the ethanol to produce hydrogen and the feeding of hydrogen to an intermediate SOFC.



Table 3: Saccharification of Cellulose reactions

Chemical Reaction Equations	Conversion (%)
Cellulose + water \Rightarrow glucose	90
Cellulose + 0.5water \Rightarrow 0.5cellobiose	1.2
Cellobiose + water \Rightarrow 2glucose	95

The co-fermentation process was configured to use a strain, *Z.mobilis* ZM4 (pZB5) which has the ability to ferment both pentose (C5) and hexose

(C6) sugars at the same time (Majidian et al. 2018). The condition for co-fermentation is presented in Table 4 below:

Table 4: Operating Conditions for Co-fermentation

Fermenter Parameters	Values
Total Solids (wt %)	0.198
Insoluble Solids (wt %)	0.051
Temperature ($^{\circ}$ C)	32
Pressure (atm)	1
Residence Time (days)	1.5
Inoculum level	10 vol% of production vessel size
Batch time	24h
Fermenter turnaround time	12h
Number of trains	2
Number of fermenter stages	5
Maximum fermenter volume	757 m ³
Corn steep liquor (CSL) loading (wt %)	0.5
Diammonium phosphate (DAP) loading	0.65 g/L Fermentation broth

The chemical reactions considered in the saccharification of cellulose process are presented in Table 5. The reaction kinetics for the SSCF were adapted from literature (Hari Krishna et al, 2001). The reactant for the biochemical changes were

commonly glucose and xylose sugars. The process of converting from reactant to product; ethanol and other byproducts, was with the help of *Z.mobilis* ZM4 (pZB5), which is a gram-negative bacterium (Singh and Harvey 2009).

Table 5: Co-fermentation biochemical reactions (Singh and Harvey 2009)

Chemical Reaction Equations	Typical Conversion (%)
Glucose	
Glucose \Rightarrow 2EtOH + 2CO ₂	90
Glucose + 2water \Rightarrow 2glycerol + O ₂	0.5
Glucose + 2CO ₂ \Rightarrow 2succinic acid + O ₂	0.6
Glucose \Rightarrow 3acetic acid	1.5



0.55 Glucose ==> 0.33yeast + 1.11water + 0.45CO2	2
Xylose	
3Xylose ==> 5EtOH + 5CO2	85
3Xylose + 5water ==> 5glycerol + 2.5O2	0.3
Xylose + water ==> xylitol + 0.5O2	4.6
3Xylose +5CO2 ==> 5succinic acid + 2.5O2	0.9
2Xylose ==> 5acetic acid	1.4
0.66Xylose ==> 0.33yeast + 1.11water + 0.45CO2	4

The resulting ethanol in the form of fermentation broth from the co-fermentation process was introduced as feed to the distillation section. The broth was filtered in “Beer column” so as to separate unconverted solid and lignin which are sent for combustion. The CO₂ in the feed was sent to the “Scrubber” while the liquid production of the “Beer column” was sent to a second column tagged “Rectification column” in a bid to increase concentration >90%. The bottoms of the “Rectification column” was sent for the production of cellulase.

The ethanol steam reformer (ESR) was configured as a multitubular reactor, with the ESR catalyst inside the tubes and hot gases deriving from ethanol combustion in the shell side. A burner was configured as external unit to compute the heating of the ESR reactor. The product of the ESR reactor was first purified from CO in a high temperature water gas shift reactor (HTWGS), followed by a low temperature one (LTWGS) and a methanator (METH). The heat available through cooling of the outlet of the HTWGS reactor, as well as the heat generated by the reactor was used to preheat the feed through proper heat exchangers. The same holds for heat recovery from the LTWGS and METH blocks. Final cooling of the reformat stream to allow conditioning the feed for the separator B3 takes place. Condensed water was then separated. The gaseous product was sent to the intermediate SOFC. The combustion products (stream 71) serve to preheat the incoming air in the ‘HEATX1’ block and the ethanol/water feed mixture.

4.0 CONCLUSIONS

Process configurations for the generation of hydrogen from sugarcane bagasse through gasification and ethanol steam reforming were explored. The resulting hydrogen steam was configured to fuel an intermediate Solid Oxide Fuel Cell. A process simulation of the configurations using Aspen Plus or Aspen HYSYS is

recommended in a bid to inform process design. However, the operating conditions must be informed by recent findings that guided the conceptualization of the configurations.

References

1. Din, Z. U., and Zainal, Z. A. (2015). Biomass integrated Gasification SOFC systems Technology overview. *Renewable and Sustainable Energy Reviews* 53, 1356-1376. <http://dx.doi.org/10.16/j.rser.2015.09.013>.
2. Humbird, D. e. (2011). Process design and economics for biochemical conversion of lignocellulosic biomass to ethanol: dilute-acid pretreatment and enzymatic hydrolysis of corn stover. National Renewable Energy Laboratory, Golden, co.
3. Hussain, S. (2009). A Numerical Evaluation of the Design of an Auto thermal Reformer for the On-board Production of Hydrogen from Iso-octane. M.Sc. Thesis, Department of Mechanical and Materials Engineering, Queen’s University Canada. 3- 8.
4. Koster, V. (2012). How do fuel work. Weinhein. Retrieved from <http://www.chemistryviews.org/details/education/1458465>.
5. McGlocklin, K. H. (2006). Economic Analysis of Various Reforming



- Techniques and Fuel Sources for Hydrogen Production. M.Sc Thesis University of Alabama. 6, 24. Retrieved from <http://pdfs.semanticscholars.org/.../fe7580e5b0e1af1ed140bd035eeef594C77a.pdf>
6. Nahar, G., and Dupont, V. (2012). Recent Advances in Hydrogen Production via Auto-thermal Reforming Process (ATR). A Review of Patents and Research Articles. *Recent Patents on Chemical Engineering*, 6 (1), 8 - 421. <http://dx.doi.org/10.2174/2211334711306010003>
 7. Ramadhani, F. M., A Hussain, H. Mokhlis and S. Hajimolana (2017). Optimization Strategies of Solid Oxide Fuel Cell (SOFC) Application: *Renewable and Sustainable Energy Reviews*, 76, 460-484, <http://dx.doi.org/10.1016/j.rser.2014.03.052>.
 8. Wiyaratn, W. (2010). Review on Fuel Cell Technology for Valuable Chemicals and co-generation. *Engineering Journal*, 14(3), 28. doi:10.4186/ej.2010.14.3.1.
 9. Suleiman, B., Abdulkareem A. S., Musa, U., Mohammed, I. A., Olutoye, M. A., and Abdullahi, V. I. (2016). Thermo-economic Analysis of Proton Exchange Membrane Fuel Cell. *Energy Conversion and Management* 117, 228-244. <http://doi.org/10.1016/j.enconinman-2016.03.033>.
 1. K. McGlocklin, Auburn University, (2006).
 2. S. Hussain, Queen's University, Kingston, Ontario, Canada (2009).
 3. B. Suleiman *et al.*, Thermo-economic analysis of proton exchange membrane fuel cell fuelled with methanol and methane. *Energy Conversion and Management* 117, 228-240 (2016).
 4. Z. Ud Din, Z. A. Zainal, Biomass integrated gasification-SOFC systems: Technology overview. *Renewable and Sustainable Energy Reviews* 53, 1356-1376 (2016).
 5. ChemistryViews. (WILEY-VCH Verlag GmbH & Co. KGaA, Weinheim, 2012), vol. 2023.
 6. W. Wiyaratn, Reviews on Fuel Cell Technology for Valuable Chemicals and Energy Co-Generation. *Engineering Journal* 14, (2010).
 7. F. Ramadhani, M. A. Hussain, H. Mokhlis, S. Hajimolana, Optimization strategies for Solid Oxide Fuel Cell (SOFC) application: A literature survey. *Renewable and Sustainable Energy Reviews* 76, 460-484 (2017).
 8. G. Nahar, V. Dupont, Recent advances in hydrogen production via autothermal reforming process (ATR): a review of patents and research articles. *Recent Patents on Chemical Engineering* 6, 8-42 (2013).
 9. D. Humbird *et al.*, *Process Design and Economics for Biochemical Conversion of Lignocellulosic Biomass to Ethanol: Dilute-Acid Pretreatment and Enzymatic Hydrolysis of Corn Stover*. (2011).



P093 - A REVIEW ON SUSTAINABLE LOW-DENSITY POLYETHYLENE (LDPE) WASTE MANAGEMENT: POSSIBILITIES FOR NIGERIA

Sokoga Victor ATEGBE^{1*}, Johnson Nsuhoridem Aniekan², Musa Aminat Ummih³, Maryam Nasir⁴, Jibrin Abdulkadir⁵, Simon Istifanus Adamun⁵, Opeoluwa Olusola Fasanya⁵, Elizabeth Winful⁵, Bridget Nwobi⁵, Mahmood Abdullahi⁵, Victor Ochigbo⁵

Department of Chemical Engineering, Ahmadu Bello University Zaria

Department of Biochemistry, Ahmadu Bello University Zaria

Department of Microbiology, Ahmadu Bello University Zaria

Department of Microbiology, Kaduna State University, Kaduna

Industrial and Environmental Pollution Department, National Research Institute for Chemical Technology, Zaria

Corresponding author email: ategbesokoganevdan@gmail.com

ABSTRACT

This study addresses the pressing issue of LDPE waste management in Nigeria, highlighting the adverse environmental consequences resulting from improper disposal and the lack of essential data regarding plastic pollution. The research explores various plastic waste management practices, including advanced thermal, chemical, and biological processes, with a focus on LDPE recycling through dissolution, precipitation, and pyrolysis methods. The study underscores the urgent need for comprehensive waste management strategies, recycling initiatives, increased public awareness, and effective policy measures to promote sustainability alternatives. Additionally, it outlines the significant challenges currently faced in LDPE recycling in Nigeria, including inadequate infrastructure, informal practices, limited awareness, economic viability concerns, and quality control issues. The study also delves into effective recycling techniques, such as sorting, mechanical recycling, and chemical recycling, showcasing their roles in enhancing recycling rates and offering solutions to address LDPE waste challenges. In conclusion, the research advocates for ongoing research and development efforts to enhance recycling methods, infrastructure, and sustainability practices, ultimately contributing to a more responsible and sustainable LDPE waste management approach in Nigeria and beyond.

KEYWORDS

INTRODUCTION

Plastics are a diverse group of synthetic materials with a foundation in polymer chemistry. These materials are primarily composed of long polymer chains created through the process of polymerization. The specific monomers used in this process, as well as the conditions of polymerization, determine the type and properties of the plastic produced. The versatility of plastics is a key attribute, as their properties can be tailored to a wide array of applications thus making plastics an indispensable part of everyday life. Plastics can be lightweight or rigid, durable and resistant to corrosion, electrically insulating, and even transparent. The incorporation of various additives like plasticizers, stabilizers, colorants, and fillers further enhances their utility. However, this

versatility comes with environmental concerns, as the persistence of plastic waste in the environment has raised issues of pollution and sustainability. Addressing these concerns has become a critical focus for the ongoing development of plastics and their responsible use in a rapidly changing world.

In Nigeria, plastic consumption and invariably waste generation has increased steadily in tandem with world plastic consumption rates. As of 2020, It was estimated that 20% of the total solid waste generated in Nigeria is comprised of plastics(1). This amounts to approximately 8.4 million tonnes per annum which is composed of short life products such as bottles and water sachets amongst others(2). On the African continent, Egypt, Nigeria and South Africa were the highest importers of plastics as well as the highest ranking countries for mismanaged plastic waste(3). In Nigeria there is



difficulty finding harmonized data with regards to the composition of plastic waste generated.

LDPE (low density polyethylene) is a thermoplastic polymer is composed of carbon and hydrogen atoms. Its chemical structure consists of repeating units of ethylene, which contain two carbon atoms (C_2H_4). Carbon forms the backbone of the polymer chain, and hydrogen atom are bonded to the carbon atom in the ethylene monomers creating the CH_2 along the polymer chain, they are linked together through covalent bonds to form the long chain of polyethylene polymer. It has low density and high degree of branching, they contain additives such as plasticizers, stabilizers and pigment which can affect its properties and behaviour during biodegradation, it is known for its flexibility, durability and also resistance to moisture making it widely used for our everyday products such as packaging materials and end up as litters (4).

LDPE pollution in Nigeria is mostly caused by improper disposal and management of LDPE waste. overtime LDPE waste can breakdown into micro plastic which can be ingested by aquatic organisms, it causes detrimental effect on the environment including soil, water contamination blockage of drainage and also harm to wild life (5).

Plastic waste is managed through practices like open air burning, dumping and landfilling (6). There is also more advanced method such as thermal, Chemical and biological processes which are used for treatment and utilization of plastic, although it leads to emission of greenhouse gases, noxious fumes and toxins (6). LDPE can be recycled through dissolution or precipitation method which involve dissolving the polymer in a solvent and reprecipitating it in a non-solvent. Pyrolysis is another thermochemical recycling technique that can be used to recycle LDPE which involve heating in the absence of oxygen (7).

Many developed and developing countries are improving their approaches to plastic waste disposal, collection and recycling of plastic waste into valuable materials such as carbon nanomaterials, polymeric composite materials, chemicals, and plasma conversion etc. (2).

In Nigeria a country around 186million inhabitants theirs a notable lack of data regarding the use of plastic materials in urban areas and management of recycling plastic causes immediate and future risk in the environment (2).

Addressing LDPE pollution in Nigeria require comprehensive waste management strategies, recycling initiatives, public awareness, and policy measures to reduce plastic use and promote sustainability alternatives on long and short term impact on human health, safety and environment in Nigeria (2).

CURRENT CHALLENGES IN LDPE RECYCLING IN NIGERIA

Recycling low-density polyethylene (LDPE) plastic materials has historically been less prevalent compared to other commonly consumed materials like glass, paper, ceramics, and aluminium. This is due to the inherent complexity of LDPE recycling processes, which encompass sorting, disposal, distribution, and usage stages (8).

Nigeria currently faces numerous challenges in the recycling of Low-Density Polyethylene (LDPE) materials. The foremost issue is the lack of adequate recycling infrastructure, which encompasses the absence of recycling facilities, organized collection systems, and efficient transportation networks for recyclable LDPE waste. Without the essential infrastructure in place, the effective collection, processing, and recycling of LDPE materials remain formidable challenged (6).

The recycling sector in Nigeria remains predominantly informal, characterized by numerous small-scale recyclers operating in an unregulated manner. This informality often leads to suboptimal recycling rates, as these entities lack the necessary resources and technology for efficient LDPE recycling (6).

Limited public awareness and education regarding the significance of recycling and proper LDPE waste disposal continue to pose significant obstacles. Without widespread awareness and education initiatives, it remains difficult to encourage individuals and businesses to participate actively in recycling programs (8–10).

Furthermore, Nigeria still grapples with the absence of comprehensive government policies and regulations supporting and promoting recycling. The government's role in regulating the recycling industry and creating a conducive environment for recycling initiatives remains minimal in many instances (11).

Market demand for products made from recycled LDPE materials remains low, as businesses remain hesitant to use them due to concerns about quality



and consistency (8). This hesitation is influenced by factors such as the quality of collected LDPE, sorting processes, and doubts regarding the viability of recycled materials.

Inefficient waste management practices, including improper disposal and littering, continue to contribute to the accumulation of LDPE waste in the environment, exacerbating recycling challenges. Additionally, limited investment in research, development, recycling technology, and equipment hinders the growth of the LDPE recycling industry (12).

Quality control and contamination also persist as issues, as maintaining the purity and quality of recycled LDPE materials can still be compromised by contamination from other materials and improper sorting processes (13, 14). Moreover, Nigeria's vast size and sometimes inadequate transportation infrastructure continue to pose logistical challenges in collecting and transporting LDPE waste to recycling facilities, particularly in remote or underserved areas.

Finally, the economic viability of LDPE recycling remains a concern, as the cost of recycling LDPE materials sometimes exceeds the market value of the resulting recycled products, making it financially challenging for recycling businesses to thrive (12).

Addressing these challenges continues to require a multifaceted approach involving government intervention, public awareness campaigns, investment in recycling infrastructure, and collaboration among various stakeholders. It is essential for ongoing efforts to focus on improving the LDPE recycling landscape in Nigeria and addressing these challenges to create a more sustainable and environmentally responsible waste management system.

EFFECTIVE RECYCLING TECHNIQUES FOR LDPE WASTE

LDPE plastic waste can be recycled through chemical, mechanical, or thermal methods. Initially, LDPE plastic waste is subjected to sorting, often facilitated by various technologies such as fluorescence, electrostatics, infrared, floatation, and spectroscopy (8).

Sorting

The difficulty and cost of sorting LDPE based on its properties hinder recycling. LDPE's covalent C-C

bonds demand high-temperature and catalyst-intensive decomposition. Olefin-based plastics like LDPE suffer from low recycling rates due to their economic inferiority. Yet, over 50% of plastic waste comprises olefin-based plastics, while LDPE dominates (13).

Various sorting methods are used in LDPE and plastic recycling, each with unique advantages and limitations. These systems contribute significantly to recycling efforts, providing options for different scenarios. Following sorting, plastics can be repurposed for valuable materials or energy generation. (15) describes major methods of sorting. Thermal-adhesion sorting which relies on temperature differences but struggles with thermosetting plastics; Float-sink sorting separates by specific gravity but faces challenges with minimal differences; Dry zig-zag sorting uses air flow and shares similar limitations. Electrostatic sorting is cost-effective but can only sort one plastic from two. Froth flotation sorting relies on hydrophobicity and handles plastics with specific gravity differences below 0.1 but needs surface treatment. NIR (near infrared) spectra sorting identifies and separates mixed plastics but comes with higher equipment costs.

(16) introduced a novel model based on seven parameters for waste segregation and management. This model aimed to enhance recyclability rates, reduce environmental impact, and facilitate direct communication between recyclers and waste generators. Compared to other methods, the proposed model demonstrated higher recyclability rates, positioning it as an effective waste management and recycling solution.

Automatic waste collection systems, including RFID (Radio-Frequency Identification) technology and IoT (Internet of Things), can improve waste collection and sorting (14). RFID-enabled trucks weigh bins and use RFID tags for household identification. IoT and wireless sensor networks enhance monitoring, utilizing low-power sensors, cloud computing, and machine learning. Energy-autonomous IoT-based waste management systems offer smart interfaces. Recycling methods include source separation and centralized sorting facilities like MRFs (Materials Recovery Facility) and MBT (Mechanical Biological Treatment) plants. AI-based sorting uses sensors and cameras for accurate material separation. Tracer-based sorting (TBS) with fluorescent markers enhances purity. Blockchain technology facilitates payments, rewards, and waste tracking, promoting recycling



and circular economy practices. Combining IoT, AI, and blockchain drives innovation in waste management. Technologies like RFID tags in packaging improve material sorting but face cost and contamination issues. CPS, blockchain, and IoT integration offer new opportunities (14). Sorting performance relies on indicators like recovery rates, product quality, polymer quality, and diversity indexes for recycling optimization.

The value of recycled plastic depends on the end product, and sorting and recycling methods have different costs based on waste volume. Coordinating these strategies is vital for efficient plastic recycling as a renewable energy source, improving economic viability, and reducing environmental harm from landfilling and incineration.

Mechanical Recycling

Mechanical recycling is a common approach, involving processes like shredding and grinding, although it is often deemed less efficient than incineration due to the intricate nature of LDPE waste mixtures (8). Nevertheless, mechanical recycling remains the prevailing method due to its speed and efficiency.

Products that can be created through the mechanical recycling of low-density polyethylene (LDPE) include plastic bags and films, plastic lumber, playground equipment, park benches, plastic pallets, trash cans, outdoor signage, traffic cones, garden hoses, drip irrigation tubing, drainage pipes, trash bags, plastic buckets and containers, shipping envelopes, car parts like underbody shields and wheel arch liners, and synthetic fibers for clothing and textiles. These applications demonstrate the versatility of LDPE in contributing to a more sustainable and circular economy by repurposing this plastic material into a wide range of useful items while reducing environmental waste.

Mechanical recycling (MR) is a crucial aspect of sustainable plastic waste management, encompassing primary, secondary, tertiary, and quaternary recycling stages (17). Primary recycling aims for plastics to retain their original properties, secondary recycling accepts some property loss, tertiary recycling focuses on chemical component recovery, and quaternary recycling extracts energy from plastic waste. Various techniques like sink-float flotation, melt filtration, and sorting methods remove contaminants during MR (14). After sorting, plastics undergo grinding and remelting

while preserving polymerization energy for high-quality recycled materials. Challenges include hazardous additives, polymer degradation, and market barriers. Achieving high-quality recycled plastic and fostering market demand are key goals for MR's sustainability and growth. Ongoing research and innovation are essential for its advancement.

Plastics in Construction

The construction industry, a cornerstone of national economies, has an opportunity to enhance sustainability by incorporating LDPE waste materials into construction practices (8, 18). The principles of a circular economy aim to maintain product efficiency and value throughout their lifecycles while reducing the environmental burden of LDPE plastic waste. Examples include utilizing recycled LDPE waste materials to create durable wall and floor tiles or incorporating LDPE aggregates into construction materials such as self-consolidating concrete (SCC) to enhance their properties (19). By converting it into granules, LDPE can be integrated into concrete mixes, effectively substituting some of the sand content. This not only results in lightweight but also durable concrete (20). LDPE's unique characteristics, such as its low density and specific surface properties, make it well-suited for this purpose. This innovative approach aligns with circular economy principles, promoting sustainability by reducing waste and conserving resources. Moreover, LDPE's versatility allows it to function as a binder, aggregate, or fiber in cement-based composites, unlocking a multitude of construction possibilities (8, 19–21). This not only addresses waste management challenges but also tackles the problem of resource depletion in the construction sector.

Concrete, a major construction material, has substantial environmental impacts and CO₂ emissions. (22) showed that enhancing Recycled Waste Plastic (RWP) recyclability in cement using 2–4% EVA and 1% nS improves compatibility. EVA-nS (Ethylene-Vinyl Acetate and nano-silica) improves RWP recyclability, pseudo ductility, and reduces strength reductions (>4% in compressive and >2% in flexural strengths). This is due to EVA's elastic polymeric films formed when reacting with water and a more porous microstructure. The study concludes that EVA-nS enhances RWP recyclability and waterproofing, positively impacting microstructure by reducing porosity by 25% through nanofilling. 3D I-XCT images demonstrate EVA's air-entraining effect, aligning



with prior research (22). Future work should explore specific transport mechanisms and engineering parameters using contrast-enhancement agents like Cesium Iodide (CsI) to further improve RWP cementitious composites.

Incorporating LDPE waste and stone dust into composite concrete improves its mechanical strength but increases water absorption, making it more vulnerable to water damage. The ideal mix is 30% LDPE waste and 40% stone dust, offering a greener construction option (21).

The utilization of waste plastics, both thermoplastics and thermosets, as modifiers for asphalt mixtures presents a promising avenue, albeit with challenges related to their high melting temperatures and storage stability (23). Recycling methods vary, with mechanical-physical approaches commonly employed for thermoplastics, while chemical treatments like aminolysis enhance their utility. For waste thermosets, mechanical processing into fine powders remains the primary recycling solution.

Plastic Composites

The addition of waste plastic generally enhances the strength and durability of asphalt binders and mixtures, but the degree of improvement depends on factors such as the method of incorporation, plastic dosage, and chemical nature. Plastics with low melting points are suitable for wet mixing, while high melting point plastics are better for dry mixing. Environmental concerns include fume emissions during construction, with factors like temperature and wind speed influencing their impact (24). Additionally, leaching of contaminants from waste plastics raises health and environmental risks. A comprehensive life cycle assessment (LCA) is crucial to evaluate the social, environmental, and economic aspects of incorporating waste plastics into asphalt mixtures, guiding optimal application methods. Successful pilot projects worldwide demonstrate the feasibility of large-scale implementation, offering a viable recycling outlet for waste plastics while addressing the challenges and concerns associated with their use in asphalt pavements.

The study by Priyantha and Sampath (25) investigated waste-based composites (WBC) using banana stalk fibers and waste low-density polyethylene (LDPE) as a sustainable solution for waste management. Banana fibers, both pre-treated with a 5% NaOH solution (mercerized) and

untreated, were incorporated into LDPE matrices at varying weight percentages. The study evaluated WBC properties through density, uniaxial tensile, and water absorption tests. The results indicated that banana fiber reinforcement improves density, Young's modulus, yield stress, maximum stress, resilience modulus, and water absorption capacity while reducing yield strain, failure strain, and toughness modulus compared to unreinforced LDPE sheets. Optimal fiber additions are found to be 20% for pre-treated fibers and 15% for untreated fibers, with mercerization positively influencing WBC characteristics. This research demonstrated the potential of WBC with banana fiber and waste LDPE as a sustainable waste management solution, enhancing physical and mechanical properties.

Yalwaji and co-workers(26) introduced green composites by combining recycled low-density polyethylene (RLDPE) with Egg Shell Nanoparticles (ESp) for engineering applications. Notably, adding 10% ESp to RLDPE led to a 68% increase in tensile strength, with 52% and 19% enhancements in flexural strength and hardness at 12% ESp additions, alongside a slight reduction in impact energy. The research highlighted the potential of ESp to improve the mechanical properties of RLDPE composites, supported by findings from previous studies, and a regression model validated the tensile strength results.

Chemical Recycling

Chemical recycling of Low-Density Polyethylene (LDPE) is a process that involves the transformation of LDPE plastic waste into its constituent monomers or other valuable chemicals. This method typically starts with depolymerization, breaking down LDPE into simpler compounds through processes like pyrolysis, hydrolysis, or catalytic cracking (17, 27). Pyrolysis, for instance, uses high temperatures in the absence of oxygen to disintegrate LDPE into smaller hydrocarbon molecules, while hydrolysis relies on water to cleave polymer chains. The resulting chemicals can serve as feedstock for various chemical synthesis processes, enabling the production of new plastics or other chemical products.

LDPE chemical recycling holds promise for reducing the environmental impact of plastic waste by diverting it from landfills and incineration. However, it faces challenges such as the need for specialized equipment and addressing contamination issues. Ongoing research and development efforts aim to enhance the efficiency



and cost-effectiveness of LDPE chemical recycling methods, contributing to a more sustainable approach to plastic waste management.

Pyrolysis of LDPE using Fly Ash Catalyst

The utilization of thermo-chemical processes, specifically catalytic pyrolysis, offers a promising avenue for converting waste plastics, such as low-density polyethylene (LDPE), into valuable fuels and chemicals. This approach by (28) employs fuel oil fly ash as an effective and cost-efficient catalyst, demonstrating its potential in enhancing the production of kerosene, CH₄, H₂, and valuable hydrocarbons from LDPE waste. The process also yields a solid char product. Thorough preparation of the LDPE feedstock and the use of a carefully designed reactor setup contribute to controlled experimental conditions. This catalytic LDPE pyrolysis not only offers a sustainable waste management solution but also promotes energy production and supports a circular economy, aligning with environmental conservation goals. The resulting pyrolysis oil exhibits properties comparable to diesel, making it a valuable product for various applications.

Pyrolysis of LDPE using Table Salt Catalyst

Shaker *et. al*(29) introduced an innovative chemical recycling approach using table salt (NaCl) as a catalyst for mixed and metallized plastics, focusing on a polyolefin blend resembling common plastics found in US municipal solid waste. Pyrolysis experiments conducted at various conditions demonstrated that NaCl-assisted pyrolysis was highly efficient, achieving a 100% conversion of the polyolefin blend into oil (86%) and gas (14%) products, surpassing the performance of expensive Pt catalysts. When applied to metallized films, NaCl contributed to a pyrolysis product comprising 84% oil and gas, which increased to 91% when used with Pt/carbon catalyst. This discovery presents a transformative opportunity for cost-effective and efficient chemical recycling, potentially revolutionizing the processing of mixed plastics and metallized film waste into valuable hydrocarbon products and enhancing the sustainability of plastic recycling. Further research is underway to expand the applicability of table salt to diverse waste streams.

Pyrolysis of LDPE using Zinc Oxide as Catalyst

Efforts to address the challenge of reversing polymerization in LDPE, have led to the utilization

of catalytic pyrolysis with zinc oxide (ZnO) as a catalyst. LDPE-based materials are globally prevalent and generate significant waste, making methods for converting them into valuable products highly advantageous. Rajan *et al* (27) demonstrated that catalytic pyrolysis, as opposed to thermal pyrolysis, improved oil yield, with 0.6 g of ZnO identified as the optimal dosage for a 50 g batch of LDPE waste. The process achieved a 67.30% conversion of plastic into oil, but further optimization is required to reduce wax and gas production and increase efficiency to around 90%. Additional investigations are needed regarding pyrolysis oil purification, its performance in internal combustion engines, and detailed chemical analysis of oil fractions to identify potential applications. Exergy analysis indicated enhanced process efficiency with ZnO compared to other catalysts, warranting further temperature-based experiments for validation. This research presents a promising approach to addressing LDPE waste and converting it into valuable resources.

Chemical Upcycling

Alali *et al* (30) focused on the upcycling of LDPE plastic waste into valuable chemicals, specifically alkyl aromatics. LDPE plastic waste poses significant environmental challenges when incinerated or buried. Traditional depolymerization methods for recycling LDPE often demand substantial energy consumption. But this study proposes a more energy-efficient solution by employing controlled partial depolymerization, which transforms LDPE waste into high-quality products at temperatures around 400 °C. The plant design outlined in this study optimizes energy utilization, process efficiency, and product quality, making it a sustainable approach to managing LDPE plastic waste and reducing environmental pollution. The project aims to combat LDPE plastic pollution while simultaneously creating value from LDPE waste, offering eco-friendly alternatives for various applications.

Performance Analysis of LDPE in Gasification Process using MCDM Techniques

Hasanzadeh and co-workers (31) analysed the performance analysis of plastic wastes in gasification processes using Multi-Criteria Decision-Making (MCDM) techniques. Specifically, Technique for Order Preference by Similarity to Ideal Solution (TOPSIS) and Grey Relational Analysis (GRA) were employed, supplemented by a comprehensive sensitivity



analysis. The findings revealed that LDPE demonstrated the most promising performance in air gasification exhibiting the highest lower heating value of syngas and favourable outcomes in terms of cold gas and exergy efficiencies. Both TOPSIS and GRA techniques concurred on LDPE's superiority in the context of air gasification. However, the selection of the optimal plastic waste for steam gasification proved to be more complex. TOPSIS suggested high-density polyethylene (HDPE), while GRA favoured LDPE as the preferred feedstock. Sensitivity analyses further underscored LDPE as the top choice for air gasification, while for steam gasification, LDPE and HDPE emerged as competitive options. These findings provide valuable insights into LDPE's performance in both air and steam gasification processes, aiding in the selection of the most suitable feedstock based on MCDM techniques. Despite some limitations, this study contributes significantly to advancing knowledge about LDPE's potential in gasification and its environmental benefits.

In the comparative analysis of thermochemical technologies for low-density polyethylene (LDPE) waste depolymerization, including gasification, hydrothermal liquefaction (HTL), pyrolysis, hydrogenolysis, and hydrocracking by Kots *et al.*, (32), several key findings and recommendations were identified. Notably, technologies that produced higher-value products, such as olefins for lubricant oils, were deemed more profitable. Increasing the selectivity of catalytic processes was highlighted as a means to enhance economics by generating more high-value products and reducing separation costs, necessitating further research to improve catalyst stability and selectivity. Plant scale was found to play a pivotal role, with even modest-scale facilities demonstrating profitability for value-added products. Pilot plants were deemed essential for demonstrating and de-risking technologies. Effective waste management logistics, particularly waste collection and sorting, significantly influenced the economics of plastic recycling. Challenges and opportunities in catalysis were identified, including the need to reduce reactor costs, eliminate Precious Group Metals (PGMs), and lower hydrogen pressure. In terms of environmental considerations, hydrogenolysis and hydrocracking were found to be more environmentally friendly in terms of CO₂ emissions, followed by pyrolysis. Reducing nitrogen use in pyrolysis and exploring alternative heat sources were suggested to further decrease

emissions, with electrification as a potential avenue. Overall, these findings emphasized the importance of value-added product generation, product selectivity, plant scale, waste management logistics, and environmental considerations in advancing LDPE waste depolymerization technologies, highlighting the need for continued research and development efforts in this field.

Suitability for implementation in Nigeria.

In Nigeria, the adoption of effective recycling techniques for Low-Density Polyethylene (LDPE) waste can have significant real-life applications. Implementing effective LDPE waste recycling strategies in Nigeria is essential to tackle the growing problem of plastic waste. Leveraging advanced sorting technologies, such as fluorescence, electrostatics, and spectroscopy, can improve the efficiency of LDPE waste segregation, making the recycling process more cost-effective. Automation through RFID-enabled waste collection systems and IoT-based sensors streamlines waste management, particularly in urban areas. Centralized sorting facilities like Materials Recovery Facilities (MRFs) and Mechanical Biological Treatment (MBT) plants can enhance the purity and recovery rates of LDPE plastics. Integrating block chain technology for waste tracking and rewards can incentivize participation in recycling.

Nigeria's growing construction sector can benefit from incorporating LDPE waste materials into construction practices. By converting LDPE into granules and integrating it into concrete mixes, construction companies can create lightweight yet durable concrete. This innovative approach not only addresses waste management challenges but also tackles resource depletion issues in the construction sector. Additionally, LDPE's versatility allows it to serve as a binder, aggregate, or fiber in cement-based composites, unlocking a multitude of construction possibilities. By promoting the sustainable use of LDPE waste in construction, Nigeria can reduce its environmental footprint, conserve resources, and foster a more circular and eco-friendly construction industry.

Furthermore, promoting the use of LDPE in chemical recycling can create a sustainable circular economy, reducing environmental harm and enhancing economic viability. Collaboration, regulation, and community engagement are key components of a comprehensive approach to



address LDPE waste in Nigeria, fostering a cleaner and more sustainable environment.

CONCLUSION

This review casts a spotlight on the urgent and critical issue of LDPE waste management in Nigeria, unveiling the harsh environmental consequences that result from improper disposal practices. It serves as a clarion call for immediate and comprehensive action: the development of waste management strategies, the implementation of recycling initiatives, the amplification of public awareness, and the enforcement of effective policy measures that foster sustainable alternatives. Amidst the formidable challenges posed by insufficient infrastructure, informal recycling practices, and economic viability concerns, this review also offers a glimmer of hope through innovative recycling techniques, including sorting, mechanical recycling, and chemical recycling. These methods hold the key to elevating recycling rates and tackling the LDPE waste predicament. As we march forward, it becomes paramount to channel resources into further research and development, refining recycling methods, enhancing infrastructure, and bolstering sustainability practices. In essence, this study is a pivotal milestone in the pursuit of responsible and sustainable LDPE waste management practices in Nigeria and beyond, safeguarding our environment and illuminating the path toward a greener, more sustainable future.

RECOMMENDATION

This study underscores the pressing need for comprehensive strategies to address the current challenges and promote sustainable practices. To mitigate the adverse environmental impact caused by improper disposal, it is imperative to invest in robust recycling infrastructure, including recycling facilities and efficient transportation networks. Concurrently, raising public awareness through extensive campaigns is essential to foster a culture of responsible LDPE recycling. The government and regulatory bodies should play a more active role by enacting and enforcing policies that support and incentivize LDPE recycling. Furthermore, research and innovation efforts must be intensified to enhance recycling methods, improve quality control, and explore emerging markets for recycled LDPE materials. Chemical recycling, particularly catalytic pyrolysis, holds significant promise and should be further investigated and optimized. The integration of circular economy principles into

industries, such as construction and asphalt production, can reduce waste and promote resource conservation. Strengthened waste management logistics, comprehensive environmental impact assessments, collaborative initiatives, and pilot programs will collectively contribute to a more sustainable and responsible LDPE waste management system in Nigeria and beyond.

REFERENCES

1. E. Dumbili, L. Henderson, "Chapter 22 - The challenge of plastic pollution in Nigeria" T. M. B. T.-P. W. and R. Letcher, Ed. (Academic Press, 2020); <https://www.sciencedirect.com/science/article/pii/B9780128178805000220>, pp. 569–583.
2. R. U. D. E. E. I. J. A. Ibekwe, Challenges and prospects of plastic waste management in Nigeria. (2019).
3. O. D. Akan, G. E. Udofia, E. S. Okeke, C. L. Mgbachidinma, C. O. Okoye, Y. A. B. Zoclanclounon, E. O. Atakpa, O. O. Adebajo, Plastic waste: Status, degradation and microbial management options for Africa. *J. Environ. Manage.* **292**, 112758 (2021).
4. S. K. Sen, S. Raut, Journal of Environmental Chemical Engineering Microbial degradation of low density polyethylene (LDPE): A review. **3**, 462–473 (2015).
5. B. Yalwaji, H. O. John-nwagwu, T. O. Sogbanmu, Plastic pollution in the environment in Nigeria : A rapid systematic review of the sources , distribution , research gaps and policy needs. **16** (2022).
6. B. B. Nyakuma, Emerging trends in sustainable treatment and valorisation technologies for plastic wastes in Nigeria : A concise review. doi: 10.1002/ep.13660 (2021).
7. D. S. Achilias, C. Roupakias, P. Megalokonomos, A. A. Lappas, E. V Antonakou, Chemical recycling of plastic wastes made from polyethylene (LDPE and HDPE) and polypropylene (PP). doi: 10.1016/j.jhazmat.2007.06.076 (2020).
8. E. N. Kalali, S. Lotfian, M. E. Shabestari, S. Khayat-zadeh, C. Zhao, H. Y. Nezhad, ScienceDirect Green and Sustainable Chemistry A critical review of the current progress of plastic waste recycling technology in structural materials. (2023).
9. A. Dey, C. Vilas, D. Priyanka, S. Arushi, Challenges and possible solutions to mitigate the problems of single-use plastics used for



- packaging food items : a review. (2020).
10. A. Chun, M. Loy, J. Yau, B. Shen, C. Loong, S. Sow, M. Lock, Science of the Total Environment Rethinking of the future sustainable paradigm roadmap for plastic waste management : A multi-nation scale outlook compendium. **881** (2023).
 11. *Circular Economy and the Law*.
 12. T. Abbasi, N. Jaafarzadeh, H. Fard, F. Madadzadeh, H. Eslami, Environmental Impact Assessment of Low-Density Polyethylene and Polyethylene Terephthalate Containers Using a Life Cycle Assessment Technique. (2023).
 13. H. Jung, G. Shin, H. Kwak, L. Tan, J. Jegal, H. Jeong, H. Jeon, J. Park, D. X. Oh, Chemosphere Review of polymer technologies for improving the recycling and upcycling efficiency of plastic waste. **320** (2023).
 14. K. Bernat, Post-Consumer Plastic Waste Management : From Collection and Sortation to Mechanical Recycling. (2023).
 15. J. Lim, Y. Ahn, J. Kim, Optimal sorting and recycling of plastic waste as a renewable energy resource considering economic feasibility and environmental pollution. **169**, 685–696 (2023).
 16. S. V Dharia, A. J. Khushwah, C. M. Choudhari, M. S. Kavre, Optimum source segregation bin for household solid waste and waste plastic recycling. (2023).
 17. K. Ragaert, L. Delva, K. Van Geem, Mechanical and chemical recycling of solid plastic waste. (2017).
 18. C. Tsala-mbala, K. S. Hayibo, T. K. Meyer, N. Couao-zotti, P. Cairns, J. M. Pearce, Technical and Economic Viability of Distributed Recycling of Low-Density Polyethylene Water Sachets into Waste Composite Pavement Blocks on. (2022).
 19. V. Athithan, L. Thilagam, Reuse of plastic waste as building materials to enhance sustainability in construction : a review. (2023).
 20. M. Jawaid, B. Singh, L. K. Kian, S. A. Zaki, A. M. Radzi, ScienceDirect Processing techniques on plastic waste materials for construction and building applications. (2023).
 21. Investigating the Use of Post-Consumer LDPE Waste and Stone Dust in Sustainable Concrete Composites.
 22. A. Al-mansour, R. Yang, C. Xu, Y. Dai, Y. Peng, J. Wang, Q. Lv, L. Li, C. Zhou, Z. Zhang, Q. Zeng, S. Xu, Materials & Design Enhanced recyclability of waste plastics for waterproof cementitious composites with polymer-nanosilica hybrids. **224** (2022).
 23. P. Kumar, A. Sreeram, X. Xu, P. Chandrasekar, Closing the Loop : Harnessing waste plastics for sustainable asphalt mixtures – A comprehensive review. **400** (2023).
 24. K. R. Vanapalli, B. Samal, B. K. Dubey, J. Bhattacharya, 12 Emissions and Environmental Burdens Associated With Plastic Solid Waste Management. (2019).
 25. S. S. W. Priyantha, H. M. C. C. S. D. S. Sampath, Synthesis and characterisation of waste - based composites from banana fibre and low - density polyethylene. (2023).
 26. B. Yalwaji, H. O. John-nwagwu, T. O. Sogbanmu, F. A. C. Sanchez, H. Boudaoud, M. Camargo, J. M. Pearce, K. R. Vanapalli, B. Samal, B. K. Dubey, J. Bhattacharya, M. Shamsuyeva, H. Endres, M. I. Din, R. U. D. E. E. I. J. A. Ibekwe, S. Adekunle, N. Kolawole, M. Yinka, M. Kayode, J. Adekunle, K. Adekunle, M. Olanrewaju, V. Shanmugam, R. Afriyie, M. Försth, G. Sas, Á. Restás, C. Addy, Q. Xu, L. Jiang, R. Esmacely, S. Singha, G. George, T. J. E, F. Berto, M. S. Hedenqvist, O. Das, S. Ramakrishna, Journal of King Saud University – Engineering Sciences Eggshell nanoparticle reinforced recycled low-density polyethylene : A new material for automobile application. **6** (2021).
 27. K. P. Rajan, I. Mustafa, A. Gopanna, S. P. Thomas, Catalytic Pyrolysis of Waste Low-Density Polyethylene (LDPE) Carry Bags to Fuels : Experimental and Exergy Analyses. (2023).
 28. A. Khan, N. Iqbal, Sustainable Energy & Fuels Conversion of low-density polyethylene plastic waste into valuable fuels using fly ash as a catalyst †. doi: 10.1039/d3se00779k (2023).
 29. M. Shaker, V. Kumar, C. M. Saffron, M. Rabnawaz, Revolutionizing Plastics Chemical Recycling with Table Salt. **2300306**, 1–8 (2023).
 30. S. A. S. Alali, M. K. M. B. J. Aldaihani, K. M. Alanezi, applied sciences Plant Design for the Conversion of Plastic Waste into Valuable Chemicals (Alkyl Aromatics). (2023).
 31. R. Hasanzadeh, P. Mojaver, T. Azdast, S. Khalilarya, A. Chitsaz, M. A. Rosen, Decision analysis for plastic waste gasification considering energy , exergy , and environmental criteria using TOPSIS and grey relational



- analysis. **174**, 414–423 (2023).
32. P. Kots, E. Selvam, D. G. Vlachos, M. G. Ierapetritou, Techno-Economic and Life Cycle Analyses of Thermochemical Upcycling

Technologies of Low-Density Polyethylene Waste. (2023).



P094 - ANTIMICROBIAL ACTIVITIES OF CALOTROPIS PROCERA: A REVIEW

H. S. Abdullahi¹, A. M. Dikko², A. P. Olorundare², F. L. Auwal³, G. O. Idakwo⁴, E. Winful⁵, B. E. Nwobi⁵, M. Abdullahi⁵, V. Ochigbo⁵.

Department of Biological Science, Ahmadu Bello University, Zaria, Nigeria¹.

Department of Microbiology Zaria, Ahmadu Bello University, Kaduna state².

Department of Biochemistry, Ahmadu Bello University, Zaria, Nigeria³.

Department of Microbiology Federal University of Lafia, Nasarawa state, Nigeria⁴.

National Research Institute for Chemical Technology Zaria Kaduna State⁵.

Corresponding author's email: * aishadikko360@gmail.com

ABSTRACT

Abuse of antimicrobial has led a to the rising cases of drug-resistant microorganisms and concerns resulting from these drugs resistant microorganism is currently gaining global awareness. A blend of ethnomedicine and green chemistry is currently gaining attention in research as a promising solution to this crisis caused by antimicrobial resistance. This approach involves using environmentally friendly processes to synthesize new drugs from plants that can overcome the resistance of pathogenic microorganisms. Green chemistry offers several advantages over traditional methods, including the use of less toxic solvents and reducing waste production. This review looked at some research works done on the antimicrobial activity of bioactive components extracted using various solvents from different parts of the plant *Calotropis procera* over a ten (10) year period. The results showed that various parts of the plant after extraction conferred significant antimicrobial activities thus suggesting that *Calotropis procera* is a potential source that can be explored for new antimicrobial.

KEYWORDS

Calotropis procera, antimicrobial, drug resistance, ethnomedicine, green chemistry

INTRODUCTION

The goal antibiotics is meant to achieve is greatly threatened by the development of antimicrobial resistance (AMR) in both medical and community settings(1). AMR usually arises as a result of misuse or overuse of drugs especially antimicrobials, as well as poor infection prevention and control. At present, as a way of tackling AMR, ethnomedicine is gaining a lot of awareness. Research carried out by the World Health Organization (WHO) in over 91 countries showed that the number of available medicinal plants are nearly 21,000 (2). It has also been widely observed and accepted that the medicinal value of plants lies in the bioactive and phytochemical present in the plant. Various formulations of medicinal plants have been used either to inhibit or eliminate infections resulting from bacteria, fungi, viruses, protozoa, etc. (3).

Calotropis, a medicinal plant of interest distributed largely throughout the tropics and warm temperate climates has about 4555 species of which *Calotropis procera* (Rakta arka), *Calotropis gigantia* (Sweata arka), *C. sussuela* and *C. acia* (4) are some of common available species.

Calotropis procera which is the specie of focus in this review can be readily found in Indonesia, Malaysia, China and India as wasteland weed. It's flower, leaves, roots, root barks, stem, stem bark is said to have antifungal activity against approximately 27 different fungi and yeast (5, 6). Therefore, the aim of this review is to investigate various works done on the antimicrobial activity of *Calotropis procera* (4, 7) as potential source for new antimicrobials.

BOTANICAL DESCRIPTION

Calotropis has 4555 species distributed largely throughout the tropics but also in warm temperate climates and the common species are *C. procera*



(Rakta arka), *C. gigantean* (Sweata arka), *C. sussuella* and *C. acia* (4, 7). *Calotropis procera* (Rui Tree) is an erect, tall large, highly branched, and perennial shrub or small tree that grows to 3 -6' high. Its leaves are usually dark green in color and the veins inside the leaves are white in color it can be as long as 7-18 centimeter and as broad as 5-13 centimeter. Its leaves arrangement is opposite, flower size 2", color is white to purple, and the fruit is follicle. *C. procera* is an ayurvedic plant with important medicinal properties. The Common names for the plant include Apple of Sodom, Sodom apple, king's crown, rubber bush, Ark, Swallow wart or milkweed and rubber tree. It is known by various vernacular names such as Swallow-Wort (English), Madar (Hindi), Alarka (Sanskrit), Tumfafiya (Hausa), Ewe Bomubomu (Yoruba) (8).

GEOGRAPHICAL DISTRIBUTION

C. procera is drought-resistant and salt tolerant to a relatively high degree. It quickly becomes established as a weed along degraded roadsides, lagoon edges, and in overgrazed native pastures. It has a preference for and often dominant in areas of abandoned cultivation especially sandy soils in low rainfall areas (9). Hence commonly found in Indonesia, Malaysia, China and the Indian as wasteland weed and also found in North Africa, tropical Africa, Western Asia, South Asia, and Indochina, Kenya, Nigeria and Niger (8).

PHYTOCHEMISTRY AND MEDICINAL VALUE.

Extensive literature review shows that *C. procera* contains many bioactive components such as cardenolides, steroids, tannins, glycosides, phenols, terpenoids, flavonoids, alkaloids and saponins (10, 11). It has exhibited many pharmacological effects like antimicrobial, antihelmintic, anti-inflammatory, immunological, antidiabetic, cardiovascular, hypo-lipidemic, gastro protective, hepatic protective, renal protective, antidiarrheal, antioxidant, anticonvulsant, enhancement of wound healing, smooth muscle relaxant, schizonticides, analgesics etc., (12-14).

Extracts and latex from different parts (flowers, leaves, roots, root bark, stems, and stem bark) of *C. procera* showed *in vitro* antifungal activities against approximately 27 different fungi and yeasts (5, 15). It is also utilized as an arrow poison, molluscicide, a fungicide, an anti-syphilitic, an anti-inflammatory, antipyretic, a purgative, as well as in the treatment

of leprosy, diabetes, bronchial asthma, ulcers, tumors, piles, applied to painful joints and swelling (8, 13, 16) etc. The leaf of *C. procera* contains an enzyme called calotropain, which is also perceived as a valuable antidote for snakebite, sinus, rheumatism, mumps, etc. The root barks are used to treat a variety of illnesses such as leprosy, menorrhagia and high fever. Flowers are used as health tonic, cough, dog/jackal bite (rabies), epilepsy, asthma, bronchitis, liver and spleen disorder. The fruits are used for Eye disorder and anemia (5, 9, 17). Phenolic acid has effective role against the binding of parasites against teeth and urinary bladder lining and, in this way, it inhibits the risk of (UTI) urinary tract infection and dental cares (10, 12).

SOME WORKS DONE ON *C. PROCERA*.

Studies carried out by Gomah (2013), explored the plant's antimicrobial activity of which *C. procera* was sourced from the arid region near Najran province, Saudi Arabia. The leaves underwent a 10-day air-drying process at a controlled temperature of $28\pm 2^{\circ}\text{C}$, followed by powdering. These powdered samples were securely stored in dry bags. A portion of the sample was subjected to maceration using methanol, petroleum ether, and chloroform, with regular shaking over 7 days. The resulting extracts were filtered, treated with anhydrous sodium sulfate for drying, and concentrated under vacuum, ensuring the temperature did not exceed 65°C (18).

A 2019 study conducted by Radwan *et al.*, to investigate the impact of *C. Procera* plant extract on seed germination and microbial growth. The study explored the antibacterial activity of *C. procera* extracts using the disc diffusion method on microbial strains such as *Escherichia coli* and *Staphylococcus aureus* (19).

In 2014, Hussein *et al.*, investigated the antimicrobial properties of latex silver nanoparticles derived from *C. Procera* latex. The latex was separated into rubber, serum, and lipids using centrifugation. A mixture was created by diluting the latex serum with deionized water and adding silver nitrate. This mixture was heated and incubated to produce latex silver nanoparticles (LAg-Nps). During the experiment, bacterial growth in nutrient broth media was assessed by inoculating fresh colonies into the broth, which was then incubated at 37°C . The growth was measured at 600nm intervals using a UV-vis spectrophotometer over one-hour periods (20).



A research study conducted by Shah, *et al.* (2022) utilized *C. procera* leaf extract for synthesizing copper oxide nanoparticles (CuONPs). The leaves were collected, dried, and powdered, followed by mixing with distilled water and boiling. After filtration and centrifugation, CuONPs were stored at 4°C. These nanoparticles were then tested for their antifungal properties against *Rhizopus Oryzae* (E1D5). Various concentrations of CuONPs were added to PDA media to evaluate their fungicidal effectiveness (21).

In 2016, a study conducted by Karale and Karale aimed to identify bioactive compounds such as Flavonoids, Tannins, Glycosides, Alkaloids, Steroids, Triterpenoids, and Saponins in *C. Procera* leaves. The leaves were dried, powdered, and extracted with chloroform, methanol, and ethanol using a Soxhlet Extractor (22).

Bioactive compounds from *C. Procera* root were extracted and incorporated into chitosan and polyvinyl alcohol (CS-PVA) carriers for effective delivery to support wound healing. This research, conducted by Abbas *et al.*, (2022), utilized plant roots sourced from Jhang, Pakistan. After drying and grinding the roots into a fine powder, they were extracted using methanol for over 48 hours at 25°C. The extracted bioactive compound underwent further processing at 60°C with continuous stirring for 30 minutes, followed by filtration and centrifugation for 20 minutes. The resulting extract was loaded onto CS-PVA membranes for wound healing applications, including the treatment of induced dorsal skin wounds in rabbits (23).

In 2020 a study conducted by Bilal *et al.*, on the antibacterial properties of the methanolic extract from *C. procera* leaves were investigated. The extract was tested against several bacteria, including *Proteus mirabilis*, *Pseudomonas aeruginosa*, *Bacillus cereus*, *Escherichia coli*, *Klebsiella pneumonia*, *Salmonella typhi*, and *Enterococcus faecalis*, using the disc diffusion method. Various concentrations of the extract were applied to filter discs, which were then placed on nutrient agar plates inoculated with the bacteria. After 24 hours of incubation at 37 °C, the zones of inhibition were measured to determine the antibacterial activity (24).

In 2015, Shetty *et al.*, reported tha freshly harvested leaves of *C. procera* were air-dried and ground into a fine powder. The resulting powder was used to prepare aqueous extract and extracts in different organic solvents like ethanol, methanol, acetone,

and ethyl acetate. After maceration, the liquid extracts were filtered and then dried. The study utilized bacterial isolates such as *Bacillus subtilis*, *Micrococcus aureus*, *Pseudomonas aeruginosa*, and *Escherichia coli*, all maintained on nutrient agar plates at 4°C. Positive controls such as Tetracycline, Streptomycin, Polymyxin-B, and Gentamycin were employed for specific bacterial strains, while Dimethyl sulfoxide served as the negative control. Each bacterial strain had its own set of controls using pure solvents. The agar plates were incubated at 37°C for 48 hours, and the sensitivity of the bacterial strains to various extracts was evaluated by measuring the zone of inhibition using the agar well diffusion assay. This experiment was performed in triplicates for each test organism, and the results were analyzed accordingly (3).

In 2022, a study led by Saddiq *et al.*, investigated the antimicrobial properties of *C. procera* against harmful microorganisms. Leaves of *C. procera* and soil from its rhizosphere were collected. The leaves were dried, powdered, soaked in hydroethanol, and then filtered. The resulting ethanolic extract was evaporated and lyophilized. Actinobacteria were isolated from the rhizosphere using soil-extract medium with glycerol and starch-casein agar medium. Antimicrobial activity of plant and actinobacterial extracts against bacteria (*E. coli*, *K. pneumonia*, *B. subtilis*, *S. aureus*), yeast (*C. albicans*), and fungus (*Aspergillus fumigatus*) was determined using agar well-diffusion assays. Growth media and controls were utilized, and all experiments were conducted in triplicate (25).

DISCUSSION

Experiment conducted by Gomah (2013) showed the bioactive extracts gotten from the three solvents (methanol, petroleum ether and chloroform) to be four flavonoid glycosides. Fractions of methanol extract were found to be the 3-O-rufinosides of isorhamnetin, quercetin, and kaemferol, besides flavonoid 5-hydroxy-3,7- dimethoxyflavone-4'-O-B-glycopyranoside. When tested for antimicrobial activity, the result indicated that methanol, petroleum ether and chloroform extract showed considerable antimicrobial activity against some tested organisms. However, they differ significantly in their action against bacteria with diameter of inhibition ranging between 8.5 and 28.5mm while fungi ranging between 10.5 to 30mm. The result also indicated that among the organic solvents used, methanol extract exhibited superior antimicrobial activity while no antibacterial activity was observed in some cases of the petroleum ether and



chloroform extract. The crude flavonoid showed the strongest activity against both bacteria and fungi (18).

This work also coincides with work done by Radwan *et al.*, (2019) that revealed the main components of *C. procera* to be phenolic compounds and flavonoids. These compounds were suspected to be responsible for seed germination and activity against pathogenic microbes. Assessment of the activity of aqueous extract of *C. procera* on microorganisms noted that an increase in concentration of the extract negatively affected the growth of the microorganisms. However, the difference is that work done by Radwan *et al.*, (2019) focused mainly on the aqueous extract and it was deduced that the extract has broad spectrum activity against both gram negative and positive bacteria. While for work done by Gomah (2013), most gram-positive bacteria showed resistance (18, 19).

Research on the synthesis of latex silver nanoparticles (Lag-NPs) from *C. procera* and silver nitrate was conducted based on the biogenic synthesis approach. The nanoparticles when studied using TEM and other characterization techniques revealed to be highly stable spherical shaped particles with strong antimicrobial and antifungal activity (20). These nanoparticles exhibited good antimicrobial activity against Gram negative bacteria in the likes of *E. coli*, *Serratia species* and *P. aeruginosa* and also antifungal activity against dermatophytes and phytopathogenic fungi. The synthesized NPs also showed higher effect in comparison with crude latex. However, no prominent activity was detected in other microorganisms tested. The latex serum NPs was shown to contain various organic compounds that play a vital role in reduction of silver nitrate to silver thereby escalating the antimicrobial activity of the particles.

Similar work was conducted by Shah *et al.*, (2022) on green synthesis and characterization of copper oxide nanoparticle (CuONPs) using leaf extract of *C. procera*. These NPs also exhibited antimicrobial potential when tested using standard disc diffusion against Gram negative (*E. coli*). Increase in the diameter of zones of inhibition was seen in extracts containing nanoparticles then leaf extract lacking nanoparticles. Previous studies reported that the bacterial effect of the CuONPs is due to small particle size which give it more surface area and also the presence of organic functional groups of the *C. procera* extract on the surface of the

nanoparticle. This statement is in accordance with the report by Hussein *et al.*, (2014) stating the strong antimicrobial activity of the synthesized NP depends on the large surface area of the NP which give it more area for interaction with the organism. In vitro activity of CUONPs showed that higher concentration was found to effectively prevent spread of fungal infection. This higher activity was due to the presence of biomolecules in the leaf extract used which are the flavonoids, glycosides, saponins, phenolic compounds and tannin (20, 21).

Similarly, the work of Karale and Karale, (2016) on the phytochemical screening of various extracts of leaf of *C. procera* prove the presence of this bioactive compounds with the addition of protein and alkaloids. The presence of all these in the organic extract indicated that the plant possesses medicinal value. Another experiments with resemblance to this was conducted to assess the phytochemical presence in the aqueous extract of the whole plant (19, 22).

The potential of this medicinal plant isn't limited to only its antimicrobial aspect, research by Abbas *et al.*, (2022) proved that *C. procera* extract have promising potential and could possibly be a potential agent for wound dressing in combination. The extracts of this plant act as an antioxidant, anti-inflammatory and antimicrobial agent which are applied for skin damage treatment. This plant produces secondary metabolites which are well known for their bioactivity. The CS-PVA membrane loaded with *C. procera* extract proved to be highly for wound healing, which is also in accordance with already documented studied that material loaded with bioactive material showed higher wound healing capacity versus their individual efficient counterparts (23).

Result of the investigation conducted by Bilal *et al.*, (2020) on the antimicrobial activity of methanolic extract of *C. procera* leaf on some strains of bacteria showed activity against *P. mirabilis*, *P. aeruginosa* and *B. cereus* whereas, *E. coli*, *K.pneumonia*, *S.typhi* and *E. feacalis* showed resistance. Hence it was deduced that the plant extract has different effect at different concentration against a specific bacterium. The investigation also provided a comprehensive profile of the phytochemical analysis and antibacterial activity of *C. procera* (24).

The work carried out by Shetty *et al.*, (2015) to analyze the phytochemical of leaf extracts (methanol, ethyl acetate, athanol, acetone and



aqueous) and their antimicrobial activity revealed the presence of alkaloid, saponin, flavanoids, sterols, terpenoids cardiac glycosides, proteins and sugar. Reducing sugar were found to be absent in acetone. Aquoeus extract showed antimicrobial activity against Gram positive organisms like *B. subtilis* and Gram-negative bacteria like *E. coli*. Acetone and ethanol extracts exhibited maximum activity against both Gram positive and negative bacteria. Ethyl acetate and methanol extracts showed moderate inhibitory effect. When tested for minimum inhibitory concentration (MIC), the ethanol extracts showed lowest MIC value followed by acetone and methanol extracts. Ethyl acetate extract exhibited higher MIC value and was deducted to be less effective. Among the various bacteria strains tested, lower MIC values were obtained for *B.subtilis* and *E.coli* indicating that they are more susceptible (3).

From the work of Saddiq *et al.*, (2022), four actinobacterial strains named (CALT-1, CALT-2, CALT-3 and CALT-4) were discovered to be related to streptomyces strain via the 16s rRNS sequences analysis. For the antimicrobial activity determination, the result revealed that the ethanolic extract of *C. procera* possessed potential antimicrobial activity. The leaf extract showed significant activity against all tested microorganisms when compared with standard antibiotics gentamycin and Ketoconazole. Most antibacterial activity was recorded in *Staphylococcus aureus* and *Klebsiella pneumoniae* followed by *Bacillus subtilis* and *Escherichia coli*. The leaf extract also showed significant activity against *Candida. albican* and *Aspergillus fumigatus* when compared with Ketoconazole. The ethanolic extract also exhibited high fungistatic activity and bacteriostatic effective against Gram negative bacteria compared with the four actinobacterial extracts. However, the actinobacterial extract were more effective against Gram positive bacteria than *C. procera* extracts (25).

CONCLUSION

A blend of ethnomedicine and green chemistry is currently gaining attention in research as a promising solution to this crisis caused by antimicrobial resistance. Conclusions drawn from the above findings shows that the various part of *C. procera* are potential sources for new drugs especially in the field of pharmacognosy. It is therefore recommended that the yet to be researched fractions of the various phytochemicals contained in *C. procera* should be greatly explored

as a promising approach to tackling the rise in antimicrobial resistance.

REFERENCES

1. S. M. Bairagi, P. Ghule, R. Gilhotra, Pharmacology of Natural Products: An recent approach on *Calotropis gigantea* and *Calotropis procera*. (2018).
2. I. A. Ziblim, K. A. Timothy, E. J. Deo-Anyi, Exploitation and use of medicinal plants, Northern Region, Ghana. *Journal of Medicinal Plants Research* 7, 1984-1993 (2013).
3. V. G. Shetty, M. G. Patil, A. S. Dound, Evaluation of phytochemical and antibacterial properties of *Calotropis procera* (Ait) R. Br. Leaves. *Int J Pharm Pharm Sci* 7, 316-319 (2015).
4. L. M. Hassan, T. M. Galal, E. A. Farahat, M. M. El-Midany, The biology of *Calotropis procera* (Aiton) WT. *Trees* 29, 311-320 (2015).
5. S. Sagadevan *et al.*, Exploring the therapeutic potentials of phyto-mediated silver nanoparticles formed via *Calotropis procera* (Ait.) R. Br. root extract. *Journal of Experimental Nanoscience* 15, 217-231 (2020).
6. U. Saher *et al.*, Soluble laticifer proteins from *Calotropis procera* as an effective candidates for antimicrobial therapeutics. *Saudi Journal of Biological Sciences* 30, 103659 (2023).
7. M. Lakhdar, CALOTROPIS PROCERA (AIT) R. BR, A VALUABLE MEDICINE PLANT: A REVIEW. *Advances in Biology & Earth Sciences* 8, (2023).
8. M. S. Akhtar, S. Hussain, AN OVERVIEW: IDENTIFICATIONS AND ACTIVITIES OF CALOTROPIS PROCERA LEAVES. (2019).



9. A. Ogundola *et al.*, Evaluation of nutrients in leaves and seeds of calotropis procera (linn): A multipurpose plant. *Journal of Pharmacy and Nutrition Sciences* **2**, 33-39 (2021).
10. U. Farooq, S. Nisar, A. B. Merzaia, M. W. Azeem, Isolation of Bioactive components from Calotropis procera Plant Latex-A Review. *International Journal of Chemical and Biochemical Science* **11**, 95-101 (2017).
11. S. Kundu, A mini review on Calotropis procera and tapping its phytochemical and pharmacological potential. *The Journal of Phytopharmacology* **10**, 277-280 (2021).
12. R. P. Mali, P. S. Rao, R. Jadhav, A review on pharmacological activities of Calotropis procera. *Journal of Drug Delivery and Therapeutics* **9**, 947-951 (2019).
13. I. Pavani, S. Udayavani, A REVIEW ON CALOTROPIS PROCERA (AIT) AND ITS PHARMACOLOGICAL ACTIVITIES. (2020).
14. E. H. Naser, A. M. Kashmer, S. A. Abed, Antibacterial activity and phytochemical investigation of leaves of Calotropis procera plant in Iraq by GC-MS. *IJPSR* **10**, 1988-1994 (2019).
15. M. Suba Sri, M. Subhashini, M. K. Devi, R. J. Devi, R. Usha, Green synthesis of nanohydroxy apatite using Calotropis procera and Wrightia tinctoria plant latex serum extract for biomedical application. *Biomass Conversion and Biorefinery*, 1-15 (2023).
16. H.-L. Han, C. W. Kwon, Y. Choi, P.-S. Chang, Antifungal activity of α -helical propeptide SnuCalCpII15 derived from Calotropis procera R. Br. against food spoilage yeasts. *Food Control* **133**, 108628 (2022).
17. B. D. Wadhvani, D. Mali, P. Vyas, R. Nair, P. Khandelwal, A review on phytochemical constituents and pharmacological potential of Calotropis procera. *RSC advances* **11**, 35854-35878 (2021).
18. G. Nenaah, Antimicrobial activity of Calotropis procera Ait.(Asclepiadaceae) and isolation of four flavonoid glycosides as the active constituents. *World Journal of Microbiology and Biotechnology* **29**, 1255-1262 (2013).
19. A. M. Radwan, H. Alghamdi, S. K. M. Kenawy, Effect of Calotropis procera L. plant extract on seeds germination and the growth of microorganisms. *Annals of Agricultural Sciences* **64**, 183-187 (2019).
20. M. H. Nadia, I. A. Mady, A.-M. M. Wael, Antimicrobial activity of latex silver nanoparticles using Calotropis procera. *Asian Pacific Journal of Tropical Biomedicine*, 876-883 (2014).
21. I. H. Shah *et al.*, Green synthesis and Characterization of Copper oxide nanoparticles using Calotropis procera leaf extract and their different biological potentials. *Journal of Molecular Structure* **1259**, 132696 (2022).
22. P. Karale, M. Karale, Preliminary phytochemical screening of various extracts and fractions of leaves Calotropis procera (AIT) R. BR. *Int. J. Life Sci. Res* **2**, 158-161 (2016).
23. M. Abbas *et al.*, Chitosan-polyvinyl alcohol membranes with improved antibacterial properties contained Calotropis procera extract as a robust wound healing agent. *Arabian Journal of Chemistry* **15**, 103766 (2022).



24. H. Bilal *et al.*, Biological evaluation of antimicrobial activity of *Calotropis procera* against a range of bacteria. *Journal of Pharmacognosy and Phytochemistry* **9**, 31-35 (2020).
25. A. A. Saddiq, H. M. Tag, N. M. Doleib, A. S. Salman, N. Hagagy, Antimicrobial, antigenotoxicity, and characterization of *Calotropis procera* and its rhizosphere-inhabiting Actinobacteria: In vitro and in vivo studies. *Molecules* **27**, 3123 (2022).



P095 - EFFECT OF ACETYLATION AND FATTY ACID TREATMENT ON OLEOPHILICITY OF KENAF FIBRES

Ozogu A. Nanadeinboemi^{1*}, Opeoluwa O. Fasanya², Olusegun A. Ajayi³, Adegboyega S. Olawale³, and Michael. S. Olakunle³.

¹*Petrochemical and Allied Department, National Research Institute for Chemical Technology, Basawa-Zaria, Kaduna State, Nigeria.*

²*Industrial and Environmental Pollution Department, National Research Institute for Chemical Technology, Zaria, Nigeria.*

³*Chemical Engineering Department, Ahmadu Bello University, Zaria, Nigeria.*
Corresponding author email: donagbe@yahoo.com

ABSTRACT

Kenaf fibre is one of the popular natural fibres used as reinforcement in polymer matrix composites, and during chemical modification, it loses more hydroxyl groups and become more hydrophobic. The kenaf fibres were extracted using water retting method, and were subjected to acetylation and fatty acid treatment at 120°C for 3 h and 75°C 1 h respectively. FT-IR analysis was used to observe the chemical changes in the kenaf fibres after treatment. The FTIR spectra shows peaks within 2346-2360 cm⁻¹, which is attributed to C=O stretching of the acetyl group, and peaks around 1746-1745 cm⁻¹ is attributed to the C=O stretching of carbonyl in the ester bonds, these peaks were observed in both acetylation and stearic acid treated kenaf fibres, but were not found on the non-treated fibres. The appearance of these bonds signifies that acetylation and fatty acid treatment has induced hydrophobicity on the fibres. Acetylation and fatty acid treated fibres absorbed crude oil in a similar capacity, while the non-treated gives different capacity. Acetylation and fatty acid treated sorbent materials showed an increase in sorbent capacity with time until attainment of equilibrium. While the non-treated fibre attained maximum capacity within the first 15 minutes and lost capacity as time progressed. Fatty acid treated fibres had a maximum capacity of 90%, acetylation 86%, and non-treated fibres had 64%. Therefore, the acetylation and fatty acid treated kenaf fibres can be used for effective absorbents in crude oil spill effluent, but fatty acid treated fibres were more effective than acetylated fibres.

KEYWORDS:

Acetylation, Kenaf fibre, Fatty acid, Modification, Bast fibre

INTRODUCTION

For the past decades, there is an increasing demand for natural fibres over synthetic fibres due to their renewable and biodegradable nature. Natural fibres often derived from renewable sources such as plants, animals, and minerals (1). Researchers suggest that the natural fibres are more cost-effective in the long run with inherent advantages such as being produced from renewable resources that are abundant and cheap (1). Currently, there is growing interest in finding inexpensive, abundant, and effective materials as oil spill sorbents in water with a lot of focus being cast on natural organic sorbents mainly from agriculture. A wide variety of cellulosic materials such as corn stalk (2), cotton (3), kenaf fibres (4), orange peel (5), palm fibres (6), sawdust (7), sugarcane bagasse (8), and walnut shell (9) have shown good results, making them

potential candidates for oil spill treatment. Although, natural based materials are low cost, abundant, eco-friendly, and support proper utilization of waste, their sorption efficiency is inferior compared to some synthetic materials. Their main disadvantages stem from their poor oleophilic/hydrophobic properties. This is due to the chemical structure of natural fibres (such as kenaf) which is mainly of hydrophilic moiety (mainly OH), which will cause high polar characteristic. In order to improve these characteristics, the sorbents can be modified using mechanical (10), thermal (10), and chemical (11) methods. Kenaf (*Hibiscus cannabinus L.*) is a warm season annual fibre crop closely related to cotton, okro and jute. Historically, kenaf has been used as a source of fibre to produce twine, rope and sackcloth (12). It is used mainly as a jute substitute.



Nowadays, there are various new applications for kenaf including paper products, building materials, absorbents, and animal feeds.

The kenaf stem consists of two types of fibres known as bast fibre (the outer layer) and the core fibre (the inner layer) respectively (13). The bast constitutes 40% of the plant, and the fibre cells are about 2–6 mm long and slender with cell wall thick (6.3 μm). The core is about 60% of the plant and has thickness ($\approx 38 \mu\text{m}$), but short (0.5 mm) and thin-walled (3 μm) fibre cells (14).

Amongst the different ways of inducing hydrophobicity, acetylation and fatty acid treatment methods are rather popular. Acetylation is a technique for increasing hydrophobicity in naturally hydrophilic materials. In acetylation, the

hydroxyl groups in the cellulose structure are converted to oleophilic acetate groups (O-CO-CH_3) through reaction with acetic anhydride in the presence of catalysts such as N-bromosuccinimide, N-methylpyrrolidone, and 4-dimethylaminopyridine. Acetylation lowers the hydrophilic properties of the sorbent and enhances the oleophilic properties (11 and 15). The principle of fatty acid treatment such as stearic acid or oleic acid is that, the carboxyl group of fatty acid reacts with the hydroxyl groups of the fibre through an esterification reaction, thus, reduces the hydroxyl groups number available to bond with water molecules (16). One more advantage of treatment with fatty acid is that it is not sensitive to oxidation during the processing temperatures of natural fibre/polymer composites (17).



Figure 1: Fresh and Dry Kenaf Plants (18).

In this study, changes in chemical structure as well as sorption capacity of kenaf fibres when acetylated and treated with fatty acids was compared.

MATERIALS AND METHODS:

Materials:

The kenaf fibre were sourced from Textile Technology Department, National Research Institute for Chemical Technology (NARICT), Zaria, Kaduna State. The chemicals include; acetic anhydride ($\text{C}_4\text{H}_6\text{O}_3$), N-bromosuccinimide ($\text{C}_4\text{H}_4\text{BrNO}_2$), ethanol ($\text{C}_2\text{H}_5\text{OH}$) (99.7%), acetone ($(\text{CH}_3)_2\text{CO}$) (99%), stearic acid ($\text{C}_{18}\text{H}_{36}\text{O}_2$), and

deionized water. All the chemicals used were an analytical grade, and used without further purification.

Extraction of Kenaf Fibres:

Water retting method was applied to extract the kenaf fibres (19). About 10 kg of the dry kenaf plants was soaked in a 50 L plastic drum with tap water for about 3 weeks to separate the core from the bast. The extraction was done by combing with normal small hair combs. The fibres were dried under sunlight for 24 hr.

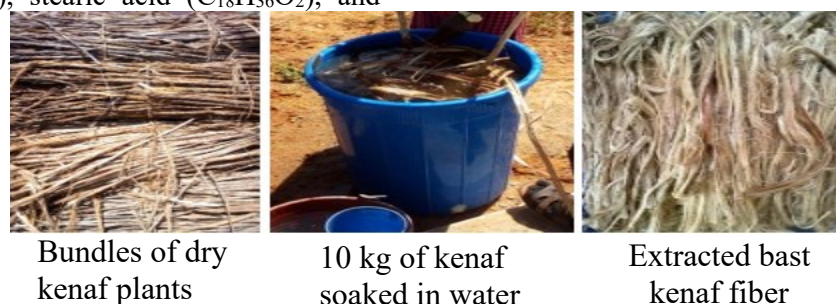


Figure 2: Extraction of Kenaf Fibres.



Preparation of Kenaf Fibres:

About 10 g of the Kenaf fibres were size reduced to ~ 2 mm and blended with a kitchen blender to powder. It was washed with deionized water, sun dried for 7 h, and oven dried for 24 h at 80°C.

Acetylation of Kenaf Fibres:

Acetylation was carried out using the method described by Sun *et al* (20). About 5 g of the kenaf fibres was placed in a two neck round bottom flask, 150 mL of acetic anhydride was added into it to submerge the fibres, and 1% N-bromosuccinimide (NBS, catalyst) was also added. The flask was then placed in an oil bath, fitted with a reflux condenser. The required temperature for the reaction was 120°C for 3 h. After the reaction time, the flask was removed from the oil bath, and the hot reagent was decanted off, and the treated fibres were washed with a mixture of acetone and ethanol 3 times. The fibres were then dried in an oven at 60°C overnight, and characterized with FTIR to observe chemical structural changes.

Fatty Acid Treatment:

Fatty acid treatment was carried out using the method described by Salem *et al* (21). A total mass of 4 g of stearic acid was added to 100 mL of distilled water in a beaker and heated up at 75°C to form a suspension. Kenaf fibres amounting to a total mass of 5 g was immersed in the suspensions containing stearic acid and stirred for 60 min at 75°C. The treated kenaf fibres were then washed with distilled water until a pH value of 7 was attained. The fibres were then dried in an oven at 60°C overnight, and characterize with FTIR.

Oil Sorption Test:

Simulated oil spills were used for oil sorption experiments in the laboratory; 2.5 g of crude oil was added to a beaker filled with 100 mL of distilled water. About 0.2 g of the acetylated fibres were added to the mixture and shake on a rotary shaker for 5, 10, 15, 20, and 25 minutes. The fibres were then collected using a sieve net and left to drain in an oven for at least 6 hours at 60°C. The weight of the drained fibres was recorded. This procedure was applied to the fatty acid and non-treated fibres. The sorption capacity of the fibres was evaluated using equation 1.

$$\text{Oil Sorption Capacity} = \frac{\text{New weight Gained}}{\text{Original Weight}} \times 100$$

RESULTS AND DISCUSSION:

FT-IR Analysis of Functional Groups of Acetylation, Fatty Acid, and Non-Treated Kenaf Fibres:

FTIR was used to confirm whether chemical modification took place in the kenaf at the range of 4000 to 600 cm^{-1} and presented in Figure 3. The absorption peaks at 3409 cm^{-1} which correspond to free O-H stretching (22), peaks within 1644-1637 cm^{-1} are attributed to the carbonyl group of the acetyl ester ($-\text{C}=\text{C}-$ stretching) in hemicellulose and the carbonyl aldehyde in lignin (23), all these peaks appeared in all the three spectra. Peaks around 2919-2857 cm^{-1} are attributed to stretching of C-H groups of cellulose (24), peaks within 1324-1460 cm^{-1} is attributed to C=O stretch of acetyl group of lignin is reduced (24), peak at around 1154 cm^{-1} is probably associated with absorbed water in crystalline cellulose (24), peaks within 1030-1040 cm^{-1} is C-O stretching vibrations in cellulose, peaks within 888-977 cm^{-1} representing the β -glucosidic linkages between the sugar units in hemicelluloses and celluloses (25), and peaks within 602-670 cm^{-1} are attributed to COOH, all these peaks are observed in both acetylation and non-treated kenaf fibres. Peak at 1541 cm^{-1} is attributed to the C=C aromatic in plane vibrations in lignin (26), peak at 702 cm^{-1} is attributed to aromatic C-H out-of-plane bend, these peaks are found only in fatty acid treated kenaf fibres. Peaks within 2346-2360 cm^{-1} is attributed to C=O stretching of the acetyl group, and peaks around 1746-1745 cm^{-1} is attributed to the C = O stretching of carbonyl in the ester bonds (27), these peaks were observed in both acetylation and stearic acid treated kenaf fibres. But peak at 1154 cm^{-1} disappears only in fatty acid treated fibres, this shows that water content is been removed completely on the fatty acid treated fibres. The appearance of these bonds signifies that some level of acetylation has taken place, and fatty acid too has enhanced some oleophilic properties on the fibre.



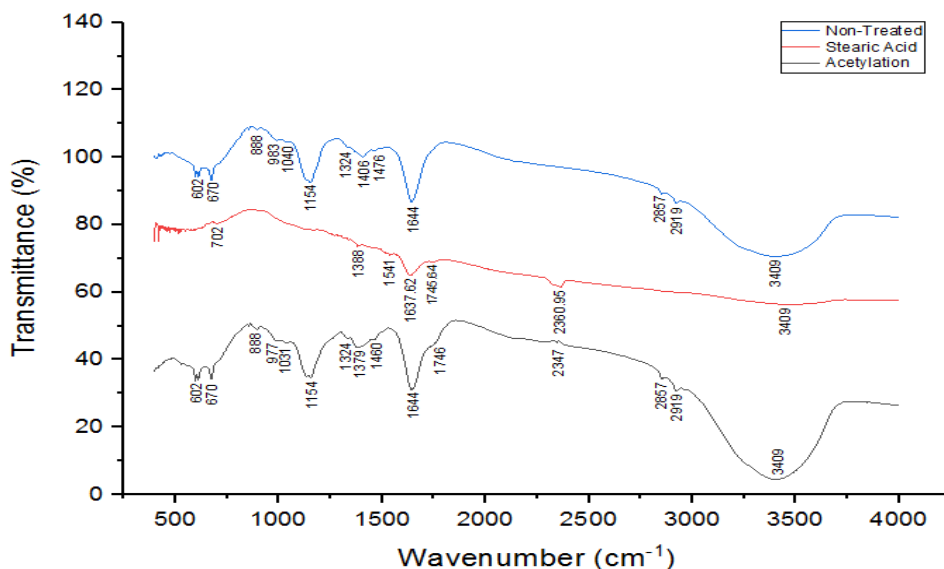


Figure 3: FTIR Spectra of Acetylation, Fatty Acid, and Non-Treated Kenaf Fibres.

Oil Sorption Test:

Figure 4 shows the sorption capacity of acetylated, fatty acid, and non-treated kenaf fibres with time. Acetylation and fatty acid treated sorbent materials showed an increase in sorbent capacity with time until attainment of equilibrium. But, fatty acid treated fibres absorbed oil faster to attain

equilibrium than that of acetylation. While the non-treated fibre attained maximum capacity within the first 15 minutes and lost capacity as time progressed. Fatty acid treated fibres had a maximum capacity of 90%, acetylation 86%, and non-treated fibres had 64%. This indicates that modified fibres would have better sorption capacity than non-treated fibres.

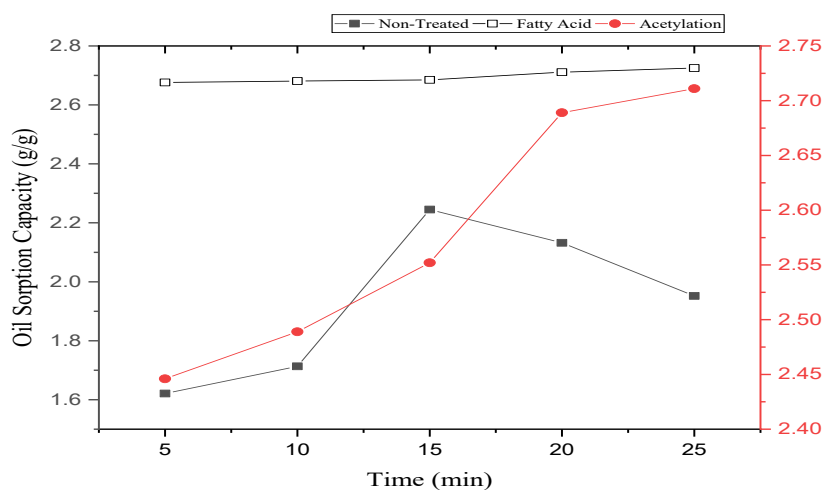


Figure 4: Sorption Capacity of Acetylation, Fatty Acid, and Non-Treated Kenaf Fibres with Time.

CONCLUSION:

Oil sorbent materials were successfully synthesized from kenaf plant fibres. The final sorbent materials are hydrophobic in nature based on FTIR analysis. The FTIR spectra revealed that acetylation and fatty acid treatment of kenaf fibres was successful. The

differences in sorption capacity of the non-treated, fatty acid and acetylated samples were rather significant. The treated fibres presented higher sorption capacity than the non-treated fibres. Therefore, it was concluded that, both fatty acid and acetylated kenaf bast fibres can be used as low-cost



alternative to commercial adsorbents for effective wastewater and crude oil spill effluent treatment.

REFERENCES:

1. H. M. Akil, M. F. Omar, A. A. M. Mazuki, S. Safiee, Z. A. M. Ishak, and B. A. Abu. Kenaf fibre reinforced composites: A review. *Materials and Design* 32(8-9):2011, 4107-4121.
2. M. Hussein, A. A. Amer, A. El-Maghraby, and N. Hamedallah. Oil spill removal from water by using corn stalk: Factors affecting sorption process. *Int. J. Environ. Waste Manag.* 16, 2015, 281.
3. S. Cao, T. Dong, G. Xu, and F. Wang. Oil Spill Cleanup by Hydrophobic Natural Fibres. *J. Nat. Fibres.* 14, 2017, 727-735.
4. Z. Miltiadis, T. Dimitrios, D. Vassilios, and I. Theophilos. Application of Sorbents for Oil Spill Cleanup Focusing on Natural-Based Modified Materials: A Review. *Molecules.* 25, 2020, 4522; doi:10.3390/molecules25194522.
5. I. A. El-Gheriany, E. F. Ahmad, E. R. A. A. Abdul, and M. Hussein. Oil spill sorption capacity of raw and thermally modified orange peel waste. *Alex. Eng. J.* 59, 2020, 925-932.
6. O. Abdelwahab, S. M. Nasr, and W. M. Thabet. Palm fibres and modified palm fibres adsorbents for different oils. *Alex. Eng. J.* 56, 2017, 749-755.
7. M. Mojžiš, T. Bubeníková, M. Zachar, D. Kačíková, and J. Štefková. Comparison of natural and synthetic sorbents' efficiency at oil spill removal. *BioResources.* 14, 2019, 8738-8752.
8. R. Behnood, B. Anvaripour, N. Jaafarzadeh, and M. Farasati. Oil spill sorption using raw and acetylated sugarcane bagasse. *J. Cent. South Univ.* 23, 2016, 1618-1625.
9. A. Srinivasan and T. Viraraghavan. Removal of oil by walnut shell media. *Bioresour. Technol.* 99, 2008, 8217-8220.
10. M. Hussein, A. A. Amer, A. El-Maghraby, and N. A. Taha. Availability of barley straw application on oil spill clean-up. *Int. J. Environ. Sci. Technol.* 6, 2009, 123-130.
11. J. C. Onwuka, E. B. Agbaji, V. O. Ajibola, and F. G. Okibe. Treatment of crude oil-contaminated water with chemically modified natural fiber. *Appl. Water Sci.* 8, 86. 2018.
12. A. M. E. Mohd, M. A. B. A. Hazizan, and M.I. Z. Ariffin. Chemical modification of kenaf fibres. *Materials Letters* 61 (2007) 2023-2025.
13. S. Mutasher, A. Poh, A. M. Than, and J. Law. The effect of alkali treatment mechanical properties of Kenaf fibre epoxy composite. *Key Engineering Materials* 471-472: 2011, 191-196.
14. H. Nanko, A. Button, and D. Hillman. *The World of Market Pulp.* Appleton, WI, USA: WOMP, LLC. ISBN 0-615-13013-5. 2005, p. 258.
15. J. O. Nwadiogbu, P. A. C. Okoye, V. I. Ajiwe, and N. J. N. Nnaji. Hydrophobic treatment of corn cob by acetylation: Kinetics and thermodynamics studies. *J.*



- Environ. Chem. Eng. 2, 2014, 1699–1704.
16. A. Tijjani and U. Hashim. Highly sensitive silicon nanowire biosensor with novel liquid gate control for detection of specific single-stranded DNA molecules, *Biosensors and Bioelectronics*. 67(2015a) 656–661.
 17. A. Tijjani and U. Hashim. Design and fabrication of micro-mixer with short turns angles for self-generated turbulent structures, *Microsystem Technologies*, 1-8, 2015b.
 18. <https://www.fibre2fashion.com>.
 19. I. K. Mazharul. Kenaf Fibre: Properties, Cultivation, Production, Uses and Advantages. 2021. <https://textilelearner.net/kenaf-fibre-properties>.
 20. X. F. Sun, R. C. Sun, and J. X. Sun. Acetylation of sugarcane bagasse using NBS as a catalyst under mild reaction conditions for the production of oil sorption-active materials. *Bioresource Technology* 95 (3), 2004, 343–50.
 21. I. A. S. Salem, A. R. Rozyanty, B. O. Betar, T. Adam, M. Mohammed, and A. M. Mohammed. Study of the effect of surface treatment of kenaf fibre on chemical structure and water absorption of kenaf filled unsaturated polyester composite. *IOP Conf. Series: Journal of Physics: Conf. Series* 908 (2017) 012001.
 22. J. Moran, V. Alvarez, V. Cyras, and A. Vazquez. Extraction of cellulose and preparation of nanocellulose from sisal fibres. *Cellulose*, 15, 2008, 149–159.
 23. N. E. Zafeiropoulos, G. G. Dijon, C. A. Baillie. A study of the effect of surface treatments on the tensile strength of flax fibres: Part I. Application of Gaussian statistics. *Composites: Part A* 38: 2007, 621–628.
 24. I. M. Süleyman, D. K. Emine, and M. Nigar. Effect of the Ecological Methods on the Surface Modification of the Kenaf Fibres. ISSN 1392–1320 MATERIALS SCIENCE (MEDŽIAGOTYRA). Vol. 22, No. 3. 2016.
 25. L. Manzato, L. C. A. Rabelo, S. M. Souza, C. G. Silva, E. A. Sanches, D. Rabelo, and J. Simonsen. New approach for extraction of cellulose from tucuma's endocarp and its structural characterization. *Journal of Molecular Structure*. 2017, 1143.
 26. S. Kubo and J. F. Kadla. Hydrogen bonding in lignin: A Fourier transform infrared model compound study. *Biomacromolecules*, 2005, 6, 2815–2821.
 27. J. Mehdi, P. M. Aji, M. A. Mahnaz, D. M. Majid, and O. Kristiina. A Comparison of Modified and Unmodified Cellulose Nanofibre Reinforced Poly(lactic Acid) (PLA) Prepared by Twin Screw Extrusion. *J Polym Environ*, 2012. DOI 10.1007/s10924-012-0503-9.



P096 - SYNTHESIS OF HIERARCHICAL ZSM-5 ZEOLITE WITH IMPROVED MESOPOROSITY

Abubakar Ganiyu, Baba Yakubu Jibril, Abdulazeez Yusuf Atta, Benjamin Olorunfemi Aderemi & Bello Mukhtar

emailganiyu@gmail.com

ABSTRACT

Hierarchical H-ZSM-5 zeolites were synthesized by modifying nanocrystalline ZSM-5 zeolite with aqueous sodium hydroxide (NaOH) and Cetyltrimethylammonium bromide (CTAB) solution using desilication-reassembly methods. The dissolution and reassembling effects of NaOH and CTAB treatments were respectively investigated. The treated samples were characterized using XRD, XRF, FTIR, and BET techniques. Five important variables were optimized by estimating the percentage crystallinities of the samples. The parameters optimized were hydrothermal reassembly time, NaOH concentration, NaOH treatment time, desilication-reassembly pH, and CTAB concentration. BET surface area analysis revealed an increase in mesoporous and total surface areas from 39.9 m²/g and 373 m²/g to as much as 248 m²/g and 425 m²/g respectively. Micropore volume was slightly decreased from 0.150cm³/g to 0.093cm³/g representing retention of 62% microporosity.

Keywords: *ZSM-5 Desilication-reassembly, characterization, Crystallinity*

Introduction

Zeolites are a unique microporous crystalline aluminosilicates built from tetrahedrally bonded TO₄ (T=mostly Al, Si or P) via corner sharing of oxygen leading to formation of rings, cages, channels and 3D frameworks with pore diameters less than 2nm (Van laak et al, 2011; Li and Yu, 2021; Li and Yu, 2014). The framework structure and chemical composition are primarily responsible for its unique properties such as well-defined microporosity, high thermal stability, intrinsic acidity and good shaped selectivity. These properties have made zeolites applicable in many industrial processes such as water treatment, adsorption and separation, and catalysis (Sang et al, 2004). Zeolites can either occur naturally or chemically synthesized. Among synthetic zeolites, MFI structured ZSM-5 receives a lot of attention as a catalyst due to the high thermal stability, resistance to deactivation, high acidic activity, cation-exchange capability, well-ordered pore

network, and molecular shape selectivity arising from a unique framework structure (Thubsuang et al. 2012; Alipour et al, 2014).

The ZSM-5 zeolite is a synthetic zeolite with a framework structure consisting of one straight (0.54 nm×0.56 nm) and one sinusoidal (0.51 nm×0.55 nm) intersecting channel, with a 10-membered ring opening (pentasil zeolite) (Bjørgen et al, 2008; Karimi et al, 2012; Alipour et al, 2014). It is applied in a wide area of industrial processes such as catalytic cracking, dewaxing, alkylation, isomerization and aromatization (Adewuyi et al. 1995; Kim et al. 2006; Ren et al. 2011).

Aromatization is a process of thermal and catalytic conversion of hydrocarbons or oxygenates into aromatics such as Benzenes, Toluene, and Xylenes (BTX). BTX have wide applications as raw materials for many industrial chemicals such as styrene, phenol and gasoline blendstocks (Akhtar et al, 2012; Jia, et al, 2017; Pinilla-Herrero et al, 2018). Presently, BTX is industrially produced by naphtha



reforming of crude oil (Zhang et al, 2014). Researchers have been working to replace crude oil with an economic and commercial feedstock in order to reduce the environmental impact of aromatic synthesis. Aromatics are produced over ZSM-5 because of its strong acidity, thermal stability and its pore structure. The small pore architecture associated with micropores are beneficial but causes diffusion limitations of larger reacting species, giving rise to restrictions in the catalyst activity and lifetime (Wang et al, 2016). Researchers have over the years done great work in order to overcome this problem. Shortening of diffusion path length in zeolites is considered as effective and can be achieved by one these four main strategies (Ivanova et al, 2013).

The first strategy involves reducing the particle size of zeolites (Schmidt et al, 2000; Biemmi and Bein, 2008). In the second strategy, materials typically referred to as mesoporous zeolites are simply single zeolite crystals with irregular intracrystalline mesopores. The introduction of mesopores into zeolitic crystals are post-synthetically carried out by treatments such as solid or supramolecular templating, dealumination and/or desilication procedures (Pérez-Ramírez et al 2008; Ogura, 2008; Meng et al, 2009; Chal et al, 2011; Lopez-Orozco et al, 2011; Groen et al, 2004; Groen et al, 2006). Desilication yields tailored mesoporosity by altering concentration of alkali, the Si/Al ratio of the parent zeolites, the reaction temperature and reaction time. Application of this method is quite cost efficient and facile.

So much works have been carried out in finding the best conditions for desilication. Extensive studies carried out to vary NaOH concentration, dissolution temperature and time revealed optimum conditions to be 0.2M, 65° C and 30 minutes respectively (Groen et al, 2004; Groen et al, 2006; Groen et al, 2007; Meunier et al, 2012). Desilication, however, has the problem of relative unselective mesopore formation and loss of zeolite material due to the leaching process (Rahmani and Taghizadeh, 2017). To solve this problem, an approach that helps to reassemble the leached material is employed. This approach referred to as dissolution and reassembly method, gives rise to micro-mesoporous materials and simultaneously improves the intrinsic crystallinity and acidity while also helping to reduce the diffusion constraints.

This contribution is therefore aimed at synthesis of hierarchical zeolite by NaOH dissolution and CTAB reassembly method for improved acidity and transport properties.

2. Material and Methods

2.1 Synthesis of ZSM-5-based mesostructures

ZSM-5-based hierarchical micro-/mesoporous materials were synthesized from commercial MFI-type zeolites by the combined method of dissolution and self-assembly based on the procedure reported elsewhere (Peng et al, 2016). The parent zeolite used in this study was a commercial H form ZSM-5 with SiO₂/Al₂O₃ mass ratio = 50 (Zeolyst International Inc.).

Typically, (3.000±0.005) g ZSM-5 was first mixed with a series of aqueous solutions containing varied concentrations of NaOH. Vigorous agitation of the solution occurred at 353 K for 2 h and then (4.500±0.005) g CTAB that was dissolved in 60 mL of deionized H₂O and then added to the dissolution system. The pH was then adjusted to 10.5 by addition of 2.0 mol/L sulphuric acid solution. The slurry was then transferred into a Teflon-lined stainless-steel autoclave for self-assembly at 383 K for 24 h. The solid product was filtered and washed with excess deionized water, dried in an oven at 383 K, and subsequently calcined at 823 K for 6 h. The resulting materials were ion-exchanged with 1 mol/L ammonium chloride (Chemical Reagent Co. Ltd) at 353 K for 1 h and repeated three times.

2.2 Characterization

Powder X-ray diffraction (XRD) patterns were measured using PANalytical X'Pert PRO MPD diffractometer equipped with Cu K radiation ($\alpha = 0.1541$ nm), 40 kV voltage and current strength of 30 mA in the 2θ range of 5-60° (wide-angle XRD patterns) at room temperature. The relative crystallinity of MFI phase in ZSM-5-based mesostructures was calculated using 7-10° and 22.5-25°, respectively.

The Fourier transform infrared (FT-IR) analysis of the samples was done in order to detect surface functional groups by Agilent MicroLab Instrument. XRF



analysis was carried out with EDXRF Analyzer with geological calibrated oxide.

N₂ adsorption–desorption experiments have been performed on an ASAP 2020, V4.02 at liquid nitrogen temperature of -195.8°C. Prior to analysis, each sample was evacuated at 300 °C in vacuum for 8 h. The micropore area and volume were calculated by the t-plot method. The mesopore areas were obtained by subtracting the micropore area from the BET surface area, and the mesopore volumes were calculated by subtracting the micropore volume from the total volume at 0.9915 P/P₀, according to the methods reported in literature (Oseke, et al, 2020). The values reported for mesopores consisted of the contributions from the external surface of particles which includes mesopores and macropores. The pore size distributions of the solids were derived from the adsorption

branch of the isotherm using the BJH model.

Thermal gravimetric analysis of the used samples was carried out on TGA instrument. Measurements were conducted by scanning from room temperature to 800°C with a heating rate of 10 C min⁻¹ under nitrogen flow.

3. Results and Discussions

3.1 XRD Analysis

3.1.1 Effects of CTAB Concentration on Crystallinity of Zeolite

The crystallinities are confirmed from XRD. All samples are previously calcined before analyses. Regardless of the concentration of CTAB, ZSM-5 crystalline phase were present. The observed diffraction peaks are characteristic of the MFI zeolite (Figure 1). As can be observed from figure 1, an increasing the molar concentration of CTAB from 0 to 0.05M under hydrothermal temperature of 110°C leads to a corresponding increase in crystallinity from 44% to 62%. The increase in the relative crystallinity observed over this concentration range was attributed to the dissolution of some amorphous phase contained in commercially available zeolites and also to the recovery of zeolitic phase due to the healing of some defects in the zeolite framework under recrystallization conditions (Ivanova et al,2011; Konnov et al, 2012; Ordonsky et al, 2012; Bouhadjar et al, 2015).



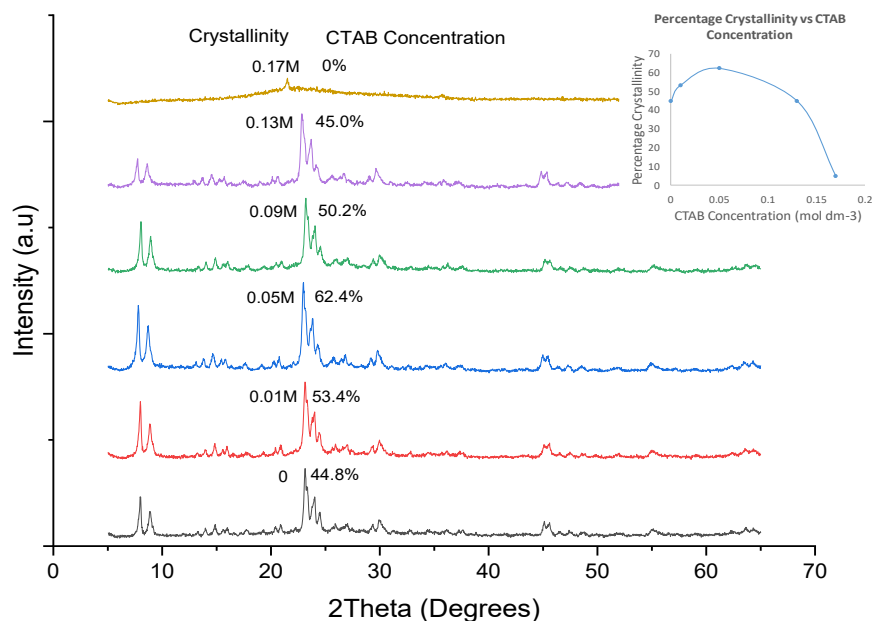


Figure 1. XRD results showing percentage crystallinity at varying CTAB concentrations Inset is the corresponding crystallinity curve for CTAB concentration.

Note: All Samples were treated at desilication conditions of fixed NaOH concentration at 65°C for treatment time in minutes and reassembly/hydrothermal conditions of 110°C and 17 hours reassembly time

At CTAB concentrations above 0.05M, however, relative crystallinity (RC) decreases. This is in agreement with results obtained in the literatures (Xu et al, 2014; Jin et al 2014). A CTAB concentration range of 0.01–0.05M has been found to be perfect for ZSM-5 formation (Xu et al, 2014). However, higher values result in a reduction of crystallinity of ZSM-5 leading to formation of mesoporous amorphous species (Xu et al, 2014; Jin et al 2014).

This observation may be due to the fact CTAB displays a self-assembly effect for the synthesis of hierarchical MFI-type zeolites. Negatively charged zeolite moiety, resulting from the basic reaction media is attracted by the hydrophilic cationic head group of CTAB through ionic interactions, thereby promoting assembly. This good affinity between the two species is responsible for the crystal growth inhibition, thus reducing crystallinity and promoting formation of large pores (Mcheik et al, 2021). As established in the literature, formation of these species (mesoporous molecular sieves) occurs by liquid crystal templating mechanism. According to this mechanism, the liquid crystal mesophase

aggregates into rodlike micelles before the addition of the reactants, followed by migration and polymerization of silicate anions thereby resulting in the formation of mesoporous molecular sieves. Self-assembly of the liquid crystal-like structures then occurs as a result of mutual interactions between silicate anions in the basic mixture and the surfactant cations in the solution leading to an ordered liquid crystal phase (Ahmed and Ramli, 2014).

3.2 XRF Analysis

This observed trend in crystallinities dependence on concentration is in agreement with the results of XRF elemental analysis shown in Table 1. An increase in Si/Al ratio is an indication of reassembly of silica species and most likely an increased crystallinity. As seen from the table, there is an increase in the Si/Al ratio from 22.9 to 27.3 for an increase in concentration from 0 to 0.05M. There is however a decrease in this ratio from 29.3 to 23 as concentration increases 0.09 to 0.17M

Table 1. XRF analysis of Zeolite samples



Sample	HZ	0	0.01	0.05	0.09	0.13	0.17
SiO ₂	93.0	85.1	90.3	88.1	87.9	88.0	57.1
Al ₂ O ₃	4.2	6.3	5.2	5.5	5.1	5.2	4.2
Si/Al	37.6	22.9	29.2	27.3	29.3	28.7	23.0

3.3 Analysis of FT-IR spectra

The FT-IR spectra of the CTAB reassembled samples, 0M, 0.01M, 0.05M, 0.09M, 0.13M and 0.17M samples were recorded in the range of 400–4000 cm⁻¹.

Fig. 2 shows the FT-IR spectra of the catalysts in spectral region of 400–2500 cm⁻¹.

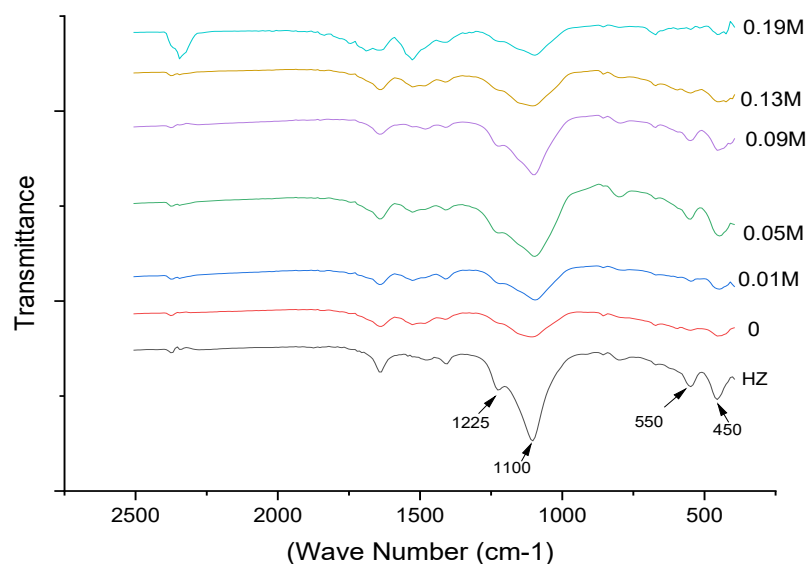


Figure 2. FTIR results at varying CTAB concentrations

The framework vibration near 450, 550, 800, 1100 and 1225 cm⁻¹ which identifies ZSM-5 zeolite structure is observed in all samples (Koekkoek et al, 2011; Rahmani and Taghizadeh, 2017). However, sample treated at 0.19M CTAB seem to have lost its crystallinity due to excess amount of CTAB. The IR band near 450 cm⁻¹ is related to T–O (T = Si or Al) vibration of TO₄ internal tetrahedral units. The band at 550 cm⁻¹ indicates ZSM-5 formation with five-membered rings (D5R). The intensity ratio of the 550 and 450 cm⁻¹ bands is known as an estimation for ZSM-5 zeolite crystallinity (Koekkoek et al, 2011). The IR bands at 800 and 1100 cm⁻¹ indicate symmetric stretching of external linkage and internal asymmetric stretching vibration of Si–O–T linkage, respectively. The IR band around 1225 cm⁻¹ is

structure-sensitive (Shukla and Pandya, 2007). This band (1225cm⁻¹) which is due to external asymmetric stretching vibration is clearly present in IR spectra of ZSM-5 zeolite with four chains of five-membered rings (Koekkoek et al, 2011). As shown in Figure 2, the intensity of this band gradually increases as the concentration of CTAB is increased from 0 to 0.05M. This increment corresponds to increase in crystallinity and is in agreement with the results obtained from XRD analysis. The band intensity thereafter decreases as CTAB concentration is increased from 0.09M to 0.17M.

3.4 Porosimetric Studies



The effect of the concentrations of basic solutions and pore directing agent solutions

(NaOH/CTAB) on the pore system of the synthesized samples was studied. Figure 3 shows the N₂ adsorption and desorption isotherms at 77 K for the parent commercial ZSM-5 (H) and samples treated with NaOH and CTAB (0M, 0.01M, 0.05M, 0.09, 0.13M, and 0.17M).

The parent zeolite material exhibits a type I isotherm with high N₂ uptake at low relative pressures, confirming its microporous nature (Sadowska et al, 2013). Porosity assessment of samples treated with NaOH and CTAB solutions revealed a sharp increase in the relative pressure region 0.4 < P/P₀ < 0.9 leading to an isotherm representing both types of I and IV behaviour resulting to the formation of a large number of mesopores (Fig. 3).

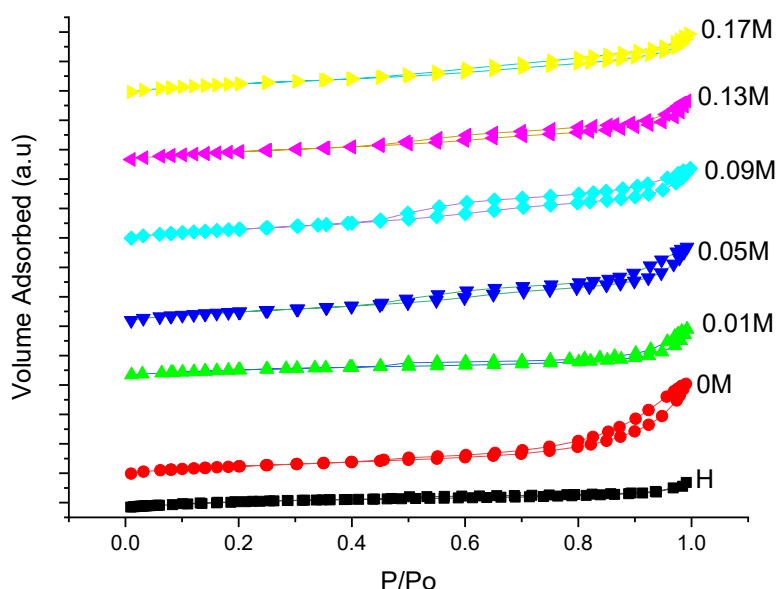


Figure 3. N₂ Isotherms at 77 K of the Commercial ZSM5 (Parent) and the NaOH/CTAB-Treated ZSM-5 samples at varying CTAB concentrations

It is worthy to note that a steeper increase in the high relative pressure region of the adsorption and desorption branches was observed for the desilication products as compared to samples treated with NaOH and CTAB solutions. This suggests that larger mesopores sizes are present in the desilication products, compared to the

desilication/re-assembly products (Lee et al, 2001). This observation also suggests the presence of both micro and mesoporosity as reported in the literatures (Wang et al, 2010; Van laak et al, 2011).



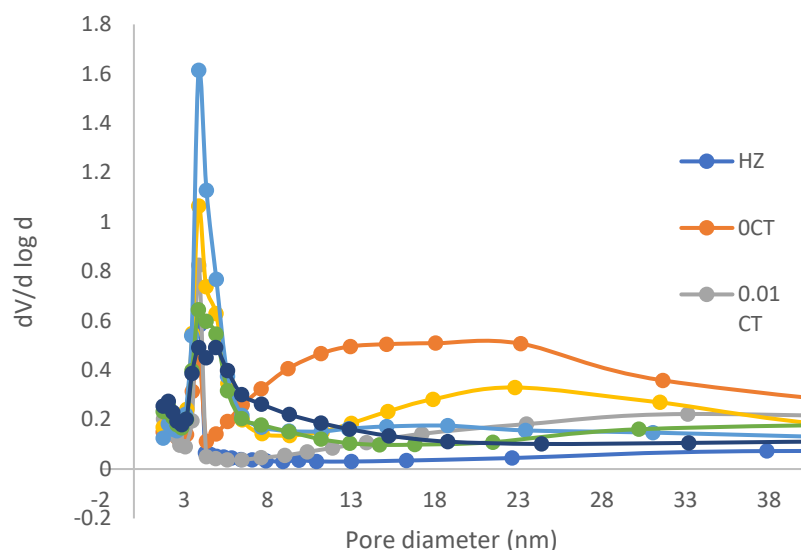


Figure 4: Pore Size Distribution (BJH desorption curves) curves of the Hierarchical ZSM-5 catalysts

For pure alkaline treatment in the absence of CTAB (0M), a wide pore diameter distribution of about 4-32nm was obtained by the BJH model applied to the adsorption branch (Fig. 4).

The majority of these pores are concentrated at about 10 nm average, agreeing with the results reported in the literature (Groen et al, 2007). In contrast to the purely alkaline treated material, the surfactant

assisted templating results in a material, with very narrow mesopore size distribution ranging from 3–7 nm. The narrow mesopore size distributions (at 0.05-0.2 M CTAB concentration) suggest that a restructuring took place during the alkaline treatment with CTAB (Verboekend et al, 2012). These smaller-size mesopores are considered to be similar to the micellar size of CTAB surfactant.

Table 3: Textural characteristics of the as-prepared samples

Sample	S _{BET} ^a (m ² /g)	S _{micro} ^b (m ² /g)	S _{ext} ^b (m ² /g)	V _{tot} ^c (cm ³ /g)	V _{micro} ^d (cm ³ /g)	V _{meso} (cm ³ /g)	Pore Width ^e (nm)	% Meso	Meso/Micro Ratio	Crys (%)	IHF ^f
H	373.0	333.1	39.9	0.226	0.150	0.076	-	10.7	0.12	100	-
0 M	390.2	190.3	199.9	0.621	0.100	0.521	10.1	51.2	1.05	44.8	0.77
0.01M	339.6	179.3	160.3	0.379	0.095	0.284	7.9	47.2	0.89	53.4	0.59
0.05M	425.1	176.8	248.3	0.542	0.093	0.449	6.9	58.4	1.40	62.4	0.89
0.09M	431.2	172.2	259.1	0.523	0.090	0.433	6.3	60.1	1.50	50.2	0.90
0.13M	409.0	174.3	234.8	0.462	0.092	0.37	6.3	57.4	1.35	45	0.83
0.17M	409.6	168.5	241.0	0.457	0.089	0.368	6.1	58.9	1.43	0	0.83

Conclusion



In this work, mesoporous H-ZSM-5 zeolites were synthesized using desilication-reassembly methods. Important parameters considered during synthesis were hydrothermal reassembly time, NaOH concentration, NaOH treatment time, desilication-reassembly pH, and CTAB concentration. The work revealed the optimum values of 17 hours reassembly time, 0.3M NaOH

concentration, 1-hour NaOH treatment time, pH of 11.5 and CTAB concentration of 0.05M. Techniques like XRD, FTIR, XRF and BET were employed to characterize the synthesized samples. The surface area analysis revealed an increase of total surface area from 373 m²/g to 425 m²/g with a corresponding micropore volume decrease from 0.150 cm³/g to 0.093 cm³/g.

References

- Adewuyi, Y. G., Klocke, D. J., & Buchanan, J. S. (1995). *Effects of high-level additions of ZSM-5 to a fluid catalytic cracking (FCC) RE-USY catalyst. Applied Catalysis A: General*, 131(1), 121–133. doi:10.1016/0926-860x(95)00124-7
- Ahmed, S. and Ramli, A. (2021). *Effects of surfactant concentration on the physico-chemical characteristics on mesoporous molecular sieve. Journal of Applied Sciences*, 11(7), 1178–1184. doi: 10.3923/jas.2011.1178.1184
- Akhtar, M. N., Al-Yassir, N., Al-Khattaf, S., & Čejka, J. (2012). *Aromatization of alkanes over Pt promoted conventional and mesoporous gallosilicates of MEL zeolite. Catalysis Today*, 179(1), 61–72. doi:10.1016/j.cattod.2011.06.03
- Alipour, S. M., Halladj, R., & Askari, S. (2014). *Effects of the different synthetic parameters on the crystallinity and crystal size of nanosized ZSM-5 zeolite. Reviews in Chemical Engineering*, 30(3). doi:10.1515/revce-2014-0008
- Biemmi, E., & Bein, T. (2008). *Assembly of Nanozeolite Monolayers on the Gold Substrates of Piezoelectric Sensors. Langmuir*, 24(19), 11196–11202. doi:10.1021/la8009892
- Boukoussa, B., Aouad, N., Hamacha, R., & Bengueddach, A. (2015). *Key factor affecting the structural and textural properties of ZSM-5/MCM-41 composite. Journal of Physics and Chemistry of Solids*, 78, 78–83. doi:10.1016/j.jpics.2014.11.006
- Björger, M., Joensen, F., Spangsberg Holm, M., Olsbye, U., Lillerud, K.-P., & Svelle, S. (2008). *Methanol to gasoline over zeolite H-ZSM-5: Improved catalyst performance by treatment with NaOH. Applied Catalysis A: General*, 345(1), 43–50. doi:10.1016/j.apcata.2008.04.02
- Chal, R., Gérardin, C., Bulut, M., & van Donk, S. (2010). *Overview and Industrial Assessment of Synthesis Strategies towards Zeolites with Mesopores. ChemCatChem*, 3(1), 67–81. doi:10.1002/cctc.201000158
- Chang, C. D., & Bell, A. T. (1991). *Studies on the mechanism of ZSM-5 formation. Catalysis Letters*, 8(5-6), 305–316. doi:10.1007/bf00764192
- Cheng, Y., Liao, R. H., Li, J. S., Sun, X. Y., & Wang, L. J. (2008). *Synthesis research of nanosized ZSM-5 zeolites in the absence of organic template. Journal of Materials Processing Technology*, 206(1-3), 445–452. doi:10.1016/j.jmatprotec.2007.1
- Choi, M., Cho, H. S., Srivastava, R., Venkatesan, C., Choi, D.-H., & Ryoo, R. (2006). *Amphiphilic organosilane-directed synthesis of crystalline zeolite with tunable mesoporosity. Nature Materials*, 5(9), 718–723. doi:10.1038/nmat1705



- Choi, M., Na, K., & Ryoo, R. (2009). *The synthesis of a hierarchically porous BEA zeolite via pseudomorphic crystallization. Chemical Communications, (20), 2845.* doi:10.1039/b905087f
- Cundy, C. S., & Cox, P. A. (2005). *The Hydrothermal Synthesis of Zeolites: Precursors, Intermediates and Reaction Mechanism. ChemInform, 36(37).* doi:10.1002/chin.200537220
- Egeblad, K., Christensen, C. H., Kustova, M., & Christensen, C. H. (2008). *Templating Mesoporous Zeolites†. Chemistry of Materials, 20(3), 946–960.* doi:10.1021/cm702224p
- Groen, J. (2004). *On the introduction of intracrystalline mesoporosity in zeolites upon desilication in alkaline medium. Microporous and Mesoporous Materials, 69(1-2), 29–34.* doi:10.1016/j.micromeso.2004.01.
- Groen, J. C., Moulijn, J. A., & Pérez-Ramírez, J. (2006). *Desilication: on the controlled generation of mesoporosity in MFI zeolites. J. Mater. Chem., 16(22), 2121–2131.* doi:10.1039/b517510k
- Groen, J. C., Zhu, W., Brouwer, S., Huynink, S. J., Kapteijn, F., Moulijn, J. A., & Pérez-Ramírez, J. (2007). *Direct Demonstration of Enhanced Diffusion in Mesoporous ZSM-5 Zeolite Obtained via Controlled Desilication. Journal of the American Chemical Society, 129(2), 355–360.* doi:10.1021/ja065737o
- Holland, B. T., Abrams, L., & Stein, A. (1999). *Dual Templating of Macroporous Silicates with Zeolitic Microporous Frameworks. Journal of the American Chemical Society, 121(17), 4308–4309.* doi:10.1021/ja990425p
- Lechert, H., *The pH-value and its importance for the crystallization of zeolites: In Verified Syntheses of Zeolitic Materials, 2nd Revised Edition*
- Ivanova, I. I., Kuznetsov, A. S., Knyazeva, E. E., Fajula, F., Thibault-Starzyk, F., Fernandez, C., & Gilson, J.-P. (2011). *Design of hierarchically structured catalysts by mordenites recrystallization: Application in naphthalene alkylation. Catalysis Today, 168(1), 133–139.* doi:10.1016/j.cattod.2010.11.09
- Ivanova, I. I., & Knyazeva, E. E. (2013). *Micro-mesoporous materials obtained by zeoliterecrystallization: synthesis, characterization and catalytic applications. Chem. Soc. Rev., 42(9), 3671–3688.* doi:10.1039/c2cs35341e
- Jesudoss, S. K., Vijaya, J. J., Kaviyarasu, K., Kennedy, L. J., Jothi Ramalingam, R., & Al-Lohedan, H. A. (2018). *Anti-cancer activity of hierarchical ZSM-5 zeolites synthesized from rice-based waste materials. RSC Advances, 8(1), 481–490.* doi:10.1039/c7ra11763a
- Jia, Y., Wang, J., Zhang, K., Feng, W., Liu, S., Ding, C., & Liu, P. (2017). *Nanocrystallite self-assembled hierarchical ZSM-5 zeolite microsphere for methanol to aromatics. Microporous and Mesoporous Materials, 247, 103–115.* doi:10.1016/j.micromeso.2017.03
- Jin, L., Liu, S., Xie, T., Wang, Y., Guo, X., & Hu, H. (2014). *Synthesis of hierarchical ZSM-5 by cetyltrimethylammonium bromide assisted self-assembly of zeolite seeds and its catalytic performances. Reaction Kinetics, Mechanisms and Catalysis, 113(2), 575–584.* doi:10.1007/s11144-014-0743-x
- Karimi, R., Bayati, B., Charchi Aghdam, N., Ejtemaee, M., & Babaluo, A. A. (2012). *Studies of the effect of synthesis parameters on ZSM-5 nanocrystalline material during template-hydrothermal synthesis in the presence of chelating agent. Powder Technology, 229, 229–236.* doi:10.1016/j.powtec.2012.06.03
- Kasyanov, I. A., Maerle, A. A., Ivanova, I. I., & Zaikovskii, V. I. (2014). *Towards understanding of the mechanism of stepwise zeolite recrystallization into micro/mesoporous materials. J. Mater. Chem. A, 2(40), 16978–16988.* doi:10.1039/c4ta03681f
- Kim, S. D., Noh, S. H., Park, J. W., & Kim, W. J. (2006). *Organic-free synthesis of ZSM-5 with narrow crystal size distribution using two-step temperature process. Microporous and Mesoporous Materials, 92(1-3), 181–188.* doi:10.1016/j.micromeso.2006.01
- Koekkoek, A. J. J., Xin, H., Yang, Q., Li, C., & Hensen, E. J. M. (2011). *Hierarchically structured Fe/ZSM-5 as catalysts for the oxidation of benzene to phenol. Microporous and Mesoporous Materials, 145(1-3), 172–181.* doi:10.1016/j.micromeso.2011.05
- Konnov, S. V., Ivanova, I. I., Ponomareva, O. A., & Zaikovskii, V. I. (2012). *Hydroisomerization of n-alkanes over Pt-modified micro/mesoporous materials obtained by mordenite recrystallization. Microporous*



and Mesoporous Materials, 164, 222–231. doi:10.1016/j.micromeso.2012.08

Lee, J., Sohn, K., & Hyeon, T. (2001). Fabrication of Novel Mesocellular Carbon Foams with Uniform Ultralarge Mesopores. *Journal of the American Chemical Society*, 123(21), 5146–5147. doi:10.1021/ja015510n

Lopez-Orozco, S., Inayat, A., Schwab, A., Selvam, T., & Schwieger, W. (2011). Zeolitic Materials with Hierarchical Porous Structures. *Advanced Materials*, 23(22-23), 2602–2615. doi:10.1002/adma.201100462

Magdalane, C. M., Kaviyarasu, K., Vijaya, J. J., Siddhardha, B., & Jeyaraj, B. (2016). Photocatalytic activity of binary metal oxide nanocomposites of CeO₂/CdO nanospheres: Investigation of optical and antimicrobial activity. *Journal of Photochemistry and Photobiology B: Biology*, 163, 77–86. doi:10.1016/j.jphotobiol.2016.08.01

Mcheik, Z., Pinard, L., Toufaily, J., Hamieh, T., & Daou, T. J. (2021). Synthesis of Hierarchical MOR-Type Zeolites with Improved Catalytic Properties. *Molecules*, 26(15), 4508. doi:10.3390/molecules26154508

Meng, X., Nawaz, F., & Xiao, F.-S. (2009). Templating route for synthesizing mesoporous zeolites with improved catalytic properties. *Nano Today*, 4(4), 292–301. doi:10.1016/j.nantod.2009.06.00

Meunier, F. C., Verboekend, D., Gilson, J.-P., Groen, J. C., & Pérez-Ramírez, J. (2012). Influence of crystal size and probe molecule on diffusion in hierarchical ZSM-5 zeolites prepared by desilication. *Microporous and Mesoporous Materials*, 148(1), 115–121. doi:10.1016/j.micromeso.2011.08

Ogura, M. (2008). Towards Realization of a Micro- and Mesoporous Composite Silicate Catalyst. *Catalysis Surveys from Asia*, 12(1), 16–27. doi:10.1007/s10563-007-9037-x

Ordonsky, V. V., Murzin, V. Y., Monakhova, Y. V., Zubavichus, Y. V., Knyazeva, E. E., Nesterenko, N. S., & Ivanova, I. I. (2007). Nature, strength and accessibility of acid sites in micro/mesoporous catalysts obtained by recrystallization of zeolite BEA. *Microporous and Mesoporous Materials*, 105(1-2), 101–110. doi:10.1016/j.micromeso.2007.05.0

Ordonsky, V. V., Ivanova, I. I., Knyazeva, E. E., Yuschenko, V. V., & Zaikovskii, V. I. (2012). Cumene disproportionation over micro/mesoporous catalysts obtained by recrystallization of mordenite. *Journal of Catalysis*, 295, 207–216. doi:10.1016/j.jcat.2012.08.011

Oseke, G. G., Atta, A. Y., Mukhtar, B., Jibril, B. Y., & Aderemi, B. O. (2020). Highly selective and stable Zn–Fe/ZSM-5 catalyst for aromatization of propane. *Applied Petrochemical Research*, 10(2), 55–65. doi:10.1007/s13203-020-00245-9

Peng, P., Wang, Y., Rood, M. J., Zhang, Z., Subhan, F., Yan, Z., ... Gao, X. (2015). Effects of dissolution alkalinity and self-assembly on ZSM-5-based micro-/mesoporous composites: a study of the relationship between porosity, acidity, and catalytic performance. *CrystEngComm*, 17(20), 3820–3828. doi:10.1039/c5ce00384a

Peng, P., Wang, Y., Zhang, Z., Qiao, K., Liu, X., Yan, Z., ... Komarneni, S. (2016). ZSM-5-based mesostructures by combined alkali dissolution and re-assembly: Process controlling and scale-up. *Chemical Engineering Journal*, 302, 323–333. doi:10.1016/j.cej.2016.05.027

Pérez-Ramírez, J., Christensen, C. H., Egeblad, K., Christensen, C. H., & Groen, J. C. (2008). Hierarchical zeolites: enhanced utilisation of microporous crystals in catalysis by advances in materials design. *Chemical Society Reviews*, 37(11), 2530. doi:10.1039/b809030k

Pérez-Ramírez, J., Verboekend, D., Bonilla, A., & Abell³, S². (2009). Zeolite Catalysts with Tunable Hierarchy Factor by Pore-Growth Moderators. *Advanced Functional Materials*, 19(24), 3972–3979. doi:10.1002/adfm.200901394

Pinilla-Herrero, I., Borfecchia, E., Holzinger, J., Mentzel, U. V., Joensen, F., Lomachenko, K. A., ... Beato, P. (2018). High Zn/Al ratios enhance dehydrogenation vs hydrogen transfer reactions of Zn-ZSM-5 catalytic systems in methanol conversion to aromatics. *Journal of Catalysis*, 362, 146–163. doi:10.1016/j.jcat.2018.03.032

Prokešová, P., Mintova, S., Čejka, J., & Bein, T. (2003). Preparation of nanosized micro/mesoporous composites via simultaneous synthesis of Beta/MCM-48 phases. *Microporous and Mesoporous Materials*, 64(1-3), 165–174. doi:10.1016/s1387-1811(03)00464



- Rahmani, M., & Taghizadeh, M. (2017). *Synthesis optimization of mesoporous ZSM-5 through desilication-reassembly in the methanol-to-propylene reaction. Reaction Kinetics, Mechanisms and Catalysis, 122(1), 409–432.* doi:10.1007/s11144-017-1204-0
- Ren, N., Bronić, J., Subotić, B., Lv, X.-C., Yang, Z.-J., & Tang, Y. (2011). *Controllable and SDA-free synthesis of sub-micrometer sized zeolite ZSM-5. Part 1: Influence of alkalinity on the structural, particulate and chemical properties of the products. Microporous and Mesoporous Materials, 139(1-3), 197–206.* doi:10.1016/j.micromeso.2010.10
- Sachse, A., & García-Martínez, J. (2017). *Surfactant-Templating of Zeolites: From Design to Application. Chemistry of Materials, 29(9), 3827–3853.* doi:10.1021/acs.chemmater.7b0059
- Sadowska, K., Wach, A., Olejniczak, Z., Kuśtrowski, P., & Datka, J. (2013). *Hierarchical zeolites: Zeolite ZSM-5 desilicated with NaOH and NaOH/tetrabutylamine hydroxide. Microporous and Mesoporous Materials, 167, 82–88.* doi:10.1016/j.micromeso.2012.03.04
- Sang, S., Chang, F., Liu, Z., He, C., He, Y., & Xu, L. (2004). *Difference of ZSM-5 zeolites synthesized with various templates. Catalysis Today, 93-95, 729–734.* doi:10.1016/j.cattod.2004.06.09
- Schmidt, I., Boisen, A., Gustavsson, E., Ståhl, K., Pehrson, S., Dahl, S., ... Jacobsen, C. J. H. (2001). *Carbon Nanotube Templated Growth of Mesoporous Zeolite Single Crystals. Chemistry of Materials, 13(12), 4416–4418.* doi:10.1021/cm011206h
- Schmidt, F., Lohe, M. R., Büchner, B., Giordanino, F., Bonino, F., & Kaskel, S. (2013). *Improved catalytic performance of hierarchical ZSM-5 synthesized by desilication with surfactants. Microporous and Mesoporous Materials, 165, 148–157.* doi:10.1016/j.micromeso.2012.07
- Shukla, D. B., & Pandya, V. P. (2007). *Estimation of crystalline phase in ZSM-5 zeolites by infrared spectroscopy. Journal of Chemical Technology & Biotechnology, 44(2), 147–154.* doi:10.1002/jctb.280440206
- Song, C.-M., Jiang, J., & Yan, Z. (2007). *Synthesis and characterization of MCM-41-type composite materials prepared from ZSM-5 zeolite. Journal of Porous Materials, 15(2), 205–211.* doi:10.1007/s10934-007-9121-7
- Van laak, A. N. C., Zhang, L., Parvulescu, A. N., Bruijninx, P. C. A., Weckhuysen, B. M., de Jong, K. P., & de Jongh, P. E. (2011). *Alkaline treatment of template containing zeolites: Introducing mesoporosity while preserving acidity. Catalysis Today, 168(1), 48–56.* doi:10.1016/j.cattod.2010.10.10
- Verboekend, D., Mitchell, S., Milina, M., Groen, J. C., & Pérez-Ramírez, J. (2011). *Full Compositional Flexibility in the Preparation of Mesoporous MFI Zeolites by Desilication. The Journal of Physical Chemistry C, 115(29), 14193–14203.* doi:10.1021/jp201671s
- Verboekend, D., & Pérez-Ramírez, J. (2014). *Towards a Sustainable Manufacture of Hierarchical Zeolites. ChemSusChem, 7(3), 753–764.* doi:10.1002/cssc.201301313
- Verboekend, D., Vilé, G., & Pérez-Ramírez, J. (2012). *Mesopore Formation in USY and Beta Zeolites by Base Leaching: Selection Criteria and Optimization of Pore-Directing Agents. Crystal Growth & Design, 12(6), 3123–3132.* doi:10.1021/cg3003228
- Wang, L., Zhang, Z., Yin, C., Shan, Z., & Xiao, F.-S. (2010). *Hierarchical mesoporous zeolites with controllable mesoporosity templated from cationic polymers. Microporous and Mesoporous Materials, 131(1-3), 58–67.* doi:10.1016/j.micromeso.2009.12.001
- Wang, X., Zhang, J., Zhang, T., Xiao, H., Song, F., Han, Y., & Tan, Y. (2016). *Mesoporous ZnZSM-5 zeolites synthesized by one-step desilication and reassembly: a durable catalyst for methanol aromatization. RSC Advances, 6(28), 23428–23437.* doi:10.1039/c6ra03511f
- Xia, Y., & Mokaya, R. (2004). *On the synthesis and characterization of ZSM-5/MCM-48 aluminosilicate composite materials. Journal of Materials Chemistry, 14(5), 863.* doi:10.1039/b313389c
- Xu, D., Feng, J., & Che, S. (2014). *An insight into the role of the surfactant CTAB in the formation of microporous molecular sieves. Dalton Trans., 43(9), 3612–3617.* doi:10.1039/c3dt53308e



Yoo, W. C., Zhang, X., Tsapatsis, M., & Stein, A. (2012). *Synthesis of mesoporous ZSM-5 zeolites through desilication and re-assembly processes*. *Microporous and Mesoporous Materials*, 149(1), 147–157. doi:10.1016/j.micromeso.2011.08

Zhang, G. Q., Bai, T., Chen, T. F., Fan, W. T., & Zhang, X. (2014). *Conversion of Methanol to Light Aromatics on Zn-Modified Nano-HZSM-5 Zeolite Catalysts*. *Industrial & Engineering Chemistry Research*, 53(39), 14932–14940. doi:10.1021/ie5021156



P097 - DEMULSIFICATION EFFICIENCY OF THREE FATTY ACID BASED DEMULSIFIERS ON NIGERIAN CRUDE OIL EMULSIONS

D. C. Nwakuba^{1*}, I.A Mohammed-Dabo², H. Ibrahim³, and O. O. Fasanya¹

¹National Research institute for chemical technology, (NARICT), Zaria Nigeria,

²Chemical engineering department, Ahmadu Bello university, Zaria

³Chemical engineering department, Kaduna state polytechnic

Corresponding author email: chidimmanwakuba@gmail.com

ABSTRACT

Synthetic chemicals often have adverse effects on the environment. Exposure of humans to hazardous chemicals effect has resulted in ailments that lead to death. Synthetic demulsifiers though effective are often toxic with adverse effects on flora and fauna. Some naturally occurring materials have been found to have demulsification effects. Due to this and the need to develop local content, three demulsifiers were produced from different vegetable oils namely mahogany, neem and calabash. A total of 30 demulsifier formulations were produced using starch, paraffin oil, camphor and detergent. Synthetic oil field brine was prepared by mixing Bonny light crude oil from Kaduna Refining and Petrochemical Company, (KRPC) with brine. 0.5, 1.0, 1.5, 2.0, and 2.5 ml of these demulsifiers were mixed thoroughly with crude oil and allowed to settle. Mahogany and neem based demulsifiers containing 10 % oil had the highest separation of 78 and 77% respectively.

Keyword: production, mahogany oil, neem oil, crude oil, demulsifier, calabash.

1.0 Introduction

Demulsification or emulsion breaking is one of the methods used to treat the problem of water-in-oil emulsion [1]. Due to more and more severe environmental challenges, there is a need in the oil production to limit the use of chemicals and to utilize safer formulations which are less toxic and also as efficient as chemical demulsifiers. According to Oseghale *et al.*, [2] Emulsion of oil and water is one of many problems encountered in the petroleum industry. During production, crude oil normally mixed with water requiring separation before processing. In most cases, the water is dispersed in water as tiny droplets called emulsion of oil in water [3]. However, the emulsion of water in oil is aided by some chemical agents which at one end attract water (hydrophilic end) and at the other end attracts oil (lipophilic end). The component of emulsion agents that attract water is ionic in nature while the other component is a hydrophobic organic component [4]. These agents called surfactants locate themselves at the water-oil interface thereby forming interfacial films. The stability of the emulsion depends on its viscosity and droplet size. The higher the viscosity of emulsion and the thinner the droplet size lead to an increase in emulsion stability [4]. Some common naturally occurring emulsifiers are lecithin, proteins, gums and fatty

acid esters. Their Hydrophilic Lipophilic Balance (HLB) determines the type of emulsion formed. HLB 1-6 favours water in oil emulsion while HLB greater than 8 favours oil in water emulsion [4]. In petroleum refining, water-oil emulsion is also formed by washing oil in the desalting unit of crude oil processing [5]. This washing is necessary to avoid corrosion of the machine during the refining process due to the presence of some metal particles in the crude. Emulsion breaking is achieved as a result of three main mechanisms known as flocculation, coagulation and coalescence.

Commercial demulsifiers are generally polymeric surfactants such as copolymer of polyoxyethylene and polypropylene or alkylphenol formaldehyde resins or blends of various surface-active substances which contains methylbenzene, a chemical that causes damage to the organisms of the surrounding environment. After the treatment with the commercial demulsifier, the waste water is discharged into the water bodies. Due to this discharge, underground water and aquatic life are directly exposed to these chemical substances contained in the water. These water have become acidified as well as have some unacceptable level of alkaline property and therefore highly toxic. During crude oil processing, packaging and delivery process, land and air can be contaminated by these chemicals which are mainly caused by chemical spillage [6].



The use of natural oils for demulsifier synthesis is theorized to have less toxic effect on the environment. This research is focused on production of demulsifier for crude oil using locally sourced vegetable oils mahogany, neem and calabash. These oils are relatively low cost and are environmentally friendly as compared to synthetic surfactants used in commercial demulsifiers.

2.0 Materials and Methods

2.1 Materials

Materials used in this study include; Mahogany oil, neem oil, calabash oil, camphor, paraffin oil, starch, liquid soap and distilled water. The apparatus used were; density bottle, hot plate magnetic stirrer, weighing balance, beakers, syringe, graduated bottles, centrifuge machine, thermometer, plastic buckets and water bath.

2.2 Experimental

2.2.1 Preparation of Oil Field Brine

Bonny light crude oil which was obtained from KRPC was dissolved in 3 g of sodium chloride solution to prepare synthetic oil field brine. This is done to obtain similar salinity with that of crude used in KRPC which is about 2.4% [7] as presented in equation 1

$$Y = 8.3566x - 0.3582 \dots \dots \dots (1)$$

Y = Salinity (%w/w); % in per thousand

X = NaCl concentration (g/100 mL)

2.2.2 Emulsion Preparation

Distilled water amounting to a volume of 50 mL was mixed with 50 mL of oilfield brine in the ratio (1:1v/v). A mechanical stirrer was operating at a speed of 1300 rpm was used to agitate the mixture for 3 hours to get a stable emulsion.

2.2.3 Extraction of Oil

Apart from calabash seed which was bought from Katsina, mahogany and neem seeds were harvested within NARICT environs. The seeds were dehauled and extracted in the NARICT neem laboratory using mechanical press.

2.2.4 Production of Liquid Soap from Locally Sourced Materials

A solution of 192 g of Sodium Laurel Sulphate (SLS), 270 g Sodium Trioxocarbonate (IV) (Na₂CO₃) and 520 g of Sulphonic acid was prepared in a bowl and set aside. 125 g of Sodium Hydroxide (NaOH) was soaked in 150 g of distilled water for 24 hours in a bowl. Meanwhile, the solution of sodium hydroxide and distilled water, including the prepared sulphonic acid was then added to the solution of sodium laurel sulphate, sodium Trioxocarbonate (IV) and sulphonic acid. The mixture was gently stirred and more distilled water was added to produce a homogeneous mixture of 10 litres with a pH of 9.0.

2.2.5 Production of Local Starch from Cassava

Cassava starch was made by purchasing some quantity of dry cassava starch from a local market around Sabon Gari market in Zaria. Some quantity of distilled water was made to boil on a gas burner at 100 °C and 262 g of the dry cassava starch which was dissolved in 261 g of cold distilled water to form a solution was added. 300.9 g of the boiled distilled water was then added to the starch solution and gently stirred to form a paste-like solution.

2.2.6 Production of Local Demulsifiers

The production of the demulsifier involved three steps. First, formation of the lipophilic end, then the hydrophilic end, and lastly, the addition of the binder to bind the above two ends. 25 g of camphor powder was measured and poured into a beaker containing 15 g of mahogany oil, placed on a heated hot plate at a regulated temperature of 40 °C and gently stirred to completely dissolve the camphor. 10 g of paraffin oil was then added to the hot camphorated Mahogany oil. Next, 30 g of prepared cassava starch was added to the mixture while stirring still continued. Finally, 20 g of prepared liquid soap was added to the entire mixture and stirred gently for 60 minutes on the heated hot plate to obtain a homogenous blend of local demulsifier. This same method was also applied to Neem and Calabash oils. Ten formulations of each of the three vegetable oils were prepared with different ratio of the components as presented in Tables 1, 2 and 3 respectively.

Table 1: Formulation of Demulsifier from Mahogany Oil

Components	M1	M2	M3	M4	M5	M6	M7	M8	M9	M10
------------	----	----	----	----	----	----	----	----	----	-----



Oil	35	15	34	20	33	20	32	10	31	0
Camphor	5	5	6	0	7	15	8	10	9	20
Starch	5	25	6	10	7	10	8	0	9	10
Paraffin oil	25	25	24	35	23	35	22	40	21	50
Soap (g)	30	30	30	35	30	20	30	40	30	20

Table 2: Formulation of Demulsifier from Neem Oil

Components	N 1	N 2	N 3	N 4	N 5	N 6	N 7	N 8	N 9	N 10
Oil (g)	35	15	34	20	33	20	32	10	31	0
Camphor (g)	5	5	6	0	7	15	8	10	9	20
Starch (g)	5	25	6	10	7	10	8	0	9	10
Paraffin oil (g)	25	25	24	35	23	35	22	40	21	50
Soap (g)	30	30	30	35	30	20	30	40	30	20

Table 3: Formulation of Demulsifier from Calabash Oil

Components	C1	C2	C3	C4	C5	C6	C7	C8	C9	C10
Oil (g)	35	15	34	20	33	20	32	10	31	0
Camphor (g)	5	5	6	0	7	15	8	10	9	20
Starch (g)	5	25	6	10	7	10	8	0	9	10
Paraffin oil (g)	25	25	24	35	23	35	22	40	21	50
Soap (g)	30	30	30	35	30	20	30	40	30	20

3.0 Results and Discussion

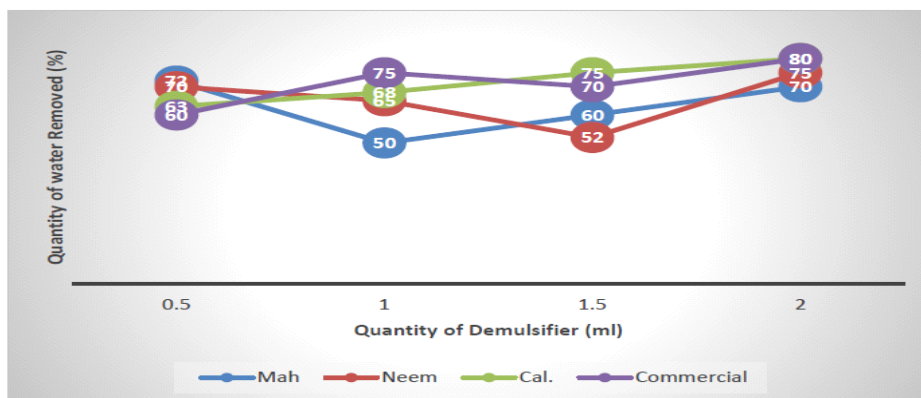


Figure1: Static Test Performance of bio-demulsifiers and commercial demulsifier



3.1 Static Test Performance

The result of the static test demulsification of Nigerian crude oil by bio-demulsifiers and commercial demulsifier shows good performance. Calabash seed oil demulsifier at 2 mL concentration had an equal performance as commercial one with 80% of quality water removal. This was closely followed by Neem seed oil with 75% quality water removal with the same quantity as depicted in Figure 1 unlike the other samples which depicted hazy water with these results, in terms of quality water removal, Calabash seed oil demulsifiers can conveniently replace commercial demulsifiers. For the sake of environmental degradation, Neem seed oil demulsifiers can also be considered to be better than the commercial ones.

3.2 Thermal Test

In the thermal test, all the bio-demulsifiers performed very well especially the calabash seed oil demulsifier which exhibited the same performance as commercial. Both have their best performance of 80% water removal with the quantity of 2 mL when subjected to same temperature and time. closely followed by Neem demulsifier, 75% and Mahogany 70%. Though Mahogany demulsifier is the best when considered with respect to the concentration of demulsifier used, its thermal performance is 72% water removal with 0.5 mL which was the highest at that quantity among demulsifiers as depicted in Figure 2.

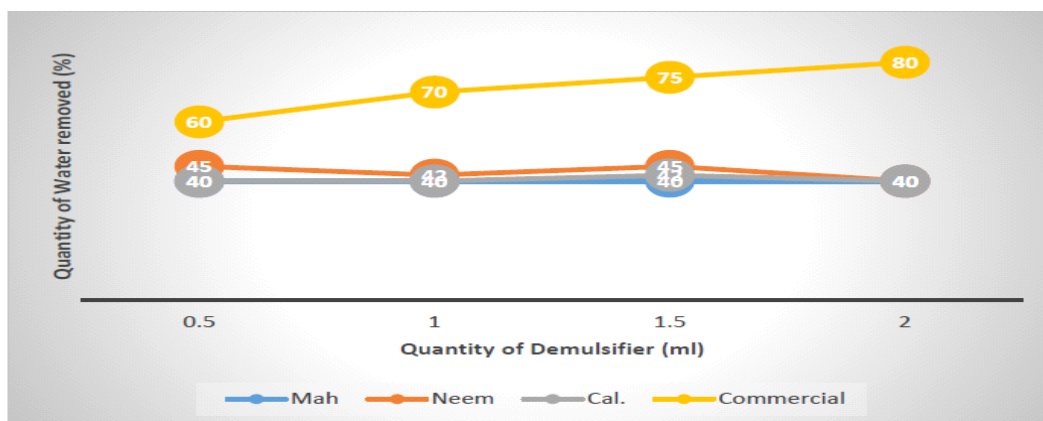


Figure 2: Thermal Test Performance of bio-demulsifiers and commercial demulsifier

3.3 Basic Sediment and Water Removal Test

Basic sediment and water removal test is to determine the least amount of demulsifier used. In this result, Neem seed oil demulsifier shows very good performance very close to commercial

demulsifier. 1.5 mL Neem seed oil demulsifier had 75% basic sediment and water removal while commercial demulsifier had its best with 1.0 mL quantity separated 78% basic sediment and water as shown in Figure 3.

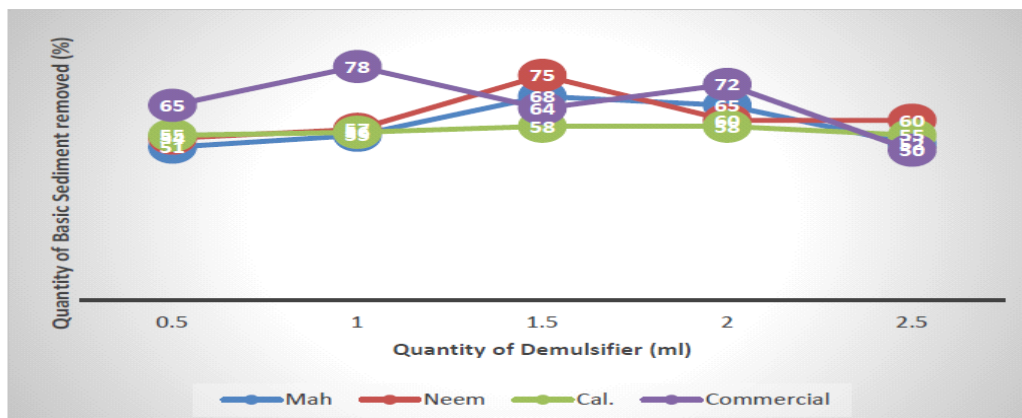


Figure 3: Basic Sediment and water Performance of bio-demulsifiers and commercial demulsifier.



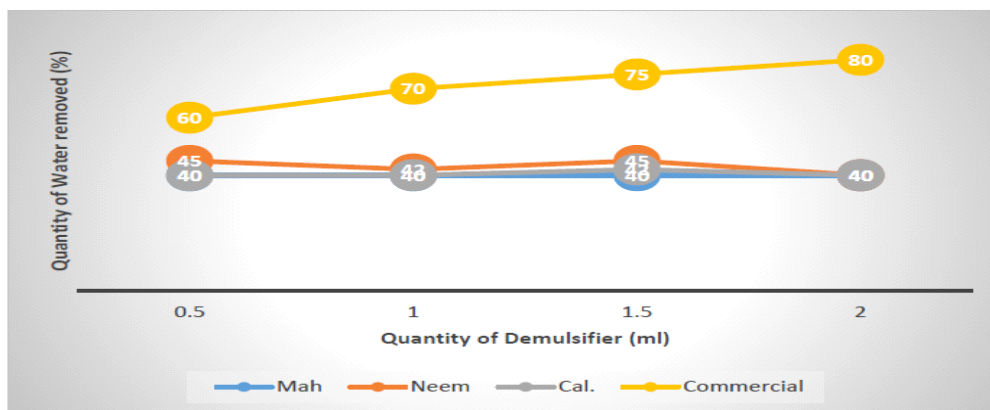


Fig 4. Dynamic test

3.4 Dynamic Test

None of the bio-demulsifiers could be compared with commercial demulsifiers for dynamic test performance because this test is to determine the amount of water being separated in a short space of time. The commercial demulsifier had a performance of 60% water removal with 0.5 mL and this increases with its quantity to 80%. The bio-demulsifiers had a very low performance with the highest of 45% water removal by Neem seed oil demulsifier with 0.5 and 1.5 mL. The other two had their highest performance of 40% water removal as depicted in Figure 4.

3.5 Demulsification Efficiency

When the three best performing demulsifiers and the commercial (imported) one were tested for water separation performance under the same conditions of temperature and time, the amount of water separated, the quality of water separated and the amount of demulsifier used, their performances were compared as presented in Figure 5. The performance exhibited by the Mahogany demulsifier was almost the same as that of the commercial demulsifier with the difference of 0.5%. This also conformed to the result obtained by [1]. Due to the higher ester content of mahogany and neem, Mahogany demulsifier is good enough for desalting Nigeria crude oils followed by neem oil demulsifier.

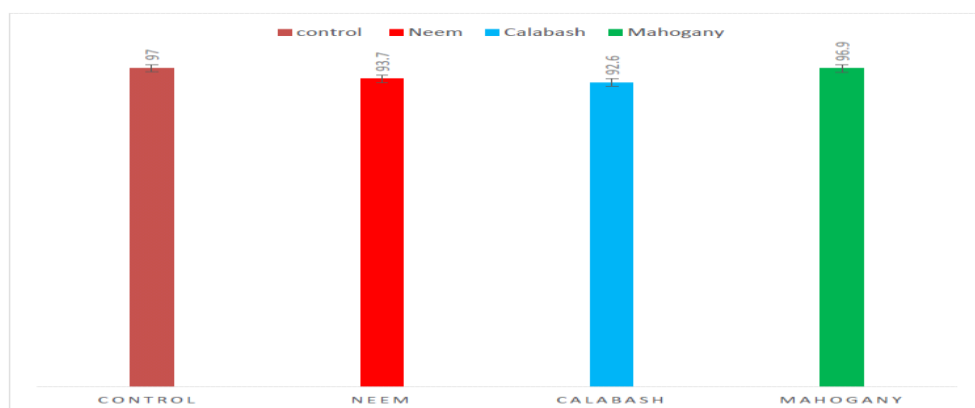


Figure 5: Efficiency test

4.0 Conclusion

The three oils were used to produce demulsifier which was used to demulsify Nigerian crude oil. The mahogany based demulsifier formulation showed the best performance at a density of 0.96 g/cm³ and a viscosity of 137 cP though the pH of the control demulsifier is 8.79 higher than the pH

3.8 of the emulsion. The density and viscosity of the emulsion is relatively low at 0.86 g/cm³ and 76.4 cP respectively which may have given rise to the result according to [8]. A demulsifier without addition of oil was produced and tested; the highest water removal was 65% from the formulation 0.5:50. Comparing the efficient test of the three local demulsifiers with imported commercial



demulsifier, mahogany demulsifier is good enough to replace the former. Mahogany separated 96.5% while commercial separated 97% with a margin of 0.5%.

5.0 References

1. P. C. N. Ejikeme, E. M. Ejikeme, and J. O. Okechukwu. Demulsification of Emulsified Crude Oil Using Local Demulsifier And Urea, 2019. <http://www.sciencepub.net/researcher>.
2. C. I. Oseghale, E. J. Akpabio and G. Udotong. Breaking of Oil -Water Emulsion for the Improvement of Oil Recovery Operations in the Niger Delta Oilfields. *International Journal of Engineering and Technology* Volume 2 No. 11, November, 2012.
3. T. Erfando, S. Chlahyam and R. Novia, The Utilization of Citrus hystrix and citrus liomnas an organic demulsifier formulation. *IOP Conference Series: Material Science and Engineering*. Doi:1088/1757-899x, 2019, pp1-10.
4. J. P. Clark. Emulsions: when oil and water do mix. *Food Technol*, 67(8), 2013, 1-9.
5. H. A. A. R. Ali. Preparation and evaluation of demulsifiers agents for Basra crude oil. *Applied Petrochemical Research*, 1(1), 2012, 29-33.6. B. Y. Abu and A. S Aliyu, performance assessment of plant extract as green demulsifier. *Journal of japan petroleum institute* 60, 4, 2017, 189 193.
7. O. A. Falode and O. C. Aduroja, Development of Local Demulsifier for Water-in-Oil Emulsion Treatment. *International Journal of Sciences: Basic and Applied Research (IJSBAR)* ISSN 2307-4531, 2015. pp301-318.
8. V. Venkatesham, M. Nasal, M. J. Robin, and G. Ginto. Studies on demulsification of crude oil emulsion using plant extracts as green demulsifiers. *Asian J Appl Sci Technol*, 2, 2018, 999-1004.



P098 - APPLICATION OF DEEP EUTECTIC SOLVENTS IN REMEDIATION OF CONTAMINATED WATER – A MINI REVIEW

Ugochi Judith Okoduwa^{1,2}, Edith Bolanle Agbaji², Victor Olatunji Ajibola², Adamu Uzairu², Zaharaddeen Sani Gano³, Jeffery Tsware Barminas¹.

Industrial and Environmental Pollution Department, National Research Institute for Chemical Technology, P.M.B 1052, Basawa Zaria.

Department of Chemistry, Ahmadu Bello University, Zaria.

Petrochemicals and Allied Department, National Research Institute for Chemical Technology, P.M.B 1052, Basawa Zaria

Email of corresponding author: judithsplendour@gmail.com

ABSTRACT

Water is a valuable resource that humanity has been blessed with. Overtime, its availability and purity have been of utmost concern as it affects every sphere of life. The need for potable water can therefore not be overemphasized as it forms the basis for human and animal life. Contamination of water bodies has been an issue over time and research is still ongoing in trying to curb this menace with regards to the particular types of contaminants. This review focuses on the removal of contaminants from water bodies using a green approach, deep eutectic solvents. Results show that this approach is feasible, safe, economical and perform better than conventional approaches.

Key words: *Deep eutectic solvents (DES), Micro wave, freeze drying, green chemistry, liquid liquid extraction (LLE)*

1.0 INTRODUCTION

The use of toxic chemicals to solve environmental problems has over time led to pollution of same (water, air and land), loss of arable land for farming, death of aquatic animals, man, and introduction of diseases which persist over time. These chemicals while helping to remove harmful contaminants from the affected environment, also leave some negative chemical foot prints which may take longer if ever to remove completely. These contaminants are usually lethal in very small quantities, are none biodegradable and have the tendency to bioaccumulate. In other to curb the use of toxic chemicals, scientists are beginning to look into new and novel ways of stemming the tide of destruction of life and the environment. In searching out better and safer methods, several factors come into play such as sample preparation methods involving very small quantities of reagents, the use of equipment that are selective, sensitive and very robust, minimizes waste, does not expose the

worker to harm, saves time, cost and energy (1, 2).

Clean water also known as potable water is a basic necessity for the well-being of man, plants and animals. Access to clean water has remained a major challenge in several parts of the world even though it occupies 70% of the Earth's crust. Water is life and its need cannot be over emphasized. It is used for domestic activities such as cooking, washing, bathing, drinking. Farmers need water for proper plant growth, industrially it is used to cool heavy machinery.

Over the years water has been contaminated most times due to the activities of man which include but not limited to agricultural practices (run off containing fertilizers and pesticides), improper waste management, oil spills, radioactive waste discharge, chemical waste dumping. This contaminated water has led to health challenges, poor crop production, death of aquatic animals that sometimes lead to wiping off of species, loss of livelihood for fishermen, loss of revenue especially if such water bodies have been a tourist destination.



Water can be contaminated as a result of any one or more of the following

- i. Naturally occurring chemicals (argon, radon, uranium, fluoride) – Though beneficial in certain limits, the increase beyond acceptable limits poses a problem to the well-being of aquatic animals, crops where such water is applied, and ultimately humans who drink the water or use it for domestic purposes (3, 4).
- ii. Emerging contaminants- These are contaminants that have a new source and an alternate route to people or novel treatment approaches (5). The effluent from waste water treatment plants (WWTP) is one of the major sources of emerging contaminants which further finds its way into surface waters, sediments, soil and ground water (6). An example of these emerging contaminant which dates back to 2000 years ago is lead. This was as a result of the over exploitation of lead mines by the Romans and Greeks. Emerging contaminants include but are not limited to nanomaterials, personal care products, pesticides, plasticizers, household cleaning products, industrial compounds, medicines and a host of others. These contaminants have also been defined as those contaminants who until recently have been regulated but there are still concerns about their impact on humans and the environment ((7).
- iii. Local land use practices (fertilizers, pesticides)- The use of fertilizers, pesticides, herbicides have also introduced harmful substances that find their way into water which in turn contaminates the ground water.
- iv. Manufacturing processes – Several companies make use of manufacturing processes that end up leaving traces of heavy metals and likely introduce contaminants to the water. Abandoned military sites, shooting ranges, hazardous waste sites play host to quite a number of toxic chemicals which find

their way to water sources like ground water (4)

- v. Sewer overflows or waste water releases- Poorly built and maintained sewage systems often experience overflows and release of its content which pollutes the environment. These waste water could be pharmaceutical in nature from hospitals/medical companies or even industries. Research has shown that untreated or poorly treated waste from sewage spills or overflows often elevates concentration of nutrients, pathogens, endocrine disruptors, heavy metals and pharmaceuticals in natural ecosystems (6, 8).
- vi. Oil spills – In different parts of the world, oil spills have remained a major cause of environmental pollution. Several methods have been used to curb or remediate this menace but sometimes, the methods employed have done more harm than good as can be seen years later in the health and welfare of inhabitants in the affected places (9). The BP deep-water horizon spill that occurred in 2010 is a typical example where there was a well blow out and millions of gallons of oil was spilled into the gulf coast. This led to death of aquatic animals, loss of source of income for fishermen, health challenges like rashes on the skin, muscle cramps, migraines, pneumonia and cough on the coastal citizens (10-13). High level of anxiety, depression which lasted for several years after the spill were also experienced by those living on the Gulf coast. Suffice to say that these health effects came years after the spill had been cleaned up.

1.1 Water decontamination technology

Several methods have been introduced in making water clean and healthy. Some of these methods are boiling, addition of chlorine and iodine, distillation, electron deionization, reverse osmosis, solar purification, activated carbon, clay vessel filtration and using a water



purifier. All these methods have shown ability in making contaminated water clean.

Activated carbon is a broad term used to describe amorphous carbonaceous adsorbents with a well-defined form and internal pore structure obtained by carbonization/roasting of any organic material (coconut shells, corn cobs, wheat straw, rice bran etc) and activation of its organic contents shells at very high temperature 800-1000°C to activate it (14, 15).

Reverse osmosis is a filtration technique which hinders the passage of a wide range of impurities to a high degree by using the particular properties of reverse osmosis membrane. Naturally the water with low concentration of contaminants will tend towards that of high concentration but the reverse is the case here where by applying pressure, the movement is opposite of what it normally would have been as it passes through a semi permeable membrane (16). Reverse osmosis is capable of removing up to 99% of dissolved particles, colloids, organics, bacteria, pyrogens and contaminants from feed water (17, 18)

Distillation being one of the oldest methods of water purification, involves the use of heat source to vaporize water from water systems thereby leaving organic contaminants such as arsenic, lead, barium, cadmium, nitrate, sodium, sulphate to mention but a few behind.

The use of UV light prevents the growth of micro-organisms and also removes organic compounds by oxidizing them to acidic species and finally converting them to carbon dioxide. UV light can also be used to remove chlorides and chloramine species from water(19). This is achieved in two ways. UV light at wavelength 253.7nm destroys DNA and RNA polymerase at low doses preventing replication while a lower wavelength of 185nm has a strong oxidizing action breaking down large organic molecules to smaller ones and then to carbon dioxide (20).

The main aim of the afore mentioned methods is to ensure that water is safe for whatever use

it might be put to and that aquatic life is preserved.

Green Chemistry seeks to introduce safe and healthy alternatives in chemical processes. It encourages the use of green alternatives that are in agreement with the principles of Green Chemistry which include the following (21)

- i. Prevention of waste to the barest minimum.
- ii. Atom economy whereby synthetic methods should be designed to maximize incorporation of all materials used in the process into the final product.
- iii. Where possible, synthetic methods must not result in hazardous chemical synthesis with detrimental effect to man or the environment.
- iv. Designing safe chemicals while maintaining efficacy and function.
- v. As much as possible, it is recommended to use safer solvents while working.
- vi. The entire chemical process must be designed for energy efficiency by operating under ambient temperature and pressure.
- vii. The use of renewable feedstock. This will ensure availability and biodegradability of such which will in turn not adversely affect the environment.
- viii. Reduce derivatives- Quite a number of syntheses require protecting or blocking steps which require extra reagents and in turn generate waste, the application of green chemistry suggests the use of enzymes that are specific in action thereby eliminating the need for derivatives.
- ix. Catalysis- A catalyst lowers the energy barrier of a reaction thereby speeding it up without being changed in the process. Hence catalysts are usually used in small quantities and can be used over and over again without generating waste.



- x. Design for degradation- Chemical products should be designed in a way that after performing the required function, they break down into harmless materials that will not persist in the environment.
- xi. Real time analysis for pollution prevention. Analytical methods where processes can be monitored in real time before the production of hazardous substances are produced is encouraged.
- xii. Safer chemistry for accident prevention. Substances used for chemical processes should be safe to eliminate or minimize harm in terms of releases, explosion, and fire to the worker.

1.2 Innovative Techniques in water remediation

The search for safer and greener solvents by scientists gave rise to the discovery of Ionic liquids (ILs) and Deep Eutectic Solvents (DES).

1.2.1 Ionic Liquids

Ionic liquids were introduced as a green alternative to the use of toxic chemicals. They are salts that remain liquid below 100°C or at room temperature(22). It's usually a combination of organic cations and organic or inorganic anions. Ethyl ammonium nitrate was the first ionic liquid reported in literature in 1914 (23).

Ionic liquids have the following characteristics (24)

- i. Very low vapor pressure under ambient conditions.
- ii. They remain liquid over a wide temperature.
- iii. They have excellent lubricating and hydraulic properties.
- iv. They possess tunable basicity and acidity trends.
- v. They are mostly colorless and polar in nature.
- vi. They can take in and release gases.
- vii. They are mostly hydrophilic.

- viii. They possess very low viscosity.

The limitations with the Ionic liquids which include but are not limited to poor biodegradability, significant toxicity, large amount of salts and reagents to completely exchange the anions, high cost of common ILs, synthesis and purification (25) which hampers their use in industry gave rise to deep eutectic solvents which have superior qualities to ionic liquids .

1.2.2 Deep Eutectic Solvents (DES)

The discovery of deep eutectic solvent began with Abbott and his co-workers looking for liquids that could overcome the moisture sensitivity and high cost of some common ionic liquids (26-28). In their study, quaternary ammonium salts and metal salts were tested. Choline chloride, zinc in ratio 1:2 presented the lowest freezing point of between 23°C to 25°C. They further investigated eutectic mixtures of quaternary ammonium salts and hydrogen bond donors and named them DES (27). The term eutectic is gotten from the Greek word eutektos which means easily melted. The eutectic point is the temperature and chemical composition at which a mixture of two solids become fully molten at the lowest melting temperature relative to that of either compound.

DES is a class of solvents made up of a combination of two or more compounds at room temperature which may be all solids or a combination of liquids and solids made up of a hydrogen bond donor (HBD) and a hydrogen bond acceptor (HBA) forming a eutectic liquid upon mixing, with melting point lower than that of the starting materials (29).



Zhang et al. 2012 defined DES as a composition of two or three safe and cheap components which are capable of associating with each other through their hydrogen bonds to form a eutectic mixture. It can be represented by the general formula $R_1R_2R_3R_4N^+X^-Y^-$ (30). They are usually formed by Lewis or Bronsted acids and bases which may contain a variety of anionic and/or cationic species.

A deep eutectic solvent is prepared by mixing two or more components which are capable of associating with each other through their hydrogen bond interactions. An example is Choline chloride (302°C) and urea (133°C) at 1:2 molar ratio giving a liquid mixture with a melting point of 12°C.

This phenomenon of having a product with a lower melting point was explained by (31) as a balance formed by all the species (choline chloride and urea) as a result of their intermolecular hydrogen bonding forces. The chloride is strongly affiliated with the choline and urea in an orderly manner while ensuring that crystals are not formed. Choline chloride also exhibits anisotropy which enables it to change or assume different properties. The lower melting point is also due to formation of intermolecular hydrogen bonding between the chloride anion of choline chloride and hydrogen bond donor (32) the presence of bulky, non-symmetrical ions with small lattice energy and

charge delocalization between the halide ion and Hydrogen bond donor (8, 32, 33).

Deep eutectic solvents have the following properties which make them more acceptable in recent times safe, easy to prepare, environmentally friendly, biodegradable, relatively cheap starting materials, reusable, greater designability with a wide range of HBDs and HBAs and molar ratios (34, 35).

DES have been classified into four as summed up in Table 1 and highlighted below (30, 36):

Type I DES comprises a combination of a quaternary salt with a metal chloride represented as $Y = MCl_x$ where $M = Zn, Sn, Fe, Al, Ga$.

Type II DES comprises a combination of a quaternary salt and a hydrated metal chloride represented as $Y = MCl_x \cdot yH_2O$, where $M = Cu, Co, Fe, Cr, Ni$

Type III DES comprises a hydrogen bond donor and hydrogen bond acceptor represented as $Y = R_5Z$ with $Z = -COOH, -OH, -CONH_2$

Type IV DES $Y =$ Metal chlorides (e.g $ZnCl_2$) mixed with HBDs such as urea, ethylene glycol, acetamide.

Type V DES HBA + hydroxyl compound attached to an aromatic ring e.g phenol

Table 1: Classes of DES(30, 36)

Types	General Formula	Terms	Example
I	$Cat^+X^- + MCl_x$	$M = Zn, Sn, Al, Ga$	$C_2mimCl + AlCl_3$
II	$Cat^+X^- + MCl_x \cdot yH_2O$	$M = Cr, Ni, Cu, Fe, Co$	$ChCl + MgCl_2 \cdot 6H_2O$ $ChCl + CrCl_3 \cdot 6H_2O$
III	$Cat^+X^- + R_5Z$	$Z = OH, COOH, CONH_2$	$ChCl + Urea (U)$
IV	$MnCl_x + RZ$	$M = Zn, Al$ $Z = OH, CONH_2$	$ZnCl + Urea (U)$
V	HBA + Hydroxyl compound		Thymol+ hexadecenoic acid Thymol+camphor

Cat^+ = any phosphonium, ammonium or sulfonium cation, X^- = a Lewis base, generally a halide anion, MCl_x = metal chloride, RZ = organic compound.

Deep eutectic solvents have found use in the fields of Chemistry, Pharmacy, as pharmaceuticals, Chemical Engineering, (36) as catalysts (37, 38), drug delivery system (39,

40), absorbents (41, 42), in biosensor development (43, 44), electrochemistry (45, 46), nanoscience, solvent extraction/separation (47), hydrometallurgy, polymer synthesis, CO_2



capture (48, 49), catalysis and electroplating , gas separation, removal of sulphur compounds (50), and a host of other applications.

2.0 SYNTHESIS OF DES

DES can be prepared by mixing a Hydrogen Bond Acceptor (HBA) and Hydrogen Bond Donor (HBD) in suitable ratios and at a suitable temperature. It can be synthesized by several methods which include:

2.1 Heating and stirring method

The components are placed in a beaker with a stirring bar and heated on a heating mantle to about 80°C until a liquid is formed. The process takes place in less than two hours (51, 52)

2.2 Evaporating Method

Components are dissolved in water and evaporated at 50°C using a rotary evaporator. The liquid obtained is collected, bottled and kept in a desiccator till when needed (52, 53).

2.3 Microwave Method

One of the most promising techniques for the development of more environmentally benign processes is the microwave method. It boasts of advantages such as i. higher yields ii. milder reaction conditions iii. shortest reaction times. In 2018, a group of researchers experimented with three different Natural Deep Eutectic Solvents (NADES) which were prepared and compared with those obtained by the heating, stirring method. The results showed comparable chemical and physical properties. Although synthesis time (time to form NADES) was 20secs and energy consumption was 650 times lower. (52, 53).

2.4 Freeze drying

In this method, choline chloride and urea in ratio 1:2 with a 5wt% solute content were prepared by mixing separate aqueous solutions of same. Subsequently, the mixed solutions were

frozen at 77 and 253K and freeze dried to produce a clear viscous DES (52, 54).

It can also be obtained by combining a quaternary ammonium salt and metal salts or HBD (urea, carboxylic acids) that has the ability to form a complex with the halide ion of the quaternary ammonium salt (30).

The use of DES not only allows the design of safer processes but also provides a straight forward access to new chemicals and materials.

3.0 DEEP EUTECTIC SOLVENTS IN EXTRACTION PROCESSES

The use of DES in remediating contaminated water have been researched by several workers. These types of DES are called Hydrophobic DES (HDES) because of their ability to not interact with water or their water hating character. They are a new generation of water immiscible solvents presented in literature for the first time in 2015 (55, 56).

The first time HDES was used was in the removal of Volatile Fatty Acids (VFA) from water. The HDES was based on a combination of decanoic acid and quaternary ammonium salts was used. In the end, this combination showed better extraction than the conventional industrial standard trioctyl amine. The extraction efficiency also increased with increase in the chain length of the VFA (56)

In 2016, Van Osch et al removed alkali and transition metal ions from water using ion exchange resin. In the research organic solvents like dodecane, toluene and kerosene were replaced with hydrophobic deep eutectic solvents consisting of decanoic acid and lidocaine in molar ratios 2:1, 3:1 and 4:1. The highlights of this study were i. all metals



could be extracted with high distribution coefficients. ii. low mass fractions of deep eutectic solvents. iii. maximum extraction efficiency was attained in 5s. iv. regeneration is possible (57).

Some other workers developed hydrophobic deep eutectic solvents for the removal of 4 neonicotinoids namely imidacloprid, acetamiprid, nitenpyram and thiamethoxam from dilute aqueous solutions. The DES used were DL Menthol and natural neutral organic acids such as acetic acid, hexanoic acid, octanoic acid, decanoic acid and dodecanoic acid. The other group of DES was quaternary ammonium salts (Tetrabutyl ammonium bromide) and organic acids such as levulinic acid, pyruvic acid, butyric acid. DL Menthol and TBAB formed the HBAs which were dried in a vacuum pump at 40°C for at least 4 days, the carboxylic acids were used without further purification. Stock solutions of the pesticides in Milli-Q water in different concentrations were prepared and used to plot a calibration curve $R^2 \geq 0.997$. Equal mass of each one of the aqueous solutions of the pesticides and the prepared HDES were put in contact and vigorously stirred for 4h at room temperature and left to settle for 24h to ensure complete separation of phases. A needed syringe was used to take a sample from the water rich phase for easy reading using UV-Vis (58)

HBA and HBD were mixed in a jacketed glass vessel, stirred at 350rpm and a temperature of 353.15K until a

homogenous liquid with no solids in it was obtained. The HBA and HBD were combined in ratios ranging from 1:1, 1:2, 2:1. The results showed extraction efficiencies up to 80% for the four pesticides using water stable DES based on DL Menthol and organic acids. Only chemically stable DES were used for extraction of the pesticides in order to prevent contamination of the water cycle while ensuring the possibility of reuse of the DES.

(29) used DES to purify water contaminated with ciprofloxacin which has been identified as one of the top ten micropollutants in water environments. The DES used consisted of a combination of DL Menthol and fatty acids (octanoic and decanoic acids etc) and those based on quaternary ammonium salts [N7777]Br, [N8888]Br, [N8881]Br and natural fatty acids. The solubility of ciprofloxacin in DES and the miscibility of water and DES were determined. Liquid liquid extraction was used to extract the micropollutant from water by first of all preparing stock solutions of the ciprofloxacin and plotting a calibration curve of micropollutant $R^2 \geq 0.993$. The HDES and water containing the ciprofloxacin were stirred at room temperature and left to settle for a minimum of 12h to ensure complete phase separation. Using a needed



syringe, a sample of the water rich phase was taken and analysed with a UV-Vis spectrophotometer. The results showed C12:C10 gave the best extraction efficiency of ciprofloxacin and it also displayed highest solubility value and lowest water solubility value of ciprofloxacin. In conclusion, the research showed excellent extraction efficiencies when cheap, neutral and natural DESs were used.

In another publication DES was used to remove Bisphenol A from water. Bisphenol A is an endocrine disruptor that sometimes mimics oestrogen in the body. Conventional water plants are not able to remove it completely. Bisphenol A has been used in packaging plastic medical devices and as a plasticizer in food and drink packaging. Ionic and neutral DESs were used for this research. Influential experimental parameters like stirring speed, contact time, initial concentration of Bisphenol A (BPA), DES/water ratio were optimized using Central Composite Design (CCD). All the selected HDES gave good extraction efficiencies due most likely to the hydrophobicity of the DES. It was observed that extraction efficiencies increased with increase in the alkyl chain length in both the fatty acid and quaternary ammonium salt. The best performance for all the studied systems

was achieved using the lowest HBA:HBD molar ratio (1:2) and initial concentration of BPA greatly influenced extraction efficiency which decreased as the concentration of BPA decreases (29).

Another set of workers removed Pb(II) from water using choline chloride based deep eutectic solvents functionalized carbon nano tubes (59). The presence of lead (Pb) in water has led to a variety of health problems especially in children. The effects can be so bad as it affects the nervous system which causes brain disorders. Lead contamination could be as a result of corrosion of plumbing material of waste disposal associated with certain industries.

In this work, DES was synthesized by combining Choline chloride as hydrogen bond acceptor (HBA) with ethylene glycol (EG), Diethylene glycol (DEG), glycerol (Gly), triethylene glycol (TEG), Urea (U), Malonic acid (MA) all serving as Hydrogen bond donor (HBD) stirring at 400rpm and 80 °C until a DES is formed as a clear liquid without precipitates. At the end of the research, the optimum Pb (II) removal condition were found to be pH 5, adsorbent dosage of 5mg and contact time of 15minutes. Pb (II) adsorption system fitted excellently to a pseudo second order kinetics model.



Other methods have been employed in removing Pb from water. Top on the list is the use of adsorbent materials such as maize cobs, rice husks, saw dust (60), aquatic plants (61), kaolinitic clay, giru clay (62).

The same workers researched the removal of mercury from water using Ally triphenyl phosphonium bromide based DES- functionalized carbon nanotubes (63). Mercury has been identified as one of the most toxic elements in nature which affects neurologic, gastrointestinal and renal systems. It can be found in different forms such as a metallic element, organic salt and an inorganic salt (64). As a result of the toxic nature of mercury the WHO allowable limit in water is $1\mu\text{gL}^{-1}$ (65). Several techniques such as extraction, precipitation, ion-exchange, reverse osmosis, coagulation, photo remediation have been used to decrease mercury pollution in water overtime. Carbon nano tubes (CNTs) despite their draw backs have been successfully utilized in removing cadmium (66), zinc (67), lead (68) and copper (67). Functionalization with DES was performed by sonicating 200mg of P-CNTs, K-CNTs, N-CNTs separately with 7ml of DES for 3h at 65°C . This resulted to PA- CNTs, KA-CNTs, NA-CNTs respectively. The result of their work showed functionalization with Ally

triphenyl Phosphonium bromide (ATPB) based DES significantly increases the removal percentage of mercury at pH 2.0 and 6.0. Removal increased with increasing pH. Of all the combinations (P-CNTs, K-CNTs, N-CNTs, PA-CNTs and NA-CNTs) used, KA-CNTs achieved the highest removal percentage.

4.0 CONCLUSION AND FUTURE OUTLOOK

From peer reviewed journals in literature, there is no doubt that incorporating DES in the removal of contaminants from aqueous environments is not only feasible but safe and can be used repeatedly in several cycles meaning it is of economic value and in most cases perform better than conventional methods. It is therefore expedient that further research be carried out with different combinations of HBAs and HBDs to test for their ability in remediating contaminated water.

REFERENCES

1. T. Huang *et al.*, An overview of graphene-based nanoadsorbent materials for environmental contaminants detection. *TrAC Trends in Analytical Chemistry* **139**, 116255 (2021).
2. T.-L. Chen *et al.*, Implementation of green chemistry principles in circular economy system towards sustainable development goals: Challenges and perspectives. *Science of the Total Environment* **716**, 136998 (2020).



3. M. B. Shakoor *et al.*, Human health implications, risk assessment and remediation of As-contaminated water: a critical review. *Science of the Total Environment* **601**, 756-769 (2017).
4. R. P. Schwarzenbach, T. Egli, T. B. Hofstetter, U. Von Gunten, B. Wehrli, Global water pollution and human health. *Annual review of environment and resources* **35**, 109-136 (2010).
5. R. Kumar *et al.*, A review on emerging water contaminants and the application of sustainable removal technologies. *Case Studies in Chemical and Environmental Engineering* **6**, 100219 (2022).
6. M. Taheran, M. Naghdi, S. K. Brar, M. Verma, R. Y. Surampalli, Emerging contaminants: Here today, there tomorrow! *Environmental Nanotechnology, Monitoring & Management* **10**, 122-126 (2018).
7. T. Rasheed, M. Bilal, F. Nabeel, M. Adeel, H. M. Iqbal, Environmentally-related contaminants of high concern: potential sources and analytical modalities for detection, quantification, and treatment. *Environment international* **122**, 52-66 (2019).
8. Y.-L. Loow *et al.*, Deep eutectic solvent and inorganic salt pretreatment of lignocellulosic biomass for improving xylose recovery. *Bioresource technology* **249**, 818-825 (2018).
9. B. Ordinioha, S. Brisibe, The human health implications of crude oil spills in the Niger delta, Nigeria: An interpretation of published studies. *Nigerian medical journal: journal of the Nigeria Medical Association* **54**, 10 (2013).
10. M. A. D'Andrea, G. K. Reddy, The development of long-term adverse health effects in oil spill cleanup workers of the Deepwater Horizon offshore drilling rig disaster. *Frontiers in Public Health* **6**, 117 (2018).
11. B. Laffon, E. Pásaro, V. Valdiglesias, Effects of exposure to oil spills on human health: Updated review. *Journal of Toxicology and Environmental Health, Part B* **19**, 105-128 (2016).
12. J. Nriagu, E. A. Udofia, I. Ekong, G. Ebuk, Health risks associated with oil pollution in the Niger Delta, Nigeria. *International journal of environmental research and public health* **13**, 346 (2016).
13. O. I. Akinbobola, Environmental worry of River State residents in the Niger delta region, Nigeria. *Psychology* **5**, 32 (2014).
14. A. Bhatnagar, W. Hogland, M. Marques, M. Sillanpää, An overview of the modification methods of activated carbon for its water treatment applications. *Chemical Engineering Journal* **219**, 499-511 (2013).
15. R. I. Kosheleva, A. C. Mitropoulos, G. Z. Kyzas, Synthesis of activated carbon from food waste. *Environmental Chemistry Letters* **17**, 429-438 (2019).
16. M. Abd El-Salam, Membrane techniques| applications of reverse osmosis. (2003).
17. S.-k. Park, J. Y. Hu, Assessment of the extent of bacterial growth in reverse osmosis system for improving drinking water quality. *Journal of Environmental Science and Health Part A* **45**, 968-977 (2010).
18. A. E.-C. Lopera, S. G. Ruiz, J. M. Q. Alonso, Removal of emerging contaminants from wastewater using reverse osmosis for its subsequent reuse: pilot plant. *Journal of Water Process Engineering* **29**, 100800 (2019).
19. R. James, Dechlorination by ultraviolet radiation: a suitable alternative to activated carbon in dialysis water systems? *Journal of Renal Care* **35**, 205-210 (2009).
20. J. P. Chen, L. Yang, L. K. Wang, B. Zhang, in *Advanced physicochemical treatment processes*. (Springer, 2006), pp. 317-366.
21. P. T. Anastas, J. B. Zimmerman. (ACS Publications, 2003).



22. A. Benedetto, Room-temperature ionic liquids meet bio-membranes: the state-of-the-art. *Biophysical reviews* **9**, 309-320 (2017).
23. S. Sugden, H. Wilkins, CLXVII.—The parachor and chemical constitution. Part XII. Fused metals and salts. *Journal of the Chemical Society (Resumed)*, 1291-1298 (1929).
24. S. K. Singh, A. W. Savoy, Ionic liquids synthesis and applications: An overview. *Journal of Molecular Liquids* **297**, 112038 (2020).
25. A. El-hoshoudy, F. Soliman, E. Mansour, T. Zaki, S. Desouky, Experimental and theoretical investigation of quaternary ammonium-based deep eutectic solvent for secondary water flooding. *Journal of Molecular Liquids* **294**, 111621 (2019).
26. A. P. Abbott *et al.*, Preparation of novel, moisture-stable, Lewis-acidic ionic liquids containing quaternary ammonium salts with functional side chains Electronic supplementary information (ESI) available: plot of conductivity vs. temperature for the ionic liquid formed from zinc chloride and choline chloride (2: 1). See <http://www.rsc.org/suppdata/cc/b1/b106357j>. *Chemical Communications*, 2010-2011 (2001).
27. A. P. Abbott, G. Capper, D. L. Davies, R. K. Rasheed, V. Tambyrajah, Novel solvent properties of choline chloride/urea mixtures. *Chemical communications*, 70-71 (2003).
28. A. P. Abbott, D. Boothby, G. Capper, D. L. Davies, R. K. Rasheed, Deep eutectic solvents formed between choline chloride and carboxylic acids: versatile alternatives to ionic liquids. *Journal of the American Chemical Society* **126**, 9142-9147 (2004).
29. C. Florindo, F. Lima, L. s. C. Branco, I. M. Marrucho, Hydrophobic deep eutectic solvents: a circular approach to purify water contaminated with ciprofloxacin. *ACS Sustainable Chemistry & Engineering* **7**, 14739-14746 (2019).
30. Q. Zhang, K. D. O. Vigier, S. Royer, F. Jérôme, Deep eutectic solvents: syntheses, properties and applications. *Chemical Society Reviews* **41**, 7108-7146 (2012).
31. O. S. Hammond, D. T. Bowron, K. J. Edler, Liquid structure of the choline chloride-urea deep eutectic solvent (reline) from neutron diffraction and atomistic modelling. *Green Chemistry* **18**, 2736-2744 (2016).
32. F. Chemat, H. Anjum, A. M. Shariff, P. Kumar, T. Murugesan, Thermal and physical properties of (Choline chloride+ urea+ l-arginine) deep eutectic solvents. *Journal of Molecular Liquids* **218**, 301-308 (2016).
33. A. Mohsenzadeh, Y. Al-Wahaibi, A. Jibril, R. Al-Hajri, S. Shuwa, The novel use of deep eutectic solvents for enhancing heavy oil recovery. *Journal of Petroleum Science and Engineering* **130**, 6-15 (2015).
34. Q. Wen, J.-X. Chen, Y.-L. Tang, J. Wang, Z. Yang, Assessing the toxicity and biodegradability of deep eutectic solvents. *Chemosphere* **132**, 63-69 (2015).
35. C. Florindo, L. C. Branco, I. M. Marrucho, Quest for green-solvent design: from hydrophilic to hydrophobic (deep) eutectic solvents. *ChemSusChem* **12**, 1549-1559 (2019).
36. E. L. Smith, A. P. Abbott, K. S. Ryder, Deep eutectic solvents (DESs) and their applications. *Chemical reviews* **114**, 11060-11082 (2014).
37. H. Mąka, T. Szychaj, J. Adamus, Lewis acid type deep eutectic solvents as catalysts for epoxy resin crosslinking. *RSC advances* **5**, 82813-82821 (2015).
38. S. Khandelwal, Y. K. Tailor, M. Kumar, Deep eutectic solvents (DESs) as eco-friendly and sustainable solvent/catalyst systems in organic transformations. *Journal of Molecular Liquids* **215**, 345-386 (2016).



39. S. Emami, A. Shayanfar, Deep eutectic solvents for pharmaceutical formulation and drug delivery applications. *Pharmaceutical development and technology* **25**, 779-796 (2020).
40. N. R. Mustafa, V. S. Spelbos, G.-J. Witkamp, R. Verpoorte, Y. H. Choi, Solubility and stability of some pharmaceuticals in natural deep eutectic solvents-based formulations. *Molecules* **26**, 2645 (2021).
41. L. Moura *et al.*, Deep eutectic solvents as green absorbents of volatile organic pollutants. *Environmental Chemistry Letters* **15**, 747-753 (2017).
42. K. Chandran, C. F. Kait, C. D. Wilfred, H. F. M. Zaid, A review on deep eutectic solvents: Physicochemical properties and its application as an absorbent for sulfur dioxide. *Journal of Molecular Liquids* **338**, 117021 (2021).
43. W. da Silva, M. E. Ghica, C. M. Brett, Biotoxic trace metal ion detection by enzymatic inhibition of a glucose biosensor based on a poly (brilliant green)-deep eutectic solvent/carbon nanotube modified electrode. *Talanta* **208**, 120427 (2020).
44. R. Svirgelj, N. Dossi, C. Grazioli, R. Toniolo, Deep eutectic solvents (DESs) and their application in biosensor development. *Sensors* **21**, 4263 (2021).
45. H. Cruz *et al.*, Alkaline iodide-based deep eutectic solvents for electrochemical applications. *ACS Sustainable Chemistry & Engineering* **8**, 10653-10663 (2020).
46. C. M. Brett, Deep eutectic solvents and applications in electrochemical sensing. *Current Opinion in Electrochemistry* **10**, 143-148 (2018).
47. D. V. Wagle, H. Zhao, G. A. Baker, Deep eutectic solvents: sustainable media for nanoscale and functional materials. *Accounts of chemical research* **47**, 2299-2308 (2014).
48. G. García, S. Aparicio, R. Ullah, M. Atilhan, Deep eutectic solvents: physicochemical properties and gas separation applications. *Energy & Fuels* **29**, 2616-2644 (2015).
49. Y. Zhang, X. Ji, X. Lu, in *Novel materials for carbon dioxide mitigation technology*. (Elsevier, 2015), pp. 87-116.
50. S. Sun, Y. Niu, Q. Xu, Z. Sun, X. Wei, Efficient SO₂ absorptions by four kinds of deep eutectic solvents based on choline chloride. *Industrial & Engineering Chemistry Research* **54**, 8019-8024 (2015).
51. Y. Dai, J. van Spronsen, G.-J. Witkamp, R. Verpoorte, Y. H. Choi, Natural deep eutectic solvents as new potential media for green technology. *Analytica chimica acta* **766**, 61-68 (2013).
52. A. P. Santana *et al.*, Sustainable synthesis of natural deep eutectic solvents (NADES) by different methods. *Journal of Molecular Liquids* **293**, 111452 (2019).
53. F. J. Gomez, M. Espino, M. A. Fernández, M. F. Silva, A greener approach to prepare natural deep eutectic solvents. *ChemistrySelect* **3**, 6122-6125 (2018).
54. M. C. Gutiérrez, M. L. Ferrer, C. R. Mateo, F. del Monte, Freeze-drying of aqueous solutions of deep eutectic solvents: a suitable approach to deep eutectic suspensions of self-assembled structures. *Langmuir* **25**, 5509-5515 (2009).
55. D. J. Van Osch, C. H. Dietz, S. E. Warrag, M. C. Kroon, The curious case of hydrophobic deep eutectic solvents: A story on the discovery, design, and applications. *ACS Sustainable Chemistry & Engineering* **8**, 10591-10612 (2020).
56. D. J. van Osch, L. F. Zubeir, A. van den Bruinhorst, M. A. Rocha, M. C. Kroon, Hydrophobic deep eutectic solvents as water-immiscible extractants. *Green Chemistry* **17**, 4518-4521 (2015).
57. D. J. van Osch *et al.*, Removal of alkali and transition metal ions from water with hydrophobic deep eutectic



- solvents. *Chemical Communications* **52**, 11987-11990 (2016).
58. C. Florindo, L. Branco, I. Marrucho, Development of hydrophobic deep eutectic solvents for extraction of pesticides from aqueous environments. *Fluid Phase Equilibria* **448**, 135-142 (2017).
 59. M. K. AlOmar *et al.*, Lead removal from water by choline chloride based deep eutectic solvents functionalized carbon nanotubes. *Journal of Molecular Liquids* **222**, 883-894 (2016).
 60. N. Abdel-Ghani, M. Hefny, G. A. El-Chaghaby, Removal of lead from aqueous solution using low cost abundantly available adsorbents. *International Journal of Environmental Science & Technology* **4**, 67-73 (2007).
 61. N. R. Axtell, S. P. Sternberg, K. Claussen, Lead and nickel removal using *Microspora* and *Lemna minor*. *Bioresource technology* **89**, 41-48 (2003).
 62. F. F. Orumwense, Removal of lead from water by adsorption on a kaolinitic clay. *Journal of Chemical Technology & Biotechnology: International Research in Process, Environmental AND Clean Technology* **65**, 363-369 (1996).
 63. M. K. AlOmar *et al.*, Allyl triphenyl phosphonium bromide based DES-functionalized carbon nanotubes for the removal of mercury from water. *Chemosphere* **167**, 44-52 (2017).
 64. L. R. Goldman, M. W. Shannon, C. o. E. Health, Technical report: mercury in the environment: implications for pediatricians. *Pediatrics* **108**, 197-205 (2001).
 65. D. Mohan, V. K. Gupta, S. Srivastava, S. Chander, Kinetics of mercury adsorption from wastewater using activated carbon derived from fertilizer waste. *Colloids and Surfaces A: Physicochemical and Engineering Aspects* **177**, 169-181 (2001).
 66. M. Ruthiraan *et al.*, Comparative kinetic study of functionalized carbon nanotubes and magnetic biochar for removal of Cd²⁺ ions from wastewater. *Korean journal of chemical engineering* **32**, 446-457 (2015).
 67. N. Mubarak, J. Sahu, E. Abdullah, N. Jayakumar, Removal of heavy metals from wastewater using carbon nanotubes. *Separation & Purification Reviews* **43**, 311-338 (2014).
 68. Y.-H. Li *et al.*, Lead adsorption on carbon nanotubes. *Chemical physics letters* **357**, 263-266 (2002).



P099 - COMPUTATIONAL ESTIMATION OF HEXANE SELECTED THERMODYNAMIC PROPERTIES: USING PROCESS AND ATOMIC-SCALE SIMULATIONS IN CONTRAST WITH EXPERIMENTS

Odih Charles^{1,2}, Umar M. Mogaji^{1,2}, Raliat Abdullahi^{1,2}, Lucia C. Kuyet^{1,2}, Olorunfemi Sharon^{1,2}, Amina Abbas^{1,2}, Abdu Gerson^{1,2}, Abubakar M. Salihu^{1,2}, Muhammad G. Haruna^{1,2}, and Toyese Oyegoke^{2,*}

¹The C2 and C6 Group of 2023 ProMolSim – Process Thermodynamic Subjects, Pencil Team. ²Chemical Engineering Department, Faculty of Engineering, Ahmadu Bello University Zaria, Nigeria.

*Corresponding author email: OyegokeToyese@gmail.com

ABSTRACT

Thermodynamics is a fundamental cornerstone in chemical processes and product design, encompassing property prediction, process simulation, energy integration, and feasibility studies. This study focuses on estimating thermodynamic properties, specifically targeting hexane, through a dual approach employing process simulations and atomic-scale simulations. The investigation aims to assess the accuracy of these methods in representing hexane's behavior in gaseous and liquid phases. The results highlight DFT, particularly the B3LYP model, as remarkably precise in capturing hexane's vibrational characteristics, outperforming the semi-empirical PM3 method. However, the choice of simulation method depends on the prevailing phase conditions, with process simulations, notably COCO, closely mirroring experimental values, especially for entropy and enthalpy in the liquid phase. In contrast, DWSim exhibits limitations in accuracy. In conclusion, this study emphasizes the pivotal role of accurate thermodynamic property predictions in diverse industrial applications. It underscores the need to select the most suitable simulation method based on the specific phase conditions, offering valuable insights into the reliability of different techniques for estimating thermodynamic properties.

KEYWORDS

Process, Modeling, Simulation, DFT, PM3, Thermodynamics, Property, Alkane.

1.0 INTRODUCTION

The significance of thermodynamics to the design of chemical processes and products cannot be overemphasized. Some vital applications of thermodynamics to chemical process engineering include compound properties prediction, process simulation, process modeling, energy integration, chemical process feasibility studies, and more (1–3). In the design of chemical products, especially via atomic-scale modeling and simulation, it aids helps in the scale-up process of obtaining the macroscopic thermodynamic properties from their respective molecular properties (4–7).

A survey of the works reported in the literature shows that several thermodynamic models have been developed to predict molecules or compounds' properties. These thermodynamic models include Wilson, UNIFAC, NRTL, Peng Robinson (PR), Raoult Law (RL), UNIQUAC, and more (1, 3, 5, 8). These thermodynamic models could be categorized into either equation-of-state or activity coefficient-based models. They have shown better fitting for

predicting some selected compounds that are either gaseous or liquid, polar or non-polar, and a lot more. The subject of what thermodynamic model best suits the process simulation of a particular process has continued to be a subject in process modeling and simulation. Likewise, the issue of best approximating the molecular properties for gas-phase, liquid-phase, or surface species into macroscopic thermodynamic properties during the atomic-scale simulation like density functional theory, semi-empirical theory, and molecular mechanics calculations (1, 9, 10).

In the realm of chemical engineering and molecular research, the accurate estimation of thermodynamic properties holds a central role and is crucial. These properties are vital to unraveling the intricacies of chemical processes across a wide range of industries, from energy to pharmaceuticals and environmental sciences. This investigation uses computational simulations to estimate selected thermodynamic properties of hexane using process and atomic-scale simulation.



2.0 COMPUTATIONAL MATERIALS AND METHODS

2.1 Material Employed in the Study

In the study, we deployed both process and molecular simulators. A choice of two freeware process simulators, DWSim (11) and COCO v3.7 (12), while the selection of Spartan v20 (13) as the only molecular simulator was made.

2.2 Computational Methods and Details

In the modeling and simulating of the thermodynamic properties using process simulation, the technique or procedure generally reported in the literature (8) was employed across the two simulators (DWSim and COCO) (11, 12). In the analysis, we assessed using some selected thermodynamic models like Peng Robinson (PR) and Solvay Redlich–Kwong (SRK) from the equation of state model types (5, 14). In contrast, the NRTL and UNIQUAC models from activity coefficient model types (1, 5) were evaluated.

Moreover, we employed the use of the atomic-scale modeling approach via the use of DFT (B3LYP, 6-31G*) and Semi-empirical (PM3) models (15) to calculate the infrared spectrum, electronic energies, and other molecular properties of hexane, including the thermodynamic properties. The molecule was built using the Spartan v20 software (13), and their

various IRs, which will be seen in the later sections, were calculated, and other molecular properties using the earlier mentioned models. The experimental spectra were sourced from an online Spartan database, which was used to fit the calculated spectrum by the DFT and PM3 models. The automatically computed thermodynamic properties (Enthalpy, Entropy, and Heat capacity) from Spartan v20 (13) for using DFT (B3LYP, 6-31G*) and Semi-empirical (PM3) were compared with the experiment and the process simulation outputs.

3.0 RESULTS AND DISCUSSIONS

Here, we present our findings from the validation of the model used at atomic-scale simulation, the predicted properties obtained from both the process and atomic-scale simulation in contrast with the experiment for hexane molecule.

3.1 Model Validation Using IR Spectra

The modeling and calculation of the infrared spectrum of hexane molecules with a corresponding match of an experimental spectrum accessed via an online database are generally presented in Figure 1. The approach of matching the IR spectra computed with experimental ones was to assess the model's (B3LYP or PM3) (15) ability to successfully represent the experimental hexane spectra in our simulation at the atomic scale.

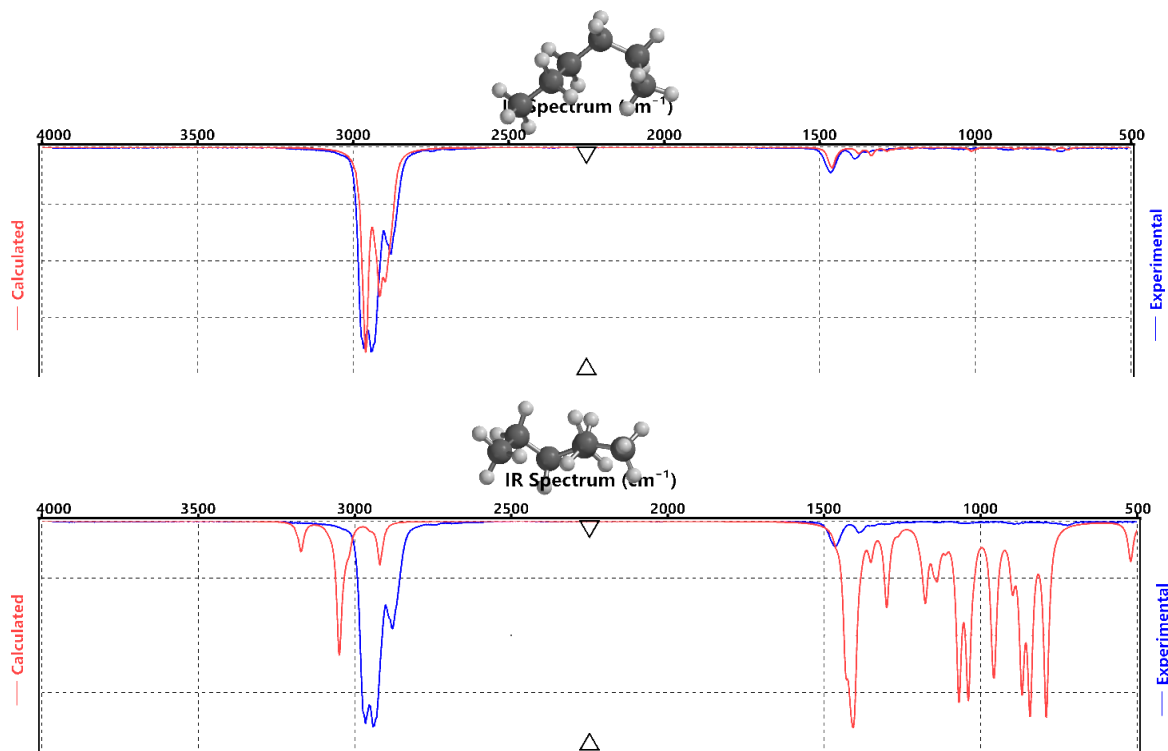


Figure 1: Hexane (C6-alkane) IR spectra obtained for B3LYP (above) and PM3 (below) in DFT and Semi-empirical calculations, respectively, with experimental spectra (13, 16).

Analysis of the result obtained for the hexane infrared (IR) spectra calculation using the DFT (B3LYP) calculation shows a better match and a good agreement with the one reported in the experiment, as shown in Figure 1. Contrary to the spectra trend obtained for DFT, the use of semi-empirical calculation (PM3) calculations only shows a repeated mismatch was obtained for the peaks within the 1000-1500 cm⁻¹ (in experiment/PM3), a shift in the IR spectra peaks was observed within 2500-3500 cm⁻¹ (in experiment/PM3), while other parts of the spectra match well. The poor match of the PM3 could be associated with the approximations present in its calculation, unlike the case of DFT, which has lesser approximations. Comparing the spectra with the one reported in the literature (16) reveals that the PM3 computed spectra correlated better with the liquid phase hexane. In contrast, DFT correlated well with its gas phase form.

The computational time shows that the PM3 was fast due to the higher level of approximations or parameterization implemented to facilitate calculations. This approximation could be responsible for its deviation from the experimental data, and the lesser level of approximation in B3LYP must have aided its good match (15). Therefore, the analysis suggests using DFT in our further research to estimate the thermodynamic properties of hexane.

Table 1: Entropy (J/mol/K) of hexane molecule.

Simulator	PR	SRK	NRTL	UNIQUAC	DFT	NIST _L	NIST _G
COCO	297.28	295.40	296.42	296.42	350.47	296.06	388.82
DWSim	-91.45	-93.33	-105.84	-105.84	350.47	296.06	388.82

Moreover, the result obtained for using DFT in Table 1 showed a better agreement with the experimental results reported by NIST (16) for the gas phase of the hexane. This suggests that the automatic computation of species' thermodynamic properties in Spartan software treats the species as a gas phase species, accounting for a full degree of freedom for all contributions like rotation,

3.2 Estimation of Thermodynamic Properties

Here, the results obtained for the comparison of thermodynamic properties predicted for the use of the process simulation (DWSim and COCO) (11, 12), atomic-scale simulation, and experimental values reported in the NIST (16) online database. Tables 1 to 3 present the entropy, enthalpy, and heat capacity. The process simulation output confirmed that all hexane streams modeled at 298.15 K and 1 atm showed a vapor fraction 0. This suggests that the hexane at that condition would be liquid, which agrees with the literature (17) that shows that hexane exists in the liquid phase at room temperature.

3.2.1 Entropy Estimation

Analysis of the results collated for the estimation of hexane entropy in Table 1 using COCO (12) and DWSim (11) process simulators shows closely related values across the different thermodynamic packages assessed in the study, except for the result reported for DWSim, which only showed similarity across the equation of state models (5) like PR and SRK, and activity coefficient models (1) like NRTL and UNIQUAC. However, values obtained for COCO (12) showed a good relationship with the reported by NIST (16) for its liquid phase as 296.06 J/mol/K. A wide range of disagreement accounted for the entropy values reported for using DWSim (11) with the experimental result reported by NIST (16).

translation, vibration, and electronic effects in its calculation, which differs when treating liquid. Hence, Spartan automatic thermodynamic property estimators would not be advised for use in future analyses, not in the gas phase.



3.2.2 Enthalpy Estimation

Similar to the findings made for the analysis of entropy in Table 2, DWSim (11) needs to improve its thermodynamic properties prediction accuracy

due to the repeated difference or disagreement obtained for its predicted value for the hexane enthalpies using different thermodynamic models failed in comparison with the experimental value reported by NIST (16).

Table 2: Enthalpy (kJ/mol) of hexane molecule (**heat of formation).

Simulator	PR	SRK	NRTL	UNIQUAC	DFT**	NIST _L	NIST _G
COCO	-198.17	-198.80	-198.51	198.51	-164.30	-198.70	-167.20
DWSim	-31.23	-31.86	-31.56	-31.56	-164.30	-198.70	-167.20

The enthalpies reported for using different thermodynamic models in the COCO simulator (12) show a close agreement with the experimental values reported by NIST (16) for the liquid phase of

the hexane. The value obtained for using the DFT (18) consistently shows a better agreement with the values reported by NIST (16) for the hexane gas phase as -167.20 kJ/mol.

3.2.3 Heat Capacity Estimation

Moreover, Table 3 further shows the need for the DWSim (11) thermodynamic properties prediction model design to be improved due to its repeated disagreement with the experimental values reported in the literature, either for the liquid or gaseous phase of hexane. Contrary to the better prediction obtained for COCO (12), where the equation of state model (PR and SRK) shows a close relation to each other, likewise, the activity coefficient models

(UNIQUAC and NRTL). The different models analyzed in COCO (12) showed better agreement with the reported experimental value for liquid in the literature. The SRK model showed the best agreement with the experiment in the hexane liquid phase using the COCO simulator (12), which also agreed with the report of Nasri and Binous (19) that established the suitability of the SRK model for the prediction of liquid and gas phase properties of a molecule.

Table 3: Heat capacity (J/mol/K) of hexane molecule.

Simulator	PR	SRK	NRTL	UNIQUAC	DFT	NIST _L	NIST _G
COCO	187.85	192.56	208.86	208.86	135.93	197.64	142.6
DWSim	2.08	2.10	2.28	2.28	135.93	197.64	142.6

The DFT calculation results show a better agreement with the gas phase value reported by NIST (16), contrary to the COCO case (12), which offers better agreement with the liquid phase hexane. This was due to the vapor phase of hexane in process simulation being zero (0), indicating a liquid phase, while Spartan automatically computes the thermodynamic properties with the assumption that all species are in the gas phase, which will not be accurate in reality in some cases.

4.0 CONCLUSIONS

In conclusion, this study meticulously validated the use of atomic-scale simulations, specifically employing DFT (B3LYP and PM3) to estimate the thermodynamic properties of hexane molecules. The validation process involved comparing the computed infrared spectra with experimental data, highlighting the superior performance of DFT over the semi-empirical PM3 method. With its lesser approximations, DFT proved to be a more reliable



choice for accurately representing hexane's vibrational behavior.

Further investigation into the estimation of thermodynamic properties through process simulations using COCO and DWSim unveiled some interesting disparities. Notably, the COCO simulator demonstrated closer agreement with experimental values, especially in the case of entropy and enthalpy. DWSim, however, exhibited limitations in its accuracy, with substantial discrepancies between its predictions and experimental data.

The choice of which simulation method to employ depends on the specific phase conditions of hexane. For gas-phase estimations, DFT was found to be more reliable, whereas COCO, with its closer alignment to liquid-phase experimental values, is a better choice for situations involving hexane in a liquid state. It is imperative to consider the phase conditions of the system when selecting the appropriate simulation method. Overall, this study provides valuable insights into the reliability of different simulation techniques for estimating thermodynamic properties, offering a foundation for informed choices in future applications.

5.0 CONFLICT OF INTEREST

The authors declare no conflict of interest.

6.0 ACKNOWLEDGEMENTS

The authors wish to acknowledge the support of Wavefunction Inc, Irvine, CA, USA for the help of providing the license for Spartan v20 and for supporting the 2-week 2023 ProMolSim Training program organized between 6-20 October 2023 by Pencil Team Leadership at the Chemical Engineering Department, Ahmadu Bello University Zaria-Nigeria. In addition, the authors greatly appreciate the DWSim and COCO process simulator developers' support in making their software free of charge.

7.0 REFERENCES

1. J. Gmehling, M. Kleiber, B. Kolbe, J. Rarey, *Chemical Thermodynamics for Process Simulation* (Wiley VCH, ed. 2nd, 2019; <https://www.wiley.com/en-us/Chemical+Thermodynamics+for+Process+Simulation%2C+2nd%2C+Completely+Revised+and+Enlarged+Edition-p-9783527809448>).
2. S. A. Subramanian, P. R. Naren, "Elucidating Concept of Separation techniques and Thermodynamics in process development using DWSim" in *The First National Conference on Chemical Process Simulation*, M. P. Kannan, P. R. Naren, W. Daniel, Eds. (NCCPS Proceedings, Bombay, 2018; https://static.fosee.in/dwsim/proceedings/NCCPS-2018_proceedings.pdf), pp. 12–16.
3. T. Oyegoke, F. N. Dabai, S. M. Waziri, B. Y. Jibril, A. Uzairu, 1 Computational study of propene selectivity and yield in the dehydrogenation of propane via process simulation approach. *Sustainable Chemistry Research*, 1–16 (2023).
4. G. Li, D. Deng, Y. Chen, H. Shan, N. Ai, Solubilities and thermodynamic properties of CO₂ in choline-chloride based deep eutectic solvents. *J Chem Thermodyn* **75**, 58–62 (2014).
5. J. M. (Joseph M. Smith, H. C. (Hendrick C.) Van Ness, M. M. Abbott, *Introduction to Chemical Engineering Thermodynamics*. (McGraw-Hill, 2005).
6. T. Oyegoke, COCO, a process simulator: Methane oxidation simulation & its agreement with commercial simulator's predictions. *Chemical Product and Process Modeling aop* (2023).
7. M. I. Uzochukwu, T. Oyegoke, R. O. Momoh, M. T. Isa, S. M. Shuwa, B. Y. Jibril, Computational insights into deep eutectic solvent design: Modeling interactions and thermodynamic feasibility using choline chloride & glycerol. *Chemical Engineering Journal Advances* **16**, 100564 (2023).
8. T. Oyegoke, F. Dabai, Techno-economic feasibility study of bioethanol production from a combined cellulose and sugar feedstock in Nigeria: 1-modeling,



- simulation and cost evaluation. *Nigerian Journal of Technology* **37**, 913–920 (2018).
9. P. W. (Peter W. Atkins, J. De Paula, *Physical Chemistry : Thermodynamics, Structure, and Change* (2014).
 10. *Thermodynamics and Chemistry - Second Edition - Open Textbook Library* (Howard DeVoe, Maryland, 2019); <https://open.umn.edu/opentextbooks/textbooks/715>).
 11. K. Tangsriwong, P. Lapchit, T. Kittijungjit, T. Klamrassamee, Y. Sukjai, Y. Laonual, DWSIM – The Open Source Chemical Process Simulator – Just another WordPress site, *DWSim Report* (2023). <https://dwsim.org/>.
 12. van B. Jasper, B. Richard, K. Harry, T. Ross, M. B. Jr. William, COCO - the CAPE-OPEN to CAPE-OPEN simulator, *COCO-COFE Web Report* (2023). <https://www.cocosimulator.org/index.html>.
 13. Wavefunction, Spartan v20, *Wavefunction, Inc.* (2023). <https://www.wavefun.com/>.
 14. E. E. Peter, A. Y. Atta, B. Mukhtar, B. O. Aderemi, B. J. El-Yakub, Thermodynamic analysis of products distribution for propane aromatization process. *Journal of King Saud University - Engineering Sciences* **33**, 447–458 (2021).
 15. J. Frank, *Introduction to Computational Chemistry* (John Wiley & Sons Ltd., Second edition., 2007).
 16. NIST, n-Hexane, *NIST Chemistry WebBookm SRD 69* (2023). <https://webbook.nist.gov/cgi/cbook.cgi?ID=110-54-3>.
 17. Air Liquide, Hexane, *Gas Encyclopedia* (2023). <https://encyclopedia.airliquide.com/hexane>.
 18. W. J. Hehre, *A Guide to Molecular Mechanics and Quantum Chemical Calculations* (Wavefunction, 2003).
 19. Z. Nasri, H. Binous, Applications of the Soave–Redlich–Kwong Equation of State Using Mathematica®. *JOURNAL OF CHEMICAL ENGINEERING OF JAPAN* **40**, 534–538 (2007).

P100 - CORROSION MITIGATION STRATEGIES: INTEGRATING CLUSTER MODEL STABILITY & MATERIAL SCREENING FOR ENHANCED METAL PROTECTION IN ATOMIC-SCALE SIMULATIONS

Mikailu Z. Mainasara^{1,2}, Olatunde Abdulsobur^{1,2}, Usman Dunderere^{1,2}, Paul Abraham^{1,2}, Shofiyyullah M. Yusuf^{1,2}, Abubakar Abdulrasheed^{1,2}, Damudi N. Omeiza^{1,2}, Jatto Mustapha^{1,2}, Toyese Oyegoke^{2,*}

¹The C3 and C5 Group of 2023 ProMolSim – Corrosion Subjects, Pencil Team. ²Chemical Engineering Department, Faculty of Engineering, Ahmadu Bello University Zaria, Nigeria.

*Corresponding author email: OyegokeToyese@gmail.com

ABSTRACT

This study delves into the corrosion resistance of copper and the potential for selected compounds to serve as effective corrosion inhibitors. Through a rigorous screening of cluster models, a stable copper cluster was identified as a basis for subsequent analysis. The adsorption of water on the copper surface unveiled its vulnerability to corrosion, emphasizing the urgency of robust prevention strategies. Examination of compound adsorption on the copper surface, encompassing both physisorption and chemisorption, highlighted the effectiveness of chemical adsorption in inhibiting corrosion activity. Notably, styrene (SP6) demonstrated



exceptional inhibition capabilities. These findings provide significant insights into corrosion prevention, with practical implications for safeguarding metal infrastructure and components from corrosion-induced deterioration, promising innovative solutions for diverse industrial applications.

KEYWORDS

Process, Modeling, Simulation, DFT, PM3, Thermodynamics, Property, Alkane.

1.0 INTRODUCTION

Corrosion, an age-old adversary of materials and infrastructure, silently erodes the integrity of metals and alloys, undermining their strength and durability (1, 2). It's a phenomenon that impacts various sectors, from transportation and energy production to manufacturing and construction. The economic toll of corrosion is substantial, with estimates reaching billions of dollars annually in maintenance, repairs, and replacements.

In this relentless battle against corrosion, researchers and engineers seek innovative solutions to protect critical assets and extend the service life of materials. This quest has led to the development of corrosion inhibitors, compounds designed to impede or even halt the corrosive processes. These inhibitors act as shields, mitigating the impact of environmental factors that accelerate corrosion. Several works in the literature (1–3) have evaluated a series of materials for possible application in corrosion inhibition promotion in metals and related materials.

In this study, we likewise explored corrosion science, integrating two critical dimensions of corrosion prevention. Firstly, the stability of cluster models for metals, exemplified by copper, is scrutinized to establish a foundation for further analysis. The screening of cluster models (4, 5) not only highlights the importance of stability criteria but also sets the stage for the subsequent evaluation of corrosion resistance. Secondly, molecular compounds are assessed for their potential as corrosion inhibitors, offering a multifaceted approach to combat metal degradation.

Our study delves into the corrosion phenomenon, from the atomic and molecular scale to the practical implications for diverse industrial applications. To be precise, we deployed a semi-empirical (PM3)

method to rapidly evaluate the potentials of the various compounds selected for our study. The single-point energy calculation was further deployed using the DFT (B3LYP) method. We did that by combining the assessment of cluster models with the analysis of molecular compounds; our goal is to share insight on this kind of study strategy and contribute to the advancement of corrosion prevention strategies, fostering innovation in safeguarding metal assets and infrastructure.

2.0 COMPUTATIONAL MATERIALS AND METHODS

2.1 Material Employed in the Study

In the study, we deployed Spartan v20 (6) to model and simulate the corrosion inhibition study. Relevant cluster models employed in this study were adapted from published literature (4, 5).

2.2 Computational Methods and Details

The calculations employed the use of Semi-empirical (PM3) methods (7, 8) to compute the electronic energies and other molecular properties of relevant species involved in the analysis. A single point energy calculation using DFT (B3LYP, 6-31G) calculation was used to re-evaluate the PM3 computed energies. Some of these species include the selected potential inhibitors, water, and cluster models (adapted from the literature (9)). The species structures were built directly in the Spartan v20 (6) working environment.

3.0 RESULTS AND DISCUSSIONS

Here, we present our findings for the screening of the cluster models adapted from the literature (4, 5), the analysis of copper corrosion resistance, and the potential of the selected inhibitors to prevent corrosion activity on its surface.



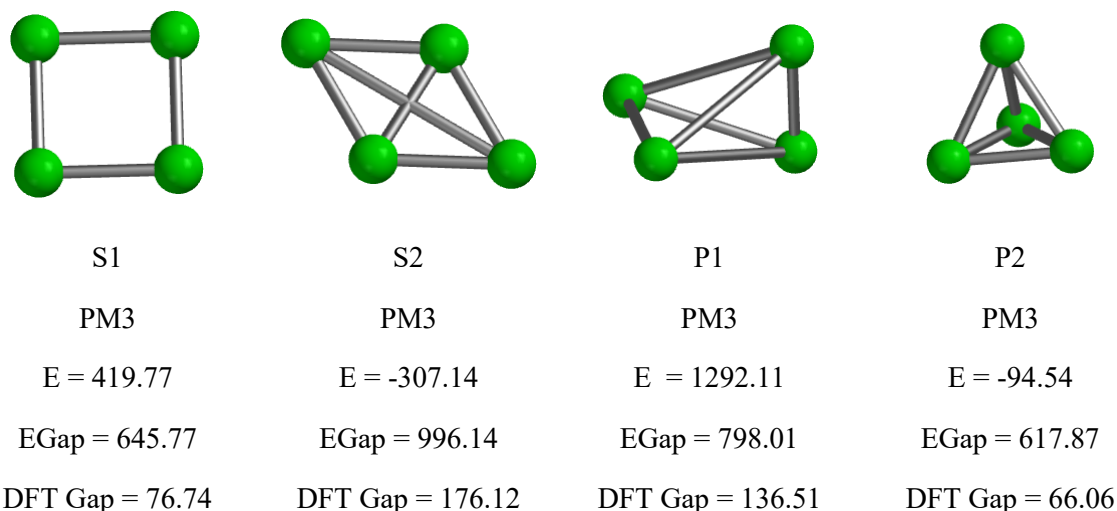


Figure 1: The cluster model for the copper metal: square (S1/S2) and pyramid (P1/P2) model. Note that E is electronic energy, EGap is the energy band gap, and all the energy values are in kJ/mol.

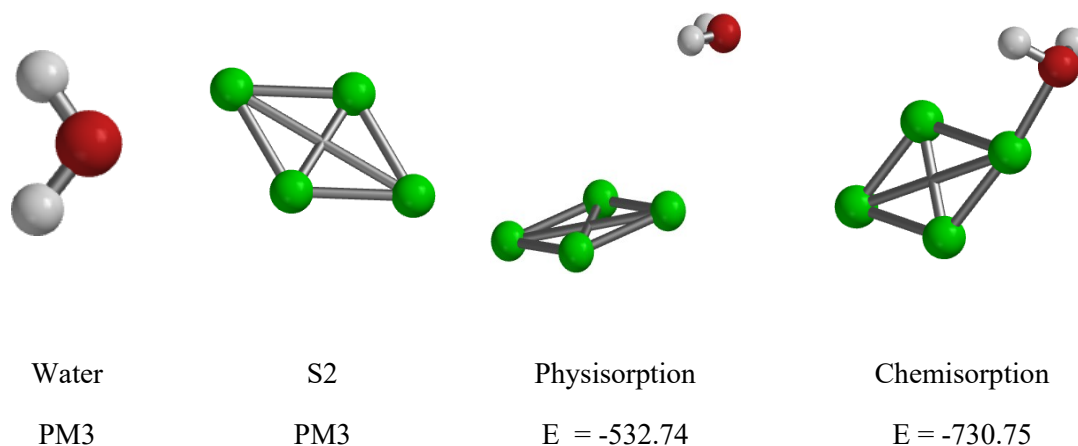
Screening of the Cluster Models

The adapted cluster models for copper, limiting it to ones with only four Cu atoms, were reported to be in either form of a squared or pyramid-like shape, as shown in Figure 1 and literature (4, 5).

The cluster models were screened using the stability of the models. The stability criteria include the use of electronic energies and energy band gap (1), where the cluster model with square-shaped cluster model (S2) shows the highest negative electronic energy and wider energy band gap than the other pyramid-shaped cluster model, which confirms S3 model to be the most stable cluster out of the two models. Hence, further analysis for the corrosion inhibition studies resolved to focus on the use of the said most stable cluster model for the copper metal.

adsorption of water on the copper cluster model was employed to probe the corrosion resistance of the copper metal. The corrosion resistance of a metal probe was approximated to be equal to the ability of the metal to repel the adsorption of water from its surface, in agreement the literature (10, 11) that said water and oxygen has to be present before corrosion can hold.

3.2 Analysis of Copper Corrosion Resistance



$E = -223.54$ $E = -307.14$ $D = 3.7\text{\AA}$, $E_{\text{ads}} = -2.0$ $D = 1.9\text{\AA}$, $E_{\text{ads}} = -200.07$
 $E_{\text{Gap}} = 1580.11$ $E_{\text{Gap}} = 996.14$ (PM3), -15.15 (DFT) (PM3), -62.11 (DFT)

Figure 2: The geometrical structure of water adsorption on the copper metal using the S2 square-shaped model. Note that E is electronic energy, E_{Gap} is the energy band gap, and all the energy values are in kJ/mol.

The negative adsorption energy (-200 kJ/mol in Figure 2) obtained for the adsorption of water predicts the ease of copper initiating corrosion activity. So, the analysis shows that copper metal is liable to corrode easily in the presence of water, which agrees with existing literature(12) that reports on the need to review better measures for preventing corrosion activity on the metal.

3.3 Evaluating the Potential of Selected Compound for Inhibiting Corrosion Activity

Compounds like acrylic acid, methyl acrylate, butyl acrylate, methyl methacrylate, butyl methacrylate, and styrene were selected for our analysis from the literature (9) and are hence tagged with code of SP1 to SP6, respectively as shown in Figure 3.

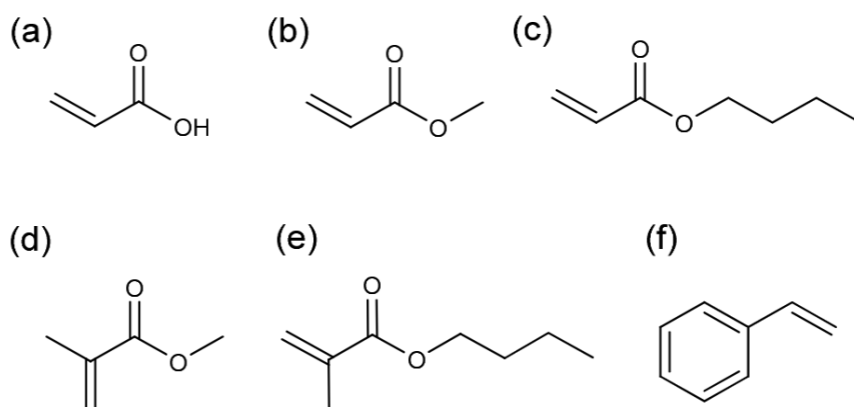


Figure 3: (a) SP1, (b) SP2, (c) SP3, (d) SP4, (e) SP5, and (f) SP6 are the selected compounds to be screened for potential corrosion inhibition activity on copper.

Table 1 presented the adsorption energies obtained for the binding or interaction of the selected compounds with the copper surface, showing the different modes of adsorption evaluated in the study. The adsorption modes include the physisorption and chemisorption modes. From

which the analysis of the result in Table 1 shows that the physical adsorptions were found to have weaker strength across the selected compounds except for the SP6, which shows a much stronger interaction (without introducing any chemical bonding) than other compounds evaluated.

Table 1: Adsorption energy of the selected compound on the stable copper cluster (S2) model.

Compound	Method	Physisorp.	Singly-Bonded	Doubly-Bonded	Strongest	Weakest
Water	PM3	-2.06	-200.07	N/C	-200.07	-2.06
SP1	PM3	-7.26	-154.22	-279.20	-279.20	-7.26
SP2	PM3	-7.57	-456.45	-257.88	-456.45	-7.57



SP3	PM3	-9.32	-160.03	-293.21	-293.21	-9.32
SP4	PM3	-12.33	-136.62	-237.39	-237.39	-12.33
SP5	PM3	-9.92	-129.99	-262.88	-262.88	-9.92
SP6	PM3	-588.04	-604.89	-589.75	-604.89	-588.04
Water	DFT	-15.15	-62.11	N/C	-62.11	-15.15
SP1	DFT	-11.29	-66.63	-47.88	-66.63	-11.29
SP2	DFT	-10.43	18.12	-44.72	-44.72	18.12
SP3	DFT	-14.56	-73.8	-62.2	-73.8	-14.56
SP4	DFT	4.58	-50.08	-45.24	-50.08	4.58
SP5	DFT	11.16	-53.03	-24.11	-53.03	11.16
SP6	DFT	-111.88	39.01	N/C	-111.88	39.01

Note: **N/C means not-computed

Chemical adsorption of the potential inhibitors was found to have shown a stronger interaction across all the compounds evaluated in Table 1, where a large number of the compounds feasibly adsorbed

with a double bond, while a few compounds like SP2 and SP6 better adsorbed using a single bond interaction.

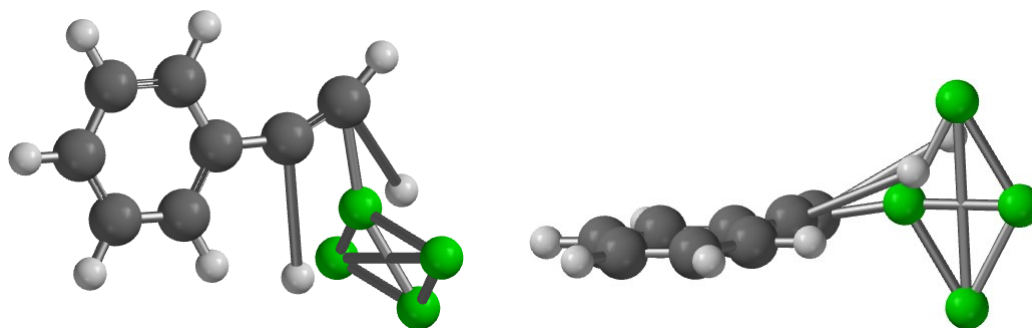


Figure 4: Geometrical structure view of the chemisorbed SP6 compound (styrene) to copper.

Cross-evaluation shows a stronger binding strength (-604.89 kJ/mol) than that the copper had with the water as -200 kJ/mol for the PM3 results and, likewise, the DFT. This suggests that all the evaluated compounds would facilitate the inhibition of corrosion activity on copper metal, where the SP6 compound (styrene) would best protect the copper metal due to its stronger interaction reported for the adsorption strength in line with the established procedures often deployed in the literature (2, 13, 14) in such evaluation. The stronger adsorption strength shown by SP6 would easily displace water molecules from the copper

surface and better present water to access the copper surface to initiate corrosion.

4.0 CONCLUSIONS

In this study, we explored the corrosion resistance of copper and the potential of selected compounds to inhibit corrosion activity on its surface. We identified the most stable copper cluster through a systematic screening of cluster models, providing a solid foundation for further analysis.

Our findings revealed that copper is susceptible to corrosion when exposed to water, emphasizing the



need for effective corrosion prevention measures. To this end, we evaluated the adsorption of various compounds on the copper surface, considering both physisorption and chemisorption modes. The results demonstrated that chemical adsorption, characterized by strong interactions, holds promise for inhibiting corrosion activity on copper. Styrene (SP6) emerged as a potent corrosion inhibitor due to its robust adsorption strength. Suggesting that styrene-based material could potentially prevent corrosion activity on the copper metal.

This study contributes valuable insights into corrosion inhibition, offering a pathway for enhancing the protection of copper and, potentially, other metals. Identifying effective inhibitors and understanding their adsorption mechanisms lay the groundwork for practical applications in safeguarding metal infrastructure and components from corrosion-related degradation. Further research in this direction can lead to innovative solutions for addressing corrosion challenges in various industries.

5.0 CONFLICT OF INTEREST

The authors declare no conflict of interest.

6.0 ACKNOWLEDGEMENTS

The authors wish to acknowledge the support of Wavefunction Inc, Irvine, CA, United States for the help of providing the license for Spartan v20 and for supporting the 2-week 2023 ProMolSim Training program organized between 6-20 October 2023 by Pencil Team Leadership at the Chemical Engineering Department, Ahmadu Bello University Zaria-Nigeria.

7.0 REFERENCES

1. M. A. Erteeb, E. E. Ali-Shattle, S. M. Khalil, H. A. Berbash, Z. E. Elshawi, Computational Studies (DFT) and PM3 Theories on Thiophene Oligomers as Corrosion Inhibitors for Iron. *Am. J. Chem.* **2021**, 1–7.
2. A. Toghan, A. Fawzy, A. Al Bahir, N. Alqarni, M. M. S. Sanad, M. Khairy, A. I. Alakhras, A. A. Farag, Computational Foretelling and Experimental Implementation of the Performance of Polyacrylic Acid and Polyacrylamide Polymers as Eco-Friendly Corrosion Inhibitors for Copper in Nitric Acid. *Polymers (Basel)*. **14**, 4802 (2022).
3. B. U. Ugi, V. M. Bassey, M. E. Obeten, S. A. Adalikwu, E. C. Omaliko, D. N. Obi, Acetylcholine and Rivastigmine as Corrosion Inhibitors of Cu – Sn - Zn – Pb Alloy in Hydrochloric Acid Environment: DFT & Electrochemical Approach. *J. Appl. Sci. Environ. Manag.* **25**, 1441–1448 (2021).
4. U. J. Rangel-Peña, R. L. Camacho-Mendoza, S. González-Montiel, L. Feria, J. Cruz-Borbolla, Nonconventional C–H···Cu Interaction Between Copper Cun Clusters (n = 3–20) and Aromatic Compounds. *J. Clust. Sci.* **32**, 1155–1173 (2021).
5. P. Jaque, A. Toro-Labbé, Polarizability of neutral copper clusters. *J. Mol. Model.* **20**, 1–8 (2014).
6. Wavefunction, Spartan v20, *Wavefunction, Inc.* (2023). <https://www.wavefun.com/>.
7. J. Frank, *Introduction to Computational Chemistry* (John Wiley & Sons Ltd., Second edition., 2007).
8. W. J. Hehre, *A Guide to Molecular Mechanics and Quantum Chemical Calculations* (Wavefunction, 2003).
9. J. Cyrene, M. Jones, R. A. Milescu, T. J. Farmer, J. Sherwood, C. R. McElroy, J. H. Clark, Cyrene™, a Sustainable Solution for Graffiti Paint Removal. *Sustain. Chem.* **4**, 154–170 (2023).
10. H. R. Copson, Effects of Velocity on Corrosion by Water. *Ind. Eng. Chem.* **44**, 1745–1752 (2002).
11. A. Royani, S. Prifiharni, G. Priyotomo, J. Triwardono, Sundjono, “Corrosion of carbon steel in synthetic freshwater for water distribution systems” in *IOP Conference Series: Earth and Environmental Science* (Institute of Physics Publishing, 2019)vol. 399.



12. Elhuyar Foundation, Study of the corrosive effects of water, *EU Research Results* (2023).
<https://cordis.europa.eu/article/id/96045-study-of-the-corrosive-effects-of-water>.
13. T. Oyegoke, F. N. Dabai, S. M. Waziri, A. Uzairu, B. Y. Jibril, Impact of Mo and W on CrXO₃ (X = Cr, Mo, W) Catalytic Performance in a Propane Non-oxidative Dehydrogenation Process. *Kem. u Ind.* **71**, 583–590 (2022).
14. O. Ademola, T. Oyegoke, J. John Olusanya, Computational Study of CO Adsorption Potential of MgO, SiO₂, Al₂O₃, and Y₂O₃ Using a Semiempirical Quantum Calculation Method. *Niger. J. Mater. Sci. Eng.* **11**, 52–57 (2021).



P101 - ANTIMICROBIAL PROPERTIES OF GARLIC (*ALLIUM SATIVUM*): A MINI REVIEW

SHUAIB, Muneerah A.^{1*}, YAHAYA, Isma'il S.¹, YAKA, Miria¹, MUHAMMAD, Amina K.², IDOWU, Olanipekun O.³, OCHIGBO, Victor⁴, NWOBI, Bridget E.⁴

¹Department of Microbiology, Ahmadu Bello University Zaria.

²Department of Biochemistry, Ahmadu Bello University Zaria.

³Scientific and Industrial Research Department, National Research Institute for Chemical Technology Zaria.

⁴Industrial and Environmental Pollution Department, National Research Institute for Chemical Technology Zaria.

*Corresponding author's email: neerahchenyo@yahoo.com

ABSTRACT

With the increase of viral and fungal-related illnesses, parasitic threats to human health, and resistant microbes, there is a need for alternative treatment methods, or more natural remedies. *Allium sativum* has been acknowledged by several civilizations throughout history for its possible application in the prevention and treatment of various illnesses. The effects of *A. sativum* and its extracts in a variety of applications are supported by various research studies. Different compounds in *A. sativum* have been shown to have anti-microbial effects, even against multi-drug-resistant *Staphylococcus aureus* (MRSA). This mini review considers the various reported therapeutic effects of *A. sativum* and its fractions and extracts against bacteria, fungi, viruses, and parasites.

Keywords: Antimicrobial, Garlic, *Allium sativum*, Allicin, Ajoene.

1.0 INTRODUCTION

Antimicrobial resistance has been identified as an immediate and serious danger to human health, forcing the development of innovative and effective antimicrobial agents by scientific researchers. Several scientific studies and medical experience publications have reported that the prevalence of microbial infections brought on by multidrug-resistant bacteria has drastically grown during the past few decades (1-4). The term "multidrug resistance" (MDR) refers to a microorganism's capacity to withstand the effects of an antimicrobial drug even after having previously shown sensitivity to it. This has become a significant public health threat, as almost all antimicrobial agents available are subject to the problem. Furthermore, due to the recent rise of bacterial strains that are resistant to traditional antibiotics, researchers are working to identify

new medications (1). One approach to resolving this issue appears to be a combination of antibiotics already on the market with *A. sativum* extracts, with the two drugs either fully or partially synergizing (1, 5).

Allium sativum L., commonly called garlic (English), tafarnuwa (Hausa), galiki (Igbo), ata ile (Yoruba), is a common herbaceous cooking spice and flavouring ingredient that has been used for ages in different cultures all over the world to treat a variety of diseases, primarily bacterial infections (2, 5, 6). *A. sativum* is a member of the Liliaceae family, which also includes onions (7, 8). *A. sativum* is cultivated all over the world with a per-capita consumption of about one kilogram per year (5). *A. sativum* is believed to provide health advantages due to its antifungal, antiviral, antibacterial, and antiparasitic properties (2, 5, 9). The compounds contained in *A. sativum* synergistically influence each other so that they can have different effects (10). The active ingredients of garlic include enzymes (e.g. *alliinase*), sulfur-containing compounds such as alliin and compounds produced enzymatically from alliin



(e.g. allicin) (11, 12). Therapeutic use of *A. sativum* has been recognized as a potential medicinal value for thousands of years to different microorganisms (2, 13, 14).

Allium sativum antibacterial properties were initially described by Louis Pasteur in 1858, and several other investigations have followed over the years (14-17). *A. sativum* extracts were reported to exhibit activity against both Gram-negative bacteria (e.g., *Escherichia coli*, *Salmonella* species, *Shigella* species *Vibrio* species, *Enterobacter*, and *Enterococcus* species) (1, 17) and Gram-positive bacteria (e.g., *Clostridium difficile*, *Staphylococcus aureus* and *Streptococcus*) (1, 2, 5) all of which are causes of morbidity worldwide (2). Hyun-Joo *et al.* (18), showed that low-density lipoprotein (LDL) oxidation and lipid peroxides may both be reduced and reactive oxygen species (ROS) removed by the natural antioxidants found in garlic.

Antiviral therapies are essential for the prevention and management of viral infections, but many antiviral drugs have significant side effects. As a result, there has been growing interest in the potentials of natural antiviral agents such as *Allium sativum* extract, which has been used for centuries as a remedy. It has long been used traditionally to treat many viral diseases (6, 19-21), and is the second most commonly recommended herb in the traditional treatment of a number of viral illnesses, including hepatitis, gastroenteritis, retroviruses, and viruses that cause the common cold (19). In numerous scientific studies, garlic isolates, or compounds have demonstrated antiviral activity (19, 20, 22, 23).

An interesting *in vivo* experiment by El-Saber *et al.* (24), demonstrated the antiviral activity of *Allium sativum* extract, and it was reported that *A. sativum* improved the production of neutralizing antibodies when given to mice, protecting against influenza viruses. This activity was based on the presence of several phytochemicals, including ajoene, allicin, allyl methyl thiosulfinate, and methyl allyl thiosulfinate (24, 25). The virucidal chemicals in garlic were reported in the following order: ajoene > allicin > allyl methyl thiosulfinate > methyl allyl thiosulfinate; no activity was observed for the polar portions alliin, deoxyalliin, diallyl disulfide, or diallyl trisulfide (26). This mini-review considers the various reported antimicrobial activities about *A. sativum*.

1.1. Bioactive Compounds of *Allium sativum*

Among other bioactive compounds of *Allium sativum*, the major active components of these compounds are its organosulfur compounds, such as ajoene (E-ajoene and Z-ajoene), diallyl thiosulphinate (allicin), diallyl sulphide (DAS), diallyl disulphide (DADS), diallyl trisulphide (DATS), and S-allyl-cysteine sulphoxide (alliin). Allicin is one of the most dominant compounds present in it (27, 28).

2.0 ANTIMICROBIAL ACTIVITIES OF *Allium sativum* EXTRACT.

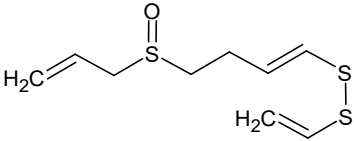
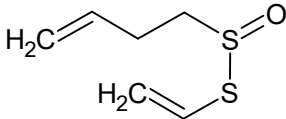
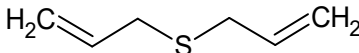
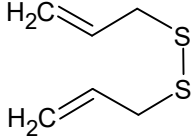
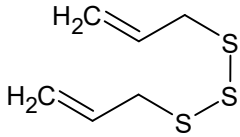
In addition to being commonly used to improve the flavour of food, *Allium sativum* has long been used to treat a variety of illnesses in many different cultures and traditions (5, 14, 29). Several studies have evaluated the antimicrobial activities of various *A. sativum* preparations (3, 5, 6, 8, 16, 26). *A. sativum* extract may be a natural alternative for preventing and treating tooth plaque and related disorders like periodontitis, instead of synthetic antibacterial medications (8). Additionally, it possesses antifungal effects against *Candida albicans* and *Aspergillus niger* (8, 30). Further research suggests that *A. sativum* extract also shows antiviral properties against the respiratory syncytial virus (RSV) and *Herpes simplex* virus type 1 (HSV-1) (8, 14). Although the exact mechanisms by which *A. sativum* exerts its antimicrobial effects are unknown. Other research studies have shown that *A. sativum* may be effective by obstructing different phases of viral replication (31, 32). Various sulphur-containing molecules generated from cysteine are responsible for the majority of the health beneficial properties of *A. sativum*, of which the most active compound was reported to be allicin and ajoene (5, 6, 33). *A. sativum* could be used as an adjuvant therapy for bacterial infections in addition to antibiotics, i.e., when ciprofloxacin and *A. sativum* extract work together synergistically (8). An inhibitory synergism was observed when *A. sativum* extract were used in combination with tobramycin, and vancomycin, thereby enhancing their susceptibility to microbial illnesses (14, 34). Sushma *et al.* (5), reported that allicin along with allyl methyl and methyl allyl mixture exhibited activity against *Helicobacter pylori* (a spiral-shaped bacterium that lives in the digestive tract, and it's been linked to a number of different diseases,



including stomach ulcer) and showed synergy when used together. The table below list the most

effective bioactive compounds of *A. sativum*, and their mechanism of action.

Table 1: Some antimicrobial compounds of *A. sativum*

Name	Extract	Activity against	Mechanism	Structure
Ajoene	Ethanol	Protozoa	Inhibits glutathione reductase (human) and trypanothione reductase (<i>Trypanosma cruzi</i>)	
Allicin (Diallyl-thiosulfinate)	Ethanol	Bacteria, Fungi, Protozoa, Virus	Chemical interaction with enzymes containing thiol	
Diallyl sulphide	Hexane	Bacteria	Membrane disruption.	
Diallyl disulfide	Ethanol, Water	Bacteria, Virus, Fungi	Membrane disruption.	
Diallyl trisulfide	Dichloro-methane	Bacteria, Virus, Fungi	Membrane disruption.	

2.1. Antibacterial Activities of *Allium sativum* Extracts.

Allium sativum extracts have been reported to have a wide-range of effects on bacteria. Fresh extract (FE) of *A. sativum* has been reported to show activity against a wide range of bacteria, including some resistant bacteria (3, 5, 6, 26). Xing-Yang *et al.* (35), reported that FE also showed good antimicrobial activity against five multi drug resistant strains (*E. coli*, *Pseudomonas aeruginosa*, *Klebsiella pneumoniae*, *Serratia marcescens* and multi-drug resistant *Staphylococcus aureus* [MRSA]). Other research shows that FE may be used to inhibit the growth of endospore-forming bacteria (e.g., *Clostridium* species) (5, 36). Furthermore, in a clinical trial, Shang *et al.* (27), reported that a treatment of raw *A. sativum* inhibited *Helicobacter pylori* in the stomach of patients with *H. pylori* infection.

Allium sativum extracts have shown a tremendous effect on bacterial biofilms (37, 38). Biofilms are commonly associated with many health problems, such as otitis media, periodontitis, and urinary tract infections. Previous studies have shown the effect of various *A. sativum* preparations, either FE or individual components on bacterial biofilms (30, 37, 39). Two components, Allicin and ajoene, appear to work in a variety of ways to prevent the growth of bacterial biofilm. The two most researched areas of these are the inhibition of polysaccharide intercellular adhesin (PIA) synthesis and quorum sensing (35, 37).

The mechanisms of action of the bioactives of *A. sativum* extracts are not fully understood. Previous research suggests that the antibacterial activities of FE are as a result of the enzyme *alliinase*, sulphur-containing compounds such as alliin and compounds produced enzymatically from alliin (e.g., allicin) (3, 36). It has also been reported that



allicin has sulfhydryl modifying activity, and is capable of interacting with sulfhydryl enzymes (14, 40) e.g., thioredoxin reductase, RNA polymerase, and alcohol dehydrogenase. Allicin is thought to achieve this by oxidizing cysteine or glutathione residues under physiological conditions (6). Since it is reported that allicin interferes with RNA production, then protein synthesis might be severely affected (40).

Various *A. sativum* extracts (aqueous, chloroform, methanolic, and ethanolic extracts) were reported to inhibit the growth of several pathogenic bacteria with varying degrees of susceptibility. For instance, a study revealed that ethanolic extract showed higher inhibitory effect against *E. coli* and *S. typhi* than the aqueous extract that showed little or no inhibitory effect (6). The effectiveness of *A. sativum* extract, may therefore, depend on the methods and solvents used in the extraction. Temperature and pH are other factors that determine the effectiveness of *A. sativum* extracts.

2.2. Antiviral Activities of *Allium sativum* Extract

A. sativum isolates or compounds have been shown to have antiviral action (6, 19, 21, 32). Extracts or isolates include chemical constituents that can attack different stages of the viral life cycle e.g., inhibiting the virus's admission stage into cells. Both encapsulated and non-enveloped pathogens can be destroyed by this technique. *A. sativum* and its potent organosulfur components have shown a great antiviral activity by interacting with and destroying receptors on the surface of viruses. They may also affect genetic material inside the virion by changing how the viral genome is translated in the host cell, and affecting viral RNA polymerase, which is required for viral replication. They can also prevent the viral process that changes the host cell's signalling pathway and prevent viral multiplication (19).

A wide variety of birds, most notably domestic chickens, are susceptible to the extremely contagious and deadly Newcastle disease (23, 41-43). The virus that causes it is a member of the paramyxoviridae family. In the poultry sector, the disease could result in significant financial losses. All birds are anticipated to be prone to infection, with varied clinical symptoms and results. *A. sativum* oil which was extracted from dried garlic using the Soxhlet setup was tested *in vitro* as an antiviral to Newcastle disease virus (23). The results were validated by the inoculation of

embryonated chicken eggs with the virus and *A. sativum* oil. The results showed that *A. sativum* oil has a great ability to eliminate the virus by destroying receptors on the surface of the virus and the genetic material inside. In addition, it was found that there was no toxicity or pathological effects of this oil on the animals (23).

It was reported by Tudu *et al.* (19), that very low concentrations (as low as 0.01 mg/ml) of aqueous *A. sativum* extract was found to be effective in inhibiting the progression of a Measles morbillivirus infection, possibly by blocking viral receptors and preventing cell adsorption (19). Additionally, the flavonoid quercetin, which is commonly found in fruits and vegetables (including *A. sativum*) has shown antiviral activity against the avian H1N1 influenza virus by altering viral attachment to the surface of the host cell (44).

Even if the virus enters the host cell, there are still various steps suitable for its inhibition. One of these represents inhibition in the viral replication step. Replication may occur in the cytoplasm or in the nucleus of the host cell. In the current history, numerous investigations have proven the ability of *A. sativum* to prevent viral proliferation (19). The host cell's nucleus or cytoplasm might both be the site of replication. Numerous studies conducted in recent years have demonstrated the capacity of *A. sativum* to stop viral growth (19, 22, 24, 44-46).

2.3. Antifungal Activities of *Allium sativum* Extracts

Antifungal activity of *Allium sativum* extract was first established in 1936 by Schmidt and Marquardt (47), whilst working with epidermophyte cultures. Both the aqueous garlic extract and the concentrated garlic oil showed an inhibitory effect against *Aspergillus* (11). Allicin showed a fungicidal effect against numerous yeasts and fungi, including *Candida albicans*, *Cryptococcus trichophyton*, *Histoplasma capsulatum*, and *Cryptococcus neoformans*. *A. sativum* has been shown to inhibit the growth of fungal diseases (48-50).

Allium sativum extracts were shown to decrease the oxygen uptake, reduce the growth of the microorganisms, inhibit the synthesis of lipids,



proteins and nucleic acids and damage membranes (51). Many fungi appear to be susceptible, including *Candida*, *Trichophyton*, *Cryptococcus*, *Aspergillus*, *Trichosporon* and *Rhodotorula* (11). A sample of pure allicin was shown to be antifungal (47). Recently, garlic extract was found to inhibit *Meyerozyma guilliermondii* and *Rhodotorula mucilaginosa* germination and growth (52). Another study reported the antifungal activity of various *A. sativum* extracts against human pathogenic fungi such are *Trichophyton verrucosum*, *T. mentagrophytes*, *T. rubrum*, *Botrytis cinerea*, *Candida species*, *Epidermophyton floccosum*, *Aspergillus niger*, *A. flavus*, *Rhizopus stolonifera*, *Microsporium gypseum*, *M. audouinii*, *Alternaria alternate*, *Neofabraea alba*, and *Penicillium expansum* (4).

The *A. sativum* extract acted by affecting the fungal cell wall and causing irreversible ultrastructural changes in the fungal cells, which lead to loss of structural integrity and affected the germination ability (53). Moreover, allicin and *A. sativum* oil showed potent antifungal effects against *Candida albicans*, *Ascospaeraapisin*, and *A. niger* and they acted by penetrating the cellular membrane as well as organelles membranes like the mitochondria and leading to organelles destruction and cell death (54). A concentrated *A. sativum* extract containing 34% allicin, 44% total thiosulfates, and 20% vinylidithiins possessed potent in vitro fungistatic and fungicidal activity against three different isolates of *Cryptococcus neoformans*. The minimum inhibitory concentration of the concentrated *A. sativum* extracts against 1×10^5 organisms of *C. neoformans* ranged from 6 to 12 $\mu\text{g/mL}$ (55). In addition, in vitro synergistic fungistatic activity with *amphotericin B* was demonstrated against all isolates of *C. neoformans*, pure allicin was found to have a high anticandidal activity with a minimum inhibitory concentration of 7 $\mu\text{g/mL}$ while another report shows that pure allicin was effective in vitro against species of *Candida*, *Cryptococcus*, *Trichophyton*, *Epidermophyton*, and *Macrospore* at low concentration (minimal inhibitory concentrations of allicin was between 1.57 and 6.25 $\mu\text{g/mL}$). Allicin inhibits both germination of spores and growth of hyphae (53).

2.4. Antiparasitic Activities of *Allium sativum* Extracts

Parasitic infections are a major concern globally, especially in poor countries. Malaria, caused by parasites of the genus *Plasmodium*, is one of the

leading infectious diseases in many tropical regions, including Nigeria (56). Ajoene was reported to be active against malaria caused by *Plasmodium berghei* in mice (57). Coppi *et al.* (58), later reported that allicin was active against *P. falciparum*. The mechanism of action was thought to be inhibition of the protozoan cysteine protease, which significantly reduced parasitaemia in infected hosts. This was also reported by Feng *et al* (59).

Trypanosoma brucei is a parasite that causes, if not treated, a deadly sleeping sickness in Africa (9). *Leishmaniasis* is a disease caused by the protozoan parasite *Leishmania*, which results in up to 30,000 deaths each year (9). *A. sativum* extracts and its phytochemicals have been shown in several studies to have anti-protozoal efficacy against a number of protozoan parasites (6, 33). Allicin may act by interfering with the synthesis of parasite RNA, DNA and protein. Examples of these parasites reported to be susceptible to allicin are *Entamoeba histolytica*, *Leishmania* species, *Trypanosomas* species, *P. falciparum*, *Babesia* species, *T. brucei*, and *Giardia lamblia* (6, 7, 26). In addition, ajoene also exhibited antiparasitic activity by inhibiting *Trypanosoma cruzi* trypanothione reductase (6).

In an *in vitro* study by El-Saber *et al.* (6), the ethanolic extract of *A. sativum* was the most effective against the helminth *Haemonchus contortus* (the causative agent of anaemia and weight loss in infected animals), while the aqueous extract of *A. sativum* was highly active against the helminths *Trichuris muris* (a whipworm that is capable of causing significant pathology, including diarrhoea, anaemia, and weight loss) and *Angiostrongylus cantonensis* (a lungworm parasitic nematode, that infect human with a symptoms such as fever, headache, and neurological symptoms, such as paralysis).

3.0 CONCLUSION

This research demonstrates that *Allium sativum* can be used alongside existing antibiotics to enhance their effectiveness and reduce the risk of antimicrobial resistance. Multi-drug resistant *Staphylococcus aureus* (MRSA) which was found to develop resistance factors against other antimicrobial, has been proven to be susceptible to *A. sativum* extract. *A. sativum* has the potential to be efficient in fighting infectious diseases. Its antibacterial, antiviral, antifungal and antiparasitic properties makes it a promising route for the development of new antimicrobial therapies.



Though further research is needed to fully explore the potentials of *A. sativum* in this aspect, since the mechanisms of action of *A. sativum* is yet to be well understood, but the findings of this study are a promising step forward.

4.0 References

1. A. Magryś, A. Olender, D. Tchórzewska, Antibacterial properties of *Allium sativum* L. against the most emerging multidrug-resistant bacteria and its synergy with antibiotics. *Arch Microbiol* **203**, 2257-2268 (2021).
2. D. Daka, Antibacterial effect of garlic (*Allium sativum*) on *Staphylococcus aureus*: An in vitro study. *African journal of Biotechnology* **10**, 666-669 (2011).
3. A. Tesfaye, Revealing the Therapeutic Uses of Garlic *Allium sativum* and Its Potential for Drug Discovery. *The Scientific World Journal* **2021**, 8817288 (2021).
4. M. Arbach *et al.*, Antimicrobial garlic-derived diallyl polysulfanes: Interactions with biological thiols in *Bacillus subtilis*. *Biochimica et Biophysica Acta (BBA)-General Subjects* **1863**, 1050-1058 (2019).
5. S. B. Bhatwalkar *et al.*, Antibacterial properties of organosulfur compounds of garlic (*Allium sativum*). *Frontiers in Microbiology* **12**, 1869 (2021).
6. G. El-Saber Batiha *et al.*, Chemical Constituents and Pharmacological Activities of Garlic (*Allium sativum* L.): A Review. *Nutrients* **12**, 872 (2020).
7. M. R. Sahidur, S. Islam, M. H. A. Jahurul, Garlic (*Allium sativum*) as a natural antidote or a protective agent against diseases and toxicities: A critical review. *Food Chemistry Advances* **3**, 100353 (2023).
8. F. Azmat *et al.*, Valorization of the phytochemical profile, nutritional composition, and therapeutic potentials of garlic peel: a concurrent review. *International Journal of Food Properties* **26**, 2642-2655 (2023).
9. S. Krstin, M. Sobeh, M. S. Braun, M. Wink, Anti-Parasitic Activities of *Allium sativum* and *Allium cepa* against *Trypanosoma b. brucei* and *Leishmania tarentolae*. *Medicines* **5**, 37 (2018).
10. R. Arreola *et al.*, Immunomodulation and anti-inflammatory effects of garlic compounds. *Journal of immunology research* **2015**, (2015).
11. D. Ayodhya, G. Veerabhadram, Green synthesis of garlic extract stabilized Ag@CeO₂ composites for photocatalytic and sonocatalytic degradation of mixed dyes and antimicrobial studies. *Journal of Molecular Structure* **1205**, 127611 (2020).
12. M. A. Adetumbi, B. H. Lau, *Allium sativum* (garlic)—a natural antibiotic. *Medical hypotheses* **12**, 227-237 (1983).
13. D. Atsamnia, M. Hamadache, S. Hanini, O. Benkortbi, D. Oukrif, Prediction of the antibacterial activity of garlic extract on *E. coli*, *S. aureus* and *B. subtilis* by determining the diameter of the inhibition zones using artificial neural networks. *LWT-Food Science and Technology* **82**, 287-295 (2017).
14. L. Bayan, P. H. Koulivand, A. Gorji, Garlic: a review of potential therapeutic effects. *Avicenna journal of phytomedicine* **4**, 1 (2014).
15. P. Avato, F. Tursi, C. Vitali, V. Miccolis, V. Candido, Allylsulfide constituents of garlic volatile oil as antimicrobial agents. *Phytomedicine* **7**, 239-243 (2000).
16. M. Banerjee, P. K. Sarkar, Inhibitory effect of garlic on bacterial pathogens from spices. *World Journal of Microbiology and Biotechnology* **19**, 565-569 (2003).
17. C. Chen *et al.*, Broad-spectrum antimicrobial activity, chemical composition and mechanism of action of garlic (*Allium sativum*) extracts. *Food Control* **86**, 117-125 (2018).
18. H.-J. Jang *et al.*, Antioxidant and antimicrobial activities of fresh garlic and aged garlic by-products extracted with



- different solvents. *Food science and biotechnology* **27**, 219-225 (2018).
19. C. K. Tudu *et al.*, Traditional uses, phytochemistry, pharmacology and toxicology of garlic (*Allium sativum*), a storehouse of diverse phytochemicals: A review of research from the last decade focusing on health and nutritional implications. *Frontiers in Nutrition* **9**, 929554 (2022).
 20. D. Chakraborty, A. Majumder, Garlic (Lahsun)—an immunity booster against SARS-CoV-2. *Biotica Res Today* **2**, 755-757 (2020).
 21. M. M. Donma, O. Donma, The effects of allium sativum on immunity within the scope of COVID-19 infection. *Medical Hypotheses* **144**, 109934 (2020).
 22. R. Rouf *et al.*, Antiviral potential of garlic (*Allium sativum*) and its organosulfur compounds: A systematic update of pre-clinical and clinical data. *Trends in Food Science & Technology* **104**, 219-234 (2020).
 23. M. M. Hizam, F. T. M. Al-Mubarak, W. A. Al-Masoudi, Antiviral efficacy of garlic oil against newcastle disease virus. *Basrah Journal of Veterinary Research* **18**, 234-247 (2019).
 24. G. El-Saber Batiha *et al.*, Chemical constituents and pharmacological activities of garlic (*Allium sativum* L.): A review. *Nutrients* **12**, 872 (2020).
 25. A. Yusuf, S. Fagbuaro, S. Fajemilehin, Chemical composition, phytochemical and mineral profile of garlic (*Allium sativum*). *J. Biosci. Biotechnol. Discov* **3**, 105-109 (2018).
 26. G. Gebreyohannes, M. Gebreyohannes, Medicinal values of garlic: A review. *International Journal of Medicine and Medical Sciences* **5**, 401-408 (2013).
 27. A. Shang *et al.*, Bioactive Compounds and Biological Functions of Garlic (*Allium sativum* L.). *Foods* **8**, (2019).
 28. E. Subroto *et al.*, Bioactive compounds in garlic (*Allium sativum* L.) as a source of antioxidants and its potential to improve the immune system: a review. *Food Res* **5**, 10.26656 (2021).
 29. S. Adaki, R. Adaki, K. Shah, A. Karagir, Garlic: Review of literature. *Indian journal of cancer* **51**, 577-581 (2014).
 30. B. Sadanandan *et al.*, Aqueous spice extracts as alternative antimycotics to control highly drug resistant extensive biofilm forming clinical isolates of *Candida albicans*. *PLOS ONE* **18**, e0281035 (2023).
 31. N. D. Weber *et al.*, In vitro virucidal effects of *Allium sativum* (garlic) extract and compounds. *Planta Med* **58**, 417-423 (1992).
 32. E. Lissiman, A. L. Bhasale, M. Cohen, Garlic for the common cold. *Cochrane Database Syst Rev* **2014**, Cd006206 (2014).
 33. H. Yavuzcan Yildiz, Q. Phan Van, G. Parisi, M. Dam Sao, Anti-parasitic activity of garlic (*Allium sativum*) and onion (*Allium cepa*) juice against crustacean parasite, *Lernantropus kroyeri*, found on European sea bass (*Dicentrarchus labrax*). *Italian Journal of Animal Science* **18**, 833-837 (2019).
 34. E. Buommino, M. Scognamiglio, G. Donnarumma, A. Fiorentino, B. D'Abrosca, Recent advances in natural product-based anti-biofilm approaches to control infections. *Mini reviews in medicinal chemistry* **14**, 1169-1182 (2014).
 35. X. Y. Zhu, Y. R. Zeng, Garlic extract in prosthesis-related infections: a literature review. *J Int Med Res* **48**, 300060520913778 (2020).
 36. M. Majewski, *Allium sativum*: facts and myths regarding human health. *Rocz Panstw Zakl Hig* **65**, 1-8 (2014).
 37. V. M. Girish *et al.*, Anti-biofilm activity of garlic extract loaded nanoparticles. *Nanomedicine: Nanotechnology, Biology and Medicine* **20**, 102009 (2019).
 38. N. Hassan, S. Firdaus, S. Padhi, A. Ali, Z. Iqbal, Investigating natural antibiofilm components: a new therapeutic perspective against candidal vulvovaginitis. *Medical Hypotheses* **148**, 110515 (2021).



39. Q. Q. Zhang *et al.*, Comparative antibacterial and antibiofilm activities of garlic extracts, nisin, ϵ -polylysine, and citric acid on *Bacillus subtilis*. *Journal of Food Processing and Preservation* **43**, e14179 (2019).
40. S. Durairaj, S. Srinivasan, P. Lakshmanaperumalsamy, In vitro antibacterial activity and stability of garlic extract at different pH and temperature. *Electronic journal of Biology* **5**, 5-10 (2009).
41. B. Adjei-Mensah, B. Quaye, O. Opoku, C. C. Atuahene, Antiviral potentials of garlic (*Allium sativum*) in poultry production: A mini review. *Veterinary Medicine and Science*, (2023).
42. D. J. Alexander, Newcastle disease in the European Union 2000 to 2009. *Avian pathology* **40**, 547-558 (2011).
43. V. R. Brown, S. N. Bevins, A review of virulent Newcastle disease viruses in the United States and the role of wild birds in viral persistence and spread. *Veterinary research* **48**, 1-15 (2017).
44. W. Wu *et al.*, Quercetin as an antiviral agent inhibits influenza A virus (IAV) entry. *Viruses* **8**, 6 (2015).
45. T. Arify, S. Jaisree, K. Manimaran, S. Valavan, A. Sundaresan, Antiviral effects of garlic (*Allium sativum*) and nilavembu (*andrographis paniculata*) against velogenic strain of newcastle disease virus-an in ovo study. *Int. J. Livest. Res* **8**, 157 (2018).
46. H. YOSHIDA *et al.*, Antimicrobial Activity of the Thiosulfates Isolated from Oil-Macerated Garlic Extract. *Bioscience, Biotechnology, and Biochemistry* **63**, 591-594 (1999).
47. K. M. Lemar, M. P. Turner, D. Lloyd, Garlic (*Allium sativum*) as an anti-Candida agent: a comparison of the efficacy of fresh garlic and freeze-dried extracts. *Journal of Applied Microbiology* **93**, 398-405 (2002).
48. G. E.-S. Batiha *et al.*, Application of natural antimicrobials in food preservation: Recent views. *Food Control* **126**, 108066 (2021).
49. R. Heras-Mozos *et al.*, Development and optimization of antifungal packaging for sliced pan loaf based on garlic as active agent and bread aroma as aroma corrector. *International journal of food microbiology* **290**, 42-48 (2019).
50. M. Robles-Martínez *et al.*, Antimycotic Activity Potentiation of *Allium sativum* Extract and Silver Nanoparticles against *Trichophyton rubrum*. *Chemistry & Biodiversity* **16**, e1800525 (2019).
51. R. M. Khounganian *et al.*, The Antifungal Efficacy of Pure Garlic, Onion, and Lemon Extracts Against *Candida albicans*. *Cureus* **15**, e38637 (2023).
52. Y.-x. Li *et al.*, Antimicrobial mechanisms of spice essential oils and application in food industry. *Food Chemistry* **382**, 132312 (2022).
53. A. Tesfaye, Revealing the Therapeutic Uses of Garlic (*Allium sativum*) and Its Potential for Drug Discovery. *The Scientific World Journal* **2021**, 8817288 (2021).
54. G. El-Saber Batiha *et al.*, Chemical Constituents and Pharmacological Activities of Garlic (*Allium sativum* L.): A Review. *Nutrients* **12**, (2020).
55. M. M. El-Azzouny, A. S. El-Demerdash, H. G. Seadawy, S. H. Abou-Khadra, Antimicrobial Effect of Garlic (*Allium sativum*) and Thyme (*Zataria multiflora* Boiss) Extracts on Some Food Borne Pathogens and Their Effect on Virulence Gene Expression. *Cell Mol Biol (Noisy-le-grand)* **64**, 79-86 (2018).
56. J. O. Adebayo, A. U. Krettli, Potential antimalarials from Nigerian plants: A review. *Journal of Ethnopharmacology* **133**, 289-302 (2011).
57. H. A. Perez, M. D. I. Rosa, R. Apitz, In vivo activity of ajoene against rodent malaria. *Antimicrobial Agents and Chemotherapy* **38**, 337-339 (1994).
58. A. Coppi, M. Cabinian, D. Mirelman, P. Sinnis, Antimalarial activity of allicin, a biologically active compound from garlic



cloves. *Antimicrob Agents Chemother* **50**, 1731-1737 (2006).

59. Y. Feng *et al.*, Allicin enhances host pro-inflammatory immune responses and

protects against acute murine malaria infection. *Malar J* **11**, 268 (2012).



P102 - THE PHYSICAL PROPERTIES AND EFFECT OF ACRYLIC POLYMER DISPERSIONS ON WATER VAPOUR PERMEABILITY OF FINISHED LEATHERS

S. A. Abdulkadir¹, S. A. Amina², B. I. Mbonu³, S. H. Haruna⁴, A. Shamsiyya⁵,

¹Department of polymer and Textile Engineering, Ahmadu Bello University, Zaria, Nigeria

^{2,3,4,5}Department of polymer and Textile Engineering, Ahmadu Bello University, Zaria, Nigeria

Corresponding Author: abdul2sure4real@gmail.com: +2347060731593

ABSTRACT

The research study some physical properties and effect of acrylic polymer dispersions on the water vapour permeability of finished leather. An acrylic based commercial binder AE 558 Nycil has been characterized and its effect when applied in a finish formulation on some of the physical properties of originally retanned leathers was investigated. The binder was found to have an intrinsic viscosity of 227 dL/g, and a viscosity molecular weight (Mv) of 4.03×10^5 . This was obtained by conducting a solution viscosity measurement of the solid polymer in toluene at 25°C. The melting temperature of the solid binder has been found to be in the range 361.7°C - 370 °C. The results of these physical properties suggest that there is a very high molecular weight polymer with high thermal stability. Formulations for leather finishing was prepared containing the binder at varied proportions of A125g, B150g, and C175g, and was applied on the leather substrates corresponding to samples A1, A2, and A3 respectively. Tests on some of the physical properties of these coated samples were conducted. The water vapour permeability of the originally retanned (uncoated) leathers was reduced significantly after the finish was applied. A1 has the lowest permeability at 125 g of the binder in the formulation, while A3 has the highest permeability at 175 g of the binder in the formulation. Generally, the water vapour permeability of the coated leathers increases as the factor varied in this experiment was increased. A2 had the highest Shore A value at 150g of the binder in the formulation while A3 has the lowest Shore A value at 175 g of the binder in the formulation. Distension and Bursting strength of the uncoated leathers was improved after the leathers were coated. The results shows that the fastness of the coated samples generally increased as the quantity of the binder in the finish formulations was increased with sample A3 having the best resistance to wet rub action.

KEYWORDS

Acrylic polymer, Water vapour permeability, Finished leathers, Shore A Hardness Tester, Lastometer test

INTRODUCTION

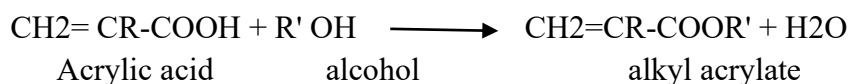
Acrylic polymers containing hydroxyl groups that are utilized in base coats as binders, which bind the pigments together, usually by a catalysed cross-linking mechanism with a polyisocyanate hardener, providing a chip-resistant coating. These coatings are usually two-component systems, meaning the binder and cross-linker are stored separately and mixed to form a pot mix prior to application also the binder are synthesized by emulsion polymerization (Eid *et al* 2017). Acrylic polymers, when applied as coatings or treatments to substrates like leather, textiles, or films, can influence these properties in various ways. Knowing that Leather is a durable

and versatile material that holds a significant place in human history and culture (Hirose, *et al.*, 2019). It is derived from the tanning and processing of animal hides or skins, resulting in a material with remarkable properties and applications. Leather has been utilized for various purposes, from clothing and accessories to upholstery and industrial goods. Its distinct attributes of strength, texture, and aesthetics have contributed to its enduring popularity. The effect of acrylic polymer dispersion on water vapor permeability and other physical properties such as hardness, rub fastness, and lastometer performance can be a complex and significant aspect of material development (Abd El-Ghaffar, *et al.*, 2017).



The research problem of the study based on the interest stemmed from the increasing incidence of worn shoe complaints involving lack of finish fastness, and other performance defects thus leading to investigation of the influence of finish components, and impregnating resins. It would be impossible to investigate a comprehensive range of resin dispersions, thus simple formulations of acrylic based binder have been selected.

This research is aimed at preparing a formulation of acrylic polymer dispersions suitable for application in leather finishing. The aim and objectives of this research was to prepare acrylic polymer formulations, apply it on the retanned leather and carry out Testing on the finished leathers to determine the water vapour permeability, and other physical properties of the leathers, the research will justify that various leather finishing materials, acrylic resin finishing agents are popular in leather industry due to its good film-forming performance, good adherence, simple production process and low production cost, large market share in both product kinds and yields, and has a bright market prospect, application prospect and its ability of being able to exclude water and allow air and water vapour to pass through the cross-section of the upper which is a basis of foot comfort (El-Nahass, et al.,2017).



The major monomers used are ethyl acrylate, methyl methacrylate and butyl acrylate, as well as non-acrylic monomers such as vinyl acetate and styrene which behave similarly.

Viscosity measurement of the resin binder

The solution viscosity measurement of the Binder was carried out at 25 °C using toluene as the solvent. 1 g of the solid polymer was dissolved in 50ml of the solvent to give a stock solution of 0.02 g/dl. The stock solution was divided into four portions, one was left that way while the other three were diluted by adding the solvent in the order 5 ml, 10 ml, and 15 ml. 10 ml of the pure solvent was introduced into the viscometer and the elution time, t_0 was obtained. This was repeated for each solution and the corresponding elution time was obtained and recorded as t_1 , t_2 , t_3 , and t_4 respectively.

Melting point determination of the resin binder

A melting point capillary was used. A tiny sample of the resin Binder was placed on a piece of weighing paper. The samples were placed into three

MATERIALS AND METHODS

Materials

The Leather made from the skin of goat was used for this research it was obtained from Nigerian Institute of Leather and Science Technology (NILEST) Samara Zaria.

Equipment's

Mettler, Lastometer (Muver, Model 5077-ET), Durometer, Gray scale, Water vapour permeabilimeter (Muver Model 5011), Rub fastness Tester, Barnstead Electrothermal A9100 (UK) and Cutter Machine

Finishing Consumables

Resin Binder (Nycil, AE 558), Wax (Lepton-Wax A, Basf), Penetrating agent (EE 8044, Pixel Colour), Liquid Syntan (Syntan-Re, Smit-zoom), Powdered Syntan (Syntan-SA, Smit Zoom), Bagaruwa (Vegetable Tannin), Wet Blue sheep skins and Toluene.

METHODS

Monomers were prepared by a reversible reaction between an acrylic acid and an alcohol:

melting point capillaries which have been previously sealed at one end. The capillaries containing the samples were then inserted into sample compartment of the melting point apparatus Barnstead Electrothermal A9100 (UK), and the instrument was switched on with a set temperature of 0-400 °C. The capillaries containing the samples were heated slowly and the temperatures at which melting occurred was observed and read out from the scale of the instrument.

Preparation of leather substrate

Three (3) pieces of sheep skins in the blue state was weighed (4.5 Kg) and then soaked in 9 Kg of water (i.e. 200 % of the sheep skins) at 50 °C for 15 minutes. The leather samples were then neutralized under this condition with 1 % NaHCO_3 for 45 minutes and the resulting pH of the bath was determined at the end of the operation. The samples were then rinsed with 200 % water at 50 °C for 15 minutes. The leather samples were then retanned using the following retanning agents: liquid syntan (4 %) for 20 minutes, powdered syntan (6 %) for 10 minutes, and bagaruwa (6 %) for 60 minutes



sequentially in accordance with established procedures in 200 % water at 60 °C. Finally, 6 % of fatliqour was added in 80 % water at 60 °C for 30 minutes. The leathers were then horsed up overnight, hanged to dry at room temperature for 45 minutes. The samples were then conditioned and

hand staked before finishing. The leathers were cut into two groups of three leathers each in order to finish them according to one with the finish labeled A1, A2, and A3 the other without a finish labeled B1, B2, and B3 respectively



Plate 3.1 B Samples



A Samples

Preparation of the finish formulations

The ingredients for the preparation of the finish formulations were weighed in grams (g) using an

electronic weighing balance and were introduced into five containers and was stirred vigorously for proper mixture. three different quantities of the resin binder were incorporated as shown in Table 3.1.

Table 3.2: Finish Formulations

Additives/Ingredients (g)	Formulations		
	A1	A2	A3
Acrylic Resin	125	150	175
Pigment	6.25	6.25	6.25
Water	50	50	50
Penetrator	6.25	6.25	6.25
Wax dispersions	8.75	8.75	8.75



Pigments

Plate 3.3 Cream Pigment

Application of finish formulations on the prepared leather substrate

A spray gun was used to apply the finish on the prepared leathers at room temperature under a fume



Acyclic formulations

Black Pigment

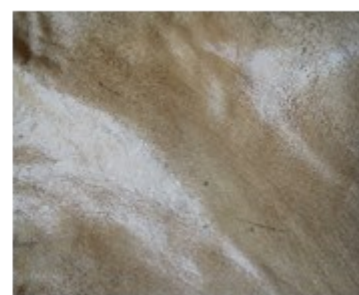
hood. The finish formulations were applied on the retanned leathers three times in order to obtain adequate cover and were allowed to dry at normal temperature and after which it was plated using a hot electric pressing iron.



Plate 3.4. Sample A1



Sample A2



Sample A3

Water vapour permeability Test

This test is used to determine the effect of the surface coat on porosity of the leathers. Weighed coated leather samples were placed inside thermostated sample holders containing 20 cm³ of water in water vapour permeabilimeter (Muver Model 5011) for 1 hr. The test sample capsules

together with the leathers were weighed again to take the difference in accordance with IUP 15. Water vapour permeability (P_{wv}) is calculated as: $P_{wv} \text{ (mg/cm}^2\text{/hr)} = 7640 M/d^2xt$, where, M= mass gain between weighings in milligrams; d² = area of diameter of sample in cm², t = time in minutes between first and second weighing.





Plate 3.5 Watber vapour Permeability test machine
Lastometer Test

Circular samples of the coated and uncoated leathers were cut and placed on an electronic lastometer (Muver, Model 5077-ET) respectively and were tested for distension and grain burst strength in accordance with official methods (SLTC, 1996). The forces (Kg) and displacement (mm) at burst was obtained from

Mettler

the corresponding digital print-out. Distension as a good index of film strength is a measure of the extent to which the film will extend before film breaks. The film strength in Kg/mm is established as the product of the force at break per unit area of the net distensions, i.e., grain film strength (Kg/mm) = Force (Kg)/Distension (mm).



Plate 3.6 Lastometer Machine



Tested Samples

Shore A (°) hardness test

The grain side of the leather was placed on the Shore A Hardness Tester/Durometer (Muver Model: 5019/5023-1/5023-A) to measure the degree of hardness.





Plate 3.7: Durometer Machine

Wet rub fastness Test

A rectangular piece of the leather samples was cut, and for each track 20 mm wide. The grain side of the leather to be tested was rubbed with pieces of standard wool felt under pressure with a given number of forward and backward motions. The SATRA machine was used, the samples was examined after 32, 64, 128, 256, 512 and 1024 revolutions of the dry and wetted pad and given

scores of 0, 1, 1/2, 2,2/3, 3, 3/4, 4, 4/5, and 5 when compared with a standard grey scales. A score of 1 is given to a sample with very poor resistance to rubbing effect while a score of 5 is ascribed to a sample with excellent resistance to rubbing effect. 0 is applicable to samples that were damaged due to the rubbing effect



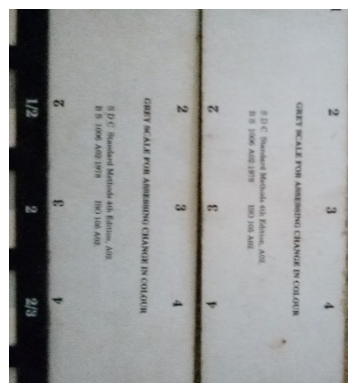
Tested Samples



Rub Fastness Machine



Grey Scale



Grey Scale



Felt

RESULTS AND DISCUSSION

Physical Testing of the Finished Leather



Water Vapour Permeability of Leather

Water vapour permeability tests on the coated and uncoated acrylic resin finished leathers were conducted and the results are shown in Table 4.1

Table 4.1: Effect of Acrylic Dispersion on Water Vapour Permeability of Leather

WEIGHT WATER VAPOUR PERMEABILITY ($\text{gcm}^{-3}\text{h}^{-1}$)									
Sample	0	1	2	3	1	2	3	Average	S.DEV
Coated									
A1	137.4 515	137.42 88	137.4035	137.3960	42.501	47.369	14.042	34.638	14.6981
A2	138.1 358	138.11 33	138.0896	138.0833	42.127	44.561	11.608	32.765	14.9932
A3	138.4 492	138.39 18	138.2583	138.2014	107.470	249.953	106.534	154.652	67.386
A	136.2 006	135.91 33	135.3578	134.6897	537.913	1040.06 5	1254.256	944.078	300.2189
Uncoated									
B1	138.6 242	137.80 00	136.5674	136.0698	1543.15 3	2307.80 2	931.568	1594.304	562.9668
B2	139.8 710	139.60 80	139.0865	138.5405	491.105	977.717	1022.278	830.367	240.5829
B3	137.0 437	136.21 93	135.0840	134.6876	1543.52 7	2125.62 7	742.181	1470.445	567.1484
B	135.3 739	135.06 96	134.5470	134.0622	569.742	978.466	907.693	817.634	178.3489

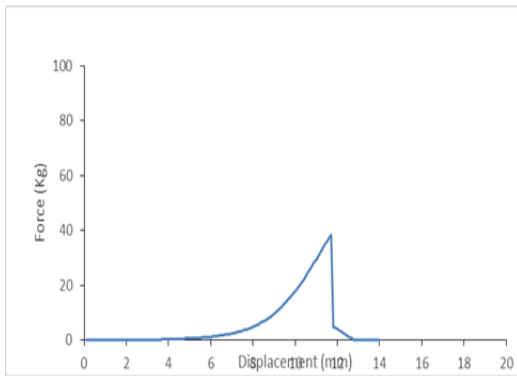
Lastometer Tests on Leather Samples

Lastometer Tests on the coated and uncoated acrylic resin finished leathers were conducted and the results are shown in Table 4.2.

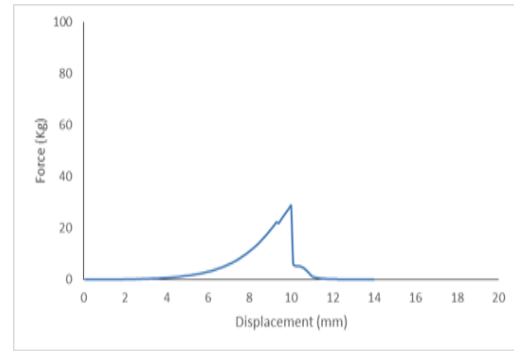
Table 4.2: Lastometer Tests on Leather Samples



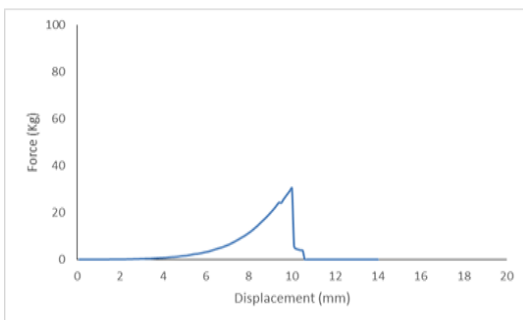
Sample	Force (kg) (Maximum)	Displacement (mm) (Maximum Value)
Coated		
A1	36.67	11.02
A2	37.35	11.28
A3	36.67	12.77
A	38.53	11.69
Uncoated		
B1	31.11	10.06
B2	29.10	10.04
B3	30.74	11.25
B	33.76	11.06



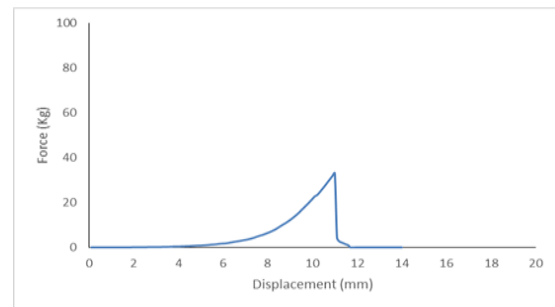
Sample A1



Sample A3

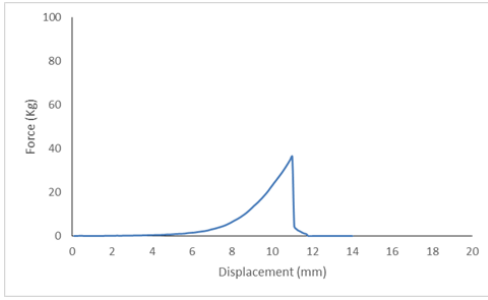


Sample A2

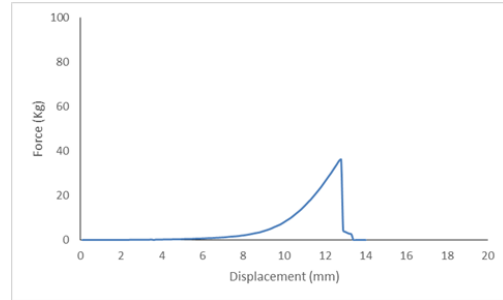


Sample A

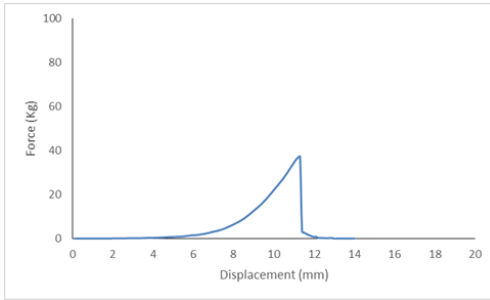




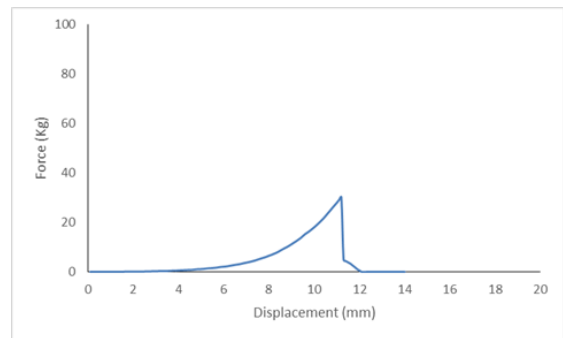
Sample B1



Sample B3



Sample B2



Sample B

Shore A (°) hardness of finished leather and melting point of binder

Film hardness of the acrylic resin coated and uncoated leathers and the melting point of the

binder was carried out on the acrylic resin coated leathers and the results are presented in Table 4.3 below.

Table 4.3: Determination of Shore A (°) of Finish Film and Melting Point of Resin Binder

SAMPLE ID	DUROMETER READING					MEAN	SDEV
	1	2	3	4	5		
A1	77.0	76.0	76.0	74.0	74.0	75.0	1.1
A2	72.0	75.0	72.0	76.0	75.0	74.0	1.6
A3	66.0	71.0	71.0	69.0	70.0	69.4	1.5
D	74.0	75.0	74.0	77.0	75.0	75.0	0.8
B1	79.0	79.0	80.0	79.0	78.0	79.0	0.4
B2	78.0	80.0	79.0	75.0	75.0	77.4	1.9
B3	80.0	78.0	75.0	78.0	77.0	77.6	1.3
D	75.0	77.0	73.0	72.0	78.0	75.0	2.0

Melting temperature (°C) 361.72-370



Wet rub fastness

Wet rub fastness tests were carried out on the acrylic resin coated leathers and the

results of counts in seconds and the corresponding Grey Scale ratings are presented in Table 4.4.

Table 4.4: Effect of Finish Formulations on Wet Rub Fastness of the Coated Leathers

Sample	Acrylic Offer (g)	Score	Count
A1	125	3	512
A2	150	4	512
A3	175	5	512
A	200	1	512

DISCUSSION

Permeability to water vapour is a property of major importance in garment leather, upper leather articles of clothing in general. It is this properties which permit escape of perspiration from the body and thus contributes to the comfort of wearer. Table 4.1. shows the effect of acrylic finish on the water vapour permeability of the original retanned leathers. It also tried to demonstrate the effect variations in the quality of the acrylic offer (g) in the formulations had on the water vapour permeability of the finished leathers. First, it is worthy to point out that the water vapour permeability of leathers especially for upper shoe determines the level of foot conform obtainable when shod. For this particular test, the general average of this result is surprisingly high. This is partly by the fact that the quantity of the finish applied are not large enough in order to obtain adequate cover, or probably the pores were not properly closed (contribution from retannage). However, the permeability of uncoded samples was significantly reduced by the application of the finished formulation when compared of that of the coated leather (Figure 4.2.) sample A1, which has the lowest quantity of the resin binder in the formulation, was expected the least permeable with the water vapour permeability of $137.4288 \text{ (gcm}^{-3}\text{h}^{-1}\text{)}$ and sample A3 with the $138.1133 \text{ (gcm}^{-3}\text{h}^{-1}\text{)}$ was the most permeable. For coated samples increase the amount of the acrylic offer in the formulations

produced a corresponding increase in water vapour permeability of the finish leathers. The uncoated samples generally as expected to produce much larger water vapour permeability of the originally retanned when compared with their finished counterpart. **Lactometer:** the result of the force an displacement of both coated and uncoated samples is shown in table 4.2. the displacement (MM) coated acrylic binders are higher than that of uncoated acrylic binders i.e. the coated samples A1, A2, and A3 have higher displacement than uncoated samples B1, B2 and B3. And also, there is an increase in the displacement of coated samples from A1, A2 and A3 (11.02 mm, 11.28 mm and 12.77 mm) and there is a decrease in the uncoated samples from B1 to B2 (10.06 mm and 10.04 mm) but B3 is higher than B1 and B2.

Shore hardness (⁰) harness of the acrylic coated leathers was determine and the melting point of the resin binder were carried out and their result are in table 4.3. the shore A value range between 60° to 77° and shore B value range between 70° to 80° . the uncoated samples i.e. B1, B2 and B3 (control samples) are harder than the coated sample A1, A2 and A3 (finished samples). The hardness of surface coating film is determined by the glass transition temperature (Tg). Tg. Occurs at a temperature where polymer changes from hard, brittle, glassy substance to soft and flexible one. (i.e. below Tg) and above room temperature, the polymer will hard and rigid.



Acrylic binder: Acrylic binder are known to have high Tg than other binder e.g. polyurithene and polybutadiene (Weijun, 2019), and the harder film should have higher Tg and versa-versal. In leather finishing where the binder is of the soft type with low Tg, during hot plating these film are very tacky and the finish formulation will require a plate release agent. The melting point (T_m) of a polymer is a temperature at which the crystalline melt and polymer becomes a viscos liquid (Hirose,*et.al.*2019). The melting point of acrylic was in the range of 3462-371⁰ table 4.3. Dry rub fastness: sample A1 with the acrylic resin 125g and score 3 have fire resistance to rubbing effect sample A2 with acrylic resin 150 g have score 4 have very good resistance to rubbing while sample A3 with acrylic resin 175 g have score 5 with excellent resistance rubbing effect. Therefore between A1, A2 and A3 samples, A3 sample have excellent resistance to rubbing effect due to good finish formulations and finishing.

CONCLUSION

The acrylic resin binder is a hard binder with a very large molecular weight, and has a melting temperature in the range 361-370 °C. This shows that the binder is a high polymer and possesses the properties suitable for application in leather finishing. The effect of the resin formulations on some physical properties of the originally retanned leathers have been studied and it is obvious that the finish had significant effect on such properties as water vapour permeability, lastometer, Shore A hardness, and wet rub fastness.

The results showed that the finished leathers were better than their unfinished counterpart. Increasing the quantity of the acrylic resin in the formulations also increased the water vapour permeability and wet rub fastness of the finished leathers except for the lastometer tests and shoreA hardness where there was no specific trend in behaviour. All the formulations showed better and adequate response to all the properties tested when compared to that of the unretanned leathers. Sample A1 (125 g resin offer), however would not be suitable for use in leather finish formulations where wet rub fastness is a priority. Aesthetic properties are very important, but finishes must be durable and standards for upper leathers and must include an assessment of finish properties. This has been highlighted in literatures because of the increasing incidence of worn shoe complaints involving lack of finish fastness, and this report has shown that the

quantity of components in finish formulations play an important part in determining wet rub resistance.

Acknowledgment: The authors expressed their gratitude to the H.O.D, staffs and the 2021/2022 final year Students of department of Polymer and Textile Engineering and the laboratory staff of Polymer and leather of the Nigerian Institute of Leather and Science Technology (NILEST) Samara Zaria, for their workshops, equipment used in the work.

Recommendations: As finishing plays an important role in water vapour permeability in order to improve the water vapour permeability of leathers, studies should be done on how to improve the water-absorbing capacity of finishing agent. On the other hand, if the water absorbing capacity of finishing agent is too high, the wet rubbing resistance may be decreased. So the work should be done to find a balance to improve the water absorbing capacity without decreasing the wet rubbing resistance of leathers

Declaration of conflicting interests: The authors declared no potential conflicts of interest with respect to the research, authorship, and/or publication of this article

REFERENCES

- Abd El-Ghaffar, M.A., El-Sayed, N. H., and Masoud, R. A., (2017). Modification of Leather Properties by Grafting. I. Effect of Monomer Chain on the Physico-Mechanical Properties of Grafted Leather"; *Journal of Applied Polymer Science*, 89 (6): 1478–1483.
- Anzlover, A., and Zigon, M., (2018). Semi-interpenetrating Polymer Networks with Varying Mass Ratios of Functional Urethane and Methacrylate Prepolymers, *Acta. Chem. Slov.*52: 230-237.
- Barrere, M., and landfester, K., (2016). High Molecular Weight Polyurethane and Polymer Hybrid particles in Aqueous



- Miniemulsion, *Macromolecules*, 36:5119-5125.
- Biemond, G.J.E., Braspenning, K., Gaymans, R.J., (2017). Polyurethanes with Monodisperse Rigid Segments Based on a Diamine-Diamine Chain Extender, *Journal of Applied Polymer Science*, 107: 2180-2189.
- Eid, M. A., Nashy, E.H.A., (2017). Speciation of Chromium Ions in Tanning Effluents and Subsequent Determination of Cr (VI); ICP-AES, *Journal of American Leather Chemists Association*, 97, 451.
- El-Nahass, M.M., Kamel, M.A., El-Barbary, A.A. et al., (2017). Spectrochem. Acta. A, 111, 37. In Rashid, S., Ahmad, A., and Fahim, A.Q., (2017). Synthesis and Application of Eco-Friendly Amino Resins for Retanning of Leather under Different Conditions, *Society of Leather Technologists and Chemists*, 98:8-15.
- Fan, H.J., and Shi, B., (2019). The Synthesis of Cationic Acrylic Resin for Water-based Leather Finish, *Chemistry*, 11: 722-726.
- Fekete, E., Foldes E. and Pukanszky, B., (2018). Effect of Molecular Interaction on the Miscibility and Structure of Polymer Blends, *European Polymer Journal*, 41, 727-736.
- Hirose, M., Zhou, J.H., Nagai, K., (2019). The Structure and Properties of Acrylic-Polyurethane Hybrid Emulsions, *Progression in Organic Coatings*, 38:27-34.
- Ibrahim, M.A. and Gawad, A.E.A., (2017). *J. Comput. Theor. Nanosci.*, 9: 1120, In Rashid, S., Ahmad, A., and Fahim, A.Q., (2017). Synthesis and Application of Eco-Friendly Amino Resins for Retanning of Leather under Different Conditions, *Society of Leather Technologists and Chemists*, 98:8-15
- Ibrahim, M., Mahmoud, A.Z., Osman, O. et al., (2017), *Spectrochem. Acta. A*, 81:724. In Rashid, S., Ahmad, A., and Fahim, A.Q., (2019). Synthesis and Application of Eco-Friendly Amino Resins for Retanning of Leather under Different Conditions, *Society of Leather Technologists and Chemists*, 98:8-15.
- Weijun D., (2019). Synthesis of Alkali-Soluble Copolymer (butyl acrylate/acrylic acid) and its Application in Leather Finishing agent"; *European Polymer Journal*, 44: 2695–2701.



P103 - REVIEW ON PHEROMONES IN AGRICULTURE: DISCOVERY, SYNTHESIS, AND ADVANCEMENTS FOR SUSTAINABILITY, ECONOMICS, AND CROP ENHANCEMENT

Adams, A.A.^{1,*}, Titus, O.M², Salisu, Z.M³, Ilyasu, A³

¹*Institute of Natural and Applied Science, Necmettin Erbakan University, Konya, Türkiye*

²*Mersin üniversitesi, Yenisehir, Türkiye*

³*National Research Institute for Chemical Technology, Zaria, Nigeria*

Corresponding Author: * adamsadeizaabdulrauf@gmail.com, philicbil101kd@gmail.com

ABSTRACT

This article examines the pivotal role of pheromones in revolutionizing sustainable agricultural practices, offering a promising solution to the challenges posed by conventional farming methods. The study addresses urgent need for environmentally friendly strategies in tackling the world's food concerns. In 19th-20th centuries, scientists had worked on phenomena that recognized as pheromones. However, since the amounts emitted by an individual animal were very small, these scientists could not easily identify the pheromones due to the limitations of the techniques available at that time. In 1959, the chemist Adolf Butenandt and his team identified the first pheromone, the silk moth's sex pheromone bombykol (Butenandt et al. 1959). This discovery prompted the creation of the word "pheromone" (from the Greek: *pherein*, to carry or transfer hormone, to excite or stimulate). Butenandt's discovery also established that chemical signals between animals exist and can be identified by researcher. This study highlights the need for pheromone manufacturing and application in the context of precise agriculture while appreciating the extraordinary contributions of pheromones in pest management and crop security. The broad adoption of pheromone-based practices with other integrated biological and cultural pest management as a cornerstone of global agricultural sustainability, serving as a beacon of hope in the pursuit of food security and environmental preservation.

Keywords: *pheromones, pest management, agricultural, environment, sustainability.*

1.0 INTRODUCTION

Addressing the world's food concerns requires a strong focus on agriculture. In order to ensure that everyone has access to food as the world's population continues to increase, production must be increased immediately. In order to maximize agricultural production yield, the use of fertilizers to nourish the soil and enhance crop growth, implementing effective management controls like the use of pesticides to safeguard crops from potential damage and ensure healthy harvest, good farm practice system like crop rotation have been adopted over the recent years. However, the use of pesticide has been found to be disrupting the natural ecosystem, not environmentally friendly, posing health risk and development of resistance by the targeted organism have been identified as a major setback.

Pheromones have attracted the attention of researchers as chemical messengers in the natural world. The purpose of this article is to discuss the function of pheromones in agriculture and their potential for crop sustainability and economics. The potential of pheromones to manage pests in horticulture, forestry, and stored goods has been thoroughly investigated (1). These specific behaviour-modifying substances have been applied to control insect populations, monitor insect populations, and protect plants and animals from insects. Pheromones and other semi chemicals can help manage sustainable and provide food security for a growing population (1). In addition to their role in pest management, pheromones also have the potential to be used in plant signalling for crop protection (2).

The synthesis of pheromones has been a significant area of research, with notable contributions from Professor Kenji Mori (3). His work in pheromone



synthesis and stereochemistry has laid the foundation for the practical application of insect pheromones in integrated pest management (3). Understanding the synthesis of pheromones is crucial for their development and application in agriculture.

This research aims to evaluate the importance contribution of pheromones in agriculture, understanding their nature and how they work as a chemical messenger, their roles in crop protection and sustainability, how they are used for crop enhancement, their synthesis, possible challenges that might be encountered during their synthesis and Innovative strategies to counter its setback, their economic and environmental benefits and future direction. Hence, the study showcases comprehensive conclusion and provides recommendations.

2.0 PHEROMONES: NATURE'S CHEMICAL MESSENGERS

Pheromones are chemical signals released by animals to communicate with members of the same species. They play a significant role in various behaviors and interactions within the animal kingdom (1). Pheromones have been classified into different types, this including sex pheromones, aggregation pheromones, alarm pheromones, and more (4). Sex pheromones are released to attract mate by animals of the same species and initiate reproductive behaviors. Members of the opposite sex may sense these pheromones, which causes particular behavioral reactions and mating interactions (4). Animals employ aggregation pheromones to establish groups or colonies and attract members of their own species. These pheromones aid in group activity coordination and social organization (4). When there is a threat or hazard, alarm pheromones are released. They serve as warning signals to alert other members of the species about potential risks or predators. Alarm pheromones can trigger defensive behaviors and help in group survival (5). Pheromones are used by animals in the animal kingdom for a variety of actions, including mating and marking territory. Pheromones, for instance, are essential for communication within the hive in honey bees. The queen bee secretes the "queen substance," a chemical that prevents worker bees from developing ovaries and preserves the colony's social order (6).

Researches have also shown that pheromones have been identified to cause anxiety. Research

conducted by Inagaki *et al.* (7), in 2014 shows that when a rat can release a specific odour into the air when stressed, this can increase anxiety levels in other rats. Pheromones are not only limited to insects and mammals, they have been found across the animal kingdom, from insects and crustaceans to fish and mammals. They are present in various habitats, both on land and underwater, and are involved in communication between different species (4). While pheromones are well-established in the animal realm, there is still disagreement over their function in human communication. Researchers are still investigating the vomer nasal organ (VNO), which is responsible for detecting pheromones in a variety of animals, including humans (8). However, chemical communication does occur among humans, although not all examples meet the proposed definition of pheromone communication.

3.0 DISCOVERY, SUSTAINABILITY AND ROLES OF PHEROMONES IN AGRICULTURAL SYSTEM

The discovery and application of pheromones in agriculture have transformed pest control strategies. Early accounts of pheromone-like effects in agricultural contexts provided the background for further studies in this area. The use of pheromones in agriculture has greatly benefited from advances in the identification and isolation of pheromones that affect interactions between plants and insects. Researchers have made significant progress in understanding the function and role of volatile organic compounds (VOCs) in plant signalling and how they can be employed in crop protection. One key study by Witzgall *et al.* (1) focused on the use of sex pheromones as a means of pest management in agriculture, where they looked at the possibilities of species-specific behaviour-modifying compounds, such as sex attractants for suppressing noxious insects was successful and appreciated.

This study highlighted the importance of pheromones in disrupting insect mating behaviours and reducing pest populations. Pickett and Khan (2) discussed about using plant volatiles to deliver signalling in agriculture. They stressed the use of next-generation genetic modification (GM) techniques and companion cropping as efficient ways to leverage plant signaling for long-term crop protection. Their research has made it possible to include pheromones into pest control methods. Witzgall, Pickett and Khan are notable researchers in this area whose work has considerably advanced the use of pheromones in agriculture. The discovery



of pheromones and their application in agriculture have had a profound impact on pest management strategies.

Pheromones have been used to interrupt insect mating and manage pest populations in agriculture. The mating behavior of pests can be interrupted, resulting in a decrease in their number, by releasing synthetic pheromones that replicate the natural chemical signals used by insects to attract mates. This approach, known as mating disruption, has been successfully implemented in various crops, such as apples, pears, and grapes (1). Using pheromones in pest management offers several benefits as compared to traditional chemical pesticides. Firstly, pheromones are species-specific, meaning they exclusively attack the targeted pest species, leaving harmless insects alone. This methodically focused strategy lessens the negative effects on non-target organisms and promotes the ecological stability of agricultural environments (1).

Nanotechnology have also played a significant role in precision agriculture by offering the potential for controlled release and targeted delivery of pheromones to give a better result (9). For instance, using nano- fertilizers to increase the effectiveness of nutrient delivery to crops can increase crop productivity and sustainability (9). These chemical signals released by organisms to communicate with

each other, have also shown potential in enhancing pollination and crop yield beyond their traditional use in pest control. Pheromones have been studied for their potential to improve crop quality and output by encouraging plant growth, root development, and stress resistance. However, the use of pheromones in promoting plant growth, root development, and stress resistance has been studied.

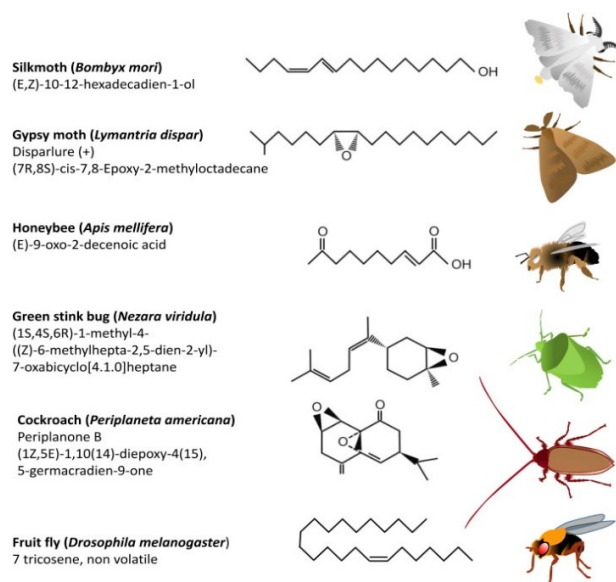


Figure 1 shows some insect sex pheromone molecules illustrating the diversity of chemical structures (10)

SYNTHESIS OF PHEROMONES: CHALLENGES AND INNOVATIONS

Synthesizing pheromones in the laboratory for mass production involves several steps and

Recent discoveries in molecular biology and neurology have illuminated how insects like the silk moth *Bombyx mori* recognize sex pheromones in a precise and sensitive manner. The detection of sex pheromone signals take place through pheromone receptors expressed in olfactory receptor neurons in the pheromone-sensitive *sensilla trichodea* on male antennae. The antennal lobe receives these signals, which are subsequently processed further in higher centres to produce orientation behaviour toward females (12).

challenges. Researchers use a variety of methods to reproduce the chemical structure and composition of naturally existing pheromones in order to synthesize them (11).



Figure 2 shows how insect have been trapped in the field with pheromones

Understanding the genetic underpinnings of pheromone synthesis is one of the difficulties in producing complex pheromones. Recent advances in genetic and genomic studies have revealed key genes and pathways involved in pheromone synthesis in eusocial insects. For example, studies have identified candidate genes, such as cytochrome P450 (CYP) genes, that are differentially expressed between queens and workers in ants. These genes are likely involved in the synthesis of queen pheromones, which play a crucial role in social communication within ant colonies (11).

The procedures used to create pheromones have been considerably streamlined and enhanced because of technological. The breakthrough covers all level of analysis, from molecular to behavioural, enabling a thorough examination of pheromone recognition processes. For example, researcher have identified candidate genes involved in pheromone synthesis among differentially expressed cytochrome P450 genes in eusocial insects (11). These developments have aided in the development of more effective and affordable techniques for the mass manufacture of pheromones while also improving the understanding of pheromone synthesis.

The development of biosynthetic pheromone production has shown significant importance in offering affordable and efficient alternatives to conventional chemical synthesis techniques. These improvements make use of acyl-CoA oxidase complexes and insect fatty acid-modifying enzymes. Insect fatty acid-modifying enzymes play an important role in the biosynthesis of pheromones derived from fatty acids. The precise positioning of double bonds in the produced fatty acid chain, which is necessary for the unique configuration of the pheromone, is accomplished by these enzymes (13).

4.0 FUTURE DIRECTIONS AND INNOVATIONS:

Ongoing research in pheromone application is focused on exploring new technologies and potential breakthroughs to enhance the effectiveness and efficiency of pheromone-based strategies in various fields, including agriculture and pest management. According to Benelli *et al.*(14), Sex pheromone aerosol devices have also been developed for mating disruption, and provides

an effective and environmentally friendly approach to pest control.

Integration of cutting-edge technologies like nanotechnology and biotechnology with pheromone delivery systems is another area of research. Nanotechnology offers the potential to develop novel nanoscale pheromone dispensers that can provide more accurate and controlled release of pheromones (15). These nanoscale dispensers can improve the longevity and stability of pheromones, ensuring a sustained release over an extended period. This technology has the potential to enhance the efficacy of pheromone-based strategies by optimizing the timing and dosage of pheromone release, leading to improved pest control and crop protection.

Biotechnology is also playing a significant role in advancing pheromone application. To increase the production of pheromones in organisms or create genetically engineered crops that can produce their own pheromones to attract or repel pests, genetic engineering techniques can be used. This approach offers the potential for sustainable and self-contained pest management systems, reducing the reliance on external pheromone sources and minimizing the need for additional applications. Pheromone-based monitoring systems can be combined with sensor technologies to detect and identify pest populations in real-time. This information can then be used to initiate the release of pheromones or other pest control measures, ensuring timely and effective pest control.

CONCLUSION

In conclusion, it is not impossible to overestimate the tremendous role that pheromones have played in changing sustainable agriculture. The use of pheromone-based techniques has demonstrated their efficiency in pest management as well as their tremendous potential for reducing the negative environmental effects of conventional chemical pesticides. Recognizing the crucial part pheromones can play in influencing the future of agriculture is imperative in solving both global food security and environmental issues. This necessitates a collective effort for the research institutes, universities, policymakers, and agricultural stakeholders to intensify their efforts by fostering collaboration, and invest in the research and development of pheromones-based approaches. By utilizing pheromones, it tends to increase crop yields, providing a sustainable solution for food availability in the world's expanding population and



maintaining the ecosystem. It is incumbent upon us to adopt this cutting-edge environmentally friendly technology, ensuring that pheromone-based approaches are at the top of our global agricultural agenda. In addition, pheromones usage can be practice alongside other integrated pest management practices, such as crop rotation, biological control, and cultural practices.

REFERENCES

1. P. Witzgall, P. Kirsch, A. Cork, Sex pheromones and their impact on pest management. *Journal of chemical ecology* **36**, 80-100 (2010).
2. J. A. Pickett, Z. R. Khan, Plant volatile-mediated signalling and its application in agriculture: successes and challenges. *New Phytologist* **212**, 856-870 (2016).
3. H. Takikawa, S. Kuwahara, Overview of Kenji Mori's pheromone synthesis series. *Journal of Pesticide Science* **48**, 1-10 (2023).
4. T. D. Wyatt, *Pheromones and animal behavior: chemical signals and signatures*. (Cambridge University Press, 2014).
5. V. C. Norman, T. Butterfield, F. Drijfhout, K. Tasman, W. O. H. Hughes, Alarm pheromone composition and behavioral activity in fungus-growing ants. *Journal of Chemical Ecology* **43**, 225-235 (2017).
6. D. Baracchi *et al.*, Pheromone components affect motivation and induce persistent modulation of associative learning and memory in honey bees. *Communications Biology* **3**, 447 (2020).
7. H. Inagaki *et al.*, Identification of a pheromone that increases anxiety in rats. *Proceedings of the National Academy of Sciences* **111**, 18751-18756 (2014).
8. M. Meredith, Human vomeronasal organ function: a critical review of best and worst cases. *Chemical senses* **26**, 433-445 (2001).
9. R. Raliya, V. Saharan, C. Dimkpa, P. Biswas, Nanofertilizer for precision and sustainable agriculture: current state and future perspectives. *Journal of agricultural and food chemistry* **66**, 6487-6503 (2017).
10. E. Jacquin-Joly, A. T. Groot, in *Encyclopedia of Reproduction (Second Edition)*, M. K. Skinner, Ed. (Academic Press, Oxford, 2018), pp. 465-471.
11. H. Yan, J. Liebig, Genetic basis of chemical communication in eusocial insects. *Genes & development* **35**, 470-482 (2021).
12. T. Sakurai, S. Namiki, R. Kanzaki, Molecular and neural mechanisms of sex pheromone reception and processing in the silkworm *Bombyx mori*. *Frontiers in physiology* **5**, 125 (2014).
13. M. Tupec, A. Buček, I. Valterová, I. Pichová, Biotechnological potential of insect fatty acid-modifying enzymes. *Zeitschrift für Naturforschung C* **72**, 387-403 (2017).
14. G. Benelli, A. Lucchi, D. Thomson, C. Ioriatti, Sex Pheromone Aerosol Devices for Mating Disruption: Challenges for a Brighter Future. *Insects* **10**, 308 (2019).
15. C.-L. Tsai *et al.*, Genetic differentiation and species diversification of the *Adoxophyes orana* complex (Lepidoptera: Tortricidae) in East Asia. *Journal of Economic Entomology* **116**, 1885-1893 (2023).



P104 - PHYSICOCHEMICAL CHARACTERIZATION OF LAUNDRY WASTEWATER AND ITS ENVIROCHEMICAL IMPACT ON SOILS AND WATER

¹Feka D.P., ²Patrick B.T., ³Adegboro N.N., ⁴Ityo S. D., Patrick K.

¹Department of Science Laboratory Technology, Nigerian Institute of Leather & Science Technology Zaria

²Department of Industrial Chemical Processing Technology, Nigerian Institute of Leather & Science Technology Zaria

³Department of Polymer Technology, Nigerian Institute of Leather & Science Technology Zaria

⁴Center for Food Technology and Research (CEFTR), Benue State University Makurdi, Nigeria

Correspondence: fekepaschal@yahoo.com; +2347067821907

ABSTRACT

The influence of greywater on the physicochemical properties of surrounding soil and water was evaluated. Laundry wastewater was collected from students (male and female) at Nigerian Institute of Leather and Science Technology (NILEST) Zaria. Physicochemical parameters and some metal contaminations were studied. Control sample for the work was collected from borehole water at the hostel. pH and TDS, EC and Temp. were within the WHO tolerable limits. At room temperature, the laundry wastewater from the hostels for male and female had an average of 2245 mg/L TDS, 3.2 $\mu\text{S}/\text{cm}$ EC, and pH of 10.3. Cadmium (Cd), chromium (Cr), nickel (Ni) and Zinc (Zn) were evaluated in the samples and control, average concentration of 0.304 mg/L of Cr, 0.189 mg/L of Cd, 1.514 mg/L of Ni, and 1.784 mg/L of Zn were present.

Keywords: greywater, wastewater, metal enrichment

1.0 INTRODUCTION

The composition of laundry detergents is generally complex due to the numerous factors that have to be taken into consideration to ensure fresh clean garments at the end of the wash process (1).

Soap, detergents and water are important because they are frequently utilized in day-to-day activities of people. They are used in bathing, washing hands and clothes (2).

Among pollutants, detergents have been highlighted as an important source of industrial, commercial and domestic pollution, especially in large urban centres (3). Pollution discharges containing surfactants cause severe changes to biota because the activities of many aquatic organisms depend fundamentally on water surface tension. Anionic surfactants can bind to peptides, enzymes, and DNA. Binding to proteins and peptides may change the folding of the polypeptide chain and the surface charge of a molecule. This may modify the biological functions of biota (4, 5).

Tariq *et al.* (6) opined that laundry wastewater contains varying levels of suspended solids, salts, nutrients, organic matter and pathogens, that arise from clothes and laundry detergents and fabric softener residents. These pose precarious situation with regard to population health and environmental conservation. Thus, it is imperative that characterization of the wastewater, as well as development of an economically viable and efficient technology that allow for an improvement of sanitary conditions. Such characterization should reveal physicochemical properties like organic matter, pH, redox potential, TDS and other nutrients. Giagnorio *et al.* (7) have studied the environmental impact of different detergents used in the industrial laundry processes.

2.0 METHODOLOGY

2.1 Sample Collection

Samples of wastewater were taken from students' laundry for several types of hand-washed clothes (mixed, white, black, and colored). Polyethylene bags were used to collect soil samples, and plastic containers were used to collect wastewater samples, the containers were thoroughly cleaned by washing them in non-ionic detergent. After thoroughly



rinsing the 250 cm³ capacity sample bottles three times with sample water, they were filled to the brim at a depth of one meter below the wastewater from each sampling station and then brought to the lab for examination.

2.2 Experimental

2.2.1 Determination of pH, TDS, and Conductivity

This was carried out using a multi-meter (HI9813-61) with relevant probes inserted into the solution of the wastewater, and the reading on the machine was reported.

2.2.2 Heavy metal analysis

All measurements were performed using Agilent 4210 MP-AES. The sample introduction system consisted of PVC peristaltic pump tubing (white/white and blue/blue), a

single pass cyclonic spray chamber and the nebulizer. The Agilent MP Expert software was used to automatically subtract the background signal from the analytical signal, following this, the blank solution's background spectrum was recorded, and this was automatically deducted from each of the standards and sample solutions investigated. The software was also applied to improve both the nebulization pressure and viewing position for each of the designated wavelength in order to maximize sensitivity. Owing to this optimization, and also in view of all determinations were carried out successively, each analyte was determined under enhanced settings. A standard reference solution was employed to quickly and easily optimize the considerations. This was carried out following the instrument manufacturers' instruction.

3.0 RESULTS

Table 1: Physicochemical properties of laundry wastewater collected from student hostel

Samples	pH	TDS (mg/L)	EC ($\mu\text{s}/\text{cm}$)	Temp ($^{\circ}\text{C}$)
Control (borehole water)	6.84	410	60	22.8
Female hostel laundry wastewater	10.42	2040	290	23.3
Male hostel laundry wastewater	10.18	2450	350	24.4

WHO Limits: pH (6-9), conductivity (1000.0 $\mu\text{s}/\text{cm}$), TDS (2000.0 mg/L), temperature (40 $^{\circ}\text{C}$),

Table 2: Physicochemical properties of soils collected from points in NILEST

Parameters	pH	Temp ($^{\circ}\text{C}$)	EC ($\mu\text{s}/\text{cm}$)	TDS (mg/L)
Sample C: Control	7.09	26.50	0.090	0.13
Sample A: Male's hostel	8.85	24.20	1.04	730
Sample B: Female's hostel	8.42	23.20	3.31	2290

WHO Limits: pH (6-9), conductivity (50-500 $\mu\text{s}/\text{cm}$), TDS (2000 mg/L)

Table 3: Heavy metals concentration in water samples

Samples	Elements (mg/L)			
	Cr	Cd	Ni	Zn



Control (borehole water)	0.014	0.098	0.363	0.366
Male hostel laundry wastewater	0.234	0.184	2.528	1.503
Female hostel laundry wastewater	0.374	0.194	1.039	1.524

WHO limit (mg/L): Zn (300), Cd (0.01), Ni (1.0), Cr (0.5)

4.0 DISCUSSION

The mean concentration of physicochemical parameters and trace metals is given in Tables 1-3. The wastewater samples analysed were of dark brown colour for sample from female's hostel and blackish colour in sample from male hostel. The pH for the samples 6.84 – 10.42 in table 1, and 7.02 – 8.84 in table 2, indicating that analyzed wastewater samples fall within allowable pH range (i.e., 6–9) as stated by the World Health Organisation (WHO) (8). The pH values recorded for the control sample (borehole water) is 6.84, sample from female hostel gave 10.42 and 10.18 was recorded sample from male hostel respectively. Greywater was collected from students after laundry hostels are at the alkaline region, while the control sample is neutral.

The most significant property of soil is its pH level, its effects on all other parameters of soil. Therefore, pH is considered while analysing any kind of soil. If the pH is less than 6 then it is said to be an acidic soil, the pH ranges from 6-8.5 it's a normal soil and greater than 8.5 then it is said to be alkaline soil. Soil irrigated with untreated greywater has shown an elevation in pH value due to the contents of alkaline detergents

The result reveals heightened values for TDS (organic salt and small amount of organic matter dissolved in water), in the laundry wastewater from the male hostel and laundry wastewater from the female hostel. This reveals that the laundry wastewater contains high level of contaminants (TDS) compared to the control (borehole water). High TDS is harmful to aquatic life and soil organisms as well.

soil's samples from male' and female' hostel 730 and 2270, and outside the hostel control sample C has 0.13 sample B has highest values, sample A lower while sample C lowest values. The result obtained in this study was lower that maximum limit of the soils parameter which was collected (WHO) recommended 50 mg/L.

Electrical conductivity (EC) is usually related to the amount of dissolved solids or minerals (ions). It means the proficiency of water to pass out an electric current. The EC value (Table 1) of all the

wastewater samples is 290 and 350 $\mu\text{s}/\text{cm}$, indicating that the samples (>83%) were within the standard limits, i.e., <1000 $\mu\text{s}/\text{cm}$, this very very high when compared to the control sample (60 $\mu\text{s}/\text{cm}$). our result showed there is evidently and amplification of the concentration of ions by the presence of detergents.

Another crucial aspect of soil is its electrical conductivity, it is useful in assessment of a soil's quality. It measures the amount of ions in a solution; an increase in ion concentration causes a soil solution's electrical conductivity to rise. It is an indicator of how many ions are in a solution. Checking the health of soils can be done quickly, easily, and affordably with electrical conductivity (9). For soil samples from male hostel and female hostel (1.04 $\mu\text{s}/\text{cm}$ and 3.31 $\mu\text{s}/\text{cm}$ respectively) and the control sample (0.090 $\mu\text{s}/\text{cm}$), higher (EC) may linked to higher sodium content, an abundant element in the tripolyphosphate of detergents (10) WHO limit which is accepted before wastewater is discharged is 500 $\mu\text{s}/\text{cm}$ at maximum.

The pH, conductivity, and TDS environmentally acceptable limits by WHO were not exceeded by any of the samples.

4.1 Heavy Metals Analysis

The amounts of specific heavy metals (zinc, nickel, chromium, and cadmium) detected in the wastewater samples under analysis are shown in Table 3.

The control sample's concentration of metal chromium (Cr) is 0.014, whereas wastewater from the hostels for male and female has a concentration of 0.234 and 0.374 mg/kg, respectively. According to the analysis's findings, wastewater from the hostels for male and female has higher Cr concentrations than the control sample. The wastewater samples from the female' hostel was the most contaminated by chromium. Chromium levels was exceeded by all samples but in closely acceptable amount (0.014 mg/L) in the control sample, while laundry wastewater from male hostel and female hostel show a high enrichment for Cr. The values recorded are over 100 % when compared to the control sample.



As reported by Tariq *et al.* (6), chromium may experience oxidation, reduction, sorption, and precipitation in aquatic environments. Furthermore, chromium's solubility is pH-dependent, meaning that at acidic pH levels, it tends to solubilize; at pH levels greater than 7, on the other hand, Cr (III) precipitates. Furthermore, dichromate and Cr (VI) chromate are very soluble in all pH ranges. In the end, increased solubility leads to increased bioavailability of chromium; yet, even at low concentrations—roughly 0.5 to 5.0 mg/L in nutrient solution and 5 to 100 mg/g in soil—it is extremely hazardous.

The result for Cadmium (Cd) shows that the control sample, laundry wastewater from the male and female hostels has concentrations of 0.98 mg/L, 0.184mg/L and 0.194mg/L respectively. The results from the laundry wastewater from the male and female hostels has the highest value of contaminants Cd than the control sample.

Zinc (Zn) evaluated shows that the control sample, laundry wastewater from the male hostel and laundry wastewater from the female hostel has the value of 0.366 mg/L, 1.503 mg/L and 1.524 mg/L respectively. The result from the laundry wastewater shows Zn enrichment.

The control sample showed the least amount of Ni (0.363 mg/L), while laundry water from male hostel was the most (2.528 mg/L). Findings from this study discloses obvious enrichment of Ni in the wastewater from the male and female hostel. The most polluting metal was Ni with a maximum concentration of 2.528 mg/L male hostel, 1.039 mg/L concentration recorded in female hostel was slightly above the WHO environmental standard.

All samples did not exceed the WHO threshold for Cr (0.5 mg/L), Cd(3.0 mg/L), Ni (50.0 mg/L) and Zn (300.0 mg/L), but it is worth stating their continues discharge of these greywater will lead to elevated concentrations in surrounding soils, and thus pose an ecological risk.

5.0 CONCLUSION

The results of the study show that laundry wastewater raises pH, TDs, electrical conductivity, and levels of several heavy metals (Cr, Cd, Ni, and Zn). According to this study, laundry wastewater contains contaminants that are bad for the environment. Discharging detergents-containing wastewater into soils increased phosphorus and sodium content, and raise pH and electrical

conductivity. There is a serious risk to the residents of the sample area's health. Therefore, it is highly advised to switch to detergents that are both environmentally friendly and biodegradable.

REFERENCES

1. O. Lade, Z. Gbagba, Sustainable water supply: Potential of recycling laundry wastewater for domestic use. *Journal of Civil Engineering and Environmental Sciences* **4**, 056-060 (2017).
2. F. O. Abulude, S. D. Fagbayide, S. A. Olubayode, E. A. Adeoya, Assessment of Physicochemical Properties of Soaps, Detergents and Water Samples Originated from Nigeria. *CONTINENTAL JOURNAL SUSTAINABLE DEVELOPMENT* **18**, 55-67 (2017).
3. J. K. Braga, M. B. A. Varesche, Commercial laundry water characterisation. *American Journal of Analytical Chemistry* **2014**, (2014).
4. S. O. Badmus, H. K. Amusa, T. A. Oyehan, T. A. Saleh, Environmental risks and toxicity of surfactants: overview of analysis, assessment, and remediation techniques. *Environmental Science and Pollution Research*, 1-20 (2021).
5. T. Ivanković, J. Hrenović, Surfactants in the environment. *Arh Hig Rada Toksikol* **61**, 95-110 (2010).
6. M. Tariq *et al.*, Physicochemical and bacteriological characterization of industrial wastewater being discharged to surface water bodies: significant threat to environmental pollution and human health. *Journal of Chemistry* **2020**, 1-10 (2020).
7. M. Giagnorio, A. Amelio, H. Grüttner, A. Tiraferri, Environmental impacts of detergents and benefits of their recovery in the laundering industry. *Journal of Cleaner Production* **154**, 593-601 (2017).



8. WHO, pH in Drinking-water. *WHO Guidelines for Drinking-water Quality*. 2007.
9. K. S. Tale, S. Ingole, A review on role of physico-chemical properties in soil quality. *Chemical Science Review and Letters* **4**, 57-66 (2015).
10. J. J. Scheibel, The evolution of anionic surfactant technology to meet the requirements of the laundry detergent industry. *Journal of surfactants and detergents* **7**, 319-328 (2004).



P105 - EXTRACTION OF BITUMEN FROM TAR SANDS OBTAINED FROM LODA, ONDO STATE, NIGERIA FOR APPLICATIONS IN CONSTRUCTIONS AND PETROCHEMICALS

N. A. Ozogu¹, A. A. Osigbesan¹, A. F. Ade-Ajayi^{1*}, E. A. Audu¹, N. Ashade¹, Z. Sani. Gano¹, O. U. Ahmed², and J. T. Barminas¹

National Research Institute for Chemical Technology, Zaria, Kaduna State, Nigeria.

²Department of Chemical and Petroleum Engineering, Bayero University, Kano State, Nigeria.

Corresponding author email: pheemmistic@gmail.com

ABSTRACT

Nigeria is blessed with vast deposit of tar sand containing bitumen in the South-Western part along the Ondo-Edo-Ogun-Lagos belt. These deposits are in a shallow subsurface of this region, and have not less than 42 billion barrels of extrapolated reserve of bitumen. Bitumen was extracted from tar sand obtained from four different locations in Loda, Ondo State by Soxhlet extraction method using Cyclohexane as the solvent. The bitumen obtained was analysed by Fourier Transform Infrared Spectroscopy (FTIR) technique, the components were further separated by into group components of Saturates, Aromatics, Resins and Asphaltenes (SARA). The highest bitumen yield obtained from the different samples was 18.0 % while the lowest was 7.6%. The results of SARA analysis of the samples showed that there are more of aromatics (above 50%), followed by resins (17 -29%), and saturates (11 – 18%). The FTIR analysis of the bitumen showed the presence of functional groups like C-H, OH, N-H, P-O-C. therefore, based on outcomes of the analyses conducted so far on the extracted bitumen samples, their applications are promising in the constructions and petrochemical industries.

KEYWORDS: *Tar sand, Bitumen, Solvent technique, Extraction, Unconventional resources.*

1.0 INTRODUCTION

The global demand for energy is rapidly increasing, and conventional oil reserves will not be able to meet up the demand. The need to exploit unconventional resources which include tar sand, shale oil, shale gas and tight gas, is being considered globally (1). Currently, crude oil produced from light oil deposits comprises only one third of all world oil reserves. The other two thirds belong to heavy and extra heavy oil, of which only one percent is being exploited (2). Tar sands are found in several countries around the world, such as former Soviet Union, Venezuela, Cuba, Indonesia, Brazil, Jordan, Madagascar, Trinidad, Colombia, Albania, Rumania, Spain, Portugal, Argentina, and Nigeria. The estimated worldwide resources of tar

sands are about three times the known petroleum reserves (3). The world's largest deposit of tar sands is found in Athabasca, Alberta, Canada, which have 2.4 trillion barrels in reserve (4).

Tar sands (also known as oil sands) are sands or carbonates containing bitumen or other hydrocarbons that are immobile due to their high viscosity under normal reservoir temperatures. In order to utilized tar sand, the hydrocarbons can be mined or extracted from the rock by the use of steam or solvents (5). Tar sand is composed of a mixture of about 10 - 20% bitumen, about 70 - 85% mineral matter including sands, clays, and 4 - 6% water (5). There are two major ways to extract bitumen from tar sands depending on the depth of the deposit; in-situ extraction and surface mining.



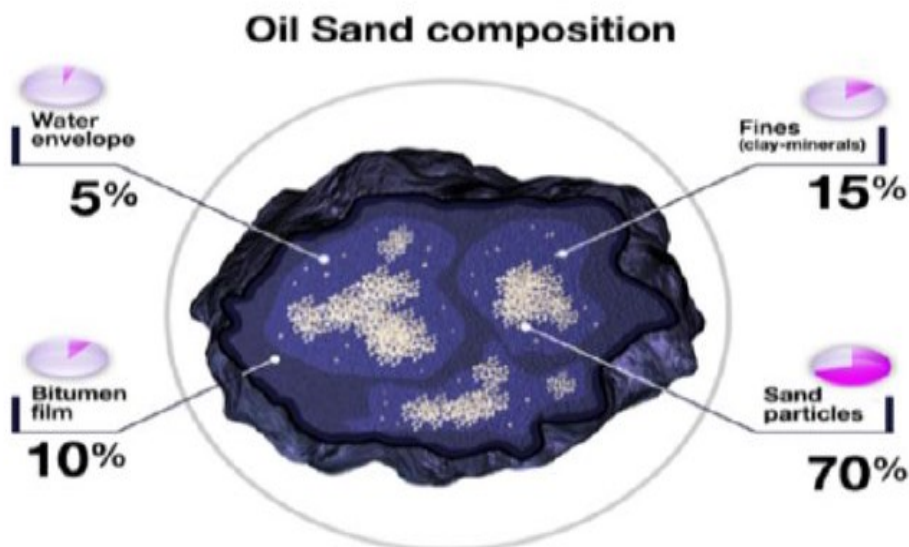


Figure 1: Composition of Tar Sand (Oil Sand) (1).

Nigeria's bitumen deposit belt is found in four states; Edo, Ondo, Ogun, and Lagos, according to geo-physical surveys carried out since 1901 when it was first discovered by the Germans, and have not less than 42 billion barrels of extrapolated reserve. Nigeria's bitumen is documented to rank sixth in the world (5). In Ondo state, major tar sand deposits are located in Okitipupa, Agbabu, Loda, and Ilubinrin. The exploitation of the bitumen in tar sand deposit according to experts would open a new source of foreign exchange earnings for the nation's oil dependent economy, but they have largely remained unexploited due to the availability of the conventional oil in the neighbouring oil rich Niger Delta of the country (1).

Tar sand consists of a mixture of bitumen, water, quartz sand, clays, and other minerals which is either oil or water wet. Nigerian tar sands are water-wet having chemical composition as shown in Table 1. Tar sands have found applications in different areas such as in road construction, buildings, production of petroleum products like gasoline, diesel, kerosene, benzene, xylene, etc. (1).

The purpose of this research is to extract bitumen from tar sands using solvent extraction techniques. This study intends to promote the exploration and exploitation of bitumen from Nigerian tar sands which can aid in further revenue in the country.

Table 1: Chemical Composition of Nigerian Tar Sands (5).

Element	Nigeria's Composition (%)
Carbon	85
Hydrogen	10.7
Nitrogen	0.5
Oxygen	1.7



2.0 MATERIALS AND METHOD:

2.1. Materials and Equipment:

Tar sand samples were collected from four different locations in Loda, Ondo State, Nigeria.

Cyclohexane (C_6H_{12}), silica gel, chloroform, methanol, Rotary evaporator (RE300 model), FTIR (analytica 3000 model). All chemicals were of analytical grade and were used without further purification.

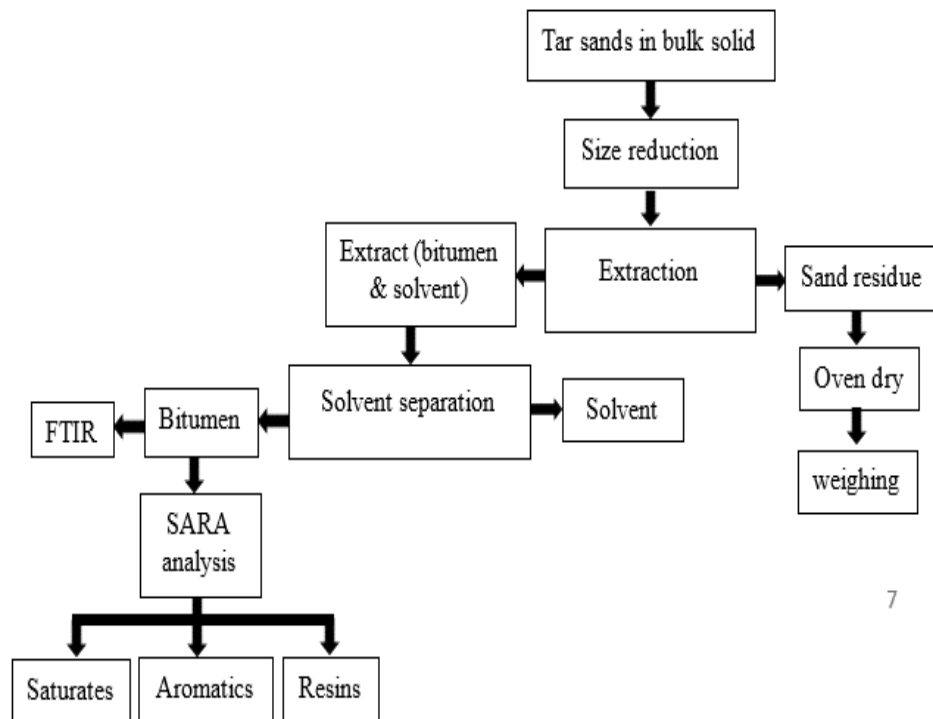


Figure 2: Block Diagram for the Extraction Process.



Figure 3: Tar Sands Samples.

2.2. Experimental Procedure:

Sample preparation:

The collected tar sand samples were crushed using ceramic mortar and pestle.

Extractions of Bitumen Oil:

Bitumen was extracted from the tar sand samples (1A, 1B, 2A and 2B) using soxhlet extraction method. Tar sand sample 1A was loaded into a thimble and 300 mL of Cyclohexane was used for the extraction. Subsequently, the bitumen oil was recovered using a rotary evaporator. The residue



was then dried in an oven at 60 °C overnight in order to determine the percentage yield of bitumen extracted. This procedure was applied to the other three samples.

$$Y = \frac{W_i - W_f}{W_i} \times 100$$

.....
 (1)

The percentage yield (Y) was calculated as;

Where W_i is the initial weight of the sample, and W_f is the final weight of the sample.



Figure 4: Recovered Bitumen oil

SARA Analysis:

The bitumen oil sample was separated into saturates, aromatics and resin components by the SARA technique which was carried out using a silica gel packed column of height 7 cm. The saturates (aliphatic component) was eluted using Cyclohexane, while the aromatic component was obtained using 3:2 cyclohexane to chloroform ratio; and the resin was obtained using 1:1 chloroform to methanol ratio. These components were collected and the solvents were allowed to evaporate at room temperature. This SARA technique was carried out according to the ASTM D4124-09 adapted from Shi et al., 2017 (6), and repeated for the other three

samples. The percentage composition of each component was calculated.

3.0 RESULTS AND DISCUSSION:

The percentage yield for the extracted bitumen from tar sands for each sample was calculated and presented in Figure 5. The result showed that sample 1A had the highest percentage yield of 18% while sample 2B had the lowest percentage yield of 7.57%. This suggest that the tar sand collected from location 1A is richest in bitumen when compared with the samples from other locations (1B, 2A and 2B).



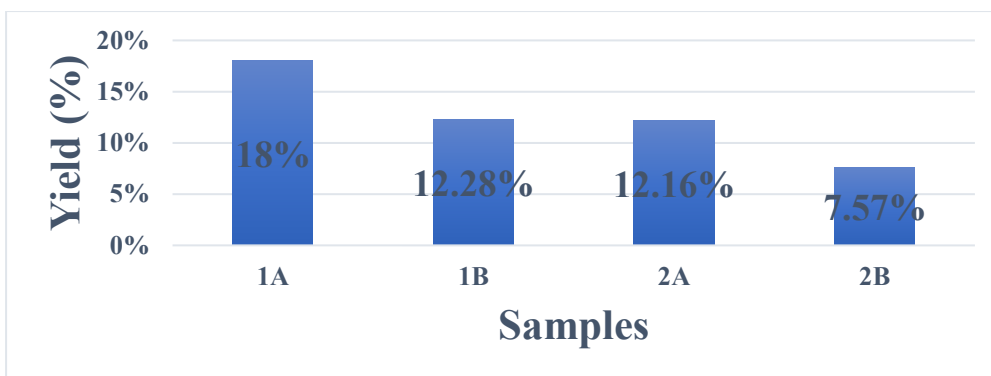


Figure 5: Percentage Yield of the Extracted Bitumen from Tar Sands.

3.1. SARA Analysis:

The result of SARA analysis is presented in Figure 6. Findings from the results showed that the percentage of aromatics is highest and above 50% in all the samples compare to the percentages of the

saturates and resins which are between 11 – 18% and 20 – 37% respectively. This result conforms with the result of Shadrach *et al.*, 2018, on a tar sands from Yegbata and Agbabu, Ondo State, (saturates 7.59 and 46.35%, aromatics 64.39 and 21.63%, and resins 28.01 and 32.02)(I).

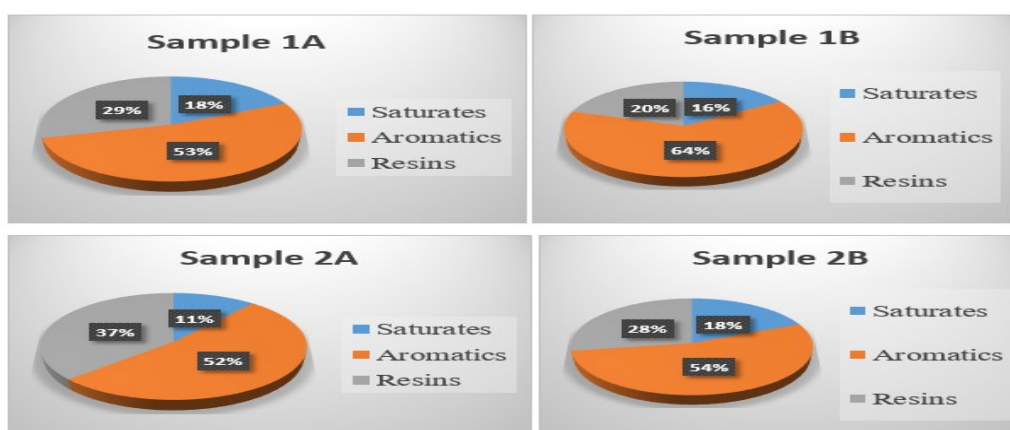


Figure 6: SARA Results of the Four Samples 1A, 1B, 2A, and 2B.



3.2. FTIR spectra of bitumen:

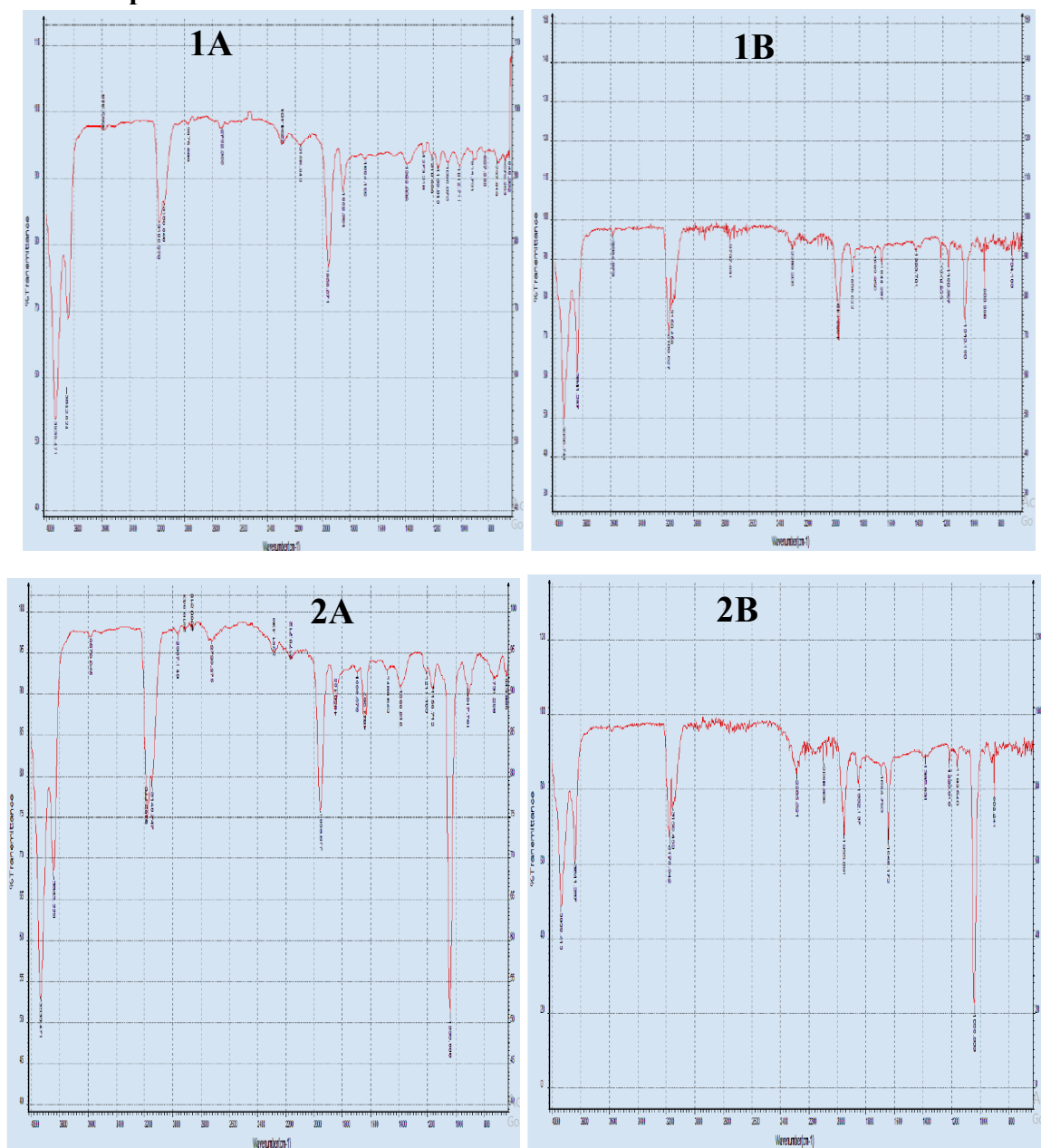


Figure 7: FTIR spectra of the bitumen samples 1A, 1B, 2A, and 2B.

The FTIR spectra of the bitumen samples were collected in the range of 4000 to 600 cm^{-1} and presented in Figure 7. Sample 1A, 1B, 2A and 2B showed similar absorption peaks within 3936 and 3842 cm^{-1} corresponding to OH stretching (7), the peaks within 3186 and 3160 cm^{-1} corresponds to the intermolecular hydrogen bonds (OH, NH) stretching vibration (8), while the peaks within 1958, 1852, and 1694 cm^{-1} suggest characteristic of C=O stretching vibration. Sample 1A and 1B shows similar peaks within 1012 cm^{-1} corresponds to

aliphatic phosphates (P-O-C stretching), 914 cm^{-1} suggesting aromatic phosphates group (P-O-C stretching) and 704 cm^{-1} denotes a C-H bend in alkyl group (9). Sample 2A and 2B showed similar peaks within 1644 cm^{-1} suggesting a C-C stretching (in ring) aromatics (9), 1038 cm^{-1} suggests the presence of S-O stretching and peaks 917 to 904 cm^{-1} suggest an aromatic phosphate (P-O-C stretching). However, the peak at 643 cm^{-1} corresponds to an alkyne C-H bend is found only in 2A.



4.0 CONCLUSIONS:

Bitumen was successfully extracted from tar sands obtained from Loda, using cyclohexane as solvent. Sample 1A showed higher percentage of bitumen compared to the other samples. The SARA analysis showed aromatic to have the highest percentages in all the samples. The FTIR analysis revealed peaks corresponding to paraffinic, aldehydic, anhydric, aromatic, and hetero-atomic-containing compounds. Hence, based on the information obtained from the characterization of the extracted bitumen, it can find applications in petrochemicals and allied industries, construction and building.

REFERENCES:

1. S. Ogiriki, M. Agunloye, A. Gbadamosi, A. Olafuyi, exploitation of bitumen from Nigerian tar sand using hot-water/steam stimulation process. *Petroleum and Coal* **60**, 217-224 (2018).
2. H. Alboudwarej *et al.*, Highlighting heavy oil. *Oilfield Review* **18**, 34-53 (2006).
3. I. Ohenhen, O. A. Olafuyi, S. S. Ikiensikimama, paper presented at the SPE Nigeria Annual International Conference and Exhibition, 2015.
4. P. H. Phizackerley, L. O. Scott, in *Developments in Petroleum Science*, G. V. Chilingarian, T. F. Yen, Eds. (Elsevier, 1978), vol. 7, pp. 57-85.
5. F. Afolabi, T. Ojo, S. G. Udeagbara, A. Gbadamosi, Bitumen extraction from tar sands using solvent techniques. *International Journal of Scientific and Engineering Research* **08**, 783-790 (2017).
6. H. Shi, T. Xu, P. Zhou, R. Jiang, Combustion properties of saturates, aromatics, resins, and asphaltenes in asphalt binder. *Construction and Building Materials* **136**, 515-523 (2017).
7. C. Yang *et al.*, Investigation of physicochemical and rheological properties of SARA components separated from bitumen. *Construction and Building Materials* **235**, 117437 (2020).
8. L. Ma, A. Varveri, R. Jing, S. Erkens, Chemical characterisation of bitumen type and ageing state based on FTIR spectroscopy and discriminant analysis integrated with variable selection methods. *Road Materials and Pavement Design* **24**, 506-520 (2023).
9. O. Hassan, H. Bakare, A. O. Esan, O. Olabemiwo, Characterisation of Agbabu Natural Bitumen and Its Fractions Using Fourier Transform Infrared Spectrometry. **7**, (2015).



P106 - ENHANCEMENT OF THE ANTIBACTERIAL ACTIVITIES OF AMPICILLIN BY SCHIFF BASE FORMATION AND COMPLEXING WITH METAL(II)-IONS OF CU, FE AND ZN.

Umar M¹., Umar I.A¹, J.D Lawiye¹ and Yelwa J.M².

¹ Department of Science Laboratory Technology, Gombe State Polytechnic, Bajoga

² Department of Scientific and Industrial Research, National Research Institute for Chemical Technology, Zaria.

Corresponding Author E-mail: umaralkemyst@gspb.edu.ng

ABSTRACT

The Schiff base of ampicillin with salicylaldehyde was synthesized according to standard established procedures. The synthesized Schiff base and its corresponding Metal (II)-ions of Cu, Fe, Mn and Zn were characterized using FTIR, UV-Visible Spectroscopy, Molar conductivity, melting point and Solubility in: distilled water, methanol, ethanol, acetone, chloroform, DMSO and Petroleum ether respectively. The FTIR result confirmed the formation of the Schiff base with an azomethine group (C=N) absorption band at 1633.71cm⁻¹. The synthesized Schiff base and its metal complexes were found to be soluble in DMSO and the molar conductivity result was found to be low in all the complexes which indicates their non-electrolytic nature. The in-vitro antibacterial activity test of Schiff base and its Metal complexes on gram-positive (*Staphylococcus aureus* and *Streptococcus pyrogen*) and gram-negative (*Pseudomonas aeruginosa* and *Salmonella typhi*) showed an enhanced antibacterial activity than that of the control (Ampicillin) with a zone of inhibition ranging from 17-28mm at a concentration of 100mg/ml. The control (Ampicillin) showed inhibition zones ranges of 18-25mm on *S. aureus*, *S. pyrogen*, *P. aeruginosa* and *S. typhi*. This study therefore substantiates the use of Schiff base in improving the efficacy level of antibiotic drugs to which resistant has been developed.

Key words: Ampicillin, Schiff Base, Synthesis, Antibacterial, Enhancement

1.0 Introduction

Ampicillin is a beta-lactam antibiotic that is widely used to treat bacterial infections clinically such as *Escherichia coli*. It belongs to the group of aminopenicillins having a molecular formula of C₁₆H₁₉N₃O₄S with a molecular mass of 349.41g/mol. It's chemically regarded as 6[-2-amino-2-phenylacetyl]amino)-3,3-dimethyl-7-oxo-4-thia-1-azabicyclo[3.2.0]neumoni-2-carboxylic acid. It has a strong broad spectrum action that was extended to both gram-positive and gram-negative bacteria by suppressing its cell wall synthesis (1).

Schiff bases are synthetic compounds obtained by condensation of primary amine and carbonyl compounds (aldehydes and ketones). They are important category of pharmacological active molecules that have a great concern by medicinal Chemists because they possess a variety of pharmacological properties. Large number of Schiff base derivatives have been reported to exhibit significant antibacterial, antifungal, antitubercular,

antitumor, antileishmanial, DNA-binding activities etc (2).

Schiff base inorganic complexes having transition metal ion possesses broad range of pharmacological activities like antiviral, anticancer, antibacterial, antifungal, anticonvulsant and anti-inflammatory activities that can be well explained by several commercially available drugs containing their functional group (3). Large number of drugs exhibits modified pharmacological and toxicological properties preferably Schiff base containing compound possessing wide range of biological activities and complexation of metal in the form of complexes exhibits some degree of antibacterial, antifungal, antitumor and anti-inflammatory activities (4).

2.0 Material and Method:

All the chemicals used were of analytical grade from Sigma-Aldrich and BD and used without further purification. The metal salts used are in their chloride form. Melting point of the synthesized compounds were carried out by an open capillary method using electrothermal melting point apparatus. The Fourier-Transform Infrared (FTIR) spectrometric was recorded on Perkin-Elmer in the

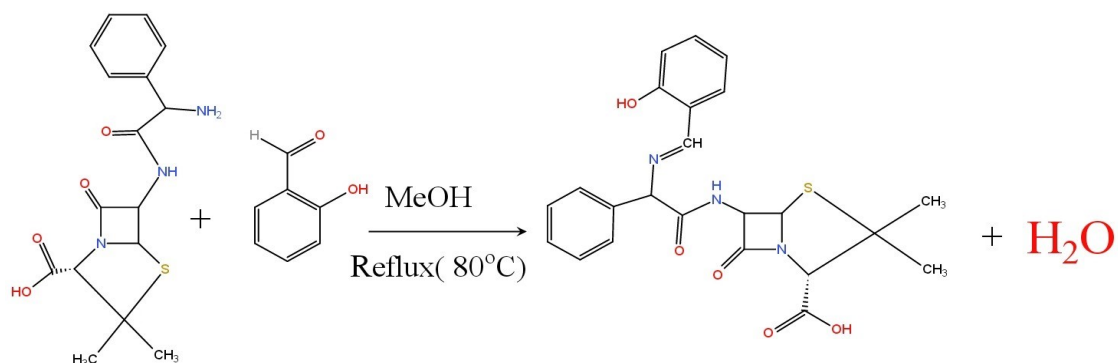


wavelength range of and the UV-Visible spectrum of the

2.1 Synthesis of Schiff Base ligand (HL¹)

The Schiff base was prepared by using a method as described by Reiss *et al.* (5), in which 0.349g (1mmol) of ampicillin was dissolved in 25 mL methanol and mixed with 0.122g (1mmol) salicylaldehyde dissolved in 15mL of Methanol. In order to obtain the pH value between 7 to 8, then

few drops of 1M NaOH solution was added and the mixture was refluxed for 2 hours at 80°C. The volume of the solution was reduced to one half by evaporation and an orange precipitate was formed. It was filtered, washed with methanol and dried in vacuum at room temperature under anhydrous CaCl₂ in desiccator. Recrystallization from a mixture of ethanol – water (50:50) gave the Schiff base.



Scheme 1: Synthesis of HL¹

2.2 Synthesis of Schiff Base Metal Complex

The Cu(HL¹)₂ complexes was synthesized by using a method as describe by Reiss *et al.* (5), in which 0.907g (2.0mmol) of the synthesized Schiff base dissolved in 25 mL methanol was mixed with 0.135g (1.0 mmol) of the Copper(II)-Chloride (CuCl₂). The mixtures pH value was adjusted between 7 to 8 by adding few drops of 1M NaOH solution and then the mixture was refluxed for 2 hours at 75°C. Finally, the volume of solutions was

reduced to one half by evaporation, and an occurrence of coloured precipitate was formed. It was filtered, washed with methanol and dried in desiccator. Recrystallization from hot methanol gave the metal complex. The same procedure was repeated with Iron(II)-Chloride and Zinc(II)-Chloride to obtain their complexes.

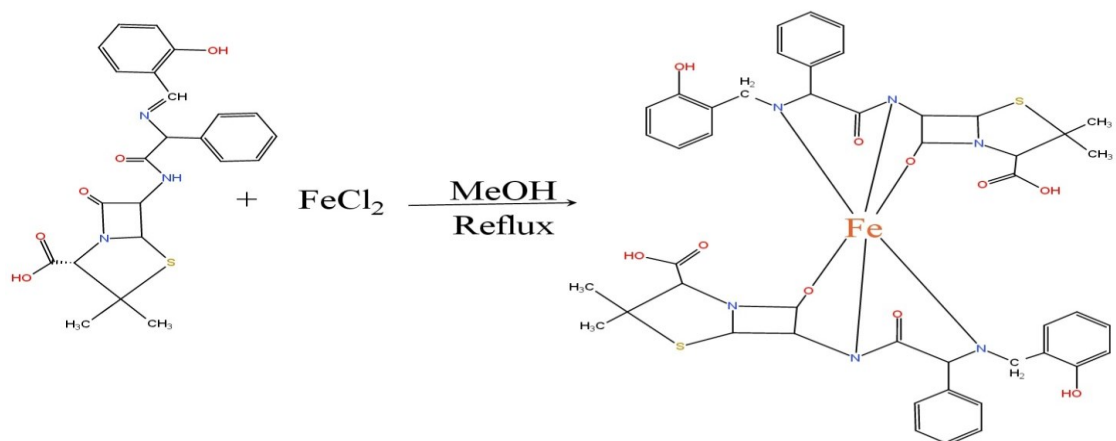
3.1 Physical Characterization

From Table the synthesized Schiff base ligands and their metal complexes show different colours

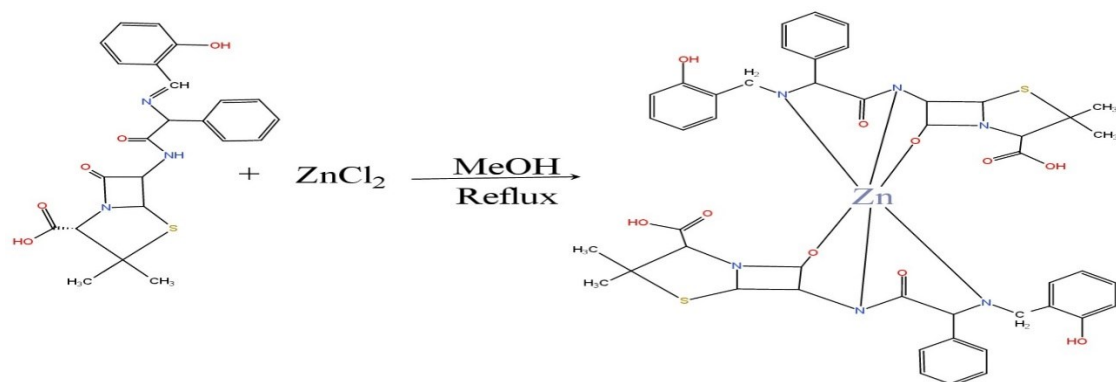
3.0 RESULT AND DISCUSSION

ranging from brown, orange, yellow, grey, blue to green. The Schiff base HL¹ is orange in colour. The HL¹ complexes of Cr, Fe and Zn are green, brown and grey in colour respectively.





Scheme 2: Synthesis Of Fe(HL¹)₂ Complex



Scheme 3: Synthesis Of Zn(HL¹)₂ Complex

TABLE: Physical Characterization Results						
COMPOUND	MOLECULAR		COLOUR	YIELD (%)	MELTING POINT (°C)	MOLAR CONDUCTIVITY (Scm ² mol ⁻¹)
	FORMULAR	WEIGHT				
HL ¹	C ₂₃ H ₂₃ N ₃ O ₅ S	453.53g/mol	Orange	68.95	238	57.8
Cu(HL ¹) ₂	[Cu(C ₂₃ H ₂₃ N ₃ O ₅ S) ₂]	970.61g/mol	Blue	51.25	252	39.3
Fe(HL ¹) ₂	[Fe(C ₂₃ H ₂₃ N ₃ O ₅ S) ₂]	959.85g/mol	Brown	56.12	276	49.1
Zn(HL ¹) ₂	[Zn(C ₂₃ H ₂₃ N ₃ O ₅ S) ₂]	969.41g/mol	Grey	60.32	265	38.6



The HL¹ metal complexes of Cu, Fe and Zn has a percentage yield of 51.25, 56.12 and 60.32% respectively. This is in agreement with the percentage yield values obtained by Abdulsada *et al.* (2). The low yield may be attributed to the incomplete reaction of the ligand with the metal ion.

The melting point show that the HL¹ and its metal complexes had a melting point range of 238-276°C and are in agreement with the values obtained from the Yahaya *et al.* (6). The free HL¹ ligand has lower melting point than that of its correspondent complexes of Cu, Fe and Zn respectively.

The molar conductivities of HL¹ and its metal complexes in DMSO showed that Cu, Fe and Zn

complexes had conductivity values of 39.3, 49.1 and 38.6 respectively while the free ligand had a conductivity value of 57.8, the lower value of molar conductivity in the complex of Zn is an indicative of its non-electrolytic nature (7).

3.2 Fourier Transform Infrared Spectroscopy (FTIR)

The FTIR spectra of the synthesized Schiff bases and their metal complexes were recorded on Perkin Elmer spectrum version 10.03.09 in the wave number range of 450-4000cm⁻¹ and the result obtained was recorded on the Table 2:

TABLE : FTIR Result of the ligands and their metal complexes

COMPOUND	$\nu(\text{O-H})$	$\nu\text{C=C}$	$\nu\text{C=N}$	$\nu\text{M-N}$	$\nu\text{M-O}$
HL ¹	3194.82	1525.16	1633.71		
Cu(HL ¹) ₂	3435.00	1531.27	1614.56	697.55	527.78
Fe(HL ¹) ₂	3486.76	1457.22	1650.97	526.00	453.97
Zn(HL ¹) ₂	3479.30	1525.16	1645.00	526.00	466.62

From Table 2 the absorption band at 1633.71cm⁻¹ is assigned to $\nu(\text{C=N})$ (azomethine) group of HL¹. This data confirmed the formation of HL¹ schiff base through the -C=N- bond and this is in line with the result obtained by Reiss *et al.* (5). In HL¹ metal complexes the $\nu(\text{C=N})$ was moved to higher values of 1650.97cm⁻¹ for Fe and 1645.00 cm⁻¹ for Zn respectively, while Cr moved down to a lower wave number of 1614.56cm⁻¹ and this shift in absorption of the free ligand with that of the metal complexes is an indicative of the coordination of the Schiff base ligands with the metal ions. This is in line with the work of Abdulsada *et al.* (2), who find out that upon complexation of the free ligand with the metal ion the absorption band of azomethine shift to lower or higher wavenumber. In the free ampicillin the $\nu(\text{C=N})$ absorption band is lacking because the ampicillin does not have the azomethine group.

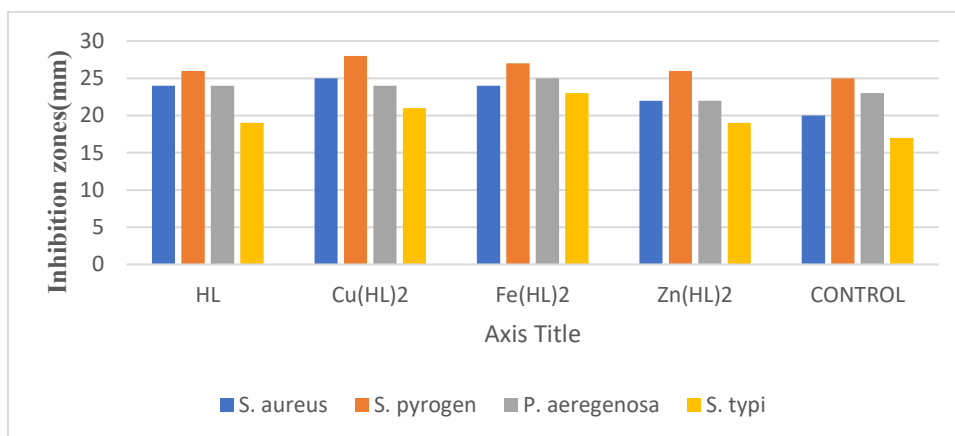
assigned to $\nu(\text{M-O})$ and this also correspond to that of Yahaya *et al.* (6).

The presence of strong absorption band at 3194.82 cm⁻¹ in the spectrum of HL¹ was assigned to $\nu(\text{O-H})$ vibration. The band was shifted to 3435.00 cm⁻¹, 3486.76 cm⁻¹ and 3479.30 cm⁻¹ upon complexation with Cu, Fe and Zn respectively which is indicative of coordination with metal ions. This is in line the reported literature of Nasiru *et al.* (6), who found out that on complexation of ligand with metal ions the absorption band shifts to longer frequencies. Furthermore, in free ampicillin the $\nu(\text{OH})$ appeared at 3445.43 cm⁻¹ due to the presence of OH group attached to the carboxylic group of the ampicillin. In the complexes there is an existence of weak bands at 527.00 cm⁻¹, 526.00 cm⁻¹, 547.87 cm⁻¹, 500.40 cm⁻¹, 561.79 cm⁻¹, 526.47 cm⁻¹ and 578.79cm⁻¹ which are assigned to $\nu(\text{M-N})$ while the absorption bands at 453.97 cm⁻¹, 466.62 cm⁻¹, 518.27 cm⁻¹, 467.01 cm⁻¹, 485.94 cm⁻¹, 467.39 cm⁻¹ and 464.24cm⁻¹ were

3.3 Antibacterial activity

The antibacterial activities of the Synthesized Schiff base and its corresponding metal complexes was conducted according to standard procedures and the result obtained were presented in the subsequent figure:





From figure 3 the measured zone of inhibition of HL¹ and its metal complexes of Cu, Fe and Zn against *Staphylococcus aureus*, *Streptococcus pyogenes* (gram positive), *Pseudomonas aeruginosa* and *Salmonella typhi* (gram negative). The activity of the ligand and the metal complexes were found to be slightly higher than that of the control drug on *Staphylococcus aureus* (gram positive), *Pseudomonas aeruginosa* and *Salmonella typhi* (gram negative) and *Streptococcus pyogenes* in all the metal complexes. The result is in agreement with the one obtained by Abdulsada *et al.* (2), who found that metal complexes of copper with terephthalaldehydeampicillin and terephthalaldehydecephalexin inhibit the bacterial activity of *E.coli*, *S.aureus* and *P.aeruginosa* than the free ligands.

CONCLUSION

This study therefore substantiates the use of Schiff base in improving the efficacy level of antibiotic drugs to which resistant has been developed.

REFERENCES

1. B. G. Katzung, *Basic and clinical pharmacology*. (McGraw-Hill, New York, Longman Medical Books, ed. 8th, 2012).
2. A. H. Abdulsada, N. H. Nasser, A. K. Hussein, Design Synthesis and Preliminary Antibacterial Evaluation of Schiff Base Metal Complexes of Ampicillin and Cephalixin. *Acta Chimica and Pharmaceutica Indica* **8**, 123 (2018).
3. S. Y. Ebrahimipour, B. Machura, M. Mohamadi, M. Khaleghi, A novel cationic cobalt (III) Schiff base complex: Preparation, crystal structure, Hirshfeld surface analysis, antimicrobial activities and molecular docking. *Microbial pathogenesis* **113**, 160-167 (2017).
4. A. Xavier, N. Srividhya, Synthesis and study of Schiff base ligands. *IOSR Journal of Applied Chemistry* **7**, 06-15 (2014).
5. A. Reiss, A. Samide, G. Ciobanu, I. Dabuleanu, Synthesis, spectral characterization and thermal behaviour of new metal (II) complexes with Schiff base derived from amoxicillin. *Journal of the Chilean Chemical Society* **60**, 3074-3079 (2015).
6. N. P. Yahaya *et al.*, Synthesis and partial characterization of two Schiff base ligands with (2 and 4-nitroaniline) and their transition metal (II)(Co and Cu) complexes. *Dutse Journal of Pure and Applied Sciences* **4**, 584-591 (2018).
7. T. A. Al-Diwan, Synthesis and characterization of some divalent transition metals complexes of Schiff bases derived from salicylaldehyde diamine derivatives. *Al-Mustansiriyah Journal of Science* **22**, 101-108 (2011).





P107 - PRODUCTION AND CHARACTERIZATION OF ORGANIC POTASH FROM AGRICULTURAL WASTES IN FOOD AND FERTILIZER APPLICATIONS: A CASE STUDY OF CORNCOB AND GUINEA CORN HUSK

*Samuel, Alkali Akuso; Kabiru, Mu'azu; Etukessien, S. Akpan; Joseph, O. Otsai; Mohammed Salisu, Lois, Zinas Clement

National Research Institute for Chemical Technology (NARICT), Zaria, Kaduna State, Nigeria

*Corresponding Author: alkaliakuso@gmail.com

ABSTRACT

The rapid growth in the world's population has caused a corresponding increase in the demand for food, shelter and social amenities. This in turn has encouraged the generation of huge quantities of agricultural wastes in the environment and its surroundings. The production of organic potash from agricultural wastes ash via evaporation technology, and characterizing same product using XRF, XRD and FTIR analytical tools have been studied. Open air burning of agricultural wastes in open fields often constitutes serious pollution to the environment couple with further destruction on soil nutrients and microorganisms. Subsequently, mining of inorganic potash from the ground leads to serious problems such as; reduction in farm land, swamping and enormous cost of beneficiation which all results in high cost of potash. Therefore, the production of organic potash from agricultural wastes ash (i.e. guinea corn husks and corncobs) presents an alternate means of environmental hygiene, wealth creation and a good waste management disposal system. XRF analysis showed that the compositions of guinea corn husks and corncobs potash are potassium-based salt having 61.63% & 73.33% concentrations respectively. Thus, making each suitable as an ingredient either in food seasoning and condiments or fertilizer production. XRD analysis showed that the minerals present in the guinea corn husks and corncobs potash samples are mixtures of the chlorides of Na and K and oxides of Si, Mg and Ca with potassium having the highest chemical composition (31% & 66% respectively) in both the potash produced, while the FT-IR spectra analysis identified strong bands of potash with vital functional groups of O-H, C-H, N-H and C-O.

Keywords: *Corn cob, guinea corn husk, potash, food, fertilizer, XRF, XRD, FTIR*

1.0 INTRODUCTION

The rapid growth in the world's population has culminated in increased demand for food, shelter and social amenities which in turn has led to the generation of huge/large quantities of agricultural wastes in the environment and fields. According to Capanoglu *et al.* (1), Obi *et al.* (2), Sabiiti (3) and Abou Hussein and Sawan (4), agricultural waste are by-products of agricultural production following the different harvesting activities carried out within the period. Agricultural wastes are commonly available, nontoxic, renewable and almost free; hence they can be a potential material for value added products.

Agricultural wastes constitute a significant percentage of environmental pollution worldwide, due to greenhouse gas effects on the environment and society at large. Researches have been focused on the conversion of these agricultural wastes into value added products. The residues of agricultural wastes include manure and animal carcasses (animal waste); corn stalks, corncob, rice and hungry rice stalks, wood, sugar cane bagasse, drops and culls from fruits and vegetables, and crop waste (1), crop residues (residual stalks, straw, leaves, roots, husks, shells etcetera) and animal waste (3); By implication, an increase in agricultural production will significantly increase the amount of agricultural wastes in fields with an estimated value of about 998 million tonnes of agricultural waste produced yearly (2, 5).





a. Corn cob



b. Corn cob ash



c. Guinea corn husks



d. Guinea corn husk ash

Plates 1(a-d): Shows images of corncob, corncob ash, guinea corn husk and guinea corn husk ash.

Generally, agricultural wastes are either burnt, incinerated or landfilled. Combustion incineration process still happens to be the most acceptable method of agricultural waste disposal and accounts for more than 95% of all agricultural waste handling today (2). Most of these agricultural wastes are under-utilized, and left to rot or subjected to open-air burning with its accompanying environmental consequences such as greenhouse gas effects and degradation or loss of precious nutrients in soil. (6, 7).

Employing suitable conversion technologies, agricultural wastes can be transformed into useful products like potash, fertilizer, biogas, animal feed etc. The use of firewood often results in the accumulation of wood ash in most rural homes. According to Chris Koziicki (8), wood ash is a valuable asset used as manure (green fertilizer) to increase crop yield, food preservation, cooking food, wounds healing, explosives powder, pest control, black soap production, pottery, stain and odour removers, and even cosmetics etc.

Before the coming of industrial evolution, potash was processed by leaching the filtrate from wood ash in a pot, the filtrate obtained was either used to

produce black soap, stain and odour removal, and explosive powder. It was then evaporated by boiling to produce crystalline salt known as potash (K_2CO_3). Sarkar *et al.* (9), in their 2017 study discovered that organic potash is the best micronutrient for sustainability of soil health and crop yield rate which is far better than inorganic potash.

Organic potash, also known as *botok ranrinya* in (Koro), *Kaun* (Yoruba), *Akanwa* (Igbo) or *Kanwa* (Hausa) does not only improve soil fertility but also increase crop output. Potash is a colourless and odourless crystalline residue obtained from burning and processing organic wastes matter. Potash has broad areas of applications ranging from household uses (food seasoning and condiments) and has also been found as relief to hypertensive patients, in the agricultural sector potash is one of the sources of fertilizer and animal feed production; while in the industries, potash is used for the manufacture of soaps, glass, baked goods and gunpowder, brewing of beer, textiles, catalyst for synthetic rubber manufacturing, and pharmaceuticals (10). Global potash consumption in 2021 for fertilizers production was estimated to have increased to 45



million tons from 44 million tons as recorded in 2020. This potash demand has been on the increase due to high population growth. Asia and South America are the leading consuming countries.

According to Vera Koester (11), the composition of K_2CO_3 in wood ash is 14-19 %, also ash from other sources such as corn stalks, rice straws, potato weed, bean stalks, corncobs, vines, seaweed, reeds, hungry rice stalks are suitable for the production of organic potash.

2.0 MATERIALS AND METHODS

The equipment used for the research work are; incinerator, beakers, hot plate, oven, measuring cylinder, filter paper, suction pump, weigh balance, funnel, retort stand, spatula and muffle furnace.

2.1. Material Sourcing and Preparation

The materials for this study are corncobs, guinea corn husks, and tap water. These items were gotten from National Research Institute for Chemical Technology, (NARICT), Zaria, Kaduna State. The corncobs and guinea corn husks were pre-treated and sun dried for 48 and then ashed in an incinerator to white ash. The white ashes were freed from any

pieces of charcoal and 140g of the ash was recovered from 26kg of corncobs, while that of the guinea corn husks ashes 128g was recovered from 23kg of guinea corn husks. Both powders were separately mixed with clean tap water and leached to dissolve out the soluble components into an alkaline solution.

The respective alkaline solutions were boiled to evaporation at $100^\circ C$ under continuous stirring. Finally, the amount of potash produced from corncobs was 85g, while that of guinea corn husk was 103g. The potash produced from the ashes are meant to be hydroxides of alkali metals (Na or/and K), but in most cases, it contains other water-soluble non-alkali substances such as calcium, chloride and sulphate salts (10). The whitish powders were packed in a dry container and allowed to cool. In some instances, potash could be greyish/reddish brown or blackish in colour due to the presence of trace elements or other impurities (12, 13).

Figures 1, 2 & 3 below shows the set-up for the production process of organic potash from agricultural biomass.



Figure 1: Set-up for ashing of corncob and guinea corn husks using an improvised incinerator

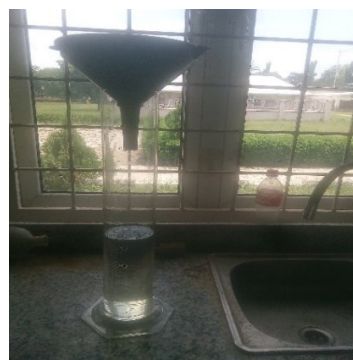


Figure 2: Set-up for the leaching of alkaline solution from guinea corn husks and corncob ashes



Figure 3: Set-up for the production of organic potash from guinea corn husks and corncob



The plates below show samples of organic potash produced from guinea corn husks and corncob

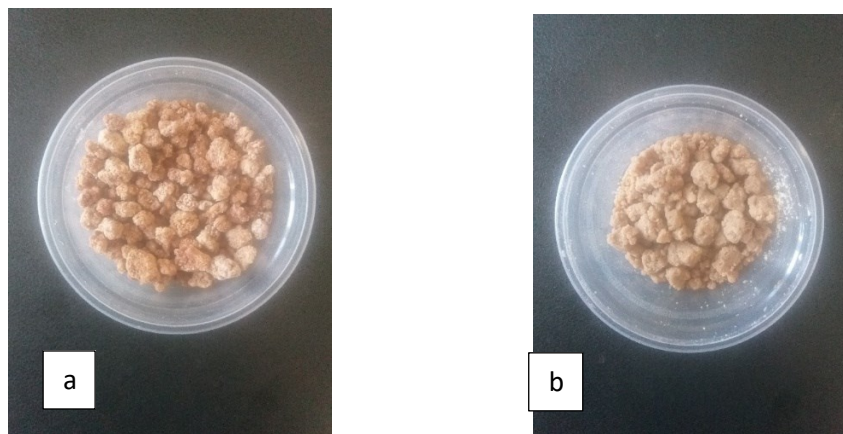


Plate 2 (a- b): Shows samples of organic potash produced from guinea corn husks and corncob

Figure 4 shows process flow diagram of potash production from guinea corn husks and corncob

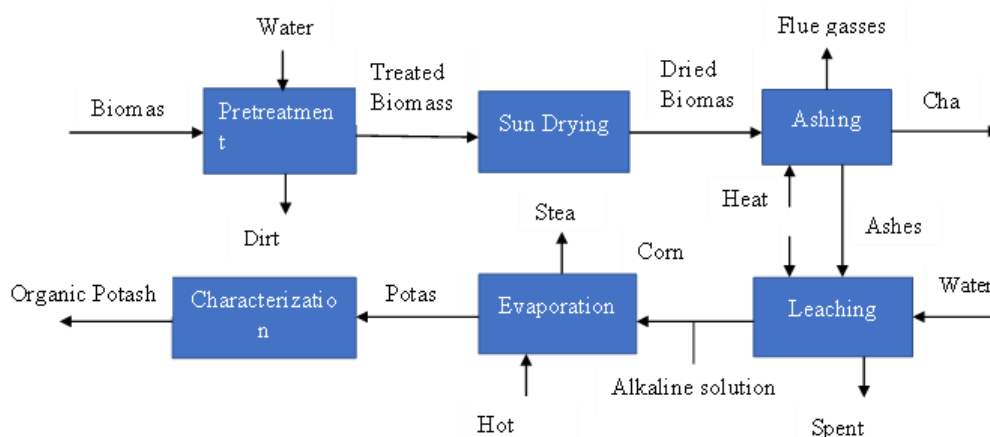


Figure 4: Process flow diagram for the production of organic potash from guinea corn husks and corncobs

RESULTS AND DISCUSSION

X-Ray Fluorescence (XRF) Analysis of Organic Potash derived from Guinea Corn Husks and Corncobs Potash

The XRF analysis of guinea corn husks and corncobs potash were carried out using Genius IF – Xenometrix XRF equipment at National Steel Raw Materials Exploration Agency (NSRMEA), number 18 Rabah Road, Malali Village, Kaduna, Nigeria. The samples received were crushed and pulverized to $-75\mu\text{m}$ and submitted for XRF Analyses. The pulverized aliquot was analyzed using Genius IF -

Xenometrix XRF Equipment. Duplicate analyses performed to obtain average values.

X-Ray Refractive Diffractometer (XRD) Analysis of Organic Potash obtained from Guinea Corn Husks and Corncobs

The XRD analysis of guinea corn husks and corncobs potash were carried out at National Steel Raw Materials Exploration Agency (NSRMEA), number 18 Rabah Road, Malali Village, Kaduna, Nigeria. The samples received were crushed and split into two equal halves. One crushed portion was pulverized to 100% passing through $75\mu\text{m}$ sieve, split into two portions with one portion further



submitted for XRD Analysis while the other half was kept as reference sample. The pulverized fraction was analyzed using Rigaku Miniflex 600 XRD equipment employing Cu-K α radiation at 2 θ angle 2 $^{\circ}$ – 70 $^{\circ}$.

The results were presented as peak positions at 2 θ and x-ray counts in the form of a spectra that reveals the compound's name, mineral name, chemical formula, empirical formula, and with the crystallographic parameters.

The crystalline phases, chemical formula and concentrations detected by XRD for guinea corn husks and corncobs potash are as shown in Tables 1 & 2 with their quantitative values and accompanying diffractogram shown in Figures 5 & 6, respectively.

Table 1: XRF results of guinea corn husks and corncobs potash in percentage concentrations composition of elements (%).

S/N	Sample	Si O ₂	V ₂ O ₅	Cr ₂ O ₃	Nb ₂ O ₃	Fe ₂ O ₃	Cu O	K ₂ O	W O ₃	Mg O	Ag ₂ O	Al ₂ O ₃	Zn O	Ta ₂ O ₅	Zr O ₂	Co ₃ O ₄	Mn O	Sn O ₂	Cl	S O ₃	P ₂ O ₅	B D L
1	A	3.51	0.01	0.01	0.05	0.13	0.06	61.63	0.01	10.01	7.59	4.15	0.04	0.01	0.01	0.01	0.01	6.76	4.42	0.89	-	0.69
2	B	4.21	0.003	0.01	0.01	0.19	0.05	73.33		3.52	0.02	3.84	0.01	0.01	0	0.02	0.01	4.19	4.89	0.80	4.53	4.76

A and B, represents organic potash from guinea corn husks and corncobs.

BDL: Below detection limit

Table 1 above shows that potash produced from different source contain varying level of chemical composition. The XRF analysis of the compositions of guinea corn husk and corncob potash showed that it is a potassium-based salt having the highest percent concentrations in the two source

Fourier Transform Infra-Red (FTIR) Analysis of Organic Potash Derived from Guinea Corn Husks and Corncobs

Fourier Transform Infrared spectroscopy (FTIR) is a technique that uses infrared light to observe properties of solid, liquid, or gas to detect functional groups and characterized bond formation in a sample. Analysis was carried out using Shimadzu (Japan) – 8400S equipment at National Research Institute for Chemical Technology, Km 4, Basawa, Zaria, Kaduna State, Nigeria.

Table 1 shows the results of XRF of potash from guinea corn husk and corncob. It revealed the percentage concentrations composition of the compounds (%) present in the potash produced from guinea corn husk and corncob.

agricultural wastes. The result obtained agreed with the findings of (14)

From the XRD analysis of guinea corn husk and corncob potash, Tables 2 & 3 shows the chemical formula and chemical name and concentrations of the minerals present.

Table 2: Chemical formula of the mineral phases (%) as determined by XRD Analysis of guinea corn husks potash

S/N	Mineral	Chemical Formula	Concentration (%)
1	Quartz	SiO ₂	2.0
2	Periclase	MgO	12.0
3	Sylvine	KCl	31.0
4	Sodalite	Na ₄ Al ₃ ClSi ₃ O ₁₂	28.0
5	Lime	CaO	27.0

Table 3: Chemical formula of the mineral phases (%) as determined by XRD Analysis of corncobs potash

S/N	Mineral	Chemical Formula	Concentration (%)
-----	---------	------------------	-------------------



1	Quartz	SiO ₂	10.0
2	Periclase	MgO	8.0
3	Sylvine	KCl	66.0
4	Sodalite	Na ₄ Al ₃ ClSi ₃ O ₁₂	3.0
5	Lime	CaO	13.0

Figures 5 and 6 are the spectrum for the chemical formula and compound name for the guinea corn husk and corncob potash. The spectrum revealed that the potash produced after thermal combustion of guinea corn husk and corncob in an incinerator into ashes under normal atmospheric pressure contains different phases of minerals.

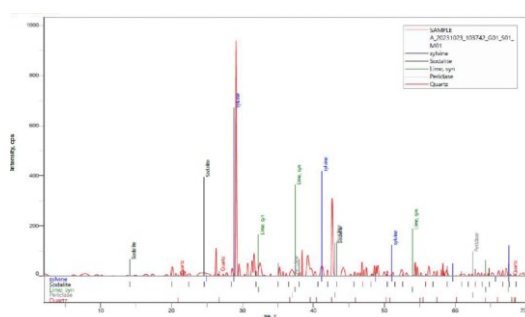


Figure 5: Guinea corn husk potash XRD spectra: Compound name

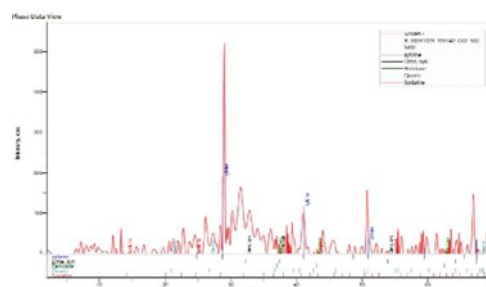


Figure 6: Corncob potash XRD spectra: Compound name

From the chemical formula and the minerals present in the guinea corn husk and corncob potash are the oxides of silicon, magnesium and calcium and chlorides of potassium and sodium with the quantitative value of the minerals; SiO₂ is 2.0%, MgO is 12.0%, KCl is 31.0%, Na₄Al₃ClSi₃O₁₂ 28.0% and CaO is 27.0% for guinea corn husk, while that of corncob is SiO₂ 10.0%, MgO is 8.0%, KCl is 66.0%, Na₄Al₃ClSi₃O₁₂ 3.0% and CaO is 13.0% as reported in Tables 2 & 3 above. Therefore, it could be deduced that the minerals present in the guinea corn husks and corncobs potash samples are mixtures of the chlorides of Na and K and oxides of

Si, Mg and Ca. It helps maintain fluid levels in the body and also supports the proper functioning of the kidneys, heart, muscles, and nervous system. An acceptable intake of potash is about 3,400 mg and 2,600 mg per day for a healthy adult male and female respectively, while for pregnant and breastfeeding mothers it is recommended at 2,900 mg and 2,800 mg per day respectively. consequently, potash salts help to improve both the uptake of nitrogen from the soil, proper growth of plant parts like the root strength, disease resistance, conversion of nitrogen in the plant to amino acids and ultimately protein content and high yield.

Fourier Transform Infra-Red (FTIR) Analysis of Guinea Corn husk and corncob potash

Figures 7 & 8 shows below spectral of guinea corn husk and corncob potash.



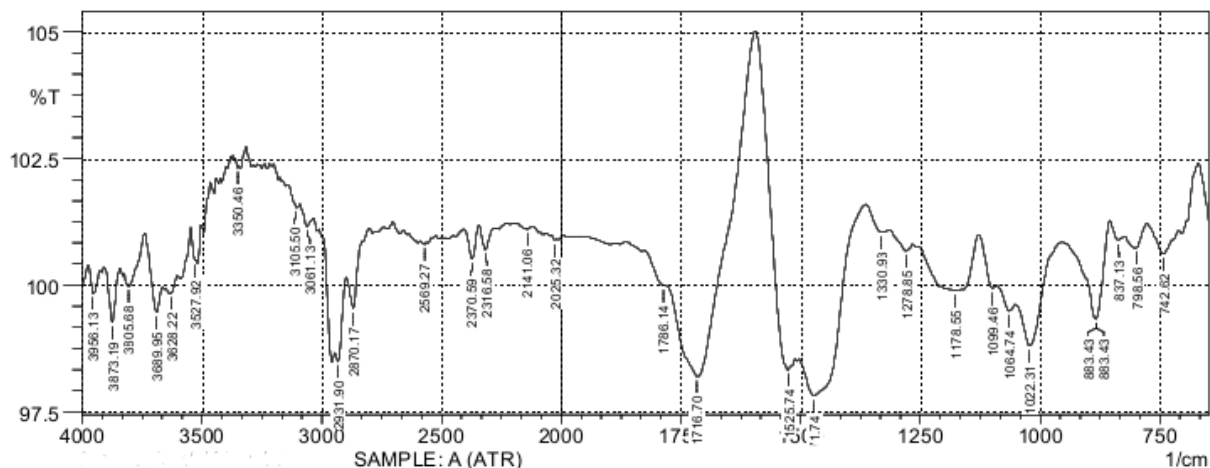


Figure 7: FTIR spectra of guinea corn husk potash

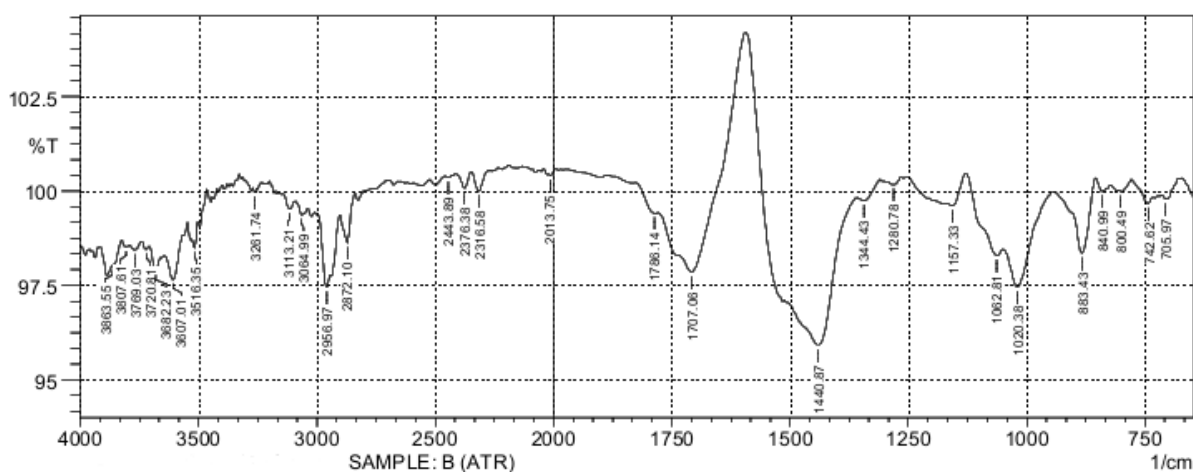


Figure 8: FTIR spectra of corncob potash

The spectra analysis for guinea corn husk and corncob potash are shown in Figures above. One of the most vital functional groups present on the potash are; O-H, C-H, N-H and C-O. FTIR analysis shows absorption bands at 3873.19 cm^{-1} , 3863.55 cm^{-1} , 3805.68 cm^{-1} , 3807.61 cm^{-1} , 3689.95 cm^{-1} , 3682.23 cm^{-1} , 3607.01 cm^{-1} , 3628.22 cm^{-1} , 3527.92 cm^{-1} and 3516.35 cm^{-1} which are associated with N-H stretched groups in amines and amides; bands at 3350.46 cm^{-1} and 3261.74 cm^{-1} are associated with the stretched vibration of the O-H and N-H groups in carboxylic acids, amides, alcohols and phenols, while bands at 3061.50 cm^{-1} and 3113.21 cm^{-1} are associated with the stretch vibration of the O-H and N-H groups in carboxylic acids, phenols and primary amines, bands at 3061.13 cm^{-1} and 3064.99 cm^{-1} which are associated with the stretch vibration of the C-H and O-H groups in alkenyl and carboxylic acids. Also, bands at 2956.97 cm^{-1} ,

2931.90 cm^{-1} , 2870.17 cm^{-1} and 2872.10 cm^{-1} are associated with the stretched vibration of the C-H groups in alkyl and aldehyde groups, bands at 2376.38 cm^{-1} , 2370.59 cm^{-1} and 2316.58 cm^{-1} are associated with the stretched vibration of the O-H groups in carboxylic acids, bands at 1716.70 cm^{-1} and 1707.06 cm^{-1} are associated with the stretched vibration of the C=O groups in carboxylic acids and ketones, bands at 1440.87 cm^{-1} and 1471.74 cm^{-1} are associated with the stretched vibration of the H-C-H groups in alkanes. Spectrum bands at 1344.43 cm^{-1} and 1330.93 cm^{-1} are associated with the stretched bend of N=O groups in nitromethane. Bands at 1278.85 cm^{-1} and 1280.78 cm^{-1} are associated with the stretched vibration of C-O groups in esters and ethers. Bands at 840.99 cm^{-1} , 837.13 cm^{-1} , 800.49 cm^{-1} , 798.56 cm^{-1} and 742.62 cm^{-1} are associated with the stretched of alkanes, alkynes and aromatic. While bands at 1178.55 cm^{-1}



¹, 1157.33 cm⁻¹, 1099.46 cm⁻¹, 1062.81 cm⁻¹, 1064.74. cm⁻¹, 1060.91 cm⁻¹, 1022.31 cm⁻¹ and 1020.38 cm⁻¹ are associated with stretched of C-O in esters and ethers. These functional groups determine the activities of the compounds or molecules present in the potash.

3.0 CONCLUSION

The XRF analysis of the compositions of guinea corn husk and corncob potash showed that it is a potassium-based salt having the highest percent concentrations of KCl content in corncob (73.33 %) and guinea corn husk (61.63). It helps maintain fluid levels in the body and supports the functioning of the kidneys, heart, muscles, and nervous system. Also, it helps improve both the uptake of nitrogen from the soil, proper growth of plant like root strength, disease resistance, conversion of nitrogen in the plant to amino acids and ultimately protein and high yield.

The XRD analysis revealed that guinea corn husk and corncobs potash have chemical compositions of minerals presence of SiO₂, MgO, KCl, Na₄Al₃ClSi₃O₁₂ and CaO that formed the mixtures of Quartz (SiO₂), Periclase (MgO), Sylvine (KCl), Sodalite (Na₄Al₃ClSi₃O₁₂) and Lime (CaO), which can find uses in various areas of application such as food seasoning and condiments, relief to hypertensive patients, production of green fertilizer and animal feed, production of black soaps, water softener, gun powder, deicer (snow and ice melting), drilling of oil well mud, pharmaceuticals, water softening, tooth ache relief, preservatives, fertilizer production, constipation relief, stomach ache etcetera.

The FTIR spectra analysis for guinea corn husk and corncob potash has the following most vital functional groups; O-H, C-H, N-H and C-O. These functional groups are found in the chemical minerals present in the potash. Therefore, agricultural wastes are potential raw material for the production of organic potash that is beneficial to human as a common food seasoning and condiments and to boost agricultural output and soil fertility. This calls for public awareness on the benefits of organic potash in food and fertilizer applications will reduce potash mining and increase farm land.

4.0 RECOMMENDATION

An immediate pilot or industrial scale up of the production process of organic potash which has demonstrated several value additions to hitherto

agricultural wastes should be given due consideration.

REFERENCES

1. E. Capanoglu, E. Nemli, F. Tomas-Barberan, Novel approaches in the valorization of agricultural wastes and their applications. *Journal of Agricultural and Food Chemistry* **70**, 6787-6804 (2022).
2. F. O. Obi, B. O. Ugwuishiwu, J. N. Nwakaire, Agricultural waste concept, generation, utilization and management. *Nigerian Journal of Technology* **35**, 957-964 (2016).
3. E. N. Sabiiti, Utilising agricultural waste to enhance food security and conserve the environment. *African journal of food, agriculture, nutrition and development* **11**, (2011).
4. S. D. Abou Hussein, O. M. Sawan, The utilization of agricultural waste as one of the environmental issues in Egypt (a case study). *Journal of Applied Sciences Research* **6**, 1116-1124 (2010).
5. P. Vispute, S. Dabhade, A Review: Utilization of Agricultural Waste in India. *International Journal of Science and Research* **7**, 1879-1883 (2018).
6. S. Babu *et al.*, Exploring agricultural waste biomass for energy, food and feed production and pollution mitigation: A review. *Bioresource Technology*, 127566 (2022).
7. A. S. Olufemi, O. O. Olayebi, D. E. Makpah, A novel process for the production of potash from plant ash: leaching technique. *Journal of Advancement in Engineering and Technology* **5**, 1-5 (2017).
8. C. Kozicki, in *Process Systems Engineering & Manufacturing Handbook*. (FEECO International Inc., 2023), pp. 71.



9. M. I. U. Sarkar, M. N. Islam, A. Jahan, A. Islam, J. C. Biswas, Rice straw as a source of potassium for wetland rice cultivation. *Geology, Ecology, and Landscapes* **1**, 184-189 (2017).
10. O. I. Ogunwede, M. S. Abolarin, A. S. Abdulrahman, O. A. Olugboji, J. B. Agboola, Production and Characterization of Potash from Maize Stovers Ash Neutron Activation by Analysis and X-Ray Diffraction. *Nigerian Journal of Scientific Research* **17**, 1-8 (2018).
11. V. Koester, Potash. *Chemistry Views*. 2020.
12. F. Akindejoye, T. B. Hammed, M. K. C. Sridhar, Potassium recovery potential of selected agroforestry and organic wastes in ibadan, Nigeria. *Euro. Sci. J.* **13**, 1857-7881 (2017).
13. T. B. Momoh, C. A. Yaro, S. O. Usuman, V. A. Iyeh, Effect of potash on the tenderness and phytochemical constituents of *Cajanus Cajan*. *Trends Applied Sciences Research* **14**, 278-282 (2019).
14. M. H. Shagal, Analytical study of local potash around Yola metropolis of Adamawa state. *Journal of Physical Sciences and Innovation* **3**, 24-35 (2011).



P108 - EFFECT OF OPTIMUM PROCESS CONDITIONS FOR DETOXIFICATION OF PHORBOL ESTER (PE) AND ANTI-NUTRIENTS REDUCTION OF *JATROPHA CURCAS* SEED CAKE (JSC) BY *LENZITES BETULINA*.

*Bala S.¹, Salihu A.², Ameh D. A.², Musa H.², Abdulkadir J.¹, Abdulwaliyu I.¹, Ochigbo V.¹, Idowu O.¹, and Arekemase S.¹

¹National Research Institute for Chemical Technology Zaria, Nigeria

²Ahmadu Bello University Zaria, Nigeria

*Corresponding author's mail address: suleimanbala240821@gmail.com, +2347031272034

ABSTRACT

The *Jatropha curcas* seed cake is a by-product generated from the oil extraction of *J. curcas* seeds, which is rich in protein, and the presence of high concentration of phorbol ester and anti-nutrients limit its utilization in food and feed formulation. This study is aimed at detoxifying phorbol ester and anti-nutritional factors of *J. curcas* seed cake (JSC) under the optimized process condition by solid state fermentation using *Lenzites betulina*. The anti-nutrients and PE content of the seed cake were determined according to the standard analytical methods. The PE content was extracted and quantified by HPLC using phorbol-12-myristate-13-acetate as an external standard. The anti-nutritional analysis showed that *J. curcas* seed cake contained $0.90 \pm 0.01\%$ tannin, $5.30 \pm 0.47\text{mg}/100\text{g}$ phytate, $119.88 \pm 0.94\text{mg}/100\text{g}$ oxalate, $0.35 \pm 0.66\%$ saponin, 74.27 ± 0.83 TIU/mg trypsin inhibitor and $0.33 \pm 0.01\text{mg}/\text{g}$ phorbol ester. This study equally showed that after fermentation with *L. betulina* (6% v/w) for 12 days, phorbol ester, phytic acid, saponin, oxalate, tannin, and trypsin inhibitor were significantly ($p < 0.05$) reduced by 93.94, 81.01, 71.09, 98.34, 80.06 and 98.20% respectively under the optimum process conditions. The findings of this study showed that *Lenzites betulina* aids in the detoxification of JSC hence, improving the nutritional status of the detoxified JSC and promotes its utilization for possible inclusion in animal feed production.

KEYWORDS

Phorbol ester, *Lenzites betulina*, Anti-nutrient, *Jatropha curcas*.

1.0 INTRODUCTION

The *Jatropha curcas* seed cake (JSC) is a lignocellulosic residue rich in minerals, protein, anti-nutrients and the toxic PEs, which is generated during biodiesel production (1). Zanzi *et al.* (2) reported that for every 2.85 tons of *J. curcas* seeds, only 1 ton of oil can be extracted using solvent or mechanical extraction methods, with the remaining ending up as JSC. However, the de-oiled *J. curcas* seed cake contains anti-nutritional substances, which include trypsin inhibitors, tannins, saponins, phytates and toxic factors - phorbol esters (PEs), which restricts the wider utilization of the seed cake. The PEs have been identified as the main toxicants in JSC, which cannot be destroyed even by heating at 160°C for 30 mins (3). Phorbol esters are 20 carbon tetracyclic diterpenoids made up of four isoprene units (4). Tiglain is the main alcohol moiety in the phorbol esters. Hydroxylation of this basic tiglain structure at different positions and its esterification with various acid moieties results in

the formation of large varieties of PE compounds mainly responsible for the toxicity in *Jatropha* (5).

Therefore, the seed cake is considered toxic due to the presence of PEs and other anti-nutrients (6),(7), (5, 8), and when ingested can be very toxic to human beings, mice, rats, goats, sheep, calves, chicks, pigs, fish and snails (9). Similarly, PEs irritate the epidermal cell, promote cancer, cause burning sensation and pain in the mouth and stomach as well as watery or bloody diarrhoea (10). Hence, JSC cannot be used directly as animal feed without detoxification (10); and if left to decay, the cake/biomass will add to the existing environmental problems (6, 11). Thus, its safe disposal or meaningful utilization is currently an important issue to be addressed. However, there is an increased demand globally for sustainable protein source for animal feed, hence the use of agricultural residues appear as a viable, economical and sustainable alternative to address this challenge (12).



White-rot fungi (WRF) are well known as suitable detoxifying agents due to their environmental friendliness, Generally Accepted as Safe (GRAS) nature, and efficient enzyme systems (13). Based on the available literature, *Lenzites betulina* has not been explored in the reduction of PE and anti-nutrient contents of JSC. Thus, JSC if detoxified can serve as a nutrient dense feedstock for various applications

MATERIALS AND METHOD

Sample collection

Jatropha seeds were obtained from NARICT plantation, Basawa Zaria in Sabongari Local Government Area of Kaduna State. The seed cake was obtained after extraction of oil from oil extraction plant. The JSC was dried in an oven at 55°C, finely powdered then sieved using STSJ-4 digital high frequency sieve shaker (Okhard Machine Tools Ltd, Nigeria), to obtain 0.20mm mesh size. The powdered sample was autoclaved at 120°C, 15psi for 20 minutes. This was then preserved in a polythene bag at 4°C for further analysis (14).

The selected microorganism, white rot fungi (WRF) "*Lenzites betulina*" was obtained from Mycology Laboratory of the Department of Biological Sciences, Ahmadu Bello University Zaria. This was maintained on potato dextrose agar slants at 4°C and sub-cultured every 15 days.

Methods

Culture and Inoculum preparation

The WRF, *Lenzites betulina* was grown on potato dextrose agar plates for 5 days at a temperature of 25 ± 2°C. Spores were harvested by adding 10 ml of sterile saline containing 0.1% (v/v) Tween-80 on to the culture plate. The surface was gently scraped with a sterile wire loop to gently dislodge the spores

from the agar plate and filtered. The spore suspension was used as the inoculum. The spores were counted in a Hemocytometer (Neubauer-improved, Paul Marienfeld GmbH & Co. KG Germany) as 1.4 x 10⁶/L.

Solid State Fermentation (SSF)

The *Lenzites betulina* was cultivated in disposable petridishes containing 10g deoiled *J. curcas* seed cake. For typical SSF, the seed cake was adjusted at different moisture levels with sterile water, and seeded with different concentration of mycelium spores and incubated in 65% relative humidity in a humidity-controlled BOD incubator at temperature 30°C. Samples were aseptically withdrawn at different time intervals for determination of anti-nutrients and phorbol ester content.

In above protocol, single-factor experiment was performed to select the best moisture percentage, inoculum size, incubation time and pH for detoxification of JCS by the microorganism. The aliquots of the samples were aseptically withdrawn at various time intervals for the quantitative determination of PEs and anti-nutrient assessment (15). The fermented substrate was oven dried at 70°C to terminate the fungi growth.

Determination of anti-nutrients and PE contents

Determination of other anti-nutrients

The PE content was extracted and quantified by modified method (16) with HPLC using phorbol - 12-myristate-13-acetate as an external standard. Trypsin Inhibitor was determined using the spectrophotometric method described by (17). Phytic acid was determined using the procedure described by (18); Oxalate was determined by the titration method described by Day and Underwood (19); Tannin content was estimated according to the method described by Makkar *et al.* (20); Saponin content was determined using the AOAC method described by Uematsu *et al.* (21).

2.0 RESULT AND DISCUSSION

Table 1: Effect of Moisture content on Anti-nutrients and Phorbol Ester composition in JSC-based substrate

	Tannin (%)	Trypsin inhibitor (TIU/mg)	Saponin (%)	Oxalate (mg/100g)	Phytate (mg/100g)	Phorbol ester (mg/g)
55	0.613 ± 0.030 ^c	59.400 ± 0.72 ^d	0.202 ± 0.021 ^c	78.728 ± 0.628 ^c	4.280 ± 0.027 ^d	0.314 ± 0.002 ^d



60	0.361 ± 0.020 ^c	53.333 ± 0.808 ^c	0.160 ± 0.190 ^b	67.030 ± 0.070 ^b	4.099 ± 0.041 ^c	0.306 ± 0.007 ^b
65	0.293 ± 0.040 ^a	32.800 ± 0.40 ^a	0.151 ± 0.026 ^a	65.003 ± 0.410 ^a	3.365 ± 0.116 ^a	0.302 ± 0.001 ^a
70	0.33 ± 0.010 ^b	40.467 ± 0.611 ^b	0.163 ± 0.021 ^c	66.343 ± 0.595 ^b	3.890 ± 0.027 ^b	0.307 ± 0.007 ^{bc}
75	0.371 ± 0.060 ^d	52.533 ± 0.222 ^c	0.174 ± 0.027 ^d	79.718 ± 0.178 ^d	4.188 ± 0.284 ^{cd}	0.309 ± 0.001 ^c

Values with different superscripts down the column differ significantly at $p < 0.05$

Table 2: Effect of inoculum concentration on anti-nutrients and Phorbol ester reduction in JSC-based substrate

Inoculum conc. (%)	Tannin (%)	Trypsin inhibitor (TIU/mg)	Saponin (%)	Oxalate (mg/100g)	Phytate (mg/100g)	Phorbol ester (mg/g)
2	0.547 ± 0.021 ^c	70.733 ± 0.808 ^c	0.158 ± 0.202 ^c	69.076 ± 0.73 ^c	4.675 ± 0.038 ^c	0.313 ± 0.002 ^c
4	0.513 ± 0.014 ^d	69.200 ± 0.600 ^d	0.152 ± 0.050 ^d	63.833 ± 0.55 ^d	4.294 ± 0.119 ^d	0.310 ± 0.005 ^d
6	0.28 ± 0.015 ^a	51.650 ± 0.723 ^a	0.129 ± 0.179 ^a	51.391 ± 0.09 ^a	3.207 ± 0.052 ^a	0.295 ± 0.003 ^a
8	0.439 ± 0.035 ^b	60.667 ± 0.461 ^b	0.146 ± 0.225 ^c	56.340 ± 0.46 ^b	3.655 ± 0.144 ^b	0.303 ± 0.001 ^b
10	0.482 ± 0.025 ^c	64.800 ± 0.346 ^c	0.145 ± 0.122 ^b	60.166 ± 0.21 ^c	3.952 ± 0.076 ^c	0.306 ± 0.076 ^c

Values with different superscripts down the column differ significantly at $p < 0.05$

Table 3: Effect of initial pH on anti-nutrients and PE reduction in JSC- based substrate

Initial pH	Tannin (%)	Trypsin inhibitor (TIU/mg)	Saponin (%)	Oxalate (mg/100g)	Phytate (mg/100g)	Phorbol ester (mg/g)
Uncontrolled pH*	0.254 ± 0.098 ^a	48.567 ± 0.208 ^a	0.103 ± 0.108 ^a	53.726 ± 0.353 ^a	2.912 ± 0.080 ^a	0.272 ± 0.010 ^a
pH 4	0.424 ± 0.057 ^d	55.133 ± 0.416 ^d	0.114 ± 0.070 ^d	58.725 ± 0.203 ^c	3.932 ± 0.041 ^d	0.287 ± 0.002 ^{cd}
pH 5	0.402 ± 0.061 ^c	53.450 ± 0.739 ^c	0.112 ± 0.151 ^c	58.478 ± 0.281 ^c	3.628 ± 0.053 ^c	0.285 ± 0.020 ^c
pH 6	0.377 ± 0.061 ^b	50.333 ± 0.503 ^b	0.107 ± 0.100 ^b	54.585 ± 0.525 ^b	3.247 ± 0.056 ^b	0.278 ± 0.015 ^b
pH 7	0.452 ± 0.027 ^c	59.600 ± 1.000 ^c	0.117 ± 0.040 ^c	60.705 ± 0.810 ^d	4.277 ± 0.060 ^e	0.288 ± 0.072 ^d



pH 8 0.474 ± 0.076^f 63.001 ± 0.346^f 0.117 ± 0.045^c 62.708 ± 0.309^c 4.632 ± 0.039^f 0.292 ± 0.030^c

Values with different superscripts down the column differ significantly at p < 0.05

***pH 5.8**

Table 4: Effect of Temperature on Anti-nutrients and Phorbol Ester Content of JSC-based substrate

Temperature (T°C)	Tannin (%)	Trypsin inhibitor (TIU/mg)	Saponin (%)	Oxalate (mg/100g)	Phytate (mg/100g)
30	0.342 ± 0.030 ^b	44.467 ± 0.611 ^b	0.157 ± 0.147 ^b	46.403 ± 0.490 ^b	2.837 ± 0.042 ^b
35	0.304 ± 0.070 ^a	40.800 ± 1.386 ^a	0.125 ± 0.108 ^a	41.025 ± 0.654 ^a	2.450 ± 0.871 ^a
40	0.356 ± 0.012 ^b	49.867 ± 1.137 ^c	0.291 ± 0.051 ^c	48.127 ± 0.309 ^c	3.120 ± 0.027 ^c

Values with different superscripts down the column differ significantly at p < 0.05

Table 5: Effect of Incubation Period on Anti-nutrients and Phorbol Ester Reduction in JSC-based substrate

Incubation period (Day)	Tannin (%)	Trypsin inhibitor (TIU/mg)	Saponin (%)	Oxalate (mg/100g)	Phytate (mg/100g)	Phorbol ester (mg/g)
Day 0	0.902 ± 0.015 ^c	74.533 ± 1.220 ^f	0.344 ± 0.266 ^c	120.553 ± 0.467 ^c	5.172 ± 0.220 ^d	0.332 ± 0.007 ^f
Day 2	0.894 ± 0.012 ^c	74.067 ± 1.701 ^f	0.321 ± 0.416 ^d	120.620 ± 0.374 ^c	5.143 ± 0.374 ^d	0.331 ± 0.018 ^f
Day 4	0.619 ± 0.017 ^d	71.267 ± 0.306 ^e	0.145 ± 0.211 ^c	85.333 ± 0.539 ^d	3.327 ± 0.132 ^c	0.300 ± 0.03 ^e
Day 6	0.336 ± 0.013 ^c	39.133 ± 0.306 ^d	0.345 ± 0.503 ^b	15.797 ± 0.247 ^c	1.593 ± 0.737 ^b	0.288 ± 0.001 ^d
Day 8	0.281 ± 0.015 ^b	31.067 ± 0.503 ^c	0.120 ± 0.05 ^a	5.917 ± 0.204 ^b	1.080 ± 0.692 ^a	0.255 ± 0.007 ^c
Day 10	0.176 ± 0.030 ^a	17.267 ± 0.306 ^b	0.110 ± 0.02 ^a	2.340 ± 0.179 ^a	1.003 ± 0.635 ^a	0.140 ± 0.03 ^b
Day 12	0.175 ± 0.029 ^a	1.333 ± 0.115 ^a	0.100 ± 0.05 ^a	1.980 ± 0.142 ^a	1.003 ± 0.635 ^a	0.020 ± 0.005 ^a
Day 14	0.175 ± 0.039 ^a	1.334 ± 0.306 ^a	0.101 ± 0.06 ^a	1.980 ± 0.107 ^a	1.002 ± 0.133 ^a	0.020 ± 0.006 ^a

Values with different superscripts down the column differ significantly at p < 0.05

Table 6: Validation of the Optimum Process Condition for the Reduction of Anti-Nutrients and PEs Contents in JSC-based substrate

Anti-nutrient	Untreated JSC	Treated JSC	% reduction
Saponin (%)	0.35 ± 0.66	0.10 ± 0.05	71.09
Phytate (mg/100g)	5.29 ± 0.46	1.00 ± 0.64	81.09
Tannin (%)	0.90 ± 0.010	0.18 ± 0.11	80.06
Oxalate (mg/100g)	119.88 ± 0.94	1.99 ± 0.14	98.34
Trypsin inhibitor	74.27 ± 0.83	1.34 ± 0.12	98.20
PE (mg/g)	0.33 ± 0.007	0.02 ± 0.01	93.94

Optimum Conditions: Moisture 65%, Inoculum 6%, Initial pH 5.8, Temperature 35°C and Incubation Period 12 days.



Table 1 indicates the highest reduction of PE and anti-nutrient contents at 65% moisture level. The lower reduction of anti-nutrient and PEs content due to moisture level below the optimal may be due to insufficient moisture to enhance growth for substrate utilization and enzyme production. The increase in moisture level above the optimal is believed to reduce the porosity of the substrate, thus limiting oxygen transfer.

Table 2 showed the optimum inoculum concentration (6%) on the reduction of PEs and anti-nutrient content. There was significant difference ($p < 0.05$) in the mean PE and anti-nutrient reduction. Inoculum concentration has an important role in biological pre-treatment since the time required for the colonization of the substrate is clearly influenced by the type and amount of inoculum (22). The low anti-nutrient and PEs reduction observed below the optimal inoculum concentration may be due to insufficient inoculum concentration to enhance the growth, whereas a low anti-nutrient and PE reduction above the optimal inoculum concentration may be due to competitive inhibition because of interrupted nutrient availability (23)

The pH is one of the important parameters in fungal cultivation. The optimal pH for maximum anti-nutrient and PE reduction were attained at uncontrolled pH 5.8. As seen in Table 3. It can be seen that there is lower reduction in the PE and anti-nutrients content below and above the optimal pH. This could be attributed to the fact that, changes in pH may have altered the three-dimensional structure of the enzymes (24). Enzymes originated from fungi was reported to be active at pH 3.9 to 5.2, but the optimal pH for fungi is from 4.5 to 6.0 (25).

Effect of temperature in the reduction of PE and anti-nutrients content as showed in table 4 revealed significant difference ($p < 0.05$) in the mean PEs and anti-nutrient content. However, the highest reductions were observed in temperature 35°C while the least reduction were observed in 40°C. The low reduction of anti-nutrient and PEs due to increase in temperature may be due to the fact that high temperature above optimal denature the protein. Temperature is of much significant in the SSF systems, because during fermentation, there is a general increase in the temperature of the fermenting mass due to respiration (26). It has

impact on microbial growth and enzyme production.

Effect of incubation time in the reduction of PE anti-nutrients content as showed in Table 5 revealed significant different ($p < 0.05$) in the mean PEs and anti-nutrient content. The highest reductions were observed at day 12 while beyond day 12, there were no significant reductions in the PE and anti-nutrients content. Also, no further increase in fungal biomass was observed, since production of ligninolytic enzymes occurred during their secondary metabolism of growth phase (27). Time course study is one of the most critical factors that govern the value of the process along with product formation. The pattern of growth after a specific incubation time is characteristics to each species (28).

Table 6. showed the validation of the optimum conditions in the reduction of PE and anti-nutrients which indicate that; Saponin, Phytate, Tannin, Oxalate, Trypsin inhibitor and PE contents of JSC were significantly ($p < 0.05$) reduced by 71.09, 81.09, 80.06, 98.34, 98.20 and 93.94% respectively. The reduced tannin content (0.18%) in table 6 is lower than the reported value (0.35%) when treated with *Absidia spinosa* (29). The value is equally lower than the range of the recommended deleterious dose of 0.75 - 0.95% (30). Tannin are complex polyphenol found widely in the plant kingdom. It forms complexes, precipitating dietary proteins, and digests enzymes (31). The saponin value (0.10%) of the detoxified JSC in Table 6 is lower than 0.23% report by (29). This value is far below the acceptable limit of 3.4% for making the seed cake non-toxic (32). The presence of saponins could confer bitter and astringent characteristics on the material. Saponin are known astringent components of food materials and this could lead to reduced palatability (33). The phytate value (1.0mg/100g) in table 6 after fermentation is in agreement with 0.8mg/100g in *Absidia spinosa* culture (27). This value is far below the acceptable limit for making the seed cake non-toxic (32). Phytic acid is a strong chelator and is the principal storage form of phosphorous and other minerals and trace minerals in many plant tissues (34). The detoxification of phytic acid by *Lenzites betulina* may be favoured due to the production of phytase and other enzymes (34). The oxalate content of 1.99mg/100g in the detoxified JSC (table 6) is lower than the value (1.49mg/100g) reported by (35) after 7 days incubation period. Oxalate is found



in nature in some plants in the form of soluble and insoluble salts and as oxalic acid, the simplest organic acid (36). It affects calcium and magnesium metabolism and reacts with protein to form complexes which have an inhibitory effect on peptic digestion (37). The value (1.34 TIU/mg) of trypsin inhibitor after 12 days incubation in *Lenzites betulina* in JSC-based substrate is in agreement with 1.12 TIU/mg reported (38). This is far lower than the acceptable limit 26.5 TIU/mg (32). It destructively alters trypsin thereby rendering unavailable to bind with proteins for the digestion process (39).

The PE value (0.02mg/g) showed in Table 6 in JSC-based substrate for 12 days incubation period is lower than the reported value of 0.03mg/g (40). This value obtained is however below the reported acceptable limit of 0.11mg/g (32). The PE has been reported to affect many enzymatic activities through its interaction with protein-kinase C (PKC) (41). The differences in these determinations of anti-nutrients and the PE content reduction could be attributed to the type of the organisms, substrate used and the fermentation conditions.

3.0 Conclusion

This study demonstrated that *Lenzites betulina* was able to reduce phorbol ester from *J. curcas* seed cake from the initial concentration of 0.33mg/g to 0.02mg/g, which is lower than 0.11mg/g reported as safe in the non-toxic seed varieties. There was significant reduction (>70%) in all the five (5) anti-nutrients (saponin, phytate, tannin, oxalate, and trypsin inhibitor) considered in this study under the optimum condition. Thus, the increase in protein content coupled with significant reduction in PE and anti-nutrients of JSC could allow its usage as a potential feedstock in animal feed formulation.

REFERENCES

1. R. Zanzi, J. Perez, P. Soler, in *Proceedings of the 3rd international congress university-industry cooperation, Ubatuba, Brazil*. (2008).
2. M. Baldini, E. Bulfoni, C. Ferfuaia, Seed processing and oil quality of *Jatropha curcas* L. on farm scale: A comparison with other energy crops. *Energy for sustainable development* **19**, 7-14 (2014).
3. H. Makkar, A. Aderibigbe, K. Becker, Comparative evaluation of non-toxic and toxic varieties of *Jatropha curcas* for chemical composition, digestibility, protein degradability and toxic factors. *Food chemistry* **62**, 207-215 (1998).
4. Y. Ito *et al.*, Epstein-Barr virus activation by tung oil, extracts of *Aleurites fordii* and its diterpene ester 12-O-hexadecanoyl-16-hydroxyphorbol-13-acetate. *Cancer letters* **18**, 87-95 (1983).
5. G. Goel, H. P. Makkar, G. Francis, K. Becker, Phorbol esters: structure, biological activity, and toxicity in animals. *International journal of toxicology* **26**, 279-288 (2007).
6. K. Rakshit *et al.*, Toxicity studies of detoxified *Jatropha* meal (*Jatropha curcas*) in rats. *Food and Chemical Toxicology* **46**, 3621-3625 (2008).
7. G. El Diwani, S. A. El Rafei, S. Hawash, Ozone for phorbol esters removal from Egyptian *Jatropha* oil seed cake. *Advances in Applied Science Research* **2**, 221-232 (2011).
8. X. Liu *et al.*, Quantitative determination of phorbol ester derivatives in Chinese *Jatropha curcas* seeds by high-performance liquid chromatography/mass spectrometry. *Industrial Crops and Products* **47**, 29-32 (2013).
9. C. Joshi, P. Mathur, S. Khare, Degradation of phorbol esters by *Pseudomonas aeruginosa* PseA during solid-state fermentation of deoiled *Jatropha curcas* seed cake. *Bioresource technology* **102**, 4815-4819 (2011).
10. P. SORGELOOS, C. Rémiche-Van Der Wielen, G. Persoone, The use of *Artemia nauplii* for toxicity tests—a critical analysis. *Ecotoxicology and environmental safety* **2**, 249-255 (1978).



11. M. Nakao, G. Hasegawa, T. Yasuhara, Y. Ishihara, Degradation of Jatropha curcas phorbol esters derived from Jatropha oil cake and their tumor-promoting activity. *Ecotoxicology and environmental safety* **114**, 357-364 (2015).
12. M. B. Guimarães *et al.*, Evaluation of Bio-detoxification of jatropha curcas seed cake and cottonseed cake by basidiomycetes: nutritional and antioxidant effects. *Waste and Biomass Valorization*, 1-16 (2022).
13. A. Akinfemi, O. Adu, O. Adebisi, Use of white rot-fungi in upgrading maize straw and, the resulting impact on chemical composition and in vitro digestibility. *Livestock research for rural development* **21**, 162 (2009).
14. M. Belewu, M. Azeez, Replacement of Fungus treated jatropha curcas seed meal for Soybean meal in the diet of rat. *Green Farming Journal* **2**, 154-157 (2008).
15. X. Zhang, Z. Yang, J. Liang, L. Tang, F. Chen, Detoxification of Jatropha curcas seed cake in solid-state fermentation of newly isolated endophytic strain and nutrition assessment for its potential utilizations. *International Biodeterioration & Biodegradation* **109**, 202-210 (2016).
16. W. Haas, M. Mittelbach, Detoxification experiments with the seed oil from Jatropha curcas L. *Industrial crops and products* **12**, 111-118 (2000).
17. G. Onwuka, Food analysis and instrumentation. *Theory and Practice. Naphthali Prints*, 140-146 (2005).
18. G. Lucas, Phytic acid and other phosphorous compounds of lima beans (Phaseolus lunatus). *Journal of Agriculture and Food Chemistry* **23**, 13-15 (1975).
19. R. A. Day, A. L. Underwood, *Qualitative Analysis*. (Prentice-Hall Publications, New Delhi, India, ed. 5th, 1986).
20. H. P. Makkar, M. Blümmel, N. K. Borowy, K. Becker, Gravimetric determination of tannins and their correlations with chemical and protein precipitation methods. *Journal of the Science of Food and Agriculture* **61**, 161-165 (1993).
21. Y. Uematsu, K. Hirata, K. Saito, I. Kudo, Spectrophotometric determination of saponin in Yucca extract used as food additive. *Journal of AOAC International* **83**, 1451-1454 (2000).
22. S. J. van Kuijk, A. S. Sonnenberg, J. J. Baars, W. H. Hendriks, J. W. Cone, Fungal treatment of lignocellulosic biomass: Importance of fungal species, colonization and time on chemical composition and in vitro rumen degradability. *Animal Feed Science and Technology* **209**, 40-50 (2015).
23. A. Sabu, A. Pandey, M. J. Daud, G. Szakacs, Tamarind seed powder and palm kernel cake: two novel agro residues for the production of tannase under solid state fermentation by Aspergillus niger ATCC 16620. *Bioresource Technology* **96**, 1223-1228 (2005).
24. M. Shulter, F. Kargi, Bioprocess engineering basic concept. *New Delhi: Parentice-Hall of India Pvt Ltd*, (2000).
25. C. F. Thurston, The structure and function of fungal laccases. *Microbiology* **140**, 19-26 (1994).
26. N. K. Roy, S. Panda, G. Dey, Engineering a sustainable protein revolution: Recent advances in cultured meat production. *Food Bioengineering*, (2023).
27. X. Zhou, X. Wen, Y. Feng, Influence of glucose feeding on the ligninolytic enzyme production of the white-rot fungus



- Phanerochaete chrysosporium. *Frontiers of Environmental Science & Engineering in China* **1**, 89-94 (2007).
28. P. Senthilkumar, C. Uma, P. Saranraj, Amylase production by *Bacillus* sp. using cassava as substrate. *International journal of Pharmaceutical and Biological archives* **3**, 274-280 (2012).
 29. G. Sanusi *et al.*, Changes in chemical composition of *Jatropha curcas* kernel cake after solid-state fermentation using some selected fungi. *Global J. Biol. Agric. Health Sci* **2**, 62-66 (2013).
 30. O. Aletor, G. Oboh, S. Ojo, Antinutrient content, vitamin constituents and antioxidant properties in some value-added Nigerian traditional snacks. *WIT Transactions on Ecology and the Environment* **170**, 209-220 (2013).
 31. G. Oboh, A. Akindahunsi, Biochemical changes in cassava products (flour & gari) subjected to *Saccharomyces cerevisiae* solid media fermentation. *Food chemistry* **82**, 599-602 (2003).
 32. E. Aregheore, K. Becker, H. Makkar, Detoxification of a toxic variety of *Jatropha curcas* using heat and chemical treatments, and preliminary nutritional evaluation with rats. *The South Pacific Journal of Natural and Applied Sciences* **21**, 51-56 (2003).
 33. V. Enujiugha, T. Oluwole, J. Talabi, A. Okunlola, Selected bioactive components in fluted pumpkin (*Telfairia occidentalis*) and Amaranth (*Amaranthus caudatus*) leaves. *American Journal of Experimental Agriculture* **4**, 966-1004 (2014).
 34. T. Santos, C. Connolly, R. Murphy, Trace element inhibition of phytase activity. *Biological trace element research* **163**, 255-265 (2015).
 35. C.-F. Chang, J.-H. Weng, K.-Y. Lin, L.-Y. Liu, S.-S. Yang, Phorbol esters degradation and enzyme production by *Bacillus* using *Jatropha* seed cake as substrate. *International Journal of Environmental Pollution and Remediation (IJEPR)* **2**, 30-36 (2014).
 36. N. Ilelaboye, I. Amoo, O. Pikuda, Effect of cooking methods on mineral and anti nutrient composition of some green leafy vegetables. *Archives of Applied Science Research* **5**, 254-260 (2013).
 37. K. E. Akande, U. D. Doma, H. Agu, H. Adamu, Major antinutrients found in plant protein sources: their effect on nutrition. (2010).
 38. D. Saetae, W. Suntornsuk, Toxic compound, anti-nutritional factors and functional properties of protein isolated from detoxified *Jatropha curcas* seed cake. *International Journal of Molecular Sciences* **12**, 66-77 (2010).
 39. C. J. Farady, C. S. Craik, Mechanisms of macromolecular protease inhibitors. *Chembiochem* **11**, 2341-2346 (2010).
 40. M. Belewu, R. Sam, Solid state fermentation of *Jatropha curcas* kernel cake: proximate composition and antinutritional components. (2010).
 41. U. Testa, M. Titeux, F. Louache, P. Thompoulos, H. Rochant, Effect of phorbol esters on iron uptake in human hematopoietic cell lines. *Cancer research* **44**, 4981-4986 (1984).
 41. AOAC. *Official Method of Analysis*, 15th Ed., Association of Official Analytical Chemists, Washington, DC, 1990.
 42. R.A. Day, A.L. Underwood, Quantitative analysis 5th ed. Prentice. Hall publication p. 701, (1986).





P109 - THE INDUCED DAMAGE TO LIVER AND KIDNEY OF WISTAR RAT BY SPENT VEGETABLE OIL AND THE AMELIORATING POTENTIALS OF COCONUT OIL

*Simon I. A¹; Solomon M.D.²; Sangodare R.S.A¹; Dabak J.D.²; Abubakar A.¹; Abdulkadir J.¹

1 National Research Institute for Chemical Technology, PMB 1052. Basawa, Zaria, Kaduna State, Nigeria.

2 Department of Biochemistry University of Jos Plateau State, Nigeria.

**Corresponding author: adamunistifanuss@gmail.com ORCID no:0000-0002-4552-986X*

ABSTRACT

It has been a regular practice in this part of the world to continually use spent edible oil and consumed it without knowing the harmful effects of such. Heating results in the formation of free reactive oxygen species (ROS) which is responsible for oxidative stress and changes to various organs in the body. The study aimed at investigating the changes caused on liver and kidney by consumption of repeatedly used (spent) oil and possible ameliorating potential of virgin coconut oil (VCO) on spent vegetable oil-induced liver and kidney changes in Wistar albino rats. Blood samples were obtained and assayed for biomarkers of liver and kidney damage; It was observed that spent vegetable oils induced severe damage on liver and kidney. While administration of virgin coconut oil significantly ($p < 0.05$) reversed the changes induced by the spent oil as observed in the biomarkers AST, ALT, ALP, Urea, Creatinine, Uric acid, Total serum protein, Albumin. These findings suggest that VCO could ameliorate the adverse effect of consumption of spent oil on liver and kidney indices in rats.

KEYWORDS: *Spent Vegetable Oil, Ameliorating, Coconut Oil, Oxidative Stress, Liver, Kidney*

1.0 INTRODUCTION

The repeated use of spent vegetable oil is the most common and one of the oldest methods of food preparation worldwide especially in developing nation like Nigeria. In order to reduce expenses, oils tend to be used repeatedly for frying. When heated repeatedly, changes in physical appearance of the oil will occur such as increased viscosity and darkening in colour (1), this may alter the fatty acid composition of the oil. Heating causes the oil to undergo a series of chemical reactions like oxidation, hydrolysis and polymerization (2). During this process, many oxidative products such as hydroperoxide and aldehydes are produced, which can be absorbed into the fried food (3). Findings indicates that chronic consumption of repeatedly used vegetable oils could be detrimental to health. In rats given alcohol plus heated sunflower, an apparent liver damage as well as increased cholesterol level were observed (4).

Spent vegetable oils promotes the generation of free radicals such as ketones, aldehydes, alcohols, hydrocarbons, peroxides, epoxides, and cyclic polymers, these may play an important contributory role in pathogenesis of several conditions.

In this study, repeatedly heated palm oil is used to mimic the situation that happens where people fry foods using the same oil multiple times. This practice is common among Malaysian, as a means to cut expenses. Previous research done by Azman et al., (2012) showed that even though night market vendors agreed that repeatedly heated cooking oil is harmful to health, they still continued the practice of using the same cooking oil repeatedly.

Nowadays, virgin coconut oil (VCO) has become popular due to its beneficial effects. VCO has been shown to have anti-inflammatory, analgesic, and antipyretic properties (5). VCO has been shown to decrease lipid levels in serum and tissue as well as LDL lipid peroxidation (6). Consumption of VCO enhances antithrombotic effects related to inhibition of platelet coagulation and low cholesterol level (7). VCO has been known to have higher antioxidant activity compared to refined coconut oil (8). It has also been proven that VCO enhances antioxidant activity and inhibits lipid peroxidation in rats (9). Therefore, it is of great interest for us to investigate whether VCO is able to prevent hypertension in male rats given repeatedly heated palm oil.

2.0 MATERIALS/EQUIPMENT

The equipment used were Chemistry Auto Analyzer Mindray Bs-120, Centrifuge 800D, un-heparinized capillary tubes, STP 120 Thermoscientific, needle



and syringe (21G), plain sample bottles, microm HM340E Thermoscientific, SLEE MPS/P2, cotton wool, surgical gloves and nose mask.

2.1. Sample preparation

Spent Vegetable Oil from fish vendor (SVOF) and Spent Vegetable Oil from beans cake vendor (SVOB) used were obtained from different locations within Jos Metropolis while frying, while 1 liter of vegetable oil and palm oil were purchased from local markets in Jos. The VCO was freshly extracted.

Single dosage of 14.4mls and double dosage of 28.8mls of spent palm and spent vegetable oils were prepared by mixing with the rat feeds.

2.2. Experimental Animals

Wistar Albino rats weighing between 110-250g were obtained from the Animal House, University of Jos.

2.3. Methods

The method of Gornal *et al* (1949) was employed for the determination of serum total protein. Urea in serum was measured spectrophotometrically by Berthelots reaction at 546 nm. Determination of serum albumin was carried out according to modified method of Bartholomew and Delaney method, (1966)

The method of King-Armstrong (1934) was used in the determination of serum alkaline phosphatase. Serum AST activity was estimated according to the method of Reitman and Frankel (1957) and Serum Alanine Aminotransaminase (ALT) activity was estimated according to the method of Reitman and Frankel (1957). The method of Hare (1950) was used in the determination of serum creatinine. Concentration of serum uric acid was carried out using Randox Kit

RESULT AND DISCUSSION

Effect of Virgin Coconut Oil (VCO) on serum total protein and albumin of rats fed with Spent Palm Oil Single dose (SPOS) and Spent Palm Oil Double dose (SPOD).

Table 1

Group	Treatment	Serum Total Protein (g/L)	Albumin (g/L)
Normal control (NC)		77.24±1.02	36.51±0.96
SPOS		70.46±1.01 ^{ac}	30.96±0.43 ^{ac}
SPOD		63.72±0.32 ^{abd}	25.82±0.53 ^{abd}
SPOS + VCO		75.71±0.27 ^{bcd}	35.75±0.26 ^{bcd}
SPOD + VCO		65.51±0.14 ^{abd}	27.64±0.93 ^{abd}

Values are expressed as mean ± SD, n= 5 for each group

^a values are significantly different from the NC group (p<0.05)

^b values are significantly different from SPOS (p<0.05)

^c values are significantly different from SPOD (p<0.05)

^d values are significantly different from SPOS + VCO (p<0.05)

Where NC= Normal Control, SPOS= Spent Palm Oil Single dose, SPOD= Spent Palm Oil Double dose.

Result of effect of VCO on serum total protein and albumin shown on Table 1 indicates that there was significant (p<0.05) decrease in the level of the serum total protein and albumin of the rats given spent palm oil compared with the control rats (Table

Effect of VCO on serum total protein and albumin of rats fed with Spent Vegetable Oil Single dose (SVOS) and Spent Vegetable Oil Double dose (SVOD)

1). The administration of 1ml of VCO significantly (p<0.05) increased the level of serum total protein and albumin in rats when compared with the rats given spent palm oil only.

Table 2

Group	Treatment	Serum Total Protein (g/L)	Albumin (g/L)
-------	-----------	---------------------------	---------------



NC	77.24±1.02	36.51±0.96
SVOFS	67.17±1.20 ^{acfg}	29.48±0.56 ^{acfg}
SVOBS	65.43±0.30 ^{abfh}	27.06±0.58 ^{abfh}
SVOFD	61.07±0.37 ^{abfg}	24.37±0.35 ^{abfg}
SVOBD	59.35±0.33 ^{abfh}	24.09±0.41 ^{abfh}
SVOFS + VCO	70.26±0.27 ^{abfg}	30.42±0.51 ^{abfg}
SVOBS + VCO	68.25±0.44 ^{abfh}	29.52±0.41 ^{abfh}
SVOFD + VCO	63.40±0.36 ^{abeg}	25.82±0.17 ^{abeg}
SVOBD + VCO	59.50±0.18 ^{ab}	24.02±0.32 ^{ab}

Values are expressed as mean ± SD, n= 5 for each group

^a values are significantly different from the NC group (p<0.05)

^e values are significantly different from SVOBD (p<0.05)

^f values are significantly different from SVOFS+VCO (p<0.05)

^g values are significantly different from SVOBS (p<0.05)

^h values are significantly different from SVOFD+VCO (p<0.05)

Where NC= Normal Control, SVOFS= Spent Vegetable Oil Fish Vendor Single dose, SVOFD= Spent Vegetable Oil Fish Vendor Double dose, SVOBS= Spent Vegetable Oil Beans Cake Vendor Single dose SVOBD= Spent Vegetable Oil Beans Cake Vendor Double dose.

Result of effect of VCO on serum total protein and albumin.

There was significant (p<0.05) decrease in the level of the serum total protein and albumin of the rats given spent vegetable oils compared with the control rats (**Table 2**). The administration of 1ml of VCO significantly (p<0.05) increased the level of serum total protein and albumin in rats when compared with the rats given spent vegetable oils only.

Effect of VCO on liver biomarkers of rats fed with spent palm oil single dose (SPOS) and spent palm oil double dose (SPOD).

Table 3

Group	Treatment	ALT(U/L)	AST(U/L)	ALP(U/L)
NC		9.84±0.40	13.82±0.65	228.33±1.37
SPOS		16.89±1.20 ^{acd}	20.56±0.66 ^{acd}	274.33±1.86 ^{acd}
SPOD		24.14±0.13 ^{abcd}	28.85±0.28 ^{abcd}	313.00±3.23 ^{abcd}
SPOS + VCO		15.58±0.20 ^{abc}	17.66±0.26 ^{abc}	225.00±2.37 ^{abc}
SPOD + VCO		21.57±0.50 ^{abd}	29.43±0.37 ^{abd}	351.00±1.79 ^{abd}

Values are expressed as mean ± SD, n= 5 for each group

^a values are significantly different from the NC group (p<0.05)



^b values are significantly different from SPOS (p<0.05)

^c values are significantly different from the SPOD (p<0.05)

^d values are significantly different from SPOS + VCO (p<0.05)

Result of effect of VCO on some liver biomarkers.

There was significant (p<0.05) increase in the level of biomarkers (ALT, AST and ALP) of the rats administered spent palm oil compared with the control rats (**Table 3**). The administration of 1ml of VCO significantly (p<0.05) decreased the level of

biomarkers (ALT, AST and ALP) in rats when compared with the rats given spent palm oil only.

Effect of VCO on liver biomarkers of rats fed with spent vegetable oil single dose (SVOS) and spent vegetable oil double dose (SVOD).

Group	Treatment	ALT(U/L)	AST(U/L)	ALP(U/L)
NC		9.84±0.40	13.82±0.65	228.33±1.37
SVOFS		20.10±0.97 ^{abf}	23.33±0.52 ^{abf}	287.33±1.37 ^{abf}
SVOBS		22.41±0.31 ^{abf}	25.33±0.52 ^{abf}	320.67±1.37 ^{abf}
SVOFD		26.46±0.10 ^{abfg}	31.30±0.54 ^{abfg}	373.67±1.37 ^{abfg}
SVOBD		29.11±0.35 ^{abfh}	36.33±1.03 ^{abfh}	387.33±0.52 ^{abfh}
SVOFS + VCO		20.03±0.30 ^{abf}	21.67±0.52 ^{abfg}	281.67±2.25 ^{abf}
SVOBS + VCO		20.95±0.50 ^{abfh}	23.00±0.00 ^{abfh}	310.33±0.52 ^{abf}
SVOFD + VCO		24.30±0.27 ^{abfgi}	29.43±0.37 ^{abfgi}	361.00±1.55 ^{abfg}
SVOBD + VCO		29.33±0.41 ^{abf}	36.00±0.89 ^{abf}	287.00±0.89 ^{abf}

Values are expressed as mean ± SD, n= 5 for each group

^a values are significantly different from the NC group (p<0.05)

^f values are significantly different from SVOFS + VCO (p<0.05)

^g values are significantly different from SVOBS + VCO (p<0.05)

^h values are significantly different from SVOFD + VCO (p<0.05)

ⁱ values are significantly different from SVOBD + VCO (p<0.05)

Result of effect of VCO on liver biomarkers.

There was significant (p<0.05) increase in the level of the liver biomarkers (ALT, AST and ALP) of the rats given spent vegetable oils compared with the control (**Table 4**). The administration of 1ml of VCO significantly (p<0.05) decreased the level of biomarkers (ALT, AST and ALP) in rats when compared with the rats given spent vegetable oils only.

The fact that there was a significant (p<0.05) decrease in the serum total protein and albumin of groups fed with repeatedly used (spent) vegetable oils diets shows that it may alter protein synthesis in the liver, The decrease in serum total protein and albumin levels associated with the test rats indicate impairment in the normal function of the liver, but on oral gavages administration of VCO at 1 ml for 14 days there was significant increase in the serum

total protein and albumin which shows an increase in the protein synthesis of the liver.

The plasma ALP, AST and ALT activities of the groups fed with repeatedly used (spent) vegetable oils diets increased when compared with the control groups in, Table 3 and 4. An evidence of hepatic damage was also reported with a significant elevation of aspartate and alanine transaminases, the marker enzymes for liver function in rats that were given combination of heated soy and rapeseed oils (10). The increase in ALP appears to be lipid-dependent, ingestion of fat leads to an increase in ALP synthesis by rat intestinal mucosa ((11); (12); (13)). Serum ALP is a sensitive



detector for early intrahepatic and extrahepatic bile obstruction. The presence of infiltrative diseases of the liver (14). The increase ALP, AST and ALT activities in the serum observed might be due to alterations in membrane architecture of the cells of the liver of rats fed with repeatedly used (spent) vegetable oils diets and hence, an effect on the liver

integrity, but on oral administration of VCO there was decrease in level of the serum ALP, AST and ALT which shows that biomarkers leak out and their free circulation is reduced in the liver.

Effect of VCO on kidney biomarkers of rats fed with Spent Palm Oil Single dose (SPOS) and Spent Palm Oil Double dose (SPOD).

Table 5

Group	Treatment	UA(μmol/l)	Urea(mmol/l)	Creatinine (μmol/l)
NC		227.75±0.31	4.59±0.21	67.78±0.83 ^a
SPOS		266.09±1.83 ^{ac}	5.42±0.15 ^{ac}	98.54±0.33 ^{ac}
SPOD		301.42±1.61 ^{abd}	8.80±0.12 ^{abd}	132.86±1.33 ^{abd}
SPOS + VCO		268.52±0.67 ^{abd}	4.97±0.09 ^{abd}	78.12±0.94 ^{abd}
SPOD + VCO		289.29±0.85 ^{abd}	7.68±0.05 ^{abd}	123.53±0.94 ^{abde}

Values are expressed as mean ± SD, n= 5 for each group

^a values are significantly different from the NC group (p<0.05)

^b values are significantly different from SPOS (p<0.05)

^c values are significantly different from the SPOD (p<0.05)

^d values are significantly different from SPOS + VCO (p<0.05)

Result of effect of VCO on uric acid, urea and creatinine.

There was significant (p<0.05) increase in the level of uric acid, urea and creatinine of the rats given spent palm oil compared with the NC rats

(Table 5). The administration of 1ml of VCO for 14 days significantly (p<0.05) decreased the level of uric acid, urea and creatinine in rats when compared with the rats given spent palm oil only

Effect of VCO on kidney biomarkers of rats fed with Spent Vegetable Oil Single dose (SVOS) and Spent Vegetable Oil Double dose (SVOD).

Table 6

Group	Treatment	UA(μmol/l)	Urea(mmol/l)	Creatinine (μmol/l)
NC		227.75±0.31	4.59±0.21	67.78±0.83
SVOFS		273.26±0.22 ^{abf}	6.47±0.04 ^{abf}	106.87±1.35 ^{abf}
SVOBS		285.82±2.30 ^{abf}	6.89±0.11 ^{abf}	128.10±1.18 ^{abf}
SVOFD		331.71±1.22 ^{abfg}	9.06±0.09 ^{abfg}	138.88±0.58 ^{abfg}
SVOBD		345.77±1.92 ^{abfh}	9.86±0.19 ^{abfh}	142.81±0.78 ^{abfh}
SVOFS + VCO		271.44±1.32 ^{abf}	6.39±0.05 ^{abf}	107.78±1.61 ^{abf}
SVOBS + VCO		276.17±2.28 ^{abfh}	6.96±0.07 ^{abf}	118.55±0.80 ^{abfh}
SVOFD + VCO		326.08±0.56 ^{abfgi}	9.09±0.10 ^{abfg}	139.24±0.60 ^{abfgi}
SVOBD + VCO		336.85±1.21 ^{abfh}	9.84±0.06 ^{abfh}	141.37±0.05 ^{abfh}

Values are expressed as mean ± SD, n= 5 for each group

^a values are significantly different from the NC group (p<0.05)

^e values are significantly different from SVOBD (p<0.05)



^f values are significantly different from SVOFS + VCO (p<0.05)

^g values are significantly different from SVOBS + VCO (p<0.05)

^h values are significantly different from SVOFD + VCO (p<0.05)

Result of effect of VCO on uric acid, urea and creatinine.

There was significant (p<0.05) increase in the level of uric acid, urea and creatinine of the rats given spent vegetable oils compared with the control rats (**Table 6**). The administration of 1ml of VCO for 14 days significantly (p<0.05) decreased the level of uric acid, urea and creatinine in rats when compared with the rats given spent vegetable oils only.

The increase observed in the serum urea, creatinine and uric acid concentrations in groups of rats fed with repeatedly used (spent) vegetables oils diets, and likewise the double dose of repeatedly used (spent) vegetables oils diet (and) when compared with control groups. There was decrease in serum urea, creatinine and uric acid of groups' rats after the administration of VCO, which indicates a recovery process of proper function of the kidney.

CONCLUSION

From our results it's suggested that virgin coconut oil could Our results show ameliorating potential of virgin coconut oil. for the prevention of oxidative stress induced hepato-renal toxicities in spent vegetable oil induced liver and kidney damage in Wistar rats. Consumption of spent vegetables oil diets had deleterious effects on biochemical indices in rats. The effects were most pronounced in rats fed with double dosage of the spent vegetable oil. Therefore, considering the harmful and detrimental effect associated with consumption of spent vegetable oil of any kind as observed from the finding of this work it is therefore imperative to avoid such practice.

Limitations

There wasn't any control of the type of spent vegetable oil used since it was bought from different vendors that varied in different preparation methods, times and periods used for the frying purposes and the various ingredients used in frying. Secondly, the period of this study might be too short to fully ascertained the ameliorating potentials of the VCO oil on the induce damage to liver and kidney of wistar rat by spent vegetable oils.

Recommendation

The findings suggest the avoidance of spent vegetable oils in diet due to its possible deleterious effect on health, the findings also suggest that fresh vegetable oils and coconut oil do not have detrimental effects but possibly has a positive effect on health.

Further research is required for the establishment of detailed ameliorating potential of virgin coconut oil for their hepatorenal protective and antioxidative efficacy.

REFERENCES

1. A. K. S. Rani, S. Y. Reddy, R. Chetana, Quality changes in trans and trans free fats/oils and products during frying. *European food research and technology* **230**, 803-811 (2010).
2. E. Choe, D. Min, Chemistry of deep-fat frying oils. *Journal of food science* **72**, R77-R86 (2007).
3. E. Choe, D. B. Min, Mechanisms and factors for edible oil oxidation. *Comprehensive reviews in food science and food safety* **5**, 169-186 (2006).
4. P. Latha, D. Chaitanya, R. Rukkumani, Protective effect of *Phyllanthus niruri* on alcohol and heated sunflower oil induced hyperlipidemia in Wistar rats. *Toxicology Mechanisms and Methods* **20**, 498-503 (2010).
5. S. Intahphuak, P. Khonsung, A. Panthong, Anti-inflammatory, analgesic, and antipyretic activities of virgin coconut oil. *Pharmaceutical biology* **48**, 151-157 (2010).
6. K. Nevin, T. Rajamohan, Virgin coconut oil supplemented diet increases the antioxidant status in rats. *Food chemistry* **99**, 260-266 (2006).



7. K. Nevin, T. Rajamohan, Influence of virgin coconut oil on blood coagulation factors, lipid levels and LDL oxidation in cholesterol fed Sprague–Dawley rats. *e-SPEN, the European e-Journal of Clinical Nutrition and Metabolism* **3**, e1-e8 (2008).
8. A. Marina, Y. Che Man, S. Nazimah, I. Amin, Antioxidant capacity and phenolic acids of virgin coconut oil. *International journal of food sciences and nutrition* **60**, 114-123 (2009).
9. K. G. Nevin, T. Rajamohan, Wet and dry extraction of coconut oil: impact on lipid metabolic and antioxidant status in cholesterol coadministered rats. *Canadian journal of physiology and pharmacology* **87**, 610-616 (2009).
10. N. Totani, M. Burenjargal, M. Yawata, Y. Ojiri, Chemical properties and cytotoxicity of thermally oxidized oil. *Journal of Oleo Science* **57**, 153-160 (2008).
11. R. Glickman, D. Alpers, G. Drummey, K. Isselbacher, Increased lymph alkaline phosphatase after fat feeding: effects of medium chain triglycerides and inhibition of protein synthesis. *Biochimica et Biophysica Acta (BBA)-General Subjects* **201**, 226-235 (1970).
12. K. Izui, A lipid requirement for induction of alkaline phosphatase, one of periplasmic enzymes, in *Escherichia coli*. *Biochemical and Biophysical Research Communications* **45**, 1506-1512 (1971).
13. J. J. Kaneko, J. W. Harvey, M. L. Bruss, *Clinical biochemistry of domestic animals*. (Academic press, 2008).
14. D. Owu, E. Osim, P. Ebong, Serum liver enzymes profile of Wistar rats following chronic consumption of fresh or oxidized palm oil diets. *Acta tropica* **69**, 65-73 (1998).



P110 - DESIGN OF 200KG/DAY ZEOLITE ODOUR ABATEMENT PILOT PLANT FROM KAOLIN (CLAY)

David Ayeni

Nigerian Universities Commission

danayenco2005@yahoo.com

ABSTRACT

Odour pollution presents significant environmental challenges in various industries, particularly in wastewater treatment and waste management. This study introduces zeolite-based odor abatement as an innovative and sustainable solution. Zeolites, known for their exceptional surface area and adsorption capacity, offer an eco-friendly approach to remove odorous compounds. The paper focuses on the design and energy balance of a pilot plant capable of handling 200 kilograms of odorous compounds daily. The material balance outlines the input and output of materials, emphasizing the importance of efficient zeolite use. The energy balance analysis assesses the plant's energy efficiency, demonstrating its capacity for high odor removal efficiency while minimizing energy input. The study underscores the potential of zeolite-based odor abatement as a cost-effective and environmentally conscious solution to combat odor pollution.

KEYWORDS

Zeolite, odor abatement, pilot plant, design, energy balance, regeneration, sustainability.

1.0 INTRODUCTION

Odor pollution poses a formidable environmental challenge, with far-reaching implications across industries, most notably in sectors such as wastewater treatment and waste management. The noxious emissions of odorous compounds not only disrupt the quality of life for neighboring communities but also threaten the overall environmental balance (1,2). To address this issue, the scientific community has been diligently exploring innovative technologies that can effectively mitigate odor emissions. One such technology, zeolite-based odor abatement, has gained significant attention in recent years (3).

Zeolites, crystalline aluminosilicate minerals, have garnered substantial recognition for their exceptional surface area and adsorption capacity. These unique properties make zeolites an ideal candidate for the removal of odorous compounds from industrial effluents. Unlike conventional methods, zeolite-based odor abatement presents a more sustainable and eco-friendly solution, making it an area of substantial interest for environmental scientists and engineers. This paper focuses on the design and energy balance of a pilot plant meticulously engineered to showcase the practicality, feasibility, and efficacy of zeolite-based odor removal technology (4).

This study seeks to address the pressing need for efficient odor control in industrial settings, with a specific emphasis on the significance of our pilot plant design. By exploring the intricacies of this design and the associated energy balance, we aim to demonstrate the immense potential of zeolite-based odor abatement as an environmentally conscious and cost-effective solution to this pervasive problem. The pilot plant's architecture, meticulously tailored to handle a daily load of 200 kilograms of odorous compounds, signifies a significant step forward in the battle against odor pollution, opening new avenues for clean and sustainable industrial operations (2,5).

2.0 Design Overview

The pilot plant represents a comprehensive solution to the pervasive challenge of odor pollution in industrial settings. The design encapsulates several vital components that synergistically work towards efficient odor abatement. These components include an odor inlet system, zeolite adsorption beds, a regeneration unit, and an emission control system. The collective integration of these elements ensures not only the efficient removal of odorous compounds but also minimal energy consumption,

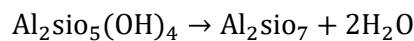


a paramount consideration in the design philosophy.

The cornerstone of the pilot plant's design is its ability to handle a daily odor load of 200 kilograms. This capacity is a critical feature, as it empowers the technology to cater to the needs of a diverse range of industries, from smaller-scale operations to medium-sized enterprises. Such adaptability and scalability make the design an appealing solution for a variety of applications. Whether it's a wastewater treatment facility or a waste management plant, the pilot plant provides an effective and versatile means of tackling odor issues.

By encompassing the entire odor abatement process, from the initial intake of odorous emissions to their final emission control, the design ensures a holistic approach to the problem. This not only maximizes the efficiency of odor removal but also minimizes any potential release of pollutants into the environment.

3.0 MATERIAL AND ENERGY BALANCE



The reaction temperature of 600⁰c was used as optimal temperature for maximum yield of metakaolin.

Table 1 Component molecular weight

Component	Molecular Mass(g)
Meta-kaolin	222.0
Water/Steam	18.0
Kaolin	258.0
NaOH	40.0

3.1 MATERIAL BALANCE

The material balance in the design of 200kg/day zeolite odour abatement pilot plant is a crucial aspect of the process. It ensures that we account for all materials entering and leaving the system accurately. The primary material involved in this process is the zeolite feedstock

3.1.1 Furnace

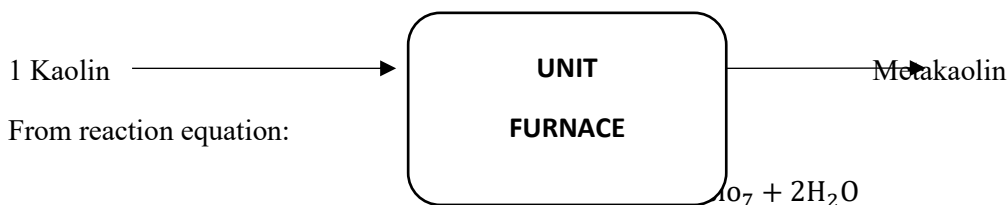
The furnace is the first unit in the design of 200kg/day zeolite odour abatement pilot plant and plays a crucial role in the overall process. Its primary purpose is to provide the necessary heat for the activation of the zeolite material.

Basis of Calculation:

Meta-kaolin basis of 0.25g/s was used to estimate the kaolin amount used as starting material, using the conversion reaction of kaolin to Meta-kaolin;

Al₂SiO₅ to Meta-kaolin Al₂SiO₇ will be obtained as in the reaction below;

UNIT: FURNACE



Metakaolin basis rate is given as; $= \frac{0.25\text{g/s}}{222.0\text{g/mol}}$

$$= 0.001126126126 \text{ mol/s}$$

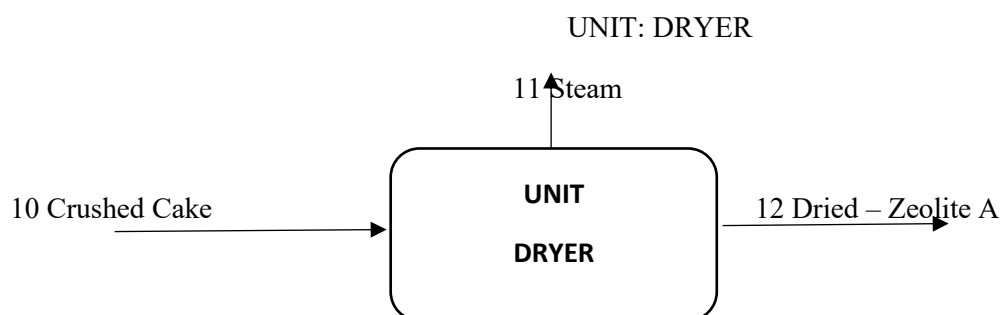
One hundred percent (100%) of conversion is assumed to have taken place in the furnace due to the use of the optimal conversion temperature of 600⁰c.



Table 2: Furnace Material Balance Summary

Component	Input Mass(mol)	Input Mass(g/s)	Output Mass (mol/s)	Output Mass (g/s)
Metakaolin	0.0000	0.0000	0.0011261261261	0.25
kaolin	0.0011261261261	0.2905405405	0.0000	0.0000
NaOH	0.0000	0.0000	0.0000	0.0000
Steam	0.00000	0.00000	0.002252252	0.04054054054
Water	0.0000	0.0000	0.0000	0.0000
Total	0.0011261261261	0.2905405405	0.003378378	0.2905405405

3.1.2 Dryer



Zeolite A (wet) is dried to the needed moisture content.

Total moisture content of zeolite A is given as =
Steam + Water

$$0.04054054054 + 0.0498(\text{g/s})$$

$$0.09034054054\text{g/s}$$

Assuming that 35% of the feed moisture is removed from cake, moisture removed will be

$$0.09034054054\text{g/s} \times \frac{35}{100}$$

$$0.031611918919\text{g/s}$$

$$\text{Final Zeolite A product moisture} = 0.09034054054\text{g/s} - 0.031611918919\text{g/s}$$

$$0.05872862162\text{g/s}$$

Table 3: Material Balance Summary for Dryer

Component	Input Mass(g/s)	Output Moisture removed Mass (g/s)	Output Dried Cake Mass (g/s)
Metakaolin	0.25	0.0000	0.25
Kaolin	0.0000	0.0000	0.0000
Steam	0.04054054054	0.031611918919	0.008928621
NaOH	1	0.0000	1
Water	0.0498	0.0000	0.0498
Total	1.3087286216	0.031611918919	1.308728621



3.2 ENERGY BALANCE

To ascertain the energy efficiency and sustainability of the pilot plant, a comprehensive energy balance analysis has been carried out. This analysis serves as a critical lens through which we assess the energy requirements associated with the entire odor abatement process, encompassing odor adsorption, regeneration, and any auxiliary processes. The results obtained from this analysis provide a strong

foundation to demonstrate the plant's capacity for high odor removal efficiency while minimizing energy input.

The chemical components' heat capacity coefficients used in the research are as outlined in Table 4.

Table 4: Heat Capacity Coefficient (J/mol)

Component	a	b	C	d
kaolin	4.871	-1.728×10^{-2}	3.748×10^{-5}	
Metakaolin	4.871	-1.728×10^{-2}	3.748×10^{-5}	
Steam	32.24	0.1923×10^{-2}	1.055×10^{-5}	-3.595×10^{-9}
NaOH	1.780	38.0633×10^{-2}	8.8647×10^{-5}	
Water	18.296	47.212×10^{-2}	-133.88×10^{-3}	

The energy balance equation is given as

$$\Delta H = n \times \int_{T_r}^{T_s} C_p(T) dt \quad (1)$$

Where ΔH = Change in enthalpy (J/mol)

T_r = Reference temperature (k)

T_s = System temperature (k)

$C_p(T)$ = Heat capacity $\left(\frac{J}{\text{mol} \cdot \text{k}}\right)$

n = Amount of substance mol/s

For equation involving the reactions,

$$\Delta H = n \times \int_{T_r}^{T_s} C_p(T) dt + h_f \quad (2)$$

C_p is expressed in terms of heat capacity coefficients, a, b, c and d as expressed in equation 3

$$C_p = a + bT + cT^2 + dT^3$$

The energy balance equation therefore becomes

$$\Delta H = n \times \int_{T_r}^{T_s} (a + bT + cT^2 + dT^3) dt$$

Furnace

For Stream1 Enthalpy H_{s1}



Specific Enthalpy calculation at 30⁰C reference temperature in kelvin is

$$T_r = 30 + 273 = 303\text{k} \text{ and } T_2 = 600^{\circ}\text{C} \text{ is equivalent to } T_2 = 600 + 273 = 873\text{k}$$

$$\begin{aligned} \Delta H_{\text{Fur}(s1)} &= n \times \int_{303}^{873} (4.871 + (-1.728 \times 10^{-2})T + 3.748 \times 10^{-5})dt \\ &= 1.593 \times 10^{-3} \times \int_{303}^{873} (4.871 + (-1.728 \times 10^{-2})T + 3.748 \times 10^{-5})dt \\ &= 7.88481\text{J/s} \end{aligned}$$

Total Enthalpy going into furnace is given as $\Delta H_{\text{in}2} = \Delta H_1$

$$\Delta H_{(s1)} = 7.88481\text{J/s}$$

7.88481
0
0
0
0
0

Total Enthalpy going into the furnace = 7.88481 J/s

For stream 2, Enthalpy, H_{s2}

$$T_1 = 302^{\circ}\text{C}, T_2 = 873\text{k}$$

Metakaolin and steam leaving the furnace the Enthalpies are calculated separately.

$\Delta H =$

$$\begin{aligned} n \times \int_{303}^{873} (a + bT + cT^2)dt \\ &= 1.593 \times 10^{-3} \times \int_{303}^{873} (a + bT + cT^2)dt \\ &= 1.593 \times 10^{-3} \times \int_{303}^{873} (4.871 + (-1.728 \times 10^{-2}T + 3.748 \times 10^{-5}T^2))dt \\ &= 7.88481\text{J/s} \end{aligned}$$

0
7.88481
0
0
0

For Steam:

$$\begin{aligned} \Delta H &= 3.186 \times 10^{-3} \\ &\times \int_{303}^{873} (32.24 + (0.1923 \times 10^{-2}T) + 1.055 \times 10^{-5}T^2 + (-3.595 \times 10^{-9}T^3))dt \end{aligned}$$

$$= 66.1056 \text{ J/s}$$

0



7.88481
66.1056
0
0

$$\begin{aligned} \text{Total Enthalpy out of Furnace} &= 7.88481 + 66.1056 \\ &= 73.990 \text{ J/s} \end{aligned}$$

$$\begin{aligned} \text{Heat load } \Delta H &= \Delta H_{\text{out}} - \Delta H_{\text{in}} \\ &= 73.990 - 7.884816 \\ &= 66.1056 \text{ J/s} \end{aligned}$$

Dryer

Enthalpy of stream 11

$$\begin{aligned} \Delta H &= 2.48 \times 10^{-3} \int_{313}^{325} (a + bT + cT^2 + dT^3) dt \\ &= 2.48 \times 10^{-3} \int_{313}^{325} (32.23 + 0.1923 \times 10^{-2}T + 1.055 \times 10^{-5}T^2 + 3.595 \times 10^{-9}T^3) dt \\ &= 1.006196 \text{ J/s} \end{aligned}$$

Stream 12

$$\Delta H_{\text{out}} = \Delta H_{\text{in10}} = -574.54 \text{ J/s} = \Delta H_{11} + \Delta H_{12}$$

Therefore, Enthalpy into Dryer = -574.54 J/s

$$\begin{aligned} \Delta H_{12} &= 7.018 \times 10^{-4} \times \int_{313}^{325} (a + bT + cT^2 + dT^3) dt \\ &= 7.018 \times 10^{-4} \int_{313}^{325} (32.23 + 0.1923 \times 10^{-2}T + 1.055 \times 10^{-5}T^2 + 3.595 \times 10^{-9}T^3) dt \\ &= 0.284737 \text{ J/s} \end{aligned}$$

0
0.0606
1.2926
56.1210
-632.0235

$$\Delta H_{12} = -574.54 \text{ J/s}$$

Total Enthalpy out of Dryer;

$$\begin{aligned} \Delta H_{\text{in10}} &= \Delta H_{11} + \Delta H_{12} \\ &= 1.006196 + (-574.54) \\ &= -573.5338 \text{ J/s} \end{aligned}$$



$$\begin{aligned}
 \text{Heat load} &= \Delta H_{\text{out}12} - \Delta H_{\text{in}11} \\
 &= -574.54 - 1.006196 \\
 &= -2071.965\text{J/s}
 \end{aligned}$$

4.0 CONCLUSIONS AND RECOMMENDATION

The design of the pilot plant, with its ability to handle a daily load of 200 kilograms of odorous compounds, represents a significant step forward in addressing odor pollution. This adaptability and scalability make it a versatile solution for a wide range of industrial applications, from wastewater treatment to waste management. The holistic approach, encompassing the entire odor abatement process, ensures not only efficient odor removal but also minimizes the release of pollutants into the environment.

The material balance analysis ensures the efficient use of zeolite feedstock, while the energy balance analysis highlights the plant's energy efficiency, emphasizing its capacity for high odor removal efficiency with minimal energy input. It also provides a promising and environmentally conscious approach to combat odor pollution, offering new avenues for clean and sustainable industrial operations.

Based on the findings and insights from this study, we make the following recommendations:

1. **Scale-Up and Implementation:** The promising results of the pilot plant design and the material and energy balance analyses suggest the need for further research and development to scale up and implement zeolite-based odor abatement technology in industrial settings. Collaboration with industry partners and environmental agencies is recommended to facilitate the practical application of this technology.
2. **Regeneration and Recycling:** Further research into the regeneration of spent zeolite and the

recycling of byproducts should be conducted. This will enhance the sustainability of the technology and reduce waste generation.

REFERENCES

1. N. F. David, T. J. Henry, J. D. H. Sprayberry, Odor-Pollution From Fungicides Disrupts Learning and Recognition of a Common Floral Scent in Bumblebees (*Bombus impatiens*). *Frontiers in Ecology and Evolution*. 10 (2022), doi:10.3389/fevo.2022.765388.
2. N. V. Syrchina, Л. В. Пилип, Т. Ya. Ashikhmina, Control of odor pollution of atmospheric air (review). *Theoretical and Applied Ecology*, 26–34 (2022).
3. F. Buttignol, D. Rentsch, I. Alxneit, A. Garbujo, P. Biasi, O. Kröcher, D. Ferri, Aging of industrial Fe-zeolite based catalysts for nitrous oxide abatement in nitric acid production plants. *Catalysis Science & Technology*. 12, 7308–7321 (2022).
4. Y. Li, J. Yu, Emerging applications of zeolites in catalysis, separation and host–guest assembly. *Nature Reviews Materials*. 6, 1156–1174 (2021).
5. Y. Wang, H. Zhang, W. Wang, Z. Wu, X. Xu, X. Kang, O. Zhan, F. Lü, P. He, Double membrane gasholder for biogas storage: Odor pollution risk and permeation characteristics. *Journal of Cleaner Production*. 352, 131644 (2022).



P111 - THEORETICAL INVESTIGATION OF THE EFFECTS OF SOLVENTS ON ELECTRONIC AND NON-LINEAR OPTICAL PROPERTIES OF SUMANENE MOLECULE BASED ON DFT

Bashir Mohammed Aliyu^{1,2*}, Rabiun Abubakar Tafida², Joshua Adeyemi Owolabi², Abdulkadir Shuaibu Gidado³

¹National Research Institute for Chemical Technology Zaria-Nigeria, ²Nigerian Defence Academy Kaduna, ³Bayero University Kano

Corresponding author email: bmaliyu59@gmail.com

ABSTRACT

Sumanene (C₂₁H₁₂) is an organic semiconductor, specifically polycyclic aromatic hydrocarbons which is said to be a bowl-shaped molecule with C_{3v} symmetry composed of alternating benzene rings. It has various applications such as organic photovoltaic cells, hydrogen storage, and field effect transistors. In this work, a theoretical study on the effects of solvent on Sumanene molecule was investigated and reported based on the Density Functional Theory (DFT) as implemented in Gaussian 09 package using B3LYP/6-311++G(d,p) basis set. Different solvents (methanol, acetone, toluene, chlorobenzene) have been introduced to investigate their effects on the electronic and nonlinear optical properties. The HOMO, LUMO, energy gap, global chemical index, and NLO properties of Sumanene molecule were obtained to determine the reactivity and stability of the molecule. The results showed that the solvents have effects on the electronic and non-linear optical properties of the molecule. The optimized bond length revealed that the molecule has strong bond in methanol and acetone, both having the smallest bond length of about 1.0853Å (C₁₀-H₁₉) than in both gas phase and the remaining solvents. The molecule in gas phase was found to be more stable with HOMO-LUMO energy gap and chemical hardness of 4.655eV and 2.3275eV, respectively. Computed results agreed with the literature. The NLO properties indicate that Sumanene molecule has highest total dipole moment (μ_{tot}) and first order hyperpolarizability (β_{tot}) of 3.4981Debye and 0.67704×10^{-30} (esu) respectively, in methanol than in gas phase and remaining solvents which are 3 and 2 times higher compared with prototype urea (1.3732 Debye and 0.3728×10^{-30} esu) molecule. These results show that careful selection of solvents and basis sets can tune the frontier molecular energy gap of the molecule and can be used for organic optoelectronic devices.

KEYWORDS

Gaussian 09, Sumanene, DFT, Solvents, Non-linear Optical Properties

1.0 INTRODUCTION

1.1. Background of the Study

Organic semiconductors have received a lot of attention because of their applications in electronic and optoelectronic devices like solar cells, sensors, organic thin-film transistors, and light-emitting diodes (OLEDs) (1). Although organic materials have many applications, carbon molecules such as Fullerenes and Carbon nanotubes (CNT) are of particular interest. While the basic organic materials discovered are known as insulators and metals, we will concentrate on novel material " π -bowls," also known as buckybowls, which are now considered to be another group of key materials in the science of non-planar π -conjugated carbon systems (2).

Organic π -conjugated molecules have been the focus of organic semiconductor development over

the last decade due to their ability to afford high operating speeds, large device densities, low cost, and large-area flexible circuits. The key step in developing a suitable candidate for an electronic system, such as an organic field-effect transistor (OFET), is the design of a molecule with optimal charge carrier ability (3, 4). A bucky bowl is a bowl-shaped molecule in which a portion of a fullerene or the top portion of a carbon nanotube (CNT) is cut off. It can be used to apply the asperity interaction of fullerene (5). Since the discovery of C₆₀ fullerene in 1985, buckybowls have attracted much attention due to their physical properties, not only as model compounds for fullerenes but also as unique bowl-shaped aromatic compounds (5).

Corannulene and sumanene are two types of buckybowls studied. A corannulene molecule is a fragment of a fullerene that has been cut to leave a five-membered benzene ring, known as the first



buckybowl to exist. The sumanene molecule is the second buckybowl and has a structure in which a fullerene is cut to leave a six-membered ring (6).

Sumanene ($C_{21}H_{12}$) is a bowl-shaped (hexagonal), π -conjugated molecule with C_{3v} symmetry, composed of alternating benzene rings and cyclopentadiene rings centered on a benzene ring (7). In comparison to corannulene, $C_{20}H_{10}$, Sumanene has three benzylic positions that allow further functionalization and deepen the molecular bowl (1.11 Å), whereas corannulene has only one (0.87 Å) (8). Sumanene has been discovered to be quite useful in the production of novel building blocks for molecular switches, chemical machines, molecular motors, ferroelectric memories, molecular devices, and sensory materials due to its bowl-to-bowl inversion. Surprisingly, electronic switching, thermal transport, and thermoelectric properties all exist (7). As of 2018, Della and Suresh discovered that Bucky bowls are bowl-shaped fullerene fragments that have many applications in synthetic organic chemistry and

electronic device fabrication. According to their studies, sumanene has comparable adsorption efficiency to graphene layers, carbon nanotubes, and C_{60} fullerene for molecules such as CO, CO_2 , NH_3 , CH_4 , and C_2H_2 (5, 9). The improved optical and electronic properties of these diverse sumanene derivatives make them promising candidates for the production of electronics and optical materials. Priya Kumar and Sastry reported an ab initio and pure and hybrid density functional theoretical study before the synthesis of sumanene (10). They have explained the structure, inversion barrier, suitability of various theoretical procedures, vibrational spectra, population and charge analyses, and strain energy calculation using isodesmic equations.

As a result, at the moment, density functional theory (DFT) is the only viable option for accounting for the effects of dynamic electron correlation. Thus, the use of density functional methods for electronic structure calculations has reached a new high in recent years.

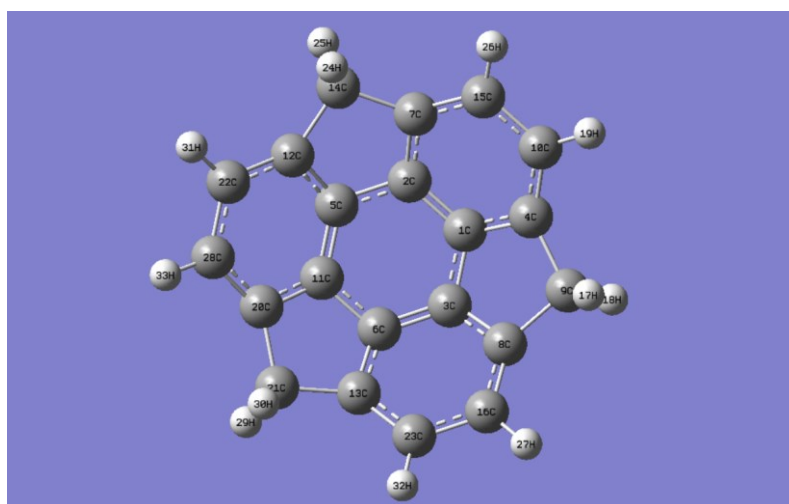


Figure 1: Optimized Sumanene Structure

1.2. Theoretical Background

1.2.1. Density Functional Theory (DFT)

Density Functional Theory (DFT) is a computational method and quantum mechanical technique used to investigate the structural and electronic properties of many body systems in physics and chemistry (11). DFT has proven to be extremely effective in describing structural and electronic properties in a wide range of materials, including atoms, molecules, clusters, and bulk materials, as well as simple crystals and complex extended system. Due to its high computational

efficiency and excellent accuracy for the structure of molecules, crystals, surfaces, and their interactions, the DFT method has become the most widely used ab-initio method in Computational Material Science (CMS) and Solid-state Physics (12). The energy of the molecule in the DFT method is a function of the electron density. However, DFT is one of the most widely used and versatile methods in condensed matter physics, computational physics, and computational chemistry (13). The ground state energy in DFT can be calculated using the density relation given (14)



$$\rho(r) = \sum_{i=1}^n |\psi_i(r)|^2 \quad (1)$$

This relationship is used to calculate the ground state energy of the molecules.

1.2.2. Molecular Orbitals

Molecular orbitals and their properties such as energy are used to explain various types of reactions and to predict the most reactive position in conjugated systems. The energies of the Highest Occupied Molecular Orbital (HOMO) and the Lowest Unoccupied Molecular Orbital (LUMO) are

Furthermore, according to Koopmans' theorem, the energy gap, E_{gap} , is defined as the difference between HOMO and LUMO energy and is given by

$$E_{gap} = (E_{LUMO} - E_{HOMO}) \approx IP - EA \quad (2)$$

Where $IP = -E_{HOMO}$ is the ionization potential and $EA = -E_{LUMO}$ is the electron affinity of the molecule.

1.2.3. Global Quantities

Global reactivity descriptors such as chemical potential, chemical hardness-softness, electronegativity and electrophilicity index are useful quantities in predicting and understanding global chemical reactivity trends. The Chemical hardness is given by half of the energy band gap (15)

$$\eta = \frac{IP - EA}{2} \quad (3)$$

The softness of a molecule can be obtained by taking the inverse of its chemical hardness

$$S = \frac{1}{\eta} \quad (4)$$

The chemical potential is given by;

$$\mu = -\left(\frac{IP + EA}{2}\right) \quad (5)$$

The electronegativity is given by;

$$\chi = \frac{IP + EA}{2} \quad (6)$$

The mean first hyperpolarizability is defined as ();

$$\beta_{tot} = (\beta_x^2 + \beta_y^2 + \beta_z^2)^{1/2} \quad (10)$$

where β_x , β_y and β_z are defined as (17);

the most important orbitals in a molecule. HOMO can be through the outermost orbital containing electrons and tends to give these electrons such as an electron donor. LUMO, on the other hand, can accept electrons through the innermost orbital with free places. The HOMO energy is proportional to the ionization potential, whereas the LUMO energy is proportional to the electron affinity. The energy difference between the HOMO and LUMO orbitals is known as the energy gap, and it is an important parameter that determines structural stability. The energy gap is also used to calculate molecular electrical transport properties (13)

The electrophilic index is expressed as (15);

$$\omega = \frac{\mu^2}{2\eta} \quad (7)$$

1.2.4. Non-Linear Optical Properties (NLO)

The nonlinear optical properties of an isolated molecule in an electric field are described by the electric dipole moment (μ), polarizabilities (α), first (β) and second (γ) order hyperpolarizability (16).

The dipole moment is defined as

$$\mu_{tot} = [\mu_x^2 + \mu_y^2 + \mu_z^2]^{1/2} \quad (8)$$

Polarizability is the measure of a molecule's distortion in an electric field. The following equation is used to calculate polarizability (α) (17)

$$\alpha = \frac{1}{3}(\alpha_{xx} + \alpha_{yy} + \alpha_{zz}) \quad (9)$$

The quantities α_{xx} , α_{yy} and α_{zz} are known as principal values of the polarizability tensor. It measures the strength of molecular interactions (e.g., dispersion forces, long-range intermolecular induction).

The first-order hyperpolarizability is also a tensor that can be represented by $3 \times 3 \times 3$ matrices. The 27 components of the 3-D matrix can be reduced to 10 due to the Kleinman symmetry. The following is the complete equation for calculating the total static first-order hyperpolarizability magnitude of Gaussian output (13).

$$\beta_x = \beta_{xxx} + \beta_{xyy} + \beta_{xzz}$$

$$\beta_y = \beta_{yyy} + \beta_{xxy} + \beta_{yzz}$$

$$\beta_z = \beta_{zzz} + \beta_{xxz} + \beta_{yyz} \quad (11)$$



The β_x , β_y and β_z refer to the components of hyperpolarizability along x , y and z components of molecular dipole moment.

$$\beta_{tot} = ((\beta_{xxx} + \beta_{xyy} + \beta_{xzz})^2 + (\beta_{yyy} + \beta_{xxy} + \beta_{yzz})^2 + (\beta_{zzz} + \beta_{xxz} + \beta_{yyz})^2)^{1/2} \quad (12)$$

The second-order hyperpolarizability is given by (17);

$$\gamma_{tot} = \frac{1}{5} (\gamma_{xxxx} + \gamma_{yyyy} + \gamma_{zzzz} + 2(\gamma_{xxyy} + \gamma_{xxzz} + \gamma_{yyzz})) \quad (13)$$

2.0 COMPUTATIONAL METHODS

Geometrical structure of TTF was optimized with no symmetry constraint using Becke's three parameter hybrid exchange combined with LeeYang-Parr's gradient-corrected correlation (18) functional (B3LYP) method with 6-31++G (d, p) basis set. All the parameters were fully allowed to relax and each of the calculations converged to an optimized geometry which corresponds to a true energy minimum.

For the study of solvation effects, a Self-Consistent Reaction Field (SCRF) approach based on Polarizable Continuum Model (PCM) was employed. The effects of four solvents (toluene, acetone, acetonitrile and dichloromethane) were investigated by means of the SCRF method based on PCM as implemented in the Gaussian 09(19, 20). The optimized geometries were then used to obtain the HOMO-LUMO energy gap, chemical hardness, chemical softness, chemical potential, electronegativity, electrophilicity index, dipole

moment, polarizability, anisotropic polarizability, hyperpolarizability, entropy and the specific heat capacity of the investigated molecule at the same level of theory (B3LYP/6-31++G(d,p). All calculations were performed within the framework of Density Functional Theory (DFT) as coded in Gaussian 09 package (20)

3.0 RESULTS AND DISCUSSION

3.1. Optimized Parameter

The outcomes of these calculations are detailed in Tables 1 and 2. The term "bond length" refers to the separation between the nuclei of bonded atoms, while "bond angle" indicates the angle formed by two neighbouring bonds connected to an atom within the molecule (17). They are expressed in Armstrong and degrees respectively.

From Table 1, slight variations are observed in the bond lengths of Sumanene when subjected to optimization using methanol, acetone, toluene, and chlorobenzene, as compared to the gas phase. The findings indicate that the most minimized value, at 1.0853Å, was achieved in methanol and acetone. However, upon comparing these findings with the outcomes from a previous study involving a regular Sumanene molecule conducted by (21), it becomes evident that the bond lengths in the current study exhibit a slightly similar tendency. It is worth noting that, the smaller the bond length, the higher the bond energy and stronger the bond (16).

From Table 2, There is a slight decrease in the bond angles of the studied molecule in solvents in comparison with the gas phase. Based on this finding, the results attained in methanol is slightly less than those obtained in the gas phase and other solvents.

Table 1: Selected Bond Lengths of the optimized structure of Sumanene in the gas phase and in different solvents using B3LYP/6-311++G(d,p) basic set

Tag	Bond length	Gas phase	Methanol	Acetone	Toluene	Chlorobenzene
1	C ₁ -C ₂	1.3852	1.3858	1.3858	1.3856	1.3856
2	C ₁ -C ₃	1.4324	1.4332	1.4332	1.4326	1.433
3	C ₈ -C ₉	1.5523	1.5519	1.552	1.5523	1.552
4	C ₁₀ -H ₁₉	1.0855	1.0853	1.0853	1.0854	1.0854
5	C ₂₈ -H ₃₃	1.0855	1.0853	1.0853	1.0854	1.0854

Table 2: Selected Bond angles of the optimized structure of Sumanene in the gas phase and in different solvents using B3LYP/6-311++G(d,p) basic set

Tag	Bond length	Gas phase	Methanol	Acetone	Toluene	Chlorobenzene
-----	-------------	-----------	----------	---------	---------	---------------



1	C ₂ -C ₁ -C ₃	119.995	120.0024	119.9977	119.9954	119.999
2	C ₄ -C ₉ -C ₈	102.6375	102.5937	102.6003	102.6018	102.6019
3	H ₂₄ -C ₁₄ -H ₂₅	107.0954	106.9298	106.95	107.045	106.9764
4	C ₂₁ -C ₂₀ -C ₂₈	134.4573	134.3994	134.4485	134.4148	134.4273
5	C ₂₂ -C ₂₈ -H ₃₃	117.5204	117.5196	117.515	117.5176	117.5131

3.2. Frontier Molecular Orbital Energies (FMOEs)

Table 3 presents the Highest Occupied Molecular Orbital (HOMO) and Lowest Unoccupied Molecular Orbital (LUMO), along with the Energy Gap (E_{gap}), all measured in electron volts (eV) for the studied molecule. These results were obtained in both the gas phase and in some solvents, and computed using DFT/B3LYP approach with the 6-311++G(d, p) basis set. The computed HOMO, LUMO, and HOMO-LUMO energy gap values signifies the chemical activity of the molecule (12). The higher HOMO-LUMO energy gap, the more stable the compound will be (13). Taking solvation effects into account brings about changes in the energies of molecular orbitals as shown in Table 3. In a solution, the values differ from those in a gaseous state as a result of polarization effects.

In this work, the order of stability of the molecule is more in the gas phase > toluene > chlorobenzene > methanol > acetone for both basis sets. The result shows that Sumanene has higher band gap energy in gas phase (4.655eV) than in the remaining solvents. It can be observed that it is more difficult to remove an electron from gas phase < toluene < chlorobenzene < acetone < methanol. Similarly, it is more difficult to add an electron in terms of their EAs to the molecule in the gas phase > toluene > chlorobenzene > acetone > methanol.

Table 3: Calculated HOMO, LUMO, IP, EA, and Energy gap in (eV) of the Optimized Structure of Sumanene in gas phase and different solvents using B3LYP basis set

Solvents	HOMO (eV)	LUMO (eV)	IP (eV)	EA (eV)	Egap (eV)
Gas Phase	-5.8325	-1.1774	5.8325	1.1774	4.655
Methanol	-5.9511	-1.3031	5.9511	1.3031	4.648
Acetone	-5.9438	-1.2968	5.9438	1.2968	4.647
Toluene	-5.8703	-1.2193	5.8703	1.2193	4.651
Chlorobenzene	-5.9122	-1.262	5.9122	1.262	4.650

3.3. The Global Chemical Indices

The global chemical indices such as chemical hardness (η), softness (f), chemical potential (μ), electronegativity (χ) and electrophilicity index (ω) of the molecule in the gas phase and in different solvents were reported in Table 4 using the frontier molecular orbital energy. Chemical hardness is linked to the stability and reactivity of a chemical system. According to the frontier molecular orbital approach, chemical hardness is proportional to the energy gap. From Table 4, Sumanene molecule in the gas phase with slightly higher value of chemical hardness of 2.3275eV for both basis sets are considered to be harder and more stable than in the

different solvents. Hence, Sumanene in the gas phase is more stable. Electronegativity and chemical potential are important parameters in quantum chemical reactions. Sumanene in methanol exhibits higher electronegativity than other solvents and maximum chemical potential in gas phase. The electrophilicity index value was used to determine the chemical reactivity of molecules. A higher reactive nucleophile has a lower value of ω (2.6391). Sumanene in gas phase is considered to be a more reactive nucleophile, so it is considered to be a good nucleophile. However, sumanene in methanol is a good electrophile, having the highest (ω) value (2.8304eV).

Table 4: Global chemical indices for Perylene in the gas phase and in different solvents.

Solvents	η (eV)	f (eV)	χ (eV)	μ (eV)	ω (eV)
Gas Phase	2.3275	0.4296	3.505	-3.505	2.6391



Methanol	2.324	0.4303	3.6271	-3.627	2.8304
Acetone	2.3235	0.4304	3.6203	-3.620	2.8204
Toluene	2.3255	0.4300	3.5448	-3.545	2.7017
Chlorobenzene	2.325	0.4301	3.5871	-3.587	2.7672

3.4. Non-Linear Optical Properties

Table 5 shows the non-linear optical properties of Sumanene in the gas phase and in some solvents calculated at the DFT/B3LYP level in the 6-31+G(d) and 6-311++G(d,p) basis sets. It can be observed that there is an increase in values of total

dipole moment (μ_{tot}), first-order hyperpolarizability (β_{tot}), and second-order hyperpolarizability (γ_{tot}), while the mean polarizability $\langle\alpha\rangle$ decreases due to the effects of the solvents. From the results obtained, methanol has the highest value of dipole moment with a value of 3.4981 Debye.

Table 5: Non-linear Optical Properties (in electrostatic unit, esu) and Dipole Moment in (Debye) of the optimized structure of Sumanene in the gas phase and in different solvents using B3LYP basis set.

Solvents	μ_{tot} (Debye)	$\langle\alpha\rangle \times (-10^{-23})$ (esu)	$\beta_{\text{tot}} \times 10^{-30}$ (esu)	$\gamma_{\text{tot}} \times (-10^{-36})$ (esu)
Gas Phase	2.5114	1.7134	0.53656	1.0408
Methanol	3.4981	1.6855	0.67704	1.0229
Acetone	3.4848	1.6866	0.67082	1.0237
Toluene	2.8938	1.7020	0.59044	1.0336
Chlorobenzene	3.2190	1.6932	0.63518	1.0278

However, from the result, Sumanene molecule in methanol has slightly higher value of first-order hyperpolarizability (0.67704×10^{-30} esu). This shows that, there is an increase in the value of the first-order hyperpolarizability in the order of gas-phase < toluene < chlorobenzene < acetone < methanol. Therefore, the result indicates that the first order hyperpolarizability of Sumanene increases with increase in the polarity of the solvents. The results for μ and β obtained as compared with that of prototype urea (1.3732 Debye and 0.3728×10^{-30} esu) molecule (22) is approximately 3 and 2 times higher respectively.

4.0 CONCLUSIONS AND RECOMMENDATION

In this study, we investigated the optimised parameters, electronic properties, thermodynamic parameters, and non-linear optical properties of sumanene in solvents and in gas phases using B3LYP methods under 6-311++G(d,p) basis set. Global descriptors were used to investigate the reactivity of the molecule in different solvents. The obtained descriptors could also provide more information and may contribute to a better understanding of the electronic structure of this compound. The HOMO–LUMO energy gap of

4.655eV shows that the titled compound is more stable in the gas phase than in the remaining solvents. The energy gap was compared with that reported in the literature (4.759eV). We calculated and reported the ionization potential, electron affinity, chemical potential, electronegativity, hardness, softness, and electrophilicity of the studied molecule. The high stability and low reactivity of the molecule in chemical reactions indicate its good electrophile. Therefore, it can be used for solar cell applications.

We recommend further study of the ionic and charge distribution properties of this molecule to give a deeper insight into its relevance in organic semiconductor applications. Finally, we believe that the systematic use of this theoretical approach can be employed to predict the optoelectronic properties of other organic materials and to design novel materials for organic solar cells.

REFERENCES

1. O. Ostroverkhova, Organic Optoelectronic Materials: Mechanisms and



- Applications. *Chem. Rev.* **116**, 13279–13412 (2016).
- S. Higashibayashi, H. Sakurai, Synthesis of Sumanene and Related Buckybowls. *Chem. Lett.* **40**, 122–128 (2011).
 - X. Zou, S. Cui, J. Li, X. Wei, M. Zheng, Diketopyrrolopyrrole Based Organic Semiconductor Materials for Field-Effect Transistors. *Front. Chem.* **9**, 671294 (2021).
 - J. Yang, Z. Zhao, S. Wang, Y. Guo, Y. Liu, Insight into High-Performance Conjugated Polymers for Organic Field-Effect Transistors. *Chem* **4**, 2748–2785 (2018).
 - K. Kanagaraj, K. Lin, W. Wu, G. Gao, Z. Zhong, D. Su, C. Yang, Chiral Buckybowl Molecules. *Symmetry* **9**, 174 (2017).
 - A. Muraoka, M. Hayashi, Electronic structure of sumanene-type Buckycatcher by DFT calculations. *Chemical Physics Letters* **748**, 137393 (2020).
 - T. Amaya, T. Hirao, Chemistry of Sumanene. *The Chemical Record* **15**, 310–321 (2015).
 - S. Mebs, M. Weber, P. Luger, B. M. Schmidt, H. Sakurai, S. Higashibayashi, S. Onogi, D. Lentz, Experimental electron density of sumanene, a bowl-shaped fullerene fragment; comparison with the related corannulene hydrocarbon. *Org. Biomol. Chem.* **10**, 2218 (2012).
 - B. M. Schmidt, D. Lentz, Syntheses and Properties of Buckybowls Bearing Electron-withdrawing Groups. *Chem. Lett.* **43**, 171–177 (2014).
 - U. D. Priyakumar, G. N. Sastry, First ab Initio and Density Functional Study on the Structure, Bowl-to-Bowl Inversion Barrier, and Vibrational Spectra of the Elusive C_{3v} -Symmetric Buckybowl: Sumanene, $C_{21}H_{12}$. *J. Phys. Chem. A* **105**, 4488–4494 (2001).
 - Density functional theory, *Wikipedia* (2023). https://en.wikipedia.org/w/index.php?title=Density_functional_theory&oldid=1174426409.
 - A. B. Suleiman, A. Maigari, A. S. Gidado, C. E. Ndikilar, Density Functional Theory Study of the Structural, Electronic, Non-Linear Optical and Thermodynamic Properties of Poly (3-Hexylthiophene-2, 5 - Diyl) in Gas Phase and in Some Solvents. *PSIJ*, 34–51 (2022).
 - A. S. Gidado, L. S. Taura, A. Musa, SOLVENT EFFECTS ON THE ELECTRONIC STRUCTURE AND NON-LINEAR OPTICAL PROPERTIES OF PYRENE AND SOME OF ITS DERIVATIVES BASED ON DENSITY FUNCTIONAL THEORY. *FJS* **4**, 236–251 (2021).
 - V. P. Gupta, “Density Functional Theory (DFT) and Time Dependent DFT (TDDFT)” in *Principles and Applications of Quantum Chemistry* (Elsevier, 2016; <https://linkinghub.elsevier.com/retrieve/pii/B9780128034781000054>), pp. 155–194.
 - K. Chandrakumar, S. Pal, The Concept of Density Functional Theory Based Descriptors and its Relation with the Reactivity of Molecular Systems: A Semi-Quantitative Study. *IJMS* **3**, 324–337 (2002).
 - N. M. Sulaiman, L. S. Taura, A. Lawal, A. S. Gidado, A. Musa, Solvent Effects on the Structural, Electronic, Non-Linear Optical and Thermodynamic Properties of Perylene Based on Density Functional Theory.
 - R. N. Muhammad, N. M. Mahraz, A. S. Gidado, A. Musa, Theoretical Study of



Solvent Effects on the Electronic and Thermodynamic Properties of Tetrathiafulvalene (TTF) Molecule Based on DFT. *AJR2P*, 42–54 (2021).

18. A. D. Becke, Density-functional thermochemistry. III. The role of exact exchange. *The Journal of Chemical Physics* **98**, 5648–5652 (1993).

19. Frisch A., Nielson A. B., *Gauss View User-Manual* (Gaussian Inc., Pittsburg, PA, 2000).

20. Frisch, M. J., Trucks, G. W., Schlegel, H. B., et al., *Gaussian 09, Revision A11.4* (Gaussian Inc., Pittsburg, PA, 2009).

21. S. Armaković, S. J. Armaković, J. P. Šetrajčić, S. K. Jaćimovski, V. Holodkov, Sumanene and its adsorption properties towards CO, CO₂ and NH₃ molecules. *J Mol Model* **20**, 2170 (2014).

22. H. Abbas, Mohd. Shkir, S. AlFaify, Density functional study of spectroscopy, electronic structure, linear and nonlinear optical properties of l-proline lithium chloride and l-proline lithium bromide monohydrate: For laser applications. *Arabian Journal of Chemistry* **12**, 2336–2346 (2019).



P112 - SYNTHESIS OF AZO DYE AND ITS IRON COMPLEX DERIVED FROM 3-AMINOPHENOL

M. L. Batari¹, B. Myek², I. Abdulwalyu¹, S.O. Arekemase³, V. Ochigbo⁴, O. B Adeshina⁴, O.H Olabimtan⁴, A. Bakare⁵, F. O Aliyu⁶

¹Department of Scientific and Industrial Research, National Research Institute for Chemical Technology, Zaria, Nigeria

²Department of Pure and Applied Chemistry, Kaduna State University, Kaduna, Nigeria

³Petrochemical and allied department, National Research Institute for Chemical Technology, Zaria, Nigeria

⁴Department of Industrial and Environmental Pollution, National Research Institute for Chemical Technology, Zaria, Nigeria

⁵Department of Chemistry, Ahmadu Bello University Zaria, Kaduna State, Nigeria

⁶Department of Biochemistry, Ahmadu Bello University Zaria, Kaduna State, Nigeria

*Corresponding author E-mail: musalatayo@gmail.com

ABSTRACT

An azo dye derived from 3-aminophenol and its iron complex have been synthesized and characterized using IR spectroscopy and UV-Visible absorption spectroscopy. The ligand exhibits an absorption maximum at 445.50nm. Upon binding with the Fe, forming the complex, the maximum absorption band was shifted to 359.50nm suggesting an interaction of the Fe with the ligand. The IR spectra showed the values of —N=N— stretching frequency at 1460 cm^{-1} for azo dye while in the complex the value increased to 1558 cm^{-1} indicates its involvement in co-ordination to the metal. The percentage yield of the azo dye calculated was found to be 85% while that of the iron complex is 58%. The decreased in yield for iron complex may be attributed to some interferences during the course of the experiment.

Key words: Complex, 3-aminophenol, Ligand, Azo Dye, Diazotization

1.0 INTRODUCTION

Azo dyes constitute by far the most important chemical class of commercial organic colorant. They account for around 60—70% of the dyes used in traditional textile applications and they occupy a similarly prominent position in the range of classical organic pigments. Azo colorants, as the name implies, contain as their common structural feature the azo (—N=N—) linkage which is attached at either side to two sp^2 carbon atoms. Usually, although not exclusively, the azo group links two aromatic ring systems. The majority of the commercially important azo colorants contain a single azo group and are therefore referred to as monoazo dyes, but there are many which contain two (disazo), three (trisazo) or more such groups. In

terms of their colour properties, azo colorants are capable of providing virtually a complete range of hues. There is no doubt though that they are significantly more important commercially in yellow, orange and red colors (i.e. absorbing at shorter wavelengths) than in blues and greens [1].

Azo compounds are continuously receiving attention in scientific research [2, 3]. The dyes are widely used in the textile industry and are the largest and most versatile group of synthetic organic dyes, with a tremendous number of industrial applications [4]. They are used in many industries like textile, leather, plastics, paper, food, cosmetics as a coloring agent and in optical recording medium [5].

Metal complex dyes plays a significant role in the textile industry. Cr (III) and Co(III) complexes are used most frequently for the dyeing of wool and synthetic polyamides. Metal complex dyes are applied to the wool either in the pre-metallized form or a complex is prepared "*in situ*" in the fiber by the treatment of dyed wool with chromate or dichromate (Cr (VI)) salts [6]. Metal complex dye is used in textile, lips, eye shadow, inks, leather finishing and coloring for metals and plastics.

Traditionally used cobalt and chromium complex dyes have very good wet fastness and also light fastness. It is known that some iron (Fe (II) and Fe (III)) complex dyes have comparable fastness properties. Since iron salts are not considered toxic, they present little or no pollution challenge for the users [7].

Aim

The aim of this work is to prepare new azo dye and its iron complex by coupling diazotized 3-aminophenol with saccharine.



2.0 Experimental

2.1 Reagents

3-aminophenol, sodium nitrite (NaNO_2), Concentrated Tetraoxosulphate(VI) acid (H_2SO_4), saccharine, sodium hydroxide (NaOH) were obtained from National Research Institute for Chemical Technology (NARICT) Bassawa, Zaria Kaduna State, Nigeria. The chemicals were used without further purification.

2.2 Procedure for synthesis of an azo dye

2.88g of 3-aminophenol was weighed and dissolved in a conical flask (A) containing 30cm^3 of distilled water. Thereafter 3cm^3 of concentrated HCl was added slowly with constant stirring until complete dissolution. The solution was cooled in an ice bath until its temperature was below 5°C . 3.5g of saccharine was weighed and dissolved in 20cm^3 of distilled water in a conical flask (B). The solution was stirred until it dissolved; the solution was then cooled in an iced bath to a temperature below 5°C . 0.40g was weighed and transferred into a test tube (C) and 5cm^3 of distilled water was added and stirred. The solution of sodium nitrite in test tube (C) was transferred into 3-aminophenol solution in beaker (A) above. 10g of crushed ice was weighed in a 100cm^3 beaker (D) and 3cm^3 of Conc. HCl was added. The solution of 3-aminophenol with sodium nitrite in flask (A) was transferred into beaker D and stirred to form the diazonium salt. Flask (B) and its content was transferred into beaker (D) and stirred. The solution was then kept for 24 hours before it was filtered, washed with distilled water and dried.

2.3 Procedure for synthesis of metal complex dye

Method of Ali [4] was adopted with slight modification as follows: 0.25g of unmetallized azo dye was weighed and transferred into a beaker and 50cm^3 of methanol was added to it. 0.45g of FeCl_3 was dissolved in 70cm^3 of methanol in a beaker. The two solutions were mixed together and the pH

was adjusted to 8 using NaOH (0.1M). The solution was stirred and then heated on a hot plate at 70°C for 30 mins. The mixture was kept for 24hrs before it was filtered and then washed with methanol and dried.

2.4 Instruments

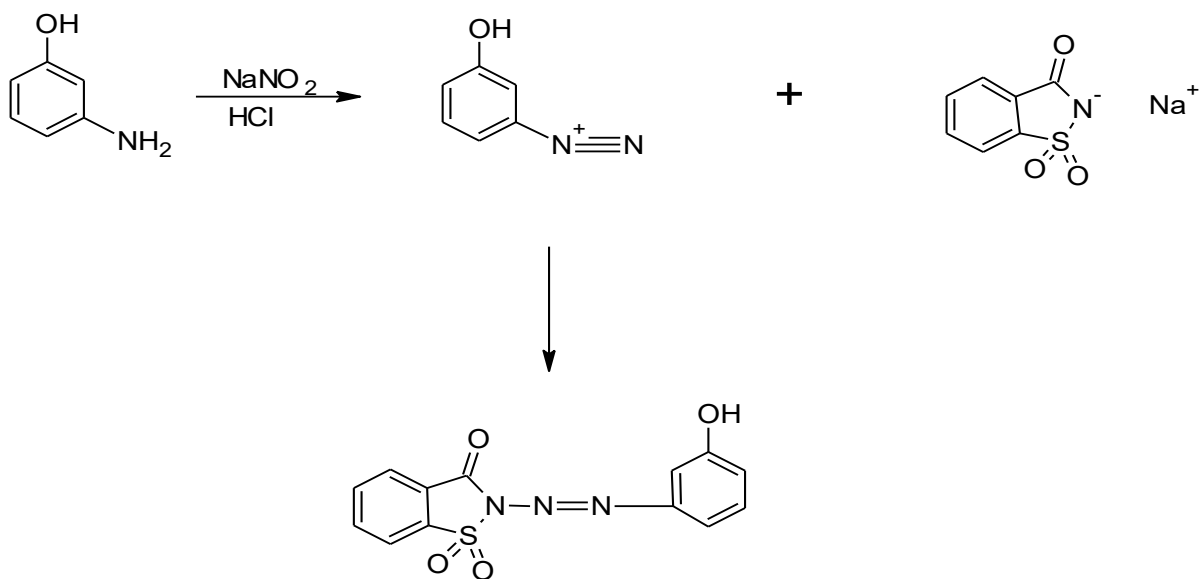
Shimadzu FTIR-8400S and UV-Vis 2550 Shimadzu spectrophotometer

3.0 Results and discussion

An azo dye was synthesized by coupling diazotized 3-aminophenol with saccharine. Its metal complex was formed by reacting the dye which serves as a ligand with iron (III) chloride. The infrared spectra of the azo dye and its iron complex were obtained using Shimadzu FTIR-8400S. The appearance of the azo band at ($1450\text{-}1600\text{ cm}^{-1}$) confirmed that the synthesized dye and its iron complex contained azo group [4]. Figure 1 and 2 are the FTIR results for azo dye and its metal complex. The IR spectra showed the values of -N=N- stretching frequency at 1460 cm^{-1} for azo dye while in the complex the value increased to 1558 cm^{-1} indicates its involvement in coordination to the metal. The carbonyl group C=O stretching frequency in azo dye is 1721 cm^{-1} while in its iron complex the value is 1649 cm^{-1} , indicating its participation in the coordination. Change in the position of O-H stretching shows that it involved in coordination between the dye and its complex [4]. The ligand (azo dye) exhibits an absorption maximum in methanol solution of 445.50 nm , upon binding with the Fe(III) , forming complex, the maximum absorption band was shifted to 359.50 nm , suggesting an interaction of the Fe(III) with the ligand. These results are in agreement with those reported in the literature [8 - 11] which indicates that the band shift is caused by the binding of the metal ion. The percentage yield of the azo dye calculated was found to be 83% while that of the iron complex is 58%. The decreased in yield for iron complex may be due to some interferences during the course of the experiment.

Scheme 1: Reaction scheme showing the synthesis of an azo dye





2-[(3-hydroxyphenyl)diazenyl]-1,2-benzothiazol-3(2H)-one 1,1-dioxide

Scheme 2: Proposed Complex dye

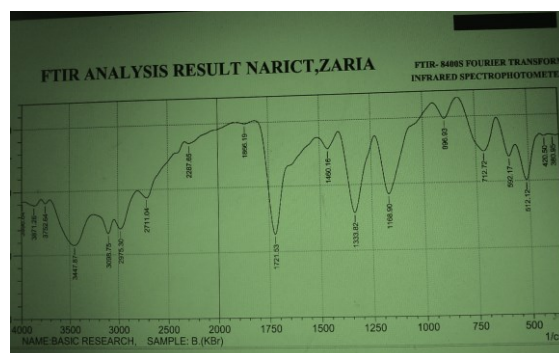
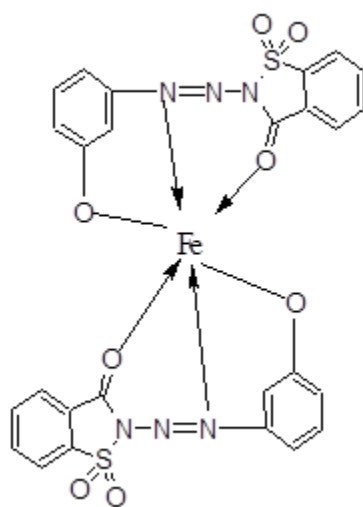
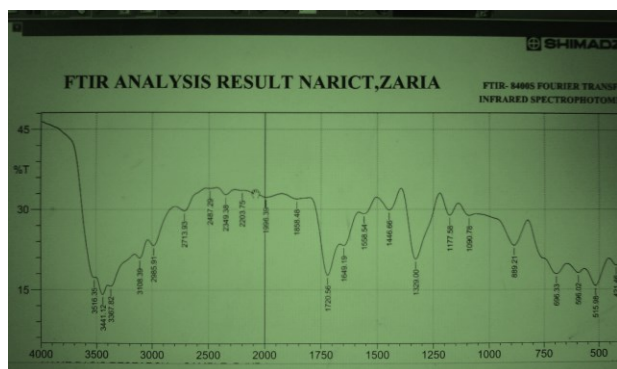


Figure 1: Infrared spectrum for azo dye



Conclusion

We were able to synthesize an azo dye by coupling diazotized 3-aminophenol with saccharine. Its iron complex was also produced and characterized using UV and FTIR. The proposed structure of the dye and its metal complex were established based on the results of FTIR analysis.

Acknowledgements

The authors wish to appreciate the National Research Institute for Chemical Technology for providing the facilities for this research.

References

- [1] R. M. Christie. Colour Chemistry. Heriot-Watt University, Scottish Borders Campus, Galashiels, UK. Published by the Royal Society of Chemistry, Thomas Graham House, Science Park, Milton Road, Cambridge CB4 0WF, UK, **2011**, 45.
- [2] Kirkan, B. and Gup, R. Synthesis of New Azo Dyes and Copper (II) Complexes Derived from Barbituric Acid and 4-Aminobenzoylhydrazone. *Turk. J. Chem.* **2008**, 32: 9-17
- [3] Seferoglu, Z. A study on tautomeric equilibria of new hetarylazo-6-aminouracils. *ARKIVOC*, **2009**, 42 -57
- [4] Ali A. I., Abdul Z. Synthesis, characterization and spectroscopic properties

Figure 2: Infrared spectrum for complex dye

of new azo-dyes and azo-metal complexes derived from 8-hydroxyquinoline. *Basrah Journal of Science*, **2011**, 28(1): 15-36.

[5] Otutu J. O. Synthesis and application of azo dyes derived from 2-amino-1,3,4-Thiadiazole-2-Thiol on polyester Fibre. *IJRRAS*, **2013**, 15(2): 292-296.

[6] Zollinger, H. Color Chemistry. Syntheses, Properties, Application of Organic Dyes and Pigments. Third revised edition. Wiley-VCH, **2003**.

[7] Reife A, Weber, E and Freeman, H.S. Chentech October 1997: *J. Am. Chem. Soc.*, 1997, 17.

[8] Escandar, G. M.; Sala, L. F. Complexing Behavior of Rutin and Quercetin *Can. J. Chem.*, **1991**, 69: 1994-2001.

[9] Yogeewaran, G.; Viswanathan, P.; Sriram, V. Sensitive spectrophotometric assay for 3-hydroxysubstituted flavonoids, based on their binding with molybdenum, antimony, or bismuth. *J. Agr. Food Chem.* **2000**, 48: 2802-2806.

[10] Budzisz, E.; Keppler, K.; Giester, G.; Wozniczka, M.; Kufelnicki, A.; Nawrot, B. Synthesis, crystal structure and biological characterization of a novel palladium(II)



complex with a coumarin-derived ligand. *Eur. J. Inorg. Chem.*, 2004, 22, 4412-4419

[11] De Giovani, W. F.; De Souza, R. F. V.
Synthesis, spectral and electrochemical

properties of Al(III) and Zn(II) complexes
with flavonoids. *Spectrochim. Acta Part A*,
2005, 61: 1985-1990.



P113 - ISOLATION AND CHARACTERIZATION OF *ASPERGILLUS NIGER* AND *SACCHAROMYCES CEREVISIAE* FOR BIOETHANOL

Abubakar A*, Arekemase S.O., Adegbola Olubukola, Uduakobong Ime Idio, Ozogu Agbe N., Nwakuba D. C., Zaharaddeen sani Gano Jeffrey Tsware Barminas.

National research institute for chemical technology, Basawa zaria.

Corresponding author: daddysadi@gmail.com

ABSTRACT

The supply and demand of energy determine the course of global development in every sphere of human activity. Conversion and utilization of biomass to energy source have become means of mitigating the current global energy crisis. Brewers' spent grain used was pre-treated with 0.5 M alkaline and washed severally till a neutral pH was obtained. The alkaline treated sample was dried and the functional properties were determined using FTIR-8400S, which reveals the ester bonds existing in the cellulose chain. This work is aimed at isolation and characterisation of *Aspergillus niger* and *Saccharomyces cerevisiae* for the production of bioethanol from brewery spent grain. The *Aspergillus niger* isolated have a wide zone of cellulose hydrolysis of 1.56cm while The Isolated *Saccharomyces cerevisiae* strains were screen for ethanol production based on thermo-tolerance, ethanol tolerance, osmo-tolerance, assimilation of various carbon compound, and growth in 5% yeast extract. The isolated *Aspergillus niger* showed a good potential for cellulose hydrolysis while *Saccharomyces cerevisiae* was able to ferment sugars.

KEYWORDS

Brewers' spent grain, *saccharomyces cerevisiae*, *Aspergillus Niger*, Isolation, biomass.

1.0 INTRODUCTION

The world energy demand is expected to grow at an average annual rate of 1.2% by 2035 (1). This increase in energy demand is expected to gradually contribute in the depletion of world oil resources such as fossil fuel, solar, wind, thermal, hydroelectric, and biomass (2). One of the largest renewable and sustainable energy source worldwide with considerable potential that can mitigate the current energy crisis, increase global stability and economic prosperity is the utilization and conversion of biomass (2). Nigeria is known commercially as a producer of energy crops and fruits whose residues can be used in promoting the production of second generation biofuels (3). Some of these energy crops (sugar cane, cassava, maize, rice, wheat sorghum, etc) are used in the brewery industry for the production of alcoholic and non-alcoholic drinks. The brewery industry generates significant amounts of brewer's spent grain (BSG), which is the major by-products of the industry that can be converted to a more useful bio-products (3). Brewery industries in Nigeria produced more than

750 thousand tons of spent grains annually, hence making BSG a readily available low-cost by-product as well as a valuable resource for industrial exploitation (4). The Proper management of this biomass wastes may bring about economic benefits and help to protect the environment from pollution caused by its excessive accumulation (2). However, Microbial degradation of this biomass is a key component of the global carbon cycle (5). This bioconversion could also provide industrial energy sources, such as ethanol, methane gas etc. (5). One of the abundant microorganism with a strong biodegradable ability is *Aspergillus niger*, it is known for its biomass degrading ability and has proven useful in degradation of lignocellulose biomass. *Aspergillus niger* is one of the saprobic fungus and produces many extracellular enzymes to degrade the plant biomass efficiently into hexose and pentose sugars (6).

Fungi have been well studied for their ability to produce high levels of degradative enzymes, such as cellulases and hemicellulases. However, these enzymes help to hydrolysed the cellulose in the lignocellulosic biomass into simple sugars like



hexoses and pentoses. With the help of fermenters such as *Saccharomyces cerevisiae* (brewer's yeast), which help to ferment the simple sugars to bioethanol *saccharomyces cerevisiae* have rapid fermentative potential, improved flocculating ability, appreciable osmotolerance, enhanced ethanol tolerance and good thermotolerance (7). This work is tailored towards isolation and characterization of *Aspergillus niger* and *Saccharomyces cerevisiae* for bioethanol.

2.0 MATERIAL AND METHODS

2.1 Isolation and characterisation of *Aspergillus niger*

Soil samples were collected within Jatropa and Moringa plantation of National Research Institute for Chemical Technology Zaria. *Aspergillus niger* was isolated and characterised as described by (8-10).

2.1.1 Screening of *Aspergillus niger* for Cellulase production (plate assay method)

Isolates, identified to be *Aspergillus niger* were screened for their capacity to produce cellulase enzyme as described by (11, 12).

2.2 Isolation, Characterisation and Screening of *Saccharomyces cerevisiae* from palm wine sample

Local beer (burukutu) used in this research for the isolation of *Saccharomyces cerevisiae* was obtained from Mami market in Basawa barracks, Zaria, Kaduna State Nigeria. *Saccharomyces cerevisiae* was isolated from burukutu using the method of Ogbo and Igwilo, (2018) (13). Pure isolates thus obtained were characterized following standard

procedures as described by Barnett and Hunter, 1999 (9). The isolated *Saccharomyces cerevisiae* strains were screened for ethanol production based on thermo-tolerance, ethanol tolerance, osmotolerance, nitrogen assimilation, assimilation of various carbon compounds, and growth in 5% yeast extract as described by (14, 15).

3.0 RESULT AND DISCUSSION

3.1 Macroscopic and microscopic Characteristics of *Aspergillus niger* isolate

In the macroscopic characterisation, the isolate appeared woolly at the initial stage, appearing as a white to yellow colour which turned into a black granular mass on PDA plates. Colour on the reverse side of the plates was yellow/brown as shown in Plate I below. *Aspergillus niger* isolates stained with lactophenol cotton blue dye viewed microscopically, have hyphae with septate blue-black and a transparent substratum plate II. Isolate had globular head conidia on the hyphae growing from the stratum using the slight culture technique as seen in plate III. *Aspergillus niger* has a good cellulolytic activity (1.56cm) and a good cellulose production potential which is very important in cellulose hydrolysis plate IV. The macroscopic and microscopic identification of the fungi was based on the colour of their colony and the structure of the conidial head as classified by Brandt et al. (2011) (16) and Olawale et al. (2021) (17), who reported that colonies of *Aspergillus niger* are carbon black with a dark globular conidial head. *Aspergillus niger* strain isolated from soil samples were found to have good amylase production potential, which is essential for breaking down starch (17).

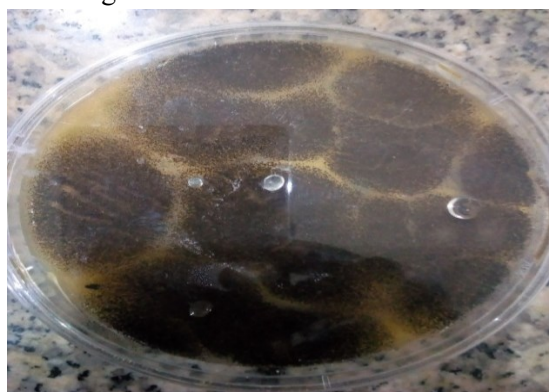


Plate I: pure sub-culture of *Aspergillus niger* on potatoes Dextrose Agar plate



Plate II: A portion of young culture of *Aspergillus niger* viewed using X 40 objective lens

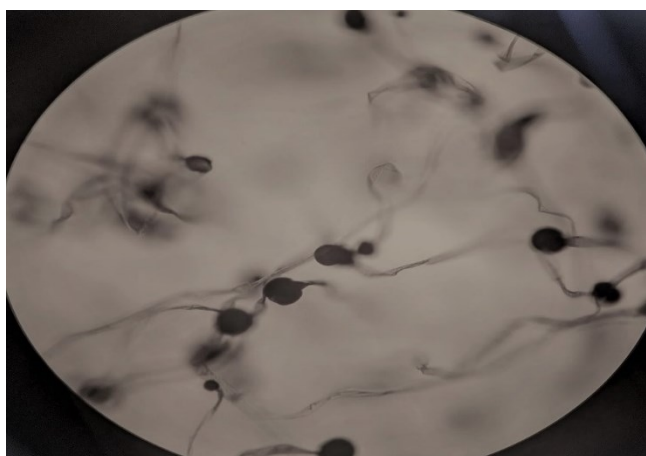


Plate III: A portion of a young culture of *Aspergillus niger* from slide culture viewed under the microscope using x40 objectives.

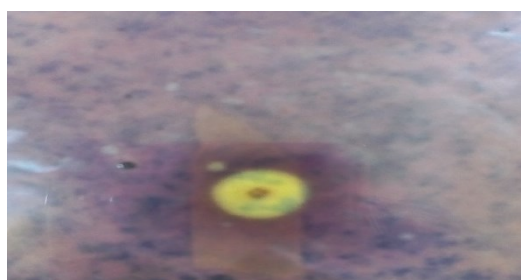


Plate IV: Zone of Clearance Due to Hydrolysis of Cellulose by Screened *Aspergillus niger* Isolates

3.2 Macroscopic and Microscopic Characteristics of *Saccharomyces cerevisiae*

The cultural characteristics of the yeast isolate on YEPG + Chloramphenicol medium were found macroscopically to be milky in colour, spherical in

shape, moist, and had alcoholic odour typical of *Saccharomyces cerevisiae* (Plate V). Microscopic view of the yeast cell after 48 hours of incubation at 30°C shows that the cell is ovoid or spherical in shape and the budding arrangement of the cells are multilateral and transparent in colour.





Plate V: sub-culture of pure isolate of *Saccharomyces cerevisiae*

Table 1: Thermotolerance of the yeast isolate after 48 hours

S/N	Temperature (T°C)	Growth extent	inference
1	25	+	Scanty growth
2	30	++	Heavy growth
3	35	++	Heavy growth
4	40	+	Moderate growth
5	45	-	Scanty growth

Table 2: ethanol tolerance of the yeast Isolate at 48 hours

S/N	Ethanol concentration (v/v)	OD of Isolate (600nm)
1	3	1.805
2	6	1.656
3	9	1.531
4	12	1.261
5	15	0.986
6	18	0.586

Table 3: growth of *S. cerevisiae* in 10 to 50 % of glucose concentration (Osmotolerance)

% Glucose concentration	Optical density	Inference
10	2.514±0.01	Luxuriant growth
30	1.680±0.032	Luxuriant growth
50	0.834±0.011	Luxuriant growth

The Isolate was able to tolerate various stress situations of temperature, ethanol concentration, high glucose concentration as seen in table 1,2 and 3; it was also able to utilise various sugars of glucose, fructose, galactose maltose, and sucrose except for lactose table 4. S₄ had the best sugar assimilation capacity produces acid and gas for all the sugars mention bellow except for lactose The isolate was grown in a medium containing 3, 6, 9,

12, 15, and 18% v/v of ethanol. The optical density was found to decrease with increased ethanol concentration, as seen in Table 2. These agrees with the work of Andrietta *et al.*, (2007) (18) and Olawale *et al.*, (2021) (17) , who reported that *Saccharomyces cerevisiae* is a yeast capable of withstanding stressful conditions and has high fermentation efficiency, effective sugar usage, tolerance to high ethanol concentration,



osmotolerance and thermotolerance, which are fundamental for industrial used. The yeast isolate was unable to ferment lactose. This is in agreement of the report by Olawale *et al.*, (2021) (17) that species of *Saccharomyces cerevisiae* cannot

ferment lactose as they lack the enzyme lactase but were found to ferment different types of sugars such as glucose, fructose, maltose, sucrose, and galactose with the evolution of gas in the Durham tubes except lactose.

Table 4: sugar fermentation characteristic of the Isolate after 48 hours' incubation

Isolate	Maltose	Sucrose	Glucose	Galactose	Fructose	Lactose	Inference
S1	--	--	+-	--	--	--	<i>S. cerevisiae</i>
S2	--	--	+-	--	+-	--	<i>S. cerevisiae</i>
S3	+-	++	++	++	++	+-	<i>S. cerevisiae</i>
S4	++	++	++	++	++	--	<i>S. cerevisiae</i>
S5	-	--	+-	--	--	--	<i>S. cerevisiae</i>

Key: ++ = acid and gas production, -- = no acid and gas production +- = acid production no gas production

Fourier-Transform Infrared Spectroscopy (FTIR) Spectra of Dignified Brewery Spent Grain:

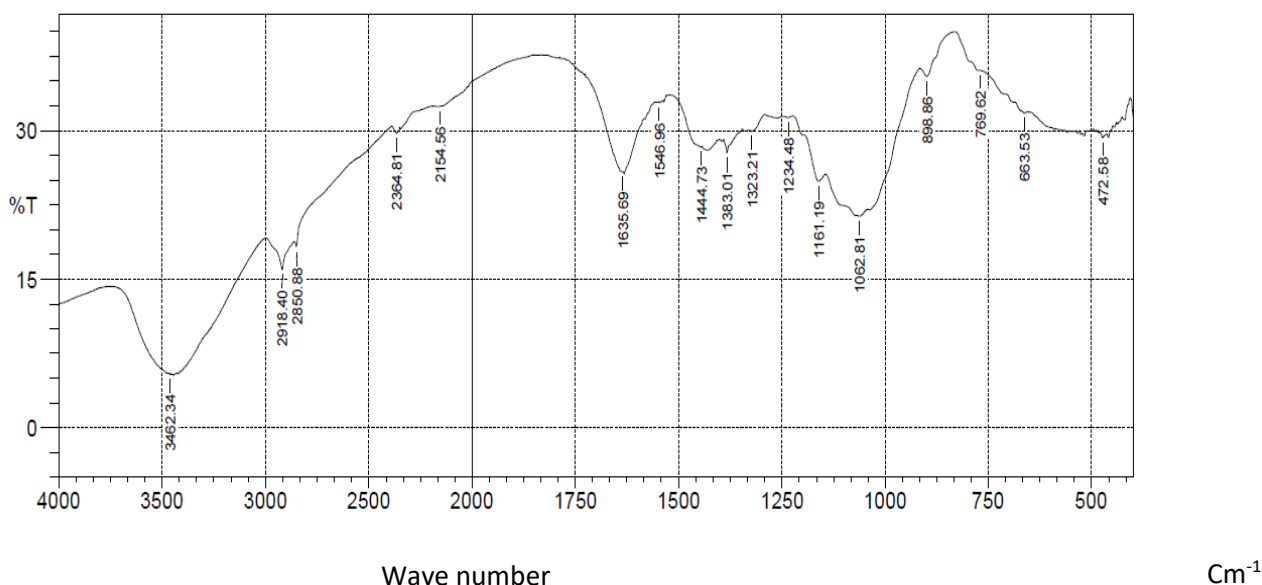


Fig. 1. FTIR spectra of dignified brewery spent grain

3.3 FTIR Spectra of dignified brewery spent grain (BSG)

The FTIR spectra of brewery spent grain (BSG) treated with NaOH is shown in Figure 1 above. Only major peaks on cellulose were considered. The absorption bands are observed in two wave number regions of 3462.3 cm^{-1} to 2154.56 cm^{-1} , and 1635.69 cm^{-1} to 472.58 cm^{-1} respectively. The peaks on the spectra of the cellulose from BSG in the wave number range of 3462.3 cm^{-1} to 2154.56 cm^{-1} is a characteristic for stretching vibration of O-H and C-H bands in a polysaccharide. This peak

includes also intramolecular and intermolecular hydrogen band vibration in cellulose. Bands at 2918.40 cm^{-1} and 1383.01 cm^{-1} are assigned to stretching and deformation vibrations of C-H group in glucose unit. The signal at 1062.81 cm^{-1} is assigned to -C-O- group of secondary alcohols and ethers functions existing in the cellulose chain backbone. The absorption band at 898.86 cm^{-1} is characteristic of β -glycosidic linkage between glucose units. The absorption bands at 1428, 1367, 1334 cm^{-1} and 896 cm^{-1} belong to stretching and bending vibrations of -CH₂ and -CH, -OH and C-O bonds in cellulose (19, 20).



4.0 CONCLUSION

This study showed that *Aspergillus niger* and *Saccharomyces cerevisiae* had potential for cellulose hydrolysis, and the ability to ferment sugar to bioethanol. The functional properties of the alkaline treated BSG was also determine using FTIR and reveals the ester bond existing in the cellulose chain.

5.0 REFERENCE

1. D. J. Rodriguez, A. Delgado, P. DeLaquil, A. Sohns, Thirsty energy. (2013).
2. P. Arauzo *et al.*, Effect of protein during hydrothermal carbonization of brewer's spent grain. *Bioresource technology* **293**, 122117 (2019).
3. A. Gwandu, A. Farouq, A. Baki, D. Peni, PRODUCTION OF BIOETHANOL FROM RICE AND MILLET HUSKS. *Journal DOI* **7**, (2021).
4. S. I. Mussatto, M. Fernandes, I. M. Mancilha, I. C. Roberto, Effects of medium supplementation and pH control on lactic acid production from brewer's spent grain. *Biochemical Engineering Journal* **40**, 437-444 (2008).
5. K. L. Anderson, in *Glycomicrobiology*. (Springer, 2002), pp. 359-386.
6. Z. Wu, Mixed fermentation of *Aspergillus niger* and *Candida shehatae* to produce bioethanol with ionic-liquid-pretreated bagasse. *3 Biotech* **9**, 41 (2019).
7. M. Kechkar *et al.*, Isolation and identification of yeast strains from sugarcane molasses, dates and figs for ethanol production under conditions simulating algal hydrolysate. *Brazilian Journal of Chemical Engineering* **36**, 157-169 (2019).
8. D. A. Animasaun *et al.*, Molecular identification and phylogenetic analysis of fungi contaminants associated with in vitro cultured banana based on ITS region sequence. *HAYATI Journal of Biosciences* **29**, 288-300 (2022).
9. H. Barnett, B. Hunter, Illustration genera of imperfect fungi. *American Phytopathological Society Minnesota*, (1998).
10. D. H. Ellis, S. Davis, H. Alexiou, R. Handke, R. Bartley, *Descriptions of medical fungi*. (University of Adelaide Adelaide, 2007), vol. 2.
11. M. Camassola, A. J. Dillon, Effect of different pretreatment of sugar cane bagasse on cellulase and xylanases production by the mutant *Penicillium echinulatum* 9A02S1 grown in submerged culture. *BioMed research international* **2014**, (2014).
12. R. C. Kasana, R. Salwan, H. Dhar, S. Dutt, A. Gulati, A rapid and easy method for the detection of microbial cellulases on agar plates using Gram's iodine. *Current microbiology* **57**, 503-507 (2008).
13. F. Ogbo, I. Igwilo, Shelf Life Extension In Burukutu, A Nigerian Alcoholic Beverage Using Antimicrobiologically Active Spices. *The Bioscientist Journal* **6**, 1-12 (2018).
14. G. Z. Breisha, Production of 16% ethanol from 35% sucrose. *Biomass and bioenergy* **34**, 1243-1249 (2010).
15. W. Borzani, A. Gerab, G. De La Higuera, M. Pires, R. Piplovic, Batch ethanol fermentation of molasses: a correlation between the time necessary to complete the fermentation and the initial concentrations of sugar and yeast cells. *World journal of Microbiology and biotechnology* **9**, 265-268 (1993).
16. M. E. Brandt, B. L. Gomez, D. W. Warnock, Histoplasma, Blastomyces, Coccidioides, and other dimorphic fungi causing systemic mycoses. *Manual of clinical microbiology*, 1902-1918 (2011).
17. S. A. Olawale, Biosorption of heavy metals from aqueous solutions: an insight and review. *Arch. Ind. Eng* **3**, 1-31 (2021).
18. S. R. Andrietta, C. Steckelberg, M. d. G. S. Andrietta, Study of flocculent yeast performance in tower reactors for bioethanol production in a continuous



- fermentation process with no cell recycling. *Bioresource technology* **99**, 3002-3008 (2008).
19. K. Fackler *et al.*, FT-IR imaging microscopy to localise and characterise simultaneous and selective white-rot decay within spruce wood cells. (2011).
20. F. Xu, J. Yu, T. Tesso, F. Dowell, D. Wang, Qualitative and quantitative analysis of lignocellulosic biomass using infrared techniques: a mini-review. *Applied energy* **104**, 801-809 (2013).



P114 - PRODUCTION OF BIOETHANOL FROM SAWDUST USING CO-CULTURE OF ASPERGILLUS NIGER AND SACCHAROMYCES CEREVISIAE



P115 - EFFECT OF SULPHURIC ACID CONCENTRATION ON COPPER LEACHING FROM METAL SCRAPS FOR COPPER SULPHATE SYNTHESIS

Olabimtan O. H*, Usman Y. O, Fasanya O. O, Batari M. L, Otsai J. O, Akpan E. S, Adesina O. B, Ochigbo V, and Barminas J. T

National Research Institute for Chemical Technology, Zaria
Corresponding author email: olabode4angel@gmail.com

ABSTRACT

The study investigates the leaching process of copper scrap to produce copper sulfate pentahydrate crystals using analytical and industrial grade sulphuric acid under controlled experimental conditions. The research examines the impact of key parameters, including copper scrap mass, acid concentration, nucleation temperature, and undigested scrap percentage, on the percentage yield of copper sulfate crystals. From the copper scrap, XRF analysis reveals high percentage of Cu of 89%. With an increase in the sulfuric acid concentration from 15.40 M to 15.63 M, the percentage of copper sulphate yield increased from 235.43% to 240.49% at 100 g/600 mL solid to liquid ratio for industrial grade acid A and analytical grade acid respectively. Also, an increase in the sulfuric acid concentration from 15.10 M to 15.63 M, the percentage of copper sulphate yield increased from 224.10% to 240.49% at 100 g/600 mL solid to liquid ratio for 4hrs at 270 °C for industrial grade acid B and analytical grade acid respectively. The XRF result of the copper sulphate produced has CuO (48.07 %) and SO₃ (39.64 %) as the dominant oxides among all other metal oxide impurities.

KEYWORDS

Copper recovery, leaching, sulphuric acid, sustainable sourcing, recycling, locally sourced materials.

1.0 INTRODUCTION

Copper, a fundamental element in industrial applications, has witnessed a surge in demand worldwide, driven by emerging technologies and global infrastructure development(1). Copper sulfate is used on a large scale across the globe in view of the multiplicity of its application and industrial uses. Copper sulphate is used as a starting material for the production of a variety of copper salts. It can also be used as a mordant for dyeing and electroplating as well as numerous agricultural uses. In agriculture it can be used as fungicide, correction of copper deficiency in soils and animals, molluscicide for destruction of snails and slugs and also fattening of pigs and broiler chickens. Furthermore, copper sulphate also finds application in production of anti-fouling paints and colouring of glass while the mining industry uses it as an anti-frothing agent. As a result of this, the demand for the chemical is increasing yearly. The worldwide market for copper sulfate pentahydrate is expected to grow at a roughly 2.3% rate over the next five years, will reach \$1.150 billion in 2024, from \$1 billion in 2019(2).

In the context of sustainable resource management and environmental responsibility, the recovery and recycling of copper from scrap metal have gained prominence as a viable source for the production of copper sulfate. The efficient recovery of copper from low-grade ores, scraps, and industrial residues is a pressing concern.

Copper recovery from locally sourced copper scraps in Nigeria has gained attention due to its potential for contributing to sustainable resource management and reducing reliance on imported copper. Nigeria, like many other countries, has witnessed a surge in copper recycling initiatives. Small and medium-scale recycling businesses have emerged, particularly in urban areas, to recover copper from various sources, including electrical cables, electronic waste, and industrial scraps (3). In Nigeria, the copper sulfate requirement is mostly met through importation despite its wide application across various industries. "In view of the high level of building going on in the country, Nigeria expends more than ₦7 billion to import wood preservatives for use in the building and construction industry in 2018(4).



However, the informal copper recycling sector in Nigeria faces significant challenges. Lack of appropriate technology, limited safety measures, and inadequate regulatory oversight have raised concerns about health and environmental risks(5). Additionally, inefficiency in the informal sector can lead to suboptimal recovery rates. Some case studies have explored the economic viability of copper recovery in Nigeria. While copper recycling can be profitable due to the high market demand for copper, the profitability depends on factors such as the scale of operations, copper scrap availability, and market prices (6). The environmental impact of copper recovery in Nigeria has been a topic of concern. Inefficient recycling processes, improper disposal of waste, and the release of pollutants can pose environmental risks(7).

Sulphuric acid, a commonly employed leaching agent, plays a pivotal role in these processes. Its ability to solubilize copper-bearing minerals and compounds has made it a preferred choice for copper recovery(8). Recent studies have highlighted the significance of optimizing sulphuric acid leaching processes to enhance copper recovery yields. Researchers have examined the impact of various parameters, such as acid concentration, temperature, particle size, and leaching time, on leaching efficiency (9). This quest for efficiency aligns with the broader goals of sustainability and resource conservation.

This present study seeks to contribute to this body of knowledge by comparing the yield of Copper (II) Sulphate Pentahydrate from locally sourced copper scraps using both analytical and industrial grades of sulphuric acid.

2.0 MATERIALS AND METHODS

2.1 Materials and Reagents

Locally sourced copper scraps were collected and thoroughly cleaned to remove contaminants, rust, and any non-copper materials. The cleaned copper scraps were then characterized for composition and impurities.

Analytical-grade H_2SO_4 with a purity of at least 95% and industrial grade H_2SO_4 from three different manufacturers was used for leaching experiments. The acids were used without further purification and stored in a controlled environment to prevent contamination.

2.2 Methodology

2.2.1 Sample Preparation

Copper scraps were cut into uniform pieces and weighed to achieve consistent experimental conditions. A representative sample was selected for characterization before leaching.

2.2.2 Determination of Acid Concentration

To determine sulphuric acid strength, titration was carried out using NaOH. The molarity of the NaOH was used to calculate volume of NaOH used and subsequently the strength of sulphuric acid. Phenolphthalein was used as indicator

2.2.3 Sulphuric Acid Leaching

A predetermined mass of cleaned copper scraps was placed in four leaching vessels for each run. In each vessel a volume of either Analytical-grade sulphuric acid or industrial grade sulphuric acid was added to the labelled vessel in the desired concentration. The leaching vessels was sealed to prevent evaporation and contamination. The reaction mixture was maintained at a controlled temperature for a defined period. Samples were periodically collected to assess copper concentration in the leachate. Experimental conditions for all experiments were uniform and as follows: 100 grams of copper scrap, 600 mL of acid volume, 270 °C temperature for a duration of 4-hour duration.

Characterization

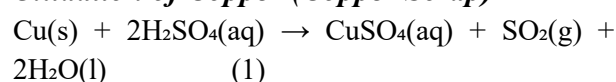
The copper scraps were analysed using XRF to determine the composition before leaching.

The product was analysed using an XRF.

3.0 RESULTS AND DISCUSSION

The production of copper sulfate pentahydrate from copper scrap and concentrated sulfuric acid involves several chemical reactions (8). Here are the key reactions step by step.

Oxidation of Copper (Copper Scrap)



In this reaction, copper (Cu) from the copper scrap reacts with concentrated sulfuric acid (H_2SO_4) to form copper sulfate ($CuSO_4$), sulfur dioxide gas (SO_2), and water (H_2O).



Dilution and Addition of Water:

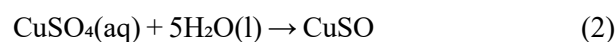


Figure 1. copper scrap



Figure 2. Copper sulphate pentahydrate

Table 1: XRF Analysis of copper scraps

Metal	%	Metal	%	Metal	%
Si	1.16	Cu	89.14	Al	2.96
V	0.01	Nb	2.45	Ta	Nil
Cr	0.01	W	0.07	Ti	0.08
Mn	0.14	P	Nil	Zn	0.28
Fe	0.16	S	Nil	Zr	0.36
Co	0.06	Ca	0.64	Ag	Nil
Ni	0.01	K	0.09		

The above results show that the copper scrap material is primarily composed of copper (Cu), with various other elements present in smaller quantities. Some of these elements could be intentional alloying components, while others may be impurities from previous uses or sources. The absence of phosphorus and sulfur is beneficial for

the quality of the copper, and the absence of silver and tantalum may have specific implications for its intended use (10). This XRF analysis provides valuable insights into the elemental composition of the copper scrap, which can be crucial for recycling or repurposing the material in various industrial applications(11).

Table 2: CuSO₄ yield

Grade	Cu Scrap(g)	Acid conc.(M)	Nucleation point (deg C)	Yield of crystals (%)	Undigested scrap (g)
Analytical	100	15.63	45	240.49 ± 0.01	0
Industrial A	100	15.40	55	235.43 ± 0.1155	28.21 ± 0.0116
Industrial B	100	15.10	56	224.10 ± 0.1000	29.34 ± 0.0058

Table 2 presents the yield of CuSO₄ after the leaching process. The analytical grade H₂SO₄ had the highest yield of crystals leaving behind no undigested scrap metal. Both industrial grade

H₂SO₄ had appreciable amount of residue undigested.

Table 3 shows the XRF analysis of the copper sulphate produced using analar grade sulphuric acid. XRF analysis for CuSO₄ produced using



industrial grade sulphuric acid are unavailable as of preparation of this manuscript.

Table 3 XRF analysis of produced copper sulphate

Metal	%	Metal	%	Metal	%
SiO ₂	2.10	BaO	0.09	MnO	-
V ₂ O ₅	-	WO ₃	0.05	TiO ₂	-
CaO	0.10	Ag ₂ O	-	Cl	0.72
Nb ₂ O ₃	3.68	Al ₂ O ₃	4.11	SO ₃	39.64
Fe ₂ O ₃	0.16	ZnO	0.18	ZrO ₂	0.93
CuO	48.07	Ta ₂ O ₅	0.06		
K ₂ O	-	Co ₃ O ₄	0.01		

The nucleation point which is the temperature at which crystals begin to form, is 45°C for the analar grade sulphuric acid as seen in Table 2. This temperature is 10 degrees lower than the nucleation temperature of industrial grade sulphuric acids.

In other words, the percentage recovery is based on the mass of the recovered product relative to the initial amount of the copper scrap. If the crystals are forming with a higher weight than expected, it can lead to a yield percentage that exceeds 100%. Several factors such as supersaturation, slow cooling, nucleation points, reaction kinetics, and concentration of reactants can contribute to the growth of crystals with a higher weight (12, 13).

Similarly, several factors could contribute to some parts of the copper scrap remaining undigested during the leaching process. The incomplete dissolution of the scrap may be due to the following reasons such as Insufficient reaction time, inadequate mixing or agitation, passivation or surface oxides, inadequate acid, concentration or volume, variations in scrap composition, temperature fluctuations, presence of protective films, mechanical obstructions and experimental errors.

Generally, acid concentration plays a crucial role in the leaching process of copper from copper scraps. The concentration of the leaching agent, in this case, sulphuric acid, affects the rate and extent of copper dissolution.

Higher acid concentrations provide more hydrogen ions (H⁺), which actively participate in the leaching reaction. The increased concentration of H⁺ ions enhances the dissolution of copper compounds, such as copper oxides or sulphides, from the surface of the copper scraps(14). This results in higher

copper concentrations in the leachate, indicating improved leaching efficiency.

4.0 CONCLUSION

The analytical grade sulphuric acid leaching of copper scrap enables better leaching of copper and other minor metals than the industrial grade sulfuric acid leaching base on its high quality and concentration.

The analytical grade sulphuric acid, yielded 240.49% of copper sulphate at 100 g/600 mL solid to liquid ratio under the optimum conditions of 270°C for 4 h. Conversely, the industrial grade sulfuric acid enables the leaching of copper scrap to yield 235.43% and 224.10% copper sulphate for A and B industrial grade sulphuric acid respectively, at 100 g/600 mL solid to liquid ratio under the optimum conditions of 270°C for 4 h.

The effect of acid concentration was also observed as the nucleation point varies with increase in acid concentrations.

There however appears to be a correlation between the molar acid concentration and the amount of metal left undigested. Further investigation with generation of more empirical data is however required to establish these relationships adequately.

5.0 REFERENCES

1. D. Dong *et al.*, Scenarios for anthropogenic copper demand and supply in China: implications of a scrap import ban and a circular economy transition. *Resources*,



- Conservation and Recycling* **161**, 104943 (2020).
2. B. W. Schipper *et al.*, Estimating global copper demand until 2100 with regression and stock dynamics. *Resources, Conservation and Recycling* **132**, 28-36 (2018).
 3. T. R. Ayodele, M. A. Alao, A. S. O. Ogunjuyigbe, Recyclable resources from municipal solid waste: Assessment of its energy, economic and environmental benefits in Nigeria. *Resources, Conservation and Recycling* **134**, 165-173 (2018).
 4. V. E. Akpan, D. O. Olukanni, Hazardous Waste Management: An African Overview. *Recycling* **5**, 15 (2020).
 5. C. Egbuna *et al.*, Emerging pollutants in Nigeria: A systematic review. *Environmental Toxicology and Pharmacology* **85**, 103638 (2021).
 6. T. Wang, P. Berrill, J. B. Zimmerman, E. G. Hertwich, Copper Recycling Flow Model for the United States Economy: Impact of Scrap Quality on Potential Energy Benefit. *Environmental Science & Technology* **55**, 5485-5495 (2021).
 7. W. Zhang *et al.*, Analyzing the environmental impact of copper-based mixed waste recycling-a LCA case study in China. *Journal of Cleaner Production* **284**, 125256 (2021).
 8. K. Yoo, Y. Park, S. Choi, I. Park, Improvement of Copper Metal Leaching in Sulfuric Acid Solution by Simultaneous Use of Oxygen and Cupric Ions. *Metals* **10**, 721 (2020).
 9. M. Gericke, Y. Govender, Bioleaching strategies for the treatment of nickel-copper sulphide concentrates. *Minerals Engineering* **24**, 1106-1112 (2011).
 10. S. Liu *et al.*, Recycling the domestic copper scrap to address the China's copper sustainability. *Journal of Materials Research and Technology* **9**, 2846-2855 (2020).
 11. M. Houllberghs *et al.*, Evolution of the crystal growth mechanism of zeolite W (MER) with temperature. *Microporous and Mesoporous Materials* **274**, 379-384 (2019).
 12. J. Zhao, H. Miao, L. Duan, Q. Kang, L. He, The mass transfer process and the growth rate of NaCl crystal growth by evaporation based on temporal phase evaluation. *Optics and Lasers in Engineering* **50**, 540-546 (2012).
 13. J. N. Sherwood, R. I. Ristic, The influence of mechanical stress on the growth and dissolution of crystals. *Chemical Engineering Science* **56**, 2267-2280 (2001).
 14. R. Padilla, P. Pavez, M. C. Ruiz, Kinetics of copper dissolution from sulfidized chalcopyrite at high pressures in H₂SO₄-O₂. *Hydrometallurgy* **91**, 113-120 (2008).



P116 - OPTIMIZATION OF THE EPOXIDATION PROCESS PARAMETERS OF BAOBAB SEED OIL

ABSTRACT: Pure baobab seed oil was epoxidized via in situ conventional method using hydrogen peroxide and formic acid. Optimization of the effect of process parameters such as time, temperature, and concentration of hydrogen peroxide and formic acid was studied using Response Surface Methodology (RSM). The optimal condition for the predicted oxirane value, 5.96%, was obtained at a reaction time of 2 hours, at temperature of 50°C and 0.5 mol concentration of formic acid and hydrogen peroxide. The resultant epoxide product was confirmed using Fourier transform infrared spectroscopy (FTIR) (at 2900 cm^{-1}). These findings demonstrated the effects of process parameters on the rate of epoxide formation and the possibility to synthesize bio-based resin from baobab seed oil.

KEYWORDS: *Baobab seed oil; Optimization; Formic acid; Response surface methodology; Oxirane value.*

INTRODUCTION

Plant (vegetable) and animal oils are natural renewable materials that differ in structure and unsaturation. Vegetable oil is a class of plant oil that is abundant, inexpensive, biodegradable, environmentally benign, and offers varying degrees of unsaturation depending on the nature of the plant [1]. Vegetable oil, such as groundnut, sunflower, melon, Karanja, soybean, castor, linseed, okra seed oil, etc. are considered unreactive chemical materials that can be made reactive through chemical modification [2]. They are triglycerides, which contain saturated fatty acids such as palmitic or stearic acids, and unsaturated fatty acids such as palmitoleic, oleic, linoleic, or linolenic acids, containing one, two, or more double bonds between two carbon atoms. The unsaturated fatty acids are the reactive sites for chemical modification in vegetable oils, hence the more unsaturated the fatty acids, the more reactive the oil [3].

Baobab tree (*Adasonia digitata*) offers shelter, clothing, medicine and a source of nutrition as well as raw material for many useful items. The flesh of fruit white has the taste of acid, it used as juice which is very rich of vitamins C, A, E and calcium. Seeds contain averagely 35-40% oil, which is used in cooking, medicine and cosmetics [4]. The seeds are not suitable for human

consumption and so its industrial applications do not deplete the food supply. The oil is unsaturated and exhibits a semidrying property, hence it can be used in the manufacture of paint, soap, alkyd resin, and wood polish, same as other plant oils. [5,6]

Various chemical modifications on the double bonds (reactive sites) of these vegetable oils have been done. In the chemical industry, the most common value-adding chemical modification of vegetable oils is epoxidation and hydroxylation. [7]. Epoxidation of fatty acids is a reaction of a C=C double bond with active oxygen to form a three-membered oxirane ring or epoxide group [8,9].

Industrial methods usually involve the reaction of these unsaturated C=C double bonds with a peracid (that is, an acid with additional oxygen). This acid is formed by the reaction of an ordinary carboxylic acid (e.g. acetic acid) with hydrogen peroxide. The epoxides formed can be used as raw materials to synthesize cross-linkable bio-resins [10].

The epoxides obtained from higher alkenes, esters, and triglycerides of unsaturated fatty acids are intermediates for the preparation of oligoesters, glycols, hydroxy ethers, alcanolamines. Without further modifications, they are used as plasticizers and stabilizers for plastics, inks, coatings,



and cutting fluid for metalworking processes or coatings obtained by UV initiates cross-linking [3, 7, 11-15]. Recent studies have attempted to improve the efficiency of epoxidation under slighter conditions that reduce by-product formation, reaction time, increase the rate of peracid formation using a catalyst and optimize the process parameters [16]. Table 1 below show the physicochemical characteristics of baobab seed oil as reported by wang *et al.* [5] which is a pointer to the fact that it can be suitably epoxidized. The kinetics and thermodynamic studies of vegetable oils indicated that an increase in temperature increased the rate of epoxide formation it was validated by Tai *et al* [17]. Optimization of the process parameter of some vegetable oils like canola, soya bean, rapeseed, and sesame seed oil has been investigated by [18-21] respectively. Comparative analysis of different epoxidation procedures of *Cynara cardunculus* seed oil has been carried out by Turco *et al* [22]. Hence this work investigates the optimum epoxidation condition for baobab seed oil varying the process parameters such as time, temperature, and concentration of hydrogen peroxide and formic acids.

EXPERIMENTAL SECTION

Materials:

Pure baobab seed oil used in this study was manually extracted using cold press extraction method; formic acid (99%) and hydrogen peroxide (30wt %) obtain from Cardinal Scientific Supplies.

Table 1: Physico-chemical characteristics of baobab seed oil

Iodine value (gI ₂ /100g)	86
Specific gravity (30°C)	0.9999
Acid value (MgKOH/g)	0.5
Free fatty acid (% oleic acid)	37.7
Peroxide value (meq/kg)	2.94
Saponification value (MgKOH/g)	209.28

Source; Sigma oil seed (2020)

Equipment Used

Water bath, three-necked round bottom flask, thermometer, condenser, feed funnel, mechanical stirrer, measuring cylinder, weighing balance, separation funnel, rotary evaporator.

Design of Experiment

The experiment was designed with Box Behnken considering 4 factors (temperature, time, concentration of formic acid and hydrogen peroxide) and 2 responses (iodine value and oxirane value) comprising of 16 experimental runs using Design Expert Software.

Epoxidation procedure

The epoxidation method reported by Goud *et al.* (2012) was used with little variation in the procedure and was repeated for all the experimental runs with the same stirring speed while varying reaction time, temperature, hydrogen peroxide and formic acid concentration. 30g of baobab seed oil was placed in a three necked bottom flask, 15g of formic acid was added to the flask after about 5 min, the mixture was stirred continuously for 30 min. Then 30g of 30 wt% aqueous hydrogen peroxide was added dropwise to the reaction mixture, as oxygen donor, at a rate such that the hydrogen peroxide addition was completed within half an hour. The mole ratio of the components used is 1:1:0.5; H₂O₂ : HCOOH. After the complete addition of hydrogen peroxide, the mixture was heated at the same desired temperature (50 °C) for 2 h with rapid stirring. A liquots of the reaction mixture was cool to room temperature. The oil was extracted with ethyl acetate, separated and washed with warm water until acid free and dried over sodium sulphate.



Analytical techniques;

Iodine value of epoxidized baobab seed oil

The iodine value of the test oil sample was determined by the Wijs method for iodine value [The American Oil Chemist's Society Official Method]. 0.5 g of the sample was poured into a conical flask. 10 ml of carbon tetrachloride was added to the oil and was shaken to allow the oil to dissolve. Also, 20 mL of the Wijs iodine solution was later added to the mixture. It was stirred vigorously, stoppered, and kept in the dark for 30 minutes. Subsequently, 15 ml of potassium iodide solution followed by 100 ml of distilled water was added. The mixture was titrated against 0.01N sodium thiosulphate solution. A reagent black was titrated as well. The iodine value of epoxidized samples was calculated after analysis using the formula:

$$IV = \frac{(B - S) \times M \times 12.69}{W} \quad 1$$

Where:

IV = Iodine value of samples

S = Volume of Na₂S₂O₃ used for sample (ml),

B = Volume of Na₂S₂O₃ used for blank (ml),

W = Weight of sample used (g),

M = Molarity of the Na₂S₂O₃ used.

Oxirane Oxygen content

The percentage of the oxirane oxygen was determined using equation 2.

$$OO_{\text{exp}} = \left[\frac{\left(\frac{IV_0}{2A_i}\right)}{100 + \left(\frac{IV_0}{2A_i}\right)A_o} \right] A_o \times 100 \quad 2$$

Where A_i (126.9) and A_o (16.0) are the atomic weights of iodine and oxygen, respectively, and IV₀ is the original iodine value of oil sample per 100 g of oil.

FT-IR analysis

The pure and epoxidized rubber seed oil was characterized using Fourier Transform InfraRed (FT-IR) Spectroscopy Technique to determine surface functional groups present. The FT-IR analyses were carried out on the samples using Shimadzu FT-IR-8400S Spectrophotometer with a resolution of 4 cm⁻¹ in the range of 4000 - 500 cm.

RESULTS AND DISCUSSION

Statistical analysis of data for epoxidation of rubber seed oil

The results of the iodine and oxirane value presented in Table 2 were determined using Equations 1 and 2, respectively. The varying responses are indications that the process parameters considerably affected the iodine and oxirane value. The minimum iodine value of 11.56g /100g oil was obtained at a temperature of 50°C after 6 h. The maximum oxirane value of 5.87% was obtained at a 50°C of temperature for 2 h is in line with what was reported by Paul *et al.* [25], hence this is an indication that the iodine and oxirane values from the epoxidation of baobab seed oil were affected by process conditions. The statistical analysis for epoxidation of baobab seed oil was done using analysis of variance (ANOVA). Table 3 shows the ANOVA results for baobab seed oil epoxidation for oxirane value. The multiple regression analysis of the experimental data gives a second-order polynomial equation. The quadratic model developed depicts the interaction between the oxirane value respectively (Y) and the coded values of the independent variables A, B, C and D (time, temperature, concentration of formic acid and hydrogen peroxide).

$$Y = 2.65 - 0.2292A - 0.6267B - 0.4933C - 0.4567D - 0.0579AB - 0.3579AC + 0.3904AD + 0.5096BC + 0.4329BD + 0.4671CD + 0.000A^2 + 0.00B^2 + 0.00C^2 + 0.00D^2 \quad 3$$

Where Y represents response variable oxirane value measured in %



Table 2: Experimental design layout for iodine and oxirane value of epoxidised baobab seed oil

Run	Factor 1 Formic Acid conc. (mol)	Factor 2 Hydrogen peroxide conc. (mol)	Factor 3 Time (hr)	Factor 4 Temperature (°C)	Response 1 Iodine Value g/100g of oil	Response 2 Oxirane value %
1	0.5	0.5	2.00	50	92.76	5.87
2	1.0	0.5	2.00	50	89.46	5.30
3	0.5	2.0	2.00	50	45.01	2.75
4	1.0	2.0	2.00	50	39.73	2.36
5	0.5	0.5	6.00	50	50.55	3.94
6	1.0	0.5	6.00	50	24.36	1.57
7	0.5	2.0	6.00	50	37.79	2.36
8	1.0	2.0	6.00	50	11.56	0.73
9	0.5	0.5	2.00	60	39.72	2.46
10	1.0	0.5	2.00	60	57.98	3.50
11	0.5	2.0	2.00	60	15.55	0.99
12	1.0	2.0	2.00	60	31.73	1.94
13	0.5	0.5	6.00	60	34.01	2.00
14	1.0	0.5	6.00	60	29.86	1.60
15	0.5	2.0	6.00	60	44.76	2.69
16	1.0	2.0	6.00	60	39.09	2.39

Adequacy of the model

The significance of the model is that; it can be used to predict the Oxiran Oxygen Content during experimental set up prior to conducting physical experiment.

Moreso, the adequacy of the model was further ascertain using its R^2 value which was compare with the adjusted R^2 to be 0.9849 instead of 0.9954.

Table 3. shows the ANOVA result for epoxidation of baobab seed oil. As shown in the table, the model is significant as the probability greater than F-value, which is <0.0001 is less than 0.05. Also, the model terms A, B, C, D and others are all significant because their Prob>F value are less than 0.05. The lack of fit as shown in Table 4.4 is not significant as the prob > F value of 1.72 is greater than 0.05.

Table 3: Analysis of variance for baobab seed oil epoxidation

Source	Sum of Squares	DF	Mean Square	F-value	p-value	
Model	29.54	10	2.95	99.14	< 0.0001	significant
A-FA	0.8402	1	0.8402	28.20	0.0032	
B-HP	6.28	1	6.28	210.87	< 0.0001	
C-time	3.89	1	3.89	130.70	< 0.0001	
D-tempt	3.34	1	3.34	111.98	0.0001	
AB	0.0536	1	0.0536	1.80	0.2374	



AC	2.05	1	2.05	68.79	0.0004
AD	2.44	1	2.44	81.84	0.0003
BC	4.16	1	4.16	139.45	< 0.0001
BD	3.00	1	3.00	100.63	0.0002
CD	3.49	1	3.49	117.16	< 0.0001
A ²	0.0000	0			
B ²	0.0000	0			
C ²	0.0000	0			
D ²	0.0000	0			
Lack of fit	0.0999	1	0.0999		1.72
					Not significant
Residuals	0.1490	5	0.1642		
Cor Total	29.69	15			

The model generated is shown in Equation 4

$$Y = 2.65 - 0.2292A - 0.6267B - 0.4933C - 0.4567D - 0.0579AB - 0.3579AC + 0.3904AD + 0.5096BC + 0.4329BD + 0.4671CD + 0.000A^2 + 0.00B^2 + 0.00C^2 + 0.00D^2 \quad 4$$

As presented in Equation 4, the Y represents the Oxiran Oxygen Content, A is the formic acid, B is hydrogen peroxide, C represents the operating time while D is the time of the reaction. The significance of the model is that; it can be used to predict the Oxiran Oxygen Content during experimental set up prior to conducting physical experiment.

As presented in the figure 1, the experimental data are in good and close agreement with the predicted data as all the data points are very close or superimposed along the regression line.

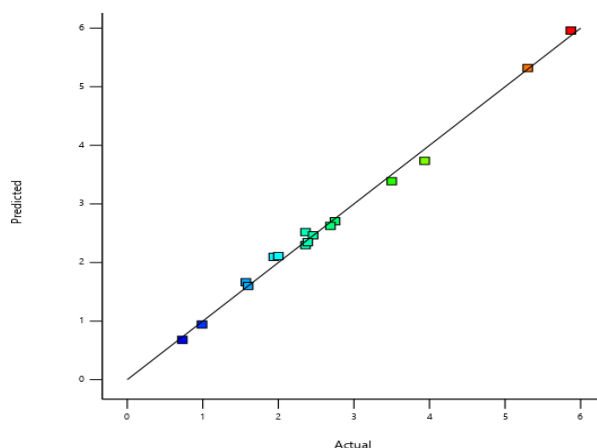


Figure 1: Relationship between the predicted and experimental data of the oxiran oxygen content.

Also, as show in Figure 2, the four independent parameters (formic acid, H₂O₂, operating time and temperature) are in virtuous interface with each other as confirmed from the reference point they meet each other.



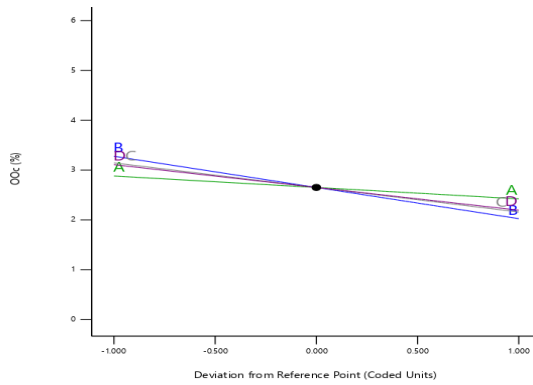


Figure 2: perturbation plot of the independent parameters

FT-IR graphs

In the FT-IR spectra in figure 3, it can be seen that the presence of carbon-carbon double bonds (C=C) in the unepoxidized baobab seed oil was indicated by the appearance of peaks at 2022 cm^{-1} with also a lot of unstrengthening peaks at around 3500 cm^{-1} . The absorption band for the epoxy group in the epoxidized baobab seed oil was indicated by the single peak at 1750 cm^{-1} and 2900 cm^{-1} this peaks were missing in the unepoxidised oil. Hence, an indicator to the fact that the oil has been suitably epoxidized.

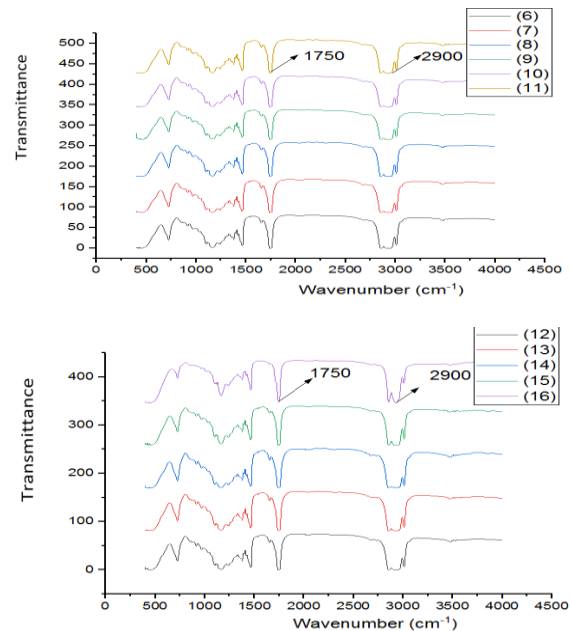
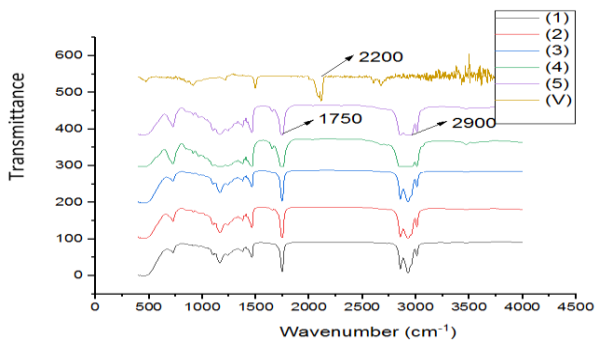


Figure 3: The FT-IR spectroscopy of the Baobab, a) Pure baobab seed oil (b and c) Epoxidized baobab seed oil.

Hence, a pointer to the fact that the oil has been suitably epoxidized. The acrylate epoxy resins of baobab seed oil were obtained at the wavenumber of 2900 cm^{-1} to form the acrylic group, which indicates that it has been modified and can be applied in biobased thermoset development.

CONCLUSIONS

The development of epoxidized baobab seed oil was demonstrated and the formation of epoxy groups was confirmed by FT-IR spectroscopy

analysis. The result of the investigation shows that baobab seed oil can be successfully utilized for epoxidation using peroxy acid generated in situ. The optimal condition for the predicted oxirane value of 5.96 %, was obtained at a reaction time of 2 hours, temperature of $50\text{ }^{\circ}\text{C}$, and concentration of 0.5 mol of both acid and hydrogen peroxides. Results of the statistical analysis showed that the process parameters (concentration, time, and temperature) have significant effects on the response. Hence these findings are for possible utilization of baobab



seed oils in the production of thermosets and composite materials.

REFERENCES

- [1] Petrovic Z.S., *Polymers from Biological Oils, Contemporary Materials*, 1: 39-50 (2010).
- [2] Saurabh T., Patnaik M., Bhagat S. L., Renge V.C., *Studies on the Synthesis of Biobased Epoxide using Cottonseed Oil*, *Int. J. Adv. Eng. Res. Stud*, 1(2): 279284 (2012).
- [3] Jabar J.M., Olagboye S.A., *Kinetics Studies on Epoxidation of Jatropha Curcas and Thevetia Peruviana Oil*, *Journal of Sustainable Technology*, 8(1): 117-127 (2017).
- [4] Nwankwo B.A., Aigbekaen S.G.A., "Estimates of Rubber (ev) Seed Production in Nigeria". in: "Industrial Utilization of Natural Rubber, Seed Latex, and Wood", *Proceedings of Natural Conference* (Ed: Ephraim E. Enabor). *Rubb. Res. Inst. of Nigeria*.;78-87 (1985)
- [5] Okieimen F. E., Bakare O. I., Okieimen C.O., *Studies on the Epoxidation of Rubber Seed Oil, Industrial Crops, and Products*, 15: 139-144 (2002)
- [6] Ramadhas A. S., Jayaraj S., Muraleedharan C., *Biodiesel Production from High FFA Rubber Oil*, *Fuel*, 84(4): 335-340 (2009).
- [7] Goud V. V., Patwardhan A. V., Pradhan N. C., *Studies on the Epoxidation of Mahua Oil (Madhumica indica) by Hydrogen Peroxide*, *Bioresource Technol.*, 97: 1364-1371 (2006).
- [8] Dinda S., Patwardhan A. V., Goud V.V., Pradhan N. C., *Epoxidation of Cottonseed Oil by Aqueous hydrogen Peroxide Catalyzed by Liquid Inorganic Acids*, *Bioresource*. 99 (9): 3737-3744 (2008).
- [9] Rios L.A., Weckes P.P., Schuster H., Hoelderich W.F., *Resin Catalyzed Alcoholysis of Epoxidized Fatty Esters: Effect of the Alcohol and the Resin Structures*, *Applied Catalysis A: General*, 284: 155161 (2005).
- [10] Nwosu-Obieogu K., Kalu U.C., *In Situ epoxidation of Sesame Seed Oil for the Synthesis of a Bio-Based Resin*, *European J. Sustainable Dev.*, 4(3): em0121 (2020).
- [11] Latif F.E.A, Abidin Z.Z., Cardona F., Awang Biak K.A., Tahir P.M., Ern L.K., *Bio-Resin Production Through Ethylene Unsaturated Carbon Using Vegetable Oils, Processes.*, 8(48): 1-15 (2020).
- [12] Metzger J.O., Bornscheuer U., *Lipids as Renewable Resources. Current State of Chemical and Biotechnological Conversion and Diversification*, *Appl. Microbiol. Biotechnol.*, 71: 13–22 (2006)
- [13] Quinchia L.A., Delgado M.A., Reddyhoff T., Gallegos C., Spikes H.A., *Tribological Studies of Potential Vegetable Oil-Based Lubricants*, *Tribol. Int.*, 69: 110–117 (2014).
- [14] Dinda S., Ravisankar D., Puri P., *Development of Bio-Epoxide from Nahor (Mesua ferrea Linn) Oil*, *Journal of the Taiwan Institute of Chemical Engineers*, 65: 399-404 (2016).
- [15] Silviana S., Anggoro D.D., Kumoro A.C., *Kinetic Study of Waste Cooking Oil Epoxidation with Peroxyacetic Acid Using Acid Catalysts*, *Rasayan J.Chem.*, 12(3): 1369-1374 (2019).
- [16] Thames S.F., Yu H., *Biopolymer from Renewable Resources*, *Surf. Coat. Technol.*, 115: 208-214 (2009)
- [17] Obanla O.R., Udonne J.D., Ajani O.O., Ojewumi M.E., Omodara O.J., Oni B.A., *Studies of the in-Situ Epoxidation of Rubber (Hevea Brasiliensis) Seed Oil by Performic Acid*, *J. Phys. Conf. Ser.* 1378, 1-8. (2019).
- [18] Musik M., Milchert E., *Selective Epoxidation of Sesame Oil with Peracetic Acid, Molecular catalysis*, 433: 170-174 (2017).
- [19] Matusiak M., Milcher, E., *Optimization of Selective Epoxidation of Canola Oil with in Situ Generated*



- Peracetic Acid, *Journal of Advanced Oxidation Technologies* 21(1): (2018).
- [20] Sinadovic-Fiser S., Milovan J., Zoran S., Kinetics of in Situ Epoxidation of Soyabean Oil in Bulk Catalyzed by Ion Exchange Resin, *Kansas Polymer Research*, 78(7): 725-731 (2001). [20] Arumugam S., Sriram, G., Rajmohan, T., Multi-Response Optimization of Epoxidation Processparameters of Rapeseed Oil Using Response Surface Methodology(RSM)-Based Desirability Analysis, *Arab. J. Sci. Eng.*, 39: 2277-2287 (2014).
- [21] Turco R., Tesser R., Russo V., Vitiello R., Fagnano M., Di Serio M., Comparison of Different Possible Technologies for Epoxidation of Cynara cardunculus Seed Oil, *Eur. J. Lipid Sci. Technol.*, 1900100, pp 1-8 (2019).



P118 - DEVELOPMENT OF BEEHIVE-GINGER/SISAL POLYESTER HYBRID COMPOSITE FOR BUILDING AND FURNITURE INDUSTRIES

Audu H. I*, Shehu U., Gano Z. S., Ade-Ajayi A. F.

National Research Institute for Chemical Technology, P.M.B 1052, Zaria, Nigeria

*Correspondence to: E-mails: auduidowu3@gmail.com

ABSTRACT

Over the span of time, the development of environmentally friendly materials to shield the environment from health risk and pollution caused by the discharge of conventional waste materials, has become a major concern in the research and industries. These drawbacks had ignited the interest of the researchers toward the development of recyclable, cheap, biodegradable and eco-friendly materials. Though mono natural fiber reinforced polymer composites are environmentally friendly, renewable and lightweight, however, there are limitations to which these materials can be used due to decrease in strength and high moisture absorption. Thus, this study focused on the development of beehive-ginger/sisal polyester hybrid composite material that have application in building and furniture industries. The effect of different loadings of 100/0, 90/10, 80/20, 70/30, 60/40 and 50/50 on the mechanical properties such as tensile strength, impact strength, flexural strength and hardness of beehive-ginger/sisal fiber reinforced polyester hybrid composites were determined according to ASTM standards and the results were obtained as 75.29 MPa, 70.69kJ/m², 183.2 MPa and 87.9 shore D respectively. Water absorption of the material were obtained as 12.65, 72.90, 56.80, 52.74, 40.70, 35.93 and 23.71% respectively.

KEYWORDS:

Reinforced composites, Polyester, Methyl ethyl ketone peroxide, Cobalt naphthanate, Tensile strength, Flexural strength

1.0 INTRODUCTION

Composites are multipurpose material that provide properties that are lacking in other materials (1). They are developed using different methods such as hand lay-up etc via combination of two or more materials of different compositions (2). The reinforcement in these materials can be natural or synthetic and sometimes combination of the two (3).

Synthetic fiber reinforced composites are commercially appealing because of their outstanding properties to meet different diversity of applications. However, these materials caused environmental imbalance during production and upon disposal (4). Because of this reason, couple with the growing rate of environmental challenges as a result of synthetic composites materials being discharged on environment, the attention of the researchers had been shifted toward the use of renewable and recyclable natural fibers as reinforcement to develop eco-friendly materials which can be used in different industries (5). This has influenced the increasing demand for lighter-weight, stiffer, fire repellent and less expensive materials for industrial application (6).

Lignocelulosic fibers reinforced polymer composites has the potential and opportunity to reduce the environmental problems via incorporation of natural fibers such as sisal, beehive-ginger, wood particles etc., in place of synthetic fibers such as aramid, carbon glass in composite development (7). Despite the benefits in mono fiber reinforced composites, they can still not be used in some areas of applications (8). Therefore, the need to develop a novel material that plays vital role in most of engineering applications.

Although many research had been carried out and still on-going on the use of cellulosic fibers as reinforcement in composite, there are lot of fibers that are not explored in which beehive-ginger fiber is one of them. The Beehive-ginger fiber plant (*Zingiber Spectablis*) is native to many countries: New Guinea, Southeast Asia, Nigeria etc., and belongs to grass fibers family like bamboo, India grass, bagasse etc. For the reason, this study focused on development of beehive-ginger/sisal fiber reinforced polyester hybrid composite that can be used in various areas.

2.0 MATERIALS AND METHODS



2.1 Material

Unsaturated polyester resin, Cobalt naphthenate and methyl ethyl ketone peroxide (MEKP) and glass-fiber were procured from Tony Nigeria Enterprise Ojota, Lagos State. Beehive-ginger (*Zingiber spectabilis*) fibers were sourced at Iyamoye, Ijumu L.G.A, Kogi State, while the Sisal fibers were extracted from its plant gotten from National Research Institute for Chemical Technology (NARICT), Zaria.

2.2 METHODOLOGY

2.2.1 Beehive-ginger/ Sisal Fibers Extraction

The beehive-ginger fibers were extracted via local mechanical decortications, cleaned, washed, and sun dried for 7 hours to remove the moisture content. Also, sisal fibers were extracted from the leaves of the plant *Agave sisalana*, using the local extraction method. This involves gradual hitting of the leaves with stick and subsequently sun dried for 10 minutes. The hitting process stopped when almost all the impurities: lignin, wax, pectin and other compounds binding the fibers together had been removed. Finally, the extracted fibers were sun dried for 5 hours and hence combed in order to stretch them perfectly

2.2.2 Mould preparation

A locally fabricated mould of dimensions 120 x 80 x 6mm was used in this research. The mould cavity was cleaned and then coated with releasing agent for easy demolding of the developed composite. The fabrication was carried out by hand lay-up and compression technique.

2.2.3 Fibers Preparation

The 70 grams of beehive-ginger and 45 grams of sisal extracted were chopped into 20 mm length. Based on the following ratio: 100/0, 90/10, 80/20, 70/30, 60/40, 50/50 and 0/100, total fiber loading of 15 grams established was divided into 15/0, 1.5/13.5, 3/12, 4.5/10.5, 6/9, 7.5/7.5 and 0/15 grams respectively.

3.0 BEEHIVE-GINGER/SISAL POLYESTER HYBRID COMPOSITE PREPARATION

Based on 15 wt% of total loading initially established, 15g of beehive-ginger were measured and loaded randomly in prepared mold. Load of 10 kN were applied for 10 minutes, after which the estimated solution of unsaturated polyester, (prepared by adding 1ml of MEKP and 1ml cobalt naphthenate to a calculated amount of unsaturated polyester), was pure on the fiber inside the mold, spread with brush and then allow to gel for 1 hour before subjecting it to a load of 10 kN under hydraulic press for 24 hours. Further post curing of the composite occurred in an oven operating at 70 °C for another 2 hours to enhance complete curing. Above procedures were repeated on 1.5/13.5, 3/12, 4.5/10.5, 6/9, 7.5/7.5 and 0/15 grams respectively. The composites formed were characterized.

3.1 Determination of Mechanical Properties of Developed Hybrid Composite

3.1.1 Tensile strength test

Tensile strength of the composite specimens was determined according to ASTM D638 using an Instron Machine Model 3369, System Number 3369K1781, Maximum speed 500mm/min, Capacity 50 kN, located at Center for Energy Research and Development (CERD) OAU Ile-Ife(9).

3.1.2 Impact strength test

The impact test was conducted according to ASTM D256 using the charpy V-notch impact testing machine. The dimensions, gauge length and V-notch were chosen according to the standard. Flexural strength of the hybrid composite specimens(10).

3.1.3 Flexural test.

The flexural test was carried out based on ASTM D790 an Enerpac universal material testing machine located at the Department of Mechanical Engineering, Ahmadu Bello University Zaria. The flexural modulus (MOR), was estimated using Equation 5 (10).

$$MOR = \frac{3Px}{2ht^2} \quad 5$$

Where, x is the span length of the sample (gauge length). P is the load applied; h and t are the width and thickness of the specimen respectively

3.1.4 Water absorption test

The water absorption test was conducted using the procedure outlined according to ASTM D570-98.



Equation 6 was used to establish the percent water absorbed.

$$M_t = \frac{M_a - M_b}{M_b} \times 100\% \quad 6$$

where m_b is initial weight of the dry sample and m_a is the final weight of the wet sample.

3.1.5 Hardness test

The hardness test was conducted according to ASTM D2240 using a Shore Duro-meter testing

machine. The dimensions and gauge length were chosen according to the standard. The sample was cut into 25 x 25 x 10 mm square strips for the test that was performed by gradually pressing presser foot of the diamond-tipped indenter which penetrated to a certain depth on the specimen (9).

4.0 RESULTS AND DISCUSSION

4.1 Effect of beehive-ginger-sisal fibers loading on impact strength of the composite

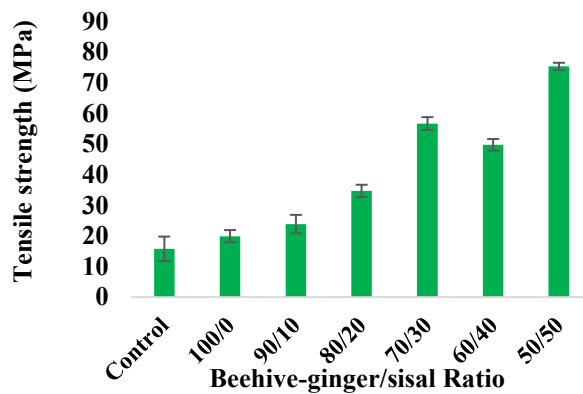


Figure 1: Effect of Beehive-ginger/sisal hybridization on Tensile strength of the composite

The unreinforced unsaturated polyester plate has the lowest average tensile strength, when compared with 100 wt% beehive-ginger reinforced polyester composite and 10,20,30 and 40 wt% sisal reinforced polyester hybrid composites. The mono fiber reinforced composite (100 wt% beehive fiber) was 91.80% higher when compared with unreinforced polyester plate. The increase in the tensile strength observed between the reinforced composites and unreinforced polyester plate might be as a result of good adhesion of the fiber to the matrix. The 50/50 wt% beehive-ginger/sisal fibers

reinforced polyester hybrid composite has the highest tensile strength of 75.29 MPa, which is 377.42% better than unreinforced polyester plate.

The 65.29 MPa obtained at 50 wt% of sisal was higher the optimal value of 10.4 MPa for Dum palm fiber-polyester composites (11) but lower when compared with 255 MPa reported by (12) at 50:50 ratios for sisal-glass fiber reinforced epoxy composite. The variations observed could be associated with the difference in the matrix and fiber type used.

4.2 Effect of beehive-ginger-sisal fibers loading on impact strength of the composite



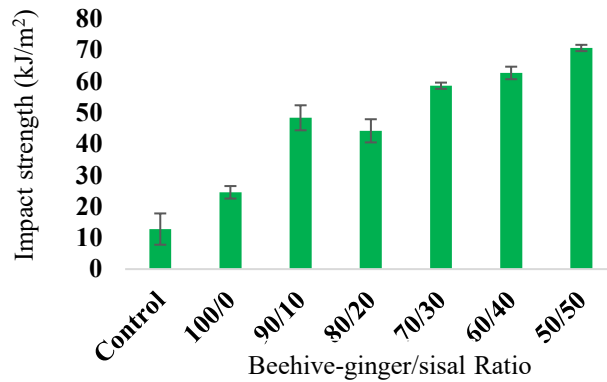


Figure 2: Effect of beehive-ginger/sisal hybridization on the Impact strength of the composite

The effect of beehive-ginger/sisal fiber on impact strength of the composite is shown in Figure 2. As the percentages of sisal content increases, there is remarkable improvement in the impact strength of the hybrid composite when compared the value with unreinforced polyester plate. The hybrid composite of 50:50 fibers reinforcements exhibited the highest impact strength of 70.69 kJ/m² which is 452.27% higher than unreinforced polyester plate and 187.94%, 46.14% and 12.72% higher than the impact strength value obtained from 100:0, 90:10,

and 60:40 composites respectively. These significant improvements in the impact strengths of the composites with increase in sisal fiber content may be due to a better resistance property of the sisal as compared to beehive-ginger fiber (13).

4.3 Effect of beehive-ginger-sisal fiber loading on flexural strength of composite

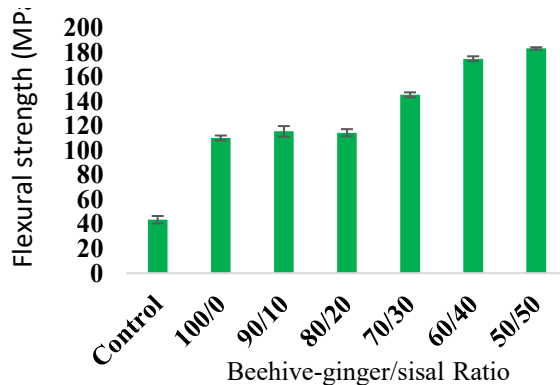


Figure 3: Effect of beehive-ginger/sisal hybridization on the Flexural strength of the composite

Figure 3 shows the effect of beehive-ginger/sisal fiber loading on the flexural strength of the hybrid composite. It was observed that the unreinforced polyester plate has the lowest flexural strength of 43.60 MPa. On addition of the fiber, there was significant increase in flexural strength of the composite. The major reason for this improvement might be attributed to the favourable entanglement of the polymer chain because of proper interlocking of fiber and the matrix with increase in fiber content (14). The composites with 50:50 fiber ratios gave the highest flexural strength of 183.20 MPa.

This is 320.18% higher than the un-reinforced polyester plate and 65.49%, 58.48%, 60.0%, 25.99% and 4.81% higher than 100:0, 90:10, 80:20, 70:30, and 50:50 composites. This observed result is attributed to good fiber - fiber interactions in the composite (10).

The observed result of 183.20 MPa obtained at 50:50 fiber ratio in this study is higher than 45.77 MPa reported by (11) on luffa fiber reinforced polyester composite at the same ratio but lower than 200.80 MPa reported by (12) at 20:20 sisal/glass



fiber for sisal/glass fiber reinforced polyester composite. The variation of loading, nature of the reinforcement, fabrication, and fiber-matrix interaction could be the cause of the observed variations in the results (15).

4.4 Effect of beehive-ginger-sisal fibers loading on the hardness of the composite

The effect of Beehive-ginger/sisal fiber ratio on the hardness of the Composite is showed in figure 4. As the sisal fiber contents increasing, the degree of penetration of the indenter into the composite material decreases due to increase in hardness of the material. The highest value of 87.9 Shore-D was obtained at 50:50 beehive-ginger/sisal fiber ratios which is 133.16% higher when compared with unreinforced polyester plate and 66.79%, 32.58% and 16.27% higher than 100:0, 80:20, and 60:40 reinforced composites respectively. This significant improvement with increase in sisal fiber content

4.5 Effect of beehive-ginger-sisal fibers loading on water absorption of the composite

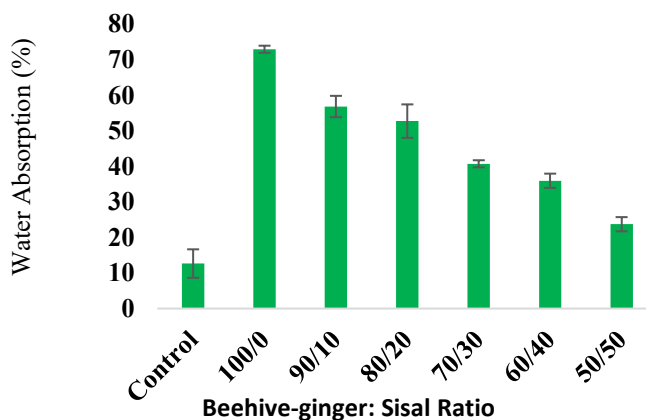


Figure 5: Effect of Beehive-ginger/sisal hybridization on the Water absorption of the Composite

Figure 5 shows the beehive-ginger/sisal fiber loading effect on the water absorption of the hybrid composite. There was a clear linear decrease in the percentage of water absorbed by the composite with decrease in beehive-ginger fiber content. The observed sharp increase in water absorption in beehive-ginger composite may be due to high hydrophilic nature of beehive-ginger fiber. The

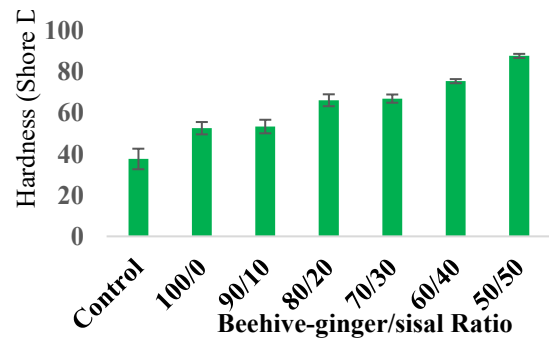


Figure 4: Effect of beehive-ginger/sisal hybridization on the Hardness of the composite

might be due to the proper distribution of the test load within the fibers and the stiffness of sisal fiber(12)

The highest hardness value of 87.9 shore D recorded in this study at 50:50 beehive-ginger/sisal composite was higher than the 85.33 shore D reported by (9) at 50:50 sisal/baobab LDPE hybrid composite. The observed changes could be associated with the nature of the fibers, difference in matrix used and interfacial bonding of the fiber to the matrix (10).

observed reduction in water absorption in the case of hybrid composites could be attributed to proper binding of the fiber to the matrix at the interface (16).

This study showed higher water absorption of 25.90% when compared with 2.58567% reported by (10) at 50:50 Okro/glass fiber ratios composite. The



observed result is attributed to the difference in fiber used and proper adhesion of the fiber to the matrix(17).

5.0 CONCLUSIONS

The mechanical properties of beehive-ginger/sisal fibers reinforced polyester hybrid composites was investigated in this study, by varying beehive-ginger/sisal fibers loading using hybridization ratio of 100:0,90:10, 80:20, 70:30, 60:40, 50:50. Based on the results obtained from the study, the following conclusions were made: Beehive-ginger and Sisal fibres were successfully used as reinforcement to develop polyester hybrid composites.

The baobab/sisal fibres hybridization ratio of 50:50 exhibited the highest mechanical properties, with tensile strength, flexural strength, impact strength and hardness as 75.29 MPa, 183.20 MPa, 70.69 kJ/m and 87.90 Shore D respectively. The water absorption capacity of 23.70% was obtained at the same ratio. Based on ASTM standard requirements and results obtained from this study, the developed composite can be used in building and furniture industries.

6.0 REFERENCES

1. R. Venkatesh *et al.*, Effect of fiber layer formation on mechanical and wear properties of natural fiber filled epoxy hybrid composites. *Heliyon* **9**, (2023).
2. L. Natrayan *et al.*, Statistical experiment analysis of wear and mechanical behaviour of abaca/sisal fiber-based hybrid composites under liquid nitrogen environment. (2023).
3. S. N. Sarmin, in *Green Hybrid Composite in Engineering and Non-Engineering Applications*. (Springer, 2023), pp. 15-29.
4. K. Sadashiva, K. Purushothama, Physical and Mechanical Properties of Bio Based Natural Hybrid Composites. *J. Mater. Environ. Sci.*, *14* (1), 131 **140**, (2023).
5. S. Baladivakar, M. Starvin, J. B. Raj, Performance Evaluation of Natural Composites Made from Banyan and Cotton Fibers for Sustainable Thermal Insulation Applications. *Journal of Natural Fibers* **20**, 2123881 (2023).
6. V. U. Siddiqui, S. M. Sapuan, T. Jamal, Mechanical, Morphological, and Fire Behaviors of Sugar Palm/Glass Fiber Reinforced Epoxy Hybrid Composites. *Pertanika Journal of Science & Technology* **31**, (2023).
7. M. El-Wazery, M. El-Elamy, S. Zoalfakar, Mechanical properties of glass fiber reinforced polyester composites. *International journal of applied science and engineering* **14**, 121-131 (2017).
8. R. P. Kumar, G. K. Chandan, R. Ramamoorthi, Fabrication and testing of natural fiber hybrid composites. *International Journal of Engineering Research* **5**, 285-288 (2016).
9. U. Shehu, O. Aponbiede, T. Ause, E. Obiodunukwe, Effect of particle size on the properties of polyester/palm kernel shell (PKS) particulate composites. *J. Mater. Environ. Sci* **5**, 366-373 (2014).
10. U. Sule, M. Isa, A. Ameh, O. Ajayi, O. Omorogbe, Studies on the properties of short okra/glass fibers reinforced epoxy hybrid composites. *The International Journal of Science and Technoledge* **2**, 260 (2014).
11. S. Aminu, O. Sunmonu, K. Bello, Effect of Chemical Modification on Mechanical Properties of Luffa Guord and Dum Palm Reinforced Composite. *Standard Scientific Research and Essays* **2**, 541-545 (2014).
12. S. Rangunath, C. Velmurugan, T. Kannan, S. Thirugnanam, Evaluation of tensile, flexural and impact properties on sisal/glass fiber reinforced polymer hybrid composites. (2018).
13. K. Palanikumar, M. Ramesh, K. Hemachandra Reddy, Experimental investigation on the mechanical properties of green hybrid sisal and glass fiber reinforced polymer composites. *Journal of Natural Fibers* **13**, 321-331 (2016).
14. B. Katla, W. A. Ravindra, S. K. Kota, S. Raju, RAP-added SMA mixtures: How do they fare? *Journal of Materials in Civil Engineering* **33**, 04021199 (2021).



15. M. Maache, A. Bezazi, S. Amroune, F. Scarpa, A. Dufresne, Characterization of a novel natural cellulosic fiber from *Juncus effusus* L. *Carbohydrate polymers* **171**, 163-172 (2017).
16. I. i. Mukhtar, Z. Leman, E. S. Zainudin, M. R. Ishak, Hybrid and nonhybrid laminate composites of sugar palm and glass fibre-reinforced polypropylene: Effect of alkali and sodium bicarbonate treatments. *International Journal of Polymer Science* **2019**, (2019).
17. M. Thiruchitrabalam, D. Shanmugam, Influence of pre-treatments on the mechanical properties of palmyra palm leaf stalk fiber–polyester composites. *Journal of Reinforced Plastics and Composites* **31**, 1400-1414 (2012).



P119 - EFFECT OF DIFFERENT PROCESSING METHODS ON THE PROXIMATE AND FUNCTIONAL PROPERTIES OF *DETARIUM SENEGALENSE* (TALLOW) SEED FLOUR

*¹Adamu H., *²Nzelibe, H.C., ³Adamu, Z., ⁴Arekemase S.O., ¹Abubakar, F.S., ¹Shehu, A.B.

¹Food Technology and Home Economics Department, NAERLS/A.B.U Zaria, Kaduna State Nigeria

²Department of Biochemistry Ahmadu Bello University Zaria, Kaduna State Nigeria

³Department of Biochemistry Federal University of Technology Minna, Niger State Nigeria

⁴Department of Petrochemical, Energy Division, National Research Institute for Chemical Technology, Zaria.

*Corresponding Author: ahussaina45@gmail.com

ABSTRACT

Detarium senegalense JF Gmelin (Caesalpiniaceae) seed, commonly known as tallow, it is used traditionally in food, medicine and other commodities. Despite its high protein content, its seed is under-utilized due to limited information on its nutritional and functional properties. This study investigated the effect of different processing methods on the proximate composition and functional properties of *Detarium senegalense* seed flour. Freshly purchased seeds were washed and grouped into unprocessed (raw) and processed (soaked, boiled, roasted, autoclaved and microwaved). The samples were analyzed using standard procedures. Data obtained were statistically analyzed using Analysis of variance (ANOVA). Duncan's multiple range tests were used to compare the means. Significance was accepted at ($p \leq 0.05$). Moisture contents ranged from 7.83% to 11.47%, ash contents ranged from 1.97% to 2.36% and protein contents ranged from 16.43% to 19.84%. The highest value for fat was obtained in microwaved samples 1.76% while the lowest was obtained in boiled samples 1.68%. Crude fibre was highest with roasting (2.06%) while boiling gave the lowest value 1.87%. Carbohydrate contents ranged from 64.52% to 68.69%. The oil and water absorption capacity, swelling index, emulsion capacity and bulk density were significantly ($p \leq 0.05$) increased by boiling, roasting and microwaving. The soaked and boiling method of processing is the best as it enhances protein and functional properties higher than the other methods. The properties of *Detarium senegalense* seed flours evaluated suggest its potential for application as both nutritional supplements and functional ingredients in the preparation of baked and complementary food products.

KEYWORDS:

Proximate composition, functional properties, *Detarium senegalense*.

INTRODUCTION

Studies on the utilization of legumes continue to gain attention due to the worldwide increasing demand for cheap and acceptable dietary protein, particularly for the low-income groups. The need to search for unconventional legumes therefore attracts research in this direction (Balogun and Olatidoye, 2012). *Detarium senegalense* is one of such unconventional legumes which studies have shown that together with other conventional legumes can be used for combating protein malnutrition prevalent in the third world (Ndulaka *et al.*, 2017). It is an important legume found in West and Central Africa; it belongs to the family *Caesalpiniaceae*, *Phylum spermatophyte* and the order *Fabaceae* (Dossa *et al.*, 2020). It is known by various tribal

names as 'Ofor' (Igbo), 'Taura' (Hausa) and 'Ogbogbo' (Yoruba) (Nwozo *et al.*, 2016). It is also a useful plant that finds applications in food, medicine and other commodities (Akah *et al.*, 2012, Dossa *et al.*, 2020). There is limited information on the effects of processing on the nutritional properties and functional properties of this seed flours which could improve its nutritional value and therefore their utilization (Peters and Olapade, 2018).

This experimental study was therefore carried out to determine the effect of soaking, boiling, roasting, autoclaving and microwaving on the proximate composition and functional properties of *Detarium Senegalense* seed flour.



MATERIALS AND METHODS

Seed collection and processing: The seeds of *Detarium senegalense* were obtained from a private farm in Umuaga, Udi Local Government Area Enugu State and identified and authenticated at the herbarium Unit, Botany Department, Ahmadu Bello University, Zaria, Kaduna State.

Six Kilograms of *Detarium Senegalense* seeds was divided into 6 equal portions. One portion was left unprocessed and the other portions were (1) soaked in de-ionized water (1:3) at room temperature (25±2 °C) for 12 hours (2) boiled in a seed to water ratio of 1:10 w/v for 30 min (3) roasted at temperature of 120°C for 40 min in a hot air oven (Model DHG 9101 ISA) (4) autoclaved in a seed to water ratio of (1:10, w/v) for 20 minutes at a temperature of 121°C and pressure of 15 atmospheres in an autoclave (Model 75HG, Britain, UK) (5) microwaved in a seed to water ratio of 1:10, w/v for 20 min in a microwave oven (Model 4915, Philips). All samples were each dehulled, spread on the trays

and dried in a hot air oven (Model DHA 9101 ISA) at 60°C for 8 hours, ground into flour in an attrition mill and sieved through a 500-micron mesh sieve and packaged (Adamu and Nzelibe, 2022)

Proximate analysis: proximate composition (moisture, ash, crude protein, crude fat and crude fiber) of the unprocessed and processed *Detarium senegalense* samples were determined by the method of (AOAC, 2006) while carbohydrate content was determined by difference (AOAC, 1990).

Functional Properties: The water absorption capacity, oil absorption capacity, swelling capacity, foaming capacity and bulk density were determined by the method describe by (Yellavila *et al.*, 2015).

Statistical analysis

The analysis was carried out in triplicates for all determinations. The data were analyzed by one-way analysis of variance (ANOVA). A multiple comparison procedure of the treatment means was performed by Duncan's multiple range test with $P < 0.05$ as the accepted level of significance.

RESULTS

Table 1: Effect of Processing on the Proximate Composition of Detarium senegalense Seed Flour

Parameters (%)	Unprocessed	Soaking	Boiling	Roasting	Autoclave	Microwave
Moisture content	9.77±0.03 ^c	10.17±0.02 ^d	11.4±70.04 ^e	7.83±0.01 ^a	9.68±0.05 ^b	9.70±0.02 ^b
Ash content	2.77±0.02 ^c	2.73±0.04 ^e	1.97±0.04 ^a	2.28±0.01 ^b	2.36±0.05 ^c	2.25±0.03 ^b
Crude protein	21.80±0.29 ^f	20.43±0.04 ^e	16.43±0.85 ^a	17.41±0.50 ^b	19.84±0.60 ^d	19.35±0.73 ^e
Crude fat	1.93±0.07 ^c	1.81±0.01 ^c	1.68±0.01 ^a	1.70±0.06 ^{ab}	1.73±0.05 ^b	1.76±0.01 ^c
Crude fiber	2.15±0.12 ^d	2.16±0.05 ^b	1.87±0.16 ^a	2.06±0.17 ^c	1.89±0.11 ^{ab}	1.92±0.08 ^b
Carbohydrate	61.58±2.89 ^a	62.70±0.07 ^b	66.55±5.93 ^c	68.69±4.56 ^f	64.52±3.18 ^c	65.03±5.58 ^d

Results are expressed as Mean ± SD (n=3).

Values in the same row with different superscripts are significantly ($P < 0.05$) different.

Table 2: Effect of Processing on the Functional Properties of *Detarium senegalense* Seed Flour

Parameters	Unprocessed	Soaked	Boiled	Roasted	Autoclave Microwave	Microwaved
WAC(g/g)	1.33±0.04 ^{ab}	1.29±0.07 ^a	1.59±0.09 ^c	1.27±0.06 ^a	1.35±0.04 ^{ab} 1.46±0.11 ^b	1.46±0.11 ^b



SI	2.19±0.07 ^b	1.93±0.10 ^a	2.06±0.04 ^{ab}	2.05±0.06 ^{ab}	1.93±0.13 ^a 2.14±0.04 ^b	2.14±0.04 ^b
FC (%)	14.68±0.16 ^d	13.29±0.17 ^c	11.82±0.28 ^a	12.69±0.16 ^b	11.77±0.12 ^a 12.58±0.18 ^b	12.58±0.18 ^b
BD(g/ml)	0.65±0.07 ^a	0.63±0.03 ^a	0.60±0.12 ^a	0.57±0.12 ^a	0.57±0.05 ^a 0.58±0.06 ^a	0.58±0.06 ^a
EC (%)	23.32±1.58 ^c	21.77±0.19 ^b	19.29±0.23 ^a	19.41±0.03 ^a	18.77±0.14 ^a 18.32±0.12 ^a	18.32±0.12 ^a
OAC(g/g)	1.17±0.04 ^b	1.06±0.03 ^{ab}	1.09±0.18 ^{ab}	0.98±0.03 ^a	1.05±0.04 ^{ab} 1.02±0.07 ^{ab}	1.02±0.07 ^{ab}

Results are presented as Mean ± SD (n=3).

Values across the rows with different superscripts are significantly different (P< 0.05).

WAC= water absorption capacity, SI=Swelling index, FC= Foaming capacity, BD=Bulk density, EC= Emulsion capacity, OAC=Oil absorption capacity

DISCUSSION

Moisture content is critical for predicting the shelf life of food products. In this study, the moisture contents of *Detarium senegalense* seed flours were found to be between 7.83 and 11.47% which is appreciable for the inactivation of microbial growth (Beruk, 2013). However, the higher moisture content in boiled and soaked could be attributed to the absorption of a large quantity of water by the seeds during boiling and soaking while the lower moisture content in roasting is expected and could be due to loss of water during roasting. These observations were in agreement with the report of Peters and Olapade (2017) where the boiled and soaked method had the highest moisture content and roasted the least. The variation in the ash contents of the various samples could be attributed to the leaching and degradation of food minerals during the processing of the seed (Babalola and Giwa, 2012). The high ash in the autoclave is suggestive of high retention of minerals just as it was reported that cooking under pressure (autoclaving) gave the lowest reduction in the elements Na, Mg and Fe, which may be attributed to cooking by steam only (Mubarak, 2005). The Protein composition of the raw and processed *Detarium senegalense* seed flour (16.43-21.80%) was higher than some legumes (*Mucuna flagelipes* 16.18%, *Detarium microcarpum* 16.02%, *Brachystegia eurycoma* 15.25% and *Afzelia africana* 15.20% (Ndulaka *et al.*, 2017). The denaturation of the protein matrix which took place during the heat-treated method could have reduced proteins in the autoclave, microwave, roasted and boiled samples which also makes it more palatable for human consumption (Nwosu *et al.*, 2011). Among the heat processed, autoclave and microwave methods showed higher amounts of protein than boiled and roasted. Khatoun and

Prakash (2004) reported that microwave cooking and pressure cooking do not affect the nutrient composition of eight different legumes studied. Fat is an important “vehicle” for fat-soluble vitamins and a high energy-yielding nutrient (Balogun and Olatidoye, 2012). This study showed that the seeds of *Detarium Senegalense* contain low crude fats (1.68-1.93%) like other legumes (Ndulaka *et al.*, 2017). The results showed that heat processed method significantly reduced fat which means that exposure to heat causes a reduction in fat probably because of loss of volatile fatty acids. Aside from low-fat content, the boiled also contain low fiber content, although fiber content of *Detarium senegalens* seed flours were reduced significantly (p<0.05) by all processing methods. These might be due to the degradation of fiber into simpler sugars initiated by endogenous enzymes. This observation is in agreement with the studies in chickpea, mungbean, kidney bean and quality protein maize-based complementary food (Beruk, 2013). The soaked method with the highest fiber content than the other methods implies a higher lowering of nutrient bioavailability while the boiled method with the lowest fiber content implied that boiling could have caused the soluble fiber such as pectin and gums to solubilize out in the boiling water more than in the other samples similar to the result of Amandikwa *et al.*, (2015) on processed *Detarium microcarpum* seed flour. Carbohydrate ranged from 61.58% to 68.69% favorable with the acceptable range mean values for legumes (20 to 60%) (Nwafor *et al.*, 2017), and is comparable to that of other legumes (Ndulaka *et al.*, 2017) but higher as compared to that of *C. ensiformis*, *Glycine max*, *Mucuna utilis* and *A. pavonina* (Nwafor *et al.*, 2017). The carbohydrate content indicated that the seeds of *Detarium Senegalense* can be considered a rich source of energy and can supply the daily energy requirements for the body in children and



adults (Balogun and Olatidoye, 2012). However, the heat-treated samples (roasted, boiled, microwaved and autoclaved) had higher carbohydrate contents than the non-heat-treated sample (unprocessed and soaked) due to increased solubility during thermal processing. The results obtained were in agreement with the report of Adegunwa *et al* (2012).

Functional properties have been reported to be improved through processing methods such as fermentation, sprouting, cooking, and soaking (Amandikwa *et al.*, 2015). Findings from this study revealed that the boiled method of processing possesses better water and oil absorption capacity than the other methods. This is in contrast with the work of Peter and Olapade (2017) where roasted samples showed higher water and oil absorption capacity. The high water and oil absorption capacity suggests the boiled comprises of high polar amino acid and high hydrophobic residue on the protein molecules, respectively. Therefore, the boiling method could be used for food formulation such as baked products, sausages, cheese, meat extenders and soups (Olaofe *et al.*, 1998). The high oil absorption capacity also makes the flours suitable for facilitating enhancement in flavour and mouth feel when used in food preparation (Beruk 2013). The soaking method possesses a high foaming capacity. This could be attributed to its high protein. High protein content increases viscosity which encourages the formation of cohesive protein layers (Amandikwa *et al.*, 2015). Interestingly, the soaked sample has a high emulsion capacity compared to the other methods sample; this could imply that it contains both polar and nonpolar amino acids which

REFERENCES

- Adamu H and Nzelibe H.C. (2022). Effect of Different Processing Methods on the Amino acid profile, Mineral and Antinutrient content of *Detarium senegalense* (tallow) Seed [Flour Journal of Agriculture and Agricultural Technology](#), 8(2), 12-14.
- Adegunwa M.O., Adebowale A.A. and Solano E.O. (2012). Effect of Thermal Processing on the Biochemical Composition, Antinutritional Factors and Functional Properties of Beniseed (*Sesamum indicum*) Flour. *American Journal of Biochemistry and Molecular Biology*, 2(3), 175-182.
- Akah, P., Nworu, C., Mbaoji, F., Nwabunike, I. and Onyeto, C. (2012). Genus *Detarium*: Ethnomedicinal, Phytochemical and Pharmacological Profile. *Phytopharmacology*, 3(2), 367-375.
- Amandikwa, C., Bede, E.N., Eluchie, C.N. (2017). Effects of Processing Methods on Proximate Composition, Mineral Content and Functional Properties of Ofor (*Detarium microcarpum*) Seed Flour. *International Journal of Science and Research*, 6(5), 2319-7064
- AOAC (2006) Official Methods of Analysis. 15th edition, Association of Official Analytical Chemists, Washington DC.
- AOAC (1990) Official Methods of Analysis. Association of Official Analytical Chemists.
- Babalola, R. O. and Giwa, O. E. (2012). Effect of fermentation on nutritional and antinutritional properties of fermenting Soy beans and the antagonistic effect of the

increases the interaction between both oil and water molecules. Proteins can function as an emulsifier since they have both hydrophobic and hydrophilic properties that can interact with oil and water in food systems (Mao and Hua, 2012). Bulk density explains the packaging capacity of food material. The low bulk density of all the methods except soaked implies that less quantity of them would be packaged in constant volume, therefore, ensuring economic package. The lower bulk density value in this study would also give an advantage in the formulation of complementary foods as it promotes easy digestion of food materials (Beruk 2013). Microwave exhibited a higher swelling index than the other samples. The Swelling index determines the amount of water that would be absorbed and the degree of swelling within a stipulated time. The Swelling index is influenced by temperature, water availability, carbohydrate, and protein (Yellavila *et al.*, 2015). The high swelling index of the microwave could be as a result of high protein content.

CONCLUSION

Different processing methods adopted in this study have been proven to have significant effects on the nutritional and functional properties of *Detarium senegalense* seed flour, a highly nutritious and neglected legume. Furthermore, this study revealed that the seeds, when properly processed, have high nutritional values that can be exploited and considered as an alternative source of nutrients to reduce malnutrition among economically weaker categories of people in developing countries.



- fermenting organism on selected pathogens. *International Research Journal of Microbiology*, 3(10), 333-338.
- Balogun, I.O. and Olatidoye, O.P. (2012). Chemical composition and nutritional evaluation of velvet bean seeds (*Mucuna utilis*) for domestic consumption and industrial utilization in Nigeria. *Pakistan Journal of Nutrition*, 11, 116-122.
- Beruk, B (2013). Formulation of Nutritionally Improved Complementary Food: The case of Shebedino Woreda, Southern Ethiopia. MSc Thesis, Hawassa University, Hawassa.110pp.
- Beruk, B. D (2015). Effect of Soaking and Germination on Proximate Composition, Mineral Bioavailability and Functional Properties of Chickpea Flour. *Food and Public Health*, 5(4), 108-113
- Dossa, B.A.K., Ouinsavi, C., Towanou, H. and Sourou, B.N. (2020). Knowledge Points and Research Perspectives on *Detarium Senegalense*, A Vulnerable Species in Benin” *International Journal of Research Studies in Biosciences (IJRSB)*, 8(2), 4- 12. DOI: <http://dx.doi.org/10.20431/2349-0365.0802002>
- Khatoon, N., Prakash, J., 2004. Nutritional Quality of Microwave-Cooked and Pressure-Cooked Legumes. *International Journal of Food Sciences and Nutrition*, 55, 441–448.
- Mao, X. and Hua, Y. (2012). Composition, Structure and Functional Properties of Protein Concentrates and Isolates Produced from Walnut (*Juglans regia* L.). *International Journal of Molecular Science*. 13, 1561– 1581
- Mubarak, A.E. (2005). Nutritional Composition and Anti-nutritional Factors of Mung bean Seeds (*Phaseolus aureus*) as Affected by Some Home Traditional Processes. *Food Chemistry* 89, 489–495
- Ndulaka, J.C., Ekaiko, M.U., Onuh, E.F and Okoro, O.A. (2017). Comparative Studies on the Nutritional and Anti – Nutritional Properties of Indigenous Seeds Used as Soup Thickeners in South-East Nigeria. *Journal of Biotechnology and Biochemistry*,3(5), 39-44
- Nwafor,F.I., Egonu,S.N., Nweze, N.Oand OhabuenyiS.N (2017). Effect of Processing Methods on the Nutritional Values and Anti-nutritive Factors of *Adenanthera pavonina* L. (Fabaceae) Seeds. *African Journal of Biotechnology*, 16(3), 106-112.
- Nwosu, J. (2011). The Effect of Storage Condition on the Rheological/Functional Properties of Soup Thickner *Mucuna sloanei* (Ukpo). *Researcher*, 3, 6-10.
- Nwozo, S O, Adebowale, T.L. and Oyinloye, B.E. (2016). Defatted *Detarium senegalense* seed-Based Diet Alters Lipid Profile, Antioxidants Level and Sperm Morphology in Male Albino Rats. *International Journal of Biological and Chemical Science* 10(3), 928-943
- Olaofe, O., Arogundad, L.A., Adeyeye, E.I. and Falusi, O.M. (1998). Composition and food of the variegated grasshopper. *Tropical Science*, 38, 233-237.
- Peters, D.P. and Olapade, A. A. (2018). Effects of Some Processing Methods on Antinutritional, Functional and Pasting Characteristics of *Detarium microcarpum* Seed Flours. *Annals. Food Science and Technology*, 19(1) 69-78.
- Yellavila, S.B., Agbenorhevi, J.K., Asibuo, J.Y. and Sampson, G.O. (2015). Proximate Composition, Minerals Content and Functional Properties of Five Lima Bean Accessions. *Journal of Food Security* 3(3), 69– 74



P120 - ISOLATION AND AUTHENTICATION OF RHIZOBIA FROM RHIZOSPHERE AND ROOT NODULES OF SOYBEAN PLANTS

Mohammed H. A^{1,2}., Atta H. I²., Machido D. A².

¹National Research Institute for Chemical Technology, PMB 1052, Basawa, Zaria

²Ahmadu Bello University, Zaria

Corresponding author email: hauwa3014@gmail.com

ABSTRACT

A significant challenge in many developing countries is the limited nitrogen (N) content in the soil, which hampers sustainable and high crop production. The nitrogen-fixing symbiosis between legumes and rhizobia plays a crucial role in providing an adequate supply of nitrogen for leguminous and subsequent non-leguminous crops. To develop effective bioinoculants, it is essential to characterize rhizobia strains. This study aimed to isolate and confirm the presence of rhizobia that form nodules on soybeans and were previously present in soybean-cultivated fields. Twenty rhizobia isolates were obtained from soybean root nodules and soil samples taken from farmlands. These isolates were cultured on Bradyrhizobium Jopanicum Selective Medium (BJSM) and then sub cultured on plates of Yeast Extract Mannitol Agar (YEMA). Fourteen isolates were authenticated as rhizobia since they successfully formed nodules between 3-17 nodules on soybean roots grown in sterile river sand.

KEYWORDS

Nitrogen, Bradyrhizobia, Rhizobia, Nodule, Yeast Mannitol Agar

1.0 INTRODUCTION

Rhizobium is a type of soil microorganism that can thrive on plant remains (as saprophytes), inside plants (as endophytes), or in proximity to plant roots (as rhizo-bacteria) (Geniaux *et al.*, 1993). Rhizobia play a vital role in supplying nitrogen to various soil ecosystems by fixing nitrogen in collaboration with legumes. They are categorized into slow (*Bradyrhizobium*) and fast-growing rhizobia based on their nitrogen-fixing capabilities. The process of rhizobia colonizing the rhizosphere, infecting roots, and fixing nitrogen contributes to plant growth and enhances grain yield (Appunu *et al.*, 2008). The method of capturing atmospheric nitrogen for plant assimilation is not widely utilized by small-scale African farmers, mainly due to their lack of understanding about its mechanism and proper management (Rao And Ansari, 2013) For instance, although 95% of farmers in East and Southern Africa were aware of legume root nodules, only 26% recognized their benefits (Woomer *et al.*, 2014)

According to Dilworth (2016), stated that one way to enhance the process is by discovering native rhizobia strains that possess excellent symbiotic and competitive capabilities, and incorporating them in large quantities into inoculants. This approach leverages the diverse range of indigenous rhizobia populations (Rao and Ansari, 2013) The natural adaptability of these indigenous rhizobia to their surroundings enhances their ability to compete and thrive, particularly in saprophytic conditions (Maureen, 2013). Continuously identifying new and superior isolates provides an opportunity to enhance biological nitrogen fixation with specific geographical precision, as reported by Appunu and Dhar (2008). Consequently, maintaining a broad variety of rhizobia isolates ensures a sustainable supply of strains for future commercial applications (Appunu *et al.*, 2008).

The primary method of biological nitrogen fixation is performed by symbiotic nitrogen-fixing organisms like rhizobium, which holds significant agricultural and ecological



importance (Peoples *et al.*, 1995). Some previous studies suggest that biological nitrogen fixation could be a viable solution for Nigerian soybean farmers, given that soybean crops can fix between 54 to 300 kg N/ha when associated with *Bradyrhizobium*. This process contributes over 15 kg N/ha to the soil where soybeans are grown (Onwualu, 2008). Currently, nitrogen needs in agriculture are primarily met through industrially produced nitrogen fertilizers, leading to ecological issues and health concerns (Iwe, 2003).

Biological nitrogen fixation, facilitated by rhizobia interacting with leguminous plants, is a cost-effective and environmentally friendly approach (Dilworth, 2016). Research has shown that the presence of rhizobia enhances plant productivity without adverse effects on human health and the environment as in the case of inorganic fertilizer (Machido *et al.*, 2011). Therefore, cultivating leguminous plants, which replenish atmospheric nitrogen through symbiosis with rhizobia, in rotation with non-leguminous plants is crucial for maintaining soil fertility (Abubakar, 2015). Thus, this study aims to isolate and authenticate native Nigerian Rhizobia from the rhizosphere and root nodules of soybean plants.

2.0 MATERIALS AND METHODS

2.1 Description of study area

Soil samples for this study were collected from three (3) agricultural farmlands at National research institute for chemical technology (NARICT) Basawa, Zaria. Kaduna state Nigeria. These farmlands were previously used for soybean cultivation and also from bed of a river located also at NARICT.

2.1.1 Sample collection and sample preparation

On each of the selected field, 2.0 kg soil samples were collected at five (5) different points in each field, 2.0 kg of soil sample from

0-15 cm soil depth using auger (Ofori, 2016). The samples were packaged in clean polythene bags labelled appropriately and transported to the laboratory at Department of Microbiology ABU, Zaria. The five (5) sub-samples were bulked together and mixed thoroughly to obtain one composite sample representing the field sampled. The composite soil sample was air dried, crushed and passed through a 2 mm sieve. The composite sample was stored in new black polythene bags for screen house studies (Machido, 2010).

Ten (10kg) samples of sand were also collected from the bed of a river using a hand trowel. The sand sample was placed in clean polythene bags as described earlier and also transported to the laboratory at Department of Microbiology, Ahmadu Bello University, Zaria. The sand sample was sun dried, passed through 2mm sieve and store in new black polythene bags for later use.

2.1.2 Planting of soybean to obtain root nodules

This was carried out following the plant trap technique described by Machido *et al.* (2011). Plastic pots (13cm x 8cm)/soil were perforated at the bottom. A Whatman filter paper was placed at the bottom of each plastic pot to prevent too much water from draining out and 1kg of the soil samples was weighed and placed into each pot. Single super phosphate and muriate of potash was applied to each pot at the rate of 15.9 mg/kg (P_2O_5) and 11.4 mg/kg (K_2O) per hectare. The treated soil was moistened until the water starts draining out and then left to stay overnight. Five clean seeds of soybean were sown in each pot at a depth of 2cm. The soil with the seeds was watered daily with the correct amount of water before and after the seedlings sprouted, over a span of 6 weeks. To minimize the loss of root nodules, the experimental plants were harvested by rinsing off the soil under a gentle stream of tap



water (Machido, 2010). The nodules formed on the roots of the trap plants were harvested for the isolation of *Rhizobium* spp.

2.1.3 Isolation of rhizobia from root nodules

This was carried out following a slightly modified method described by Nahar *et al.* (2017) (Nusrat *et al.*, 2017). Healthy, unbroken, and pink root nodules from plants grown in each of the soil samples were randomly selected for isolation of rhizobia. Selected nodules were surface sterilized in a laminar flow cabinet by immersion in ethanol (95% v/v) for 30 seconds followed by immersion in 3.8% sodium hypochlorite for 4-minute and finally were rinsed with six changes of sterile distilled water. The nodules were then crushed in 100 μ l of sterile normal saline using sterilized blunt forceps. One loopful of each nodule suspension was aseptically streaked onto freshly prepared plates of *Bradyrhizobium Japonicum* selective medium (BJSJ). The cultured plates were wrapped in aluminum foil and incubated aerobically at ambient temperature for 5 days. Also, to isolate rhizobia from the soil samples, serial dilution of the samples was carried out and 1mL of the 10^{-1} , 10^{-2} and 10^{-3} dilutions of the soil suspensions were inoculated on triplicate plates of freshly prepared *Bradyrhizobium japonicum* Selective Medium (BJSJ) (Tong and Sadowsky, 1994). Inoculated plates were then incubated aerobically at ambient temperature for 5 days.

2.2 Morphological characterization

Culture plates were examined for tiny white colonies typical of *Rhizobium* on BJSJ. Such colonies were then subculture on plates of Yeast Extracts Mannitol Agar (YEMA) and thereafter on slants of YEMA incubated at 28°C for further authentication.

2.2.1 Authentication of isolates

In this approach, the process of plant infection, specifically the ability of an isolate to infect and create nodules on soybean plant roots was used to serve as a criterion for identifying the isolate (Dilworth, 2016).

Preparation of inocula

The isolates, initially identified as *Bradyrhizobium* sp based on their cultural traits on BJSJ, were introduced into 50mL of freshly prepared Yeast Extract Mannitol Broth medium (YEMB) in 100ml conical flasks. They were then aerobically incubated on a rotary shaker at room temperature for 5 days. The broth cultures were preserved for the subsequent phase of the plant infection process (Pervin *et al.*, 2017).

Preparation of Sand culture of Soybean

This procedure included placing 1kg of river sand, prepared as previously mentioned, in perforated plastic pots with Whatman No 4 Filter paper at the bottom to prevent leakage. The sand was dampened with a nitrogen-free plant nutrient solution and left overnight. In each of these prepared sand cultures, five healthy, surface-sterilized soybean seeds were planted. The planted seeds were watered with nitrogen-free plant nutrient solution both before and after the seedlings emerged, spanning a period of fourteen days post-emergence (Dilworth, 2016). The pots containing the soybean seedlings were identified with labels matching the code numbers of the isolates to be confirmed. These pots were then treated with the inoculum derived from the respective isolates. The inoculated plants were carefully attended to, receiving daily irrigation with a plant nutrient solution for duration of six weeks (Dilworth, 2016).

After 6 weeks, the plants from the experiment were collected by rinsing away the sand under gently flowing tap water. The roots were then inspected for the presence of root nodules. Isolates capable of forming nodules on the



experimental plant roots were identified as *Bradyrhizobium* sp. These specific isolates were purified and preserved on YEMA slants under refrigerated conditions (Dilworth, 2016).

2.3 Data Analysis

Data obtained from this study were analyzed using Statistical Package for Social Sciences (SPSS) version 25 for statistical analysis and presented in the form of tables, charts and figures where appropriate.

(Dilworth, 2016). (Rao And Ansari, 2013) (Maureen, 2013)

3.0 RESULTS

A total of twenty (20) isolates presumed to be *Rhizobium* spp were isolated from both soil and root nodules of the soybean plants, of this, five

(5%) were isolated from the soil and fifteen (75%) from root nodules of the soybean plants as presented in Figure 1

Similarly, the results of the morphological characteristics of the colonies isolated in this study are presented in Plate 1 and Plate 3. The colonies appeared creamy and translucent with large and small colonies formed with a diameter range of 2-5mm after five days incubation period on both BJSM and YEMA. Some isolates (2) formed pink colonies after 24hrs of incubation as showed in Figure.

Sixteen (16) isolates of the *Rhizobium* spp were authenticated based on their potential to form root nodules on the soy beans plants as presented in Table 2. Seven (44%) out of the sixteen isolates did not form nodules while nine (56%) isolates formed nodules.

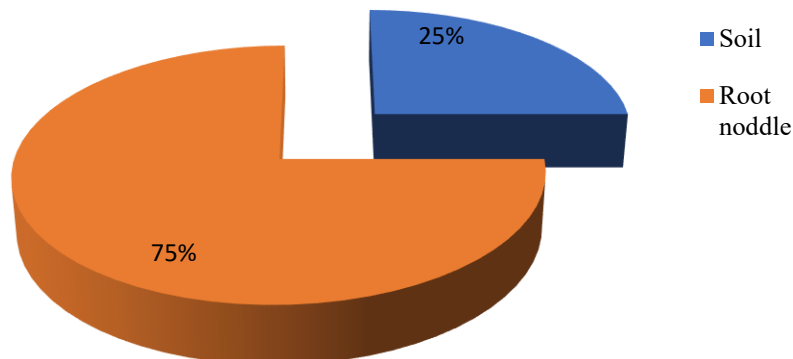


Figure 1: Percentage of *Rhizobium* spp Isolated From Soil and Root Nuddles of Soyabean Plant



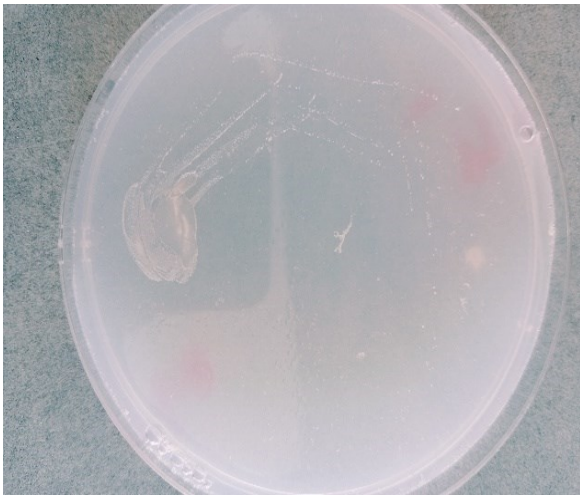


plate1: Growth of *Bradyrhizobium japonicum* on *Bradyrhizobium japonicum* Selective Medium (BJS)



Plate 2: Growth of *Bradyrhizobium japonicum* on Yeast Extract Mannitol Agar (YEMA)

Table 1A: Growth Characteristics on BJSM and YEMA

Isolates	Growth on BJSM	Growth on YEMA	Growth Rate
F14	White and translucent, slightly elevated	White, buttery, translucent, elevated slimy and scanty colonies	+
F231	White and translucent, slightly elevated	Creamy large mucoid translucent colonies, slightly raised growth after 5days	+
F322	White distinct tiny colonies with smooth margins	Creamy large mucoid translucent colonies, slightly raised growth after 24hrs	+++
F22	Creamy mucoid translucent colonies	Creamy large mucoid translucent colonies, slightly raised growth after 5days	++
F34	White buttery, translucent	White, buttery, translucent, elevated slimy and scanty colonies	+
F2	Creamy mucoid translucent colonies	Creamy mucoid translucent colonies, slightly raised growth	+
F24	White and translucent, slightly elevated	Creamy mucoid translucent colonies, slightly raised growth	+
F11S	Creamy mucoid translucent colonies	Creamy large mucoid translucent colonies, slightly raised growth	++
F12	White distinct tiny colonies with smooth margins	Creamy large mucoid translucent colonies, slightly raised growth after 24hrs	+++
F14	Creamy mucoid translucent colonies	White, buttery, translucent, elevated slimy and scanty colonies	+

Key: +++: Fast Growing Isolates (within 24 hours); ++: slow Growing isolates (growth after 3days); +: Slow Growing Isolates (growth after 5days); YEMA: Yeast Extract Mannitol Agar; BJSM: *Bradyrhizobium jopanicum* Selective Medium.



Table 1B: Growth Characteristics on BJSM and YEMA

Isolates	Growth on BJSM	Growth on YEMA	Growth Rate
F21S	White distinct tiny colonies with smooth margins	Creamy large mucoid translucent colonies, slightly raised growth after 24hrs	+
F33	Creamy mucoid translucent colonies	White, buttery, translucent, elevated slimy colonies	++
F13	Creamy mucoid translucent colonies	White, buttery, translucent, elevated slimy and scanty colonies	+
F31	Creamy mucoid translucent colonies	Creamy large mucoid translucent colonies, slightly raised growth	++
F3 2S	White distinct tiny colonies with smooth margins	Pink mucoid translucent colonies after 24hrs with large rough edges	+++
F21	White distinct tiny colonies with smooth margins	Milky mucoid colonies after 24hrs with large colonies	+++
F2S2	White distinct tiny colonies with smooth margins	Creamy large mucoid translucent colonies, slightly raised growth after 24hrs	+++
F31S	White distinct tiny colonies with smooth margins	Pink mucoid translucent colonies after 24hrs with large rough edges	+++
F311	Creamy mucoid translucent colonies	White, buttery, translucent, elevated slimy and scanty colonies	+
F3	Creamy mucoid translucent colonies	White, buttery, translucent, elevated slimy and scanty colonies	+

Key: +++: Fast Growing Isolates (within 24 hours); ++: slow Growing isolates (growth after 3days); +: Slow Growing Isolates (growth after 5days); YEMA: Yeast Extract Mannitol Agar; BJSM: *Bradyrhizobium jopanicum* Selective Medium.



Table 2: Potential of *Rhizobia spp* isolates to form nodules

Isolates Codes	Nodule Formation	Nodule Abundance
F ₁ 4	Formed	8
F ₂ 3 ₁	Formed	10
F ₃ 2 ₂	Formed	12
F ₂ 2	Formed	6
F ₃ 4	Formed	13
F ₂	Formed	15
F ₂ 4	Not formed	0
F ₁ 1S	Formed	8
F ₁ 2	Not formed	0
F ₁ 4	Formed	12
F ₂ 1S	Not formed	0
F ₃ 3	Formed	9
F ₁ 3	Formed	8
F ₃ 1	Formed	10
F ₃ 2S	Formed	16
F ₂ 1	Formed	3
F ₂ S ₂	Formed	8
F ₃ 1S	Formed	17
F ₃ 1 ₁	Not formed	0
F ₃	Not formed	10
F ₁ 4	Not formed	0
Control	Not formed	0



Plate 3: Root nodules formed by *Rhizobia spp* Isolates

4.0 DISCUSSION

This study reports on the isolation and authentication of *Rhizobia* isolated from root nodules of soy beans and also from farmlands previously cultivated with soy beans. A total of twenty (20) suspected *Bradyrhizobium* strains were isolated from BJSM showing a characteristic feature of very small whitish

colonies on the medium. Growth was very slow appearing only after 10 days of incubation. Then transferred to YEMA for cultural identification, 13 of the isolates were found to grow within a period of 5-7 days while 7 grew within 24hours. This finding contradicts the findings of Rao and Ansari (2013) where they recorded growth characteristics from 7-10 days



this is probably because growth rates are generally faster from subcultures, presumably because the bacterial metabolism for growth on artificial media has already been expressed (Dilworth, 2016).

Furthermore, the twenty (20) isolates exhibited different colonial morphology ranging from creamy/buttery/whitish to mucoid/slimy and most were raised colonies (Table 1A and B). All the colonies were translucent. Such colonial morphology was also observed in the *Bradyrhizobia* isolated in the study by of Rao and Ansari (2013) where majority of the slow growers were translucent and slightly raised. Fourteen (14) isolates were authenticated to be rhizobia as they nodulated the soybean roots grown in sterile river sand (Table 2). Maureen (2013) suggested that an isolate cannot properly be regarded as a species of *Rhizobium* until its identity has been confirmed through plant infection test on an appropriate host as recorded in this study.

5.0 CONCLUSION

This research revealed the existence of root-nodulating bacteria in both the rhizosphere and root nodules of soybean plants. Rhizobia are not only present in leguminous plants but also in the surrounding soil, aiding in soil fertilization. Unlike conventional chemical fertilizers, this method has minimal environmental impact. Consequently, it is crucial to isolate effective native nitrogen-fixing rhizobia for soybeans and produce them as inoculants to enhance legume production in the country.

REFERENCES

Geniaux, E., Laguerre, G., Amarger, N (1993). Comparison of geographically distant populations of *Rhizobium* isolated from root

nodules of *Phaseolus vulgaris*. *Molecular Ecology* **2**, 295–302.

Mujahidy et al, Isolation and characterization of *Rhizobium* spp and determination of their potency for growth factor production. *Int. Res. J. Biotechnol.* **4**.

Woomer, P. L., Mahmadi, D., Max, N (2014). A New Legume Inoculant in West Africa p. 26.

Appunu, C., N'Zoue, A., Laguerre, G. (2008). Genetic Diversity of Native Bradyrhizobia Isolated from Soybeans (*Glycine max* L.) in Different Agricultural-Ecological-Climatic Regions of India. *Appl Environ Microbiol* **74**, 5991–5996.

Peoples, M.B., Herridge, D.F., Ladha, J.K. (1995). Biological nitrogen fixation: An efficient source of nitrogen for sustainable agricultural production? *Plant Soil* **174**, 3–28.

Iwe, M. O., *The Science and Technology of Soybeans Chemistry, Nutrition, Processing, Utilization* (Rojoint Communications Services Ltd, Umuahia, Nigeria).

Onwualu, A. P., Issues on innovational strategies in agribusiness. Proceedings of a workshop on innovation strategies in agribusiness. *Raw Materials Research and Development Council (RMRDC), Abuja.*

Machido, D.A., Olufajo, O.O., Yakubu, S.E., Yusufu, S.S. (2011). Enhancing the contribution of the legumes to the N- fertility of soils of the semi-arid zone of Nigeria.

Abubakar, F. J. (2015). Isolation And Characterisation Of Indigenous Rhizobia And Response To Inoculation By Promiscuous Soybean In The Nigerian Savanna.

Ofori, P., (2016). Yield response of soybean and cowpea to rock phosphate fertilizer blend



and rhizobia inoculation on two benchmark soils of Northern Ghana.

Machido, D. A., (2010). Effects of fungicides on population size and activities of nitrifying and nitrogen fixing bacteria under screen house conditions.

Nusrat, N., Ridwan, B.R., Anowara, B. and Humaira, A. (2017). Isolation, identification and molecular characterization of Rhizobium species from *Sesbania bispinosa* cultivated in Bangladesh. *Afr. J. Agric. Res.* **12**, 1874–1880.

Tong, Z., Sadowsky, M.J., (1994). A Selective Medium for the Isolation and Quantification of *Bradyrhizobium japonicum* and

Bradyrhizobium elkanii Strains from Soils and Inoculants. *Appl Environ Microbiol* **60**, 581–586.

Dilworth, M.J. (2016). *Working with Rhizobia* (Australian Centre for International Agricultural Research, Canberra, p 78.

Pervin, S., Jannat, B., and Sanjee, S.A. (2017). Characterization of Rhizobia from Root Nodule and Rhizosphere of *Lablab purpureus* and *Vigna sinensis* in Bangladesh. *Turkish JAF Sci.Tech.* **5**, 14 (Pervin *et al.*, 2017).

Maureen N.W. (2013). Identifying Elite Rhizobia for Commercial Soybean (*Glycine Max*) Inoculants. p 45.



P121 - ASSESSMENT OF ELEMENTAL COMPOSITIONS OF EXTRACTED DATE PALM (*PHOENIX DACTYLIFERA L*) SYRUP VARIETIES OBTAINED FROM WUKARI MARKET, TARABA STATE

Raymond Bwano Donatus and Archibong Christopher Sunday

Department of Chemical Sciences, Federal University Wukari, Nigeria

Corresponding email: donatus_r28@yahoo.com

ABSTRACT

The fruit of the Date Palm (*Phoenix dactylifera L.*), represents a crucial nutritional source for individuals residing in Northern Nigeria. Within the confines of this investigation, the researchers collected samples of date fruit from Sample A (Targali), Sample B (Agadaz), and Sample C (Dan Mali), recognizing the potential health benefits and the pivotal role they play in furnishing vital nutrients. The team conducted an elemental composition analysis of the samples, which entailed analyzing the syrup of date palm species acquired from Wukari market. With regards to the syrup samples, the researchers used warm water maceration at 50°C for 15 minutes to extract samples from three mature date fruits. The preliminary evaluation of the physicochemical properties of the date palm syrups showed that the moisture contents were, Sample A (Targali) 7.81 g, Sample B (Dan Agadaz) 6.90 g, and C (Dan Mali) 6.84 g respectively. The ash content values indicated 6.90 g, 4.40 g, and 5.20 g samples A, B and C respectively. Finally, the pH analysis for the sugar syrups yielded pH values of 4.17, 4.20, and 4.19 for samples A, B, and C, accordingly. To facilitate the elemental evaluations, the Buck Scientific Flame Atomic Absorption Spectroscopy (FAAS) 210 VGP instrument was employed to determine the component elements, recording Cadmium (Cd), Lead (Pb), Iron (Fe), Zinc (Zn), Copper (Cu), Manganese (Mn), Nickel (Ni), Chromium (Cr), Cobalt (Co), Potassium (K), Sodium (Na), and Magnesium (Mg). The study findings were significant, revealing that the sampled dates contained considerable quantities of these vital elements that are crucial to human health.

Keywords: Elemental composition, Date Syrup, Date Palm, Phoenix dactylifera, Atomic Absorption

1.0 INTRODUCTION

The *Phoenix dactylifera L.*, commonly known as the date palm, serves a crucial ecological, financial, and societal function for many individuals residing in semi-arid and arid regions of the biosphere. The date palm is the most important fruit-bearing crop in arid regions of the Middle East and North Africa, including Iran (Dehghanian et al. 2022). Overall, the date palm plays a significant role in the environmental, economic, and social aspects of the regions where it is grown. The *Phoenix dactylifera L.*, commonly known as the date palm, serves a crucial ecological, financial, and societal function for many individuals residing in semi-arid and arid regions of the biosphere. The fruit of the date palm is widely consumed across the globe and is deemed an indispensable dietary component, particularly in numerous Arab nations (Al-Farsi & Lee, 2008). With a history spanning over 6000 years, it is considered one of the earliest cultivated plants. The global production of dates has increased from 4.60 million tons in 1994 to approximately 7.680 million tons in 2010, with projections indicating a continued growth trajectory (Al-Farsi & Lee, 2008). While there are around 2000 recognized producers

of date palms worldwide, only a few have been evaluated for their fruit quality and overall performance. The nutritional significance of fruits has garnered the attention of many researchers worldwide, particularly in Nigeria (Anhwange et al., 2004; Hassan & Umar, 2004; Umar et al., 2007). Although the government has made efforts to promote food production, malnutrition remains Africa's leading health issue, with protein-energy malnutrition being one of the most prevalent nutritional concerns among children and infants (Achu, 2004). The *P.dactylifera L.* is classified under the *Palmae (Arecaceae)* family. As the importance of maintaining a healthy lifestyle, including dietary habits, continues to grow, there has been an increased interest in identifying products that are rich in nutrients, vitamins, and micro and macronutrients. The date palm fruit meets these requirements and possesses several health-promoting properties. The principal constituent of dates is carbohydrates, ranging from 44 to 88%, contingent upon the stage of maturation and the species of the dates (Al-Shahib & Marshall, 2003). These carbohydrates are not subject to digestion, but are rather immediately utilized by the



human body. As such, dates are an optimal energy source for athletes prior to exercising. Moreover, dates are abundant in protein, ranging from 2.3 % to 5.6 % (Sulieman et al. in 2012). The protein component in dates is more noteworthy than that found in other fruit plants, such as bananas, oranges, and apples, where the protein component does not surpass 1% (Maqsood et al. 2020). Additionally, specific amino acids, including serine, aspartic and glutamic acid, threonine, proline, alanine, and glycine, are almost exclusively present in dates (Al-Shahib & Marshall, 2003; Sulieman et al. in 2012; Al-Showiman, 1998). The exceptional nutritional value of dates is also linked to the remarkable fiber component. In addition to accelerating intestinal motility and preventing constipation, it also impedes the reduction of total LDL cholesterol levels in the bloodstream along with the sugar level (Kritchevsky, 1988; Al-Shahib & Marshall, 2002). The work by Al-Shahib and Marshall (2002), scrutinized 13 species of dates from diverse countries and disclosed that the fiber component varies from 6.4 to 11.5%, contingent upon the species and degree of maturity. Dates palms are a good source of minerals and nutritional components, however, research showed that the concentration of minerals in the date's fruit is affected by soil fruitfulness, variety and maturing stage (Marzouk & Kassem 2011; Cui et al. 2021). The presence of pectin in dates, ranging from 0.5% to 3.9%, has been demonstrated to mitigate risk factors associated with diabetes and heart disease. Specifically, it aids in reducing cholesterol levels in the bloodstream (Echegaray et al. 2021). Furthermore, dates are effective in reducing triglyceride levels and preventing atherosclerosis by improving lipid profile (Fayadh & Al-Showiman 1990; Rock et al. 2009; Djaoud et al. 2020). Moreover, research has shown that consumption of dates by healthy individuals results in a decrease in serum triacylglycerol levels and serum basal oxidative pressure without adversely affecting serum lipoprotein or glucose levels (Rock et al. 2009). Dates have been extensively studied for their beneficial properties, and it has been found that they possess remarkable antibacterial effects against a variety of pathogens including *Streptococcus pyogenes*, *Pseudomonas aeruginosa*, *Escherichia coli*, *Shigella flexeneri*, *Staphylococcus aureus*, and *Bacillus subtilis* (Perveen et al. 2012). Additionally, the flavonoids present in dates have been shown to be responsible for their antifungal activity against *Candida albicans* and *Candida krusei* (Orhan et al. 2010). Fruit tree species represent an incredible source of biologically active molecules important

for the human diet, such as carbohydrates, vitamins, minerals and antioxidant compounds (Sabbadini et al. 2021). Therefore, it is imperative to estimate and understand the mineral components of the date palm for the sake of human health and safety. In this study, the sampled date palm (Sample A (Targali), Sample B (Dan Agadaz), and C (Dan Mali) were procured from Wukari market in Wukari Local Government Area, Taraba State, Nigeria. The Date Palm holds a significant place in human life as it serves various purposes. However, the Date Palm industry in Nigeria, including production, processing, and marketing, faces a number of challenges such as a lack of data on dietary information on the Date Palm species consumed in and around Wukari, Taraba State, Nigeria. The different applications of dates and their co-products in different foods demonstrates that it is a very versatile fruit whose revaluation can help the palm industry to produce in more sustainable manner, promoting the circular economy in the food chain, and increasing their profits (Muñoz-Tebar et al. 2023).

2.0 Materials and Methods

About 1000 g of dry date (*Phoenix dactylifera*) fruit flesh pieces samples prepared from variety of each sample, (sample A, Targali; sample B, Dan Agadaz; and sample C, Dan Mali) from Wukari market, Taraba State. Buck Scientific Flame Atomic Absorption Spectrometer (FAAS) 210 VGP. Centrifuge model RC 28 S USA, Blender, Clean laboratory glass wares, distilled water, plastic storage bottles. All reagents used are of analytical grade. The glass wares were cleaned and dried on standard base guidelines for use.

2.1 Extraction of Date Syrup

The method of El-Shaunorby et al. (2014) was adopted with little modifications in time of centrifugation. The dry date variety weighed 100 g each, cut to small pieces with a sharp knife and crushed, and dry within laboratory room temperature. The dried date's pieces was blended for 5 minutes using a kitchen blender, and extracted twice with water, using 1:2 ratio of flesh powder water rate at 70 °C for 30 minutes. Following the post-heating process, the mixture underwent filtration through an improvised clean filter cloth, facilitated by a hand press, with the intention of eliminating any sizable impurities and insoluble substances. The raw date syrup was centrifuge at



8000 rpm for 15 minutes and supernatant decanted, weighed and refrigerated in clean air tight plastic bottles until when used.

2.2 Determination of moisture content

The moisture content of the 20 g dates sample was observed by drying the sample in an electric oven at 110 °C till constant weight was obtained. The loss in weight after drying is moisture. The difference in the initial and final weights gave the moisture content (AOAC, 2000).

$$\text{Moisture content} = \frac{\text{Initial weight} - \text{final weight}}{\text{Initial weight}} \times 100$$

2.3 Determination of ash content

The samples are heated at 500°C to burn up all the organic matter according to (AOAC, 2006).

$$\text{Ash (\%)} = \frac{\text{Initial weight} - \text{Final weight}}{\text{Initial of ash}} \times 100$$

2.4 Determination of fibre content

Fibre content was determined according to (AOAC, 2006).

$$\text{Crude fibre content (\%)} = \frac{A-B}{C}$$

2.5 Determination of pH

The pH values of dissolved 100 g of each sample in 75 ml distilled water done according to Mathew et al. (2015).

2.6 Specific gravity

The specific gravity of the sampled syrups, being its densities to that of water at 25 °C, was done according to the method of Dhir et al. (2018).

$$\text{Specific gravity} = \frac{\text{Density of Date Syrup}}{\text{Density of distilled water}} \text{ g/cm}^3$$

2.7 Elemental Composition

The elemental composition was determined using Buck Scientific Flame Atomic Absorption Spectroscopy (FAAS) 210. Samples were digested as follow,

3.0 Results and Discussions

The extraction of date syrup from the date flesh yielded sample A (7.81 g), sample B (6.9 g), and Sample C (6.48 g).

Table 1: Physicochemical Properties

Parameters	Sample A	Sample B	Sample C
Moisture content	13.75%	14.5%	12.4%
Fibre content	64%	59.5%	62%
Ash content	34.7%	22%	26%
pH Value	4.17	4.20	4.19

3.1 Physicochemical Properties Date Syrups

Table 1 showed results for the physicochemical (moisture, fibre content, ash content, pH) properties of the Dates Palm fruits samples. The moisture content ranged between 32.4- 39.1%. Sample A, revealed 39.1% (7.81 g), sample B 34.5% (6.9 g), and Sample C 32.4% (6.48 g)

This work revealed moisture content results similar to earlier reports, 9.2 % to 30.1% Ahmed *et al.* (1995). Al-Shahib & Marshal 2003 reported moisture content of species at mature stages between 15-25 %; Moisture content was also reported in several species of date palm fruit that ranged between 10 % -30% Aidoo, et al; 1996 and Pavi et al. 2015 also reported lower moisture content value between 13.2-14.1% in dry date fruit



from Bangladesh. The moisture proportion is diverse in date species, ranging from 9.2 to 23.1%. A difference in moisture content of various dates species at several mature stages, at ripening Tamar stage moisture ranged from 15 % – 25 % (). Semi-dry dates possessed more than 30 % moisture and less than 10 % dry dates during the Tamar period (Abdessalam et al. 2008).

The ash results indicated a dry date's content of 6.94 g (34.7 %), around 34 - 70 % of the date fibre ash's total weight (20.00 g). Our results of ash are nearly the same and agreed with the discoveries of other scientists working on diverse date species in which the ash proportion in diverse dry date species. Al-Shahib and Marshal (2003) stated that ash content in diverse date species ranged within the values stated in this work. The results of the current study, closely corresponds to the conclusion of investigation work conducted in previous studies. The ash and moisture percentage variance has been described among several species producing in the same country or the same variety in diverse areas, primarily due to the variances in harvest and postharvest skills indicated diverse moisture levels.

3.2 FAAS Analysis of Date Syrups

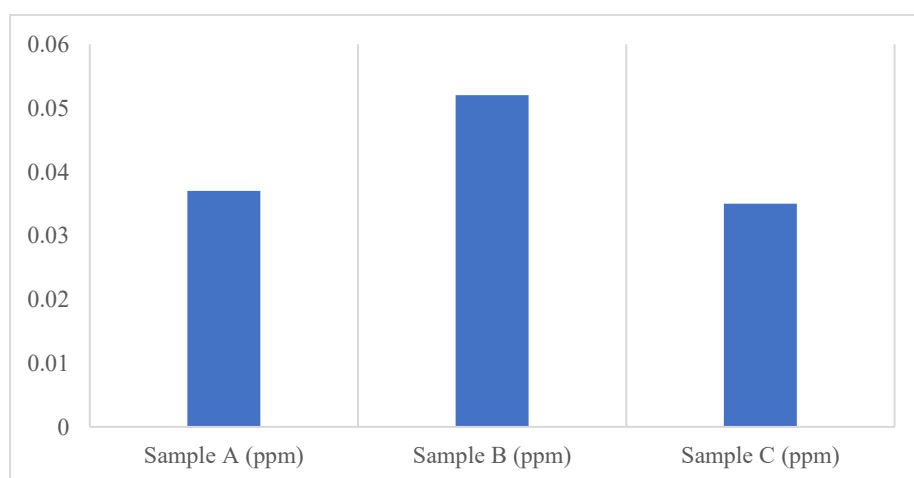


Figure 2; Concentration of Cadmium (Cd) in date samples A, B and C

The moisture content results revealed that the high percentage of moisture content will enable spoilage of date fruits, and low moisture per cent will lead to dry dates not proper to consumers. However, dry dates can be stored for an extended period, compared to semi-dry dates with low moisture content in dates to avert the growth of yeast and moulds (Ahmed, 1981).

The pH value of the date syrup for sample A is 4.17, sample B is 4.19 and sample C is 4.20, which is slightly acidic with a specific gravity of 1.4016 at ambient temperature. Nagga and Abd El-Tawab (2012) reported a pH of 4.8 from Egyptian dates syrup extracted. The high level of acidity in syrups contributed to its stability against microorganisms (Hawraa *et al.*, 2017)

Muñoz-Tebar, N.; Viuda-Martos, M.; Lorenzo, J.M.; Fernandez-Lopez, J.; Perez-Alvarez, J.A (2023). Strategies for the Valorization of Date Fruit and Its Co-Products: A New Ingredient in the Development of Value-Added Foods. *Foods*. 12, 1456.



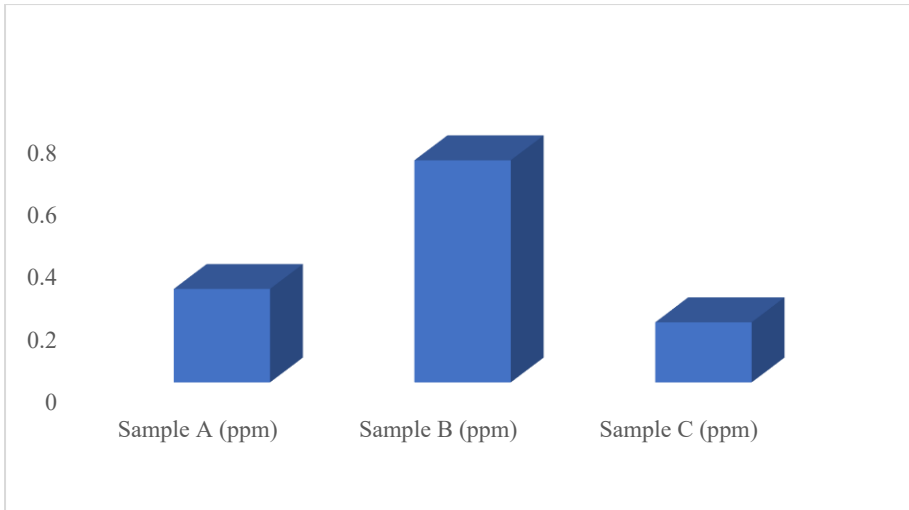


Figure 3; Concentration of Lead (Pb) in date samples A, B and C

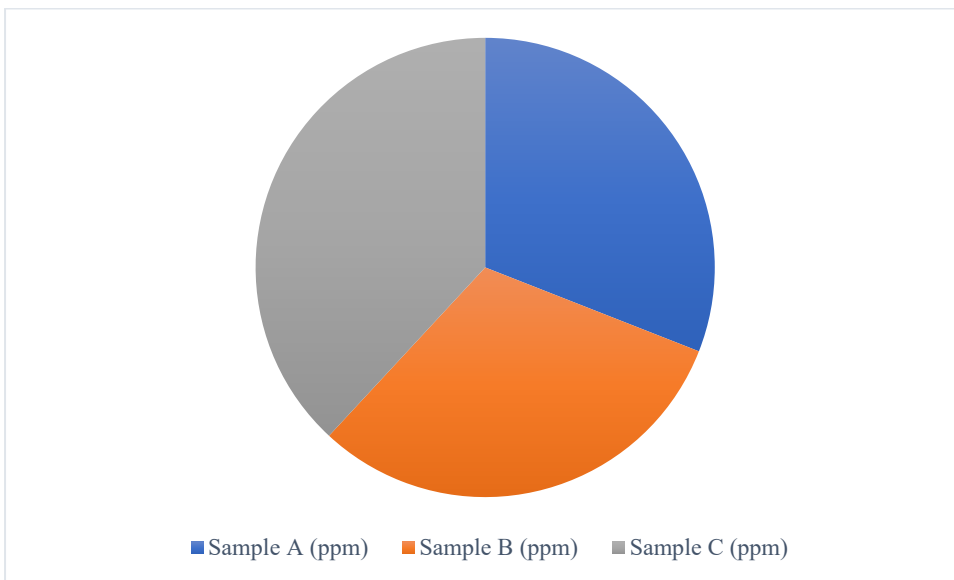


Figure 4; Concentration of Iron (Fe) in Date Sample A, B and C



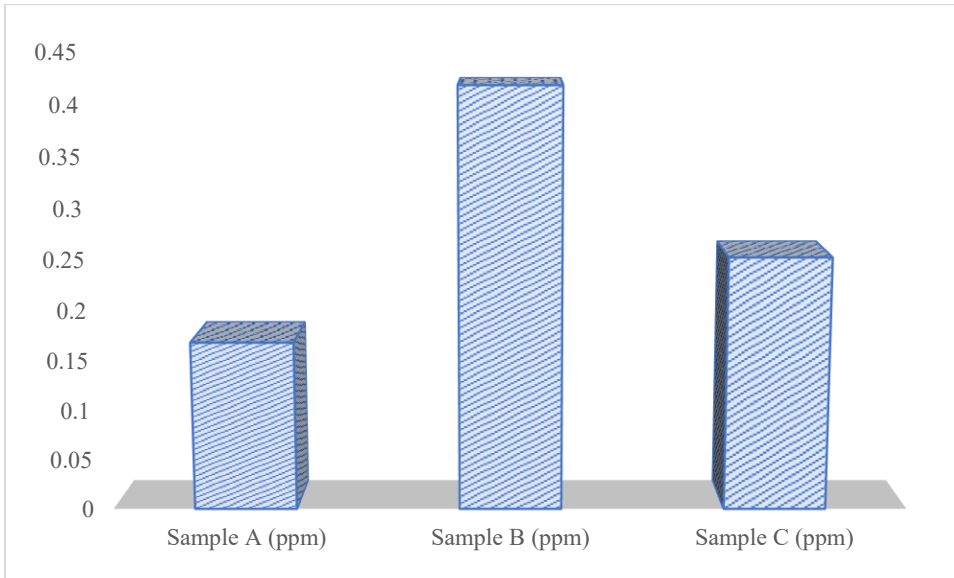


Figure 4.5; Concentration of Zinc (Zn) in date samples A, B and C

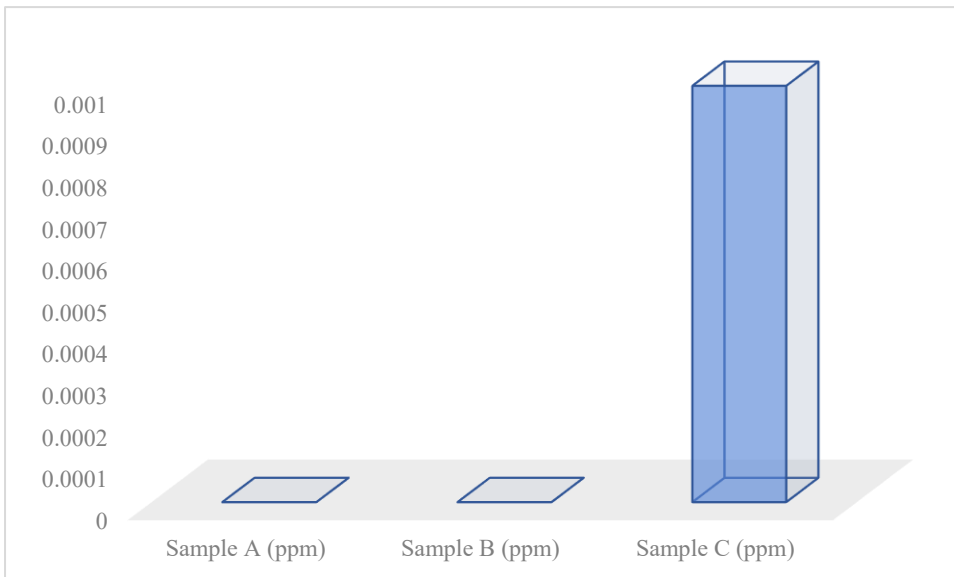


Figure 4.6; Concentration of Copper (Cu) in date samples A, B and C



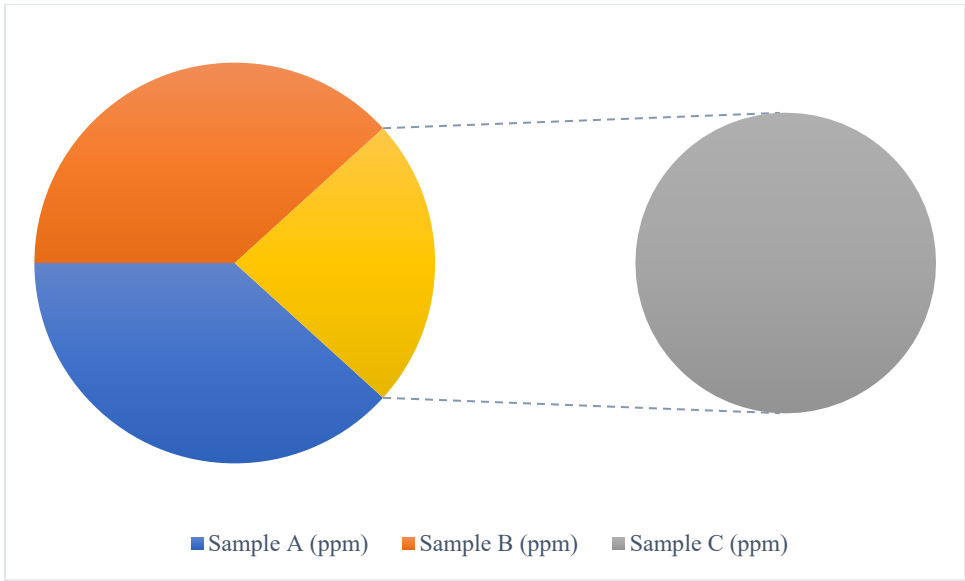


Figure 4.7; Concentration of Manganase (Mn) in date samples A, B and C

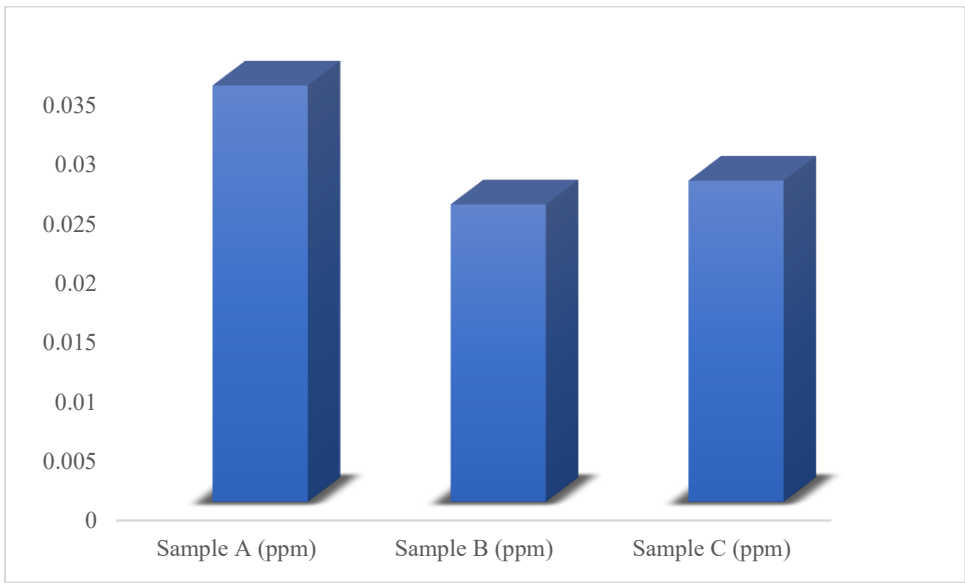


Figure 4.8; Concentration of Nickel (Ni) in date samples A, B and C



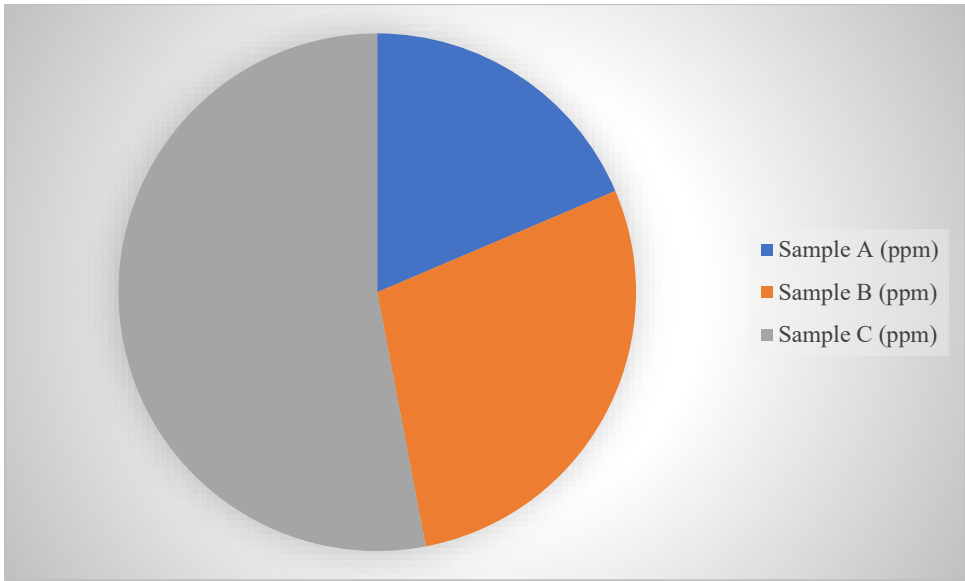


Figure 4.9; Concentration of Chromium (Cr) in Date samples A, B and C

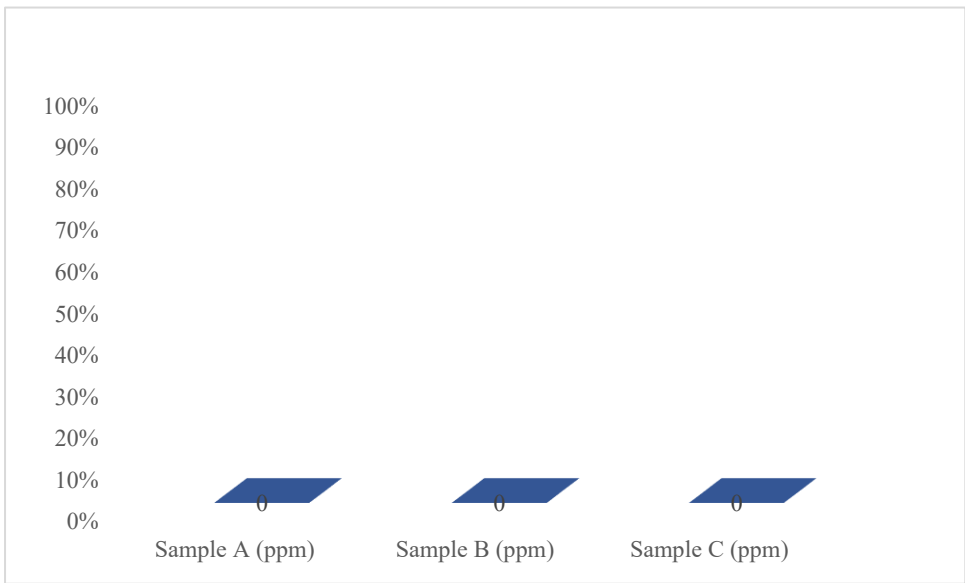


Figure 4.10; Concentration of Cobalt (Co) in Date Sample A, B and C



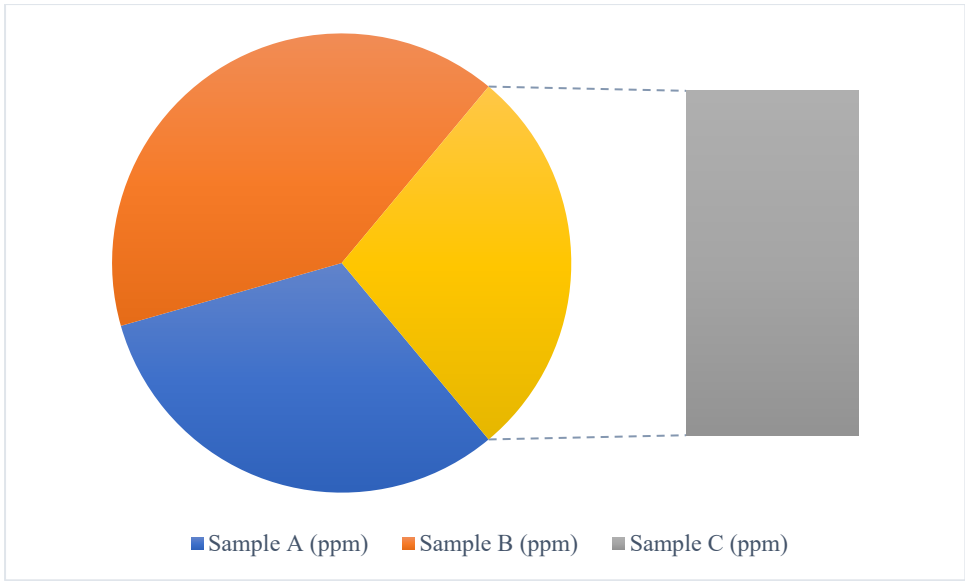


Figure 4.11; Concentration of Potassium (K) in Date Sample A, B and C

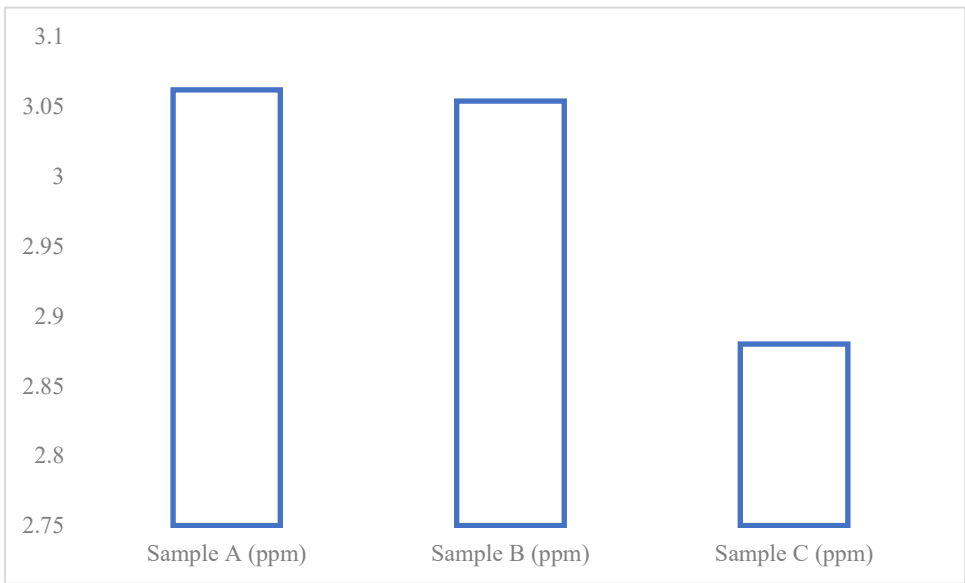


Figure 4.12; Concentration of Sodium (Na) in Date Samples A, B and C



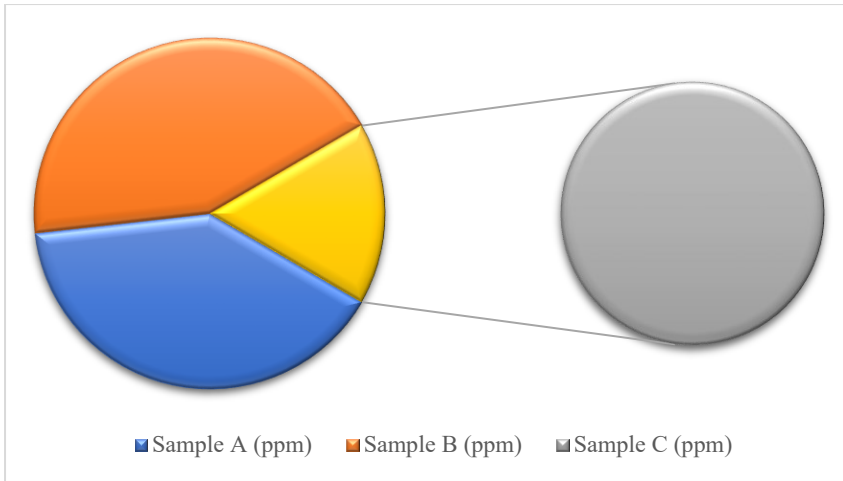


Figure 4.13; Concentration of Magnesium (Mg) in Date Sample A, B and C

Table 2; Average value of FAAS results for Sample A, B and C in (ppm)

Elements	Sample A (ppm)	Sample B (ppm)	Sample C (ppm)
Cd	0.037±0.002	0.052±0.001	0.035±0.002
Pb	0.300±0.005	0.713±0.036	0.193±0.003
Fe	0.13±0.026	0.13±0.006	0.16±0.01
Zn	0.168±0.001	0.418±0.004	0.252±0.002
Cu	0.00±0.001	0.000±0.000	0.001±0.001
Mn	0.044±0.002	0.044±0.003	0.027±0.002
Ni	0.03±0.0025	0.025±0.0015	0.027±0.002
Cr	0.1137±0.0048	0.1735±0.0040	0.3239±0.0155
Co	0.000±0.000	0.000±0.000	0.000±0.000
K	174.9±0.833	223.7±1.026	154.2±1.060
Na	3.062±0.003	3.054±0.013	2.880±0.013
Mg	10.84±0.056	11.81±0.035	4.56±0.065

From the result obtained in Fig. 4.1, sample A, it is clear that lead has the highest quantity (0.300 ppm) followed by Zinc (0.168 ppm), Iron (0.13 ppm), Chromium (0.1137 ppm), Manganese (0.044 ppm), Cadmium (0.037 ppm) and Nickel (0.035 ppm) while Copper and Cobalt is said to be absent for heavy metals, its similar to result discussed by Shaymaa *et al.*, (2015). However, for essential elements in Fig. 4.2 sample A, potassium has the highest quantity (174.9 ppm), which is by far more

than magnesium (10.84 ppm) and sodium (3.062 ppm).

Fig. 4.3 has some similarities with the result obtained in Fig. 4.1, above. However, there are some irregularities in the amount of Fe (0.13 ppm) compared to Fig. 4.1, above. Pb has the highest amount (0.713 ppm), followed by Zn (0.4183 ppm), Cr (0.1735 ppm), Fe (0.13 ppm), Mn (0.044 ppm) and lastly, Ni (0.025 ppm). Cu and Co are absent, as seen in Fig. 4.3 above. K is highest concentration



(223.7 ppm), followed by Mg (11.81 ppm), while Na (3.054 ppm) is the least concentration for essential metal. The results obtained from this study work falls within the concentration range in mg/kg of Cd, 0.0005; Pb, 0.005; Fe, 0.1; Zn, 0.2; Mn, 0.02; Ni, 0.005; and Cr, 0.005 reported by Shaymaa *et al.*, (2015) for heavy metals.

In Fig. 4.5, there is a remarkable difference between Fig. 3 and others (fig 4.1 and 4.3), figures in concentration of the heavy elements, chromium (0.3239 ppm), zinc (0.252 ppm), lead (0.193 ppm) Iron (0.16 ppm), cadmium (0.035 ppm), manganese (0.027 ppm) and nickel (0.027 ppm). This shows a decreasing trend from Cr to Ni: (Cr > Zn > Pb > Fe > Cd > Mn > Ni). For essential elements, sodium indicated (2.880 ppm) and magnesium's (4.56 ppm) are relatively low, while potassium showed (154.2 ppm) present in abundance. This trend (K > > Mg > Na) is precisely the same for all tested samples. Potassium showed higher concentration while magnesium and sodium contents were less than the previous data reported for Egyptian and Saudi dates. Al-Tamim (2014). The Egyptian dates reported K 154.2 ppm, Mg 4.56 ppm, and Na 2.880 ppm; However, Saudi dates species reported 66.33 mg/g, Mg 81.7 mg/g, K 55.11 mg /100 g, respectively. In preference for naturally flavoured foods, dates represent a promising alternative to replace chemical additives, giving products good nutritional properties and good acceptability by consumers (Muñoz-Tebar *et al.* 2023).

4.0 Conclusion

The physicochemical and elemental analysis of syrup extract from varieties of *P. dactylifera* includes moisture content, ash content, fibre content and pH. Flame atomic absorption spectroscopy was used to determine the concentration of Cadmium (Cd), lead (Pd), iron (Fe), zinc (Zn), Manganese (Mn), Nickel (Ni), Chromium (Cr), Potassium (k), Sodium (Na), and Magnesium (Mg), which possess antioxidant, antimutagenic, and immunomodulatory properties.

In addition to its nutritious importance, in folklore, dates are whispered to have medicinal properties such as aphrodisiac, boost immunity, and provide strength, fitness and relief against pains and protection against many diseases. Based on the findings of this research work, the following recommendations were made. Further study is therefore required to explore the health benefits of date syrup in some varieties consumed around Taraba. Adequate concern with the cooperation of the government and private sectors is also required for increased development of the Nigerian date palm industry.

References

- Abdessalam, M. Ali, F.C. Nizar, C. Ben, S.M. Mohammad, B. Threadgill, M.P. (2008). Physio-chemical characteristics and total utility of date palm varieties grown in the southern of Tunisia. *Pak. J. Bio. Sci.*, 11 (7): 1003-1008.
- Abdu, S.B (2011). The protective role of Ajwa date against the hepatotoxicity induced by Ochratoxin A. *Egypt J Nat Tox* 8: 1-15.
- Ahmed, M.S.H. (1981). Investigation on insect disinfestations of dried dates by using gamma radiation- A review. *Date Palm J. I.*, 107-116.
- Ahmed, I.A., Ahemed, A.W.K., Robinson, R.K. (1995). Chemical composition of date varieties as influenced by the stage of ripening. *Food Chemistry* 54: 305-309.
- Aidoo, K.E., Tester, R.F., Morrison, J.E., Macfarlane, D. (1996). The composition and microbial quality of pre-packed dates purchases in Greater Glasgow. *International Journal of Food Science and Technology* 31: 433-438.



- Al-Kharusi, L.M., El-Mardi, M.O., Ali, A., Al-Said, A.F., Kadir, M. (2009). Effect of minerals and organic fertilisers on the chemical characteristics and quality of date fruits. *International Journal of Agriculture and Biology* 11(3): 290–296
- Al-Farsi, M. Lee, C.Y. (2008). Nutritional and functional properties of dates: A review. *Critical Review in Food Science and Nutrition* 48: 877–884.
- Al-Farsi, M., Alasalvar, C., Morris, A., Baron, M., Shahidi, F. (2005b). Comparison of antioxidant activity, anthocyanins, carotenoids, and phenolic of three native fresh and sun dried date (*Phoenix dactylifera* L.) varieties grown in Oman. *Journal of Agriculture and Food Chemistry* 53: 7592–7599.
- Al-Farsi, M., Alasalvar, C., Morris, A., Baron, M., Shahidi, F. (2005b). Comparison of antioxidant activity, anthocyanins, carotenoids, and phenolic of three native fresh and sun dried date (*Phoenix dactylifera* L.) varieties grown in Oman. *Journal of Agriculture and Food Chemistry* 53: 7592–7599.
- Al-Farsi, M., Alasalvar, C., Morris, A., Baron, M., Shahidi, F. (2005a). Compositional and sensory characteristics of three native sundried date (*Phoenix dactylifera* L.) varieties grown in Oman. *Journal of Agriculture and Food Chemistry* 53: 7586–7591.
- Al-Hooti, S., Sidhu, J.S., Qabazard, H. (1995). Studies on the physico-chemical characteristics of date fruits of five U.A.E. cultivars at different stages of maturity. *Arab Gulf Journal of Scientific research* 13: 553–569.
- Al-Hooti, S., Sidhu, J.S., Qabazard, H. (1997). Physicochemical characteristics of five date fruit cultivars grown in United Arab Emirates. *Plant Foods for Human Nutrition* 50: 101–113.
- Ali Ahmed, Naheed Bano., Muhammad Tayyab (2016). Phytochemical and Therapeutic Evaluation of Date (*Phoenix dactylifera*) A Review. *Journal of Pharmacy and Alternative Medicine*. 9. 2222-4807 (online) ISSN 2222-5668.
- Al Tamim E. A. (2014). Comparative study on the chemical composition of Saudi Sukkari and Egyptian Swei date palm fruits. *J. American Science*, 10 (6); 149–153.
- Ali, A. Yusra, M. Al-Kindi, Al-Said, F. (2009). Chemical composition and glycemic index of 3 varieties of Omani dates. *International Journal of Food Science and Nutrition* 60(S4): 51–62
- Allaith, A.A.A. (2008). Antioxidant activity of Bahreini date palm (*Phoenix dactylifera*) fruit of various cultivars. *International Journal of Food Science and Technology* 43(6): 1033–1040.
- Almana, H.A., Mahmoud, R.M. (1994). Date-palm seeds as an alternative source of dietary fibre in Saudi bread. *Ecology Food Nutrition* 32: 261–270.
- Al-Shahib, W., Marshall, R.J. (2002). Dietary fibre content of dates from 13 varieties of 9 date palm *Phoenix dactylifera* L. *International Journal of Food Science and Technology* 37: 719–722.
- Al-Shahib, W. Marshal, R.M (2003). The fruit of the date palm: Its possible uses as the best food for the future. *Intr. J. Food Sci. Nutr.* 54: 247-259.



- Al-Showiman, S.S. (1990). Chemical composition of date palm seeds (*Phoenix dactylifera* L.) in Saudi Arabia. *Journal of the Chemical Society* 12: 15–24.
- Al-Showiman, S.S. (1998). *Al Tamr, Ghetha was Saha* (date, Food and Health). Saudi Arabia: Dar Al-Khareji Press.
- AOAC (Association of Official Analytical Chemists) (2006). *Official Methods of Analysis*, 15th edn. (Gaithersburg, S. edn). AOAC Press, Washington DC., USA. pp. 78- 90.
- Babich, H., Sedletcaia, A., Kenigsberg, B. (2002). In-vitro cytotoxicity of protocatechuic acid to cultured human cells from oral tissue: Involvement in oxidative stress. *Pharmacology Toxicology* 91: 245–253.
- Barreveld, W.H. (1993). *Date-Palm Products*. Bulletin No 101. Rome, Italy: Food and Agriculture Organization of the United Nations
- Ben-Amotz, A. Fishler, R. (1998). Analysis of carotenoids emphasising 9-cis- β -carotenes of vegetables and fruits commonly consumed in U.K. *Food Chemistry* 62: 515–520.
- Biglari, F., Abbas, F.M., Alkarkhi, F.M., Azahar, M.E. (2008). Antioxidant activity and phenolic content of various date palm (*Phoenix dactylifera*) fruits from Iran. *Food Chemistry* 107: 1636–1641.
- Boudries, H., Kefalas, P., Hornero-Mendez, D. (2007). Carotenoid composition of Algerian date varieties (*Phoenix dactylifera*) at different edible maturation stages. *Food Chemistry* 101: 1372–1377.
- Cui, J. Zhao, C. Feng, L. Han, Y. Du, H. Xiao, H. Zheng, J. (2021). Pectins from fruits: relationships between extraction methods, structural characteristics, and functional properties, *Trends Food Sci. Technol.* 110, 39–54.
- Cummings, J.H., Bingham, S., Heaton, K.W., Eastwood, M.A. (1992). Fecal weight, colon cancer risk, and dietary intake of non-starch polysaccharides (dietary fibre). *Gastroenterology* 103: 1783–1789.
- Cuvelier, M.E., Richard, S., Berset, C. (1992). Comparison of the antioxidant activity of some acid phenols: Structure–activity relationship. *Bioscience, Biochemistry and Biotechnology* 56: 324–325.
- Dehghanian, M., Sheidai, M., (2022). Genetic structure and diversity of date palm (*Phoenix dactylifera* L.) cultivars in Iran revealed by re-map genotyping. *Acta Botanica Hungarica*, 64 (3-4), 259-271.
- Djaoud, N Boulekbache-Makhlouf, L. Yahia, M. Mansouri, H. Mansouri, N. Madani, K. Romero, A (2020). Dairy dessert processing: effect of sugar substitution by date syrup and powder on its quality characteristics, *J.Food Process.Preserv.* 44 (5), e14414.
- Echegaray, N., Gull' on, B., Pateiro, M., Amarowicz, R., Misihairabgwi, J.M., Lorenzo, J.M. (2021). Date fruit and its by-products as promising source of bioactive components: a review, *Food Rev.Int.* 1–22.
- Elmer, P. (2017). Sensitivity, Background, Noise and Calibration in Atomic Spectroscopy— Effects on



- Accuracy and Detection Limits, Perkin Elmer, Inc., Shelton, CT.
- Elleuch, M., Basbes, S., Roiseux, O., Blecler, C., Deroenne, N., Driera, E., Attia, H. (2008). Date flesh: Chemical composition and characteristics of dietary fibre. *Food Chemistry* 111: 676–682.
- El-Sharnouby G.A, Aleid S.M, Al-Otaibi M.M (2014) Liquid Sugar Extraction from Date Palm (*Phoenix dactylifera* L.) Fruits. *J Food Process Technol* 5: 402
- El-Zoghbi, M. (1994). Biochemical changes in some tropical fruits during ripening. *Food Chemistry* 49:33–37.
- Fayadh, J.M., Al-Showiman, S.S. (1990). Chemical composition of date palm (*Phoenix dactylifera* L.). *Journal of the Chemical Society of Pakistan* 12: 84–103.
- Fennema, O.R. (1996). *Food Chemistry*, 3rd edition. New York: Dekker.
- García, R., Ba'ez, V. (2012). Atomic absorption spectrometry (A.A.S.), in: D.M.A. Farrukh (Ed.), *Atomic Absorption Spectroscopy*, InTech.
- García, R. Báez, A. P. (2012). Atomic Absorption Spectrometry (A.A.S.), *Atomic Absorption Spectroscopy*.
- Guan, S., Ge, D., Liu, T.Q., Ma, X.H., Cui, Z.F. (2009). Protocatechuic acid promotes cell proliferation and reduces basal apoptosis in cultured neural stem cells. *Toxicology In-vitro: An International Journal Published in Association with BIBRA* 23(2): 201–208.
- Guo, C., Yang, J., Wei, J., Li, Y., Xu, J., Jing, Y. (2003). Antioxidant activities of peel, pulp and seed fractions of common fruits as determined by FRAP assay. *Nutrition Research* 23: 1719–1726.
- Hannaford, P. (2000). Alan Walsh 1916–1998. *Hist. Rec. Aust. Sci.* 13 (2) 179–206.
- Hill, S.J., Fisher, A.S. (2017). Atomic absorption, methods and instrumentation, in: J.C. Lindon, G.E. Tranter, D.W. Koppenaal (Eds.), *Encyclopedia of Spectroscopy and Spectrometry*, third ed., Academic Press. 37–43.
- Ishurd, O., Kennedy JF (2005). Anti-cancer Activity of Polysaccharides prepared from Libyan Dates (*Phoenix dactylifera* L.). *Carbohydr. Polym.*, 59: 531-535.
- Ishurd, O., Zahid, M., Xiao, P., Pan, Y. (2004). Protein and amino acid contents of Libyan dates at three stages of development. *Journal of Science, Food and Agriculture* 84: 481–484.
- Ismail, B., Haffar, I., Baalbaki, R., Mechref, Y., Henry, J. (2006). Physico-chemical characteristics and total quality of five date varieties grown in United Arab Emirates. *International Food Science and Technology* 41: 919–926.
- Karasawa, K., Uzuhashi, Y., Hirota, M., Otani, H (2011). Matured fruit extract of date palm tree (*Phoenix dactylifera* L.) stimulates the cellular immune system in mice. *J. Agri. Food Chem.*, 59(20): 11287-11293
- Khan, M., Sarwar, A., Wahab, M., Haleem, R. (2008). Physio-chemical characterisation of date varieties using multivariate analysis. *Journal of Food Agriculture* 88: 1051–1059.



- Lim, Y.Y., Lim, T.T., Tee, J.J. (2007). Antioxidant properties of several tropical fruits: A comparative study. *Food Chemistry* 103(3): 1003–1008.
- Liu, S., Willett, W.C., Stampfer, M.J., Hu, F.B., Franz, M., Sampson, L., Hennekens, C.H., Manson, J.A.A. (2000). Prospective study of dietary glycemic load, carbohydrate intake and risk of coronary heart diseases in U.S women. *American Journal Clinical Nutrition* 71: 1455–1461.
- Makki, M., Hamooda, A., Al-Abri, A. (1998). *The Date Palm, Culture, Operation and Maintenance*. Muscat, Oman: Modern Color Publishers.
- Mansouri, A., Embarek, G., Kokkalou, E., Kefalas, P. (2005). Phenolic profile and antioxidant activity of the Algerian ripe date palm fruit (*Phoenix dactylifera*). *Food Chemistry* 89: 411–420.
- Maqsood, S. Adiamo, O. Ahmad, M. Mudgil, P. (2020). Bioactive compounds from date fruit and seed as potential nutraceutical and functional food ingredients, *Food Chem.* 308, 125522.
- Marlett, J.A., Mc Burney, M.I., Slavin, J. (2002). Position of the American Diabetic Association: Health implications of dietary fiber. *Journal American Diabetic Association* 102: 993–1000.
- Mathew J.T., Ndamitso, M.M., Otori, A.A., Shaba E.Y., Inobeme, A., Adamu, A (2014). Proximate and Mineral Compositions of Seeds of Some Conventional and Non Conventional Fruits in Niger State, Nigeria. *Acad. Res. Int.* 5(2):113-118.
- Mathew, J.T., Ndamitso M.M., Shaba E.Y., Mohammed S.S., Salihu A.B., Abu Y (2015). Determination of the Nutritive and Anti-Nutritive Values of *Pelophylax esculentus* (Edible Frog) Found in Hanyan Gwari, Minna Niger State, Nigeria. *Adv. Res.* 4(6):412-420.
- Mossa, J.S., Hifnawy, M.S., Mekkawi, A.G. (1986). Phytochemical and biological investigation on date seed (*Phoenix dactylifera L.*) produced in Saudi Arabia. *Arab Gulf Journal of Science and Research* 4: 495–501.
- Muñoz-Tebar, N., Viuda-Martos, M., Lorenzo, J.M., Fernandez-Lopez, J., Perez-Alvarez, J.A (2023). Strategies for the Valorization of Date Fruit and Its Co-Products: A New Ingredient in the Development of Value-Added Foods. *Foods*, 12, 1456.
- Myhara, H.M., Karkala, J., Taylor, M.S. (1999). The composition of maturing Omani dates. *Journal of the Science of Food and Agriculture* 47: 471–479.
- Okolo, E.C., Okwagwu, C.O., Ataga, C.D. (2000): "Flowering and Fruiting Pattern of Date in Nigeria" In: *Proceedings of the Date palm International Symposium, Wind Hoek Namibia* 22 – 25.
- Ramadan, B.R. (1995). Preparation and evaluation of Egyptian date syrup. *Food Science & Technology Dept., Faculty of Agric. Assuit Univ. Assuit, Egypt*
- Regnault-Roger, C., Hadidan, R., Biard, J.F., Boukef, K. (1987). High performance liquid and thin chromatographic determination of phenolic acids in palm (*Phoenix dactylifera L.*). *Food Chemistry* 25: 61–71.
- Shahidi, F., Naczk, M. (2004). *Phenolics in Foods and Nutraceuticals*. Boca, Rotan, FL: CRC Press.



- Shaymaa S. Abdrabo; Guillermo Grindlay; Luis Cras; Juan Mora (2015) Multi-Elemental Analysis Of Spanish Date Palm (*Phoenix Dactylifera L*) By Inductively Coupled Plasma-Based Techniques. Discrimination Using Multivariate Statistical Analysis. 8(5): 1268-1278.
- Shinwari, M.A. (1993). Date palm. In Encyclopedia of Food Science. Food Technology and Nutrition, Macrae, R., Robinson, R.K., and Sadler, M. (eds). London, UK: Academic Press Limited,1300–1305
- Shivashankara, K.S., Isobes, S., Al-Haq, M.I., Takenaka, M., Shinha, T. (2004). Fruit antioxidant activity, ascorbic acid, total phenol, quercetin, and carotene of Irwin mango fruits stored at low temperature after high electric field treatment. Journal of Agriculture and Food Chemistry 52:1281–1286.
- Silvia Sabbadini., Franco Capocasa., Maurizio Battino., Luca Mazzoni., Bruno Mezzetti (2021). Improved nutritional quality in fruit tree species through traditional and biotechnological approaches. Trends in Food Science & Technology, 1-14.
- USDA National database for standard Reference, United States Department of Agriculture: http://www.nal.usda.gov/fnic/foodcomp/cgi-bin/list_nut_edit.pl
- Vayalil, P.K. (2002). Antioxidant and antimutagenic properties of aqueous extract of date fruit (*Phoenix dactylifera L. Arecaceae*). Journal of Agriculture and Food Chemistry 50: 610–617(s).
- Vinson, J.A., Zubik, L., Bose, P., Samman, N., Proch, J. (2005). Dried fruits: Excellent in vitro and in vivo antioxidants. Journal of the American College of Nutrition 24: 44–50.





TRUSTWORTHY & RELIABLE SERVICES

National Research Institute
for Chemical Technology, Zaria
P.M.B 1052
Km 4, Old Kano Road,
Basawa, Zaria, Kaduna State,
Nigeria

NARICT ANALYTICAL SERVICES

Our Services

PETROLEUM PRODUCTS TESTING ◆

WATER ANALYSIS & QUALITY CONTROL ◆

PHYTOCHEMICAL ANALYSIS ◆

PHYSICOCHEMICAL ANALYSIS ◆

MATERIAL CHARACTERIZATION ◆

TEXTILE ANALYSIS ◆

INDUSTRIAL EFFLUENT ANALYSIS ◆

ENVIRONMENTAL ANALYSIS ◆

Why Us

The National Research Institute for Chemical Technology, Zaria is equipped with state of the art equipment manned by trained and highly professional scientists & engineers catering to the chemical analysis needs of Industry and Academia both within and outside Nigeria.

At NARICT, we ensure that analyses are carried out using present day standards and guidelines. Good Laboratory Practices are also strictly adhered to.

Call Us :

+234 8065162971

+234 8066039966

+234 8023783939

email: analyticals@narict.gov.ng

NARICT ANALYTICAL SERVICES

Trustworthy & Reliable Services

ANALYTICAL EQUIPMENT

Gas Chromatograph with Flame Ionization Detector (GC-FID)

BET Surface Area and Porosity Analyser

Fourier Transform Infrared Spectrometer (FTIR)

UV-Visible Spectrometer (UV-Vis) with ISR for solid material analysis

Brookefield Rheometer | Densitometer

High Performance Liquid Chromatograph (HPLC)

Atomic Absorbance Spectrometer (AAS)

Amino Acid Analyzer (AAA)

Universal Testing Machine (UTM)

Gas analysers for CO, CO₂, H₂S, NH₃, NO₂ and H₂ analysis

Gas chromatography with mass spectrometer (GC-MS)

Thermogravimetric Analyzer (TGA)



Chemical Analysis
Materials Characterization
Petroleum Products Testing
Water Analysis
Heavy Metal Analysis

National Research Institute
for Chemical Technology, Zaria
Km 4, Old Kano Road
Basawa, Zaria, Kaduna State,
Nigeria
P.M.B 1052

+234 806 6039966
+234 806 516 2971

analyticals@narict.gov.ng
<https://www.narict.gov.ng>

NARICT ANALYTICAL SERVICES



PHYTOCHEMICAL & PHYSICOCHEMICAL ANALYSIS

Tannins
Saponins
Glycosides
Alkanoids
Flavinoids
Phenols
Oxalates
Phytates

Specific Gravity
Refractive Index
Free Fatty Acid
Acid Value
Ester Value
Iodine Value
Relative Density
Peroxide Value



Trustworthy
& Reliable Services



Call to find out more

+234 806 516 2971
+234 806 603 9966



National Research Institute
for Chemical Technology, Zaria
Km 4, Old Kano Road,
Basawa, Zaria, Kaduna State
PMB 1052

email: analytics@narict.gov.ng
<https://www.narict.gov.ng>